

Proceedings of the

First

Joint Conference

on Point Detection

for Chemical and

Biological Defense



DISTRIBUTION STATEMENT A
Approved for Public Release
Distribution Unlimited



**Reproduced From
Best Available Copy**

23-27 October **2000**

**The Williamsburg Hospitality House
Williamsburg, Virginia**

20011010 103

REPORT DOCUMENTATION PAGE			Form Approved OMB No. 0704-0188	
Public reporting burden for this collection of information is estimated to average 1 hour per response, including the time for reviewing instructions, searching existing data sources, gathering and maintaining the data needed, and completing and reviewing the collection of information. Send comments regarding this burden estimate or any other aspect of this collection of information, including suggestions for reducing this burden, to Washington Headquarters Services, Directorate for Information Operations and Reports, 1215 Jefferson Davis Highway, Suite 1204, Arlington, VA 22202-4302, and to the Office of Management and Budget, Paperwork Reduction Project (0704-0188), Washington, DC 20503.				
1. AGENCY USE ONLY (Leave blank)		2. REPORT DATE 23 - 27 Oct 2000		3. REPORT TYPE AND DATES COVERED Proceedings - 23 - 27 Oct 2000
4. TITLE AND SUBTITLE Proceedings of the First Joint Conference on Point Detection for Chemical and Biological Defense			5. FUNDING NUMBERS DAAD05-00-P-7443	
6. AUTHOR(S)				
7. PERFORMING ORGANIZATION NAME(S) AND ADDRESS(ES) Joint Science and Technology Panel on Chemical and Biological Defense AMSSB-RRT (JSTPCBD) Aberdeen Proving Ground MD 21010-5424			8. PERFORMING ORGANIZATION REPORT NUMBER	
9. SPONSORING/MONITORING AGENCY NAME(S) AND ADDRESS(ES) Joint Science and Technology Panel on Chemical and Biological Defense AMSSB-RRT (JSTPCBD) Aberdeen Proving Ground MD 21010-5424			10. SPONSORING/MONITORING AGENCY REPORT NUMBER	
11. SUPPLEMENTARY NOTES				
12a. DISTRIBUTION AVAILABILITY STATEMENT Approved for Public Release; distribution is unlimited			12b. DISTRIBUTION CODE	
13. ABSTRACT (Maximum 200 words) This proceedings contains 75 unclassified papers presented at the First Joint Conference on Point Detection for Chemical and Biological Defense (1JCPD), held at the Williamsburg Hospitality House, Williamsburg, Virginia, 23 - 27 Oct 2000. The Conference was organized by the Joint Science and Technology Panel on Chemical and Biological Defense (JSTPCBD) in cooperation with the U.S. Army, Navy, Air Force, and Marine Corps, and other CB Agencies. Mr. Kirkman Phelps, U.S. Army SBCCOM, was the Conference Chair. Keynote addresses were given by Dr. Anna Johnson-Winegar, Deputy Assistant to the Secretary of Defense (CBD), and COL(P) Patricia Nilo, Commandant, U.S. Army Chemical School.				
14. SUBJECT TERMS			15. NUMBER OF PAGES 633	
			16. PRICE CODE	
17. SECURITY CLASSIFICATION OF REPORT Unclassified	18. SECURITY CLASSIFICATION OF THIS PAGE Unclassified	19. SECURITY CLASSIFICATION OF ABSTRACT Unclassified	20. LIMITATION OF ABSTRACT SAR	

Proceedings of the

**First Joint Conference on
Point Detection for Chemical
and Biological Defense**

23-27 October 2000

The Williamsburg Hospitality House
Williamsburg, Virginia

PREFACE

This proceedings contains 75 unclassified papers presented at the First Joint Conference on Point Detection for Chemical and Biological Defense (1JCPD), held at The Williamsburg Hospitality House, Williamsburg, Virginia, 23-27 October 2000. The papers contained in this document have also been made available on CD-ROM.

The Conference was organized by the Joint Science and Technology Panel on Chemical and Biological Defense (JSTPCBD) in cooperation with the U.S. Army, Navy, Air Force, and Marine Corps, and other CB Agencies. Mr. Kirkman Phelps, U.S. Army SBCCOM, was the Conference Chair. Keynote addresses were given by Dr. Anna Johnson-Winegar, Deputy Assistant to the Secretary of Defense (CBD), and COL(P) Patricia Nilo, Commandant, U.S. Army Chemical School.

Acknowledgment is made of the support and cooperation of the Steering Committee and Technical Committee, keynote speakers, session chairs, and presenters during 1JCPD. Logistical support for the conference was provided by Science and Technology Corp.

SPONSORS

SERVICES:

U.S. Army

- Edgewood Chemical Biological Center, SBCCOM, Aberdeen Proving Ground, Maryland
- Medical Research Institute of Infectious Diseases, Ft. Detrick, Maryland

U.S. Navy

- Naval Surface Warfare Center, Dahlgren, Virginia
- Office of Naval Research, Arlington, Virginia
- Naval Research Laboratory, Washington, D.C.

U.S. Air Force

- Air Force Research Laboratory, Wright-Patterson AFB, Ohio
- 311 Human System Wing, Brooks AFB, Texas

U.S. Marine Corps

- Marine Corps Systems Command, Quantico, Virginia

JOINT:

- Joint Project Office – Bio Defense, Falls Church, Virginia
- Defense Threat Reduction Agency, Dulles, Virginia
- Joint Service Material Group, Aberdeen Proving Ground, Maryland
- Joint Service Integration Group, Ft. Leonard Wood, Missouri

Steering Committee:

Mr. Kirkman Phelps, Conference Chair
COL Edwin Armitage, Medical
LTC Donald Buley, JPO-BD
Mr. Merlin Erickson, ECBC
Mr. Gary Kwitkoski, DTRA
Dr. S. Randolph Long, SBCCOM
Mr. David Lueck, JSIG
Mr. Jose Martinez, 311 HSW
Mr. Michael Pompeii, NSWCDG
Ms. Julie Redfern, USMC
Dr. I. Gary Resnick, DTRA
Dr. Peter Schmidt, ONR
Dr. Ngai Wong, AFRL
Dr. Edward W. Stuebing, ECBC

Technical Committee:

Dr. Edward W. Stuebing, Chair, SBCCOM
Mr. Adam J. Becker, MARCORSYSCOM
Dr. Steven D. Christesen, SBCCOM
Mr. Terry Creque, DTRA
Dr. Dan Driscoll, NSWC
Dr. Jay Eversole, NRL
Mr. Michael T. Goode, SBCCOM
COL Erik A. Henchal, USAMRIID
Ms. Janet L. Jensen, SBCCOM
Mr. Jerry Pate, DTRA
Dr. Peter Stopa, SBCCOM
LTC Mark Weitekamp, DOE

Conference Coordinator:

Diana McQuestion
Science and Technology Corporation
Meeting Services International
10 Basil Sawyer Drive
Hampton, Virginia 23666-1393
Telephone: 757/766-5831
Telefax: 757/865-8721
Email: mcquestion@stcnet.com

TABLE OF CONTENTS

	Page
Preface	iii
Sponsors	iv
– SESSION A. PLENARY SESSION –	
Opening Remarks	1
<i>Mr. Kirkman R. Phelps</i> , Chairman, Commodity Area Manager	
Overview of the JSMG Program	9
<i>Dr. Ngai Wong</i> , U.S. Air Force Research Laboratory and <i>Dr. S. Randolph Long</i> , U.S. Army Edgewood Chemical Biological Center, Co-Chairmen	
Overview of Requirements	17
<i>Lt. Col. Leslie Koch</i> , Joint Services Integration Group	
Key Note Address	25
<i>COL(P) Patricia Nilo</i> , Commandant, U.S. Army Chemical School	
Key Note Address: The DoD Chemical and Biological Defense Program	28
<i>Dr. Anna Johnson-Winegar</i> , Deputy Assistant to the Secretary of Defense (CBD)	
– SESSION B1: OVERVIEWS I –	
Joint Biological Point Detection System (JBPDS) Requirements and Design Interplay	41
<i>LTC Timothy Moshier</i> and <i>Tom Buonaugurio</i> , Joint Biological Point Detection System, APG, MD	
JBPDS Block I EMD Program: Overview and Summary	52
<i>Wolf P. Altman</i> and <i>Donald R. Hohe</i> , Battelle, Columbus, OH	
M22 Automatic Chemical Agent Alarm	61
<i>Rob Howard</i> , Graseby Dynamics Ltd., Watford, Herts, United Kingdom; <i>Daniel M. Nowak</i> , U.S. Army Soldier and Biological Chemical Command, APG, MD	
– SESSION B2: OVERVIEWS II –	
Biological Detection Systems: The Industry Experience	64
<i>Peter J. Day</i> , Graseby Dynamics Ltd., Watford, Herts, United Kingdom	
Ion Mobility Spectrometry – Past, Present and Future	75
<i>Alan M. Brittain</i> and <i>John Brokenshire</i> , Graseby Dynamics Ltd., Watford, Herts, United Kingdom	

– SESSION B3: OVERVIEWS III –

The Block II Chemical Biological Mass Spectrometer – Point Detection for Both Chemical and Biological Warfare Agents	81
<i>Wayne H. Griest, Marcus B. Wise, Kevin J. Hart and Stephen A. Lammert, Oak Ridge National Laboratory, Oak Ridge, TN; Alexander P. Hyrncewich and David W. Sickenberger, U.S. Army Soldier and Biological Chemical Command, APG, MD</i>	
Point Detection Chemistry at the U.S. Army Research Office	92
<i>Stephen J. Lee, U.S. Army Research Laboratory – Army Research Office, Research Triangle Park, NC</i>	

– SESSION C: NEW CONCEPTS – GENERAL –

Development of a Corona Discharge Source to Generate Ions in Chemical Agent Detector	94
<i>George Lozos and Doug Green, Environmental Technologies Group, Inc., Baltimore, MD; and Rod Wilson, Graseby Dynamics Ltd., Watford, Herts, United Kingdom</i>	
Canary B-Cell Sensor for Rapid, Sensitive Identification of Biological Agents	102
<i>Todd H. Rider, Albert M. Young, Martha S. Petrovick, Frances E. Nargi, Ann E. Rundell, Richard H. Mathews, Jae H. Kyung, Timothy Stephens, Linda M. Mendenhall, Steven T. Palmacci, Laura T. Smith, Bernadette Johnson, and Mark A. Hollis, MIT Lincoln Laboratory, Lexington, MA; Jianzhu Chen, MIT Department of Biology, Cambridge, MA</i>	

– SESSION D: NEW CONCEPTS - NANOTECHNOLOGY FOR CB DETECTION –

Luminescent Sensors for the Detection of Chemical Agents in Water	109
<i>Amanda Jenkins and Ray Yin, U.S. Army Research Laboratory, APG, MD; Dujie Qin, Janet Jensen, and H. Dupont Durst, U.S. Army Edgewood Chemical Biological Center, APG, MD</i>	
Nanostructure Enhanced Raman Scattering	116
<i>Paul D. Pulaski, David Burckel, and S.R.J. Brueck, University of New Mexico, Albuquerque, NM</i>	

– SESSION E1: SMALL DETECTORS I –

Side-by-Side Comparison of Small, Hand-held Ion Mobility Spectrometers and Surface Acoustic Wave Devices	122
<i>Charles S. Harden, Dennis M. Davis, Donald B. Shoff, and Vincent M. McHugh, U.S. Army Edgewood Chemical Biological Center, APG, MD; Gretchen Blethen, Geo-Centers, Inc., APG, MD</i>	

– SESSION E2: SMALL DETECTORS II –

Residual Life Indicators – Point Chemical Detectors Used to Measure the Capacity of Activated Carbon in Protective Garments, Gas Mask Filters, and Collective Protection Filters.....	123
<i>Joseph E. Roehl, Timothy W. Caraher, Kimberly A. Kalmes, and Elizabeth A. Isley, Scentczar Corporation, Fredericksburg, VA</i>	
Development of μChemLab™/CB for Detection of Biotoxins	131
<i>Julia Fruetel; Ronald Renzi, Robert Crocker, Victoria VanderNoot, Scott Ferko, Jamie Stamps, Isaac Shokair, Dan Yee, and Charlie Hasselbrink Sandia National Laboratories, Albuquerque, NM</i>	
Miniature Chemical Analysis System (μChemLab) for Chemical Agent Detection	140
<i>Patrick R. Lewis, Gregory C. Frye-Mason, Richard J. Kottenstette, Ronald P. Manginell, George R. Dulleck, Douglas R. Adkins, Edwin J. Heller, Curtis D. Mowry, David Martinez, Darryl Y. Sasaki, and Lawrence F. Anderson, Sandia National Laboratories, Albuquerque, NM</i>	

– SESSION F: OPTICAL METHODS FOR CHEMICAL DETECTION –

Chemical Detection Based on Photo-Induced Energy Transfer	145
<i>Guangming Li, Larry W. Burggraf, and William Baker, Air Force Institute of Technology, OH</i>	
Surface-Enhanced Raman Spectroscopy as a Rapid Field Detector for Chemical and Biological Defense	151
<i>James M. Sylvia, Jeremy M. Raelin, James A. Janni, Savvas C. Makrides, Andrew A. Guzelian, and Kevin M. Spencer, EIC Laboratories, Inc., Norwood, MA</i>	
Monitoring Low Levels of Ionic Pollutants in Water Using Attenuated Total Reflectance Infrared Spectroscopy	158
<i>Matthew A. Odom, Gretchen N. Hebert, Brady J. Clapsaddle, and Steven H. Strauss, Colorado State University, Fort Collins, CO</i>	
Trace Chemical Vapor Detection by Photothermal Interferometry	168
<i>Nicholas F. Fell, Jr., Paul M. Pellegrino, and James B. Gillespie, U.S. Army Research Laboratory, Adelphi, MD</i>	

– SESSION G: BIOAEROSOL TRIGGERS –

The BioCounter: A Hand-Held Biodetector and Sampler Based on Fluorescence Particle Sizing	175
<i>Greg A. Luoma, Pierre P. Cherrier, Carol Y. Zheng, Marc A. Piccioni and Alex S. Wong, Bio-Defence Systems, Calgary, Canada; Richard K. DeFreez, Michael A. Potter, Kenneth L. Girvin, and Ronald B. Whitney, Pacific Scientific Instruments, Grants Pass, OR</i>	

– SESSION H: GENETIC ASSAYS –

Identification of Anthrax-Specific Signature Sequence from <i>Bacillus anthracis</i>	185
<i>Vipin K. Rastogi</i> , Geo-Centers, Inc., APG, MD; <i>Tu-chen Cheng</i> , U.S. Army Edgewood Chemical Biological Center, APG, MD	
Design and Optimization of Fluorogenic 5'-Nuclease Assays for <i>Bacillus anthracis</i> and <i>Yersinia pestis</i>	195
<i>Deanna R. Christensen</i> , <i>Melissa S. Frye</i> , <i>Stephen B. Kerby</i> , <i>Laurie J. Hartman</i> , <i>Tammy R. Gibb</i> , <i>Erik A. Henchal</i> , and <i>David A. Norwood</i> , U.S. Army Medical Research Institute of Infectious Diseases, Fort Detrick, MD	
A Frozen Bacteria Collection as a Source of Quality Reference Material	199
<i>Jeffrey D. Teska</i> , <i>Cindy M. Allan</i> , <i>Stephanie L. Redus</i> , and <i>John W. Ezzell</i> , U.S. Army Medical Research Institute of Infectious Diseases, Fort Detrick, MD	

– SESSION J: IMMUNOASSAYS –

Recombinant Antibodies for the Detection of Bacteriophage MS2 and Ovalbumin	204
<i>Kevin P. O'Connell</i> , <i>Peter A. Emanuel</i> , <i>Akbar S. Khan</i> , and <i>James J. Valdes</i> , U.S. Army Edgewood Chemical Biological Center, APG, MD; <i>Timothy J. Stinchcombe</i> and <i>Robert Shopes</i> , Tera Biotechnology Corp., La Jolla, CA; <i>Maha Khalil</i> and <i>Mohyee E. Eldefrawi</i> , University of Maryland School of Medicine, Baltimore, MD	
Immunomagnetic One-Step Assay for Detection of Biological Agents	212
<i>Deborah L. Menking</i> , <i>Michael T. Goode</i> , and <i>Alan W. Zulich</i> , U.S. Army Edgewood Chemical Biological Center, APG, MD; <i>Emily D. Myers</i> , <i>Bruce T. Voelker</i> , and <i>Rebecca L. Tanner</i> , Science and Technology Corporation, Edgewood, MD	
Development and Testing of an Electrochemiluminescent Platform for the Diagnosis of Infectious and Non-Infectious Disease	222
<i>Cindy A. Rossi</i> , <i>Todd M. Kijek</i> , <i>Erik A. Henchal</i> , <i>Mary E. Brock</i> , and <i>George V. Ludwig</i> , U.S. Army Medical Research Institute of Infectious Diseases	
Development of an Autonomous Pathogen Detection System	227
<i>Richard G. Langlois</i> , <i>Steve Brown</i> , <i>Bill Colston</i> , <i>Les Jones</i> , <i>Don Masquelier</i> , <i>Pete Myer</i> , <i>Mary McBride</i> , <i>Shanavaz Nasarabadi</i> , <i>Albert J. Ramponi</i> , <i>Kodumudi Venkateswaran</i> , and <i>Fred Milanovich</i> , Lawrence Livermore National Laboratory, Livermore, CA	

– SESSION K: MASS SPECTROMETRY AND ION MOBILITY SPECTROMETRY –

Shipboard Automatic Chemical Agent Detector and Alarm	235
<i>Gregory P. Johnson</i> , Naval Surface Warfare Center, Dahlgren, VA	
Force Protection from Biological Aerosols Using a Portable Hyphenated Analytical System	242
<i>A. Peter Snyder</i> , U.S. Army Soldier and Biological Chemical Command, APG, MD; <i>Waleed M. Maswadeh</i> , <i>John A. Parsons</i> , and <i>Ashish Tripathi</i> , Geo-Centers, Inc., APG, MD; <i>Henk L. C. Meuzelaar</i> , <i>Jacek P. Dworzanski</i> , and <i>Man-Goo Kim</i> , University of Utah, Salt Lake City, UT	
Automated Sample Processing for Mass Spectrometric Identification of Biological Agents	252
<i>Thaiya Krishnamurthy</i> and <i>Rabih Jabbour</i> , U.S. Army Edgewood Chemical Biological Center, APG, MD; <i>Dennis C. Roser</i> , Geo-Centers, Inc., APG, MD; <i>Remco Swart</i> and <i>Bruno Laine</i> , LCPackings, Amsterdam, The Netherlands; <i>Jean-Pierre Salzmann</i> , LCPackings USA, San Francisco, CA	

The Use of Ion-Ion Chemistry in an Electrospray Ion Trap Mass Spectrometer for the Detection and Identification of Chemical/Biological Threats	263
<i>James L. Stephenson and Stephen A. Lammert, Oak Ridge National Laboratory, Oak Ridge, TN</i>	
Biodetection by Identification of PCR Products Using Electrospray Ionization Mass Spectrometry and Tandem Mass Spectrometry	272
<i>Yvette A. Johnson, Madan Nagpal, Mark T. Krahmer, Karen F. Fox, and Alvin Fox, University of South Carolina School of Medicine, Columbia, SC</i>	
Rapid Response Chem/Bio Detection System Based on Photoionization Mass Spectrometry	277
<i>Matthew D. Evans, Karl A. Hanold, and Jack A. Syage, Syagen Technology, Inc., Tustin, CA</i>	
– SESSION L: IMPROVING DETECTOR PERFORMANCE –	
Strategies for the Detection of Unknown Biological Materials	289
<i>Peter J. Stopa, U.S. Army Edgewood Chemical Biological Center, APG, MD</i>	
– SESSION M: TEST AND EVALUATION METHODOLOGY –	
Aerosol Generation for Testing BW Detectors	294
<i>Jerold R. Bottiger, Edward W. Stuebing, and Paul J. Deluca, U.S. Army Edgewood Chemical Biological Center, APG, MD</i>	
Test Protocol and Algorithm Development	309
<i>Gary Bodily, MRC Corp., Logan UT; John V. Mathews, J. Jarez, and Joel Dubow, University of Utah, Salt Lake City, UT</i>	
– SESSION N: CB COLLECTION, SAMPLING, AND SAMPLE PROCESSING –	
Bioaerosol Sampling Systems	318
<i>S.A. Lee, J.S. Haglund, H. N. Phan, S. Chandra, and Andrew R. McFarland, Texas A&M University, College Station, TX; R.S. Black and M.J. Shaw, Battelle Columbus Laboratories, Columbus, OH</i>	
Performance Characterization of Developmental and Next Generation Bioaerosol Collectors	328
<i>Agnes Akinyemi, Jerold Bottiger, Robert Doherty, Jana Kesavan, Edward Stuebing, Daniel Weber, and Daniel Wise, U.S. Army Edgewood Chemical Biological Center, APG, MD</i>	
Surface Sampling Capability for Chemical Point Detection Systems	336
<i>Elizabeth S. Catalano, U.S. Army Edgewood Chemical Biological Center, APG, MD</i>	
BioHaz: A Concept for First Responders	341
<i>Peter J. Stopa and Philip A. Coon, U.S. Army Edgewood Chemical Biological Center, APG, MD; David Trudil, New Horizons Diagnostics Corporation, Columbia, MD; David Gray and Randy Bright, EAI Corporation, Abingdon, MD</i>	

Rapid Lysis and Release of Nucleic Acid from Microbial Agents for TAQMAN-PCR-Based Real-Time Identification	346
<i>Sanjiv R. Shah, Misty H. Lindsey, Rebecca L. Tanner, and Heena S. Beck, Science and Technology Corporation, Edgewood, MD; Michael T. Goode and Alan W. Zulich, U.S. Army Edgewood Chemical Biological Center, APG, MD</i>	

POSTER SESSION

– P1: CB SAMPLE COLLECTION AND SAMPLE PROCESSING –

Purification of MS2 Bacteriophage from Complex Growth Media and Resulting Analysis by the Integrated Virus Detection System (IVDS)	357
<i>Charles H. Wick, U.S. Army Soldier and Biological Chemical Command, APG, MD; Patrick E. McCubbin, Optimetrics, Inc., Forest Hill, MD</i>	

Rapid Extraction and Amplification of Bacterial DNA from Soil Samples	369
<i>Darrel E. Menking, Peter A. Emanuel, James J. Valdes, U.S. Army Soldier and Biological Chemical Command, APG, MD; Suzanne K. Kracke, Geo-Centers, Inc., APG, MD; Calvin Chue, Battelle, Bel Air, MD</i>	

Comparison of the Schleicher and Schuell Isocode PCR DNA Sample Isolation Device and the Qiagen QIAAMP DNA Purification Systems	373
<i>Fred K. Knauert, Philip D. Craw, Susan R. Coyne, David R. Shoemaker, and Erik A. Henchal, U.S. Army Medical Research Institute of Infectious Diseases, Fort Detrick, MD</i>	

A Procedure for Preparing PCR-Amplifiable DNA from <i>Bacillus Anthracis</i> Spores in Soil Samples	377
<i>Susan R. Coyne, Philip D. Craw, Jeff D. Teska, John W. Ezzell, Erik A. Henchal and Fred K. Knauert, U.S. Army Medical Research Institute of Infectious Diseases, Fort Detrick, MD</i>	

Honey Bees Scavenge Airborne Bacteria from the Atmosphere	380
<i>Kevin Prier, Microbial Aerosol Research Laboratory, LLC, Monmouth, OR; Bruce Lighthart and Jerry Bromenshenk, University of Montana, Missoula, MT; Gerald Loper, USDA, Carl Hayden Bee Center, Tuscon, AZ</i>	

– P2: GENETIC ASSAYS –

An Integrated Fiber-Optic System for Identifying Biological Agents	390
<i>Yifu Guan, Jeffrey T. Ives, and James H. Bechtel, TACAN Corporation, Carlsbad, CA</i>	

– P3: IMMUNOASSAYS –

Production of Monoclonal Antibodies: Validation of Processes and Products for Critical Reagent Repository	399
<i>Tracy H. Coliano, Ameneh M. Arasteh, and Peter Emanuel, U.S. Army Edgewood Chemical Biological Center, APG, MD; Jun T. Park, Karen S. Heroux, Sarah Cork, and Suzanne K. Kracke, Geo-Centers, Inc., APG, MD</i>	
Peptide Epitopes and Mimetics	401
<i>Roy G. Thompson, Akbar S. Khan, Ameneh M. Arasteh, and James J. Valdes, U.S. Army Soldier and Biological Chemical Command, APG, MD</i>	
RAPTOR: A Portable, Automated Biosensor	408
<i>George P. Anderson, Chris A. Rowe-Taitt, and Frances S. Ligler, Naval Research Laboratory, Washington, DC</i>	
Demonstration of a Rapid, Portable Evanescent Wave Biological Agent Identifier	415
<i>Stephen J. Krak, Richard L. Hall, and Herbert S. Bresler, Battelle Memorial Institute, Columbus, OH; Anthony A. Boiarski, BioSense Consulting</i>	
Dissociation Enhanced Lanthanide Fluoroimmuno Assays (DELFI[®]) for Detection of Foodborne Pathogens and Agents of Biological Origin	423
<i>Emily D. Myers, Science and Technology Corporation, Edgewood, MD; Deborah L. Menking, Michael T. Goode, and Alan W. Zulich, U.S. Army Edgewood Chemical Biological Center, APG, MD</i>	

– P4: MASS SPECTROMETRY –

Microorganism Identification by Mass Spectrometry and Protein Database Searches – An Analysis	432
<i>Ravi P. Lall and A. Peter Snyder, U.S. Army Edgewood Chemical Biological Center, APG, MD</i>	
Advancements in Detection Capabilities and Data Analysis with the Improved Pyrolysis Gas Chromatography-Ion Mobility Spectrometer Biodetector	442
<i>Ashish Tripathi and Waleed Maswadeh, Geo-Centers, Inc., APG, MD; Philip Coon, and A. Peter Snyder, U.S. Army Soldier and Biological Chemical Command, APG, MD</i>	

– P5: ION MOBILITY SPECTROMETRY –

Upgrading a Chemical Monitor into a Biodetector	459
<i>Waleed M. Maswadeh, Ashish Tripathi, and John Parsons, Geo-Centers, Inc., APG, MD; Ken Barry, Charles S. Harden, and A. Pete Snyder, U.S. Army Soldier and Biological Chemical Command, APG, MD</i>	

– P6: OPTICAL METHODS FOR CB DETECTION –

Semi-Selective Optical Sensors for Real-Time Detection of Biological Warfare Agents	471
<i>Han Chuang, AnCheng Chang, Laura Taylor, and Mary Beth Tabacco, Echo Technologies, Inc., Boston, MA</i>	
Demonstration of Surface Enhanced Fluorescence with Bacterial Biosensors	479
<i>Han Chuang, Jaimie Russo, and Mary Beth Tabacco, Echo Technologies, Inc., Boston, MA; Jim Gillespie, Army Research Laboratory, Adelphi, MD</i>	
Non-Intrusive Analysis of Chemical Agent Identification Sets (CAIS) Using a Portable Fiber-Optic Raman Spectrometer	486
<i>Steven D. Christesen, Brian MacIver, Lawrence Procell, and David Sorrick, U.S. Army Edgewood Chemical Biological Center, APG, MD; Michael Carrabba and Job Bello, EIC Laboratories, Inc., Norwood, MA</i>	
Detection and Identification of Chemical Agents in Water Using Surface Enhanced Raman Spectroscopy (SERS) on Gold and Silver Doped Sol-Gels	494
<i>Steven D. Christesen and Kate K. Ong, U.S. Army Edgewood Chemical Biological Center, APG, MD; M. Edward Womble, Raman Systems Inc., Richard Clark and Ranjith Premasiri, Boston University Photonics Center</i>	
Detection of Chemical and Biological Agents of Death with Molecular Specificity Through Quantified Raman Spectroscopy (QRS)	498
<i>J. Kirchoff, J. Lucke, S. McLeod, F. Nottke, D. Obergh, and J. Pollard, Pima Community College, The University of Arizona Optical Sciences Center and Opto-Forensic Technologies/Wizard of Ink & Co. (OFT/WOI), Tucson, AZ</i>	
Porphyrins as Detectors of CB Agents	505
<i>H. James Harmon, Oklahoma State University, Stillwater, OK</i>	
Rotational Signatures of Chemical Agents and Related Compounds	515
<i>R.D. Suenram, A.R. Hight Walker, G.T. Fraser, D.F. Plusquellic, R.S. DaBell, P.M. Chu, and G.C. Rhoderick, National Institute of Standards and Technology, Gaithersburg, MD; A.C. Samuels, J.O. Jensen, M.W. Ellzy, and J.M. Lochner, U.S. Army Edgewood Chemical Biological Center, APG, MD</i>	
Infrared, Far Infrared, and Millimeter Wave Spectroscopic Measurements on Biological Materials: Bacterial Spores, Pollens, and Mold	522
<i>Alan C. Samuels, James O. Jensen, William R. Loerop, Michael Ellzy, J. Michael Lochner, Dorothea Paterno, and Kate K. Ong, U.S. Army Edgewood Chemical Biological Center, APG, MD; Dwight Woolard, Army Research Office, Research Triangle Park, NC; Tatiana Globus, University of Virginia, Charlottesville, VA</i>	
Artificial Neural Networks for Infrared Spectral Classification	533
<i>Howard T. Mayfield, Air Force Research Laboratory, Tyndall Air Force Base, FL, Larry Burggraf, and DeLyle Eastwood, Air Force Institute of Technology, Wright Patterson Air Force Base, OH</i>	

Polarized Light Scattering to Provide Size Distributions of Microorganisms	542
<i>Burt V. Bronk</i> , Air Force Research Lab, APG, MD; <i>Merrill E. Milham</i> , U.S. Army Edgewood Chemical Biological Center, APG, MD; <i>Zhao Z. Li</i> and <i>Jozsef Czege</i> , USUHS, Bethesda, MD	
– P7: CHEMICAL AGENT DETECTION –	
Shipboard Automatic Liquid Agent Detector (SALAD)	552
<i>Diane LaMoy</i> , Naval Surface Warfare Center, Dahlgren, VA	
– P8: BIO BACKGROUNDS –	
Ambient Background Characterization Web Site	565
<i>Dorothea Paterno</i> , U.S. Army Edgewood Chemical Biological Center, APG, MD; <i>Allen Smith</i> , Oak Ridge National Laboratory, Oak Ridge, TN	
BW Detection and the Background Bioaerosols – Issues, Problems and Recommendations	573
<i>Amnon Birenzvig</i> and <i>Charles H. Wick</i> , U.S. Army Soldier and Biological Chemical Command, APG, MD	
– P9: INFORMATION DISSEMINATION –	
Chemical and Biological Agent Point Detector Data Acquisition Using the Environmental Systems Management Analysis and Reporting Network	586
<i>Anthony Gattuso</i> and <i>Roger Schlicht</i> , General Atomics, San Diego, CA; <i>Joel Roark</i> and <i>Bob Hilley</i> , Nomadics, Stillwater, OK; <i>John D. Mills</i> , Tinker Air Force Base, OK; <i>Bruce J. Nielsen</i> and <i>Dennis Bernia</i> , Tyndall Air Force Base, FL	
List of Participants	597
Author Index	617



FIRST JOINT CONFERENCE ON POINT DETECTION FOR CB DEFENSE



OPENING REMARKS

PRESENTED BY
KIRKMAN R. PHELPS, PE
CHAIRMAN

410-436-2675

Kirkman.Phelps@sbccom.apgea.army.mil

JSMG-961022.1



FIRST JOINT CONFERENCE ON POINT DETECTION FOR CB DEFENSE



STEERING COMMITTEE

Kirkman Phelps, Chair
Ngai Wong, AFRL
David Lueck, JSIG
Gary Resnick, DTRA
Donald Buley, JPO-BD
Gary Kwitkoski, DTRA
Edwin Armitage, Medical

S. Randolph Long, ECBC
Michael Pompeii, NSWCDG
Merlin Erickson, PM-NBC
Julie Redfern, USMC
Jose Martinez, 311 HSW
Peter Schmidt, ONR
Dr. Ed Stuebing, SBCCOM

JSMG-961022.1



FIRST JOINT CONFERENCE ON POINT DETECTION FOR CB DEFENSE



Technical Committee

Edward W. Stuebing, Chairman
Erik A. Henchal, USAMRIID
William H. Capozzoli, USMC
Adam J. Becker, USMC
Daniel C. Driscoll, USN
Eugene L. Berger, USAF
Jerry Pate, DTRA (Chem)
Terry Creque, DTRA (Bio)

Michael Goode, SBCCOM
Peter Stopa, USMC
Steve Harden, SBCCOM
Janet Jensen, SBCCOM
Steven Christesen, SBCCOM
Jeff Stiefel, JPO-BD
Eric Kaufman, DOE

JSMG-961022.1



FIRST JOINT CONFERENCE ON POINT DETECTION FOR CB DEFENSE



SPECIAL THANKS TO:

Ngai Wong & Randy Long
Ed Stuebing
Dan Davis
Diana McQuestion

JSMG-961022.1



Contamination Avoidance



RDA, Industrial Base
Logistics and Threat

Joint Service Materiel Group (JSMG)

**Chemical and Biological Defense
Contamination Avoidance**
Kirkman R. Phelps
DSN 584-2675/Com 410-436-2675

**Other Members of
Commodity Team**
SOFCOM
CMO

Commodity Area Team

U.S. Army Rep
Donald H. Edler
DSN 584-4028
Com 410-436-4028

U.S. Marine Corps Rep
Julie A. Redfern
DSN 278-5897
Com 703-784-5897

U.S. Navy Rep
Alan E. Moore
DSN 332-8841
Com 703-602-8841

U.S. Air Force Rep
Jose A. Martinez
DSN 240-4320
Com 210-536-4320

JSIG Rep
David Lueck
DSN 676-7763
Com 573-596-0131
EXT 37763

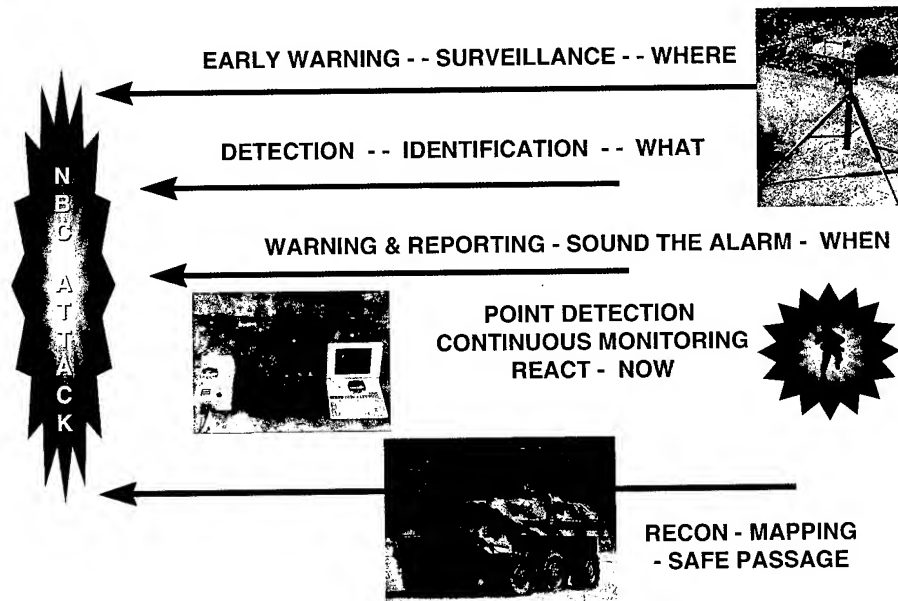
JSTPCBD Rep
Ngai M. Wong
DSN 584-3111
Com 410-436-3111

JPO-BD Rep
MAJ(P) Jeff Stiefel
DSN 761-9678
Com 703-681-9678

Integrated Product Teams & Working Groups



Contamination Avoidance

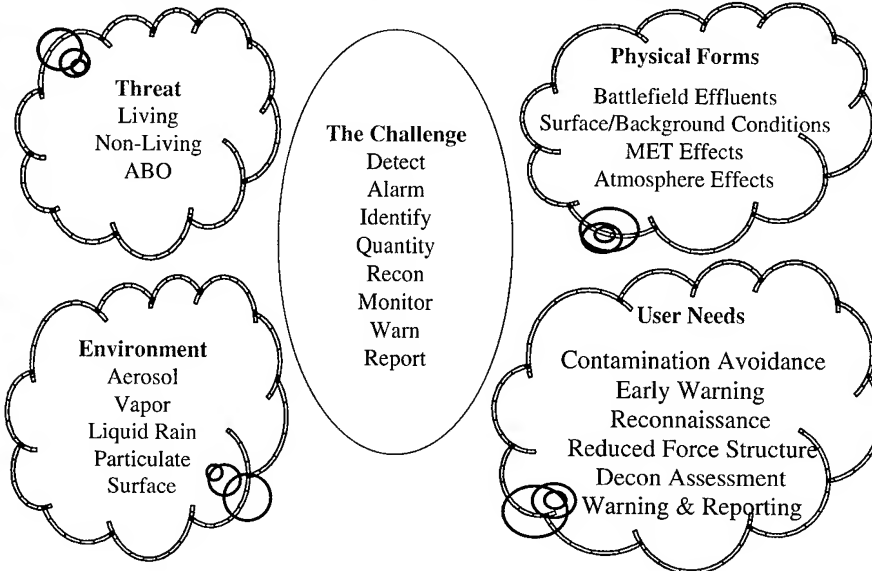




Contamination Avoidance



Overall Objective: Provide CB Situational Awareness



Contamination Avoidance SUB AREAS



THREE PILLARS:

- **Point Detection** - Goal is to provide Real-Time Detection, Monitoring, Identification, Quantification, and Local Warning *1JCPD Oct 00*
- **Standoff Detection** - Goal is to provide the above capabilities plus Early Warning, Area Over Watch, and Mapping *4JCSD Oct 01*
- **Battle Management** - Goal is to provide Warning and Reporting, Sensor Fusion, Situational Awareness, Commander Decision Support, and Mission Planning and Assessment Tools *1JCBM Oct 02*



CONTAMINATION AVOIDANCE PRODUCTS



Technology Base	Production/Deployment
<p>Miniature Standoff Agent Detector (MSAD)</p> <p>JS Warning & Identification LIDAR Detection (JSWILD)/Artemis</p> <p>Joint Warning & Reporting Network III (JWARN III)</p> <p>Joint Biological Point Detection System, Blk II (JPBDS Blk II)</p> <p>Joint Biological Standoff Detection System (JBSDS)</p> <p>Joint Service Agent Water Monitor (JSAWM)</p> <p>JS CBR Integrated Detection System (JSCBRIDS)</p> <p>Joint Modular CB Detector (JMCBD) JS Wide Area Detection</p> <p>Surface Monitoring Liquid Surface Detection WideSpec</p> <p>HyperSpectral Imaging Joint Point & Standoff Radiacs</p>	<p>M8/M9 Paper</p> <p>M256A1 Detector Kit M272A1 Water Test Kit</p> <p>M8A1 Chemical Agent Alarm AN/KAS-1</p> <p>Biological Integrated Detection System (BIDS), NDI & M31</p> <p>Chemical Agent Point Detection Systems (CAPDS)</p> <p>Individual Chemical Agent Detector (ICAD)</p> <p>Improved Point Detection System (IPDS)</p> <p>Chemical Agent Monitor (CAM/ICAM)</p> <p>M21 Remote Sensing Chemical Agent Alarm (RSCAAL)</p> <p>NBC Reconnaissance System (NBCRS), M93 & Blk I</p> <p>Automatic Chemical Agent Detector & Alarm (ACADA)</p> <p>AN/VDR-2 Radiac Set</p> <p>AN/PDR-75 Radiac Set</p> <p>AN/PDR-77 Radiac Set</p> <p>Multi-Function Radiac Set</p> <p>AN/UDR-13 Pocket Radiac</p>
Development	
<p>NBC Reconnaissance System, Blk II (NBCRS Blk II)</p> <p>JS Lightweight NBC Reconnaissance System (JLNBCRS)</p> <p>CB Mass Spectrometer (CBMS)</p> <p>JS Lightweight Standoff Chemical Agent Detector (JSLSCAD)</p> <p>Joint Warning & Reporting Network II (JWARN II)</p> <p>Joint Biological Point Detection System (JBPDS)</p> <p>Interim Biological Agent Detection System (IBADS)</p> <p>Joint Chemical Agent Detector (JCAD)</p>	



Contamination Avoidance FY02-07 - Key Capabilities



- **Chemical Point Detection/Monitoring/Recon**
 - **Automatic Chemical Agent Detector Alarm (ACADA)**
 - Unit detector to replace the M8A1 alarms
 - **Improved (Chemical Agent) Point Detection System (IPDS)**
 - Shipboard Detector
 - Automatic detection of CW vapors and aerosols
 - Replaces CAPDS Alarm
 - **Improved Chemical Agent Monitor (ICAM)**
 - Improved maintenance without affecting performance
 - Twice the operational life over the CAM. Reduced operating costs
 - **Joint Chemical Agent Detector (JCAD)**
 - Small, lightweight detector to detect, identify, quantify and warn to lower levels of CW vapors
 - **NBC Reconnaissance System (NBCRS)**
 - Armored NBC Recon with improved detection (M21 RSCAAL & CBMS)
 - Improved logistics and reduced manpower
 - **JSLNBCRS**
 - USMC version of NBCRS (Mounted on LAV)





Contamination Avoidance FY02-07 - Key Capabilities

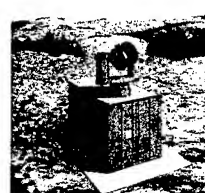


- **Chemical Stand-Off/Warning and Reporting**

- **Joint Service Lightweight Standoff Chemical Agent Detector (JSLSCAD)**
 - Range up to 5 km; Capable of remote, aerial, and on-the-move operation
- **Joint Service Warning and Identification LIDAR (JSWILD)**
 - Automatically detect, range, and map CW agents at up to 20 km
 - Scan to detect vapors, airborne liquids and particles
 - Stand-off capability for fixed site and reconnaissance
 - Rapid agent concentration mapping *Warning and Reporting*
- **Joint Warning and Reporting Network (JWARN)**
Comprehensive analysis and response capability to:
 - Interface with all NBC detectors and sensors & interoperability with all service C2 systems
 - Generate NBC reports, and automatically transmit NBC alarm and data
 - Vehicle or man-portable operations



JSLSCAD



JSWILD



JWARN



Contamination Avoidance FY02-07 - Key Capabilities



- **Biological Detection**

- **Portal Shield - XM99**
 - Identifies 8 BW agents in less than 25 minutes
 - Network for Automated BW detection in support of fixed sites
 - Chemical Sensor Interface
- **Joint Biological Point Detection System (JBPDs)**
 - Modular Bio point detection suite integrated on service platforms to replace BIDS and IBAD
 - Identify BW agent in 15 min or less after detection
 - Full automated detection/identification operation
- **Joint Biological Remote Early Warning System (JBREWS)**
 - Advanced Concept Technology Demonstration (ACTD)
 - Enhances overall BW protection system in theater with sensors significantly further upwind, closer to BW agent release point
 - Exploits power of networked sensors
 - Automated immunoassay reader
 - Low-power samplers
- **Joint Biological Standoff Detection System (JBSDS)**
 - Provides detect to warn capability
 - Maps Biological cloud
 - Vehicle, ship and fixed site applications



XM99



JBPDs



JBREWS



JBSDS
Early Prototype



Past, Present, Emerging (Chemical Detection)



1991 (Desert Storm)

♦ Limitations:

- No Organic Communication
- Limited standoff detection capability
- Limited liquid agent detection
- Limited recon
- Limited HD detection
- No individual detectors
- High false alarm rate potential

Today (FY00)

♦ Improved capabilities fielded:

- Improved Chemical Agent Monitor (ICAM)
- Automatic Chemical Agent Detector Alarm (ACADA)
- Remote Sensing Chemical Agent Alarm (RSCAAL)
- AN/KAS-1A
- M93A1 - NBCRS
- Improved (Chemical) Point Detection System (IPDS)

Future (FY07)

♦ Fielded in FYDP

- Joint Service Light-weight Chemical Agent Detector (JSLSCAD)
- Joint Chemical Agent Detector (JCAD)
- Joint Warning and Reporting Network (JWARN)
- NBCRS Block I Upgrade
- JSLNBCRS



Past, Present, Emerging (Biological Detection)



1991 (Desert Storm)

♦ Limitations:

- Single Technology
- No Organic Communication
- No Doctrine
- No Crew Protection
- Slow response time to higher HQs (hours)
- False alarms



Today (FY00)

♦ First time capabilities fielded:

- Biological Integrated Detection System (BIDS)/P3I
- Interim Biological Agent Detector (IBAD)



- Critical Reagents
- Portal Shield
 - Bio defense for critical fixed sites

Future (FY07)

♦ Fielded in FYDP

- Joint Biological Point Detection System
 - to supersede BIDS, BIDS P3I and IBAD
- Joint Biological Standoff Detection System (JBSDS)



Concluding Thoughts



CONTAMINATION

AVOIDANCE:

- Goal is to Provide Real-Time Capability to Detect, Identify, Characterize, Locate, and Warn Against ALL CB Warfare Threats
- Key to Rapid Maneuver and Survival on the Battlefield
- Enhances Situational Awareness and Influences Strategic/Operational Decision Processes
- Largest Force multiplier in the NBC Battlespace

Point Detection is the Central Pillar

Joint Science & Technology Panel for Chemical Biological Defense DETECTION BUSINESS AREAS OVERVIEW BRIEFING

23 October 2000

UNLIMITED DISTRIBUTION: Statement A (Public Release)

Business Areas



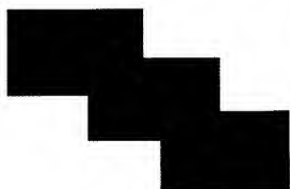
Chemical Detection
Dr. Ngai Wong (AF)



Biological Detection
Dr. Randolph Long (A)



Protection
Mr. Tony Ramey (N)



Modeling & Simulation
Dr. Ronald Ferek (N)



Supporting Science & Technology
Dr. Edward Stuebing (A)

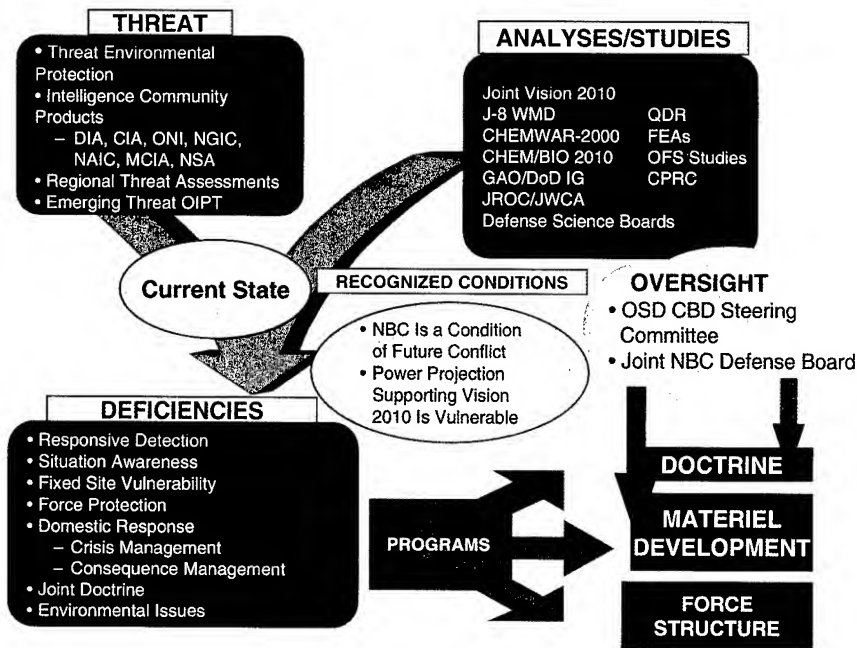


6.1 - Basic Research
Dr. James Baker (A)

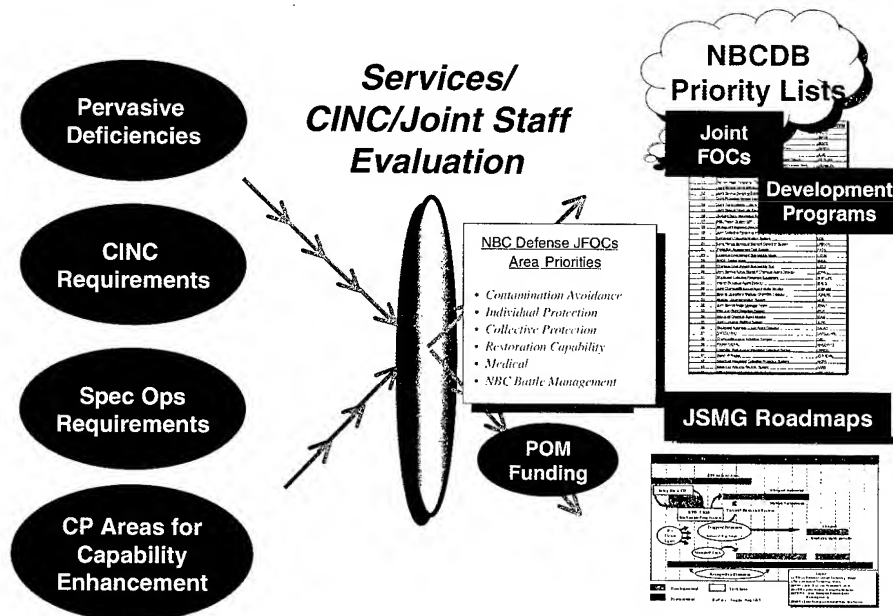


Decontamination
Dr. John Weimaster (A)

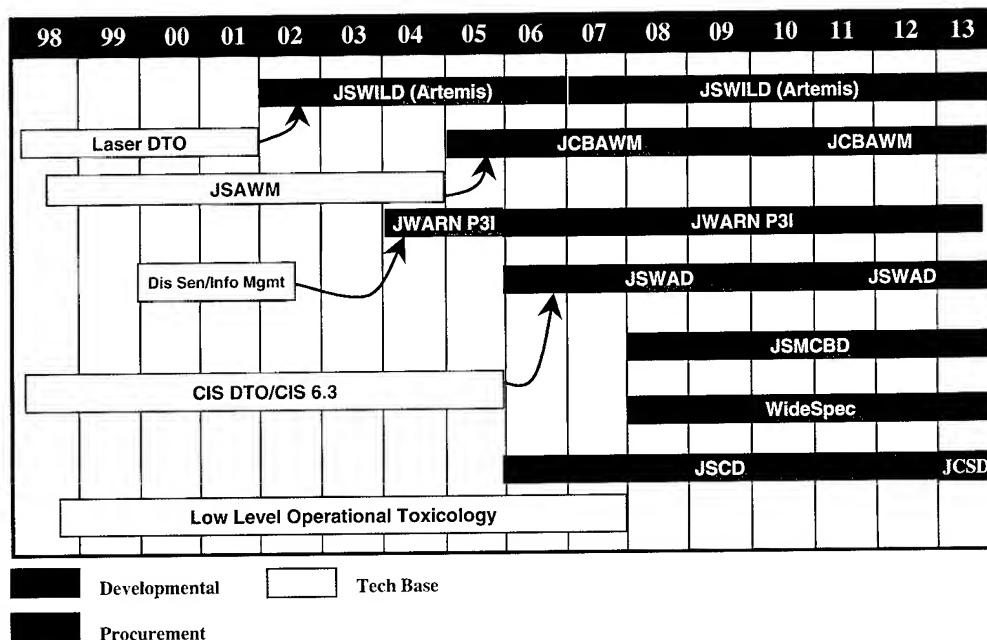
DoD Joint CB Defense Program: The Process



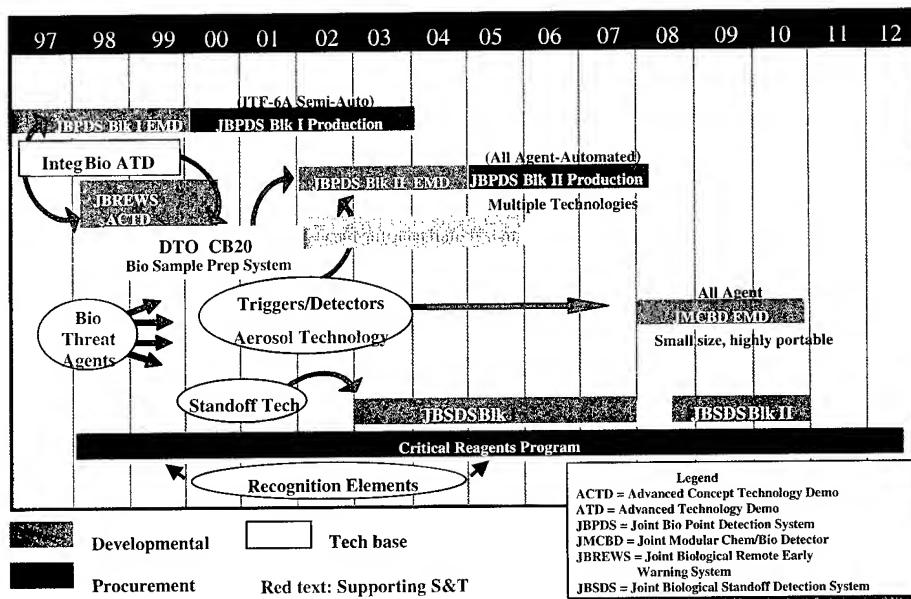
Joint NBC Defense Board Priority List Development for the CBDP



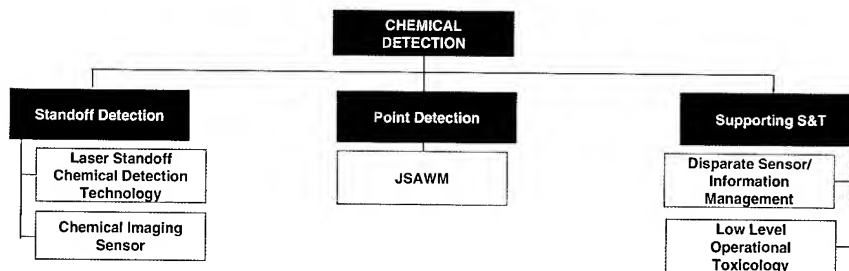
Chemical Detection Road Map



Tech Base Overlay on Roadmap



Chemical Detection Efforts - FY00



JFOCs

- | | |
|---------------------------------|---|
| (1) Increase sensitivity limits | (5) Non-standard TICs & TIMs |
| (2) Decrease response times | (6) Integration of chem/bio sensors |
| (3) Standoff is a priority | (7) Integration of point and standoff sensors |
| (4) Miniaturization of sensors | |

Chemical Detection Thrusts

Standoff Detection

Objectives: Develop and demonstrate passive and active concepts for remote detection, identification, ranging, and mapping of chemical clouds in all physical forms

Challenges:

- High speed interferometry; focal plane arrays
- Rapid data processing, software
- Laser technology to reduce size, weight of active systems



Chemical Imaging Sensor



JS Warning ID Lidar

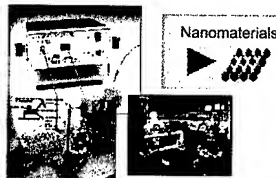
❖ Demonstrated 100 scan/sec operation in field with 9-pixel array passive CIS spectrometer

Point Detection

Objectives: Provide the capability to detect, identify, and quantify chemical and biological contamination in potable water

Challenges:

- Non-traditional threat environment
- Immature technologies
- Sampling low level toxics



❖ Model technology downselect process utilized fair assessment of technology candidates from all sources

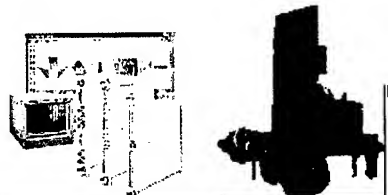
Chemical Detection Thrusts (cont.)

Disparate Sensors

Objectives: Develop NBC Information Management (IM) processes and products to enhance assessment and integration of Disparate Sensors (DSI)

Challenges:

- Defining/designing NBC IM Tools
- Assessing sensor utility
- Coordination



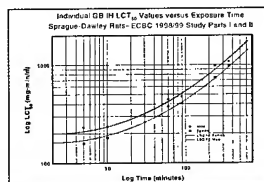
❖ *Developed model relevant to validated operational scenario*

Low-Level Toxicity

Objectives: Develop sound values for exposure levels having physiological impact below acute response levels to guide development of detectors and protective equipment

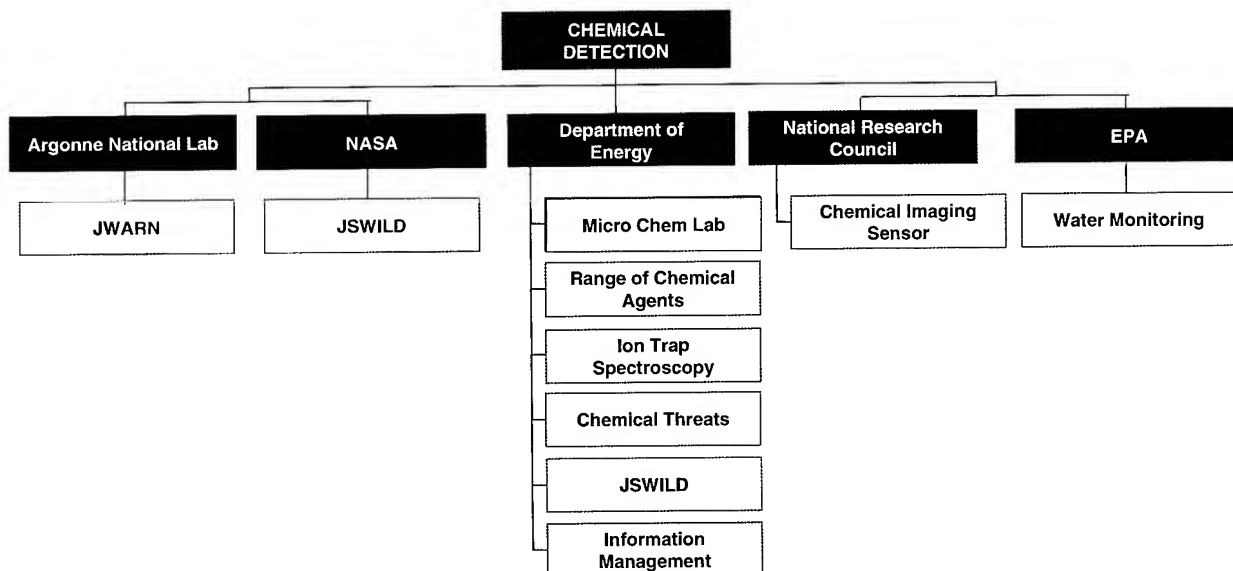
Challenges:

- Identifying physiological indicators of low level exposure
- Developing exposure methodologies
- Extrapolating to human response

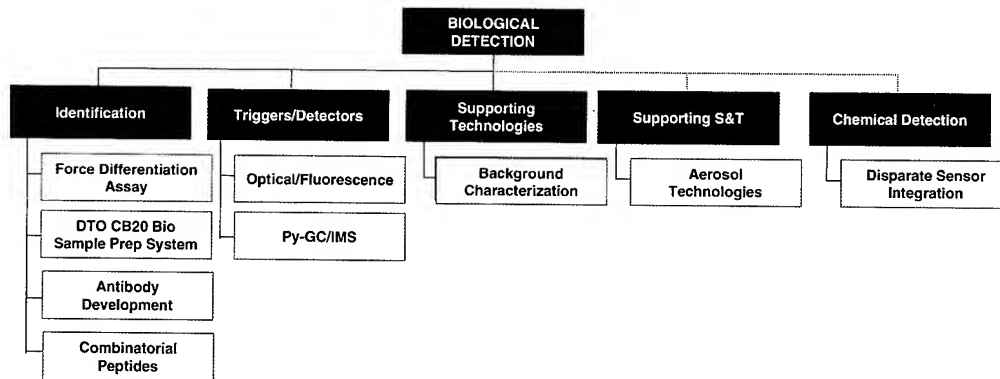


❖ *Extend CT range for acute effects*

Chemical Detection Program Leveraging



Biological Detection Efforts - FY00



JFOCs Point Detection

- (1) Increase no. standard agents
- (2) Lower detection response time
- (3) Minimize false positives
- (4) Non-standard ABOs, TIBs

JFOCs Early Warning

- (1) EW detection/ID standard ABOs
- (2) EW detection/ID non-standard ABOs

Biological Detection Thrusts

Point Identification

Objectives: Develop fully automated sample prep and analysis systems for unattended monitoring of air samples; transition FY02 to JBPDS

Challenges:

- fluidics
- biomarker extraction/cleanup
- background interference



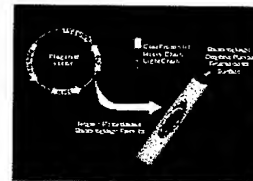
❖ Demonstrated detection of mass and genetic markers of JPBDS requirement levels

Reagent Development

Objectives: Develop improved reagent candidates for implementation in fielded and developmental identifiers via Critical Reagent Program

Challenges:

- specificity
- shelf life
- reproducibility



❖ Demonstrated improved sensitivity of recombinant antibodies vs available monoclonals; initiated assessment of combinatorial peptide

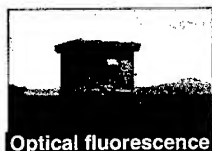
Biological Detection Thrusts (cont.)

Triggers / Detectors

Objectives: Develop technologies which reduce false triggers/alarms by enhancing discrimination against ambient bio background

Challenges:

- signatures/database
- reduce size, weight
- requires commensurate improvements in air sampling technologies



Optical fluorescence



Pyrolysis-GC/IMS

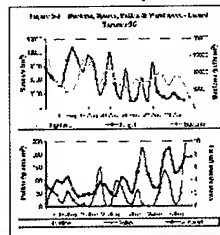
❖ Demonstrated detection of spores in field tests near requirement levels using Py-GC/IMS

Supporting Studies

Objectives: Assemble database of available ambient background data and analyze for key heuristics

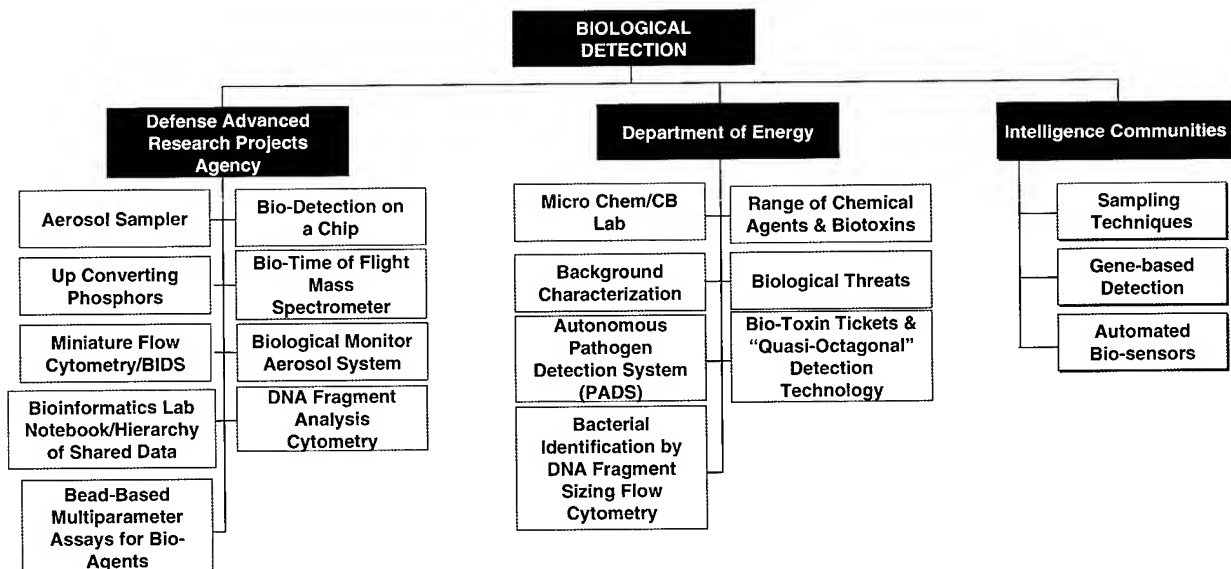
Challenges:

- multiple sources of data
- disparities in collection parameters

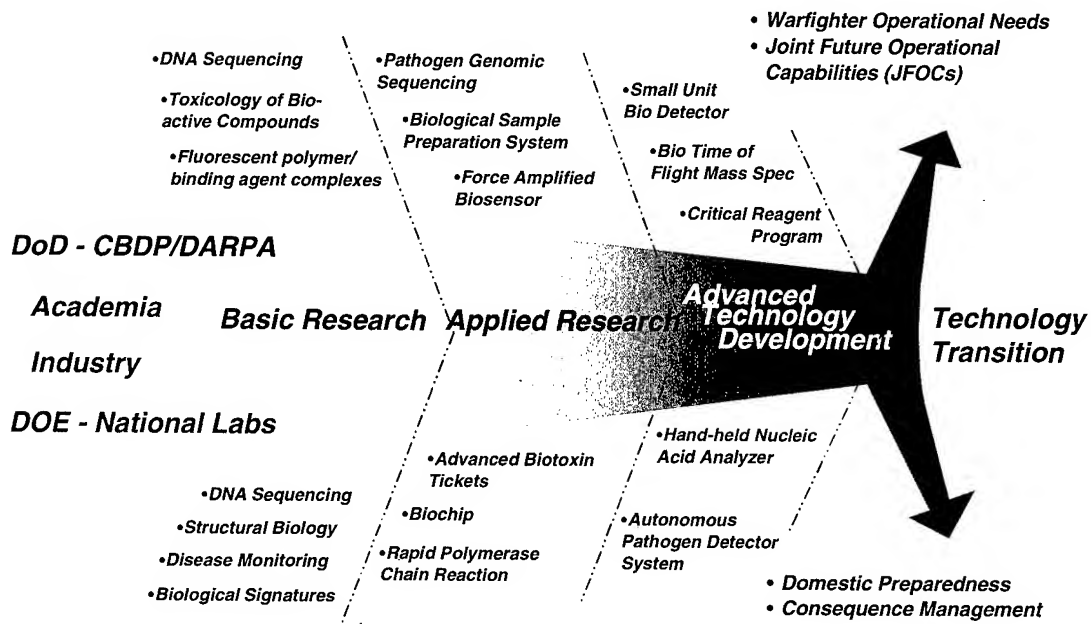


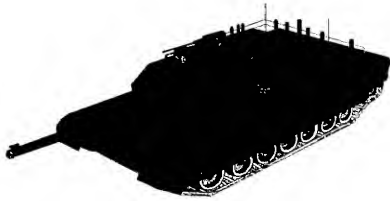
❖ Established joint DoD/DOE/TTCP website; data loading and analysis in process

Biological Detection Program Leveraging



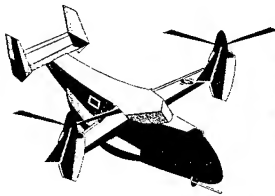
DARPA and DOE S&T Partnerships: Biological Detection



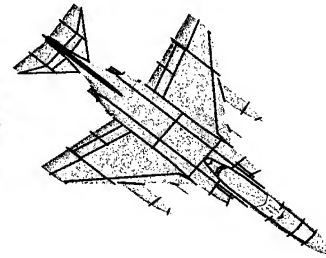


FIRST JOINT CONFERENCE ON POINT DETECTION FOR CHEMICAL AND BIOLOGICAL DEFENSE

23 OCTOBER 2000



**JOINT INTEGRATION
STARTS HERE**



LtCol Leslie R. Koch
Director, Joint Service Integration Group
Kochl@wood.army.mil

JOINT NBC DEFENSE CONCEPT



JOINT USER NEEDS

- FUTURE OPERATIONAL CAPABILITIES (JFOC)
- MISSION AREA ANALYSIS (MAA)
- MISSION NEED STATEMENT (JMNS)
- OPERATIONAL REQUIREMENTS DOCUMENTS (ORD)

CB POINT DETECTION JOINT FOCs

- **CHEMICAL AND BIOLOGICAL POINT DETECTION**
 - PROVIDE THE CAPABILITY TO DETECT AND IDENTIFY THE PRESENCE OF ALL CHEMICAL AND BIOLOGICAL AGENTS.
 - PROVIDE THE CAPABILITY TO CONFIRM AND VALIDATE ALL CHEMICAL AND BIOLOGICAL SAMPLES.
- **SENSOR INTEGRATION**
 - PROVIDE CAPABILITY FOR ALL NBC AGENT DETECTION USING A SINGLE INTERFACE.
 - PROVIDE CAPABILITY TO INTEGRATE WITH OTHER NON-NBC SENSORS.
- **MEDICAL SURVEILLANCE/VETERINARY SUPPORT**
 - CAPABILITY TO ID ALL NBC AGENTS IN CLINICAL SPECIMENS.
 - DEPLOYABLE, RAPID ID OF NBC AGENTS IN FOOD AND WATER.

JOINT MNS

- **NBC Battle Management - Challenges**
 - Real-time NBC battle management system is not available.
 - Consolidated modeling and simulation does not adequately predict and track NBC and TIM impacts.
 - Information from point/stand-off sensors and medical info is not automatically and electronically integrated.
- **Contamination Avoidance - Challenges**
 - Point and stand-off sensors not miniaturized into one suite.
- Automatic integration of med and non-med information into warning and reporting systems does not exist.
 - Limited military TIM detection capability.
 - Detection Capability for full range of threats and sensitivity levels associated with long term effects does not exist.
 - Stand-off capabilities severely limited.
 - Detection capability of CBW agents in food, water, body fluids and surfaces is required.

CB POINT DETECTION JORDs

JBCRD – JOINT BIOLOGICAL AGENT DETECTION AND WARNING
CAPSTONE REQUIREMENTS DOCUMENT

JBPDS – JOINT BIOLOGICAL POINT DETECTION SYSTEM

JBTDS – JOINT BIOLOGICAL TACTICAL DETECTION SYSTEM

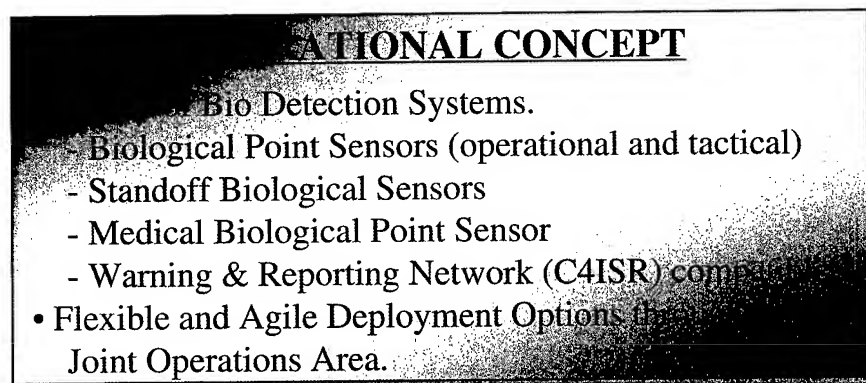
JBAIDS – JOINT BIOLOGICAL AGENT IDENTIFICATION AND
DIAGNOSIS SYSTEM

JCAD – JOINT CHEMICAL AGENT DETECTOR

JMCBDS – JOINT MODULAR CHEMICAL/BIOLOGICAL DETECTION
SYSTEM

JCBAWM – JOINT CHEMICAL/BIOLOGICAL AGENT WATER MONITOR

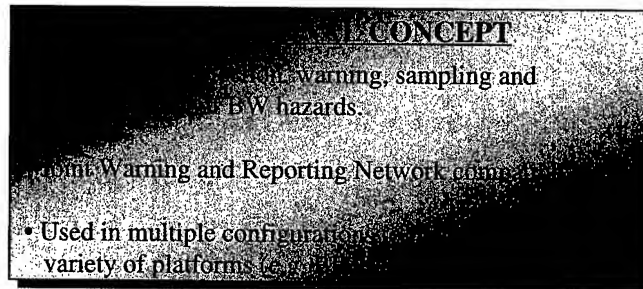
Joint Bio Agent Detection Capstone Requirement Document (JBCRD)



CAPABILITIES REQUIRED

- Automated real-time detection, identification, warning and reporting.
- Acquire samples to support agent confirmation.
- Supports reconnaissance, surveillance and early warning modes.
- Supports medical diagnosis and treatment.
- Define spatial extent of agent hazard and predict downwind hazards.
- Archiving of agent attack and post-attack data.

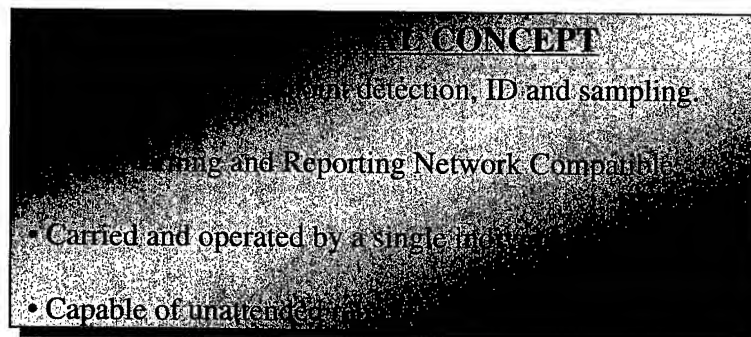
Joint Biological Point Detection System (JBPDS)



CAPABILITIES REQUIRED

- BW detection sensitivity equal to or greater than IBADS and/or BIDS.
- ID probability equal to or greater than 98% within 15 min. (10 min. obj.).
- Capable of simultaneous ID of multiple BW agents.
- Capable of modification to identify future threat agents.
- ID false positive response less than 2 % (.1 % obj.).
- Meet size/weight constraint of platforms. Man-portable variant (2 persons).

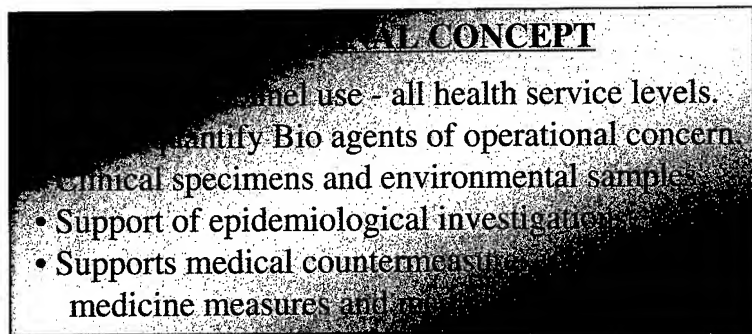
Joint Biological Tactical Detection System (JBTDS)



CAPABILITIES REQUIRED

- 90% Probability of detection of BW agents (95% obj.).
- An objective to identify all Threat List BW agents as to genus and species.
- Capable of being field modified to identify new threat agents.
- Operate on-the-move and stationary from ground, air and shipboard platforms.
- False alarms to be less than or equal to 2% of detections.
- Can be installed, operated and moved by 5th to 95th percentile.

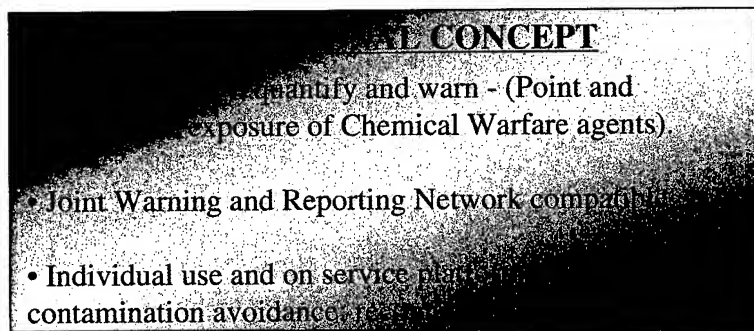
Joint Biological Agent ID and Diagnosis System (JBAID)



CAPABILITIES REQUIRED

- ID and quantify biological agents (ITF-6A) and diseases of concern to the WHO.
- Simultaneous ID of at least 8 agents (all agents is an objective).
- Programmable capability to address future threats.
- Sample processing < 20 min. (10 min. obj.); Sample analysis < 25 min.
- Means to protect and preserve selected samples for later analysis.
- Set up and operating by one person within 30 min. (10 min. obj.).

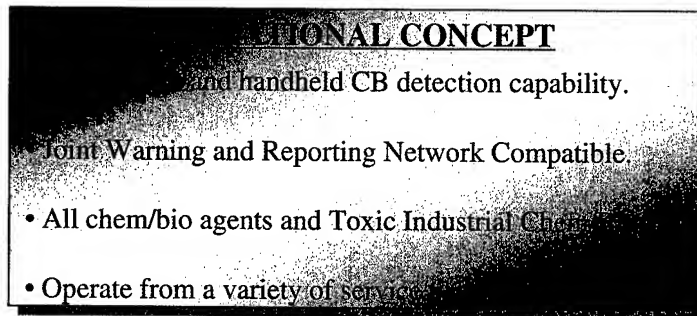
Joint Chemical Agent Detector (JCAD)



CAPABILITIES REQUIRED

- Detect, ID and quantify (by class) nerve, blister and blood agent vapors.
- Liquid, particulate, specific agent and TIC detection is an Objective.
- Be operational within one minute of power on.
- False alarms will be minimized; MTBFA > 168 hours.
- Capable of rejecting battlespace interferants.
- Will not exceed two (2) pounds and forty (40) cubic inches.

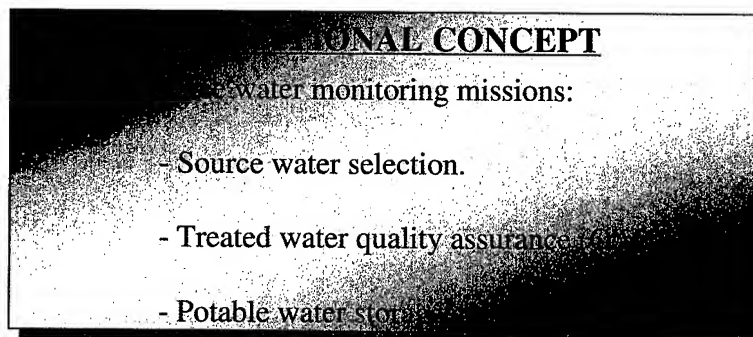
Joint Modular Chemical/Biological Detection System (JMCBDS)



CAPABILITIES REQUIRED

- Automatically detect CW agents by class and Toxic Industrial Chemicals (TIC).
- Automatically detect BW agents and Biological hazards.
- Objective is to identify and quantify CW agents, BW agents and TIC/TIBs.
- Capable of being modified to detect future Chem/Bio threats.
- Capable of distinguishing and rejecting battlespace and environmental interferences.
- Will not exceed 10 lbs. and 50 cu. inches (2 lbs. And 40 cu. inches obj.).

Joint Chemical/Biological Agent Water Monitor (JCBAWM)

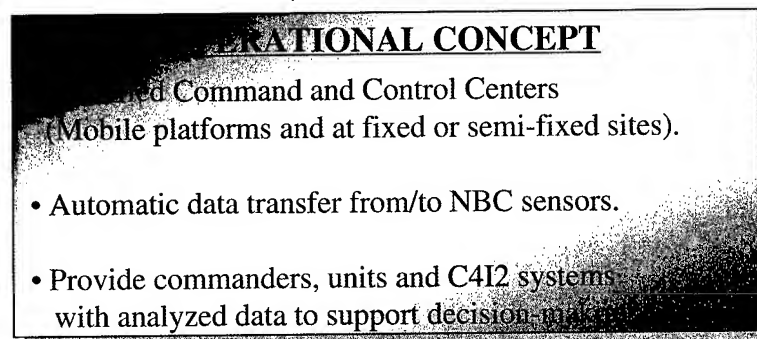


CAPABILITIES REQUIRED

- Detect, ID by class and quantify all known Chem and BIO agents.
- ID of specific CB agents and TICs/TIBs is an Objective requirement.
- Detection levels consistent with Tri-Service long term consumption standards.
- Be operational (set-up thru results) within 10 minutes of arrival at location.
- MTBFA = or > most effective current point detector.
- Portable by one individual; Objective is to minimize size and weight.

BACKUP CHARTS

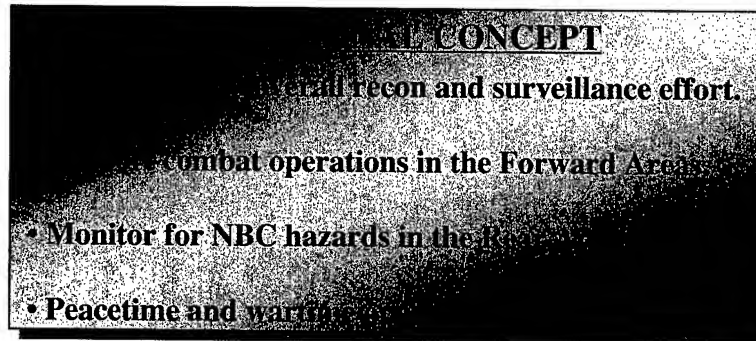
Joint Warning and Reporting Network (JWARN)



CAPABILITIES REQUIRED

- Interface with service C4I2 and DoD/Global C4I2 architecture.
- Interface with all legacy and co-developmental NBC detectors/sensors.
- Collect, model, generate, edit, and disseminate NBC information.
- Consistent with ratified version of NATO ATP-45B and AEP-45.
- Provide data base info, operational unit updates and risk assessment software.
- Automatic/manual transmittal of hazard ETA/ETD to all locations.

Joint Service Light NBC Reconnaissance System (JSLNBCRS)



CAPABILITIES REQUIRED

- Stationary and moving (up to 45 kph) operations.
- Vehicle mounted or dismounted operations for point and stand-off detection.
- CWA point detection/monitoring and on-the-move stand-off detection.
- BWA point detection and ID (stand-off /on-the-move detection is an objective).
- Integration of POS/NAV and Met data; Equipped with sampling and marking.
- Electronic mapping, on-board displays and collective protection.

First Joint Conference on Point Detection For Chemical and Biological Defense
COL(P) Pat Nilo Keynote Address
23 October 2000

Good morning. It is an honor and a privilege to help open this first point detection conference. This is an area where we need to pay very close attention in order to ensure that we will have the right mix of capability to satisfy Services' needs to protect the Force.

It has been said many times that we are living in a world that is the most dangerous it is has ever been with respect to chemical and biological agents. Not only do we have to be concerned about warfare agents, but also, given where we are deployed and can potentially be fighting, we need to be concerned with non-warfare chemical and biological agents present in the environment. We refer to these as toxic industrial material or TIM's.

With the rapid advancements in technology, it is becoming an increasingly difficult task to maintain the edge on bad actors who continue to explore ways to circumvent treaties or threaten us with the potential of technological surprise.

As Joint Vision 2020 describes, we must be prepared to operate across the entire spectrum of conflict. Operations such as Operation Desert Storm are examples of a conflict occurring at the mid and high ends of the conflict spectrum. The recent conflict in the former Republic of Yugoslavia exemplifies the type of conflict at the low end of the spectrum. And today, we also have the added responsibility of Homeland Security.

We are in the business of winning our Nation's wars. We need to be prepared to counter any threat. There is a new breed of adversary that understands our power and will look for every opportunity to force us into conflict characterized by asymmetry.

Asymmetric warfare focuses whatever comparative advantages one side has against the other side's relative vulnerabilities or weaknesses. A defining and distinguishing aim of asymmetric warfare is to create conditions where an enemy's relative advantage cannot be applied, is degraded or is neutralized.

Joint Vision 2020 tells us that these asymmetric threats are dynamic and subject to change, and the US Armed Forces must maintain the capabilities necessary to deter, defend against, and defeat any adversary who chooses such an approach. To meet the challenges of the strategic environment in 2020, the joint force must be able to achieve full spectrum dominance. Threats to U.S. forces range from terrorist use of Weapons of Mass Destruction to the use of CB weapons by a conventional military force. The psychological impact of the use, or threat of use, of this weaponry and toxic industrial materials allows countries and/or non-state actors to have substantial influence with a small stockpile.

The stated or implied possession of WMD could have a major strategic impact across the entire spectrum of conflict. Even limited amounts of chemical or biological weapons can produce a

significant shift in the regional balance of power at a much cheaper price than a buildup of conventional forces.

The ability of individuals and states to develop and acquire these weapons has altered the battlespace calculus, and lowered the threshold for their employment.

Particularly ominous is the fact that states working the hardest to develop chemical and biological weapons are, for the most part, located in unstable regions of the world. Bitter and unresolved rivalries in these locations have erupted into war in the past and hold the prospect of doing so again. Future adversaries may employ chemical and biological agents against our power projection operations to maximize their political and psychological impact and cripple our effectiveness of troop deployment.

The complexity of the modern battlespace, makes a digitally linked integrated detection capability necessary to protect the force. New methods of rapidly detecting, identifying, and reporting hazards must be integrated throughout the battlespace. This networking connectivity starts with integration of sensors and reporting networks within each Service and extends across the Force. This integrated networking is an important part of information superiority. Without this improved capability, units and their commanders will not have the situational awareness to make a rapid and well-informed decision based on the threat.

Integrated detection is a function of both battle management and contamination avoidance. This process is not solely equipment driven. For example, as we increase the numbers of sensors in the battlespace and the amount of information flow, we need to ensure that we are building enough infrastructure within each Service to be able to quickly analyze, process, and disseminate meaningful and accurate data.

The linkage of what the sensor can detect and when they are operational is central for integrated NBC networking planning and cross platform integration. Currently, we have rudimentary networking capabilities. But as we look to and plan our modernization, we need to keep in mind several factors.

First, we need to strive to have a capability that combines the detection and identification of chemical and biological hazards. Although this is difficult, it is not impossible. We need to continually demand that the research and development community stretch to reach this objective.

In addition to being multi-purpose, these systems need to be small and light weight, have minimum impact on the logistics base and require less power. With our added responsibilities for homeland security, these systems must show a versatility that will allow them to be used for homeland security missions as well as combat.

We need to look for ways to establish symbiotic relationships with non-NBC sensors. For example, by using unmanned aerial vehicles or UAV intended for Military Intelligence missions to also gather NBC information. We widen our ability to establish situational awareness, don't proliferate NBC unique equipment, and have someone else assume the cost of operation and training, in addition to the cost to develop, and procure the platform.

We need to carefully examine the differences in operations of the Services to ensure we have the right sensors in the right places. For example, emplaced sensors may meet the needs of fixed sites but as we look at the operations of the maneuvering ground forces, there may need to be the development of low cost sensors that can be scattered or dropped off throughout the battlefield in large numbers to augment high cost, low-density sensors that are more analytical. This combination increases the depth of understanding of the environment and allows rapid maneuver.

We must be able to detect low levels of agents. But, a key factor must be that as systems become more sensitive to detect low levels of agent, false alarm rates must be kept to an absolute minimum, or better, eliminated.

Overall, our program needs to be commander friendly and operationally relevant. Our value must be expressed in terms of our capability as a combat multiplier. We must carefully manage the program to ensure that we are pursuing avenues that will give us the "best bang for our buck" and get products out to the Force in the shortest amount of time. The field is getting very impatient for improved capability. Our attention needs to be on evolving technology and we must have the courage to recognize when we may be going down the wrong path and not cling to our programs just because. And, if there is a better mousetrap on industry's shelf, than we ought to go after it.

In conclusion, we must keep looking for technologies that provide maximum capability and reliability with minimum logistics burden that ensure we can operate effectively in all environments. The user community needs to work more closely with the developers to make the hard decisions that if a requirement cannot be met in a reasonable timeframe that we look together for a lesser solution as an interim capability until the objective system can be produced. Our ultimate goal together, must be to provide the right capability in a timely manner to the Force to permit it to easily achieve and maintain Full Spectrum Dominance - - To Win Our Nations Wars.
Thank You.

The DoD Chemical and Biological Defense Program

Anna Johnson-Winegar, Ph.D.

**Deputy Assistant to the Secretary of Defense for
Chemical and Biological Defense**

**First Joint Conference on Point Detection
for Chemical and Biological Defense, Williamsburg, VA**

23 October 2000

Outline

- **DoD Chemical and Biological Defense Program**
- **The chemical and biological warfare threat**
- **Responding to the Threat**

Outline

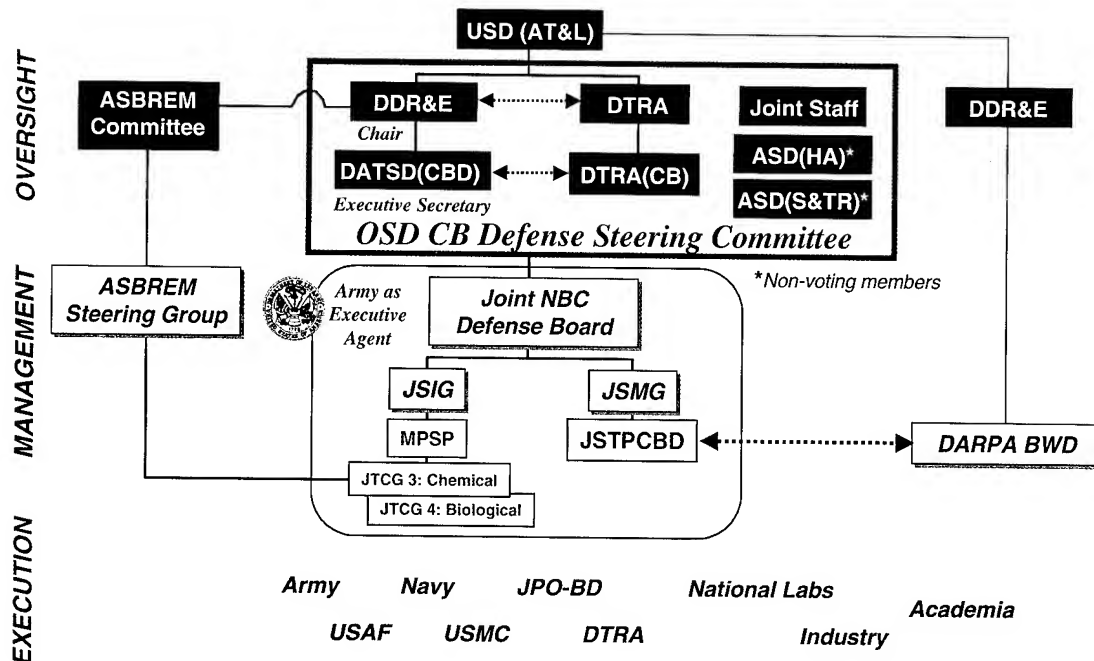
- **DoD Chemical and Biological Defense Program**

- The chemical and biological warfare threat
- Responding to the Threat: Development and Procurement of Systems and Technologies

Creation of the CBDP

- **Established by Congress**
 - Fiscal Year 1994 National Defense Authorization Act
Public Law 103-160, Sect. 1703 (50 USC 1522)
- **“The Secretary of Defense shall ... Assign responsibility for overall coordination and integration of the chemical and biological warfare defense program and the chemical and biological medical defense program to a single office within the Office of the Secretary of Defense.”**
 - Provides visibility for many, relatively low-cost items
 - Eliminates redundancy

DoD Chemical and Biological Defense Program Organization (50 USC 1522)

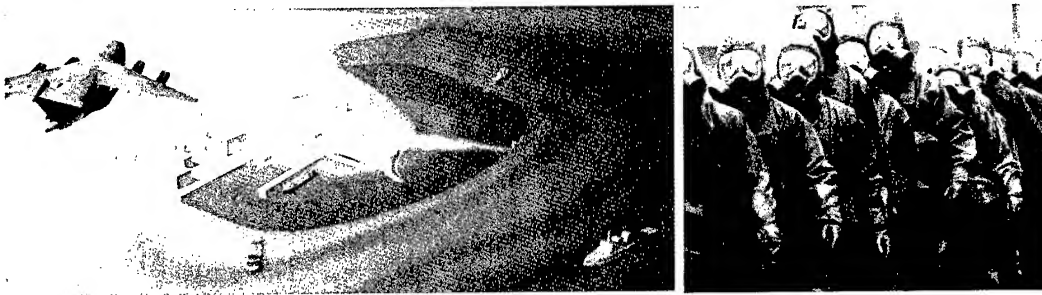


Scope of the Chemical and Biological Defense Program

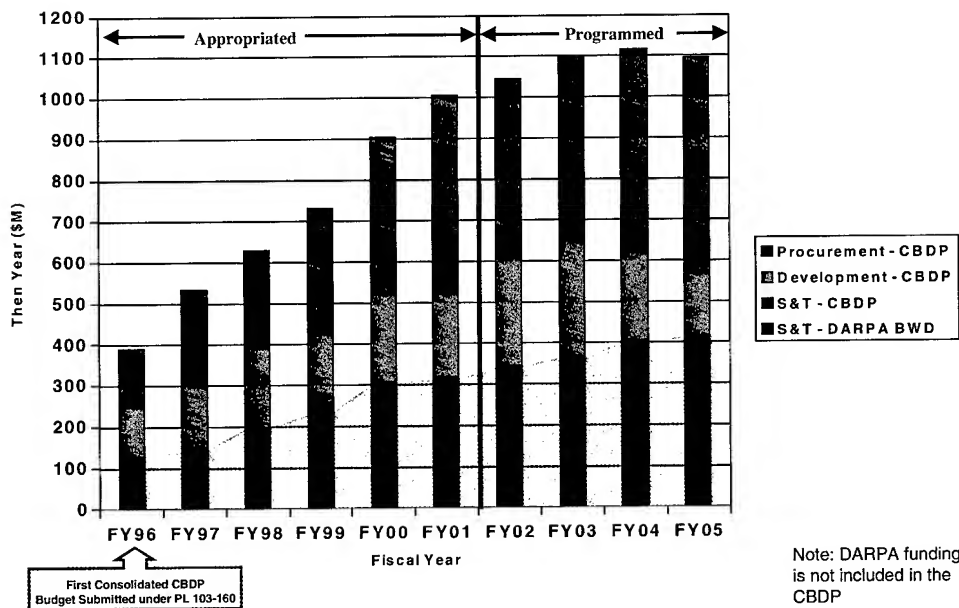
- **Integrates and controls funding for:**
 - Chemical and biological defense programs within DoD
 - All research, development, and acquisition funds
 - Medical and non-medical funds
- **...but not**
 - Operations & Maintenance funds (*Retained by Services*)
 - Logistics, sustainment
 - Training
 - DARPA Biological Warfare Defense projects
 - Technical Support Working Group (TSWG) programs
 - CoM-PIO CB defense programs (*Integration Plan under development*)

CBDP Mission

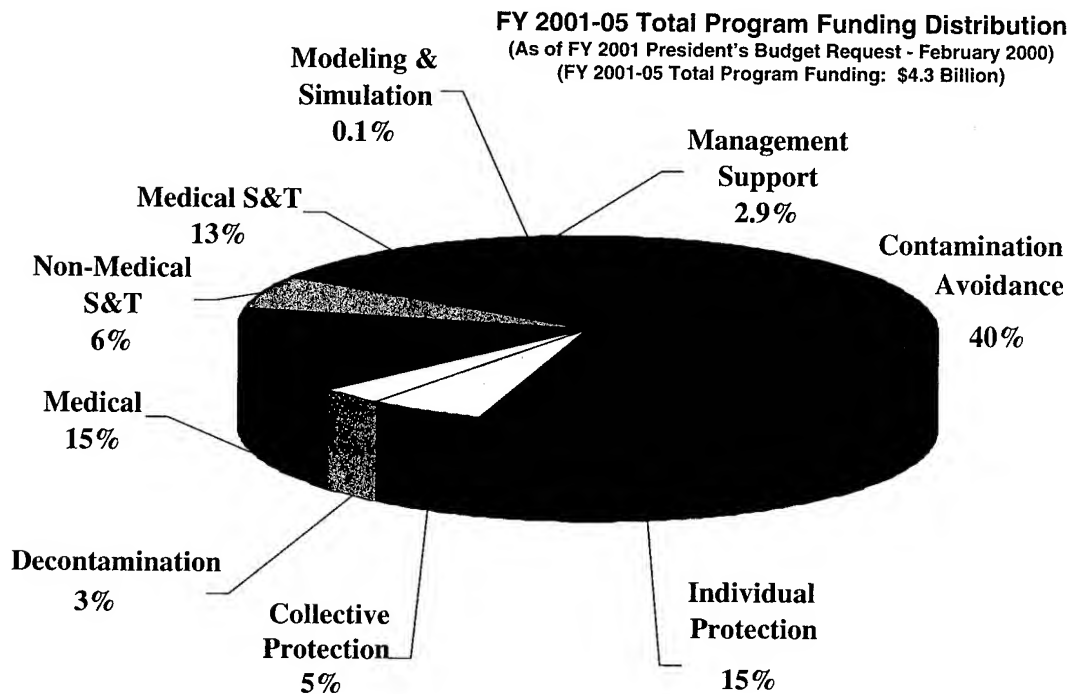
Provide CB defense capabilities to allow the military forces of the United States to survive and successfully complete their operational missions — from peacetime missions through two nearly simultaneous major theater wars — in battlespace environments contaminated with CB warfare agents.



DoD Chemical & Biological Defense Program Funding



DoD Joint Service CB Defense Program (Funding Distribution by Commodity Area)



Outline

- DoD Chemical and Biological Defense Program

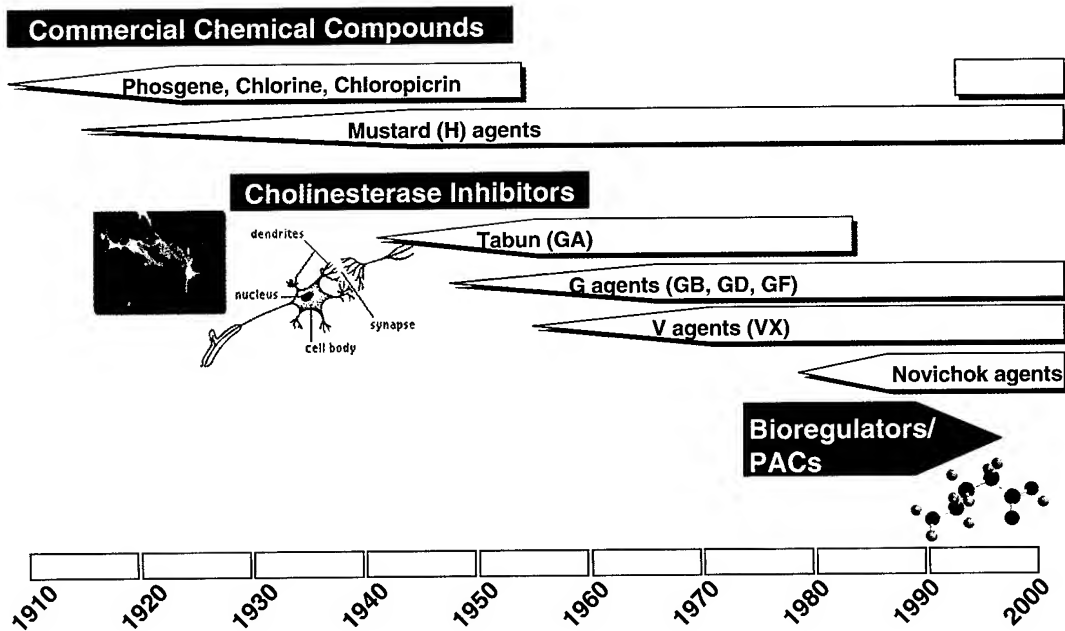
- **The chemical and biological warfare threat**

- Responding to the Threat: Development and Procurement of Systems and Technologies

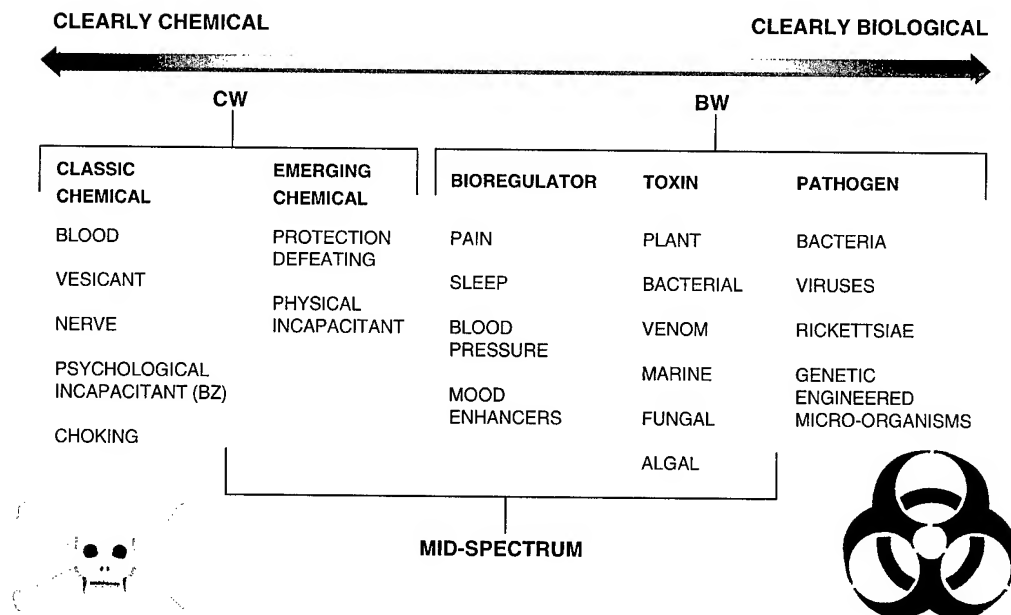
Chemical & Biological Global Proliferation

- ♦ More than 20 countries working toward CW capability
 - *Relatively cheap and readily obtainable*
 - *Blister - Nerve - Blood - Choking*
- ♦ More than 10 countries developing BW capability
 - *Equipment not unique*
 - *More potent than most deadly chemical agents*
 - *No need for large stockpiles*
 - *Easy to hide*
- ♦ At least 20 countries have delivery capabilities or are developing them
- ♦ Legitimate global trade of many precursors & equipment
 - *Difficult to limit production with export controls*

Chemical Agent Developments in the 20th Century

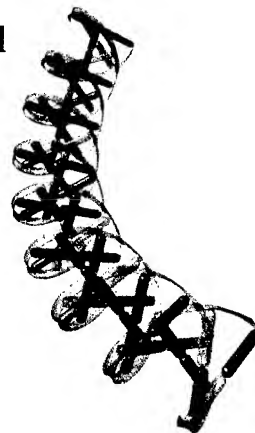


CB Agent Threat Spectrum

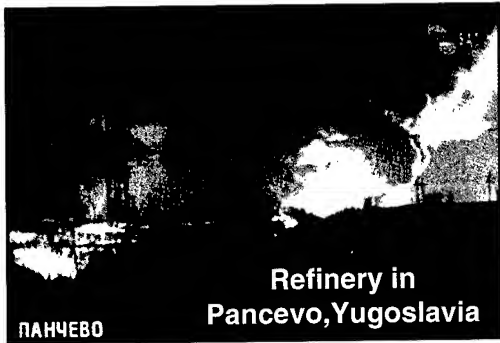


Potential Types of Novel or Engineered Agents?

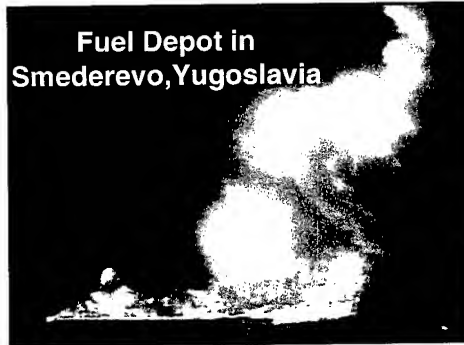
- Microorganisms with enhanced aerosol and environmental stability.
- Benign microorganisms, genetically altered to produce a toxin, venom subfraction, or endogenous bioregulator.
- Immunologically altered microorganisms able to defeat standard identification, detection, and diagnostic methods.
- Microorganisms resistant to antibiotics, standard vaccines and therapeutics.
- Combinations of above with improved delivery systems



Toxic Industrial Chemicals (TICs): A Potential Hazard in the Battlespace



Refinery in
Pancevo, Yugoslavia



Fuel Depot in
Smederevo, Yugoslavia

TICs – Any chemical with LCt_{50} less than 100,000 mg-min/m³ and produced in quantities exceeding 30 tons annually at one facility (ITF-25 definition)

Smoke from
power
stations in
Belgrade



Outline

-

-

- **Responding to the Threat: Development and Procurement of Systems and Technologies**

The TRP Process

THREAT ASSESSMENTS

- Prepared in discrete, tailored packages
- Evaluate impact on users - request requirements
 - Requirements Documents - based on validated threats

REQUIREMENTS

- Joint Service Integration Group (JSIG)
- Joint Requirements Oversight Committee (JROC)
(becoming more involved with non-major systems)

PROGRAMS

- Joint Service Materiel Group (JSMG)
- OSD CBDSC coordinates/integrates funding requests
 - Programs and technologies driven by validated threats and mission requirements, not by technologies

CB Defense Detection Deficiencies Identified in Operation Desert Storm

- Limited standoff detection
- Limited liquid agent detection
- High false alarm rate potential
- Single biodetection technology
- Limited HD detection
- No individual detectors
- No organic communication
- Slow response time to HQ



Future Concept

Handheld
Usable for
Battlefield
Detection and
Medical Diagnosis

Detects,
Identifies,
Quantifies,
Maps

Multi-Year
Usage on
Single
Battery



All Agent
Detection

Easy to Use

Low Level
Detection

No False
Alarms

Integrated with
C3 Network

Re-Programmable for New and Emerging Agents

CBDP Operational Goals

- **View NBC warfare agents within the theater area of operations**
 - *Early Warning and Stand-off Detection of NBC Agents*
- **Dominate the battlespace through reconnaissance, surveillance, and target acquisition (RSTA)**
 - *NBC Reconnaissance Systems*
- **Enhance the situational awareness of unit battlespace**
 - *Automatic Point Detection of NBC Agents, and Modeling and Simulation*
- **Provide real-time hazard information to influence current operations**
 - *NBC Battle Management and Warning & Reporting*
- **Enhance personnel and equipment survivability**
 - *Individual Detection, Individual and Collective Protection, Medical defenses, Decontamination, and NBC contamination survivability*
- **Maintain ground, air and maritime Operational Tempo**
 - *Operational Decontamination and Collective Protection*
- **Sustain operations, recovery and reconstitution efforts**
 - *Training, Readiness, and Restoration Operations*

Programmatic Issues for All Systems

- **Are they managed within the standard framework?**
 - Cost, Schedule, Performance
- **What operational capability is enhanced as a result of this system?**
- **Is it integrated with other systems?**
- **Do concepts of operation and doctrine support it?**
- **Can the program support multiple requirements?**
 - Operational/battlefield
 - Force medical protection
 - Homeland defense

Low Level Detection Issues

- **What is low level?**
- **What are the operational needs for low level detection?**
- **What are the doctrinal responses to low level exposures?**
- **Can one detector meet requirement multiple missions?**
 - Battlefield detection
 - Force health protection

Investment Strategy Summary

- Robust science and technology program is key to maintaining technological advantage and limiting technological surprise
- Science and technology focused on Joint Future Operational Capabilities
- Continued development to provide evolutionary capability enhancements
- Procurement addresses 2 MTW requirement
- Readjusts balance among short term procurement needs and long term science & technology efforts
- Strategy reviewed and updated annually

Future Directions

- ♦ Threat must drive program
- ♦ Changes within DoD a fact of life
- ♦ DoD Chemical and Biological Defense Program remains high administration priority
- ♦ Programs in place to respond to threats
- ♦ Increased awareness from public
- ♦ Continued Congressional interest

Maintain a strong R&D base that effectively transitions new products to the field

Acronyms

- ASBREM – Armed Services Biomedical Research Evaluation and Management
- ASD(HA) – Assistant Secretary of Defense for Health Affairs
- ASD(S&TR) – Assistant Secretary of Defense for Strategy and Threat Reduction
- BW – Biological Warfare
- C3 – Command, Control and Communication
- CB – Chemical and Biological
- CBDP – Chemical and Biological Defense Program
- CBDSC – Chemical and Biological Defense Steering Committee
- CW – Chemical Warfare
- COM-PIO – Consequence Management Program Integration Office
- DARPA – Defense Advanced Research Projects Agency
- DATSD(CBD) – Deputy Assistant to the Secretary of Defense for Chemical and Biological Defense
- DDR&E – Director, Defense Research and Engineering
- DTRA – Defense Threat Reduction Agency
- DoD – Department of Defense
- HQ – Headquarters
- JROC – Joint Requirements Oversight Council

Acronyms

- MILCON – Military Construction
- MPSP – Medical Programs Sub-Panel
- MTW – Major Theater of War
- JSIG – Joint Service Integration Group
- JSMG – Joint Service Materiel Group
- JSTPCBD – Joint Science & Technology Panel for Chemical and Biological Defense
- JTCG – Joint Technology Coordinating Group
- OSD – Office of the Secretary of Defense
- RDT&E – Research, Development, Test & Evaluation
- S&T – Science and Technology Base
- TICs – Toxic Industrial Chemicals
- TRP – Threats, Requirements, Programs
- USAF – United States Air Force
- USC – United States Code
- USMC – United States Marines Corps

JOINT BIOLOGICAL POINT DETECTION SYSTEM (JBPDS) REQUIREMENTS & DESIGN INTERPLAY

LTC Tim Moshier, Mr. Tom Buonaugurio
Product Manager, Joint Biological Point Detection System

We know exactly what we want. Take the single item of the tank: our requirements are simple. We want a fast, highly mobile, fully armored, lightweight vehicle. It must be able to swim, cross any terrain, and climb 30-degree hills. It must be air transportable. It must have a simple but powerful engine requiring little or no maintenance. The operating range should be several hundred miles. We would also like it to be invisible.

*General Bruce C. Clarke
September – October 1960*

There is much merit to an unconstrained requirements generation process. Requirements developers are not persuaded to be either overly conservative or over specific in their system descriptions by budgets, or current state of the art in technologies. But there must be some defining parameters used in requirements definition.

In past years, requirements were "threat based". That is, determine what the threat is, what is the threat's capabilities, and then describe a requirement to effectively counter, or defeat that threat. More recently, policy is to generate "capabilities based" requirements. Where do we want to be in the next five to ten years? Do we expect to fight from pre-positioned sites overseas, or do we expect to deploy the majority of our combat power from the continental United States? Do we want smaller forces that carry more expensive and complex equipment, but that can operate in an orchestrated fashion over relatively greater distances than today's forces? Or do we desire forces that are equipped with simpler, less costly gear? Whatever the current paradigm is, a couple of simple truths become painfully evident time and again. First, we shouldn't be pushed by a single paradigm. After all, why waste resources chasing threats that will likely never exist? Second, requirements developers and materiel developers need to be tightly synchronized during the requirements development process. Otherwise we'll be forever frustrated by unachievable requirements like those attributed to General Clarke, above (which, incidentally have yet to be realized 40 years later).

This paper will review the status of, and lessons learned from, the JBPDS Block 1 program, lessons learned from a variety of recent and on-going programs, and finally the process that we intend to use over the next year to prepare the JBPDS Block 2 program for entry into development. This paper will not spend much time describing the JBPDS itself. Mr. Altman will cover that topic in his paper and presentation.

The JBPDS Block 1 program started in 1996 with a pretty simple mission that was derived from the 1992 Mission Need Statement (MNS) for Biological Defense¹:

Develop a common, integrated suite of point biological detection components for use by all Services.

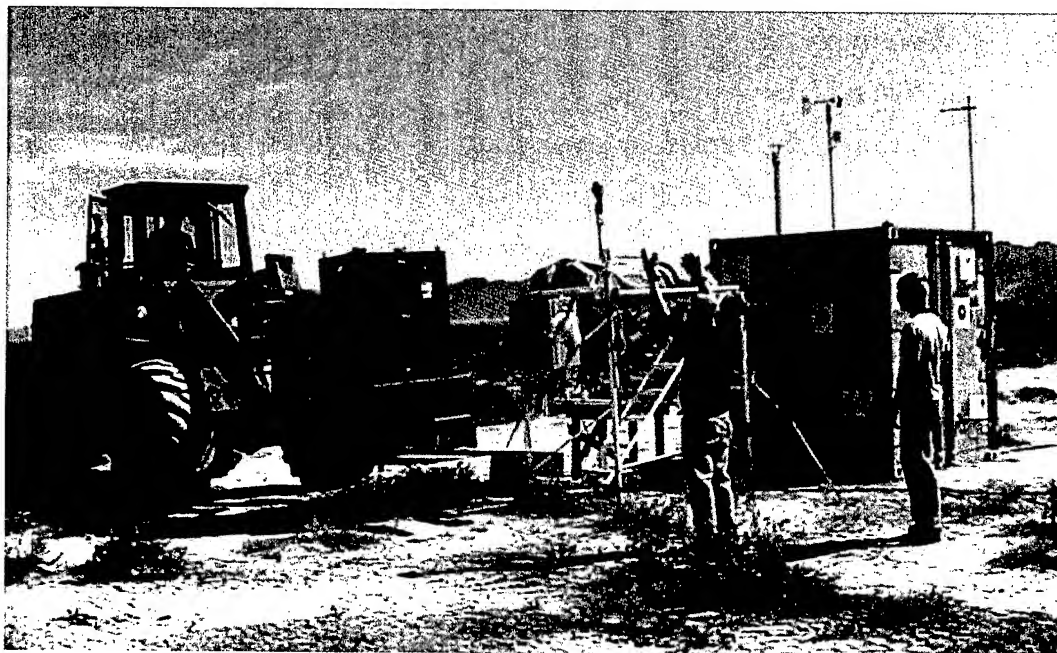


Figure 1. JBPDS Fixed Site (on forklift) being emplaced next to a referee tower and Portal Shield sensor (beige box at right).

That simple mission statement was quickly expanded into over 85 individual requirements that made up the initial performance specification for the Engineering and Manufacturing Development (EMD) phase that the Block 1 has been in since 1997. Since the beginning of the EMD effort, the requirements for the JBPDS have been both increased and better defined. For example, the JBPDS Block 1 now has to collect and hold several discrete samples after a positive identification, it must be ship-shock survivable, and capable of continuing its operational mission even after one or more of its components have become inoperable. Conversely, some requirements, like drawing a 25 milliliter sample for each positive identification were recognized as unnecessary, and costly in terms of being size and weight drivers on the system. This last requirement change highlights a fundamental truth – every requirement has a cost. Often times that cost is manifested at the physical level as increased weight and size.

The priority of requirements has also evolved somewhat. When the program first started, the main effort was to develop a fully automated system. Later, the requirement for a lower operating cost drove the program to renew its pursuit for a dry detector component. Recently

¹ Memorandum JROCM-075-92, subject: Mission Need Statement for DOD Biological Defense, dated 31 August 1992.

size and weight, and mean time between operational mission failures (MTBOMF) and maintainability, and remote operation via radio modem are becoming driving considerations.

Fortunately, most of these requirements have now been achieved, though not without considerable cost and risk. The JBPDS Block 1 program went through a major restructure just one year ago, primarily to take advantage of the Biological Agent Warning Sensor Tier 3 (BAWS-3) trigger/detector technology that was maturing out of a successful Army Advanced Technology Demonstration (ATD) called the Biological Aerosol Warning System (BAWS). (As we'll discuss later this was not the only program to feed into the JBPDS.) The BAWS allowed us to displace two major components in the original JBPDS design (the particle counter and sizer "trigger" and the flow cytometer "detector") with a single, smaller, more reliable component capable of performing both functions (see Figure 2). We'll first discuss the benefits of this action, then address the risks that we assumed by taking on this major programmatic change so late in the process.

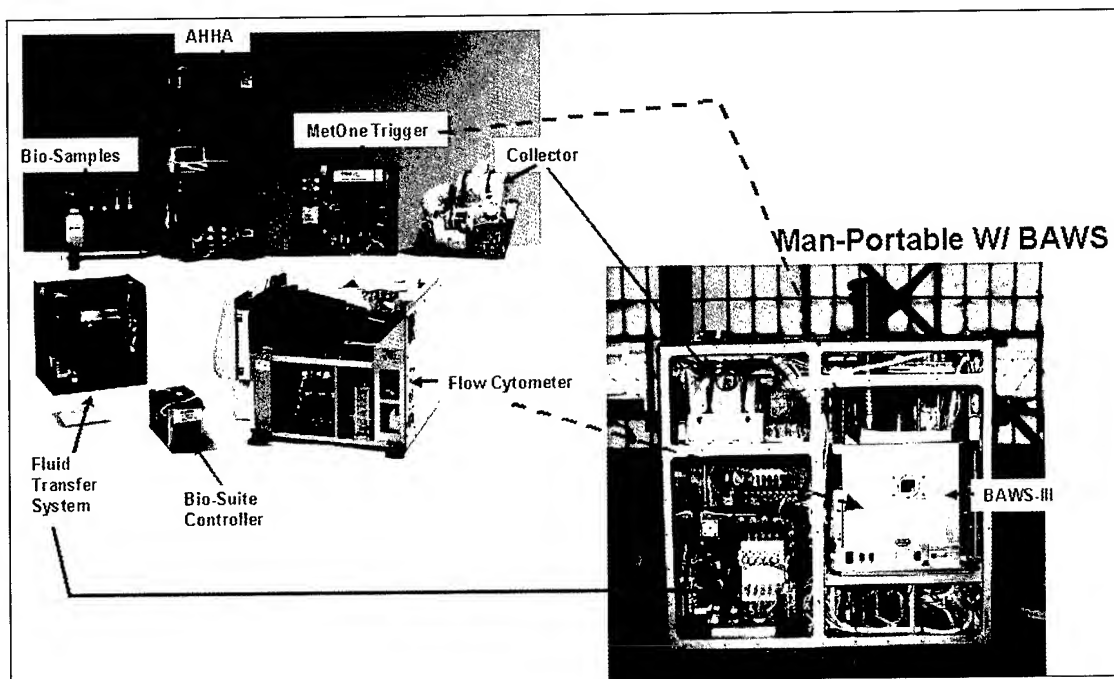


Figure 2. Components displaced by BAWS-3 enabling the downsizing of the JBDPS.

With the BAWS-3, the Portable configuration of the JBPDS (see Figure 3) was now capable of performing all required bio-detection functions, whereas previously it was not capable of performing the generic "bio/non-bio" detection function. This meant that we were now able to go from two basic bio-suite configurations, to a single, smaller bio-suite configuration that may be suitable for all applications: fixed site, portable, shipboard, and shelter. This brings us one step closer to a single instrument capable of meeting all the Services' needs, which is fully in line with Joint Vision 2010's mandate to be "... fully joint: institutionally, organizationally, intellectually, and technically. . [With] greater emphasis on common usage between Services

and increased interoperability among the Services and multinational partners.²⁹

Another benefit of the BAWS-3 is that it, along with a number of reliability and software enhancements to the rest of the system, has enabled us to drive down the JBPDS operating cost to just one-tenth of what it was in the original design. In fact even as we enter into the Low Rate Initial Production (LRIP) phase of the Block-1 program, we are continuing to make reliability and performance enhancements to the EMD instruments based on discoveries from our testing this past Spring.

While the BAWS integration effort was instrumental to getting the JBPDS program moving, it does serve as an example of the cost of requirements. The BAWS that was developed for the ATD weighed in at about 19 pounds with a power draw of about 35 watts. In order to meet the extreme environment requirements of the JBPDS (vibration, ship-shock, extreme temperatures, marine and contaminated environments) the weight of the BAWS increased by about 10 pounds, and the power requirement nearly doubled.

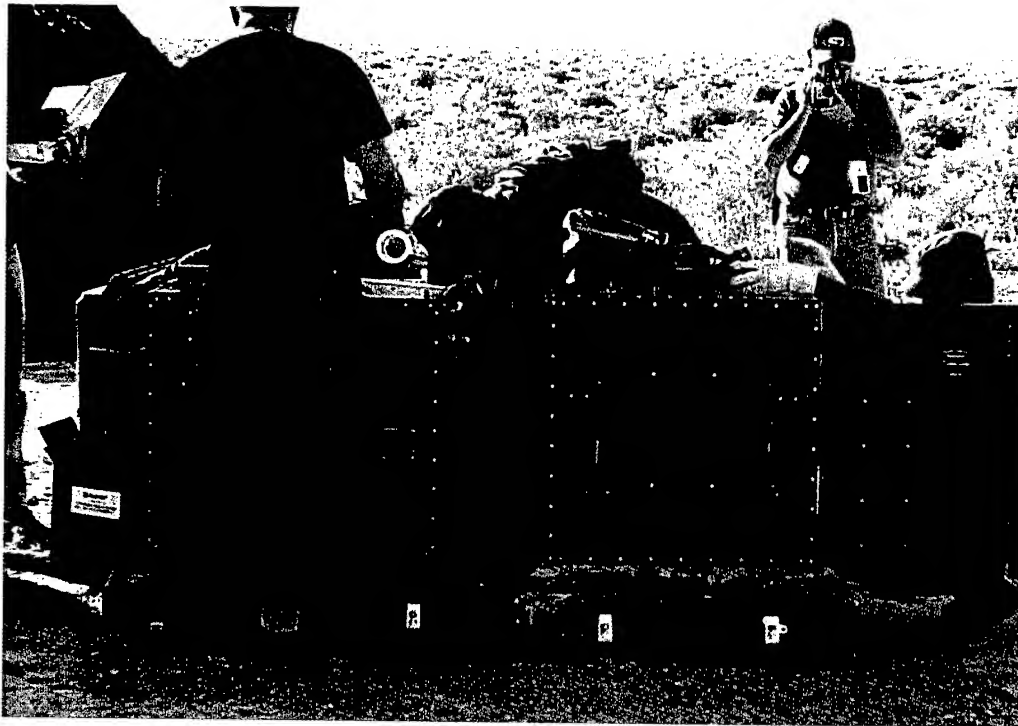


Figure 3. JBPDS Portable configuration (consisting of the two green boxes) being set-up by a team of Airmen. Note the size of the portable relative to the Fixed Site in Figure 1.

The risk of incorporating the BAWS into the JBPDS can be summed up in a single word – “Schedule”. As noted earlier, we are continuing to make improvements and conduct testing on the EMD prototypes even as we prepare to enter LRIP. The reasons why we are doing this

² Joint Chiefs of Staff, *Joint Vision 2010*, as found on the Internet at <http://www.dtic.mil/doctrine/jv2010/jvpub.htm>, page 9, 32.

include the users' stated requirements for fielding as soon as possible, and the scope of the changes that we've made to the JBPDS design. Fully one-third of the JBPDS's bio detection functionality (considering trigger, detect, collect, identify, sample, alarm as being the fundamental requirements on the JBPDS) has been pulled out and replaced with a new technology. That alone may not seem too great until one considers the considerable interface development work that has to take place in a fully automated system, and the BAWS-3 had yet to be hardened to JBPDS standards. On top of the huge efforts that had to be made just to make the necessary design changes, were the testing, analysis and programmatic decision cycle requirements. To look at this another way, we had about 10 months to revamp one-third of a system that already been in development for three years. Not a trivial task.

And concurrent with the BAWS integration effort, we had a lot of other corrections to make from findings made during Engineering Development Testing (EDT). We knew that we weren't going to be able to fit all the effort into the limited time that we had, but by working with the Service representatives on the JBPDS team we were able to develop a prioritized list of things to accomplish. Among the top priorities was ensuring that the JBPDS was safe to operate in all its intended environments. Next we worked on the bio-performance of the system. Unfortunately, we got caught short on time, and we missed a couple of correctable issues on the BAWS, and were caught in a transition between assemblers of the identifier's (AHHA in Figure 2) assay carriers. (Yet again the risk of Schedule!) Fortunately, all of these bio-performance issues have fixes already identified. Next priority was reliability, though we knew there were some hardware and software changes that we couldn't do without making major redesigns to the system, we were able to demonstrate that at the machine level we were meeting or exceeding threshold requirements. Lastly, we worked on human factors and maintainability. The majority of improvements in this area require major redesigns, and so were put off till after the PQT/OA test.

In fact, our strategy, and what was communicated to potential bidders on the JBPDS Block 1 production contract was the need to emphasize human factors engineering and logistic supportability in their proposed designs. This was an example of where we were willing to accept risk in the PQT/OA in order to meet the users' stated requirement to field the JBPDS as soon as possible. This approach has also translated a fair degree of risk to the LRIP contractor. Instead of getting a 95% solution from the Government, we're asking the contractor to redesign a significant portion of the JBPDS. This moderate to high risk approach is very unpopular within DOD.

The JBPDS' calendar driven schedule, versus an event driven schedule, is a condition that Department of Defense (DOD) has identified as a risk driver to the program (and rightly so). Of course, anyone who is even casually involved with biological and chemical defense is aware of the real and tangible biological warfare (BW) threats that exist. So logically one would conclude that we need to get an effective biological detection system to the users as soon as possible. Right – given that requirements are kept under strict control, and the users are willing to accept the “80% solution” immediately, trading time to effectively address the more challenging 20% of requirements. This is partly the reasoning behind another principle in acquisition – evolutionary development. It's also a driving consideration in our approach to the Block 2 program – get the users involved early to better define and translate their needs into a successful design.

To accommodate both available resources and schedule, we started this past year's work with a strategy of "test-fix-test" (see Figure 4). This approach not only gave us the opportunity to flush out problems early; it also gave us the opportunity to sort out "good ideas" from "not so good ideas". That is, which requirement changes to the JBPDS made sense and which didn't. This fact illuminates on a small scale the value of keeping dialog going between requirements writers and materiel developers early and continuously through the development process. In fact, those good ideas, some of which have already been enumerated, are what we have been working on since June, and what have been driving the perceived risk with EMD and LRIP overlap efforts. In a field as new as biological defense, every opportunity to use hardware, even experimental hardware, gives new insight into how actual bio defense operations may best be conducted.

As the JBPDS Block 1 is fielded, the combat and materiel developers need to look at the value of conducting war-fighting experiments to better define where the future of bio-detection should go, what it should look like, and what the impact is on forces and doctrine. Like the introduction of the tank and the airplane in World War I, and the introduction of the voice radio just prior to World War II, the armed services are about to receive a fundamentally new capability that they now need to learn to use.

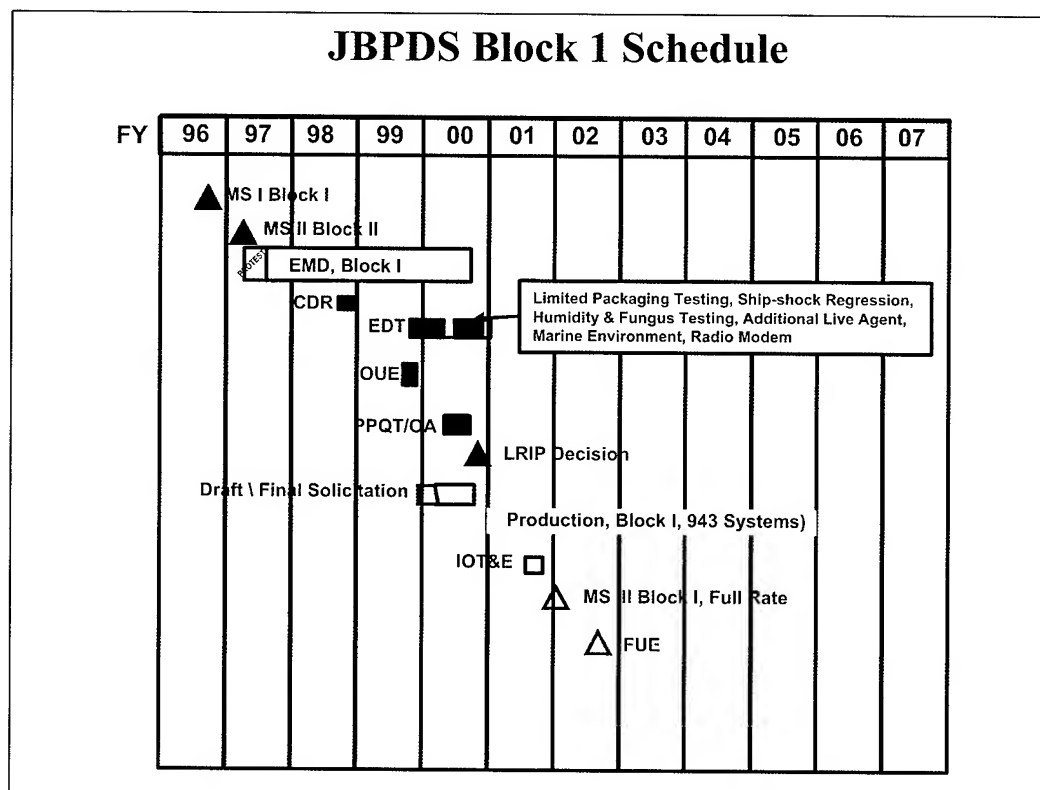


Figure 4. JBPDS Block 1 Schedule.

Learning from deployments and deployed systems is actually going on right now, at least on a limited scale. The Army's BIDS and the Portal Shield systems have already been deployed overseas, and in the case of the Portal Shield, domestically. Some of the lessons learned include:

- Biological detection assets must compete with other high priority systems and cargo during the build-up phase of the operation. Ideally, the biological detection assets will already be in theater, or are easily deployable (i.e., they don't take up a lot of weight and space, and can be easily prepared for transport). Regional commands like European Command have expressed a preference for systems that are portable and flexible in their employment over larger, vehicle-based systems.
- In-theater support for unique items (like biological detection systems) will likely be austere. In the case of the 1998 deployment of BIDS and Portal Shield, both systems supported each other (as well as did the Navy's Forward Deployed Lab and the Army's Theater Army Medical Laboratory). This fact supports the wisdom of developing systems that maximize commonality amongst the Services. Ideally, the biological detection system will be designed to take advantage of whatever resources are available in-country (e.g., local power, commercial carriers, commercial parts supply (i.e., COTS), etc.)
- Each environment is unique; every environment is complex. The Joint Program Office for Biological Defense (JPO-BD) has both conducted specific efforts in background characterization, as well as gleaned relevant data from operational deployments to give us a better understanding of the environments and the biological backgrounds that our systems are required to operate in. For a detailed discussion on their findings, see their document Joint Program Office for Biological Defense: Assessment of Biological Detection. The bottom line finding from the study is that the local biological and aerosol background at any single point will vary widely over the course of the day, the seasons, and through weather changes. Local fluctuations may also be very local (i.e., confined to a few tens of meters), and that argues for the use of biological detectors in multiples. A concept not too foreign to the military as we always deploy our combat assets as teams; never as single entities. Portal Shield and BIDS both operate as networks or arrays. Obviously, this means that more is better (at least to a point), so the systems need to be economically supportable.
- Systems should exploit the use of complimentary, or orthogonal, technologies to reduce the probability of false detections. As noted above, the background that biological detection devices have to work in is extremely challenging. A way to enhance the "signal to noise" aspect of an actual BW attack over the ambient environment is to use two or more technologies that are looking for independent signatures in the biological agents. For example, fluorescence with immunochemistry, multi-dimensional aerosol analysis with immunochemistry, or mass spectrometry with gene-based combinations. A positive hit for a single suspect event greatly increases the confidence that the event was actually a BW attack and not just a natural fluctuation.
- Another benefit of the use of complimentary technologies is that single point failures won't prevent you from completing your mission. The BIDS P3I has two completely

independent instruments that are capable of continually monitoring the air. The JBPDS Block 1 has a number of "degraded" modes that it will go into automatically should one of the LRUs become inoperative (for example, if the BAWS goes down, the JBPDS will automatically start taking periodic samples and delivering them to the identifier for analysis).

- Perhaps one of the most important lessons learned, is that transfer, or evolution, of technologies is instrumental to the success of developmental programs. For example: the basic design of the Navy IBAD fed the Portal Shield design, the use of complimentary technologies from the BIDS fed both the Portal Shield and the JBPDS, the basic Portal Shield design fed the JBPDS, the BAWS ATD contributed the BAWS-3 to the JBPDS, the HHAs from the IBAD feed into every biodetection program. Now the JBPDS lessons learned and technologies may be used to launch future programs, if the programmatic bridges and detection strategy will accommodate that.

So now where do we go with the JBPDS Block 2 program? The original JBPDS strategy was to build a fixed number of Block 1 systems and then use the Block 2 development effort to finish off emerging technologies that would meet the objective requirements. Block 1 technologies on a per-line replaceable unit (LRU) basis would then be replaced by the Block 2 LRU(s) into the existing Block 1 frames; no new systems were to be built. The current direction, however, is to build completely new Block 2 systems and the Block I JBPDS units would not be upgraded (unless additional funds became available). Additionally, the September 1999 draft Joint Operational Requirements Document (JORD) appears to be asking for multiple JBPDS designs. The Block 2 JORD, under the type of system proposed states, "...the JBPDS may include multiple biological detection and identification solutions into platform specific configurations."

These are fundamental differences from the current strategy and our goal, as material developers, must be to ensure that they are in accord with the users' concepts of employment.

Some other questions that have emerged with respect to the Block 2 program include:

- Will the hand held JBPDS variant be the same as the Joint Biological Tactical Detection System (JBTDS)?
- Is the JBPDS expected to work in different environments and roles from those the Block 1 is designed to?
- Can the requirements for size, weight, mission duration etc., be decreased by reducing the environmental requirements such as a weatherproof enclosure or length of time for unattended operation (i.e. volume of consumables required to complete a mission)?

An extremely important consideration in the design of the Block 2 is trying to identify where the trade spaces are, or conversely which characteristics are most important to the user? Knowing those characteristics that are most important to the system users will allow us to best allocate our limited resources (like time and money). To get an appreciation for the importance of trade

space, consider the following:

- At what level could we reduce system complexity and cost by being a less sensitive detector? A 1 ACPLA (Agent Containing Particle per Liter of Air) challenge may not be a significant threat to an otherwise healthy soldier since the exposure required to get an effective dose is so high (see Figure 5) (1 ACPLA is the current JBPDS objective requirement for sensitivity). Note that only a small proportion of particles are actually deposited in the lung for each breath.

Human Response

Tidal volume (air exchange)

Ex: For Male 20-30 yr old.

(0.5 L/breath)(15 breath/min)

= 7.5 L/min

Only 10-20% of Tidal volume of air replaces

The residual volume in the lung. (Hatch, 1961)

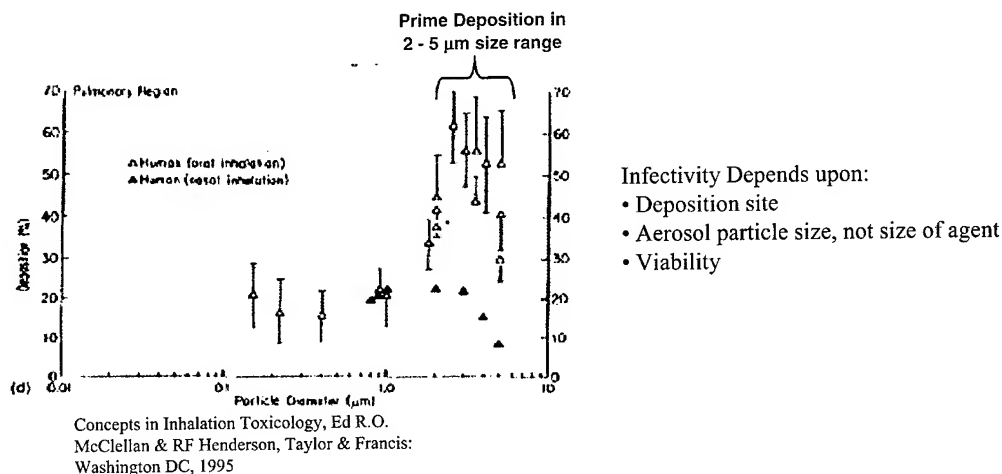


Figure 5. Deposition of aerosol particles in the human lung.

- When you consider the actual exposure required to get a lethal dose, you get a much better appreciation for detector sensitivity requirements. Figure 6 compares current JBPDS responsivity to two aerosol clouds, one three micron mean diameter (yellow curves) and the other one micron mean diameter (green curves), to a BW challenge required to produce an effective infection or intoxication (red curves).

Human Response versus JBPDS Block 1 Response to a LD50 Challenge

Consider a typical gaussian 10 minute cloud

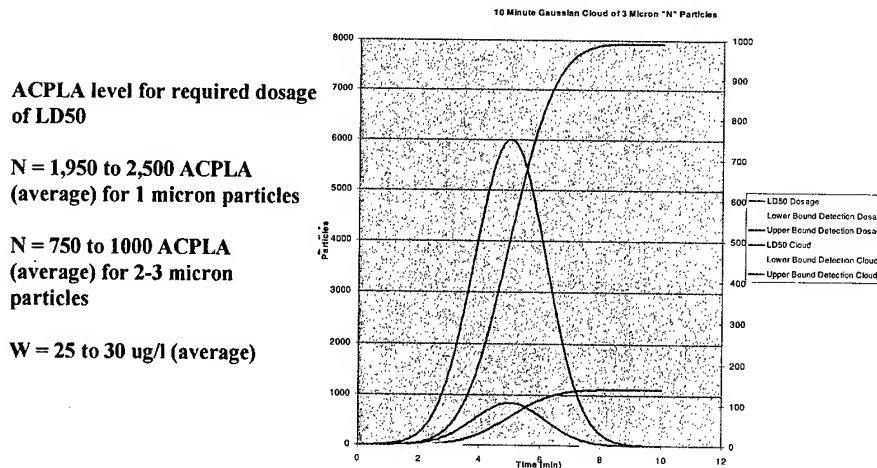


Figure 6. JBPDS Responsivity Compared to an LD50 Challenge. "N" and "W" are two BW agents shown here for demonstration.

- The importance of this analysis is that it may allow us to trade sensitivity (which typically costs processing time, power, size and cost) for speed (i.e., time to respond to a lethal or incapacitating challenge, smaller size and weight, and lower cost detectors. The real payoff of this to the commander in the field is that he/she could afford to deploy many more detectors, and that means that the chance of a local attack being successful is greatly reduced. Another benefit of decreased requirements for sensitivity is that false positive detection rates can then be dramatically lowered (sensitivity and specificity are typically inversely related).

Trade space analyses also have to extend to the inter-service requirements. How are requirements and precedence mediated over competing service needs? For example, the USMC need for a man portable JBPDS (where weight and size are prime considerations) may not be in accord with the Air Force or Navy requirements for EMI, ship shock, extended unattended operations, etc., which add considerable weight to the JBPDS.

In returning to the opening quote on the requirements for the tank, the following is a synopsis of its introduction during WWI.

The tactical situation was that fighting had pretty much bogged down into static trench warfare, but soon a new capability would emerge to help break the quagmire, the tank! On 15 Sep 1916, of 60 tanks sent to France, only 49 could be sent forward with 32 reaching the front lines. At the start of the attack 23 were able to depart, 5 became

stuck in the mud, but 9 were able to complete their mission. While on the surface a success ratio of 15% is hardly encouraging, the impact was so impressive that this new capability took hold and shaped the beginnings of mobile warfare in less than a generation.

In summarizing this paper, with its historical analogy, a sense of how much progress has been made in the last few years emerges. In the post WWII period, tactical biological defense consisted principally of sampling and collection, basically the Q-Tip in a tube. This capability did not change substantially in the field for more than 45 years. The beginnings of Operation Desert Shield in 1990, resulted in a limited capability to have near real time detection and identification, but it was a manual process, requiring a skilled operator. This October marks 86 years since the tank's introduction and will also mark the introduction of the JBPDS under the Limited Rate Initial Production phase to all the services!

There are many similarities to the introduction of any new defense system and while tactical biological detection has not been an easy task, recent events have shown that in unconventional warfare and terrorist attacks the U.S. could be vulnerable to this type of attack. Therefore the conclusion is that efforts to improve Biodetection and Identification are in the best interests of the Department of Defense. The JBPDS has undergone the most rigorous testing of any Biological Detector to date and the results prove that the JBPDS is impressive. The JBPDS is lighter, faster, cheaper and better protecting our service men and women as we progress into the new era of defense.

But to make the JBPDS the best possible system for our military, we need the active participation of those that will actually use it right now in the design phase. We need to know what are their driving concerns, and what have they learned from bio detection systems that are being used now. The tank has undergone a remarkable evolution; an evolution that has been driven by technology, lessons learned from actual use, the threat, and anticipations of future required capabilities. We intend to use an analogous process over the next year by forming a working group composed of tech base representatives, user representatives, systems experts from national labs, and modeling and simulation. At the conclusion of this effort we expect to have a clear definition of what the user actually expects from the JBPDS Block 2, and candidate designs that offer the best opportunities for meeting those expectations. We will provide these designs, along with the concepts of operation and lessons learned, to the Block 2 Development contractor(s) next year to mitigate their risk in successfully developing the next state-of-the-art bio detection system.

JBPDS BLOCK I EMD PROGRAM OVERVIEW AND SUMMARY

Wolf P. Altman and Donald R. Hohe
Battelle
505 King Avenue
Columbus, Ohio 43201

Abstract

The Joint Biological Point Detection System (JBPDS) Block 1 EMD program has been recently completed and provides the new benchmark against which future systems will be measured. This system is intended to meet the needs for the four military services and provides an automated, integrated biodetection system for deployment in shelters, around airbases and naval ports, on board ships and by forward fighting units. By providing a common set of components, logistical support savings is accomplished. Human factors design inputs have made the system easy to set up and operate. Implementation of high sensitivity, low false alarm rate trigger/detector life cycle costs have been dramatically reduced. This paper will provide an overview of the design of the system as well as operating performance characteristics. A demonstration of the system will also be provided.

Introduction

Ever since Operation Desert Storm (ODS) highlighted the critical need to develop biodetection systems, the four services in the United States (Army, Air Force, Navy, and Marines) have been developing various approaches to meet this challenge. The M31 Biological Integrated Detection System (BIDS) was Type-Classified in 1995 as the first biological alarm. The BIDS, developed by the Army, consists of a suite of equipment to detect, collect and analyze ambient aerosols for pathogenic agents, housed in a HMMWV (High Mobility Multipurpose Wheeled Vehicle) mounted shelter. One of the design principles that emerged in the development of the BIDS was to exploit complementary technologies (e.g., flow cytometry, mass spectrometry, and antibody based identification) to reduce the risk of false detections. The first BIDS unit was the Army Reserves' 310th Chemical Company created in Ft. McClellan.

The Navy deployed the first Interim Biological Agent Detector (IBAD) in September 1994 aboard the USS LaSalle. The IBAD is composed of a particle sizer/counter to automatically initiate the collector (based on unusual changes in the background aerosol), particle wet cyclone sampler and a manual Hand Held immunochromatographic Assay (HHA) identifier. The system can detect and identify a sample in less than 20 minutes. The system also produces a sample for later confirmatory laboratory analysis. One IBAD system weighs <200 lbs and occupies a volume of 7.5 cubic feet. Both the BIDS and IBAD require manual intervention by an operator(s) to meet their mission objectives.

To protect airbases and naval ports, the Joint Program Office for Biological Defense (JPO-BD) developed the Portal Shield Advanced Concept Technology Demonstration (ACTD). Portal Shield is a network of automated systems consisting of triggers, collectors and automated handling of Handheld immunochromatographic assays (HHAs). Their good performance is based upon a novel alarm algorithm that leverages networking of the sensors. Networking acts as another, complimentary technology to straight particle counting and sizing as it adds the dimensions of time and space correlated to local wind conditions. In contrast to the BIDS and IBAD, the Portal Shield, is highly automated. To meet the rigors of the extreme environments encountered in the field, the Portal Shield is housed in a shelter, comparable in size of the BIDS shelter. Several of these units have been successfully deployed to various locations in Northeast Asia and Southwest Asia.

To meet the needs for all four services with one system, in April 1997 the JPO-BD initiated a contract for the development of the Block I Joint Biological Point Detection System (JBPDS). In addition to the objective of meeting the needs for all four services as a battlefield biodetection system, the objectives of this system included:

- automating the biodetection process (triggering the system, collecting a sample of airborne aerosols into a liquid medium, identifying the collected sample against a list of 10 agents and providing a confirmatory sample) as much as possible
- providing a common logistics basis for all services – e.g., common technical manuals, Line Replaceable Units (LRUs) for sparing, and common consumables
- meeting or exceeding the capabilities of existing fielded equipment – i.e., BIDS and IBAD

This paper summarizes the Engineering and Manufacturing Development (EMD) program to develop the Block I JBPDS.

Requirements

The JBPDS is required to meet 85 performance requirements. These requirements can be divided into:

- 11 Reliability, Availability & Maintainability Requirements – e.g. Mean Time Between Operational Mission Failure (MTBOMF) and Mean Time to Repair (MTTR)
- 15 Interface Requirements – e.g. interfaces to other systems such as JWARN (Joint Warning and Reporting Network) and man-machine interface issues (audible and visual alarms)
- 21 Physical and Environmental Requirements – e.g. operation during or after exposure to temperature, shock, and vibration extremes
- 12 Transportability, Design and Safety Requirements – e.g. safe operation, workmanship, and transportability issues (i.e., can the system be transported via intratheater systems like the C-130 aircraft, and rail cars).
- 26 Performance Requirements – e.g. detection/identification sensitivity levels, probability of detection, response time, false positive rate

Technology Selection

During the first few months of the project, a trade-off analysis was performed to identify the technologies that could best meet the performance requirements described above. This analysis defined the technologies that would be engineered to meet all 85 performance requirements. This began with the identification of over 60 technologies that were reduced to approximately 20 technologies that were deemed potentially viable for the JBPDS. Virtually of these technologies had first been evaluated during the Joint Field Trials (JFT) that are sponsored by the Joint Program Office for Biological Defense. The JFT is an annual, open invitation to governmental, industry, academia and foreign technology developers to demonstrate their technologies in an objective, refereed environment. The candidate technologies are shown in Table 1.

These remaining technologies were subsequently combined into 99 systems that were evaluated using an Analytical Hierarchy Process. Considerations included: performance, size weight, power consumption, life cycle costs, level of automation, and developmental maturity. After the objective analysis was utilized, a subjective discussion among the participants decided upon the recommended technologies for the JBPDS.

JBPDS Components

Figure 1 shows a block diagram of the BioSuite Component Assembly. It is composed of five key biological sensors that are integrated with the BioSuite Controller to allow the JBPDS to meet its performance specification sensitivity requirements. The BioSuite Component Assembly consists of the BAWS LRU, the Collector LRU, the Identifier LRU, BioSuite Controller (BCS) LRU and fluidics. Their functions are:

- BAWS LRU
The purpose of the BAWS is to continuously monitor the background air and to notify the BioSuite Controller when a suspect biological aerosol is detected.
- Collector LRU
The purpose of the Collector is to collect and concentrate background aerosol particles in a liquid medium. These liquid samples will be used by the Identifier and to provide a confirmatory sample for use by in theater and U.S. laboratories.
- Identifier LRU
The purpose of the Identifier is to positively identify a BW agent the species and toxin type level.
- BioSuite Controller LRU
The purpose of the BioSuite Controller is to control the operations of the Biological Sensors.

Table 1 – Initial Candidate Components

TRIGGERS	COLLECTORS	Detectors	IDENTIFIERS
Ultraviolet Aerodynamic Particle Sizer (UV APS)	Carousel Liquid Sampler (CRLS)	Fluorescence Aerodynamic Particle Sizer (FLAPS)	Chemical/Biological Mass Spectrometer (CBMS)
Fluorescence Aerodynamic Particle Sizer (FLAPS)	IBADS Wetted-Wall Cyclone Sampler	Aerosol Shape Analysis System (ASAS)	Biological Detection Kit (BDK)
High Volume Aerodynamic Particle Sizer (HVAPS & HVAPS II)	Spincon	Biological Aerosol Warning System (BAWS)	Hand-Held Assays
Interim Biological Agent Detection System (IBADS) APS	Biological Inertial Collector/Concentrator (BICC)	Single Particle Fluorescent counter (SPFC)	Light Addressable Potentiometric Sensor (LAPS)
Aerosol Shape Analysis System (ASAS)	Research International 1, 2 Collectors	Surface Transverse Wave (STW)/Shear Horizontal-Acoustic Plate Model	IGEN Origen
Met One Particle Counter	Phllaas	Chemical/Biological Mass Spectrometer (CBMS)	Fiber Optic Wave Guide (FOWG)
BIO-TEST Particle Measuring System	RECON test system PM-10	Model 4700 Bio-Luminometer	Biological Detector (BD)
Aerosizer	French Cyclone	Model 3550 Bio-Luminometer	Mini-PCR
		IDEXX Lightning Bio-Luminometers	Enzyme Linked Immuno Sorbant Assay (ELISA)
		Coulter Flow Cytometers	
		LANL Flow Cytometer	
		Becton-Dickenson Flow Cytometers	
		Bio-Rad BRYTE Flow-Cytometer	
		LLNL Flow Cytometer	

- **Fluidics**

The fluidics is composed of four (4) LRUs: the Fluid Transfer System (FTS), the Consumable LRU, the Waste LRU and the Confirmatory Sample LRU. The purpose of the FTS is to collect samples from the Collector, temporarily store them for analysis and to transfer portions of the samples to the appropriate LRUs. The Consumable LRU holds all the liquids used during the normal operation. The Waste LRU is used to store all waste fluids and to hold the detergent used to clean the system at the end of a mission. The Confirmatory sample LRU is used to store samples for future analysis.

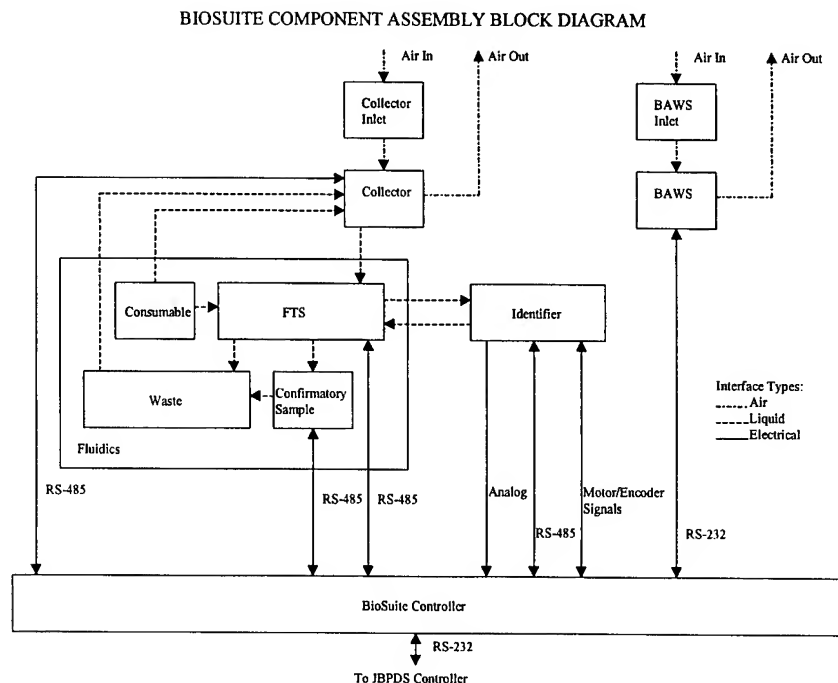


Figure 1 JBPDS BioSuite Component Assembly Block Diagram

In order to meet the JBPDS Block I EMD Performance Specifications requirements, the JBPDS was designed to continuously monitor particles in the air for suspect biological material. When suspect biological material is detected, the JBPDS will collect aerosol particles into a liquid sample for analysis. If a BW agent is identified, the sample will then be sent to a confirmatory sample vial that will be used for future analysis. In order to assure that a BW agent will not be missed (for example, during periods of heightened alert), the JBPDS is designed to continuously collect a sample for analysis in five minute batches.

In the event of a BW agent identification, the JBPDS will alarm via the M42 interface. The interface to the operator is controlled via the Local Control System (LCS) and External Control System (ECS). The ECS, along with the integral fiber optic and radio modems, allow a single operator to control one or more remote JBPDS systems. Through the LCS and ECS the operator is able to start-up, set the operating mode, shutdown, and monitor the status of the system. Communication between the JBPDS and the ECS can be performed via optical link or radio modem. In addition to the biological detection status, the JBPDS is also equipped with a GPS and weather sensor to provide additional information.

Configurations that are designed to operate in a stand-alone configuration are equipped with an Environmental Control Unit (ECU) that provides temperature and power conditioning control for the system.

Detector LRU

The Biological Agent Warning Sensor – Tier III (BAWS III) performs the triggering and detection functions for the JBPDS. Figure 2 shows a picture of the BAWS. The BAWS was developed by MIT-Lincoln Labs.

The BAWS utilizes a laser-induced fluorescence technology to determine the presence of biological material in the atmosphere. It is designed to continuously monitor the air at approximately 100 L/min for particles less than 10 microns and to monitor for variations in background that indicates a biological agent has been disseminated. Besides the improved detection sensitivity, the BAWS does not require the use of consumables, which greatly reduces the JBPDS operating costs. In addition, the response time of the BAWS is less than one minute.

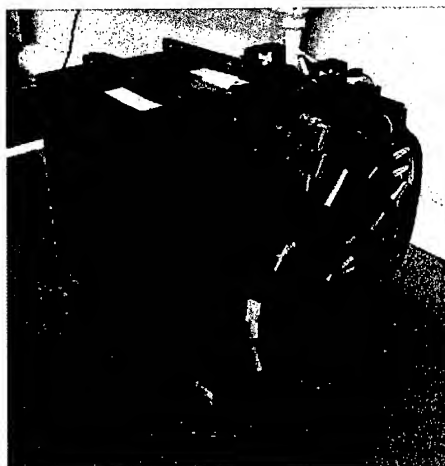


Figure 2 BAWS (Detector) LRU

COLLECTOR LRU

The WWC technology was originally used by the US Navy and Canadian Government in their early biological sensor programs. Battelle took the lessons learned from these designs and modified them to meet the needs of the JBPDS program. Modifications included reducing the size envelope, improving the collection efficiencies and developing the fluidic and electrical components so it could be integrated into the JBPDS.

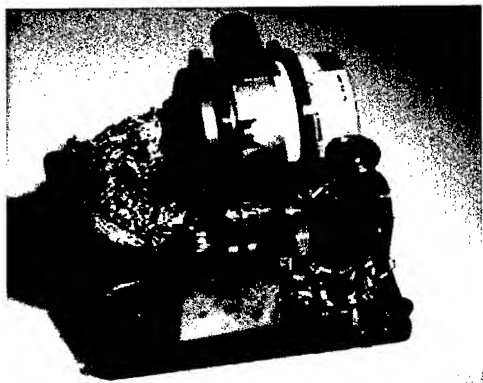


Figure 3 WWC (Collector) LRU

Figure 3 shows a picture of the WWC LRU. It is designed to collect particles at a rate of 800 L/mn of air and supply an output liquid flow rate of 1mL/min. The actual performance (concentrating factor) of the Collector is determined by the air flow, output liquid flow rate and the Collector efficiency.

IDENTIFIER

The HHA was originally designed as a manual test for BW agent. It consists of a strip that has been treated with antibodies that will react when a specific BW agent is present. By visually observing the presence of two lines on the strip when it has been inoculated with approximately 100 uL of sample and allowed 15 minutes to react with the sample, an operator is able to identify the presence of a BW agent. The first line observed is the control line that

appears when the strip is inoculated. This allows the operator to know that the sample has been processed. The second line is the test line that only appears if a specific BW agent is present. The presence of the test line on the HHA supplies positive identification that a specific BW agent has been identified.

To allow the HHA to be integrated into the JBPDS system an automated inoculator and reader had to be developed. Figure 4 shows a picture of the Automated Hand Held Assay (AHHA) LRU. It is capable of inoculating and reading a carrier containing a number of HHA. Each HHA has been treated with antibodies specific to a particular BW agent. The AHHA is capable of holding up to 75 carriers during a single mission.

The AHHA operates by automatically inoculating the AHHA Carrier strips with 100 uL of collected sample. At approximately 15 minutes after inoculation the strips are read by the AHHA. The AHHA reads the lines by a looking at the reflection of the strips from an optical diode. The intensity of the reflected light is read and converted by an analog-to-digital converter into data stored by the BCS. The BCS is equipped with an algorithm that processes the data and determines if the control and test lines are present.

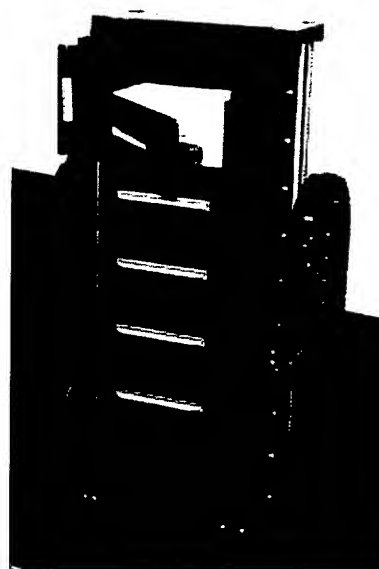


Figure 4 AHHA (Identifier)

System Testing

The JBPDS has undergone many months of testing to confirm its ability to meet the performance requirements. This has included:

- Engineering Design Tests conducted by the contractors to confirm the system readiness to be tested by the Government. These tests included:
 - human factors tests to evaluate the design in terms of ease of operation and man-machine interfaces
 - bio-performance tests to determine the sensitivity and false alarm rates
 - reliability growth tests to evaluate the MTBOMF of the system
 - environmental testing to confirm the ability to operate under the natural and induced environmental extremes of temperature, shock, and vibration
- Production Qualification Tests conducted by the Government at Dugway Proving Ground to test the system against numerous simulant and agent challenges with and without interferant backgrounds
- Operational Assessments and Limited User Tests to rate the training and ease of operation for long periods of time with actual military operators

Performance

The JBPDS Engineering Design Test (EDT) and Production Qualification Tests (PQT) verified the system is able to meet its performance requirements. Table 2 shows the performance data of the key JBPDS requirements.

Table 2. JBPDS Key Performance Requirements

Parameter	Requirement	Measured
Trigger Level	25 ACPLA	<25 ACPLA
Detection Time	5 minutes	~30 seconds
Sensitivity (Bacteria)	500 cfu/Lair	500 cfu/Lair for wet BG
Sensitivity (Virus)	500,000 pfu/Lair	250,000 pfu/Lair for MS2
Sensitivity (Toxin)	0.5 ng/Lair	<0.35 ng/Lair for Ov
Identification Time	15 minutes	15 minutes

During normal operations the JBPDS continuously monitors the background air and triggers the system when the concentration of up to ten micrometer sized particles in the sampled air causes a significant change with respect to average background levels. Because the BAWs is a particle fluorescence sensor it detects the presence of suspect biological agents based upon the quantity and characteristics of particles in the air. As a result a conversion table was required between colony forming units (cfu), plaque forming units (pfu), nanograms of toxin per liter of air and the quantity of agent containing particles per liter of air (ACPLA). It was decided at the start of the program to use the U.S. Army conversion table that was developed during the BIDS program. It defines a 25 ACPLA threat to be equivalent to 500 cfu/Lair, 500,000 pfu/Lair or 0.5 ng/Lair.

The BAWs LRU was configured to detect the presence of suspect biological material at the 25 ACPLA threshold. The actual sensitivity of the BAWs detector can be significantly improved by increasing the number of false triggers allowed during a 12 hour mission. During the Governments PQT testing at Dugway the JBPDS system only experienced about 1 false alarm every two hours. This would result in the JBPDS turning on the Collector LRU to collect a liquid sample for positive identification. The sample would then be sent to the AHHA for identification. Because there was no simulant dissemination at these times the JBPDS would report a negative identification and no alarm would occur.

The JBPDS is required to perform the detection function within 5 minutes of a biological threat being present. Because the BAWs LRU is able to directly monitor the background air it is able to detect the presence of suspect biological material in approximately 30 seconds of an event. This allows early warning for the operator while the system performs the identification function. The limiting factor on the Identifier's response time is the 15 minute processing time required for the Hand Held Assay (HHA).

The objective of the JBPDS system was to have sensitivity greater than 25 ACPLA. The testing at Dugway verified that the system is capable of identifying bacteria and toxins at the required sensitivities. Because of weather conditions the system's performance with viruses could not be verified; however, laboratory test of MS2 during EDT verified the performance to be below the required thresholds for viruses.

Summary

The JBPDS Block I EMD program has met its objectives by developing and demonstrating an automated biodefense system suitable for use by the four services of the U.S. military government. This system is planned to go into production in FY01 with fielding of hundreds of units shortly thereafter. It will become the new benchmark against which future biodefense systems will be evaluated.

Acknowledgements

The success of the JBPDS Block I EMD program could not have been accomplished without the contributions of many organizations and their dedicated staff. The BAWs was developed by MIT-Lincoln Laboratories (Lexington, MA) with a team lead by Michael Languirand. The BAWs was originally intended as an Advanced Technology Demonstrator, not intended to meet the environmental extremes required of the JBPDS. Nonetheless, MIT-LL was able to upgrade their design in a very brief matter of time and met the allocated requirements.

The system software was developed and documented by Ricciardi Technologies Inc. (Fairfax, VA) with a team lead by David Godso. Their attention to detail and dedicated efforts, especially at the second half of the program when they took over overall responsibility for the software was critical to meeting the schedule objectives.

Finally, the program was operated as an Integrated Product Team (IPT) lead by the Government. This environment established early in the program is indicative of the acquisition reform movement with the military. The success of the program was largely due to this approach to managing the individual contributing organizations in a team-oriented manner.

Contact Information

Wolf P. Altman
Battelle
505 King Avenue
Columbus, Ohio 43201
Tel: 614-424-4342
altmanb@battelle.org

Donald R. Hohe
Battelle
505 King Avenue
Columbus, Ohio 43201
Tel: 614-424-4892
hohed@battelle.org

M22 AUTOMATIC CHEMICAL AGENT ALARM

Rob Howard and *Daniel M. Nowak*

Graseby Dynamics LTD Bushey, Watford, Herts United Kingdom
And

U.S. Army Soldier and Biological Chemical Command
Project Manager for Nuclear, Biological and Chemical Defense Systems
Aberdeen Proving Ground, MD 21010-5424

ABSTRACT

(U) The newest chemical agent point detection system is now on the battlefield. The M22 Automatic Chemical Agent Alarm (ACADA) is currently being fielded to the U.S. Armed Forces and other Government Agencies. The M22 is capable of detecting nerve and blister agents simultaneously and provide a warning when these agents are present. It can be interfaced with automated warning systems. The detector is man portable, lightweight and easy to operate. It can be operated in an area-warning role, within Collective Protective Equipment and in and on vehicles.

(U) The ACADA detection technology is based on Ion Mobility Spectrometry and several unique features have been incorporated into the detector to improve agent sensitivity and interference rejection over the range of required environmental operating conditions. These features will be described along with the components which make up the system. The system has been extensively tested and has demonstrated satisfactory operational suitability. An overview of the scope of the test program will be presented.

(U) Within the presentation the Ion Mobility Spectrometry technology will be described along with the unique features incorporated in the detector. The operational roles will be highlighted and the varied uses and applications will be described to include specific mounted applications on various vehicles.

(U) The use of Chemical Warfare agents continues to be a viable threat to U.S. Forces. In an interview for the United States Navy Surface Warfare magazine, Major General Wooten, Former Commandant of the U.S. Army Chemical School stated "The chemical/biological threat is real, more so than the nuclear threat right now. Before the demise of the Soviet Union, we believed the chemical/biological threat was contained. But when "the wall" crumbled, there was no more central control; chemical/biological weapons and weapon delivery systems proliferated. Intelligence estimates 25-27 countries have either chemical or biological weapons." (ref. 1) Chemical Agents have been called "poor man's nuclear weapon". The manufacture of chemical warfare agents in small quantities by terrorists is an ongoing threat but the manufacture and use of military quantities of chemical warfare agents for delivery against U.S. Forces during military missions is always a potential. The delivery of chemical weapons against our ground and mechanized forces could cause disruption of communications and a degradation of command and control.

There are numerous defense strategies for countering these threats and the newest tool in ameliorating the tactical effects of chemical agents is the M22 Automatic Chemical Alarm, ACADA (Slide 1). The M22 ACADA is the Joint Services most advanced chemical agent detector. It is a point detector which is

capable of quickly warning our troops that a chemical attack has occurred or that our forces have traversed a chemically contaminated area. With sufficient warning, military personnel can take protective measures to reduce the chances of inhaling these chemical warfare agents, thereby preventing or reducing casualties (Slide 2). The M22 ACADA, when employed properly, will provide this warning capability. The M22 is a point detector which simultaneously senses vapors of Nerve and Blister agents and provides an alarm. The M22 system consists of the M88 detector, transit case, removable battery pack and M42 remote alarm unit. Auxiliary equipment includes the M28 power supply and M281 vehicle mount with an M42 mounting bracket (Slide 3).

(U) The ACADA (M88 Detector) (Slide 4) detects the nerve agents GA, GB, GD, VX and Blister Agents HD and L in under two minutes at low concentration requirements. At higher concentrations the response time is typically 10 seconds. After detection the ACADA provides both a visual (flashing red light) and audible alarm. The detector simultaneously detects and displays both Nerve and Blister alarms. The size and weight of the ACADA and auxiliary equipment allows for easy transport and is one person portable.

(U) The M88 Detector is powered by two BA5590 LiSO₂ batteries providing +24 Volts DC. The detector also can be powered from 115/220 VAC line power using the M28 Power Supply. The detector can also be powered from vehicles using the M281 Vehicle Mount.

(U) The M22 (Slide 5) and its auxiliary equipment has been tested and operates over a wide range of environmental conditions and is operable in all military environments. The M88 Detector has an RS232 communications port, is compatible with MICAD and is adaptable to other reporting systems. Finally, the M22 and its auxiliary equipment is easy to operate and requires minimal (8 hours) of training for any operator (Non-Military Operational Specialty specific).

(U) The detection technology (Slide 6) within the M88 Detector is Ion Mobility Spectrometry (IMS). The unique features within the detector design include: dual Ion Mobility Spectrometers, heated membrane, heated cell, heated inlet, pressure sensors and temperature sensors. The detector IMS tubes are independent and allows for simultaneous detection of Nerve and Blister Agents. The heated elements of the system enhance the transport of less volatile agents thereby reducing response times for agent detection. The pressure and temperature sensors provide information to the microprocessor which calculates the absolute mobility (K_0) of detected spectra (ion peaks). The mobility of the detected ion peaks are then compared to the agent library. A match of agent spectra of sufficient amplitude then triggers an alarm. The algorithm is optimized for agent detection and interference rejection. The final unique feature of the M88 Detector cells is the addition of ammonia to the cells via a permeation tube located in the air stream of the IMS cells. This addition of ammonia improves interference rejection and allows for operation of the ACADA within Collective Protection Equipment where higher than ambient ammonia concentration may be present.

(U) M22 is designed for 3 operational roles. These roles include area warning, monitoring collective protective equipment (CPE) and operation on and in vehicles. In the area warning role, the M22 is employed up to 400 meters upwind and is operated by a battery pack (Slide 7). The hard wired M42 alarm unit is emplaced with the troops to be alerted. Once operational, set-up and break-down times are typically a few minutes, making the system highly mobile for changing tactical situations. In the CPE monitoring role (Slide 8) the M88 detector is used with the M28 power supply to allow long term monitoring of the air. This operational role will indicate if the "clean" environment has been breached by incoming contaminated personnel or equipment, or if the chemical filters have failed.

(U) In the vehicular role (Slide 9) the M88 detector is used with the M281 vehicle mount and powered from vehicle power. In this application the M88 detector can be installed at an appropriate location on the exterior or interior of the vehicle. Both applications require the M281 vehicle mount which provides vibration and shock isolation for the detector. The M42 is connected to the M88 alarm and located near crew members to provide an audible and visual alarm. The M88 is the detector used with the Multi-Purpose Integrated Chemical Agent Alarm (MICAD) system. The MICAD system is used for communication to the immediate crew and surrounding command and control units that a chemical agent has been detected in or around a particular vehicle. The M88 detector is easily removed from the M281 vehicle mount to allow for area warning around the vehicle.

(U) The M22 system is the most extensively tested chemical detector fielded to U.S. Forces (Slide 10). The 2 year test program included all military environmental and intended operational roles. Test conditions included operation at temperature extremes of -30 degrees Centigrade to +55 degrees Centigrade, rain, dust, salt spray and electro-magnetic interference including high altitude electro-magnetic pulse. Extensive vehicular tests (Slide 11) were conducted at the Test and Evaluation Command test sites in Alaska, Panama, Yuma, and Aberdeen. The detectors were mounted on the exterior of the vehicles to demonstrate reliability and survivability. In the Arctic, the SUSV and HMMWV were tested at temperatures down to -45 degrees and were driven a total of 200 vehicular miles. At the Tropic Test Center, the M22 was mounted on the HMMWV and operated in driving rain and in tropic conditions for a total of 1,182 vehicular miles. At the Desert Test Center, the M22 was mounted on the M113 and operated in dusty conditions and at temperatures up to 50 degrees Centigrade. At this location, a total of 2,760 vehicular miles were accumulated. At the Aberdeen Test Center (ATC), testing consisted of the M22 being mounted on the outside of the M113 armored personnel carrier and at the center console of the HMMWV. Both vehicles accumulated a total of 10,000 vehicular miles while being driven over the Perryman Cross-Country vehicle qualification course. In all cases, the M22 and its vehicle mount, operated successfully and without false alarm. An additional test conducted (Slide 12) at ATC to qualify the M22 for attack vehicles. The M22 was mounted both inside and outside the M1A1 Abrams Battle Tank using the vehicle mount. The M1A1 cannon was fired to determine if the blast, shock and combustion effluents would effect the operation of the M22. The M22 operated successfully throughout the test.

(U) The M22 is rugged, not prone to interferences and is very sensitive to chemical agents. Its application on vehicles is the next step for providing our mechanized forces with the warning and information essential to protect the crew and to avoid contamination of their equipment. Currently, the M22 (Slide 13) is being installed in all FOX vehicles and the M22 is a requirement on the Bradley C2V, the AAV and Light NBC Recon. The M22 can be applied to many types of platforms including the M113, HMMWV, Crusader, Paladon, Future Scout Vehicle, SUSV, M2 Bradley, and M1 Abrams. Applications on other vehicles are also viable.

(U) The ACADA team is dedicated to product support and we have several (Slide 13) publications available or in development to assist operators and users in the deployment and operation of the M22. These include technical manuals, bulletins, a CD ROM, and an operator's video.

Reference:

1. Surface Warfare Magazine, November/December 1996, "The Battle of NBC", p. 16 (U).

BIOLOGICAL DETECTION SYSTEMS: THE INDUSTRY EXPERIENCE

Peter J. Day

Graseby Dynamics Limited

Park Avenue, Bushey, Watford, Hertfordshire WD23 2BW England

Abstract

The UK Ministry of Defence has fielded a Prototype Biological Detection System (PBDS) to give the UK armed forces a biological detection capability until the Integrated Biological Detection System (IBDS) enters service. Graseby Dynamics Limited (GDL) was responsible for the provision of the chemical and biological detection systems for PBDS. Under the Full Development and Production contract for IBDS, currently in mid / late development, GDL is again responsible for the chemical and biological detection systems. For both systems GDL has drawn heavily on the foundation work of CBD Porton Down, which is the subject of a separate paper at this conference.

The PBDS and IBDS systems are described in outline. The rationale for the selection of the detection technologies is discussed with respect to programme risk and through life costs.

Particular engineering problems associated with a mobile military application are discussed and the solutions described. Particular attention is given to the physical containment of instruments for the purposes of crew protection.

A very high efficiency Sample Collection System is described. The SCS is based on a novel modification to the wetted wall cyclone. The wall of the cyclone is manufactured from a permeable sintered stainless steel surrounded by a water jacket. Pumping the collection liquid through the cyclone wall causes a continuous film to be formed which significantly increases collection efficiency as compared to other traditional cyclone designs.

Finally, experiences of the project definition phase of the IBDS programme, the PBDS in service and the current IBDS development programme, the desirable key characteristics of the next generation of biological detectors are examined.

Introduction

These PBDS and IBDS programmes were won on a competitive tender basis by a tripartite consortium in which Graseby Dynamics Ltd. had responsibility for the biological and chemical detection systems and associated ancillary equipment.

The PBDS contract called for the design and build of a small number of vehicles. The detection system comprises existing commercial equipment and prototype bio-warfare agent instruments.

The IBDS is the subject of a development and production contract and is at an advanced development stage. The IBDS will contain a fully integrated, designed for purpose, fully automated detection system.

The rapid introduction of PBDS into service and the strong base from which IBDS is being developed is the result of the Ministry of Defence, Defence Procurement Agency funding of a number of

preparatory programmes at CBD Porton Down. The foundations laid by these two bodies is fully acknowledged. This paper should be read in conjunction with that of Dr. A. Bell, of CBD Porton Down.

Prototype Biological Detection System

The Prototype Biological Detection Systems arose from an Urgent Operational Requirement (UOR) contract placed by the Defence Procurement agency (DPA). The PBDS was based on a set of recommendations in the Invitation to Tender (ITT) as to which technologies were appropriate. A number of vehicles were delivered to the customer in about twenty weeks. The equipment fitted to PBDS consists of commercial equipment, and further builds of what can be regarded as prototypes of instruments in the IBDS lineage.

Collection System

The sample collection system, a Horizontal Wetted Wall Cyclone (HWWC) is a purpose designed equipment contributed by CBD Porton Down. The HWWC consists of a conventional cyclone with peristaltic pumps to supply the water spray in the air inlet to the cyclone and to scavenge the particle bearing liquid from the cyclone. An air / liquid interface provides a mechanism for the de-bubbling of the sample and prevents pressure changes in the fluid system. The fluid level in the a/l interface is controlled by a sensor switched peristaltic pump. The HWWC inlet is provided by a commercial PM10 sampler acting as a filter. The PM10 performance is insensitive to wind direction and wind speed within adequate limits.

Detectors

Aerosol Shape Analysis System: An ASAS, the BM10, designed and manufactured by Bristol Industrial Research Associates Ltd., is the non-specific detector. This unit is in effect the prototype for the ASAS for IBDS. The ASAS counts the number of particles in a continuous air sample and provides information on the size and shape of each particle. By observing changes in the count, size and shape characteristics of the particles over time, an assessment can be made as to whether a change is occurring in the sample that could be attributable to an artificially generated aerosol. An ASAS inlet system was commissioned from CBD Porton Down. Sample airflow from the environment is induced in a vertical inlet pipe by a fan drawing air from a concentric plenum. The ASAS draws its sample from the vertical inlet by means of an isokinetic sample nozzle. Coarse filtering is achieved by vertical alutration augmented by a bug screen.

Continuous Flow Luminometer: The CFL is the generic detector. The build standard is that of a laboratory prototype intended for use in a reagent development programme at CBD Porton Down. This unit is the precursor to the IBDS CFL. The CFL uses a liquid sample. The sample is split into two equal streams, each stream being then combined with an extractant. One extractant removes all the adenosine tri phosphate (ATP) in the sample, the other removes all the ATP except bacterial ATP. Each stream is then injected with an enzyme that luminesces in the presence of ATP. The emitted light is measured by photomultiplier tubes (PMT) and the difference between the signals from the PMTs indicates the amount of bacterial ATP present. The process is continuous and significant changes in the signal above the expected level are taken as an indication of a possible event.

Resonant Mirror: The RM is a commercial instrument re-cased for this application. Advantage was taken of spare space within the unit to mount the sample feed and scavenge peristaltic pumps and a computer driven valve. The valve controls the flow of a regeneration agent over the cuvette surface. These components are used to create an automated system. The RM is an optical biosensor, used in this

application as the specific detector for toxins. Antibodies are bonded to the surface of a prism. The prism is mounted in an assembly such that a sample well is formed with the prism forming the lower surface. When antigen / antibody bonding occurs there is a change of refractive index at the prism surface. This change is measured by means of a gimballed laser that illuminates the underside of the prism.

Manual Threshold: A standard commercial equipment manufactured and supplied by Molecular Devices Inc. The light addressable potentiometric sensor (LAPS) of the Manual Threshold is the sensor element of the Bio Detector used in the IBDS. The general principle of both devices is described below.

Plate Reader: A standard commercial equipment manufactured by Labsystems Affinity Sensors.

Fraction Collector: A commercial equipment used to collect sample for the purposes of the Sampling and Identification of Biological and Chemical Agent (SIBCA) process. The sample is automatically distributed into cells in a collection block. Each cell holds five minutes worth of sample. The block can be taken away for laboratory analysis and concentration / time profiles derived from that analysis.

Chemical Warfare Agent Detector: A Graseby Dynamics GID-3 was fitted. This is currently being supplied to several nations, including the US. A standard vehicle mount is utilised. A sample intake designed for an armoured vehicle was modified slightly to account for the greater thickness of wall on the PBDS soft-skinned vehicle.

Ancillary Equipment: The detection equipment, with the exception of the ASAS, is mounted in a containment designed in accordance with the principles pertaining to microbiological safety cabinets. The design is an expanded version of a portable isolator designed for, and used by, the Royal Army Medical Corp. The containment is provided with glove ports as appropriate and hinged hatches for replenishment and maintenance purposes. A plate sealer is provided as a means of sealing the fraction block prior to storage and despatch. A domestic refrigerator is installed for the storage of reagents and SIBCA samples. A laboratory water purification equipment is installed to supply water for the HWWC and rehydration of reagents. This is modified to work in a 100% recovery mode.

Integrated Biological Detection System

The First Decisions

As our activity in the IBDS bidding process got underway it became apparent fairly rapidly that there were several key issues of a strategic nature that would require resolution during the programme. The first of these was whether to follow the path beaten for us by CBD Porton Down in respect of detector technology. The spur for considering alternative approaches was the perceived high running costs of some elements of detector suite and, in the case of one detector system, perceived difficulties in the practicalities of use in the field. The trade-off was of the risk of introducing new technologies which would be cheaper to run and of less certain performance, against the in-depth knowledge available for the particular technologies described to contractors in the Invitation to Tender (ITT). This trade-off was set against a background of a competitive tendering situation and an ambitious requirement for the in-service date. The overall novelty of the programme, the first purpose designed, integrated biological detection system into service, heavily influenced the decision. On balance the view was taken that the route forward was that of utilising technologies for which there was maximum background knowledge in this application. Later in the programme specific packets of work were undertaken to reduce the running costs of the system in terms of bio-consumables usage.

The Detector Suite

During the study phase and early part of the development programme the IBDS detector suite evolved into the following set of equipment:

- An Aerosol Shape Analysis System (ASAS) – the non-specific detector.
- A particle collection system / intake for the ASAS (ASASCS)
- A Sample Collection System (SCS) – particle collector for the “wet assays”.
- A Continuous Flow Luminometer (CFL) – the generic detector.
- A Resonant Mirror (RM) – the specific detector for toxins.
- A Bio Detector (BD) – the specific detector for the bacterial and viral agents.
- A facility for acquiring a liquid sample to provide evidence of BW attack: (The SIBCA sample).
- A Biological Hazard Control System (BHCS) – a microbiological and chemical containment system to protect the crew from exposure to harmful agents.
- A GID-3 – the specific detector for chemical warfare agents.

In addition the following ancillary equipment forms a part of the vehicle fit:

- A refrigerator – for the storage of bio-consumables.
- A water purification system – to supply water for the SCS and rehydration of certain reagents.

Graseby Dynamics are also responsible for the design and supply of Bio-consumable Battlefield Mission resupply packs (BBFMP). The consumable items include the reagents for the wet assays and disposable items such as gloves, wipes, etc.

General Configuration

The IBDS vehicle is a standard UK four tonne flat-bed truck. A container provides accommodation for the crew and equipment. The IBDS vehicle is fully equipped for extended deployment, with the crew working in a “shirt sleeve” environment.

The detectors, mounted within the BHCS are located at the rear of the vehicle along the right hand wall. The SCS is mounted externally on the rear face of the container.

The Biological Hazard Control System

Subassemblies of the SCS and three of the four detectors use a wet sample that could result in some aerosolisation, the fourth detector requires the transport of air sample from the general environment into the crew area. It was clear that some form of protection was required for the crew. This protection was demanded both by the Customer's requirement and by UK health and safety legislation. The BHCS takes the form of a microbiological safety cabinet. The design parameters are taken where practical from the relevant British Standard and its Euro equivalent. Adherence to these requirements wherever possible greatly simplifies the preparation of the detector suite safety case. Some of the requirements are not practical in this application. The standards for microbiological safety cabinets are written around fixed installations, and not all the requirements expressed in those standards can be applied to a situation where there is very limited availability of space, weight and power. Consequently the BHCS exchanges air with the crew compartment.

Although not specifically intended to do so, it is anticipated that the SCS will entrain into the sample, some proportion of any chemical agent that passes thorough the SCS. Therefore, in addition to the

biological filters there are chemical agent filters in the exhaust air path to remove any traces of chemical agent.

As a general safety principle the minimum of equipment is introduced to biological safety cabinets. It is also desirable to minimise the equipment isolated for ease of maintenance and repair. Consequently only those elements of the detectors that have to be in contact with the sample are mounted inside the BHCS. The remaining elements, generally printed circuit cards, are mounted in a racking system located beneath the BHCS.

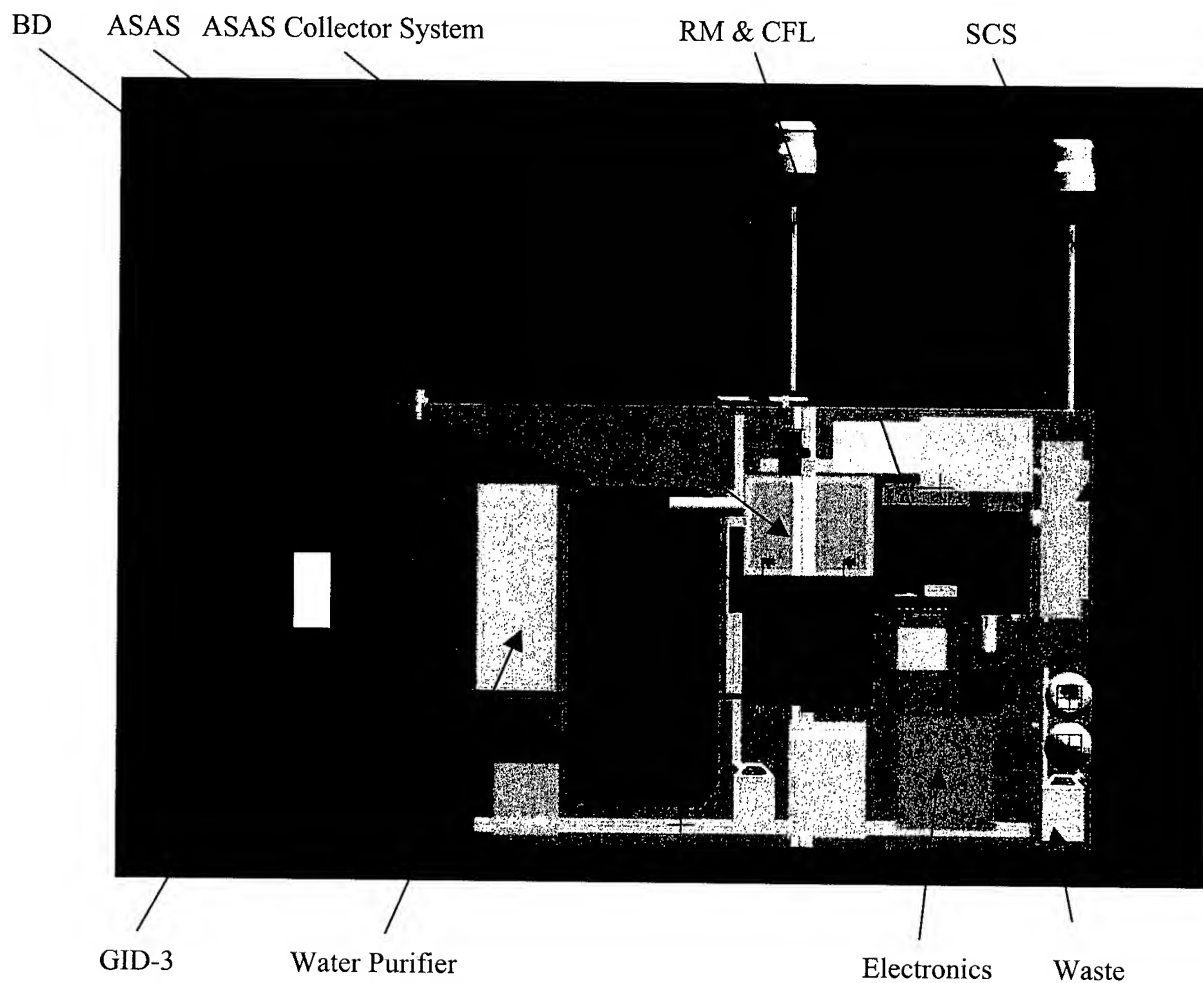


Figure 1 - The Detector Suite Disposition

The problem of passing consumable items, spares and samples for evidence into and out of the BHCS has been solved by the provision of a docking canister system; essentially a small removable airlock, these are commercially available accessories for microbiological safety cabinets. Wherever possible components have been selected for size to be compatible with the docking canister.

The Aerosol Shape Analysis System

The Aerosol Shape Analysis System for IBDS is a development of that used for PBDS. The IBDS ASAS has extended performance and has been re-engineered in form to satisfy the need to minimise the component count that could be exposed to agents. The design is such that all the routine maintenance

and resupply can be carried out with one hand via a standard glove port in the BHCS. There has also been an increase in sensitivity at the lower end of the particle size range.

The ASAS Collection System

The function of the ASASCS is to provide a representative sample of air from the general environment to the ASAS after removal of those particles which are too large to be of interest and which could clog the system.

The particles that are outside the upper size limit, bugs and other objects that are not of interest are removed by vertical alutiation. A supplementary bug screen is provided for the more persistent and suicidal insects. The airflow is induced in the vertical inlet pipe by a fan drawing air from a concentric plenum. The ASAS draws its sample from the vertical inlet by means of an isokinetic sample nozzle.

The ASASCS assembly is topographically external to the crew compartment, except for the inlet to the ASAS. The functional components of the ASASCS are sealed within a "bath tub" let into the vehicle roof. The topographical arrangement is such that no credible single breach of the ASAS / ASASCS system will hazard the crew.

The Sample Collection System

The performance of the SCS is a key factor in any detector system, particularly so in a system such as IBDS where three of the four detectors use a liquid sample from the SCS. Any increase in the collection efficiency reflects immediately as a sensitivity enhancement for all parts of the system which use the sample.

Some considerable effort was expended in the selection of the technology to be used in IBDS. A trade-off study between cyclones and impactors showed the former to be preferred.

The precursor cyclone work undertaken by CBD, centred on a vertical cyclone using water or buffer solution sprayed into the inlet. A wetting agent was used in an attempt to ensure a continuous film over the cyclone wall. The collection of particles is effected by the "scrubbing effect" of fluid droplets on the air, that is by the entrapment of particles by collision with droplets of the collection fluid, and the subsequent impact of the droplets on the cyclone wall. The film of sample on the wall drains to the bottom of the cyclone where it is pumped away for use. An additional mechanism for the collection of particles is the entrapment of those particles by impact into the film of collection liquid on the cyclone wall.

The first prototype SCS incorporated a glass cyclone and the observation was made that the fluid on the wall did not form a continuous film despite the use of the wetting agent. The fluid stayed in droplets and rivulets that covered a small percentage of the surface of the cyclone wall. These patches of liquid migrated around the wall of the cyclone under the influence of the airflow. It was apparent that one of the two supposed mechanisms of particle capture was to some extent non-effective. Means were sought of forcing a continuous film on the cyclone wall, and the idea of a permeable wall surrounded by a water jacket was mooted. The permeable, or transpired wall was to be used either in conjunction with an inlet spray or as the sole collection method. A sintered stainless steel was selected as the cyclone wall material and this has proved to be successful in all testing to date. The transpired wall cyclone (HTWWC) is the subject of patents applications.

Some extension of performance to lower ambient temperatures may be achieved for the cyclone by heating the water jacket and, directly or indirectly, the permeable cyclone wall. As the heat requirement is that to prevent freezing of the thin film of fluid on the cyclone wall it is anticipated that there will be a reduced power requirement compared to heating the sampled air.

It is desirable to keep the inlet tract straight as particles tend to impact on the walls of bends and collection efficiency is thereby reduced. The IBDS cyclone has been turned on its side to eliminate the 90° curve in the inlet that is otherwise necessary. Somewhat counter-intuitively the liquid sample still collects at the same point in the cyclone and is pumped away as before.

Like the ASASCS, the SCS uses vertical alutriation at the inlet to eliminate the larger particles, bugs and other gross and unwanted detritus from the sample. This is a distinct advantage over the PBDS that uses an impactor for this purpose. The elimination of the impactor means a reduced workload for the operators, as there is no impaction plate requiring routine cleaning and regreasing. This is also a health and safety benefit and there is a reduced supply burden in respect of consumables and/or impaction plates.

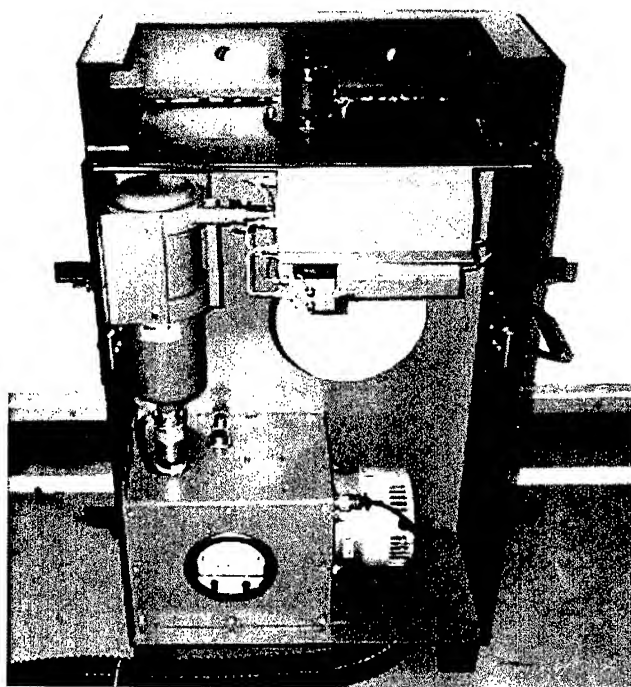


Figure 2 – Sample Collection System

The Continuous Flow Luminometer

The Continuous Flow Luminometer in its prototype form has proven to be a reliable and rugged device. Relatively little reengineering has been necessary to produce an item of equipment suitable for service use. The main tasks have been:

- To rationalise the fluidic circuit and reduce the component count.
- To reselect the key components for reliability under extreme mechanical environments.
- To separate the detection elements from the processing in order to minimise the component count within the BHCS.
- To improve the lower limit of detection by improvements in both the instrument and the reagents.

- To reduce reagent consumption.
- To develop easy change, foolproof reagent cartridges.

The Resonant Mirror

Like the CFL the Resonant Mirror is a fundamentally reliable and rugged device, as proven by its reliability in the deployed PBDS vehicles and by environmental testing applied to the prototypes.

For IBDS the RM the main re-engineering tasks have been as follows:

- To increase the number of agents that can be detected.
- To increase instrument sensitivity.
- To separate the detection elements from the processing in order to minimise the component count within the BHCS.
- To design and produce an automated facility for the printing of antibodies onto the cuvette.

The Bio Detector

The Bio Detector (BD) is a modified version of the instrument that is in service with the US BIDS system. The BD will be familiar to the great majority of people working in the field of biological warfare agent detection, and there is a significant amount of information available on this instrument elsewhere, including the web site of the Environmental Technologies Group who manufacture the instrument.

The Bio Detector is an automated version of the Manual Threshold. The detector in the Manual Threshold (MT) and the BD is a light addressable potentiometric sensor (LAPS). The LAPS is a semiconductor electrode that detects changes in potential in the presented sample, these changes being due to chemical reactions.

The BD and MT both have essentially the same chemistry, with the BD automating the whole process. The assay proceeds in three stages, incubation/reaction, separation and detection. In the first stage, the antibody and target antigen are incubated together and the specific detection reaction takes place. The specificity of the antibody determines the antigen that can be detected, which can be bacteria, virus or toxin.

In the separation stage, the incubation mixture is passed through a biotinylated membrane, that 'captures' the antibody / antigen complex. On the BD this is automated, using the membrane on a roll of tape assembled into a cassette format. On the MT this involves manual effort using vacuum to capture the reaction onto the individual MT 'sticks'.

In the detection phase, a second enzyme labelled antibody is added, that detects if either the whole antibody/antigen complex is present (positive sample), or just the antibody alone if no antigen is present in a negative sample. Again, this is a manual addition on the MT that is automated on the BD.

Finally a urea substrate is added, so that if the enzyme labelled antibody is present, it will initiate a reaction to change the pH of the solution that can be detected by the LAPS sensor. The sensor then gives results measured as a rate of change, in uV per second.

In the case of a negative reaction, there will be no enzyme labelled antibody available, consequently no pH change and no signal. Although the measurement is automatic on the BD, for the MT this stage involves transferring the 'stick' to the reader section containing the LAPS device.

MT and BD results are directly comparable, although due to the automation standardising incubation times, and reagent manipulation, the BD is considered the more sensitive device.

A number of modifications have been made to suit the IBDS application. The two front access doors have been replaced with a "sash window" like arrangement that reduces the operating envelope and enables the BD to be contained within a reasonably sized BHCS. The BD's operating software has been augmented to allow remote operation of the BD. Remote operation brings this facet of the BD into line with the general philosophy that the detection equipment should be isolated from the crew and that the crew should have the absolute minimum exposure to potentially contaminated equipment during operation, replenishment and maintenance. The User's control panel has been replaced by a blanking panel as it was no longer required.

Chemical Warfare Agent Detector:

A Graseby Dynamics GID-3 will be fitted. The installation derived for PBDS using standard accessories has proved to be entirely satisfactory in use in PBDS and so the same configuration will be retained for IBDS.



Figure 3 - GID-3 Chemical Warfare Agent Detector PBDS & IBDS

Bioconsumable Battlefield Mission Resupply Packs

The most significant items in the Bioconsumable Battlefield Mission Resupply Packs are the reagents (including antibodies, Ab). Considerable work has been undertaken and is planned for the future support of the IBDS. A brief description of the reagent programme is as follows.

Validation Programmes: A series of tests using both simulants and live agents carried out using progressive build standards of each detector. These tests provide the proof that the system meets the design requirements.

Life Determination Programmes: The life of each reagent and antibody is of significance both in the planning of the support of the IBDS and in terms of its successful function in the field. A series of sub-programmes determine the likely life of the reagents in the following forms:

1. In "deep" storage, i.e. not in ready to use form (particularly applicable to antibodies).
2. In ready to use form.
3. In transit from the storage point to the fielded vehicle.
4. Life when reagents are in use in the vehicle.

Life Confirmation Programmes: It is anticipated that there will be batch-to-batch variation in the life of reagents. Therefore monitoring programmes are planned that will confirm that the material held in store at any moment is still active within specified limits.

Reagent Supply Modelling and Control: The manufacturing processes for the reagents, particularly for the antibodies, are complex and for some materials quite lengthy. There are also various possible manufacturing process routes that can be used and the optimum route is likely to change depending on prevailing circumstances. It has proved necessary for sophisticated modelling tools and techniques to be adopted in order to optimise the manufacturing plan in terms of its cost effectiveness in relation to the many potential patterns of demand.

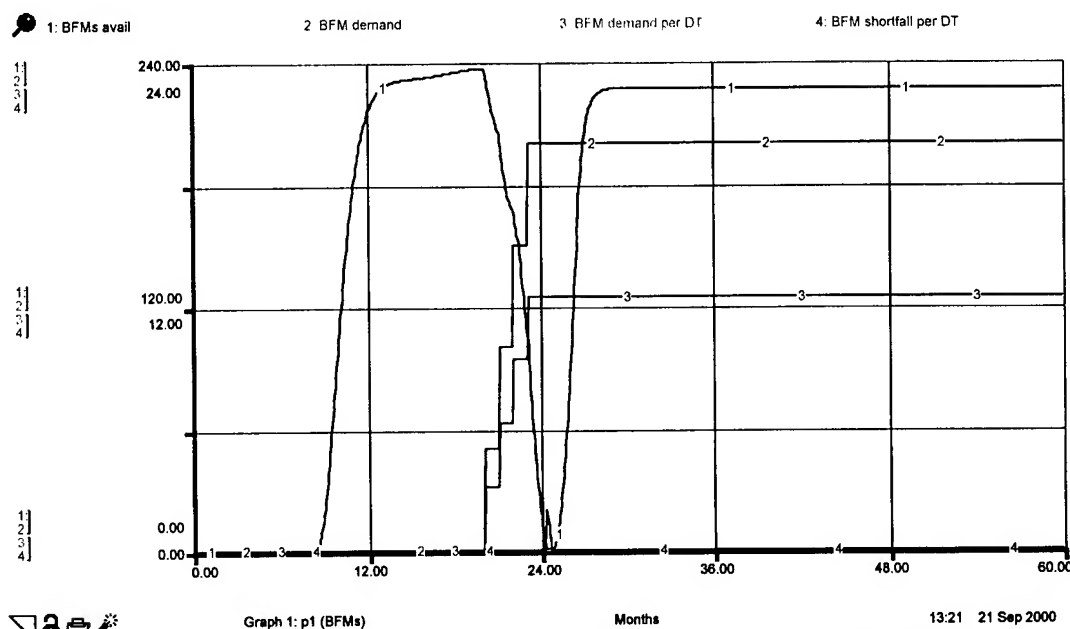


Figure 4 - Bio Consumable Supply Modelling and Management Software

Biological Warfare Agent Detection – The Next Generation

It is clear that BWA detection is in its infancy. Whereas CWA detection can be achieved with small, light, pocketable detectors, an equivalent (or even lesser) performance in BWA requires a four tonne truck full of equipment. In addition the truck requires regular supplies of reagents and other consumables, the CWA detector requires occasional recharging of its batteries and replacement of a sieve pack at extended intervals. The current logistic burden for BWA detection is significant. The reagents and antibodies are relatively delicate, and relatively short lived materials that require a considerable industrial commitment.

The following table gives estimates of the factors and levels of improvement that need to be achieved before BWA detection systems enjoy a similar utility to that of CWA detectors as they are today.

Factor	Improvement	Degree / Comment
Weight	Reduce	Two orders min.
Size	Reduce	Two orders min.
Power Consumption	Reduce	Three orders min.
Reagents & Antibodies	Eliminate	Or develop detectors that use cheap, long life, temperature insensitive reagents.
Sensitivity	Increase	

A large reduction in power consumption should result as and when detection techniques are developed which are not temperature sensitive. At present a significant use of power is the maintenance of temperature in the region where bio reactions occur. Significant power reduction should also result from increased sensitivity. Sensitivity improvements will mean a reduced requirement for sample and hence less energy will be required to collect the sample. Given the low concentrations of some agents at a level that poses a threat, then the collection of BWA will require the processing of large quantities of air. Reducing the power consumption of the collection system will be a significant challenge for future BWA detection systems.

ION MOBILITY SPECTROMETRY – PAST, PRESENT AND FUTURE

Alan Brittain and *John Brokenshire*

Graseby Dynamics Ltd.

Watford, Herts. WD23 2BW, U.K.

Introduction

The future requirements for chemical and biological (CB) agent detectors, encompass the needs of both the military and civilian authorities, and include times of conflict, the performance of peace keeping roles, the occurrence of civil emergencies and acts of terrorism. In view of this widely expanding range of possible roles, the performance characteristics of detection equipment have to keep pace. The requirement is typically to detect a range of CB agents under a wide range of environmental conditions, in the presence of materials which could induce either false positive or false negative responses. As a result of the need to provide a greater detection capability over a wider base, the need for personal and integrated detectors has rapidly expanded. The goal is to provide these enhanced performance characteristics within detection suites, which can be simply adapted to meet the full range of operating requirements.

Existing Detectors

Typical military chemical warfare agent detectors are illustrated in Figure 1. These include the Chemical Agent Monitor (CAM™), a handheld, real time monitor which is used once the presence of chemical agents has been confirmed. It determines the presence and vapour hazard level of selected agents, the effectiveness of decontamination procedures, the safety margins for relaxation of protective measures, and locates areas free from agent contamination. ACADA is a more sophisticated version of CAM™, which is primarily for use in vehicles by mobile infantry, but can be dismounted and used as a man-portable detector or deployed upwind to provide early warning of the presence of chemical agents. The GID-2A detector is a fixed installation detector for ships, and is used to monitor the outside environment, or to monitor the inside of the ship's citadel, once it has been closed down following the detection of chemical agents.

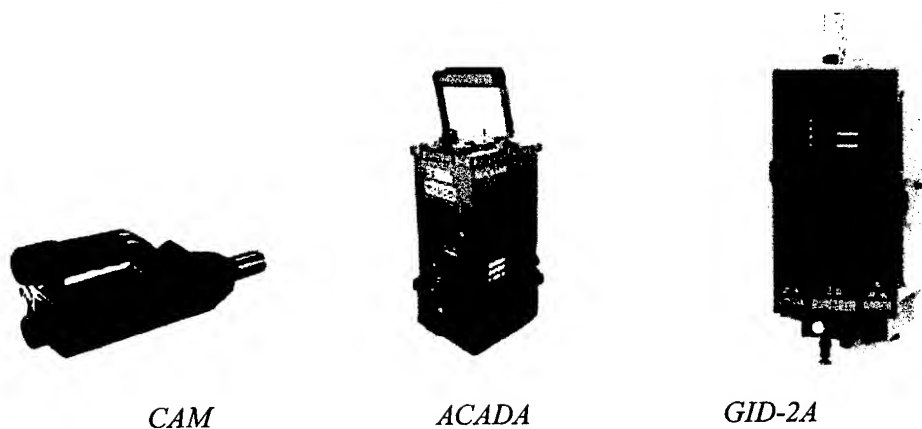


Figure 1 Militarised CWA Detectors

Detectors of this type are typical of the current range of chemical agent detectors deployed by many armed services worldwide. There are tens of thousands of CAMs, thousands of GID-3s and hundreds of GID-2As in service with many different countries around the world. All of these detectors use the same detection principle – namely ion mobility spectrometry, and this detection technique will be used as a benchmark to illustrate the challenges in meeting future requirements.

Ion Mobility Spectrometry

In ion mobility spectrometry, ion clusters formed by fast ion-molecule reactions are subjected to time-of-flight measurements at atmospheric pressure. Analysis of the resultant mobility spectrum is used to determine the identity and concentration of materials present in the sample. A typical configuration is shown in Figure 2.

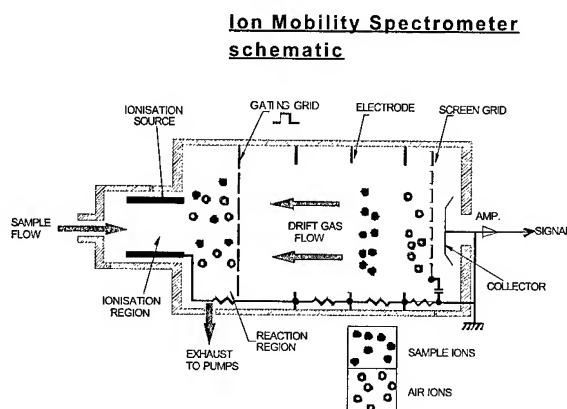


Figure 2 IMS Detector Schematic

In order to achieve the levels of performance necessary, the detector has to be operated in clean, dry air, and this is often achieved by recirculating air through drying agents using a pump. Sample is then introduced into the device through a semi-permeable membrane, which preferentially transmits many materials of interest compared with water, effectively transferring the sample to a dry air environment. Ionisation is traditionally carried out using a beta emitter such as ^{63}Ni , which results in the very fast formation of ion-molecule clusters. These clusters are acted upon by an applied longitudinal electric field which drives the ions towards a shutter grid. By electrically pulsing the grid, it can be either 'open' or 'closed'; in the 'open' configuration it is electrically transparent, and ions can pass through. By repetitively pulsing the grid, packets of ions are allowed to pass through, and then drift towards a collector electrode under the influence of the longitudinal field. The time of arrival of a particular ion species is determined by its shape and mass. Because the device is at atmospheric pressure, collision phenomena dictate performance, and unlike mass spectrometry, it is the shape which has the greater influence. In addition there is far less fragmentation than in mass spectrometry, and hence much less detailed information concerning chemical structure. A typical mobility spectrum is shown in Figure 3.

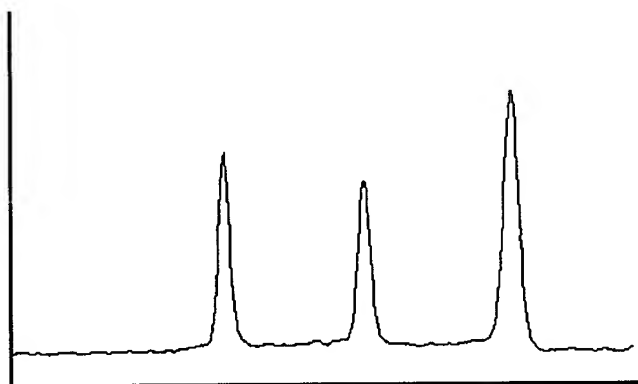


Figure 3 Positive ion mobility spectrum

The mobility spectrum, which is typically generated in 20 milliseconds, is averaged to improve the signal to noise ratio. Approximately once per second the averaged spectrum is subjected to peak measuring routines, and resident software used to determine the appropriate hazard level, which is then displayed.

There are various possible configurations of ion mobility spectrometers. Materials may produce ion-molecule clusters which are either positively or negatively charged; most nerve agents produce positively charged ions because of their high proton affinity, whereas blister agents produce negatively charged ions due to their high electron affinity. CAM is a single mode ion mobility spectrometer, and in its original configuration would be used in one mode and then manually switched to the other mode. More recent versions can automatically perform rapid switching, giving the impression of working in both modes simultaneously. In addition, variable averaging within the detection cycle enables fast alarms at high concentrations, while lower concentrations may be monitored with slower alarms. ACADA has two completely independent spectrometers including ionisation sources, and detects both positive and negative ions simultaneously. GID-2A has two mobility spectrometers in tandem with a single ionisation source to perform simultaneous detection.

Where Next?

The next generation of detectors must be capable of detecting more materials, with the ability to select individual or groups of materials by the operator. In some applications lower levels of detection may be necessary, such as miosis levels for selected nerve agents. The drive towards zero false alarms almost inevitably means the use of multiple detection techniques or arrays of detectors utilising the same detection principle. The simultaneous detection of both chemical and biological materials may necessitate different sampling techniques. The combination of these requirements with economic realities, determine that the drive will be towards miniaturisation of detection techniques coupled with the extraction of the maximum amount of information from every element of the detection suite. In addition to all this is the need to link every single detector to a central database to enable mapping and threat prediction to be undertaken.

How does IMS need to develop?

The drive to miniaturisation means that the major performance characteristics need to be critically examined to determine the extent to which miniaturisation is possible, while at the same time enhancing performance characteristics wherever possible. The three major performance features are sensitivity, response and recovery characteristics, and selectivity. Each of these factors needs to be considered in detail.

Sensitivity: Since IMS is primarily an ionisation detection method, sensitivity is determined by the amount of sample, and the efficiencies of ionisation and ion collection. Traditionally IMS devices use semi permeable membranes for sample introduction, and although they achieve the desired effect of sample transfer to a dry medium there are drawbacks. There is an attenuation factor – only a small proportion of sample is transferred; the temperature is important - higher temperatures favour rapid transfer (fast response and recovery) characteristics, while lower temperatures favour amount of transfer (increased sensitivity). Because of the need to heat the membrane there is a power burden. The use of increased averaging allows miosis level detection with increased response time. Sample size may be increased by the use of direct inlet systems, but there is a penalty in the rate of desiccant consumption. Ionisation efficiency is limited in the case of ^{63}Ni sources, partly by self absorption, where increasing the level of activity beyond a certain point does not result in an increase in the population of ions. Radioactive sources are unlikely to be acceptable in detectors used for the personal monitoring role, but they have the advantage of being self-sustaining, requiring no power input and having long life, and high reliability. Alternative ionisation sources may provide greater ionisation efficiencies and be more acceptable, but need power, are lifed and therefore carry a logistic burden. Once ions have been formed, in order to maximise sensitivity, it is necessary to produce mobility peaks with maximum amplitude. This means that the device needs to transport ion clusters through the drift tube as rapidly as possible to avoid diffusion effects, whilst at the same time avoiding space charge effects which lead to inevitable peak broadening.

Response and Recovery: In IMS devices the ionisation processes are essentially instantaneous, and the response and recovery characteristics are therefore determined by the efficiency with which sample is introduced to and removed from the detector. As previously mentioned, the performance of membrane inlets is a compromise between sensitivity and speed of response and recovery. The rate of transfer is determined by the thickness of the membrane and its temperature. The effect of thickness is a square dependency - in order to halve the lag time the thickness has to be decreased by a factor of four. There is a limit to how thin membranes can reliably be made without pinholing or becoming vulnerable to sudden pressure changes. The use of direct inlet systems overcomes these difficulties and removes the power burden. Response times below 250 milliseconds are practically achievable, which are useful for fast moving platforms such as UAVs. The efficiency of sample introduction and removal is one of design and material choice. The goal is to find a solution which obviates the need to supply heat, thus removing a power burden - which is not easy in view of the high surface affinity of some of the less volatile chemical agents.

Selectivity: In IMS devices, selectivity is determined by a number of factors. The chemistry within the ionisation region determines the ion-molecule reactions which take place. This chemistry can be controlled by deliberately introducing materials called dopants, which can suppress or enhance specific reactions thereby directly affecting selectivity. The use of dopants requires a method of generating and control, which again affects miniaturisation. Resolution within the device is governed by the 'sharpness' of the peaks within the mobility spectrum, and this is to a large extent determined by the voltages applied to the drift tube. This is again a square relationship and to double the resolution requires the applied voltage to increase by a factor of four. Since the field strength has to remain constant, the length of the drift tube has to increase by a factor

of four, and this means that the drift times increase by a factor of four. Practically only limited improvements in resolution are possible when miniaturisation is considered. The final factor which can improve selectivity is the signal processing, which incorporates algorithms to separate the desired responses from the background. There are numerous techniques for improving the sophistication of signal processing. Recently it has been suggested that mobility spectra carry more structural information than previously thought, suggesting that improved selectivity may be possible with additional processing.

Inevitably there are limits and compromises to what can be achieved in terms of sensitivity, response and recovery, and selectivity characteristics. Where it is not possible to achieve the desired performance, then hyphenated techniques have to be considered involving the use of preconcentration and preseparation techniques. Although considerable work is being conducted in this area, such devices are not yet compatible with miniaturised detectors for personal use.

Summary of Requirements

Detectors must meet the requirements of the Joint Services, including the Army, Navy, Air Force and Marines, as well as the Civil Authorities including Fire Services, Police and Civil Defence, under all conditions that these organisations may face. Materials to be detected include CB agents, environmental industrial hazards (EIHs) and toxic industrial chemicals (TICs). It must be possible to easily select individual substances or groups of materials for detection, while maintaining acceptable levels of false positive and negative responses. In general the Civil requirements for interference rejection are more demanding than those of the military. Detectors must have low life cycle costs, since it is now generally recognised that it is not the initial purchase price of detectors which determines their affordability. It must be possible to configure detectors for the personal detection role, which means that they must be capable of being carried or worn by individuals without degradation of their operational role. Additionally it must be possible to adapt detectors to operate on and integrate with a range of platforms, including unattended vehicles. Other features, which are desirable but not necessarily mandatory, are the ability to log data for post incident analysis, and to provide individual substance identification, even when monitoring groups of materials.

Comments on Performance Specifications

Detection: Usually the detection requirements are spelled out as a list of materials which must be detected, the sensitivity required, and the minimum response and recovery characteristics at various levels. As the list of materials gets longer the possibility of false alarms (positive and negative) increases, since the requirement is leading towards producing a near universal detector with almost complete selectivity.

Environmental: The conditions under which the detectors must operate is defined in a whole raft of requirements. These include high temperature - high humidity, low temperature - low humidity, blowing rain, sand, dust and fine mist. The ability to withstand immersion, shock and vibration, exposure to nuclear and electromagnetic effects, both high and low air pressures are also required features. Over-specification can result in unnecessary compromises.

Other considerations: In addition to the detection and environmental requirements, there is the need to ensure that the detector is simple to operate and understand and can be maintained by unskilled operators, without the use of special tools, and as close to the operational situation as possible. There is also the need to utilise all available information to assess developing threat situations. This requires that all detectors be linked to a central control station, such that each detector can be interrogated on demand, by means of two way communication.

State of the Art Miniaturised CWA IMS Detectors

Figure 4 shows the latest IMS device for personal use, in which all of the factors highlighted previously have been considered in great detail. The features of this device are that it has a direct sample inlet system, with a dual-cell ion mobility detector operating from a single non-radioactive ionisation source, and has dopant controlled chemistry. It is capable of monitoring nerve, blister, blood and choking agents simultaneously, and displaying the hazard to the operator in real time. It is packaged to meet the full range of environmental requirements associated with military hardware. It has data ports which enable data to be transmitted for further analysis or archiving. Future versions will continue to enhance the performance characteristics and add further features.

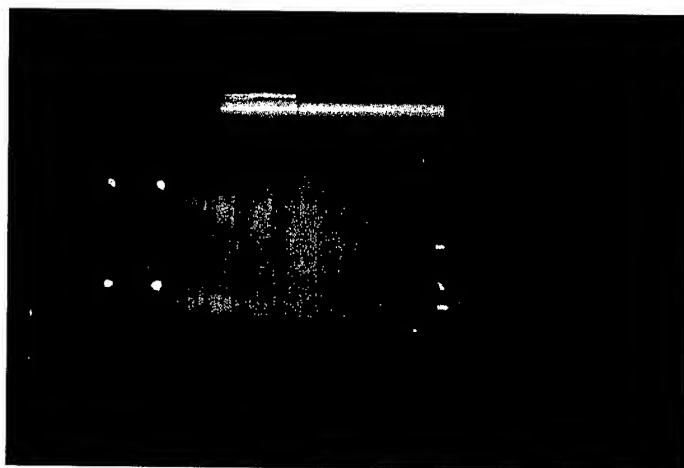


Figure 4 LCD2 Miniaturised IMS Detector

THE BLOCK II CHEMICAL BIOLOGICAL MASS SPECTROMETER – POINT DETECTION FOR BOTH CHEMICAL AND BIOLOGICAL WARFARE AGENTS

Wayne H. Griest, Marcus B. Wise, Kevin J. Hart and Stephen A. Lammert
Oak Ridge National Laboratory
Oak Ridge, TN

and

Alexander P. Hryniewicz and David W. Sickenberger
U.S. Army Soldier and Biological Chemical Command
Aberdeen Proving Ground, MD

ABSTRACT

The Block II Chemical Biological Mass Spectrometer (CBMS) is a new instrument for point detection that integrates the detection and identification of both chemical warfare (CW) and biological warfare (BW) agents into a single compact unit. It is based upon a direct-sampling ion trap mass spectrometer interfaced to three sampling systems and is operated in full scan and tandem mass spectrometry (MS/MS) using ethanol chemical ionization (CI) or electron ionization (EI) modes.

INTRODUCTION

The Block II CBMS is a new vehicle-borne point detection (as well as reconnaissance) instrument that integrates chemical and biological warfare agent detection and identification into a single unit that is lighter, smaller, and less power-intensive than separate detectors. The instrument is soldier-friendly in operation and self-diagnosing in fault location, and resists nuclear radiation, temperature extremes, vibration and shocks from wheeled vehicle transport. New capabilities of the Block II instrument compared to the Block I instrument include the ability to rapidly switch between chemical and biological agent detection via the mode valve, *in situ* derivatization of biomarkers, a direct capillary inlet, inclusion of CW vapor detection, a vacuum system equipped with a turbomolecular pump, an ion trap mass spectrometer capable of using chemical ionization, automatic switching between full scan and MS/MS scans and between EI and CI by novel multiscan functions (MSF) with broadband notches for multiple ion detection and confirmation.

INSTRUMENT

The Block II CBMS consists of four major modules – the Mass Spectrometer Module, the Sample Introduction Module (SIM), the Bioconcentrator Module and the Soldier Display Unit (SDU). Collectively, the four major modules occupy a volume of 5.8 ft³ and weigh ca. 170 lbs. Preliminary power figures indicate that the unit draws less than 500 Watts (average) of power under stabilized operating conditions. The following sections briefly describe the instrument. Greater detail is reported elsewhere¹.

Mass Spectrometer Module

The mass spectrometer module is divided into two halves that separately house the mass spectrometer assembly and the electronics card cage. The mass spectrometer assembly consists of an open-

split capillary interface, an ion trap mass analyzer, turbomolecular pump and diaphragm rough pumps, and a manifold for the CI reagent and mass calibration gas. The electronics card cage is based on a 6U compact-PCI (CPCI) chassis to minimize the amount of external wiring harnesses. The 6U chassis houses a computer board that contains the CPU for low level instrument control (the Low Level Controller or LLC). Three additional 6U circuit card assemblies incorporate the broadband arbitrary waveform generator (including the high voltage rf control circuitry), the multifunction interface board (containing the temperature measurement subsystem, the RF-ramp generator, and much more of the general use analog and digital I/O circuitry), and the electrometer interface board (containing the control circuits for the ion-source lenses and filament, and related analog interface circuits).

Sample Introduction Module

The SIM module contains the hardware components for selecting one of the three sample introduction lines. These sample paths are controlled using a micro-electric multiposition valve actuator and 4-position valve (Valco Instruments Co., Inc, Houston, TX), referred to as the mode select valve, that allows one of the three sample inlets to be switched to the inlet of the open-split capillary vacuum interface. The three agent sample paths are described below. The SIM also houses the pyrolyzer.

Chem Ground Line: The Fox reconnaissance vehicle uses a pair of silicone wheels to alternately sample the ground surface for liquid CW agents and transport any adhering or adsorbed material to a heated desorption probe head mounted on the ground probe, which extends to the outside of the vehicle hull. The desorbed material is transported via a 2-meter heated capillary transfer line to the analysis instrument, which, in the case of the Fox vehicle, is currently a Bruker MM-1 Quadrupole Mass Spectrometer. The Block II design takes the effluent from the existing heated transfer line and directs the flow into the 4-port mode select valve and, when selected, to the CBMS Block II open-split vacuum interface.

Chem Air Line: A heated 1/16" Silicosteel™ (Restek Corp., Bellefonte, PA) line provides an interface with a port in reconnaissance vehicles to sample the outside air for CW agents at a rate up to ca. 100 mL/min. Results of a study comparing different materials for transfer lines indicates that the Silicosteel™ lines are particularly well suited for air sampling because these lines were found to be less adsorptive than Nylon™, polyethylene and Teflon™ lines and provide an opportunity to be resistively heated². As is the case for the other agent inlets, effluent from this line can be routed by the mode select valve to the open-split vacuum interface.

Bioconcentrator/Pyrolyzer: The Block II CBMS monitors for BW agents using an opposed jet virtual impactor particle concentrator and pyrolysis mass spectrometry. The bioconcentrator (MSP Corp., Minneapolis, MN) draws 330 L/min of air. A scalper with a 10 µm particle diameter cut point passes 300 L/min to the opposed jet virtual impactor stages and discards all particles with effective aerodynamic particle diameters greater than 10 µm to a venturi exhaust line coupled with the main pump exhaust. A two-stage opposed jet virtual impactor subsequently reduces the flow rate from 300 L/min to 1 L/min while retaining between 50% to 95% of all particle aerodynamic diameters between 2 µm and 10 µm. The improved efficiency for particle transmission is due in part to the opposed jet impactor design developed by MSP. The 1 L/min flow from the Biosampler is then transferred to a quartz pyrolysis tube in the Sample Interface Module where the particles are deposited. After a sampling period of 2 minutes or longer, the flow from the Bioconcentrator is terminated to allow initiation of the pyrolysis cycle.

Toward the end of the biocollection, the pyrolyzer body heater is engaged to heat the pyrolyzer body to ca. 250 °C. This step requires approximately 1 minute to complete so it is important to begin this step

prior to the completion of the collection of the sample to maintain a ca. 4 minute duty cycle for the bio monitoring mode. The temperature of the pyrolyzer body is then maintained at the elevated temperature until the end of the data acquisition (ca. 60 s). The temperature inside the pyrolysis tube is only raised ca. 20-30 °C when the pyrolyzer body is heated to 250°C. The particles in the pyrolysis tube are then treated *in situ* with ca. 1-2 uL of 0.015 – 0.03 M tetramethylammonium hydroxide (TMAH) or tetrabutylammonium hydroxide (TBAH) using a newly designed automated injector. The pyrolysis tube is then ballistically heated to ca. 550 °C over 14-18 s where the polar components of the sample (e.g. the bacterial fatty acids) are derivatized using the reagent. The resulting derivatized pyrolysis products are then continuously transported via heated 1/16" Silicosteel™ lines through the mode select valve to the inlet of the open-split capillary vacuum interface. A pump establishes a flow of ca. 1.3 mL/min from the pyrolyzer tube to the open-split interface when in the Bio Mode. A more typical flow rate of 10 mL/min has been used for the Chem Air and Chem Ground Modes. Data acquisition begins at the start of the pyrolysis cycle.

Software and Soldier Display Unit

In addition to the Low Level Controller, another CPU running Microsoft Windows NT Workstation 4.0 is dedicated to high level control of experimental design and data analysis software (High Level Controller – HLC). Communication between the two CPUs is accomplished using a TCP/IP ethernet connection. There are two options for the HLC. One option uses a ruggedized notebook computer running a full standard release of Windows NT and an expert level user interface. The second option uses an embedded version of Windows NT (Microsoft Windows NT Embedded) running on a Soldier Display Unit described below.

The expert level software is much more flexible for research and development purposes and includes a "research grade" scan function editor (SFE) interface. The SFE provides controls for instrument settings and allows the user to control the timing of signals to the ion trap electrodes (i.e. a scan function). The SFE also has the ability to display mass spectra, total ion profile and selected mass profile graphs during data acquisition. An additional tool has also been developed to provide offline analysis of data including the display and background subtraction of mass spectra, total ion profiles and selected mass profiles from data that are saved in either the same datafile or in different datafiles (separate runs). There are also options to automate instrument response calibration and quantitation. The work described in this paper was pursued using the expert user software.

The Soldier Display software is intended for end users with little or no knowledge of ion trap mass spectrometry and is being programmed using an instrument control language tailored to the Block II CBMS design. The Block II CBMS operator interface, referred to as the Soldier Display Unit (SDU), consists of the HLC single board computer and a gas plasma display in a box approximately 12" W X 7.5" H X 4.25" D. The SDU uses a gas plasma display because of the extreme, low temperature range specification. Mass storage includes several solid state devices to provide this ruggedized design and includes a 40 MB IDE compatible flash drive for the operating system, a removable 40 MB PC Card for the application software and a removable 4 MB PC Card for a mission log. PC Cards were utilized to allow rapid software upgrades and to provide a removable mission log. The front panel of the SDU has a bank of LEDs that show instrument status and configuration information in the upper left quadrant. There are three user-input buttons on the right side of the plasma display that allow the user to interact with the CBMS in a manner similar to an automatic teller machine. The modes of operation are selected using these buttons. On the bottom of the SDU is a row of buttons that select the pages that are displayed to the user (e.g. the alarm page, the configuration page, etc.). The SDU software engages an audio and visual alarm, displays a message on the alarm page of the SDU that consists of the inlet source (i.e. BIO mode), the agent (i.e. BG), the agent

classification (i.e. bacteria) and a scaled bar graph that denotes relative intensity and sends a report message via a serial line.

PERFORMANCE

Bio/Air Mode

Ethanol CI in both full scan and MS/MS modes was selected to provide maximum selectivity and sensitivity to BW (as well as CW) agents in the presence of common battlefield interferents such as diesel engine exhaust and fuel. The ability of CI to minimize interferents in full scan MS is illustrated by comparison of the EI and CI full scan spectra shown in Figure 1. Raw diesel engine exhaust from an old bus with a "dirty" 7 L diesel engine was sampled directly into the bioconcentrator of a Block II CBMS operated in EI or CI modes. A considerable reduction in the diesel exhaust signal is apparent in the CI mode versus the EI mode. For comparison with an agent spectrum, a full scan CI spectrum (TMAH derivatization) in Figure 2(A) shows the full scan CI spectrum of an aerosol of Gram negative organisms at about 31 agent-containing particles (3.2 μm aerodynamic diameter) per L of air. Biomarkers ranging from the 10:0 to 24:0 acids are readily visualized, and even lower aerosol concentrations could be detected. Figure 2(B) shows the spectrum of a 200 ng sample of a crude protein preparation introduced by direct liquid injection. Ions from an important biomarker are labeled.

Earlier biomarker work^{3,4} focused on fatty acid methyl esters produced by TMAH derivatization, but the very low intensities of unique fragment MS/MS product ions of fatty acid biomarkers severely limited CI MS/MS sensitivity to about 1% of the full scan CI. In addition, the methyl esters of unsaturated and cyclic fatty acids also fragment severely in full scan CI, as shown in Figure 2(B). Comparison of different esters identified the butyl derivatives as having good full scan MS and MS/MS properties. The unique MS/MS fragment ions are 10 to 70% as intense as their precursors, and the TBAH is being considered as a drop-in replacement for the TMAH. The full scan CI spectrum of TBAH-derivatized Gram negative organisms in Figure 3 (A) shows the expected 10:0 through 24:0. In Figure 3(B), the MS/MS spectrum of the protonated molecular ion of the 22:0 fatty acid (m/z 397) illustrates the two intense diagnostic product ions and the clean MS/MS spectrum. Higher line temperatures were required to transmit the heavier fatty acid butyl esters. Spectral libraries of the target BW agents are now being collected.

Chem/air Mode

The second operational mode of the Block II CBMS provides a means to monitor air for the presence of CW agent vapors via a heated Silicosteel® line. The line is typically heated to 180°C. A solution of a simulant, dimethylmethyl phosphonate, was injected on the tip of the Chem/Air line to demonstrate a typical instrument response. The extracted mass profile for the protonated molecular ion of DMMP (m/z 125) is shown in Figure 4(A). Three blank injections of methanol were followed by 3 injections of 10 ng and 50 ng of DMMP dissolved in methanol. Another test was performed using methyl salicylate (MS) diluted in a Tedlar bag at concentrations of 0.01 and 0.1 mg/m^3 . The mass profile obtained while the Tedlar bag was attached to the Chem/Air line is shown in Figure 4(B). The protonated molecular ion of MS at m/z 153 is clearly discernable at this level.

Chem/Ground Mode

Considerable work has been devoted to evaluating the detection of CW agent liquids sampled using the laboratory version of the ground probe. The data illustrate the selectivity which can be achieved for CW

agent detection in the CI MS/MS mode of operation. Figure 5 shows mass profiles for tests using fog oil or no. 2 diesel fuel (DF2) with and without added agents GB or HD. Figure 5(A) shows the mass profile for m/z 99 (product ion from the protonated GB molecular ion of m/z 141) for 10 ug of fog oil (alone) and two runs of 120 ng of GB with 10 ug of fog oil. Figure 5(B) shows the mass profile for m/z 123 (product ion from the protonated HD molecular ion of m/z 159) for 10 ug of DF2 (alone) and then two runs of 132 ng HD with 10 ug DF2. Both CW agents are easily detected in the presence of ca.100-fold mass excess of fog oil or DF2, and there is very little or no ion activity from the interferents. This indicates the ability of CI MS/MS to minimize false negatives and positives. Even greater excesses of interferent can be tolerated, but a clear-out period is necessary before agent can be detected. Ten ng of MS have been detected within 2 min. of applying a road wheel dipped in DF2 to the lab probe head.

STATUS

Design and testing has been performed to ensure that the fielded instrument can survive temperature extremes and shock and vibrations from wheeled vehicle transport. The capability to survive radiation from a tactical nuclear event has been developed using specially selected components (where feasible) and custom-designed circumvention circuits. Tests have been performed at the White Sands Missile Range to confirm the radiation tolerance of critical components and subsystems⁵.

The Block II CBMS is undergoing tests with biological and chemical agents, and it participated in the JFT-6 trials at the Defense Research Establishment Suffield. It has been selected for trials on the JSLNBCRS HMMWV and LAV platforms and on the Block II FOX.

CONCLUSIONS

The development and preliminary testing of the Block II CBMS is being completed this year. Its sensitive and selective detection of BW and CW agents will provide improved protection to US and allied forces.

ACKNOWLEDGEMENTS

This research was sponsored by the U.S. Army Soldier and Biological Chemical Command, DOE No. 2182-K011-A1, U.S. Department of Energy under contract DE-AC05-00OR22725 with Oak Ridge National Laboratory, managed and operated by UT-Battelle LLC. The authors wish to acknowledge the CBMS Program Team in the development of the Block II: colleagues at ORNL for their design and testing of the instrument, MSP Corporation for their design of the biosampler, Colorado School of Mines for their work on identifying biomarkers and developing the reagent injector, and Orbital Sciences Corporation for their instrument design work and fabrication of preproduction units.

REFERENCES

1. K. J. Hart, M. B. Wise, W. H. Griest, and S. A. Lammert, "Design, Development and Performance of a Fieldable Chemical & Biological Agent Detector," *Field Analytical Chemistry and Technology*, 4 (22-3), 93-110 (2000).
2. C.V. Thompson, M.B. Wise and M.R. Guerin, "Effects of Transfer Line on MS Sampling and Analysis of VOC's in Air", *Proceedings of the 43rd ASMS Conference on Mass Spectrometry and Allied Topics*, Atlanta, GA, May 21-26, 1995, p. 831.

3. S.A. Barshick, D.A. Wolf and A.A. Vass, "Differentiation of Microorganisms Based on Pyrolysis-Ion Trap Mass Spectrometry Using Chemical Ionization", *Anal. Chem.*, 71, 633-641 (1999).
4. F. Basile, M.B. Beverly, C. Abbas-Hawks, C.D. Mowry, T.L. Hadfield and K.J. Voorhees, "Direct Mass Spectrometric Analysis of in Situ Thermally Hydrolyzed and Methylated Lipids from Whole Bacterial Cells", *Anal. Chem.*, 70, 1555-1562 (1998).
5. R. M. Brady, "Initial Nuclear Radiation (INR) Detailed Test Report for the First Article Test (FAT) on the Block II Chemical/Biological Mass Spectrometer Electronics Test Stands (Block II CBMS)," TECOM Project No. 8-CO-410-000-052, White Sands Missile Range, White Sands, NM (July, 1998), and following reports.

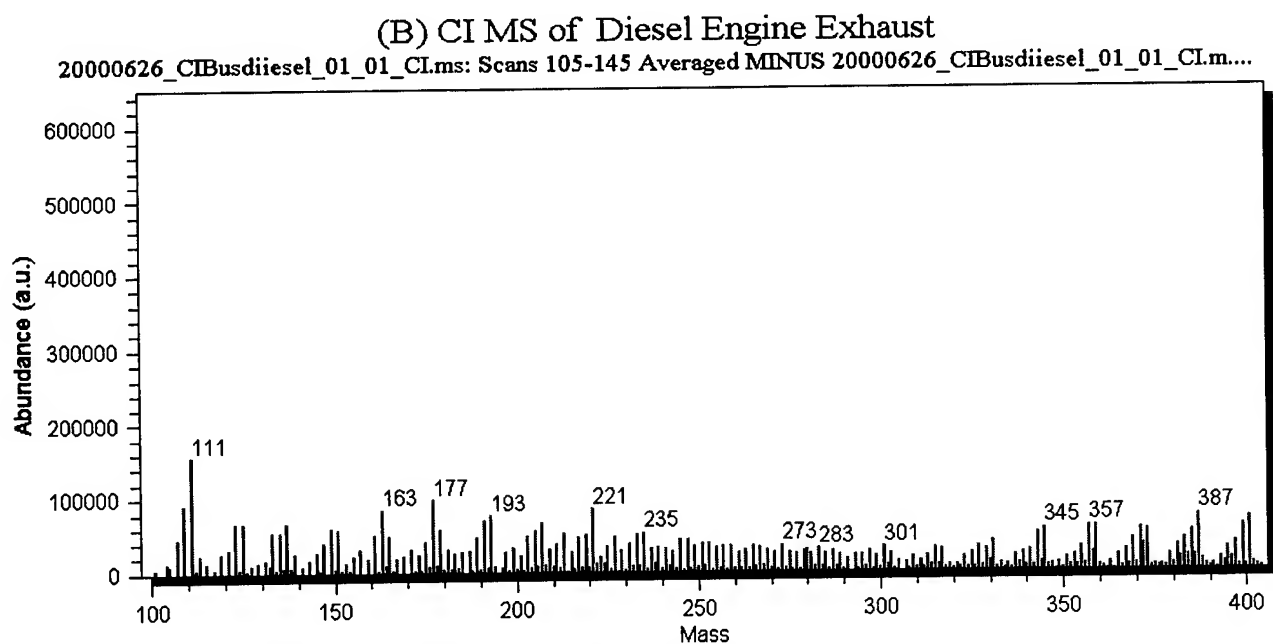
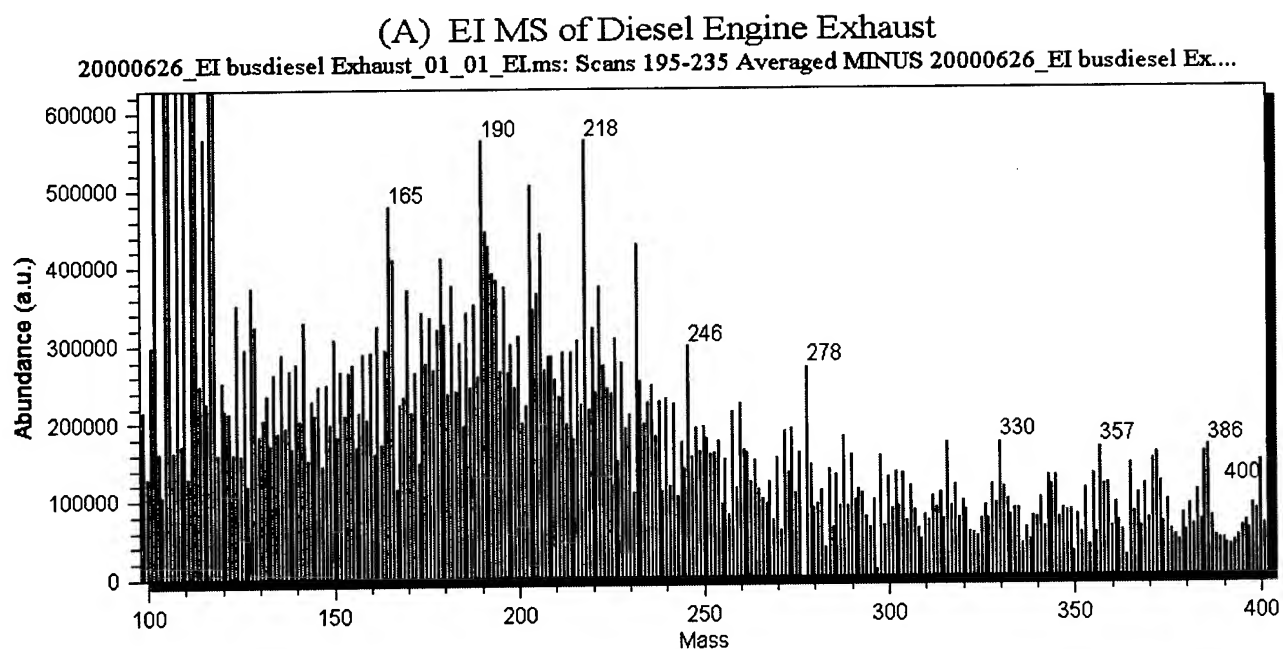
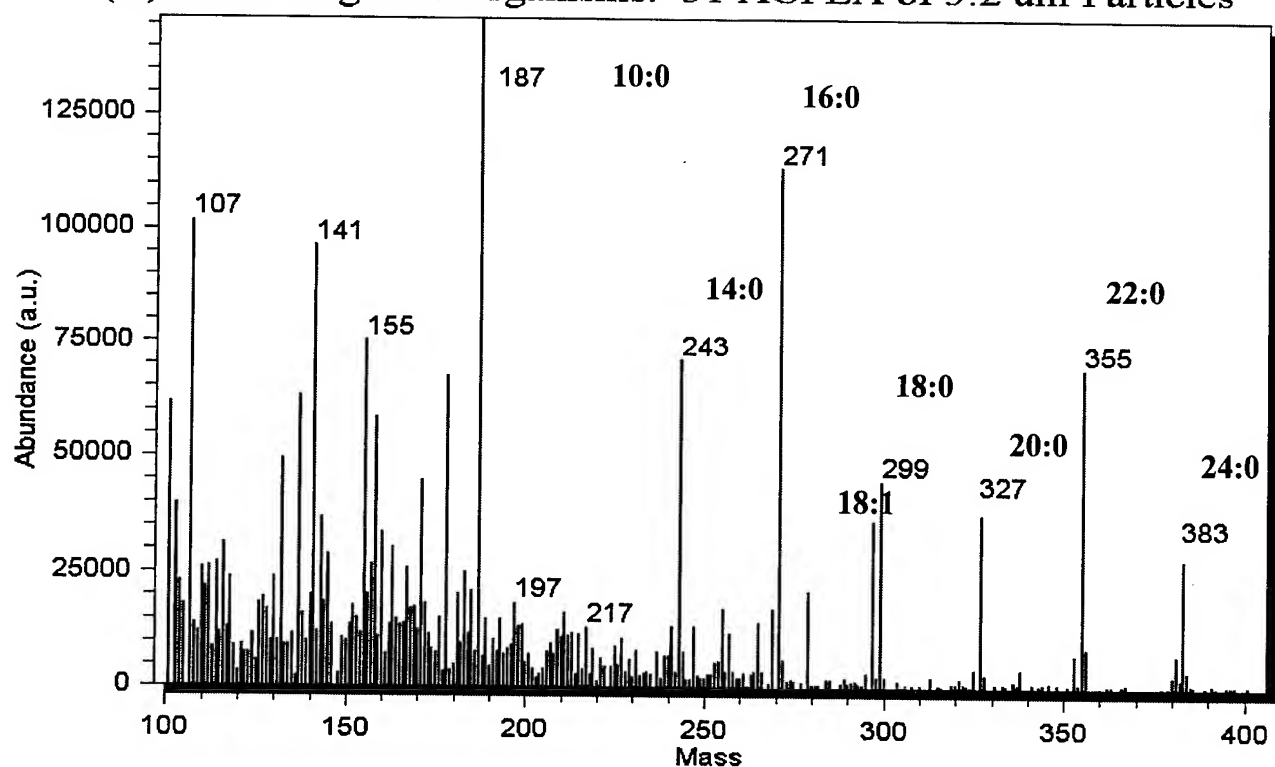


Figure 1. Comparison of EI and CI MS of diesel engine exhaust as TMAH derivatives.

(A) Gram Negative Organisms: 31 ACPLA of 3.2 μ m Particles



(B) Crude Protein Preparation, 200 ng Direct Injection

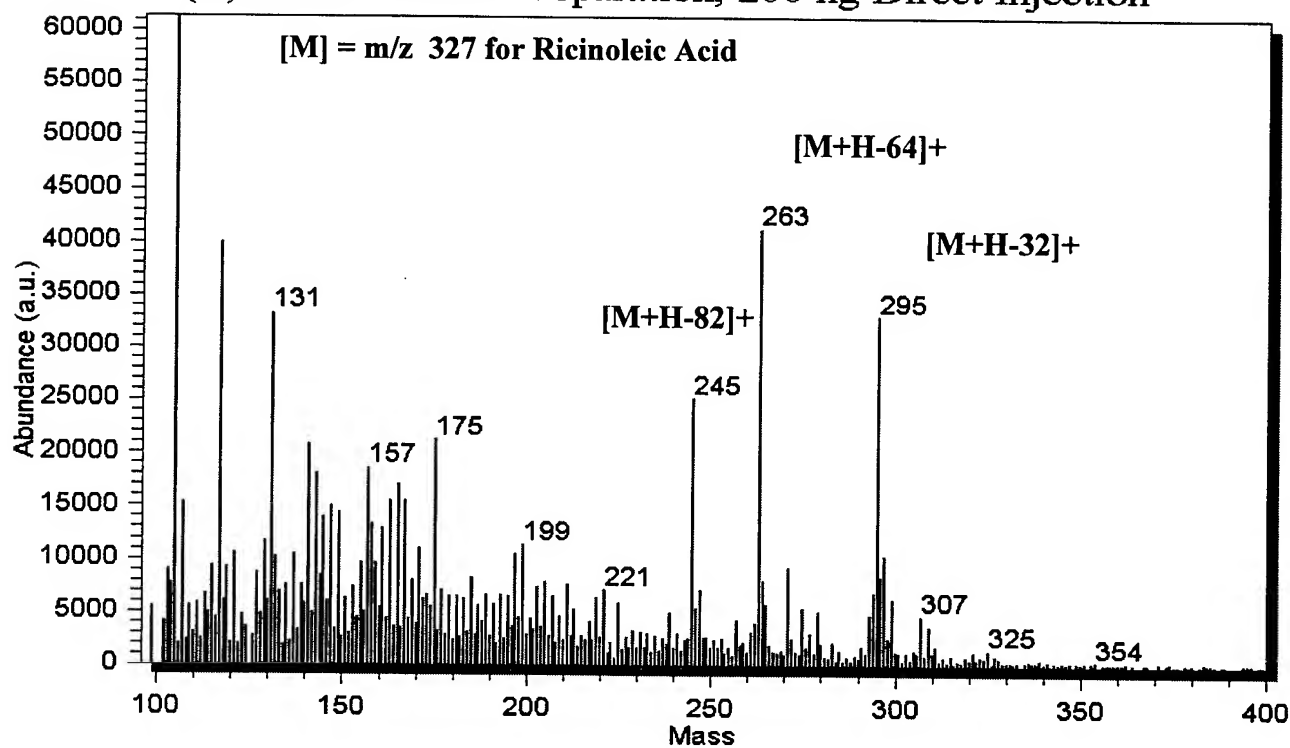


Figure 2. CI MS spectra of a bacterial aerosol and an injected crude protein as TMAH Derivatives.

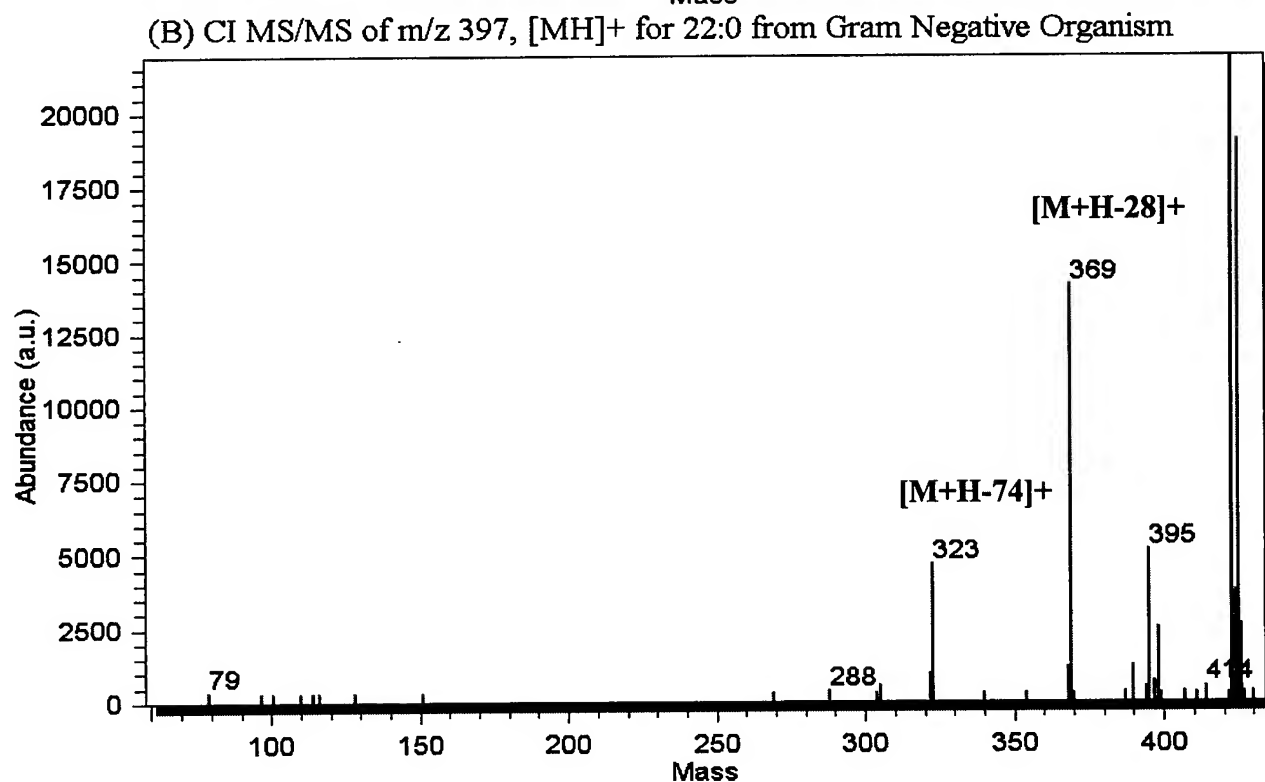
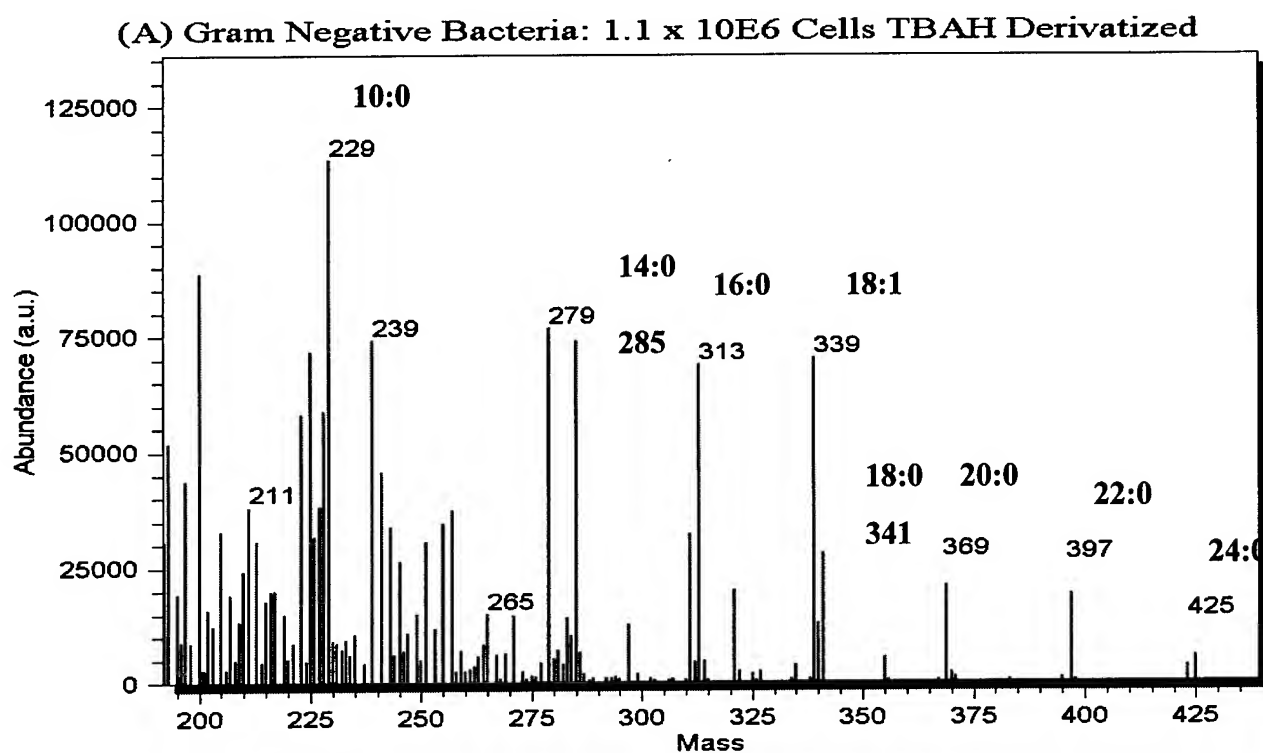
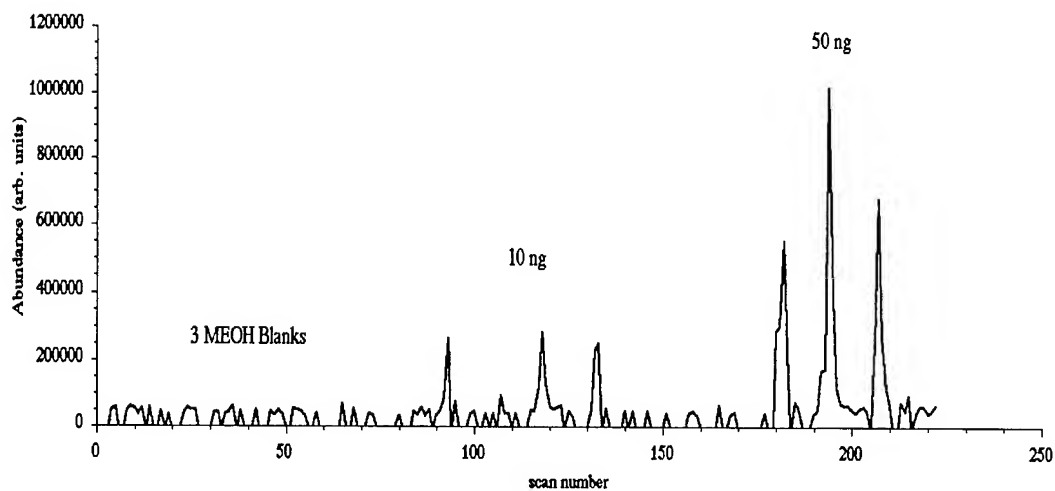


Figure 3. CI-MS of Gram Negative Bacteria and CI MS/MS of 22:0 fatty acid as TBAH derivatives.

(A) Mass profile (m/z 125) for injection of methanol, 3 x 10 ng and 3 x 50 ng of DMMP



(B) Mass profile (m/z 153) for MES vapors at 0.01 and 0.1 mg/m^3 from Tedlar bag

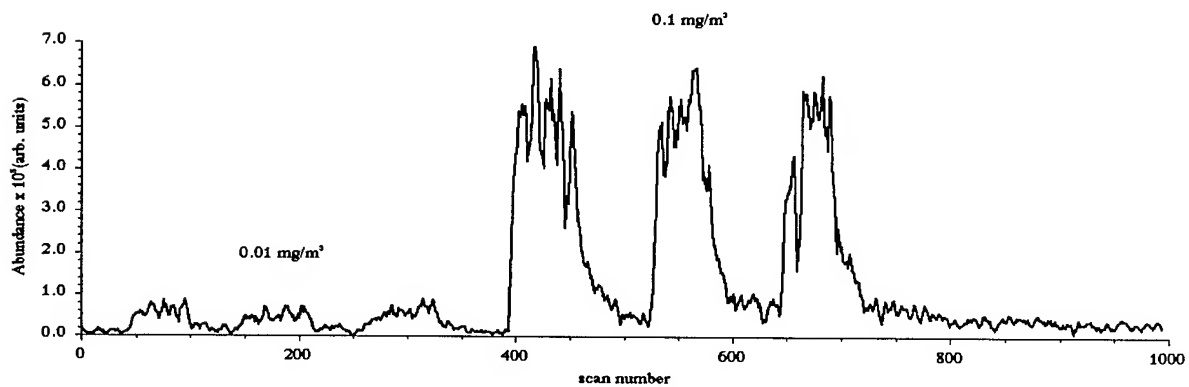
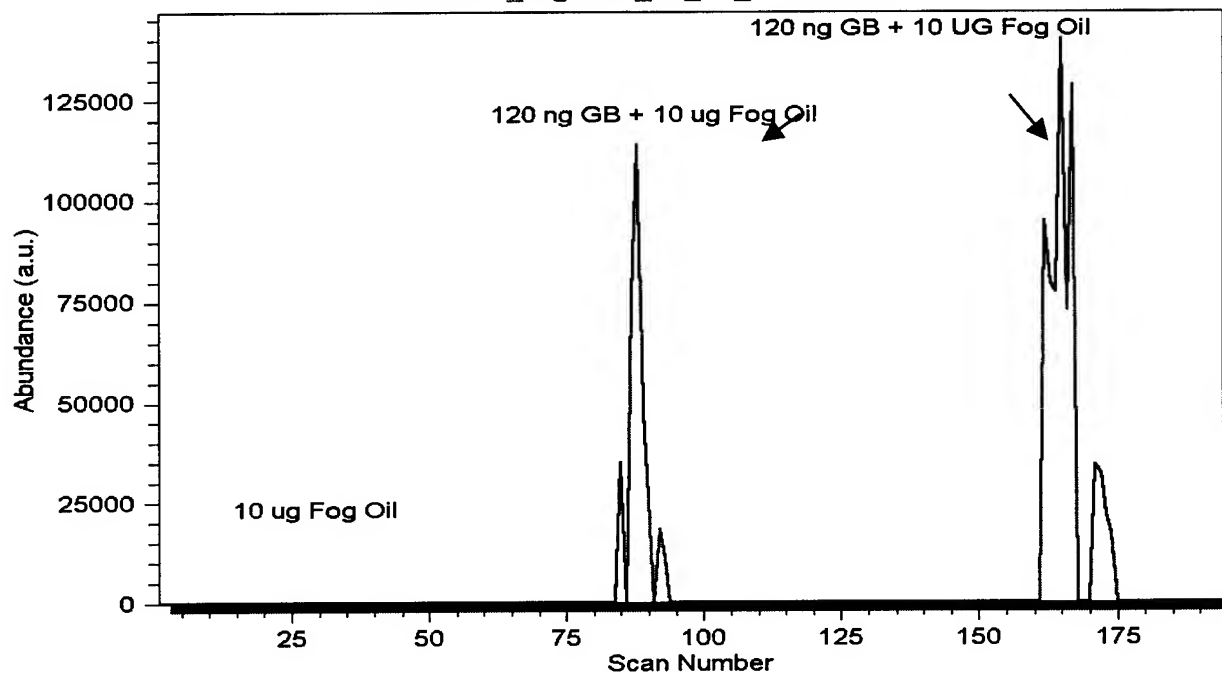


Figure 4. Simulant tests using Chem/Air sampling line and full scan CI MS mode.

(A) CI MS/MS (m/z 141 to 99) of Fog Oil and GB with Fog Oil
20000811_ccgb007_06_01_ci-msms/99



(B) CI MS/MS (m/z 159 to 123) of DF2 and HD with DF2
20000831_cchd009_03_01_ci-msms/123

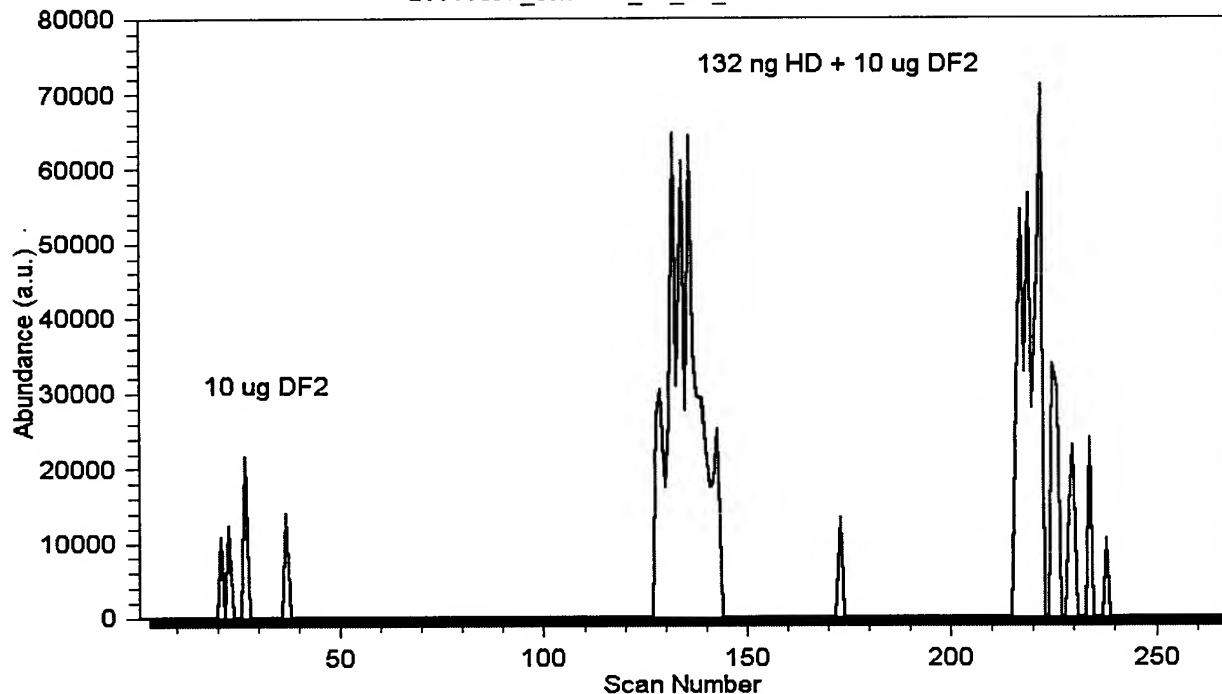


Figure 5. Mass profiles from CI MS/MS tests using GB, HD and battlefield interferents on lab probe.

POINT DETECTION CHEMISTRY AT THE U.S. ARMY RESEARCH OFFICE

Stephen J. Lee

U.S. Army Research Laboratory – Army Research Office
PO Box 12211, RTP, NC 27709

The U.S. Army Research Office (ARO) mission is to seed scientific and far reaching technological discoveries that enhance DoD capabilities. Basic research proposals from educational institutions, nonprofit organizations, and private industry are competitively selected and funded. The Army Research Office has a long-term research investment in the field of Chemical and Biological Defense. The chemistry program at ARO supports CBD research in the areas of microemulsions, catalysts, adsorbents, reactive fabrics and materials, solution chemistry, and reactive nanoparticles. In the field of detection the Army Research Office supports basic research in sensing of agents in water through Surface Enhanced Raman Spectroscopy research in collaboration with ECBC, enzyme-based detection technologies, and multifunctional detection and decontamination technologies.

The U.S. Army Research Office (ARO) mission is to seed scientific and far reaching technological discoveries that enhance DoD and Army capabilities. The Army Research Office has a long-term basic research investment in the field of detection and sensors.

The chemistry program at ARO supports Chemical and Biological Defense basic research in the areas of microemulsions, catalysts, adsorbents, reactive fabrics/coatings and polymeric materials, solution chemistry, reactive nanoparticles, and fuel cells.

In the field of detection the Army Research Office supports basic research in sensing of agents in water through Surface Enhanced Raman Spectroscopy research in collaboration with ECBC, enzyme-based detection technologies, and multifunctional detection and decontamination technologies.

Current detection research includes the following university programs:

- Testing a High-Sensitivity ATR-FTIR Water Monitor for Ionic CWA Breakdown Products - Steven Strauss, Colorado State University supported with help from the JSAWM program and ECBC.
- Prototype of On-Chip Signal Processing for Handheld Chemical Agent Sensors - Charles Ih, University of Delaware supported with help from ARL-WMRD
- Concept Studies of Micro-Pump for Chemical Concentration in Handheld Micro Sensors - Jian Sun, University of Delaware supported with help from ARL-WMRD
- Nanocomposite/Hybrid Materials of Electroactive Polymers with Inorganic Oxides for Biosensor Application - Yen Wei, Drexel University supported with help from ARL-WMRD.
- Novel SERS Substrates via Templated Assembly of Colloidal Particles - Abraham Lenhoff, University of Delaware
- Quantitative and Qualitative Determination of Organics in Water Using Electrospray Ionization Coupled with Ion Mobility Spectrometry - Herbert H. Hill, Washington State University
- Metallo-Nucleic Acid Sequences for Analyte Detection - Mark Grinstaff, Duke University
- Nanoworkbench for Analysis, Manipulation and Excitation of Individual Nanostructures - John Yates, Jr., University of Pittsburgh
- New Catalytic Molecules and Materials for Decontamination and Detection - Craig Hill, Emory University
- A Colorimetric Sensor Array for Odour Visualization - Kenneth S. Suslick, University of Illinois at Urbana-Champaign (ARO-Kiserow-MURI)

- Surface Chemistry of Enzymes for Detection and Decontamination of Organophosphorus Compounds - Roger Leblanc, University of Miami-Coral Gables
- Simultaneous Signaling and Decontamination of Chemical Agents - David Jaeger, University of Wyoming

Upcoming ARO supported workshops and conferences relevant to detection include:

- Enzyme 2001: International Symposium on Applications of Enzymes in Chemical and Biological Defense, May 13-18, 2001, Orlando, FL
- Gordon Research Conference on Chemical Sensors and Interfacial Design, May 2001, Il Ciocco, Barga, Italy, <http://www.grc.uri.edu/>
- International Workshop on Bioanalytical Sensors, Biochips, and Nanobiotechnology, December 12-15, 2001, Autrans, France, <http://www-chimie.ujf-grenoble.fr/LEOPR/congres/>

Basic research proposals from educational institutions, nonprofit organizations, and private industry are competitively selected and funded. Potential applicants are encouraged to review the ARO website (WWW.ARO.ARMY.MIL) and discuss ARO research with relevant program managers. In general the first step in application is to prepare a one to two page preproposal which clearly defines the goals of the research, contains some technical detail, level of support needed, and any special equipment requirements.

DEVELOPMENT OF A CORONA DISCHARGE SOURCE GENERATE IONS IN A CHEMICAL AGENT DETECTOR

Dr. George Lozos and Dr. Doug Green, PE
Environmental Technologies Group, Inc
1400 Taylor Ave
Baltimore, MD 21234

Dr. Rod Wilson
Graseby Dynamics Ltd.
Park Avenue, Bushey
Watford, WD2 2BW, UK

Currently most chemical agent detectors are based on Ion Mobility Spectrometry (IMS) which use a radioactive source to generate the reactant ions. These sources are subject to extensive regulatory controls for reasons of health and safety. The logistics burden becomes more significant when such detectors are used to protect a civilian population against terrorist activities. To alleviate this, effort is underway to replace the standard Ni⁶³ beta particle source with a non-radioactive corona discharge source. This paper describes the nature of corona discharge ionization, the physical electrodes, electronics needed to control the system and the ion chemistry involved. The critical end result is a consistent comparison of detected product ions generated with the new non-radioactive corona source and the old standard radioactive source.

1. Introduction

The Graseby developed CAM has for the last 15 years been the equipment of choice in most chemical agent monitoring scenarios. The CAM contains a small radioactive source. Equipment containing such sources can in many territories, particularly in the more civilian type applications, be the subject of exhaustive regulatory controls for reasons of health and safety. The logistics burden demanded by this fact is becoming far more significant for many users. This has lead to the development of a Non-radioactive Enhanced Chemical Agent Monitor (ECAM) using Graseby's dual point corona discharge technology as an alternative means of ionisation to a the standard Ni⁶³ beta particle source. A CAM system has been developed which retains the operational characteristics of the standard ECAM without the need for the radioactive source. This paper presents the details of the development and explains why the ECAM is considered the ideal framework on which to develop this system with demilitarisation applications in mind.

2. The Technology.

The detection technology most frequently associated with detection of CW agent is Ion Mobility Spectrometry. Ion Mobility Spectrometry (IMS) involves creating ions from the vapours of a target material and measuring the mobility of the ions at atmospheric pressure. On the early CAM developments with the UK MoD (Porton Down), back in the early 1980's, Graseby Dynamics Ltd (GDL) exploited this method to detect CW vapours at trace levels (low parts per billion). Since that time, GDL have developed a range of detectors based on IMS to become one of the leading experts in the application of this technology.

2.1 Principles of Ion Mobility Spectroscopy.

DRIFT TUBE

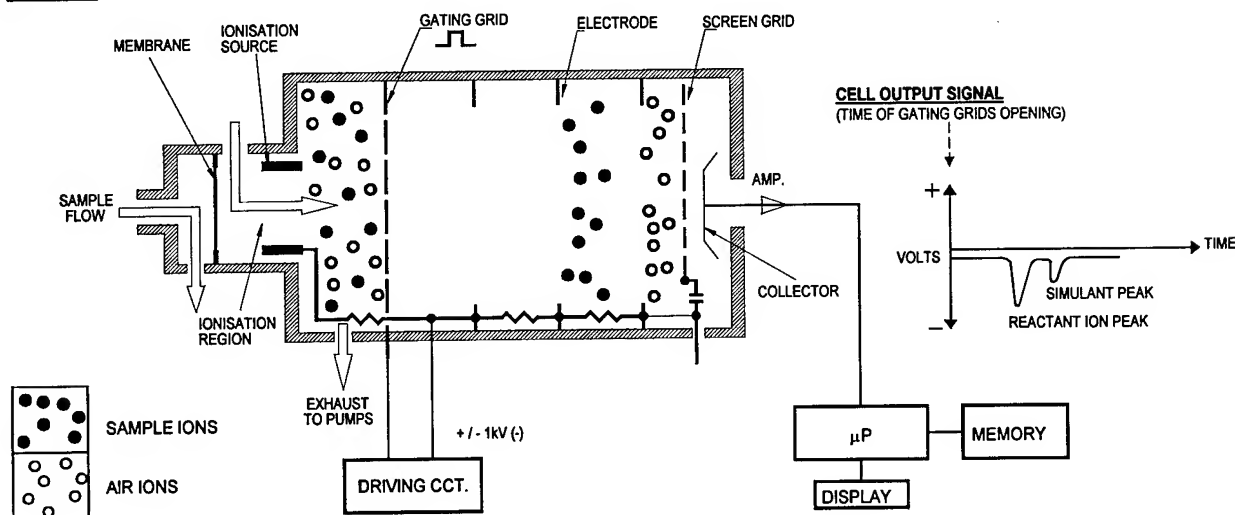


Figure 1. Schematic of Ion Mobility Spectroscopy.

An IMS detector is shown schematically in Figure 1. Ion species created via interactions with high energy electrons (positive ions) or thermal electrons (negative ions) move toward the ion gate under the influence of an extracting electric field. The gate allows a narrow pulse of ions to pass into the drift region, it typically opens for only a few 100 μ s.

In the drift region the sample ions move under the influence of the applied electric field. Due to the collisions between the sample ions and the drift gas molecules, separation takes place depending on the mobility of the sample ions. Ions with a higher mobility traverse the length of the drift region in a shorter time than ions with a lower mobility. The mobility of the ions will depend on their size, mass and shape and the resulting drift time are typically up to 20ms.

The performance of such systems depends on the ability of a particular material to form relatively stable, long lived ions with mobilities which are discrete from the normal ions produced by clean air. Experience has shown that only materials that have either very high proton or electron affinities can be reliably identified under these conditions. The standard target materials for the detection of CWA fall into these categories. For an IMS system to operate with a Non-radioactive source similar ions must be generated.

2.2 Ion Molecule Reactions.

2.2.1 Radioactive source based systems

Using a ^{63}Ni radioactive source in air, complex ion-molecule reactions lead to the formation of ion clusters with the predominant ions as illustrated. These ions are called reactant ions:

Positive Ions $[H^+. (N_2)_x. (H_2O)_y]$

Negative Ions $[(O_2)_a. (N_2)_x. (H_2O)_y]^-$

Monitoring the Collector Electrode allows the arrival of ions following pulsing of the shutter to be observed, resulting in the generation of the complete Ion Mobility Spectrum. Typical spectra for positive and negative ions are shown in Figure 2.

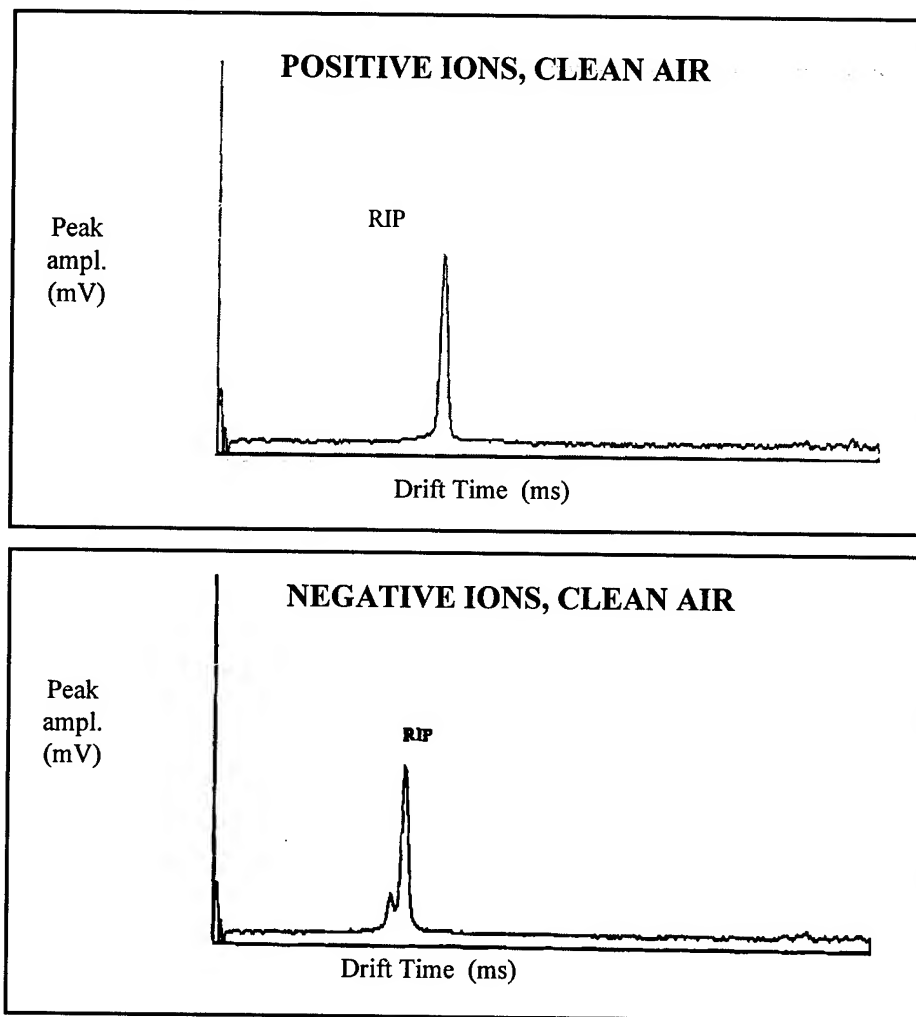
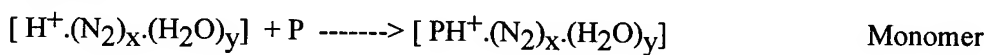


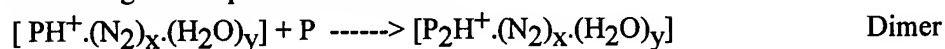
Figure 2. Typical Clean Air IMS Spectra.

The introduction of a material with a high proton or electron affinity into the Ionisation Region will result in the formation of product ions as illustrated:

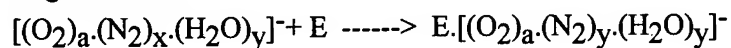
Positive Ions:



And at higher sample concentrations :



Negative Ions:



When these product ions are larger and more massive than the original reactant ions and therefore of lower mobility; this results in longer drift times as illustrated by Dipropyleneglycol-monomethylether (DPM) and Methyl salicylate (MS) in Figure 3

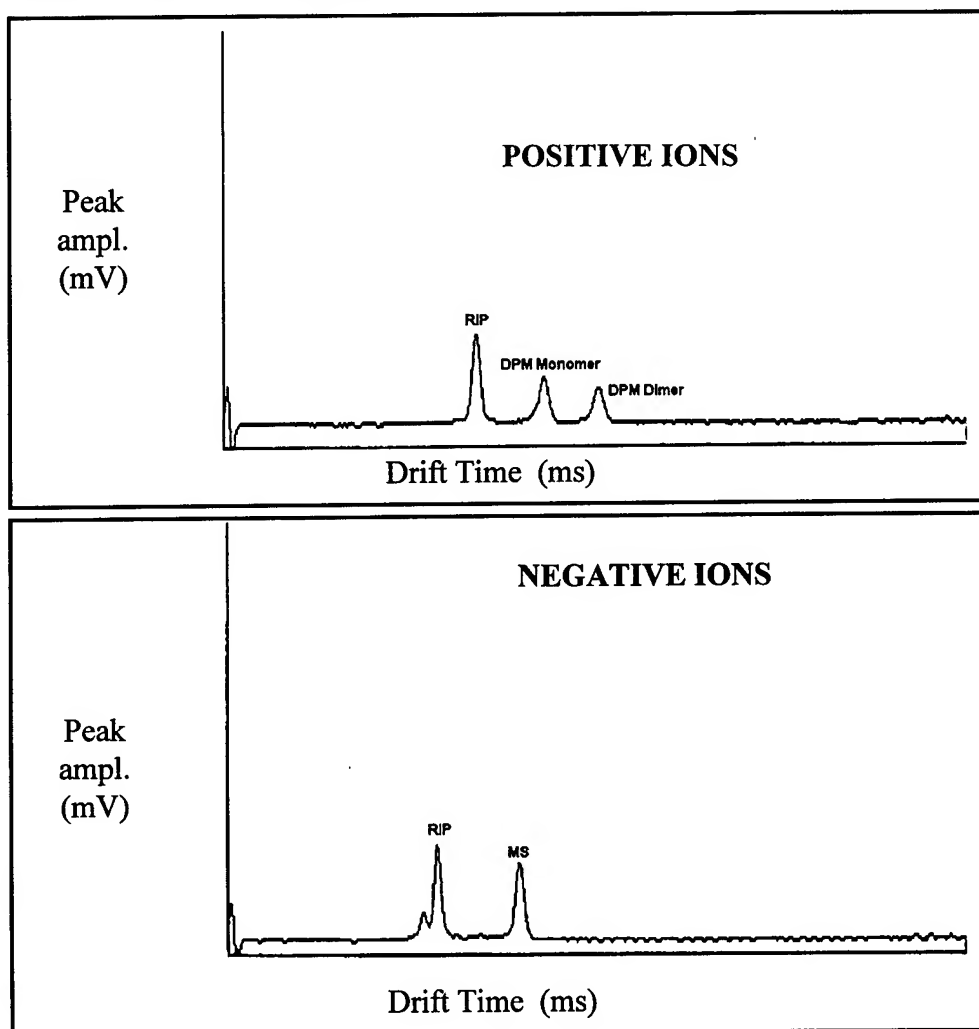


Figure 3. Typical Product Ion IMS Spectra.

The positive mode spectrum shows the formation of both protonated monomer and dimer ions. The negative mode spectrum shows the formation of a single adduct ion.

The performance of ion mobility detectors is primarily dependent upon the ion-molecule chemistry occurring in the ionisation region. It is therefore possible to modify this performance by controlling this

chemistry in order to suppress certain reactions or enhance others. The ion-molecule chemistry is best manipulated by the deliberate introduction of chemical modifiers (dopants) at controlled levels, which will either enhance certain ion-molecule reactions or suppress others as mentioned above. Virtually all successful fielded ion mobility spectrometers use dopants, for CAM the dopant used is acetone. Again for a Non-Rad CAM to operate as the standard CAM then the same dopant ion chemistry must apply.

2.2.2 The Corona Discharge Ionisation Source.

Until recent developments, the mechanisms of ionisation in the GDL CAM have been via interactions of air/dopant molecules with Beta particles from a Ni^{63} radioactive source (typically 10mC). In a corona discharge source the ions are created when a high voltage (typically 5keV) is applied to a fine wire point.

In the source developed by GDL (U.K. PAT. No. GB 2127212; U.S. PAT No. 5,162,652) this source takes the form of a dual point system, referred to as the primary and secondary points, where the secondary point is held permanently at a set voltage and the primary point is pulsed to a higher voltage.

The secondary point can be considered to be seeding charge into the ionisation region to stabilise the creation of the true corona that is created when the high voltage pulse is applied to the primary pulse.

In order to be able to use the corona discharge source in a similar way to the previous radioactive source, and carry the confidence in detection associated with the rad-sourced system across to the new corona discharge based system, it is essential that the same fundamental chemistry is involved in the creation of the target ions. This demands that the similar reactant ions are generated as for the radioactive system and similar product peaks created. Tests on corona based systems have shown this to be the case and live agent test support the basis that the same basic chemistry is associated with a corona discharge IMS system as with a rad-source based IMS system.

A typical spectrum from a corona-based IMS system is shown in figure 4.

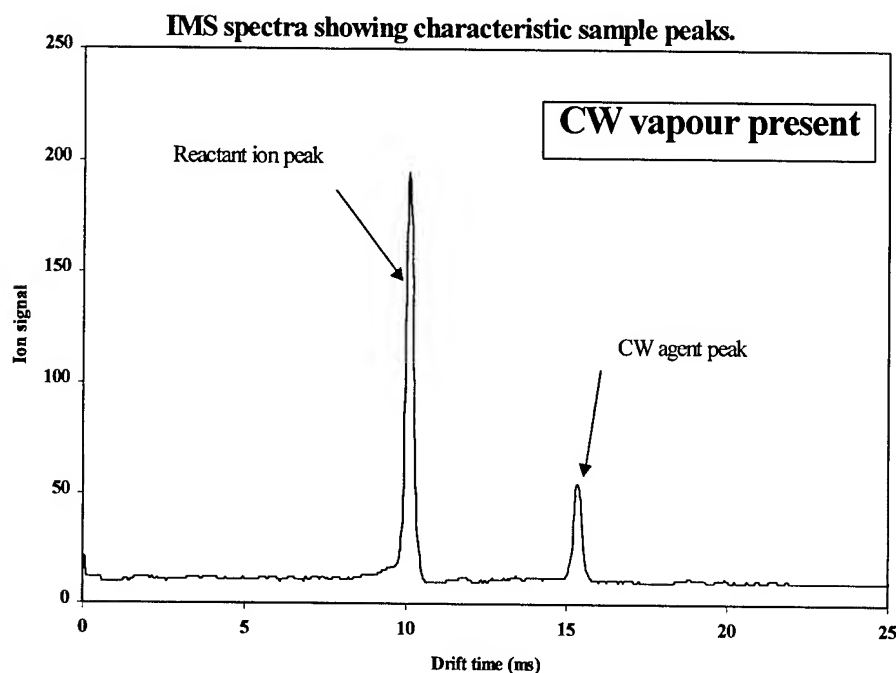


Figure 4. Typical spectrum from a corona based IMS detection system.

Although current studies performed using agent simulants and live agents suggest the chemistry of Non-Rad based systems to be similar to Rad-source based systems detailed studies are now underway using a tandem IMS-Mass Spectrometer to determine to detailed nature of the chemistry associated with the corona ionisation process.

Experimentation over many years with CAM systems has shown that the most sensitive materials are detectable in the 0.1 - 1 ppb level (by volume) in real time. Recent tests with corona-based systems have shown similar performance characteristics.

3. The Non-Rad Enhanced Chemical Agent Monitor.

Like the original CAM the ECAM (Enhanced Chemical Agent Monitor) is a field operable hazardous vapour detection system. The ECAM was the equipment of choice on which to based GDLs Non-radioactive CAM development. The rad-source based ECAM grew out of an initial development of CW detectors for the Swiss Department of Defence. A lengthy and detailed evaluation of the available technology resulted in the placement of a large production contract with GDL in late 1997. The whole development was the result of over eight years of collaboration between GDL and the Swiss Government and their technical laboratory, AC laboratorium, Spiez.

The Non-Rad ECAM is like the standard ECAM with the addition of the corona source as an easily replaceable module with a separate control PCB. Tests to determine the life of the corona points indicate that it is in excess of several thousand hours of continuous use. It would therefore add little to the logistics burden of the system to check/replace the corona points with other consumable items, like filter-packs that have typically 2000-3000hr of operation life.

3.1 The Primary Operational Role

The ECAM is primarily aimed at a role based around Civil Defence. In this role there are envisaged to be two main operational scenarios:

- Post incident threat evaluation
- Contamination monitoring in decontamination procedures.

This is defined by the technical specification as; the system is "design to indicate either, the absence in the air of all blister and nerve agents," or "for contamination monitoring". This basic role was considered to best match the civilian operational roles for which it is envisaged that the corona-source based CAM systems would find most application.

3.2 The Non-Rad ECAM operational characteristics.

These are:

- Detection capability using proven IMS technology in-line with existing Rad-CAM.
Rad-CAM has been more widely evaluated by the world's leading CW laboratories than any other CW detection system and more than 50,000 units have been sold.
- Tried and Tested Human Interface.
This includes a simple display of hazard level and a design compatible with operation in full NBC protection clothing.
- Field proven ruggedness and reliability.

- Proven during operations including deployment during the Gulf conflict.
- Widely integrated into operational environment.
This includes confidence samples, dust filters and a full package of support accessories for operation and field support.
- Dual detection modes which meet the requirements of the proposed roles.
- Rapid deployment following long unattended storage periods, up to 20yrs.
- Easily interchangeable corona source for minimal additional support requirement.

3.3 Operation.

The ECAM/Non-Rad ECAM uses a new software system with two separate detection modes. These two modes referred to as "AUTO" and "SCAN" are represented by the flow diagram presented below. The AUTO mode is most applicable to post incident evaluation reporting the level of threat from both nerve and blister agents from a detection cycle activated with a single key press, whilst the "SCAN" mode gives the near real-time response characteristics for each agent separately required for effective decontamination monitoring.

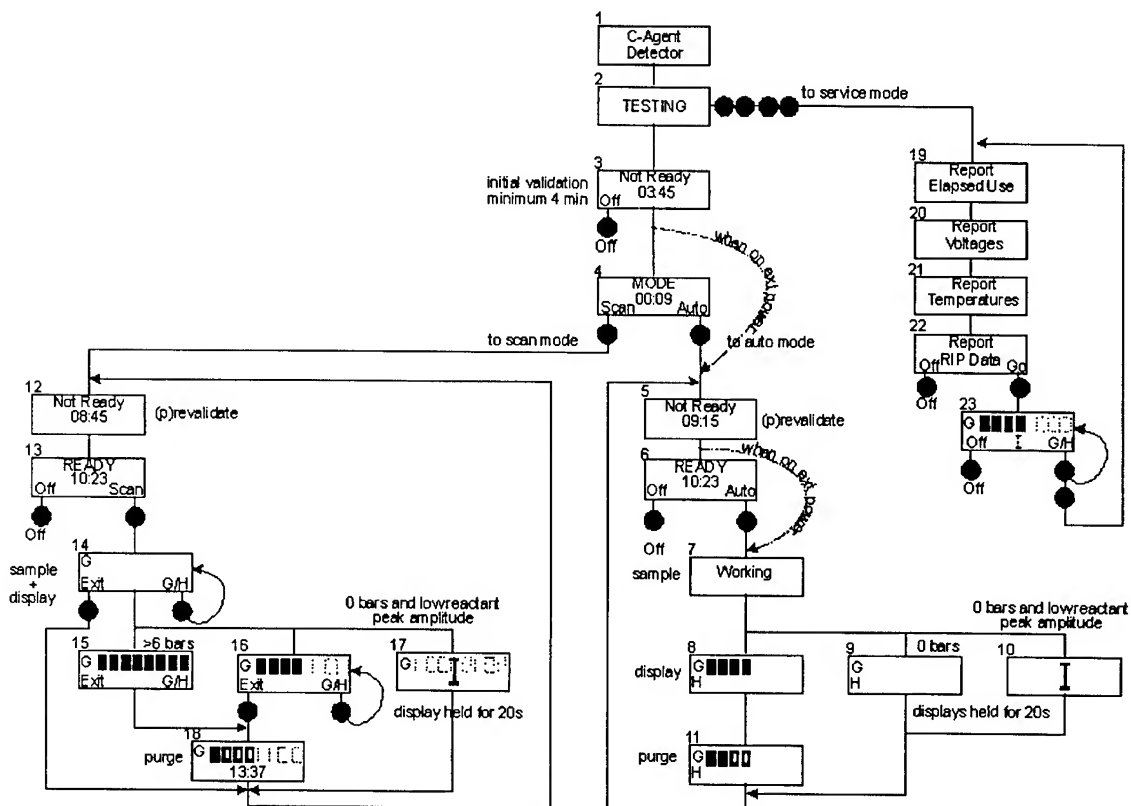


Figure 5 Flow diagram representing the two operating modes of the ECAM.

The need to be able to put the system into deployment rapidly following long unattended periods of storage periods, where the storage period could be up to 20yrs, present a significant engineering challenge. This required that the dopant source, which is essential to achieve the detection and false

alarm rejection capability of the existing CAM, is stored separately and then can be inserted quickly, easily and without any special-to-type tooling. The only tooling deemed suitable for this being the standard issue Swiss Army knives or similar hand tool. The dopant source is introduced through the base of the CAM directly into the filter pack.

The new main ECAM PCB and software offers some additional features to previous CAMs. These include a special service mode activated through a non-standard key press sequence. This gives the field service engineer access to data on runtime of the system and read-out of system sensor measurements, enabling the engineer to readily determine remaining sieve pack and corona point life. As well as this, by connecting the unit to a PC through a RS232 link the service engineer can view and record full spectral information and control many of the system parameters (display contrast, solenoid valve operation, heater operation, etc). The serial output also allows a user log data through an operational mission the data then being readily transferable to standard spreadsheet packages.

Also, when powered remotely through the rear socket (as opposed to battery powered) the ECAM will enter an auto-cycling mode continuously sampling and reporting in both modes. With the PC data logging system this is ideal for continuous background monitoring, in the classical detector role.

One of the other advantages provided by the new PCB is the facility to re-programme software into the system through the PC RS232 link. This allows future up grades to software to offer, say the targeting for new agent threats can be done easily.

Acknowledgements.

Special thanks goes to Vicky Oakham of GDL and Linda Gathwright of ETG who contributed to this paper and accompanying presentation.

CANARY* B-CELL SENSOR FOR RAPID, SENSITIVE IDENTIFICATION OF BIOLOGICAL AGENTS†

Todd H. Rider, Albert M. Young, Martha S. Petrovick, Frances E. Nargi,
Ann E. Rundell, Richard H. Mathews, Jae H. Kyung, Timothy Stephens, Linda M. Mendenhall,
Steven T. Palmacci, Laura T. Smith, Bernadette Johnson, and *Mark A. Hollis*

MIT Lincoln Laboratory
244 Wood Street, Lexington, MA 02420-9108

and

Jianzhu Chen

MIT Department of Biology
Cambridge, MA 02139

A novel bioelectronic sensor is being developed to identify bacteria and viruses in less than one minute with a sensitivity on the order of a few bioparticles. This approach uses aequorin-expressing B-cell lines specific for various bioagents. Crosslinking of a B cell's antibodies by the correct bioagent will cause the cell to emit light. Cells specific for different bioagents can be maintained in a sensor and monitored with an avalanche photodiode (APD) or other photodetector. The feasibility of this concept has been demonstrated by engineering B cells with a fast, strong, and specific bioluminescent response and demonstrating that the cells are robust to contaminants. A compact, fieldable sensor prototype is now being developed.

*Cellular Analysis and Notification of Antigen Risks and Yields.

†This work was sponsored by DARPA/DSO under Air Force Contract F19628-00-C-0002. Opinions, interpretations, conclusions, and recommendations are those of the authors and are not necessarily endorsed by the United States Air Force.

SENSOR APPROACH

We are developing a new bioelectronic sensor that can identify pathogenic bacteria and viruses for applications such as biological agent detection and medical diagnostics. B lymphocytes, white blood cells that function within animals to detect pathogens, respond in a fashion that is more rapid, sensitive, and specific than currently available man-made sensors. Therefore, our approach is to directly integrate live B cells with microelectronics. Because this project uses a biological system to warn of hazardous substances in the environment, it is called CANARY: Cellular Analysis and Notification of Antigen Risks and Yields.

CANARY utilizes B cells that have been genetically engineered to produce aequorin, a calcium-sensitive bioluminescent protein originally found in the *Aequorea victoria* jellyfish¹. As illustrated in Fig. 1, the system works as follows: (1) The B cells can be exposed to suspected bioagents or other pathogens from an air sample, blood sample, or other source. (2) The B cells have antibodies specific for certain bioagents. If one of those agents is present in the sample, it will bind to the antibodies on the surface of an appropriate B cell. (3) Crosslinking of a B cell's antibodies by a bioagent triggers an intracellular enzymatic cascade that releases calcium inside the cell². (4) In the presence of calcium, the aequorin emits blue light. (5) Light from stimulated B cells can be detected using an avalanche photodiode (APD) or other photodetector.

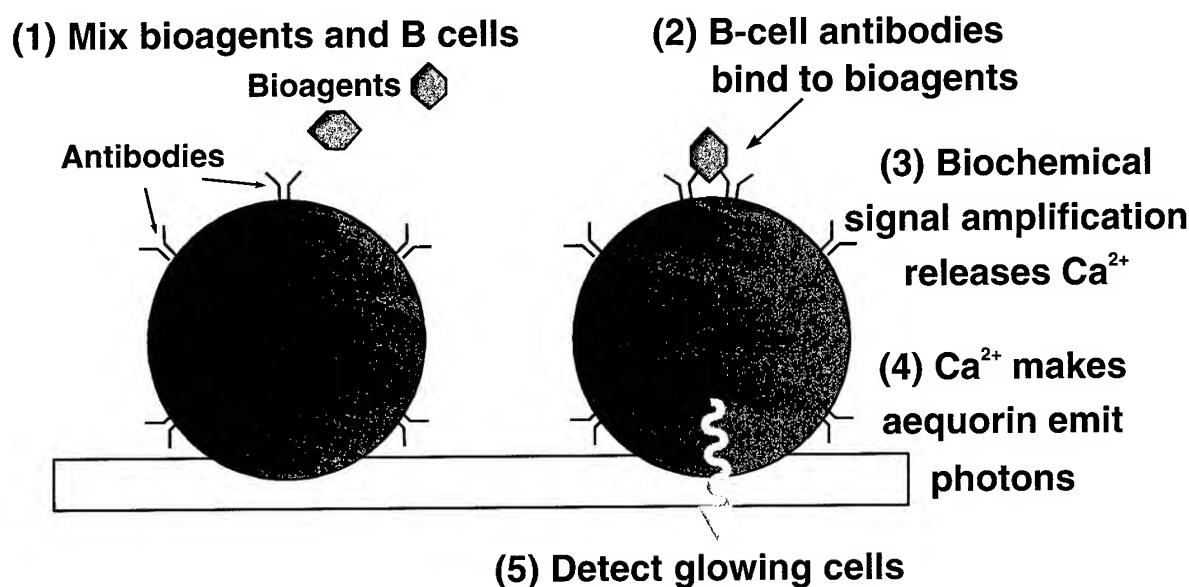


Figure 1. Fundamental principles of CANARY bioelectronic sensor. Genetically engineered B cells emit photons in response to specific bioagents, and a photodetector measures the luminescence.

The B cells can be used in a sensor architecture such as that shown in Fig. 2. Air samples can be impinged on a solid surface to deposit bioagents that might be in the samples. By using a collection tape for this deposition surface, collected samples can be moved into a reader stage, where B cells can be added to the samples and the resulting luminescence measured. B cells with different specificities can be deposited onto samples to identify bioagents. The cells can be easily maintained in separate chambers and replaced whenever necessary. To minimize operation of the CANARY identifier, air samples can be pre-screened by a bioparticle detector such as MIT Lincoln Laboratory's Biological Aerosol Warning Sensor (BAWS)³.

This overall architecture has several attractive features, including a simple, automated air-to-identifier interface, minimal usage of consumables, and efficient interactions of B cells with bioagents.

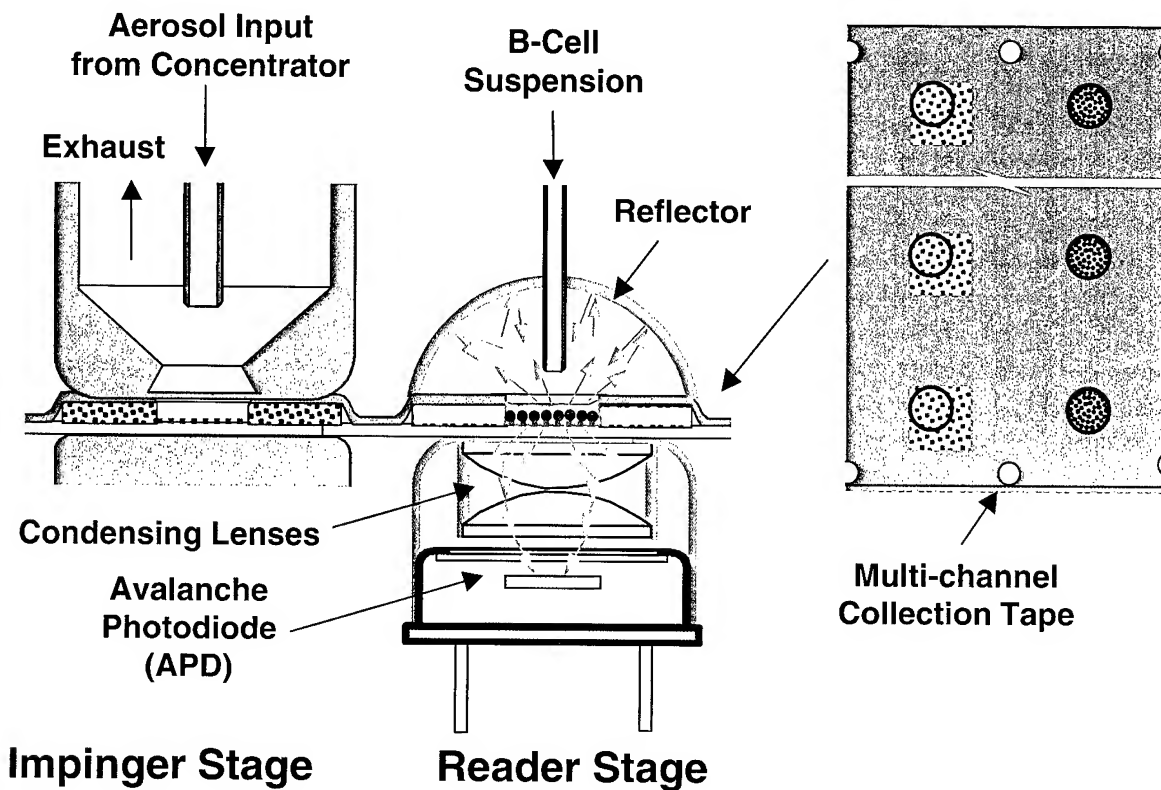


Figure 2. Approach for identifying bioagents in air samples using CANARY concept. A stream of environmental air containing potential bioagents impinges on a collection tape, and droplets of B cells can be added to the tape to identify bioagents.

Relative to other pathogen-detection approaches (for examples, see Ref. 4), CANARY should have several advantages. Because the signaling process within B cells is so fast, it is possible to detect bioagents in less than a minute. Since detection is accomplished via antibodies, the sensor can be made highly specific for particular agents by choosing the appropriate antibodies. If desired, this approach could be made even more accurate by checking for different epitopes on the surface of a given type of pathogen. Because aequorin actually emits photons instead of merely fluorescing, a CANARY sensor could be smaller and less expensive than sensors that use fluorescent reagents and hence require a laser or other light source to excite them optically.

The final and perhaps most important advantage of this approach is its potential sensitivity. A B cell typically has $\sim 10^5$ antibodies, all of which are specific for the same epitope⁵. Since a virus may have up to 10^3 copies of a given epitope on its surface and a bacterium may have at least 10^4 copies of a surface epitope⁶, it is possible for one pathogen particle to crosslink a large number of antibodies on a B cell. In addition, the enzymatic cascade inside the B cell greatly amplifies the signal. Computer modeling indicates that with the collection tape approach described above, the B cells should be able to detect bioagent cloud concentrations as low as 2 ACPLA (agent-containing particles/liter of air) in <1 minute.

TESTING

To verify the feasibility of the CANARY concept, suitable B cells were genetically engineered and shown to have very rapid, vigorous, and specific responses. The M12g3R B-cell line, which had already been transfected with antibodies specific for phosphorylcholine (PC)⁷, was stably transfected with aequorin, and the cells' responses to PC and other antigens were tested in a bioluminescence assay. As shown in Fig. 3, when the cells were exposed to PC molecules conjugated to an ovalbumin carrier, their photon emission rate increased by a factor of 130 in approximately 40 seconds. In contrast, when the cells were exposed to just PC, there was very little response, since individual PC molecules were unable to crosslink antibodies on the B cells. Unconjugated ovalbumin or bovine serum albumin also produced little or no response, verifying that the specificity is for the PC antigen. Furthermore, the cells did not respond to common contaminants that might be present in environmental samples, such as Gram-positive bacteria (*Bacillus subtilis*), Gram-negative bacteria (*Escherichia coli*), yeast (*Saccharomyces cerevisiae*), a virus (phage M13), and sand.

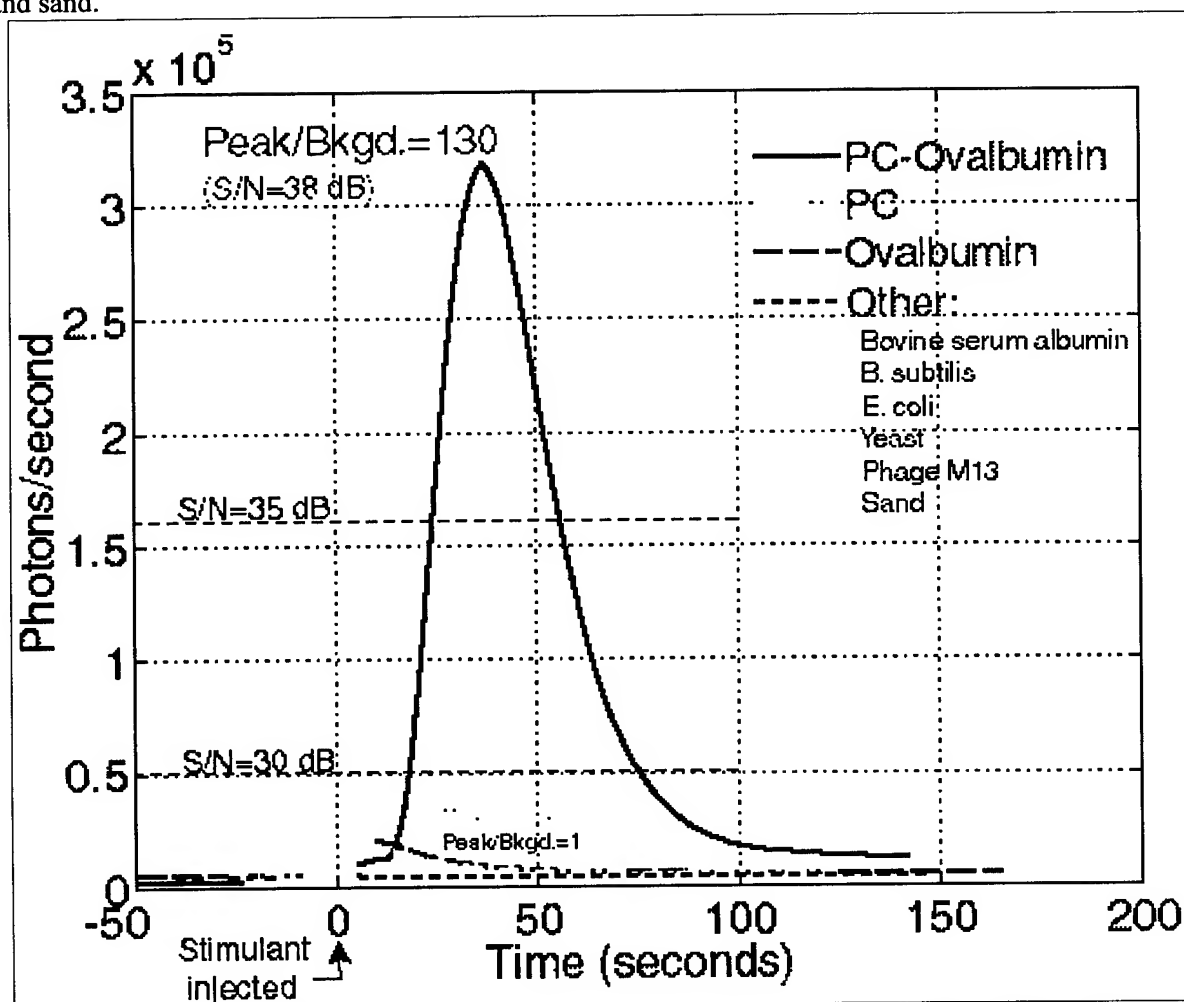


Figure 3. Specificity of bioluminescent B-cell response, with several signal/noise ratios indicated for reference. Cells were cultured in RPMI medium using standard techniques⁸ and transfected with the pCMV.AEQ.IRES.NEO plasmid⁹ using electroporation¹⁰. For testing, these genetically engineered cells were prepared as in Ref. 9 and assayed using a Hamamatsu HC125-08 photomultiplier tube. 40 μ l of sand or 20 μ l of PC-ovalbumin¹¹ or the other substances was added to 60 μ l of cells.

Figure 4 demonstrates that the cells can remain fully functional even in the presence of contaminants or after prolonged periods of culture in a sensor. These three curves show the bioluminescent response of B cells to crosslinking by 10^{-6} M anti-IgM after incubation in a microfluidic chip under various conditions for several days. For curve A, the cells were exposed for one hour to concentrated diesel exhaust, then incubated for three days. As may be seen from the graph, the cells still responded to crosslinking with a 50-fold increase in bioluminescence within 50 seconds. Since biological contaminants may also be a concern, curve B shows that even three days after the chip was inoculated with 10^7 *E. coli* bacteria, the B cells still responded to crosslinking with over a 50-fold increase in bioluminescence within 40 seconds. The B cells were also very robust to other tested contaminants, such as chimney soot, particulate matter collected from urban air samples, and soil samples of montmorillonite, silt loam, clay loam, and barnyard muck (data not shown). To show the effect of prolonged incubation in the chip (without contaminants), the cells were cultured for 7 days (curve C), and they still gave over a 100-fold bioluminescence increase within 40 seconds after stimulation.

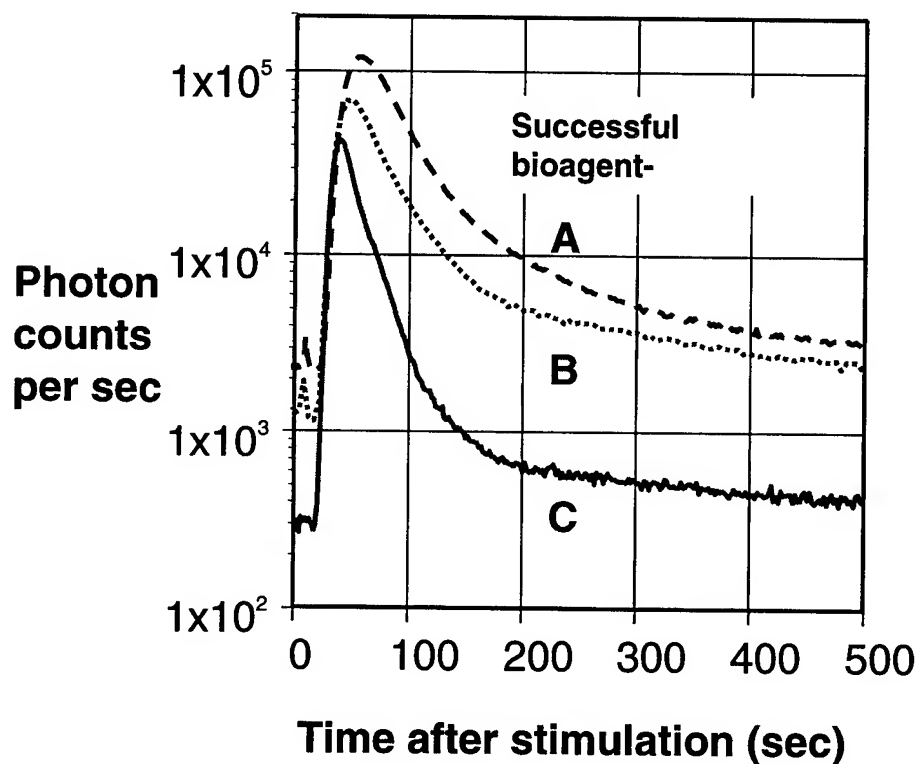


Figure 4. Performance of B cells in the presence of contaminants. (A) Response of cells to stimulation 3 days after a 1-hour exposure to full-strength diesel exhaust. (B) Response of cells to stimulation 3 days after contamination with 10^7 *E. coli*. (C) Response of cells to stimulation after 7 days of culture in a microfluidic chip.

Continuing work is focused on developing CANARY into a fieldable sensor prototype. We are currently engineering several B-cell lines that are specific for a variety of bacteria and viruses, including *Bacillus globigii*, plague, tularemia, Venezuelan equine encephalitis, foot-and-mouth disease virus, Q fever, and anthrax. We are also developing and testing components to deposit particles from air samples onto a surface and present them to the B cells. Finally, we are developing algorithms to optimize the sensitivity of this detection system.

CONCLUSIONS

Implementation of a robust detect-to-protect doctrine in the presence of typical biological background aerosols is only possible if a rapid and sensitive *identification* sensor is available. We are developing such a sensor, known as CANARY, that potentially offers substantially improved response time (<1 minute) and detection sensitivity (few bioparticles). This sensor uses B cells, or white blood cells, that have been genetically engineered to bind to specific bioagent particles via the antigen-antibody reaction and then emit photons when triggered by this binding event. Proof-of-concept experiments have shown photon emission within a few seconds after antigen is introduced to the B cells, with excellent signal-to-noise ratio and specificity. High sensitivity arises from the fact that one bioagent particle can fire one B cell, and one of our B cells presently emits about 210 photons over a 30-second period after it is triggered. We have also experimentally demonstrated that B cells are robust and operative in the presence of common battlefield interferents such as smoke soot, fuel exhaust, soils, muck, urban particulate matter, and ambient bacteria. Temperature control of the B cells is not critical, and they operate well about room temperature. We have developed collaborations with NMRC, CDC, USDA, and USAMRIID to engineer B-cell lines for specific bioagents and simulants, and are presently developing cell lines for *Bacillus globigii*, plague, tularemia, Venezuelan equine encephalitis, and foot-and-mouth disease. We have developed a sensor architecture that uses minimal consumables and should, according to simulations, be able to detect and identify bioagent cloud concentrations as low as 2 ACPLA (agent-containing particles/liter of air) in <1 minute in the presence of background biological and nonbiological interference.

ACKNOWLEDGEMENTS

We appreciate the generous donations of the M12g3R mouse B-cell line by P. W. Tucker (U. Texas at Austin), the pCMV.AEQ.IRES.NEO aequorin plasmid by D. Button (Stanford), and PC-ovalbumin by J. L. Claflin (U. Michigan). We are grateful for the advice and assistance of: D. Blanchard, M. Boes, B. Cho, L. Filip, J. Harper, A. M. Lee, H.-R. Lee, A. Leed, K. Molvar, G. Paradis, L. Parameswaran, T. Schmidt, C. Wang, and C. Whitehurst. This work was supported by the Defense Advanced Research Projects Agency's Defense Sciences Office (DARPA/DSO).

REFERENCES

1. M. J. Cormier, D. C. Prasher, M. Longiaru, and R. O. McCann, *Photochem. Photobiol.* **49**, 509 (1989).
2. A. L. DeFranco, in *Fundamental Immunology* (Raven, New York, 3rd ed., 1993), Chap. 14.
3. F. L. Reyes, T. H. Jeys, N. R. Newbury, C. A. Primmerman, G. S. Rowe, and A. Sanchez, *Field Analytical Chem. Tech.* **3**, 240 (1999).
4. B. M. Paddle, *Biosens. Bioelectron.* **11**, 1079 (1996).
5. P. W. Kincade and J. M. Gimble, in *Fundamental Immunology* (Raven, New York, 3rd ed., 1993), Chap. .
6. W. K. Joklik, H. P. Willett, D. B. Amos, C. M. Wilfert, *Zinsser Microbiology* (Appleton & Lange, Norwalk, CT, 20th ed., 1992).

7. V. S. Parikh, C. Nakai, S. J. Yokota, R. B. Bankert, and P. W. Tucker, *J. Exp. Med.* **174**, 1103 (1991).
8. R. I. Freshney, *Culture of Animal Cells* (Wiley, New York, 3rd ed., 1994).
9. D. Button and M. Brownstein, *Cell Calcium* **14**, 663 (1993).
10. L. Davis, M. Kuehl, and J. Battey, *Basic Methods in Molecular Biology* (Appleton & Lange, Norwalk, CT, 2nd ed., 1994), pp. 636-646.
11. J. George, S. J. Penner, J. Weber, J. Berry, and J. L. Claflin, *J. Immunol.*, **151**, 5955 (1993).

LUMINESCENT SENSORS FOR THE DETECTION OF CHEMICAL AGENTS IN WATER

*Amanda L. Jenkins**, Ray Yin

US Army Research Laboratory, Attn: AMSRL-WM-MA Bldg. 4600, Aberdeen Proving Ground, MD 21005

Dujie Qin, Janet Jensen, H. Dupont Durst,
US Army Edgewood Biological Chemical Center, Attn: AMSSB-RRT,
Aberdeen Proving Ground, MD 21010

Novel polymeric materials containing artificial recognition sites for pesticide and chemical agent detection in water have been prepared. The materials are designed to selectively detect phosphonate-containing species such as pesticides, insecticides and nerve agents. They are based on molecular imprinting techniques combined with sensitized lanthanide luminescence and function by selectively binding the phosphonate group to a functionality-imprinted polymer possessing a bound luminescent lanthanide ion. The polymer is coated onto a multi-mode optical fiber, and the luminescence excited using a 465.8nm laser and monitored between 550-700nm. A miniature fiber-optic spectrometer is used to monitor the changes in lanthanide luminescence that result when the analyte is reversibly bound to the co-polymer. Several of these fibers, each coated with a polymer for a specific analyte will be bundled together. The limits of detection for this type of sensor are in the low parts per trillion (ppt) in solution with linear ranges from low parts per trillion to parts per million. The sensors exhibit the same recognition characteristics over several months of use with response times of less than 15 minutes. Selectivity of the sensors against other pesticides and chemically similar compounds has been demonstrated.

Introduction

The use of chemical and biological weapons as agents of war has been banned, and the production and stockpiling of such weapons prohibited. Nevertheless, several countries, including the United States and the former Soviet Union, are known to have manufactured and stockpiled such weapons and toxins.¹ Two nerve gases of particular concern are the organofluorophosphorus compounds Sarin and Soman. These are the agents used on troops in the Iran/Iraq War, and currently leaking from stockpiles of aging weapons in the United States.² Many pesticides are so chemically similar to nerve agents that they trigger the same decrease in the enzyme plasma cholinesterase as the agents themselves do. Growing concerns over possible contamination of water supplies by nerve agents and pesticides has prompted the desire for small portable devices that can quickly detect trace amounts of these substances in water.

Despite today's technology, few methods can be used to quickly detect these compounds at the required levels. Much of the technology being used, such as gas chromatography - mass spectroscopy (GC-MS), liquid chromatography-MS and high performance liquid chromatography (HPLC), are large (not portable), expensive or require sophisticated, often extensive analysis procedures.^{3,4,5} These methods are only effective for laboratory analysis. The devices that do meet needs of real time analysis, such as surface acoustic wave devices (SAW), typically lack selectivity, especially between chemically similar pesticides and insecticides, making false positive readings a major concern.^{6,7,8} The technology currently being fielded for analysis of chemical warfare agents is enzyme based. These techniques while very specific can take 20-30 minutes to respond and are not reusable.^{9,10}

The sensors described here are fiber optic probes utilizing a luminescent europium complex.

The use of lanthanide ions as spectroscopic probes of structure and content is an established technique. The narrow excitation and emission peaks of lanthanide spectra, (typically on the order of 0.01 - 1 nm full width at half max.) provide for highly sensitive and selective analyses.^{11, 12} Lanthanide complexes exhibit long luminescent lifetimes and are intensely luminescent when complexed by appropriate ligands. Proper ligand choice, used to both immobilize the lanthanide probe and provide the enhancements needed for trace analysis, has been shown to provide limits of detection in the parts per trillion (ppt), or lower.¹³ Europium has been utilized as the probe ion since its luminescence spectrum is the least complex. Detection is based upon the changes that occur in the spectrum when the analyte is re-coordinated to Eu^{3+} . The combination of molecular imprinting and luminescence detection provides multiple criteria of selectivity to virtually eliminate the possibility for false positive readings.

Experimental

Reagents. Unless otherwise indicated, materials were obtained from commercial suppliers and used without further purification. Analytical reagent grade chemicals were used along with deionized water to prepare solutions. Pinacolylmethylphosphonate (PMP), sodium phosphate, europium(III) oxide, polystyrene, AIBN, and vinyl benzoate were obtained from Aldrich (Aldrich, Milwaukee, WI 53233). Neat analytical standards of the pesticides were obtained from Supelco (Supelco Chromatography Products, Bellefonte, PA 16823). Malathion, thionazin, and dibutyl chlorendate were obtained as neat liquid standards from Radian (Radian International, Austin, TX 78720).

Instrumentation. Luminescence was excited using a model 60X-argon ion laser (MWK Industries, Corona, CA). A 488nm holographic filter (Kaiser Optical Systems, Ann Arbor, Michigan) turned to pass the 465.8nm line, was used to exclude all other laser lines. Spectra were collected using an f/4, 0.5 m DKSP240 monochromator with a direct fiber coupler (CVI Laser Corp., Albuquerque, NM 87123) equipped with a Model ST-6 CCD (Santa Barbara Instruments Group, Santa Barbara, CA) using Kestrel Spec Software (K&M Co., Torrance, CA, USA). Spectra were also obtained with an Ocean Optics S2000 Miniature Fiber Optic Spectrometer (Ocean Optics, Dunedin, FL 34698) equipped with a 1200 line holographic grating, permanently installed 100 micron slits and a 440 nm cutoff filter. Spectra were plotted and calculations performed using Igor Pro Software (WaveMetrics Inc., Lake Oswego, OR 97035).

Compound Preparation. Pesticides were divided into 4 different groups depending on their functionality¹⁴, aliphatic organothiophosphates, pyridine organothiophosphates, organophosphates, and pyrimidine organothiophosphates. Candidate pesticides from each group were chosen, along with pinacolyl methyl phosphonate (the hydrolysis product of the nerve agent Soman). Compounds were synthesized, using a stoichiometric ratio of one mole europium to one mole of pesticide and 3 moles of the vinyl benzoate ligating molecule. (The number of ligating species was chosen to accommodate the 9 coordinate Eu^{3+}). $\text{Eu}(\text{NO}_3)_3$ was prepared by dissolving the oxide in water with just enough nitric acid to produce a clear solution. The calculated amount of each pesticide was diluted/dissolved in a 50/50 water-methanol mixture to which the vinyl benzoate monomer was subsequently added. The resulting solution was added to the $\text{Eu}(\text{NO}_3)_3$ and the pH adjusted to between 9 and 10 for complexation. The resulting solutions were stirred on low heat approximately 4 hours, then covered with a watch glass and left to crystallize overnight. The crystals were then filtered, dried and sealed in glass vials. Spectra were interpreted to determine the symmetry changes associated with analyte inclusion.

Fiber Optic Sensors. The fiber optic sensors consisted of a 200 micron optical fiber (Thor Labs, Newton, NJ, 07860) with the polymeric sensing element chemically bound on the distal end. The fibers were prepared by terminating one end with an SMA connector and removing the cladding from and polishing the distal end using the procedures outlined in the "Thor Labs Guide to Connectorization and Polishing of Optical Fibers". The sensing portions of the fibers were tapered by heating them in an air/acetylene flame and manually pulling the end. (Tapered fibers are much more efficient at coupling

the evanescent field to the polymer.) The tapered tips were dipped into the chemically initiated viscous copolymer leaving a uniform layer on the fiber.

Polymers were prepared by dissolving 3 mole percent complex compound in 95 mole percent styrene with approximately 0.1 mole percent azobisisobutyronitrile (AIBN) added as an initiator, and 2 mole percent divinyl benzene (DVB) added as a crosslinking agent. The resulting solutions were placed in glass vials, purged with nitrogen, and sealed using parafilm and screw on tops. The polymers were sonicated at 60°C for 2-4 hours until they became viscous. (Sonication is believed to help maintain homogeneity in the polymer¹⁵.) The partially polymerized material was then dip coated on the fibers and cured under a small UV lamp for 2 hours. Once cured, the polymers were swelled in water with gradually increasing amounts of methanol to remove unreacted monomer and expand the polymer pores which produces accessible sites and facilitates the removal of the imprinting ion.¹⁶ The imprinting ion was removed by washing with 1.0M nitric acid to facilitate the removal of the analyte and leave in its place a weakly coordinated nitrate.

Analysis. Measurements for the calibration data, pH study, response time and interference testing were all performed using the same fiber. The analytical figures of merit were obtained using serial dilutions of the standards in 0.01M NaOH. The luminescence was excited using the argon laser and the active end of the sensor was placed in a cuvette containing one of the sample dilutions. Spectra were collected at each concentration after the sensor had equilibrated for 15 minutes. The sensor was rinsed with deionized water between each sample. Standards were analyzed in order of both increasing and decreasing concentration in order to demonstrate the reversibility of the sensor. Calibration curves were obtained and linear regressions were performed.

The response time of the sensors and the pH dependence was evaluated using a method similar to the one described above. A series of standards with pH values ranging from 4.5 to 13.0 were prepared from the stock standard through the addition of 1.0 M nitric acid or 1.0 M sodium hydroxide. The sensor was placed in a cuvette with each solution and spectra collected at a variety of exposure times. Response was evaluated through a comparison of peak area at each time and pH.

Pesticide and insecticide standards were tested as possible interferences for the sensors. Standard 100 ppm solutions were prepared by the dissolution and/or dilution of the samples in deionized water when possible. The pesticides with limited solubility in water were prepared using a 50:50 water/methanol mixture. The pH of each of the solutions was adjusted to 10.5 using 1M sodium hydroxide. Spectra from the fibers for each analyte were taken at regular intervals for 30 minutes, and then compared with the response from the imprinted analyte. The sensor was rinsed with deionized water between each analysis.

Results and Discussion

Preparation of the Sensors. The sensors were prepared using 200 μm multimode optical fibers. (Larger fibers although able to pass more light, did not provide the resolution necessary to isolate the analyte band.) Differing thickness of the polymeric coating were used in order to evaluate the effects of polymer thickness on response time, background signal and signal intensity. Thickness was controlled by the number of times the fiber was dipped into the viscous polymer. It was observed that increasing the thickness of the coating increased the time required for response¹⁵. This is consistent with the fact that thicker coatings have cavities that are deeper in the polymer and are relatively inaccessible. Thus, a larger amount of analyte could remain trapped in the polymer increasing the residual peak. A thickness of four coats, 100 μm was determined to be optimal for the design of the sensors since it gives an 80% response within a reasonable time (less than 15 minutes).

Excitation. Two argon ion excitation wavelengths 465.8 and 488 nm, were used with the polymers. The spectrum of the sensors excited with the 465.8 nm laser line displayed increased luminescence intensity and greater spectral resolution of the analyte peaks from the parent europium.

This increase indicates that excitation using the 465.8 nm line results in a near resonant excitation transition from the ground 7F_0 level to the 5D_2 level of the europium. As a result, 465.8 nm was chosen as the excitation wavelength for the sensor.

Analytical Figures of Merit. The performance of the fiber optic sensors with the 1/2 meter monochromator was evaluated to obtain figures of merit. Using 1mW of (465.8 nm for excitation) 200 micron slits on the monochromator, and an exposure time of 25 seconds, the luminescence spectrum of the sensors in a series of analyte solutions at pH 10.5, was obtained. The response of the sensor to increasing concentrations of analyte exhibits an increase in the luminescence intensity of the spectra. This increase in luminescence is indicative of rebinding the analyte into the coordination sphere of the lanthanide and the exclusion of water.

The resulting peak areas in the 609 to 621 nm spectral region were calculated using Igor Pro Software, and plotted as a function of concentration. Peak areas have been shown to provide a longer, more linear calibration curve than direct peak height, since the bandwidths as well as the peak heights of the lanthanides increase as a function of concentration. Linear regression was performed and the limits of detection calculated. The analytical figures of merit for the sensors with the benchtop apparatus are given in Table 1. Some residual bands remain visible even when the sensors are cleaned, and should be subtracted out with the background for application purposes. Variations in the residual peak, the background, or other slight differences between sensors appear to have little effect on the overall calibration curve, linear dynamic range and limit of detection.

TABLE 1.
Analytical Figures of Merit for the Sensors

	PMP	Ethion	Chloropyrifos Methyl	PMP Mini-System
Limit of Detection	660 ppq	8 ppt	5 ppt	7 ppt
Linear Dynamic Range	750 ppq to 10 ppm	100 ppm to 8 ppt	100 ppm to 5 ppt	10 ppt to 10 ppm
Correlation Coefficient	0.9984	0.9935	0.9996	0.9973
Slope	1.949 counts ppt ⁻¹	1.391 counts ppt ⁻¹	1.528 counts ppt ⁻¹	1.484 μ V ppt ⁻¹
80% Response Time	8 minutes	11 minutes	13 minutes	8 minutes

Response Time and pH Dependence. The response time of the sensor is the most crucial characteristic of detectors and sensors for real-time monitoring.¹⁷ The sensor must be fast enough to provide a warning with enough time for an appropriate response such as evacuation of the area. A study was performed using a sensor with a 200 micron coat to determine the effect of pH on the response time. The study was performed on solutions with pH values ranging from 4.5 to 13 over a period of 30 minutes. Figure 1 demonstrates the response of the sensor over the initial 30 minute time period. The sensors show a positive response to the presence of PMP after 3 minutes for all pH values from 6 to 12, and a positive response after 1 minute for the solution with a pH of 13. At low values of pH (below 6), the response of the sensor is indicative of the removal of PMP from the sensor. This demonstrates the washing process that occurs under acidic conditions. Neutral and slightly basic values (pH from 6-11) provide a steeper, more linear response that is consistent over the entire pH range.

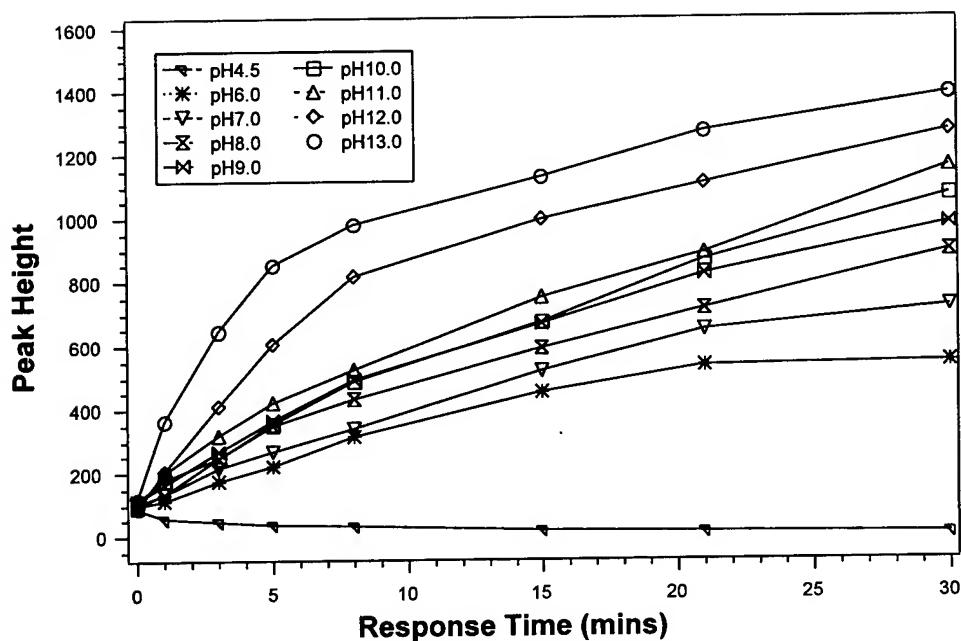


Figure 1. Effect of pH on the temporal response of the sensor.

The effect of coating thickness on the response time of the sensor was also evaluated. Figure 2 shows the response with a 100 and 200 micron coated sensors to a 10 with the 80% response time less than 14 minutes. (Response times are typically reported as the time it takes the sensor to reach 80% of maximum⁹.) The 80% response time of the 100-micron coated fiber decreased to 8 minutes. For an on-line monitor, the time for initial response is the most important factor. Using pH = 10.5, a distinct response occurs within 1 minute.

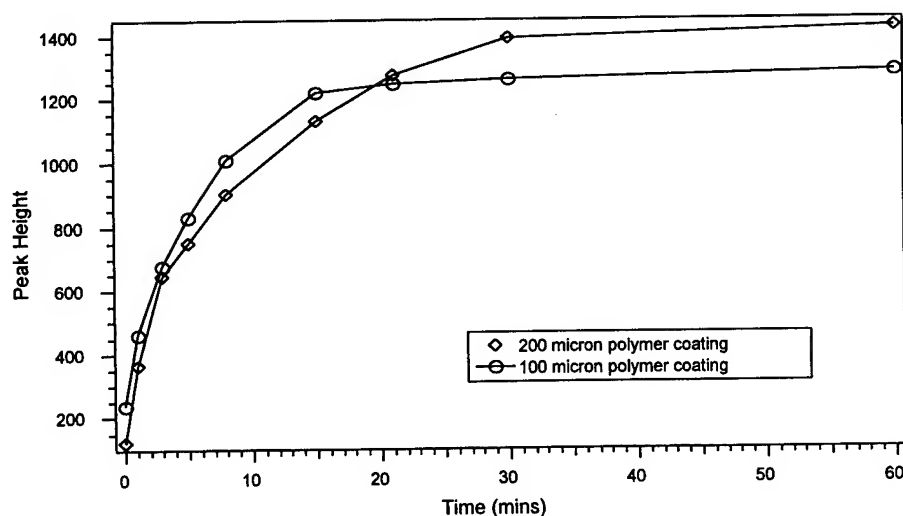


Figure 2. Effect of the thickness of the polymer coating on the temporal response.

Interferences. Many pesticides, insecticides, and nerve agents are chemically analogous. These compounds exist as liquids, oils or solids at ambient temperatures. Common pesticides, insecticides and herbicides were tested using the sensors in order to determine the degree of interference. The concentration used for screening interferences, 100 ppm, is much higher than typically found in water systems even with runoff from nearby agriculture. Each of the pesticides and a sodium phosphate solution at pH 10.5 was exposed to the sensor for 1/2 hour with measurements taken during scheduled intervals.

The polymer imprinted for chlorpyrifos methyl, a small pyridine organothiophosphate pesticide not only discriminates against other classes of pesticides but also can distinguish against other larger members of its own class such as chlorpyrifos ethyl. The spectra resulting from the exposure of selected pesticides at 100ppm are shown in Figure 4 with the spectrum of 1 ppm chlorpyrifos methyl shown for comparison purposes. (Figure 3)

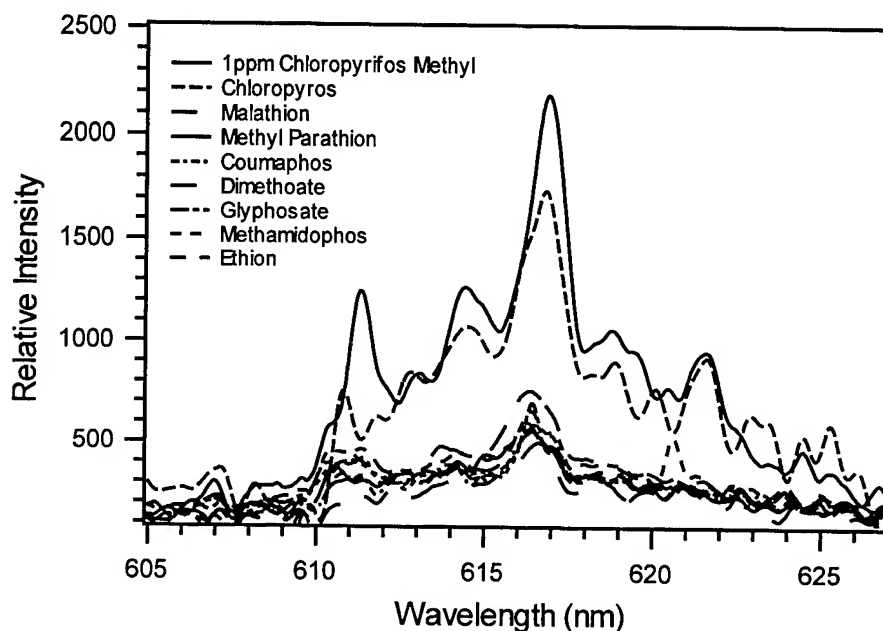


Figure 3. Response of the Chlorpyrifos-methyl sensor to 100ppm pesticide interferences.

None of the pesticides tested against the PMP hydrolysis product sensor responded as interferents. The influence of these chemicals was apparent as indicated by the changing intensity of the major 617 nm europium luminescence band, however none produced a luminescence peak in the 610nm region. Since the chemicals that are the most likely interferences do not cause false positive readings, other less similar compounds should be unlikely to interfere. In addition, none of the pesticides screened irreversibly bound to the sensors so poisoning is not a concern.

Miniaturization. A miniaturized version of the PMP sensor was designed using an Ocean Optics miniature spectrometer. This sensor fit on a board 3.5' x 2.5', and showed promise for both sensitivity and selectivity in detecting the PMP. The limit of detection for this device was determined to be 7 parts per trillion using conditions previously described. The linear dynamic range is from 7 ppt to 1ppm using a 100 μ m coated fiber. Signal averaging and smoothing using the Savitzsky-Goulay method was kept to a minimal 3-point average to get the required resolution. Figures of merit for this device are presented in Table 1.

Conclusions

Sensors for hazardous materials are characterized in terms of sensitivity, selectivity, response time, adaptability and portability. The devices described here show benefits in all of these areas. The benchtop and portable versions provide a detection limits in the low parts per trillion. The sensors are both sensitive and selective combining both chemical and spectroscopic selectivities making them less prone to false positives. The 80% response time of the sensors is less than 14 minutes. The main size-limiting factor for the device is the argon laser and its power supply. However, recent advances in the field of blue LEDs are eliminating the need for the "large" laser and further miniaturization is underway.

The technology developed here is very adaptable, and could be modified to detect new agents or species as they become available. Adaptation would include the design of new molecularly imprinted polymers. Several of these devices can be coupled together to allow simultaneous detection for a wide array of chemical species. Devices such as the one described here could be used to detect the presence of chemical agents or pollutants near battlefields, in hospitals or military installations, or in community water supplies. The pesticide sensors could also be used in agricultural applications to optimize the amounts of the pesticides applied.

References

- (1) Crelling, J. K. "Chemical Warfare Capabilities-The Warsaw Pact," U. S. Army Foreign Science and Technology Center, 1979.
- (2) "Decaying Sarin-filled Rockets Spark Fears", *Jane's Defense Weekly* 1996, 25(20), 3.
- (3) D'agostino, P. A.; Provost, L. R.; Brooks, P. W. *Journal of Chromatography* 1991, 541, 121-130.
- (4) Black, R. M.; Clarke, R. J.; Reid, M. J. *Journal of Chromatography* 1994, 662, 301-321.
- (5) Martinez, R.C.; Gonzalo, E.R.; Garcia, F.G.; Mendez, H.J.; *J. Chromatogr.*, 1993, 644, 49-58.
- (6) Balog, P. P.; Stanford, T. B.; Nordstrom, R. J.; Burgener, R. C. "Feasibility Assessment of Piezoelectric Crystals as Chemical Agent Sensors," HQ Aerospace Medical Division, 1986.
- (7) Nieuwenhuizen, M. S.; Hartevelt, J. L. N. *Talanta* 1994, 41, 461-472.
- (8) Grate, J.W., Martin, S.J., White, R.M.; *Anal. Chem.* 1993, 65(21), 940-948.
- (9) Report "Assessment of Chemical and Biological Sensor Technologies," National Research Council, 1984.
- (10) Trettnak, W.; Reininger; Zinterl, E.; Wolfbeis, O.S. *Sensors and Actuators B*. 1993, 11, 87-93.
- (11) Jenkins, A.L. Masters Thesis, University of Maryland Baltimore County, 1996.
- (12) Evans, C.H.; "Biochemistry of the Lanthanides", Plenum, New York, 1990.
- (13) Jenkins, A. L.; Murray, G. M. *Analytical Chemistry* 1996, 68, 2974-2980.
- (14) "Compendium of Pesticides", <http://www.hclrss.demon.co.uk/index.html>
- (15) Jenkins, A. L.; Uy, O.M., Murray, G. M. *Analytical Chemistry* 1999, 71(2), 373-378.
- (16) Helfferich, F. *Ion Exchange*; McGraw-Hill: New York, 1962, pp. 511.
- (17) Yang, Y.-C.; Baker, J.; Ward, R. *Chemical Reviews* 1992, 92, 1729-1743.

NANOSTRUCTURE ENHANCED RAMAN SCATTERING

Paul D. Pulaski, David Burckel, S.R.J. Brueck
Center for High Technology Materials, UNM
1313 Goddard SE
Albuquerque, NM 87106

I. ABSTRACT

Recently here at CHTM, we have observed a significant enhancement of the Raman scattered radiation from the surface of small pitch ($<1\text{ }\mu\text{m}$) silicon gratings compared to bulk silicon substrates. Silicon grating samples with pitches ranging from $0.34\text{ }\mu\text{m}$ to $1\text{ }\mu\text{m}$ were fabricated via interferometric lithography and post-processing etching techniques which produced different grating depths for the various pitches. These gratings exhibited Raman enhancement factors of the integrated intensity of the spectral peaks, an order of magnitude greater than the bulk samples (for the smallest pitch and deepest grating depths).

II. INTRODUCTION

There are two types of "enhancement" that can occur for Raman scattered radiation emission from nanostructure materials. First there is the enhancement of the Raman emission from nanostructured dielectric materials such as silicon¹, which is due to coupling of dipole emission with the waveguide modes of very thin ($<\text{wavelength}$) dielectric slabs². The second type is the more common Surface-Enhanced Raman Scattering (SERS), which occurs in chemical and biological molecules that are adsorbed onto the surface of textured and colloidal metals³⁻⁵. In this case, the electric field from the incident radiation is resonant with the localized surface-plasmon frequency of the metal structure and couples to the Raman-active molecules to produce an enhancement that depends on the wavelength of the incident light and the geometry of the metal particles⁶. In general, higher aspect ratios yield large enhancement factors. Most of the SERS work has been done on randomly textured surfaces, however there has been some work performed on regularly patterned surfaces⁷⁻⁸. The patterns have been fabricated by using various lithographic techniques such as electron-beam⁸, nanoparticle⁹, and interferometric⁷ lithography. Here at CHTM, in addition to the silicon gratings, we have begun fabricating an array of metal gratings and posts with a range of pitches and aspect ratios via interferometric lithography, which will be used for subsequent SERS studies. We plan to adsorb chemical and biological simulants onto both silicon and metal nanostructures for comparison SERS measurement with the potential for biosensor applications.

III. THEORY

Raman scattering is a two-photon process whereby incident light excites the vibrational modes in a medium shifting the frequency of scattered light ($\sim 520\text{ cm}^{-1}$ for silicon). The intensity of the Raman scattering radiation in a bulk crystal structure depends on the Raman cross section and the polarization of the incident light relative to the crystalline axes (the polarization of the scattered light depends on the polarization of the incident light):

$$I_R = C |\vec{p}' \cdot \mathbf{R} \cdot \vec{p}|^2 I_o$$

where C is a constant related to the Raman cross section, \vec{p}' and \vec{p} are the incident and scattered light polarizations respectively and \mathbf{R} is a three-dimensional Raman tensor relating the incident and scattered light polarization vectors, which depends on the crystalline structure of the medium¹⁰.

IV. EXPERIMENTAL METHODS

Silicon grating samples with pitches ranging from 0.34 μm to 1 μm were fabricated via interferometric lithography and post-processing etching techniques, which produced different grating depths for the various pitches. There were three different grating depths for each grating pitch by etching the silicon with a reactive ion etcher (RIE) for 6, 12 and 24 minutes (200 nm, 450 nm, 700nm respectively). These gratings exhibited Raman enhancement factors of the integrated intensity of the spectral peaks an order of magnitude greater than the bulk samples (for the smallest pitch and deepest grating depths).

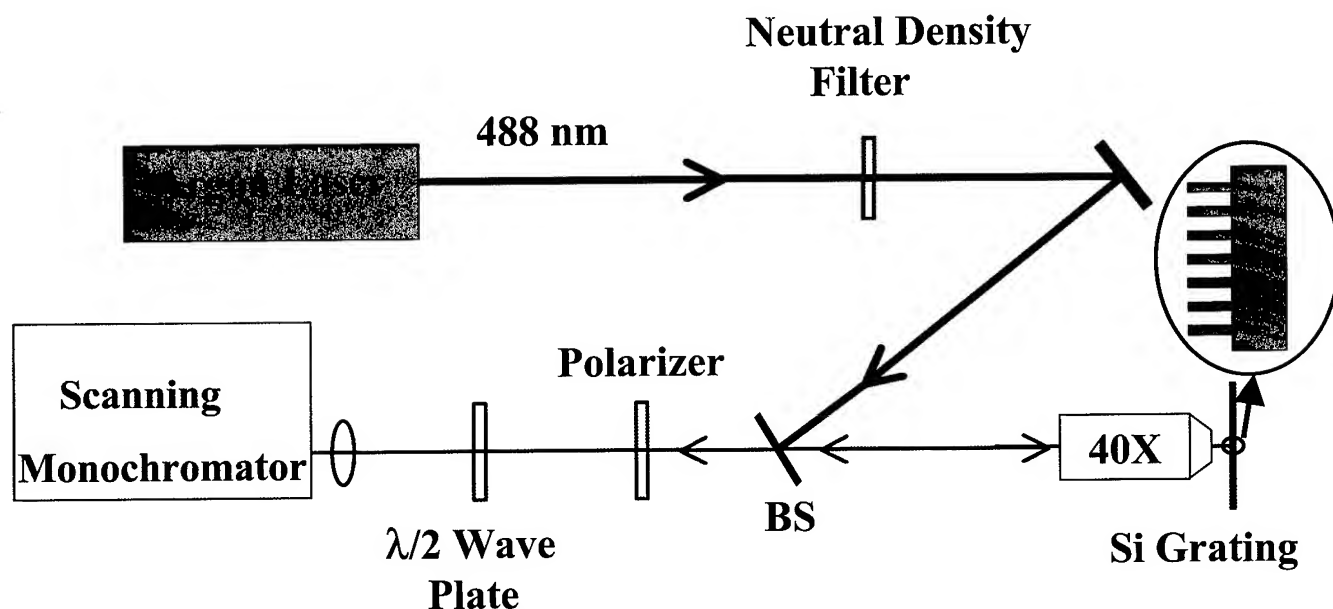


Figure 1: Experimental Setup for Raman spectroscopy

The Raman scattered radiation was measured using a standard backscattering geometry (Fig. 1) by focusing 488 nm light from an argon-ion laser onto the samples with a 40X microscope objective and collecting the scattered light with a 2 m double-pass scanning monochromator. The input polarization was fixed at a position parallel to the plane of the setup and the sample stage was constructed so that the

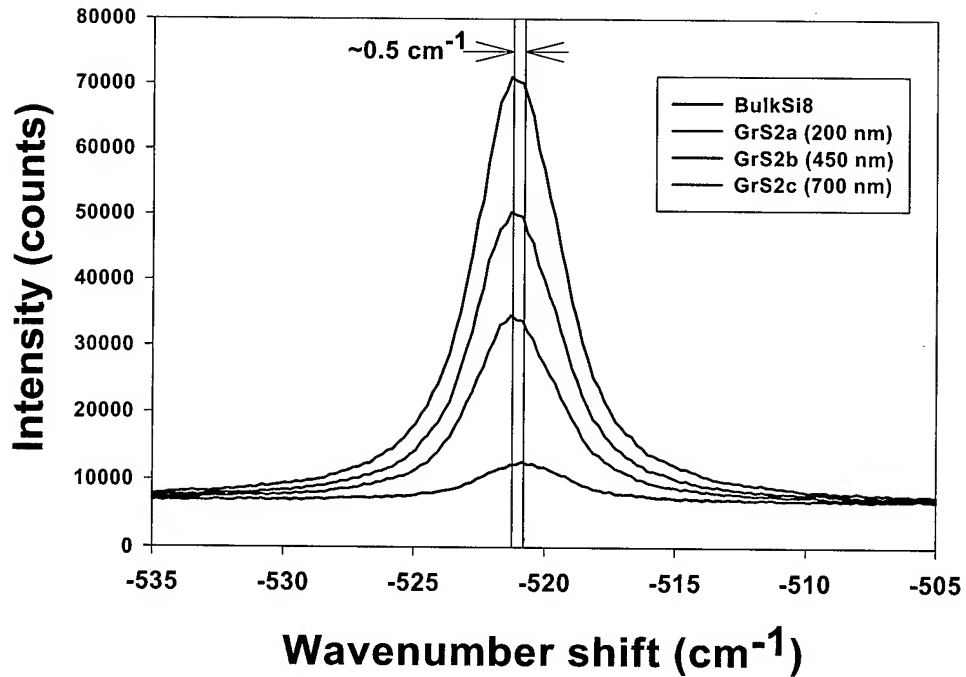


Figure 2: Raman Spectrum for (H/H) orientation

sample holder can be rotated about any fixed position on the grating sample. The scattered light polarization was detected with a high-extinction ratio Glan-Thompson polarizer and a half-wave plate was placed at the input of the spectrometer to rotate the polarization to the optimum for the spectrometer. The Raman polarization selectivity in silicon was tested on a bulk silicon wafer with a $\langle 100 \rangle$ orientation with no measurable polarization scrambling from the optics used to collect the scattered light.

In order to determine the Raman enhancement factor, we first measured the Raman spectrum on a bulk silicon sample as a reference. Then for each grating sample, we measured the Raman spectrum using four different polarization orientations. The incident and scattered light polarizations were oriented either parallel (H) or perpendicular (V) to the grating “lines” and the half-wave plate insured that the same optimum polarization was incident on the spectrometer independent of the position of the polarization analyzer. Therefore the four polarization orientations are: (H/H), (V/V), (H/V), (V/H) where the notation stands for (“incident”/“scattered”).

V. DISCUSSION

Calculating the area under the Raman intensity spectral peak (Fig 2-3) and comparing it to the area of the bulk silicon Raman peak determined the enhancement of the Raman signal from the gratings. The calculated enhancement factor is the ratio of integrated intensities of the spectral peaks (grating/bulk) and was calculated for each grating in the (H/H) orientation, which yielded the maximum enhancement factor compared to the other polarization orientations. Incidentally there was no enhancement measured for the (H/V) and (V/H) cases. The enhancement of the integrated intensity as a function of the grating pitch and RIE time can be seen in Fig. 4. In addition, the shift of the Raman peak in the gratings compared to bulk silicon indicates that the Raman emission is from the grating fingers (Fig 2).

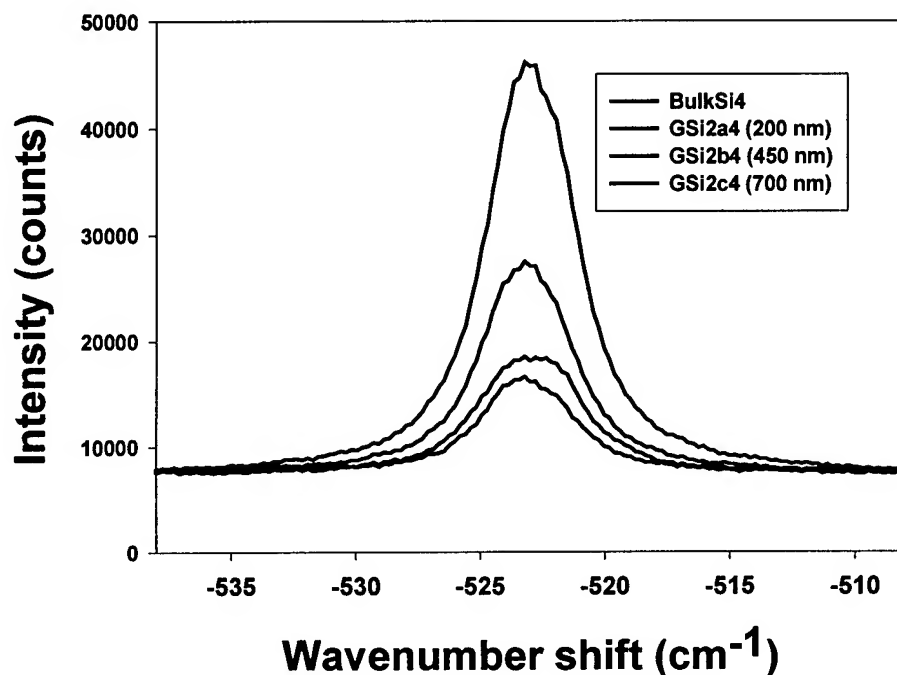


Figure 3: Raman Spectrum for (V/V) orientation

The maximum enhancement factor of about 11.5 was measured on the shortest pitch grating ($0.34\ \mu\text{m}$) with the deepest depth ($\sim 700\ \text{nm}$). This trend suggests that even shorter pitch and deeper gratings will yield larger enhancement factors. The grating linewidth and profiles of the fingers also affects the intensity of the Raman scattered light. According to a recent theoretical model², the maximum enhancement can be obtained when the grating linewidth is approximately $\lambda/2$.

Comparison of the experimental results of the enhancement factor with the theoretical model relating the spontaneous Raman emission from the grating “fingers” to a dipole radiation emission from dielectric slabs will be discussed in a separate publication. This model suggests that the enhancement of the Raman scattered light for two-dimensional structures will be significantly larger than for the one-dimensional gratings. Therefore, future work includes an extension of the fabrication to 2-D structures (i.e. “posts”) along with a systematic study of the Raman enhancement as a function of pitch, grating/post height, and linewidth.

In addition, previous work of Raman emission from chemical molecules adsorbed onto metal ellipsoids such as gold or silver has shown very large Raman enhancements for increasing axial ratios⁶. This enhancement is strongly dependent on the wavelength of the incident radiation used to stimulate the Raman scattered light. The maximum enhancement shifts to longer incident wavelengths for increasing axial ratios of the metal ellipsoids. Therefore, in light of these new results in the silicon nanostructures and the previous work on SERS in metal ellipsoids, we have begun to extend this research by fabricating metal nanostructures such as two-dimensional silver posts using interferometric lithography and standard liftoff procedures (with the potential for large aspect ratios). We plan to explore the issues related to the

Raman enhancement as a function of incident wavelength and aspect ratio of the silver and silicon posts. Furthermore, biological molecules will be adsorbed onto the surface of the nanostructured metals and silicon for subsequent SERS measurements that could lead to more sensitive sensors of harmful chemical and biological agents.

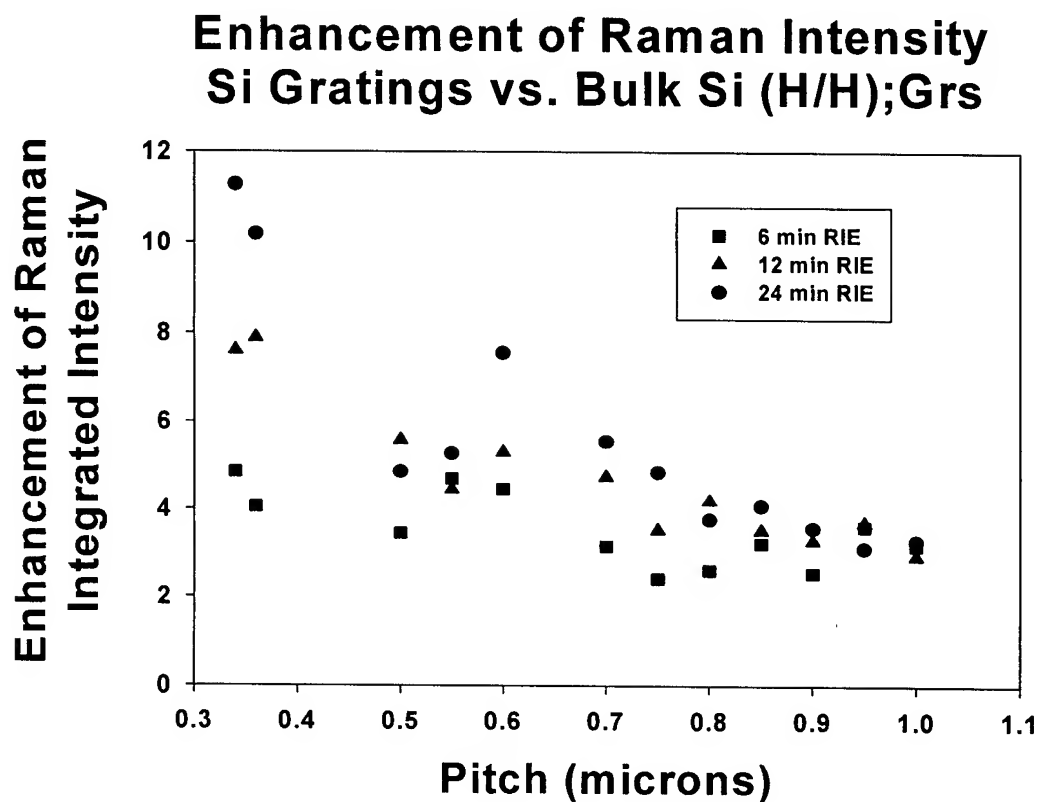


Figure 4: Plot of Raman enhancement factor for silicon gratings

CONCLUSIONS

Enhancement of the integrated intensity of the Raman scattered radiation from silicon gratings compared to bulk silicon has been demonstrated. The enhancement factor of the integrated intensity of the Raman peak has been measured as a function of grating pitch and depth. These results suggest that even greater Raman enhancements can be achieved with smaller pitch, deeper grating depth and narrower linewidth. This research will be extended to two-dimensional nanostructures (ie.silicon and metal posts) with varying aspect ratios for subsequent Raman enhancement measurements in silicon and SERS studies in both silicon and metal nanostructures to determine the optimum material and relative

dimensions of the patterned surfaces which will lead to the maximum enhancement of the Raman emission from adsorbed chemical and biological simulants.

REFERENCES

1. S.H.Zaidi *et al.*, J. Appl. Phys. **80**, 6997, (1996)
2. S.R.J. Brueck, *to be published*
3. M. Fleischmann *et al.*, Chem. Phys. Lett., **26**, 163, (1974)
4. D.L. Jeanmaire *et al.*, J. Electroanal. Chem., **84**, 1, (1977)
5. M.G. Albrecht *et al.* J. Am. Chem. Soc., **99**, 5215, ((1977)
6. M. Moskovits, Rev. of Mod. Phys., **57**, 783, (1985)
7. P.F. Liao *et al.*, Chemical Physics Letters, **82**, 355, (1981)
8. M. Kahl *et al.*, Sensors and Actuators, **51**, 285, (1998)
9. J.C. Hulteen *et al.*, J. Vac. Sci. Tech. A, **13**, 1553, (1995)
10. R. Loudon, Adv. Phys., **13**, 423, (1964)

SIDE-BY-SIDE COMPARISON OF SMALL, HAND-HELD ION MOBILITY SPECTROMETERS AND SURFACE ACOUSTIC WAVE DEVICES

Charles S. Harden, Dennis M. Davis, Donald B. Shoff and Vincent M. McHugh

Research and Technology Directorate
U.S. Army Edgewood Chemical Biological Center
Aberdeen Proving Ground, MD 21010 USA

Gretchen Blethen
GEO-Centers, Incorporated
Aberdeen Proving Ground, Maryland 21010-5424, USA

Within the U.S. Military, there has been a long-term and on-going debate with respect to the relative attributes of Ion Mobility Spectrometry (IMS) and Surface Acoustic Wave (SAW) technology for the detection and identification of chemical warfare agent. Almost all of the claims that have been made in favor of one technology or the other have been made on the bases of experimental data gathered in unrelated tests. Because of the on-going technology debate and because the U.S. Department of Defense has entered into a significant development program aimed at production of small, unobtrusive CW detectors, side-by-side evaluations of prototype IMS and SAW field instruments have been performed at the U.S. Army Edgewood Chemical Biological Center. Of particular interest in these evaluations were small field prototype instruments that will fit in the palm of a human hand -- instruments that are $\leq 40 \text{ in}^3$ (655 cm^3) in volume and weigh ≤ 2 pounds (900 gm).

The purpose of the evaluation was to describe relative performance characteristics of devices based on the two technologies in experiments consisting of exposures to the same sample conditions at the same time — arguments resulting from possibilities of different analyte concentrations, water vapor concentrations and sample gas temperatures would be eliminated. Analytes included toxic organophosphorus analytes were studied (the so-called "nerve" agents), organosulfur analytes ("mustard gas"), and hydrogen cyanide (a "blood" agents). Analyte concentrations ranged from about 10 ppb to 10's of ppm, water vapor concentrations were intentionally kept high to stress the technologies, and sample gas temperatures ranged from about 25 to 36 C. The prototype devices were simultaneously exposed to analyte vapors in air and in mixtures of air and other substances that were known to cause undesirable responses in both IMS and SAW devices. IMS spectra were compared with SAW crystal frequency shifts for each of the analyte - interference - water vapor mixtures. Figures of relative merit to be reported include limits of detection, response time, ability to distinguish analytes by group and by type within a group, and ability to distinguish between analytes of interest and potentially interfering substances.

The state-of-the-art in development of small, hand-held field detection devices based on IMS and SAW technologies will be reviewed.

RESIDUAL LIFE INDICATORS – POINT CHEMICAL DETECTORS USED TO MEASURE THE CAPACITY OF ACTIVATED CARBON IN PROTECTIVE GARMENTS, GAS MASK FILTERS, AND COLLECTIVE PROTECTION FILTERS

Joseph E. Roehl, Timothy W. Caraher, Kimberly A. Kalmes, Elizabeth A. Isley
Scentczar Corporation
213 Taylor Street
Fredericksburg, VA 22405-2909

Abstract

Activated carbon is used in Nuclear, Biological, and Chemical (NBC) protective garments, gas mask filters, collective protection filters, and battlefield chemical alarms to adsorb chemical warfare agents. Common battlefield environmental contaminants such as cigarette smoke, jet fuels, and diesel exhaust have been shown to contain chemicals that displace chemical agents in activated carbon or inhibit their adsorption and are of concern. We will describe the problem and three approaches to estimating the residual utility or remaining capacity of carbon beds under development at Scentczar Corporation using chemical sensors and a communications system that could be interfaced with digital communications systems.

Introduction

Activated carbon beds are used as an adsorbant in many military field devices including garments, filters, and alarms. Users have understood for many years that activated carbon beds can become contaminated or "loaded" with environmental chemicals making them ineffective at adsorbing chemical warfare (CW) agents. Strategies for dealing with this problem have usually involved protecting the carbon in a sealed container until it is actually required in the field. In addition a number of breakthrough detectors appear in the patent literature that sense the breakthrough of a particular contaminant as the carbon bed, especially in a gas mask filter, is expended. To our knowledge none of these devices has been implemented by the U.S. military. Scentczar Corporation is developing three separate specialized Residual Life Indicator (RLI) technologies for the U.S. military that are designed to remain in intimate contact with CW protective gear using carbon beds and provide CW adsorption capacity information to the battlefield commander or chemical officer. We originally received funding for this work through a subcontract with Du Pont Fabrics and Separation Systems in Old Hickory, Tennessee. Du Pont's contract was with Natick Laboratories in Natick Mass. Du Pont's project used Battelle Memorial Institute to evaluate the contaminants that are adsorbed by carbon and actually cause the problem and other subcontractors, including Scentczar Corporation, to develop specific chemical detector technologies. Later we received funding from the U.S. Marine Corps to continue development of our approach and refinement of our detector through a Small Business Innovation Research (SBIR) phase I program. We are currently anticipating award of the phase II.

Background

Carbon is the key adsorption material in gas mask filters, protective garments, and collective protection filters used in the military, and in many civilian process applications requiring the adsorption of Volatile Organic Chemicals (VOCs). In CBW applications the efficiency of the carbon as an adsorbent is dependent on the exposure of the carbon to other materials. Adsorption is an exothermic, reversible, process and an adsorption isotherm is used to describe carbon adsorption. Carbon's ability to adsorb a particular material is related to its exposure to other materials that may be present or may have

previously been present in the background environment. Carbon responds to materials on an ordered scale. Materials higher on the scale will make adsorption of materials lower on the scale difficult or impossible. Because of concern over this phenomenon warfighters are forced to change carbon beds, including filters and protective suits on a very conservative time schedule. Example applications where this is a concern are:

1. Gas masks,
2. Collective Protection Filters for tents, shelters, aircraft, ships, and other safety enclosures,
3. Instruments requiring a carbon filter in order to introduce a clean gas sample for reference or clear down purposes, for example Ion Mobility Spectrometers (IMS) such as CAM or ACADA, ionization detectors such as the M8A1, and even the original M8 wet chemical system, require an air sample assumed clean because it has been passed through an activated carbon filter,
4. Ship citadel systems,
5. Chemical protective garments with an embedded carbon matrix,
6. Numerous industrial processes utilizing a carbon bed to adsorb volatile organic compounds from manufacturing, painting, and other processes requiring the use of solvents.

Work performed for Natick at Battelle Memorial Research Laboratories through a Du Pont subcontract points to four contaminants, present in military environments that load the activated carbon rendering it ineffective. Figure 1 below illustrates chemical structures for the four chemicals that are components of complex contaminants such as diesel smoke, jet fuel, and cigarette smoke.

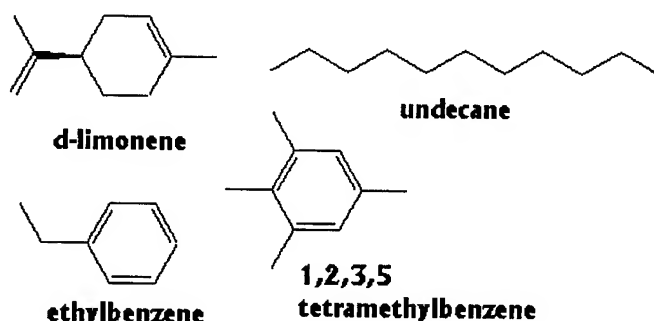


Figure 1 - Chemicals present in battlefield contaminants that have been shown to interfere with CW agent adsorption

Activated carbon is a micro-porous, carbonaceous material made from various raw materials, such as wood, coal, lignite, and coconut shells. The raw materials are converted into activated carbon using steam or acid. This activation process creates an internal pore network and deploys specific surface chemistries inside each particle, thus giving the carbon unique filtering capabilities. Different activated carbon products made from different raw materials using different processes will have different pore structures and adsorb different VOCs preferentially. The unique structure of carbon produces a very large surface area. One pound of granular carbon typically provides a surface area of 125 acres. The carbon surface is non-polar which results in an affinity for non-polar adsorbates such as VOC's. Adsorption arises as a surface phenomenon in which an adsorbate is held onto the surface of the carbon by electrostatic Van der Waals forces and saturation is represented by an equilibrium point. Adsorption occurs via condensation of the adsorbate in the adsorbent pores and a larger total pore volume will therefore result in a higher maximum adsorption capacity. Carbon is also capable of chemisorption, whereby an irreversible chemical reaction takes place at the carbon interface, thus changing the state of the adsorbate. Parameters that influence adsorption properties include surface area, pore size, particle

size, temperature, concentration of adsorbate, pH, contact time, ash, and apparent density. Different CW protection devices utilize different activated carbon products and will have different adsorption characteristics including VOC adsorption preference.

The Life Cycle of a CW adsorbent bed used in Military applications

Activated carbon used as an adsorbent has a history beginning with its manufacture and ending with its disposal that must be taken into account in ensuring its effectiveness. A number of problems can occur throughout its life cycle that may render it ineffective. In addition CW protective items are made in very large quantity and keeping track of them is a major concern. For example, according to public figures available from Natick, over 1.5 million M40 gas masks were made during the years 1987 through 2000. Each of the M40 masks used in the field requires a constant stream of filter cannisters during use. During peacetime cannisters exposed to agent are discarded after 30 days and cannisters not exposed to agent are discarded after one year. Figure 2 illustrates a simplified life cycle for a CW protective item.

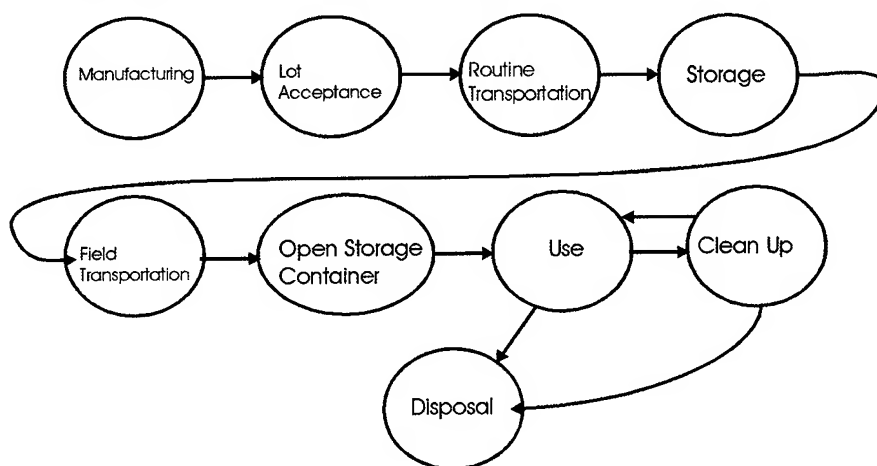


Figure 2 - Life Cycle of a Carbon Bed used in a CBW Protection Device

Items are manufactured, packaged in a protective container or bag, and organized into lots. Some of the items are chosen for lot acceptance. The lot is accepted and placed in storage. When required the items are transported to the field, perhaps after years of storage. The package is opened which may be considered final acceptance. Based on discussions at the First Residual Life Indicator Symposium held at Natick, bags are sometimes found to be open when received in the field presenting troops with the dilemma of whether to use them. The item is used in a difficult and rapidly changing battlefield environment. Some items may be cleaned, for example garments, and re-used. All items end their life with disposal. Contamination of the activated carbon bed can occur anywhere in the process from manufacturing to disposal. Two pieces of information would be useful to users:

1. The capacity remaining on the activated carbon at any particular time, and
2. The identity of the item

The following useful tasks could be accomplished using this information:

- A. Troops could be assured that their Chemical Protective gear had adequate capacity during a mission

- B. Protective gear could be re-supplied as required rather than on a conservative time schedule by electronically determining gear status through a digital communications system and sending gear to where it is most needed
- C. If protective bags or containers are damaged the items could be tested in the field minimizing re-supply requirements
- D. Contaminated items could be tracked back through the logistics pipeline to a problem source such as a warehouse or factory.

Our Residual Life Indicator projects are focused on developing sensors that could be used to perform the tasks above.

Using a simple inexpensive Badge and a Reader to Estimate the Remaining Capacity of a Garment

Our Du Pont work was based on the assumption that we could estimate the remaining capacity of a protective garment to adsorb chemical agents by measuring the concentration of the target materials listed in figure 1 known to load the garment. This strategy is quite unlike current patents that describe systems that measure the breakthrough of the contaminant that the garment or gas mask filter is designed to protect against. We feel our new sensor system is superior because exposure to chemical warfare agents should be rare and may be at high concentration where the contaminants inhibiting CW agent adsorption build up at low concentration over a long period of time.

In order to keep the cost of the chemical sensor down we proposed building an inexpensive dosimeter that could be used to estimate exposure to the contaminants at a convenient point, say inside the garment, and a more expensive reader that could be used by a chemical officer to estimate suit loading based on an electronic reading from the badge. The reader would also serve as a data terminal transmitting suit data on a digital communications link to command headquarters where data from many suits could be integrated with threat data in order to plan re-supply efforts. During the First Residual Life Indicator Symposium at Natick we briefed this system. The military customer community reinforced our feeling that a reader-badge system would be superior to a badge that a soldier would read by eye. We have thus continued to develop our system around a separate badge and reader.

Evolution of Scentczar Corporation Residual Life Indicator Projects

Figure 3 illustrates the evolution of our work with Residual Life Indicators. Scentczar Corporation began our Residual Life Indicator development effort by attempting to develop a fluorescent sensor for the target compounds listed in figure 1. Examining the ring structure of the target compounds,

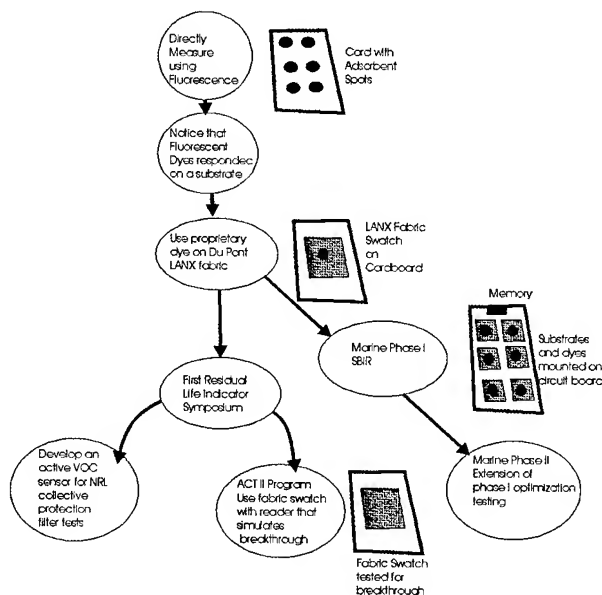


Figure 3 - RLI Evolution at Scentczar Corporation

three of the compounds have a ring structure that should fluoresce, and the fourth, undecane might be used to inhibit fluorescence. Our first concept was to use a card with adsorbent spots. Three of the spots would be used to adsorb the three fluorescent contaminants and the fourth spot would be used to detect undecane through fluorescence inhibition. As it turns out the materials did not fluoresce with sufficient intensity to make the technique practical. During this work we discovered that we could make a fluorescent dye spread on a substrate material in response to our target materials however. We spotted the material on Du Pont LANX fabric and found that it would spread over the fabric. Du Pont requested that we perform an extensive test program using badges made of fabric swatches spotted with our dye. We performed tests over a variety of temperatures and contaminant concentrations. We found two problems with this system:

1. The fabric fluoresced which created some problems with detecting the fluorescent dye, and
2. The dye tended to migrate down into the fabric rather than across its surface losing fluorescent signal.

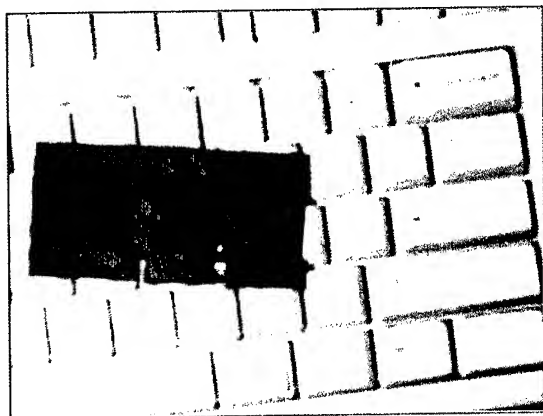


Figure 4 - Du Pont Badge

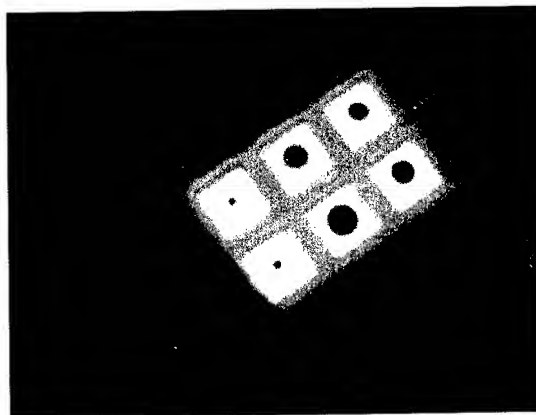


Figure 5 - Marine Corps Phase I Badge

At this time we proposed going back to the original experiments and using a simple paper substrate. This was the subject of our proposal to the Marine Corps. During our Marine Corps phase I we performed extensive tests to optimize the substrate-dye combination for detecting our chemicals of interest. Figures 4 and 5 are pictures of the original Du Pont badge and the badge delivered at the end of the Marine Corps phase I effort.

Reader Evolution

Over the course of the Du Pont project and the Marine Corps phase I project we have develop two reader designs. These are pictured in figures 6 and 7 below.

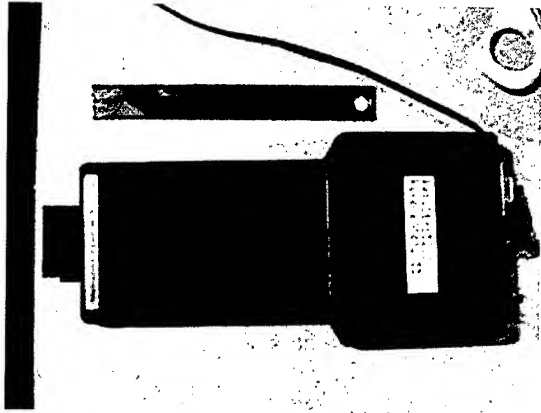


Figure 5 - Du Pont Reader

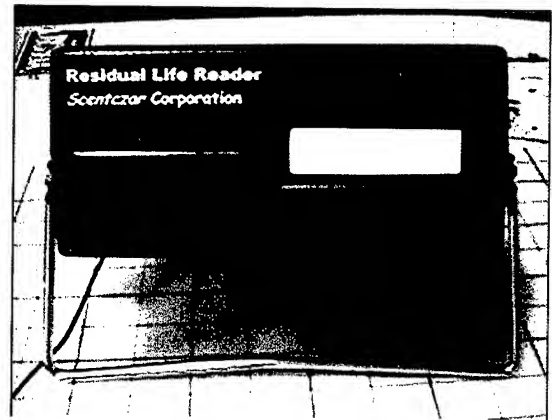


Figure 6 - Marine Corps Phase I Reader

The Du Pont reader used a pair of fluorescent lamps to illuminate the badge carrying a fabric swatch with a dye spot as it was inserted into the handle. The fluorescent signal was read by a linear array of photodiodes as the badge passed under it in the handle. The reader kept track of the badge position with an infrared sensor positioned along the side of the badge support. This system turned out to have difficulties because the position reading was noisy. The phase I reader was much better using an internal scanner. The user plugs the badge into the reader and the reader scans the badge. The phase II reader will use a camera imaging system.

Using a fabric swatch to estimate Residual Life

Our team gained extensive experience with LANX fabric while performing the Du Pont work. We became interested in another, entirely different approach to the problem. Our new approach would be to use fabric swatches directly as an indicator of garment capacity. This is the approach we proposed to the Army under their ACT II BAA program sponsored by the Battle labs. In this approach a fabric swatch is exposed to the same contaminants as the protective garment and field tested in a reader which exposes the fabric swatch to a simulant on one side and estimates breakthrough by measuring the response with a chemical sensor on the other side.

Figure 7 is a block diagram of this approach. The reader is on the left and the badge is on the right.

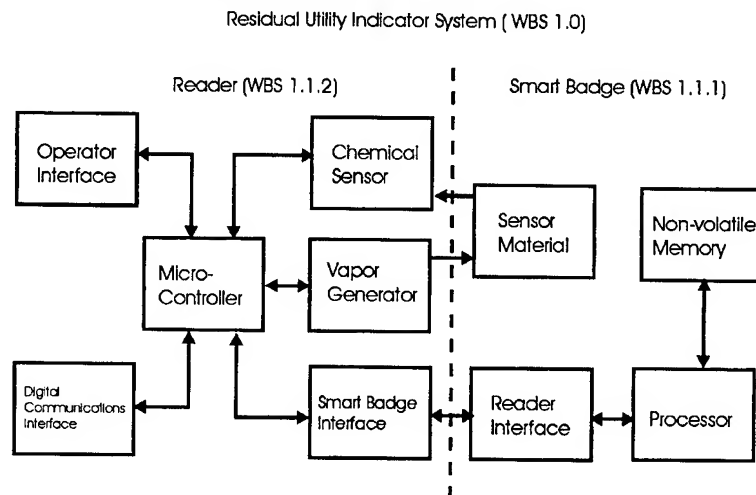


Figure 7- ACT II Concept

When the badge is inserted in the reader the vapor generator generates a small amount of vapor that exposes one side of the fabric swatch to a high concentration of simulant. The chemical sensor on the other side of the swatch monitors for simulant breakthrough. The microprocessor in the reader uses the breakthrough information to calculate the residual life of the garment.

The Active Sensor Approach

The third approach, shown in figure 8, under investigation is an active approach using a semiconductor sensor which changes its resistance with exposure to VOCs. This approach uses an active semiconductor sensor to detect contaminant build up in real time. Scentzar Corporation is currently supporting a test program at Naval Research Laboratory using this system.

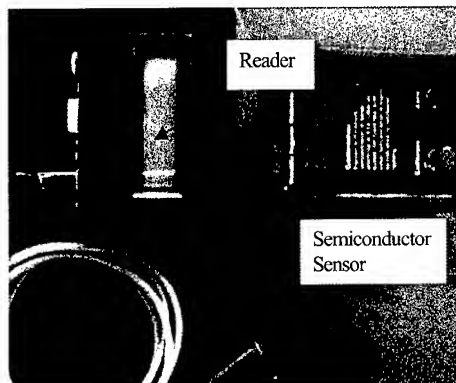


Figure 8 - Real Time Sensor

Comparing the Three Techniques

Table 1 compares three techniques described above.

Table 1 – Comparison of Three Residual Life Indicator Techniques

Technique	Advantages	Disadvantages
Miniature Passive Indicator (MPI) under development for USMC	Simple, inexpensive, chemical dosimeter sensitive to compounds known to load activated carbon bed.	Other chemicals unknown at this time may be present in the military environment and load the activated carbon beds.
Using a swatch of material as a test bed as proposed to U.S. Army under their ACT II program.	Should behave in exactly the same manner as the carbon bed that it is protecting. Readings from a swatch should be independent of the chemical that loaded the carbon bed.	Much more complex reader than the MPI requiring a device to generate simulant vapor and a detector.
Active Sensor	Accurately determine carbon bed loading in real time. Since loading is dependant on environmental conditions a real time sensor is required to track loading.	An active sensor will require a continuous source of electrical power. Practical sensors usually must be heated and can break down.

References

1. Cheremisinoff, Carbon Adsorption Handbook
2. Diederer, Michael, "Residual Life Indicator (RLI) Chemical Warfare Agent Testing of Chemical Protective Materials", Final Report for Contract LSH-84604-S, October 1999, Battelle memorial Institute, Columbus Ohio
3. Diederer, Michael, "Residual Life Indicator (RLI) Chemical Warfare Agent Additional Testing of Chemical Protective Materials", Final Report for Contract LSH-846004-S, October 1999, Battelle memorial Institute, Columbus Ohio

DEVELOPMENT OF μ CHEMLAB™/CB FOR DETECTION OF BIOTOXINS

*Julia Fruetel, Ronald Renzi, Robert Crocker, Victoria VanderNoot, Scott Ferko,
Jamie Stamps, Isaac Shokair, Dan Yee and Charlie Hasselbrink*

Sandia National Laboratories, Livermore, CA 94551-0969

ABSTRACT

We have developed a research prototype device for low level detection of SEB, ricin, botulinum toxin and ovalbumin in liquid samples. This hand-held, low power device analyzes samples by capillary zone electrophoresis (CZE) and capillary gel electrophoresis (CGE) in a parallel microchannel format, and provides sensitive detection of fluorescently-tagged analytes using miniature 392 nm diode laser-induced fluorescence. We have successfully demonstrated simultaneous parallel channel separations, fully automated high voltage control of fluidics and automated data analysis with toxin identification and semi-quantitation in the presence of aerosol backgrounds in a stand-alone self-contained unit. Tests of the fully integrated device indicate high sensitivity detection (as low as 5 nM) and cycle times of 5-10 minutes.

INTRODUCTION

As part of DOE's Chemical and Biological National Security Program (CBNP), Sandia National Laboratories is developing hand-held sensors designed to detect a broad range of chemical and biotoxin agents at high sensitivity levels and low false alarm rates. At the heart of these devices are micromachined chips that will contain arrays of parallel microseparation channels. Each channel will be designed to separate compounds on the basis of distinct chemical interactions, allowing multiple chemical properties of the compounds to be probed simultaneously. Following separation, the compounds will be detected using highly sensitive techniques, such as laser-induced fluorescence for the biotoxin separations, and arrays of surface acoustic wave sensors for the chemical agent separations. A detailed signature, generated for each compound from the analyses by multiple "orthogonal" separation techniques, will enable identification of an agent of interest based on its unique chemical and physical properties. The result will be a highly sensitive chemical sensor with a very low false alarm rate.

Two discrete devices are currently being developed: one to detect chemical agents using gas-phase analysis and another to detect biotoxins using liquid-phase analysis. Both μ ChemLab/CB devices employ modular designs to facilitate subsequent upgrades for improved performance and to detect expanded sets of target analytes. The expected result of this effort is a relatively universal sensor platform that will provide unprecedented chemical analysis capability that is compatible with the need for extensive low cost distribution, ease of use and autonomous operation.

We describe here our progress in developing a liquid-phase analysis device for low level detection of protein biotoxins (the gas-phase device for chemical agents is described elsewhere in these proceedings). Recently, a research prototype device underwent preliminary testing to validate our technological approach toward bioagent detection. At the heart of this device is electrokinetic fluid movement, whereby fluids are manipulated through microchannels by the application of high voltages (0-5 kV), enabling precise fluid handling in the absence of mechanical pumps or valves. Two separation techniques were implemented in the prototype device that separate molecules based on different, or

orthogonal, properties. The goal of the testing was to demonstrate the integration of parallel microchannel separations and ultrasensitive laser-induced fluorescence detection for the analysis of biotoxins in a miniaturized low power device. Although this system is compact and fully integrated, it is not built for field robustness. The results of this testing and an assessment of the current technology status are described.

SYSTEM DESCRIPTION

The prototype unit is a compact, fully integrated system designed to detect ricin, SEB, ovalbumin and botulinum toxin at nanomolar (10^{-9} M) concentrations (Figure 1). It is composed of a dual channel separations module with an interchangeable microfluidic reservoir module, a dual UV diode LIF detection module, an integrated multichannel high voltage power supply controller, and a main control board containing the laser diode drivers, detector amplifier, and an embedded microprocessor. Liquid samples are introduced to the device through an external syringe injection port. The prototype weighs 6 lbs and is packaged within a solid enclosure approximately 7 x 8 x 4.5 inches in size. The packaging is designed for continuous operation at room temperature and storage above 0 °C, and is sealed except for an external fan. The unit is powered by either twelve 3-volt lithium batteries, which is sufficient for about 16 hours of continuous use, or by wall plug. The user interface to the prototype consists of a four-line text LCD display and a menu-driven command interface using a four-button keypad. The system is fully automated except for sample preparation and introduction into the unit (syringe injection). An external laptop computer can be coupled to the box for chromatographic display and to download data, but is not required for operation. The unit typically requires 10 minutes to power up, self-test, and warm-up prior to analysis. The time necessary to analyze a single sample following injection is approximately 5 minutes for the CZE channel and 11 minutes for the CGE channel. These cycle times include 30-60 seconds for injection, 3-9 minutes for separation and 1 minute for analysis.

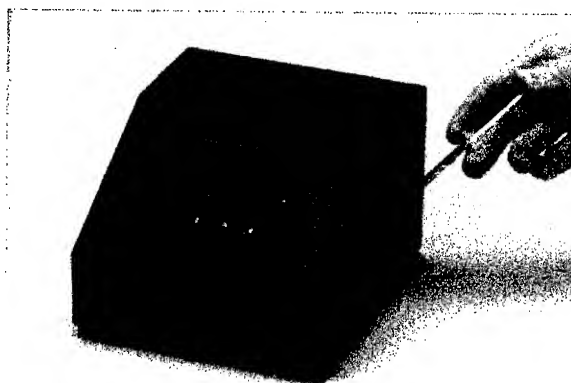


Figure 1: The μ ChemLab™/CB research prototype for biotoxin detection and analysis.

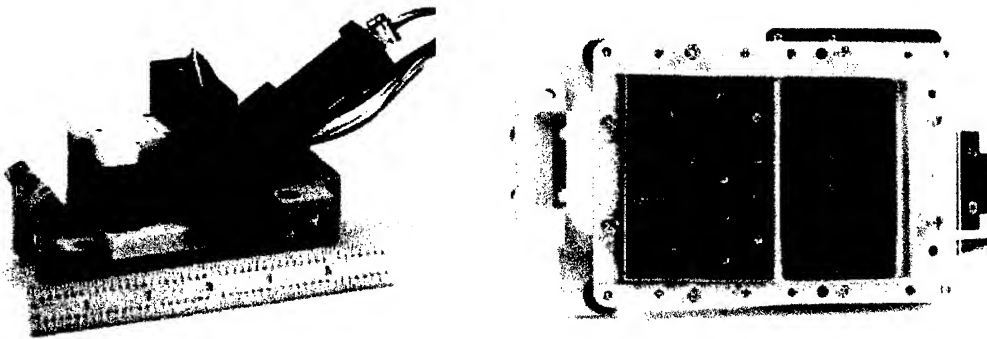


Figure 2: The separations module of $\mu\text{ChemLab}^{\text{TM}}/\text{CB}$ includes the sample introduction ports, fluid reservoirs, laser housing, photomultiplier tube, and etched fused silica wafer (close up view of wafer at right).

The separations module (Figure 2) contains two independently controlled 10-cm separation channels in a fused silica substrate: one for capillary zone electrophoresis (CZE) separation and one for capillary gel electrophoresis (CGE). Each separation channel has a sample introduction port, and sample, sample waste, buffer and buffer waste fluid reservoirs. All eight reservoirs are housed in a single cartridge for easy removal and replacement. The CZE reservoirs incorporate a novel dual-compartment design to enable extended testing (1). The integrated high voltage power supply/controller supplies up to 4500 V as needed for the separations.

Prior to syringe injection into the system, analytes are fluorescently tagged for detection. Liquid samples in pH 9 buffer containing an internal standard are labeled by adding one-tenth volume fluorescamine solution in acetonitrile and thoroughly mixing for 10 seconds. Following sample injection into the device, the system is actuated using the front keypad to begin electrokinetically introducing the sample via the injection channel (inject mode), followed by separation of the sample in the separation channel (run mode).

Detection of the analytes is accomplished by laser-induced fluorescence and employs an air-spaced modular optical design (Figure 3). Excitation light is provided by two Nichia 392 nm laser diodes (one for each channel), and fluorescence is filtered then collected onto a single



Figure 3: The optics module of $\mu\text{ChemLab}^{\text{TM}}/\text{CB}$ houses two 392 nm diode lasers, optics to filter and trim the laser beam, beam steering components to align the laser beams to the separation channels, and a single PMT to collect fluorescent signal from both channels.

photomultiplier tube (PMT) using synchronized laser pulsing and data collection. Signals from the PMT are sent to an Onset 68030-based microcontroller for on-board data processing. An LCD display on the unit provides control information and a readout of the approximate concentrations of the target agents.

Prior to the analysis of unknown samples, a series of toxins at known concentrations were run in the device to generate a database for all toxins, internal standards, and any other known interferants (excluding aerosol backgrounds). The on-board data recognition software uses the database information to detect and provide semi-quantitative biotoxin analysis of unknown samples. Peaks that correspond to species in the database are fitted to gaussian peak shapes to determine amplitudes and thus concentrations. The “goodness of fit” is determined for each fitted peak—based on signal-to-fit-error and signal-to-noise ratio—and is used to evaluate the likelihood that the detected peak corresponds to a toxin in the database.

SAMPLES

Commercially available ricin, SEB, ovalbumin and a botulinum toxin surrogate, IgG, were prepared and analyzed as provided by the commercial supplier. Indoor and outdoor aerosol samples collected at Lawrence Livermore National Laboratory using a SASS 2000 collector were run to determine the system response to background species and to assess the potential for false alarms. The samples were diluted to be equivalent to 750 L air per mL. Aerosol samples spiked with toxins were analyzed as “unknown” samples to demonstrate toxin identification and quantitation in a simulated aerosol collection sample. Blank samples were run after toxin- and aerosol-containing samples as appropriate to address contamination and carryover issues.

RESULTS

System Integration and Automation

We have successfully demonstrated simultaneous two-channel analysis in a fully automated compact device. As many as 50 runs were performed over two days with both channels operating in parallel without any serious system problems (a fluid leak at one of the reservoirs caused a minor electrical short). Extensive testing of CZE and CGE separations in single channel mode indicated that electrokinetic injection and separation together with fluorescence detection can be implemented in a hand-portable device to give reliable, interpretable results. Operation of both channels simultaneously indicates successful isolation of high voltage supplies in a compact design as well as appropriate laser modulation and signal processing in order to interpret two channel analysis with a single PMT. Data analysis of the CZE results was automated and tested in the device to give on-the-spot peak identification and semi-quantitative analysis.

Separations Performance

The two separation techniques tested in the μ ChemLab prototype device were chosen because they separate molecules by different physical properties. CZE separates molecules based on charge-to-mass ratio. The buffer chosen for the CZE separation in the device contains phytic acid (10 mM, pH 9.5), a poly-anionic buffer that ion-pairs with proteins and decreases protein interactions with the channel walls, and the zwitterionic detergent dodecyl-DAPS (2 mM), which we found to enhance the fluorescence intensity of tagged proteins as well as improving protein peak shape and resolution. CZE analysis using this buffer provides resolution of all four toxins in about 3 minutes at a separation field strength of 400 V/cm (Figure 4).

CGE, on the other hand, separates proteins based on molecular weight. The presence of high concentrations of the anionic detergent sodium dodecylsulfate (SDS) in the separation media coats the proteins such that they all have the same charge to mass ratio. Consequently, each protein electrophoreses at the same rate under these conditions, and it is the presence of sieving media (Beckman 14-200 sieving gel) which differentially retards proteins with molecular weights greater than 14 kDa. CGE analysis of the toxins is shown in Figure 5.

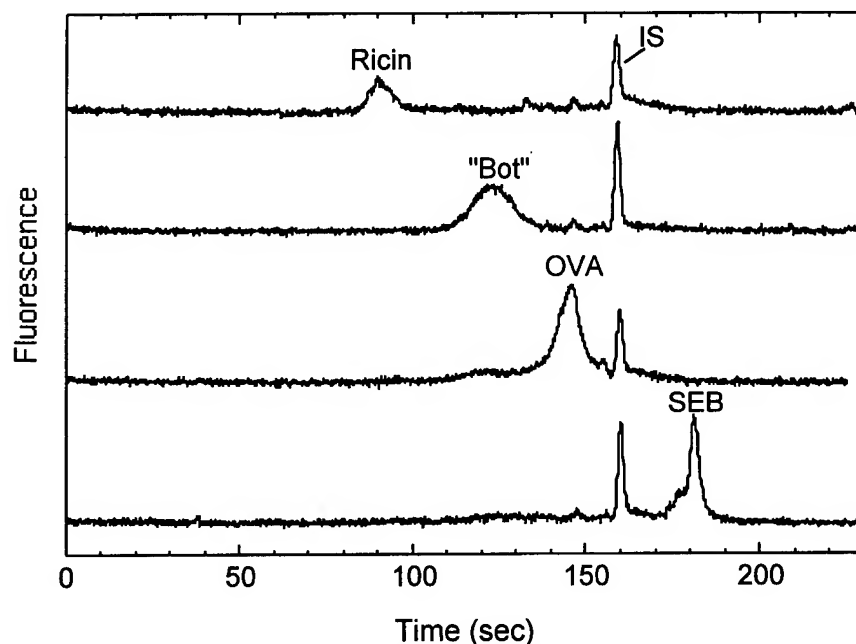


Figure 4: CZE separations of toxins in the μ ChemLab device: 50 nM ricin, 50 nM botulinum toxin surrogate, 50 nM ovalbumin and 25 nM SEB. "IS" indicates the internal standard (CCK flanking peptide).

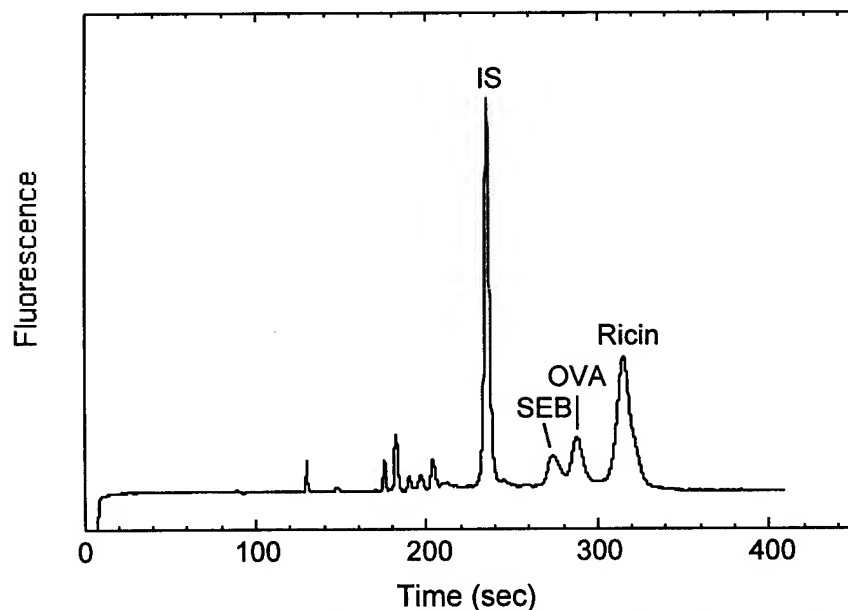


Figure 5: CGE separation of 180 nM SEB, 50 nM ovalbumin, 270 nM ricin and internal standard (-lactalbumin).

Testing over a several day period was performed with each separation in single channel mode in order to test the reproducibility of the separations. Analysis of a sample and then subsequently a buffer blank indicated some carryover was present in the next run for both types of separation. Procedurally, this was addressed by injecting each sample twice and using the data from the second run; however, system redesign is planned to better address this issue.

For the CZE channel, 35 samples were analyzed over a several day period. The reproducibility of the internal standard elution time, used as a measure of the system stability over the course of a day and from day to day, is shown in Figure 6. The results from 51 runs over a three-day period indicate variations of 3.6% RSD, and corrected retention times for the toxins showed day-to-day reproducibilities of <2%, indicating quite reasonable stability. Experience with the device indicates that elution time reproducibility is closely linked to establishing reproducible current flows in the microchannels. Once this is established, repeatable separations can be obtained for the lifetime of the fluid reservoirs.

Testing of the CGE separations indicated that although reproducible separations could be obtained, over time increased backgrounds, varying backgrounds and variable peak elution times were observed. Further improvements in system stability, such as flow monitoring and control, are expected to yield more reproducible results.

Sensitivity

Measurements of the sensitivity with the integrated device indicate that toxin concentrations as low as 5 nM are detectable. Concentration detection limits were slightly lower for CGE than CZE, which likely reflects a preconcentration effect observed for the CGE separation. Sensitivity in the presence of aerosol backgrounds is approximately the same as that observed without backgrounds due to the lack of interference of aerosol peaks at these toxin concentrations (see Figures 7 and 8).

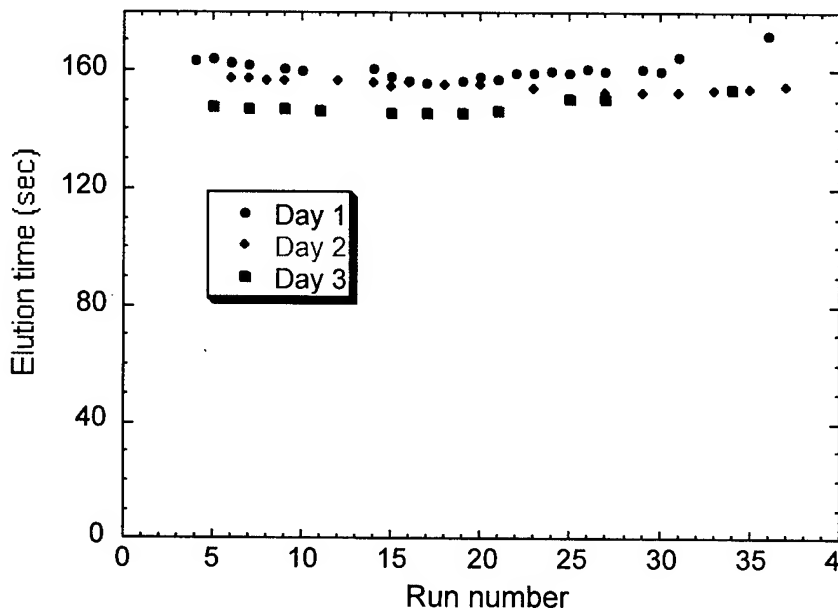


Figure 6: Plot of the CZE elution times of the internal standard versus run number for three days.

Impact of Aerosol Backgrounds on Performance

Analysis of indoor and outdoor aerosol samples by CZE and CGE indicate the presence of a few peaks of fairly narrow width (Figures 7 and 8). Separations of aerosol samples spiked with individual toxins indicate few if any of the major aerosol peaks coelute with the toxin peaks, with the exception of an aerosol peak eluting close to ricin by CZE (Figure 7). To determine if the presence of aerosol backgrounds creates a problem for identifying and quantitating toxins, preliminary data analysis was performed on 13 samples separated by CZE. Initial goodness-of-fit criteria were developed to identify biotoxin peaks in the CZE separations using a limited database of 12 samples. These criteria were then used to perform blind analyses of samples containing aerosol backgrounds spiked with and without biotoxins. Using only the results from the CZE channel, 10 out of 13 samples were correctly identified. Further characterization of the system is needed to develop robust criteria that relate the goodness-of-fit criteria with statistical confidence levels. Additionally, incorporation of the CGE data analysis will improve the true positive rate and lower the false alarm rate. However, because elution times are still variable with the CGE system, a reliable database has not yet been obtained in order to quantitate and identify unknown toxin samples. Work to improve CGE reproducibility is in progress.

Next Step Improvements

Because separations reproducibility is closely linked to reproducible fluid flows during injection and separation, techniques to better control flows in microchannels are currently being tested with the device. Additional improvements in methods reproducibility will come from elimination of sources of variation in the system, including optimization of the sample injection process and elimination of sample carryover. The sample preparation procedure used for these analyses was found to be reasonably robust. By using a large excesses of dye over protein concentration ($\sim 10^6$ -fold), reproducible and complete labeling is observed, even with subtle

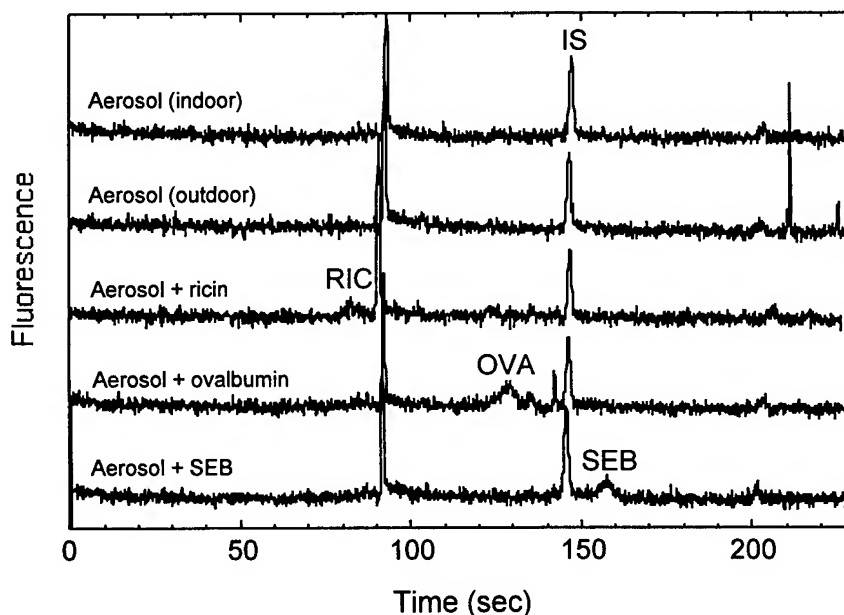


Figure 7: CZE analysis of aerosol backgrounds alone and spiked with toxins.

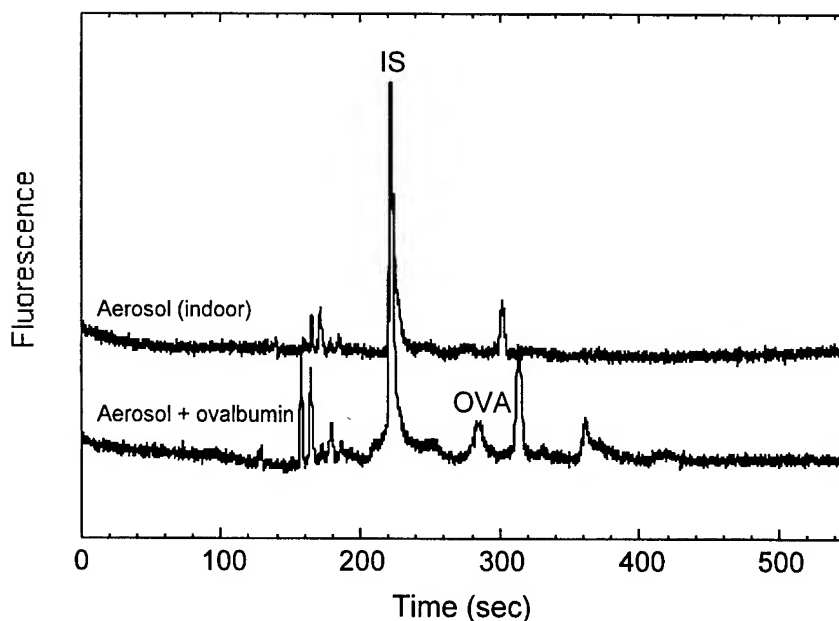


Figure 8: CGE analysis of aerosol background alone and spiked with ovalbumin.

variations in the sample preparation. The presence of aerosol species seems to have little effect on the efficiency of toxin labeling, although this will require further testing. Improvements in detection sensitivity will come with improvements in laser design/power, injector design and preconcentration techniques.

Although the lifetime of consumables in this device may be an issue for prolonged unattended operation, the implementation of the dual reservoir design greatly extended the testing period over previous designs (1). It is estimated that ~100 runs can be performed before buffer reservoirs need to be replenished in the current design.

CONCLUSIONS

We have successfully demonstrated the integration of parallel microchannel separations and ultrasensitive detection for the analysis of biotoxins in a compact low-power device. This technology shows excellent promise for becoming the basis of robust chemical and biological sensor platforms. The power of this technology lies in its applicability to a wide range of analytes and its extendibility to multiple dimensions while maintaining a microscale format. The incorporation of additional orthogonal separation channels will provide increased confidence (low false alarm rates) for analyte identification and will expand the range of analytes detectable. The use of robust, well-characterized chromatographic materials as the basis for analyte detection will enable long device lifetimes while addressing complex “real world” samples. Integration of this analysis system with an aerosol microcollector and automated sample preparation stage, together with the gas-phase chemical agent detection unit, will provide a complete stand-alone portable chem-bio detection unit.

REFERENCES

- (1) “On-Chip Separation of Explosive Compounds—Divided Reservoirs to Improve Reproducibility and Minimize Buffer Depletion,” S.R. Wallenborg, C.G. Bailey and P.H. Paul, Proceedings of the μ TAS

2000 Symposium, Enschede, The Netherlands, May 14-18, 2000; Kluwer Academic Publishers, Dordrecht, The Netherlands.

ACKNOWLEDGMENTS

Sandia National Laboratories is a multi-program laboratory operated by Sandia Corporation, a Lockheed Martin Company, for the United States Department of Energy under Contract DE-AC04-94AL85000. Funding was provided by DOE's Chemical and Biological National Security (CBNP) Program.

MINIATURE CHEMICAL ANALYSIS SYSTEM (μ ChemLab) FOR CHEMICAL AGENT DETECTION

Patrick R. Lewis (505-284-3315, prlewis@sandia.gov), Gregory C. Frye-Mason (505-844-0787, gcfrye@sandia.gov), Richard J. Kottenstette, Ronald P. Manginell, George R. Dulleck, Douglas R. Adkins, Edwin J. Heller, Curtis D. Mowry, David Martinez, Darryl Y. Sasaki, and Lawrence F. Anderson
Microsensor R&D Dept., MS-0888, Sandia National Laboratories, Albuquerque, NM, 87185-0888

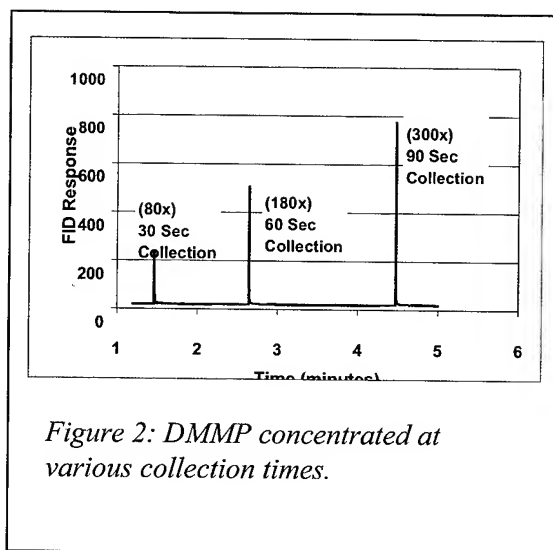
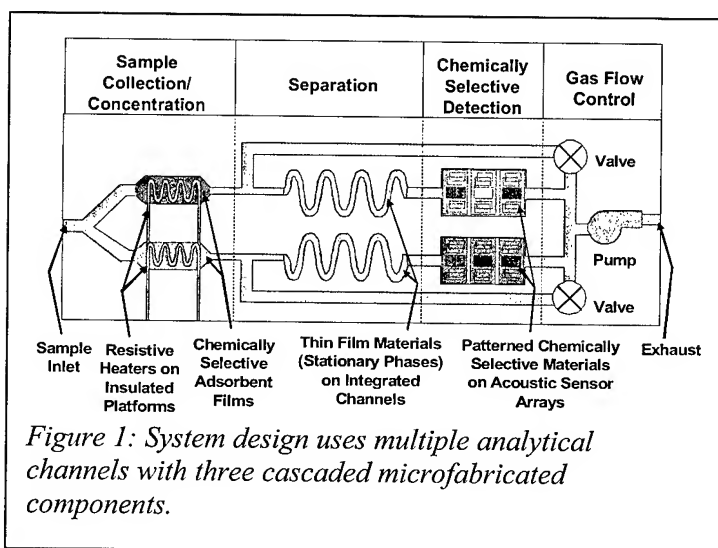
ABSTRACT

Sandia is actively developing autonomous, hand-held chemical analysis systems based on microfabricated components (μ ChemLab). Microfabrication provides small size, faster response, lower power, and the potential for low cost and improved ruggedness. Part of this program is a gas phase analysis system for detection of chemical warfare (CW) agents, initially focused on G class nerve agents and mustard gas. The system design includes three cascaded components to provide high sensitivity and chemically selective detection: (1) a sample concentrator/collector, (2) an on-chip gas chromatographic (GC) column, and (3) an array of surface acoustic wave (SAW) sensors. Our current prototype measures 8"x4"x2.8" and has been demonstrated to provide rapid (two minute) and sensitive detection of both CW simulants and actual agents.

Keywords: sample concentrator, gas chromatograph, GC, surface acoustic wave, SAW, chemical warfare

SYSTEM DESIGN

The goal of Sandia's μ ChemLab program is to use microfabrication and microsystem engineering to develop a battery operated and hand held analytical system that could provide rapid and reliable identification and detection of trace concentrations of target analytes. While the overall program includes both liquid phase and gas phase analytical trains, this paper will describe only development and results for the gas phase side, shown schematically in Figure 1. This figure shows the basic design that includes two analytical channels¹. While each channel cascades the same three parts, the parts for each channel are engineered with different chemistries. These components and their contribution to achieving the previously stated goals will be described individually below.



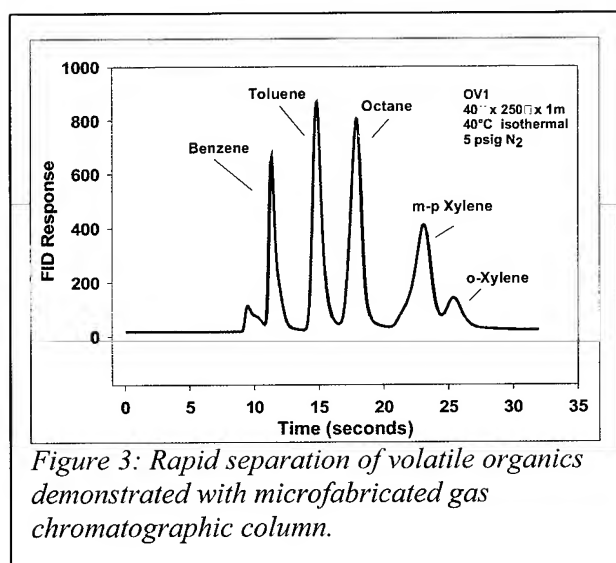
MICROFABRICATED SAMPLE CONCENTRATOR/COLLECTOR

The first component is a microfabricated sample collector/concentrator. It employs a thermally isolated membrane with a resistive heater to provide rapid and low power heating. Similar in design to micro-hotplate devices used for combustible gas sensors, these membranes can be heated to 200°C in <10 msec with <200 mW of power². Typical membrane sizes are on the order of 2.5x2.5 mm and are coated with a microporous sol-gel adsorbent. The data in Figure 2 demonstrate the sample concentrating ability of this component using a conventional GC system with a flame ionization detector (FID). A sarin (GB) simulant (dimethyl methyl phosphonate or DMMP) is present at ~200 ppb in the gas passing over the preconcentrator. The analyte collects in the sol-gel coating when the heater is unpowered. The three spikes shown are the rapid concentrated chemical pulses produced when the heater is powered. The concentration enhancements (peak height compared to unconcentrated analyte response) are 80x, 180x, and 300x for the 30, 60, and 90 second intervals. The peak widths of these pulses are typically 100-200 msec, providing sharp chemical inputs to the gas chromatographic separation stage. Another advantage of the preconcentrator is its ability to discriminate against volatile interferants. This is achieved by tailoring the sol gel coating to selectively collect and concentrate the target analytes. For example, with the preconcentrator shown in Figure 2, the semivolatile DMMP is collected and concentrated effectively while volatile organic compounds (VOCs) such as acetone, trichloroethylene, and toluene are poorly collected. Since VOCs are potential background interferants that may be present at high concentrations due to their high vapor pressures, the ability of the preconcentrator to discriminate against these compounds can provide a significant performance advantage.

HIGH ASPECT RATIO MINIATURE GAS CHROMATOGRAPHIC COLUMN

The sample collected on the preconcentrator is thermally desorbed onto a high aspect ratio microfabricated GC column. These columns are typically one meter long yet are enclosed in an area of only 1.0 to 1.5 square centimeters. The channel itself is typically 400 µm deep and has been manufactured to be 40 - 100 µm wide. Fabricated in silicon, the channel that forms the GC is deep reactive ion etched so that the walls of the channel are parallel. Next, a Pyrex lid is anodically bonded to the Si wafer to form the flow channel³. The small heat capacity allows the column

to be rapidly heated for temperature ramp chromatography using a thin platinum layer on the back of the Si chip as a resistive heater. Finally, a thin polymer stationary phase is deposited in the channel to complete the GC column. Though these GCs are only one meter long, they possess enough separating power to resolve several analytes. For example, Figure 3 shows a rapid (30 sec) separation of BTX and octane using a microfabricated GC column. Each channel of the gas phase analytical train includes a GC column of a different polarity. As in classical bench top gas chromatography, dual columns enhance the selectivity of the overall system by providing two retention times with which to identify the compounds of interest.



SURFACE ACOUSTIC WAVE ARRAY DETECTOR

The final stage of the gas phase detection train is the surface acoustic wave array. These arrays are coated with chemically selective coatings that provide a distinct pattern for different classes of compounds⁴. In addition to unique patterns for different compounds, the SAW devices also provide high sensitivity. Figure 4 shows responses for two sensors from a four sensor array selectively detecting two target analytes

separated in time by the GC column. A strong hydrogen bond acid coating (BSP3) provides selective detection of the DMMP (a sarin/GB simulant that comes out at about 15 seconds) while ethyl cellulose (EtCell) provides the largest response to methyl salicylate (a mustard/HD simulant that comes out at about 42 seconds). The data show the detection of 75 ppb DMMP and 1ppm methyl salicylate in the presence of 75 ppm of a xylene background interferant; however, only two peaks are displayed. As described above, the interfering xylene was ignored by the sample preconcentrator/collector. Due to the selectivity of the preconcentrator, the xylene does not interfere with the analysis even though it was present at a concentration almost 1000 times that for DMMP. Also, the SAW array is only required to identify one compound at a time thanks to the resolving power of the GC column. To enable the fabrication of a miniaturized SAW array detector, high frequency drive circuitry ASICs have been developed and used to assemble a hybrid detector in a package measuring only 12x14 mm. Using a unique phase detection scheme, this packaged part has only DC inputs and outputs, even though the SAW device and ASICs are operating at over 500 MHz.

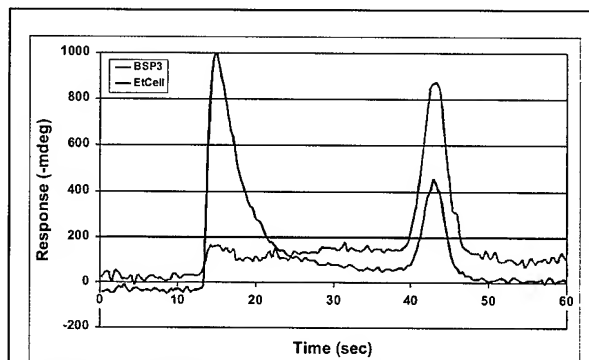


Figure 4: Chromatographically separated analytes generate a unique response pattern with a SAW array detector.

A PORTABLE TOTAL ANALYTICAL SYSTEM

Clearly, the concert of these three components provides a sensitive and selective analytical system that is sufficiently low power to be battery operated and sufficiently small to be handheld^{1,5}. Figure 5 shows the completed system, which includes the liquid phase components, assembled in an 8"x4"x2.8" box with a four button key pad and LCD display. This system consists of dual gas phase analysis channels on a 5.3x8.5 cm (2.5"x2.1") PC board. This board mates to a 8.9x8.5 cm (3.5"x3.3") PC board with all the support electronics such as temperature control circuits and 16 bit A-to-D converters for measuring the SAW detectors. A main board shown in Figure 5 has a microprocessor, memory, and a small power distribution board. The system can be operated autonomously with all system control and data acquisition and analysis being performed by the on-board microprocessor with results (agent detected and concentration) being displayed on the LCD display.

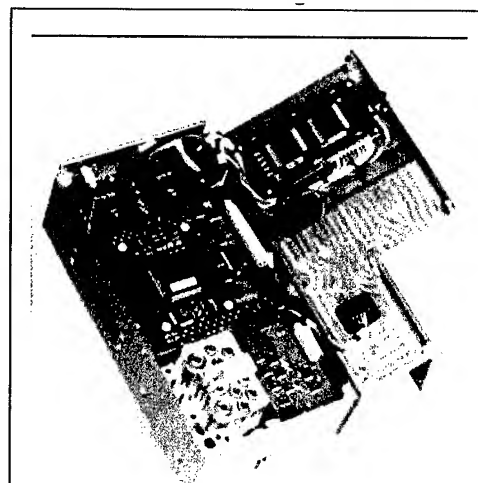
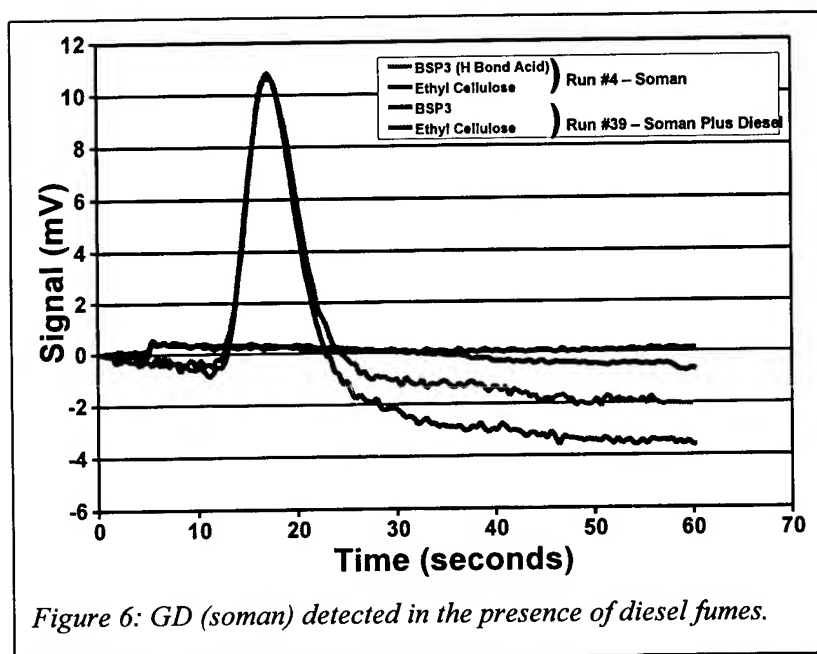


Figure 5: Picture of hand-held system being developed for gas and liquid phase analyses.

The gas phase side has been extensively tested with CW simulants (DMMP for sarin/GB, diethyl methyl phosphonate (DEMP) for soman/GD and methyl salicylate for mustard/HD). These simulants have been used both alone and in the presence of various potential interferants such as humidity, volatile organics (e.g., xylene), and semivolatiles (e.g., diesel). These tests have verified that we can separate these three simulants from each other and that we can detect them even in the presence of humidity, high concentrations of volatile interferants (up to 1000 times higher concentrations than the CW simulant), and significant concentrations of selected semivolatiles (e.g., 1% of headspace). In addition, live chemical warfare agents were performed with the Applied Chemistry Team of SBCCOM at Edgewood Chemical and Biological Center (ECBC). With the separating power of the microfabricated GCs,

μ ChemLab was able to resolve all of the G agents (GA, GB, GD, and GF were tested). Though mustard gas (HD) appeared to coelute with one of the G agents on one column stationary phase, it was separated on the other. In addition, the SAW array generated a pattern for HD that was unique compared to the G agents. μ ChemLab was also tested with live agents in the presence of interfering compounds. In one test, shown in Figure 6, GD was analyzed in the presence of 1% of saturated diesel headspace. This analysis was laid over a previous analysis of GD by itself. As can be seen in the figure, the analysis of GD was unaffected by the presence of diesel fumes. GD elutes at the same retention time and the array detected GD with the same pattern and sensitivity.



ACKNOWLEDGEMENTS

Sandia National Laboratories is a multiprogram laboratory operated by Sandia Corporation, a Lockheed Martin Company, for the United States Department of Energy under Contract DE-AC04-94AL85000. The authors would like to thank Jay Grate of Pacific Northwest National Laboratory for the BSP3 polymer, Kwok Ong and the Applied Chemistry Team of SBCCOM at Edgewood Chemical and Biological Center (ECBC), and Jeff Brinker, Randy Shul, Christi Willison, Janson Wu and Ron Renzi of Sandia. Funding was provided by Sandia's Laboratory Directed Research and

Development (LDRD) Program and DOE's Chemical and Biological Nonproliferation (CBNP) Program.

REFERENCES

1. G. A. Thomas, G. C. Frye-Mason, C. Bailey, M. E. Warren, J. A. Fruetel, K. Wally, J. Wu, R. J. Kottenstette, and E. J. Heller, " μ ChemLabTM - an Integrated Microanalytical System for Chemical Analysis using Parallel Gas and Liquid Phase Microseparations," *Proc. SPIE Unattended Ground Sensor Technologies and Applications*, **3713**, (1999), 66-76.
2. R. P. Manginell, G. C. Frye-Mason, W. K. Schubert, R. J. Shul and C. G. Willison, "Microfabrication of Membrane-Based Devices by Deep-Reactive Ion Etching (DRIE) of Silicon," *Proc. Microstructures and Microfabricated Systems IV*, Electrochemical Society: Pennington, NJ, **98-14**, (1998), 62-69.
3. C. M. Matzke, R. J. Kottenstette, S. A. Casalnuovo, G. C. Frye-Mason, M. L. Hudson, D. Y. Sasaki, R. P. Manginell, and C. C. Wong, "Microfabricated Silicon Gas Chromatographic Micro-channels: Fabrication and Performance," *Proc. SPIE Micromachining and Microfabrication Process Technology IV*, **3511**, (1998), 262-268.
4. E. J. Heller, V. M. Hietala, R. J. Kottenstette, R. P. Manginell, C. M. Matzke, P. R. Lewis, S. A. Casalnuovo, and G. C. Frye-Mason, "An Integrated Surface Acoustic Wave-Based Chemical Microsensor Array for Gas-Phase Chemical Analysis Microsystems," in *Chemical Sensors IV*, M. Butler, N. Yamazoe, P. Vanysek, and M. Aizawa, Eds., Electrochemical Society: Pennington, NJ, (1999), 138-142.
5. G. C. Frye-Mason, R. Kottenstette, P. Lewis, E. Heller, R. Manginell, D. Adkins, G. Dulleck, D.

Martinez, D. Sasaki, C. Mowry, C. Matzke, and L. Anderson, "Hand-Held Miniature Chemical Analysis Systems (μ ChemLab) for Detection of Trace Concentrations of Gas Phase Analytes," *Micro Total Analysis Systems 2000*, Kluwer Academic Publishers: Dordrecht, The Netherlands, (2000), 229-232.

CHEMICAL DETECTION BASED ON PHOTO-INDUCED ENERGY TRANSFER

Guangming Li and *Larry W. Burggraf*
Department of Engineering Physics

William Baker
Department of Mathematics and Statistics
Air Force Institute of Technology
2950 P Street, WPAFB, OH 45433, USA

ABSTRACT

Photothermal spectroscopy is demonstrated using a high-aspect-ratio multi-layer cantilever to measure adsorbed chemicals including dimethyl methylphosphonate (DMMP), which has an optical absorbance of $\sim 10^{-5}$ in the near infrared range. For non-volatile or thick adsorbates on the cantilever, the sensor deflection response comes mainly from photo-induced thermal effects, particularly thermal stress in the cantilever. For volatile adsorbates, in addition to the thermal contribution, the response includes the contribution of photodesorption, which causes dramatic changes in surface stress. Surface stress is potentially more sensitive than thermal stress for chemical detection using multi-layer cantilevers.

INTRODUCTION

The photothermal sensor based on a multi-layer reed that deflects upon absorption of light energy. It shows promise for chemical detection.¹⁻³ As pulsed electromagnetic radiation strikes molecules absorbed on the surfaces, they may be electronically or vibrationally excited depending on the wavelength of the radiation. Excitations are deactivated through luminescence, chemical reactions, or thermal processes including acoustic waves, phase transitions, and heat transfers. Various methods have been used to investigate the photo-induced surface processes. Recently, we applied a photothermal method based on bimetallic properties of a multi-layer structure for detection of photothermal processes on various solid film surfaces. The photothermal detector can be used to measure a very small temperature change as a result of resonant heating of absorbed molecules, which are strongly bound to the detector surfaces and are deactivated mainly through heat release.

THEORY

We have modeled amplitude and phase responses of cantilever sensors under the irradiation of light modulated at different frequencies. The model treats thermal transport along the reed and to a thin boundary layer of gas at the surfaces, which is largely an acoustic loss.⁴ We produced a simple dynamic model of a bimetallic cantilever, which captures the fundamental response of the cantilever as a function of source location and frequency. The modeled dependence on frequency is generally consistent with our experimental results. There is good qualitative agreement in the amplitude behavior with respect to source location and frequency. However, the phase-lag behavior deviates from experimental measurements at the reed ends.

Photothermal sensors measure the deflection of bimetallic cantilevers generally attributed to the heat-induced thermal stress. However, it is also known that surface stress of cantilevers can be changed by adsorbate atoms or molecules producing large bending of cantilevers.⁵ When a clean surface is created, the charge distribution near the surface is generally different from that in the bulk. Surface stress arises due to atom relaxation to achieve a lower energy charge distribution. For bimetallic cantilevers, the surface stresses on both sides could be different

producing net bending of the cantilever. Surface stress can be modified by surface adsorbates (molecules or atoms) causing the deflection of a bilayer cantilever. The surface stress, τ_{ij}^s , is the reversible work per area to stretch a surface elastically. Energy from cohesive intermolecular forces is coupled into surface stress of the cantilever by the equation:

$$\tau_{ij}^s = \gamma \delta_{ij} + \frac{\partial \gamma}{\partial \epsilon_{ij}}, \quad (1)$$

where γ is surface free energy, τ_{ij}^s is the surface stress and ϵ_{ij} is the strain tensor in the ij direction. For a liquid, surface stress and surface specific free energy are equal. For solid surfaces the absolute value of the derivative of the specific free energy with respect to strain can contribute to increase or decrease the surface stress. The chemisorption bonds between the surface atoms and adsorbate atoms generally cause a reduction of the tensile surface stress for heteropolar bonding with the surface. Measurements of surface stress by cantilever bending are based on Stoney's equation:

$$\tau = \frac{Et^2}{6R(1-\nu)}, \quad (2)$$

where R is the radius of curvature, E is the Young's modulus, t is the thickness of the cantilever, and ν is the Poisson ratio.

By measuring the adsorbate-induced surface stress, sub-monolayer sensitivity can be achieved. For surface adsorbates whose adsorption / desorption can be affected by resonant absorption of light, it is possible to gain spectroscopic information. Photo-induced phenomena for adsorbed molecules on solid-state surfaces have been extensively studied in the past decades because of its scientific importance and potential technological applications. As electromagnetic radiation electronically or vibrationally excites molecules on the surfaces they are quickly deactivated through light emissions, chemical reactions, or thermal processes including acoustic waves, phase transitions, and heat transfers. Photodesorption by electronic excitation has been generally explained using Menzel-Gomer-Redhead⁶ (MGR) model, while mechanisms for molecular desorption by vibrational excitation by infrared radiation are still not clear. One possible mechanism for infrared photothermal desorption involves transfer of energy from the intramolecular potential into the local surface potential enhancing desorption. In addition to direct thermal desorption, surface phonons may couple energy into the low-frequency modes of the adsorption potential. This may enhance desorption by contributing thermal energy from the substrate to the adsorbed molecules.

Desorption due to resonant absorption of IR photons by adsorbed molecules in the monolayer and multilayer coverage region was reported by J. Heidberg et al⁷. Reviews have been published by T.J.Chuang⁸. To induce IR chemistry, normally more than tens of vibrational quanta are needed. Compared to gas phase molecules, in condensed phase the efficient intermolecular energy exchange between molecules makes it difficult to accumulate tens of IR photons in one molecule to achieve multiphoton dissociation. Due to extremely fast intermolecular energy transfer selective molecular dissociation using IR radiation is difficult to obtain in the condensed phase. There is no evidence of a selective coupling between an excited vibrational mode and the adsorption potential, leading to nonstatistical surface desorption. On the other hand, it has been suggested that surface phonons may couple well with the low-frequency mode of the adsorption potential. The adsorbate bond is a bottleneck for the flow of energy from the surface modes of the substrate into the adsorbed molecules. Binding energies for intermolecular van der Waals bonds, responsible for molecular cohesion and adsorption, are in the 0.3 eV range. Therefore even an IR photon may have enough energy for a single photon process (e.g., at 3 μm). In most experiments, powerful CO_2 lasers are used and 2~3 photons are typically needed to desorb a molecule.

Our photothermal method uses a multilayer cantilever for detection of photo-induced heat flow associated with the photodesorption in the 1.2 to 2.8 μm wavelength range from a low power wide-band source. This photothermal

detector responds to resonant heating for most molecules that are strongly bound to the cantilever surface. The absorbed infrared energy deactivates mainly to heat. However, for resonant excitation of some molecules that are weakly bound to the surface we observe a significant net loss of energy from the substrate. In this paper, we illustrate the detection method by measuring DMMP and alcohol molecules in the near infrared range.

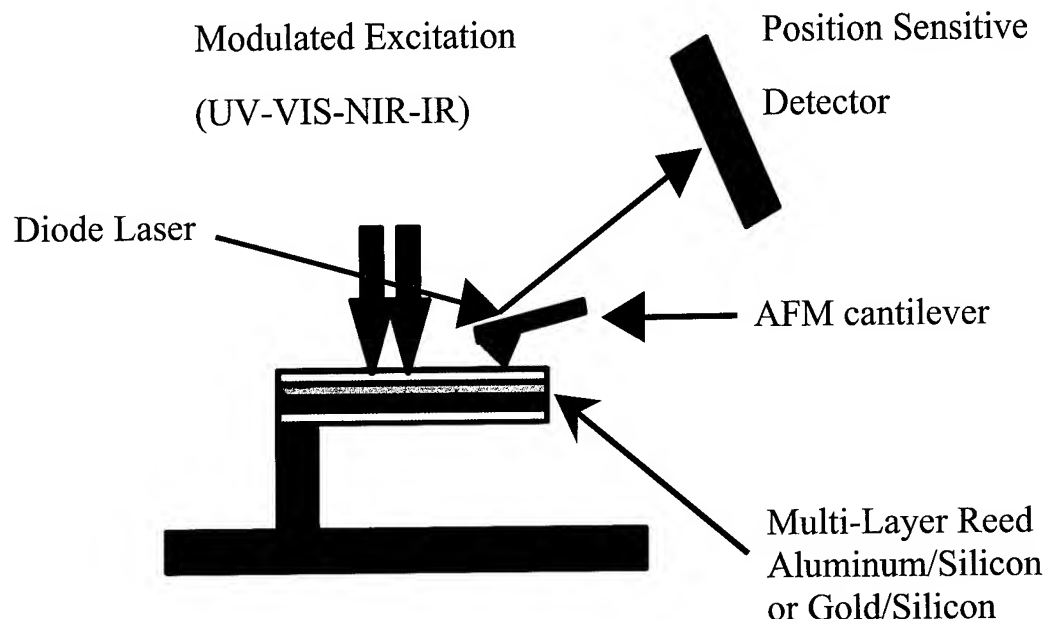


Figure 1. Experimental set-up for the photothermal spectroscopy based on multi-layer reed sensors.

EXPERIMENTAL RESULTS AND DISCUSSION

An illustration of a photothermal measurement using a multilayer rectangular cantilever sensor is shown in Figure 1. The cantilever sensor is composed of a low thermal expansion layer made of 5-10 μm thick single crystal silicon and a high thermal expansion layer made of 0.2-0.5 μm thick aluminum or a thin layer of gold. The small curvature produced by thin ($<1\mu\text{m}$) coating on the reed is inconsequential to dynamic measurements. Additional layers of gold and nano-porous sol-gel magnesium aluminate can be deposited on the reed when a high surface area is needed for chemical detection. The gold layer partially reduces light penetrating into the silicon layer, to reduce the silicon background absorption. Multilayer cantilevers are designed to have a high-surface-area host layer using sol-gel chemistry appropriate pore size for chemical selectivity. When incident ultraviolet, visible or infrared photons are absorbed by the multilayer sensor most of the absorbed energy is transformed into heat. The reed is deflected as a result of differential thermal expansion caused by the change in temperature. Long, thin cantilevers or reeds have sensitivity advantages for measurement of weak infrared optical absorption. A sensitivity of $\sim 0.32 \text{ mW}^{-1}$ has been experimentally achieved, which corresponded to a power resolution of $\sim 160 \text{ pW}$, or an energy flux resolution of $\sim 16 \text{ pJ}$. The energy absorbed is proportional to the concentration of light-absorbing chemicals on the sensor surface. The discrimination of different chemicals can be achieved based on the absorption features in optical absorption spectra together with pattern recognition techniques.

Changes in surface stress for an Al/Si cantilever upon exposure to isopropyl alcohol is shown in Figure 2. The adsorbate molecules cause the aluminum surface to contract, i.e. the surface tensile stress increases. During the adsorption process, we observed significant step-wise changes of surface stress, indicating multilayer growth of the adsorbate molecules on the surface. Figure 3 shows the changes of the amplitude and phase together with the surface stress for adsorption and desorption of isopropyl alcohol. The cantilever was illuminated with wide band light modulated at 8 Hz. The amplitude can be used as an indicator of how fast the surface stress changes with the adsorption and desorption of molecules. Given our current setup, a sensitivity of 10^{-4} ~ 10^{-5} N/m can be achieved for surface stress. On average, each layer of adsorbates was found to change the surface stress by 0.2~0.3 N/m, which corresponds to a detection sensitivity of a thousandth of a monolayer for surface adsorbates. Figure 4 gives the spectra of amplitude and phase of a cantilever under the near infrared irradiation modulated at 8 Hz, after exposure to DMMP vapor. A FTIR spectrum of liquid DMMP is given for comparison. A large signal-to-noise was observed during the near infrared scans of 10^{-11} g DMMP (in ~ 4 minutes), as shown in figure 4. Signal enhancement is attributed to stress changes accompanying photo-induced desorption of the adsorbate molecules. There are significant changes in surface stress when the sensor is illuminated by light with frequencies of resonant absorption for DMMP. We postulate that those changes are due to photodesorption of DMMP molecules from the surface. By monitoring the changes in surface stress caused by adsorption and photodesorption we can achieve both the extremely high sensitivity and good selectivity for volatile chemical detection.

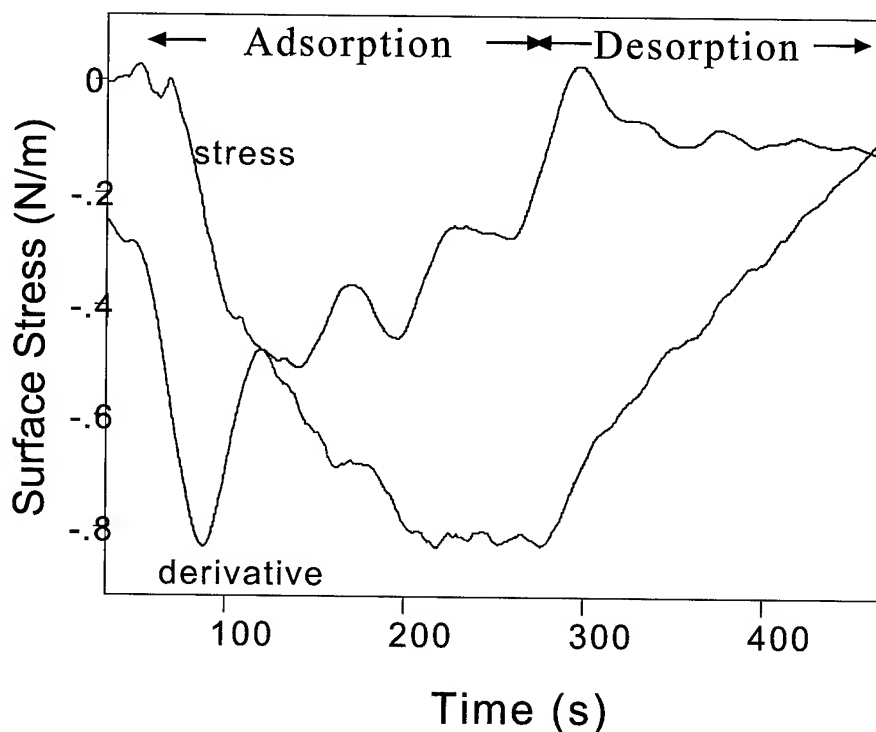


Figure 2. Surface stress change with time during adsorption and desorption of isopropyl alcohol. The derivative signal shows that successive adsorbed monolayers have decreasing influence on the surface stress.

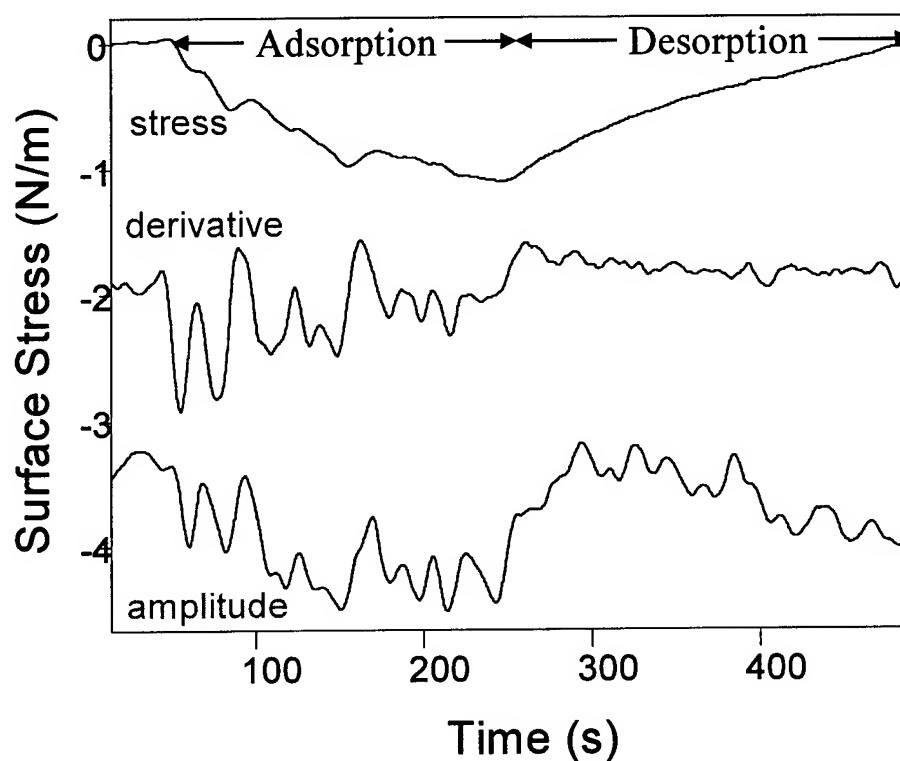


Figure 3. Change in adsorbate induced surface stress compared to amplitude and phase of cantilever response to modulated photoexcitation for isopropyl alcohol adsorbed on Al/Si cantilever. Larger stress changes associated with adsorption are due to monolayer reorganization on the surface.

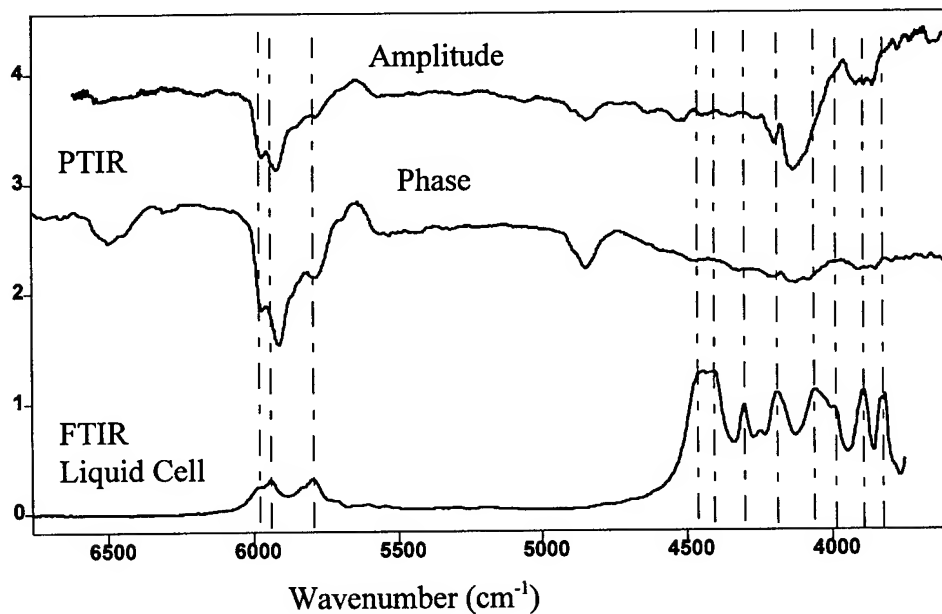


Figure 4. Photothermal desorption spectrum of dimethyl methylphosphonate (DMMP) on Al/Si cantilever.

For some combinations of cantilever materials and adsorbates the surface stress is increased, for others it is decreased. Changes in the rates of adsorption and desorption influence the signal frequency spectrum. Further study is necessary to understand the influence of adsorbate interactions on changes in surface stress.

CONCLUSIONS

Surface stress is potentially more sensitive than thermal stress for chemical detection. We have demonstrated high sensitivity of surface stress measurements for detection of sub-monolayers of adsorbates. For volatile adsorbates, in addition to the thermal contribution, the photothermal response includes the contribution of photodesorption, which causes dramatic changes in surface stress. The surface stress for volatile adsorbates can be altered by light modulation, giving a basis for spectral identification. This photothermal spectroscopy method is demonstrated using high-aspect-ratio multilayer cantilevers to measure adsorbed chemicals with absorbance of $\sim 10^{-5}$ in the near infrared range. For non-volatile or thick adsorbates on the cantilever, the sensor deflection response mainly comes from the photo-induced thermal effects or thermal stress in the cantilever.

ACKNOWLEDGEMENTS

We gratefully acknowledge sponsorship and support of the U.S. Army Edgewood Chemical Biological Center, SBCCOM, Aberdeen Proving Ground, Maryland.

The views expressed in this article are those of the authors and do not reflect the official policy or position of the United States Air Force, Department of Defense or the US Government.

REFERENCES

- ¹ J.R.Barnes, R.J. Stephenson, M.E. Welland, Ch. Gerber, and J.K. Glmzewski, Nature, 372, 79 (1994).
- ² J.R. Barnes, R.J. Stephenson, C.N. Woodburn, S.J. O'Shea, M.E. Welland, T. Rayment, J.K. Glmzewski, and Ch. Gerber, Rev. Sci. Instrum. 65, 3793 (1994).
- ³ Guangming Li, Larry Burggraf, and William Baker, Appl. Phys. Lett. 76, 1122(2000).
- ⁴ Allan Rosencwaig, *Photoacoustics and Photoacoustic Spectroscopy* (John Wiley & Sons, 1980), pp 93-124.
- ⁵ H. Ibach, Surface Science Reports 29, 193 (1997).
- ⁶ D. Menzel and R. Gomer, J. Chem. Phys. 41, 3311 (1964); P.A. Redhead, Can. J. Phys. 42, 886 (1964).
- ⁷ J. Heidberg et al., H. Stein, E. Richl, A. Nestmann. Z. Phys. Chem. (NF) 121, 145 (1980)
- ⁸ T.J. Chuang, Surf. Sci. Rep. 3, 1 (1983); Surf. Sci. 178, 763 (1986).

SURFACE-ENHANCED RAMAN SPECTROSCOPY AS A RAPID FIELD DETECTOR FOR CHEMICAL AND BIOLOGICAL DEFENSE

James M. Sylvia, Jeremy M. Raelin, James A. Janni,
Savvas C. Makrides, Andrew A. Guzelian, and *Kevin M. Spencer*

EIC Laboratories, Inc.
111 Downey St.
Norwood, MA 02062

Through improved process control, EIC Laboratories has enabled the use of SERS as a reproducible, fieldable detector for trace levels of analytes. In this paper, the advances made in SERS are applied to the detection of chemical agent simulants and whole bacteria. We present data demonstrating detection of chemical agent simulants down to the desired Joint Service Agent Water Monitor (JSAWM) detection limits. We also demonstrate detection and differentiation of whole bacteria and cell viability. Finally, we present data demonstrating the capability of our substrates to be used for multiple measurements through *in situ* surface renewal.

The Joint Service Agent Water Monitor (JSAWM) has several very challenging operational requirements for detecting and monitoring chemical and biological warfare contaminants in military water supplies.¹ The sensor must be stand-alone, lightweight, capable of constant monitoring, and provide answers in a relatively short time frame. The critical instrument design is the desired detection limits, which require very high sensitivity. Sarin requires detection at 3.2 ppb while mustard levels of 47 ppb or higher must be detected. Biological agents like Anthrax spores must be detected at limits as low as 50 counts/mL.

Time requirements for the JSAWM necessitate fieldable techniques; sampling with laboratory analysis is not an option. In addition, new chemical threats can arise requiring expansion of the database. Under these requirements, an attractive approach is to develop an instrumental method that is capable of fulfilling most if not all of the requirements in a single instrument, detecting, identifying and quantifying chemical and biological species alike. Based on the extensive SERS literature, work conducted in-house at EIC Laboratories, and reasonable extrapolations of technical feasibility, we believe that Surface Enhanced Raman Spectroscopy (SERS) can be such a universal sensor for chemical and biological defense.

When molecules are adsorbed onto specific solid substrates, an enhanced Raman signal of the adsorbate is obtained, with intensity enhancements of 10^2 - 10^{14} . In some instances, single molecule detection has been achieved.² This phenomenon forms the basis of Surface Enhanced Raman Spectroscopy (SERS). Gold, copper, and silver are the metallic surfaces for which the greatest enhancements have been observed; other metals, such as platinum, have been used but with enhancements orders below the three coinage metals. To maximize the effect, the metal must have a high degree of surface "roughness". The microroughness must be uniform and reproducible for precise results. The metal surfaces also have a positive effect of quenching fluorescence that can interfere with the Raman spectrum. Surfaces with strong SERS enhancements have been obtained by electrochemical oxidation/reduction of metals³, by vapor deposition of the metal onto a high roughness substrate⁴, by spin coating or vapor deposition onto polymer spheres⁵, and through the use of metal colloids, either as suspensions or deposited onto surfaces.⁶ The exact nature of the SERS phenomenon is still under investigation, however.

The fabrication of reproducible active sites has generally been disregarded in the literature, as most researchers have been either using SERS for physical chemical studies or strictly as a "yes/no" type of sensor. EIC Laboratories has aggressively attacked the issue of process control to create SERS substrates that can provide a high degree of sensitivity and reproducibility, enabling the acquisition of quantitative information. Recently, we performed blind tests using > 200 substrates to detect 2,4-dinitrotoluene vapors over aqueous solutions under the direction of DARPA and demonstrated reproducible detection to < 5 ppb.⁷ In this paper, we present preliminary results that indicate SERS is a promising technique for the detection of chemical and biological warfare agents.

Experimental

All Raman and SERS spectra were collected using an EIC Laboratories NIR echelle spectrograph.⁸ The NIR echelle provides a high resolution Raman spectrum over the full Raman spectral range. The excitation source was either a Spectra Diode Laboratories SDL-8530 or a Process Instruments model PI-ECL-785-350 diode laser. These external cavity diode lasers operate at 785 nm with output powers of 300 mW. The laser light was coupled into an EIC Laboratories Model RP785-08-05-FC fiber optic Raman probe. The probe serves two purposes; it is a light pipe that transfers the laser light to the sample and the Raman/SERS signals away from the sample and it serves as an optical filtering device to remove unwanted background degradation caused by the laser light. The laser light is focussed by the Raman probe onto the roughened gold or silver SERS substrates and the subsequent scattered SERS and Raman signals are directed to the NIR echelle. Data were collected on a Photometrics TE-cooled CCD (Model CH 250) and normalized, stored, and presented using in-house software. The spectral data were acquired on a Gateway 486 computer. Data manipulation and plotting were performed using either Grams (Galactic Industries, Version 5.0) or Axum (MathSoft, Version 4.1). No spectral smoothing was performed.

The SERS substrate fabrication procedure is as follows. Gold and silver foil coupons were cut to a size of $\frac{1}{4} \times \frac{1}{2}$ cm². All substrates were polished to a smooth finish using a Beuhler Ecomet V polisher. Final polishing was performed using a 0.3 μ m alumina polish. The mirror-like coupons were washed and stored in distilled water prior to electrochemical roughening. Electrochemical roughening was performed on an automated Gamry Instruments Model PC4-750 potentiostat. The roughening procedure is a slightly modified version of the method developed by DeSilvestro and Weaver.⁹ The gold electrodes were cycled 25 times at a sweep rate of 500 mV/s with upper and lower cycling limits of 1.2 and -0.3 V, respectively. The silver roughening procedure was determined in-house based on our gold results and the greater ease with which silver is roughened. The silver electrodes were cycled 20 times at a sweep rate of 10 mV/s with upper and lower limits of 0.25 and -0.6 V, respectively. The metal foil electrodes were roughened in 0.1 M KCl using a Ag/AgCl reference electrode (BioAnalytical Systems) and platinum gauze (Aldrich) as the counter electrode.

The SERS substrates were stored under distilled water after electrochemical cycling. After a minimum of an overnight soak to remove excess chloride ions, the substrates were then cleaned in a plasma cleaner (Harrick, Model PDC-3XG) for 20 minutes. The substrates employed in laboratory measurements were used immediately after plasma cleaning.

Cyanide Detection Limits

In the DARPA Dog's Nose Program, we optimized an electrochemically roughened gold SERS substrate that could detect 5 ppb 2,4-dinitrotoluene vapor.⁷ One of the significant features of the substrate preparation that enhanced detection was the addition of 10 ppm carbonate into the roughening solution. We

initiated research herein by evaluating this substrate for sensitivity to the warfare agents. Cyanide spectra proved to be highly enhanced using this substrate. We have extended the detection limit of cyanide to 1 ppb in a 0.1 μL aliquot. The SERS spectrum is presented in Figure 1. Considering a 4 mm spread of the spotting solution and a 400 μm spot size, the analyte detected has a detection limit approaching 1 fg. The spectrum of the cyanide band is weak, but detectable, and well below the 2 ppm JSAWM detection limits for cyanide.

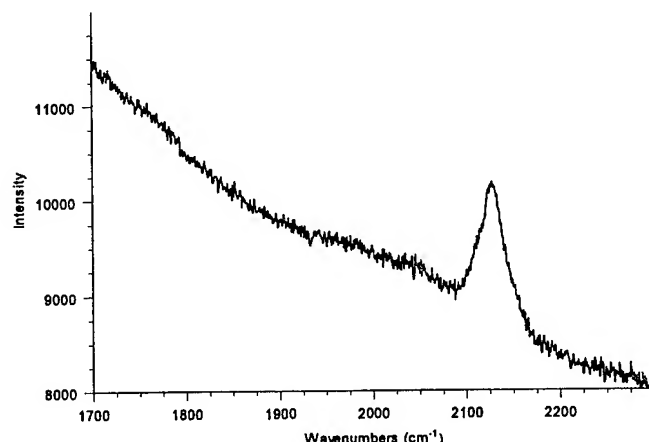


Figure 1. The SERS spectrum of 1 fg of NaCN spotted onto a gold SERS substrate. The spectrum was collected in 30 s using ~ 100 mW of 785 nm laser light.

Detection of 2-Chloroethyl Ethylsulfide (2-CEES)

2-CEES is a chemical agent simulant for sulfur mustard. As with the cyanide, the electrochemically roughened gold substrate developed for the Dog's Nose Program as well as a standard electrochemically roughened gold substrate were evaluated for detection of 2-CEES. Unlike the cyanide, the results for 2-CEES were not as sensitive, with the limit being at ~ 1 ppm. We then decided to evaluate the capability of silver to provide the desired SERS enhancement levels. We placed this silver substrate into an electrochemical cell. The purpose of the experiment was to determine if the sensitivity could be increased by applying a potential to the substrate. The cycling limits for the experiments were -1.0 V to 0.15 V. The electrode was swept slowly at 1 mV/s to enable *in situ* SERS spectral collection. An automated, multiple exposure software routine written at EIC Laboratories was employed to enable collection of SERS spectra as a function of voltage. The upper limit was determined to prevent stripping of the silver surface and changing the morphology of the SERS substrate.

Results for a 100-ppb 2-CEES solution are presented in Figure 2. The SERS spectral band at 700 cm^{-1} is clearly evident at -600 mV. As the voltage is swept more negative, the intensity of this band grows and a second band at 1000 cm^{-1} is observed. This trend continues to -800 mV, at which point the intensities begin to decrease. By -950 mV, both peaks have disappeared. Confirmation of these peaks as belonging to 2-CEES was performed in two manners. First, a blank was run with only distilled water present and no peaks were observed. Second, we spiked the 2-CEES solution with additional 2-CEES and observed an increase in the peak intensities. In addition, the two observed peaks occur in regions where SERS were observed at higher concentration. Also presented in Figure 2 is the SERS spectrum from a 50-ppb 2-CEES sample collected at -800 mV. From these results, it is evident that the detection of 2-CEES at the 47-ppb JSAWM requirement has been attained.

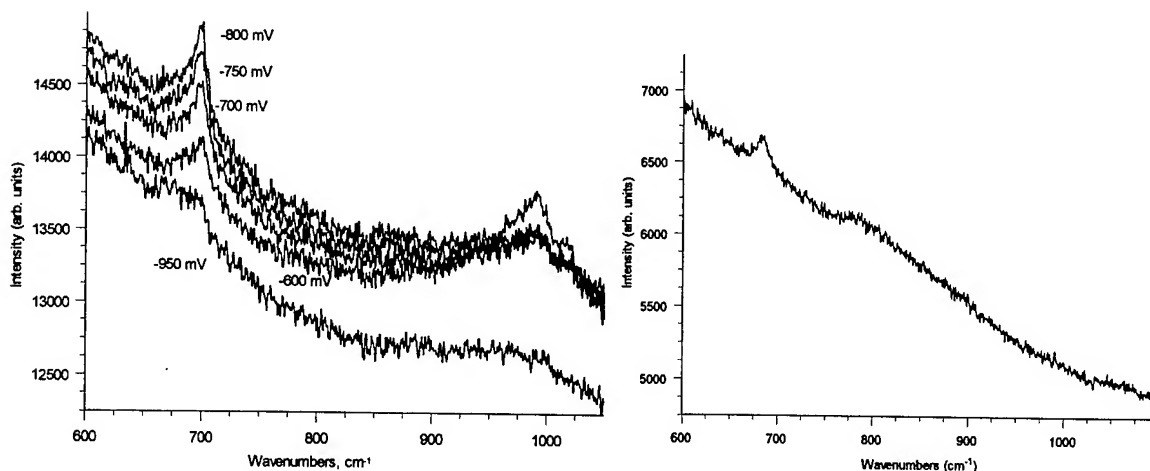


Figure 2. Left - The SERS spectra collected from a 100 ppb solution of 2-CEES as a function of electrode potential. Right - The SERS spectrum of 50 ppb 2-CEES. Each spectral acquisition was for only 30 s using ~ 100 mW of 785 nm laser radiation.

Besides meeting detection limits, this experiment also allowed demonstration of an in situ method by which the analyte can be removed without adversely affecting the surface morphology. This enables long-term usage of the SERS substrate. Multiple sweeps have been performed and the 2-CEES signal is always observed within the listed limits and disappears outside of those limits. Although the laboratory experiments were performed on an automated apparatus that could collect spectra throughout the cycling, the use of cycling was simply to determine the range of useful voltages. In the field, we believe that computer controlled application of 2 voltages, e.g. -300 mV and -800 mV, is all that will be necessary for renewing the substrate and detecting the trace levels of the agent of interest

Detection and Identification of Bacteria

One of the first issues to be determined for detection of bacteria is simple differentiation of Gram positive and Gram negative bacteria. In Figure 3, the SERS spectrum of the Gram positive species *Staphylococcus aureus* and the SERS spectrum of the Gram negative species *Pseudomonas aeruginosa* are presented. There are several features in the SERS spectra presented. From visual inspection of these spectra, there are few distinct features in each spectrum. However, there are many subtle differences in intensity distribution and spectral band width that do enable differentiation. For example, the *S. aureus* band at 750 cm^{-1} is considerably more intense with respect to the remaining spectral features than the relatively weak 750 cm^{-1} band in the *P. aeruginosa*. The latter bacterium also has a much sharper feature around 1475 cm^{-1} than the *S. aureus*. *Y. enterocolitica* also displays a broad, low intensity feature in this region. Spectral subtraction techniques were applied to a mixture of *Y. enterocolitica* and *P. aeruginosa*, with separation of these overlapping peaks clearly observed (data not shown). Although we have sampled only a small number of potential bacterial candidates, it appears that a combination of peak positions, bandwidths, and relative intensities observed in the acquired SERS spectra has the potential to differentiate bacteria.

Preliminary efforts were made at bacterial dilutions. Samples analyzed by SERS were also analyzed by scanning electron microscopy (SEM). The SEM of *S. aureus* presented in Figure 4 indicated clumping on the gold substrate. From the image, it is apparent the bacteria are clustering together into groups of 5-10 on the surface. An important feature of this SEM is the uniformity of the gold surface roughness. The uniform

roughness of this electrochemically produced substrate is the principal reason we have been able to get high sensitivity results with a high level of reproducibility. Despite the variable surface density and paucity of bacteria, we were able to collect several SERS spectra. These results indicate that low concentrations of bacteria can be determined. We are currently working on improving the delivery of the bacteria to enable accurate determination of detection limits.

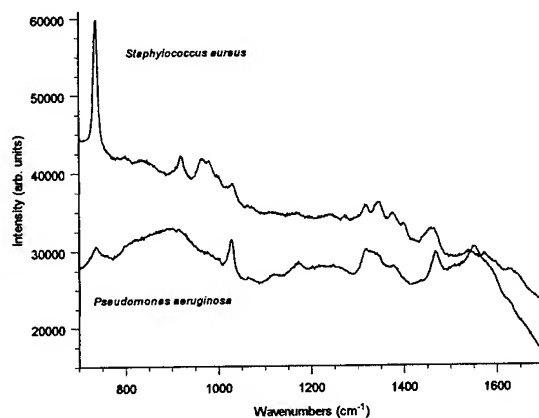


Figure 3. SERS spectra of the Gram positive species *Staphylococcus aureus* and the SERS spectrum of the Gram negative species *Pseudomonas aeruginosa*.

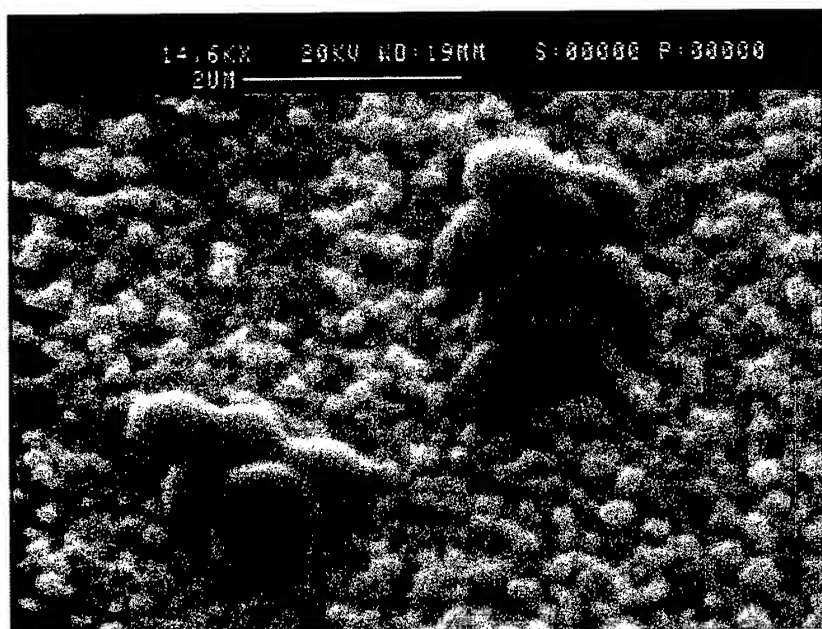


Figure 4. SEM of an electrochemically roughened gold substrate that has been exposed to *S. aureus*. The large clustered features in the foreground are groups of bacteria while the smaller, uniformly sized ridges throughout the SEM is the roughness feature of the SERS substrate.

An interesting aspect of bacterial detection is not only identifying the bacterium, but determining whether that bacterium is viable. We performed experiments to determine if SERS can differentiate between living and dead bacteria. From the spectra in Figure 5, the preliminary results are very encouraging. We first collected the SERS spectrum of *Bacillus cereus*. We then killed the bacteria by boiling for 10 minutes and then collected another SERS spectrum. As can be seen in Figure 5, the prominent spectral features disappear, providing a dramatic difference between live and dead bacteria. Similar results were obtained from *S. aureus* cells (data not shown). For the *S. aureus*, SEM photographs of the boiled cells were collected to ensure that the cells were intact. Although the mechanism for the drastic change in the SERS spectrum is not known, this ability to detect only bacteria that are viable is of significant military interest. The preliminary findings will lead to future SERS experiments using other conditions that are lethal to bacteria, such as chemical disinfectants, extreme temperature, and irradiation.

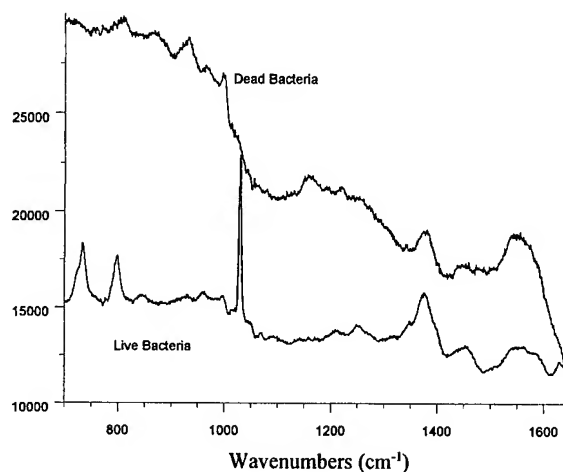


Figure 5. The SERS spectra of *Bacillus cereus* when (top spectrum) the bacteria are not viable and (bottom trace) when they are in a growth phase. The observed band at 1384 cm^{-1} is a characteristic of the gold SERS substrate and is not a function of the analyte.

CONCLUSIONS

The results presented herein clearly demonstrate that SERS has the desired sensitivity for detection of chemical warfare agents. In this preliminary work, we have already eclipsed the stated detection needs for cyanide and sulfur mustards. We have already performed preliminary research on the VX, GD, GB, and GA degradation product, methylphosphonic acid (MPA). MPA appears to have a larger SERS enhancement than 2-CEES, leading us to believe that the JSAWM detection limit for these agents will be achieved as well. The preliminary bacterial results presented herein are also very encouraging, demonstrating the potential for determining cell viability. Currently, the database is too small for conclusive results. However, the initial studies indicate that bacterial differentiation is potentially feasible. Continued research will establish the robustness of this technique, extend the range of examined bacterial species, establish limits of detection, and investigate the effects of pollens on bacterial identification. The research herein also demonstrated that the SERS substrates were reusable, enabling long-term unattended monitoring. We will be performing more research to determine the useful in situ lifetimes of these substrates.

This research is significant in that it demonstrates that SERS can achieve the technical requirements for the JSAWM. The remaining questions concern the engineering criteria. In terms of acquisition time, SERS is already stellar. All measurements presented required only 30 s. The other engineering issues concerning the size and weight of the instrument can be addressed. EIC has already created a compact, 20 lb. Raman/SERS instrument, the InPhotote, that can be made smaller and lighter through a different laser choice. These engineering details, as well as a more complete evaluation of the remaining compounds of interest for the JSAWM, are our current priority.

ACKNOWLEDGEMENTS

Financial support for this research was provided by the Chemical and Biological Defense Command Branch under contract # DAAD 13-00-C-0031.

REFERENCES

- ¹ Joint Chemical/Biological Agent Water Monitor (JCBAWM) Operational Requirement Document (ORD), 1997.
- ² (a) S. Nie and S.R. Emory, *Science*, **275**, 1102-6 (1997), and (b) K. Kneipp, H. Kneipp, I. Itzkan, R.R. Dasari, and M.S. Feld, *Chem. Rev.*, **99**, 2957-75 (1999).
- ³ (a) A.A. Tolia, C.T. Williams, M.J. Weaver, and C.G. Takoudis, *Langmuir*, **11**, 3438-45 (1995), (b) J.F. Arenas, I.L. Tocón, M.S. Woolley, J.C. Otero, and J.I. Marcos, *J. Raman Spectrosc.*, **29**, 673-9 (1998), and (c) A. Kudelski and J. Bukowska, *Chem. Phys. Lett.*, **253**, 246-50 (1996).
- ⁴ (a) G.J. Kovacs, R.O. Loutfy, P.S. Vincett, C. Jennings, and R. Aroca, *Langmuir*, **2**, 689-94, (b) P.A. Mosier-Boss and S.H. Lieberman, *Appl. Spectrosc.*, **53**, 862-73 (1999), and (c) M. Cai, M.D. Mowery, J.E. Pemberton, and C.E. Evans, *Appl. Spectrosc.*, **54**, 31-8 (2000).
- ⁵ (a) T. Vo-Dinh, D.L. Stokes, G.D. Griffin, M. Volkan, U.J. Kim, and M.I. Simon, *J. Raman Spectrosc.*, **30**, 785-93 (1999), (b) N.R. Isola, D.L. Stokes, and T. Vo-Dinh, *Anal. Chem.*, **70**, 1352-6 (1998), and (c) P.M. Tessier, O.D. Velez, A.T. Kalumbur, J.F. Rabolt, A.M. Lenhoff, and E.W. Kaler, *J. Am. Chem. Soc.*, Web Preprint (2000).
- ⁶ (a) R.G. Freeman, K.C. Graber, K.J. Allison, R.M. Bright, J.A. Davis, A.P. Guthrie, M.B. Hommer, M.A. Jackson, P.C. Smith, D.G. Walter, and M.J. Natan, *Science*, **267**, 1629-32 (1995), (b) A.A. Ooka, K.A. Kuhar, N. Cho, and R.L. Garrell, *Biospectroscopy*, **5**, 9-17 (1999), (c) A. Rupérez and J.J. Laserna, *Anal. Chim. Acta*, **335**, 87-94 (1996), (d) J. Ni, R.J. Lipert, G.B. Dawson, and M.D. Porter, *Anal. Chem.*, **71**, 4903-8 (1999), and (e) X. Dou, Y.M. Jung, H. Yamamoto, S. Dou, and Y. Ozaki, *Applied Spectrosc.*, **53**, 133-8 (1999).
- ⁷ J.M. Sylvia, J.A. Janni, J.D. Klein, and K.M. Spencer, *Anal. Chem.*, accepted for publication.
- ⁸ S. Christesen, B. MacIver, L. Procell, D. Sorrick, M. Carrabba, and J. Bello, *Appl. Spectrosc.*, **53**, 850-5 (1999).
- ⁹ J. DeSilvestro and M.J. Weaver, *J. Electroanal. Chem.*, **209**, 377-86 (1986).

MONITORING LOW LEVELS OF IONIC POLLUTANTS IN WATER USING ATTENUATED TOTAL REFLECTANCE INFRARED SPECTROSCOPY

Matthew A. Odom, Gretchen N. Hebert, Brady J. Clapsaddle, and *Steven H. Strauss**
Department of Chemistry, Colorado State University, Fort Collins, CO 80523

Abstract

When the wetted surface of a commercially available ATR-FTIR probe was coated with a number of highly selective ion-exchange compounds, the infrared spectroscopic detection limits for a variety of CWA's or their breakdown products in water were lowered by 3–5 orders of magnitude. The CWA's and other environmental pollutants studied to date include (chemical formula, current detection limit, and analysis time) cyanide (CN^- , 5 ppb, 15 min), perchlorate (ClO_4^- , 3 ppb, 60 min), PFOS ($\text{C}_8\text{F}_{17}\text{SO}_3^-$, 25 ppb, 60 min), PMPA ($\text{CH}_3\text{P}(\text{O})(\text{OCH}(\text{CH}_3)\text{C}(\text{CH}_3)_3)\text{O}^-$, 18 ppb, 75 min), EMPA ($\text{CH}_3\text{P}(\text{O})(\text{OCH}(\text{CH}_3)_2)\text{O}^-$, 12 ppm, 30 min), and MPA ($\text{CH}_3\text{P}(\text{O})(\text{OH})\text{O}^-$, 10 ppm, 4 hr).

Introduction

The recently proposed JASWM goals for the ATR-FTIR effort (i.e., exit criteria) for FY00 and FY01 are listed in Table 1. A number of these compounds of interest are monoanionic in the pH range that includes many natural waters. In addition to its use as a CWA, cyanide is also an environmental contaminant of concern (COC).^{1,2} Other monoanionic COCs that must be detected at low concentrations in aqueous media include perchlorate (ClO_4^-)^{3–6} and perfluorooctylsulfonate (PFOS, $\text{C}_8\text{F}_{17}\text{SO}_3^-$). The current EPA drinking-water standard and drinking-water reference dose for cyanide and perchlorate are 0.2 ppm^{13,14} and 4–18 ppb,⁹ respectively. The surfactant PFOS, which was formerly used in Scotchgard®-brand fabric treatments and aqueous film-forming foams (AFFFs) used to fight liquid fuel fires,^{7–11} is a major wastewater problem in that its presence can cause excessive foaming and POTW shutdowns.^{7,15}

Quantitative methods based on FTIR spectroscopy are generally considered to be insufficiently sensitive for the analysis of trace contaminants in water (i.e., < 1 ppm).^{16,17} Nevertheless, there are examples of attenuated total reflectance (ATR) crystals coated with submicron-thick layers of polymeric or sol-gel materials that enhance the sensitivity of FTIR spectrometers by concentrating an analyte in the region probed by the evanescent wave (i.e., in the coating). Most analytes that have been detected in this manner are neutral organic molecules such as atrazine (3 ppm), DDT (50 ppm), TCE (100 ppm), and benzonitrile (0.35 ppm) (the lowest aqueous concentrations studied to date are shown in parentheses).^{18–20} Only a few coatings that can concentrate ions have been reported, and none are known to detect aqueous ions at concentrations below 1 ppm.^{21–28} In this paper we report that CN^- , PMPA, ClO_4^- , and $\text{C}_8\text{F}_{17}\text{SO}_3^-$ can be detected in water at concentrations 25 ppb in one hour or less using a commercially available silicon ATR-FTIR immersion probe that has been coated with thin films of suitable organometallic ion-exchange compounds.^{29–35}

TABLE 1
JSAWM Exit Criteria for ATR-FTIR Effort, Proposed September 2000

compound of interest (aqueous analyte)	FY01 (response time 15–30 min)	FY02 ^a (response time 5–10 min)
MPA, ^b R = H	100 ppb	
PMPA, ^b R = CH(CH ₃)C(CH ₃) ₃	100 ppb	12/4 ppb
IMPA, ^b R = CH(CH ₃) ₂	100 ppb	
EMPA, ^b R = C ₂ H ₅	100 ppb	
cyanide	6/2 ppm ^a	6/2 ppm
arsenic		80/27 ppb
BZ		7/2 ppb
T-2 toxins		26/9 ppb
BSA	1 ppm	

^a Based on 1996 Short Term U.S. Tri Service Standard for 5/7 days. ^b CH₃P(O)(OR)O[−]

Methods

The compound 1,3-bis(diphenylphosphino)propanedichloronickel(II), NiCl₂(dppp), was obtained from Aldrich. The polyalkylated ferrocenium salt 1,1',3,3'-tetrakis(2-methyl-2-nonyl)ferrocenium nitrate (DEC⁺NO₃[−]) was synthesized according to a literature method.^{29,35} The europium-containing polymer (Eu-polymer) was prepared according to a literature method.^{36,37} All aqueous stock solutions were prepared in Class A volumetric glassware using distilled deionized water (Barnstead NANOpure) that had a resistivity of 18 MΩ cm. All experiments were performed at 24 ± 1 °C.

The spectrometer used was an ASI (Applied Systems) ReactIRTM-1000 equipped with either an ASI SiComp[®] or DiComp[®] ATR-FTIR probe. Data collection and manipulation was carried out using ASI ReactIRTM software (version 2.1). The SiComp[®] probe consisted of a 30-bounce silicon ATR crystal mated to a ZnSe optical focusing element and housed in a 1.5-in. long × 1-in. diameter cylindrical stainless-steel conduit. The exposed surface of the silicon ATR crystal (a circular area 1 cm in diameter) was treated with a 1 mmol/L dichloromethane solution of either NiCl₂(dppp) (80 μL) or DEC⁺NO₃[−] (20 μL). Evaporation of dichloromethane left thin-film coatings of the water-insoluble organometallic ion-exchange compounds on the surface of the ATR crystal. The DiComp[®] probe was similar except that the wetted ATR element was an 18-bounce diamond crystal.

In a typical analysis, the coated probe was immersed into a known volume of water. The coating was allowed to equilibrate with water for 10 minutes, at which time a background was collected. An appropriate amount of an analyte stock solution was then added and FTIR spectra of the resulting dilute, stirred analyte solution were collected every minute for 60 minutes (64 scans, 8 cm^{−1} resolution).

Detection limits (i.e., a signal/noise ratio • 3) for four compounds of concern are listed in Table 2. The detection limits for the uncoated and coated probes were determined in different manners. For the uncoated probe, an aqueous solution of the analyte was brought in contact with the probe and a spectrum ratioed to distilled deionized water was recorded by signal averaging continuously for 60 minutes (24,576 scans). For the coated probe, the analysis time was effectively a waiting period for ion-exchange to take place, after which a final spectrum ratioed to the coated probe immersed in distilled deionized water was recorded (64 scans). In both cases, no apodization or spectral smoothing was used, the nominal spectral resolution was 8 cm^{−1}, and the instrument gain was 1.

TABLE 2
One-Hour Detection Limits for the Uncoated and Coated ATR-FTIR Probe^a

monoanion	wavenumber monitored ^b	detection limit		
		uncoated probe	coated probe	organometallic extractant ^c
CN ⁻	2104	130 ppm	5 ppb	NiCl ₂ (dppp)
ClO ₄ ⁻	1092	288 ppm	3 ppb	DEC ⁺ NO ₃ ⁻
C ₈ F ₁₇ SO ₃ ⁻	1270	100 ppm	25 ppb	DEC ⁺ NO ₃ ⁻
CH ₃ P(O)(OR)O ⁻ ^d	1045	1,800 ppm	25 ppb	Eu-polymer

^a The detection limit is defined as the concentration at which a band with a signal/noise ratio • 3 was observed after 60 min. ^b The wavenumber monitored for the coated probe experiments; the wavenumber monitored for the uncoated probe experiments differed by a few wavenumbers in all three cases.

^c dppp = 1,3-bis(diphenylphosphino)propane; DEC⁺ = 1,1',3,3'-tetrakis(2-methyl-2-nonyl)ferrocenium cation; Eu-polymer = europium-containing polymer. ^d R = CH(CH₃)C(CH₃)₃.

Results and Discussion

Our goal was to demonstrate that ATR-FTIR spectroscopy can be used to detect polyatomic anions of interest in water at concentrations 3–5 orders of magnitude lower than current ATR-FTIR detection limits.

We accomplished this by modifying a commercially available 30-bounce silicon ATR-FTIR immersion probe with thin-film coatings of three different ion-exchange materials. No further modification of the ATR-FTIR probe, and no sample pretreatment, were necessary for the experiments reported in this paper.

For NiCl₂(dppp) and DEC⁺NO₃⁻, each thin-film coating was used for only one analysis, after which it was removed from the ATR crystal by washing with dichloromethane. In other words, the ATR crystal was re-coated with a thin film of the organometallic ion-exchange compound for each sample. Even though this simple evaporation procedure does not allow film thickness and uniformity to be precisely controlled, the authors found that different films of a given extractant afforded excellent reproducibility for multiple samples of a given aqueous analyte. By using water-insoluble but organic-soluble coatings in this manner, the authors were able to study several different ion-exchange compounds and aqueous analytes in a relatively brief period of time using only one ATR-FTIR probe. The rapid removal and reapplication of coatings would not have been possible if more robust, covalently-linked coatings had been used instead. A subsequent paper will describe experiments with a wider variety of extractants and aqueous COCs.³⁶

The europium-containing polymer^{36,37} was prepared *in situ* on the DiComp® probe by UV curing for 2 hours. This thin film extracted both PMPA and EMPA. Unlike the other two extractant coatings, the Eu-polymer coating could be regenerated by washing with 1 M aqueous hydrochloric acid. In this manner, the same coating was used for six consecutive analyses with no apparent loss of activity.

When the SiComp® probe coated with a thin film of NiCl₂(dppp) was immersed in a pH 10 aqueous solution of 5 ppb CN⁻, a new band at 2104 cm⁻¹ was clearly observed in 60 min. Since the detection limit (i.e., signal/noise • 3 at 2081 cm⁻¹) for aqueous CN⁻ with the uncoated SiComp® probe was found to be 130 ppm, the nickel-complex coating has lowered the one-hour detection limit for aqueous cyanide by a factor of 25,000. When the concentration of aqueous CN⁻ was 0.13 ppm, the time necessary to observe the band at 2104 cm⁻¹ was only 4 min. Figure 1 shows FTIR spectra recorded over time of the NiCl₂(dppp)-coated probe immersed in aqueous solutions containing 5 ppb and 0.13 ppm CN⁻.

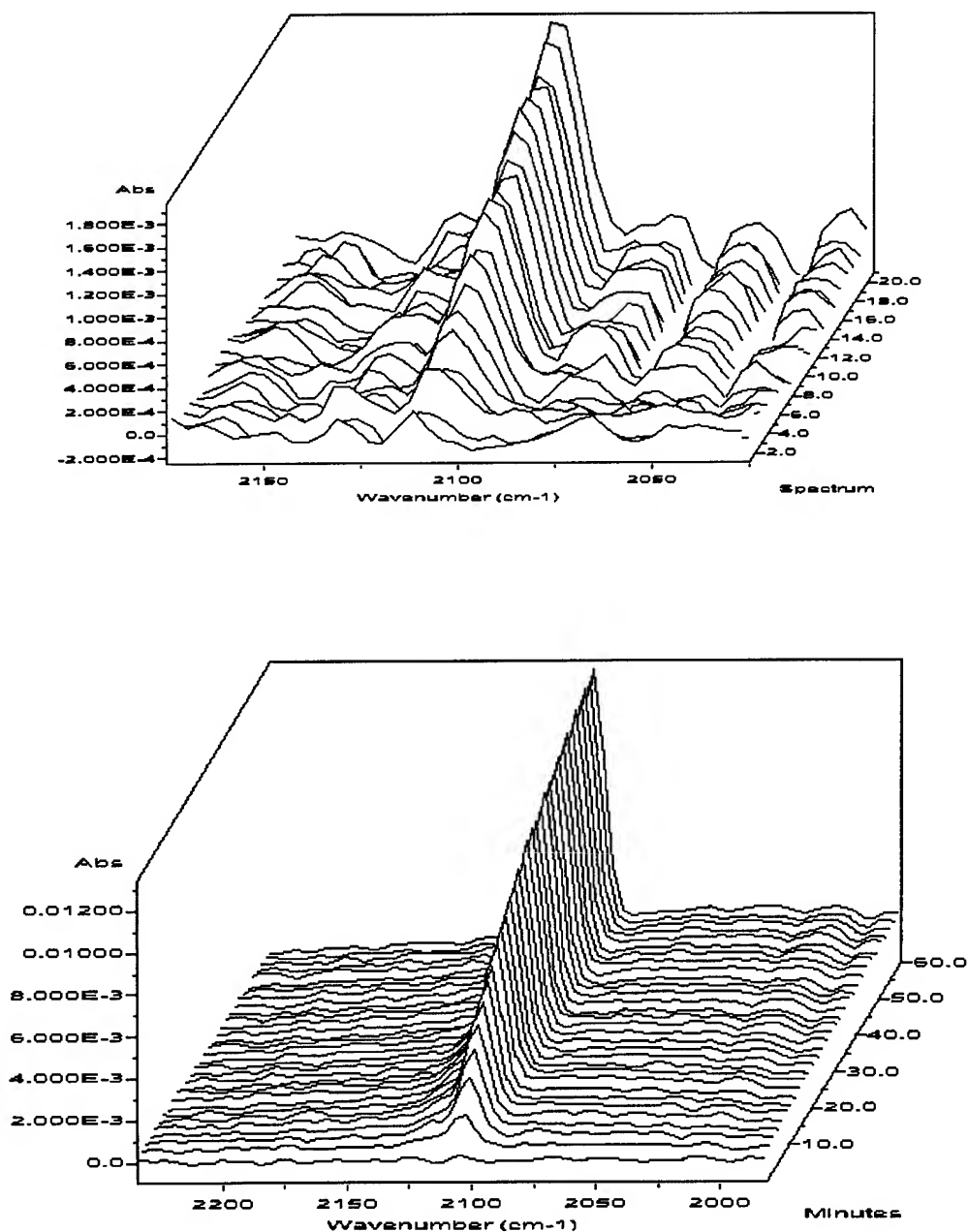
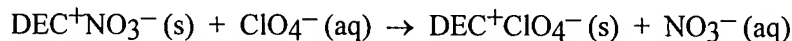


Figure 1. Time-dependent ATR-FTIR spectra of two thin films of the water-insoluble compound $\text{NiCl}_2(\text{dppp})$ on the $\text{SiComp}^{\text{®}}$ probe immersed in pH 10 aqueous KCN ($[\text{CN}^-] = 5 \text{ ppb}$ in the top spectrum; $[\text{CN}^-] = 0.13 \text{ ppm}$ in the bottom spectrum). The band that grows in over time, at 2104 cm^{-1} , is assigned to the water-insoluble compound $\text{NiCl}(\text{CN})(\text{dppp})$, which is formed throughout the film by the CN^-/Cl^- ion-exchange (ligand-exchange) reaction that occurs in the film.

Importantly, when the $\text{NiCl}_2(\text{dppp})$ -coated probe was immersed in an aqueous solution containing 0.13 ppm CN^- and 1 mol/L NaCl , the band at 2104 cm^{-1} was also observed in about 4 min. Therefore, a 20,000-fold excess of the co-contaminant Cl^- does not interfere with the detection of CN^- . This demonstrates the very high selectivity of $\text{NiCl}_2(\text{dppp})$ for CN^- and suggests that cyanide might be detectable at low concentrations in sea water (see below) and other aqueous brines using $\text{NiCl}_2(\text{dppp})$ -coated ATR-FTIR probes.

When the SiComp[®] probe coated with a thin film of $\text{DEC}^+\text{NO}_3^-$ was immersed in a solution of 3 ppb ClO_4^- in distilled deionized water (pH 5–6), a new band at 1092 cm^{-1} was observed in 60 min. This band is the T_2 -symmetry (ClO) band of the tetrahedral perchlorate ion, now concentrated in the thin-film coating *via* the following, essentially irreversible, ion-exchange reaction:



Since the detection limit for aqueous ClO_4^- ($\nu(\text{ClO}) = 1104\text{ cm}^{-1}$) with the uncoated SiComp[®] probe was found to be 288 ppm, the $\text{DEC}^+\text{NO}_3^-$ coating has lowered the one-hour detection limit for aqueous perchlorate by a factor of 96,000 (see Table 2). When the concentration of aqueous ClO_4^- was 0.5 ppm, the time necessary to observe the band at 1092 cm^{-1} was only 2 min.

Note that the related compound $\text{HEP}^+\text{NO}_3^-$ ($\text{HEP}^+ = 1,1',3,3'$ -tetrakis(2-methyl-2-hexyl)ferrocenium cation) has been used to selectively extract and recover the related tetrahedral monoanions $^{99}\text{TcO}_4^-$ and ReO_4^- from aqueous solutions containing 100,000 times as much nitrate ion.^{30,32–35} The ion-exchange process can readily be seen in Figure 2, which displays IR spectra recorded over time when the coated probe was immersed in 0.5 ppm aqueous ClO_4^- . The band at 1331 cm^{-1} (the E_u -symmetry $\nu(\text{NO})$ band of the nitrate ion) disappears at the same rate as the growth of the (ClO) band of ClO_4^- at 1092 cm^{-1} .

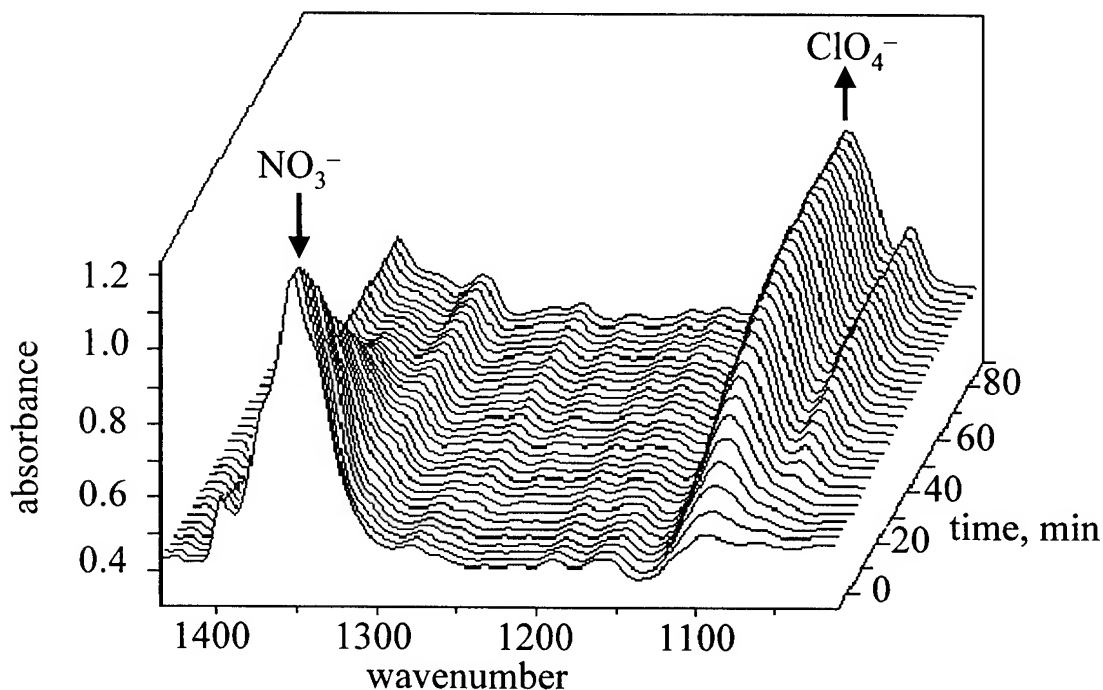


Figure 2. Time-dependent ATR-FTIR spectra of a thin film of water-insoluble $\text{DEC}^+\text{NO}_3^-$ on the SiComp[®] probe immersed in a pH 5–6 aqueous solution of LiClO_4 ($[\text{ClO}_4^-] = 0.5\text{ ppm}$). The bands at 1092 and 1331 cm^{-1} are assigned to the water-insoluble compounds $\text{DEC}^+\text{ClO}_4^-$ and $\text{DEC}^+\text{NO}_3^-$, respectively. The appearance of $\text{DEC}^+\text{ClO}_4^-$ and the disappearance of $\text{DEC}^+\text{NO}_3^-$ throughout the film are the result of a $\text{ClO}_4^-/\text{NO}_3^-$ ion exchange reaction.

The time dependence of the absorbance at 1092 cm^{-1} is shown in Figure 3. The initial rise at short times is nearly linear, and we have found that the slope of this linear region (dA/dt) is proportional to concentration over two orders of magnitude of concentration, as shown in Figure 4. Note that dA/dt appears to become constant above 10 mM ClO_4^- (260 ppb), probably because diffusion of ClO_4^- within the thin film, which is not concentration dependent, has now become the rate limiting step.

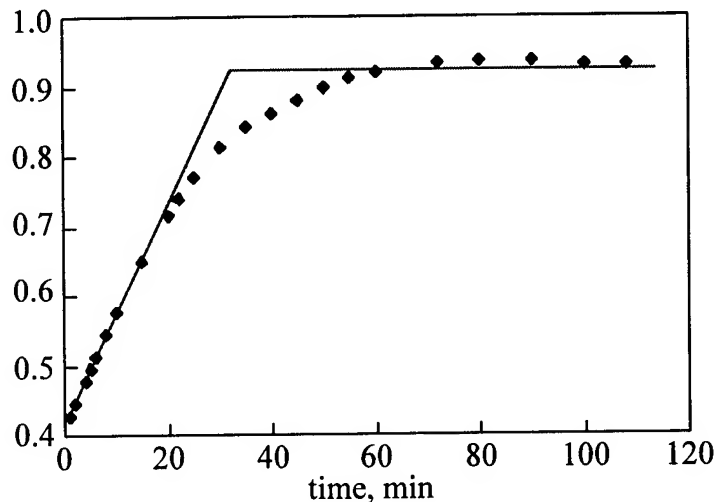


Figure 3. Plot of absorbance at 1092 cm^{-1} vs. time for a thin film of water-insoluble $\text{DEC}^+\text{NO}_3^-$ on the SiComp[®] probe immersed in a pH 5-6 aqueous solution of 0.5 ppm ClO_4^- .

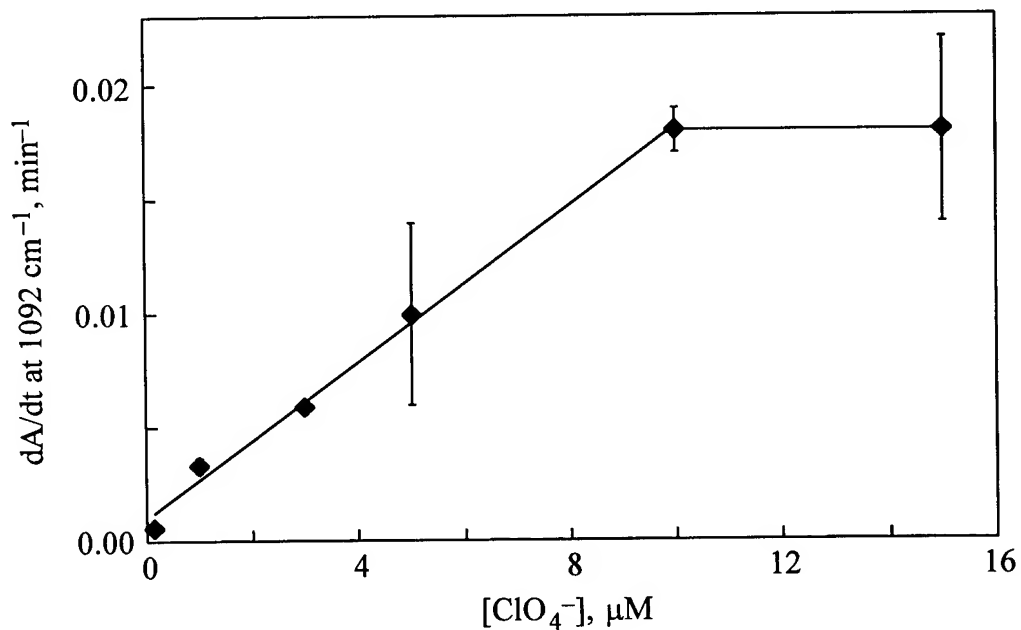


Figure 4. Calibration curve of $dA(1092\text{ cm}^{-1})/dt$ vs. perchlorate concentration from 0.1 to $15\text{ }\mu\text{M}$ (10 to 1,500 ppb).

When the SiComp[®] probe coated with a thin film of DEC⁺NO₃⁻ was immersed in a solution of 25 ppb PFOS in distilled deionized water (pH 5–6), several new bands in the fingerprint region were observed, undoubtedly due to an ion-exchange process similar to the one described above for ClO₄⁻. The most intense band, at 1270 cm⁻¹, had a signal/noise ratio • 3 after 60 min. Since the detection limit for aqueous PFOS (= 1243 cm⁻¹) with the uncoated SiComp[®] probe was found to be 100 ppm, the DEC⁺NO₃⁻ coating has lowered the one-hour detection limit for aqueous PFOS by a factor of 4,000 (see Table 2). When the concentration of aqueous PFOS was 0.25 ppm, the time necessary to observe the band at 1270 cm⁻¹ was only 4 min.

The compounds DEC⁺NO₃⁻ and HEP⁺NO₃⁻ are examples of redox-recyclable extractants, which are being developed in our laboratory for the efficient removal and recovery from water of weakly hydrated aqueous ions, even in the presence of 10⁵ times as much nitrate ion in the aqueous phase.^{29–35} The basis of redox-recyclable extraction and recovery (R²ER) is that the *neutral* extractant, in this case a hydrophobic ferrocene (Fe(Cp')₂), is the deactivated *low-affinity* form of the extractant. It is dissolved in an organic diluent or immobilized on a support. When treated with an aqueous reactivating solution, the *high-affinity* extractant Fe(Cp')₂⁺NO₃⁻ is formed within minutes. After ion-exchange equilibrium with an appropriate aqueous phase containing the target anion is complete (usually within minutes in bench-scale liquid-liquid experiments or whenever column breakthrough occurs), the R²ER phase is treated with an aqueous deactivating solution. This causes reduction of Fe(Cp')₂⁺ to Fe(Cp')₂ and release of the Y⁻ anion within minutes. Examples of reactivating solutions that have been used are aqueous Fe(NO₃)₃, Ce(NH₄)₂(NO₃)₆, and NaClO/HNO₃. Examples of deactivating solutions used are aqueous Na₂S₂O₄ and K₄Fe(CN)₆. We believe that it will be possible to recycle ATR-FTIR thin-film coatings of R²ER compounds using similar redox chemistry, once coatings that are more permanently bonded to the surface of an ATR crystal have been developed.

The results for detection of PMPA, EMPA, and MPA with the Eu-polymer coated DiComp[®] probe are summarized in Table 3, which also contains relevant results for the other analytes we have studied.

TABLE 3
JSAWM FY01 Exit Criteria vs. Current Detection Limits

analyte/compound of interest	FY01 criterion (15–30 min)	October 2000 detection limit
cyanide	2 ppm	25 ppb (15 min)
PMPA	100 ppb	180 ppb (30 min)
		18 ppb (75 min)
EMPA	100 ppb	12 ppm (30 min)
MPA	100 ppb	10 ppm (4 hr)
perchlorate		3 ppb (60 min)
PFOS		25 ppb (60 min)

The results of initial studies of matrix effects are shown in Table 4. The results for cyanide, PMPA, and triflate are promising. However, it is clear that a large excess of some interferants will affect that magnitude of dA/dt for some analytes. We will continue to test this emerging technology for reproducibility, linearity of response, tolerance of interferants, and a host of physical environmental factors.

TABLE 4
Matrix Effects (Preliminary Results of Interferant Experiments)

analyte/compound of interest	conc.	matrix	10^2 dA/dt (min ⁻¹)
cyanide	10 M	water	1.0
		seawater ^a	1.1
PMPA	100 M	water	~0.01
		0.35 M NaCl	~0.01
perchlorate	0.15 M	water	0.06
		15 M NaNO ₃	0.05
		150 M NaNO ₃	0.02
triflate (CF ₃ SO ₃ ⁻)	15 mM	water	6.3
		150 M NaNO ₃	5.9

seawater simulant (g/kg): 10.5 Na⁺; 19.0 Cl⁻; 1.3 Mg²⁺; 2.5 SO₄²⁻; 0.4 Ca²⁺; 0.4 K⁺; 0.14 HCO₃⁻; 0.06 Cl⁻; 0.02 H₃BO₃.

Acknowledgment

This research was supported initially by an R&D contract with Electrox, Inc., and subsequently by grants from the National Science Foundation (CTS-9726143) and the U.S. Army Research Office (DAAD19-00-1-0417). We thank Dr. Jeffrey J. Rack for valuable suggestions.

References

- Boening, Dean W.; Chew, Christine M. "A Critical Review: General Toxicity and Environmental Fate of Three Aqueous Cyanide Ions and Associated Ligands," *Water, Air, Soil Pollut.* **1999**, 109, 67.
- Otu, E. O.; Byerley, J. J.; Robinson, C. W. "Ion Chromatography of Cyanide and Metal Cyanide Complexes: A Review," *Int. J. Environ. Anal. Chem.* **1996**, 63, 81.
- Christen, K. "Surprising Human Health-Perchlorate Link," *Environ. Sci. Technol.* **2000**, 34, 374A (2000).
- Susarla, S.; Collette, T. W.; Garrison, A. W.; Wolfe, N. L.; McCutcheon, S. C. "Perchlorate Identification in Fertilizers," *Environ. Sci. Technol.* **1999**, 33, 3469.
- Okamoto, H. S.; Rishi, D. K.; Steeber, W. R.; Baumann, F. J.; Perera, S. K. "Using Ion Chromatography to Detect Perchlorate," *Jour. AWWA* **1999**, 91, 73.
- Urbansky, E. T. "Perchlorate Chemistry: Implications For Analysis and Remediation," *Bioremediation J.* **1998**, 2, 81.
- Moody, C. A.; Field, J. A. "Perfluorinated Surfactants and the Environmental Implications of Their Use in Fire-Fighting Foams," *Environ. Sci. Technol.*, in press.
- Moody, C. A.; Hebert, G. N.; Strauss, S. H.; Field, J. A. "Occurrence and Distribution of Perfluorinated Surfactants in Groundwater at the Wurtsmith Air Force Base Fire-Training Area Two and KC-135 Crash Site," submitted for publication.
- Tullo, A. "3M Discontinues Scotchgard Line," *Chem. Eng. News* **2000**, May 22, 9.
- Tullo, A. "3M Study Raised EPA's Concerns," *Chem. Eng. News* **2000**, May 29, 12.
- Renner, R. "Scotchgard Ban Highlights Unknowns," *Environ. Sci. Technol.* **2000**, 34, 371A.

12. Olsen, G. W.; Burris, J. M.; Mandel, J. H.; Zobel, L. R. "Serum Perfluorooctane Sulfonate and Hepatic and Lipid Clinical Chemistry Tests in Fluorochemical Production Employees," *J. Occup. Environ. Med.* **1999**, *41*, 799.
13. EPA Current Drinking Water Standards Web site. <www.epa.gov/safewater/mcl.html> (September 2000).
14. Pontius, F. W. "Regulations in 2000 and Beyond," *AWWA Jour.* **2000**, *92*, 40.
15. Darwin, R. L.; Ottman, R. E.; Norman, E. C.; Gott, J. E.; Hanauska, C. P. "Foam and The Environment: A Delicate Balance," *NFPA Jour.* **1995 May/June**, 67.
16. Urban, M. W. *Attenuated Total Reflectance Spectroscopy of Polymers. Theory and Practice*; American Chemical Society: Washington, DC, 1996.
17. Griffiths, P. R.; de Haseth, J. A. *Fourier Transform Infrared Spectrometry*; Wiley: New York, 1986.
18. Han, L.; Niemczyk, T. M.; Lu, Y.; Lopez, G. P. "Use of CLS To Understand PLS IR Calibration For Trace Detection of Organic Molecules In Water," *Appl. Spectrosc.* **1998**, *52*, 119.
19. Regan, F.; Meaney, M.; Vos, J. G.; MacCraith, B. D.; Walsh, J. E. "Determination of Pesticides In Water Using ATR-FTIR Spectroscopy on PVC/Chloroparaffin Coatings," *Analyt. Chim. Acta* **1996**, *334*, 85.
20. Göbel, R.; Seitz, R. W.; Tomellini, S. A.; Krska, R.; Kellner, R. "Infrared Attenuated Total Reflection Spectroscopic Investigations of the Diffusion Behavior of Chlorinated Hydrocarbons Into Polymer Membranes," *Vibrational Spectrosc.* **1995**, *8*, 141.
21. Barja, B. C.; Tejedor-Tejedor, M. I.; Anderson, M. A. "Complexation of Methylphosphonic Acid with the Surface of Goethite Particles in Aqueous Solution," *Langmuir* **1999**, *15*, 2316.
22. Dobson, K. D.; McQuillan, A. J. "In Situ Infrared Spectroscopic Analysis of the Adsorption of Aliphatic Carboxylic Acids To TiO₂, ZrO₂, Al₂O₃, and Ta₂O₅ From Aqueous Solutions," *Spectrochim. Acta* **1999**, *55A*, 1395.
23. Degenhardt, J.; McQuillan, A. J. "In Situ ATR-FTIR Spectroscopic Study of Adsorption of Perchlorate, Sulfate, and Thiosulfate Ions onto Chromium(III) Oxide Hydroxide Thin Films," *Langmuir* **1999**, *15*, 4595.
24. Hug, S. J. "In Situ Fourier Transform Infrared Measurements of Sulfate Adsorption on Hematite in Aqueous Solutions," *J. Coll. Interface Sci.* **1997**, *188*, 415.
25. Dobson, K. D.; McQuillan, A. J. "An Infrared Spectroscopic Study of Carbonate Adsorption to Zirconium Dioxide Sol-Gel Films from Aqueous Solutions," *Langmuir* **1997**, *13*, 3392.
26. Persson, P.; Nilsson, N.; Sjöberg, S. "Structure and Bonding of Orthophosphate Ions at the Iron Oxide-Aqueous Interface," *J. Coll. Interface Sci.* **1996**, *177*, 263.
27. Yang, Lin; & Saavedra, S. S. "Chemical Sensing Using Sol-Gel Derived Planar Waveguides and Indicator Phases," *Anal. Chem.* **1995**, *67*, 1307.
28. Ahn, D. J.; Franes, E. I. "Ion Adsorption and Ion Exchange In Ultrathin Films of Fatty Acids," *AIChE J.* **1994**, *40*, 1046.
29. Clark, D. L.; Clark, J. F.; Clapsaddle, B. J.; Chambliss, C. K.; Miller, S. M.; Anderson, O. P.; Strauss, S. H. "Synthesis and Characterization of Ferricenium Salts that are Insoluble in Water," submitted for publication.
30. Strauss, S. H. "Redox-Recyclable Extraction and Recovery of Heavy Metal Ions and Radionuclides From Aqueous Media," In *Metal Ion Separation and Preconcentration: Progress and Opportunities*. Bond, A. H.; Dietz, M. L.; & Rogers, R. D., Eds. ACS Symposium Series 716. American Chemical Society: Washington, DC, 1999, p 156.
31. Clark, J. F.; Chamberlin, R. M.; Abney, K. D.; Strauss, S. H. "Design and Use of a Redox-Recyclable Organometallic Extractant for the Cationic Radionuclides ¹³⁷Cs⁺ and ⁹⁰Sr²⁺," *Environ. Sci. Technol.*, **33**:2489 (1999).
32. Chambliss, C. K.; Strauss, S. H.; Moyer, B. A. "Comparison of the Lipophilic Redox-Recyclable

Extractant $[\text{Fe}(\text{}^5\text{-C}_5\text{H}_3(t\text{-C}_7\text{H}_{15})_2)_2][\text{NO}_3]$ with $[\text{N}(n\text{-C}_7\text{H}_{15})_4][\text{NO}_3]$ for Liquid-Liquid Anion-Exchange of Aqueous $^{99}\text{TcO}_4^-$," *Solvent Extr. Ion Exch.* **1999**, *17*, 553.

33. Chambliss, C. K.; Odom, M. A.; Morales, C. M. L.; Martin, C. R.; Strauss, S. H. "A New Strategy for Separating and Recovering Aqueous Ions: Redox-Recyclable Ion-Exchange Materials Containing a Physisorbed, Redox-Active, Organometallic Complex," *Anal. Chem.* **1998**, *70*, 757.
34. Chambliss, C. K.; Odom, M. A.; Martin, C. R.; Moyer, B. A.; Strauss, S. H. "Rapid and Selective Redox-Recyclable Anion-Exchange Materials Containing Polyalkylated Ferricenium Anion-Exchange Sites," *Inorg. Chem. Communications* **1999**, *1*, 435.
35. Clark, J. F.; Clark, D. L.; Whitener, G. D.; Schroeder, N. C.; Strauss, S. H. "Isolation of Soluble ^{99}Tc As a Compact Solid Using a Recyclable, Redox-Active, Metal-Complex Extractant," *Environ. Sci. Technol.* **1996**, *30*, 3124.
36. Hebert, G. N.; Odom, M. A.; Clapsaddle, B. J.; Craig, P. S.; Wheeler, K. E.; Strauss, S. H. "Method for the Determination of Sub-ppm Concentrations of Anions in Water," manuscript in preparation.
37. Jenkins, A. L.; Uy, O. M.; Murray, G. M. "Polymer-Based Lanthanide Luminescent Sensor for Detection of Hydrolysis Product of the Nerve Agent Soman," *Anal. Chem.* **1999**, *71*, 373.

TRACE CHEMICAL VAPOR DETECTION BY PHOTOTHERMAL INTERFEROMETRY

Nicholas F. Fell, Jr., Paul M. Pellegrino, and James B. Gillespie
U.S. Army Research Laboratory, 2800 Powder Mill Road,
Adelphi, Maryland 20783-1197

ABSTRACT

Photothermal interferometry has been demonstrated as a technique that can detect vapors with extremely high sensitivity (parts-per-trillion levels). Our present research uses a photothermal detection scheme that incorporates tunable sources and a modified Jamin interferometric design to provide high selectivity and sensitivity for organo-phosphate vapor detection. Phase shifts on microradian levels have been detected. Trace chemical vapor detection is accomplished by introducing the tunable excitation laser along the path of one interferometer beam providing a phase shift due to absorptive heating. Preliminary results indicated parts-per-billion detection of both DMMP and DIMP using ~400mW of CO₂ laser power at appropriate wavelengths.

INTRODUCTION

Monitoring trace gases in our environment has many actual and potential uses. Escalating environmental awareness has led to more restrictive regulations on air quality in both the workplace and the environment in general. Both industry and the military have expressed interest in development of more sensitive and adaptable trace gas analysis equipment. After the Tokyo subway sarin attack, the detection of CW agents became a crucial area of research in both the civilian and military arenas. Since many CW agents have low vapor pressures and are quite toxic, detection limits in the ng/mL range are required for fieldable systems. This detection limit highlights the need for extremely sensitive devices and techniques.

A more general environmental application of trace gas detection can be seen in workplace monitoring for specific pollutants. An important example involves the detection of monomethylhydrazine (MMH) and unsymmetrical dimethylhydrazine (UDMH). These materials are common components in certain types of rocket fuel as well as etchants in microstructure fabrication. Typical National Institute for Occupational Safety and Health (NIOSH) exposure levels are 30-60 parts-per-billion (ppb)¹ depending on the form of the hydrazine. This example also demonstrates that the degree of sensitivity needed in certain circumstances can exceed common limits of detection for monitoring systems.

Photothermal spectroscopy encompasses a group of highly sensitive methods that can be used to detect trace levels of gases using optical absorption and subsequent thermal perturbations of the gases. The underlying principle that connects these various spectroscopic methods is the measurement of changes in physical parameters (temperature, pressure, or density) as a result of photo-induced change in the thermal state of the sample. Photothermal methods in general are classified as indirect methods for detection of trace optical absorbance, because the transmission of the light used to excite the sample is not measured directly. Several examples of these techniques include photoacoustic spectroscopy (PAS), photothermal lensing (PTL), photothermal deflection (PTD), and photothermal interferometry (PTI). In PAS the pressure wave produced by the sample heating is measured, while the other examples sense changes in the refractive index or the refractive index directly by use of combinations of probe sources and detectors. The photothermal method we have chosen to pursue is photothermal interferometry. Recent research suggests that trace gas detection at parts-per-trillion (pptr) levels is attainable with this particular photothermal technique.^{2,3}

In the late 1960's it was recognized that optical absorption resulting in sample heating and subsequent changes in the index of refraction would induce a phase shift in light probing the heated region. McLean, Sica, and Glass⁴ were the first to demonstrate use of an interferometer to measure these photo-induced index changes. Most PTI apparatus are based on laser sources for both excitation and probe. Later Stone^{5,6} incorporated both coherent and incoherent excitation sources in a modified Jamin interferometer to measure trace absorption in liquid samples. Other notable contributions to PTI include measurements by Davis and Petuchowski,⁷ who achieved a lower limit of the infrared absorption coefficient of 10^{-10} cm^{-1} for a gaseous sample in a windowless cell. Recent research by Owens *et.al.*² demonstrated atmospheric ammonia detection at ppt levels using an apparatus similar to the Davis designs⁷. Survey of the literature both past and present indicates that a trace gas sensor with high sensitivity can be constructed using interferometer designs similar to ones previously mentioned.^{1-4,7,8}

We have designed, built, and are testing a new instrument for trace gas analysis in ambient air by PTI. The design uses a Jamin interferometer with a specialized optical coating, mid-IR excitation source, and HeNe probe source. Initial tests have established the ability to detect trace levels of two methylphosphonate compounds with modest amounts of CO₂ laser power. Methylphosphonates are well-studied simulants for nerve agents and pesticides. Our goals are to develop a PTI system with the ability to not only detect trace gases, but also to discriminate target gases from the normal atmospheric backgrounds and each other. Our work targets CW agent simulants to demonstrate the capabilities of PTI in this area. We have initially benchmarked the system performance with a waveguide CO₂ laser and plan further studies using a difference frequency generation (DFG) source. Frequency agile sources are of particular interest as they increase discrimination ability by providing absorbance information as a function of wavelength.

EXPERIMENTAL

Theory. In this section the underlying physical principles of PTI will be described in relation to our experimental system. Since PTI relies on detection of phase shifts produced by photo-induced heating of a sample, having excitation sources that overlap the peaks in the absorption spectrum of analyte gases is extremely important. Also, focusing on wavelengths that provide unique spectral information about sample strengthens the capabilities of the sensor. Due to these considerations we have chosen to probe the optical absorbance in the mid-infrared spectral region (8-12 μm). This region offers a wealth of information about the chemical structure of the CW agent simulants being investigated. A typical infrared absorption cross-section for one of these molecules, dimethyl methylphosphonate (DMMP), σ_{DMMP} , is approximately $44 \text{ atm}^{-1} \text{ cm}^{-1}$ near the 9P(26) CO₂ laser line. These large absorption cross-sections make the molecule well suited to absorption of the mid-infrared pump laser and subsequently convert the energy that is not re-emitted to heat after molecular relaxation, primarily through collisional relaxation. The collisional relaxation that occurs causes a temperature increase in the sampled gas according to,

$$\Delta T = \frac{P \sigma N}{2 f \rho C_p \pi a^2}, \quad (1)$$

where P is the IR excitation power, f is the laser modulation, ρ and C_p are the density and heat capacity of the sampled gas, respectively, N is the molecular number density, and a is the IR laser beam radius.

The rate of relaxation of the organophosphonate analytes studied can be estimated to be in the sub-nanosecond region using general gaseous thermodynamic equations⁹. The conduction of the heated air in our sample is slow relative to the relaxation time for organophosphonate samples, and the displacement due to convection of the heated gas is small compared to the radius of the laser probe beam. This implies that

we can regard the heating of the gas from the excitation source to be both instantaneous and localized within the probe beam. Modulation frequencies are chosen by considering both noise levels and the frequency dependence of the temperature change, as seen in equation (1). We modulated our CO₂ radiation in a low frequency local minimum in the noise curve appearing at ~ 600 Hz. Given the quasi-static local heating in the probe beam, the modulated index of refraction change follows the Clausius-Mossotti equation and is given by,

$$\Delta n = -(n-1)\Delta T / T_{abs}, \quad (2)$$

where T_{abs} is absolute temperature of the gas. The modulated index of refraction induces a modulated phase shift,

$$\phi_m = 2\pi l \Delta n / \lambda, \quad (3)$$

in the HeNe probe beam in one arm of the interferometer where l is the interaction path length, and λ is the wavelength of the interferometer laser. The complementary outputs of the interferometer are detected on two photodiodes. The difference in the intensities of the photodiode outputs is isolated by an instrumentation amplifier and the difference signal is sent to both the computer and a phase sensitive lock-in amplifier. The signal, S , is proportional to $\Delta\phi_m$, the difference between the complementary outputs of the interferometer, and is given by,

$$S = G \sin(\Delta\phi_m) = G(\Delta\phi_m), \quad (4)$$

with the final expression valid only for small $\Delta\phi_m$. The interferometer amplification factor, G , is a measure of the total system amplification is ~ 2 V per radian for this system. The noise encountered at the modulation frequencies investigated varied from 5-7 $\mu\text{V}/(\text{Hz})^{-1/2}$ in a typical measurement. Dividing the noise by the amplification factor gives an estimate of the interferometer sensitivity of 2.5-3.5 $\mu\text{radians}$.

Experimental Apparatus. The block diagram of the PTI beam paths and supporting analysis equipment is shown in Figure 1. The border in the diagram corresponds to an acrylic enclosure that surrounds the interferometer portion of the system. This section also rests on a 2.5-inch thick optical honeycomb board. The beam from a stabilized HeNe laser (Spectra-Physics model 117A), the probe beam, is initially directed to a steering mirror before entering the first of two specially coated etalons. The etalons have anti-reflection (AR) coatings on the front surfaces except for a centered 50/50 beamsplitting (BS) stripe while the back surfaces have high-reflection coatings. All coatings are designed for the HeNe wavelength (632.8 nm) and S polarizations. The probe beam initially enters the first etalon, is reflected off the back surface, and is subsequently split by the BS stripe. One beam exits the optic while the other beam undergoes a second reflection off the back surface before exiting. Thus, the output of the first etalon is two equal intensity beams separated by ~12 mm edge to edge. These beams define the two interferometer arms and travel through an open-ended acrylic tube (32 cm long) en route to an identical second etalon 60 cm away. The second etalon acts to recombine equal amounts of both interferometer arms into two complementary outputs of the interferometer. The modified-Jamin interferometer design gives the system superior rejection of mechanically induced noise due to the common optical path of both arms and the lack of moving parts.

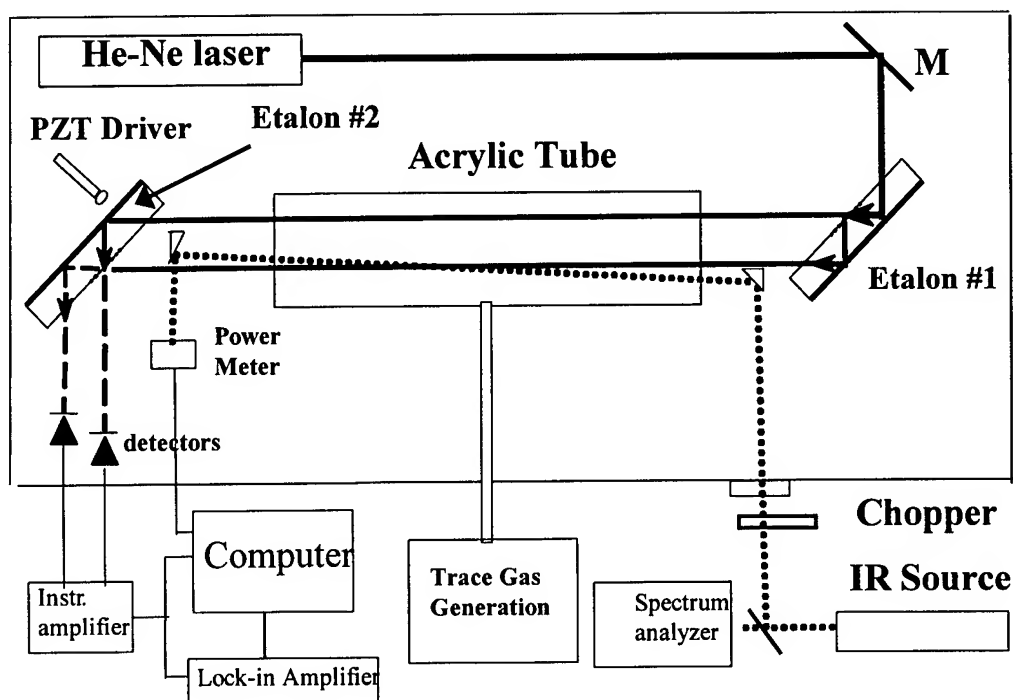


Figure 1. Experimental block diagram for modified-Jamin photothermal interferometer

The complimentary outputs are detected by two photodiodes (United Detector Technologies PIN 10DP). The signals are passed into a custom-fabricated instrumentation amplifier that provides the difference signal to both the lock-in amplifier (Stanford Research Systems SR510) and a personal computer running a LabVIEW (National Instruments) control program. The control program accepts inputs from the lock-in amplifier, instrumentation amplifier, and the power meter. A 1-second average of the DC component of the difference signal is used for feedback to control the piezo-electric driven micrometer on the second etalon. This feedback control is used to maintain the interferometer in a quadrature position, which is the most sensitive position in relation to changes in the phase shift and the center of the linear response range. The lock-in signal and the measured IR power are used to provide an excitation power normalized signal. Pure trace gases are introduced into the acrylic tube via a trace gas generator (VICI-Metronics Dynacalibrator Model 190). The gas generator is set at 100°C and pure nitrogen flows of 0.1-1.0 L/min will produce trace levels of organo-phosphate from approximately 10 ppb – 1.0 ppm depending on the length of the permeation tube in the device and the flow. The IR excitation beam is introduced from a waveguide CO₂ laser (California Laser, circa. 1984) set at wavelengths corresponding to sizeable vapor absorption cross-sections. The beam is initially split with one part entering a spectrum analyzer (Optical Engineering 16A) to provide wavelength information. The other part is modulated by a chopper ($f = 600$ Hz) before entering the enclosure through an AR coated ZnSe window. This beam glances off the gold-coated hypotenuse of a prism making a shallow crossing angle with one arm of the interferometer. Using another coated prism, the beam is directed to broadband power meter. The effective path length is estimated at 10 cm with the IR beam diameter of 3-4 mm, with a probe beam diameter not exceeding 2 mm. This mismatch in beam diameters can be attributed to poor beam quality of the waveguide CO₂ laser. This is not an inherent quality of these types of lasers, but is related to the age of our laser system. The mismatch prevents the efficient use all of our IR excitation power.

RESULTS AND DISCUSSION

Initial trials were conducted by spiking the entire acrylic enclosure with minute volumes of methanol and methanol-glycerin mixtures. Using the methanol percentage, and known volumes of both the enclosure (169 L) and liquid, a partial pressure could be calculated. Figure 2 resulted from an 18- μ L spike of pure methanol, which corresponds to 63 ppm partial pressure. The smooth line is a gaseous FTIR spectrum (EPA Public Gas Phase Database) overlaid on the experimental data taken with the PTI system. Despite gaps associated with the CO₂ laser this demonstrates the ability of the system to perform limited spectral discrimination using multiple lines of the grating-tuned CO₂ laser. Using methanol-glycerin mixtures and any of the 10P or 10R CO₂ lines as excitation, 1-ppm methanol levels were easily detected.

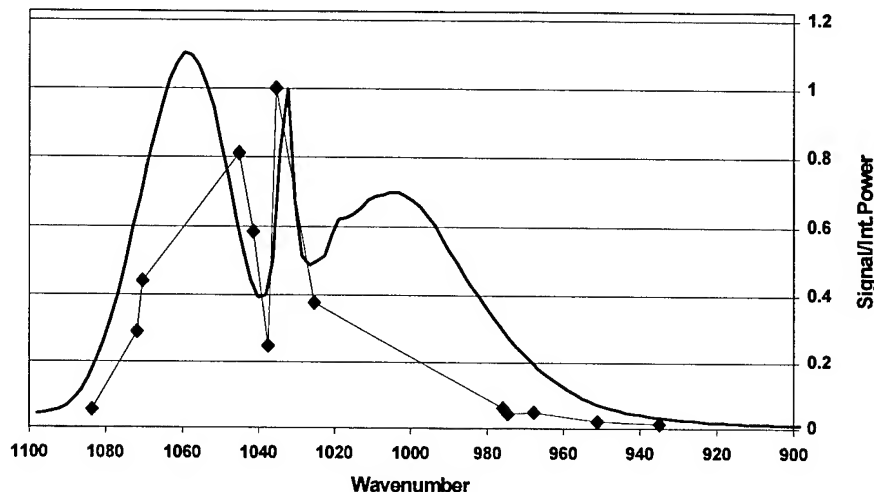


Figure 2. Spectrum of pure methanol excited with multiple CO₂ laser lines. The approximate concentration of the methanol is 63 ppm.

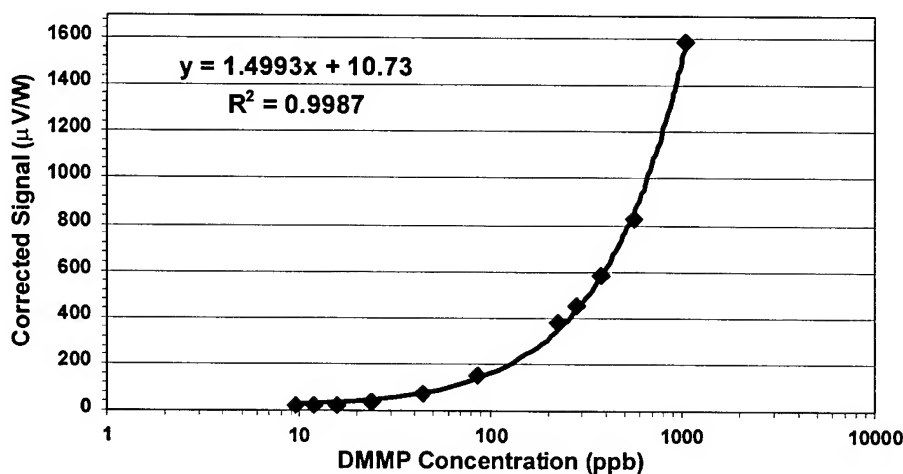


Figure 3. Semi-log plot of corrected PTI signal versus DMMP concentration

Following these initial studies both beams were enclosed by the acrylic tube seen in Figure 1 and the trace gas generator was used to investigate responses from two organophosphonate compounds. Both dimethyl methylphosphonate (DMMP) and diisopropyl methylphosphonate (DIMP) permeation tubes of varying lengths were loaded in the generator. The tube lengths and calibrated flow range of our generation system limited the concentrations available for study to 10 ppb to 1 ppm. The power-corrected signal versus concentration is shown in Figure 3 for DMMP ($\epsilon_{DMMP} \sim 44 \text{ atm}^{-1}\text{cm}^{-1}$) excited with the 9P(26) line ($P = 575 \text{ mW}$). The semi-log plot shows excellent linearity with a linear correlation coefficient (R^2) of 0.9987.

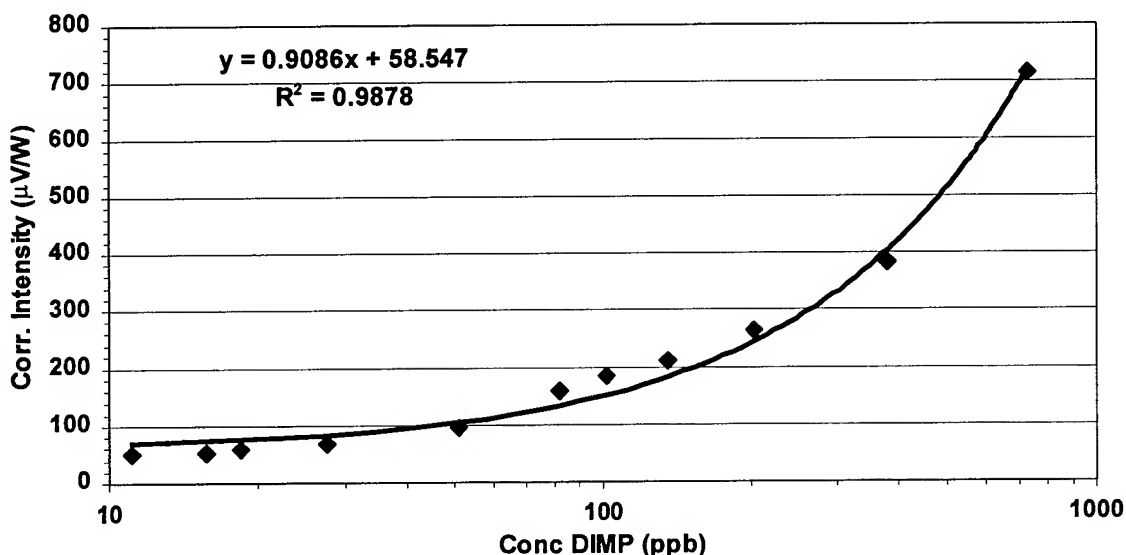


Figure 4. Semi-log plot of corrected PTI signal versus DIMP concentration

The second organophosphonate studied provided more of a challenge to our system, due to the lack of available CO_2 lines at the maximum of the DIMP IR absorption spectrum. The DIMP absorption cross-section ($\epsilon_{DIMP} \sim 27 \text{ atm}^{-1}\text{cm}^{-1}$) at the 10R(32) line is substantially weaker than the DMMP peak absorption, but was still measurable. The corrected signal versus concentration is shown in Figure 4 for DIMP excited with the 10R(32) line ($P = 400\text{mW}$). The semi-log plot of the signal shows very good linearity with an R^2 of 0.9878.

The dynamic range of our trace gas generator and the PTI system noise floor dictate the limit of our measurements on both phosphonates. The electronic noise floor of $5\text{-}7 \text{ V}/(\text{Hz})^{1/2}$ is still excessive considering the amplifier gains on the order of 10^4 V/A . This noise level is a factor of 60 above the shot noise limit of $1.0^{-7} \text{ V}/(\text{Hz})^{1/2}$ based on the systems standard parameters. Recent literature suggests that we can attain levels of noise that are factors of 3 to 4 above shot noise limits. Other noise sources (acoustical and thermal) would probably prevent full realization of the shot noise limit. The second area that requires work is the CO_2 beam size and the shallow angle overlap. The CO_2 size should be at the size of the probe beam or less to maximize use of the power that enters the interaction path. Insertion of an IR telescope to reduce the size and collimate the laser beam should make the system more efficient and aid in the alignment of the crossing.

CONCLUSIONS

We have demonstrated the ability to detect trace amounts of organophosphonate vapor using PTI. This work focused on testing the current ability of our detection system by incorporating a waveguide CO₂ as the excitation source. The measurement limits of 10 ppb for phosphonate vapors agree with the predicted sensitivity of several microradians of phase shift. Improvements on the system can be made in several key areas such as electronics and beam overlap. Future work will concentrate on system improvements and implementation of the difference-frequency-generation source.

ACKNOWLEDGEMENTS

We would like to acknowledge the efforts of two summer research students, Juan Carlos Alvarado and Ben Wun, for their work on the LabVIEW programming for the control system used in this project. We would also like to gratefully acknowledge the funding we have received for this work from the Office for Special Technology.

REFERENCES

1. D.L. Mazzoni and C.C. Davis, "Trace detection of hydrazines by optical homodyne interferometry," *Appl. Opt.* **30**, pp. 756-764, 1991.
2. M.A. Owens, C.C. Davis, and R.R. Dickerson, "A photothermal interferometer for gas-phase ammonia detection," *Anal. Chem.* **71**, pp. 1391-1399, 1999.
3. M.A. Owens, *Detection of Gas-Phase Ammonia Using Photothermal Interferometry*, University of Maryland, 1995 (dissertation).
4. E.A. McLean, L. Sica, and A.J. Glass, *J. Appl. Phys. Lett.* **13**, pp. 369, 1968
5. J. Stone, "Measurements of the absorption of light in low-loss liquids," *J. Opt. Soc. Am.* **62**, pp. 327-333, 1972.
6. J. Stone, *Appl. Opt.* **12**, pp. 1828, 1973.
7. C. C. Davis and S.J. Petuchowski, "Phase fluctuation optical heterodyne spectroscopy of gases," *Appl. Opt.* **20**, pp. 2539-2554, 1981.
8. S.E. Bialkowski, "Photothermal Spectroscopy Methods for Chemical Analysis," from *Chemical Analysis: A series of Monographs on Analytical Chemistry and Its Applications*, J.D. Wineforder, editor, Vol. 134, John Wiley & Sons, Inc., New York, 1996.
9. F. Reif, *Fundamentals of Statistical and Thermal Physics*, Chapter 12, McGraw-Hill, New York, 1965.

THE BIOCOUNTER: A HAND-HELD BIODETECTOR AND SAMPLER BASED ON FLUORESCENCE PARTICLE SIZING

Dr. Greg A. Luoma, Pierre P. Cherrier, Carol Y. Zheng, Marc A. Piccioni and Alex S. Wong
*Bio-Defence Systems, Computing Devices Canada, 1020 68th Avenue NE, Calgary, Alberta, Canada,
T2E 8P2*

*Dr. Richard K. DeFreez, Michael A. Potter, Kenneth L. Girvin and Ronald B. Whitney
Pacific Scientific Instruments, 481 California Avenue, Grants Pass, Oregon, United States, 97526*

Abstract

This presentation will describe the development to date of a new real time biological particle detector and sampler called the BioCounter. It combines a novel fluorescence particle sizer (Biological Aerosol Real Time Sensor, BARTS) with a dry sampling technology to provide a number of advantages over existing systems. These include affordable cost and small size. A discussion of the development of two discrete UV laser technologies will be discussed. Data from chamber and field trials will be presented to show that the BARTS retains the high level of technical performance of previous fluorescence particle sizers.

Introduction

The Gulf War highlighted the growing threat to the Western Alliance from biological weapons. The size and breadth of the Iraqi program to produce military quantities of biological weapons was totally unexpected, and demonstrated that even small nations could develop them as an "asymmetric" threat to counter Western dominance in more traditional warfare approaches. Revelations about the massive size and scope of the Russian program to develop biological weapons, that is now known to have involved up to 35,000 scientists in a variety of establishments, has added evidence of the growing threat. Further, the break-up of the Former Soviet Union (FSU) has resulted in a wide-spread proliferation of the technology and expertise to many rogue states and radical groups that seem to be more than willing to use biological weapons for political means. Finally, advancements in biotechnology have increased the ability to genetically modify existing agents and create new ones that can circumvent existing identification technologies and medical countermeasures. As a result, real time detection and warning are keys to avoiding exposure, since identification technologies and medical treatments cannot be relied upon in the face of the growing number of threat agents.

There are a number of significant differences in the approach to defense against biological agents between military scenarios and civilian scenarios. In general, civilian attacks in public places are expected to be smaller, less predictable, and more difficult to defend against. Most experts believe that defense against random attacks in public places will focus on consequence management after the attack rather than preventing or avoiding it. In particular, the roles of the first responders and specialist groups will be to attempt to treat the initial victims and limit the spread of contamination to avoid so-called "secondary" casualties. In this case, detection technologies are used primarily for finding the source of the release, monitoring the level of contamination in the exposure area, monitoring the spread of contamination, and determining the success of decontamination efforts.

In scenarios involving specific civilian high-risk facilities (for example, embassies) a more traditional approach to defense can be adopted because those facilities can be isolated from the outside environment

and entry can be controlled. Appropriate levels of planning can limit the potential for success of a terrorist attack, and the judicious use of detectors can help avoid or limit exposure of individuals to a release. Detectors can be part of the security system, and can be located in the high volume air system, as well as all access points to the building. They can be easily coupled with the normal intrusion alarms and other detectors such as explosive detectors.

To be effective in these roles, the detectors must be able to detect a large number of potential threat agents, not just those on a specific military threat list. This is because the small quantity of agent that is required for terrorist attacks greatly expands the potential threat list. Thus, technologies that focus on identification of specific predetermined agents will have limited effectiveness because it is very difficult to predict which agents might be used. On the other hand, generic detectors that can detect all agents and can collect a sample for analysis by more traditional identification methods will be more effective.

In addition, the detectors must respond in real time for most of the applications mentioned above. For example, when protecting high-risk facilities, only real time detection can provide the timely warning needed to avoid or minimize exposure. Also, detectors must have extremely low false alarm rates and high sensitivities because the consequences of false alarms are great. Further, they must operate autonomously for very long periods of time, so they must use no consumables. Finally, to provide maximum flexibility in applications, they must be small, portable and able to operate for extended periods on batteries.

The Role of Fluorescence Particle Detection

Of the technologies available today, fluorescence particle detection offers the greatest potential to meet these requirements. By combining airborne particle characterization with the ability to distinguish those particles that are biological, the fluorescence particle sizers are able to provide reliable, real time detection of biological agents. Two different technologies are presently incorporated into fielded biodetection systems: the Fluorescence Aerodynamic Particle Sizer (FLAPS); and the Biological Aerosol Warning System (BAWS). The two technologies use different fluorescence excitation frequencies (355 nm in FLAPS and 266 nm in BAWS) and both make use of advanced software-based alarm algorithms to improve the ability to discriminate biological agent aerosols from normal biological background aerosols. The FLAPS also has the capability to determine particle size, and this has been shown to be a valuable additional means to distinguish biological agent aerosols from other background particles.

Limitations of the FLAPS and BAWS include:

- cost;
- physical parameters (size, weight and power) that limit portability;
- lack of ruggedness (FLAPS) for some applications.

These limitations result from using expensive leading-edge ultraviolet laser technology and intricate optical assemblies to ensure that the light induces fluorescence from specific biomolecules in the aerosol particles. Therefore a major goal of this project is to develop a new fluorescence particle detector containing a low-cost UV laser producing adequate power at 355 nm combined with a simple and robust particle sizing technology. The new fluorescence particle detection technology is called the Biological Agent Real Time Sensor (BARTS). The other key goal is to integrate the detection components into a small and highly portable package that can be used in hand-held operations. A dry particle sampler will be integrated into the system to collect a sample from the exhaust of the fluorescence particle detector for identification/verification of the agent using off-line technologies. The system will also include sophisticated software to interpret the fluorescence data and provide the ability to send the data to a remote terminal by radio modem or ethernet link. The integrated detector and sampler will be called the BioCounter.

This presentation describes the development of the new fluorescence particle detector for the BioCounter, and presents results of its performance at field trials at Defence Research Establishment Suffield (DRES) and Dugway Proving Ground (DPG). The dry particle sampler technology and data analysis components will be discussed elsewhere.

Development of the UV Laser Technologies

In developing the new 355 nm UV laser technology for the BioCounter, two options were pursued: the development of a continuous wave ultraviolet laser based on a frequency-tripled Nd:YVO₄ diode laser coupled with a resonant build-up cavity to amplify the laser power; and, the development of a high frequency, long-duration pulsed laser also based on a frequency-tripled Nd:YVO₄ diode laser.

Option 1: Continuous Wave Nd:YVO₄ Laser

The key goal was to develop a reliable, compact, and inexpensive light source in the UV spectral region (330 - 370 nm) with sufficient continuous power (target >10 mW) to provide effective excitation of fluorescence from biological aerosol particles. The approach chosen was to use a frequency tripled Nd:YVO₄ laser coupled with a resonant cavity to amplify the laser power. The resonant cavity also doubles as the particle counting chamber.

To produce at least 1 mW of power at 355 nm, a diode pump laser at 808 nm was employed to produce a narrow beam width and more than 10 W of recirculating power at the fundamental frequency of 1064 nm. The light at 1064 nm was then circulated through a 3 mm thick KTP crystal to produce about 500 mW of power at the second harmonic frequency, 532 nm. A second non-linear optical frequency conversion was achieved by sequentially adding a 4 mm BBO crystal to produce about up to 1 mW of power at 355 nm. This group of crystal elements were sandwiched together to form a Monolithic Crystal Assembly (MCA) which is the key element in minimizing the size and power requirements of the new laser. A number of slight alterations to the MCA design, including varying the crystal composition, using specific crystal coatings, and inserting small air gaps in critical locations were tried in an attempt to optimize the efficiency of the frequency conversion and eliminate side bands. Figure 1 shows the laser assembly and the structure of the MCA.

The Sensor Assembly was designed to serve both as the build-up intracavity amplifier and the particle sizing/counting chamber. The design is a resonant cavity that amplifies the input beam by about 10X. It also has two output channels, one for fluorescence detection and one for scattering detection. The input beam travels through the partially reflective mirror in the first mirror assembly and is reflected back by the opposing mirror. The latter is a moveable mirror which is controlled by a piezoelectric feed-back circuit that automatically adjusts the distance between the mirrors to be an exact harmonic of the wavelength of the laser light, thereby establishing a resonator build up cavity. Alternatively, the first mirror is internal to the MCA and a window is positioned in the first mirror assembly. The sample is carefully carried through the sensor assembly that is sealed to the outside environment with the exception of clean purge air and the sample air.

This arrangement prevents contamination of the optics. The sample is introduced into the sensor through the inlet port and is detected by the electro-optical sensors. Figure 2 shows a picture of the Sensor Assembly.

A PC-104 stack containing a 12-bit A/D card, processor card and instrument control electronics is used to collect and process data. The proprietary data collection, analysis and alarming software developed for the FLAPS has been ported over to the new design to analyse the data in the same way as was done for the FLAPS. A separate PC-104 controller was used to control the laser diode current and the MCA temperature.

The same controller was used for the piezoelectric controlled resonant cavity. A sophisticated algorithm was implemented to adjust the MCA parameters for optimal UV performance.

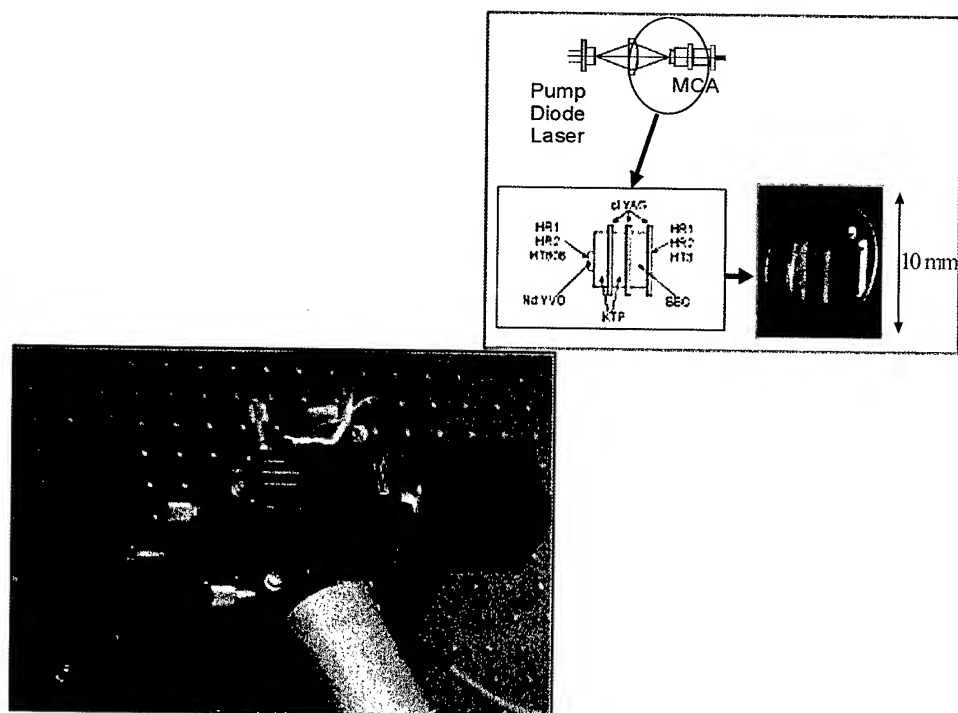


Figure 1: Pictures of the continuous wave UV laser assembly and monolithic crystal assembly (MCA) used for the frequency tripling.

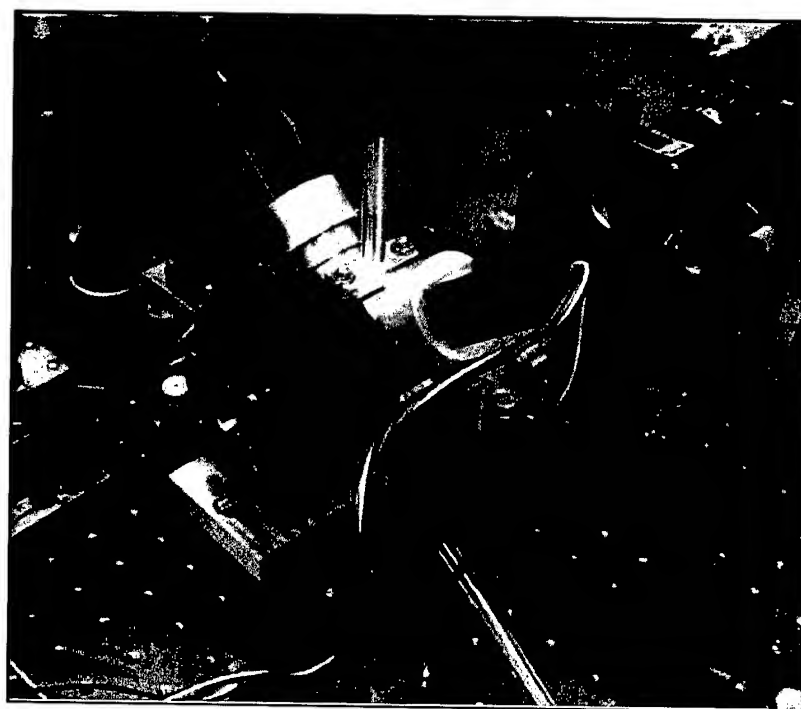


Figure 2: A picture of the optical assembly for the continuous wave laser.

Option 2: Development of a High Frequency Long-Duration Pulsed UV Laser

The development of the high frequency, long-duration pulse UV laser was undertaken to improve the stability of the laser and enhance large scale production capability by gaining enough UV power with a pulsed laser design that eliminates the need for the MCA, the fine tuning, and the resonant cavity. Here, "long-duration" means long relevant to the fluorescence lifetime of the target molecule. The main constraints in this approach were that the beam cross-section, the pulse frequency, and pulse duration had to be sufficient to ensure that every particle entering the air flow cell is interrogated at least once by the laser. Based on a flow rate of 3 liters of air per minute containing up to 10,000 particles, we determined that ensuring a pulse duration of 150 nanoseconds and a pulse repetition frequency of 100 kHz were sufficient. The average power of the laser was also specified to be 10 mW to ensure that there was sufficient power to cause efficient excitation of the fluorescence from the biomolecules in the aerosol particles.

The basic laser design uses a diode-laser-pumped frequency-tripled Nd:YVO₄ solid-state laser. The solid-state laser is actively Q-switched at 100 kHz to achieve the 150 nanosecond pulses. Efficiency of third harmonic generation to 355 nm is achieved by a proprietary multi-pass laser resonator designed and built by Applied Harmonics Corporation specifically for this program. This laser achieves sufficient power for the application with a spatially and temporally stable lowest order beam. Furthermore, this beam does not require the complexity of an external build-up resonator or its associated piezo positioning equipment and control computer. However, faster photodetection electronics had to be developed to accommodate the 150 nanosecond optical pulse duration.

Figure 3 shows a picture of the laser. Shown in the Figure (from right to left) are the diode laser heatsink, diode laser housing, coupling optics mount, solid-state laser crystal assembly, Q-switch and its holder, second and third harmonic generation optical assembly, and the fundamental resonator output mirror through which UV light is transmitted. The length of the total laser assembly is about 10 inches.

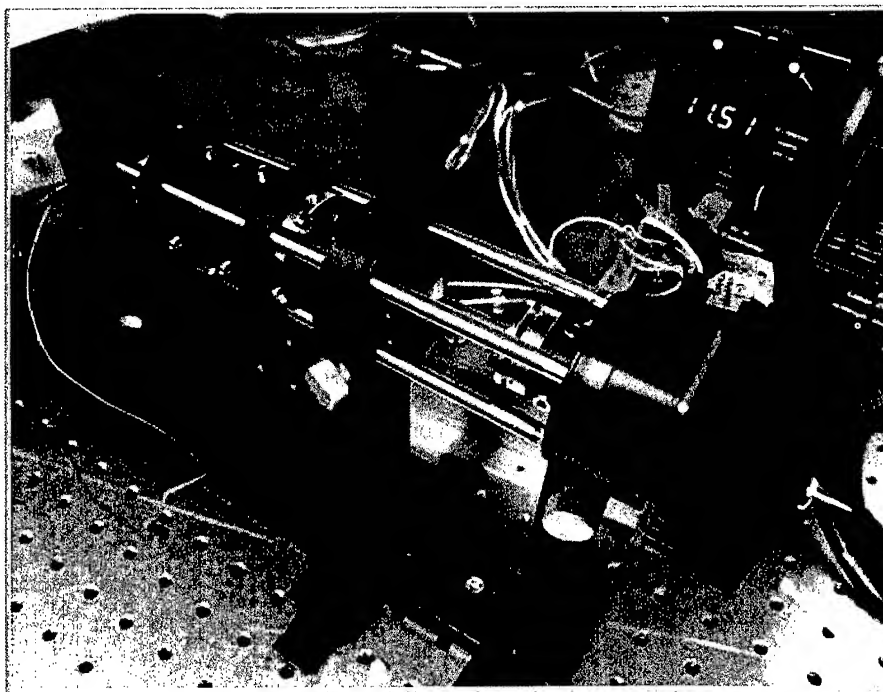


Figure 3. Actively Q-switched 100 kHz, 150 nanosecond 355 nm laser.

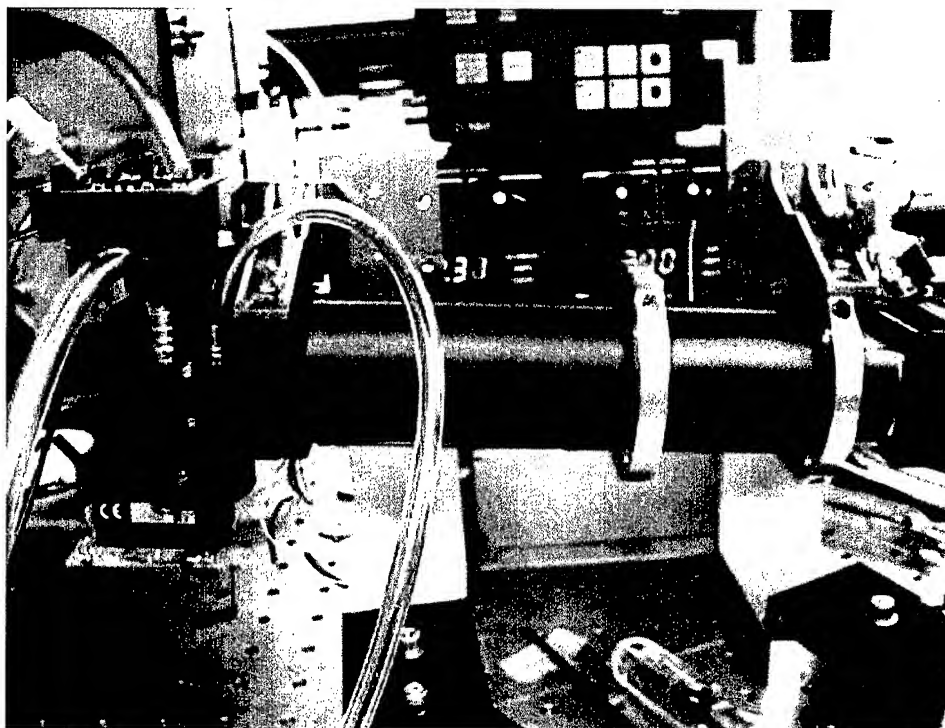


Figure 4. A picture of the high frequency long pulse duration laser attached to the BARTS sensor detection chamber.

Figure 4 is a photograph of the actively Q-switched laser attached to the BARTS sensor detection chamber. The chamber contains sample and purge jets, a vacuum exhaust port, and optical windows. Above and below, collections optics, PMT assemblies, and pre-amp boards are attached to the direct scatter and fluorescence ports of the chamber.

Field Trial of the BARTS Containing the Continuous Wave Laser

To test the performance of the BARTS containing the continuous wave laser technology, a series of field trials was conducted at Defence Research Establishment Suffield in June 2000. A total of ten releases of four simulants were conducted. In some cases, smoke was released simultaneously as an obscurant. Micron Air sprayers were deployed approximately 100 meters from the sensors. Spiral plate counters were used to collect referee samples, and a FLAPS was located near a number of BARTS sensors to provide comparative real time data. XMX concentrators were used to provide concentrated aerosol samples (input 600 liters per minute to output 3 liters per minute at 50% efficiency for 2-10 micron particle sizes) to each of the FLAPS and the BARTS. The standard FLAPS alarm algorithm was used with the BARTS to determine when the biological aerosol cloud was detected.

The ten releases of simulants included four *Bacillus globigii* (BG) (spore also known as *Bacillus subtilis* var. *niger*), two BG plus smoke obscurant, one *Erwinia herbicola* (EH) (vegetative organism), one EH with obscurant, one MS2 (virus) and one Ovalbumin (protein toxin).

The BARTS detected eight of the ten releases of simulant in real time, and the other two did not produce a high enough concentration to register on either of the referee systems (spiral counter or FLAPS). Further, the smoke obscurant did not impact the ability of the BARTS to detect either EH or BG releases.

Figure 5 shows a typical response of the various detectors and referee systems to a BG release in the presence of obscurant (most difficult case). The obscurant caused significant rises in the background particle count and would have obscured detection based on the particle data alone (top trace in each figure). However, both the FLAPS and the BARTS correctly detected this release when compared to the spiral plate count data (ACPLA in bottom trace). The FLAPS and BARTS showed remarkably similar responses, confirming that the BARTS containing the continuous wave laser detected biological agents similarly to the FLAPS.

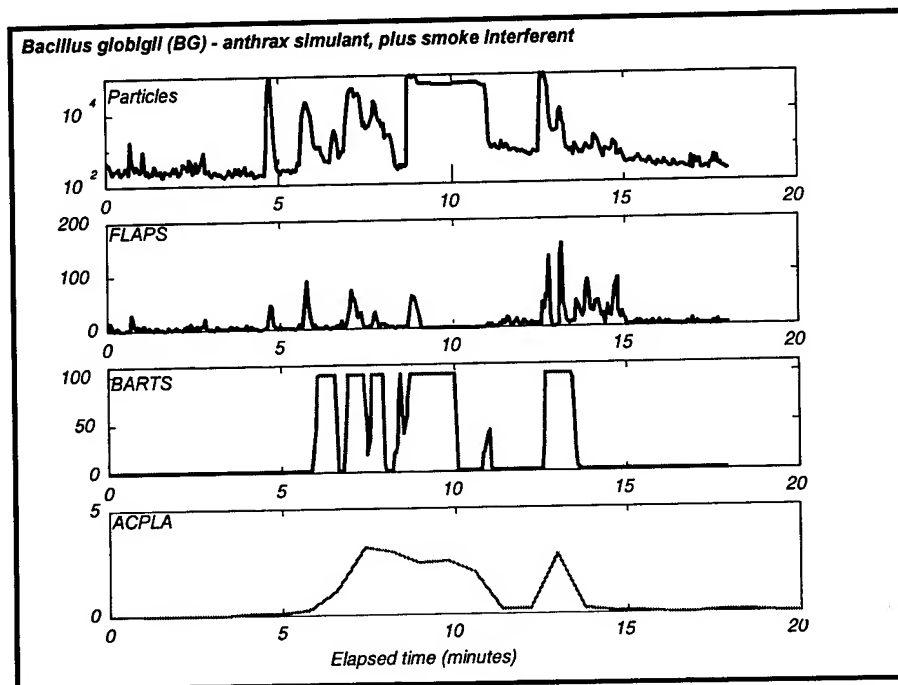


Figure 5. Field trial with BG and smoke obscurant to compare the performance of BARTS and FLAPS to referee data.

The field trials at DRES proved that the continuous wave laser version of BARTS could detect biological aerosols in the field. However, during development of the continuous wave laser design, and assembly of the eight prototype units, a number of weaknesses were identified. In particular, high quality MCAs were difficult to obtain from crystal suppliers, and the lasers required extremely accurate tuning for optimum performance. Further, in the field it was difficult to keep the lasers "in tune" for extended periods of time, and this impacted performance of the alarm algorithm. The team was concerned that the drift in the laser power would preclude producing the lasers in quantity and would greatly increase support requirements.

Field Trials of the BARTS Containing the High Frequency Pulsed Laser

Two BARTS units containing the high frequency long pulse duration laser and up-dated electronics were evaluated at field trials at Dugway, Utah, in September 2000. Because no particle concentrator was used in these trials, the BARTS sampling time interval was increased from 3 seconds to 20 seconds to increase the number of fluorescent particles in each sampling period. In the absence of the particle concentrator the BARTS samples about 3 liters of air per minute, so this represents about one liter of air per sampling period, and would result in 1 fluorescent count for every ACPLA.

The following Figures show the results from the two BARTS units deployed during September trials at Dugway responding to a specific release of dry BG. Figure 6 shows the first unit response, compared with the Portal Shield Unit response which situated in the same Tricon unit. The measurement returned from the Portal Shield unit is in particles per cubic centimeter (PPCC), and the measurement returned from the BARTS is in Total Number of Particles detected. Time scale is in minutes elapsed since test window started. It shows that using the high frequency pulsed laser does not hinder the capability of counting particles compared to a stable CW laser.

Figure 7 shows the second unit response, situated about 800 meters from the first BARTS unit, compared with the slits samplers data situated about 5 meters away from the BARTS. The measurement returned from the slits sampler plate data yields a coarse measure of biological activity (colonies per sector), and the measurement returned from the BARTS is in total number of particles detected, biological agents (i.e. fluorescent particles) detected, and the threat level returned from the alarming algorithm. Time scale is in minutes elapsed since test window started. It shows that using the high frequency pulsed laser does not hinder the capability of counting biological particles compared to a stable CW laser.

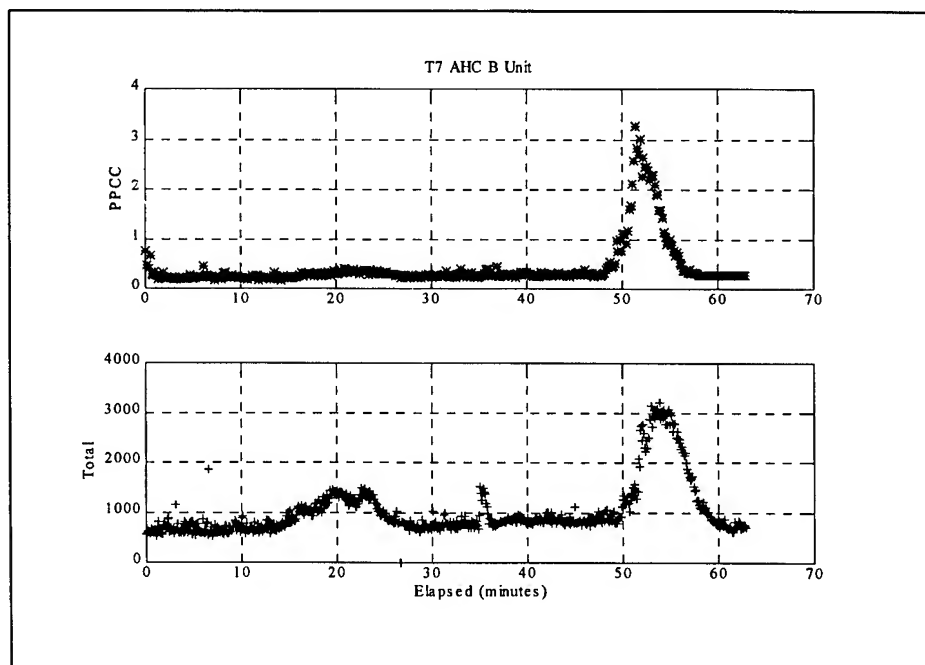


Figure 6. Field trial with BG to compare the performance of high frequency laser BARTS and Portal Shield unit (particle counting device).

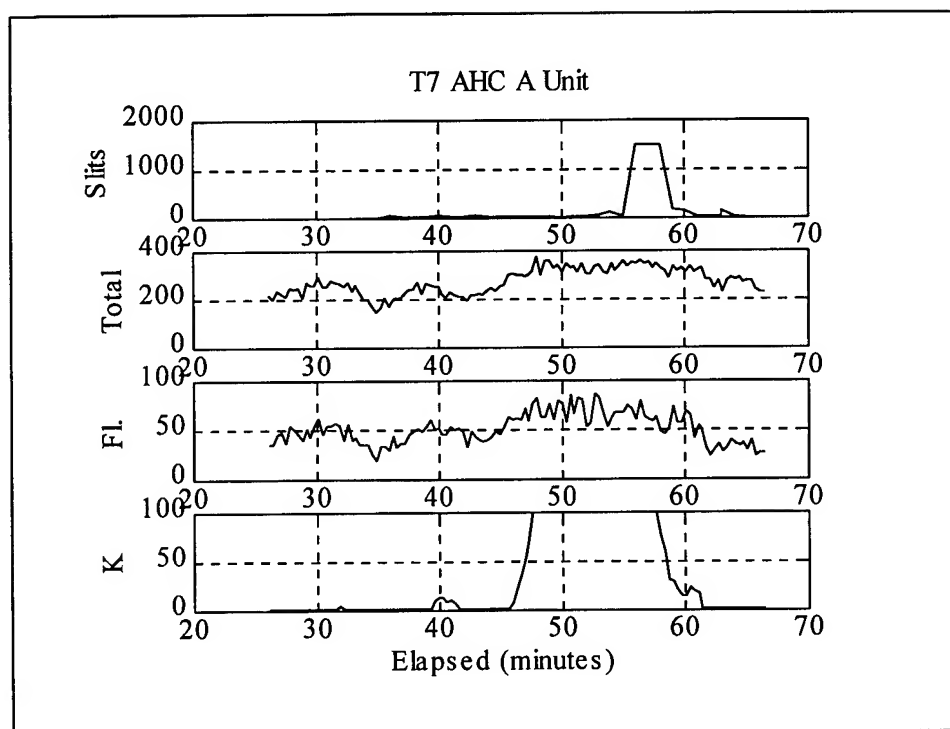


Figure 7. Field trial with BG to compare the performance of high frequency laser BARTS and referee data

CONCLUSIONS

This presentation has described the development of a new fluorescence particle detector (BARTS) based on Pacific Scientific Instruments particle counter technology and a new UV laser producing milliwatts of power at 355 nm. It represents a significant advance on existing technologies because it is much more affordable and portable than existing fluorescence particle detectors. It is suitable as an up-grade to deployed detection systems, and has the potential to be adapted as the world's first hand-held real time biological agent detector and sampler (BioCounter).

The field trial results at DRES confirm that the BARTS can detect biological agents as well as existing state-of-the-art fluorescence particle detectors (FLAPS), particularly when used in combination with a high volume particle concentrator (XMX) and a sophisticated alarm algorithm.

Two UV laser options were pursued as part of this development effort, and both have been demonstrated to elicit fluorescence from biological aerosol particles. However, the continuous wave laser coupled with the resonant cavity design of the optical cell presented problems in maintaining the tuning of the instrument and in obtaining reproducible MCAs to ensure adequate and stable power output from the laser. On the other hand, the high frequency long pulse duration laser produced excellent results, and it will be pursued further as part the BioCounter development program.

ACKNOWLEDGEMENTS

We would like to thank Defence Research and Development Canada, the Department of National Defence Canada and the Joint Program Office for Biodefense in the United States for their continued technical and financial support of this work.

IDENTIFICATION OF ANTHRAX-SPECIFIC SIGNATURE SEQUENCE FROM *BACILLUS ANTHRACIS*

Vipin K. Rastogi¹

GEO-Centers, Inc., Gunpowder Branch, APG, MD 21010¹, USA

Tu-chen Cheng^{2*}

Environmental Tech. Team, US Army, AMSSB-RTL, ECBC, APG, MD 21010², USA

Sensitive and rapid technologies for reliably detecting low numbers (1-100) of *Bacillus anthracis*, depend on availability of unique signature probes, i.e. antibody(ies) and/or DNA fragments. We have been pursuing identification and cloning of novel chromosomal DNA fragments for use as *B. anthracis*-specific markers. Towards this goal, 300 random primers were screened to locate and identify polymorphic loci on the anthrax chromosome. Amplification of such loci using random primers is referred to as RAPD (randomly amplified polymorphic DNA) technology. Five such unique polymorphic DNA fragments from anthrax chromosome were isolated and cloned. DNA sequence (genebank) analysis of one of the cloned fragment was found to contain a region of sequence, which is identical to the published chromosomal DNA sequence, Ba813 from anthrax. Presence of 1 pg quantity of anthrax had been reliably confirmed in spiked samples by PCR amplification protocols. In conclusion, we have demonstrated identification of anthrax-specific polymorphic signature sequences using RAPD technology. Amplified fragments can be used for anthrax detection on a variety of platforms including Gene-chip, Mass Spectrometer, *Taq*-man, or Capillary Electrophoresis.

INTRODUCTION

Weapons of mass destruction include both chemical warfare (CW) and biological warfare (BW) agents (Congress - OTA, 1993). In recent years, production and storage of BW agents in large quantities by a number of nations and extremist groups have raised a serious specter of their use of such in armed conflicts and civilian population around the world. Bacteria, rickettsia, viruses, and toxins are all included among BW agents, and can cause illness in humans and animals. Ten grams of anthrax spore, a BW agent, can kill as many people as a ton of CW agent, sarin. Consequently, BW agents are far more lethal than CW agents (David and Huxsoll, 1993). The degree of adverse impact on soldiers during combat or on civilian population in situations other than war can be minimized by efficient methods of early detection and identification. Current detection technology for BW agents rely on time-consuming laboratory analysis or onset of illness among people exposed the BW agent. Development of an efficient and sensitive detection capability in the battlefield environment is an important mission objective of the Edgewood Enterprise and the DoD's Biological Defense Program.

Currently, Joint Services use a BIDS (Biological Integrated Defense System) for rapid BW agent detection and warning system. In a recent ORD (Operation Requirements Document) presented to JSIG (Joint Services Integration Group), the detection system should meet following goals:

- A) automatically provide an audible or visual indication of the detected/identified BW agent;
- B) discriminate with high reliability and have minimum number of false-positives (0.98);
- C) identify in less than 15 min. (with the objective of 10 min.) with the precision of detecting 1 BW agent (10 μ in size) per liter of air volume;
- D) operational on units with static positions, onboard moving ships, or moving ground vehicles.

In theory, use of specific antibodies or distinguishing DNA probes are the two approaches to address the issue of a specific BW threat agent detection. Antibody-based detection of threat agent is subject to three

drawbacks: a) interference from other environmental contaminant precludes detection; b) detection limits at current levels fail to meet the desired goals; c) spore producing BW pathogens, such as anthrax, are poorly immunogenic. Given the limitations of small sample size in the presence of overwhelming amounts of other interfering materials, ability to amplify (front-end) and development of highly discriminatory technology are crucial. Nucleic acids, DNA and RNA, are the only biomolecules amenable to amplification, and thus offer a choice of target sites for developing signature probes for specific detection of a BW agent. Availability of highly specific polymorphic DNA probes for identification of a given bio-threat agent through PCR (polymerase cycle reaction) technology will permit development of integrated detection technology acutely needed by various defense, first-responders, and intelligence agencies.

Anthrax - primarily a disease of herbivorous animals but of rare occurrence in humans - is caused by *Bacillus anthracis*. Cutaneous anthrax is acquired via injured skin/membranes, sites where the spore germinate into vegetative cells. Proliferation of vegetative cells result into gelatinous edema. Inhalation of spores, on the other hand, results in high fever and chest pain. Both types, cutaneous and inhalation, can be fatal unless the invasive aspect of infection can be intercepted (Knusdon, 1986). Current PCR-based detection methods for *B. anthracis* rely on using primers amplifying tripartite exotoxin genes and/or the polyglutamic capsule genes (Jackson *et al.*, 1998, PNAS 95: 1224-9). Both these sets of genes comprise virulence factors, and are located on the two indigenous plasmids of anthrax bacteria, pXO1 plasmid (174 kbp; toxin) and pXO2 (95 kbp; capsule). Under normal conditions, the two plasmids, pXO1 and pXO2, in *B. anthracis* do not move across the related bacilli. However, under certain conditions, these plasmids are known to be transferred from *B. anthracis* to *B. cereus* and *B. thuringiensis* (Battisti *et al.*, 1985; Ruhfel *et al.*, 1984, J. Bact. 157: 708-11). However, *Bacillus cereus* or *B. thuringiensis* containing one or both of these plasmids do not cause anthrax. Detection of anthrax based solely on virulence factors can result in spurious determination. Clearly, information on unique regions located on the chromosome of *B. anthracis* is quite useful for an unequivocal determination. Through genome cloning and screening, two chromosomal sequences - Ba813, a 277 bp long DNA fragment (Patra *et al.*, 1996, FEMS Microbol. 15: 223-231) and *vrnA*, a region of sequence variability containing variable repeats (caa tat caa caa) - have been isolated (Anderson *et al.*, 1996, J. Bacteriol. 178: 377-84). Both these have been used for identifying presence of *B. anthracis* bacteria. Similar polymorphic loci, alternatively, can also be identified through RAPD (randomly amplified polymorphic DNA), a PCR-based technology (Williams *et al.*, 1994). Random sequence primers (ten-mers) are used in PCR protocols under low-stringency annealing temperatures with genomic DNA from a given BW agent and its close relatives. The number and sizes of amplified fragments derived from genomic DNA of a desired BW agent under these conditions depend on the ability of single primer to anneal to complementary sites on the two strands in opposite direction (5'→3' and 3'→5') within ~2500 bp of each other. Identification, cloning, and sequence information from such polymorphic DNA markers located on the chromosomal DNA comprise a library of agent-specific signature sequences.

Towards the goal of developing a sensitive technology for early detection and identification of *B. anthracis*, we have been pursuing development of specific DNA markers, which are derived from the chromosome and are polymorphic in nature, i.e. capable of distinguishing among closely-related *B. cereus* group members. Chromosomal markers in principle could also be used for distinguishing the virulent anthrax from avirulent strains (Rastogi and Cheng, 1997). Finally, successful application of DNA-based BW detection technology relies on ability to: a) purify DNA from environmental samples, soil and sludge; and b) amplify organism-specific DNA sequence in mixed samples containing overwhelming amount of non-specific DNA. Our results demonstrate that using appropriate single primers, anthrax-specific DNA could be amplified in spiked environmental sample. To our knowledge, this is the first report of anthrax detection in environmental samples using specific chromosomal DNA marker.

MATERIALS AND METHODS

1. Soil and Sludge Source: Activated sludge was obtained from Back River water treatment plant in Dundalk, Maryland, and used for isolation of genetic material. The soil samples were collected from farm area around Harford county, MD, and US Army APG, Edgewood Arsenal, Edgewood, MD.

2. Anthrax DNA and Random Primer Source: DNA from wild-type *B. anthracis* strain Sterne, was kindly provided by Dr. Tim Hoover, USAMRAID, Fort Dietrich, MD. DNA from other *B. anthracis* strains, such as VNR1-Δ1 and ΔSterne, both plasmid-free; and ΔAmes, pXO2⁺ were prepared in our laboratory following standard procedures for isolation of genomic DNA. The DNA was diluted to a concentration of 1 ng/ml, and the majority of the DNA was in the size range of about 30-50 kbp. DNA from other related bacilli, *B. cereus*, *B. thuringensis*, *B. subtilis*, and *Agrobacterium tumefaciens* were prepared following similar procedures. The random primers (10-mer) were purchased from commercial sources (University of British Columbia, Vancouver, BC, Canada).

2. Isolation and Purification of DNA: DNA from environmental samples was prepared using 'Soil DNA Isolation Kit' from MoBio Laboratory Inc. (CA, USA). Two grams of soil/sludge was processed in three replicates according to the manufacturer's protocol. Approximately 500-1000 ng total DNA was recovered, and much of DNA was ≥30-40 kbp in size.

3. RAPD - PCR Amplification: Routinely, PCR reactions were carried out in a final volume of 10 or 20 μl using 96-well tray in GeneAmp PCR System (Perkin Elmer-Cetus). The reaction mix contained 1-30 ng of DNA, 200 μM dNTPs, 2 mM MgCl₂, and 0.5 unit of Taq DNA polymerase, and 0.2 μM selected random decamer primers (Rastogi and Cheng, 1997).

4. DNA Analysis: The amplicates following PCR run were mixed with 6x loading dye in a ratio of 5:1 (DNA:dye). The samples were electrophoresced through 1.4% agarose gel submerged in 1x TAE buffer (Sambrook *et al.*, 1980) using constant voltage of 100 volts. The DNA in gels was stained with ethidium bromide (0.5 μg/ml) and destained before photographing using Polaroid film 667.

5. DNA Sequencing: Automated DNA sequencer model 373 (Perkin Elmer, Applied Biosystems Div., Foster City, CA) was used for DNA sequencing. After subcloning of the amplified DNA fragment into pCR-blunt vector (Invitrogen, Carlsbad, CA), both strands of cloned DNA fragments were sequenced following manufacturer's protocol. Computer analysis of the DNA was performed with MacVector program (Oxford Molecular Ltd., Oxford, UK).

RESULTS AND DISCUSSION

1. Quality of DNA from Soil/Sludge: Soil and sludge contain large number of diverse microorganisms, as well as genetic material released from decaying organisms. Presence of the humus material (humic acids, humates or salts of humic acid, fulvic acids and fulvates, lignite and humin) interferes with detection, measurement, and routine molecular analysis of the DNA (Thurman *et al.*, 1988; Tsai and Olson, 1992a; 1992b).

DNA isolated using 'MoBio Soil DNA Kit' was amenable to restriction digestion and ligation (results not shown). These results establish that commercially available kit is an effective procedure for removal of humus material from environmental DNA.

2. Amplification of Anthrax-specific DNA in Spiked Samples: Five random 10-mer (designated as 173, 240, 280, 290, and 361) have previously been identified to result in amplification of DNA fragment from the chromosomal DNA of wild-type anthrax. These primers did not amplify the similar-sized DNA fragments from the genomic DNA from strains related to anthrax, i.e. *B. cereus*, *B. thuringiensis*, and an unrelated strain *Agrobacterium tumefaciens* (Figure 1a and 1b). In addition, genomic DNA from wild-type anthrax and two derivative strains lacking one or both plasmids were used as target DNA. The fact that similar-sized DNA fragments are observed in the three anthrax strains, the priming sites must be located on the chromosome. The

amplification pattern derived from *A. tumefaciens* DNA was very different from *Bacillus* DNA, and therefore, this DNA was not included in subsequent experiments.

As shown in Figure 2, anthrax-specific fragments were amplified from spiked environmental sludge DNA samples, when primer #173, 241, 280, and 290 were used. The spiked samples included anthrax DNA at a concentration of 0.01 and 0.1 ng and sludge DNA mixed at 10, 50, 100, or 200 ng concentration. In general, presence of 200 ng of sludge DNA resulted in failure to amplify anthrax-specific DNA fragments. Further, primer 280 failed to amplify anthrax-specific DNA fragments even at 50 or more ng of sludge DNA. These results clearly established the specific ability of these random primers to amplify the anthrax-specific DNA fragments in sludge samples spiked with anthrax DNA.

3. Detection Limit: The spiked samples were prepared using 0.001, 0.01, 0.1 or 1 ng of anthrax DNA with 50 ng sludge DNA. These amplification assays were set up in an attempt to determine the detection limit of anthrax DNA in the presence of overwhelming amount of non-specific background DNA. Typically, in RAPD assays, low stringency annealing conditions are used to allow priming event even if the primers are not fully complementary to the priming sites, i.e. a certain level of mis-match is allowed. In an effort to determine which primers are more specific to the priming sites, an annealing temperature of 52°C was used to preclude priming events from mis-matched sites. As shown in Figure 3, primer 173 and 270 were able to amplify at high-stringency temperature even in the presence of 0.001 ng (1 pg) control anthrax DNA. This result indicates the PCR assay is highly sensitive for detection of anthrax DNA even in the presence of 5,000x non-specific DNA. Assuming 0.28 pg dry wt./bacterial cell and 3% of the dry wt to be DNA (cited in Neidhardt, 1996), ability of PCR-based technology to detect the presence of 1 pg DNA suggests that this technology would detect DNA from as many as 120-150 *B. anthracis* cells. Since the objective of JSCBD is to have a technology to detect as few as 1-10 cells, evidently, additional work is needed to make our procedures more sensitive. Despite this shortcoming, so far, no other technology has been demonstrated to be as sensitive as the PCR-based procedures detailed above.

4. Identification of Specific Chromosomal DNA Fragments: Five unique DNA fragments cloned into pCR vector were sequenced. Sequence analysis of the four fragments showed no homology to the genebank database. Part of the 5th cloned fragment has a region (Figure 4), which is highly homologous to Ba813 - an anthrax-specific DNA fragment reported earlier (Patra *et al.*, 1996). High-fidelity primers were designed from the sequence of five fragments.

5. Design and Use of High-fidelity Primers: Forward and reverse primer sets (15-20-bases in length) were designed based on the sequence of the cloned regions. The seven sets of primers, F1-B11 (290R), F1-B20 (290F), F2-B12 (280R), F1-B1 (248F), F1-B22 (173R), F1-B15 (290F), F3-B12 (280R), were selected to amplify fragments ranging in length from 144-520 bp. Total DNA isolated from environmental sources, soil and sludge, was spiked with anthrax DNA. Control DNA samples contained 1.65-1.85 ng non-specific DNA and spiked samples contained 1 pg of anthrax DNA. The ratio of non-specific DNA:anthrax DNA was about 1,600:1. Except the two primer set combinations, F1-B1 and F3-B12, the other five primer set amplified expected fragment in spiked soil/sludge samples only (Figure 5). This result established that even in the presence of overwhelming non-specific DNA, the high-fidelity primers designed in this study amplify anthrax-specific fragment.

CONCLUSIONS

In conclusion, the results summarized in this presentation established following key points:

1. Anthrax-specific DNA probes can be amplified by the random primers in the presence of excessive non-specific DNA;
2. Unprecedented sensitivity of PCR-based procedures to detect 1 pg anthrax DNA (equivalent of 120-

150 anthrax cells of in the presence of 5,000x non-specific DNA was observed.

3. Inclusion of these sequences in conjunction with virulence genes will reduce the probability of false-positive detection;

4. Such fragments/primers-based amplification can be used in various semi-automated PCR-based platforms, *Taq*-man or gene-chip, for detection of anthrax;

5. This approach of identifying unique chromosomal regions by screening random primers can also be used for obtaining signature DNA sequences from other BW threat agents.

LITERATURE CITED

1. Congress, Office of technology Assessment, Proliferation of Weapons of Mass Destruction: Assessing the Risks, Washington, D.C.: GPO, 1993: 3.
2. Huxsoll DL, The U.S. Biological Defense Research Program: In Biological Weapons, Weapons of the Future? Ed. Roberts, B, Washington, D.C.: The center for strategic and international studies, 1993, 60.
3. Jackson CR, JP Harper, D Willoughby, EE Roden, PF Churchill, A simple efficient method of humic substances and DNA from environmental samples. AEM, 1997, 63: 4993.
4. Knudson GB, Treatment of anthrax in man. History and current concepts. Military Medicine, 1986, 151: 71.
5. Neidhardt FC, ed., In: *Escherichia coli* and *Salmonella*, cellular and molecular biology, 1996, ASM Press, Washington, D.C.
6. Patra G, P Sylvestre, V Ramisse, J Therasse, J-L Guedson, Isolation of a specific chromosomal DNA sequence of *Bacillus anthracis* and its possible use in diagnosis, FEMS Imm. & Med. Microbiol., 1996, 15: 223-231.
7. Rastogi VK and T-c Cheng, Development of unique chromosomal markers for detection of *Bacillus anthracis*, 1997 ERDEC Conference on CB Defense (in press).
8. Sambrook J, EF Fritch, T Maniatis, In: Molecular cloning – A laboratory manual, 2nd ed., CSH Lab Press, CSH, NY.
9. Thurman EM, GR Aiken, M Ewald, WR Fischer, U Forstner, AH Hack, RFC Mantoura, JW Parsons, R Pocklington, FJ Stevenson, RS Swift, B Szpakowska, Isolation of soil and aquatic humic substances, In: Eds. FH Frimmel and RF Christman, Humic substances and their role in the environment, J Wiley & Sons, Ltd., NY, 1988, 31.
10. Tsai Y-L and BH Olson, Detection of low numbers of bacterial cells in soils and sediments by polymerase chain reaction, AEM, 1992a, 58: 754.

ACKNOWLEDGEMENTS

Authors would like to express thanks to Mr. Farjad Mohammadi and Mr. Jennifer Boucher for their technical assistance. Support for this work to TcC was provided through ILIR program from R&D Directorate of the ECBC, SBCCOM, US Army.

Figure 1a. RAPD amplification profile with selected random primers and genomic DNA isolated from: 1) *Agrobacterium tumefaciens*; 2) *Bacillus thuringiensis*; 3) *B. cereus*; 4) *B. anthracis* Δ Sterne (pOX1⁻/pOX2); 5) *B. anthracis* Δ Ames (pOX1⁻/pOX2⁺); 6) *B. anthracis* Ames (wild-type, pOX1⁺/pOX2⁺). Primer numbers are shown below the panel.

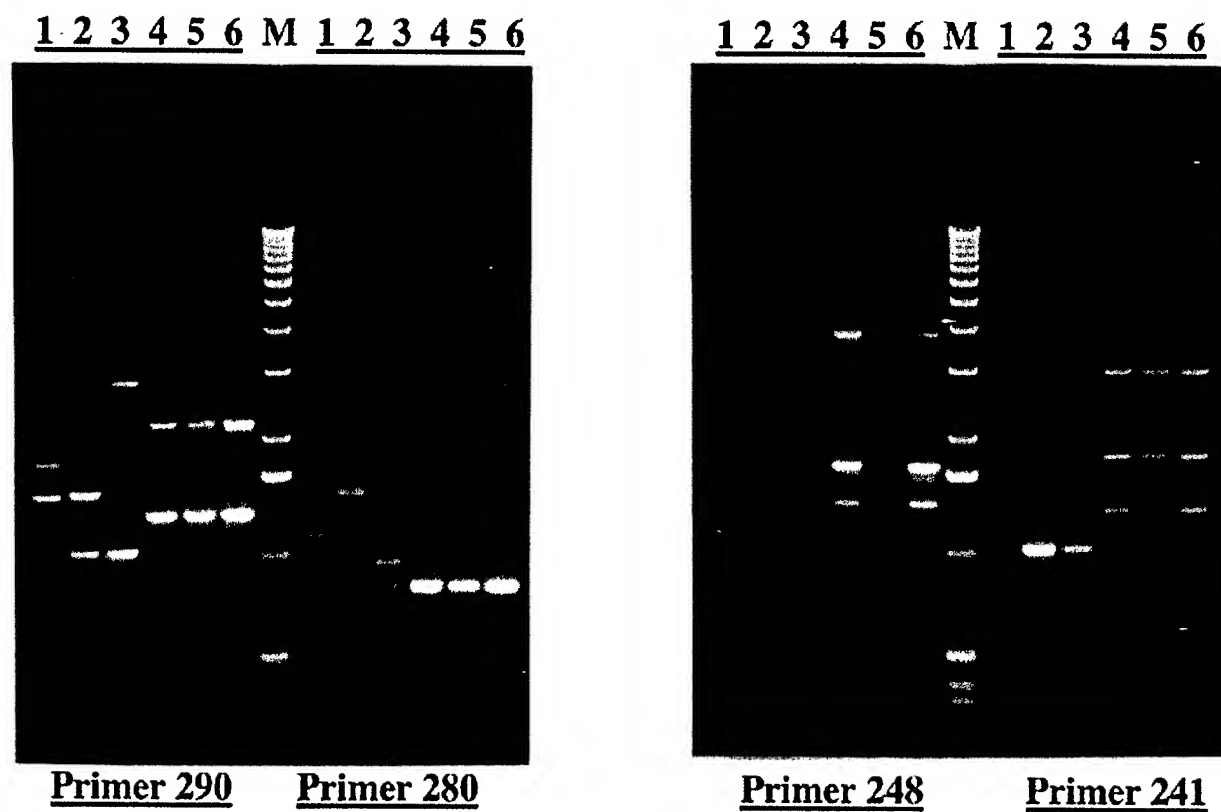


Figure 1b. RAPD amplification profile with selected random primers and genomic DNA isolated from: 1) *Agrobacterium tumefaciens*; 2) *Bacillus thuringiensis*; 3) *B. cereus*; 4) *B. anthracis* Δ Sterne (pOX1⁻/pOX2); 5) *B. anthracis* Δ Ames (pOX1⁻/pOX2⁺); 6) *B. anthracis* Ames (wild-type, pOX1⁺/pOX2⁺). Primer numbers are shown below the panel.

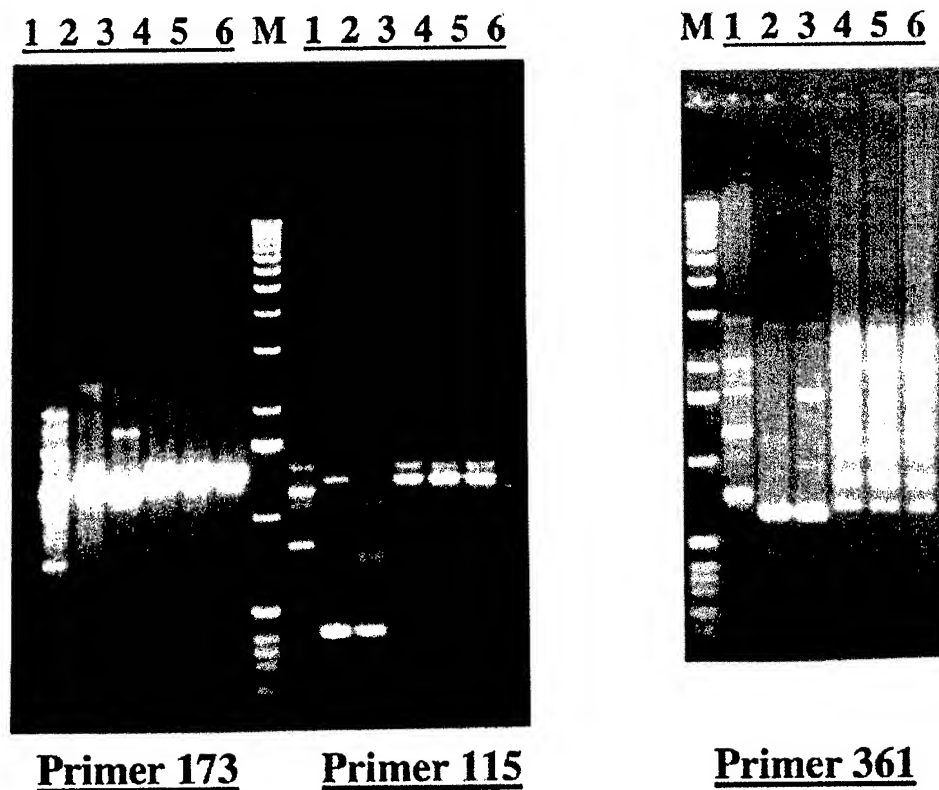


Figure 2. Amplification of anthrax-specific DNA in the presence of different amounts of non-specific environmental sludge DNA. Amount of sludge DNA was 10 ng (1), 50 ng (2), 100 ng (3), and 200 ng (4). Anthrax DNA used was 0.01 ng (1-4) and 0.1 ng (5-8).

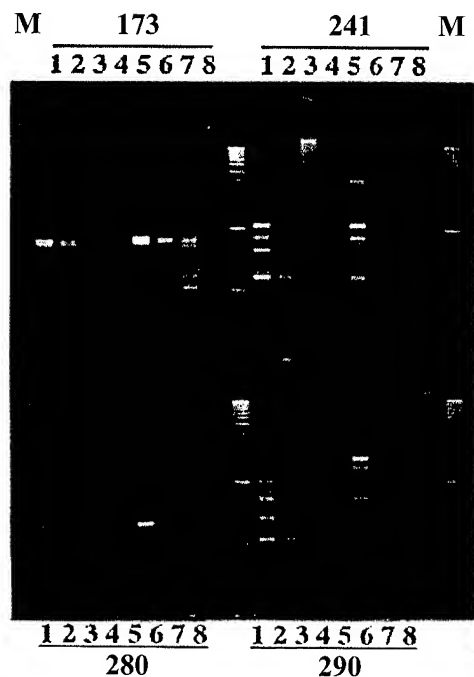


Figure 3. Detection limit of anthrax-specific DNA probes in spiked environmental samples. Four concentrations, 0.001 (lane 1), 0.01 (lane 2), 0.1 (lane 3), and 1 ng (lane 4) of anthrax DNA were used. The samples labeled as A contained only anthrax DNA and those labeled as A-S contained 50 ng of sludge DNA. Primers used are indicated on the panel.

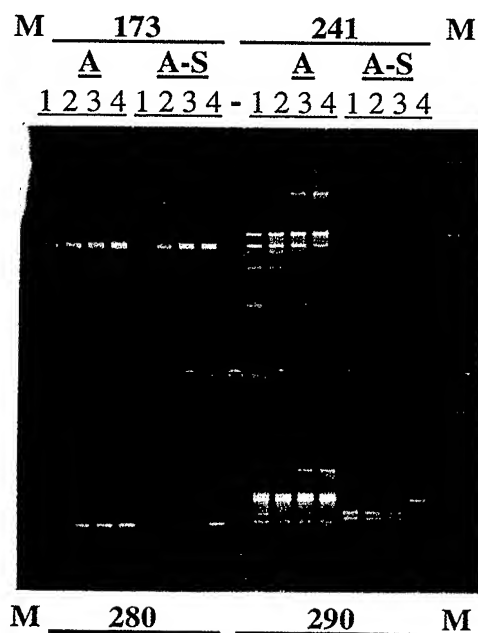


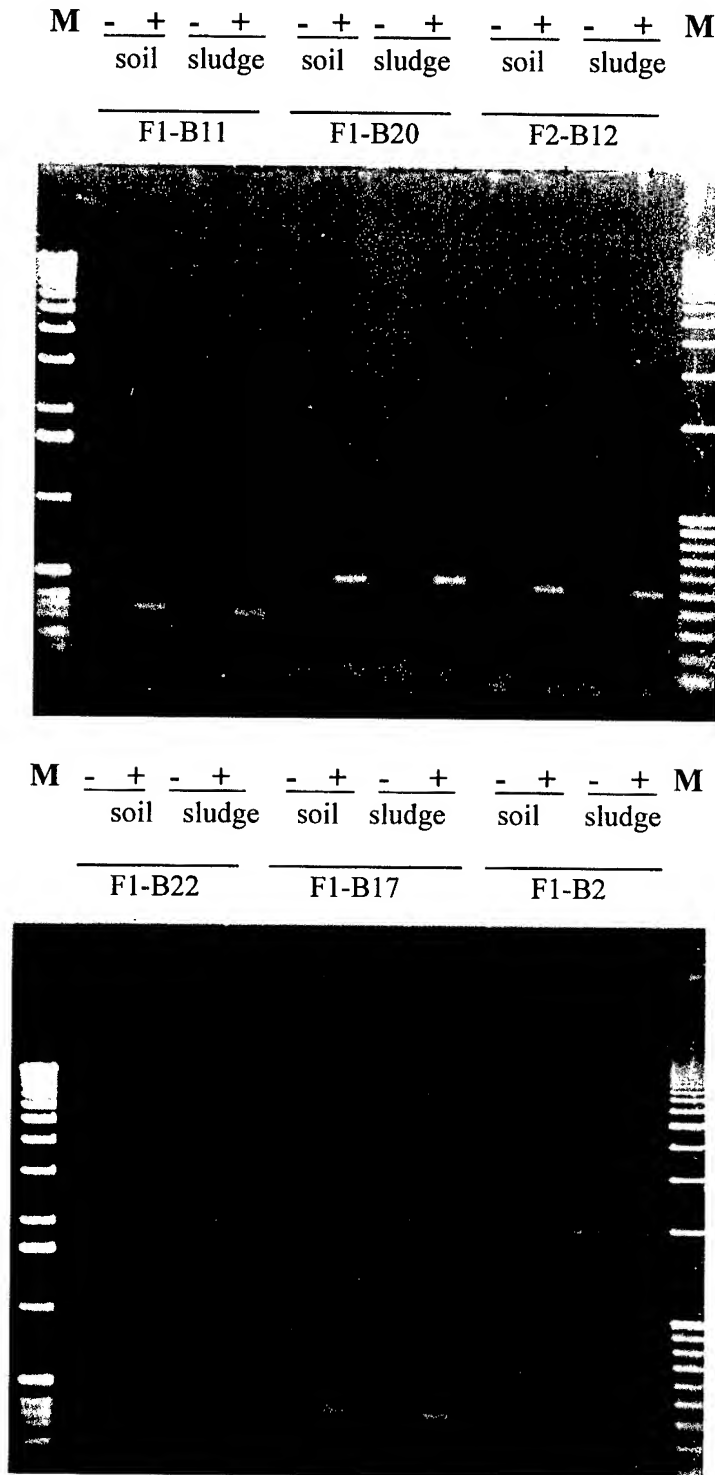
Figure 4. Nucleotide sequence in the VRTC899 homologous to the Ba813 probe from *Bacillus anthracis*. The region of homology (277 bp long) is underlined and shown in bold. The remaining sequence has no homology to the genebank and has been submitted for patent to the US patent office.

```

XXXXXXXXXXXXXXXXXXXXXXXXXXXXXXXXXXXXXXXXXXXXXXXXXXXXXXXXXXXXXXXXXXXX
1
XXXXXXXXXXXXXXXXXXXXXXXXXXXXXXXXXXXXXXXXXXXXXXXXXXXXXXXXXXXXXXXXXXXX
61
XXXXXXXXXXXXXXXXXXXXXXXXXXXXXXXXXXXXXXXXXXXXXXXXXXXXXXXXXXXXXXXXXXXX
121
XXXXXXXXXXXXXXXXXXXXXXXXXXXXXXXXXXXXXXXXXXXXXXXXXXXXXXXXXXXXXXXXXXXX
181
XXXXXXXXXXXXXXXXXXXXXXXXXXXXXXXXXXXXXXXXXXXXXXXXXXXXXXXXXXXXXXXXXXXX
241
XXXXXXXXXXXXXXXXXXXXXXXXXXXXXXXXXXXXXXXXXXXXXXXXXXXXXXXXXXXXXXXXXXXX
301
XXXXXXXXXXXXXXXXXXXXXXXXXXXXXXXXXXXXXXXXXXXXXXXXXXXXXXXXXXXXXXXXXXXX
361
XXXXXXXXXXXXXXXXXXXXXXXXXXXXATTGCACTTGCATAATATCCTTGTTTCTTTAATTCACCTG
421
CAACTGATGGGATTTCTTTCTGACTTGGAATAGCTTGCTGATACGGTATAGAACCTGGCA
481
TTAAAAGACTCATTGAGTAACTCGTTAATGCTTCAAATTCTGTGTTTGCTGTATTCCTC
541
CAAATGTAGGAGCTATCGTTTGTCCCCCTGGGAAATTCTCTGTATAACGATGTAAATTCG
601
GCACTGGATCTTCGCTAAATGAAAGATTGTTAGTTTTGTCCGATCCCAAGAAGCTTXXX
661
XXXXXXXXXXXXXXXXXXXXXXXXXXXXXXXXXXXXXXXXXXXXXXXXXXXXXXXXXXXXXXXXXXXX
721
XXXXXXXXXXXXXXXXXXXXXXXXXXXXXXXXXXXXXXXXXXXXXXXXXXXXXXXXXXXXXXXXXXXX
781
XXXXXXXXXXXXXXXXXXXXXXXXXXXXXXXXXXXXXXXXXXXXXXXXXXXXXXXXXXXXXXXXXXXX
841
XXXXXXXXXXXXXXXXXXXXXXXXXXXXXXXXXXXXXXXXXXXXXXXXXXXXXXXXXXXXXXXXXXXX
901
XXXXXXXXXXXXXXXXXXXXXXXXXXXX
961

```

Figure 5. Amplification of anthrax-specific DNA from spiked soil/sludge sample using newly-designed high-fidelity primer sets. Primer sets were derived as follows: 290R (F1-B11 and F1-B17); 290F (F1-B20); 280R (F2-B12); 173R (F1-B22); 248F (F1-B2). Control environmental samples lacking anthrax DNA are designated as (-) and those spiked with 1 pg anthrax DNA as (+). Soil or sludge DNA range from 1.7 to 1.9 $\mu\text{g}/\mu\text{l}$. The ratio of anthrax to environmental DNA is $\sim 1650:1$ in spiked sample.



DESIGN AND OPTIMIZATION OF FLUOROGENIC 5'-NUCLEASE ASSAYS FOR *BACILLUS ANTHRACIS* AND *YERSINIA PESTIS*

Deanna R. Christensen, Melissa S. Frye, Stephen B. Kerby, Laurie J. Hartman, Tammy R. Gibb, Erik A. Henchal, and *David A. Norwood

United States Army Medical Research Institute of Infectious Diseases
Diagnostic Systems Division
1425 Porter Street, Fort Detrick, MD 21702

We are optimizing sensitive and specific assays for potential biological warfare agents on two commercially available rapid nucleic acid amplification platforms, the Cepheid Smart CycTM and the Idaho Technology R.A.P.I.D. We expanded the number of gene targets for *Bacillus anthracis* and *Yersinia pestis*, and developed assays for Venezuelan Equine Encephalitis virus, and several strains of Ebola and Marburg virus. In addition, we optimized assays for *B. anthracis* and *Y. pestis* on both platforms. Currently, assay development is focused on a well-defined research path: design primers and probes, optimize assay conditions, and evaluate assay performance.

Primers and dual-labeled fluorogenic probes were designed following the guidelines set forth by Applied Biosystems Inc. to be both sensitive and specific for their targets. Primers and probes were first tested on the ABI7700 instrument and then optimized on the SmartCyclerTM and R.A.P.I.D. platforms. We used Amersham Pharmacia Biotech PCR Ready-To-GoTM bead chemistry on all three real-time PCR platforms. After initial limit-of-detection (LOD) experiments under standard conditions, we optimized assays independently on both the SmartCyclerTM and R.A.P.I.D. to maximize the potential of each assay on each system. We used well-defined protocols to determine optimal temperature profiles and concentrations of primers, probe, and MgCl₂. After optimization, another LOD experiment was performed, and blinded cross-reactivity panels were tested. If the optimized assay had a limit of detection less than or equal to 100 CFU and was specific for its target, then the assay was advanced to the evaluation phase.

Data for *B. anthracis* protective antigen and *Y. pestis* plasminogen activator assays will be presented. Results indicate that assay optimization produced a more robust assay but did not increase detection limits. The assays were specific for their targets and were relatively unaffected in a background of 5 ng of human DNA. Both platforms produced definitive results within 35 minutes and had equivalent LOD. In summary, experimental data indicate that these assays perform well on both rapid amplification platforms.

Introduction

The potential use of biological threat agents as weapons of mass destruction has become a source of anxiety and concern in recent years, especially for the armed forces. The readiness and capability of our armed forces to deal with such an event in a theater of operation will be critical to mission success. Of primary importance is the ability to detect the release of a biological agent rapidly without sacrificing precision or accuracy. The development of fluorogenic 5'-nuclease PCR chemistry resulted in real-time monitoring of nucleic acid amplification. The first machine designed for this chemistry, the ABI7700 (Applied Biosystems), is large, slow, and is incapable of displaying fluorescence during amplification. Data can only be analyzed after a run is completed, which may take from 2 to 2.5 hours. The recent development of rugged, portable amplification systems capable of rapid temperature ramping and real-time fluorescence monitoring has greatly reduced assay times. Two such platforms, the Cepheid Smart

Cycler™ and Idaho Technology R.A.P.I.D., were compared in this work. Assays were optimized independently on each platform using the same criteria. Here we present performance data for several fluorogenic 5'-nuclease assays for the detection of *Bacillus anthracis* and *Yersinia pestis*.

Methods/Results

Assays were designed specifically for rapid amplification using the guidelines set forth by Applied Biosystems Inc. for Taqman chemistry. Briefly, primers were designed with a length of 18 to 22 nucleotides, 40-60% GC content, melting temperatures (Tms) of 55-60°C, and a one to three nucleotide run of G and C (GC clamp) on the 3' end. Amplicon lengths were restricted to <200 bp to ensure extension during the rapid amplification cycles. Probes were designed with Tms 7 to 10°C above primer Tms, without G on the 5' residue, and when possible with complementary sites within 30 nucleotides of the corresponding strand's primer. Initial candidates were obtained with Primer Express software (Applied Biosystems, Inc.). Candidates were screened to reduce dimers, hairpins, long stretches of single base repeats, and false priming sites using Oligo software (National Biosciences, Inc.).

For conditions comparisons, the cycle at which fluorescence crossed a pre-defined threshold (crossing threshold or Ct value) and the fluorescence observed at the final cycle, 45 (endpoint fluorescence) were used. Assays were systematically optimized to find conditions under which assays had optimal crossing thresholds (earliest crossing threshold cycle) and generated maximum fluorescence (largest endpoint fluorescence). Assays were optimized for concentrations of primer, probe, MgCl₂, as well as temperature.

Optimization was performed using PCR Ready-To-Go beads (Amersham Pharmacia Biotech) and two step PCR. The final concentrations of bead components per reaction were 0.25 mg/ml bovine serum albumin, 2.0 units taq DNA polymerase, 10 mM Tris-HCl pH 9.0, 50 mM MgCl₂, and 200 M dNTPs. Cycling on the R.A.P.I.D. consisted of 45 cycles of 95°C for 0 seconds and 60°C for 20 seconds, while the Smart Cycler™ profile consisted of a 30 second 95°C melt followed by 45 cycles of 95°C for 0 seconds and 60°C for 20 seconds. Reaction volumes were 20 l for the R.A.P.I.D. and 100 l for the Smart Cycler™ and total run times were between 28 and 35 minutes, depending upon the anneal/extend temperature. Primer concentrations were tested by matrixing upper (forward) and lower (reverse) primers at 0.2, 0.3, 0.4, 0.5, and 1.0 M. Following the primer optimization, probe concentration was optimized in a similar manner. Because the two platforms differed in how they measure fluorescence, probe concentrations differed significantly between platforms. For the R.A.P.I.D. we initially used a probe concentration which gave a background fluorescence reading of 30 at a gain setting of 8. Probe was then diluted by 10 nm increments until five probe concentrations were tested. For the Smart Cycler™, 0.1, 0.2, 0.3, 0.4, and 0.5 M of probe was tested. The next step of optimization involved testing performance of the optimal primer and probe concentrations at various MgCl₂ concentrations. MgCl₂ was tested at 0.3, 0.4, 0.5, 0.6, and 0.7 M. Finally, optimal assay component concentrations were used to assess assay performance at 50, 55, 60, 65, and 70°C.

The performance of assays for the protective antigen gene (*pa*) of *B. anthracis* and the plasminogen activator gene (*pla*) of *Y. pestis* on the Smart Cycler™ before and after optimization are shown in table 1. Optimization produced more robust assays, resulting in increases in the amount of fluorescence produced during runs; however, detection limits did not improve and cycle threshold (Ct) values remained relatively constant. For both assays the LOD was 100 fg of total genomic DNA. Based on genome size, 100fg is equivalent to approximately 20 genomic copies.

Table 1: Limit of detection of *B. anthracis* and *Y. pestis* assays on the Smart Cycler™.

<i>B. anthracis</i> protective antigen			<i>Y. pestis</i> plasminogen activator		
Ct values			Ct values		
	Before Optimization	After Optimization		Before Optimization	After Optimization
Sample	AVE	AVE	Sample	AVE	AVE
100pg	23.84	23.90	100pg	22.05	21.70
10pg	27.37	27.97	10pg	25.57	25.29
1pg	30.12	31.89	1pg	28.84	29.82
100fg	35.36	36.07	100fg	32.00	35.08
10fg	0.00	0.00	10fg	0.00	0.00

Endpoint Fluorescence			Endpoint Fluorescence		
	Before Optimization	After Optimization		Before Optimization	After Optimization
Sample	AVE	AVE	Sample	AVE	AVE
100pg	569.73	556.80	100pg	303.70	768.21
10pg	388.66	413.83	10pg	280.94	651.44
1pg	143.85	264.98	1pg	197.58	448.17
100fg	24.17	52.61	100fg	34.37	60.55
10fg	-14.84	-2.48	10fg	0.75	-19.16

Additional LOD experiments were performed in the presence of total human genomic DNA. The presence of 5 ng of human DNA (about 1500 copies of the genome) in the assay mixture was used to determine if assay performance was compromised. Results for the *B. anthracis* assay on the Smart Cycler™ are summarized in Table 2. Assays were relatively unaffected in a background of 5 ng of human DNA. While some endpoint fluorescence values were reduced, limits of detection remained the same.

Table 2: Effect of 5 ng of human DNA on the *B. anthracis* assay on the Smart Cycler™.

<i>B. anthracis</i> protective antigen			<i>B. anthracis</i> protective antigen		
Ct values			Endpoint fluorescence		
	no spike	5 ng Hu DNA spike		no spike	5 ng Hu DNA spike
Sample	AVE	AVE	Sample	AVE	AVE
100pg	24.05	24.20	100pg	464.85	442.60
10pg	28.20	27.76	10pg	358.03	330.98
1pg	31.62	32.31	1pg	218.81	128.91
100fg	36.32	37.11	100fg	27.13	9.33
10fg	0.00	0.00	10fg	-1.67	-5.51

Blinded cross reactivity panels were used to evaluate the specificity of assays for their respective targets. Assays were performed in 1 ng of total genomic DNA from a variety of species and nearest neighbor panels. The results for a collection of 15 *B. anthracis* strains with various plasmid profiles are summarized in Table 3. Assays were specific for their targets on both platforms and no additional banding was observed on confirmatory agarose gels. Interestingly, one strain of *B. anthracis* characterized previously as not possessing the pX01 plasmid by another set of diagnostic primers was positive. The strain, Ba1017, was positive in 14 of 15 assays run on the Smart Cycler™ and R.A.P.I.D. Further

comparisons of the new fluorogenic 5'-nuclease assay primers indicated a 10-fold increase in the limit of detection when compared to the diagnostic primers previously used to characterize the strain. Coupled with the late Ct value for strain Ba1017, data suggest a low level contamination of this strain with a pX01 bearing strain of *B. anthracis*.

Table 3: Results for the *B. anthracis* assay with a blinded cross-reactivity panel on the SmartCycler™ and R.A.P.I.D.

BAPA35 Cross-reactivity							
				Ct values			
				SmartCycler		R.A.P.I.D.	
Sample	ID	pX01	pX02	AVE	CALL	AVE	CALL
1	Ba1007	+	+	23.09	POS	21.89	POS
2*	Ba1017	-	+	37.90	POS	34.73	POS
3	Ba1036	+	-	17.89	POS	16.41	POS
4	Ba1037	-	+	0.00	NEG	0.00	NEG
5	Ba0074	+	-	21.96	POS	20.95	POS
6	Ba1029	-	+	0.00	NEG	0.00	NEG
7	Ba1175	+	+	26.28	POS	24.57	POS
8	Ba1004	+	+	20.52	POS	19.01	POS
9	SPS97.13.213	+	-	25.44	POS	23.48	POS
10	Ba0068	+	-	22.31	POS	20.36	POS
11	Ba006	+	-	16.75	POS	14.62	POS
12	Ba0070	-	+	0.00	NEG	0.00	NEG
13	Ba1010	-	+	0.00	NEG	0.00	NEG
14	Ba1000	+	+	17.98	POS	15.36	POS
15	Ba0078	+	+	18.56	POS	17.41	POS

* Positive result observed in 14 of 15 assays.

CONCLUSIONS

Fluorogenic 5'-nuclease assays for the protective antigen gene of *B. anthracis* and the plasminogen activator gene of *Y. pestis* were designed and optimized to rapidly detect these agents. Assays were optimized on two rapid amplification instruments, the Idaho Technology R.A.P.I.D. and the Cepheid SmartCycler™. Both platforms produced definitive results within 35 minutes at the limit of detection. Limits of detection were 100fg (approximately 20 copies of the genomes) on both instruments. Assay optimization produced more robust assays but did not increase detection limits. The production of more fluorescence under optimal conditions during a run increases the likelihood of the assay crossing threshold at the limit of detection. Assays were specific for their targets and were relatively unaffected in a background of 5 ng of human DNA.

A FROZEN BACTERIA COLLECTION AS A SOURCE OF QUALITY REFERENCE MATERIAL

Jeffrey D. Teska, Cindy M. Allan, Stephanie L. Redus, and John W. Ezzell

Special Pathogens Branch, Diagnostic Systems Division,
U.S. Army Medical Research Institute of Infectious Diseases
1425 Porter Street, Fort Detrick, MD 21702-5011

ABSTRACT

A reference collection of bacteria was established within a quality framework, to be used as a source of well-characterized microorganisms with a clearly defined pedigree, and associated with complete and traceable production documentation. Reference strains within the collection are used as sources of quality control (QC) organisms for sample analysis, assay evaluation and validation; and for the development of microbiological, immunological, and molecular assays. The collection consists of biological safety level 3 (BSL-3) agents, BSL-2 clinical and environmental isolates, and accepted clinical QC microorganisms. Initially, a desired list of entries was prepared by using the concepts of nearest neighbor and nearest proximity. Designated entries, serving as sources of DNA for molecular assay evaluation, were divided into four specific bacteria panels, including a primary panel (80 isolates), a *Bacillus* panel (32 isolates), a *Brucella-Francisella-Yersinia* panel (46 isolates), and a *Clostridium* panel (23 isolates). Bacteria for the panels were obtained from recognized culture collections (i.e., American Type Culture Collection), commercial vendors, clinics, or unique entries from previous USAMRIID collections. Following approved procedures, entries added to the collection were grown under documented incubation conditions (i.e., defined atmosphere, temperature, time, and medium) and were checked for purity. Growth from multiple agar plates was harvested into sterile tryptic soy broth (TSB) to achieve a turbidity at least equal to a No. 3 MacFarland standard. An equal volume of TSB with 25% glycerol was then mixed with the TSB-bacterial suspension. The resulting bacterial preparation, consisting of 1 x TSB with 12.5% glycerol, was aseptically dispensed into 9 cryovials, and frozen at $-70 \pm 5^\circ \text{C}$. All vials were labeled as "SEED" with an assigned reference number, lot number, and expiration date in accordance with approved procedures. Frozen seed stocks were characterized by classical and automated microbiological methods, and then served as sources for production stocks. Production stocks were prepared by rapidly thawing one frozen seed stock vial, plating the contents on multiple agar plates, and incubating the plates under documented conditions. Growth was harvested, suspended in TSB with a final glycerol concentration of 12.5%, aseptically dispensed into 18 cryovials, and frozen at $-70 \pm 5^\circ \text{C}$. All production stock vials were labeled as "PROD" with an assigned reference number, lot number, and expiration date in accordance with approved procedures. As collection entries were requested by investigators for DNA extraction, one production stock vial was removed from the collection, thawed, and plated on multiple plates as previously described. Growth was harvested, suspended in the cryopreservative medium, dispensed into 7 cryovials, frozen at $-70 \pm 5^\circ \text{C}$, and transferred to the requesting investigator. All vials were labeled with an assigned reference number, lot number, expiration date, and 4DNA (for DNA extraction) in accordance with approved procedures. Currently, 407 seed stocks, 144 production stocks, and 130 "4DNA" stocks have been prepared. Complete documentation associated with this project is maintained by the Special Pathogens Branch as defined by our established quality guidelines.

INTRODUCTION

Point detection for biological agents is a continual process of refining and adjusting established technologies or applying novel platforms for identifying bacteria, viruses, or toxins. Current technologies strive to detect target agents in less time, with greater specificity and sensitivity, while decreasing the size of instrumentation. Those involved with technology development have become increasingly aware of the need for supporting quality documentation as a requisite for regulatory approval and advanced development. Required documentation for regulatory review typically includes performance data (i.e., sensitivity, specificity, linearity, accuracy, precision, etc.), as well as accountability for the reference material used to generate performance data. Recognizing the need for quality reference material in assay evaluation and validation, not only within the Diagnostic Systems Division (DSD) but also among biodefense investigators in general, we established and maintain a frozen culture collection to fulfill that need. From its conception, planning, and implementation, the culture collection was established with quality in mind. Before implementing the project, many quality system references were consulted for technical information, regulatory issues, and documentation guidelines. Primary sources included the National Committee on Clinical Laboratory Standards (NCCLS), the Clinical Laboratory Improvement Act of 1988 (CLIA), the College of American Pathologists (CAP), and the American Society for Clinical Pathology (ASCP). Next, a scientific approach for establishing the collection was drafted. This approach then passed a series of peer-reviews and revisions until reaching consensus approval by the DSD Coordinating Committee. Immediately before beginning work, we prepared draft standard operating procedures to cover all aspects of the project. These documents, along with detailed worksheets for recording all activities associated with the project, were reviewed and approved by USAMRIID's Quality Assurance Office, as well as senior management of DSD. Once the quality documentation was in place, work with the microbes began. The product of our labors, encompassing the complete spectrum of quality and technical issues, is a bacteria collection of reference material, constructed around a quality system framework, with consistency, traceability, and accountability for each entry. In the following, we describe the technical aspects of this collection of reference bacteria.

CULTURE COLLECTION

An initial task for establishing the collection was to obtain isolates. A selection list of desired isolates was created to provide guidance for obtaining collection entries. Criteria upon which selection was based included (1) priority agents for assay development, (2) nearest proximity, and (3) nearest neighbor. Priority agents included BSL-3 organisms producing unique virulence factors or toxins considered to be noteworthy as threats. Nearest proximity included those organisms that might be associated with a threat agent by sharing a common site (i.e., skin, nares, respiratory route, wound, etc.). Nearest neighbors included those organisms that were the same species but different strain, same genus but different species, and those organisms that are taxonomically unrelated, but genetically similar, to the target agent. One primary source for reference material was the American Type Culture Collection (ATCC; Manassas, VA). Other sources included various commercial vendors (primarily for clinical laboratory quality control organisms), clinical isolates from several health-care facilities, isolates from working collections within USAMRIID, and select isolates from cooperative agreement exchanges. Upon receipt, isolates were assigned a unique alphanumeric identifier and logged into our master list.

To prioritize work on the collection, and as a tracking system to measure progress, we established four reference panels (based on molecular assay development priorities) and assigned isolates from within the collection to each panel. Not all isolates were used for these panels, but the four panels provided a reference point for future expansion. The four reference panels include: (1) a primary panel consisting of 80 unique aerobic and anaerobic organisms, (2) a *Bacillus* panel consisting of 32 organisms (*B. anthracis* and

non-*B. anthracis*), (3) a *Brucella*/*Francisella*/*Yersinia* panel consisting of 46 organisms representing all the species within these genera, and (4) a *Clostridium* panel consisting of 23 organisms representing *C. botulinum* and other major members of the genus. A fifth panel, planned for the near future, will include members of the genus *Burkholderia*.

Lyophilized cultures were resuspended in the recommended broth and plated for growth in the appropriate medium. The majority of isolates added to the permanent collection were grown on commercially available 5% sheep blood agar and incubated at $35 \pm 2^\circ\text{C}$ for 24 ± 6 hours. Anaerobic cultures were grown in a MACS Anaerobic Cabinet (Microbiology International, Frederick, MD) at $35 \pm 2^\circ\text{C}$ for 24 ± 6 hours. After incubation, growth from each plate was harvested with sterile swabs and transferred to 6 ml of filter-sterilized tryptic soy broth (TSB). The turbidity of each TSB tube was visually adjusted to approximate at least a No. 3 MacFarland Standard. An equal volume of TSB with 25% glycerol was added to the TSB suspension, and mixed by vortex to yield a uniform suspension of bacteria in TSB with a final concentration of 12.5% glycerol. The suspension was then dispensed 1.0 ± 0.1 ml/vial into cryovials pre-labeled as "SEED" along with assigned reference number, lot number, and expiration. Nine vials of each isolate were frozen at $-70 \pm 5^\circ\text{C}$ to become our seed stock.

All entries into the culture collection were at least prepared as seed stocks; those isolates assigned to reference panels proceeded to production stocks. Production stocks were physically separated from seed stocks, but were produced from one vial of the seed stock. Each seed stock vial produced 18 vials of production stock. Production stock suspensions were dispensed in volumes of 0.5 ± 0.1 ml/vial into cryovials pre-labeled as "PROD" along with the assigned reference number, lot number, and expiration date, and frozen at $-70 \pm 5^\circ\text{C}$. Incubation, harvesting, and dispensing of production stocks were the same as for the seed stock procedure. When all of the 18 "single use" production stock vials are exhausted, another seed stock vial is removed and used to prepare 18 more production stock vials. With this procedure, each new lot of production stocks will have the same passage number and lot number of the seed stock. Before exhausting all the seed stock for a particular isolate, a new lot of seed stock will be produced. Consequently, each new lot of seed stock will have one additional passage from the previous lot.

Seed stocks are only used to produce more production stocks; therefore, production stocks are the working entities of the reference collection. These reference materials are intended to support biodefense investigators as: (1) positive and negative control material as part of assay quality control, (2) quality reference material required to complete formal assay validations under regulatory guidelines, and (3) sources of bacterial DNA for molecular assay development and evaluation. Currently, the culture collection is serving all three functions, and we anticipate that support to investigators will continue to increase.

Within the Diagnostic Systems Division, members of the Systems Development Branch are using bacteria on the reference panel as sources of DNA. Organisms on the reference panels were grown from production stocks vials. Incubation, harvesting, and dispensing of stocks destined for DNA extraction were the same as the production stock procedure. Bacterial suspensions, used for DNA extraction, were dispensed in volumes of 1.25 ± 0.1 ml/vial into 7 cryovials pre-labeled as "4DNA" along with the assigned reference number, lot number, and expiration date, and frozen at $-70 \pm 5^\circ\text{C}$. All transfers to the molecular group are documented and DNA extraction proceeds under that group's own established quality guidelines. Requests for viable cultures as reference material are also received. These requests are supplied as plate cultures, slant cultures, or frozen broth cultures according to the needs of the investigator.

CHARACTERIZATION DATA

All reference organisms added to the culture collection as seed stocks were initially characterized, by a variety of techniques, to confirm the identity of each entry. Data for each entry was added to the collection's documentation archive. Isolate characterization will be an on-going activity as investigators using the culture collection generate additional data using other technologies and platforms.

Clinical information, whenever possible, was compiled for clinical isolates obtained from several health-care facilities. Information maintained for collection entries may include clinical history, site of isolation, medium used for isolation, antibiotic susceptibility data, therapy used for treatment, unusual circumstances related to the patient, and the number of subcultures before entry into the collection. Additional information includes classical microbiology characteristics, such as growth characteristics (i.e., hemolysis, swarming), growth conditions (i.e., atmosphere, medium, temperature), colonial morphology (i.e., smooth, rough, rhizoid), cellular morphology (i.e., cocci, bacilli, arrangement of cells), Gram stain reaction, and general enzymatic reactivity (i.e., catalase, cytochrome oxidase, indole).

One technique used to characterize entries was biochemical substrate utilization profiles obtained by using the automated Vitek-32 (bioMerieux Vitek, Inc., Hazelwood, MO). With specialized, self-contained substrate cards (i.e., gram-negative identification (GNI), gram-positive identification (GPI), anaerobe identification (ANI), and *Bacillus* identification (BAC)), bacterial suspensions are loaded into the pre-selected identification card, vacuum sealed, and inserted into the instrument. Turbidity and color changes, resulting from bacterial growth and substrate metabolism, are monitored every 15 minutes for up to 15 hours. Many of the clinical isolates were identified within 4 to 8 hours. For *Bacillus anthracis*, a database entry was created using the Vitek's custom software. This organism, previously not identified by the Vitek, can now be identified with our new database entry (unpublished data).

A second technique used to characterize collection entries was whole cell fatty acid profiles obtained by using an HP6890 gas chromatograph and Sherlock® pattern recognition software (MIDI, Inc., Newark, DE). This method relies on manual sample preparation (i.e., lysis of cells, synthesis of methyl esters of the fatty acids, and MEFA extraction) followed by automated analysis. Resulting chromatographs are compared to the identification library to provide a final identification. Working closely with the MIDI technical staff, we used the custom features of the Sherlock® software to expand the identification library to include identification of *Bacillus anthracis*, *Burkholderia mallei*, and *Burkholderia pseudomallei* (unpublished data).

Specific molecular characterization of collection entries is currently restricted to those agents for which amplification primers are currently available. Future characterization may include restriction endonuclease fragment analysis obtained with the Riboprinter® from Dupont Qualicon. This technology, based on restriction enzyme digestion of the bacterial DNA and analysis of the region encoding the 16S-23S rRNA, would enhance our ability to further define our reference material. While planned for future incorporation, this technology is currently not part of our characterization procedure.

As the culture collection continues to expand, we are hopeful that this effort will become a standard. By continuing to provide investigators with quality reference material, we also anticipate that user confidence will remain high and that characterization data will continue to be added to the collection documentation files. Therefore, we shall continue to solicit user support by requesting any available user characterization data. In this way, we hope to maintain, and continue to build, a source of reference material that can benefit all.

CONCLUSION

We established a frozen bacteria collection as a source of quality reference material. The collection is maintained under established, peer-reviewed quality guidelines to ensure the pedigree, purity, consistency, and traceability of each isolate. Reference material is maintained at -70°C, and is divided into separate seed and production stocks. Seed stocks are the source for production stocks. Production stocks serve as quality control organisms, validation material, and sources of DNA for molecular assay development and evaluation. Characterization data are maintained for each entry in the collection and include passage number, clinical history, biochemical substrate utilization, whole cell fatty acid profile, and molecular information. Reference material in the collection is available to our Tri-Service partners, as well as other biodefense investigators. The Chief, Diagnostic Systems Division, approves formal requests and viable organisms and/or DNA material may be obtained. To benefit all users, we request that investigators return additional characterization data to be added to the collection documentation.

ACKNOWLEDGEMENTS

The authors thank COL Erik Henschal (Chief, Diagnostic Systems Division) for valuable contributions and critical review of all phases of this project and for continued management support. We also thank Terry Abshire, Ed Brown, Deanna Christensen, Joelle Crouch, Susan Coyne, CPT Tammy Gibb, Gerry Howe, Fred Knauert, George Ludwig, CPT David Shoemaker, and the members of the DSD Coordinating Committee for contributions associated with technical, regulatory, and quality assurance issues.

RECOMBINANT ANTIBODIES FOR THE DETECTION OF BACTERIOPHAGE MS2 AND OVALBUMIN

*Kevin P. O'Connell**, Peter A. Emanuel, Akbar S. Khan, and James J. Valdes
Edgewood Chemical Biological Center, U. S. Army Soldier Biological Chemical Command
Aberdeen Proving Ground, MD 21010

Timothy J. Stinchcombe and Robert Shopes
Tera Biotechnology Corp., La Jolla, CA 92121

Maha Khalil and Mohyee E. Eldefrawi
Department of Pharmacology and Experimental Therapeutics
University of Maryland School of Medicine
Baltimore, MD 21201

ABSTRACT

Antibodies are currently field-deployed as the biological component of sensors that detect biological threat agents. Antibodies that detect simulants of bio-threat agents are also currently incorporated into biodetection platforms for testing and evaluating new devices and materials. Previously, we developed an anti-botulinum toxin antibody using a powerful genetic technology known as phage display, in which a very large library of immunoglobulin (antibody) genes are expressed on the surface of bacteriophage (bacterial virus) particles. We describe here the isolation of additional recombinant antibodies that bind two simulants of biothreat agents: bacteriophage MS2, and the protein ovalbumin. The phage display method allows the rapid selection of genes encoding specific antibodies out of an enormous population of candidates, and the subsequent production of large amounts of the recombinant antibody in bacterial fermentations. A single anti-MS2 antibody was isolated. The screen for anti-ovalbumin antibodies yielded two independent clones with unique nucleotide and amino acid sequences. All antibodies isolated demonstrated specificity for the molecule against which their selections were targeted. A key feature of the method was the use of a recombinant antigen, cloned MS2 coat protein, for the affinity enrichment of clones in place of the intact bacteriophage target. This helped prevent bacteriophage contamination of bacterial cultures, and provided a defined, purified product for screening and subsequent characterization.

INTRODUCTION

Antibodies are the essential component in immunological sensors that detect BW (biological warfare) agents, giving them both sensitivity and selectivity for BW agents. The Army and the Joint Program Office for Bio-Defense (JPO-BD) purchase and field biosensor platforms (JBIDS, JPBDS, JBREWS, and PORTAL SHIELD systems) that incorporate antibodies produced in whole animals (polyclonal) and mammalian cell cultures (monoclonal) for biowarfare agent detection.

There is considerable lot-to-lot variability in the current production of antibodies. This is especially true for polyclonal antibodies, which require the injection of a disarmed BW agent into animals. The individual response of each animal to an agent can vary dramatically. The process of developing antibodies in animals or in mammalian cell culture is also time-consuming, which limits the capacity for "just-in-time" or surge production in time of conflict.

A recent advance in antibody production technology is the cloning of antibody genes and their expression in bacterial fermentations. This technology has been proven capable of producing antibodies for BW agent detection that are of higher quality and greater uniformity from lot to lot; therefore, their inclusion in fielded bioassays would result in greater reliability. Recombinant antibodies are also faster and potentially less expensive to produce and acquire in quantity; therefore, establishing a process for their production would improve the maintainability and supportability of fielded biodetection systems. We previously described the successful cloning and properties of a recombinant antibody that binds botulinum toxin¹.

We describe here the cloning and initial characterization of three new recombinant reagents, antibodies that bind biothreat simulants. In addition to antibodies that bind and detect BW agents, there is a need for antibodies that bind and detect organisms and substances that simulate BW agents. A panel of BW agent simulants that are non-toxic and non-pathogenic is widely used for the development and testing of biosensors and environmental samplers, in a work setting without the need for high levels of biological containment. Two such simulants are bacteriophage MS2 (a non-pathogenic virus of the bacterium *Escherichia coli*, which is used to simulate viruses) and ovalbumin (a benign protein which is used to simulate protein toxins, such as ricin). To meet the need for high-quality, inexpensive antibody reagents that bind these BW simulants, we have used a powerful technique called phage display to isolate antibody genes from immunized mice. The resulting antibody molecules are called Fabs, indicating that they are comprised of heavy and light chain antibody sequences which form the antigen-binding variable region, but do not contain the IgG constant region.

METHODS AND RESULTS

Immunization. Antibody genes for immunoglobulin library construction were obtained from B cells in the spleens of immunized BALB/c mice. Mice were immunized with MS2 and ovalbumin to increase the numbers of B cells producing anti-MS2 and anti-ovalbumin antibodies, thereby increasing the likelihood of isolating the corresponding genes. Primary immunizations were followed with three additional immunizations bi-weekly, with concurrent monitoring of antibody production in the mice by ELISA.

Antibody gene amplification and cloning. Following the immunization of BALB/c mice with a suspension of intact MS2 virions, RNA was extracted from the spleens of immunized mice by standard methods². Complementary DNA (cDNA) was synthesized from total immunized mouse spleen RNA. The resulting cDNAs were processed and amplified by PCR amplification in order to isolate individual sets of immunoglobulin genes³. PCR-amplified heavy chain genes are shown Fig. 1. Heavy and light chain gene PCR fragments were assembled by ligation (MS2) or by PCR assembly (ovalbumin) and subjected to digestion with the restriction enzymes *NotI* and *SpeI* for cloning into the phage display vectors. The primary antibody library was transformed by electroporation into cells of *E.coli* strain XL-1 Blue and then amplified by plating the library on solid Luria medium containing carbenicillin.

Display of antibodies on the surface of phage particles. The resulting primary antibody library was then expressed on filamentous phage particles by infection of the *E. coli* host cells with the helper phage VCSM13 (Stratagene, La Jolla, CA). Infection of the cells with the VCSM13 helper virus induced production of filamentous bacteriophage that express the heavy and light chain polypeptides on the surface of the virus⁴. The filamentous phages that were produced by the *E. coli* culture displayed recombinant antibodies on their surfaces, as determined by the detection of mouse kappa light chains in dot blots of the expressed phage. Filamentous phages displaying antibodies and containing the cloned antibody gene library were separated from *E. coli* cells by centrifugation, and phages were concentrated from the supernatant solution by centrifugation (Fig 2).

Expression and purification of recombinant target protein. To minimize the possibility of contaminating bacterial cultures with intact MS2 and to obtain the purest antigen possible for affinity screening, we expressed and purified a recombinant version of the MS2 coat protein. A clone of the coat protein (Dr. L. Lo, Scripps Institute, San Diego, CA) in the expression vector pET15b, contained in *E. coli* strain BL21(DE3) was induced by addition of IPTG to a three-liter batch fermentation. Cells were harvested after an overnight incubation at 37°C, and disrupted to release the coat protein by sonication. After centrifugation to remove cell debris, cell lysate was passed over a nickel affinity column. The recombinant coat protein included six histidine residues (a "6xHis" tag) on the C-terminal end, which preferentially bind metal ions. This technique gave >90% purification of the target protein in a single purification step (data not shown).

After purification, the recombinant coat protein was used to screen the antibody library for clones that bind MS2. Ovalbumin for both immunization and biopanning is was obtained commercially (Pierce Co, Rockford, IL) in highly purified form.

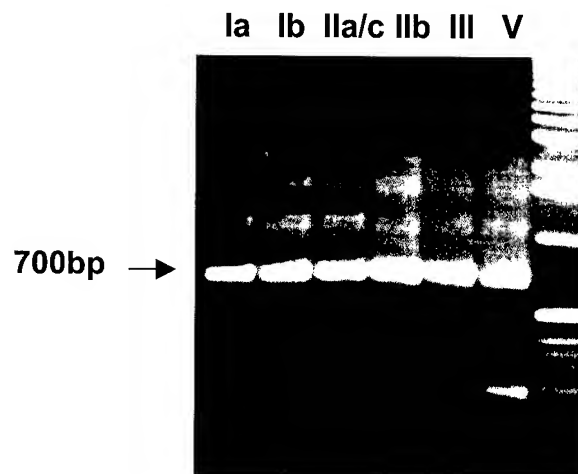


Fig. 1. Amplification of heavy chain genes. Antibodies consist of heavy and light chain proteins; both are required to bind antigen. Mammals contain several families of both heavy and light chain proteins in their antibody repertoire. To obtain the most diverse collection of antibodies from which to select desirable clones, each family of mouse immunoglobulin heavy and light chain was amplified separately using PCR primers specific to that family. Shown are amplified gene fragments of six heavy chain families (Roman numerals). The desired gene fragments are 700 bp long. Other bands represent PCR artifacts. Right lane, DNA size marker.

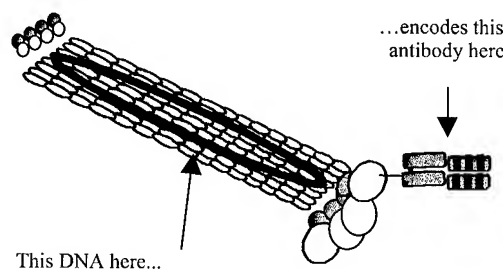


Figure 2. Schematic of antibody-displaying particle. A phage particle in the display library contains DNA encoding an antibody from the immunized mouse, and displays that same antibody on its surface. The entire repertoire of antibodies cloned from the mouse is thereby converted to a recombinant form that can be screened by applying the population to a surface coated in the antigen of interest.

Affinity enrichment ("biopanning") of antibody clones. The display of the recombinant antibodies on the surface of the phage allowed for the enrichment of antigen specific clones through biopanning against recombinant MS2 coat protein immobilized in the wells of microtiter plates. Phage particles displaying anti-MS2 or anti-ovalbumin antibodies (and containing the corresponding cloned antibody genes) were obtained by a form of affinity purification called "biopanning" (Fig. 3).

Small amounts of each antigen were immobilized on a solid surface (a well of a microtiter plate), and a population of phages displaying antibodies cloned from the corresponding immunized mice were washed across the surface. Those phage particles displaying antibodies that bind the antigen were retained on the surface, while non-specific phages were washed away. Because of the way in which the antibodies were cloned, each phage bound to antigen contains the genes that encode the antibody on the surface of that phage. Bound phages were removed from the surface, used to infect fresh cultures of *E. coli*, and reinfected with helper phage to start the next round of enrichment. Three to four rounds of biopanning were typically performed.

Subcloning and expression of the antibody genes. Following the last round of biopanning, individual phage clones containing the desired antibodies were identified by culturing individual clones and screening for binding of the appropriate antigen by ELISA. Verified positive clones were sequenced fully and from the sequence, the IgG subclass of each clone was determined. Genes for each Fab antibody were then removed from the phage display vectors (Fig. 4) and cloned into expression vectors which incorporate a 6x histidine tag on each heavy chain for subsequent expression and purification in fermentations of *E. coli*.

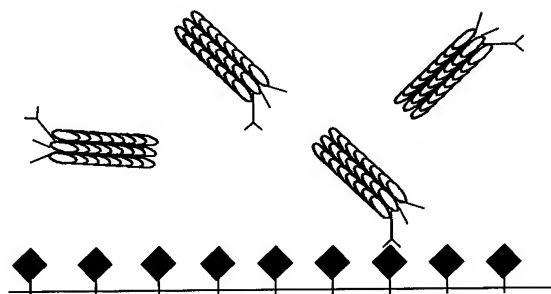


Figure 3. Biopanning. The antigen against which antibodies are desired (diamonds, above) is immobilized on a solid surface. A population of phage particles displaying a repertoire of antibodies is washed across the surface, and those phages displaying antibodies that bind the target are retained; the rest are washed away.



Figure 4. Subcloning of antibody genes. Nearly all clones obtained after several rounds of biopanning retained intact antibody genes (represented by clones 1-3, 6-9; **lower arrow** indicates 1400 base pair gene inserts, 700 bp light chain gene plus 700 base pair heavy chain gene). Some clones (4 and 5) underwent mutation or genetic rearrangement and were discarded. The remainder were used to produce antibody and were individually screened for the ability to bind ovalbumin or MS2 (depending on which antigen was used in panning). The 1400 base pair gene inserts of clones that passed successfully were removed from the phage display DNA vector (**top arrow**) and cloned into a vector that added a 6xHis tag to the carboxyl terminal of the heavy chain gene. Subsequent expression in *E. coli* fermentation and purification gives a pure recombinant antibody product. Left and right lanes, DNA size markers.

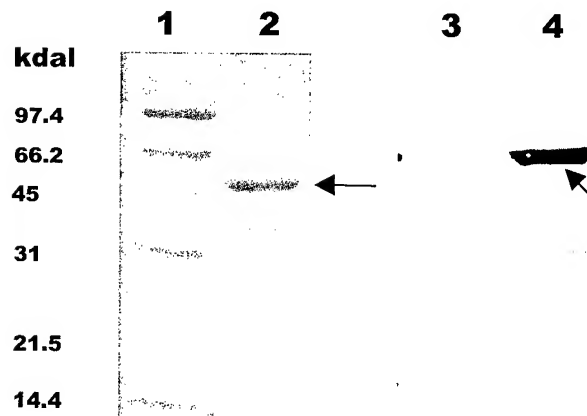


Figure 5. Purified recombinant anti-MS2 antibody. After purification as described in section 2.7, anti-MS2 antibody (lanes 2 and 4, arrows) was >90% pure as determined by SDS-PAGE and staining with Coomassie Brilliant blue (left image). Lane 1, molecular weight standard; lane 2, purified anti-MS2 antibody. Right image, experiment identical to lanes 1 and 2, but demonstrating the identity of the protein as mouse antibody by immunological detection. Lane 3, molecular weight marker; lane 4, purified anti-MS2 antibody. The anti-MS2 antibody was transferred to a nitrocellulose membrane after SDS-PAGE and detected with goat anti-mouse antibody conjugated to alkaline phosphatase, using NBT/BCIP as substrate.

Expression and purification of recombinant anti-MS2 antibody. The introduction of antibody genes into the expression vector pHis1.1 fused the heavy chain genes with a 6xHis tag. The pHis1.1 expression vector (carrying the anti-MS2 antibody genes) was introduced into an *E. coli* strain constructed to optimize protein expression (TOPP I, Stratagene). Cells were grown in a 20-liter fermentor and the compound IPTG was added to induce expression of the antibody genes. After fermentation, cells were disrupted with a sonicator to release a crude lysate containing the recombinant anti-MS2 antibodies. The crude cell lysate was applied to a column packed with Talon metal affinity resin according to the manufacturer's instructions, and eluted with imidazole buffer. Eluted anti-MS2 antibody was further purified by passage over Sephadex gel filtration columns to greater than 90% purity. Fractions were analyzed by sodium dodecyl sulfate-polyacrylamide gel electrophoresis (SDS-PAGE) and HPLC for purity and protein content. Proteins were detected by staining with Coomassie Brilliant blue and by immunoblotting (Figure 5).

Expression and partial purification of recombinant anti-ovalbumin antibodies. Genes for two anti-ovalbumin antibodies were cloned into the expression vector pHis1.1 as described above, and expressed in small-scale (3-liter) fermentations of *E. coli* strains TOPP I and TOPP II to begin optimizing a production scheme. After growth of the cultures, induction of gene expression with IPTG and cell disruption by sonication, crude lysates were passed over Talon metal affinity columns as described in section 2.7. Samples of the crude lysate, material that passed through the column, and eluted 6xHis-tagged anti-ovalbumin antibodies were obtained during purification and analyzed by SDS-PAGE and immunoblotting (Figure 6). Both antibodies were purified to approximately 30% of total collected protein after one pass over the Talon resin (antibody OVA-3 shown in Figure 6; antibody OVA-4, data not shown).

Detection of MS2 and ovalbumin with recombinant antibodies. Recombinant anti-MS2 and anti-ovalbumin antibodies were used in enzyme-linked immunosorbent assays (ELISAs) to detect their corresponding antigens. Density-gradient-purified bacteriophage MS2 (Dugway Proving Grounds, UT) and ovalbumin (Sigma, St. Louis, MO) were serially diluted and bound by adsorption to wells of Maxisorp microtiter plates (Nunc). After incubation with blocking agent (3% bovine serum albumin in Tris-buffered

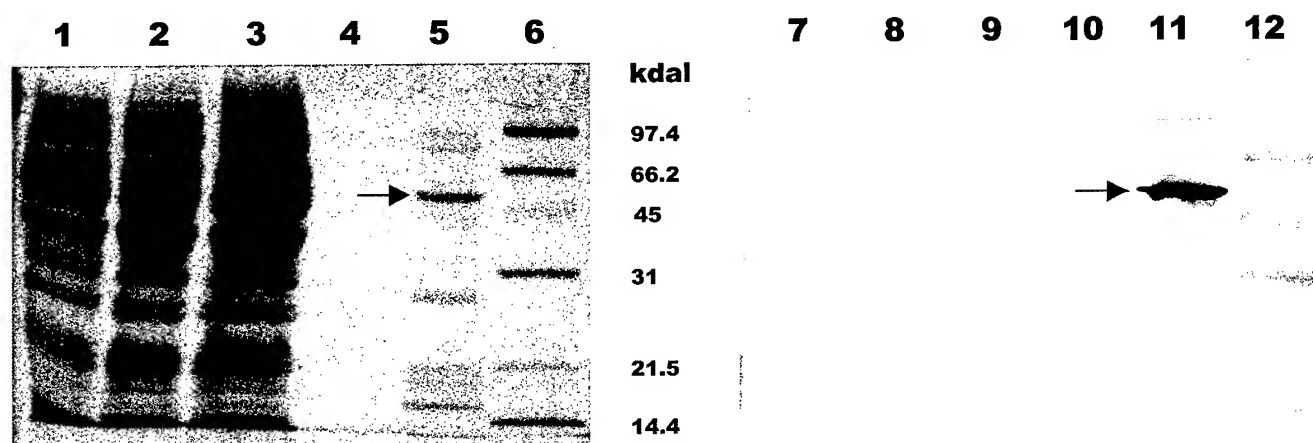


Figure 6. Partial purification recombinant anti-ovalbumin antibody (OVA-3) by metal affinity chromatography. Left image, Coomassie blue-stained gel. Lane 1, crude lysate; lanes 2 and 3, cellular proteins unbound by column; lane 4, fraction immediately preceding antibody during elution; lane 5, pooled fractions containing recombinant antibody OVA-3; lane 6, molecular weight marker. Right image, experiment identical to left image except that proteins were blotted to a nitrocellulose membrane after SDS-PAGE and detected with goat anti-mouse antibody conjugated to alkaline phosphatase, using NBT/BCIP as substrate. Lanes 7-12 identical to lanes 1-6. **Arrows** indicate position of recombinant antibody. (Sigma; working dilution 1:2500) was added to each well and incubated for 1-3 hours. Following another wash step, AP enzyme substrate solution (PNPP; para-nitrophenylphosphate, 2 mg/ml) was added to each well. Color development was measured spectro-photometrically after one hour, at 405 nm.

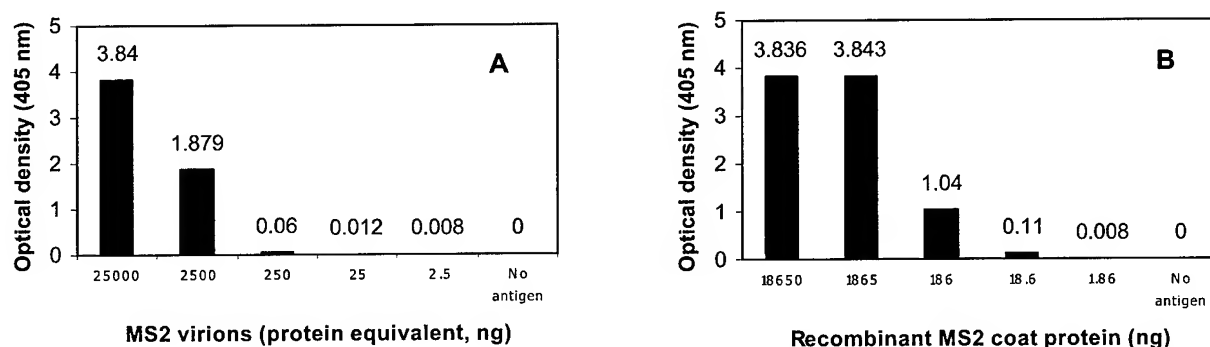


Figure 7. ELISA detection of (A) MS2 virions and (B) recombinant MS2 coat protein using purified anti-MS2 Fab antibody. Values represent the mean of duplicate measurements, adjusted by subtracting the absorbance measured in the no antigen control. The antibody appears to be more sensitive for the detection of the recombinant coat protein.

saline, pH 7.4), recombinant antibodies were applied to antigen coated wells and incubated for 2 h, followed by washing in TBS-Tween 20 (0.05%). Goat-anti-mouse IgG (Fab-specific) conjugated to alkaline phosphatase (Sigma; working dilution 1:2500) was added to each well and incubated for 1-3 hours. Following another wash step, AP enzyme substrate solution (PNPP; para-nitrophenylphosphate, 2 mg/ml) was added to each well. Color development was measured spectro-photometrically after one hour, at 405 nm.

Purified MS2 was detectable down to a level of 250 ng (protein equivalent) in this experiment (Figure 7). The recombinant coat protein used for biopanning and screening, however, was detected to a level of approximately 20 ng. This apparent greater sensitivity for the recombinant coat protein over the intact virus may reflect the isolation of the antibody using the recombinant protein as the biopanning target. Use of intact

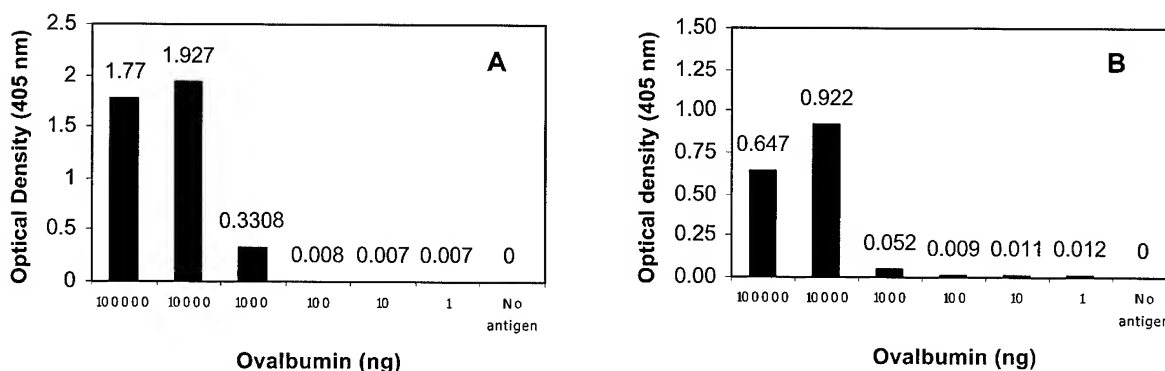


Figure 8. ELISA detection of ovalbumin using (A) recombinant antibody OVA-3 and (B) recombinant antibody OVA-4. Values represent the mean of duplicate measurements, adjusted by subtracting the absorbance measured in the no antigen control.

virions as the target, as well as performing the affinity capture of anti-body-displaying phage in solution will allow the isolation of Fabs with even greater affinity for intact MS2. Anti-MS2 did not bind phage M13, BSA, or ovalbumin (data not shown). Using partially purified recombinant antibodies OVA-3 and OVA-4, ovalbumin was detectable down to a level of 1 microgram (Figure 8).

DISCUSSION

This work is part of an overall strategy to develop an improved suite of biodetection reagents by establishing the methods for cloning, isolation and large-scale production of recombinant polypeptides. The antibodies being developed in this program complement another ongoing effort in our group to isolate and characterize small peptide aptamers that bind and detect biothreat agents. The DNA and amino acid sequences of the three antibodies described here have been determined, and each antibody displays canonical sequences flanking each of the six CDRs (complementarity determining regions) per clone. The CDRs are the portions of the antibody chains in which the greatest sequence variability is present. CDRs also form the antigen-binding pockets that determine the affinity and specificity of each antibody for its antigen.

A recombinant products approach to biodefense reagent development has several technical, logistical, and animal use advantages over traditional methods of isolating and producing antibodies.

The technical advantages include the potential to produce antibody diversity greater than that obtainable by the immune systems of mammals. Mammalian immune systems do not recognize “self” epitopes in order to avoid targeting tissues of the host animal for destruction. While beneficial for the animal, it eliminates a large number of potentially useful molecular structures as targets when making antibodies in animals, either polyclonal (the serum of immunized animals) or monoclonal (the living antibody-producing cells, fused to mouse cancer cells to make them immortal, the so-called hybridomas). Removing antibody diversity from the body of an animal allows antibody genes to be assorted and altered to increase antibody diversity by means of modern DNA manipulation techniques, and therefore increases the chances of isolating useful antibodies from a population of clones. In addition, monoclonal antibodies are generally produced by a laborious manual sorting and screening of hybridoma cells, a process that cannot handle more than several hundred clones at a time. The

biopanning procedure by its nature allows the library to self-select by allowing particles displaying a desirable antibody to bind to an immobilized target for subsequent retrieval.

Logistically, producing antibodies in bacterial fermentation offers several advantages over production in mammalian cell culture (hybridomas). Bacteria are much easier to grow, store, and manipulate genetically than mammalian cells. Microbial contamination is much less of a problem and much more easily dealt with when encountered. In general, bacterial fermentations can be scaled up more easily than mammalian cell cultures and their much more rapid growth and harvest provides the capacity for surge production. When using bacteria to produce products to be used in humans, there is no danger of viral contaminants being passed from the mammalian cell culture to human users, as such viruses cannot multiply in bacteria.

Lastly, recombinant antibody production in bacteria is in step with a growing consensus that current methods of producing monoclonal antibodies in quantity are inhumane. The production of monoclonal antibodies in quantity has traditionally been achieved by injecting hybridoma cells into animal hosts, and subsequently collecting abdominal fluids (ascites) that contain the essentially pure antibody. This method produces great discomfort in animals and is likely to be banned for large scale production in the future. Phage display library construction and subsequent cloning of antibody genes, minimizes animal use by using only those animals initially immunized in the process. All subsequent manipulation and manufacture takes place in bacterial cells, reducing the numbers of animals used from hundreds to fewer than ten per antibody cloned.

ACKNOWLEDGEMENTS

We would like to thank Sarah Cork and Dr. Jun Park of Geo-Centers, Inc. for their expert assistance in expressing and purifying the anti-ovalbumin antibodies. David Lesh of EAI. Corp. purified the anti-MS2 antibody.

REFERENCES

1. Emanuel, P., O'Brien, T., Burans, J., DasGupta, B., Valdes, J. J., and Eldefrawi, M. 1996. Directing antibody specificity towards botulinum neurotoxin with combinatorial phage display libraries. *J. Immunol. Meth.* 193:189-197.
2. Chomczynski, P. and Sacchi, N. 1987. Single step method of RNA isolation by acid guanidinium thiocyanate-phenol-chloroform extraction. *Anal. Biochem.* 162:156-159.
3. Hogrefe, H. and Shopes, B. 1994. Construction of Phagemid Display Libraries with PCR-amplified Immunoglobulin Sequences. *PCR Methods Appl.* S109-S122.
4. Parmley, S. F. and Smith, G. P. 1988. Antibody-selectable filamentous fd phage vectors: affinity purification of target genes. *Gene* 73:305-318.

IMMUNOMAGNETIC ONE-STEP ASSAY FOR DETECTION OF BIOLOGICAL AGENTS

Deborah L. Menking, Michael T. Goode, and Alan W. Zulich
U.S. Army, SBCCOM, Edgewood Chemical Biological Center
Aberdeen Proving Ground, MD 21010

Emily D. Myers, Bruce T. Voelker, and Rebecca L. Tanner
Science and Technology Corporation
Edgewood, MD 21014

ABSTRACT

A one-step process called the FASTube (patent pending) was developed by Biosensors Team to simplify and speed-up assays on a commercial electrochemiluminometer called the ORIGEN[®] analyzer without any loss of sensitivity. The paramagnetic bead-based electrochemiluminescent (ECL) sandwich immunoassay provides simple to perform yet sensitive identification of antigens in biological samples. All assay constituents (except antigen) are lyophilized in a 12 x 75 mm polypropylene test tube to simplify sequential assay chemistries for ease of use. Operator error is negligible for the 15-min assay. The method incorporates the capture of antigen to a paramagnetic streptavidin-coated polystyrene bead imbued with biotinylated capture antibody. A secondary antibody labeled with the reporter, ruthenium (II) tris bipyridyl ($\text{Ru} [\text{bpy}]_3^{2+}$) binds to the antigen to form an immunocomplex capable of emitting light when the reporter molecule is excited by an electrochemical reaction at the surface of an electrode. The versatility of the approach has been demonstrated by rapid and sensitive detection of bacterial spores and vegetative cells, viral particles, and toxins.

INTRODUCTION

In the medical, environmental, and food safety communities, immunodiagnostic testing has become the means to provide simplistic assessment and rapid identification of diseases and contaminants that are harmful to society. To prevent the occurrence of protracted illness and/or endemic disease, there is a need for simplistic confirmatory assays that provide qualitative and semi-quantitative assessment for the detection of antigen in a clinical specimen, aerosol, soil or water sample, or food. In addition, in recent years due to the realization of the threat of bioterrorism, many diagnostic tests are designed to be performed at satellite sites other than established laboratories. This scenario presents a critical need to provide very simple, reliable, and easy to use diagnostic assays that may be performed confidently by non-technical or lay personnel. Moreover, in this respect, most sophisticated bioassay platforms are useful as long as they do not require extensive operator manipulations for rapid and facile determination of the presence or absence of analyte in a clinical, environmental, or food sample. Currently, most immunoassay-based detection systems rely upon an antibody-antigen interaction that requires the addition of multiple assay components in a sequential manner to produce a detectable event. Although reliable for positive identification, present assay procedures and reagent preparation are involved and time consuming. The major drawback associated with present procedures is the sequential addition and transfer of multiple reagents to produce an assay. Each additional step in a detection assay increases the degree of difficulty for execution by the operator and is prone to misuse, thereby, resulting in a higher margin for error.

Concomitantly, the general mission of Biosensors Team is the evaluation and assay development of immunological and nucleic acid assays and their related chemistries on promising emerging biosensor

technologies. The specific mission addresses four areas: (1) the improvement of existing biosensor platforms and assays, (2) the development of assays for new bioagents, (3) the development and testing of commercial off-the-shelf (COTS) and emerging sensor technologies, and (4) the development of new or more conducive assay formats and platforms to meet Army specifications. In conjunction with mission specific goals, Biosensor Team objectives target the following operational requirements for assay development: (1) design simple, yet sensitive assay approaches for rapid detection, (2) simplify labor intensive sequential assay chemistries for *ease of use*, (3) modify and adapt assay chemistries for fieldability, and (4) minimize operator error. In this regard, Biosensors Team was responsible for assay development of toxin and pathogen immunoassays using ruthenium tris bipyridal electrochemiluminescent assays.¹

Biosensor Team has worked with the ORIGEN[®] analyzer since 1995. The system is also under investigation in a number of other government labs. To design a rapid one-step approach for immunodiagnostic testing, we selected a commercially available ECL immunoassay platform called the ORIGEN[®] analyzer developed by IGEN, Inc. (Gaithersburg, MD). The ORIGEN[®] is an extremely sensitive immunodetector but suffers from the typical multi-step assay chemistry discussed above. Biosensors Team investigated the feasibility of co-packaging all necessary ECL immunoassay constituents into a single tube assay, whereby, only the addition of an aliquot of sample would be required. This method would eliminate the separate pipetter measurements and additions necessary for the (1) specified amount of biotinylated capture antibody (2) specified amount of ruthenium-labeled reporter antibody (3) specified volume of antigen (4) incubation of immunocomplex (5) addition of specified volume of paramagnetic bead, (6) a separate incubation step required after the addition of the bead to the immunocomplex, and (7) specified volume of assay buffer.

Wet chemistry evaluations were investigated to show proof of principle for the combination of biotinylated immunoglobulin (IgG), ruthenium labeled IgG, streptavidin paramagnetic beads, and stabilizers in a single reaction tube. The concept was taken a step further by successfully lyophilizing all assay components for long-term storage in an injection-molded polypropylene reaction tube that is shatterproof and disposable. This device and method are disclosed as the FASTube assay immunodiagnostic method in U.S Patent Application Serial No. 09/433,787.

The ORIGEN[®] chemistry utilizes the electrochemiluminescence of ruthenium (II) tris (bipyridal) chelate, $\text{Ru}(\text{bpy})_3^{2+}$. In a typical immunoassay, anti-target biotinylated capture antibodies are immobilized to streptavidin-imbued paramagnetic beads, followed by the addition of anti-target antibodies conjugated to $\text{Ru}(\text{bpy})_3^{2+}$. The target antigen is added and incubated for a pre-determined amount of time for the formation of a magnetic bead-immunocomplex that contains a reporter molecule if the target has been present in solution (Fig. 1). The immune complex is aspirated into a flow cell that has been preconditioned with a buffer containing the precursor molecule tripropyl amine (TPA) to allow for electron transfer. An applied magnetic field captures the paramagnetic beads on the electrode surface where $\text{Ru}(\text{bpy})_3^{2+}$ and TPA are simultaneously oxidized on the anode resulting in TPA^+ and $\text{Ru}(\text{bpy})_3^{3+}$. Subsequently, TPA^+ is deprotonated to form the cation radical TPA^{\bullet} , which in turn creates a high energy state $\text{Ru}(\text{bpy})_3^{2+*}$. During its relaxation, $\text{Ru}(\text{bpy})_3^{2+*}$ decays to the ground state emitting a photon of light at 620 nm (Fig. 2). The amount of light emitted by the reporter molecule is quantified by a photomultiplier tube (PMT) which provides electrochemiluminescent-based detection (ECL units).²⁻⁷

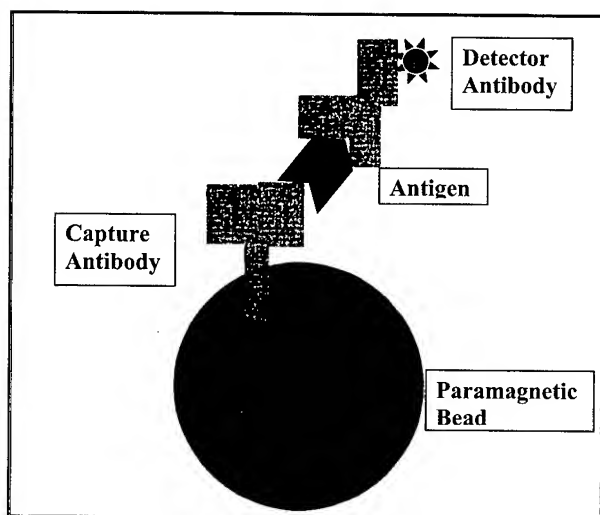


FIGURE 1. ECL immunochemistry

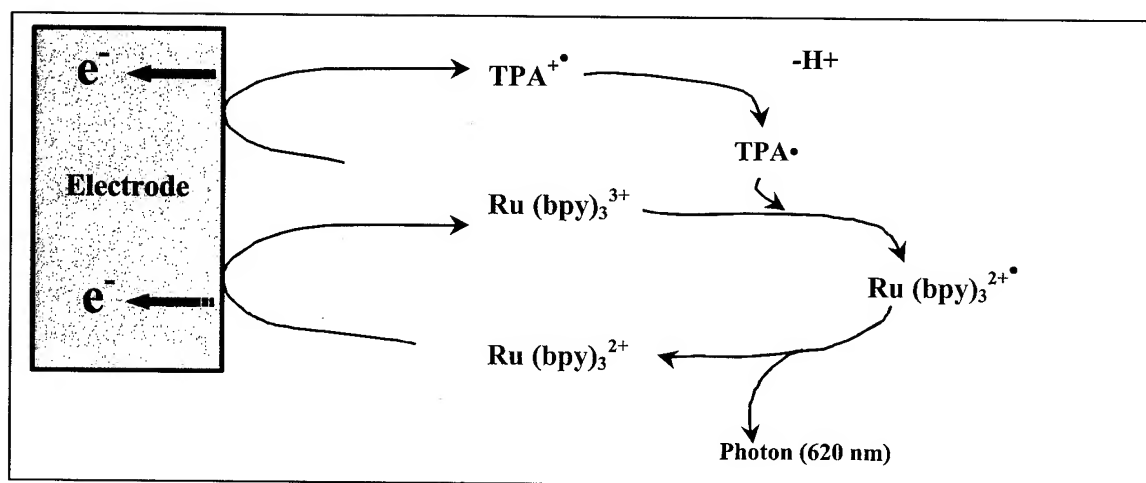


FIGURE 2. ORIGIN® electrochemistry.

The ECL FASTube concept is the cornerstone of ECL immunomagnetic assay development. One-step FASTube assays have simplified the assay process by eliminating several steps and operator manipulations by co-packaging all necessary reagents into one tube. The simplicity of this method has been enhanced by the ability to lyophilize all necessary assay constituents in a specially designed 12 x 75 mm polypropylene test tube that is capable of being hermetically sealed until use (Fig. 3). In this case, a biotinylated capture antibody, ruthenium-labeled reporter antibody, and 2.8 μ m polystyrene immunomagnetic bead are freeze-dried simultaneously in a single tube. To test for the presence of biological material in a sample, the end user places the one-step assay tube in the ORIGIN® analyzer carousel (50-site capability) and reconstitutes the tube contents with a specified volume of antigen sample, followed by a short 10 to 15 min incubation period. Once the incubation is complete, a photomultiplier tube in the analyzer reads the electrochemiluminescence. The entire assay time is approximately 15 minutes.



- Rapid and sensitive FASTube assay for ease-of-use
- Negligible operator error; homogeneous assay
- Low false positive and false negative occurrences
- Lyophilized immunoreactants optimized for sensitive detection of bacteria, toxins, and viruses
- Disposable 12 x 75mm polypropylene tube
- Cost effective assay < \$1.50
- Hermetically sealed for long-term stability of reagents

FIGURE 3. ECL FASTube format.

MATERIALS AND METHODS

ECL reagents and instrumentation. ORIGEN® ECL reagents used including streptavidin-coated paramagnetic beads (402-175-01), Assay Buffer (402-050-01), Cell Cleaner (402-006-01), and ORIGEN® ECL analyzer were from IGEN, Inc. (Gaithersburg, MD.).

Antibodies. All antibodies used for FASTube assay development were government-furnished materials: Rabbit anti-*C. botulinum*, goat anti-*C. botulinum* A, goat anti-*C. botulinum* B, monoclonal anti-Staphylococcal enterotoxin B (SEB), goat anti-SEB, rabbit anti-*B. anthracis*, rabbit anti-*Y. pestis*, monoclonal anti-*Y. pestis*, and goat anti-*B. subtilis* var. *niger* were prepared for assay development by labeling with biotin (capture) and ruthenium (reporter) for ECL assays. Protein G or Protein A purified antibodies were labeled at 1 mg/ml following a buffer exchange on Sephadex G-25 columns (17-0851-01, PD-100 from Amersham Pharmacia Biotech (Uppsala, Sweden).

Biotin-labeling. Capture antibodies were labeled with ImmunoLigand Assay (ILA) Biotin Label (# R9002), from Molecular Devices Corporation (MDC, Sunnyvale, CA.). DNP-biotin NHS ester was rehydrated with 1 ml of DMF to a final stock concentration of 0.0058 μM /μl. A molar coupling ratio (MCR) of 10:1 moles of biotin to IgG was added to a 1 mg/ml preparation of the protein. Following a 2-hr incubation in the dark at ambient room temperature (ART), the conjugates were separated on a pre-equilibrated PD-10 Sephadex G-25 column. Ten 0.5 ml fractions were eluted and absorbance reads at 280 nm and 362 nm were made using a Beckman DU 650 spectrophotometer. Molar incorporation ratios (MIRs) for protein conjugates ranged from 2.5 to 5.3 moles of biotin to protein.

Ruthenium labeling. The detector antibodies were labeled at a MCR of 12:1 with TAG NHS-ester™ (402-001-01) from IGEN, Inc. (Gaithersburg, MD). The TAG ester™ was reconstituted with 50 μl of DMSO (Fisher Scientific, # D128-500). After a 1-hr incubation at ART in the dark, the conjugate was separated on a PD-10 G25 Sephadex column in the same manner as previously described for biotin label. The absorbance of the eluate was read at 455 nm and 280 nm to determine the presence of conjugate, and the protein concentration was determined by Bradford Coomassie dye intercalation (BIO-RAD, # 500-0006). MIRs for protein conjugates ranged from 6 - 8 moles of ruthenium to protein.

Preparation of antibody dilutions. Antibody conjugates were diluted for use in 1X Assay Buffer (10 mM potassium phosphate, 150 mM sodium chloride, 0.025% Triton X-100, 0.005% sodium azide, and 1 mg/ml BSA), pH 7.0 for ORIGEN[®] assay development. Assay development consisted of determining the optimum amounts of capture and detector conjugates needed to elicit maximum endpoint sensitivity in the shortest period of time. Preliminary antibody loading studies were designed in matrix fashion by incorporating 50, 75, and 100 ng/test of each biotinylated and ruthenium-labeled conjugate pair. The dynamic range of the assay was monitored from 0 – 25 ng/ml of toxin or 0 – 1×10^7 cfu/ml for pathogen assays.

Preparation of antigens. *C. botulinum* Toxin A Soln. at 0.5 mg/ 0.5 ml (025-08173) and *C. botulinum* Toxin B Soln. (9810137) at 0.5 mg/0.5 ml were purchased from Wako Pure Chemicals Industries, Ltd. (Osaka, Japan). The antigen dilution range consisted of a fresh preparation of toxins from 0 - 25 ng/ml in Assay Buffer. *Staphylococcus enterotoxin B* (S 4881) was purchased from SIGMA (St. Louis, MO.) and reconstituted in 0.01 M Phosphate Buffered Saline (PBS) + 0.05% sodium azide for a final concentration of 1 mg/ml. The antigen dilution range consisted of a fresh preparation from 0 - 25 ng/ml of antigen in Assay Buffer. BG spores (DPG dry powdered spores 28 May 91 at 1×10^{12} spores/gm) were prepared in 0.01M PBS + 0.05% Triton X-100 (PBST) for a stock concentration of 1×10^9 cfu/ml. Serial dilutions were made in PBST ranging from 0 - 1×10^7 cfu/ml. *Yersinia pestis* Colorado 92 wild strain (lot # 1 Nov 99) was received from Dr. Ted Hadfield of the Armed Forces Institute of Pathology (AFIP) as non-viable cobalt irradiated material suspended in 0.9% saline solution. The antigen dilution range consisted of a fresh preparation of 0 - 1×10^7 cfu/ml in 0.01M PBS + 0.1% Triton X-100.

ORIGEN[®] standard assay protocol. All experiments performed on the ORIGEN[®] were 15-minute assays. Initially, 25 µl of biotinylated antibody and 25 µl of ruthenium-labeled antibody were combined in a 12 x 75 mm borosilicate glass test tube, followed by the addition of 100 µl of the respective antigen dilution (100 µl of IGEN Assay Buffer was used for the negative control) with vortexing at 70 rpm for 10 min. Following the incubation of antibody with antigen, 20 µl of Dynabeads M-280 Streptavidin at a concentration of 1 mg/ml were added to the immunocomplex and incubated for 5 min with vortexing at 70 rpm. One hundred and fifty microliters of IGEN Assay Buffer was added to each tube, and the ECL measurement was recorded. Each sample was run in triplicate and the signal to noise ratio (net signal divided by the negative control) was calculated along with statistical analyses.

Once the standard assays for each bioagent were developed and optimized for concentration, assay endpoint sensitivity, and dynamic range, the assays were transferred to the simplified FASTube version, whereby, the antibody capture and detector pair with the paramagnetic beads was lyophilized in a polypropylene tube and hermetically sealed for long term storage.

ORIGEN[®] FASTube assay protocol. FASTubes were run in triplicate with sample dilutions. The FASTubes were uncapped and placed in the ORIGEN[®] analyzer carousel. Each tube received 100 µl of the appropriate dilution series and 100 µl of negative assay buffer was added to the background tubes. The tubes were incubated for 15 minutes at ambient room temperature at 100 rpm, followed by the addition of 200 µl of IGEN assay buffer. The ECL response was recorded for each tube.

FASTube assessment. A FASTube assessment was conducted using BG FASTubes that had been previously lyophilized and pre-screened by Quality Assurance and Quality Control (QA/QC) validation studies. During the assessment, a non-technical operator was trained to perform system set up, shutdown, and FASTube analysis using known BG spore samples. The trainee ran known BG SWIPE Kit samples with the assistance of an experienced operator. The final assessment consisted of the independent operation of the system and assays by the non-technical operator. Blinded BG samples derived from SWIPE Kit samples, buffer negatives, and BG positive controls at 1×10^6 cfu/ml were evaluated in triplicate. A side-by-side evaluation of trainee and BT operator performance was monitored for all assays.

FASTube matrix effects. The effects of various matrices on FASTube efficiency was performed using *C. botulinum* A toxoid spiked into liquid samples consisting of commercial bottled apple juice and canned green bean liquid, residential tap water, and laboratory assay buffer (control). Sample preparation was a modified version of the procedure cited in the *FDA Bacteriological Analytical Manual* ⁸ with the intent of creating a sample milieu characteristic of an extraction procedure. Liquid samples of apple juice and green bean liquid were diluted 1:2 in 0.2M Phosphate Buffered Saline (PBS), pH 7.7 and sterile filtered. Liquid samples were spiked with *C. botulinum* A toxoid at 0 – 25 ng/ml. For solid food preparation, a protocol from the *USDA/FSIS Microbiology Laboratory Guidebook* ⁹ was modified, whereby, 25 g of commercial canned chicken was homogenized in 50 ml of 0.2 M PBS, pH 7.7 and clarified by centrifugation at 15,000 x g for 15 min at 5° C. The supernatant was diluted 1:10 in PBS and sterile filtered for subsequent spiking with toxoid at 0 – 25 ng/ml.

RESULTS

C. botulinum A and SEB toxins, *B. anthracis* and BG bacterial spore, and *Y. pestis* vegetative cell assays.

C. botulinum A and SEB assay endpoint sensitivity and dynamic range were determined by performing intra-assay and inter-assay ORIGIN® analyses. *C. botulinum* A and SEB toxin titrations were run in triplicate for each determination, and statistical analyses were calculated to determine the assay endpoint sensitivity and dynamic range. *C. botulinum* A toxin assay endpoint sensitivity was calculated by adding the mean background (2,438 ECL units) plus 3 times the standard deviation (3*STD: 606 ECL units) or 3,044 ECL units as the cutoff. Hence, the endpoint sensitivity was 100 pg/ml for the 15-minute assay. SEB toxin assay endpoint sensitivity was derived in the same manner with a mean background of 359 ECL units plus 3*STD (141 ECL units) or 500 ECL units as the cutoff with an endpoint sensitivity of 5 pg/ml. Both toxin assays demonstrated linear responses from 0 – 25 ng/ml and did not reveal a plateau or “hook effect” at the highest concentration range as shown in Table 1.

TABLE 1. FASTube Assay Endpoint Sensitivities for *C. botulinum* A and SEB Toxins.

Background + 3* STD: 3044 ECL units Lower Limit of Detection: 100 pg/ml Wako <i>C. botulinum</i> A Pure Toxin (# 025-08173)				Background + 3* STD: 500 ECL units Lower Limit of Detection: 5 pg/ml SIGMA SEB Pure Toxin (Cat. # S 4881)			
ng/ml	ECL Raw Signal	ECL Specific Signal	% CV	ng/ml	ECL Raw Signal	ECL Specific Signal	% CV
0	2438	-606	8.3	0	359	-141	13.1
0.013	2550	-494	12.3	0.001	484	-16	32.4
0.025	2530	-514	8.0	0.005	1339	839	13.2
0.050	2559	-485	8.5	0.010	2087	1587	3.1
0.100	3149	105	19.1	0.050	8338	7838	0.5
0.250	3795	751	9.6	0.1	16054	15554	1.9
0.500	5838	2794	7.4	0.5	77267	76767	2.7
1	9576	6532	3.9	1	147923	147423	1.7
5	40028	36984	3.9	5	701110	700610	2.8
10	76381	73337	3.0	10	1276710	1276210	0.1
25	194054	191010	3.9	25	2537954	2537454	2.1

B. anthracis and BG spore titrations were run in triplicate for each determination, and statistical analyses were calculated to determine the assay endpoint sensitivity and dynamic range. *B. anthracis* assay endpoint sensitivity was 5×10^3 cfu/ml for the 15-minute assay with a mean background of 6,776 ECL units plus 3*STD (2,561 ECL units) with 9,337 ECL units as the cutoff. The assay endpoint sensitivity for the BG spore assay was 8×10^2 cfu/ml for the 15-minute assay (Table 2).

Although the specific signal for the *Y. pestis* assay was positive at 8×10^3 cfu/ml and at 1×10^4 cfu/ml (955 and 813 ECL units, respectively), there was no evidence of titration below these points (10^1 cfu/ml and 10^2 cfu/ml) to substantiate a lower limit of detection cutoff. Therefore, the *Y. pestis* endpoint sensitivity was established at 2×10^4 cfu/ml (Table 3).

TABLE 2. FASTube Assay Endpoint Sensitivities for *B. anthracis* and BG Spores.

Background + 3 ^x STD: 9337 ECL units Lower Limit of Detection: 5×10^3 cfu/ml <i>B. anthracis</i> Sterne spore Gamma irradi. (AFIP)				Background + 3 ^x STD: 5110 ECL units Lower Limit of Detection: 8×10^2 cfu/ml <i>B. subtilis</i> spore Pine Bluff variety (DPG)			
cfu/ml	ECL Raw Signal	ECL Specific Signal	% CV	cfu/ml	ECL Raw Signal	ECL Specific Signal	% CV
0	6776	-2561	12.6	0	3163	-1947	20.5
1×10^1	6191	-3146	1.1	1×10^2	3224	-1886	3.2
1×10^2	6296	-3041	1.7	5×10^2	5089	-21	3.1
1×10^3	6981	-2356	3.9	8×10^2	5984	874	2.5
2×10^3	7982	-1355	1.6	1×10^3	6385	1275	3.4
5×10^3	10833	1496	3.5	2×10^3	10282	5175	3.1
1×10^4	15647	6310	2.6	5×10^3	22804	17694	1.6
1×10^5	50014	40677	2.5	1×10^4	42576	37466	12.0
1×10^6	208887	199550	9.1	1×10^5	273919	268809	3.2
				1×10^6	250522	245412	4.6
				1×10^7	194272	189162	1.1

TABLE 3. FASTube Assay Endpoint Sensitivity for *Yersinia pestis*.

Background + 3 ^x STD: 4018 ECL units Lower Limit of Detection: 2×10^4 cfu/ml <i>Y. pestis</i> CO92 wild strain (AFIP)			
cfu/ml	ECL Raw Signal	ECL Specific Signal	% CV
0	3097	-921	9.9
8×10^3	4973	955	11.5
1×10^4	4831	813	1.4
2×10^4	13496	9478	1.5
5×10^4	29870	25852	12.8
8×10^4	51329	47311	4.4
1×10^5	56330	52312	2.3
2×10^5	107660	103642	18.8
5×10^5	291323	287305	6.4
8×10^5	443619	439601	10.2
1×10^6	529701	525683	5.9
1×10^7	4299027	4295009	2.8

FASTube assessment. In order to be effective, the FASTube would have to meet certain qualifications and requirements necessary for biotetection: semi-automation, speed, sensitivity, moderate cost, and ease-of-use. In this regard, two-thirds of these objectives had been met by: (1) addressing assay development and optimization of ECL assay chemistries for toxin, viral, sporulated and vegetative bacterial pathogens; and, (2) designing overall simplification of the immunoassay format to provide convenient co-packaging of reagents and ease of use without sacrificing assay sensitivity. An important objective for use as a biotector was to beta test the FASTube format to assess the margin of operator error associated with non-technical operators. Table 4 describes the results of the assessment performed by a non-technical operator using BG spores and the BG FASTube in conjunction with the results obtained from a side-by-side analysis with a trained operator.

Table 4. FASTube Operator Assessment I for BG Spores:

Sample ID	Trainee		BT	
	Mean ECL	% CV	Mean ECL	% CV
Buffer Neg	3 replicates 6947	5.7	2 replicates 7365	15.6
2	701031	5.2	645992	5.6
3	630217	1.6	708264	14.5
6	622738	8.3	681051	9.4
18	7082	5.7	6164	0.5
35	6661	3.5	6094	24.7
BG Positive Cntrl	409079	2.2	359641	17.9

Sample ID	Trainee		BT	
	Mean ECL	% CV	Mean ECL	% CV
Buffer Neg	3 replicates 4028	16.8	2 replicates 6097	11.4
5	5257	11.9	6294	12
26	678249	26.3	756851	8.4
27	4183	4.8	6463	4.1
28	660101	14.2	688129	19.3
36	629708	12.5	689604	11.9
BG Positive Cntrl	396766	16.8	485142	10.7

Testing with non-technical trainees with blinded BG samples using the FASTube format demonstrated no false positive or false negative occurrences. Side-by-side analysis of non-technical operator precision as compared to experienced operator accuracy demonstrated equivalent CVs. The non-technical operator positively identified 60 blinded BG samples (20 samples x 3 replicates per sample), 12 positive controls (4 BG positives x 3 replicates per control), and 12 negative controls (4 background assays x 3 replicates) for a total of 84 determinations with no occurrence of operator error. Coefficients of variation (CVs) are somewhat higher in these assays due to particulate matter and extractables leaching out of the sponge material in the Swipe Kit.

FASTube Matrix Effects. Many detection platforms and their related chemistries are subject to matrix effects which occur due to the milieu in which the sample is presented. From the environmental perspective interfering substances such as smoke, dust, sand, soils, oils, and pollen can seriously affect the ability to detect the presence of an organism. In the clinical/medical diagnostics and food safety communities, sample extraction and/or sample preparation are critical to the success of the identification of an organism. Due to the complexity of this issue, our effort did not address an in-depth analysis of matrix effects with the ORIGIN® FASTube format; however, liquid and solid food samples were prepared to simulate a sample milieu that would be characteristic of material resulting from an extraction procedure. Therefore, the focus was not designed to address measurement of *C. botulinum* A toxoid detection based on the success or failure of pre-enrichment and/or extraction techniques; but rather, suggest the ability of this immunoassay format to yield detectable events in an environment other than a pristine laboratory buffer. For this effort, laboratory buffer spiked with *C. botulinum* A toxoid at 0 – 25 ng/ml was used as the reference control relative to the results obtained for

commercially obtained apple juice, canned green bean liquid, and canned processed chicken. Non-buffered residential tap water was spiked with the same concentration ranges of toxoid A.

A total of 296 *C. botulinum* A FASTube assays were evaluated in 5 sample milieu. Spiked buffer titrations from 0 – 25 ng/ml of toxoid A were run to establish a standard curve (endpoint sensitivity of 31 pg/ml). Detection of the spiked toxoid in sample milieu was in the low picogram range with endpoint sensitivities from 31 pg/ml to 125 pg/ml: spiked apple juice, spiked green bean liquid, and spiked residential tap water at 31 pg/ml; spiked processed canned chicken supernatant at 125 pg/ml. There was 1 false positive for spiked green bean liquid at 31 pg/ml. Figure 4 displays the assay overlays for each sample milieu evaluated.

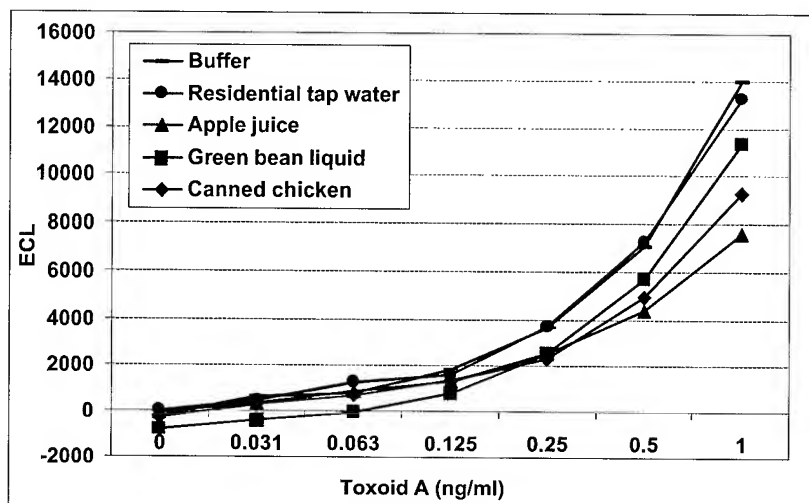


Figure 4. FASTube results of spiked *C. botulinum* A toxoid in 5 sample milieu.

CONCLUSIONS

The objective of the FASTube concept is to overcome the shortcomings of existing multi-step sandwich immunoassays by providing a method wherein a qualitative or semi-quantitative assay can be performed easily with a one-step addition of sample in a plastic tube that is easy to handle. We tailored the assay design to eliminate the dependence of numerous reagent vials and test tubes. There are no metric measurements or manual transfer of multiple reagents, pipette calibrations, etc. Biosensors Team eliminated the necessity for extensive laboratory training for reagent preparation or handling and reduced the probability of a percentage of operator error due to pipetting manipulations, reagent transfer inaccuracies, and fixed-volume transfers. We simplified overall assay procedures by eliminating complicated procedures and stringent reagent preparations. Operator handling and numerous user interactions were reduced to decrease the probability of end user error in clinical, medical, or field test situations. The FASTube concept combines the present ECL assay chemistries for inclusion into a self-contained, stand-alone plastic tube as opposed to numerous reagent combinations in the current assay format. The FASTube assay protocol is a simple one-step procedure that precludes the necessity for extensive laboratory training. The FASTube design is more cost effective and simplifies overall assay procedures. The method provides a rapid, sensitive, and uncomplicated assay format that requires only the addition of sample to a lyophilized product. The results for all ORIGEN® FASTube assays developed using the lyophilized one-step assay demonstrate a simplified and extremely sensitive format for immunoassay detection. The total assay time of approximately 15 min. is sufficient for picogram detection of toxins and <1,000 cfu for bacterial spores. The manipulations required for the assay have been reduced to a one-step addition of sample.

The FASTube concept was evaluated for ease of use, simplicity, and operator error using non-technical personnel. Twenty blinded BG samples selected at random were provided to trainees plus BG positive controls and negative controls. Three replicates were run for unknown samples and controls. Total assay time from the time the sample was presented to identification was approximately 20 min. There were no false positive or false negative occurrences in a total of 84 determinations. The FASTube ECL concept provides a high confidence level for sensitive and straightforward immunological detection coupled with low risk for operator error.

The FASTube ECL technology has potential to conserve sensitive detection capabilities in lieu of various sample matrices. Spiking of sample milieu such as commercial apple juice, canned green bean liquid, and canned processed chicken resulted in sensitive detection of *C. botulinum* A toxoid at 31 pg/ml to 125 pg/ml with no loss of detection in time or sensitivity when compared to the spiked laboratory buffer used as a reference.

These data suggest that the ORIGEN® electrochemistry, flow cell, and FASTube format are plausibly rugged and suitable for potential use in medical, clinical, environmental, and food safety communities. Additional bioagent assays under FASTube development include: *Francisella tularensis*, *Brucella melitensis*, ricin toxin, Vaccinia virus, and *Coxiella burnetti*. Current FY 00/01 efforts also include the ongoing development of two ORIGEN® FASTube assays for foodborne pathogens, namely, *Escherichia coli* O157:H7 and *Salmonella typhimurium*.

REFERENCES

1. Gatto-Menking, D., Yu, Hao, Bruno, J., Goode, M. Miller, M., and Zulich, A. 1995. Sensitive detection of biotoxoids and bacterial spores using an immunomagnetic electrochemiluminescence sensor. *Biosens. and Bioelectron.* **10**: 501-507.
2. Blackburn, G., Shah, H., Kenten, J., Leland, J., Kamin, R., Link, J., Peterman, J., Powell, M., Shah, A., Talley, D., Tyagi, S., Wilkins, E., Wu, T., and Massey, R. 1991. Electro-chemiluminescence detection for development of immunoassays and DNA probe assays for clinical diagnostics. *Clin. Chem.* **37**: 1534-1539.
3. Leland, J.K., Powell, M.J. 1990. Electrogenated chemiluminescence: an oxidative-reduction type ECL reaction sequence using tripropyl amine. *J. Electrochem. Soc.* **137**: 3127-3131.
4. Yang, H., Leland, J.K., Yost, D., and Massey, R.J. 1994. Electrochemiluminescence: a new diagnostic and research tool. *Bio/Technology* **12**: 193-194.
5. Yu, Hao, Bruno, J.G. 1995. Sensitive bacterial pathogen detection using an immunomagnetic-electrochemiluminescent instrument: potential military and food industry application. *Biomedical Products*.
6. Deaver, Daniel R. 1995. A new non-isotopic detection system for immunoassays. *Nature* **377**: 758-760.
7. Williams, Richard. 1995. Electrochemiluminescence: a new assay technology. *IVD Technology*, pp. 28-31.
8. Cook, L., Lee, W., Lattuada, C., and Ransom, G., 1998. "Methods for the detection of *Clostridium botulinum* toxins in meat and poultry products" in *USDA/FSIS Microbiology Laboratory Guidebook*, 3rd Ed., Chapter 14.

DEVELOPMENT AND TESTING OF AN ELECTROCHEMILUMINESCENT PLATFORM FOR THE DIAGNOSIS OF INFECTIOUS AND NON-INFECTIOUS DISEASE

Cindy A. Rossi, Todd M. Kijek, Erik A. Henchal, Mary E. Brock, George V. Ludwig

Diagnostic Systems Division, U.S. Army Medical Research Institute of Infectious Diseases
1425 Porter Street, Fort Detrick, MD 21702

ABSTRACT

Biological warfare (BW) agents and diagnosis of diseases caused by these agents has traditionally been detected and identified by isolating the causative agent. Because agent isolation may require days or even weeks to complete, this procedure often fails to have any direct impact on patient care. Advances in affinity-based detection technologies provide a basis for the development of immunodiagnostic platforms capable of meeting the stringent requirements for sensitivity and specificity needed to rapidly identify BW agents. These assets provide the potential to directly affect patient care. We developed a series of highly sensitive, rapid immunodiagnostic assays based upon the electrochemiluminescence (ECL).

ECL is a process in which light is generated from a voltage-dependent cyclic oxidation-reduction reaction between a ruthenium heavy metal chelate (Ru) and tripropylamine (TPA). In the presence of an electrical current, the chelate and TPA enter into a redox reaction that triggers the release of photons that are detected and assayed with a photomultiplier tube. The ruthenium chelate used is coupled to a NHS-ester that can be easily conjugated to any protein by using standard binding chemistries. Detection is facilitated in a homogeneous assay with 2.8 μm magnetic beads. The magnetic beads serve as the solid phase for the detection reaction as well as the means of drawing the specific reactants into the proximity of the electrode. The beads also provide the basis for separating and concentrating antibody-antigen complexes from potential non-specific reactants.

We demonstrated the effectiveness of the ECL system for detecting *Staphylococcus enterotoxin B* (SEB), ricin toxin, *Clostridium botulinum* toxin C fragment, *Yersinia pestis* F1 antigen, *Bacillus anthracis* PA, and Venezuelan equine encephalitis virus. The technology potentially could be used with any biological agent and is limited only by the availability of high-quality, high-affinity antibodies or other ligands. In collaboration with Edgewood Chemical and Biological Center, we are in the process of developing single tube assays for the ECL platform, which will reduce assay time to as little as 15 min.

INTRODUCTION

The threat of biological warfare (BW) has increased in the last two decades with several bioterrorist incidents reported during that time^{6,7}. While this renewed threat is alarming, it is not a contemporary problem. Classical biological threats that were part of the now defunct U.S. offensive program (terminated in 1969) include *Bacillus anthracis*, botulinum toxin, *Francisella tularensis*, *Coxiella burnetii*, Venezuelan equine encephalitis (VEE), *Brucella suis* (brucellosis), staphylococcal enterotoxin B (SEB), rice blast, rye stem rust, and wheat stem rust. The choice of these agents for the U.S. program was not accidental. Most of these agents can be cheaply produced by only moderately skilled aggressors and in sufficiently large quantities to be delivered over a wide geographic area. As a result, production and use of these weapons are within the capabilities of a greater number of potential enemies and their use may have a larger impact on both military and civilian populations than other weapons of mass destruction². The mere mention of these agents by a terrorist can cause panic and social disruption and may ultimately result in significant psychological harm to the public⁴.

Classical methods for identifying infectious agents that cause human disease have been used for over 100 years and are well established¹. These methods rely on agent cultivation, and require from 1 to 30 days. Laboratories capable of completing these analyses must be well equipped and employ well-trained, experienced personnel. To achieve rapid agent identification with a high level of confidence in the final result, a new generation of technologies will be required.

The United States Army Medical Research Institute of Infectious Diseases (USAMRIID) is the lead DoD laboratory for developing medical diagnostics for biological warfare agents. Its current policy toward agent identification and disease diagnosis incorporates a conservative approach. In other words, final diagnoses and identification depends on confirmation through concurrence between multiple, independent identification technologies. To achieve agent identification with a high level of confidence, identification strategies that use a combination of state-of-the-art immunological and nucleic acid analysis methods, as well as classical microbiological approaches, are needed to identify unknown biological agents³. The major problem with this strategy has been that the level of sensitivity for agent detection by using immunological or affinity technologies is far less than that of nucleic acid detection.

Using electrochemiluminescence (ECL) technology USAMRIID and other DoD laboratories have developed immunoassays that are capable of detecting biological agents at levels of sensitivity close to those detected by polymerase chain reaction (PCR) for the first time⁵.

ECL-BASED DETECTION

ECL is a process by which light is generated from a voltage-dependent cyclic oxidation-reduction reaction with ruthenium heavy metal chelate. In the presence of tripropylamine (TPA), the redox reaction triggers the release of photons that are detected and assayed within a photomultiplier tube. Ruthenium is used in a low molecular weight heme-like form that can be easily conjugated to any protein by standard NHS ester binding chemistries. In the conjugated form, ruthenium serves as an ideal tracer molecule because it has little or no influence on antibody-antigen interactions. Detection is facilitated in a homogeneous assay with 2.8 μm magnetic beads that serve as the solid substrate for the detection reaction. The beads also provide both the basis for the separation of antibody-antigen complexes from potential non-specific reactants and as a means to bring the specific reactants into the proximity of the electrode. A potential of only 2 volts across the electrode is required to initiate the ruthenium redox reaction. As a result of this low potential, only those ruthenium atoms within 30-50 nm of the electrode are detected, reducing the effect of non-specific reactants present in the assay suspension. The result of this process is an extremely sensitive assay exhibiting remarkable signal to noise ratios, wide dynamic range, and short incubation times.

An ECL detection system consists of an analyzer and a personal computer with menu-driven software. The system's strengths come from its speed, sensitivity, accuracy, and precision over a wide dynamic range. In a typical agent detection assay, an unknown sample is added to magnetic beads conjugated to an agent-specific capture antibody and a ruthenium-conjugated detector antibody. The analyzer draws the processed sample from a vortexing carousel, captures and washes the magnetic beads, and quantifies the electrochemiluminescent signal. The current system can be automated, uses stable reagents, and is highly sensitive into the 0.1 to 10 pg per ml range (2 to 200 fg absolute sensitivity). The current system can evaluate 50 samples in under 2 hrs. This time frame includes sample preparation, assay incubation, and instrument analysis.

We demonstrated the effectiveness of the ECL system for detecting SEB, ricin toxin, *Yersinia pestis* F1 antigen, *Bacillus anthracis* protective antigen (PA), VEE virus, and the C fragment from the toxin produced by *Clostridium botulinum* serotype A. The technology could potentially be used with any biological agent and is limited only by the availability of high-quality, high-affinity antibodies or other ligands.

METHODS AND RESULTS

Antibodies previously optimized for use in our enzyme-linked immunoassay (ELISA) platform were labeled with biotin or ruthenium by standard coupling methods. Reagents were then optimized for ECL by standard checkerboard titrations. A variety of antibody buffers, reaction volumes, incubation times, and assay formats were also evaluated. As a result of these optimizations, we chose a two-step assay format.

A two-step format was developed for a number of BW agents that employed combinations of agent-specific monoclonal-monoclonal, monoclonal-polyclonal, or polyclonal-polyclonal antibodies and includes both different and the identical antibodies on capture or detector sides of the assay. The assay was conducted at room temperature (approximately 20°C) by mixing 50 µl of sample with 25 µl of antibody-coated beads (8×10^7 beads/ml) for 15 min. A 25 µl aliquot of Ru-labeled detector antibody was then mixed to this suspension and incubated for another 15 min. The sample mixture was then read by using the ORIGEN immunoassay system (Igen International, Inc.) and the data tabulated.

Reproducible standard curves were generated in various sample matrices (PBS-0.3% tween-20, urine, serum, and 5% skim milk) and used to determine the limits of quantitation and limits of detection for each assay. Typical sensitivity, linear range, and inter-assay variation for an ECL assay are shown in table I. ECL assays were reproducible with the coefficient of variation (CV) generally less than 10% for concentrations lying within the linear range of the assay and less than 20% for concentrations above the detection limit. This held true from assay to assay and from lot to lot of reagents. Typically the linear range of the assay was between 0.1 and 100 ng/ml with a detection limit between 0.1 and 10 pg/ml (2 to 200 fg absolute sensitivity). The linear range could be used to determine quantitative results for unknowns. While the ECL assay was very reproducible in a given matrix, the nature of sample matrix did have a significant influence on overall ECL signal strength (Fig I). Despite this effect, the matrix did not affect assay sensitivity as long as matrix-specific negative control specimens were used in the assay (data not shown).

DISCUSSION

ECL represents a significant improvement over more traditional immunodiagnostic technologies both in terms of assay speed and sensitivity. The only major limitation of the ECL assay system, like most immunoassays, is the necessity for highly quality reagents. Ideally, both detector and capture antibodies should be specific and have high affinities for their respective antigens. All antibodies need to be purified to

facilitate their efficient coupling to magnetic beads and ruthenium. Sensitivity increases of 10- to 100-fold could be accomplished by replacing specific ligand-purified antibodies for Protein G- or A-purified antibodies. However, once appropriate reagents were identified and prepared, they were extremely stable, were easily lyophilized, and could readily be transported for field use. Antibodies that traditionally perform well in ELISA-based assays performed well in ECL-based assays. This makes assay development relatively easy and ensures efficient transition from ELISA to ECL. Another limitation of this system was the requirement for matrix-specific controls to ensure the accurate determination of assay cutoff values and detection limits. While this represents only an inconvenience for medical diagnosis, it could present significant problems for environmental testing where the sample matrix is more difficult to define.

The major benefit of the ECL system lies in its exquisite sensitivity. Assay sensitivities in the picogram per ml range were routinely and consistently obtained and represent a 100- to 1000-fold improvement over ELISA. ECL-based agent identification is by far the most sensitive affinity-based diagnostic technology that we have tested to date. As the ECL hardware matures, this technology will prove itself to be an important component of an integrated approach to identifying potential biological weapons both in the laboratory and in the field.

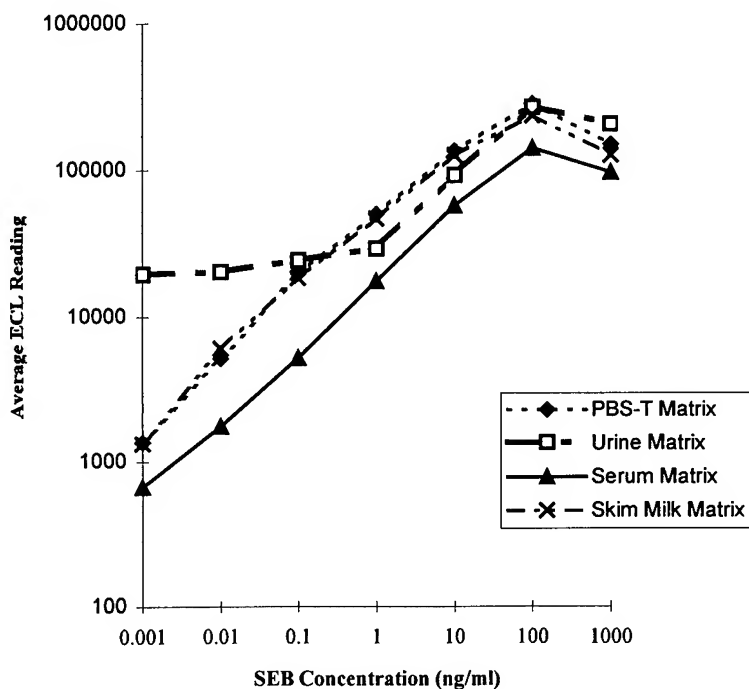


FIGURE I

SEB ECL assay and standard curves prepared in different biological matrices. SEB antibody-negative serum, urine, 5% skim milk, and PBS—0.3% Tween-20 matrices were spiked with 10-fold dilutions (1000-0.001 ng/ml) of SEB toxin. Two replicates of each dilution were used for each determination. Matrix specific cutoffs were as follows: serum, 349; urine, 1181; 5% skim milk, 53; and PBS-0.3% Tween-20, 743.

TABLE I: Sensitivity and Precision of SEB ECL Assay with 5 Replicates per Concentration.

Concentration (ng/ml)	Average ECL Reading	% CV	S/N†	Backfit Concentration (ng/ml)‡
0.001	1516	19.1	2.04	0.00005
0.01	6229	11.7	8.38	0.002
0.1	25292	5.2	34.04	0.12
1	56794	4.1	76.44	1.06
10	148111	4.2	199.34	14.78
100	269488	4.0	362.7	76.49
1000	178883	4.5	240.76	24.82

Assay cutoff = 891; n= 15

† Signal to noise Ratio (S/N) = Average ECL reading/ average ECL reading of negative values

‡ Backfit using linear portion of curve only, 0.1-100 ng/ml. R² =0.992

Bold indicates linear range.

REFERENCE LIST

1. Manual of Clinical Microbiology. 1996. ASM Press, Washington, DC.
2. **Christopher, G. W., T. J. Cieslak, J. A. Pavlin, and E. M. Eitzen, Jr.** 1997. Biological warfare. A historical perspective. J. Am. Med. Assoc. **278**:412-417.
3. **Franz, D. R., P. B. Jahrling, A. M. Friedlander, D. J. McClain, D. L. Hoover, W. R. Bryne, J. A. Pavlin, G. W. Christopher, and E. M. Eitzen, Jr.** 1997. Clinical recognition and management of patients exposed to biological warfare agents. J. Am. Med. Assoc. **278**:399-411.
4. **Holloway, H. C., A. E. Norwood, C. S. Fullerton, C. C. Engel, Jr., and R. J. Ursano.** 1997. The threat of biological weapons. Prophylaxis and mitigation of psychological and social consequences. J. Am. Med. Assoc. **278**:425-427.
5. **Kijek, T. M., C. A. Rossi, D. Moss, R. W. Parker, and E. A. Henchal.** J.Immunol.Methods, in press.
6. **Kolavic, S. A., A. Kimura, S. L. Simons, L. Slutsker, S. Barth, and C. E. Haley.** 1997. An outbreak of *Shigella dysenteriae* type 2 among laboratory workers due to intentional food contamination. J. Am. Med. Assoc. **278**:396-398.
7. **Torok, T. J., R. V. Tauxe, R. P. Wise, J. R. Livengood, R. Sokolow, S. Mauvais, K. A. Birkness, M. R. Skeels, J. M. Horan, and L. R. Foster.** 1997. A large community outbreak of salmonellosis caused by intentional contamination of restaurant salad bars. J. Am. Med. Assoc. **278**:389-395.

DEVELOPMENT OF AN AUTONOMOUS PATHOGEN DETECTION SYSTEM

Richard G. Langlois, Steve Brown, Bill Colston, Les Jones, Don Masquelier, Pete Meyer, Mary McBride, Shanavaz Nasarabadi, Albert J. Ramponi, Kodumudi Venkateswaran, and Fred Milanovich

Lawrence Livermore National Laboratory
7000 East Avenue, L-452
Livermore, CA 94551

ABSTRACT

An Autonomous Pathogen Detection System (APDS) is being designed and evaluated for use in domestic counter-terrorism. The goal is a fully automated system that utilizes both flow cytometry and polymerase chain reaction (PCR) to continuously monitor the air for BW pathogens in major buildings or high profile events. A version 1 APDS system consisting of an aerosol collector, a sample preparation subsystem, and a flow cytometer for detecting the antibody-labeled target organisms has been completed and evaluated. Improved modules are under development for a version 2 APDS including a Lawrence Livermore National Laboratory-designed aerosol preconcentrator, a multiplex flow cytometer, and a flow-through PCR detector.

INTRODUCTION

Lawrence Livermore National Laboratory (LLNL) has an ongoing program to design, fabricate and field demonstrate a fully Autonomous Pathogen Detection System (APDS). This will be accomplished by integrating a flow cytometer and real-time polymerase chain reaction (PCR) detector with sample collection, sample preparation and fluidics to provide a compact, autonomously operating instrument capable of simultaneously detecting multiple pathogens and/or toxins. The APDS will be designed to operate in fixed locations, where it continuously monitors air samples and automatically reports the presence of specific biological agents. The APDS will utilize both multiplex immuno and nucleic acid assays to provide 'quasi-orthogonal', multiple agent detection approaches to minimize false positives and increase the reliability of identification. The APDS is targeted for domestic applications in which (1) the public is at high risk of exposure to covert releases of bioagent such as in major subway systems and other transportation terminals, large office complexes, and convention centers; and (2) as part of a monitoring network of sensors integrated with command and control systems for wide-area monitoring of urban areas and major gatherings (e.g., inaugurations, Olympics, etc.). In this latter application there is potential that a fully developed APDS could add value to DoD monitoring architectures.

Technical advancements across several fronts must first be made in order to realize the full extent of the APDS. A phased approach, with increasing detection and identification capability, has been employed in the design, construction, and testing of each evolutionary version of the APDS. The version 1 system, APDS-I, which provides a single-plex immunoassay using flow cytometry, has been completed and field tested. Work is in progress on advanced modules for the second version of the APDS, APDS-II, to provide the capabilities for *automated multiplex* immunoassays and *flow-through PCR*.

DEVELOPMENT AND EVALUATION OF APDS-I

This system incorporates an aerosol collector from Research International (RI), a custom-built fluidics system, and a MicroCyte flow cytometer. The fluidic system is capable of mixing and dispensing three different

reagents for incubation with the sample before delivery to the flow cytometer. The control system utilizes LabView for instrument operation, for acquisition and data storage, and to automatically call positive samples. A direct-labeling immunoassay for B.g. was developed for the MicroCyt flow cytometer, and this assay was demonstrated for dilutions of B.g. spores in buffer, and spores in aerosol collector fluid. Figure 1 shows the completed APDS-I.

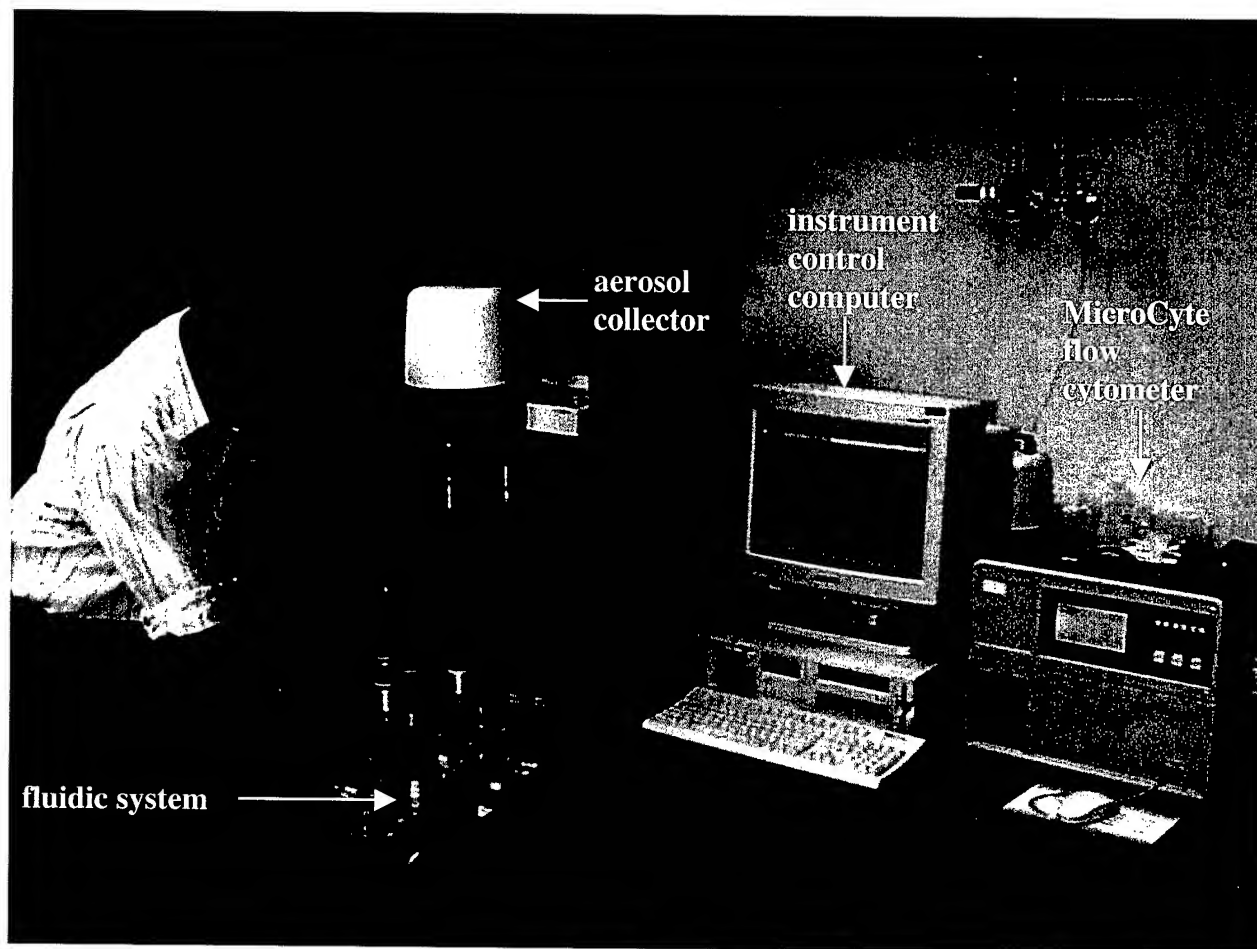


Figure 1: Version 1 Autonomous Pathogen Detection System. Minimal effort was expended to develop an integrated instrument for this proof-of-concept version of the APDS.

The integrated APDS-I instrument was transported to the Pacific Northwest National Laboratory Wind Tunnel Facility to benchmark the overall performance of the system. The APDS-I was challenged with a series of B.g. releases over a wide range of concentrations for a three day period. Highlights of these tests include a 12-hour fully automated run with results reported every 20 min.; successful detection of B.g. down to concentration levels of 50 spores per liter; and system response proportional to the aerosol spore concentration. Figure 2 shows an example of the data obtained from these wind tunnel tests.

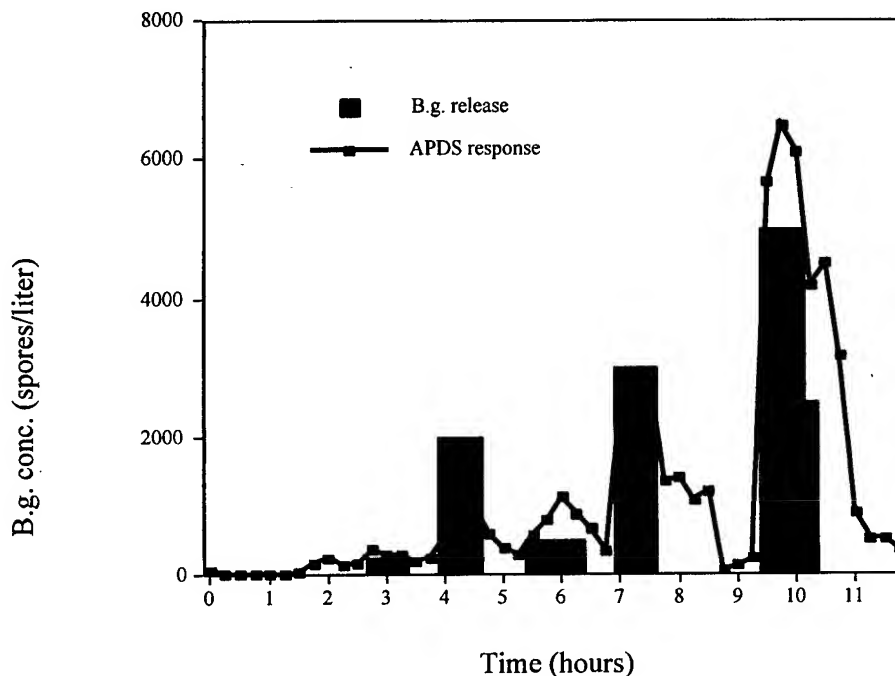


Figure 2: A 12-hour continuous APDS run at the PNNL wind tunnel

EVALUATION OF NEW MODULES FOR APDS-II

We have adopted a modular approach in our development of the APDS-II. Separation of the modules is based on their functionality (i.e., aerosol collector, sample preparation fluidics, nucleic acid assay, and multiplex flow cytometry immunoassay). This approach allows us the flexibility to develop and optimize each module before it is integrated into the final autonomous system. The first objective is to develop and demonstrate an integrated instrument containing an aerosol collector, sample preparation module (fluidics), and multiplex immunoassay. In this approach, the aerosol collected sample is added to a collection of microbeads. Each color of microbead contains a capture assay that is specific for a given bioagent. Fluorescent labels are then added to identify the presence of each agent on the bound bead. Each optically encoded and fluorescently labeled microbead is then individually read in the flow cytometer. Subsequently, in-line nucleic acid recognition (flow-through PCR) will be added to the system.

Aerosol collector

The aerosol collector used in APDS-I was the SASS-2000 cyclone sampler (Smart Air Sampler System, Research International). A custom hybrid sampler has been developed that utilizes an LLNL designed virtual impactor for selectively sampling a given particle size range coupled to a SASS-2000 aerosol collector. The performance of this LLNL/SASS Hybrid was compared with two other collectors, the SASS-2000 alone, and the SCAEP (Space Charged Atomizing Electrostatic Precipitation, Team Technologies) model PM-1B. The industrial standard All Glass Impinger; AGI-30 (Andersen Laboratories) was used as the reference sampler. Side-by-side system performance comparisons conducted in two different field trials at the Harry Reid Center for Environmental Studies, University of Nevada-Las Vegas (UNLV).

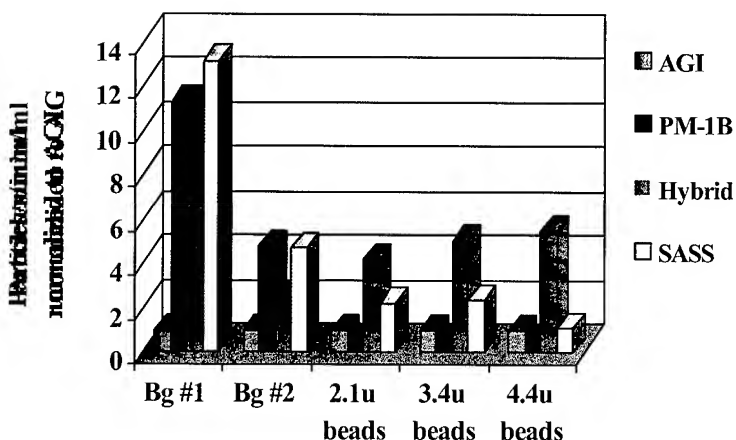


Figure 3: Side by side comparison of aerosol collectors from UNLV field trial

The results indicated that the LLNL/SASS Hybrid has the best overall collection rate for the different samples and particle sizes tested (Figure 3). Custom modifications to the LLNL/SASS Hybrid instrument for optimum adaptation to the APDS-II are nearing completion. Some of the more important upgrades to the LLNL/SASS Hybrid, include, increased air flow, variable particle size selection, smaller packaging, onboard particle counter, ruggedized design, and autonomous Labview-based control system.

Sample preparation (fluidics)

The multiplex immunoassay protocol will be used to determine the sequence of actions performed by the sample preparation module. Since engineering of the sample preparation module and assay development are necessarily parallel efforts, we defined a generalized set of operations for the sample preparation module that is flexible enough to cover virtually any defined protocol. These operations include:

- extracting a portion of the collected sample volume from the aerosol collector
- capturing the sample with antibody-labeled microbeads
- labeling the samples with fluorescent reporter antibodies
- separating, washing, and pre-concentrating microbeads to improve assay performance and prevent cross-contamination between measurements
- flowing the resulting mixture to the flow cytometer for analysis

The approach used in APDS-I was neither flexible nor modular enough to accommodate the added complexity of operations required for APDS-II. Based on experience with our previously developed in-line PCR system and some early bench testing, we adopted a technique advocated by a collaborator (Global FIA, Gig Harbor, WA) using a sequential injection analysis (SIA) platform. The basic components of this platform include: a carrier fluid; a syringe pump; a holding and mixing coil; a multi-port selection valve; reagent/sample storage; and separation cell (Figure 4). The carrier fluid is used to draw and pump fluids sequentially through the various sample ports on the selection valve. Aliquots of air are used to spatially separate the carrier from reagent and sample volumes, greatly minimizing the chance of cross-contamination. The holding/mixing coil serves to mix various assay components (i.e., sample, microbeads, reporter, etc.), to perform incubation (both heated and unheated coils are being tested), and to prevent contamination of the syringe pump. The selection valve serves as the interface between all components of the sample preparation unit, offering a flexible medium for changing and upgrading the various fluidic components. The separation cell is used to separate, wash, and/or preconcentrate the microbeads at various points in the multiplex immunoassay. A fluidics testbed with a simple serial based Labview control system and modified Global SIA hardware has been constructed to develop assay protocols.

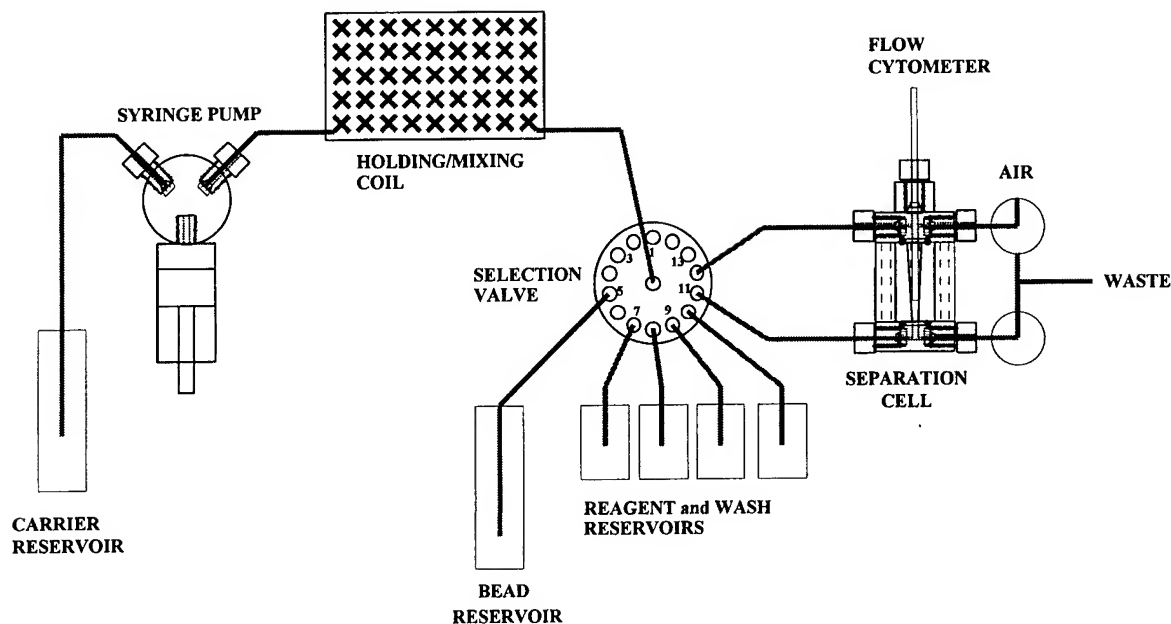


Figure 4: SIA based sample preparation module for APDS-II

Multiplex flow cytometer and immunoassays

A major advancement related to large-scale multiplex immuno-analysis is the recent release of the Luminex, model LX-100 flow cytometer. This instrument has a 100-plex target capability and constitutes the centerpiece of our development effort for incorporating multiplex flow cytometry into the APDS-II system. We have recently obtained samples of all 100 bead sets, and a mixture of all bead sets has been successfully analyzed at LLNL (Figure 5).

The current focus of our assay development is the demonstration of an automated 7-plex detection (four bioagent simulants, three controls) capability. The result shown in Figure 6 is close to achieving that goal. Bead sets were coated with specific antibodies for *Bacillus globigii* (Bg), *Erwinia herbicola* (Eh), bacteriophage (MS2), Ovalbumin (Ov), and selected fluorescent reporter dyes. We also coated two separate bead sets with reagents that provide internal positive and negative controls for each step in the sample preparation process. These controls will provide a continuous monitor of the APDS-II operation even if no target agents are detected.

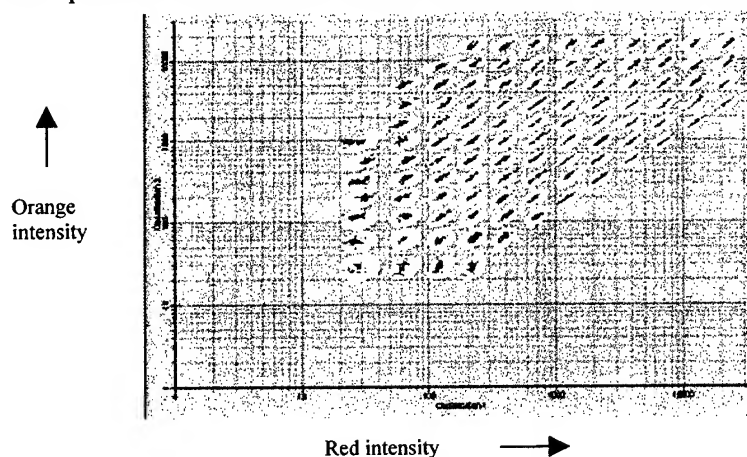


Figure 5: Dot plot of a mixture of 100 bead sets depicting adequate separation of each bead set

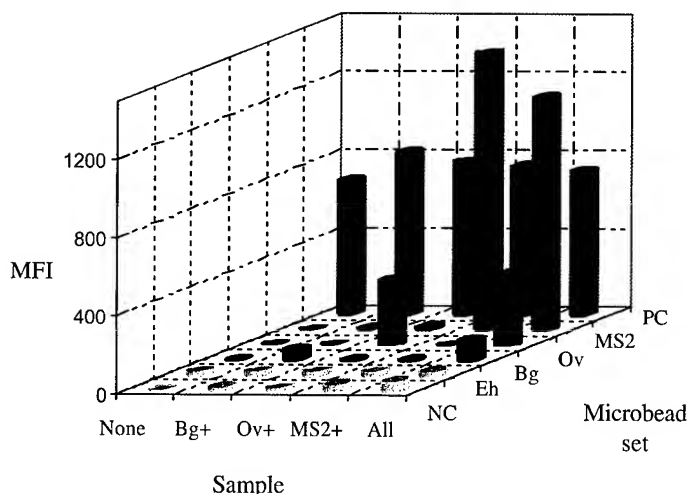


Figure 6: Luminex LX-100 analysis of 4 simulants using a 6-plex assay. Median fluorescent intensities (z-axis) of each microsphere set (y-axis) analyzed from 5 different samples (x-axis)

Flow-Through PCR

Flow-through PCR provides a method for conducting continuous, real-time nucleic acid assays. This technology will add an orthogonal detection technique to the multiplex immunoassay capability, thereby increasing the reliability of a positive identification and providing additional information regarding the origin and characteristics of a detected pathogen. The flow-through PCR system consists of a LLNL-designed, silicon-machined thermocycler mounted in-line with a sequential injection analysis system (Figure 7). The SIA system performs all necessary sample preparation functions (mixing of sample with PCR reagent components, etc.) and delivers the prepared PCR reagent/sample aliquot to the thermocycler unit. The thermocycler is designed with appropriate light sources and detectors to perform real-time TaqMan assays. After completion of the assay, the SIA system decontaminates the thermocycler chamber and all exposed fluid delivery tubes.

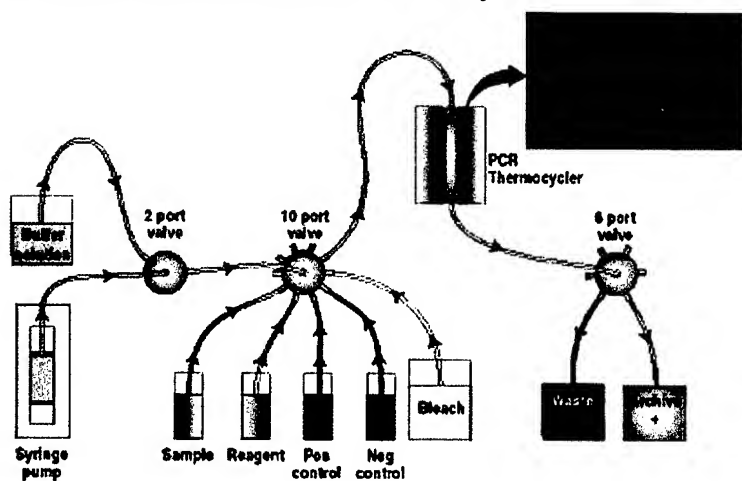


Figure 7: Flow-through PCR system

The flow-through PCR system has undergone extensive characterization during FY00. We successfully demonstrated amplification in 10^6 cfu/ml of several different bacterial species, including *Bacillus globigii* (*B.g.*), *Bacillus thuringiensis* (*B.t.*), and *Erwinia herbicola* (*E.h.*). Amplification with as little as 10 μ l of sample (7 μ l reagent, 3 μ l sample) has been successfully performed. We have also determined that the chamber and sample port can be quickly decontaminated by flushing with small volumes of bleach, making possible repeated cycling of positive and negative controls through the same sample port.

System integration

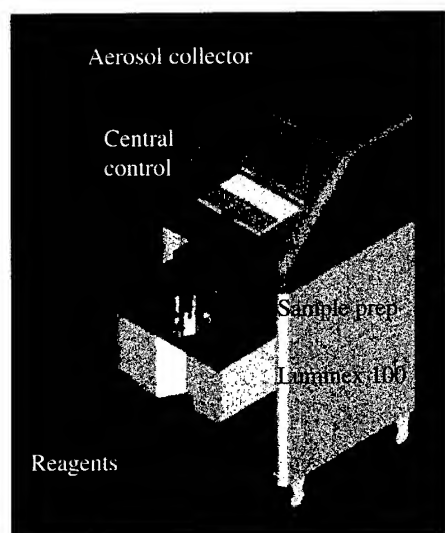


Figure 8: Integrated APDS system

We have completed a preliminary design for packaging and physically connecting the different components of the APDS-II system in a simple, "ATM" style chassis (Figure 8). Concerns such as heat transfer, vibration isolation, fluidic connections, flexibility, and user access are addressed in this design. Space for future modules, such as the in-line nucleic acid assay, has also been allocated in this chassis.

One of the most challenging tasks of the entire APDS development project is the unification of the separate components under a central control system. We chose National Instrument's Labview software as the common programming language for APDS, and have currently written software to control both the aerosol collector and sample preparation module. The largest component, reprogramming the LX100 multiplex flow cytometer in Labview, is currently in progress. The graphical user interface (GUI) is complete and currently undergoing a second round of improvements.

CONCLUSION

The successful field test of APDS-I demonstrated the feasibility of fully automated continuous environmental monitoring for pathogenic organisms. The development of bead-based immunoassays for APDS-II provides the potential for large-scale multiplex analysis that can be easily adapted to new potential threat agents. Finally, incorporation of PCR-based nucleic acid analysis should greatly increase the reliability and specificity of agent identification.

REFERENCES

- Belgrader, P., Benett, W., Bergman, W., Langlois, R., Mariella Jr., R., Milanovich, F., Miles, R., Venkateswaran, K., Long, G., and Nelson, W. (1999). Autonomous System for Pathogen Detection and Identification. SPIE Proceedings 3533, p. 198-206.
- Langlois, R.G., Kato, P., Masquelier, D., and Mariella, R. (1998). Evaluation of Flow Cytometric Methods for the Identification of Microbial Agents. Cytometry 31 (supp.9), p. 55.
- Venkateswaran, K.S., Masquelier, D., Mariella, R.P., and Langlois, R.G. (1998). Development of Flow Cytometric Methods for Simultaneous Detection of Multiple Microbial Agents. Cytometry 31 (supp.9), p. 151.
- Belgrader, P., Benett, W., Bergman, W., Langlois, R., Mariella Jr., R., Milanovich, F., Miles, R., Venkateswaran, K., Long, G., and Nelson, W. (1999). Autonomous System for Pathogen Detection and Identification. SPIE Proceedings 3533, p. 198-206.
- Langlois, R.G., Venkateswaran, K., Mariella Jr., R., and Milanovich, F. (2000). Automated system for Microbial Identification in Aerosols. Cytometry 33 (supp.10), p. 120.

Venkateswaran, K.S., Milanovich, F., and Langlois, R.G. (2000). Novel Method for Multiplex High-Throughput Flow Cytometric Analysis. *Cytometry* 33 (supp.10), p. 40.

ACKNOWLEDGEMENT

This work was performed under the auspices of the U.S. Department of Energy by the University of California, Lawrence Livermore National Laboratory under Contract No. W-7405-Eng-48, with funding from the DOE-CBNP Program.

SHIPBOARD AUTOMATIC CHEMICAL AGENT DETECTOR AND ALARM

Gregory P. Johnson

Naval Surface Warfare Center Dahlgren Division
Chemical and Biological Systems Branch (B53)
Dahlgren, VA 22448

Abstract. The Shipboard Automatic Chemical Agent Detector and Alarm (Ship ACADA) is a portable point detection system capable of identifying and alarming to low levels of chemical agent vapor both interior and exterior to ship spaces with a false alarm rate of near zero. It identifies both nerve (G and V) and blister (H) agents and has the capability to add additional agents to the algorithm to meet future threats. The main advantage of the Ship ACADA is its ability to monitor interior ship spaces in real time and alarm to low levels of chemical agent while ignoring the presence of common shipboard interferences. The system is designed around two ion mobility spectroscopy (IMS) cells. One cell operates in the positive mode with acetone as the reactant ion and the other operates in the negative mode with water as its reactant ion. Americium 241 (100 microcuries/cell) is used to ionize the air before entering the IMS drift region. The Ship ACADA IMS system is different from other typical IMS systems in the following ways:

- 1) elongated IMS cell
- 2) elevated temperature of cell and plumbing
- 3) enhanced desiccant/filter system
- 4) system pressure and flows optimized
- 5) the latest digital signal processors are used

The electronic output of the IMS cells is digitally processed to look for the presence of chemical warfare agent vapors. If agent vapor is detected, a visual display message is sent to the eight digit alphanumeric display on top of the detector and a local audible alarm is sounded. This paper will provide an overview of the design issues, testing performed, and results achieved with the Ship ACADA system.

- Overall Size of System =
0.3 ft³
- 6" x 6" x 15"
- Weight of Detector Unit =
14 lbs
- Weight of Battery Unit = 12
lbs

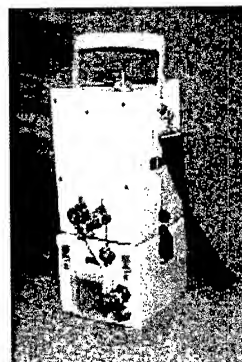


Fig. 1 Ship ACADA

The Navy identified an immediate need in FY99 for a man-portable chemical agent detector to assist post-attack shipboard recovery actions. The detector would require real-time warning in a high

interferent environment. Generally, the physical and performance characteristics for a portable ship survey monitor required that size and weight should be minimized (a maximum of approximately 25 pounds), battery powered, alarm times minimized so that survey personnel would get near real-time warning, common shipboard interferents would not cause false alarms, and it be easy to operate and maintain.

Previous experience with the design and fielding of the IMS technology-based Improved Point (Chemical Agent) Detection System (IPDS) demonstrated the ability to provide chemical agent vapor point detection of the environment surrounding the exterior of ships with a high degree of interferent rejection. IPDS was found to be acceptable for sampling exterior air and alarms to low levels of chemical agent within one minute, and testing indicated that it could possibly be optimized for interior air sampling as well. However, the IPDS detector unit was not designed for portability and could not be easily modified.

A market survey was conducted in late FY99 to see if there were detectors already available which met the requirements. No detectors, including the Army-led ACADA, were found to be acceptable for use onboard Navy ships due to false alarms from many common shipboard chemicals (e.g., aqueous film forming foam, paint, and floor wax) or electromagnetic interference. Also, in this time period, the Joint Chemical Agent Detector (JCAD) program was started with a planned fielding date for FY03. JCAD's requirements satisfy the ship survey mission, but was still at least three years away from fielding.

Since the Navy had previous success with the IPDS and some work on miniaturizing IPDS was ongoing, the Ship ACADA program was then initiated as a fast turnaround interim solution using the basic IPDS IMS cell design. The cells were long enough to provide good peak resolution. The cells were heated to elevated temperature (180F) to operate above high environmental temperatures and to aid in sample clear-down. The desiccant/filter system was designed with sufficient capacity to ensure continuous use over several weeks, if necessary. System pressures and air flows were designed to quickly introduce a sample and clear it out. The detection algorithm structure was simple enough to allow easy and rapid modification based on new signature data. New requirements not specified by the IPDS included designing a rechargeable battery system, and reducing the size of the electronics, enclosure, and plumbing. The detection software algorithm would have to be optimized to further reduce false alarms due to interferents from the ship's interior spaces. The schedule and design risks were reduced by modifying the IPDS IMS cell design and keeping the design and test efforts in-house.

Now that the requirements of Ship ACADA were laid out, the next step was to decide what design parameters could be optimized to yield the desired characteristics. A unique enclosure was designed to contain the system and ensure adequate environmental performance. A rechargeable battery assembly was designed with sufficient capability to heat cells to high temperature for several hours. The operator controls, visual display and audible alarm were designed for ease of use.

The problem most critical to the ship interior problem was detection of the agents of interest while retaining the interferent rejection capability. Some factors which were optimized to achieve the necessary IMS cell sensitivity include cell temperature, air flows, IMS peak thresholds and time windows, and membrane thickness. Initially, the parameters were set to the original IPDS parameters, and through significant testing and data collection, these parameters were set for this application.

A single prototype of the Ship ACADA was built using a power supply until the battery enclosure

was designed and built. Testing consisted of data collection and post-analysis to determine if the IMS cells were sensitive enough or the design parameters needed to be experimented with to increase sensitivity. Data collection consisted of agent testing at low and high concentrations, in-house lab testing of the headspace vapors of available interferents, and shipboard testing.

The next phase of development consisted of the in-house fabrication of 15 detector units for agent, shipboard, and environmental survivability tests. The first few units built were tested on ship in November 1999, and the units worked well with no false alarms reported. These same units were then agent tested in December 1999 and performed well for most agents and concentrations, but they did not detect the lowest required concentration of 0.1 mg/m³ of nerve agent. Analysis of the signatures indicated that only monomer peaks were produced where as dimer peaks were expected per the earlier testing which the detection algorithm exploited. The final detection software algorithm then consisted of the Dec 99 version with modifications to detect GD and GF using only monomer peaks. This could be a potential issue if there were a significant number of interferents not sampled during testing. However, since the list of interferents tested was rather extensive, there should not be many unknown interferents, and so there is only a limited risk of false alarm. In April 2000, the Ship ACADA design configuration was finalized with the optimization of three physical design parameters – (1) lowering the cell temperature to 160 F, (2) reducing the recirculating air flow, and (3) using the 0.5 mil-thick membranes. Additional shipboard and agent testing was conducted to confirm proper operation prior to going forward with a request for production approval.

A Low Rate Production Decision was made by the Navy in June 2000, and a production contract was awarded in August 2000. The rationale for acceptance included the fact that this equipment is intended to be an interim system to be used until JCAD is fielded to fill the Navy's need for a portable post-attack monitor.

Examples of typical IMS output signatures are shown in the following figures. In each of these figures, the upper view is of the negative IMS cell output and the lower view is of the positive cell output.

Figure 2 is a typical baseline IMS signature.

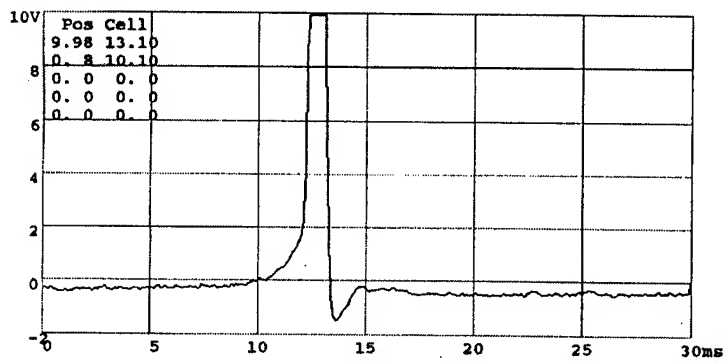
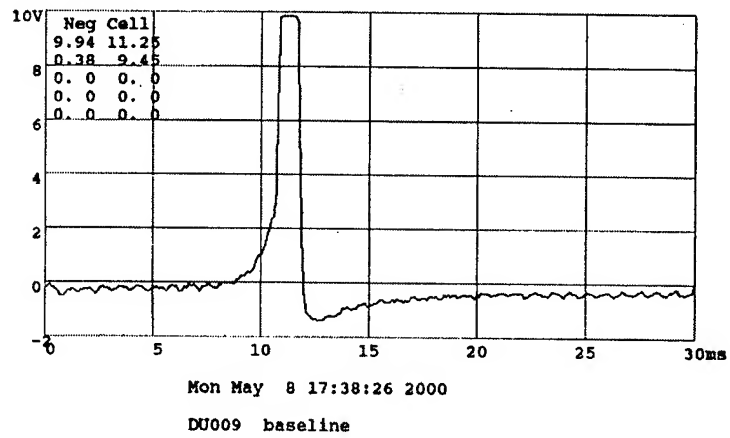


Figure 2. Typical baseline signature from Ship ACADA

Figure 3 shows the typical response to GB. Note that both monomer and dimer peaks are exploited in the detection algorithm.

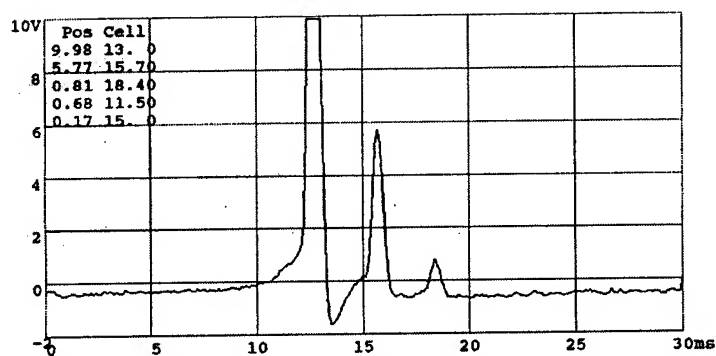
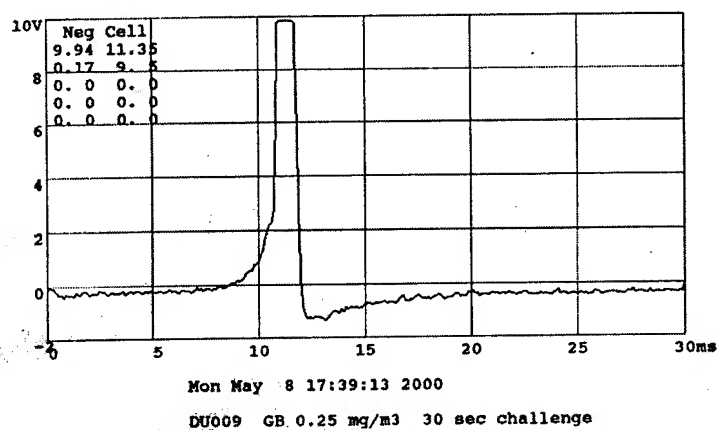


Figure 3. Typical GB signature from Ship ACADA

Figure 4 shows the typical response to aqueous film forming foam (AFFF).

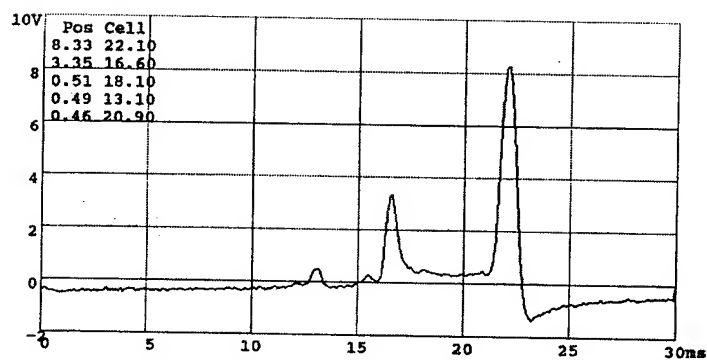
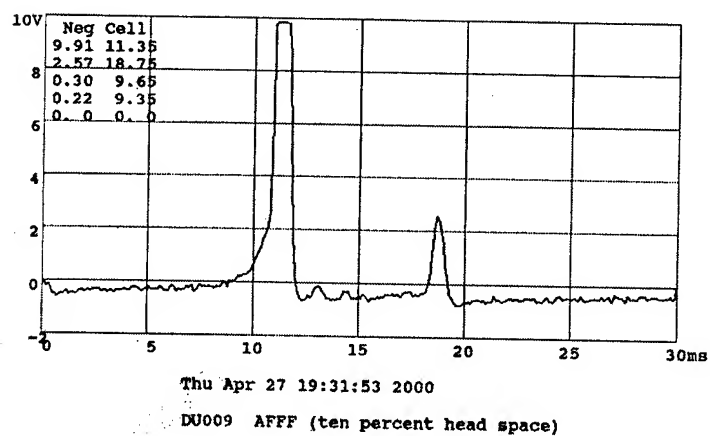


Figure 4. Typical Ship ACADA response to AFFF

CONCLUSIONS

The Ship ACADA system identifies low levels of chemical agent vapor without false alarming to common shipboard interferences. While similar in basic operation to most IMS-based systems, the primary differences that make it acceptable for shipboard use are

- 1) elongated IMS cell,
- 2) elevated temperature of cells,
- 3) enhanced desiccant/filter system,
- 4) optimized system pressure and flows, and
- 5) latest digital signal processors.

The Navy now has an interim portable chemical agent vapor detector with good interferent rejection capability that is adaptable for other uses as needed. The short development time was possible because of the corporate knowledge already in place from the IPDS development program. This capability has enabled the Navy to address an interim shortfall in detection capability.

FORCE PROTECTION FROM BIOLOGICAL AEROSOLS USING A PORTABLE HYPHENATED ANALYTICAL SYSTEM

A. Peter Snyder

U.S. Army Edgewood Chemical Biological Center, Aberdeen Proving Ground, MD 21010-5424

Waleed M. Maswadeh, John A. Parsons, Ashish Tripathi
GEO-CENTERS, INC., Gunpowder Branch, P.O. Box 68,
Aberdeen Proving Ground, MD 21010-0068

Henk L.C. Meuzelaar, Jacek P. Dworzanski, Man-Goo Kim
Center for Micro Analysis and Reaction Chemistry, University of Utah, Salt Lake City, UT 84112

ABSTRACT

A commercially-available, hand-held chemical vapor detector was modified to detect Gram-positive *Bacillus subtilis* var. *globigii* spores (BG) in outdoor field scenarios. A Chemical Agent Monitor (CAM) ion mobility spectrometry (IMS) vapor detector was interfaced to a biological sample processing and transfer introduction system. This was accomplished by quartz tube pyrolysis (Py), and the vapor was transferred by gas chromatography (GC) to the IMS detector. Gram positive spores such as BG contain dipicolinic acid (DPA), and picolinic acid is a pyrolysis product of DPA. Picolinic acid occupies a unique region in the GC/IMS data domain. An aerosol concentrator was interfaced to the Py-GC/IMS instrument, and the system was placed in an open-air, Western United States desert environment. The system was tested with BG spore aerosol releases. A Met-One aerosol particle counter was placed next to the Py-GC/IMS so as to obtain a real-time record of the ambient and bacterial aerosol challenges. In the 21 BG trials, the Py-GC/IMS instrument experienced two true negatives, no false positives, 18 true positives, and the instrument developed a software failure in one trial. A limit of detection was estimated at approximately 3300 BG spore-containing particles.

INTRODUCTION

Recent and current events around the world have highlighted the possibilities for deliberate outdoor dissemination of harmful biological substances, and at least twelve countries are known to have some degree of biological warfare program capabilities. Alleged biological terrorism attacks in Japan and threats on U.S. domestic commercial establishments have increased significantly in the past five years. Reports of alleged localized aerosol releases and hoax domestic biological terrorism in the form of postal mail packages, allegedly with spores of the pathogenic *Bacillus anthracis* and *Yersinia pestis* (bubonic plague) organisms, serve to exacerbate the problem. Desirable goals in order to effectively counter the biological warfare and terrorism applications of harmful biological agents include their ready detection and possible identification in a relatively short period of time. The detection of biological aerosols, particularly that of bacterial cells and spores, is an important component of US military biological

programs. A portion of these programs consists of analytical instrumentation to effect trigger, detection and identification responses for the presence of bacterial aerosols.

The analytical technique of ion mobility spectrometry (IMS) had its inception approximately three decades ago (1, 2). An ion mobility spectrometer can be characterized as an atmospheric pressure-based, time-of-flight system, and it is used as a detector and monitor for vapors. Atmospheric air is ionized by a ^{63}Ni ring through protonation of a neutral water molecule. The proton is transferred to a sample compound which has a higher proton affinity than water. A voltage gate pulses the resulting ions as packets into a drift tube, and the ions are detected by a Faraday plate detector. The drift time between the ion gate and Faraday detector characterizes the ions. Different molecular masses and cross-sections of ions primarily determine the drift time and degree of separation of a mixture of ions. All these phenomena take place at atmospheric pressure. Prototype portable gas chromatography (GC)/IMS concept systems were shown to successfully separate headspace vapors from complex liquid mixtures of analytes. Biological compound information was generated by a quartz tube pyrolysis (Py)-GC/IMS breadboard system under controlled sample introduction of bacterial suspensions. A compact, one-hand portable briefcase Py-GC/ion mobility spectrometer was built in-house. Aerosols were collected and concentrated by a commercially-available, air-to-air aerosol concentrator, and this was interfaced to the quartz tube pyrolysis port of the Py-GC/IMS device. The bacteria were collected on a frit inside the quartz tube and processed by pyrolysis, and a portion of the vapor was transferred through the GC separation stage. The ion mobility spectrometer analysis stage detected the separated components from the GC. Aerosols of Gram positive spores of *Bacillus subtilis* var *globigii* bacteria, which are a nonpathogenic surrogate of *B. anthracis*, were generated in an outdoor Western United States desert test site, and the aerosol concentrator-Py-GC/IMS system was used to interrogate for the presence of the aerosols.

The tandem analytical technique of GC/IMS allowed for the separation of bacterial pyrolysis products in the seconds dimension for GC and milliseconds time frame for the ion mobility spectrometer. Picolinic acid, the compound indicative of the presence of Gram positive spore bacterial aerosols, was effectively separated in a defined window in the GC/IMS data domain from other pyrolysis products. Current results provide evidence for a maturing, stand-alone, Py-GC/IMS biological point detector technology.

EXPERIMENTAL

Figure 1 presents a photograph of the briefcase Py-GC/IMS unit. The major components of the system are as follows: 1, aerosol inlet; 2, pyrex filter aerosol collector in a quartz tube/pyrolysis source; 3, high temperature 3-way GC-injection valve and pump connection to draw aerosol particulate onto the quartz filter; 4, programmable GC column ring; 5, voltage-gated ion source and ion mobility spectrometer components of the airborne vapor monitor (AVM) (Graseby-Dynamics, Watford, Herts, UK); 6, coaxial cable to radio antenna; 7, wireless transceiver; 8, RS232 connection; 9, AC power in; 10, Samsung Sens Pro 500 laptop computer with PCMCIA data acquisition card from National Instruments; 11, coaxial cable for Ethernet/serial PC Card communications; 12, dual diaphragm vacuum pump; 13, electronic hardware and power supplies; 14, 50 pin interface to PCMCIA data acquisition card; 15, molecular sieve packs; 16, 18 x 12.5 x 6 inch heavy duty briefcase.

Aerosol particulate with a diameter in the 2-10 micron range was collected by a four stage, 1000 liter/min XM-2 aerosol collector (SCP Dynamics, Minneapolis, MN 55432). The XM-2 has a 50% and

15% efficiency for aerosol collection of particulate with 5 and 2 micron diameters, respectively (unpublished data). The particulate is drawn out of the fourth stage at 250-300 ml/min and onto the quartz frit inside the quartz pyrolysis tube. The 3-way valve (#3, Figure 1) is switched to a vacuum pump (#12, Figure 1) in order to admit the particulate onto the quartz frit. The particulate was pyrolyzed at 350°C, and the high temperature 3-way valve admitted a one second pulse of pyrolysis products into the GC column. Clean, dry air was used as carrier gas, and molecular sieve packs (#15, Figure 1) were used to scrub the ambient recirculation air. The eluate was ionized by the ^{63}Ni ring at the entrance to the AVM ion mobility spectrometer. Analyte ionization is effected by proton transfer from reagent protonated water molecule clusters. Analytical parameter operation values for the Py-GC/IMS system can be found elsewhere (3). Temperature measurements of the pyrolyzer, 3-way injection valve and GC were monitored by using type K thermocouples connected to in-house constructed control electronic boards. The laptop computer in the Py-GC/IMS system was remotely-controlled from approximately 150 feet using PC ANYWHERE software (Symantec Corp., Cupertino, CA 95014) from a second Samsung Sens Pro 500 laptop computer by way of the Ethernet coaxial cable.

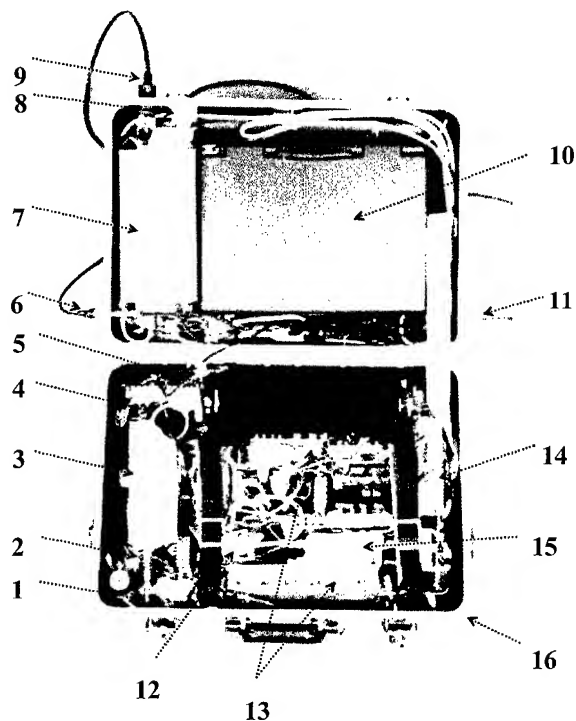


Figure 1. Picture of Py-GC/IMS briefcase unit. Refer to Experimental section for the legend

The events of a typical detection cycle started with the aerosol collection phase, and the duration was between 1-2 minutes. After the aerosol particulate was collected on the quartz frit, the latter was heated

to 120°C in 5 sec, and a subsequent 10 sec drying of the aerosol particulate was administered on the quartz frit. The pyrolysis event then occurred (9 sec) and consisted of 4 sec heating and 5 sec for temperature equilibration inside the pyrolyzer tube. At the time of the initiation of the pyrolysis event, switching of flows occurred which had a 12 sec duration. This included turning off the vacuum which admitted aerosol particulate on the frit, transfer of pyrolyzate to the 3-way injection valve, and the GC injection. The temperature programming of the GC column began at the end of the pyrolysis event, and a portion of the pyrolyzate was injected into the GC column for approximately a 1 sec duration after initiation of the GC temperature programming ramp.

A vehicle-mounted Micronair agricultural sprayer assembly disseminated bioaerosols at approximately 800 m from where the Py-GC/IMS biological detector was placed in the desert. A slurry of dry BG spores in water, stored in a reservoir tank, was drawn through a tube and forced into a spinning wire mesh. The spinning mesh partitioned the liquid slurry into approximately 50 micron droplets, and these droplets were disseminated into the air by a fan. The bacterial particles evaporated water as they traversed the 800 m distance and resulted in particle diameters in the 0.7-10 micron range. Bacterial aerosol particle counts were enumerated by the test personnel, and this was accomplished by interfacing a slit sampler to petri dishes situated on automated revolving disks. This provided an aerosol record for the temporal presence of bacterial particles. The slit sampler provided no discrimination as to the size of the particles which impacted on the petri dishes. Thus, a wide range of particle sizes was directed onto the petri dishes which included the 0.7-10 micron respirable particle size range. The dishes containing trypticase soy agar were incubated at 37°C for 24 hours, and colonies were enumerated for BG. Each bacteria-containing particle which impacted on the agar plate produced a spot or colony-forming unit (CFU) upon growth of the bacteria during incubation. The particle can contain one or more individual bacterial cells, however, only one CFU will be produced. Thus, a graph was constructed which described time vs. CFU per liter of air or analyte-containing particles per liter of air (ACPLA), and the graph was not subjected to a smoothing routine. The interpretation of an ACPLA is based on the volume of a spherical particle of a given diameter and the maximum number of analyte organisms that can fit in the spherical volume. Usually, non-biological organic and inorganic salts and debris/growth media are also contained in a representative aerosol particle generated from a bacterial suspension. Aerosol collectors such as a Met-One device measure total particles per liter of air (PLA), while an agar dish only measures particles containing viable bacteria. Thus, the Met-One aerosol information is usually equal to or higher in particle counts than that of the petri dish method. A Met-One device measures the presence of a particle when the particle intersects a helium-neon laser beam. The amount of scattered laser light determines the size of the particle. The Met-One was programmed to measure particles of 1-10 microns in diameter. The data output was smoothed by a 3-point smoothing routine. This reduced the amount of data to one-third of that of the original data set. The reduced set was then subjected to a standard cubic spline smoothing routine.

During the four week series of aerosol trials, the same GC column was used, and the pyrolysis quartz filters were replaced every 8-10 hours of operation. No significant GC column degradation was noticed (i.e.- no significant shift of analyte retention time), and the same air scrubbing molecular sieve package was used.

RESULTS AND DISCUSSION

The XM-2 aerosol concentrator-Py-GC/IMS system was placed on a table in an outdoor desert site in the Western United States. The aerosol collector/concentrator was turned on prior to a trial and then

turned off after the end of the trial window. A trial window typically encompassed a 20 minute - 1.0 hour timeframe, and a bacterial aerosol was released for a 3-14 minute duration at a selected time within the trial window. This particular time was chosen by the test directors and was not made available to the instrument operators. Thus, the aerosol concentrator/detection system was cycled in a continuous manner during a trial. A successful execution of a bacterial aerosol release from the point of dissemination to the Py-GC/IMS analytical detection device, which spanned approximately 800m, significantly relied on a steady current of wind. The series of trials consisted of 21 BG aerosol releases, and a description and conclusion of one trial and a bacterial standard analysis follow.

BG bacterial standard.

It is known that *Bacillus* spore microorganism species contain dipicolinic acid (DPA) as the calcium dipicolinate chelate at levels of 5%-15% by weight (4). Upon pyrolysis, this compound thermally fragments to picolinic acid and pyridine. Both compounds can be detected by IMS at very low amounts because of their high proton affinity. Aromatic nitrogen compounds are known to possess high proton affinities. In order to determine the signature of the BG material, a "puff" or release of approximately 24 micrograms of BG spores from a hand-held pressurized cylindrical container was directed at the entrance of the aerosol collector/ concentrator. Figure 2 shows a contour plot of the GC/IMS data domain of the pyrolysis of BG where the intensity parameter is the third dimension (out of the page). The discontinuous peak at 4.25 msec is the reactant ion peak (RIP) which consists of protonated water molecule clusters. Proton transfer from water molecules to analyte species effects the sample ionization.

The feature representing a coalescence of a number of rapidly eluting compounds between drift times (t_D) of 4.6-5.25 msec and retention times (t_R) of 1.9-4.9 seconds includes the pyridine compound (5).

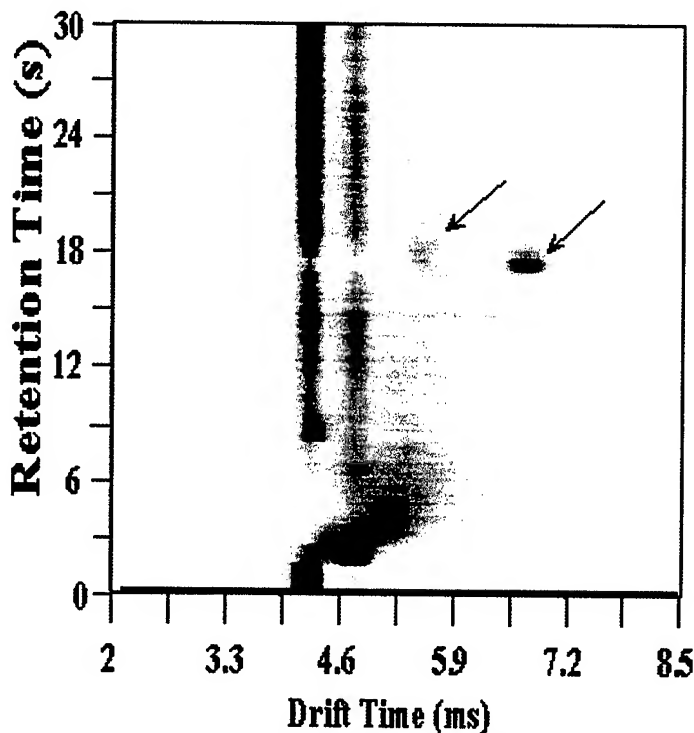


Figure 2. GC/IMS data domain of a standard BG spore aerosol challenge to the XM-2 concentrator Py-GC/IMS system

Picolinic acid can be found as weak monomer and intense dimer peaks at the drift time (t_D , msec), GC retention time (t_R , seconds) values of 5.40, 16.8 and 6.63, 16.8, respectively, in Figure 2 (arrows). A confirmation of the identity of these peaks can be found by comparing the reduced mobility (k_o) terms of the drift time values to established, documented results (5). The reduced mobility is calculated by the following equation:

$$k_o = \frac{P_{obs}}{760} \frac{273}{T_{obs}} \frac{d}{EA}$$

where k_o is reduced mobility in cm^2/Vsec ; t_D , drift time in seconds; P_{obs} , the pressure of the IMS cell in torr (520 torr); T_{obs} , the temperature of the IMS cell in degrees Kelvin (308°K); d is the effective drift cell length in centimeters measured between the ion gate and ion collector grid 3.6 cm); $E=V/d$ where V is the applied voltage (810 V) across the effective drift cell length. Inserting the monomer and dimer drift times (in seconds) into the equation yields picolinic acid monomer and dimer reduced mobility values of 1.80 and 1.46, respectively. The dimer value compares favorably to that of the field-portable prototype Py-GC/IMS system from Table 2 in reference 5 (average of 1.45). The k_o value of the picolinic acid monomer (1.80) differs from the 1.94 average value in reference 5. The 35°C temperature in the present system is considerably lower than that (64°C) used in reference 5. This decrease in temperature can cause a relative increase in clustering of water molecules about the monomer ion, and a larger ion size leads to a higher drift time (i.e.- 5.4 msec) vs. that of reference 5 (i.e.- average of 4.92 msec). Thus, the decrease in k_o in the present investigation is reasonable with respect to that at a higher IMS cell temperature. The GC column was operated at a 60°C temperature, and during an analysis cycle, the column was linearly-programmed from 60°C to 130°C @ 2.0°C/sec. Scrubbed, ambient air was used as carrier gas for all operations. Note that the bacterial pyrolyzate contains relatively few compounds with intense signals. This can be caused by the generation of relatively few compounds with a high proton affinity and/or the production of a majority of pyrolyzate compounds at low concentration. Another possibility is that most polar, high proton affinity compounds condensed on the relatively low temperature surfaces between the pyrolysis source and the ^{63}Ni ionization source/ion gate region of the IMS detector.

Trial 4.

Figure 3 presents a particle count record of Trial 4, and two significant aerosol events are labeled as peaks 1 and 2. The Py-GC/IMS chromatograms in Figure 4 provide information as to the origin of these peaks, and the contour plots provide a successive series of snapshots as to the presence/absence of the BG spore species in discrete time windows of the trial. Cycles 61 (data not shown) and 62 (Figure 4) show no biological activity while cycle 63 (Figure 4) yields an intense picolinic acid dimer signal at a t_D , t_R (msec, sec) of 6.70, 16.5. Cycle 64 shows a lower intensity picolinic acid dimer signal, and both cycles 63 and 64 correlate well in the characterization of the aerosol particle event peak labeled 2 in Figure 3. Cycle 65 shows the absence of biological aerosols. Thus, the disappearance of the picolinic acid signal from cycle 64 to 65 shows the relatively rapid cleardown time of the system. Each cycle in this trial appears as a box below the graph, and the left-hand portion of the box with respect to the tick mark represents the aerosol collection phase of that particular cycle. The right-hand portion of the box represents the pyrolysis processing and GC elution phases. This trial presents a high concentration

challenge of BG spores at 87 PLA. This value is calculated as the difference between the aerosol event maximum and average background level. Note that the Met-One aerosol background is at a level of 100 PLA and is due to the 1-10 micron diameter particles.

Cycle 60 (data not shown) occurred in the timeframe of peak 1 (Figure 3) and provided no evidence of biological presence in the GC/IMS data domain. Therefore, the origin of peak 1 may consist of non-biological aerosols such as inorganic debris and dust generated from the wheels of the moving aerosol dissemination vehicle. The close correlation of the leading edge of peak #2 and the beginning of cycle 63 observed in Figure 3 is coincidental. Likewise, the close correlation of the trailing edge of peak #2 and the beginning of cycle 64 is coincidental. The beginning of cycle 65, which is the first cycle after peak #2 where no biological marker is observed, and the trailing edge of peak #2 are separated by a gap in time which is that of cycle 64. Correlations between an aerosol event and select times in cycles are coincidental, because the timing of the Py-GC/IMS cycles is independent of the motion of the aerosol cloud, including when the cloud arrives and departs the instrument.

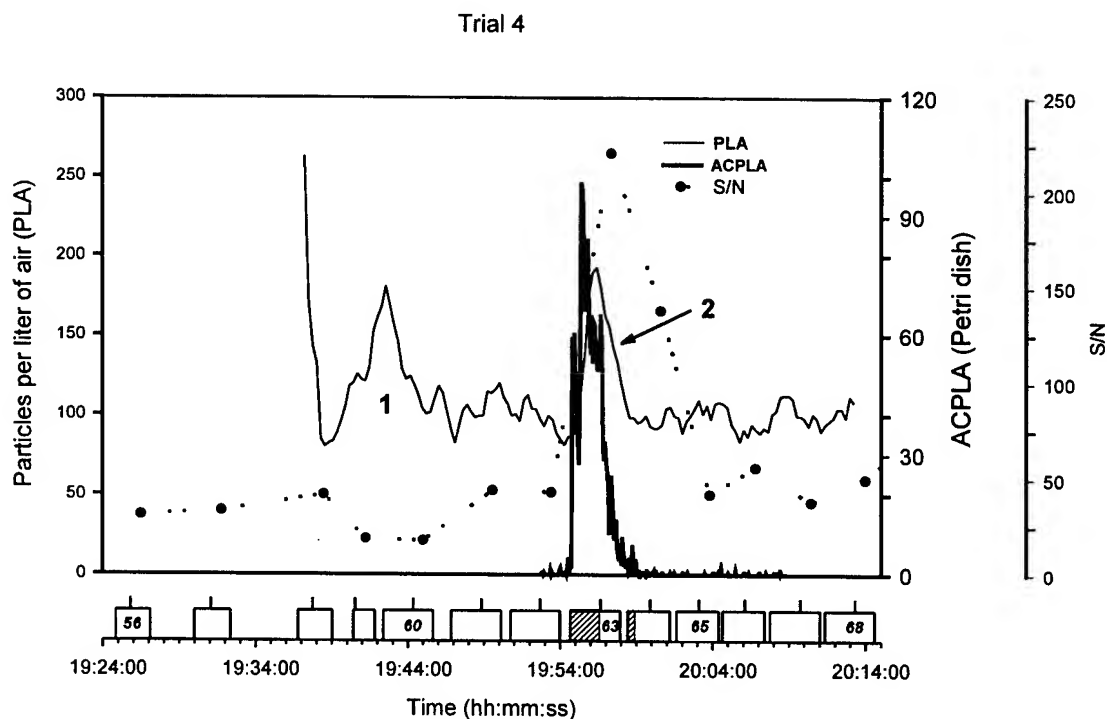


Figure 3. Met-One aerosol (PLA) and ACPLA distributions and temporal disposition of the Py-GC/IMS cycles for Trial 4.

Figure 3 provides the clock time vs PLA graph with a superimposed graph of the ACPLA distribution from the agar plate growth. Note that the ACPLA response, which shows a zero ACPLA baseline signal at the leading and trailing edges, occurs within the same general timeframe as peak #2. The shaded regions in Figure 3 represent the complete aerosol collection phase for cycle 63 and the first portion of the aerosol collection phase for cycle 64. These shaded regions overlap in time with the ACPLA aerosol distribution in Figure 3. The juxtaposition of the XM-2 aerosol collection phase in a cycle and the ACPLA aerosol distribution effects the picolinic acid indicator of biological presence in the respective GC/IMS data window. This observation reduces the degree of importance that is placed on the presence/absence of a biological aerosol event as measured by a particle counter device. Thus, without an ACPLA-cultured biological aerosol determination, the presence/absence of a bacterial aerosol cloud is predicated on the presence/absence of a biomarker signal in the GC/IMS data domain and is an alternative to the presence/absence of an aerosol event in the Met-One aerosol particle count record.

The dotted line graph in Figure 3 is a plot of the average signal intensity (S/N) of picolinic acid from its GC/IMS data window from Figure 4. Note that each point lies above the GC processing phase for each cycle. Since approximately 60 BG ACPLA were contained in the real-time ambient 87 PLA event, 69% of the ambient aerosol consisted of BG spores. Thus at least 30% of the signal in peak #2 is actually composed of non-bacterial, inorganic debris and dust. Approximately 60,000 spore-containing particles were delivered to the pyrolysis processor from the 1000 liter/min XM-2 concentrator during the two minute aerosol collection time in cycle 63 assuming particle diameters of 5 microns.

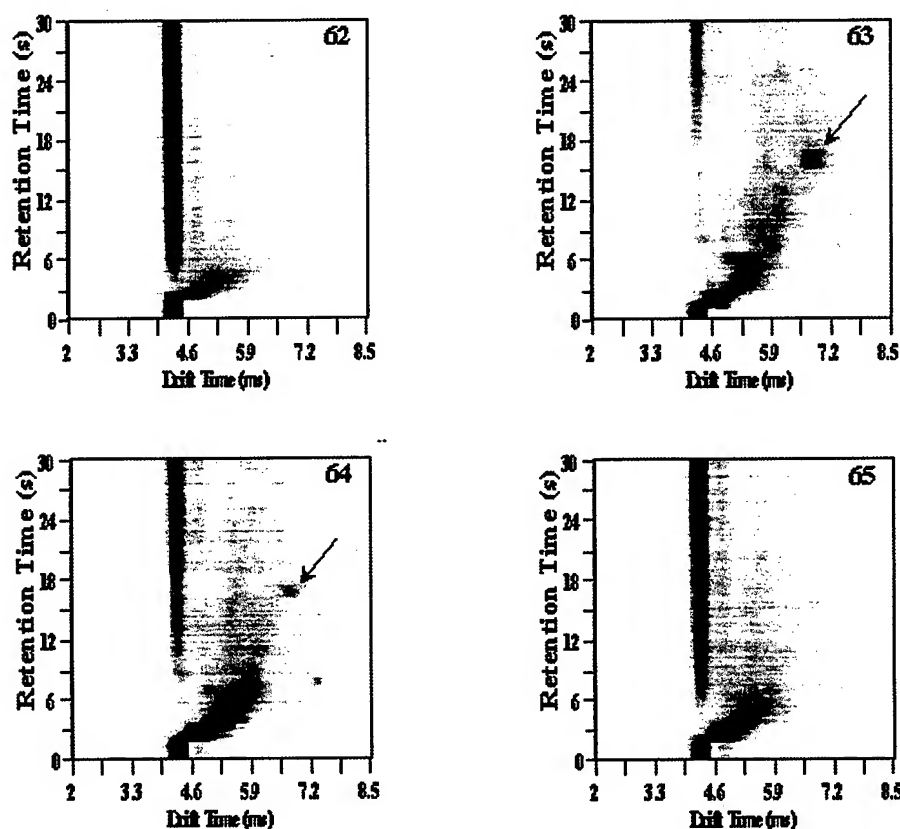


Figure 4. GC/IMS data domains of cycles 62-65 in Trial 4.

Aerosol detection limits

It was discovered that in a comparison between the presence/absence of picolinic acid in its GC/IMS data window and the presence/absence of a BG ACPLA aerosol event, a relative picolinic acid intensity value of 15% of the reactant ion peak (RIP) intensity provided a satisfactory correlation. This means that the presence of a signal in the GC/IMS data window for picolinic acid, when the intensity gain was set at 15% of that of the RIP, indicated the presence of a BG cloud, while no signal inferred the absence of a BG aerosol cloud. From these observations, a limit of detection has been estimated at approximately 3,300 BG spore-containing particles for the current version of the Py-GC/IMS system for particle diameters of 5 microns. This estimate was made in conjunction with three other ambient real-time 5 BG ACPLA (low concentration) aerosol trials (data not shown). The GC/IMS monomer and dimer picolinic acid features provided low intensity, yet relatively consistent signatures from low level biological aerosol challenges. The 3,300 particle estimate is with respect to an aerosol which also contained non-bacterial debris and inorganic dusts. As was presented, a mixture of particles containing bacterial spore and non-spore matter typically characterized the type of aerosol analyzed in the field trials. Trial 1 and 7 provided true negatives, because no picolinic acid peaks were observed in all of the cycles in each trial (data not shown). In addition, aerosol events were not observed in the PLA or ACPLA particle count recordings (data not shown).

CONCLUSIONS

Py-GC/IMS has been portrayed as an analytical technology which can provide a measure of ambient bioaerosol interrogation. The Py-GC/IMS instrument was shown to be a credible complement to an aerosol particle counter. Aerosol particle events in an aerosol record can originate from different types of materials such as biological and non-biological particles. An aerosol event can also consist of a mixture of these different kinds of materials, and different classes of biomaterials also can be present. The current Py-GC/IMS system takes advantage of the sensitive nature of IMS by detecting a substituted amine functional group compound in Gram positive bacterial spores such as the protonated form of picolinic acid. This compound was shown to be a reliable indicator of spore presence in an aerosol cloud containing as low as 5 BG ACPLA. This ambient real-time aerosol challenge yielded an effective 3,300 spore-containing particles at the analytical system's pyrolysis processor with the given aerosol concentrator parameters. The system was shown to be reliable and rugged (with the exception of the pyrolysis filter) over the testing period under outdoor temperatures routinely in the 0-5°C range. The memory effect in the Py-GC/IMS system was relatively low, and the GC column performed in a satisfactory manner despite the constant 60-130°C temperature cycling under scrubbed air carrier gas conditions for a period of three weeks. The trials spanned biological challenges from between 5-140 BG ACPLA. A summary of the four week, 21 BG field trials produced two true negatives, no false positives, and one software failure, and the remaining 18 trials were true positive determinations.

ACKNOWLEDGMENTS

We wish to thank Dr. Douglas Andersen for helpful discussions and information concerning the biological aerosol outdoor trials and Alice I. Vickers and Linda G. Jarvis for the preparation and editing of the manuscript.

REFERENCES

1. F. W. Karasek, "The plasma chromatograph," *Research/Development*, **21**, pp. 34-37, 1970.
2. M. J. Cohen and F. W. Karasek, "Plasma ChromatographyTM – A New Dimension for Gas Chromatography and Mass Spectrometry," *J. Chromatogr. Sci.*, **8**, pp. 330-337, 1970.
3. A.P. Snyder, W. M. Maswadeh, J. A. Parsons, A. Tripathi, H. L. C. Meuzelaar, J. P. Dworzanski and M. G. Kim, "Field Detection of Bacillus Spore Aerosols with Stand-Alone Pyrolysis Gas Chromatography-Ion Mobility Spectrometry," *Field Anal. Chem. Technol.* **3**, pp. 315-326, 1999.
4. G. W. Gould and A. Hurst, Eds., *The Bacterial Spore*, Academic Press, New York, 1969.
5. A. P. Snyder, S. N. Thornton, J. P. Dworzanski and H. L. C. Meuzelaar, "Detection of the Picolinic Acid Biomarker in Bacillus Spores Using a Potentially Field-Portable Pyrolysis-Gas Chromatography-Ion Mobility Spectrometry System," *Field Anal. Chem. Technol.* **1**, pp. 49-58, 1996.

AUTOMATED SAMPLE PROCESSING FOR MASS SPECTROMETRIC IDENTIFICATION OF BIOLOGICAL AGENTS

Thaiya Krishnamurthy,^{1} Remco Swart,² Dennis C. Roser,³
Bruno Laine,² Rabih Jabbour,¹ and Jean-Pierre Salzmänn⁴*

¹, US Army Edgewood Chemical & Biological Center,
Aberdeen Proving Ground (APG), MD 21010-5424, USA

², LCPackings, Baarsjesweg 154, Amsterdam, The Netherlands

³, Geo-Centers, Inc., APG, MD 21010, USA

⁴, LCPackingsUSA, 80 Carolina Street, San Francisco, CA, 94103, USA

ABSTRACT

Direct and rapid mass spectrometric (MS) methods as well as manual processes such as cell lysis, sample clean up and LC separation required prior to the MS analysis were developed for the unambiguous identification of bacterial pathogens. The optimized procedures enabled the simultaneous analysis of cellular pathogens as well as protein toxins present in unknown samples. Since total automation of the entire method is vital for field monitoring, a prototype of a biological sample processing system (BSPS) was designed and fabricated to automate the sample processing and separation procedures. Initial results indicate that the biological samples can be processed automatically and introduced into the ionization source very effectively. Optimization and testing of the processes and hardware are presently underway.

INTRODUCTION

Rapid identification of agents of biological origin (ABO) present in unknown and any suspected sites is very essential for the projection of an oncoming danger as well as decontamination and protection of the exposed personnel and sites.¹⁻² The procedures should be applicable for contaminated samples and completed within 20 minutes in order to initiate protective measures at the onset or soon after the exposure. In order to accomplish this, rugged instrumentation and fully automated analytical and data processing capabilities are required for identification of biological agents in remote areas and battlefield conditions. The ultimate system should function without human intervention for a period of at least 24 hours, which also restricts the amount of consumables and maintenance involved in the process. Since the mass spectrometric analysis and MS data processing have the potential for easier automation, we have opted to concentrate our efforts towards the development of an automated sample processor. This investigation involves the development and testing of manual sample processing method(s) and application of the optimized results towards the fabricating and testing of a totally automated biological sample processing system (BSPS). In addition, the prototype when fully developed should function on-line with any of the commercial or home built ESI-tandem mass spectrometers.

During our earlier extensive investigations, we established that bacterial proteins and other biomarkers were released from intact cells either by vortexing or ultrasonification of bacterial suspensions for less than a minute.³⁻⁶ The protein biomarkers present in the bacterial lysates were selectively detected by specific experimental MS conditions.³⁻⁶ No further sample treatment was necessary prior to the MS analysis and the entire process could be completed within 10-15 minutes.³⁻⁶

Genus, species and strain specific biomarkers were determined from the biomarkers observed for closely related microorganisms.³⁻⁶ We have demonstrated that the protein biomarkers released from the individual bacterium can be applied for the identification of the corresponding microorganism in unknown samples.³⁻⁶ In addition, we also established that the matrix assisted laser desorption ionization (MALDI) and electrospray ionization (ESI) mass spectrometric methods could be successfully applied for the analysis.³⁻⁸ By this approach, the distinction of *B.anthraxis* from its closely related non-pathogenic counterparts such as *B. cereus* and *B.thuringiensis* was accomplished with ease.³⁻⁸ In addition, the individual strains of a specific bacterium could also be differentiated.³⁻⁸ These procedures enabled us to distinguish closely related microorganisms more readily than the procedures based on other biomarkers or their pyrolysis products.⁹⁻¹⁴ Recently, other investigations based on the marker proteins of microorganisms have also been reported.¹⁴⁻²²

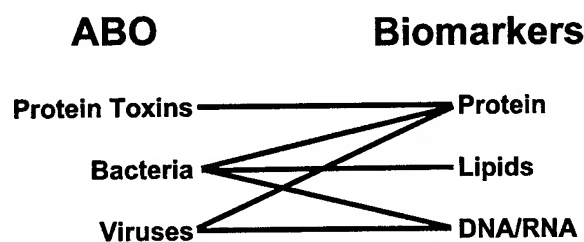


Figure 1. ABOs and biomarkers*

*, Reprinted from R. Long's unpublished work

Similarly, individual viral particles can be identified by the mass spectrometric analysis of the corresponding coat proteins.⁶ The common biomarkers among agents of biological origin (ABO) such as bacteria, viral particles and protein toxins are their corresponding marker proteins (Figure 1). Hence, the methods developed

for more complex bacterial pathogens have been found adequate for the identification of other types of biological agents as well.^{6, 23-25}

In addition, the general mass and tandem mass spectrometric methods and procedures established for structural characterization and detection of natural peptides and proteins, can be effectively applied not only for the identification of natural agents but also for characterization and detection of the modified ones. However, despite the success of this approach, it has one significant limitation. Ionizable impurities such as salts, buffers, growth media and detergents present in the samples pose a severe constraint by restricting the ionization of the samples either substantially or fully. This becomes even more pronounced under the ESI-MS conditions and demands rapid (< 3 minutes) and efficient means to remove the contaminants and concentrate the samples. We have applied a combination of ultrafiltration, reverse phase and ion exchange technologies to overcome this difficulty and simultaneously devised a scheme for the fabrication of a BSPS. We have also constructed a prototype to perform automated sample clean up, proteolytic digestion, separation, and introduction into the mass spectrometer. The optimization of these processes is presently underway. We discuss in this report, an account of our experimental results with respect to method development and the fabrication and operation of the BPS.

RESULTS AND DISCUSSION

Manual Procedures:

Cell Lysis: Intact bacterial cells were suspended in 0.1% trifluoroacetic acid and vortexed or disrupted ultrasonically for 15- 30 seconds.⁴ The lyses of the intact bacterial cells, especially spores, were more dependent on physical disruption conditions than the suspension solvents (aqueous organic acids, TRIS, PBS, water, methanol and acetonitrile).³⁻⁸ Ultrasonic disruption of the cellular suspensions in 20% acetonitrile in acidic/basic buffers were found to release the bacterial proteins most consistently.⁸ The bacterial protein mixture was mixed with sinapinic acid (MALDI matrix) to promote the detection of

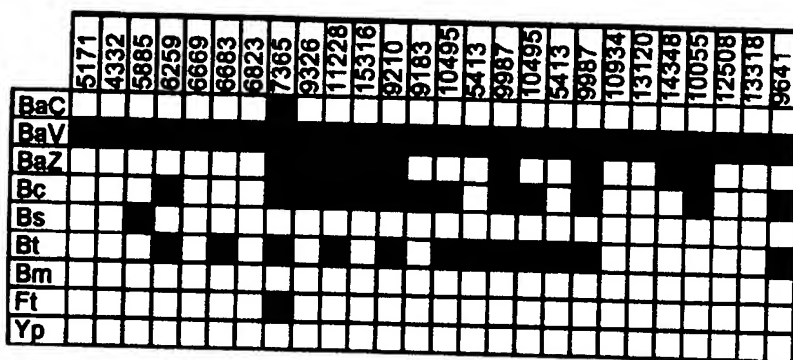


Figure 2. Protein Biomarkers for B.anthraxis, Vollum and other organisms⁸

Bc, *B.cereus*; Bt, *B.thuringiensis*; Bs, *B.subtilis*; Bm, *B.melitensis*; Ft, *F.tularensis*; Yp, *Y.pestis*

chromatography (LC)/MS analysis of the bacterial protein mixtures.^{5,8} The biomarkers assigned for a particular organism is unique enough to be applied for their identification in unknown samples (Figure 2).⁸ Simulants for sporulated bacteria (*B.subtilis*; BG), vegetative bacteria (*E.herbicola*), viral particles (MS2) and protein toxins (ovalbumin) were analyzed by adopting the same procedure during a Joint Services Field Trial held in Dugway Proving Ground, Utah. Mixture analyses were also possible.²³⁻²⁵

Clean up & Concentration: This is the most crucial step in the entire process involving analysis of biological agents. Despite the great potential for the application of developed procedures towards identification of all classes of biological agents and their corresponding simulants, some limitations remain. One limitation is due to the presence of salts, buffers, detergents, and other ionizable environmental contaminants. Another involves the lack of concentration step in the sample preparation phase. More rigorous clean up is required for the recommended technique, LC/ESI-MS, to be pursued. In order to overcome these restrictions, we needed to incorporate sample clean up as well as concentration of the analytes in a single step. It is mandatory that both should be accomplished in less than 3 minutes in a reproducible manner and the concentration capacity should be at least 50 fold. In addition, the method should be applicable in the construction and operation of the automated sample processor (BSPS).

We investigated ultrafiltration and micro-electrodialysis methods for detergent removal and the reverse phase, hydrophilic and ion-exchange adsorbents for clean up and concentration of the analytes.²⁶ Each one of the adsorbents was tested individually and in various combinations, to determine their ability to remove detergents and simultaneously concentrate the ABO proteins. The simulant mixtures containing BG, *E.herbicola*, MS2 (or myoglobin), ovalbumin (or Bovine serum albumin; BSA) or any combinations of these components in TRIS or PBS buffer containing 0.05% Triton-X were used to develop and test the clean up and concentration procedures.

The electrodialysis method was found to be adequate in cleaning up the sample but does not concentrate the analytes. In addition, it takes 20-30 minutes and considerable amount of effort to clean up a sample. Spin and micro columns containing Sephadex G10, 25 and G50 were tested. A considerable amount of detergent removal was observed (Figure 3) and G25 was found to be best suited for the clean up. Even though the process could be completed within 3 minutes, it did not contribute to the concentration of the protein biomarkers. However, in combination with other procedures, it could show great potential for the latter as well.

bacterial proteins.^{3,4}

The biomarkers specific for the genus, species and strains of *Bacillus anthracis*, *Brucella melitensis*, *Francisella tularensis* and *Yersinia pestis* were deduced from the recorded MALDI-mass spectra of numerous strains of these organisms and their counterparts.^{3,4} Similar results were observed during the direct liquid

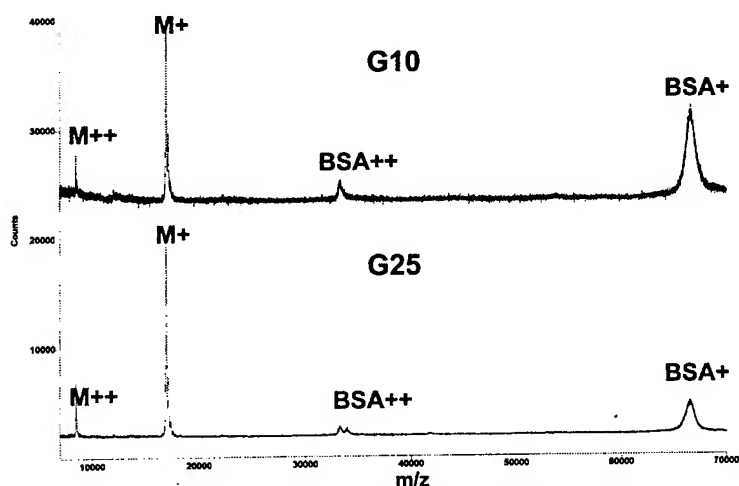


Figure 2. Clean up by ultrafiltration spin columns

M, myoglobin; BSA, bovine serum albumin

with pore size over 500 Å were found to be adequate. Aqueous formic acid solution was better suited, for eluting the analytes, than aqueous acetic or trifluoroacetic acid. Acetonitrile and methanol were found to be equally suited for the elution of the proteins. The samples were processed over G25 spin column and then over microcolumns containing C4 or C8 or mixed (C4 and C8) phase (Figure 4). The observed ratio of the detergent and myoglobin ions was 3:1 when the sample was cleaned over G25/mixed C4 and C8. Similar ratio (5:1) was observed when the samples were cleaned over G25 followed by C4 or C8. In all of these instances the concentration factor was about 50.²⁶

Strong cationic and anionic exchange columns were found to be inadequate and the recovery of the bacterial proteins was poor. Ultrafiltration followed by extraction over stacked weak anionic exchange resin and C8 phase was also examined. Considerable amount of detergent was left behind. Thus far,

ultrafiltration (G25 or G10) followed by either mixed C4 and C8 phase or stacked weak anionic exchange and C8 generated the best results.

Proteolysis: A cartridge (1mm x 15mm) packed with Porozyme trypsin (PerSeptive Biosystems) was conditioned with 50% acetonitrile in water. The sample solution containing *E.herbicola* in TRIS was passed through the conditioned Porozyme column at the rate of 100 ul/min and collected. The effluent was concentrated approximately 10 times. MS analysis of the concentrated sample indicated the absence of protein biomarkers for *E.herbicola* but several peptides indicating the completion of the proteolysis in 5-6 minutes. The

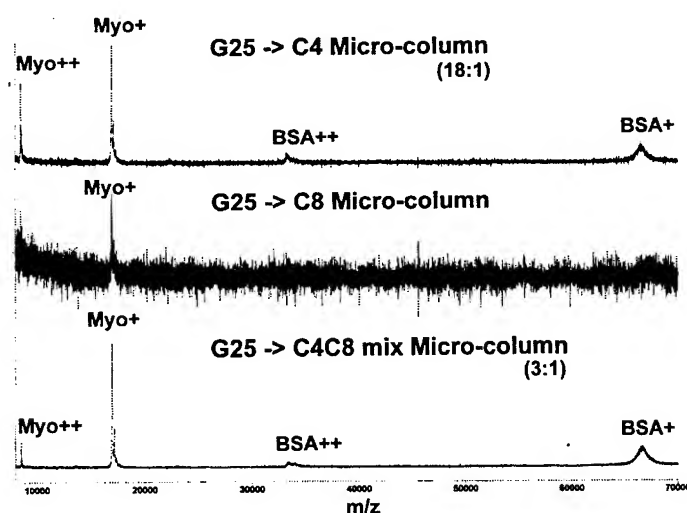


Figure 4. Clean up by subsequent treatment over ultrafiltration spin columns followed by reverse phase micro columns

Porozyme column was rejuvenated by washing with 50% acetonitrile/water. The ESI-MS analysis of the eluted sample indicated the completion of the digestion in 5-6 minutes.

Automation:

A scheme for the prototype of the BSPS was devised, based on our experimental results, to perform on-line cell lysis, filtration of the cellular debris, detergent removal, proteolysis, desalting and concentration, Nano-LC separation and introduction into the mass spectrometer (Figure 5). Duplicate

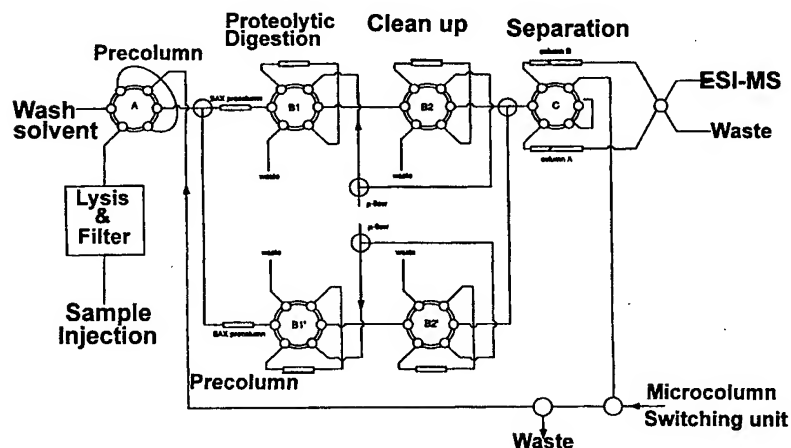


Figure 5. Schematics for biological sample processing system (BSPS)

sets of devices to perform these functions were incorporated for continuous sample processing and subsequent cleaning of the devices to avoid carry over between the analyses. Various components available in commercial (LCPackings) instrumentation (Famos, Switchos, and Ultimate) along with some new components were incorporated in the prototype (Figure 6). A ten port valve is used to connect the ion-exchange (detergent removal) and the Porozyme cartridges (proteolytic digestion) with on-line with a C8

trap column (for salt removal & concentration) and a nano separation column through a six port valve. All the following operations were conducted automatically by programming various operation and experimental parameters. A crude solution (100 μ l – 1 ml) containing a protein standard (Cytochrome C or BSA) or a bacterial sample in 0.05% Triton-X either in TRIS or PBS buffer was injected using 1 ml syringe at a rate 100 μ l/min. The sample was passed through a clean up column (0.5 x 15 mm) containing mixture of anionic and cationic exchange resins (monoS/monoQ) at an optimized rate of 100 μ l/min to remove the non-ionic detergent from the sample. The proteins were trapped in the column and the effluent containing contaminants was pumped into the waste. The column was washed and the proteins were eluted with 95% 25mM ammonium bicarbonate and 5% acetonitrile with 0.5M sodium chloride. The protein solution was pumped through the

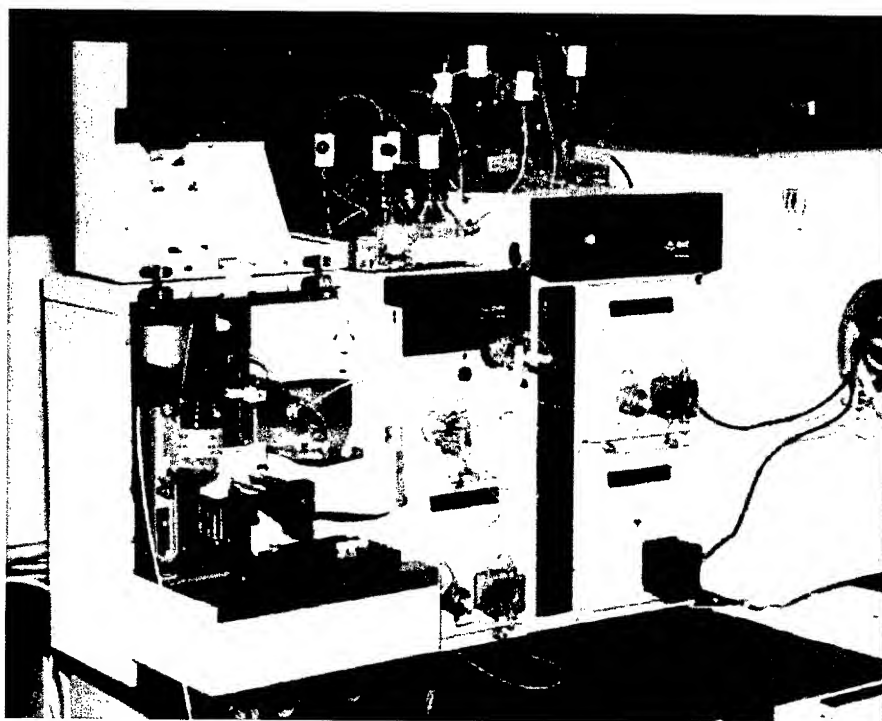


Figure 6. BSPS components

Porozyme column, maintained at 37°C, at a rate of 10 μ l/min. The digested protein solutions containing the peptides were pumped over a C8 (300 μ m x 5 mm; 5 μ m) cartridge to remove the salts. The column was washed with 5% acetonitrile in 0.1% aqueous formic acid and switched on-line with the nano C18 (75 μ m x 15 cm; 3 μ m) analytical column. Peptides were eluted with a gradient of 2-80% acetonitrile in 0.1% formic acid at a rate of 0.2 μ l/min. The effluents were sent through an UV detector and into the nanospray ionization source for subsequent analysis by mass spectrometry and tandem mass spectrometry (Figure 7 and 8). The former data provides the molecular masses of the peptides and proteins while the latter provides the information on the amino acid sequences of the peptides resulting from the proteolytic digestion of any protein including bacterial proteins. Alternatively, the cleaned up solution from the ion-exchange column can be directly pumped into the C8 cartridge for further clean up and concentration followed by the nano-LC separation and MS analysis of intact proteins.

Even though the initial scheme, fabrication of the hardware, and the operation of the prototype have been found to be adequate, the adsorbents used in the clean up and concentration phases still need to be modified and tested. The complete removal of non-ionic detergents during repeated experiments has not yet been established unambiguously. A column containing a mixture of C4 and C8 reverse phase adsorbents was found to clean up, trap and concentrate better during the manual procedure. This needs to be substituted in the trap. In addition, the Sephadex G25 ultrafiltration sorbent may have to be substituted instead of ion exchange resin for better results by avoiding the presence of sodium chloride in the elution solvent. The sodium chloride used for the elution of the trapped proteins from the ion exchange column generates difficulties during the MS analysis due to ionization suppression as well as formation of sodium adducts.

Reduction and alkylation of the proteins prior to on-line proteolytic cleavage generated better results. The results from on-line digestion was similar to the one observed during the off-line digestion procedures (Figure 9). However, consistent but limited degree of proteolysis was observed even without

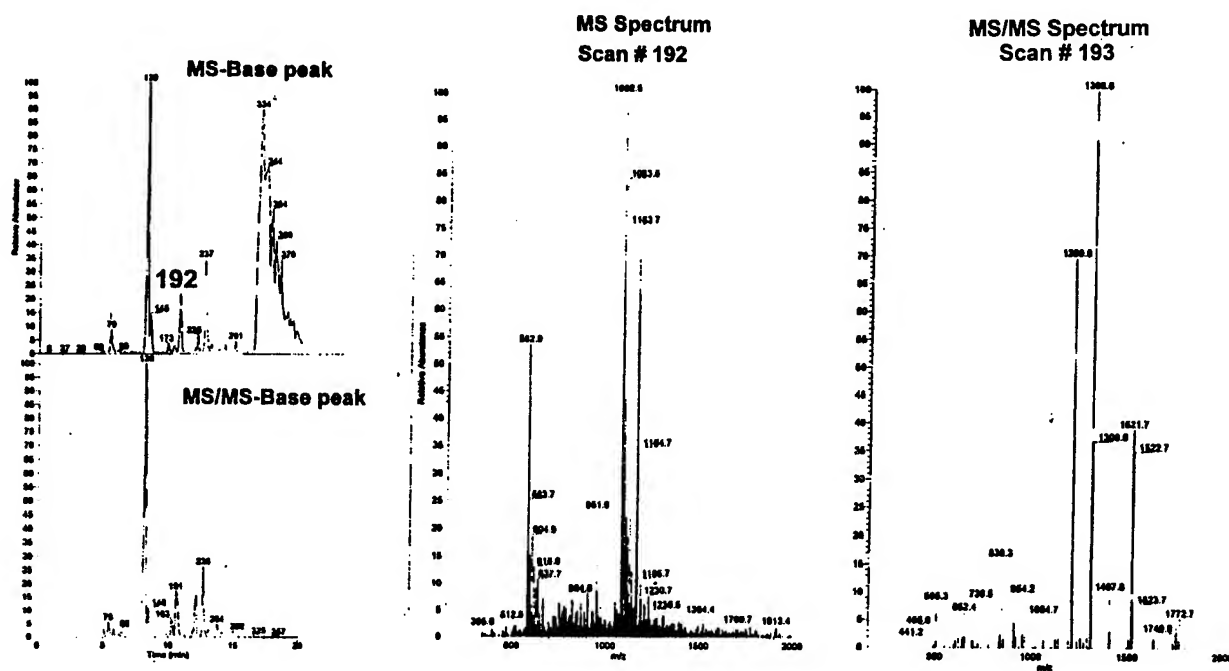


Figure 7. Subsequent electrospray-MS and MS/MS analysis of crude sample processed by BSPS

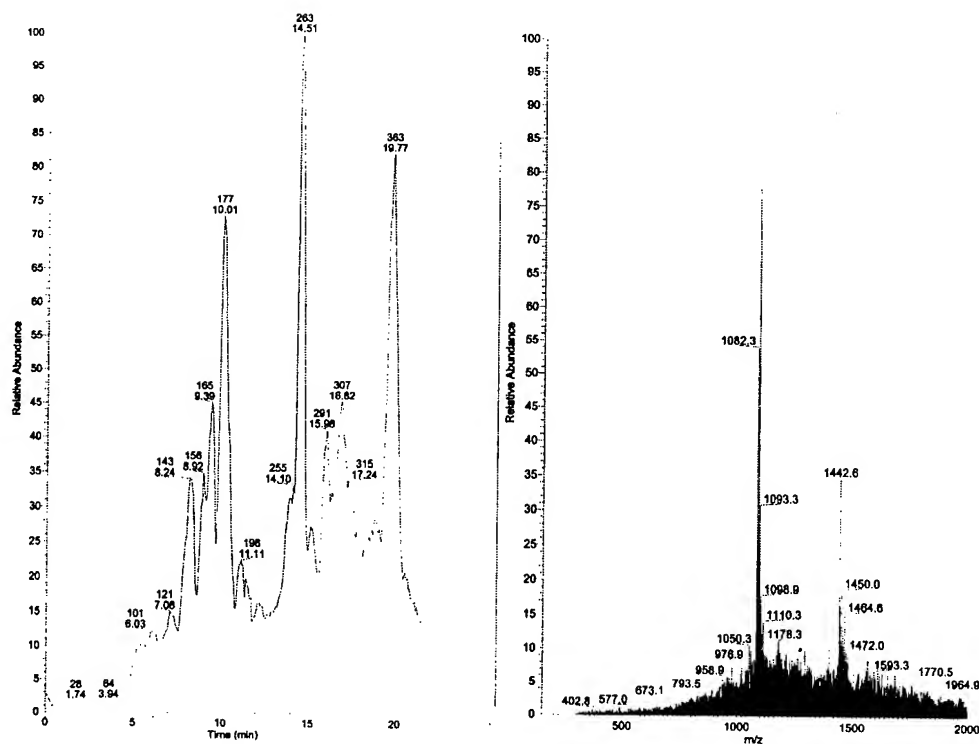


Figure 8. Sample processing (BSPS) and ESI-MS analysis of a crude B.anthraxis sample

Only slight variations were found when the temperature was raised from 37°C to 45°C and 55°C. Similarly, the resident time of a protein in the column also contributes to the digestion factor. The faster

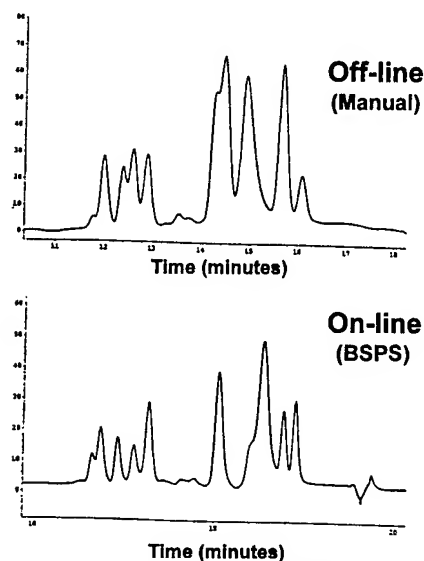


Figure 9. on-line Vs Off-line proteolytic cleavages of BSA

the flow rate is, the shorter the resident time is. The flow rate should be selected in order to maintain the resident time of protein(s) to be close to at least one minute. The effect of sodium chloride used for the elution of the bacterial proteins out of the ion-exchange (detergent removal) column, also was investigated. The clean up, proteolytic digestion, trapping and releasing and separation of the peptides were performed in the presence as well as absence of sodium chloride. The effect due to addition of salt to the system had no significant effect on the proteolytic digestion. The same peptides were observed in slightly lesser abundance in the presence of salts. (Figure10).

The adsorption and desorption of peptides and proteins from reverse phase cartridges have been well established. Even though in our automated experiments the C8 cartridges were used in the trap column, we will be substituting it to a mixture of C4 and C8 based on our manual experimental results. The flow rate was maintained at 4 ul/min. The nano separation columns (75 um ID x 15 cm), C18 for peptides and C8 for proteins, were found to be adequate and the solvents were passed through the

the reduction and derivatization of the intact proteins. Recovery of hydrophobic peptides, which have poor elution capacity, was improved by adding 5% acetonitrile to the loading solvent and the column was regenerated by increasing the organic phase to at least 60%. Experiments were conducted by varying the digestion temperatures.

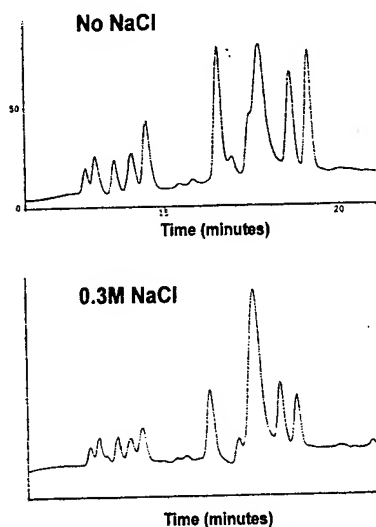


Figure 10. Effect of salt on the on-line proteolytic cleavages

based on our manual sample processing protocols, for the biological sample processing system (BSPS) is completed. At present, the prototype has the capability to perform on-line sample clean up, concentration, separation and introduction into the MS system. The operation of the individual components of the prototype was successful. Construction of a compact system (~2 cu.ft) containing all of the components is quite possible.

analytical column at a rate of 200 nl (0.2 ul)/min. Even though the BSPS hardware has been demonstrated to be adequate, optimization of the detergent removal process is still being pursued. Cartridges with different combinations of adsorbents are presently being prepared for further testing. In addition, efforts to include an on-line cell disruptor are also being pursued. A modified compact BSPS (Figure 11) is being fabricated at present. The BSPS along with the Nanospray Ion Trap Tandem Mass Spectrometer is scheduled to participate in the upcoming Joint Services Laboratory Trial.

Conclusions

Development of procedures for the manual sample preparation, MS analysis, and identification of agents of biological origin are completed. However, methods for the removal of non-ionic detergent from the crude sample need to be optimized. The fabrication of the prototype,

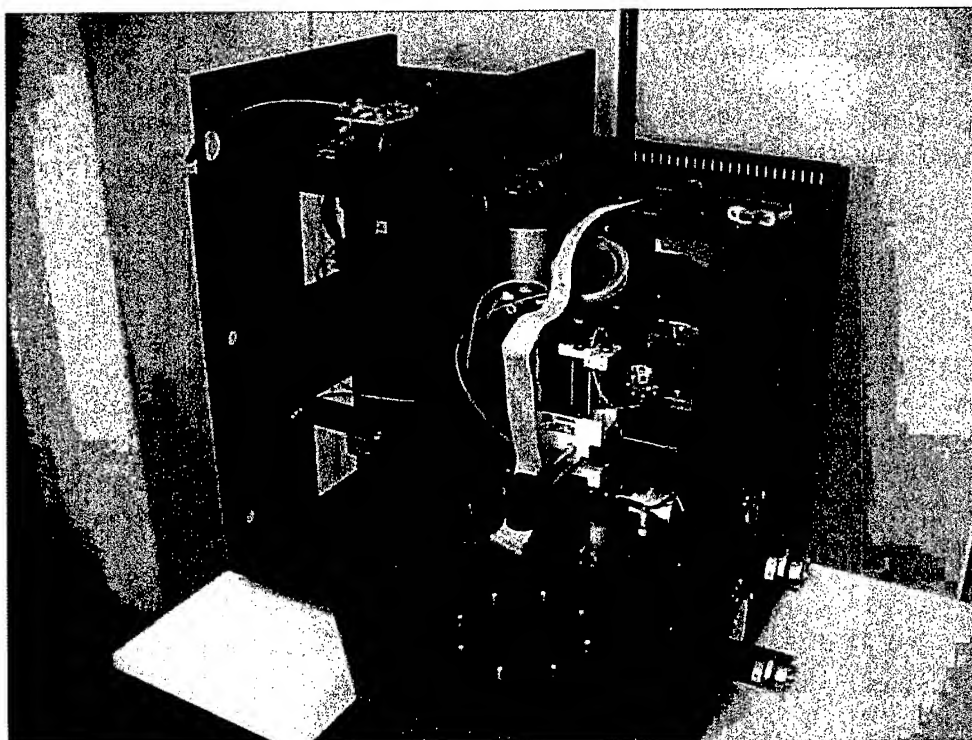


Figure 11. BSPS prototype under fabrication

ACKNOWLEDGMENTS

The authors gratefully acknowledge Dr. Asha Oroskar, Orachem, West Mont, IL, USA for supplying the packed mini clean up columns.

REFERENCES

1. Mass Spectrometry for the Characterization of Microorganisms, Fenselau, C., (Ed.), ACS Symposium Series, Volume 541, Washington, DC, 1994.
2. Tournabene, T. G., CBIAC Internal Report on the Development of Biochemical Data Base for the Bacterial Pathogens, prepared for U.S. Army Edgewood RD&E Center, Aberdeen Proving Ground, MD 1995.
3. Krishnamurthy, T., Ross, P. L., and Rajamani, U., Detection of pathogenic and non-pathogenic bacteria by matrix assisted laser desorption/ionization time-of-flight mass spectrometry, *Rapid Commun. Mass Spectrom.*, 10, 883-888, 1996.
4. Krishnamurthy, T., and Ross, P. L., Rapid identification of bacteria by direct matrix assisted laser desorption/ionization mass spectrometric analysis of whole cells, *Rapid Commun. Mass Spectrom.*, 10: 1992-1996, 1996.
5. Krishnamurthy, T., Eng, J., Yates, J., Davis, M., Lee, T. D., Rajamani, U., Wang, S., Heroux, K., Aabshire, T., Ezzell, J., Henchal, E., Bacterial Identification by Mass Spectrometry, Proceedings of the First Joint Services Workshop on Biological Mass Spectrometry, Baltimore, MD, 31-36, and 133-137, 1997.
6. Krishnamurthy, T., et al., Mass Spectral Investigations on Microorganisms, *J. Toxicology – Toxin Reviews*, 19: 95-117, 2000.
7. Krishnamurthy, T., Eng, J., Yates, J., and Rajamani, U., Field Detection of Bacterial Pathogens, Proceedings of the 45th ASMS Conference on Mass Spectrometry and Allied Fields, Palm Springs, p. 60, 1997.
8. Krishnamurthy, T., Davis, M., Stahl, D.C., and Lee, T. D., Liquid Chromatography/Microspray Mass Spectrometry for Bacterial Investigations, *Rapid Comm. Mass Spectrom.*, 13, 39-49, 1999.
9. Black, G. E., Fox, A., Fox, K., Snyder, A. P., and Smith, P. B. W., Electrospray Tandem Mass Spectrometry for Analysis of Native Muramic Acid in Whole Bacterial Cell Hydrolysates, *Anal. Chem.*, 66: 4171-4176, 1994.
10. Cole, M. J., and Enke, C.G., Direct determination of phospholipid structure in microorganisms by fast atom bombardment - triple quadrupole mass spectrometry, *Anal. Chem.*, 63: 1032-1038, 1991.

11. Wunschel, D. S., Fox, K. F., Fox, A., Bruce, J. E., Muddiman, D. C., and R. D. Smith, Analysis of double-stranded polymerase chain reaction products from the *Bacillus cereus* group by electrospray ionization Fourier transform ion cyclotron resonance mass spectrometry, *Rapid Commun. Mass Spectrom.*, 10: 29-35, 1996.
12. Hurst, G. B., Doktycz, M. J., Vass, A. A., and Buchanan, M. V., Detection of bacterial DNA polymerase chain reaction products by matrix assisted laser desorption/ionization mass spectrometry, *Rapid Commun. Mass Spectrom.*, 10: 377-382, 1996.
13. Meuzelaar, H. L. C., Kistemaker, P. G., Eshius, W., and Engel, H. W. B., Progress in Automated and Computerized Characterization of Microorganisms by Pyrolysis Mass Spectrometry, In: *Rapid Methods and Automation in Microbiology*, Newsom, S.W.B., Johnston, and H. H., Eds., p. 225-230, 1976.
14. Snyder, A. P., McClennen, W. H., Dworzanski, J. P., and Meuzelar, H. L. C., Characterization of underivatized lipid biomarkers from microorganisms with pyrolysis short-column gas chromatography/ion trap mass spectrometry, *Anal. Chem.*, 62: 2565, 1990.
15. Liang, X., Zheng, K., Qian, M.G., and Lubman, D. M., Determination of bacterial protein profiles by matrix assisted laser desorption mass spectrometry with high performance liquid chromatography, *Rapid Commun. Mass Spectrom.*, 10, 1219-1226, 1996.
16. Holland, R. D., Wilkes, J. G., Sutherland, J. B., Persons, C.C., Voorhees, K. J., and Lay, J. O. Jr., Rapid identification of intact whole bacteria based on spectral patterns using matrix assisted laser desorption ionization with time-of-flight mass spectrometry, *Rapid Commun. Mass Spectrom.*, 10: 1227-1232, 1996.
17. Claydon, M. A., Davey, S. N., Edwards-Jones, V., and Gordon, D. B., *Nature Biotechnol.*, The rapid identification of intact microorganisms using mass spectrometry, 14: 1584-1586, 1996.
18. Chong, B. E., Wall, D. B., Lubman, D. M., and Flynn, S. J., Rapid profiling of *E.coli* proteins up to 500 kDa from whole cell lysates using matrix assisted laser desorption ionization time-of-flight mass spectrometry, *Rapid Commun. Mass Spectrom.*, 11: 1900-1908, 1997.
19. Wang, Z., Russon, L., Li, L., Roser, D. C., and Long, S. R., Investigation of spectral reproducibility in direct analysis of bacteria proteins by matrix assisted laser desorption ionization time-of-flight mass spectrometry, *Rapid Commun. Mass Spectrom.*, 12: 456, 1998.
20. Li, K. W., Geraerts, W. P. M., Neuropeptide expression patterns as determined by matrix-assisted laser desorption ionization mass spectrometry, in *Methods in Molecular Biology*, Vol. 72: *Neurotransmitter Methods*, Rayne, R. C., (Ed), Humana Press, Inc., Totowa, NJ, p. 219-223, 1996.
21. Dai, Y., Li, L., Roser, D.C., and Long, S.R., Detection and Identification of Low-mass Peptides and Proteins from Solvent Suspensions of *Escherichia coli* by High Performance Liquid Chromatography Fractionation and Matrix-assisted Laser Desorption/Ionization Mass Spectrometry, *Rapid Communications in Mass Spectrometry*, 13: 73-78, 1999.

22. Demirev, P.A., Ho, Y., Ryzhov, V., and Fenselau, C., Microorganism identification by Mass Spectrometry and Protein Database Searches, *Anal. Chem.*, 71: 2732, 1999.
23. Davis, M. T., Stahl, D. C., Lee, T. D., and Krishnamurthy, Novel Microspray Methods for Rapid Biodetection by Mass Spectrometry, *Proceedings of the First Joint Services Workshop on Biological Mass Spectrometry*, Baltimore, MD, p. 133-137, 1997.
24. Krishnamurthy, Rajamani, U., and Wang, S., Unpublished results
25. Krishnamurthy, T., and Jabbour, R., Improved Procedures for Clean up & Concentration of Bacterial Samples, *Proceedings of the Annual Conference on Mass Spectrometry and Allied Fields* (1999).
26. Krishnamurthy, T., and Jabbour, R., Unpublished results.

THE USE OF ION-ION CHEMISTRY IN AN ELECTROSPRAY ION TRAP MASS SPECTROMETER FOR THE DETECTION AND IDENTIFICATION OF BIOLOGICAL THREATS

James L. Stephenson and *Stephen A. Lammert*
M/S 6365; Bldg 5510
P.O. Box 2008
Oak Ridge National Laboratory
Oak Ridge, TN 37831-6365

Abstract

The advantages of using a custom-built electrospray ion trap mass spectrometer for the analysis of toxins, viruses, bacteria, and other organisms related to biological warfare agents are discussed. The enabling feature of this instrument is the use of ion-ion reactions within the ion trap to reduce the complexity of overlapping charge states resulting from the electrospray analysis of complex mixtures. The use of ion-ion chemistry allows the reduction or elimination of many, time consuming sample processing and separation steps often required for analysis by electrospray mass spectrometry.

Introduction

Mass spectrometry has been employed by the US Army as a detector for chemical and biological warfare agents for many years now. Recently, the US Army Soldier Biological and Chemical Command (SBCCOM) has funded the development of a second-generation ion trap mass spectrometer called the Block II Chemical and Biological Mass Spectrometer¹ (or Block II CBMS) at Oak Ridge National Laboratory. This fieldable and ruggedized mass spectrometer uses pyrolysis coupled with a chemical ionization ion trap mass spectrometer to analyze the thermally liberated biomarkers. While this method works well for bacteria, the analysis of toxins and viruses is more problematic. In another program, discussed here, we have begun to investigate the advantages of using electrospray ionization and ion trap mass spectrometry for the analysis of these materials.

In order to fully understand the advantages of the electrospray ion trap approach, the limitations of the US Army's CBMS Block II must be understood. As stated earlier, the Block II CBMS uses pyrolysis (thermolysis)² to liberate the various biomarkers from the targeted agents. These biomarkers must be compatible with the gas phase, as they are transmitted through heated transfer lines to the mass spectrometer. The primary biomarkers for bacteria are the fatty acids that compose the cell wall. The analysis of fatty acids (after derivatization using a methylating agent to convert the fatty acids to their methyl esters³) for identification of bacteria is well established in the fatty acid methyl ester (FAME) analysis technique. While this method for bacteria analysis is easily translated to mass spectrometry (as the methyl esters of fatty acids can

be easily volatilized), the identification of protein toxins and viruses cannot rely on the analysis of low molecular weight biomarkers that are easily transported through the heated sample path. Currently on the Block II CBMS, protein toxins must be analyzed by determining the relative proportions of two-amino acid diketopiperazines (DKP's) that are formed in the gas phase due to decomposition of the protein. Thus the unique information of the protein (primary sequence information) is lost during this thermal degradation. The problem is the same when analyzing viruses, which are comprised primarily of proteins and RNA or DNA. Since the Block II CBMS uses relative intensities of these fragment ions, the method is especially prone to performance degradation in complex environments or if mixtures of proteins are to be analyzed.

The electrospray/ion trap mass spectrometry^{4,5} detection approach targets proteins from all three classes of biological weapons (BW) as biomarkers for the presence of a specific organism or toxin. It is proposed that proteins (either singular or in combination) can be unique to the organism and thus provide unambiguous identification. Mass spectrometry can identify proteins by employing a combination of molecular weight determination and partial protein sequencing. Electrospray mass spectrometry (using an ion trap mass spectrometer) can provide both molecular weight and partial sequence information in the same analytical method. Electrospray (ES) is designed to admit aqueous samples, and as such is an appropriate final step to on-line sample preparation techniques, most of which are best performed in the liquid phase. Electrospray is characterized by the production of a distribution of molecular ions with differing charge states. As such, it can often be difficult (especially in the presence of complex backgrounds) to determine the charge state (and thus, the molecular weight) of the target species.

The novel enabling technology under development in this program is the use of ion-ion reactions inside the quadrupole ion trap mass analyzer in order to reduce these multiply charged ions to primarily singly charged ions. In this manner, the complexity of the electrospray spectrum is reduced and the measurement of the molecular weight of the analytes becomes relatively straightforward. Partial sequence information is provided by performing MS/MS on the individual multiply charged ions (which are especially prone to decomposition due to Coulombic destabilization). The difference in mass of the resulting fragment ions corresponds to sequence amino acids from a given protein. By searching databases (either locally developed specific target libraries, or the larger, web-based databases), identification of the protein is possible using both the molecular weight and the partial protein sequence to limit the database. In this respect, this method offers the unique possibility of *a priori* identification of unknown proteins from unknown organisms.

Experimental

As stated earlier, minimal sample preparation and pre-separation is a desired outcome of using the ion-ion electrospray ion trap approach. Currently, as performed in the laboratory, the sample processing steps (and approximate times in parenthesis) can be categorized as:

- Buffering/Preparation (1 minute)
- Lysing (<10 minutes)

- Reduction/Denaturization (1 minute)
- Final Cleanup (1-2minutes)

The buffering/preparation step currently consists of adding to the sample to be analyzed 1) Tris (as a buffer), 2) dithiothreitol (to reduce the disulfide bonds), and 3) guanidine HCl (to denature the protein and allow dissolution). Currently, the lysing step is performed using a "bead beating" technique, but we are also looking at a "French press" step at 10 kpsi as an alternative to lysozyme for rapid lysing of bacteria. At this point, the solution is heated to 90°C for 1 min. A spin down step is currently employed to clean out the cellular debris followed by a quick partition of the sample by employing either a "zip-tip" pipette or dialysis (the broad applicability of both techniques is currently under study). At this point, the sample is available for ESI/MS analysis. The final volume of sample is typically about 10 μ l. This amount of sample is sufficient for several hours (though this amount of time is not required) of nanospray ESI investigation.

Instrumental

The electrospray ion trap mass spectrometer is custom-built at ORNL and consists of a nanospray syringe pump, the electrospray source (HV needle, skimmers, differentially pumped vacuum), an ion introduction lens system (for both ion desolvation and ion focusing) and the custom ion trap mass spectrometer which uses a modified Finnigan ITMS as the base system. A second, supplemental negative ion introduction source (a small, discharge source with perfluoro-1,3-dimethylcyclohexane, PDCH) administers negative ions through an aperture in the ring electrode. A schematic of this system is shown in **Figure 1**.

Results

Tobacco Mosaic Virus

The utility of this approach is demonstrated in **Figure 2**. The electrospray mass spectrum of the coat protein from Tobacco Mosaic Virus (TMV) is shown in the upper portion of the figure and contains charge states from +8 to +13. The lower portion of the figure shows the result after the ion-ion reaction. Note that the charge distribution has shifted to primarily the +1 and +2 charge state. The molecular weight of the TMV coat protein can be easily determined from the +1 charge state and the charge state determination is unambiguous.

Ion-Ion Reaction Instrumentation

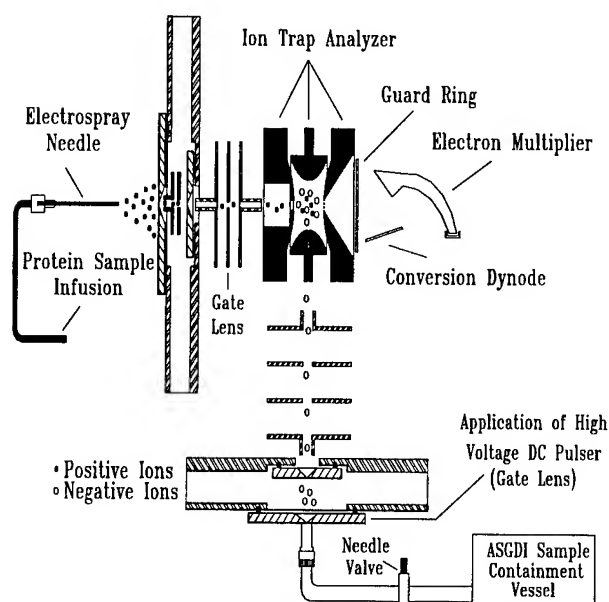


Figure 1: Schematic of the electrospray ion trap mass spectrometer modified with an atmospheric sampling glow discharge negative ionization (ASGDI) source.

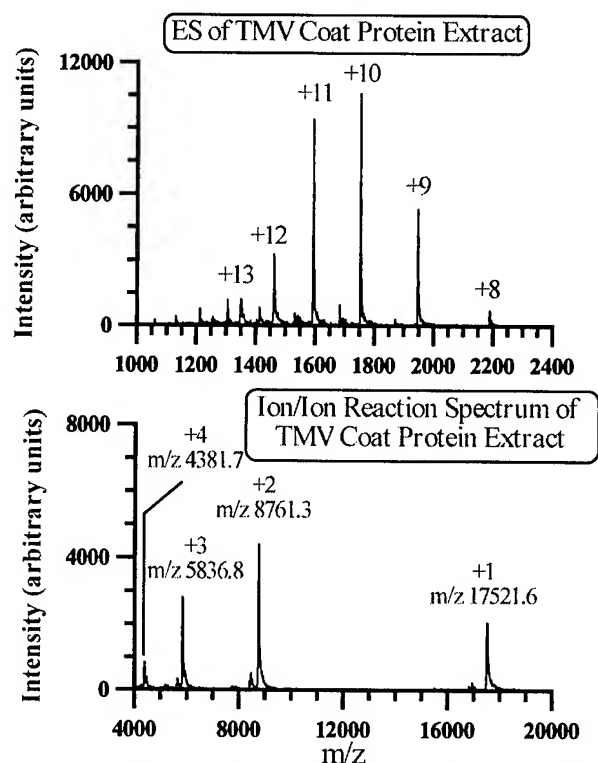


Figure 2: ESI/MS spectrum of the Coat Protein from Tobacco Mosaic Virus. Top figure shows the normal electrospray spectrum. Bottom figure shows the spectrum after ion-ion charge reduction

MS2 in *E. coli*

Bacteriophage MS2 cultures were grown in accordance with standard microbiological techniques. Samples were prepared by passing the MS2 infected media through a 100 kDa spin column and washing the resulting 1 ml fraction with several ml of deionized water. DNA/RNA was precipitated with 66% acetic acid and the resulting complex mixture of viral coat proteins and *E. coli* proteins was analyzed directly. The electrospray mass spectrum (both with and without the ion-ion charge reduction step) is shown in Figure 3 for the bacteriophage, MS2 in *E. coli*. Note again, the reduction of the charge state from the +9 (in the conventional electrospray mass spectrum) to primarily the +1 and +2 charge state (after the ion-ion reaction step).

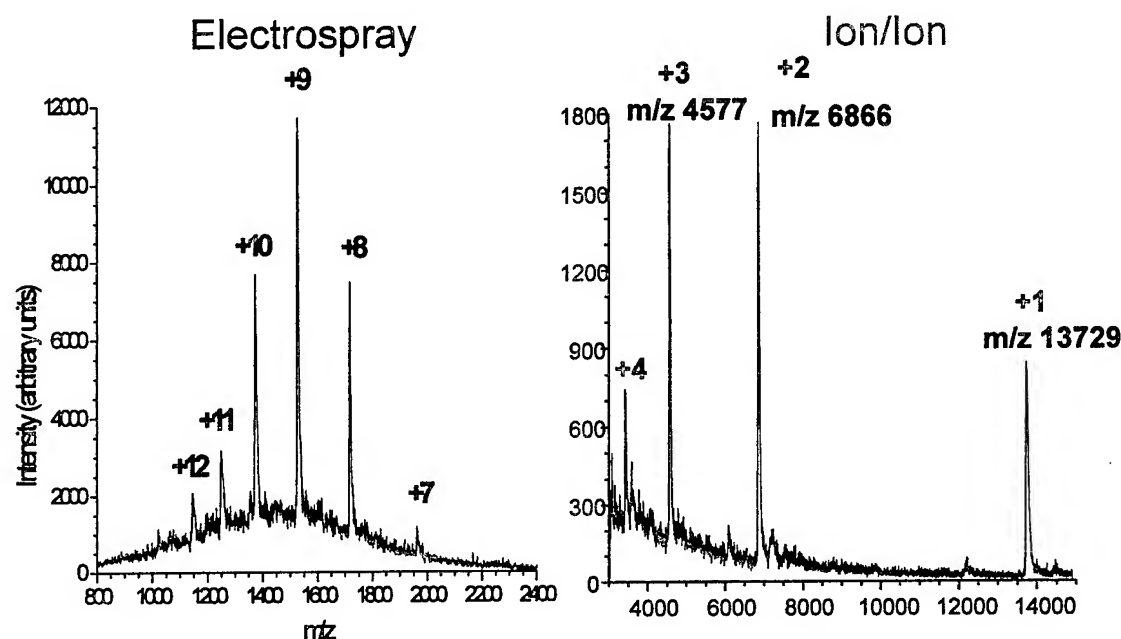


Figure 3: Conventional electrospray mass spectrum (left) and electrospray mass spectrum after ion-ion charge reduction (right) for the analysis of the bacteriophage MS2 in *E. coli*.

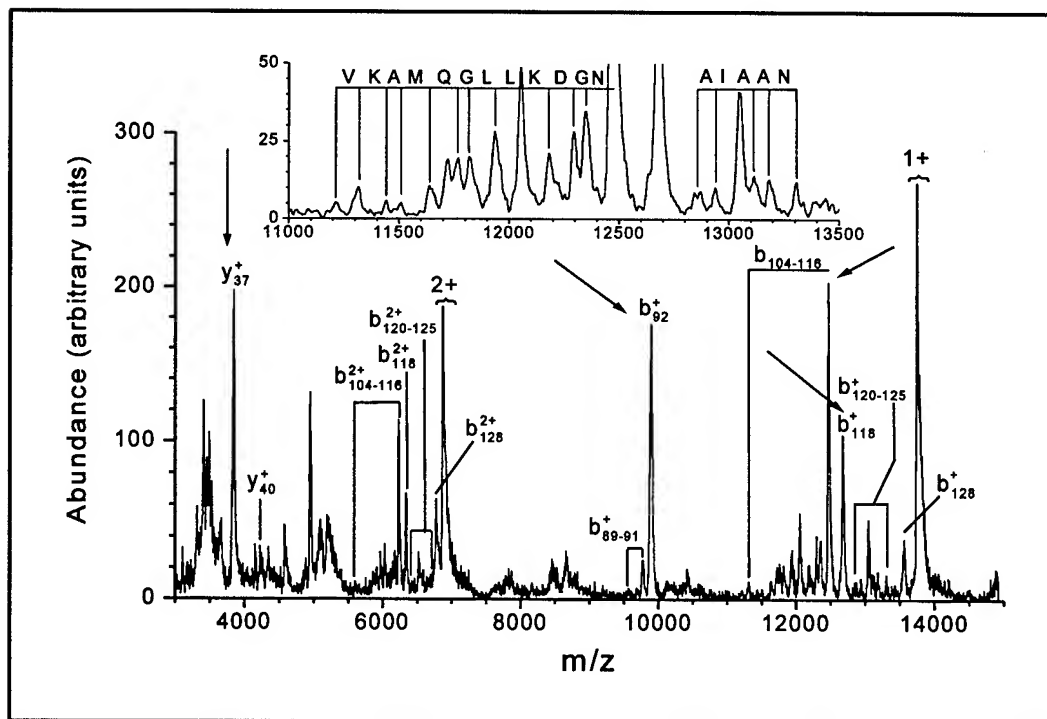


Figure 4: MS/MS of the +8 charge state of the viral coat protein of MS2 showing primary fragments and sequence tag data (see inset). Arrows indicate major fragment peaks which can be used in the database search discussed above.

By performing multiple isolation experiments in conjunction with ion/ion chemistry, a sufficient number of unwanted ions with the same m/z value of the charge state of interest can be removed prior to the MS/MS experiment. This provides the signal-to-noise ratios necessary for obtaining sequence tag information required to search protein databases. The combination of several MS/MS experiments on a variety of charge states followed by ion/ion reactions, can yield unique charge state specific fragmentation which helps identify a given protein in the database with an increased confidence level. The most directly informative structural information is obtained from those charge states that produce a series of product ions arising from fragmentation at adjacent residues. The formation of these product ions via cleavages at adjacent residues, is high dependent upon parent ion charge state. Ion/ion reaction results derived from the CID of the +8 charge state of the viral MS2 coat protein are shown in **Figure 4**. Two types of data can be derived from this spectrum. The first is the sequence tag data shown in the inset. This type of data is useful in identifying proteins regardless of whether post-translational modifications are present. It is also useful in checking for genetically modified proteins which could be engineered in an attempt to evade traditional detection technologies. The second piece of data obtained from this experiment is the presence of the larger fragment ions labeled as y_{37}^+ , b_{92}^+ , b_{116}^+ , and b_{118}^+ (see arrows in **Figure 4**).

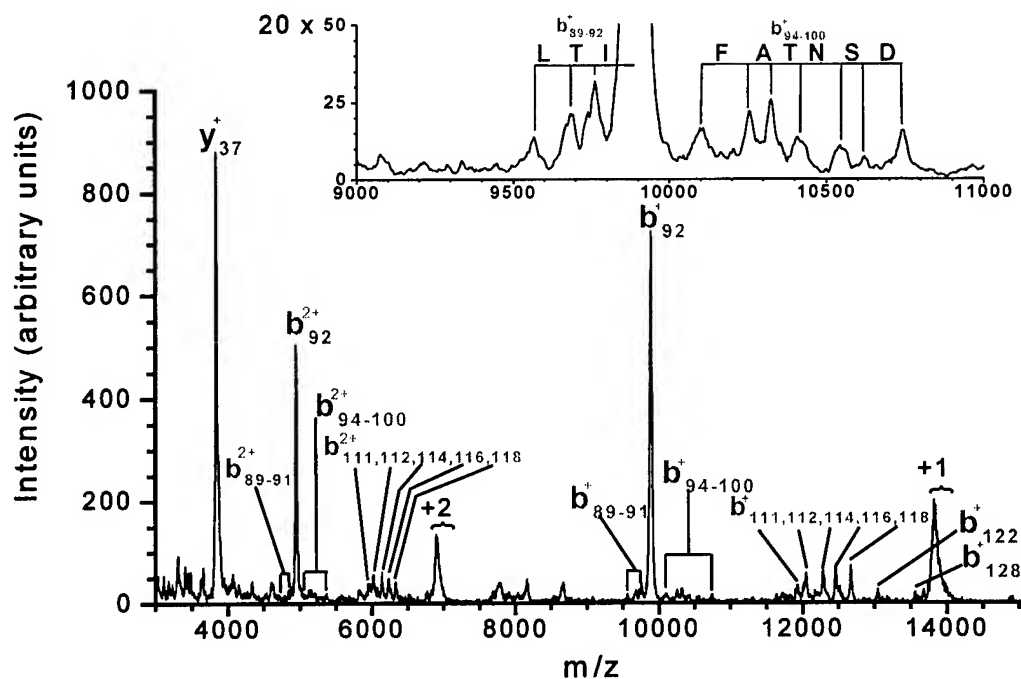


Figure 5: MS/MS of the +7 charge state of the viral coat protein of MS2 showing primary fragments and sequence tag data (see inset).

The electrospray mass spectrum in Figure 5 demonstrates the advantage of analyzing more than one charge state from the charge distribution. This figure shows the MS/MS spectrum from the +7 charge state and provides sequence information from a different portion of the protein. This information is complimentary to that obtained from the +8 charge state and aids in database searching. When the sequence information from the MS/MS spectra is combined with the molecular weight (determined from the ion-ion charge reduction step discussed previously) the data can be used to search protein databases. In this example, when the molecular weight and sequence tag generated from the +8 charge state is searched against the ExPASy Molecular Biology Server using the TagIdent Program, two hits are returned, one of them is the coat protein for MS2 (see Table 1). When the additional sequence information from the +7 charge state is included, only the MS2 entry is returned.

COAT_BPMS2 (P03612)
 COAT PROTEIN.
 pI: 8.00, MW: 13728.54
 105
 ...LTIPIFATNSDCELIvkamqgLLKDGNPIPSAIAANSIY

COAT_BPR17 (P03613)
 COAT PROTEIN.
 pI: 8.67, MW: 13727.56
 105
 ...LTIPIFATNSDCELIvkamqgLLKDGNPIPSAIAANSIY

Table 1: Results of searching the ExPASy Molecular Biology Server using the TagIdent Program.

CONCLUSIONS

The use of ion-ion charge reduction enables a strategy for the analysis of biological threats based on the direct interrogation of whole protein ions via electrospray MS/MS. The identification of the toxin or organism is based on the determination of the molecular weight and partial protein sequence for specific proteins from the target organism. The use of ion-ion chemistry with an ion trap mass spectrometer's storage and mass selection capabilities allows sufficient ion manipulation to eliminate the need to use up-front separations and enzymatic or chemical digestions of the protein. This method allows proteins to be rapidly identified from either on-system libraries or from established protein databases.

REFERENCES

1. K. J. Hart, M. B. Wise, W. H. Griest, and S. A. Lammert, "Design, Development and Performance of a Fieldable Chemical & Biological Agent Detector," *Field Analytical Chemistry and Technology*, 4 (22-3), 93-110 (2000).
2. S.A. Barshick, D.A. Wolf and A.A. Vass, "Differentiation of Microorganisms Based on Pyrolysis-Ion Trap Mass Spectrometry Using Chemical Ionization", *Anal. Chem.*, 71, 633-641 (1999).
3. F. Basile, M.B. Beverly, C. Abbas-Hawks, C.D. Mowry, T.L. Hadfield and K.J. Voorhees, "Direct Mass Spectrometric Analysis of in Situ Thermally Hydrolyzed and Methylated Lipids from Whole Bacterial Cells", *Anal. Chem.*, 70, 1555-1562 (1998).
4. Stephenson, Jr. J. L.; Cargile, B. J.; McLuckey, S. A. "Ion Trap Collisional Activation of Disulfide Linkage Intact and Reduced Multiply Protonated Polypeptides" *Rapid Comm. Mass Spectrom.* 13, 2040-2048 (1999).

5. Cargile, B. J.; McLuckey, S. A.; Stephenson, Jr, J. L. "Rapid Identification of Bacteriophage MS2 Coat Protein from E. Coli Lysates via Ion Trap Collisional Activation of Intact Protein Ions in Conjunction with Ion/Ion Reactions" *Anal. Chem.* (2000), submitted.

ACKNOWLEDGEMENTS

Supporting funding from Department of Energy NN-20 (Chemical and Biological National Security Program, CBNP). Oak Ridge National Laboratory is managed and operated by UT-Battelle, LLC, for the U.S. Department of Energy under contract DE-AC05-00OR22725.

BIODETECTION BY IDENTIFICATION OF PCR PRODUCTS USING ELECTROSPRAY IONIZATION MASS SPECTROMETRY AND TANDEM MASS SPECTROMETRY

Yevette A. Johnson, Madan Nagpal, Mark T. Krahmer, Karen F. Fox, and *Alvin Fox**.

Department of Microbiology & Immunology
University of South Carolina
School of Medicine
Columbia, SC 29208

Abstract

Detection of BW agents is possible in under seven minutes using a prototype "fluorogenic system" that combines PCR amplification and detection in a single unit. Such Taqman-type systems have the advantage of speed but disadvantage that the MW of the PCR product is not provided as in classical PCR. Knowing the MW is an important attribute in the specificity of PCR. In contrast, identification of PCR products by mass spectrometry (MS) provides both speed and MW information. Furthermore tandem mass spectrometry (MS/MS) provides a fingerprint for characterization of the PCR product, allowing additional sequence information to be obtained. There is a great potential for PCR-MS and PCR-MS/MS in biodetection.

Introduction

Selection of gene of interest for PCR, PCR-MS or PCR-MS/MS analysis.

1. Environmental analysis.

- A. *PCR without prior culture.* The power of the polymerase chain reaction (PCR) resides in amplification of only one gene sequence in a complex mixture (e.g. real-time detection of airborne anthrax particles during a biological warfare attack). The gene region selected for rapid detection must be present in the agent of interest and rarely found in other bacterial species. Otherwise, false positives will result.
- B. *PCR after culture.* However, in confirmation of an attack, culture may prove necessary, individual colonies can then be selected for analysis from environmental samples; this enormously simplifies the analysis.

2. Clinical analysis.

In infected clinical samples, after a BW attack, generally only one bacterial species would be present. This also allows greater flexibility in selection of primers for potential PCR products.

3. General Comments on PCR Markers

The selection of any one marker in the identification of *B. anthracis* has proven to be problematic. For example, the chromosomal marker, Ba813, is considered one of most distinctive for anthrax but is found in some strains of *B. cereus* and *B. thuringiensis*.¹ Virulent strains of *B. anthracis* are characterized by the presence of two plasmids (pXO1 and pXO2); the former coding for toxin components and the latter for genes involved in the synthesis of the poly-D-glutamic acid capsule. These genetic elements can be lost on culture *in vitro* complicating identification.² Furthermore, pXO2 has been shown to be present in certain uncharacterized soil isolates.³ A poly-D-glutamic acid capsule has also been shown to be produced by some strains of *B. licheniformis*.⁴ Thus the selection of multiple markers for PCR analysis may be desirable.

The interspace region between the 16S and 23S rRNA (ISR) is not subject to the same selective pressure as the rRNA structural genes and has been shown to exhibit considerable variability in sequence and also size even between closely related organisms.⁵ The ISR sequence similarity of *B. subtilis* compared to the *B. cereus* group, including *B. anthracis*^{6,7} is only 75.5-86.5%. Indeed using primers against conserved regions of the ISR, members of the *B. subtilis* and *B. cereus* groups of organisms are distinguished by PCR product size.⁸⁻¹⁰ Characterization of the ISR is useful for identification of other BW agents including *Brucella*.¹¹

Instrumental detection of PCR products

Classically, PCR products have been detected off-line by gel electrophoresis. This not only allows detection of the PCR but provides it's MW; this is an important parameter in detection of PCR products. The commercial "Taqman" system, and others based on similar principles, allow on-line detection to be completed in a relatively short time. For example, a miniature non-commercial system allows this to be done in 7 min (total analysis time, amplification and detection).¹² However, the MW of the PCR product is not provided. In contrast, rapid and precise analysis of PCR products has been achieved by electrospray ionization (ESI) MS and MS/MS.^{13,14} In this case the MW and other detailed sequence-related information is provided instantaneously. Integration of PCR and MS/MS into a single instrumental unit might improve the specificity of biodetection substantially.

PCR products can also be rapidly detected using relatively inexpensive quadrupole or ion trap mass spectrometers. *B. anthracis* (the causative agent for anthrax) was shown to be readily distinguished from *B. subtilis*; 89 base pair (bp) PCR product versus 114 base pair product (ISR marker).^{13,15,16} Strain var. *niger* is often used as a simulant for *B. anthracis*. The ISR of v. *niger* is quite distinct from *B. anthracis* and closely related to *B. subtilis*. However, v. *niger* is a member of a different species, *B. atrophaeus* (119 bp product).

More recently we have demonstrated that analysis of PCR products can be enhanced using MS/MS. Minor differences in the sequence of PCR products are readily distinguished by the product ion spectrum (chemical fingerprint).¹⁴

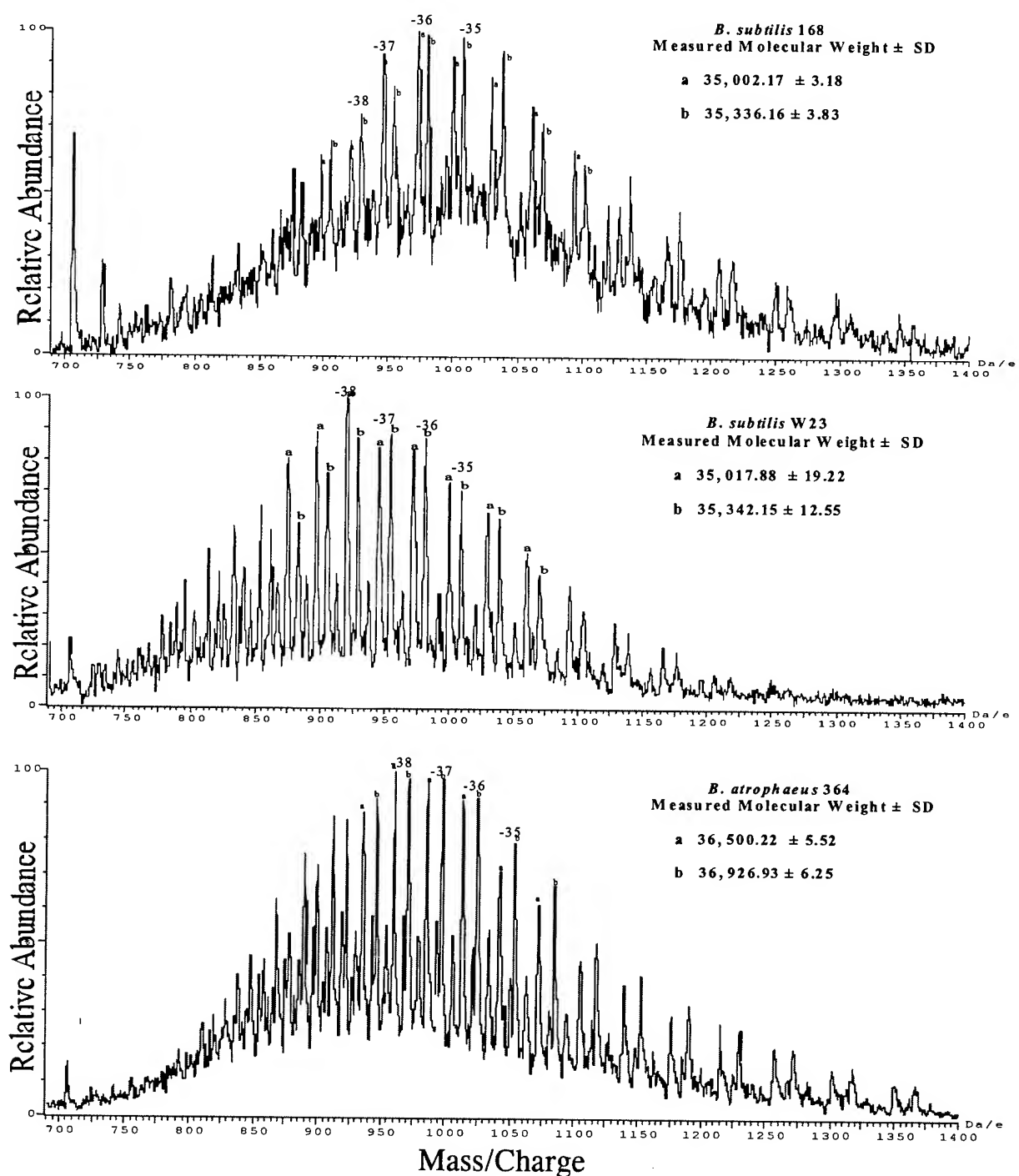


Figure 1. Electrospray ionization mass spectra of bacilli. Note the two strains of *B. subtilis* (168 and W23) are of similar MW. The PCR product of *B. atrophaeus* (strain 364, closely related to strain *v. niger*) is readily distinguishable by M.W difference from the equivalent PCR product from *B. subtilis*. The peaks labeled a and b represent the M.W. of individual strands of double stranded (dd) PCR products. Each PCR product has multiple charge states, e.g., -35 to -38 as shown in figure, depending on losses of H⁺ ions from the molecules. Thus the mass spectrum appears as a series of pairs of peaks.

CONCLUSIONS

Analysis of PCR products by MS provides a measure of MW and MS/MS provides a chemical fingerprint (product ion spectrum). Using primers against conserved regions of the 16S-23S rRNA ISR allows the potential for universal screening of BW agents (e.g. in clinical samples). However, such PCR products are unsuitable for direct analysis of environmental samples since complex mixtures of PCR products would be generated. For real-time biodetection, it is essential that each PCR product be specific for each BW agent of interest (e.g. Ba813 for *B. anthracis*). The availability of an integrated PCR-MS/MS instrument, coupled with appropriate sets of primers, would allow rapid biodetection with extremely high specificity.

ACKNOWLEDGMENTS

This research was supported by Office of Naval Research (N00014-97-1-0806).

REFERENCES

1. Ramisse, V., Patra, G., Vaissaire, J., Mock, M. 1999. The Ba813 chromosomal DNA effectively traces the whole *Bacillus anthracis* community. *J. Appl. Microbiol.* 87: 224-228.
2. Turnbull, P.C.B, Hutson, R.A, Ward, M. J., Jones, M.N., Quinn, C. P. Finnie, NJ, Duggleby, CJ, Kramer, J.M., Melling, J. 1992. *Bacillus anthracis* but not always anthrax. *J. Appl. Bacteriol.* 72: 21-28.
3. Beyer, W., Pocivalsek, S, Böhm, R. 1999. Polymerase chain reaction to detect *Bacillus anthracis* from soil samples -limitations to present published papers. *J. Appl Bacteriol.* 87: 229-236.
4. Troy, F.A. 1979. Chemistry and biosynthesis of the poly (-D-glutamyl) capsule in *Bacillus licheniformis*. *J. Biol. Chem.* 245:305-315.
5. Jensen, M.A., Webster, J.A., Straus, N. 1993. Rapid identification of bacteria on the basis of polymerase chain reaction-amplified ribosomal DNA spacer polymorphisms. *Appl. Environ. Microbiol.* 59: 945-952.
6. Green, C.J., Stewart, G.C., Hollis, M. A., Vold, B.S., Bott, K. F. 1985. Nucleotide sequences of the *Bacillus subtilis* ribosomal operon, *rrnB*. *Gene.* 37: 261-266.
7. Harrell, L. J., Andersen, G. L., Wilson, K. H. 1995. Genetic variability of *Bacillus anthracis* and related species. *J. Clin. Microbiol.* 33, 1847-1850.
8. Wunschel, D. S., Fox, K.F., Black, G.E., Fox, A. 1994. Discrimination among the *B. cereus* group, in comparison to *B. subtilis*, by structural carbohydrate profiles and ribosomal RNA spacer region PCR. *Syst. Appl. Bacteriol* 17: 625-635.
9. Nagpal, M.L., Fox, K.F., Fox, A. 1998. Utility of 16S-23S rRNA spacer region methodology: how similar are interspace regions within a genome and between strains for closely related organisms? *J. Microbiol. Meth.* 33: 211-219.
10. Johnson Y., Nagpal M., Krahmer M.T., Fox K.F., Fox A. 2000. Precise molecular weight determination of PCR products of the rRNA interspace region using electrospray quadrupole mass spectrometry for differentiation of *B. subtilis* and *B. atrophaeus*, closely related species of bacilli. *J. Microbiol. Meth.* 40: 241-254.
11. Fox, K.F., Fox, A., Nagpal, M., Steinberg, P., Heroux, K. 1998. Identification of *Brucella* by ribosomal spacer region PCR and differentiation of *B. canis* from other *Brucella* pathogenic for man by carbohydrate profiles. *J. Clin. Microbiol.* 36: 3217-3222.
12. Belgrader, B., Benett W., Hadley, D., Richards, J., Stratton, P. 1999. Raymonds M., Milanovich, F. PCR detection of bacteria in seven minutes. *Science.* 284: 449-450.
13. Krahmer, M. T., Johnson, Y.A., Walters, J.J., Fox, K.F., Nagpal, M. 1999. Electrospray quadrupole mass spectrometry analysis of model oligonucleotides and polymerase chain reaction products: determination of base substitutions, nucleotide additions/deletions and chemical modifications. *Analyt.. Chem.* 71: 2893-2900.
14. Krahmer, M. T., Walters, J. J., Fox, K.F., Fox, A., Creel, K. E., Pirisi P., Wunschel, D. S., Smith, R. D., Tabb, D. L., Yates, J. R. III. 2000. MS for identification of single nucleotide polymorphisms and MS/MS for discrimination of isomeric PCR products. *Analyt. Chem.* 72: 4033-4040.
15. Muddiman, D.C., Wunschel, D.S., Liu, C., Pasa-Tolic, L., Fox, K.F., Fox, A., Anderson, G.A., Smith, R.D. 1996. Characterization of PCR products from bacilli using electrospray ionization FTICR mass spectrometry. *Analyt. Chem.* 68:3705-3712. .
16. Wunschel, D. S., Muddiman, D.C., Fox, K.F., Fox, A, Smith, R.D. 1998. Heterogeneity in *B. cereus* PCR products detected by ESI-FTICR mass spectrometry. *Analyt. Chem.* 70: 1203-1207.

RAPID RESPONSE CHEM/BIO DETECTION SYSTEM BASED ON PHOTOIONIZATION MASS SPECTROMETRY

Matthew D. Evans, Karl A. Hanold, and *Jack A. Syage*

Syagen Technology, Inc.
1411 Warner Ave., Tustin CA 92780

ABSTRACT

This work describes a high-speed detection system for identifying chemical and biological weapons. The system is based on new innovations in mass spectrometry (MS) to achieve target molecular identification with minimal false positive responses. The core technologies are: (1) a highly efficient photoionization source and (2) a high performance mass analyzer based on the hybrid combination of quadrupole ion trap and time-of flight technologies (QitTof). The benefits of photoionization for CW detection are near universal detection efficiency, minimal ion fragmentation, and near absence of signal from air constituents and many common matrix background compounds. The detection system being developed is compact, robust and permits automated, unattended operation for real-time early warning systems, point-of-entry screening, and emergency first responder applications.

1. INTRODUCTION

This work describes a promising new chemical and biological (CB) point-detection system based on photoionization mass spectrometry (PI MS). The technology has been extensively tested on chemical agents and is giving initial promising indications for biological agent signatures.

A variety of chemical agent sensors, monitors, and point-detection systems have been developed to meet different requirements.^{1,2,3,4,5} Less adequate solutions exist for biological agent detection. The U.S. Army began the Biological Integrated Detection System (BIDS) in 1993. This project employed a battery of instruments, such as a high volume particle sizer, liquid sampler, and flow cytometer in a mobile laboratory mated to a Humvee vehicle. The BIDS vehicle was tested in June 1997 and proved capable of detecting a variety of pathogens in about 5-min, a marked improvement over previous field instruments. Added to this suite of instruments was the Chemical Biological Mass Spectrometer (CBMS). This instrument is an ion trap mass spectrometer (ITMS) capable of biological or chemical detection when connected to an aerosol collector/concentrator or chemical probe, respectively.

The above developments are large mobile laboratories. Efforts to provide man-portable detectors require innovative new technologies. Ion Mobility Spectrometry (IMS), which is used extensively for chemical detection, is being adapted for biological detection by Environmental Technology Group and by Graseby Dynamics. Mass spectrometry offers improved specificity, although developing compact, portable instruments has been a challenge. Accepted methods of biological detection include pyrolysis mass spectrometry; however, improvements are needed for this method to provide high specificity, especially for civilian use. Emerging mass spectrometry technologies for biological detection include matrix assisted laser desorption/ionization (MALDI) and electrospray ionization (ESI). MALDI is a widely used technique for large biomolecule identification; however, introducing sample is difficult, normally requiring manual

preparation and loading through a vacuum load lock. This makes MALDI challenging for automated field operation. ESI also requires a reliable and automated method of preparing and cleaning biological samples.

2. EXPERIMENTAL

2.a. PI background

Figure 1 illustrates the principle of PI MS. The Syagen PI source imparts an energy that is higher than the ionization potentials (IPs) of typical target molecules, but lower than the IPs of virtually all constituents of air as well as most common solvents. These potential interferents are not ionized, enabling significantly greater dynamic range for detecting and measuring molecules at very low concentrations. Furthermore, because molecules of interest are ionized near their IP thresholds there is minimal fragmentation to clutter a mass spectrum. These performance features provide tremendous benefits for analyzing mixtures and samples in complex matrices. The method of electron ionization (EI), by contrast, imparts energy that greatly exceeds the dissociation thresholds of most molecules. This leads to extensive fragmentation. Figure 2 compares EI MS and PI MS for the nerve agent simulant molecules DIMP and DMMP (diisopropyl methylphosphonate and dimethyl methylphosphonate). EI leads to highly fragmented spectra and weak molecular ion signal. PI, on the other hand, leads to very simple spectra with strong molecular ion signal. The simple mass spectra provided by PI is crucial to analyzing the overlapping spectra of a complex mixture of compounds.

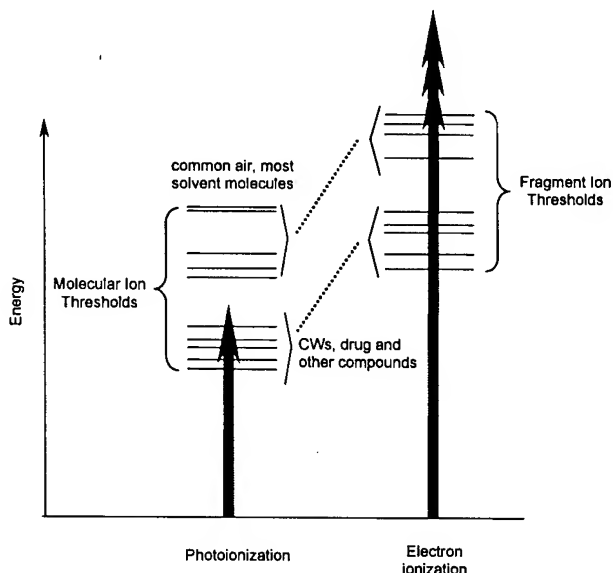


Figure 1.

Diagram showing the principle of photoionization for achieving threshold ionization of molecules. The process of electron ionization is shown for comparison.

The PI source has been described before.^{6,7} The PI light source uses a high-output gas discharge tube with a MgF_2 window for transmission of vacuum ultraviolet light into the ionization region. The fill gas is generally a rare gas and the choice of gases depends on the wavelength range of interest. Narrow band energy is available from about 8 to 12 eV, although we usually operate near 10 eV.

The principal mechanism for photoionization of molecule M is photon absorption and electron ejection to form the molecular ion M^+ . In the presence of water vapor or protic solvents, the molecular ion can extract H to form MH^+ . This tends to occur if M has a high proton affinity. This does not affect quantitation accuracy as the sum of M^+ and MH^+ is constant.

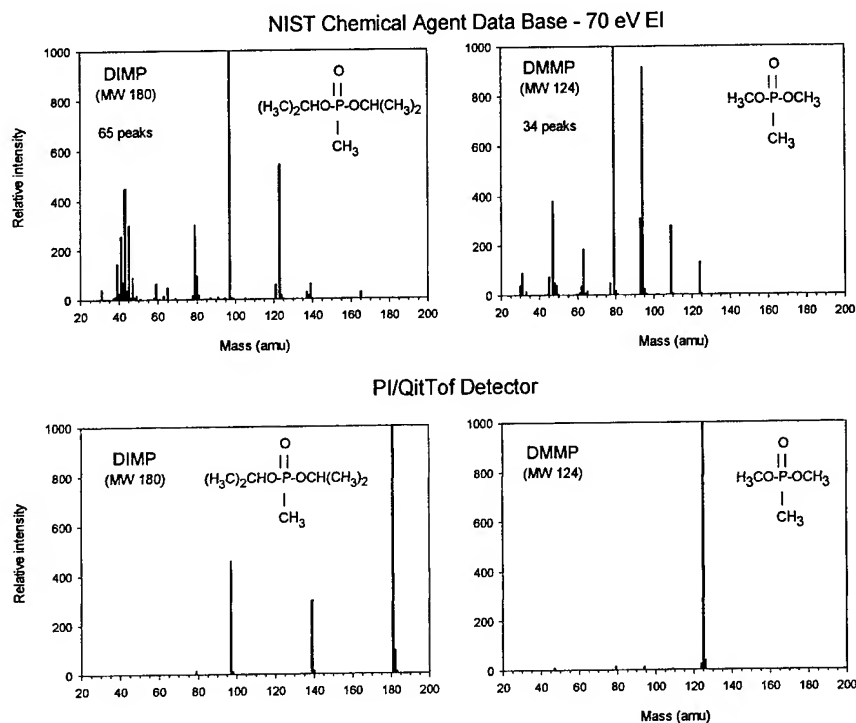


Figure 2.

Comparison of PI vs. EI mass spectra of DMMP and DIMP showing significantly reduced fragmentation and distinct signature peaks for PI mass spectra.

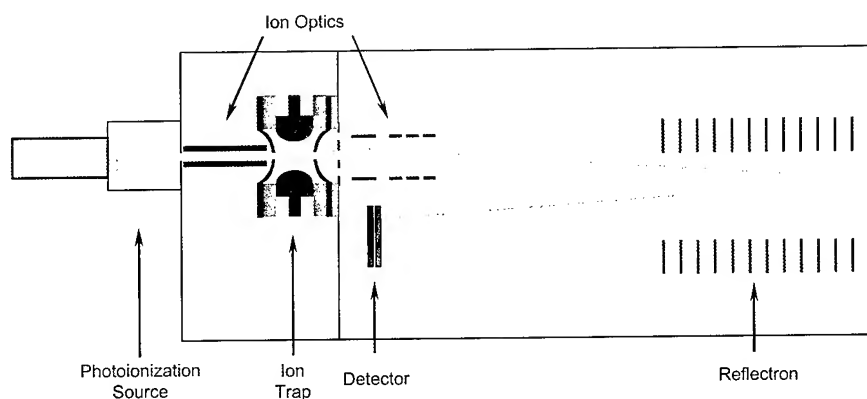


Figure 3.

Schematic diagram of the KitToF mass analyzer shown with a photoionization source.

2.b. KitToF Mass Analyzer

The ChemBio MS system employs a combination of a quadrupole ion trap and a time-of-flight mass analyzer to achieve high-speed, high-performance molecular analysis. This combination is referred to as KitToF and is also well suited for use with the PI source. A schematic showing the basic functions of PI/KitToF system is shown in Figure 3. The major benefits are outlined below:

Quadrupole Ion Trap (QIT): ^{8,9,10}

- Ability to store ions formed by a continuous ionization source followed by pulsed extraction into the TOFMS

- Option to manipulate ions, such as mass-selective isolation, followed by collisional-induced dissociation in order to fingerprint compounds (e.g., MS/MS)
- Operation at relatively high pressure, thus forming a differential pressure stage between the AS-TPI source and the TOFMS

Time-of-Flight Mass Spectrometry (TOFMS):¹¹

- Multichannel mass detection leading to efficient collection of all ions
- Large mass range of detection
- Exceptionally low instrument noise because each mass peak is detected in a narrow time window (about 20 ns)

QIT/TOFMS Combination (QitTof):¹²

- Space-charge repulsion degrades resolution in scanning QITs (ion trap mass spectrometers, ITMS), limiting trap capacity to 300-500 ions per period. Pulsed extraction and TOF analysis remove this restriction enabling >5000 ions per period (with reflectron)
- QitTof can operate at repetition rates >100 Hz vs. 20 Hz max for ITMS enabling increase in dynamic range

Furthermore, in combination with PI, the QIT can achieve significantly improved dynamic range because PI avoids ionization of common atmospheric constituents. As a result, the trap does not fill with atmospheric ions.

2.c. Deployable ChemBio MS System

Syagen has developed a pre-production quality detection system for CW and related compound detection. The system was originally developed for the Defense Threat Reduction Agency (DTRA) for Chemical Weapons Convention (CWC) treaty compliance monitoring. The currently accepted method for validating the presence of alleged CWC scheduled compounds is gas chromatography/mass spectrometry (GC/MS). The slow speed of this method limits the number of samples that can be analyzed in a given inspection time period, potentially compromising the thoroughness of a challenge inspection. The throughput can be greatly increased if a large number of samples could be rapidly screened for the presence of alleged compounds. Only those samples that test positive are then certified by GC/MS.

Figure 4 shows the mobile benchtop PI/QitTof instrument for high-speed screening of liquid samples. The integrated autosampler allows automated and unattended analysis of hundreds to thousands of samples at a time. The current sample cycle time is 45 seconds. The instrument may also be configured for air sampling by dispensing with the autosampler and making a routine change to the sample inlet. Figure 5 shows a configuration that permits rapid deployment to remote sites.

The instrument is capable of MS/MS “on-the-fly” whereby the detection of a targeted compound can trigger an excitation waveform to provide a confirmatory fragment spectrum. The entire instrument is transportable and occupies a 5 sq ft footprint. The specifications of the deployable MS system are summarized in Table I.

Another Syagen system that is currently under development (partially funded by SBCCOM) is a field-portable CB/MS system with a pyrolysis-gas chromatography (Py-GC) interface. This instrument is merging the successful methods of PI MS with the front-end Py-GC used for IMS. The PI MS system weighs between

30-40 lbs depending on configuration. A picture of the first prototype PI/QtTof MS is given in Figure 6. This paper focuses on results obtained on the portable benchtop system in Figure 4; however, the technology can be transitioned to a field-portable size with some modest reduction in specifications (e.g., factor of 3 less sensitivity). The early prototype field-portable system has been described elsewhere.^{13,14}

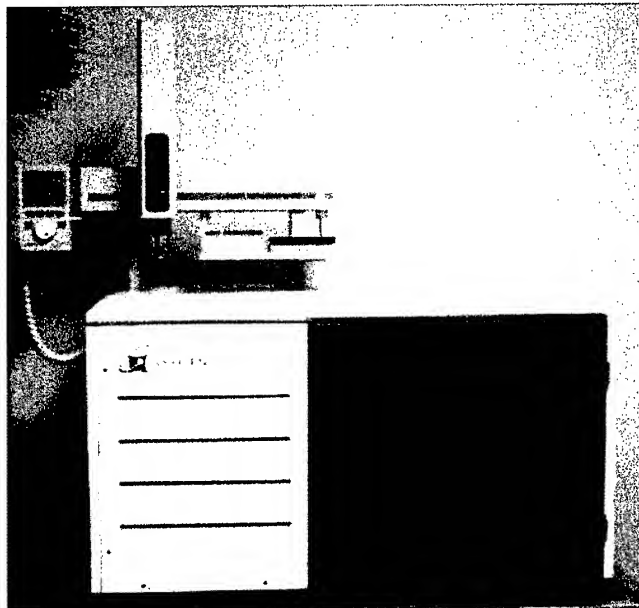


Figure 4

PI/QtTof instrument with autosampler and exterior panels.

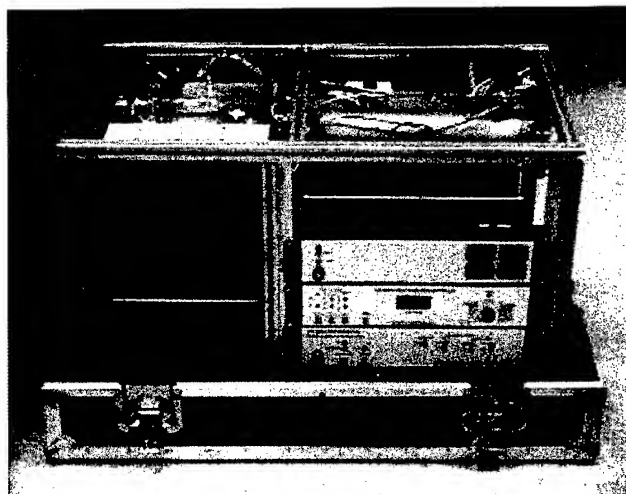


Figure 5

The PI/QtTof without panels or autosampler configured for "fly-away" applications. Computer and roughing pump not shown.

Table I. Specifications of CW analysis system

Property	Specification
Sensitivity 2-5 s sampling time, 3 σ LOD	10-100 ppb (air sampling) <1 μ g/mL, typ. (liquid sampling)
Mass Range	50-800 m/z
Mass Resolution Full width half height	~3000 at 361 m/z
Sample cycle time	45 sec for liquid autosampling 10 s for direct air sampling
Dynamic Range	3-decade linear 4-decade total
Carryover	2 to ~10%
Repeatability	short term RSD of 5% long term (hours) RSD 18-20%

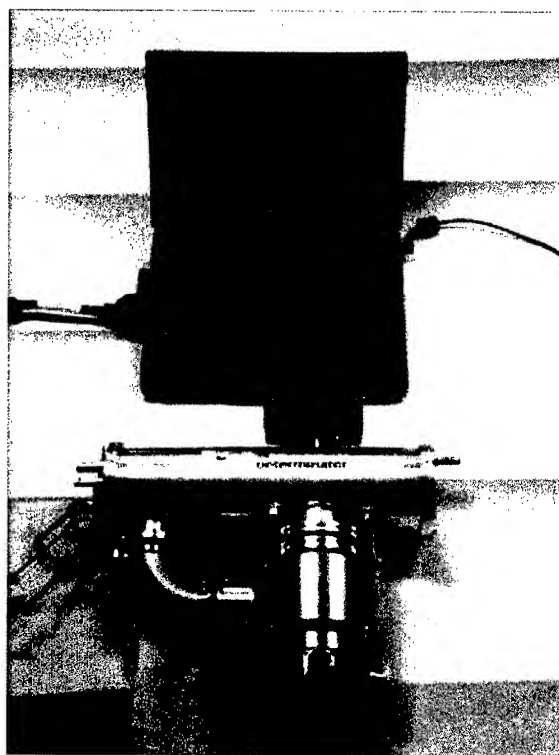


Figure 6

Picture of prototype PI/QitTof mass spectrometer and processor units. Not shown are the backing pump and electronics.

3. RESULTS AND DISCUSSION

3.a. Spectral signatures

PI mass spectra are noted for dominant molecular ion signal and minimal fragmentation. Figures 7-10 show PI mass spectra for representative nerve, blister, riot, and hallucinogenic agents. These compounds were dissolved in solvent and introduced into the MS detector by syringe injection or by direct capillary infusion. In previous experiments with live agents, sample was introduced as vapor using permeation or sorbent tubes in a mixed flow apparatus. Because the liquid samples are vaporized in the ionizer, the spectral characteristics for liquid and vapor sampling are similar. The primary difference is that protic solvents can serve as a hydrogen source that can react with molecular ion M^+ to form MH^+ .

Figure 7 shows spectra of VX recorded in conventional MS mode and using selected ion excitation of the molecular ion MH^+ (269 m/z) to give a MS/MS spectrum yielding the daughter fragment at 128 m/z. The distinct signature provided by the parent/daughter ion signals gives a definitive identification of the molecule VX. Figure 8 shows PI mass spectra of nitrogen and sulfur mustard. Both spectra show strong molecular ion signal with a characteristic 3-peak distribution for a molecule containing two chlorine atoms (^{35}Cl , ^{37}Cl). For sulfur mustard, an additional 3-peak series is observed for MH^+ , along with M^+ , due to the presence of protic solvent. Figures 9 and 10 show the riot agent CR and the hallucinogen BZ. The predominant signal for CR is the molecular ion while for BZ, the MH^+ ion dominates.

The PI/QitTof was tested for a 48-compound library of CWC treaty-scheduled compounds. 45 molecular ion signals were detected with minimal fragmentation. Table II shows the list of compounds that have been recorded by PI MS.

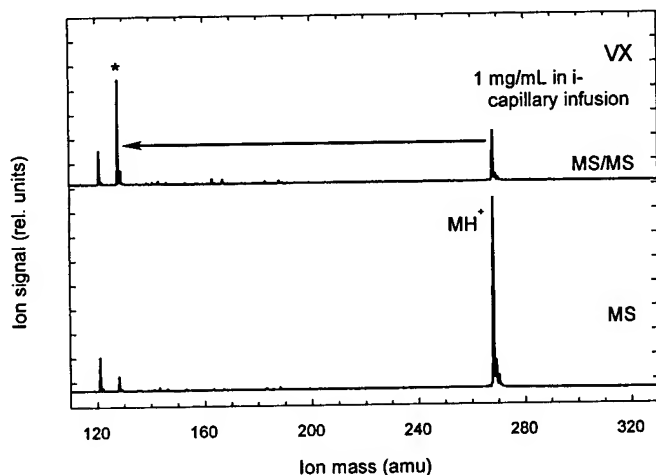


Figure 7

PI mass spectra of VX. (Bottom) MS spectrum shows a predominant molecular ion for VX. (Top) MS/MS spectrum shows mass-selective dissociation to give the confirmatory fragment signal, marked by asterisk.

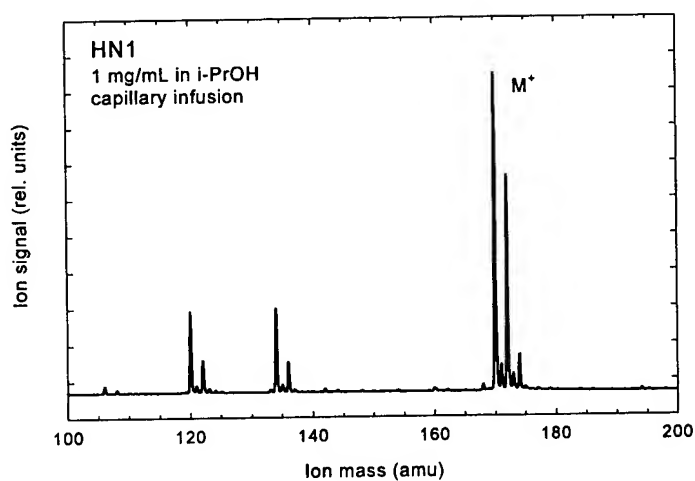
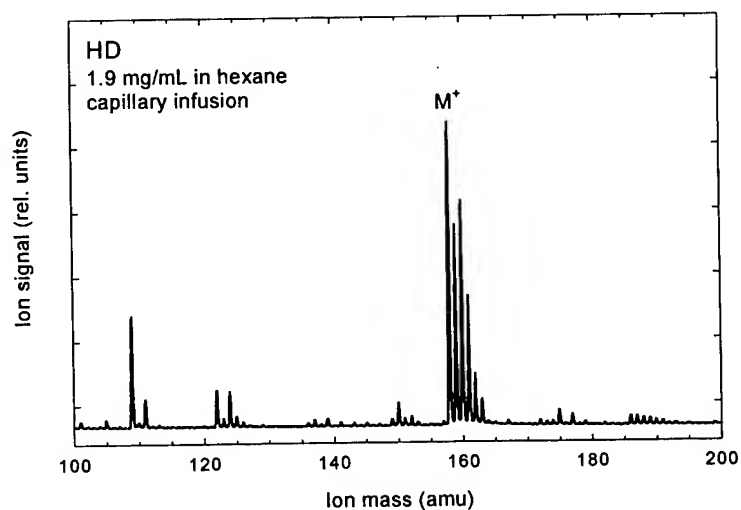


Figure 8

PI MS spectrum of HN1 and HD showing predominant molecular ion signal (isotope distribution for two chlorines) and weak singly chlorinated fragments. Note that HD also forms MH⁺.



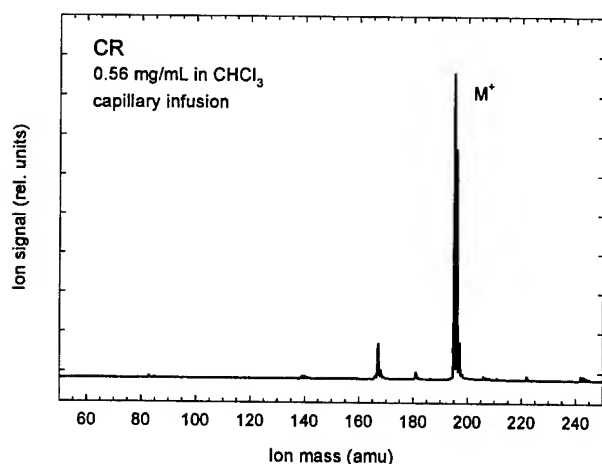


Figure 9

PI MS spectrum of CR, a riot gas. CR does not protonate in CHCl_3 .

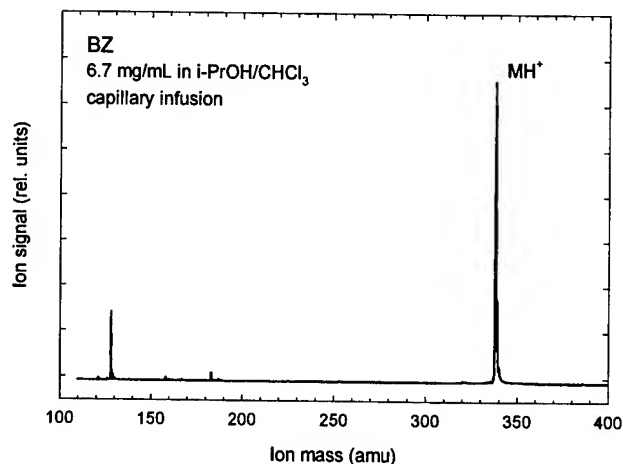


Figure 10

PI MS spectrum of BZ, a central nervous system depressant. Note that BZ ionizes and protonates.

Table II. Library of CWC-relevant compounds tested using Syagen's PI MS detector.

Schedule-1 compounds	Schedule-2 compounds	Schedule-3 compounds
Toxic	Toxic	Precursors
VX	BZ	Phosphorus oxychloride
GA (Tabun)		Dimethyl phosphite
GB (Sarin)	Precursors	Trimethyl phosphite
GD (Soman)	Diisopropyl methylphosphonate	Diethyl phosphite
GF	Diethyl methylphosphonate	Triethyl phosphite
	Dimethyl methylphosphonate	Triethanolamine
HD (sulfur mustard)	Diethyl ethylphosphonate	N-ethyldiethanolamine
HN-1 (Nitrogen mustard)	Diethyl methylphosphonothioate	N-methyldiethanolamine
HN-3	Isopropyl methylphosphonic acid	
	Cyclohexyl methylphosphonic acid	
CR	Pinacolyl methylphosphonic acid	
CS	Methyl phosphonyl dichloride	
	3-quinuclidinol	Decomposition Products
Precursors (Binary)	Benzilic acid	Methylphosphonic acid
QL	Pinacolyl alcohol	Ethylmethylphosphonic acid
DF	Thiodiglycol	EMPTA
	N,N-diethylethanolamine	2-chlorodiethylsulfide
	1,4-dithiane	
	Thiodiglycol sulfoxide	Other relevant compounds
	Methylamine	VX disulfide
	Isopropylamine	YL
	Thioxane	
Not detected: Phosgene, chloropicrin		

3.b. Application to biological agents

The key to bacterial differentiation by mass spectrometry is the release and identification of molecular signatures that are specific to different types of bacteria and other pathogens. These include DNA, proteins, lipids, and carbohydrates. A major challenge is breaking down the cell material into detectable molecular constituents. Pyrolysis mass spectrometry (Py-MS) has been demonstrated to be an effective, if not ideal, method for differentiating microorganisms.^{15,16} The principal advantages of Py as a sampling method are minimal sample preparation, speed, sensitivity, and low cost. The primary disadvantage of the Py method is that the degradation of bacterial material into a nearly undecipherable collection of molecular fragments. This problem can be compounded by current methods of MS that can further fragment these signatures, thereby destroying much of the uniqueness of the original molecular signatures.

In this work we are implementing two significant improvements to the conventional method of Py-MS. These are:

- Flash pyrolysis developed by A. P. Snyder and coworkers at Edgewood Chemical and Biological Center (ECBC). This method more rapidly heats and desorbs the cell material creating larger molecular fragments with unique signature masses.^{17,18}
- Photoionization, which is a more universal ionization source than chemical ionization (CI). PI also gives significantly less fragmentation than electron ionization (EI) for the molecular constituents of bacteria and spore pyrolysis.

The principal pyrolysis products are fatty acids and phospholipids. In addition, BG spores generate picolinic acid. A method has been developed to rapidly methylate the fatty acids to their corresponding fatty acid methyl esters (FAME).¹⁹ This in-situ derivation is important for GC separations of the pyrolysis products, a method that has been successfully demonstrated for ion mobility spectrometry (IMS).²⁰

Figure 11 shows examples of FAME compounds recorded using PI MS. These spectra show very clean ion signatures that are dominated by molecular ion signal. These results indicate that an accurate measure of different FAME relative abundances can be made, thereby providing strong signatures for identifying different bacteria.

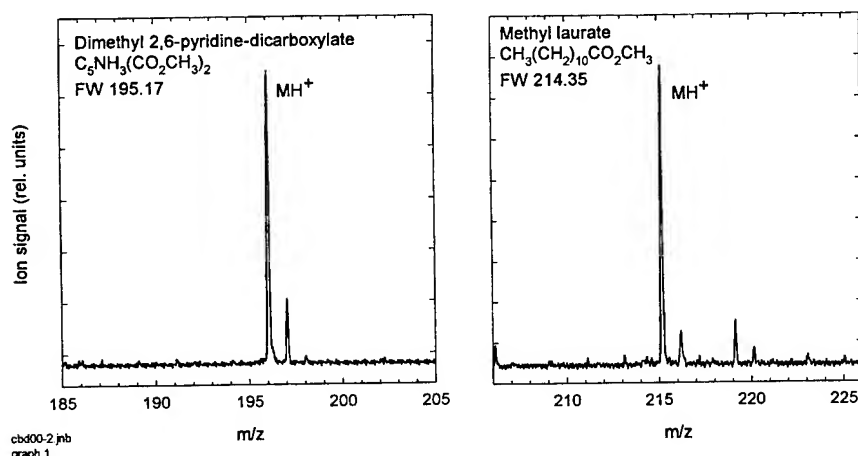


Figure 11.

PI MS of fatty acid methyl esters (FAME). These are signatures for pyrolysis of gram positive spores, such as anthrax.

3.c. Sensitivity

The various embodiments of the PI/QitTof MS instruments tested to date achieve detection limits of about 10-100 ppb with 5 s sampling periods for air sampling. Liquid sampling detection limits were <1 µg/mL in a variety of solvents (e.g., methanol and water) for direct syringe injection with typical volumes of <1 µL. Live agent testing was conducted for nerve agents, mustards and riot gas compounds at the ECBC Surety Lab. Figure 12 shows a plot of sensitivities for a variety of CWC relevant compounds. The bar intensities represent the concentration of compound in air required to give a fixed instrument signal strength (hence larger intensities represent poorer sensitivities). It should be noted that the range of sensitivities spans only about one order of magnitude and the typical variation in sensitivity between two random compounds is about a factor of 2. This is a relatively uniform response compared to other ionization methods such as ESI and APCI.

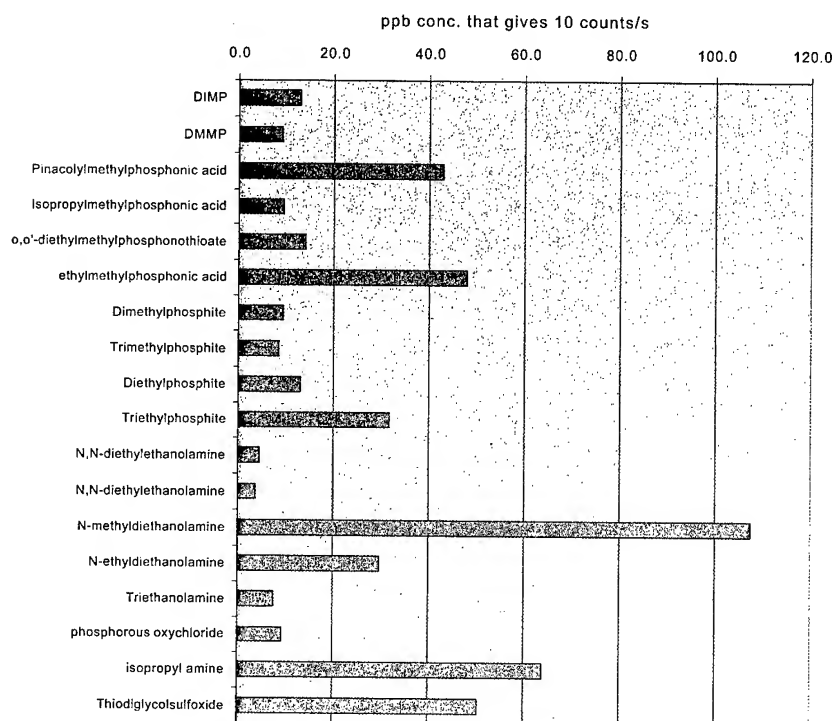


Figure 12

Plot of sensitivities for representative CWC-relevant compounds. Bar intensities represent concentration in air required to give 100 detected ion counts per second.

3.d. Dual Use Benefits

With increasing governmental regulations, environmental concerns, and military and civilian defense needs, the demand for real-time multispecies monitoring systems is growing rapidly. The specifications of the Syagen ChemBio MS instrument meet the requirements for a broad range of military and civilian applications including:

- Military force protection from threat of CB terrorism
- Chemical demilitarization, biological/toxin weapons convention verification and counterproliferation

- Emergency first response for hazardous materials
- Law enforcement for crime scene investigation requires portable detection systems
- Air quality monitoring of large public venues for civilian defense
- Environmental pollution monitoring in municipal water facilities and public waterways
- Medical diagnostics for infectious disease monitoring and for biomolecular analysis

CONCLUSIONS

Chemical and biological agents are weapons of mass destruction that are accessible to terrorists and rogue organizations because of their simplicity and low cost. In order to develop better means to counter these threats, economical, high-resolution, field-portable biological and chemical detection systems are needed. High speed is needed for rapid response in threat situations and for high throughput analysis for treaty verification and nonproliferation monitoring.

In this paper we have focused on Syagen's progress toward fielding a low-cost, high-resolution, field-portable detection systems for rapid and reliable chemical and biological (CB) agent monitoring. Effective sensors must integrate the requirements for efficient recovery of microorganisms, processing of microorganisms for detection, and molecular analysis for accurate pathogen identification. For in-field detection, the sensors must be compact, rugged, reliable, and low maintenance while achieving exceptional levels of sensitivity, specificity, and speed. The instrument criteria that this work addresses are:

- Real-time (1 min), field-portable, molecular detection system for identifying chemicals, pathogens and biological agents
- Dual chemical and biological (CB) air sampling capability with high sensitivity and specificity for low false positive and negative responses
- Automated, rugged, low maintenance operation and low upfront and recurring costs

Syagen has demonstrated the feasibility of a field-portable, ultrasensitive, real-time monitor. The ionizer/mass analyzer technology is readily adapted to front-end sample collectors, concentrators, and/or separators such as aerosol and particle collectors, thermal desorbers, gas chromatographs, etc.

ACKNOWLEDGMENTS

This work was supported by the Defense Threat Reduction Agency and by U.S. Army SBCCOM. We also acknowledge the contributions of Dr. Mark Hanning-Lee on software and Dr. Yong Liu on experimental assistance.

REFERENCES

- ¹ D. H. Tomlinson and H. L. Feller, "Improved automated analysis for nanogram quantities of organophosphorous agents GB and VX," (U.S. Army, ED-TR-76045, Aberdeen, 1976).
- ² W. R. Barger, et al., *Proc. 1985 Conf. Chem. Def. Res.*, (U.S. Army, CRDC-SP-86007, Aberdeen, 1986), p. 613.; H. Wohltjen, *Sensors and Actuators* **5**, 307 (1984); H. Wohltjen, *Anal. Chem.* **56**, 87 (1984).

- ³ F. E. Ferguson, M. W. Ellzy, and L. Gail Janes, "Analysis of VX and GB by gas chromatography / Ion trap spectroscopy," (U.S. Army, CRDEC-TR-029, Aberdeen, 1989).
- ⁴ L. R. Ember, *Chem. & Eng. News*, p. 26 (Aug. 1, 1994).
- ⁵ D. E. Riegner, et al., *Proc. Conf. Chem. and Bio. Def. Res.*, (U.S. Army, Abstract Digest, Aberdeen, 1995), p. 38.
- ⁶ J.A. Syage, M. A. Hanning-Lee, and K. A. Hanold, "A man-portable, photoionization mass spectrometer," *Field Anal. Chem. Tech.* **4**, 204 (2000).
- ⁷ J. A. Syage, M. D. Evans, K.A. Hanold, "Photoionization mass spectrometry," *Amer. Lab.*, in print (2000).
- ⁸ S. M. Michael, B. M. Chien, and D. M. Lubman, *Anal. Chem.* **65**, 2614 (1993); S. M. Michael, M. Chien, and D. M. Lubman, *Rev. Sci. Instrum.* **63**, 4277 (1992).
- ⁹ P. H. Dawson, *Quadrupole Mass Spectrometry and its Applications*, (AIP Press, New York, 1995). J. F. J. Todd, "Ion Trap Mass Spectrometry - Past, Present, and Future," *Mass Spectrom. Rev.* **10**, 3 (1991). R. G. Cooks, G. L. Glush, S. A. McLuckey, and R. E. Kaiser, "Ion Trap Mass Spectrometry," *Chem. & Eng. News* (March 25, 1991), p. 26.
- ¹⁰ S. A. McLuckey, G. J. Van Berkel, D. E. Goeringer, and G. L. Glush, *Anal. Chem.* **66**, 689A (1994).
- ¹¹ J. A. Syage, in *Lasers and Mass Spectrometry*, edited by D. M. Lubman (Oxford Univ. Press, New York, 1990), p. 468. D. M. Lubman, ed., *Lasers and Mass Spectrometry*, (Oxford University Press, New York, 1990).
- ¹² S. M. Michael, B. M. Chien, and D. M. Lubman, *Anal. Chem.* **65**, 2614 (1993); S. M. Michael, M. Chien, and D. M. Lubman, *Rev. Sci. Instrum.* **63**, 4277 (1992).
- ¹³ J. A. Syage, M. A. Hanning-Lee, and K. A. Hanold, "A man-portable, photoionization, time-of-flight mass spectrometer," *Field Anal. Chem. & Tech.*, **4**, 204-215 (2000); paper elsewhere in these proceedings
- ¹⁴ J.A. Syage, B. J. Nies, M. D. Evans, and K. A. Hanold, "Field-portable, high-speed GC/TOFMS," *J. Am. Soc. Mass Spectrom.*, submitted (2001).
- ¹⁵ S. A. Barshick, D. A. Wolf, and A. A. Vass, "Differentiation of microorganisms based on pyrolysis-ion trap mass spectrometry using chemical ionization," *Anal. Chem.* **71**, 633 (1999).
- ¹⁶ M. B. Wise, C. V. Thompson, R. Merriweather, and M. R. Guerin, *Field Anal. Chem. Tech.* **1**, 251 (1998); S. A. Lammert and J. M. Wells, *Rapid Commun. Mass. Spectrom.* **10**, 361 (1996).
- ¹⁷ A. Tripathi, R. P. Lall, L. Katsoff, K. Ong, and A. P. Snyder, *Scientific Conf. on CBD Res.* – Abstract Book, p. 83 (Nov. 1998).
- ¹⁸ A. Tripathi, A. P. Snyder, R. Lall, L. Katsoff, K. Ong, and R. Shama, "An improved quartz tube pyrolysis technique that produces approximately 1000 Dalton primary pyrolysis products from proteins, *Proc. 47th ASMS Conf. Mass Spectrom and Allied Topics* (1999).
- ¹⁹ F. Basile, T. L. Hadfield, and K. J. Voorhees, *J. Appl. & Environ. Microbiol.* **61**, 1534 (1995).
- ²⁰ Dr. A. P. Snyder, personal communication.

STRATEGIES FOR THE DETECTION OF UNKNOWN BIOLOGICAL MATERIALS

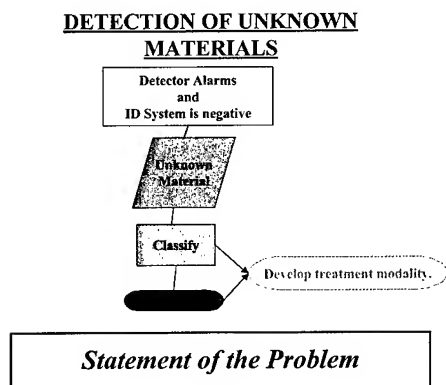
Peter J. Stopa

US Army Edgewood Chemical Biological Center, 5183 Blackhawk Road, AMSSB-REN-E-MC,
E3549, Aberdeen Proving Ground, MD 21010-5424 USA
(Peter.Stopa@SBCCOM.APGEA.ARMY.MIL)

ABSTRACT

Current strategies for the detection and identification of biological agents are largely dependent on known biological entities – specific biochemistries, specific antigens, and specific nucleic acid sequences. But what about unknown agents, either natural or man-made? Can these agents elude current or proposed detection/identification schemes? Are there strategies that can be implemented now or in the future to detect these?

Using the current template of trigger, detector, or identifier, strategies will be discussed that one can use to detect unknown materials of biological origins. For example, generic detection schemes may have a role in this area. Several recent efforts have investigated the use of pathogen receptors, such as the Gm1 ganglioside, for detection while specific nucleic acid sequences, which are known as “islands of pathogenicity”, have been proposed for identification. Perhaps these types of approaches might be exploitable in future detection/identification efforts.



Detection and identification strategies, as they might be applied to the detection of unknown materials, will be reviewed as to speed, complexity, and information generated. Trade-offs among these parameters and the introduction of new detection and identification schemes in concert with current, proposed, or futuristic technologies will be discussed.

A course for the next generation of biological detection and identification equipment will be proposed. Its intent is not to solve the problems, but perhaps to provoke new ideas, so that effective biological detection capabilities for the 21st century can be developed.

INTRODUCTION

The key to mitigating and perhaps deterring the use of biological weapons is real time detection and warning so that the appropriate protective measures can be taken. In the post attack scenario, it is even more important to identify and classify the type of agent that was used so that the appropriate medical countermeasures can be taken to minimize or eliminate casualties. Several systems have been developed to provide detection and alarm of a biological agent attack. These first generation systems provide detection of generic or specific characteristics of an aerosol cloud in order to detect changes in background aerosol content. This may be indicative of a man-made (not natural occurring) event that represents a possible attack with a biological agent or agents. Characteristics, such as particle size, shape, fluorescence, specific biochemical markers, and/or immunoreactivity, are currently utilized to obtain this initial information.

Natural vs. Man-made

Parameter	Test	Rationale	Status
Particles	Particle-size Analysis	Most man-made aerosols are > 3 um	Available (Field) - requires readjustment of existing algorithms.
	Particle-shape Analysis	May see uniform distribution of similar particle shapes.	Available (Field) - requires refinement of existing ASAS, FLAPS, BAWs, or DAWN systems.
Elemental Analysis	Spectrometric analysis	May see "unnatural" elements or ratios of elements appear.	Available (Field) - Photoionization detectors (PO ₄ , SO ₂) In Development - Sondebio System (France)
	Active/Passive Standoff	May see spectra from silica, cellulose, or other organics.	Requires investigation using existing platforms.
Propellants	Standoff Gas Analyzers IR FLIR FT-IR Spectrometers	May see propellants or other gases	Requires investigation using existing platforms

Parameters that can be used by trigger devices to differentiate between natural and unnatural aerosols.

Based on a suspected aerosol change, systems can then initiate an alarm and/or sample collection sequence for further confirmatory analysis. Today's systems typically use automated immunological identification against a specific agent list. More stringent identification techniques, utilizing nucleic acid probe technologies, are currently under development by several nations.

However, it is obvious that several parallel signatures are required to provide highly reliable information needed by unit commanders and medical personnel. No single test method is sufficient. The use of trigger, detector, and identifier modules has helped to address this issue. Therefore, one must look at technologies for these applications in concert with each other.

Encapsulants

Parameter	Test	Rationale	Status
Particle Measurements	Refractive Index	Encapsulated particles may have larger sizes, changes in refractive index, etc.	Technology exists.
	Shape		Need development or implementation program.
	Density		
	Particle Size	Could be detected by scatter.	
Absorbance	Absorbance Spectra (UV/Vis/IR)	Encapsulants may impact the absorption spectra of biological materials.	Technology exists. Needs development or implementation program. Could be implemented into existing platforms.
Composition	Mass spectrometry	Studies have shown that some encapsulant materials have unique signatures.	Technology exists.
	Py-GC-IMS Elemental analysis		Need development or implementation program.
Dissolution	Dissolution Testing followed by additional analysis.	Aqueous media may effect release of encapsulated material.	Technology exists. Need development or implementation program.

Immunoassays have been one of the most effective technologies used for accurate and rapid identification of agents to date. However, with advances in molecular biology becoming commonplace, the capability for

Strategies for the detection of encapsulated materials.

designing novel threats undetectable by immunoassay is a reality. Thus other bioanalytical methods such as genetic identification methods are required even for the currently established threat list. For example, genetically engineered threats, or bio-agents or their genes that are encapsulated in materials such as liposomes or commonly occurring organisms would not be identified by current immunoassay methods. As well, genetic identification provides complementary and confirmatory data to improve diagnostic accuracy and confidence, thereby reducing false identification of threat agents.

There are essentially two areas where an increased capability to detect unknowns is required. The first is the initial detection of bioaerosols events. There is a need to ability to clearly and reliably differentiate between naturally occurring biological events and true biological agents. This will require research to understand the attack signature of biological attacks, understanding of natural background phenomena, and the characteristics/impact of novel agents.

The second component of detection of unknowns is the ability to differentiate between harmless or benign biological content of an aerosol (either natural, man-made, or bio-attack). This would be a requirement to determine in a generic manner whether a biological is dangerous, poses a threat to health, and if medical countermeasures are required. In plain language, the detector has alarmed and determined that a significant biological event has occurred. Now how do we know what has been collected is harmful when the specific identification technologies (currently a limited list of immunoassays) do not identify the agent? For example, a timely answer such as "this is a genetically modified agent which will cause anthrax" would be most valuable!

Currently, it is expected that a sample would be taken and analyzed in a more sophisticated field lab (e.g. theater army medical lab, field lab) or at an out of theater analytical facility. This will provide an answer, eventually, but not in the time frame required to provide the commander critical information for protection and countermeasures.

Objectives for Detection of Unknowns

The objectives of a field capability to detect/identify unknown agents are to assist a commander in his decision making, including decisions on whether:

- To initiate treatment in the absence of an identification of a specific biological agent hazard;
- To implement and maintain protective postures;
- To confirm whether his forces have been subjected to an attack; and
- To differentiate between natural and artificial events.

Pathogen/non-pathogen Determination

Parameter	Test	Rationale	Status
Virulence Determination	Binding to ganglioside	A variety of pathogens and toxins bind to gangliosides, especially Gm1.	Available (Lab) - Approach has been used with cholera toxin, SEB, and others in a variety of formats. Could be integrated into a biosensor platform, possibly a bio-chip.
	Aptamer Binding	Could design aptamers to mimic pathogenic binding sites.	Concept demonstrated in the laboratory.
	Plasmid determinations by Flow cytometry pulse processing techniques.	Many virulence factors associated with bacterial plasmids.	Demonstrated in laboratory. Would have to be integrated into a platform of some type.
	Immunoassay for plasmid specific products.	Same as above.	
	Live cell assays.	Measure binding to a sentinel cell.	Demonstrated in the laboratory.

Strategies for Pathogen/non-Pathogen Detection.

Identification

Parameter	Test	Rationale	Status
Cellular Biochemistry	Metabolic Fingerprint	Routinely used for bacteriological identification.	Available (Lab) - Possibly used in field.
Virulence Factors	Immunoassays	Products of virulence plasmids can be identified by immunoassays.	Demonstrated in the laboratory.
	Nucleic Acid Analysis	Virulence plasmids can be identified by nucleic acid hybridization techniques.	Available (Field) - Fieldable nucleic acid analysis system demonstrated on several platforms.
	DNA Analysis by FCM pulse processing techniques.	Pathogenicity islands.	
Speciation Techniques: Indigenous vs. non-Indigenous strains	Chromosomal DNA analysis. RNA fingerprinting	Accepted techniques for bacterial identification.	Available (Lab) - Can be implemented into field situations.
Genetic Manipulation	Nucleic Analysis	Identify vector sequences. Identify markers associated with environmental stability.	Available (Lab) - Needs additional development to expand available library.

Parameters for Identification

- Resistance to treatment.

Other approaches may opt to interrogate for generic characteristics of biological materials, such as:

- presence of ATP;
- gram stain;
- fluorescence;
- physical properties including size, shape and density characteristics, or refractive index.

Markers that are associated with the weapon itself, that when found in conjunction of a biological aerosol change, should also be investigated as the basis for determining the presence of a BW agent. Markers may be identified as explosive residues, propellants, engine exhaust, etc.

From this discussion, it should be apparent that there are a variety of signatures that one could exploit to use as in either a trigger or detector mode to determine if there is unknown biological material in an aerosol.

Strategies to determine treatment

To meet these objectives, technological solutions must provide a timely response. In this context the technologies need to provide information in time for it to be useful to the battlefield commander.

Detection of a biological aerosol possessing *characteristics* indicative of the presence of BW agents would be a viable approach. For example, detection of:

- pathogenicity markers, or indicators of pathogenicity infectivity
- common cell responses to biological agents;
- viability, possibly through monitoring of ATP or related biochemicals, genetic techniques including rapid sequencing, or monitoring enzymatic activity, and

Treatment Modality

Parameter	Test	Rationale	Status
Antibiotic sensitivity testing	Rapid MIC on FCM	Regardless of ID result, need to know effectiveness of antibiotic therapy.	Available (Lab) - Demonstrated on the FCM (40 minute test). Commercially available systems available systems (8 hrs.)
Immune System Status	Flow Cytometer	FCM routinely used to assess immune system status.	Available (Lab) - Commercially available product.
	Luminescence	Simple ATP luminescence can be used to show clearance of bacteria from whole blood.	Demonstrated in laboratory.
	Other Biochemical test.	Other tests can be used to assess immune system function.	Commercially available products.
Antiviral Sensitivity Testing	Plaque neutralization tests	Used to assess response to antiviral drugs.	Demonstrated in lab. Not widely used.
	FCM applications	Can potentially provide a more rapid screening capability.	Needs to be investigated.

IDENTIFICATION AND MEDICAL COUNTERMEASURES

Once a determination has been made in the field that a biological event has occurred, the next step would be to retrieve the suspect samples and return them to a lab for further identification and classification. The current rationale, that one needs to know the identity of the particular agent so that the proper treatment modality can be employed, needs to be re-evaluated. In classical medicine, if one knows the identity of the organism, one can typically prescribe the appropriate course of antibiotics or other therapies. However, with the advent of genetic engineering and the relative ease that this allows an adversary to impart resistance to common antibiotics, one can no longer assume that the mere identification of the organism would be sufficient for treatment. Even in conventional medical approaches, there has been an increase in the use of susceptibility tests to determine the appropriate course of treatment. In the case of an intentional release of a biological agent by an adversary, this is even more important.

Therefore, the approach that one should take for mitigation of the event is two-fold. First of all, identification and classification of the organism is important so that the entity that we are dealing with is known. This perhaps is more important for the national command structure rather than for the battlefield treatment of the agent. Secondly, susceptibility testing should be undertaken so that the appropriate treatment modality can be determined. This is more important to the field commander and most important to the casualty.

CONCLUSIONS

From this brief discussion, it can be shown that the problem is not insurmountable; however, several things need to change.

- The user needs to become aware that the possibility does indeed exist that "unconventional" biological agents could exist and possibly could be encountered in the field.
- There are a variety of strategies that could be implemented in either trigger or detection platforms that could be used to detect signatures from unknown biological agents and possibly determine that they could present a danger to health and life.
- Although identification is important in the field, the most important thing is to provide a detector that exploits a credible signature for warning so that those in peril can take the appropriate protective measures.
- Identification may not be important for the appropriate medical countermeasures to be taken; however, other actions, such as susceptibility testing, are.
- Some of the technology exists today that can be implemented in the field for this purpose.

AEROSOL GENERATION FOR TESTING BW DETECTORS

Jerold R. Bottiger, Edward W. Stuebing, and Paul J. Deluca
U. S. Army Edgewood Chemical Biological Center
Aberdeen Proving Ground, MD

Scientists of the Aerosol Sciences Team at ECBC have developed two aerosol generation tools specifically tailored to the needs of the community developing BW detectors. The handheld "puffer" is the ultimate in portable convenient aerosol sources, and ejects a small reproducible cloud of simulant aerosol particles at the push of a button. It can be used as a quick source of particles in the laboratory, and as a confidence checker for equipment deployed in the field. The Ink Jet Aerosol Generator (IJAG) is a laboratory instrument that enables the clean and precise delivery of low concentrations of aerosols to BW detection instruments. Particles in the 1 – 10 micron range and composed of virtually any substance – simulants or live agents – can be produced and used to test the detection threshold limits of candidate instruments.

A puffer is a metered dose inhaler that, when activated, releases a 60-mg spray of its contents into the air. A typical formulation is 0.1% or 1.0 % by weight of simulant material in 1,1,1,2-tetrafluoroethane (HFA-134a) as the propellant. HFA-134a is the environmentally friendly replacement for R-12 Freon in refrigeration applications. The inhaler body is filled under pressure with liquefied 134a propellant and crimped shut with a cap that holds the metering valve. When the puffer is activated (held valve-end downward and the valve depressed) a measured volume of the contents is released to the atmosphere where it expands and evaporates instantly, leaving a small cloud of the loaded particles.

Puffers are commonly used in a semi-quantitative application, quickly checking whether a piece of detection equipment is set up and working properly by its response to the puff. The mass and characteristics of particles ejected per shot is known and quite reproducible, but generally the fraction of those particles entrained by the detector's intake is less certain. Since the shot-to-shot mass variation is small, about 10%, a puffer could also be used to fill a small chamber for more quantitative experiments.

The most popular puffers are loaded with Bg spores or ovalbumin powder. Figure 1 shows the number and mass particle size distribution of the Bg that is loaded into puffers. The peak at about 1 micron corresponds to single spores; the larger particles, evident in the mass distribution, are bits of diatomaceous earth mixed with the Bg. These data were obtained by blowing a small quantity of Bg powder with compressed air into a 2-foot diameter (118 liter) aluminum aerosol chamber. The chamber rests on top of a TSI Model 3320 Aerodynamic Particle Sizer (APS), with the APS intake nozzle protruding through a hole in the chamber bottom. Other ports in the chamber permit introduction of samples, and vacuum cleaning between runs.

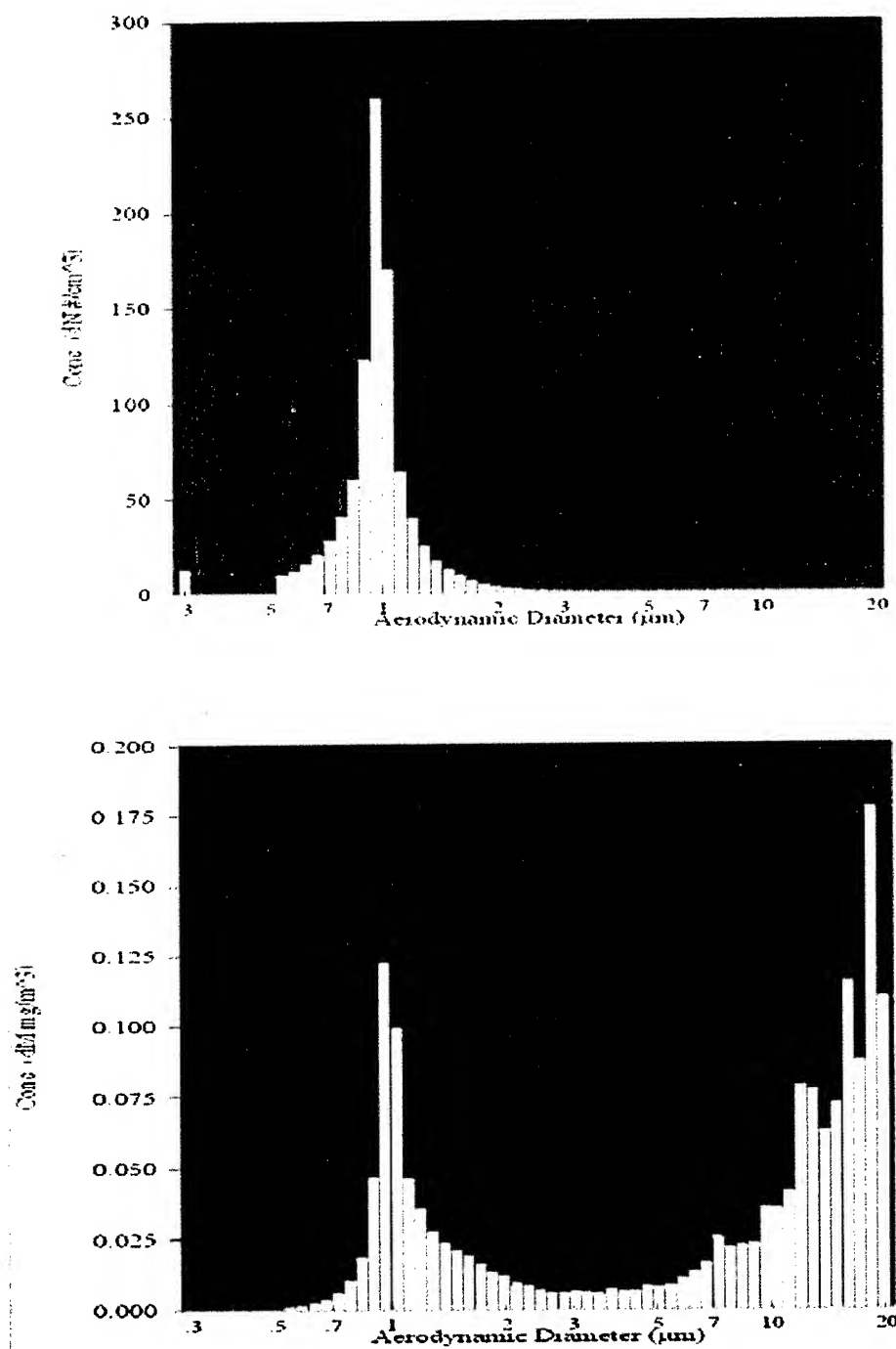


Figure 1. Number and mass particle size distribution of Bg powder.

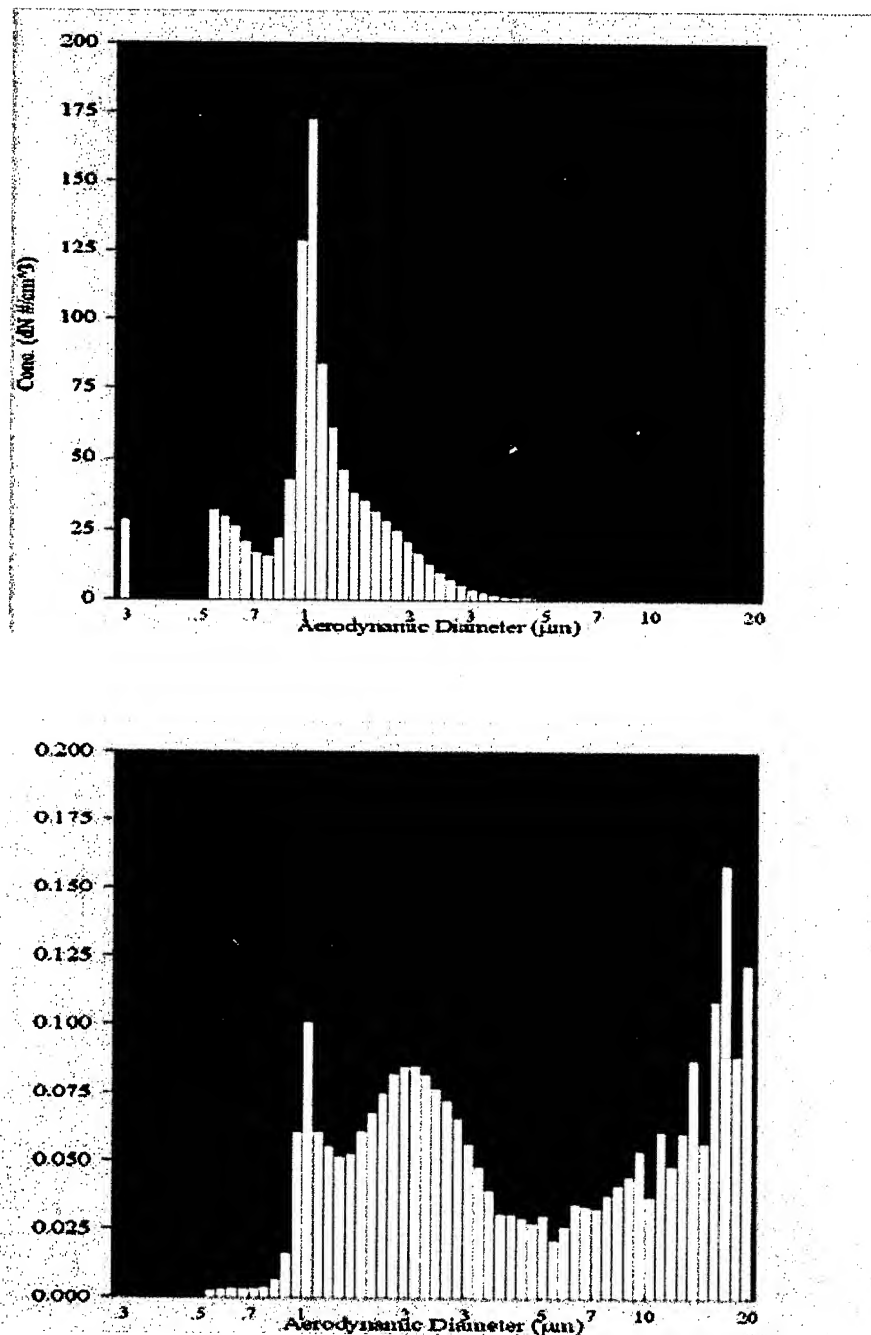


Figure 2. Number and mass particle size distribution of Bg puffer output.

Figure 2 shows the output, five shots into the chamber, of a 0.1% Bg puffer. A significant fraction of the once single spores are now found in clusters, up to 3-4 micrometers diameter. The mass peak of the new clusters is just over 2 micrometers diameter, corresponding to 10-15 spores per cluster. The number distribution shows a mode of submicron size particles that was not present in the original powder, Figure 1.

The submicron mode is shown alone in Figure 3, which is the output, three shots, from a puffer that has been loaded with nothing but propellant. Every puffer produces these particles in addition to the particles deliberately loaded. When the propellant-only puffer is sprayed onto a microscope slide we find small nonvolatile liquid droplets. We think this is an oil-like contaminant in either the propellant or the canister body. The submicron oil droplets are visible on the left side of the sprayed Bg number distribution, and may also be the residual material that binds spores together in the rapidly drying propellant spray droplets to make clusters.

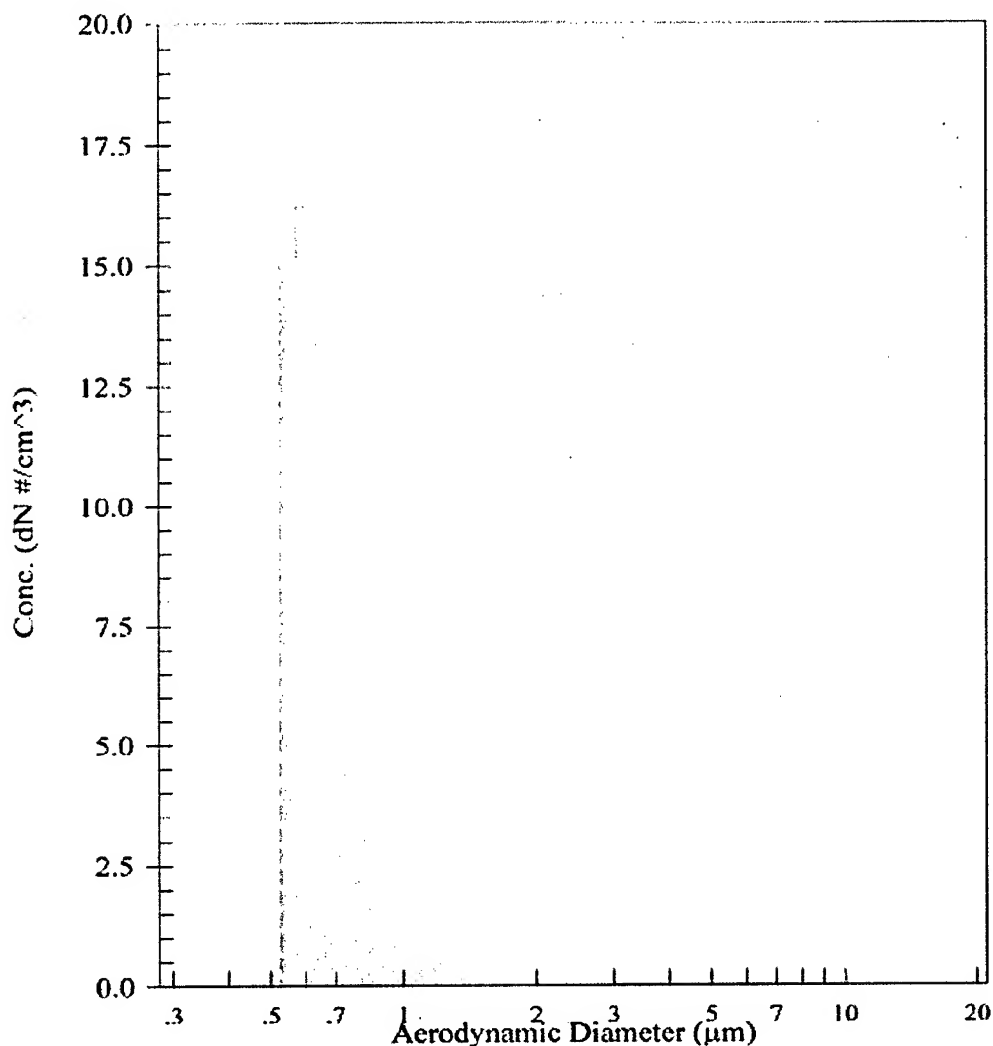
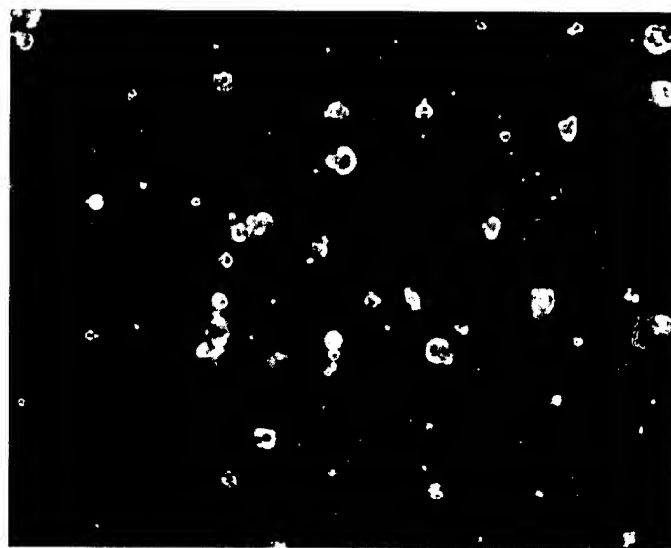


Figure 3. Number size distribution of contaminant particles from a blank puffer.

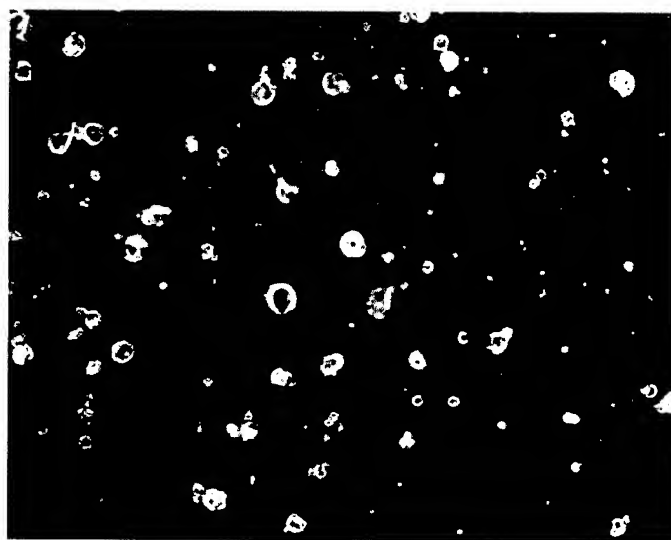
Ovalbumin puffers are loaded with Sigma Chicken Egg Albumin, Grade II, Crude, which is a light clumpy powder. Under a microscope it has the appearance of glassy sphere-like particles, with sizes

ranging from just visible (~1 micron) up to 30-40 micrometers diameter, and is clearly the product of a spray drying process. The larger particles are brittle and hollow.

Ovalbumin powder was blown into the aluminum chamber and allowed to settle overnight onto a microscope slide. A second slide was prepared by directing the spray from a 1% ovalbumin puffer onto it. The slides are compared in Figure 4, where no differences are evident.



(a)



(b)

Figure 4. Ovalbumin particles from (a) original container and (b) a puffer.

The APS particle size distribution of ovalbumin blown into the aluminum chamber is shown in Figure 5. The number distribution has a distinctive triangle shape centered at about 2 micrometers. Because there are a relatively small number of particles carrying the mass in a shot of ovalbumin, the

number particle size distribution from a puffer is dominated at low diameters by the contaminant particles noted above. Figure 6 shows the particle size distribution from an ovalbumin puffer; above about 2 micrometers the number distribution follows the pattern of the original powder, but below it the ovalbumin is obscured by the contaminant, which goes far off-scale. One cannot tell whether there has been any agglomerating of the smallest ovalbumin particles. On a mass weighting the original powder and puffer output look very similar; the contaminant peak is just barely visible.

Experimental puffers have been loaded with other materials too, including casein, kaolin, MS2, Titanium dioxide, psl spheres, and vegetative mulch.

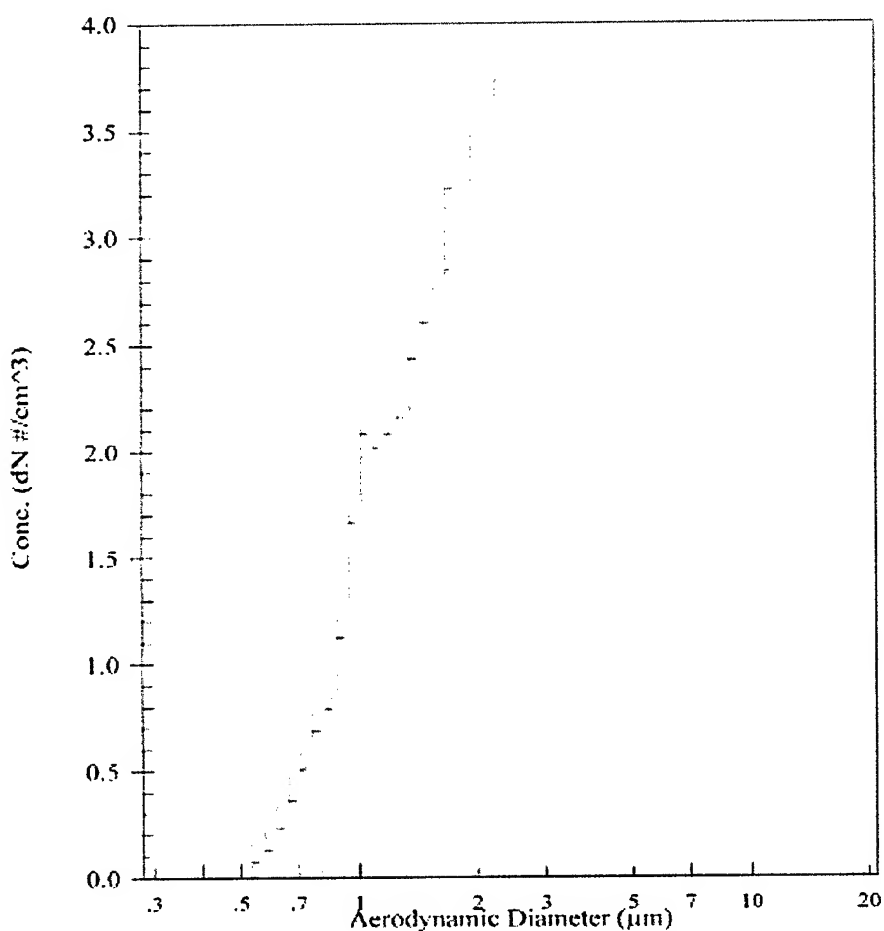


Figure 5. Number size distribution of ovalbumin particles from original container.

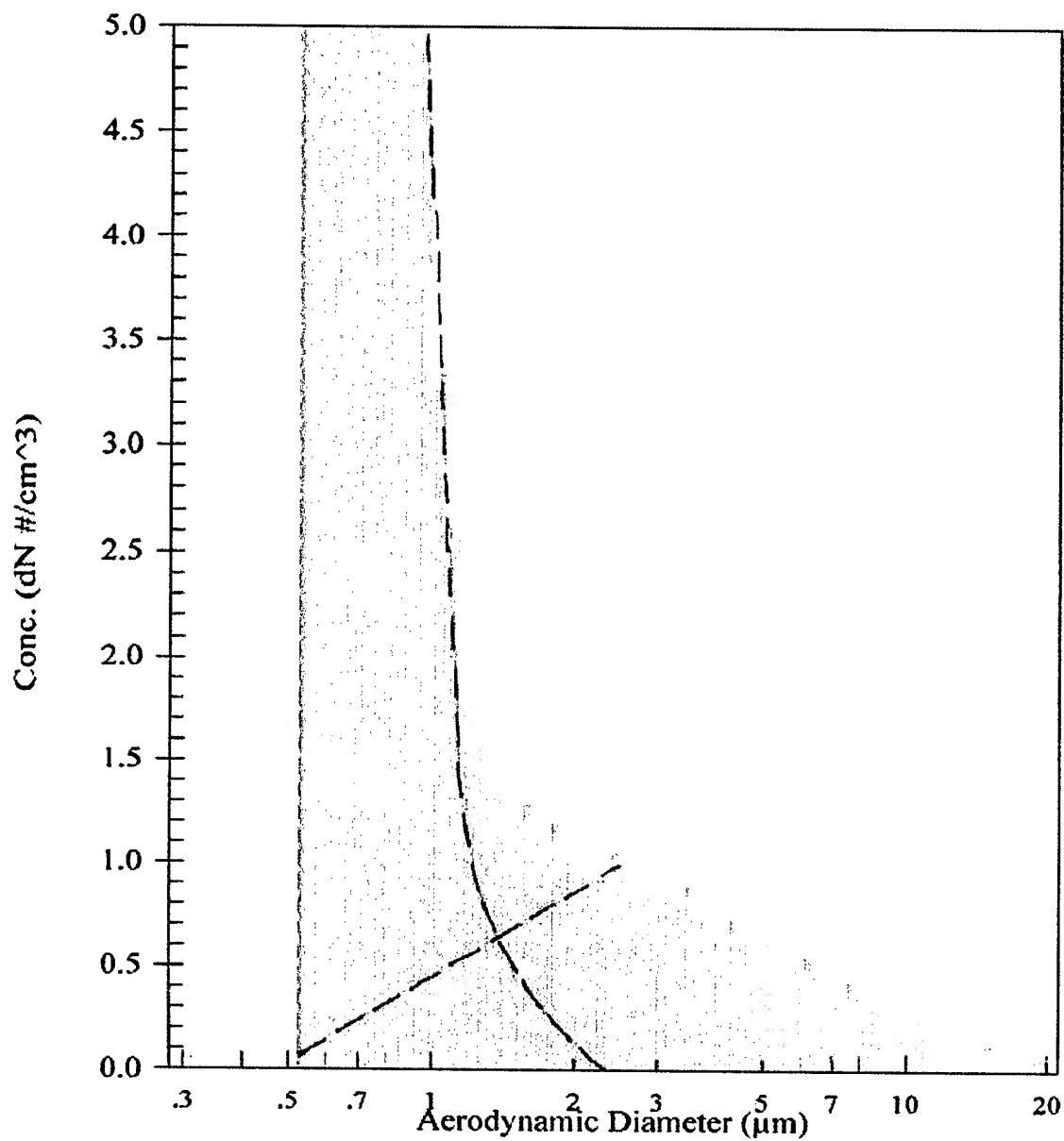


Figure 6. Number size distribution of output sprayed from an ovalbumin puffer, interpreted as the sum of submicron contaminant particles and ovalbumin particles distributed as in figure 5.

The Ink Jet Aerosol Generator (IJAG) adapts ink jet printer technology for the production of well controlled and well characterized aerosol samples. The IJAG comprises three components: the dispenser, the controller, and a computer, as shown in Figure 7.

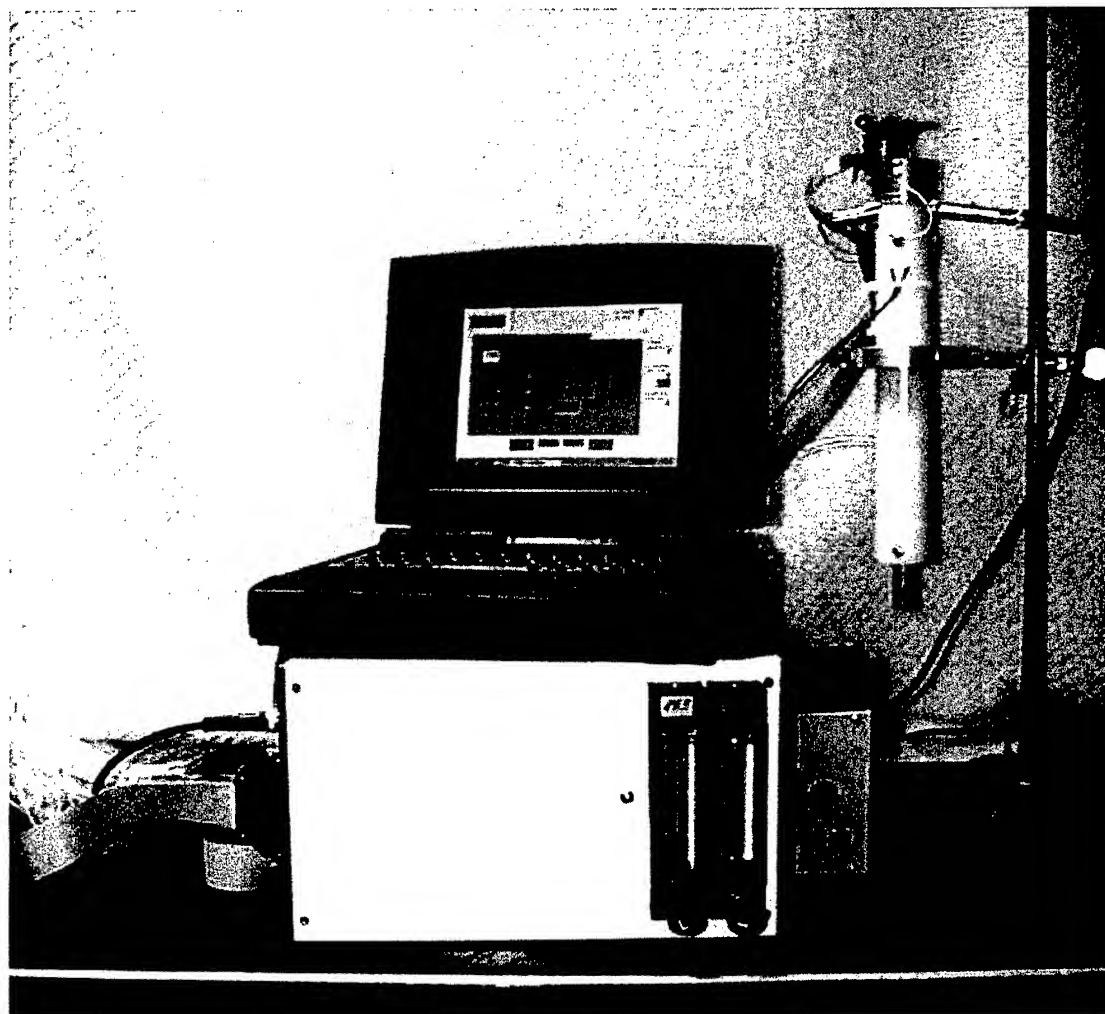


Figure 7. Computer controlled IJAG, comprising dispenser (with cartridge mounted on top), controller, and laptop computer.

The cartridge employed is the 12-nozzle model used in the old Hewlett Packard Thinkjet and Quietjet printers. We purchase the cartridges empty and load them in the lab with a slurry (or solution) of water and the material of which particles are to be made, at a concentration appropriate for the final particle size desired. The droplet emitted by this cartridge is about 50 micrometers in diameter, so, for example, to obtain a dried residue particle 5 micrometers in diameter the concentration should be 0.1%.

The loaded cartridge is mounted on the top of the dispenser, or head, and fires droplets downward through an oven that is the bulk of the dispenser. The oven is simply a brass tube, 5/8" diameter and 12" long, wrapped with heat tape and held at 250 degrees Fahrenheit. It is contained within a white delrin

tube, with the head mounted on top. As the droplets of slurry travel down the oven the water evaporates off and the non-volatile contents coagulate into compact and roughly spherical aggregates before reaching the bottom. Figure 8 is a sketch of the dispenser showing the airflows. Note that air pumped into the bottom of the dispenser is heated as it rises, and divides into two flows: most of the hot air leaves through the oven pipe, carrying the particles with it, while a smaller amount flows through an aperture into the head region and is returned to the pump. The air pump, filters and meters are within the controller.

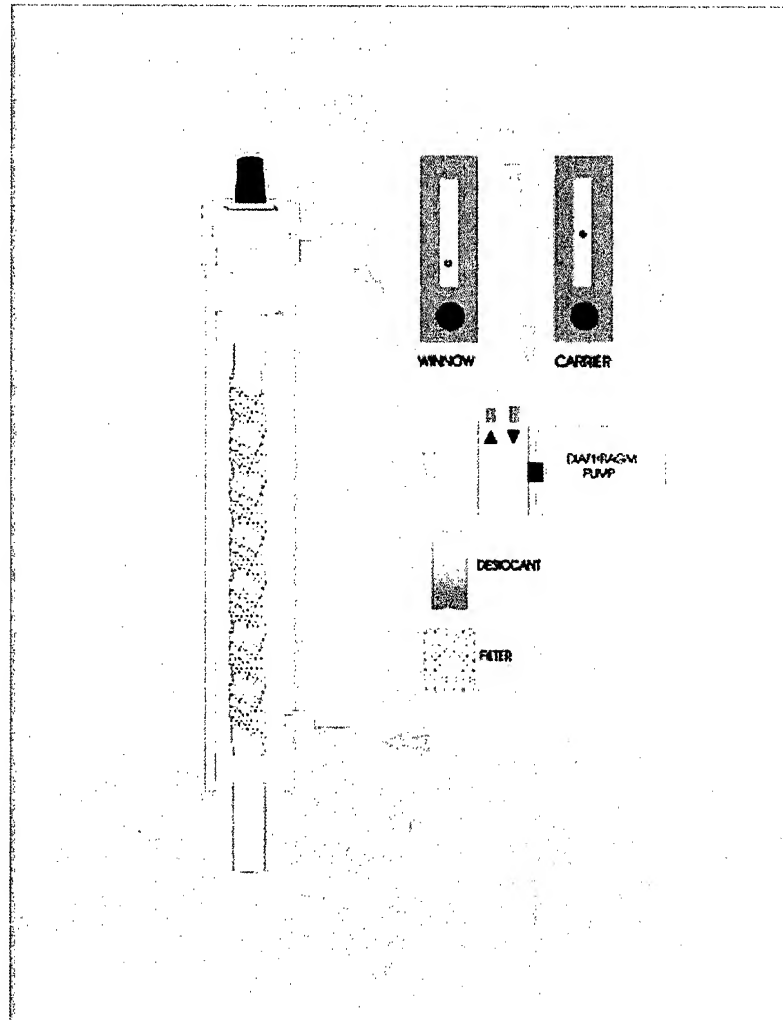


Figure 8. Cut-away sketch of IJAG dispenser, with airflows.

Inside the head are two features important for operation of the IJAG. The counterflow of air described above is used to winnow out the small satellite particles that are usually formed when an ink jet cartridge nozzle fires a droplet. The primary droplet is about 50 micrometers in diameter, while the largest of the satellite particles is about 30 micrometers. The aperture, through which particles fly downward against air moving upward, is located halfway between the primary and satellite stopping

distances. See Figure 9. So long as the velocity of the upward winnow flow exceeds the terminal settling velocity of 30 micron particles (2.7 cm/sec, or 80 ml/min through a 5/16" aperture), no satellite particles can penetrate the aperture to enter the oven. The larger primary particles, which have not yet lost all of their initial momentum, easily push through, losing only a few mm in stopping distance, and in fact not stopping until they are within the oven tube, entrained in the carrier flow.

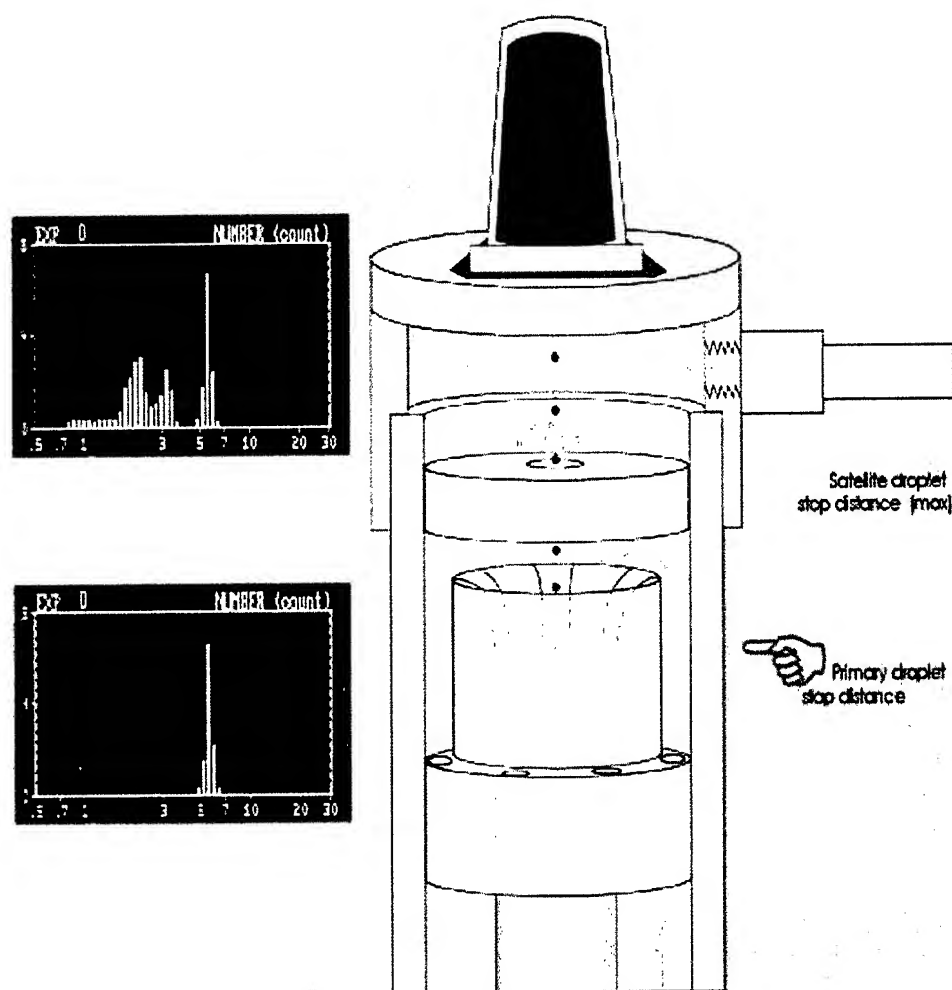


Figure 9. Satellite particles winnowed from primary particles by counter-flow.

The other feature is a light scattering based particle detector, located in the short gap (0.15") between the bottom of the aperture and the entrance to the oven tube. A laser diode with a 1mm x 4mm beam is mounted on the delrin body to direct its light across the center of the dispenser. A cylindrical

lens focuses the beam where it intersects the droplet trajectories, forming a 4mm wide thin sheet of light. On the opposite wall is a detector, comprising a lens and a photodiode, that picks up nearly-forward scattered light from the droplets as they traverse the beam to enter the drying oven. See Figure 10. Electronics in the controller box, connected by coax cable to the dispenser detector, process the photodiode output spikes to TTL pulses which are counted at the computer. The presumption is that any and every droplet that gets past the winnow aperture and crosses the light beam must continue down the oven to emerge a few seconds later as a dried particle.

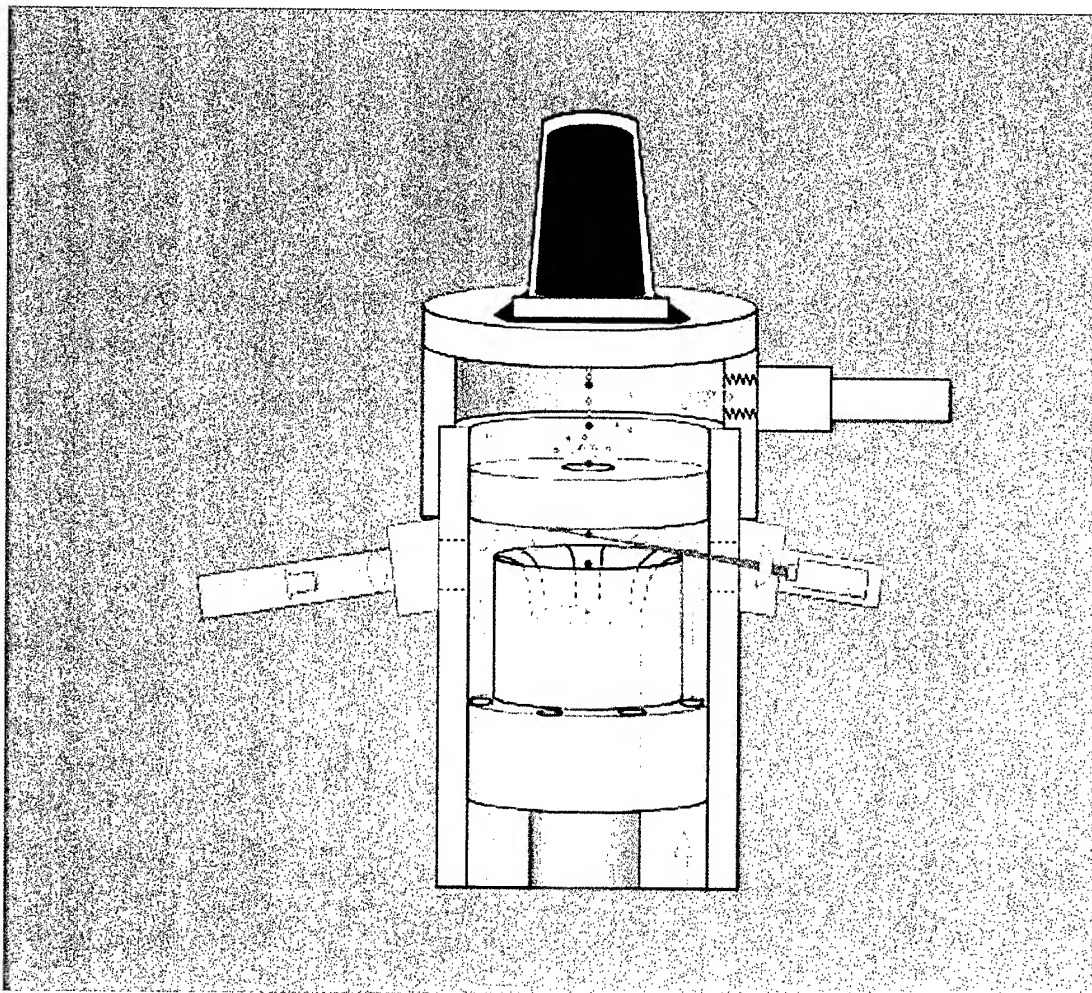


Figure 10. Light scattering detection of droplets entering the oven.

Within the controller box are two electronic circuits, the detector pulse processor just mentioned and the firing circuit that operates the cartridge heaters just under the nozzle openings. The firing circuit is paced by TTL square waves generated within the Timer/Counter interface card. On the leading (rising) edge of a pulse the next nozzle in sequence is made active via an extended decade counter, acting

similarly to a car engine's distributor. On the trailing (falling) edge the active nozzle heater is connected to 21 volts for 5 microseconds; the fluid in contact with the heater is vaporized and the expanding bubble forces a column of liquid out through the nozzle. The liquid filament has an initial velocity of about 8 m/s, and quickly fragments into a single primary droplet and 1-3 smaller "satellite" droplets. Figure 11 indicates the main IJAG components and the signals connecting them.

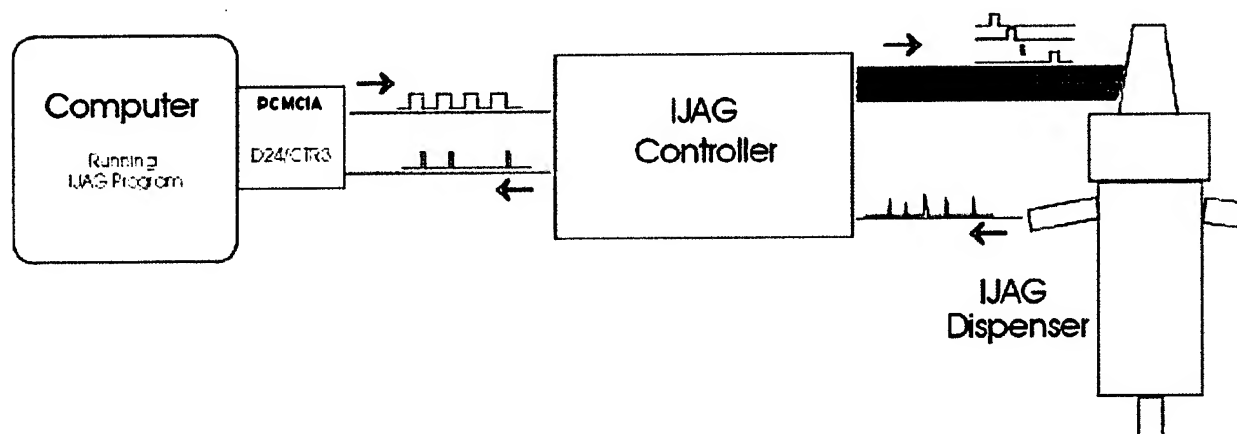


Figure 11. Flow of signals between IJAG components.

The IJAG is operated through a computer program that accepts directions from the user about what is desired and regulates the pacing square wave to carry out the user's wishes. Ideally each pulse of the square wave would produce one particle, but deterioration of the cartridge with use can cause some nozzles to fail. The program compares the number of particles detected to the number of pulses sent and calculates a correction factor to be applied to the next group of pulses. The correction is updated each second of operation.

Several modes of operation are available. The user can choose a fixed frequency of particle generation and allow the IJAG to run indefinitely, or for a set period of time, or until a set number of particles have been generated. The user can also write simple scripts of generation frequency vs. time to be executed by the program. Scripts of any complexity or length are permitted, enabling reproducible test patterns or simulations of BW clouds passing by. There is also a single particle mode that releases one particle each time the mouse is clicked.

The next three figures show photographs of particles made with the IJAG. Figure 12 is a field of 4-5 micron Bg clusters collected on a microscope slide, giving an idea of the particle shape and size dispersion. The inset is a SEM photo of one Bg cluster, just under 5 micrometers in diameter. Figure 13 shows four different sizes of Bg particles, from 4 to 9 micrometers. Cluster size is set by the concentration of the Bg slurry loaded into the cartridge. Figure 14 shows a field of yeast extract particles made with the IJAG. Yeast extract, used in culture media, dissolves readily in water, and is amorphous as it dries leaving almost perfectly spherical residue particles of very uniform size.

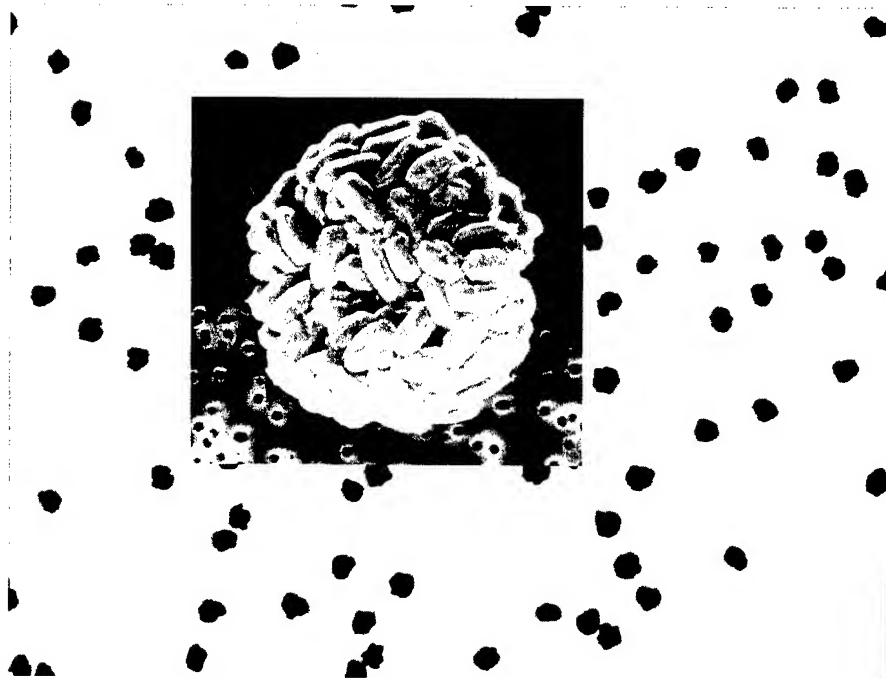


Figure 12. A sampling of 5-micrometer Bg clusters from the IJAG.

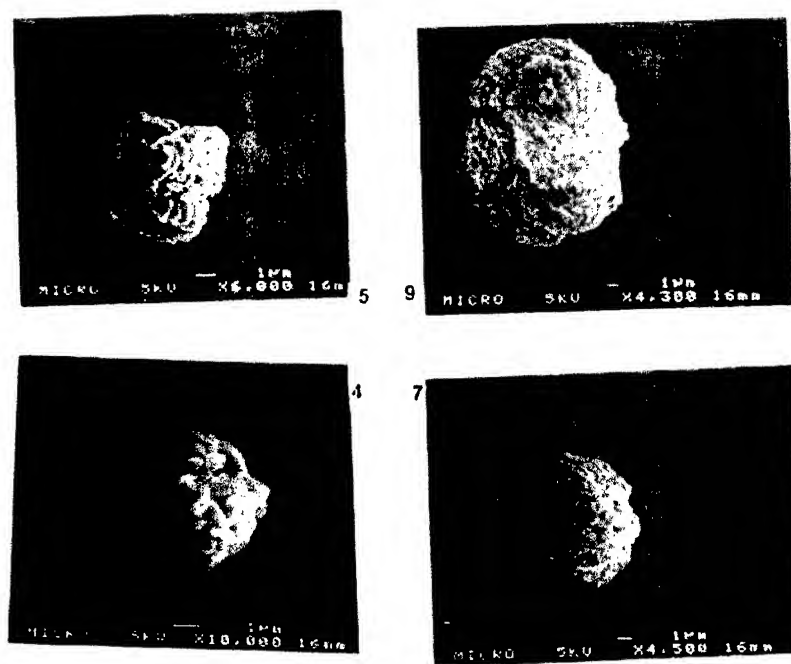


Figure 13. Bg clusters produced by the IJAG using different slurry concentrations.

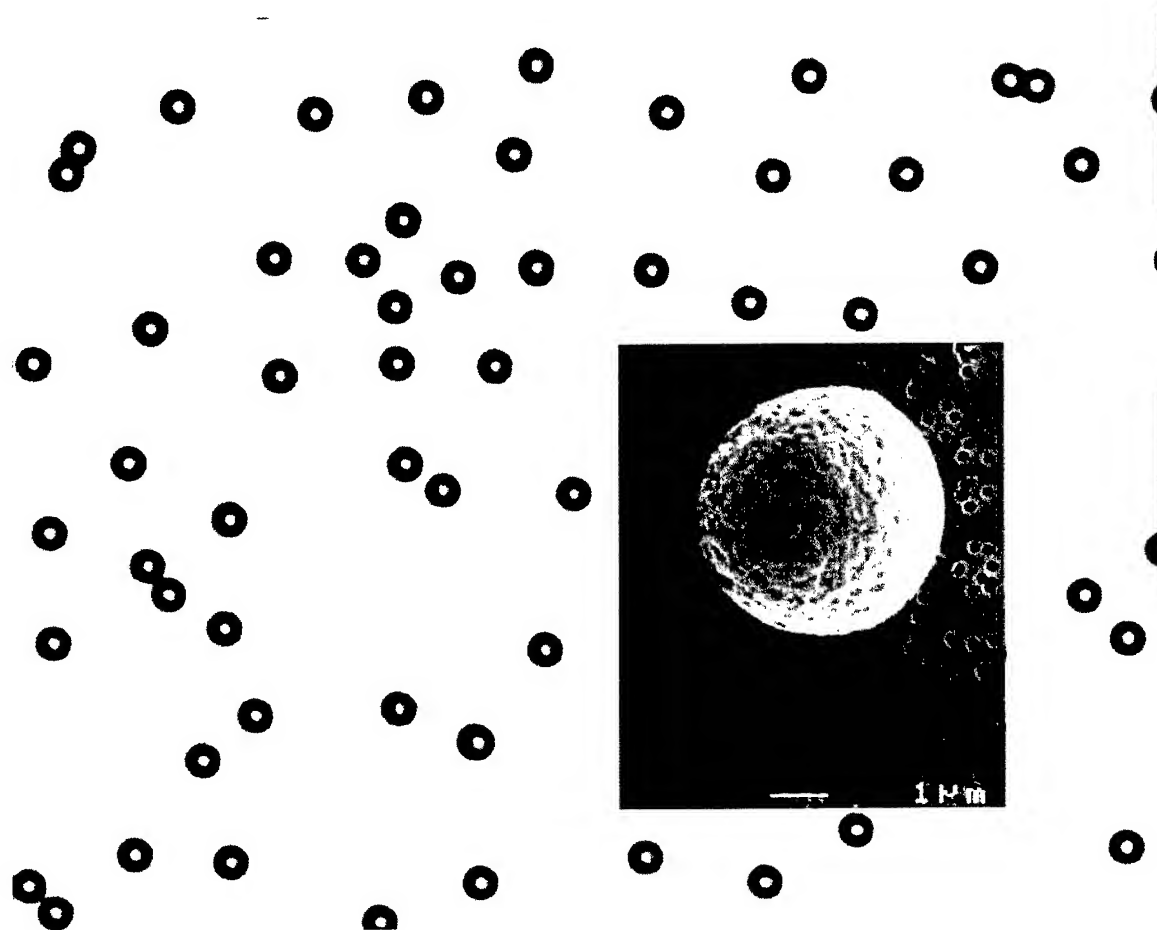


Figure 14. Nearly spherical particles made with the IJAG from yeast extract.

Figure 15 illustrates an IJAG script. It was desired to produce particles for two minutes at each of seven frequencies, from 10 particles per second to 800 particles per second. The solid line represents the scripted plan, the dots are APS counts of the IJAG output accumulated in 20- second intervals and converted to particles per second. The value of feedback in controlling the particle rate is also illustrated here, as this was an older cartridge with only seven of twelve nozzles still operating.

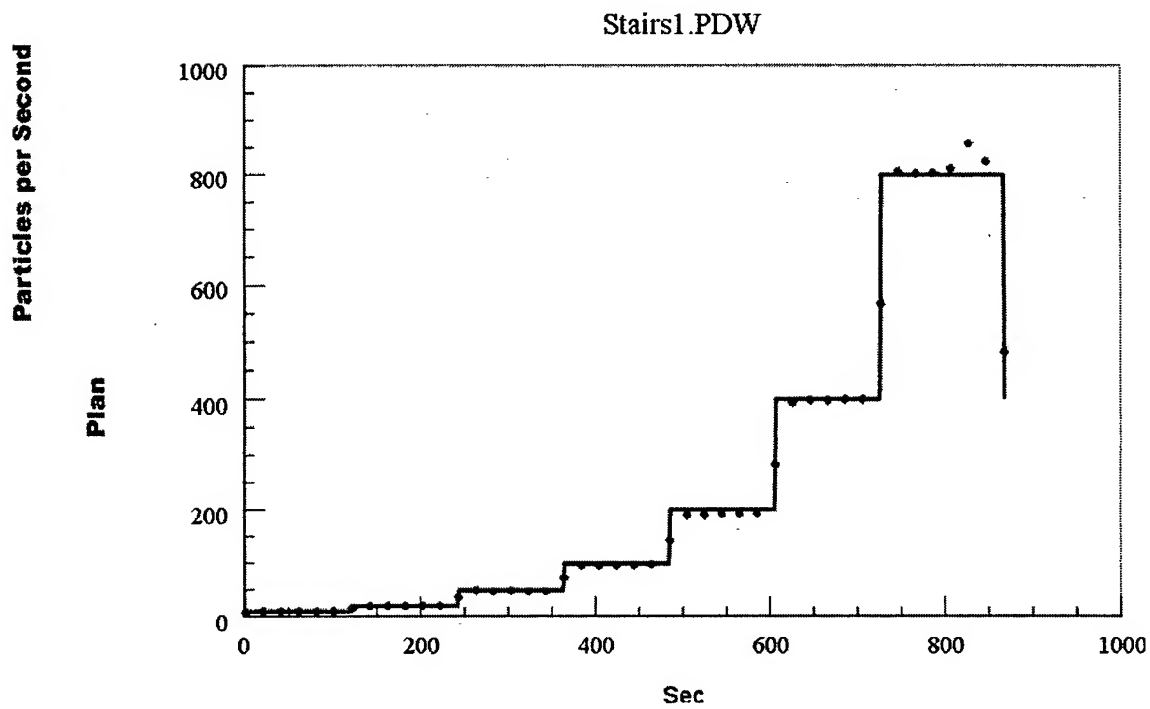


Figure 15. A test pattern of generation rate vs. time. The solid line is the intended pattern; the dots are APS count measurements of the actual IJAG output.

TEST PROTOCOL AND ALGORITHM DEVELOPMENT

G. Bodily, J.V. Mathews, J. Jarez, J. Dubow

Abstract

Testing of chemical/biological detectors is the basis of any program that attempts to understand detector operation or acquire a detector that meets specific requirements. This data is then analyzed and used as the basis of model development. Not all test protocols provide the same amount of information. The best test is simply a test that provides the most information (not necessarily the most data) for the least amount of resource expenditure. A discussion of specific test protocols is presented along with rationale as to why certain protocols are better than others. Experimental data is used to produce a dynamic model of the detector that is then used as the basis of algorithm development. Examining these models indicate it is possible for certain response characteristics to make detection algorithm development difficult. Implications of the algorithm development problem are discussed.

Background

The purpose of this paper is to suggest an approach for developing optimum methods for testing point detector systems, and provide a basic rationale for why these methods are needed. It should be apparent that algorithms are dependent on the hardware. So in the task of developing an algorithm we need to acquire information about how the sensor hardware works. In other words we need to develop a working model for the sensor that accurately reflects its performance over a specified range of conditions. To develop these models we generally run tests, and the primary purpose of running tests is to determine specific characteristics of the system. In detectors we want to learn how the sensor changes the environmental variables into signals (generally electrical) that we can read. This paper discusses a theoretical basis for general test protocols. Good test protocols will allow for dynamic models to be developed or validated. By examining a simple modeling methodology (ARMA^{1,2} models) some interesting relationships between sensor hardware and algorithms can be explored.

Linear dynamic systems were chosen because a wide range of systems can be adequately represented by linear systems, and because linear systems are well understood. It is hoped that this investigation will shed light on the directions in future work with more complex, non-linear systems.

This analysis will be applicable to all testing where there is a time component to the operation. For example a detector designed to measure O₂ concentration in the air takes a certain amount of time to register a change in the O₂ values. It also takes time to recover from upset conditions.

Linear Systems

Most of the systems of interest incorporate a digital sampling scheme. This includes any system that utilizes a digital computer in any form in its acquisition methodology. For this reason we won't use methods for continuous linear systems but will restrict our discussions to sampled linear systems. Continuous linear systems can be treated in a similar manner. We will further restrict the discussion to sampled systems where all system variables are collected at a constant rate known as the acquisition rate.

Dynamic systems are systems that have a specific time response. This includes all systems where we need to take previous history into account to accurately predict detector output. For example most chemical detectors take time to respond to a change in concentration, and take some other time to clear after the challenge is presented. Thus these chemical detectors constitute a dynamic system.

Linear systems can be represented by a finite difference equation.

A finite difference equation can be represented as

$$y_n = \sum_{i=0} b_i u_{n-i} - \sum_{i=1} a_i y_{n-i} \quad \text{Equation 1}$$

where y_n is the output at time n and u_n is the input at time n .

If we select the coefficients a and b correctly equation 1 becomes a dynamic model of the sensor. This form is an Infinite Impulse Response (IIR) filter or an Auto Regression Moving Average (ARMA) model. There are several other linear models available such as ARIMA, ARMAX, etc. These are similar to the ARMA model but are beyond the discussion of this paper and are most appropriately covered in discussion of modeling and analysis.

Notice that if we know the past history (both input and output) of the system we can predict the next output y_n . This paper discusses the problem of testing, specifically how to generate a data set that is complete enough that appropriate modeling and analysis methodology can be applied. Some specific algorithm issues are discussed.

It should be noted that most detectors are not naturally linear systems. Non-linearity includes a non-linear response or saturation of the detector. If the detector is calibrated and it is only operated within its operational range then the detector can be generally treated as a linear system. This paper assumes that the test system was designed to ensure linear methods apply. It should be noted that if we can't make use of these linear assumptions we will need a more complex (not simpler) test methodology than described herein. Thus linear based testing is the minimal test protocols we need to use and we don't expect to have a reason to use test methods less stringent than those outlined herein.

Development of an Optimum Test

This section presents some of the theoretical development necessary to understand why specific test protocols are required. A rigorous development is not included and will be the subject of a future publication.

Lets assume that we have run a test and want to perform a modeling/analysis step on the data. There are several modeling methodologies that can be used. The least square method is a simple method that has characteristics of all methods. This amounts to choosing the coefficients (a 's and b 's) to give the best fit to the data. To this end we define

$$S = \sum_m \left(\sum_{i=0} b_i u_{n+m-i} - \sum_{i=1} a_i y_{n+m-i} - y_{n+m} \right)^2 \quad \text{Equation 2}$$

This is a common definition from least squares methodologies^{1,2,3}. If S is zero we have an ideal selection of coefficients. Following least squares methodology we obtain the following matrix equation.

$$\begin{bmatrix} \sum_n u_n u_n & \sum_n u_{n-1} u_n & \cdots & \sum_n y_{n-1} u_n & \sum_n y_{n-2} u_{n-1} & \cdots \\ \sum_n u_n u_{n-1} & \sum_n u_{n-1} u_{n-1} & \cdots & \sum_n y_{n-1} u_{n-1} & \sum_n y_{n-2} u_{n-1} & \cdots \\ \vdots & \vdots & \ddots & \vdots & \vdots & \ddots \\ \sum_n u_n y_{n-1} & \sum_n u_{n-1} y_{n-1} & \cdots & \sum_n y_{n-1} y_{n-1} & \sum_n y_{n-2} y_{n-1} & \cdots \\ \sum_n u_n y_{n-2} & \sum_n u_{n-1} y_{n-2} & \cdots & \sum_n y_{n-1} y_{n-2} & \sum_n y_{n-2} y_{n-2} & \cdots \\ \vdots & \vdots & \ddots & \vdots & \vdots & \ddots \end{bmatrix} \begin{bmatrix} b_0 \\ b_1 \\ \vdots \\ a_1 \\ a_2 \\ \vdots \end{bmatrix} = \begin{bmatrix} \sum_n y_n u_n \\ \sum_n y_n u_{n-1} \\ \vdots \\ \sum_n y_n y_{n-1} \\ \sum_n y_n y_{n-2} \\ \vdots \end{bmatrix} \quad \text{Equation 3}$$

Or

$$Ax = b$$

Equation 4

where

$$A = \begin{bmatrix} \sum_n u_n u_n & \sum_n u_{n-1} u_n & \cdots & \sum_n y_{n-1} u_n & \sum_n y_{n-2} u_{n-1} & \cdots \\ \sum_n u_n u_{n-1} & \sum_n u_{n-1} u_{n-1} & \cdots & \sum_n y_{n-1} u_{n-1} & \sum_n y_{n-2} u_{n-1} & \cdots \\ \vdots & \vdots & \ddots & \vdots & \vdots & \\ \sum_n u_n y_{n-1} & \sum_n u_{n-1} y_{n-1} & \cdots & \sum_n y_{n-1} y_{n-1} & \sum_n y_{n-2} y_{n-1} & \cdots \\ \sum_n u_n y_{n-2} & \sum_n u_{n-1} y_{n-2} & \cdots & \sum_n y_{n-1} y_{n-2} & \sum_n y_{n-2} y_{n-2} & \cdots \\ \vdots & \vdots & & \vdots & \vdots & \ddots \end{bmatrix} \quad \text{Equation 5}$$

$$x = \begin{bmatrix} b_0 \\ b_1 \\ \vdots \\ a_1 \\ a_2 \\ \vdots \end{bmatrix} \quad \text{Equation 6}$$

and

$$b = \begin{bmatrix} \sum_n y_n u_n \\ \sum_n y_n u_{n-1} \\ \vdots \\ \sum_n y_n y_{n-1} \\ \sum_n y_n y_{n-2} \\ \vdots \end{bmatrix} \quad \text{Equation 7}$$

This is the basic equation we are always faced with and must solve to obtain estimates of the coefficients.

It should be noted that there are many methods to solve this problem each with their own strength or weakness. This paper will not discuss these methods except to cover how they impact the problem statement itself. Our goal is to define a test protocol that makes these equations easier to solve by any method.

Equation 3 is a very important equation in the design of dynamic testing. Matrix A primarily determines how easy the analysis will be and how much information is available. Because of the importance of matrix A, a brief review of its properties, or how easy A is to solve is included next.

Matrix A Properties

No Solution

If all elements of matrix A are equal this equation cannot be solved by any analysis methodology. Another way of generating a matrix without solution is to have the rows (or columns) to be linear combinations of each other. Simply calculating the determinant of the matrix can test for this condition.

If the determinant is zero no unique solution exists, if non-zero there is a unique solution. Another measure is the rank of the matrix. The rank is the largest sub-matrix that can be constructed that will have a non-zero determinant. If a matrix is full rank that is the same as stating it's determinant is not zero. If a test is run in such a manner as to generate a matrix that is not full rank, analysis can still be performed using pseudo inverse techniques but with significant limitations.

Ill Conditioned

It is possible to have a matrix that is full rank and hard to solve. Notice that full rank systems guarantee there is a solution, but the solution may be difficult to obtain. For example lets assume we have

$$A = \begin{bmatrix} 100.2 & 200.3 & 300.4 & 400.5 \\ 200.3 & 400.4 & 600.5 & 800.6 \\ 300.4 & 600.5 & 900.6 & 1200.7 \\ 400.5 & 800.6 & 1200.7 & 1600.8 \end{bmatrix} \quad \text{Equation 8}$$

Although this matrix has a non-zero determinant this is a very difficult problem to solve. A problem matrix can be recognized by the fact that the diagonal of numbers from the upper left corner to the lower right do not dominate the matrix. Some matrices that are not diagonal dominant can be solved easily but it's hard to tell from inspection, and the chance of successfully solving this equation gets smaller as the size of the matrix increases.

From a practical point of view an ill-conditioned number will express itself by having a very sensitive reaction to errors. For example the inverse of A is

$$A^{-1} = \begin{bmatrix} -1.2E+13 & 1.48E+13 & 6.6E+12 & -9.3E+12 \\ 2.2E+13 & -2.9E+13 & -8.8E+12 & 1.54E+13 \\ -7.7E+12 & 1.26E+13 & -2.2E+12 & -2.7E+12 \\ -2.2E+12 & 1.1E+12 & 4.4E+12 & -3.3E+12 \end{bmatrix} \quad \text{Equation 9}$$

If we change one entry in equation 8, namely the value of 1600.8 to 1601 we get the following inverse

$$A^{-1} = \begin{bmatrix} -5.9E+12 & 1.17E+13 & -5.9E+12 & 12.50269 \\ 1.17E+13 & -2.3E+13 & 1.17E+13 & -20.0054 \\ -5.9E+12 & 1.17E+13 & -5.9E+12 & 2.502685 \\ 3.333333 & -1.66667 & -6.66667 & 5 \end{bmatrix} \quad \text{Equation 10}$$

By inspection it can be seen that very small changes in some values can effect large changes in the analysis results. This is a critical point to understand; namely that the way we conduct experiments significantly affects the possible quality of the analysis. This is not a deficiency in the analysis methodology but a deficiency in how robust the test protocol is.

Experience has shown that if we conduct a test without any special effort, matrices similar to equation 8 are often generated with all the associated problems. In general any test protocol where the inputs are highly correlated in time will cause these analysis problems.

Astute readers will also note that highly correlated outputs (y's) will cause a similar problem even if the inputs are uncorrelated. This is a good observation and is correct but is not often a problem. It only becomes a problem when the outputs (y's) are not affected by the inputs (u's). It is thus possible to better design a test if the outputs can be predicted in advance, or after test data is collected. In any case the only way to uncorrelate the outputs is to drive them to values by the inputs. This is equivalent to having the inputs uncorrelated.

Although this example is contrived to make a point these types of results can, and do, occur. Specifically whenever we keep input signals static we are exiting many or all states of the system and driving the test results to yield correlated or ill-conditioned problems, and whenever we are stimulating the system with changing conditions we are driving the results away from these conditions.

These results are not very surprising when considered in context. For example in testing a car if we run a test on a car by simply running it on a straight road, at noon, in the summer, with no acceleration or deceleration, we won't learn much about the car. We will collect lots of data about the car at one test condition but will be able not be able to answer any practical questions such as how fast the acceleration is, how it climbs hills, etc. Collecting more of this same data will not add to our understanding of the car, to do that we need to perform a different test. As test costs are high we don't want to waste time generating more data that does not increase our understanding. We want our tests to be as informative as possible.

Steady State Tests

Lets take an example of a problem statement that can't be solved by any method, namely the problem of a steady state test. Steady state tests are tests where the test conditions don't change with time. These are very appealing tests to run from a testing point of view. We can stabilize the system and take any amount of time necessary to ensure we understand the test parameters. If we run this type test the values of u and y don't change for any value of n. Putting these numbers into the above matrix will result in a matrix that is not invertable. Specifically the determinant of the matrix is zero and there is not an analysis methodology that can solve this problem. Notice that this is a problem with the test methodology and not the fault of the analysis methodology, we have simply created a data set that will not yield the appropriate information. Thus we can state that steady state tests are not appropriate for detector testing.

Step Tests

Actually the steady state test is rarely achieved in practice. When we run these test we generally stabilize the conditions then introduce the stable conditions to the detector. This has the effect of introducing a step into the input concentration signal. This type of test can provide a matrix with a non-zero determinant and thus can be solved. There is a significant problem though and that arises from the fact that the input does not change much. We thus end up with the problem where $\sum_n u_n u_n$ and

$\sum_n u_n u_{n-1}$ are nearly the same number. This results in a matrix where all the elements are about the same magnitude. This results in an illconditioned matrix as discussed earlier in regard to correlated inputs. Thus we can state that step tests can provide results but lead to poorly conditioned systems that require a considerable amount of analysis to extract useable results.

Notice that we can improve this situation by repeating the step test several times. Multiple step tests generally will improve the matrix condition.

Other Tests

There are several modifications to the test protocol that can be used. Some of the popular ones are to use impulse testing, or use of a predefined test scenario. The use of a predefined scenario is attractive because we are trying to see how the detector will respond against some known challenge profile. From an information content point of view these tests can be evaluated by examining the condition of the matrix produced. The better the condition of the matrix the better the test.

Optimal Tests

An ideal conditioned matrix is a matrix where the diagonal is non-zero and all off diagonal elements are zero. The closer we can get to a matrix where all off diagonal elements are zero the better the condition of the matrix. To obtain a good condition we need for $\sum_n u_n u_n$ and $\sum_n y_{n-1} y_{n-1}$ to be large.

This is easy as this term simply says that all values should correlate highly with themselves. The fact that they do is self-evident. On the other hand we want $\sum_n u_n u_{n-1}$, $\sum_n u_n y_{n-1}$, and $\sum_n y_{n-1} y_{n-2}$ to be as small as possible. Examining these equations indicate that we want the inputs and outputs to be uncorrelated in time. Stated another way a test signal designed to stimulate all modes of the system is used to run the test. Actually a completely random function may not meet the requirements. We need a random looking signal that drives the off axis values to as small of a number as possible. We call these pseudo-random sequences. Pseudo-random test sequences must have a full frequency content and cover the entire interest range of the test item. It turns out that there is not a unique pseudo-random sequence for test protocols but many different sequences can be used. Any sequence that meets the criteria mentioned above will work.

Test Fixture Limitations

In practice it's not possible to conduct an ideal test. The reason is the test fixture has its own response characteristics and this has the effect of correlating the inputs to some degree.

In steady state tests we don't need to worry about the effect of the test fixture on the challenge profile. We can simply wait for the response transients to die out and conduct our test. In dynamic testing we don't have this luxury. By changing the conditions rapidly we make it impossible to ignore the test fixture response. This leads to the conclusion that to conduct these types of tests requires us to accurately characterize the test fixture and design test fixtures that respond rapidly. In addition the test fixture must be designed to minimize the effect of the test fixture as much as possible.

This also extends to the instrumentation used to monitor environmental conditions. Their response characteristics need to be carefully modeled. Historically we have been concerned with precision and accuracy in the CB testing world but we also need to be concerned with response.

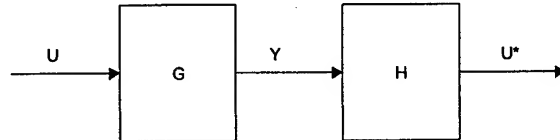
Multiple Inputs

Extensions of these tests are tests that have multiple inputs. These types of tests will have several agents changing with time. We could rigorously derive the basic equations for this case like we did for the single input case and performing this analysis leads to a similar result, namely the inputs still need to be uncorrelated. Thus we need each agent to follow a pseudo random challenge profile while also meeting the requirement that each agent profile is statistically independent from each other.

Algorithm Development

We have assumed that the primary goal of the test is to model the sensor system. Algorithm issues have been ignored to this point. After we have conducted the test correctly the next natural phase is to evaluate the sensor and determine if it meets our requirements. A specific hardware limitation has been identified that can have a significant impact on the detector development program. This limitation is known as the invertability problem. Specifically we have demonstrated it is possible to develop a sensor that is stable and sensitive but which precludes the development of an ideal algorithm. This issue is a critical issue and is discussed here to encourage development of methods to deal with the problem.

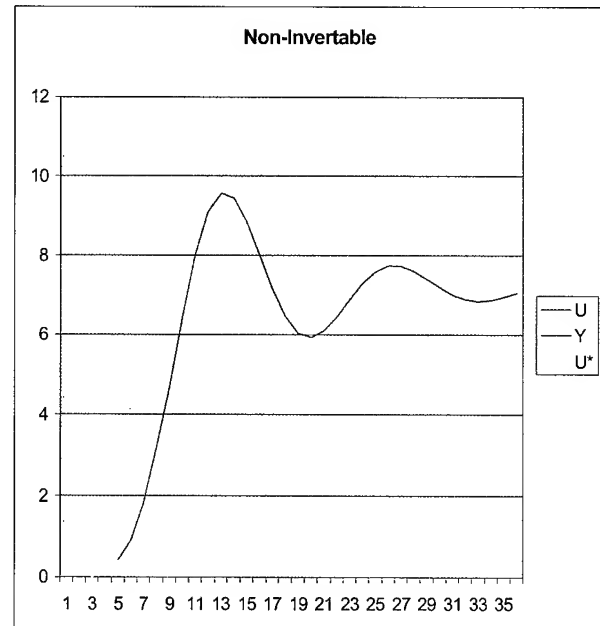
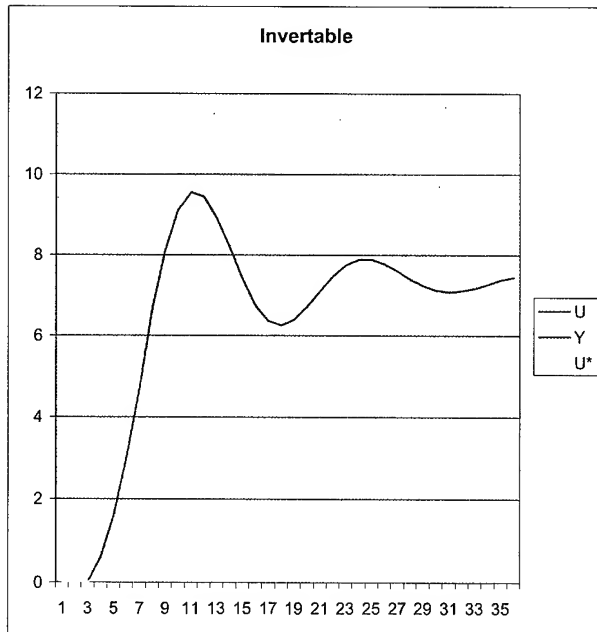
Algorithms can be understood by reference to the following figure.



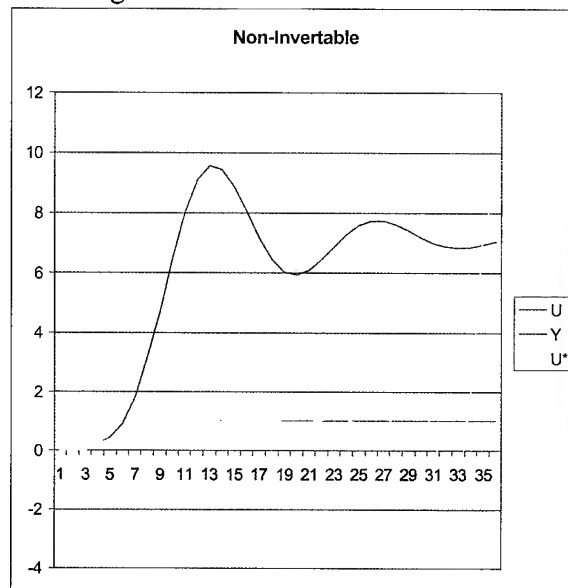
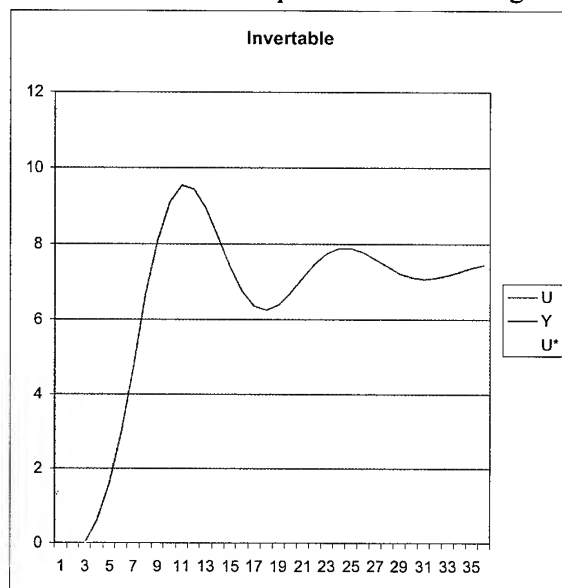
Here we have an input signal U (e.g. chemical concentration) that is modified by the detector hardware (G) to produce an electrical signal Y . The transformation of U to Y via function G is called the forward model of the detector system. The signal is processed through the inversion algorithm (H) to produce an estimate of U known as U^* . Hopefully we will have $U = U^*$. If we assume a noise free environment and can construct a function H that meets this requirement we have developed an Ideal Algorithm for this detector.

The system response of an ARMA system can be discussed by examining the poles and zeros of the function. Poles, zeros, and gain contain all the information about the system response, and poles directly affect the stability of the system. If the poles are within the stability region, the system response will be stable. Zeros can be anywhere, including unstable regions, and the system is still stable. If we use a simple inversion routine to generate H we will effectively swap the poles and zeros. The problem is a stable detector may have zeros in an unstable region that function as unstable poles in the derived algorithm. If that is the case any algorithm developed will need to compromise its performance somehow to make it stable. This implies that the error between U and U^* will not be zero. In some cases these differences are not acceptable, in other cases the differences still meet the detector requirements. In any case bounds on algorithm performance are imposed by the sensor hardware characteristics.

The differences in sensor/algorithm system response are difficult to see by simply examining the sensor response. To illustrate this two example equations (sensor models) are generated and their response (algorithm output) generated. These are ideal models generated to illustrate the problem. The poles are set identical to each other while the zeros are selected to make inversion hard and easy.



The input ramps up from zero to one. The response Y is shown along with the estimate U^* from straight inversion. As can be seen the inversion process works well and there are not significant visible differences between these two systems. These are both ideal systems with no error introduced. If we introduce a small error into point 9 of 0.1% we get the following results.



For invertable or minimum phase systems the small error is almost ignored. For the non-invertable or non-minimum phase system small error grows without bound. For some zero placements simple round off errors are enough to cause the answer to diverge. It is actually quite easy to develop an algorithm that works for the non-invertable example but not one where we get the zero error response. In fact there are an infinite number of algorithms possible depending on what we consider good algorithm performance.

CONCLUSIONS

This paper proposes a new framework for performing tests on point detector systems and provides some background as to why these new methodologies are required. More work is needed to establish standard practices for these protocols and extend their range into more non-linear cases. Specific test fixtures will need to be designed to meet the requirements suggested herein.

Algorithm development was also discussed with the observation that algorithm development must rely on a good model of the sensor. It turns out that specific sensor hardware characteristics make inversion algorithm development difficult. The practical result of this observation is that sensor response should be carefully modeled and analyzed before inversion algorithm development begins. This implies the need for testing early in the development cycle to adequately understand sensor response and allow development of robust algorithms that provide stable inversion of sensor outputs.

ACKNOWLEDGEMENTS

This paper is based on work that was performed at the University of Utah Center for Microanalysis and Reaction Chemistry (UUCMARC) funded by Dugway Proving Ground⁴. Mission Research Corporation (MRC) and UUCMARC have extended the development into the algorithm development area and provided the further insight into the algorithm development theory.

Dr. William A. Dement, Dugway Proving Ground, provided valuable comments to the final manuscript.

MRC is working with ECBC to map out future efforts and areas of mutual interest.

REFERENCES

- ¹ John, J. D'Azzo, Constantine H. Houpis, "Linear Control System Analysis & Design", McGraw Hill 1988
- ² Lennart Ljung, "System Identification : Theory for the User (Prentice Hall Information and System Sciences Series)", Prentice Hall, January 1999
- ³ Hair, Anderson, Tatham, Black, "Multivariate Data Analysis", Prentice Hall, 1998
- ⁴ Dubow, J., Mathews, J.V., Khoumovosky, E., Bodily G., "Dynamic System Models of Ion Mobility Spectrometers", Proceedings AeroSense Conference 4036, April 2000

BIOAEROSOL SAMPLING SYSTEMS

S.A. Lee⁽¹⁾, J. S. Haglund⁽¹⁾, H.N. Phan⁽¹⁾, S. Chandra⁽¹⁾,
Andrew R. McFarland⁽¹⁾, R.S. Black⁽²⁾ and Matthew J. Shaw⁽²⁾

⁽¹⁾Aerosol Technology Laboratory
Department of Mechanical Engineering
Texas A&M University
College Station, TX 77843

⁽²⁾Aerosol Science and Technology Assessment
Battelle Columbus Laboratories
505 King Avenue
Columbus, OH 43201

ABSTRACT

Particle impaction onto a liquid-transpirated collection surface is utilized for aerosol concentrating in two devices. The MMSI sampler has a cutpoint of 0.84 μm AD, operates at an airflow rate of 500 L/min and concentrates the particles in a 4 mL/min liquid film. Solid fluorescent polystyrene particles show aerosol-to-hydrosol collection efficiencies that follow the impactor fractionation curve; however, tests with 0.9 μm AD BG spores show an aerosol-to-hydrosol collection efficiency of 35.7% as compared with the predicted value of 60%. Use of transpirated surfaces that are more hydrophilic than stainless steel will be investigated to try to increase the efficiency with viable particles. This sampler has an ideal air power requirement 7.5 W. Electrical heating (200 W) is available to prevent the liquid from freezing. The second sampler (AHST) is to be used with 300-1000 L/min virtual impactor aerosol concentrators that have a cutpoints of 2.5 μm AD and coarse particle flow rates of 1 L/min. Cutpoint of the AHST is 2.0 μm AD and concentrates the aerosols into a liquid flow rate of 0.3 mL/min. Ideal power to force air across the system is about 1.4 mW and heating the flow stream from -30°C to +30°C would require 1 W.

INTRODUCTION

Two sampling devices are being evaluated, which are designed to transfer the particulate phase of bioaerosols to the hydrosol state. The principle of operation of both systems is jet impaction of aerosol onto a continuously flowing liquid film, subsequent collection of the film, and delivery of the hydrosol for bio-analysis. Both systems utilize porous collection surfaces through which liquid is transpirated, and gravitational flow of the liquid film to a location where it is aspirated and removed from the sampler. One system, which is a stand-alone device, is designed to operate at an air sampling flow rate of 500 L/min and concentrate the bioaerosol particles into a liquid flow rate of about 5 mL/min. The second system, which is intended to operate in series with a virtual impactor, will take the concentrated aerosol in the coarse particle flow stream from the virtual impactor and transfer the aerosol particles to a liquid flow rate of about 0.3 mL/min. Herein, the first unit will be referred to as a multi-mini-slit impactor (MMSI) and the second will be referenced as an aerosol-hydrosol transfer stage for a virtual impactor (AHTS).

Multi-Mini-Slit Impactor

With reference to Figure 1a, the MMSI consists of a cylindrical housing on which are mounted 8 slit impaction nozzles. Ambient air is drawn into a nozzle where it is accelerated to a velocity of 32 m/s and the jet impacts against a liquid film (Figure 1b), which is formed from liquid that is transpired through a porous collection surface (0.5 μm pore, Mott Metallurgical Corp., Farmington, CT). Aerosol particles with sufficient inertia are deposited in the liquid film, which then flows by gravity to the liquid receiver. Because aerosols used in field tests may be comprised of single spores with a size of about 1 μm aerodynamic diameter (Shaw et al., 2000) it is highly desirable for a sampler to collect particles with sizes < one micrometer. For the MMSI, a cutpoint of < 1 μm is achieved by using 0.25 mm (0.01 inch) slit widths, and a high sampling rate is achieved by using a total of 1.02 m (40 inches) of slit length. For operation in cold conditions, the system has a heater inside of the tube that contains the transpired surfaces and electrical heating of the liquid receiver.

Aerosol-Hydrosol Transfer Stage for a Virtual Impactor

Virtual impactors (Loo and Cork, 1988) are used for aerosol concentration and are employed in bioaerosol sampling applications. A virtual impactor operates on the principle of inertial impaction, but rather than collecting aerosol particles on a surface, the air jet from an impactor nozzle is directed towards an opening (receiver) where there is nearly stagnant air. Typically, circular nozzles are used and the aerosol jet is directed towards a circular receiver tube, where about 10% of the flow from the nozzle is drawn into the receiver tube. The flow in the receiver tube contains high-inertia (coarse) particles and 10% of the low inertia (fine) particles that are carried along with the transport air, which essentially produces 10X enrichment in the coarse aerosol concentration. The process can then be repeated with the coarse aerosol flow being passed through another nozzle with its coarse aerosol being collected in a second stage receiver tube. By having two stages of virtual impaction in series, the coarse particle concentration can be increased by a factor of 100 over that in the sampled air. SCP Dynamics, Inc. (Minneapolis, MN) developed a virtual impactor (Model 1001) that samples at a flow rate of 1000 L/min and concentrates the coarse aerosol particles into a flow rate of 1 L/min. The system has a cutpoint of about 2.5 μm AD, but there are significant wall losses in the virtual impactor which results in an average efficiency of less than 50% over the size range of 2.5 to 10 μm AD (Chandra et al., 1999). MSP Corporation (Minneapolis, MN) developed a system that samples aerosol at a flow rate of 300 L/min and also concentrates the coarse particles into a flow rate of 1 L/min. Both the SCP and MSP virtual impactors are designed to operate with the coarse particle flow stream containing aerosol particles in the size range of 2.5 to 10 μm aerodynamic diameter (AD). SCP also manufactures a variation of their sampler that has a coarse particle flow rate of 20 L/min and concentrates the particles into a liquid flow rate of 1 mL/min, however, there are losses in the aerosol-to-liquid collector, which result in efficiency values over the size range of 2.5 to 10 μm AD that are about $\frac{1}{2}$ of those of the system without the aerosol-liquid transfer stage (Kesavanathan, 2000).

With reference to Figure 2, the system that we are developing is matched to the design parameters of the MSP and SCP virtual impactors, i.e., the AHTS takes in air (coarse particle flow stream) at a flow rate of 1 L/min and it has a cutpoint (particle size for which 50% of the aerosol is collected in the liquid) of 2.0 μm AD. If the combination of the MSP virtual impactors and the AHTS is operated with an air sampling flow rate of 300 L/min and a liquid flow rate of 0.3 mL/min, the maximum concentration factor is 10^6 . Although the initial prototype of the AHTS was not so equipped, it is planned to heat the inflow tubing and the housing for cold weather operation. Because the airflow rate is so low, heating the entire stream from -30°C to +30°C would only require 1 watt of electrical heating.

TESTING OF SYSTEMS

Both the MMSI and the AHTS systems have been tested in the laboratory with monodisperse non-viable aerosols to obtain data on basic performance characteristics. In addition, preliminary laboratory tests have been conducted on the MMSI with *Bacillus globugii* var. *Bacillus subtilis* (BG) aerosols.

Experiments with the Multi-Mini-Slit Impactor

Fractional Collection Efficiency. Three types of experiments have been conducted to determine the fractional efficiency of the impactor as a function of particle size. First, a test fixture comprised of a single impaction nozzle and a non-transpirated aluminum collection surface was fabricated. It was tested in a wind tunnel with monodisperse oleic acid liquid aerosol particles generated with a vibrating jet atomizer (Berglund and Liu, 1973). The aerosol was tagged with an analytical tracer, fluorescein, in a mass/volume ratio of 10%. During a test, the particle size was determined microscopically using the technique of Olan-Figueroa et al. (1982). The aerosol concentration in the wind tunnel was established by using an isokinetic probe followed by a sampling filter. The aerosol that penetrated the test device was also collected on a sampling filter. Fluorescein deposited on the collection filters was eluted with a 50/50 mixture of isopropyl alcohol and water and then analyzed with a fluorometer (Model 450, Sequoia-Turner, Mountain View, CA). Aerosol deposited on the inner wall of the isokinetic probe was washed with a similar extraction solution. Sodium hydroxide (1N) was added to the extraction solutions for assurance that the pH was >8 so the fluorescent quantum yield would be maximized. Based on the mass of tracer collected from each element, and the airflow rates through the isokinetic probe and the test device, the collection efficiency of the impactor stage for a given sized particle (the fractional efficiency) could be determined.

The second type of experiment involved the use of monodisperse pre-sized solid polystyrene particles (Bangs Laboratories, Inc., Fishers, IN) that were aerosolized from a dilute hydrosol with an airblast atomizer, and detected with either an optical particle counter (Model CI-500, Climet Instruments, Inc., Redlands, CA) fitted with a multi-channel analyzer (Genie 2000, Canberra Instruments, Inc., Meridan, CT) or an Aerodynamic Particle Analyzer (Model 3010, TSI, Inc., St. Paul, MN). During a test, the fixture was operated in a flow-through chamber and the aerosol concentration was measured upstream and downstream of the device.

Monodisperse solid fluorescent polystyrene aerosol particles (Duke Scientific Corporation, Palo Alto, CA) were used in the third type of test. A complete system, with all except one nozzle blocked, was operated in a flow-through chamber. Samples of the challenge aerosol in the flow-through chamber were collected on filters, and samples of the liquid effluent from the MMSI were collected in glass beakers. The liquid used in these tests was de-opmozed distilled water with 0.2% surfactant (Tween 20, Mallinckrodt Baker, Inc., Phillipsburg, NJ) by volume, and liquid was transpired through collection surfaces under all nozzles during these tests. Comparing the concentration of fluorescent solid particles in the effluent liquid with that in the chamber allowed the overall efficiency of the sampler to be determined.

The fractional collection efficiency of the MMSI as a function of aerodynamic particle size is shown in Figure 3. It may be noted that the system has a cutpoint of $0.84\text{ }\mu\text{m AD}$ and that it has high efficiency for particles in the range of 1 to $10\text{ }\mu\text{m AD}$, indeed, the average efficiency in that size range is 98.7%. The tests with the fluorescent polystyrene particles of sizes 1.0 and $2.3\text{ }\mu\text{m AD}$ show there is effective transfer of these solid particles from the aerosol state to the hydrosol state. Approximately the same results were obtained from the aerosol-hydrosol tests as from the tests with the non-transpirated fixture.

Effect of Surfactant Concentration. Tests were conducted to determine the aerosol-hydrosol transfer efficiency of the system as a function of surfactant concentration. Here, 2.3 μm AD solid fluorescent polystyrene particles were sampled by a single slit of the complete system (all collection surfaces transpired) and the concentration of hydrosol particles was compared with those in the aerosol state to provide a measure of efficiency. Water with Tween 20 was used as the collection liquid.

The results, shown in Figure 4, indicate that surfactant is needed for aerosol-hydrosol transfer. Essentially zero collection efficiency was obtained with no surfactant and 100% collection efficiency was obtained for Tween 20 surfactant concentrations in the range of 0.03% to 1%.

Effect of Liquid Flow Rate. The MMSI, which was operated with a single nozzle and with liquid flow through all transpired collection surfaces, was used to sample 2.3 μm AD solid fluorescent polystyrene spheres. The test procedure involved aerosol being sampled by the collector for a period of 20 minutes with liquid collected continuously during this period. The airflow was then shut off, and liquid was collected in a separate vessel for a period of 10 minutes. Liquid flow rate through the sampler was varied over a range of 0.8 to 5.2 mL/min during these tests.

The results are shown in Figure 5, where aerosol-to-hydrosol transfer efficiency is shown as a function of liquid flow rate, with separate curves for the efficiency based on liquid collected during the time the aerosol was being sampled, during the post-aerosol-sampling period, and the total collection based on adding the two efficiency values. The measured total collection was 84% for a liquid flow rate of 1 mL/min, 97% for a flow rate of 2.9 mL/min, and 104% for a flow rate of about 5 mL/min. Approximately 15% of the hydrosol was collected during the post-aerosol sampling period. In a separate test, not shown in Figure 5, particle generation was stopped but airflow through the sampler was continued after the first liquid collection period. At a liquid flow rate of 4.6 mL/min, similar results were obtained to those with no airflow through the sampler during the post-aerosol generation period. Total collection was 95%, of which 5% was collected after cessation of aerosol generation.

Tests with *Bacillus Globugii* Spores. Wind tunnel tests were conducted with two prototype versions of the sampler, one having a porous surface with a width of 1.3 mm (0.050 inches) and the other a width of 2 mm (0.080 inches). The samplers were operated in a bioaerosol wind tunnel, where they were used to collect BG spores that had been generated with a Collison atomizer (May, 1973). The BG particles were essentially single cells with number median diameter of 0.9 μm AD and a geometric standard deviation of 1.3. For each test, the reference concentration of BG in the wind tunnel was established through use of an agar filter (Cat. No. 12602.047ALN, Sartorius, Goettingen, Germany) placed at the exit of a sampling probe. The aerosol-to-hydrosol collection efficiency of the sampler was characterized by comparing the reference viable BG aerosol concentration with that established from the number of viable spores collected in three liquid effluent samples. The first liquid sample was taken over a 5 minute interval during which BG spores were being generated. Two additional post-generation samples were collected to maximize recovery of the BG. The BG was incubated for 20-24 hrs at 30-32°C to obtain sufficient colony sizes for analysis.

Results, Table 1, show that the BG aerosol-to-hydrosol efficiency of the unit with the 1.3 mm wide collection surfaces was 35.7%, and that of the unit with the 2 mm wide collection surface was 20-38% depending on the test conditions. By comparison the fractional efficiency curve (Figure 3) shows that 60% of 0.9 μm AD should have been collected by the systems. Measurements of the effluent air from the unit with the 1.3 mm collection surface width shows that about 20% of the BG aerosol penetrated through the system, and another 25% was recovered from ultrasonication of the transpired tube. The difference between the results with polystyrene particles and those with BG may be that BG particles have a greater adherence to the transpired stainless steel collection surface, or it may be that the spores lose viability in the sampling process. With respect to the latter consideration, Mainelis et al. (1999) in a study of electrostatic collection of bioaerosols observed that when BG spores were collected

on agar, the bioefficiency was 50-60%, whereas the bioefficiency was 15-22% when the spores were collected on water. They defined bioefficiency as the ratio of the number of viable cells on the collection substrate of a sampler to the number of viable cells retained by the sampler (i.e., deposited on the collection substrate and inadvertent wall losses).

Ideal Power Consumption for Air Movement. The ideal power consumption of an air sampler such as the MMSI is the product of sampling airflow rate through the device and pressure drop across the system. This ideal power does not include power losses caused by the inefficiency of the blower or losses in the connecting air flow components. At a flow rate of 500 L/min, the pressure drop across the MMSI is 900 Pa (3.6 inches of water), which gives an ideal power consumption of 7.5 watts.

Aerosol-Hydrosol Transfer Stage for Virtual Impactors

Fractional Collection Efficiency. The fractional efficiency curve for the AHTS was established by testing the system with solid polystyrene aerosol particles that were generated by air blast atomization of a dilute hydrosol. The concentration of aerosol particles in the exhaust stream of the AHTS was measured with an APS, and the results compared with the aerosol concentration at the inlet plane of the sampler. With reference to Figure 6, the cutpoint is 2.0 μm AD and, if the efficiency curve is integrated over the size range of 2.5 to 10 μm AD, the average collection efficiency over that interval is 94.0%. For these tests, the collection surface was oil-soaked porous (0.5 μm pore size) stainless steel.

Effect of Surfactant Concentration. The AHTS was operated at an air sampling flow rate of 1 L/min and a liquid flow rate of 0.3 mL/min while sampling 2.9 μm AD solid fluorescent polystyrene aerosol particles. Efficiency of the sampler was determined from fluorometric measurements of the particles in the effluent liquid and those collected on sampling filters. The collection liquid was distilled water with Tween 20 added in amounts up to 0.8%.

With reference to Figure 7, if no Tween 20 was added to the water, the collection efficiency was only 17%; however, for Tween 20 concentrations $\geq 0.1\%$, the collection efficiency was approximately 90%. This behavior is similar to that observed with the MMSI.

Effect of Liquid Flow Rate. An aerosol comprised of 2.9 μm AD solid fluorescent polystyrene particles was sampled at a flow rate of 1 L/min and impacted onto a liquid film, which was set at flow rates from 0 to 0.75 mL/min. The liquid was distilled water with 0.2% Tween 20. Again, collection efficiency was determined by comparing the mass of fluorescein in the effluent liquid with that drawn into the sampler in the aerosol state.

The results, Figure 8, show that when the liquid flow rate is ≥ 0.3 mL/min, the collection efficiency is constant with a value of about 90%. A test conducted at a liquid flow rate of 0.1 mL/min yielded an efficiency of about 80%.

Response Time of the AHTS. For this test, the AHTS was used to collect 2.9 μm AD solid polystyrene aerosol particles at a flow rate of 1 L/min for 16 minutes, at which point the airflow was shutoff. Samples of the collection liquid (water plus 0.2% Tween 20), which was flowing at rate of 0.3 mL/min, were collected at one minute intervals both during the aerosol generation period and for four minutes following cessation of aerosol generation, and at two minute intervals during other periods. The hydrosol samples were analyzed fluorometrically and the results compared with the mass of sampled fluorescent aerosol to permit calculation of time-dependent collection efficiency values. Here the collection efficiency is defined as the ratio of the mass flow rate of fluorescent particles in the effluent hydrosol at any given time

to the average mass flow rate of fluorescent aerosol particles sampled by the system during the aerosol generation time period.

The results for this test are shown in Figure 9, where it may be noted the efficiency is approximately 100% at about two minutes after the start of the aerosol generation process. The data given in Figure 9 may also be used to calculate a time constant for the AHTS, where the time constant is defined as the time required for a system to undergo 63.2% of a step change. For either a step increase or decrease in aerosol concentration, the time constant is approximately 1.4 min.

Ideal Air Power. When the AHTS is operated at an air sampling flow rate of 1 L/min, the pressure drop across the device is 88 Pa (0.35 inches of water). This translates to an ideal air power of 1.4 mW. Even if the air pump had to overcome the combined pressure losses of a virtual impactor (on the order of 1 kPa for a cutpoint of 2.5 μm AD), the total power requirement would still be negligible.

Acknowledgements

Funding for the development project was provided by the Army Research Office through Battelle Research Triangle Park under Scientific Services Program Task 98-133. Dr. Edward W. Stuebing, SBCCOM, Edgewood Chemical Biological Center, Edgewood, MD, is the U.S. Army Contracting Officer's Technical Representative for the project. Funding for bioaerosols testing was provided by Battelle Columbus Laboratories under an IRAD program.

DISCUSSION

The Multi-Mini-Slit Impactor and the Virtual Impactor Aerosol-Hydrosol Transfer Stage are both based on the principle of aerosol deposition onto a liquid-transpired collection surface. Design air sampling flow rate for the MMSI is 500 L/min, at which condition the cutpoint of the fractional efficiency curve is 0.84 μm AD. The MMSI must be operated with a low surface tension liquid, as it was noted that when de-ionized distilled water was used as the transpiration fluid, the aerosol-to-hydrosol transfer efficiency was essentially 0% for 2.3 μm AD aerosol particles. However, when Tween 20 was added in the concentrations $\geq 0.03\%$, the aerosol-to-hydrosol collection efficiency was essentially quantitative. The aerosol-to-hydrosol collection efficiency for 1.0 μm AD solid polystyrene beads was approximately 80%, which is nearly the same value as the fractional efficiency for a static, non-transpired, collection surface.

Tests with BG, which has a size of 0.9 μm AD, showed an aerosol-to-hydrosol collection efficiency of 36% when an MMSI with a 1.3 mm wide collection surface was operated under normal conditions. About 20% of the aerosol penetrated through the sampler as would be expected from the fractional efficiency curve, and 44% was unaccounted. A check test showed that about 25% of the BG could be recovered by ultrasonicing the transpiration tube. We believe the aerosol-to-hydrosol collection efficiency of BG can be improved by employing a more hydrophilic surface than the stainless steel. It appears that in the manufacturing process, the pore size of the stainless steel surface, Figure 10, is controlled not by the size of the stainless steel beads from which the porous surface is formed, but rather by the external pressure applied to the surface during process. At the microscale, this results in small flat islands that are on the order of 50 μm , which, may not be wet under the action of the air jet if the stainless steel is hydrophobic. A more wettable surface, such as glass, which is formed from beads that are on the order of a micrometer in size, would provide a better transpired collection surface.

The AHTS, which is designed to transfer concentrated aerosol from a virtual impactor to the hydrosol state, operates at nominal conditions of an airflow rate of 0.3 L/min and a liquid flow rate of 0.3 mL/min. When used with a virtual impactor that has a sampling rate of 300 L/min, the theoretical concentration factor is 10^6 ; however, the virtual impactor for which the system is matched has a fractional

efficiency cutpoint of 2.5 μm AD and the AHTS has a cutpoint of 2.0 μm AD, which means that an aerosol comprised of single BG spores would not be detected.

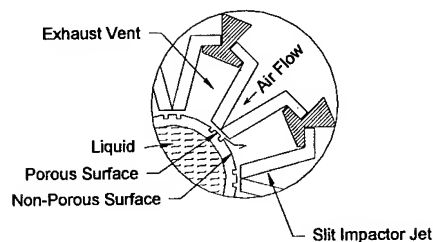
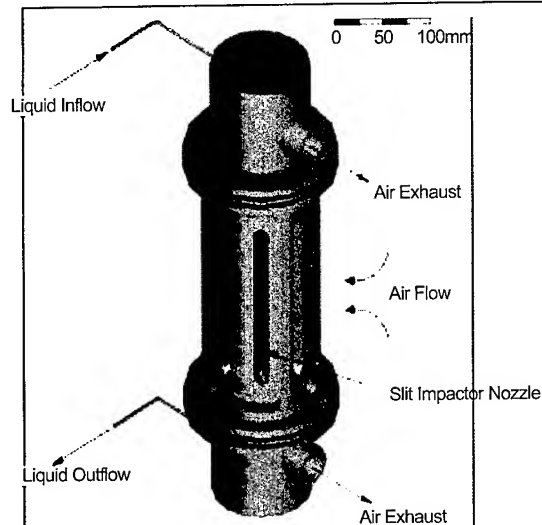
Small power requirements are a significant attraction of both the MMSI and the AHTS, as the ideal power to draw air through an MMSI is 7.5 W and that through the AHTS is about 1 mW. For operation in sub-freezing conditions, the MMSI has a 200 W heater inside the transpiration tube and a 25 W heater in the liquid collection housing. A check test of the heating system with the MMSI in a cold room at -10°C indicated no liquid freezing problems. Quantitative tests of the system need to be conducted at lower temperatures. Power to prevent freezing of the liquid in the combination of a virtual impactor and an AHTS is small because heat does not need to be added to the virtual impactor, and freezing of the liquid in the AHTS can be prevented by heating the 1 L/min air stream. To heat the 1 L/min airstream in the AHTS from -30°C to +30°C would require only 1 W.

REFERENCES

- Berglund, R.N.; Liu, B.Y.H. (1973). Generation of monodisperse aerosol standards. *Env. Sci. & Technol.* 7:147-153.
- Chandra, S.; Haglund, J.S.; McFarland, A.R. (1999). Evaluation of a bioaerosol concentrator. Report 10/99/5647. Aerosol Technology Laboratory, Department of Mechanical Engineering, Texas A&M University, College Station, TX.
- Kesavanathan, J. (2000). Personal communications with A.R. McFarland. U.S. Army Edgewood Research, Development & Engineering Center. Aberdeen Proving Ground, MD.
- Loo, B.W.; Cork, C.P. (1988). Development of high efficiency virtual impactors. *Aerosol Sci. and Technol.* 9:167-176.
- Mainelis, G.; Grinshpun, K.; Reponen, T.; Ulevicius, V.; Hintz, P.J. (1999). Collection of airborne microorganisms by electrostatic precipitation. *Aerosol Sci. and Technol.* 30: 126-144.
- May, K.R. (1973). The Collision atomizer: Description, performance and applications. *J. Aerosol Sci.* 4:235-243.
- Olan-Figueroa, E.; McFarland, A.R.; Ortiz, C.A. (1982). Flattening coefficients for DOP and oleic acid droplets deposited on treated glass slides. *Am. Ind. Hyg. Assoc. J.* 43:395-399.
- Shaw, M.; Andrews, H.; Bowdle, D. (2000). Characterization of field-generated biological aerosols. Presentation at *Scientific Conference on Obscuration and Aerosol Research*, U.S. Army Edgewood Chemical Biological Center, Aberdeen Proving Ground, MD. June 27-29, 2000.

Table 1. Results from wind tunnel testing of two MMSI samplers with single BG spores in a wind tunnel. The number median diameter of the spores is 0.9 μm AD.

Width of Porous Surfaces (mm)	Collection Liquid	Liquid Flow Rate (mL/min)	Aerosol-to-Hydrosol Collection Efficiency	Fraction of Viable BG in Effluent Air
1.3	H ₂ O + 0.2% Tween 20	4.4	35.7%	19.5%
2.0	H ₂ O + 0.2% Tween 20	5.2	26.7%	16.8%
2.0	H ₂ O + 0.2% Tween 20	5.6	20.8%	19.1%
2.0	H ₂ O + 0.2% Tween 20	10.9	38.2%	12.1%
2.0	50% H ₂ O + 50% Glycerol	6.5	25.1%	14.7%



(b)

Figure 1. Multi-Mini-Slit Impactor. a) External view. b) Region where the liquid from the transpirated cylinder flows outward collects aerosol particles impacted by the nozzles.

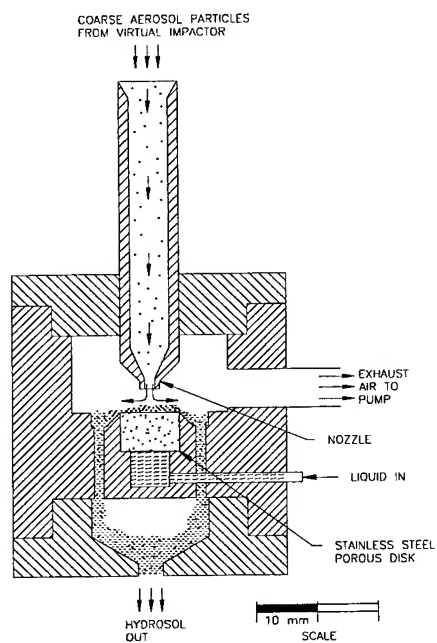


Figure 2. The aerosol hydrosol transfer stage for a virtual impactor.

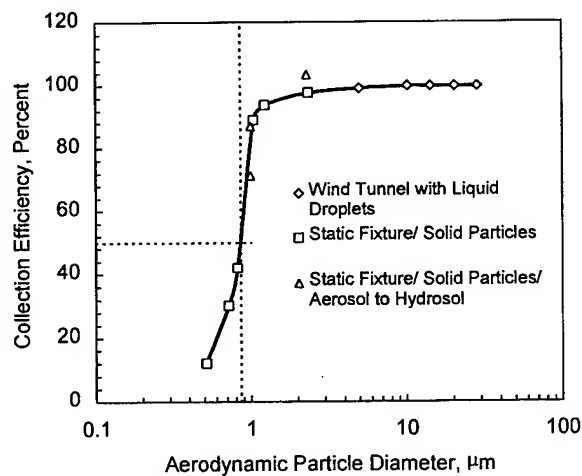


Figure 3. Fractional efficiency of the MMSI.

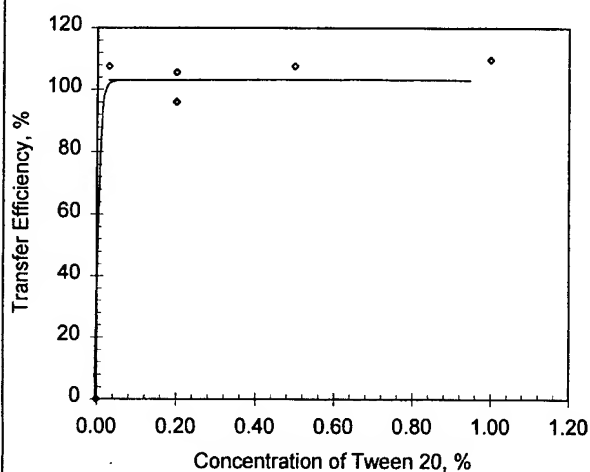


Figure 4. Effect of surfactant concentration on aerosol to hydrosol collection efficiency of the MMSI.

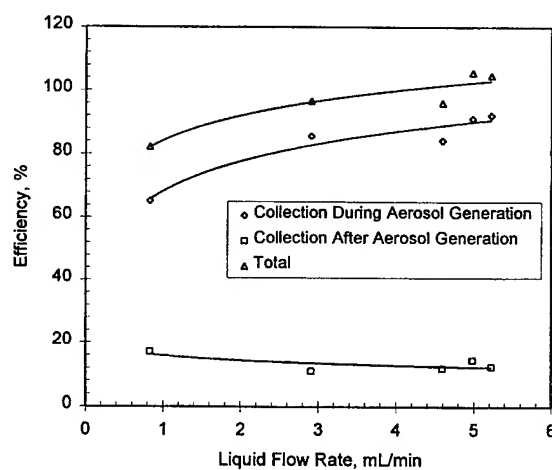


Figure 5. Aerosol to hydrosol collection efficiency of the MMSI as a function of liquid flow rate. The upper curve is the total collection for the aerosol generation and post-generation time periods.

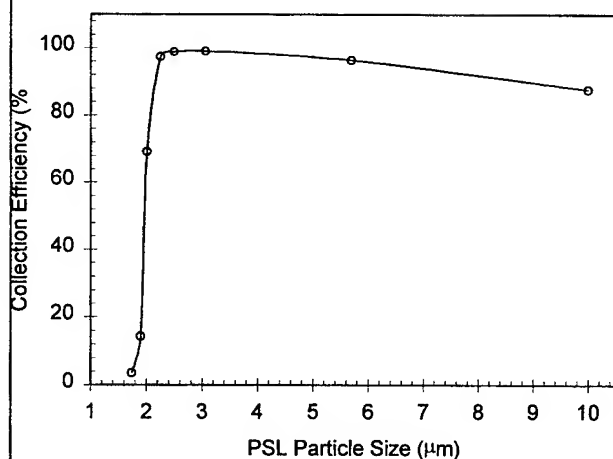


Figure 6. Fractional efficiency of the AHTS device.

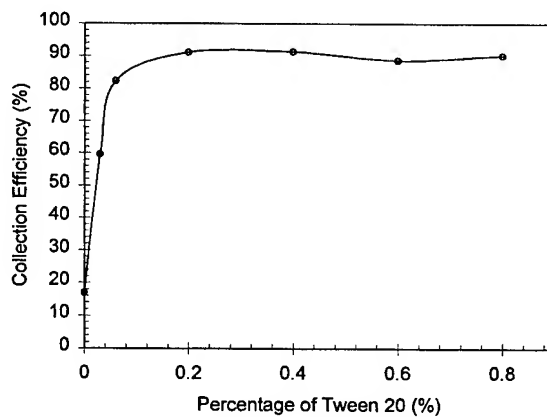


Figure 7. Effect of surfactant concentration on the aerosol to hydrosol collection efficiency of the AHTS. The test particle size was 2.9 μm AD.

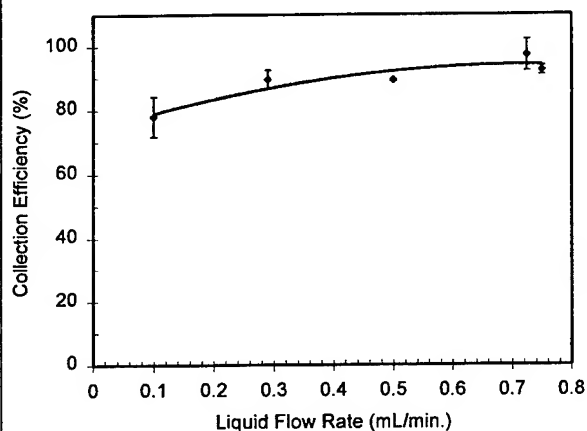


Figure 8. Effect of liquid flow rate on the aerosol to hydrosol collection efficiency of the AHTS. Test particle size was $2.9 \mu\text{m AD}$

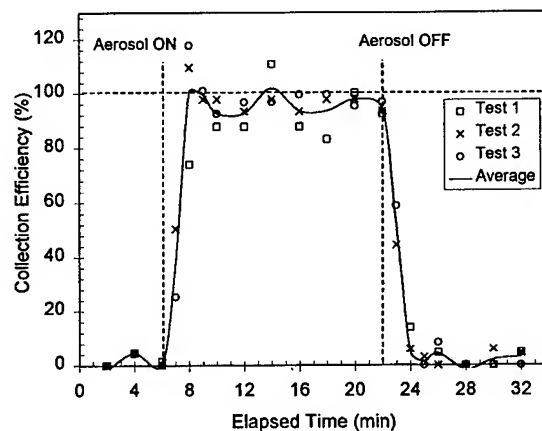


Figure 9. Time response of the AHTS to step increases and decreases of aerosol. Based on ratio of rate of particle mass collection in the liquid to that in the aerosol state.

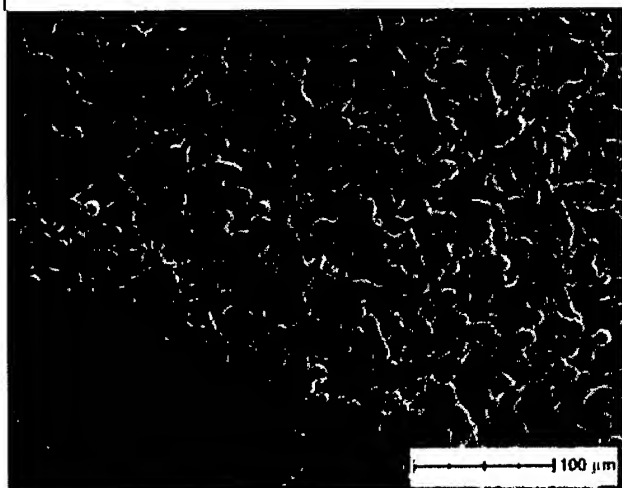


Figure 10. Electronphotomicrograph of the $0.5 \mu\text{m}$ pore size stainless steel surface. The upper surface is comprised of relatively flat globules with dimensions on the order of $50 \mu\text{m}$.

PERFORMANCE CHARACTERIZATION OF DEVELOPMENTAL AND NEXT GENERATION BIOAEROSOL COLLECTORS

Agnes Akinyemi
Jerold R. Bottiger
Robert Doherty
Jana Kesavan
Edward W. Stuebing
Daniel Weber
Daniel Wise

U.S. Army Edgewood Chemical Biological Center (ECBC)
Aberdeen Proving Ground, Maryland

1st Joint Conference on Point Detection for Chemical and Biological Defense
October 23-27, 2000
Williamsburg, VA

ABSTRACT

Biological Warfare (BW) agents and some Chemical Warfare (CW) agents are aerosols, therefore a critical component of Chemical Biological (CB) Point Detection is the aerosol collector which delivers concentrated aerosol samples from the ambient environment to the CB agent detector. Characterizing the performance of collectors used in CB defense systems is important to the assessment of the system effectiveness. Also, technological advancements to improve collection efficiencies, reduce power requirements, and develop collection media to be compatible with detection schemes, are critical future collector technology issues of the Joint Service community.

Aerosol collectors are usually comprised of air moving components, an air inlet, a sample transmission train, and some type of collection media. The Edgewood Chemical Biological Center (ECBC) has developed special aerosol test facilities and an array of test methods to evaluate the performance of aerosol collectors, and in particular aerosol inlets and sampling trains. These facilities include aerosol test chambers, flow through cells, and aerosol wind tunnels. Several collectors used in current CB defense systems and Commercial Off-the-Shelf (COTS) items were recently evaluated in the ECBC facilities. Examples of the performance data of these collectors will give perspective to the state of the art used in these systems. In addition, several advanced technology samplers will be evaluated to demonstrate the potential for performance improvement.

This presentation will discuss the basics of aerosol samplers, aerosol collector performance, and the facilities/test methods required to characterize sampling performance. The current state of collector technology and performance, as well as future needs will also be addressed.

1.0 Introduction

Biological Warfare (BW) and some Chemical Warfare (CW) agents are aerosols. They are particles suspended in air. Therefore, the Aerosol Collector is a critical component for CB Point Detection systems. Its role is to extract and concentrate the aerosol samples from surrounding environment, which can then be analyzed for detection of BW agents.

These aerosol particles have mass and a velocity vector as they are sampled. Because of the inertial properties of aerosols they resist change in velocity vector as they pass through the sampling train of a collector. Collector designs serve many purposes and must effectively address the inertial properties of aerosols for that purpose. For example, a High Volume collector means to extract a maximum number of particles from the air to generate a highly concentrated sample for analysis. It may do this at the expense of over-representing particles of a certain size. On the other hand, a representative sampler will collect an unbiased sample, which remains proportional to distribution of particles in the air. The point is that collector/sampler designs necessarily compromise performance parameters such as efficiency, sample biasing, and power requirements. Therefore characterizing the performance of collectors/samplers is important to assess point detection system effectiveness.

The terms "collector" and "sampler" are often used interchangeably in casual context. Some suggest that a "collector system" aims to extract as much aerosol as possible from the air with little regard for biasing of the sample, whereas a "sampler system" extracts unbiased samples from the air. In this presentation the terms are used interchangeably with preference to calling the overall device a "sampler" and reserving the term "collector" as designation of an aerosol collecting component within the "sampler".

2.0 Basics of Aerosol Samplers

Figure 1 is a very simple schematic of a typical sampler used in CB point detection systems. A typical sampler is comprised by some or all of the following components arranged in a sampling train. First the aerosol in the surrounding air is aspirated into the system through the inlet. It is then transmitted to the rest of the sampler, sometimes through a system of transmission tubes or ducts if the inlet is remote from the main sampler unit. The main sampler unit may include several components, such as impactors, concentrators, flow splitters, all connected by additional transmission ducts or paths. These internal components tailor the aerosol sample and deliver it to a collector device which puts the aerosol particle into a medium for the detector to analyze. Some type of air moving device, usually a fan type blower, is connected to the end of the

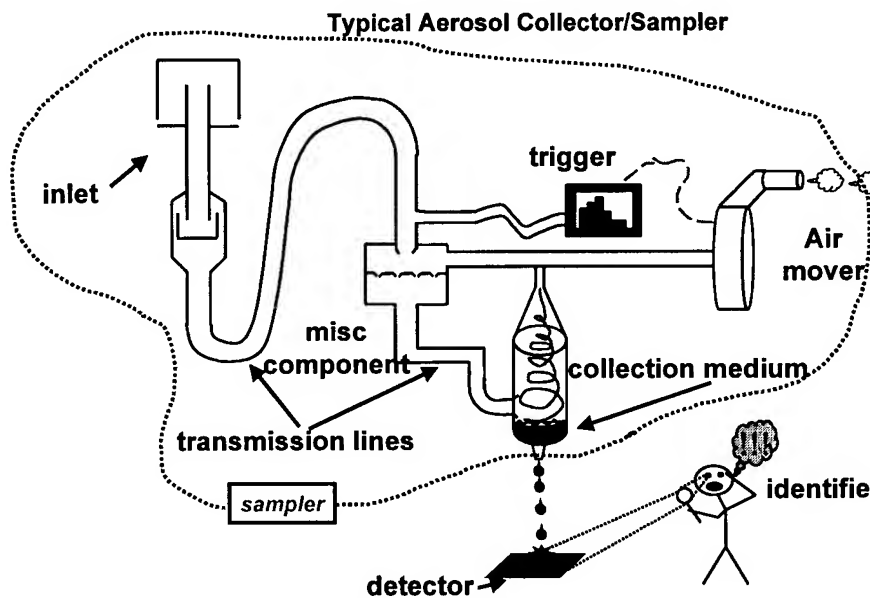


Figure 1. Sampler Schematic.

sampling train to pull the air through the system. Also, in some systems there will be a trigger component, usually some type of particle counter, which continually samples the air and initiates the blower only when a suspicious aerosol profile is sensed. This manages power expenditure and prolongs consumables. External to the sampler is the actual detector and perhaps an identifier component to complete the point detection system.

Size, weight, and performance are important considerations in selecting a sampler to be used in a point detection system. Some detection systems have more stringent size restrictions than others. Obviously a vehicle or shipboard mounted system will have limited space, whereas samplers placed in open areas are more flexible. Weight certainly is a concern if the system is portable, such as required by "first responders" in a "homeland defense" scenario. Performance issues deal with the sampler's ability to deliver aerosol to the detector. The basic performance parameters are power consumption, sampling air flow rate, Concentrating Factor, and Sampling Efficiency.

The detector requires an agent containing sample above a certain threshold concentration. It is the sampler/collector's job to get that sample to the detector. Usually it is desired in as high a concentration as possible because in the defense application the agents are in very low surrounding air concentrations. The sampler/collector's Concentrating Factor is a ratio of the concentration delivered to the detector (in current systems this means the aerosol is usually concentrated into a liquid) to the concentration of aerosol in the air. In an air to liquid collector this can be expressed as the product of the ratio of the volumetric air flow rate through the sampler to the liquid flow rate of the collector, and the efficiency by which the aerosol is captured. Therefore there are two main sampler parameters that can improve the concentrating factor other than the collection capability of the actual collector component within the sampler. First the sampler can simply take in more aerosol by increasing air flow rate. Second the efficiency of delivering the aerosol to the detector can be increased.

The first parameter, increased flow rate, comes with a high cost. Fan laws which apply to blowers used in samplers indicate that the power required to move the air is a function of the cube of the air flow rate. Small increases in flow rate will require large increases in power. The second parameter, increased efficiency, can be realized by understanding of the physics of aerosols and proper or inventive sampling train design. This is why efficiency is the focus of most sampler/collector characterizations.

Overall sampling efficiency (η_o) is the ratio of aerosol collected to the aerosol in the air. It is usually calculated as the ratio of particles collected per volume of air sampled to the concentration (C) of particles in the ambient air.

$$\eta_o = \frac{C_{coll}}{C_{air}} \quad (1)$$

Also, each element of the sampler (e.g. The inlet, tubing, collector device, etc...) has an associated efficiency (η_i). Since the flow (Q) through such elements is sometimes split for purposes of concentrating the aerosol, the efficiency equation is generalized.

$$\eta_i = \frac{C_{out} (or C_{collected}) \cdot Q_{out}}{C_{in} \cdot Q_{in}} \quad (2)$$

The overall sampling efficiency is the product of the component efficiencies.

$$\eta_o = \prod \eta_i \quad (3)$$

The overall efficiency will determine the sensitivity of the overall detection capability of the system. The individual component efficiencies will indicate where design problems exist or where sampling train improvements are most beneficial

Individual component efficiency is a function of the aerosol particle size. This is due to the inertial properties of aerosol particles; larger particles will be lost more readily to mechanisms such as surface impaction as flow curves through the sampling train, where smaller particles will not be as readily concentrated, or captured in collector devices. Aerosol particles in the 1-10 μm range are of greatest interest to samplers used in CB defense systems. In addition to particle size the efficiency of the sampler inlet is also a function of wind speed. Samplers used in point detection systems will likely operate in an outdoor environment where wind exists, for example the average wind speed in the U.S. is approximately 8 mph. In addition, several Joint Service samplers are required to operate aboard a moving platform such as Naval ships, where the wind speeds can be surprisingly high. Again, because of the inertial properties of aerosols, if they are moving along a streamline they will resist a change in the velocity vector (an acceleration) such as a curvature or the streamline as the flow moves around or through an inlet. The ability of an inlet to convey aerosol to the rest of the sampler (the inlet efficiency) is actually a combination of the ability of the inlet to aspirate the aerosol (aspiration efficiency) and the ability to transmit it to the sampler once aspirated (transmission efficiency).

$$\eta_{\text{inlet}} = \eta_{\text{transmission}} \cdot \eta_{\text{aspiration}} \quad (4)$$

Particle mass (which relates to particle size) affects the aspiration and transmission efficiencies in different ways. In terms of aspiration, small particles will follow streamlines as they move around a blunt inlet such as an inlet, whereas large particles will cross streamlines and consequently be "over-sampled" with respect to the ambient particle size distribution. However, once aspirated, the large particles will be more likely to be lost to surface impaction. These combined effects may insert a significant bias in the particle size distribution of the sample.

3.0 Sampler Performance Evaluation

Laboratory characterization of samplers largely consists of the measurement of aerosol efficiencies. Aerosol efficiencies are assessed by providing a well characterized, known aerosol challenge to the sampler or sampling component of interest and measuring the aerosol that is conveyed to the end of the component (or the amount captured by the collection components). In transmission type evaluations the aerosol through-put is collected and analyzed and ratio-ed to the challenge which is either precisely known or characterized by collection with a reference sampler. These studies require special aerosol test facilities and techniques. Sampler component efficiencies are usually examined in aerosol chambers or special test cells that deliver a known aerosol challenge to the entrance of the component. Overall sampling efficiency can be assessed in a chamber also but the inlet wind effects will not be accounted. The inlet efficiency should be determined in a realistic, but controlled wind environment. This is usually accomplished in an aerosol wind tunnel facility.

The Aerosol Science Team (AST) of the U.S. Army Edgewood Chemical Biological Center (ECBC) has developed an array of test facilities to support the development of the various Joint Service CB defense systems. The AST has both aerosol chambers and aerosol wind tunnels which are used to evaluate samplers and sampler components.

The primary chamber test facilities include a large 70 M^3 environmentally controlled chamber. This is the workhorse facility of the AST and is primarily used to evaluate full-up sampler systems. Individual component performance is accomplished through the use of what is called a "Flow-Through-Cell". This

device can simultaneously deliver the identical aerosol challenge directly to the entrance of the test component and the corresponding reference sampler. Also, the AST has fabricated a field transportable chamber for use in testing Stand-Off detection systems. In simple terms, this is a large tube on a trailer with doors on each end. An aerosol challenge is generated and circulated through the tube to create a uniform aerosol cloud contained in the tube. Doors at both ends of the tube are opened once the challenge is established to enable a stand-off system to look through the tube and sense an aerosol cloud. The stand-off device will only see the aerosol cloud, not the tube chambers itself. This quality provides the nickname "Stealth Tube" to this facility.

Wind tunnel facilities provide the realistic, controlled test conditions necessary to evaluate sampler inlets. The AST has developed two aerosol wind tunnels and is in the process of fabricating a third. The main wind tunnel has a usable test section jet that is 28-inches in diameter. The tunnel was originally designed for aerodynamic testing, however recent modifications allow it to be used for aerosol experiments. One of the recent modifications includes the use of an aerosol mixing box, described by McFarland et al to provide a uniform aerosol challenge across the entire test jet. In this configuration the tunnel can be used for inlet evaluations in the wind speed range of 10 to 60 mph. A special aerosol confinement sleeve replaces the mixing box to allow aerosol testing of items such as Unmanned Aerial Vehicle (UAV) sampling inlets at wind speeds approaching 140 mph. However in this configuration the aerosol is confined in a uniform stream directed to the test and reference inlets, not the entire test section. A smaller wind tunnel exists which is similar in configuration to the large wind tunnel but has HEPA filtered exhaust which enables the use of biosimulant aerosol challenges. The test section is an "open jet" 20-inches in diameter contained in a 48-inch chamber. The small tunnel is used to evaluate inlets in the 1 to 15 mph wind speed range. A third aerosol wind tunnel is currently being constructed to allow the testing of larger inlets in a speed range that bridges the capabilities of the two existing wind tunnels. It is basically a scaled-up version of the small wind tunnel, having a 36-inch "open jet" test section contained in a 72-inch chamber. It will be used to evaluate inlets in the 1-25 mph speed range.

Aerosol experimentation requires the generation and analysis of aerosols used to challenge the sampler hardware. The aerosol challenges used in the AST facilities falls into two general categories: inert test particles, and biosimulant aerosols. For quantitative aerosol characterizations, the inert test particles are primarily used. They may be either monodispersed or polydispersed in size distribution, depending on the type of information required and the analysis technique. For example monodispersed aerosols are used to provide characterizations at a precise aerosol size (such as in determining collector cut-points). Whereas a polydispersed aerosol can be used to provide a less precise but more inclusive characterization over a wide size range, providing the analysis technique is capable of resolving the captured samples into discreet size categories (such as hydrosol spectroscopy). The biosimulant aerosols are generally classified by the threat they represent such as bacteria, virus, or toxin. They are used to evaluate components and systems against a realistic threat aerosol. This type of evaluation is useful to prove a system's capability to handle the unique properties of the threat aerosol and is necessary to evaluate detector/identifier performance, but is less useful than test particles in determining sampler performance characterizations.

4.0 Evaluations of Current Technology Samplers/Collectors

The AST uses the aerosol test facilities it has developed to provide support the development of samplers used in point detection systems. Some examples of the evaluations are provided to gain a perspective on the state of the performance that is available from current systems. A wide array of samplers and sampler components has been recently evaluated. One focus has been on the evaluation of small, low power, commercially available collectors which may show promise as Commercially Available Off-the-Shelf (COTS) devices which can be directly included in point detection systems. The use of COTS items is attractive since it eliminates the need to develop the collector part of the detection system. These devices

are especially appropriate for systems intended to be rapidly deployed to sites where the system has to be small, light, and portable. The other focus has been working in support of fielded or soon-to-be-produced military systems. Particular attention has been in determining how a re-configuration of a basic system to meet the various Joint Service needs, will affect their performance. These systems represent the other end of the sampler spectrum as they include all elements of a point detection system. Consequently they are much bigger and consume significant power.

Significant findings of the COTS evaluations show that the commercial collectors do not have especially high efficiencies, particularly in the small size range. They are probably adequate for the purposes for which they were developed, but they may not be able to provide the aerosol sample that current military detection systems require of the current military collectors. Figure 2 compares several of the small, low power commercial collectors to a current military collector that uses similar technology. The military collector's small particle performance is much better than that available with the commercial collectors. This is not surprising since the military collector operates at a power level approximately ten times that of the commercial collectors. The small particle collection is facilitated by higher energy airflow in the collector.

The military system component studies illustrate how seemingly minor component differences made to accommodate different configurations of the same system can significantly affect sampling (and therefore detection system) performance. Figure 3 compares two identical samplers that use different collection mechanisms. Figure 4 breaks down the efficiencies of various components used in different sampling train versions of a sampler system. This study was able to identify a particular component that transmitted only 10% of the available aerosol to the rest of the sampler. This component can be completely eliminated by a 2-inch realignment of sequential sampling components.

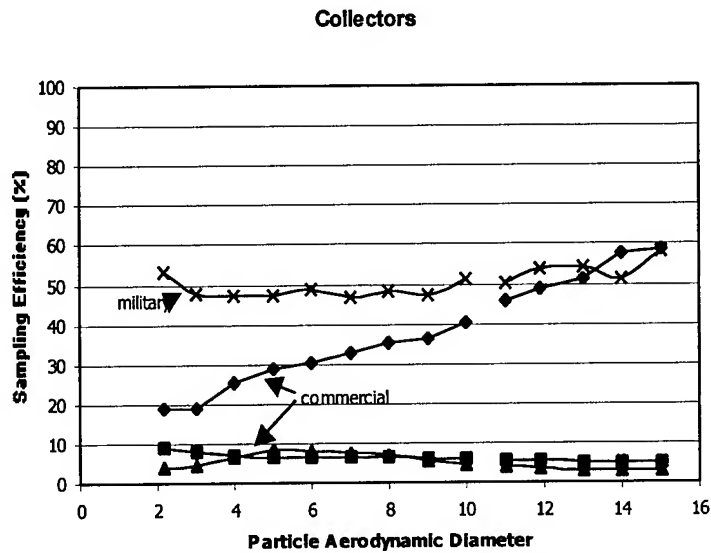


Figure 2. Collector Efficiency.

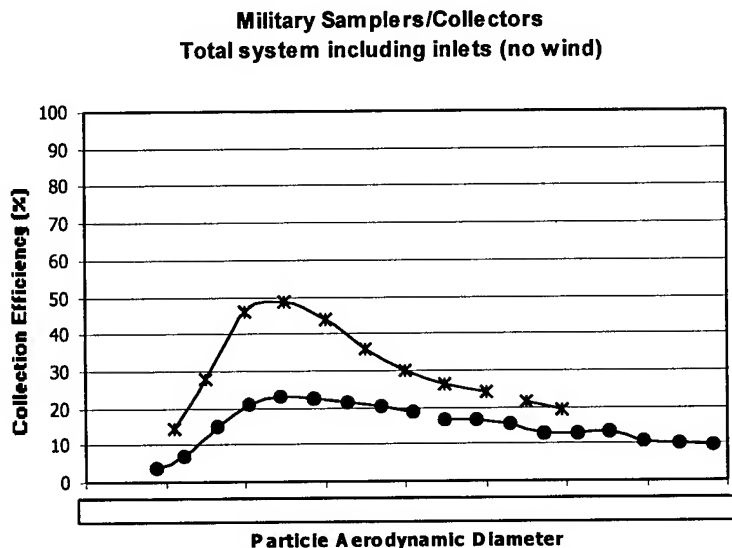


Figure 3. Military Sampler

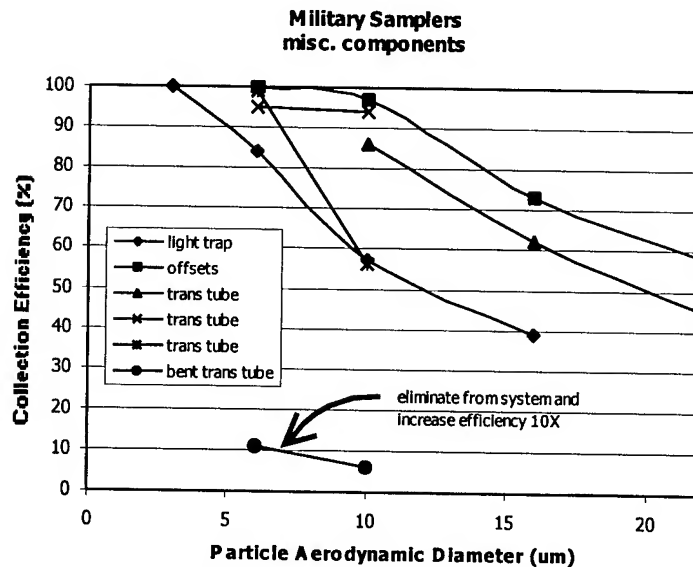


Figure 4. Military components.

Wind tunnel studies of inlets show that typical omni directional inlets used in most systems may perform very well in still air but as wind speed increases, the inlet efficiency drops significantly. For example, figure 4 indicates that in a 10 mph wind the inlet efficiency, and therefore amount of aerosol collected, will be 60 to 50 percent of what it was in still air. Note that the inlet was tested at wind speeds up to 60 mph. Although this seems very high for aerosol sampling, some Joint Service requirements for samplers have been written to include these winds as operational possibilities. In figure 5 sampling efficiency is shown for two versions of a point detection sampler inlet as a function of wind speed. A ruggedized version of a sampling inlet was required for a ship-board installation. This version uses an inlet that is scaled about 25% larger than the original. The large inlet demonstrated a noticeable increase in sampling efficiency in the 10 mph range. This is a good example of how sometimes small changes in inlet geometry can make a big difference in performance.

5.0 Advanced Technology Collectors

Improvements in collector performance will obviously yield direct benefits to the overall CB point detection system in which it is used. The Joint Service community has a great interest in future collector technologies which will reduce weight and power consumption, increase collection capability (increase efficiency and/or volume of air sampled). There are also other issues such as developing new collection media or conditioning the media to be environmentally insensitive. Also, new collection technologies that are more compatible with new detection technologies are desirable.

There are many promising concepts being proposed by collector developers. Some examples of new concepts which will be evaluated in the AST facilities in the near future include:

- Micro machined collectors which use laminar flow to reduce power consumption.
- Transpired tubes which can be used for aerosol transmission components for reduced particle deposition.
- Acoustic and thermophoretic force enhanced transmission lines which may also reduce deposition.
- Shrouded or directional inlets to improve inlet efficiencies in windy conditions.

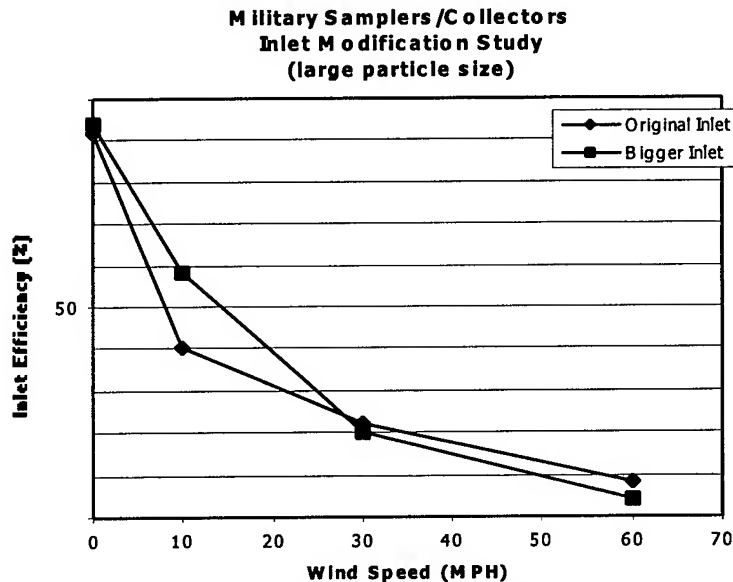


Figure 5. Inlet Efficiencies

CONCLUSIONS

Aerosol samplers are a critical component of any CB point detection system. It is the sampler's role to provide an adequate aerosol sample to the detector unit for analysis. Characterization of samplers is important to the understanding of the performance capabilities of the CB point detection system and identifying where improvements to the sampling system can be made.

Specialized aerosol test facilities and methods are used to evaluate sampler performance. Aerosol chambers are used to characterize overall collection capability and to evaluate individual components of the sampling train. However, aerosol wind tunnels are necessary to evaluate inlet efficiencies because of their wind speed dependence.

Recent sampler evaluations indicate that there is room for improvement in collector technology, especially in terms of power consumption and sampling efficiency of small particles. Even moderate improvements to sampler performance can yield large payoffs in the overall CB detection system capability.

Advanced sampler technology concepts are addressing performance issues of weight, power, and collection capability.

SURFACE SAMPLING CAPABILITY FOR CHEMICAL POINT DETECTION SYSTEMS

Elizabeth S. Catalano

U.S. Army Soldier and Biological Chemical Command
Project Manager for Nuclear, Biological, and Chemical Defense Systems
Aberdeen Proving Ground, MD 21010-5424 USA

ABSTRACT

Forces opposing the U.S. have a near all-weather ability to contaminate personnel, materiel, and terrain with chemical agents. To effectively counter this chemical agent threat, the U.S. Forces require a man portable, automatic chemical agent alarm system.

The U.S. Army has taken delivery of a new chemical agent detector, the M22 Automatic Chemical Agent Alarm (ACADA). The ACADA is the most advanced chemical warfare point detector to be fielded that can detect the most common nerve and blister agents and can be programmed to address other agents. It is a Non Developmental Item that does not have the capability for surface sampling. Currently, the U.S. Forces are dependent on chemical agent detector kits for the conduct of surface sampling. These manually operated kits are slow and require large expenditures of manpower. U.S. Forces have even used chemical agent detector paper as field expedient measures. The paper, though quicker and less labor intensive, was not adequate for surface sampling. Therefore, a Pre-Planned Product Improvement (P3I) program was initiated to develop an auxiliary component of the ACADA, the XM279 Sampler Kit.

The XM279 Sampler Kit contains the Surface Sampler Probe, which is the major component. The Surface Sampler Probe is a hand-held device that transfers suspect surface contamination to the ACADA for verification of the presence of chemical warfare agents. It is all weather operational and requires minimal maintenance that can be performed at operator level.

Within the presentation, the ACADA Program Team will briefly provide an overview of the M22 ACADA, detail the performance of the XM279, review the XM279 test program and describe the ongoing efforts of the XM279 program.

My presentation is relevant to the topic area- 1. CB Collection, Sampling, and Sample Processing. I will need the following audio visual equipment: transparency projector.

Elizabeth S. Catalano, Chemical Engineer, GS12
Telephone: 410-436-5597 FAX: 410-436-6526
E-mail: elizabeth.catalano@SBCCOM.APGEA.ARMY.MIL
Address:

Commander
U.S. Army Soldier and Biological Chemical Command
Office of Project Manager for NBC Defense Systems
5183 Blackhawk Road, Building E3549
ATTN: AMSSB-PM-RNN-A/E. Catalano
Aberdeen Proving Ground, MD 21010-5424

UNCLASSIFIED

(U) (slide 1- Title Chart) Forces opposing the U.S. have a near all-weather ability to contaminate personnel, materiel, and terrain with chemical agents. The Army was designated the lead service as part of the Joint Service Nuclear, Biological and Chemical (NBC) Defense Program to provide an automatic monitor/survey capability, an advanced point sampling chemical agent detector/alarm capability and a collective protection equipment monitor capability. The M22, Automatic Chemical Agent Alarm (ACADA) is the most advanced chemical warfare point detector and is a Non-Developmental Item (NDI). It is currently in production with several thousand systems already fielded. (slide 2- M22 chart).

(U) One of the requirements stated in the Joint Service Operational Requirements (JSOR) within the M22 is for a surface sampling capability to detect liquid chemical warfare agents (CWA) that accumulate, if sufficient agent vapor is not present. The XM279 is designed to provide this necessary capability. This surface sampling capability was a PrePlanned Product Improvement (P3I) acquisition. (slide 3- XM279 chart)

(U) The XM279 is a Joint Service program with the Army as the lead service. A purchase description was developed that further defined the surface sampling requirements for the XM279. The XM279 is to sample for CWA deposited on various surfaces and terrain and transfer the suspect CWA, in vapor form, to the M22 for analysis. It will be used to determine decontamination requirements for vehicles, equipment, and personnel and to verify the effectiveness of the decontamination. The XM279 is required to volatilize CWA within 150 seconds at surface temperatures down to -30 degrees Centigrade. It must operate for a minimum of six hours at -30 degrees Centigrade on battery power and be all weather operational. The unit is required also to use standard Army batteries.

(U) A market survey determined that no product currently existed to meet the requirements of the purchase description. Through a task

UNCLASSIFIED

UNCLASSIFIED

order contract, two concepts, the hot gas recirculation and direct heating were modeled. The direct heating infrared diode design was selected to proceed into the Engineering, Manufacturing and Development (EMD) phase. Once in EMD, the design was tested to the requirements of the purchase description and the Test and Evaluation Master Plan (TEMP). Engineering testing resulted in a mature performance purchase description and design of the Sampler Kit, Air: Chemical Agent Alarm, XM279. The XM279 Sampler Kit contains a Surface Sampler Probe, an expendable parts kit and transit case. The Surface Sampler Probe is the major component, which is a hand-held device that transfers suspect surface contamination to the M22 for verification of the presence of CWA. The surface sampler probe utilizes a BA-5800/U Lithium Sulfur Dioxide non-rechargeable battery or four BA-3030 (D-cell) batteries when used with the training battery assembly (slide 4- batteries chart). It is less than 0.10 cubic feet in size and weighs less than 5.5 pounds. The expendable parts kit (slide 5- expendable parts chart) contains the disposable tips for the surface sampler probe with tip removal tool and the detector standoffs for the M22. These expendable parts ensure that the operator, surface sampler probe, and M22 do not receive any gross contamination (slide 6- operator removing disposable tip chart). Field maintenance allows the operator to remove/replace the surface sampler probe battery, disposable tips and the detector standoff adapter. Due to the nature of the XM279 mission, warfighters will use the item wearing Mission Oriented Protective Posture (MOPP) IV protective clothing.

(U) Use of the XM279 involves three modes of operation. The first mode is the sampling of the suspect surface contamination. This operation takes approximately thirty seconds and may require that the probe end with the disposable tip be scratched lightly to obtain a decent sample. (slide 7- XM279 sampling chart) The second mode is the transferring of the

UNCLASSIFIED

UNCLASSIFIED

collected sample to the M88 detector. During this operation, the Surface Sampler Probe is held over the M88 adapter until the M88 alarms or the Transfer Light Emitted Diode on the Probe remains constant. (slide 8- XM279 transferring chart) The last mode is the Clearing Down of the probe to have ready for the next sample. During cleardown, the IR heater is continuously on for two minutes to rid the surface sampler probe of contamination. This operation may be repeated if necessary. After two attempts to cleardown, a simple decon procedure of placing the IR heater element into a container of bleach has been demonstrated and incorporated into the technical manual (slide 9- XM279 clearing down chart).

(U) The Production Qualification Testing (PQT) included agent and interferent testing and environmental extreme conditions testing. Although these tests were limited, they were successful. Follow-up with full scale testing in Production Verification Testing (PVT) will be conducted after the Milestone III decision. (slide 10- XM279 testing chart) A user demonstration was successfully conducted during PQT, which assessed the suitability of the XM279 in meeting the user's need and operational employment concept. Participants were non-specific MOS operators, 61st Ordnance Brigade, 16th Training Battalion. (slide 11- XM279 User's Demonstration Test) Two different scenerios were conducted: Survey of a warehouse for reconnaissance and Monitoring –segregation of vehicles for decontamination. (slide 12- XM279 User's Demonstration Test)

(U) The XM279 is designed for interface with the M22 Automatic Chemical Agent Alarm. No other system is planned to interface with the XM279; however, it is possible for other detection systems such as the Chemical Agent Monitor/Improved Chemical Agent Monitor (CAM/ICAM) and the Joint Chemical Agent Detector (JCAD) to use the XM279 with little modifications.

UNCLASSIFIED

UNCLASSIFIED

(U) The ACADA team is dedicated to product support and we have several publications available or in development to assist operators and users in the deployment and operation of the XM279.

(U) For more information on the XM279 program, contact either myself or Dan Nowak. (slide 13- Points of Contact chart)

UNCLASSIFIED

BIOHAZ: A CONCEPT FOR FIRST RESPONDERS

Peter J. Stopa¹, Philip A. Coon¹, David Trudil², David Gray³, and Randy Bright³

¹The US Army Edgewood Chemical Biological Center, 5183 Blackhawk Road,
AMSSB-REN-E-MC, E 3549, Aberdeen Proving Ground, MD, 21010-5424 USA,

(Peter.Stopa@SBCCOM.APGEA.ARMY.MIL), ²New Horizons Diagnostics Corporation, 9110 Red Branch Road,
Columbia, MD 21045, USA, ³EAI Corporation, 1308 Continental Drive, Abingdon, MD 21009, USA

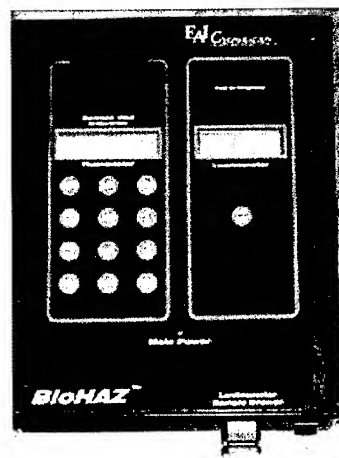
ABSTRACT

There exists a need for first responders, both military and civilian, to rapidly screen and detect the presence of a biological material in a suspect sample. This sample could consist of a letter, a fill within a suspicious device, or others. What the user needs is a way to accurately and easily obtain a sample, and then screen this sample for the presence of a biological material.

The BioHaz™ kit is being developed to fill such a need. It is intended to give the first-responder an integrated capability to sample and then screen for the presence of a biological material in an environmental sample. This allows the site commander to be aware of a potential biological hazard and call for the proper response to the situation.

This kit consists of both sampling and detection equipment. It has a variety of sampling devices to obtain solid, liquid, and aerosol samples. Samples are then screened by well-proven technology to determine the presence of biomarkers within a sample. These biomarkers include ATP, DNA, and protein. An algorithm has been developed to categorize the sample in a manner similar to the HAZCAT protocol for chemicals. This algorithm will allow the operator to determine if the sample may contain a bacteria, bacterial spore, or protein. An assessment can also be made as to the viability of the material. Samples can then be further analyzed on-site with immunoassay tickets or sent to a reference laboratory for detailed analysis.

This system can provide the first-responder with a capability that he currently does not have. The adoption of this kit by the first responder community could result in savings of time and material. It may also deter the use of biological agents since the BioHaz™ could be part of a system to mitigate the effects of a biological insult.



INTRODUCTION

There exists a need for first responders, both military and civilian, to rapidly screen and detect the presence of a biological material in a suspect sample. This sample could consist of a letter, a fill within a suspicious device, or other scenarios. The U.S. Army Edgewood Chemical Biological Center initiated an effort to develop an expedient capability for first responders to sample, detect, and identify the presence of hazardous biological materials in the environment.

Key project tasks included:

- Identify customer requirements and Concepts of Operations (CONOPS).
- Identify or develop technologies that meet mission requirements.
- Integrate these technologies into a kit.
- Test and evaluate the kit.
- Train the user in the use of the kit.
- Deliver kits to the user community.

The first step in this effort was to identify user requirements and concerns, and then to develop a Concept of Operations (CONOPS) for the use of the kit. To achieve this goal, we met with representatives of various first responder organizations at the outset of the project. Design goals and performance specifications were then established with the assistance of the customer. As a performance goal, we adopted the first generation requirements of the Biological Integrated Detection System (BIDS) that is currently fielded by the US Army for biological detection. An additional goal was that the total cost of the kit should not exceed \$20,000 per copy. The requirements of the kit were that it should provide a capability to do both air and surface sampling, but work primarily with surface samples to answer the question, "Does that white powder contain a bio-material. If it is a bacteria, is it viable?". Lastly, all of the components had to be commercially available.

MARKET SURVEY AND APPROACH

A market survey to identify technologies that meet mission requirements was then performed. Upon completion of this effort, the problem was re-evaluated. It was then decided to change the focus of the effort. The original concept consisted of a kit with sampling devices and a library of test tickets for identification purposes. However, the concept was changed to a more generic approach for a variety of reasons, some of which were:

1. A limited library of test tickets capable of identifying the agents is available. This library may miss other pathogenic biological materials that could be used by a terrorist, but may not be thought of as a battlefield agent.
2. Immunoassay test kits also have to be used within concentration and pH guidelines. Samples that are outside of these guidelines may give erroneous results. Therefore, it would be useful for field analysis to have a means to determine if the sample was within the guidelines necessary for accurate use of the kit.
3. Genetic engineering of organisms or other treatments may compromise the ability of antibody-based or nucleic acid probe-based tests to detect and/or identify pathogenic materials.

Based on our market survey, a BIDS-like approach was then adopted in which generic techniques that test for "biological traits" were implemented into a kit. The BIDS utilizes a particle counter to measure fluxes in the particle size in the environment, collects a sample, and then analyzes the sample for Adenosine Tri-Phosphate (ATP) content and for Deoxyribonucleic Acid (DNA) content. If the sample possesses certain criteria, then it is subjected to immunoassay techniques for further analysis. This scheme is based upon the:

1. ATP determination – measures presence of "living" things.
2. DNA Test – All biological materials have DNA. Although purified proteins are assumed to contain no DNA, they are often contaminated with enough residual DNA to be detectable.
3. Protein Test – All biological materials have protein.

4. Particle Size and Count determination – Most intentional, man-made particles that have viable organisms and/or biological activity are typically above 3 microns (um) in diameter.

Unlike the BIDS, a generic protein detection capability was added for proteinaceous toxins, such as Botulinum and Ricin. The same tests that are used in the BIDS are used in this kit, but because of cost, size, and weight constraints, the approach on how these tests were used was changed. For example, the BIDS uses a flow cytometer to do DNA detection. This instrument is capable of distinguishing between spore and vegetative cell DNA; however, it has a price tag of \$100,000 and weighs 300 lbs. Our approach would tell you that there was DNA in the sample, but could not tell you what type. The luminometer is comparable to the one in the BIDS. However, the BIDS luminometer measures total ATP and can not differentiate among non-bacterial ATP, vegetative bacterial ATP, or spore ATP. The Model 3550 has the capability to differentiate among these sources of DNA. Therefore, the BIDS uses the cytometer to differentiate among types of biological material- the BDK does it with the luminometer.

Sampling issues were also addressed in the kit. Since there are a variety of sampling systems in the commercial marketplace for use in different applications, it was decided to take some of these and integrate them into kits for specific purposes. Therefore, kits were developed to take large area samples (SWIPE I), sample small areas or powders (SWIPE II), liquids (SWIPE III), and air using filter systems designed for either air sampling or asbestos monitoring (SWIPE IV). In addition, a sample processing kit (SPK) was also developed.

TECHNICAL CONSIDERATIONS

Hand-Held Particle Counting/Sizing Devices

Small, Hand-held Particle sizers (Met-One Models 227A (2 channel) and 237A (6 channel), and the Bio-Test AG (4 channel)) were obtained and evaluated for use. They were tested extensively during several joint field trials held in the US. They compared relatively well to some of the more expensive devices currently available. They can be used to determine particle size and concentration in the area, and may prove to be useful in detecting sources of biological agents in structures.

ATP Luminescence Detection Devices

A market survey was conducted of ATP detection devices (luminometers) and 3 were evaluated: the IDEXX Lightning System; the New Horizons Diagnostics Model 4700, as is used in the BIDS; and the New Horizons Diagnostics Model 3550. Although other systems exist and are mainly used in food safety and sanitation monitoring, we felt that these 3 units offered some distinct advantages. The IDEXX system has all the reagents packaged in a swab device. The 4700 is used in the BIDS and would be representative of some of the other luminometers that read total ATP, and the Model 3550i. It has the advantage in that it has a separation step that allows you to eliminate non-bacterial sources of ATP. This capability was utilized to develop a test capable of detecting spores or starved bacteria. This test could not be easily achieved in some of the other instruments. The New Horizons Diagnostics, Inc., Model 3550 was implemented for the following reasons:

1. Tested by the USDA and the Polish Army Veterinary Corps (PAVC) under field conditions and found to be the only luminometer that showed good correlation with culture results.
2. FDA approved for detection of bacteria in human urine.
3. Used by several commercial companies to measure bacterial contamination in process control measurements.
4. Shown to be the least prone to interferences.
5. Allows one to use a variety of sample volumes for analysis.

The luminometer was evaluated with 5 different types of bacteria, which included gram positive spores, cocci, and rods, and gram negative rods and cocci. Detection of 10^5 CFU/ml of vegetative bacteria was achieved. We also adapted a spore test to the luminometer that could detect 10^6 CFU/ml of spores, and could repeatedly differentiate between spore and non-spore forming bacteria. This was demonstrated during a recent Joint Field Trial held in the US.

Protein Detection

The Coomassie Blue Protein Test was adopted since it is the only protein test that met time and other mission requirements. Other tests either take at least 1 hour or require boiling of the sample. However, interferences from detergents was found with this test. Field experiences with the test showed that an adoption of a cut-off of 10 ug/ml of protein from surface samples was necessary so as to minimize false positive results. 2.5 ug/ml was chosen as the cut-off value for protein in air samples. Several colorimeters were evaluated for use, and the types that are typically used for protein in water analysis were adopted. They are typically in the price range of \$200.00 to \$900.00. For evaluation purposes, the ChemMetrics VVR colorimeter was adopted for the kit.

DNA Detection

For the DNA determination, the Hoefer DNA Quantitation Kit from Pharmacia Chemicals Inc. was initially evaluated. The instrument analyzes in the UV. It was not hardened enough to be of use, showed significant variability, and the dye was too prone to interferences from the sample that could not be controlled. We then evaluated the Pico Green dye kit from Molecular Probes. This kit is readily available and gives detection limits at the required level. It is routinely used in reference labs to quantitate DNA in samples prior to PCR analysis. It does not seem to be prone to matrix interferences and has a related dye that does detect RNA (single stranded nucleic acids).

To utilize the Pico Green Dye, the Turner Instruments TD-360 Fluorometer was used. It performed well and the detection of between 10^5 and 10^6 CFU/ml of bacteria was achieved, depending on the strain.

Instrument Integration

At the conclusion of the laboratory development phase, instruments were then given to actual field users. Based on this experience, it was decided that an integrated instrument should be built. This instrument is depicted in the accompanying figure. It is currently undergoing user and field tests. Preliminary results show that it has the same performance capabilities as the individual instruments.

Another improvement that has since been made is the adoption of protein test strips rather than the Coomassie test. These strips are commonly used in urinalysis. Although the detection limit increased somewhat to about 50 ug/ml with Bovine Serum albumin, these strips are less prone to interferences than the Coomassie test.

SUMMARY OF RESULTS

A variety of tests were performed both in the laboratory and the field. The laboratory tests showed that the system could routinely detect between 10^5 and 10^6 CFU/ml of bacteria, depending on the strain and/or metabolic state of the bacteria. Interferences to common household, laboratory, and environmental interferences was also evaluated. The ATP test showed that it had no interferences from any of these materials, although the timing was crucial as to when the sample was run relative to when it was collected. The DNA test did exhibit false-positive results when tested with phosphates; however, in

the scenario under which the test kit would be used, this should not be problematic since the presence of phosphate may also be another indicator of a biological material. As previously stated the protein test, using Coomassie Blue, did give false-positive results with detergents.

The performance goal of the system was that the system should be comparable to existing biological detection platforms. The following table shows how the kit fared.

<u>Requirement</u>	<u>ATP TEST(1)</u>	<u>DNA TEST</u>	<u>PROTEIN TEST</u>
Bacteria – 5×10^5 CFU/ml	< 10^5 CFU/ml (Vegetative) ~ 10^6 CFU/ml (Spores)	~ 10^5 CFU/ml (Vegetative) ~ 10^6 CFU/ml (Spores)	NA NA
Viruses – 10^6 PFU/ml	Not applicable	~ 10^7 PFU/ml (MS2)	NA
Protein Toxins – 500 ng/ml (air)	Not applicable	See Note 2	~2500 ng/ml

CFU/ml – Colony-forming units per milliliter

PFU/ml – Plaque-forming units per milliliter

Notes:

1. The ATP test measures only live bacteria. The DNA test can measure the presence of either live or dead bacteria. It was also noted that the signal can be enhanced if detergents are used to disrupt the bacteria, the detection limit decreases. Viruses can be detected at concentrations lower than 10^7 pfu/ml if the Ribogreen™ dye is used since most viruses that are of interest contain single-stranded nucleic acids, typically RNA.
2. At protein concentrations greater than 10 ug/ml, there is detectable DNA present, which is typically $1/1000^{\text{th}}$ of the protein concentration.

These results show that the BioHaz kit meets the design specifications for bacteria, and is within a decade of performance for the other biological materials of concern. This suggests that the BioHaz can indeed do what it is designed for, minimize hoaxes from powders in envelopes, etc. Other uses can also be to survey areas of interest for hot spots, measure the effectiveness of decontamination procedures, and also for water monitoring.

CONCLUSION

The BioHaz kit can provide first responders and others with a means to screen and determine the presence of biological materials in suspect samples. It can also be used to support other missions, such as decontamination effectiveness for biological materials, and might be suitable for use by inspection teams.

RAPID LYSIS AND RELEASE OF NUCLEIC ACID FROM MICROBIAL AGENTS FOR TAQMAN-PCR-BASED REAL-TIME IDENTIFICATION

Sanjiv R. Shah, Misty H. Lindsey, Rebecca L. Tanner, and Heena S. Beck
Science and Technology Corporation
500 Edgewood Road
Edgewood, Maryland 21040, USA

Michael T. Goode and Alan W. Zulich
US Army, Edgewood Chemical Biological Center (ECBC)
Aberdeen Proving Ground, MD 21010-5424, USA

Ever increasing applications of the polymerase chain reaction (PCR) technique are no longer limited to only the clinical diagnostic field. Use of nucleic acid as a marker for rapid detection and identification of pathogens in the environment, e.g., food, water, or even air is also rapidly growing. Efficient sample preparation determines not only the fate of the technique used, but also, the sensitivity of detection of pathogens in complex biological or environmental samples. Spore forming pathogens present the greatest challenge to release the nucleic acid. A rapid protocol for the lysis of *Bacillus subtilis* spores was developed in a laboratory set up using the Cepheid Ultrasonic Lysis System. The percentage of spore lysis was determined by viable counts and the released DNA was detected by real-time TaqMan-PCR on the Smart Cycler®. For different dilutions of spores, the lysis ranged from 95% to 98%. For the release of nucleic acid from vegetative bacteria and an RNA virus, heating and ultrasonication were tested and compared. Comparable results were obtained with either of these methods. However, lysis by the ultrasonication method was found to be very rapid. Efforts are directed at the development of an automatic and portable nucleic acid analysis system that integrates fast and reliable sample processing with real-time identification of pathogens in any complex specimen and that is easy to use by a relatively unskilled operator.

INTRODUCTION

Nucleic acid-based detection and identification of pathogens typically utilizes polymerase chain reaction (PCR).^{1,2} With the advent of real-time detection of amplicons using fluorescent probes,³⁻⁵ and fast thermal cyclers coupled with fluorometers,⁶⁻¹¹ the rapidity, sensitivity, and specificity of an assay are no longer challenging issues. However, rapid, reproducible, and easy to use protocols for nucleic acid extraction, purification, and concentration from complex environmental samples in the field are yet to be developed. The complexity of these problems is further increased either by an exceptionally low number of pathogens in large samples or by a requirement to test a low volume unknown sample in multiple pathogen specific assays. Extraction, the first step in sample processing, contributes greatly to the success of subsequent steps and finally, to the high-sensitivity detection of pathogens. The effectiveness of different extraction techniques, either singly or in combination, depends on the types and sizes of cells, source of samples, method of sample collection, and the types of target nucleic acids to be analyzed. Simultaneous extraction of nucleic acids from bacterial spores, vegetative cells, and DNA-RNA viruses in a single sample has yet not been established.

While vegetative cells and most viruses in a liquid sample are easy to disrupt, spores are very difficult to break open for DNA extraction. Various extraction methods exploiting physical, chemical, and enzymatic treatments, either singly or in combination, have been tested for spore lysis in a variety of environmental and soil samples.¹²⁻²³ Usually, physical disruption methods are preferred for a relatively clean environmental sample to eliminate subsequent extensive purification procedures that are necessary when chemical and enzymatic lysis methods are used. Also, in most cases, regardless of the source and characteristics of the sample, method of sample collection, and the types of target pathogens, physical disruption methods precede other methods or treatments during sample processing. Among the physical methods, boiling,¹³ freeze-thawing,^{14, 24-25} bead mill homogenization,^{17, 25, 26-27} and ultrasonication¹² have been tested and compared. However, these procedures vary widely in time. In the recent past, ultrasonication in a minisonicator was described for rapid disruption of *Bacillus subtilis* spores for DNA-based detection.²⁸ Also reported recently was an automated and rapid spore disruption system using a microfluidic cartridge.²⁹ However, a protocol for simultaneous lysis and release of nucleic acids from bacterial spores, vegetative cells, and viruses, especially RNA viruses, in a single sample is yet to be finalized. For such a nucleic acid extraction protocol, it is imperative to include a PCR conducive RNase inhibitor to protect the target RNA of a pathogenic RNA virus from digestion by RNase(s) either released from other biological agents or present as a contaminant in a sample.

In the present study, ultrasonication and heat treatments were evaluated to rapidly extract nucleic acids from multiple types of microbial agents for TaqMan-PCR-based real-time identification. The objectives of this work were multifold. Various combinations of ultrasonication parameters such as the power and duration were evaluated to establish optimum conditions for rapid and efficient disruption of *Bacillus* spores, vegetative bacteria, and MS2, an RNA bacteriophage. The efficiency of lysis was tested by plating as well as by improvement in TaqMan-PCR-based detection in terms of sensitivity, speed, and amplitude of fluorescence signal. Ultrasonication was compared with heat treatment for the release of nucleic acid for TaqMan-PCR-based analysis. The ultrasonication protocol established for spore lysis was evaluated for its effect on heat-released nucleic acids of vegetative bacteria, and MS2 bacteriophage. All the efforts were directed at the development of protocols for a future portable, automatic nucleic acid analysis system. Such a system that is easy to use by a relatively unskilled operator in the field will integrate rapid processing of environmental samples for multiple pathogens including RNA viruses with real-time identification by TaqMan-PCR.

MATERIALS AND METHODS

Microbial Agents. Dried spores of *Bacillus subtilis* var. *niger* (formerly known as *B. globigii*), and cultures of *Erwinia herbicola* and MS2, an RNA phage were kindly provided by Dugway Proving Ground, UT. Suspensions of formalin-killed *Bacillus anthracis* (Sterne strain) and *Yersinia pestis* (Colorado 92 strain) and their respective total DNAs were kindly supplied by Ted Hadfield's group, Armed Forces Institute of Pathology (AFIP), Washington, DC.

Microbial Agent Preparation for Lysis. Ten-fold serial dilutions of each agent were prepared in ice-cold 5 mM Tris.HCl, pH 8.0. Appropriate dilutions for each agent were used for lysis followed by TaqMan-PCR-based real-time detection.

(i) *B. subtilis*. Three loop-full of spores were resuspended in 5 ml ice-cold distilled water. The spore preparation contained significant amounts of free DNA. Therefore, the spores were washed five times with water before dilution. Aliquots from appropriate dilutions were plated on Luria Bertani (LB) agar

plates to determine the number of colony forming units (cfu). Appropriate dilutions were also plated after ultrasonication to determine lysis efficiency.

(ii) *E. herbicola*. An overnight grown colony on Tryptic Soy agar was resuspended in ice-cold 5 mM Tris.HCl, pH 8.0. Aliquots from appropriate dilutions were plated on Tryptic Soy agar plates to determine count.

(iii) MS2. After serial dilutions, aliquots from appropriate dilutions were mixed with *Escherichia coli* in soft agar and plated on LB agar plates to determine the number of plaque forming units (pfu).

(iv) *B. anthracis* (Sterne). Formalin-killed spores at 1×10^8 cfu/ml concentration (AFIP) were used to prepare dilutions.

(v) *Y. pestis* (CO92). Formalin-killed cells at 1×10^8 cfu/ml concentration (AFIP) were used to prepare dilutions.

Lysis Methods. Two methods, heating and ultrasonication, were used for lysis and release of nucleic acids

(i) **Lysis by Heating.** Agent suspensions were heated either in a boiling water bath or in a heating block at 98°C. *B. subtilis* spore suspension was heated in a boiling water bath for 15 min. The spore suspension of *B. anthracis* was heated in a heating block at 98°C for 15 min. *E. herbicola* and *Y. pestis* cell suspensions were heated in a heating block at 98°C for 5-10 min. MS2 phage dilutions were heated for 10 min at 75°C with and without RNA Secure™ (Ambion, Inc.). After the heat treatment, the extracts were stored on ice.

(ii) **Lysis by Ultrasonication.** The agents were disrupted by ultrasonication in the presence of glass beads using the Ultrasonic Lysis System from Cepheid, Inc. For microbial each agent, 100 µl of suspension was pipeted into an ICORE™ (Intelligent, Cooling/heating Optics Reaction) tube (Cepheid, Inc.) containing 40 mg of 106-µm glass beads (Sigma). Different combinations of power as measured by amplitude (65, 75, or 80%) and duration (5, 10, 15, or 20 sec) were evaluated to establish optimum ultrasonication parameters for lysis of spores, vegetative bacteria, and viruses. Extracts from triplicate tubes were carefully pooled to avoid glass beads and stored on ice. To study the effect of ultrasonication on released nucleic acids, heat treated dilutions were ultrasonicated at 75-80% amplitude for 15-20 sec.

Real-Time TaqMan-PCR/RT-PCR. TaqMan-PCR and One-step TaqMan RT-PCR were conducted using the Smart Cycler® (Cepheid, Inc.). The primers and probes sequences for TaqMan-PCR assays of *B. subtilis*, *E. herbicola*, and MS2 were kindly provided by the Naval Medical Research Center (NMRC, Bethesda, MD). The primers and probes for *B. anthracis* and *Y. pestis* were designed by Dr. Ted Hadfield (AFIP) and Dr. J. P. Chambers, University of Texas at San Antonio, respectively. Ten to twenty microliter aliquots of untreated and treated dilutions were used for analyses. For a positive control, total DNA from a respective agent was used, while dilution buffer served as a negative control.

RESULTS AND DISCUSSION

Rapid Lysis of Bacterial Spores. Heating and ultrasonication methods were selected and compared for spore lysis to release DNA for TaqMan-PCR-based rapid and real-time identification. As depicted in Figure 1, even after washing the *B. subtilis* spores five times, there was enough DNA coated on the spore surface to be detected by TaqMan-PCR without any spore lysis treatment. Heating the spore suspension in a boiling water bath for 15 minutes led to a couple of cycles faster detection and a better fluorescence signal than the no treatment control suspension. Ultrasonication of spore suspension at 75% amplitude for 20 seconds using the Cepheid Ultrasonic Lysis System resulted in five cycles faster detection with a further improved fluorescence signal than the heated suspension. The fluorescence signal amplitude was more than two fold as compared to untreated spores. A major advantage of the ultrasonication method

over boiling is a short treatment time. Spore lysis by ultrasonication required less than a minute as compared to boiling for 15 minutes. Also, it is possible that *B. subtilis* spores turn non-viable after heating in a boiling water bath for 15 minutes, but remain intact and therefore, no spore DNA is released. Improved fluorescence signal and detection with heated spore suspension as compared to control may be a result of release and uniform solubilization of DNA coated on the spore surface.

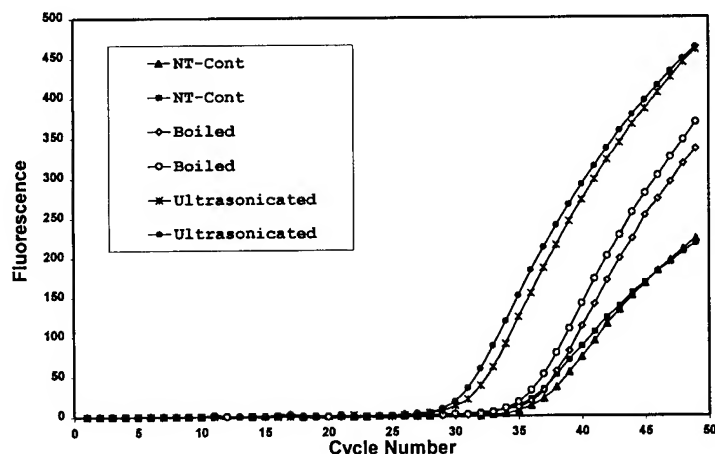


Figure 1. TaqMan-PCR-based real-time detection of *B. subtilis* spores after heat and ultrasonication treatments. Ten microliter aliquots of no treatment control (NT-Cont), boiled, and ultrasonicated spore suspensions at $7.35\text{E}+04$ cfu/ml original concentration were used in duplicate for PCR on the Smart Cycler®.

TABLE 1. *B. subtilis* Spore Lysis After Ultrasonication

Spore Concentration cfu/ml	Ultrasonication % Amplitude – Time (sec)	% Spore Lysis
1.15E+05	75 - 10	ND*
	75 - 15	89
	75 - 20	97
	80 - 10	ND*
	80 - 15	97
	80 - 20	98
1.15E+04	75 - 10	70
	75 - 15	82
	75 - 20	97
	80 - 10	67
	80 - 15	95
	80 - 20	96
1.15E+03	75 - 10	57
	75 - 15	90
	75 - 20	91
	80 - 10	67
	80 - 15	98
	80 - 20	97

ND* - Not determined because of a lawn of colonies indicating poor spore lysis.

Effectiveness of any spore lysis method is usually tested by increased sensitivity and reduced time of detection, and increased fluorescence signal amplitude. We added an additional criterion of plate count to determine the efficiency of ultrasonication. After ultrasonication using different combinations of amplitude (65, 75, and 80%) and time (5 (data not shown), 10, 15, and 20 seconds) on the Ultrasonic Lysis System, different dilutions of *B. subtilis* spores were plated on LB agar plates for the count. For $1.15\text{E}+04$ and $1.15\text{E}+05$ cfu/ml concentrations, a combination of 75% amplitude and 20 seconds duration of ultrasonication was sufficient to achieve about 97% spore lysis (Table 1). However, for a $1.15\text{E}+03$ cfu/ml concentration, ultrasonication at 80% amplitude for 15-20 sec was required for 98% spore lysis.

For the lysis of *B. anthracis* spores, heating at 98°C for 15 minutes and ultrasonication for 15 to 20 seconds at 65, 75, or 80% amplitude gave more or less similar results (Figures 2A-C). Presence of significant amount of extracellular DNA in the spore preparation, as can be seen from the untreated spores, did not allow establishment of optimum ultrasonication parameters. However, based on our results on viable *B. subtilis* counts after ultrasonication, it is safe to assume that ultrasonication at 80% amplitude for 20 seconds may be enough for *B. anthracis* spore lysis to release DNA for TaqMan-PCR-based identification. As mentioned earlier, the advantage of the ultrasonication method is the short treatment time. Ultrasonication of heat-treated spores did not show any adverse effect on heat released DNA (Figure 2D). This observation is important for a sample processing protocol which combines heating and ultrasonication methods to release nucleic acids from multiple types of microbial agents in a single sample.

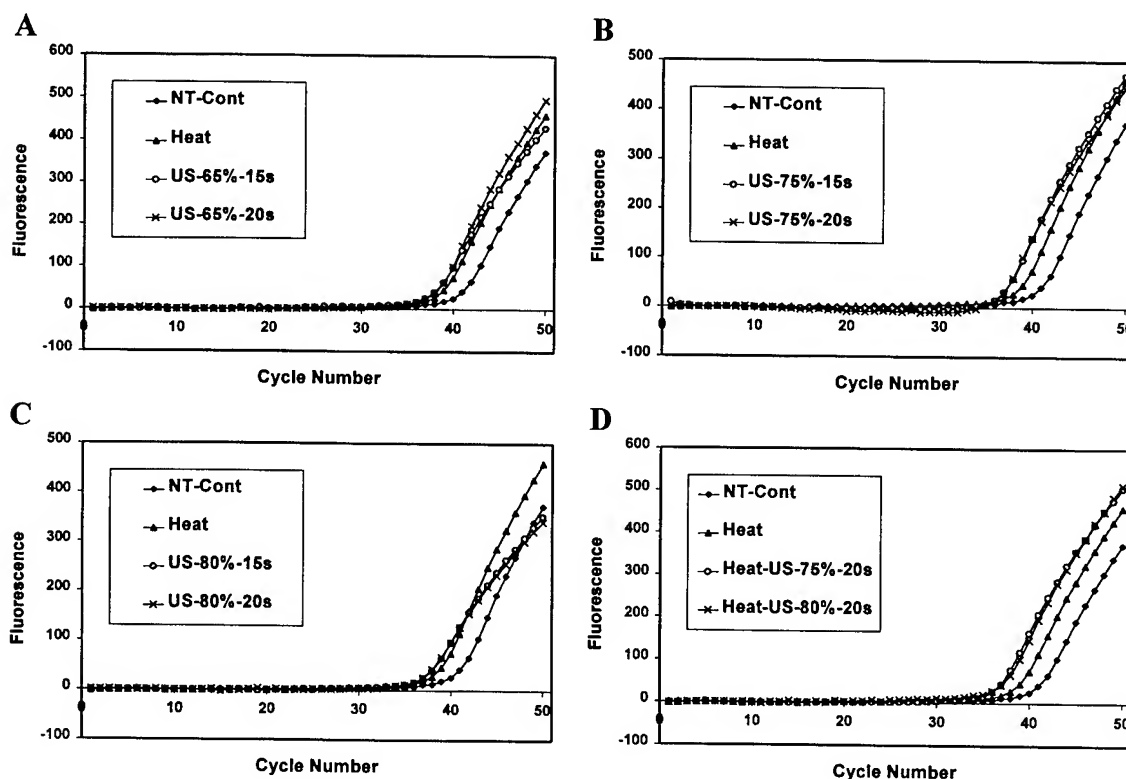


Figure 2. TaqMan-PCR-based real-time detection of *B. anthracis* spores after heat and ultrasonication treatments. Ten microliter aliquots of no treatment control (NT-Cont), heated (Heat), ultrasonicated (US) and heated-ultrasonicated (Heat-US) spore suspensions at $1.00\text{E}+03$ cfu/ml original concentration were used for PCR on the Smart Cycler®. Different combinations of ultrasonication amplitude (%) and time in seconds (s) (inset) were used for lysis.

On the basis of the spore lysis and the TaqMan-PCR results, ultrasonication is the method of choice for the rapid and efficient extraction of DNA from spores. For a maximum spore lysis and to cover low concentration samples, the ultrasonication parameters of 80% amplitude and 20 sec duration are recommended.

Rapid Lysis of Vegetative Bacterial Cells. It is a well established fact that heating at 98°C for 5 minutes is enough to disrupt vegetative cells in a PCR conducive buffer and release DNA for PCR amplification of a target gene. Lysis of *E. herbicola* and *Y. pestis* cells was tested. The ultrasonication method was compared with heating for the lysis of *E. herbicola*. Different combinations of amplitude and time of ultrasonication gave more or less similar detection results as compared to heating (Figures 3A-C). Both the methods gave a couple cycles faster detection with improved fluorescence signal than the no treatment control. Again, ultrasonication is a less time consuming method than heating. Ultrasonication of heat-treated suspensions at 75-80% amplitude for 20 sec did not show any deleterious effect on released DNA (Figure 3D). These observations are important for a sample processing protocol in which heating is to precede ultrasonication for simultaneous extraction of nucleic acid from spores and vegetative bacteria present in a single sample.

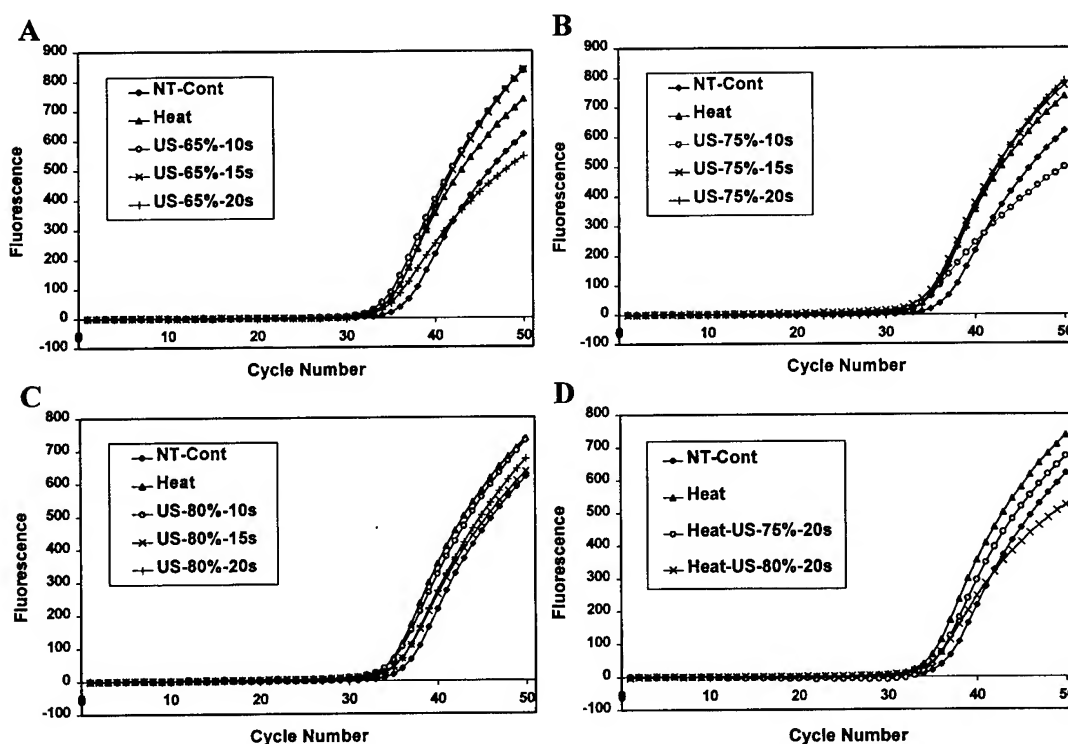


Figure 3. TaqMan-PCR-based real-time detection of *E. herbicola* cells after heat and ultrasonication treatments. Ten microliter aliquots of no treatment control (NT-Cont), heated (Heat), ultrasonicated (US) and heated-ultrasonicated (Heat-US) cell suspensions at 4.41×10^3 cfu/ml original concentration were used for PCR on the Smart Cycler®. Different combinations of ultrasonication amplitude (%) and time in seconds (s) (inset) were used for lysis.

Y. pestis cell lysis experiments indicated that for 1.00×10^3 cfu/ml concentration, ultrasonicated cell suspensions gave a couple of cycles faster detection with improved fluorescence signal by TaqMan-PCR than the no treatment control (Figures 4A-C). However, as illustrated in Figures 4D-F, a dramatic and

positive effect of ultrasonication was evident on *Y. pestis* cells at $1.00\text{E}+02$ cfu/ml concentration. While untreated cell suspension yielded a barely positive identification, a strong positive signal was obtained after ultrasonication. The amplitude of the fluorescence signal was better by 5 to 8 fold and the detection was faster by at least 6 cycles.

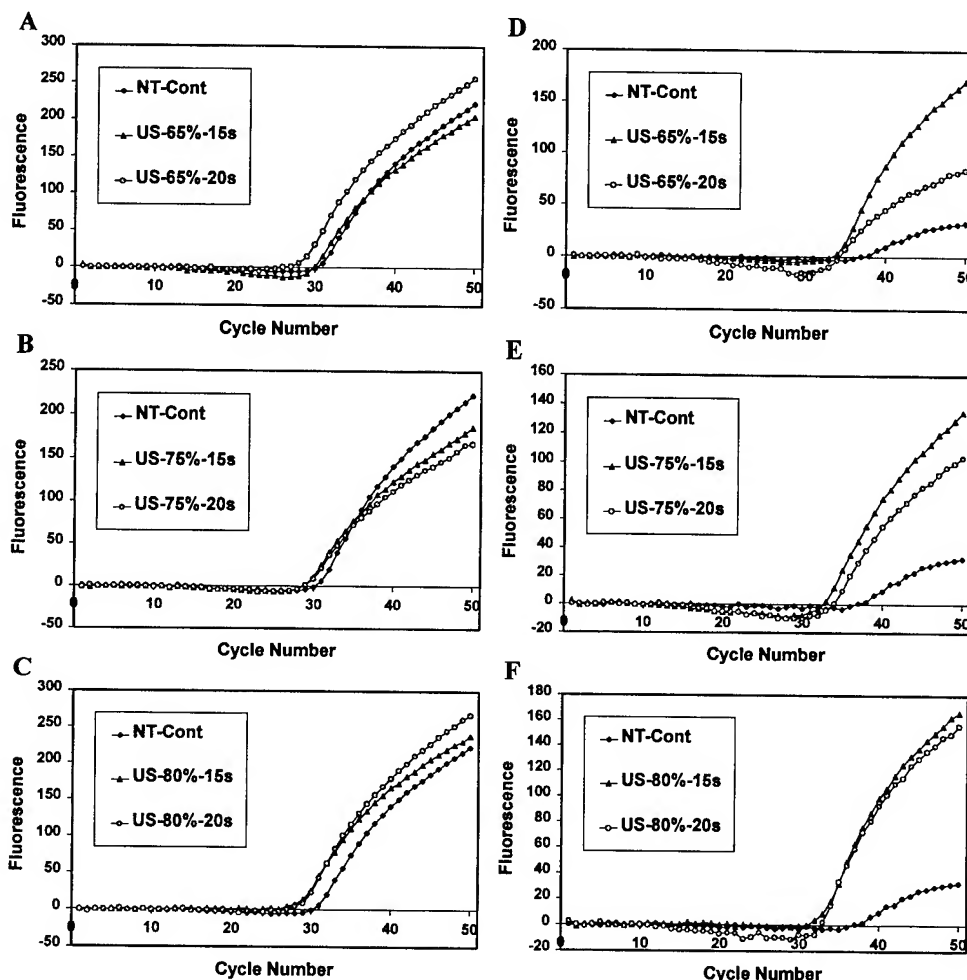


Figure 4. TaqMan-PCR-based real-time detection of *Y. pestis* cells after lysis by ultrasonication. Ten microliter aliquots of no treatment controls (NT-Cont), and ultrasonicated (US) cell suspensions at $1.00\text{E}+02$ and $1.00\text{E}+03$ cfu/ml original concentrations were used for PCR on the Smart Cycler®. Different combinations of ultrasonication amplitude (%) and time in seconds (s) (inset) were used for lysis.

The results indicate that for vegetative bacterial cells, an aliquot of a uniform cell suspension at a reasonable concentration may not require any lysis procedure for TaqMan-PCR-based detection. The first step of holding the reaction mix at 95°C and denaturation/melting step at the same temperature in the first couple of cycles in a PCR usually disrupt the vegetative cells to release DNA. However, for a sample containing a low concentration of cells, ultrasonication or heating will not only disrupt the cells but, will also allow a uniform solubilization of released DNA so that a ten to twenty microliter aliquot gives a confident identification. Also, lysis procedure improves the efficiency of purification of DNA from a complex environmental sample.

Extraction of RNA from MS2 bacteriophage. Heating at 60°C or higher temperature for 5 minutes is enough to disrupt most viruses and release nucleic acids for PCR amplification of target genes. Ultrasonication and heating methods were compared for the lysis of MS2 and release of RNA to be detected by One-Step TaqMan RT-PCR. Ultrasonication at 65% amplitude for up to 20 seconds and 75% and 80% amplitudes for up to 10 seconds gave comparable results to those obtained with control and heated phage suspensions (Figures 5A-C). However, an adverse effect in terms of delayed detection and poor fluorescence signal was observed when the phage suspension was ultrasonicated at 75 and 80% amplitudes for more than 10 seconds (Figures 5A-C).

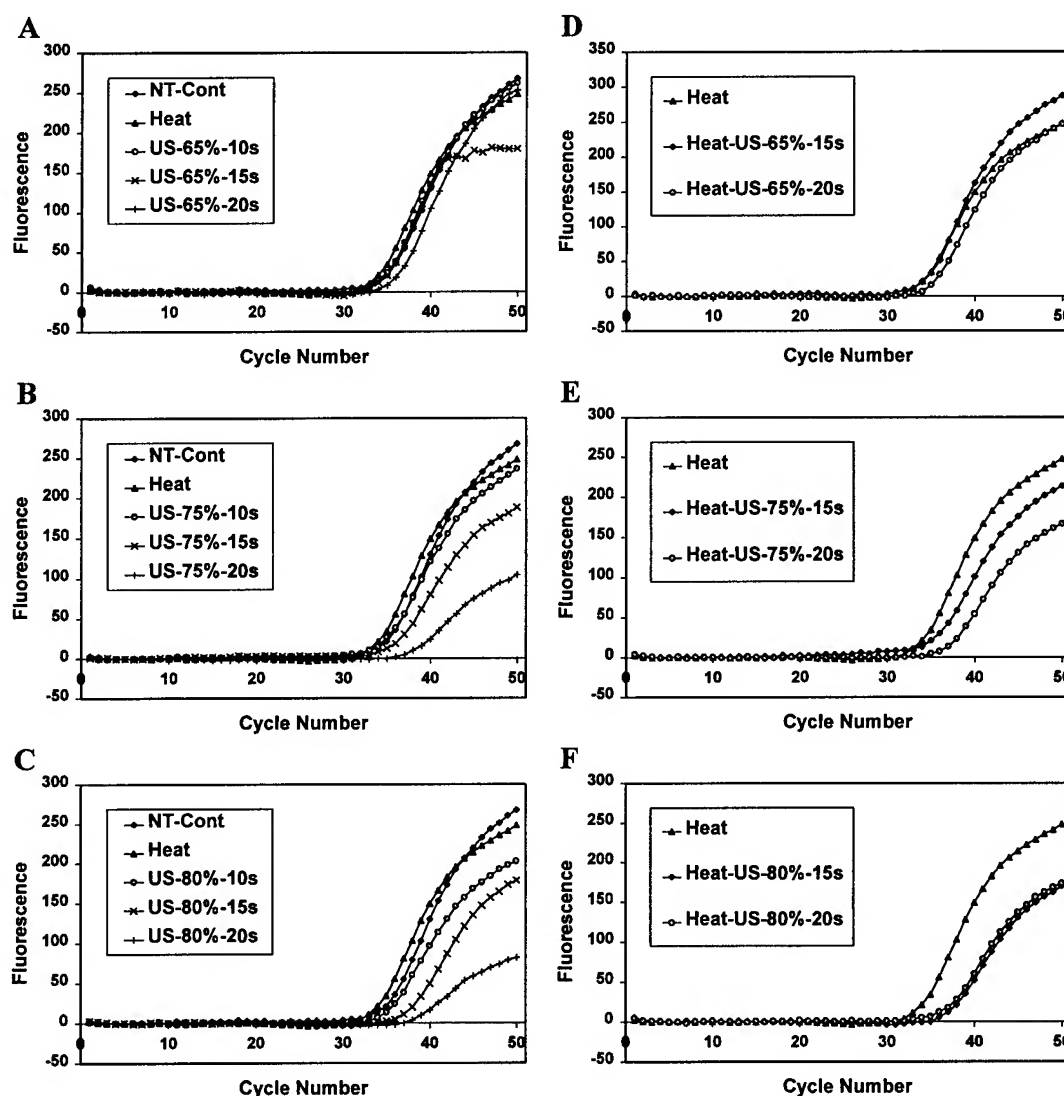


Figure 5. One-Step TaqMan-RT-PCR-based real-time detection of MS2 phage particles after lysis by heat and ultrasonication treatments. The treatments included, heating in the presence of RNA Secure™ (Heat), ultrasonication (US), and heating followed by ultrasonication (Heat-US). Different combinations of ultrasonication amplitude (%) and time in seconds (s) (inset) were used for lysis. Twenty microliter aliquots of MS2 phage suspensions at 7.94×10^4 cfu/ml original concentrations after indicated treatments were used for RT-PCR on the Smart Cycler®. NT-Cont represents the no treatment control.

A similar negative effect of such combinations of ultrasonication parameters was also seen on the phage suspensions heated in the presence of the RNA Secure™ reagent, a PCR conducive RNase inhibitor (Figures 5D-F). The adverse effect of ultrasonication at these parameters might be due to shearing of released RNA. The results further suggest that the ultrasonication parameters of 80% amplitude and 20 sec, required for an efficient lysis of spores will not be suitable for the lysis of MS2 and other similar type and size viruses.

The findings of the present investigation emphasize the need for a two-step nucleic acid extraction protocol when a sample is to be analyzed for multiple agents including RNA viruses. To protect the target RNA from RNases, the lysis protocol should include an RNase inhibitor. The RNA Secure™ used in the present study is PCR conducive. Therefore, an RNA Secure™ treated sample could be used without any further purification in the TaqMan-RT-PCR assay. A heating step (65°C or higher) required for the activation of RNA Secure™ also disrupts viruses and vegetative cells. The activated RNA Secure™ binds to heat released RNA and protects it from digestion by RNases released from other disrupted cells or contaminants in the sample. After heat treatment, an aliquot should be withdrawn to analyze the sample for the presence of an RNA virus. An aliquot may also be withdrawn at this step to analyze vegetative bacteria. The remainder of the sample should then be ultrasonicated for the lysis of spores. Alternatively, a step-by-step ultrasonication protocol should be established where in a sequential lysis of viruses followed by vegetative bacteria and spores is performed using appropriate combination of power and duration of ultrasonication. Inclusion of an RNase inhibitor (RNA Secure™ or other RNase inhibitor active at an ambient temperatures) is strongly recommended for processing field samples. On the basis of the observations of the present study, future efforts will be directed at the development of such protocols which, after further modifications will be adapted on to a portable and completely automated nucleic acid analysis system. Such a system will integrate rapid, efficient, and reliable processing of environmental samples containing multiple pathogens including RNA viruses with real-time identification using TaqMan-PCR.

CONCLUSIONS

Ultrasonication is a very rapid method for the lysis of spores, vegetative bacteria, and viruses, and release of nucleic acids for TaqMan-PCR-based identification. However, ultrasonication parameters required for an efficient spore lysis when used to disrupt viruses can cause negative (shearing) effect on small viral nucleic acids to be detected by PCR. Lysis of vegetative cells and viruses by heat treatment is comparable to ultrasonication except for a longer time of treatment. Ultrasonication parameters used for spore lysis have no adverse effect on DNA released from heat-treated vegetative cells. The results of the present investigation would lead to the development of an automated protocol for simultaneous extraction of nucleic acids from multiple types of microbial agents, including RNA viruses. Such a protocol would require either a two-step procedure including heat (for viruses) and ultrasonication (for vegetative bacteria and spores) treatments and removal of aliquots for nucleic acids analysis after each treatment, or a step-by-step ultrasonication procedure for a sequential lysis of viruses, vegetative bacteria, and spores, and removal of aliquots for analysis. Inclusion of an RNase inhibitor is strongly recommended for any sample preparation protocol to protect released RNA of a target RNA virus in a complex field sample. Such well-defined, rapid, simple, and efficient protocols have a great potential in the development of a completely automatic and field-portable nucleic acid analysis system.

ACKNOWLEDGEMENTS

We gratefully acknowledge Ted Hadfield and his colleagues (AFIP, Washington DC) for providing *B. anthracis* primers and probe sequences, and formalin-killed *B. anthracis* spores and *Y. pestis* cells along with their respective DNAs. We thank NMRC scientists for providing primers and probe sequences for simulants. The research was supported under the DTO-CB20 project on BSPS.

REFERENCES

1. Saiki, R., Scharf, S., Faloona, F., Mullis, K., Horn, G., Erlich, H., and Arnheim, N., 1985. *Science* **230**, 1350-1354.
2. Mullis, K., Faloona, F., Scharf, S., Saiki, R., and Erlich, H., 1986. *Cold Spring Harbor Symp. Quantum Biol.* **51**, 263-273.
3. Holland, P., Abramson, R. D., Watson, R., and Gelfand, D. H., 1991. *Proc. Natl. Acad. Sci. U.S.A.* **88**, 7276-7280.
4. Heid, C. A., Stevens, J., Livak, K. J., and Williams, P. M., 1996. *Genome Res.* **6**, 986-994.
5. Tyagi, S., and Kramer, F. R., 1997. *Nature Biotechnol.* **14**, 303-308.
6. Wittwer, C. T., Herrmann, M. G., Moss, A. A., and Rasmussen, R. P., 1997. *Biotechniques* **22**, 130-131.
7. Wittwer, C. T., Ririe, K. M., Andrew, R. V., David, D. A., Gundry, R. A., and Balis, U. J., 1997. *Biotechniques* **22**, 176-181.
8. Belgrader, P., Benette, B., Hadley, D., Long, G., Mariella, R., Milanovich, F., Nasarabadi, S., Nelson, W., Richards, J., and Stratton, P., 1998. *Clin. Chem.* **44**, 2191-2194.
9. Northrup, M. A., Benette, B., Hadley, D., Landre, P., Lehew, S., Richards, J., and Stratton, P., 1998. *Anal. Chem.* **70**, 918-922.
10. Ibrahim, M. S., Lofts, R. S., Jahrling, P. B., Henchal, E. A., Weedn, V. W., and Northrup, M. A., 1998. *Anal. Chem.* **70**, 2013-2017.
11. Belgrader, P., Benette, B., Hadley, D., Mariella, R., Milanovich, F., and Richards, J., 1999. *Science* **284**, 449-450.
12. Picard, C., Ponsonnet, C., Paget, E., Nesme, X., and Simonet, P., 1992. *Appl. Environ. Microbiol.* **58**, 2717-2722.
13. Carl, M., Hawkins, R., Coulson, N., Lowe, J., Robertson, D. L., Nelson, W. M., Titball, R. W., and Woody, J. N., 1992. *J. Infect. Dis.* **165**, 1145-1148.
14. Tsai, Y. L., and Olson B. H., 1991. *Appl. Environ. Microbiol.* **57**, 1070-1074.
15. Reif, T. C., Johns, M., Pillai, S. D., and Carl, M., 1994. *Appl. Environ. Microbiol.* **60**, 1622-1625.
16. Tebbe, C. C., and Vahjen, W., 1993. *Appl. Environ. Microbiol.* **59**, 2657-2665.
17. Bruce, K. D., Horns, W. D., Hobman, J. L., Osborn, A. M., Strike, P., and Ritchie, D. A., 1992. *Appl. Environ. Microbiol.* **58**, 3413-3416.
18. Poham, D. L., and Setlow, P. J. 1993. *Bacteriology* **175**, 2767-2769.
19. Johns, M., Harrington, L., Titball, R. W., and Leslie, D. L., 1994. *Lett. Appl. Microbiol.* **18**, 236-238.
20. Malik, M., Kain, J., Pettigrew, C., and Ogram, A., 1994. *J. Microbiol. Methods* **20**, 183-186.
21. Herman, L. M. F., DeBlock, J. H. G. E., and Waes, G. M. A. V. J., 1995. *Appl. Environ. Microbiol.* **61**, 4141-4146.
22. Franciosa, G., Fenicia, L., Caldiani, C., and Aureli, P., 1996. *J. Clin. Microbiol.* **34**, 882-885.
23. Zhou, J., Bruns, M. A., and Tiedje, J. M., 1996. *Appl. Environ. Microbiol.* **62**, 316-322.
24. Erb, R. W., and Wagner-Dobler, I., 1993. *Appl. Environ. Microbiol.* **59**, 4065-4073.

25. Kuske, C. R., Banton, K. L., Adorada, D. L., Stark, P. C., Hill, K. K., and Jackson, P. J., 1998. *Appl. Environ. Microbiol.* **64**, 2463-2472.
26. More, M. I., Herrick, J. B., Silva, M. C., Ghirese, W. C., and Madsen, E. L., 1994. *Appl. Environ. Microbiol.* **60**, 1572-1580.
27. Steffan R. J., Goksoyr, J., Bej, A. K., and Atlas, R. M. 1988. *Appl. Environ. Microbiol.* **54**, 2908-2915.
28. Belgrader, P., Hansford, D., Kovacs, G. T. A., Venkateswaran, K., Mariella Jr., R., Milanovich, F., Nasarabadi, S., Okuzumi, M., Pourahmadi, F., and Northrup, M. A., 1999. *Anal. Chem.* **71**, 4232-4236.
29. Belgrader, P., Okuzumi, M., Pourahmadi, F., Borkholder, D. A., and Northrup, M. A., 2000. *Biosens. Bioelectron.* **14**, 849-852.

PURIFICATION OF MS2 BACTERIOPHAGE FROM COMPLEX GROWTH MEDIA AND RESULTING ANALYSIS BY THE INTEGRATED VIRUS DETECTION SYSTEM (IVDS)

*Charles H. Wick** and Patrick E. McCubbin

Summary

Purification and concentration of viruses from the background material is required whatever the subsequent analysis methods are used. For the analysis of viruses it is essential and detection methods depend on this solution. This report demonstrates a methodology for the removal of growth media from a virus preparation. A sample of MS2 was purified using a new ultra-filtration (UF) technique with hollow fibers. A typical MS2 virus sample with a nominal stated concentration of 1.4×10^{12} plaque forming units per ml (pfu/ml) in the original growth media was used to demonstrate this method. After UF the growth media was removed the virus counted using Integrated Virus Detection System (IVDS) instrument.

This report further describes the use of this ultrafiltration procedure to remove other impurities, such as cesium chloride and albumin, from solutions containing a purified solution of MS2 bacteriophage. These solutions were also analyzed using the patented IVDS instrument¹.

Introduction

There are many inherent challenges to virus detection and analysis. One of the more important is purification and concentration from the background material. This is required whatever the detection method to be used in subsequent steps. The background loading which may contain growth media, salts, proteins and other material all make this issue a challenge. It is possible that there is little purpose to even considering detection of viruses until these steps are resolved. One step is the removal of growth media and other impurities such as salts and proteins.

¹ U.S. Patent #6,051,189; Wick, C.H., with D. Anderson, *System and Method for Detection, Identification and Monitoring of Sub-micron Sized Particles*, issued April 2000.

A sample of MS2 bacteriophage was received from the Life Sciences Division at Dugway Proving Ground (DPG). This sample was 500 ml of as grown MS2 bacteriophage, complete with growth media, at a virus concentration of 1.4×10^{12} pfu/ml. The growth media was comprised of L-B broth, 10 g Tryptone, 10 parts NaCl and 5 parts yeast extract. The MS2 solution was a dark yellow color and is clear. The sample was from Lot #98251.

The MS2 sample was analyzed using the IVDS instrument or more directly the Gas-phase Electrophoretic Mobility Molecular Analyzer (GEMMA) detector and ultrafiltration module are two stages of the IVDS instrument. The GEMMA detector consists of an electrospray unit to inject samples into the detector, a Differential Mobility Analyzer and a Condensate Particle Counter. A complete description of the IVDS system, including the GEMMA detector, can be found in the report *Virus Detection: Limits and Strategies*².

Several solutions were prepared to explore the ability of the ultrafiltration apparatus to remove contaminants and retain viruses of interest in solution. A sample of albumin, from chicken egg, was prepared at a concentration of 0.02%, by weight, in an ammonium acetate (0.02M) buffer. To this solution was added MS2 bacteriophage to a concentration of 3×10^{11} pfu/ml. A second solution was prepared containing 2.5% cesium chloride (CsCl), by weight, also in the ammonium acetate buffer. To this solution was added MS2 bacteriophage to a concentration of 5×10^{11} pfu/ml. The MS2 bacteriophage, in both cases, was a highly purified sample obtained from DPG Life Sciences Division (Lot #98110).

1.0 Laboratory Testing of MS2 Bacteriophage plus Growth Media

1.1 Results of MS2 plus Growth Media

The mixed MS2 sample, with 1.4×10^{12} pfu/ml was analyzed using the GEMMA virus detector. The sample was placed neat into the GEMMA analyzer and the results are shown in Figure 1. The growth media, with the MS2 Bacteriophage in solution, produces a graph that displays a very broad, nondescript peak across the area of interest of 24-26 nm. The size range of 24-26 nm is the expected size for a MS2 bacteriophage, as shown in Figure 2 in a micrograph by Dr. Hans Ackermann³. It is not apparent from the as received sample analysis if the sample actually contains MS2 in solution. The solution required removal of the growth media before any meaningful results could be obtained.

² Wick, C.H., Yeh, H.R., Carlon, H.R., and Anderson, D., *Virus Detection: Limits and Strategies*, ERDEC-TR-453, December 1997.

³ Micrograph located at <http://life.anu.edu.au/viruses/welcom.htm>

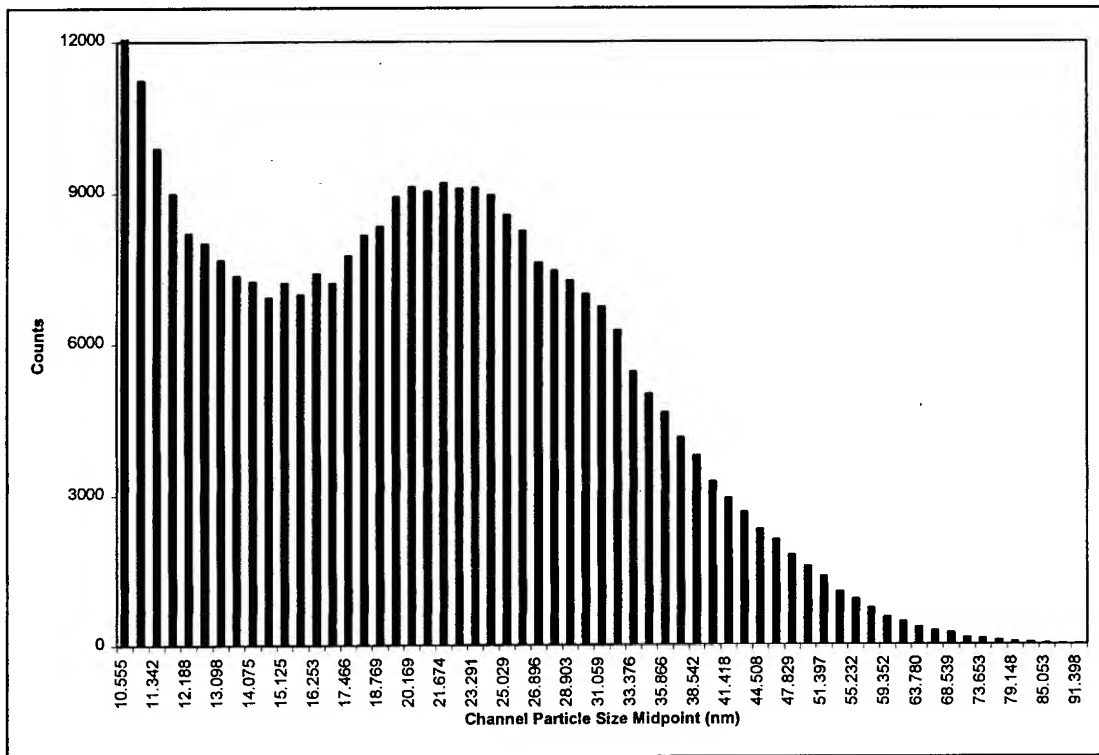


Figure 1 GEMMA Analysis of MS2 Bacteriophage plus Growth Media, DPG Lot #98251

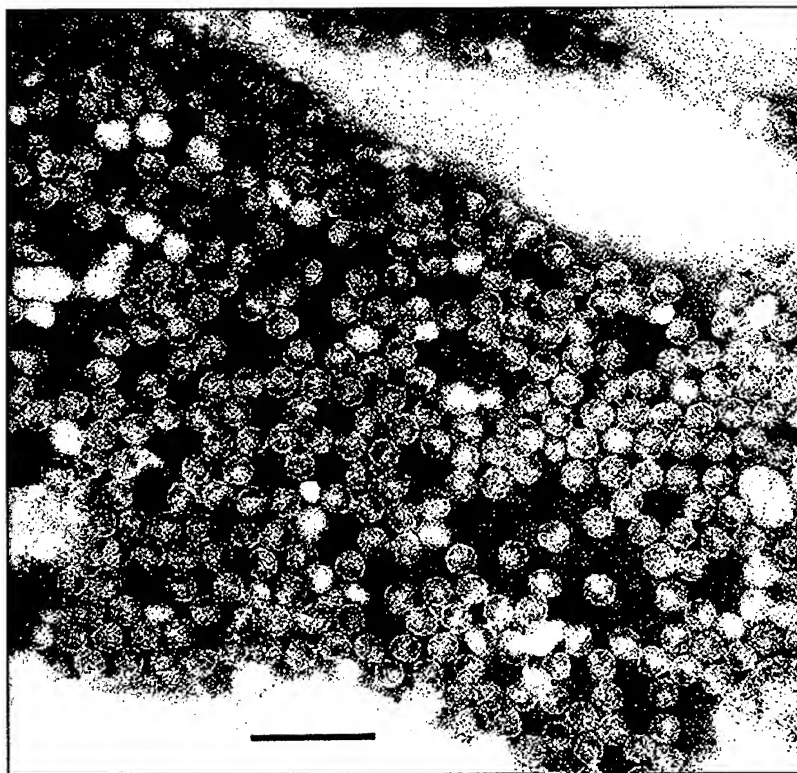


Figure 2 Micrograph of MS2 Bacteriophage (bar represents 100 nm)

1.1.2 Ultrafiltration of MS2 plus Growth Media

The virus plus growth media sample was purified and concentrated using an ultrafiltration (UF) process. The UF module, shown in Figure 3, is used for processing and retaining a virus species for further study. The UF stage is a hollow fiber-based tangential or cross flow filtration system. These filtration systems operate by pumping the feed stream through the hollow fiber, as shown in Figures 4 and 5. As the solution passes through the fiber, the sweeping action of the flow helps to prevent clogging of the fiber. A pressure differential forces the filtrate through the fiber, while the virus feed stream is purified and concentrated. There are available a wide range of pore sizes for the fibers. This filtration technique can reduce volumes from over 5 ml to 0.2 ml.

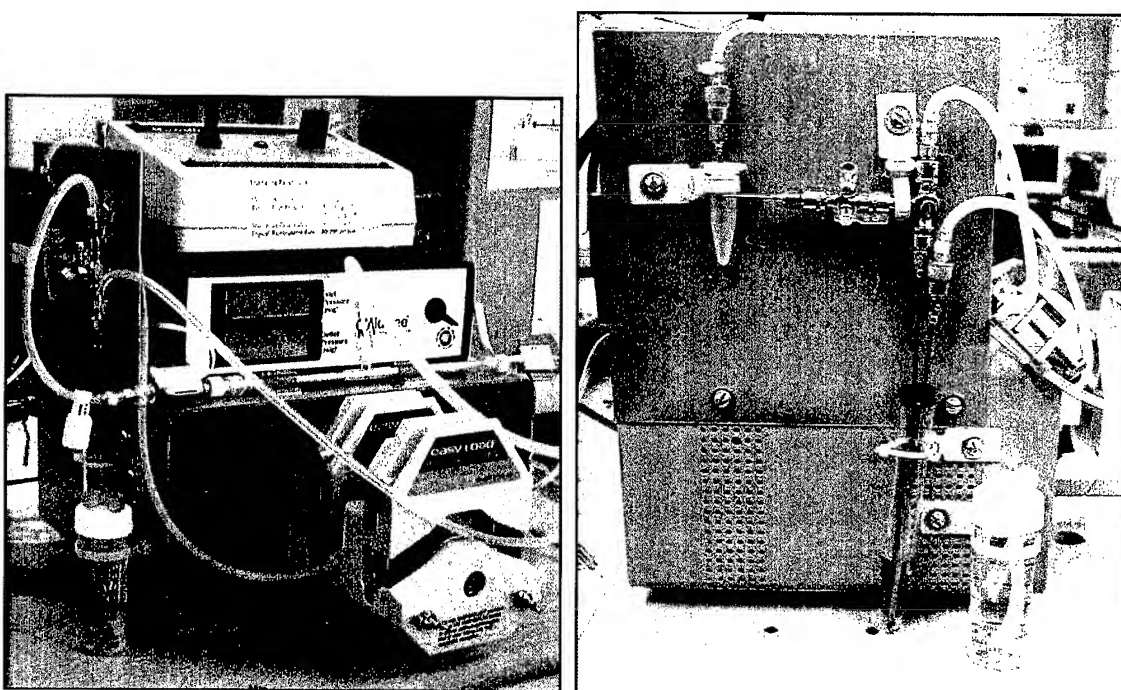


Figure 3 Front and Side View of UF Module 1

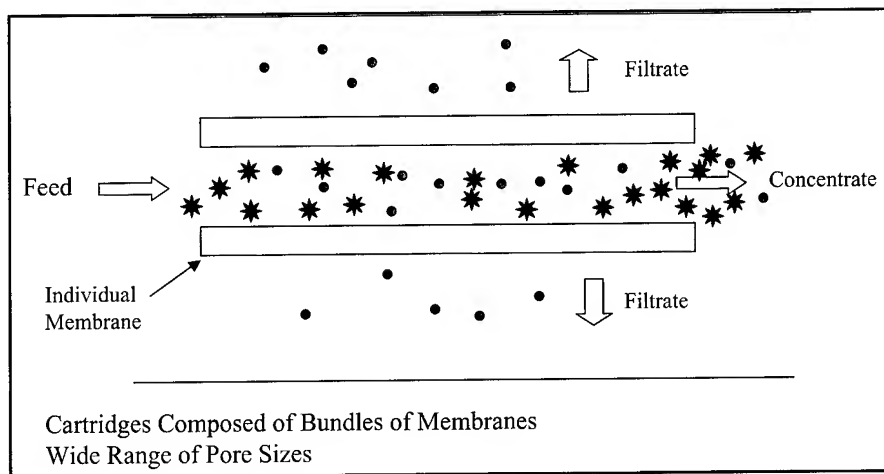


Figure 4 Graphical Representation of Cross Flow Filtration - Individual Fiber

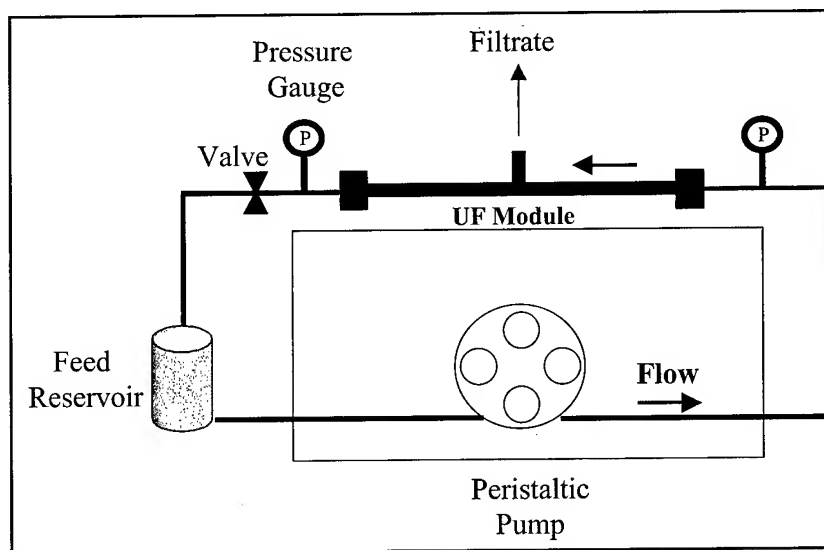


Figure 5 Flow Diagram of Ultrafiltration Apparatus Utilizing the Cross Flow Filtration Process

A sample of the DPG MS2 with growth media was then processed through the ultrafiltration apparatus. The parameters for ultrafiltration are listed in Table 1.

Table 1 UF Parameters for MS2 in Growth Media

Sample volume-initial	3 ml
Pump speed	2
Transducer pressure	15 psig
Total buffer wash volume	50 ml
Sample volume-final	2 ml
MWCO of module	500K

By continually washing the sample volume with ammonium acetate buffer (the working fluid of the GEMMA analyzer), the UF apparatus will allow the removal of ions, proteins and all other material that is smaller than the 500K molecular weight cut-off (MWCO) of the cross flow filter. The MS2 bacteriophage will be retained in the circulating solution and continue to be purified by the process. As the 500K MWCO filter will effectively retain the MS2, the total wash volume can be significantly larger than the initial sample volume. The ultrafiltration of this sample was completed in less than 10 minutes.

After ultrafiltration, the sample was then analyzed in the GEMMA. The results are shown in Figure 6. The graph shows that most if not all of the growth media has been removed and replaced with the ammonium acetate buffer, which is virtually invisible to the GEMMA analyzer. The remaining solution from the ultrafiltration apparatus is very pure and can be used for further experimentation. The numerical results, as shown in Table 2, show a very low count rate, essentially a background level, outside the area of peaks for MS2. At this level of purification and concentration, the original 500 ml of as received MS2 with growth media, could yield over 300 ml of very pure, high concentration MS2 bacteriophage in ammonium acetate.

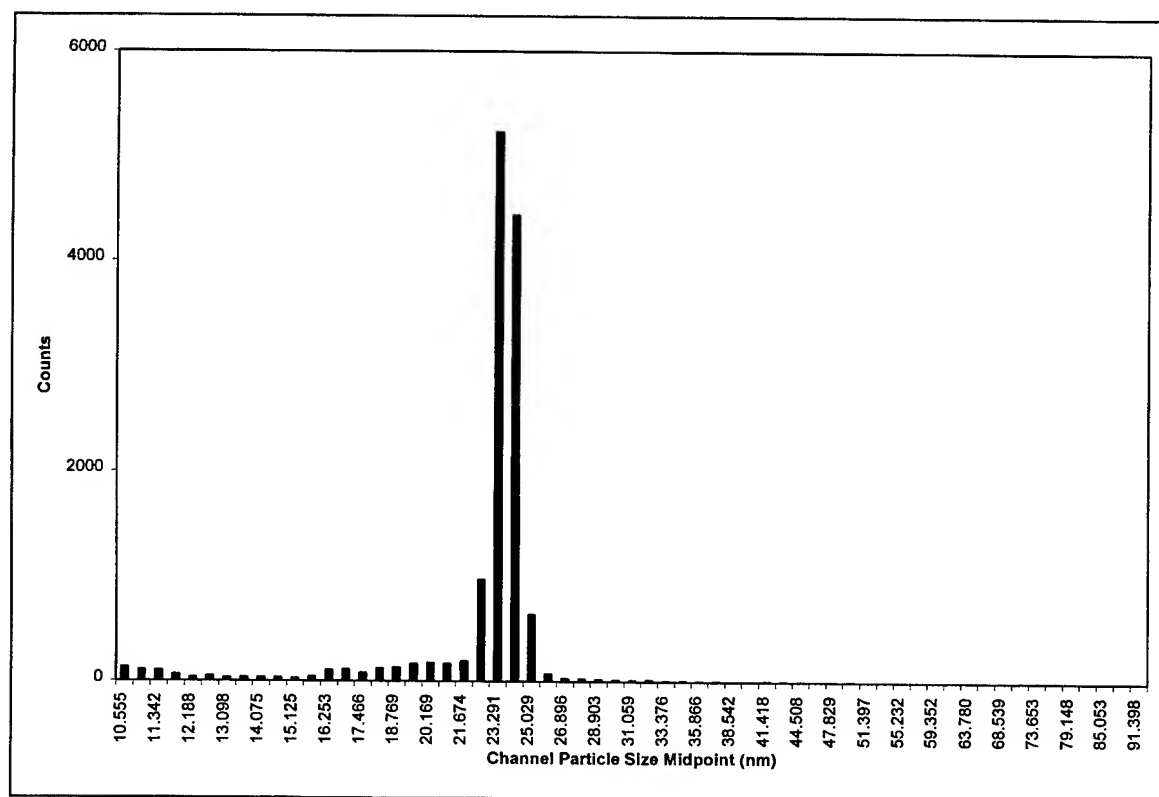


Figure 6 GEMMA Analysis of MS2 (Growth Media Sample)-Ultrafiltration Processed

Table 2 GEMMA Counts for MS2 Bacteriophage

Channel Midpoint Diameter (nm)	Counts	Channel Midpoint Diameter (nm)	Counts
10.5545	128.2	32.1968	17.5
10.9411	105.7	33.3762	8.5
11.3419	97.7	34.5989	10.5
11.7574	64.3	35.8664	7.5
12.1881	37.3	37.1803	6.5
12.6346	50.8	38.5423	2.5
13.0975	34.2	39.9542	3
13.5773	36.8	41.4178	6.8
14.0746	39.5	42.9351	2.2
14.5902	34.6	44.5079	5
15.1247	28	46.1384	2
15.6788	41.5	47.8286	1
16.2531	102.1	49.5807	2
16.8485	110.8	51.397	1
17.4658	80.3	53.2798	0
18.1056	120.7	55.2316	1
18.7688	129.4	57.2549	0
19.4564	167	59.3523	0
20.1691	175.2	61.5265	1
20.908	168.6	63.7804	1
21.6739	192.2	66.1169	0
22.4679	973.1	68.539	1
23.291	5228.2	71.0497	1
24.1442	4429.7	73.6525	1
25.0287	639.9	76.3506	0
25.9455	73.6	79.1476	1
26.896	31.4	82.047	0
27.8813	25.6	85.0526	0
28.9026	22	88.1683	2
29.9614	19.5	91.3982	0
31.059	16.2		

1.2 Results of MS2 plus Albumin

The sample of 0.02% albumin in ammonium acetate, with the addition of 3×10^{11} pfu/ml of MS2 bacteriophage, was analyzed neat in the GEMMA virus detector. As shown in Figure 7, the MS2 peak is centered around 24 nm. The albumin in the sample is displayed as a very broad peak starting below 10 nm and extending to 20 nm.

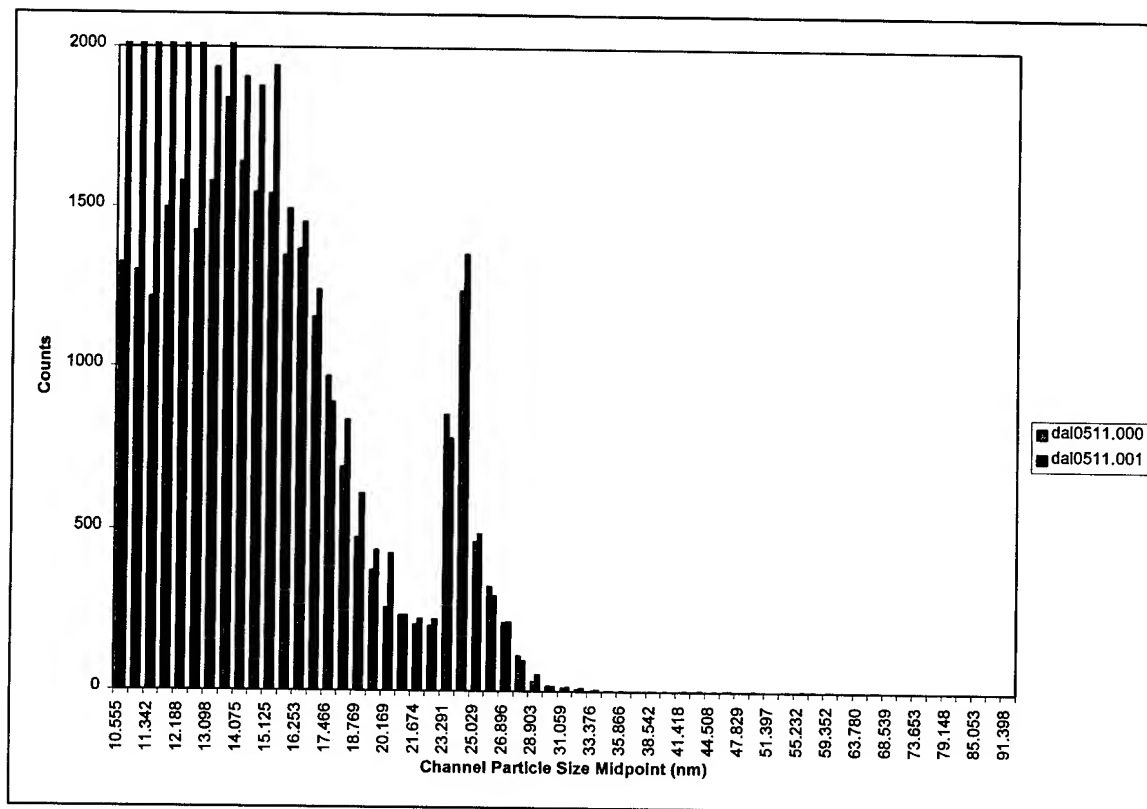


Figure 7 GEMMA Analysis of Albumin (0.02%) in Ammonium Acetate with MS2 (3×10^{11} pfu/ml)

1.2.1 Ultrafiltration of MS2 plus Albumin

The sample of albumin plus MS2 was then processed through the ultrafiltration apparatus. The parameters for the ultrafiltration are shown in Table 3.

Table 3 UF Parameters for Albumin plus MS2

Sample volume-initial	1 ml
Pump speed	2
Transducer pressure	15 psig
Total buffer wash volume	40 ml
Sample volume-final	0.4 ml
MWCO of module	500K

After processing in the ultrafiltration apparatus, the sample was examined in the GEMMA virus detector. As shown in Figure 8, the only peak in evidence is centered on 24 nm. The large peak between 10 and 20 nm was completely removed. The processing of the sample through the ultrafiltration apparatus completely removed the albumin protein, while the MS2 bacteriophage was retained.

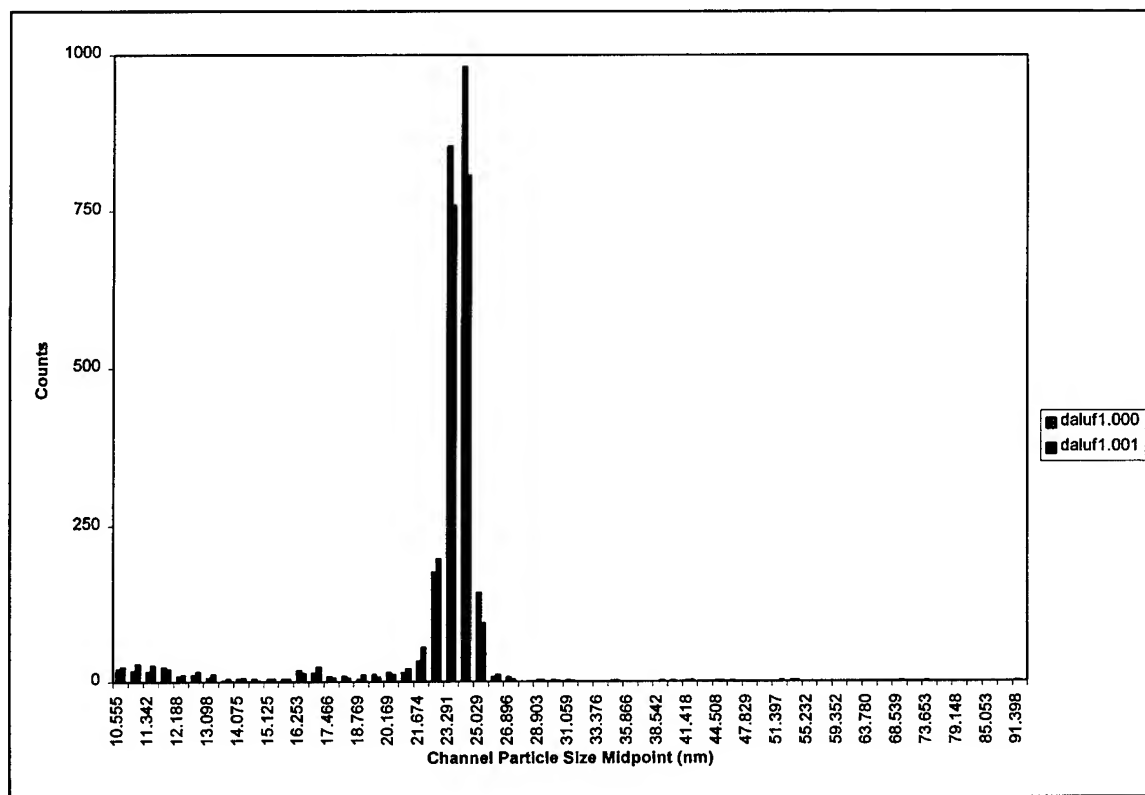


Figure 8 GEMMA Analysis of Albumin plus MS2 Bacteriophage-Ultrafiltration Processed

1.3 Results of MS2 plus Cesium Chloride

The sample of 2.5% CsCl, by weight, in ammonium acetate, with the addition of 5×10^{11} pfu/ml of MS2 bacteriophage, was analyzed neat in the GEMMA virus detector. As shown in Figure 9, the MS2 peak is centered around 24 nm. The CsCl in the sample is displayed as a very broad peak starting below 10 nm and extending to over 20 nm. Any higher concentrations of CsCl would start to obscure the MS2 peak position.

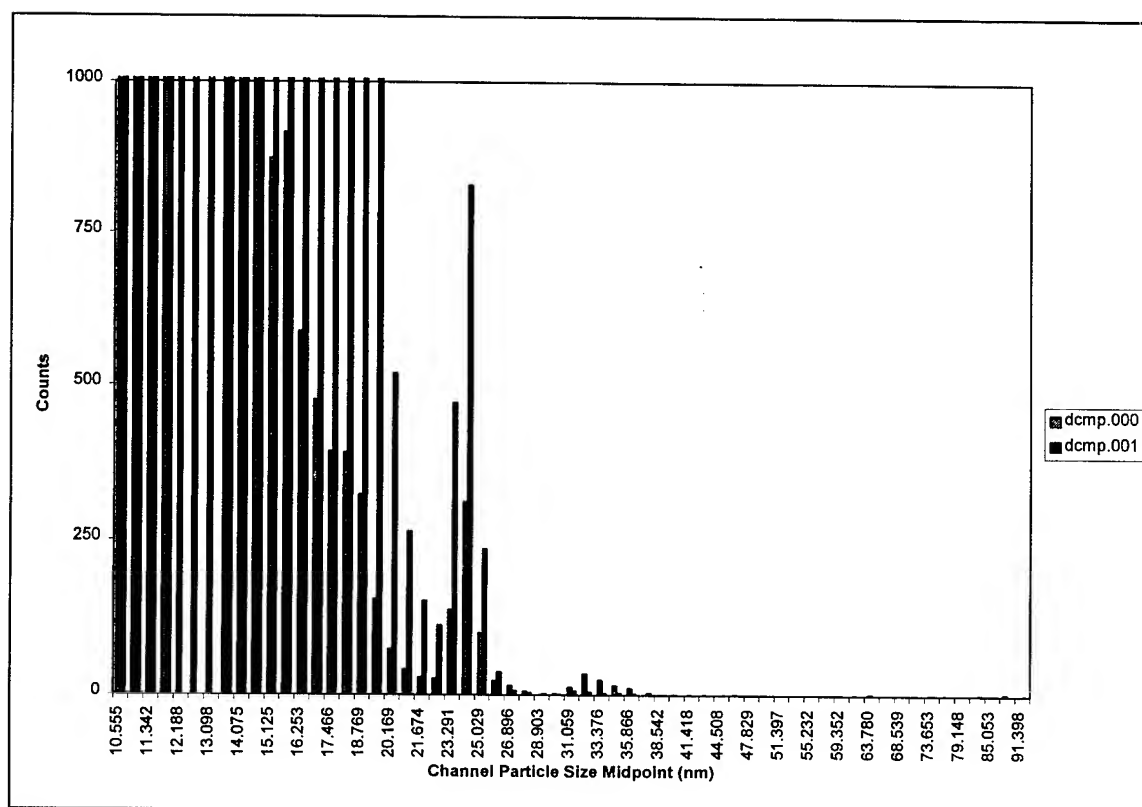


Figure 9 GEMMA Analysis of Cesium Chloride (2.5%) plus MS2 (5×10^{11} pfu/ml)

1.3.1 Ultrafiltration of MS2 plus Cesium Chloride

The sample of CsCl plus MS2 was then processed through the ultrafiltration apparatus. The parameters for the ultrafiltration are shown in Table 4.

Table 4 UF Parameters for CsCl plus MS2

Sample volume-initial	1 ml
Pump speed	2
Transducer pressure	15 psig
Total buffer wash volume	30 ml
Sample volume-final	0.5 ml
MWCO of module	500K

After processing in the ultrafiltration apparatus, the sample was examined in the GEMMA virus detector. As shown in Figure 10, the MS2 peak is shown centered on 24 nm. The large peak between 10 and 22 nm was significantly removed. There was a small remnant of the CsCl peak in the processed sample due to the smaller amount of buffer wash volume in this cycle. To completely remove the CsCl, the ultrafiltration process would only need to be continued with further washing until all of the salt was replaced with buffer solution. The processing of this sample through the ultrafiltration apparatus also retained the MS2 bacteriophage.

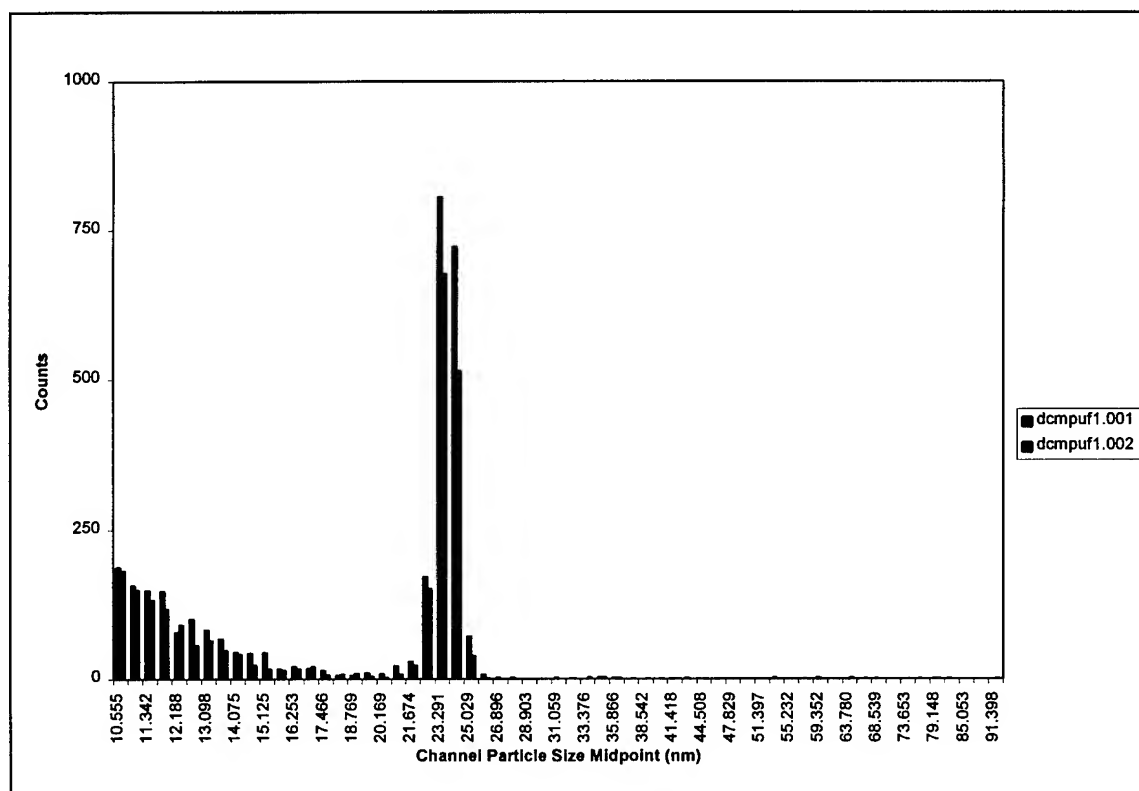


Figure 10 GEMMA Analysis of Cesium Chloride plus MS2-Ultrafiltration Processed

1.4 Analysis

The ultrafiltration apparatus was very effective in removing the growth media from the as received solution of MS2 bacteriophage. The addition of approximately ten times the amount of starting solution with ammonium acetate buffer (3 ml vs. 50 ml respectively) allowed the efficient replacement of the growth media with the buffer solution. The background of the GEMMA scan of the ultrafiltration-processed solution was very low due to the low detection of ammonium acetate. In addition, the ultrafiltration process for comparable volumes can be completed in approximately 10 minutes.

The addition of other contaminating materials in a virus solution can also be successfully removed from solution while retaining the virus. The albumin protein was almost completely removed from the MS2 containing solution by ultrafiltration. The adjustment (if necessary) of the pore size of the ultrafiltration modules allows for great flexibility in the processing of solutions.

The CsCl solution appeared to require further washing to completely remove the salt from the virus containing solution. From the few tests to date, it appears that the wash volume for the removal of CsCl in the ultrafiltration apparatus requires the initial sample volume to be washed with approximately 40-50 times the volume of buffer solution, for certain impurities, to completely remove those impurities.

2.0 Conclusions

The sample of MS2 bacteriophage containing original growth media was purified by ultrafiltration. The growth media was removed and the MS2 bacteriophage retained. The ultrafiltration module was equipped with a 500K molecular weight cut-off cross flow filter, which effectively retained the bacteriophage while allowing the removal of the growth media. The remaining solution of bacteriophage can now be further characterized and the process used as a purification step for further analysis. This technique should be compatible for removing similar material from solutions of other viruses.

Samples of laboratory produced solutions, specifically albumin protein and CsCl solutions with MS2 bacteriophage were successfully processed in the ultrafiltration apparatus that removed these typical contaminants and retained MS2.

* Corresponding Author:

Charles H. Wick
Edgewood Chemical Biological Command
Attn: AMSSB-RRT-DS Bld E3160
Aberdeen Proving Ground, MD 21010

Patrick E. McCubbin
OptiMetrics, Inc.
1 Newport Drive, Suite H
Forest Hill, MD 21050

RAPID EXTRACTION AND AMPLIFICATION OF BACTERIAL DNA FROM SOIL SAMPLES

Darrel E. Menking , Peter A. Emanuel, James J. Valdes
US Army ECBC, Attn: AMSSB-RRT, 5183 Blackhawk Rd., APG, MD 21010-5424, USA
Suzanne K. Kracke
Geo-Centers, PO Box 68, APG, MD 21010-0068, USA
Calvin Chue
Battelle, 2012 Tollgate Road, Suite 206, Bel Air, MD 21015, USA

ABSTRACT

Bacterial consortia constitute a large portion of the degrading organisms in soil. Identification of these microorganisms is hampered by lack of rapid methods of extraction from the soil. Multiple impurities such as clay and humic acid inhibit DNA amplification by Polymerase Chain Reaction (PCR). Multi-step, time-consuming methods are required to isolate the DNA from the surrounding contamination. A protocol was developed for a rapid, two-step cleanup process that delivers purified, PCR-ready DNA from soil samples in less than 30 min using the soil extraction resin from the MoBio Soil CleanUP™, followed by a 5 min DNA extraction using GeneReleaser™. DNA was successfully extracted and amplified from Artificial Soil (2×10^9 cfu/gram soil), Sassafras Sandy Loam Soil (1×10^9 cfu/gram soil), and O'Neil-Hall Sandy Loam Soil (2×10^9 cfu/gram soil).

INTRODUCTION

Field samples normally contain at least some materials that inhibit PCR; soil contains PCR inhibitors in the form of humic acid, clay, DNA from indigenous organisms, metal ions or chelators. In addition, soil contains compounds that bind protein and nucleic acids. The use of genetic material for identification of microorganisms in soil has the advantage over other identification methods in that it allows for absolute identification of indigenous and seeded organisms. Sample cleanup is imperative since PCR/DNA detection in miniaturized devices¹ requires highly purified DNA. Extraction of genetic material from soil samples has proven to be difficult². The purpose of this paper is to present rapid cleanup techniques for extraction of purified DNA from soil samples and its application toward the detection of *Bacillus anthracis* spores in soil.

MATERIALS AND METHODS

Detection of Recombinant DNA in Soil Samples.

Mo-Bio Soil CleanupTM, a one hour protocol, produces PCR-ready DNA with no additional cleanup step required. We report here the rapid extraction and amplification of plasmid DNA from recombinant *Escherichia coli* with a modified protocol (<30 min) using the resin from the Mo-Bio Soil CleanupTM and GeneReleaserTM (GR). A starting bacteria culture (1 ml) was mixed with soil (0.2-1.0 g), centrifuged and supernatant discarded. The pellet was resuspended in the resin and mixed. A 1 µl sample was removed, added to 20 µl of GR and microwaved on high for 5 min. Concentration was determined by Warburg-Christian method; purified DNA was stored frozen (-20°C). RapidcyclerTM A20, (RC, Idaho Technology, Idaho Falls, ID) was used to amplify and detect target DNA following cleanup as previously described³. The presence or absence of PCR-amplified DNA when compared to a positive control determined the inhibitory effects of soil suspensions.

Sassafras sandy loam soil (SSL), O'Neill-Hall sandy loam soil (OHSL) and Standard artificial soil (AS) used for testing purposes were obtained from the Environmental Technologies team, ECBC, APG, MD. The first round of testing determined the minimum amount of soil that inhibited PCR. Soil was suspended in distilled water and added to the PCR reaction tube (10% total vol). Suspended soil samples were serially diluted until PCR inhibition was no longer evident.

Detection of *Bacillus anthracis* (delta Ames) DNA

Bacillus anthracis (delta Ames) is a non-toxigenic strain of anthrax which lacks the plasmid-associated virulence factor pX01. The anthrax toxins and capsule, encoded by plasmids pX01 and pX02, respectively, are the only known virulence factors of *B. anthracis* and are considered essential for full virulence⁴. For these studies, the Cap A gene was PCR amplified. DNA from *Bacillus anthracis* was amplified using a modified molecular beacon probe and a TaQMan primer on the ABI PRISM 7000 Sequence Detection System. A specifically designed hybridization probe includes a fluorophore and quencher, which when in close proximity, results in no fluorescent signal. During the PCR amplification event, the probe anneals to a site within the target DNA as the primer anneals to one end of the target. The primer moves along the target DNA and replicates it. When it reaches the probe, the TAQMAN enzymatically cleaves the probe, releasing the fluorophore. The fluorophore is now un-quenched and a fluorescent signal results. The amount of fluorescence detected is directly proportional to the number of strands of DNA amplified.

RESULTS

Recombinant DNA from Soil Samples

Suspended soil was added to the PCR mix in decreasing concentrations until PCR was no longer inhibited. Figure 1 shows the level of soil inhibition by Sassafras Sandy Loam.



Figure 1. Inhibition of PCR by SSL soil. Lane 1- DNA ladder; lane 2- positive control; lane 3- 10 µg/ml soil; lane 4- 7.5 µg/ml soil; lane 5- 5 µg/ml soil; lane 6- 2.5 µg/ml soil.

Although as little as 7.5 µg/ml soil suspension in the PCR reaction inhibited PCR, the protocol developed allowed for cleanup of DNA from

soil at the following cfu/gm of soil- Sassafras Sandy Loam Soil, 1×10^9 cfu/gram soil; O'Neil-Hall Sandy Loam Soil, 2×10^9 cfu/gram soil; Artificial Soil, 2×10^9 cfu/gram soil (Figures 2-4).

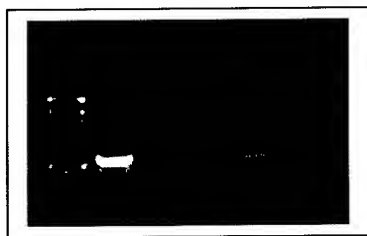


Figure 2. Sassafras Sandy Loam. Lane 1-DNA markers; lane 2- control; lane 3- 0.2g soil; lane 4- 0.4g soil; lane 5- 0.6g soil; lane 6- 0.8g soil; lane 7- 1.0g soil.



Figure 3. O'Neil-Hall sandy loam. Lane 1-DNA markers; lane 2- control; lane 3- 0.2g soil; lane 4- 0.4g soil; lane 5- 0.6g soil; lane 6- 0.8g soil; lane 7- 1.0g soil.

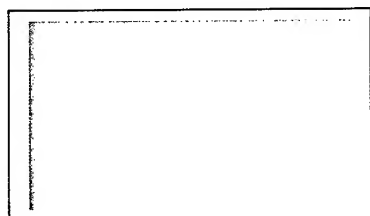


Figure 4. Artificial soil Lane. Lane 1-DNA markers; lane 2- control; lane 3- 0.2g soil; lane 4- 0.4g soil; lane 5- 0.6g soil; lane 6- 0.8g soil; lane 7- 1.0g soil.

Although 2.5×10^8 bacteria were required for extraction procedures to work, we were able to extract this from up to 0.75g soil with 0.5g being the normally used amount. This equals 5×10^8 bacteria/gram soil.

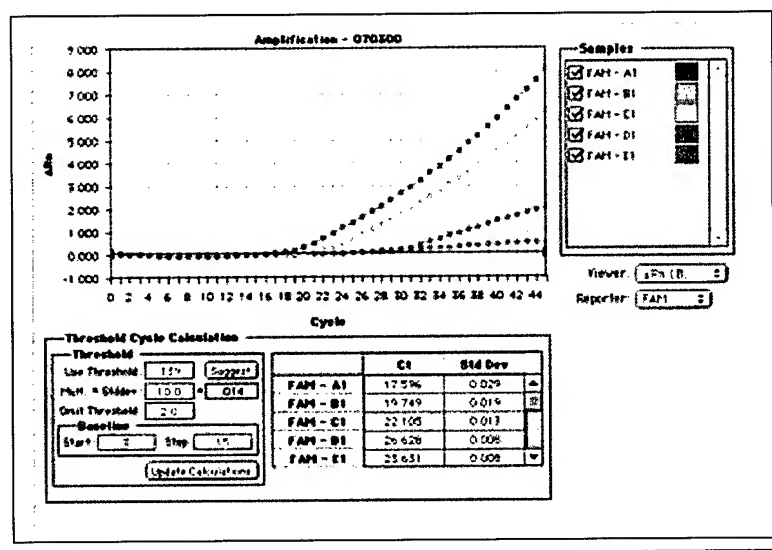


Figure 5. Amplification of raw spores using ABI Prism 7700.

The lower level of detection for raw spores is in the pg range.

CONCLUSIONS

Soil samples contain PCR inhibitors, and require multi-step, time consuming procedures. Table 1 lists current methods taken from a literature survey of DNA extraction from soil.

TABLE 1. Extraction methods for extraction of DNA from samples*

Time	Sample type	Extraction method
hr+	<i>Verticillium dahliae</i> (plant virus), in nine farm soils extraction ⁵	LN2 grinding/SDS buffer-phenol
hr+	microbial communities in soil	SDS/gels (no PCR) ⁶
hr+	soil seeded with <i>Cryptosporidium parvum</i> oocysts	Tris/SDS lysis/bead mill ⁷
hr+	soil seeded with <i>Pseudomonas putida</i> and <i>Bacillus globigii</i>	hot-detergent /bead mill ⁸

*for seeded samples, time began at time of seeding

For these studies, the assay volume was reduced by 90% and the time/cycle reduced by 75%. Detection and identification of bacteria (vegetative or spore) in complex media such as soil, ground water or bodily fluids is best accomplished via PCR. This DNA amplification process is easily disrupted by a wide range of interferents; therefore, while the amplification process itself is rapid, sample preparation adds additional critical hours. The protocol described shortens sample preparation by hours, increasing PCR sensitivity, and increases accuracy. Spore lysis has also been reported by microwave radiation⁹ and a minisonicator¹⁰. A remaining major challenge is the rapid extraction of PCR-ready spore DNA from soil samples. Future research will involve the cleanup of spores from soil and other environmental samples followed by lysis and amplification of the DNA using the ABI Prism System.

REFERENCES

1. Belgrader, P., et al., *Science*, 284:449-50, 1999.
2. Bej, A.K. and Mahbubani, M.H. *PCR Technology: Current Innovations* ed. H. and A. Griffin. CRC Press, p. 362, 1994.
3. Menking, D.E., et al., *Res. Cons. Recyl.*, 27:179-86, 1999.
4. Welkos, S.L., *Microb. Pathology*, 3:183-989, 1991.
5. Volossiuk, T., et al., *Appl. Environ. Micro.*, 61(11):3972-6, 1995.
6. Jackson, C.R., et al., *Appl. Environ. Micro.*, 63(12):4993-5, 1997.
7. Walker, M.J., et al., *Appl. Environ. Micro.*, 64(6):2281-3, 1998.
8. Kuske, C.R., et al., *Appl. Environ. Micro.*, 64(7):2463-72, 1998.
9. Vaid, A. and Bishop, A.H. *J. Appl. Micro.*, 85:115-122, 1998.
10. Belgrader P., et al., *Anal. Chem.* 19:4232-6, 1999.

COMPARISON OF THE SCHLEICHER AND SCHUELL ISOCODE PCR DNA SAMPLE ISOLATION DEVICE AND THE QIAGEN QIAAMP DNA PURIFICATION SYSTEMS

Fred K. Knauert, Philip D. Craw, Susan R. Coyne,
David R. Shoemaker, and Erik A. Henchal

US Army Medical Research Institute of Infectious Diseases
Diagnostics Systems Division
1425 Porter Street
Ft. Detrick, MD 21702-5011

The Qiagen QIAamp Tissue Kit is a reliable, robust procedure for preparing DNA from a variety of sample matrices. It has a detection limit of less than 100 CFU for *Bacillus anthracis* and it is insensitive to sample matrix effects. DNA prepared from buffer, whole blood, plasma and serum samples spiked with *B. anthracis* have the same detection limits. It has a reasonable logistics burden with only proteinase K requiring low-temperature storage. The problem with this procedure is that it is relatively complex and is labor-intensive with many hands-on manipulations. This diminishes its value as a field-useable procedure. We evaluated the Schleicher & Schuell IsoCode PCR DNA Sample Isolation Device (ISC) as an alternate method for preparing DNA. The advantage of the ISC system is that it is extremely simple. A sample is spotted onto the paper and allowed to dry. A 3-mm disk is punched out of the paper, washed briefly in water and the DNA is eluted from the paper by heating to 95 -100°C for 15 min. Either the eluate of the eluted paper can be used as a template source for PCR. In some cases it is possible to use washed paper directly in PCR without elution. In addition to its simplicity, it makes an ideal storage and shipping medium.

We evaluated the ability of the ISC to prepare DNA from a variety of sample types and found that it had a detection limit equivalent to the QIAamp procedure of less than 100 CFU of *B. anthracis* per sample and was unaffected by the sample matrix. Samples prepared from *B. anthracis*-spiked buffer, whole blood, plasma or serum had the same detection limits. The shortcoming of this procedure is that the sample size was limited to the size of the punched-out disk, which was effectively less than 10 µL. Therefore, to achieve the 100 CFU / 10 µL sample, it was necessary to start with a relatively high concentration of agent, or to be able to concentrate the sample before applying it to the ISC paper. Although this is an important limitation, there might be specific applications where the ease of use and / or storage advantages of this system make it a useful alternative to the QIAamp procedures.

Introduction

The full diagnostic potential of the polymerase chain reaction (PCR) is limited by sample preparation technology. Although exquisitely sensitive and specific, the PCR process is hindered by the paucity of rapid, simple, reliable, and efficient procedures for preparing nucleic acids from a variety of medical and environmental samples. We therefore developed and evaluated a number of sample preparation procedures. Currently, we use the Qiagen Tissue Kit to prepare samples from a variety of sample matrices. We have found it to be a reliable procedure of reasonable sensitivity that is relatively insensitive to the composition of the sample matrix. The endpoint detection limits in buffer, whole blood, plasma and serum are approximately equivalent. However, the Qiagen Tissue Kit procedure is labor-intensive with many hands-on manipulations and centrifugation steps that do not make it readily amenable to automation. We evaluated the Schleicher and Schuell IsoCard DNA purification procedure as an alternative method for preparing DNA from bacteria. The procedure was attractive because it was much simpler compared to the Qiagen Tissue Kit procedure (Table 1). After the sample is spotted and

dried on the paper, it only requires a wash and elution in water. We found that endpoint detection limits were comparable to those of the Qiagen Tissue Kit procedure and that it was also relatively insensitive to the sample matrix.

TABLE 1. Comparison of the Qiagen QIAamp Tissue Kit and S&S Isocode procedures.

<u><i>QIAampTISSUE KIT</i></u>	<u><i>S&S ISOCODE</i></u>
ATL BUFFER + SAMPLE +PROTEINASE K INCUBATE @ 55°C FOR 60 MIN +AL BUFFER INCUBATE @70°C FOR 10 MIN +ETHANOL	SPOT SAMPLE ONTO PAPER DRY 15-30 MIN @ 65°C PUNCH 3 MM DISK FROM CARD
BIND TO SPIN COLUMN BY CENTRIFUGATION	
WASH 2X WITH AW BUFFER	WASH DISK WITH WATER
ELUTE 2X WITH WATER or TE BUFFER	ELUTE FOR 15-30 MIN AT 95°C
ELUATE TO PCR	ELUATE TO PCR
TOTAL TIME ~ 2 - 2.5 HOURS	TOTAL TIME ~45-75 MIN

Materials and Methods

Sample preparation: Twofold serial dilutions of *B. anthracis* vegetative cells starting at 2.5×10^3 CFU / 10 μ l were prepared in Dulbecco's phosphate buffered saline (DPBS), whole blood, plasma, and serum. Whole blood was collected in 3-ml EDTA tubes, and plasma was prepared by centrifugation of whole blood. Serum was obtained from a commercial source. The same twofold serial dilutions of *B. anthracis* vegetative cells prepared for the QIAamp Tissue Kit were used for the IsoCode procedure.

Qiagen QIAamp Tissue Kit procedure: Ten microliters of the prepared sample was added to 170 μ l of Buffer ATL. The sample was then incubated for 60 min at 55°C with 20 μ l of proteinase K (17.8mg / ml). After the incubation, 200 μ l of Buffer AL was added and incubated an additional 10 min at 70°C. Ethanol (96-100%) was added to the sample which was then added to a QIAamp™ spin column containing a silica filter. The sample was passed through the filter by centrifugation at 6000 x g for 2 min. The spin columns were washed 2X with 500 μ l of Buffer AW. The spin columns were then placed in 1.5 ml eppendorf tubes that were preheated to 70°C. The nucleic acid was eluted from the silica membrane by adding 50 μ l of commercial molecular biological grade (MBG) water (RNase/DNase free), preheated to 70°C, by incubating for 5 min at 70°C and then centrifuging at 6000 x g for 3 min. Two eluates, E1 and E2, were collected in separate tubes.

IsoCode sample processing: Ten microliter samples of the diluted material were spotted onto IsoCards. After drying for 15-30 min, a 3-mm disk was punched from the IsoCard into a clean microfuge

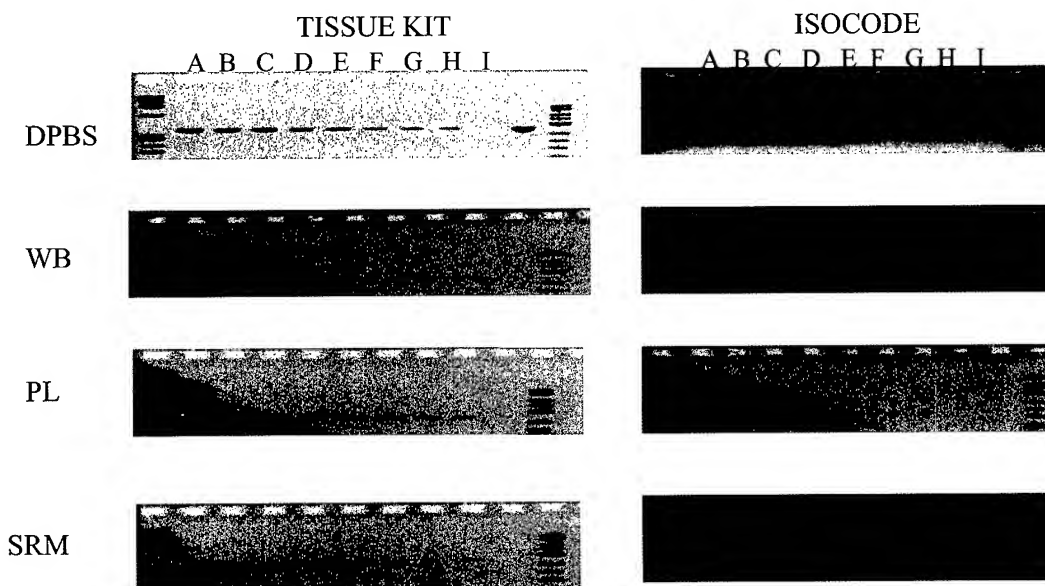
tube. The dried paper punches were washed for 5 seconds with 500 μ L of MBG H₂O. The washed punches were transferred to new microfuge tubes containing 50 μ L of MBG H₂O. The DNA was eluted from the paper punches by heating to 95°C for 15-30 min. A 10 μ L sample of the eluted material was analyzed by PCR.

PCR analysis: Eluted DNA was amplified by PCR. Master mix components for the PCR were 50 mM KCl, 10 mM Tris-HCl, pH 8.3, 0.001% gelatin, 1.5 mM MgCl₂, 200 μ M each dNTP, 100 pmol each primer, and 2.5 units of Perkin Elmer Amplitaq™ DNA polymerase per 100 μ L of reaction mix. Ten microliters of prepared sample was added per 100 μ L reaction. Thermal cycling conditions were 1 min at 95°C denaturing step, 1 min at 65°C annealing step, and 1 min at 72°C extension step. These conditions were cycled 30 times. An additional 10 min at 72°C was incorporated after the final cycle to allow the completion of initiated polymerization. After PCR, 8 μ L of product was combined with 2 μ L of 5X loading dye and electrophoresed through a 3% NuSieve™ agarose gel in TBE buffer. Photodocumentation was by a Stratagene Eagle Eye II™ Still Video system or an Alpha Inotech Photodocumentation System.

Results

Figure 1 shows that the Tissue Kit and IsoCard procedures were equivalent for preparing PCR-amplifiable DNA from *B. anthracis* vegetative cells. In both cases the endpoint detection limit was not affected by the sample matrix. It was approximately the same in DPBS, whole blood, plasma or serum.

FIGURE 1. Comparison of Qiagen QIAamp Tissue Kit and Schleicher & Schuell Isocode procedures for preparing DNA from *B. anthracis* vegetative cells in DPBS, whole blood, plasma and serum. Serial twofold dilutions starting at 2.5×10^3 CFU per 10 μ L in lane A, lane I is PCR no-template control.



CONCLUSIONS

Our data show that for preparing DNA, the Schleicher & Schuell IsoCode procedure has the same endpoint detection limit as the Qiagen Tissue Kit when starting with equivalent samples. The shortcoming of the IsoCode system is that the sample is limited to less than 10 μL since only the material from the 3-mm disk is processed. In the case of the Tissue Kit procedure, under the conditions described, it is possible to process an 80- μL sample, and by adjusting the conditions it would be possible to process over 200 μL in a 1.5-mL microcentrifuge tube. However, because the IsoCode procedure is so simple, and because it has advantages with regards to collection, storage and transportation of samples, the IsoCode method could have a special role in diagnostics applications where the concentration of target organisms is sufficient, or where samples can be appropriately concentrated. In particular it may be useful in field applications where simplicity and ease of use are desirable characteristics.

A PROCEDURE FOR PREPARING PCR-AMPLIFIABLE DNA FROM *BACILLUS ANTHRACIS* SPORES IN SOIL SAMPLES

Susan R. Coyne, Philip D. Craw, Jeff D. Teska, John W. Ezzell, Erik A. Henchal and Fred K. Knauert

US Army Medical Research Institute of Infectious Diseases
Diagnostics Systems Division
1425 Porter Street
Ft. Detrick, MD 21702-5011

Preparing DNA from *Bacillus anthracis* spores in soil samples is particularly challenging. To get maximal disruption of spores, it was necessary to first digest them with proteinase K and then mechanically disrupt the cells by agitation in the presence of glass beads. To remove degradative and inhibitory sample contaminants, we treated the sample with polyvinylpyrrolidone (PVPP) and Chelex 100. Depending on the soil, this decontamination procedure was sometimes insufficient, and it was necessary to further process the partially purified DNA sample by the Life Technologies, Inc., GlassMAX procedure, which is no longer available, or the Qiagen QIAamp Tissue Kit procedure. We tried to simplify the procedure by replacing the decontamination process with the Schleicher and Schuell IsoCode paper procedure and found that it was insufficient by itself to remove all contaminants. However, we did find that if we used this procedure in combination with the PVPP and Chelex 100 treatments, we were able to increase the amount of soil we could prepare per sample from 100 mg to 250 mg without affecting the endpoint detection limit, approximately 200 cfu / sample or less than 1000 cfu per G of soil. Thus, we were able to simplify and increase the overall sensitivity of the procedure.

Introduction

To successfully prepare DNA for the polymerase chain reaction (PCR) from *B. anthracis* spores in soil samples, two conditions must be met. First, the procedure must be able to disrupt the spore and release its DNA in both sufficient quantity and quality to support PCR. Secondly, it must remove soil contaminants that inhibit PCR, such as humic acids, or that degrade DNA, such as polyvalent metal ions. Our laboratory standard has been a modification of a procedure developed by Battelle Memorial Institute, Columbus, OH. This procedure relied on digestions with a mixture of bacterial-lytic enzymes, proteinase K and SDS in combination with mechanical disruption with glass beads to release the DNA from the organism. It also included incubation with polyvinylpyrrolidone (PVP) to remove humic acids, and a Microcon 30[™] (Amicon) step to concentrate the sample and remove low molecular weight contaminants. For certain soils, particularly those with a higher organic content, it was necessary to do an additional purification with the GlassMAX[™] system (Life Technologies, Inc.) to remove PCR inhibitory material. Because its manufacture was discontinued, we replaced the GlassMAX[™] procedure with the Qiagen QIAamp Tissue Kit procedure without any loss in endpoint detection. However, because the procedure was labor-intensive, we attempted to substitute the Schleicher and Schuell IsoCard DNA Isolation device procedure as a simpler alternative for DNA purification. We found that this procedure by itself was insufficient to completely remove PCR inhibitory contaminants. However, we found that by pre-treating the sample with polyvinylpyrrolidone (PVPP) and Chelex 100, we were able to remove the inhibitory and degradative contaminants found in the soil. The combination of pre-incubations with PVPP and Chelex 100, digestion with proteinase K, mechanical disruption and Isocode purification resulted in a simpler and more sensitive procedure for preparing PCR amplifiable DNA from *B. anthracis* spores in soil samples.

Materials and Methods

Spores used in all experiments were renograffin-purified *B. anthracis*, strain Ames, obtained by Ms. T.G. Abshire, Special Pathogens Branch, Diagnostic Systems Division, USAMRIID. The Standard Extraction Procedure and Simplified Procedure are outlined in Table 1.

TABLE 1. Summary of Extraction Methods for DNA from Soil Samples.

Standard Procedure	Simplified Procedure
Incubate with three bacterial lytic enzyme mix	Incubate with three bacterial lytic enzyme mix and PVPP
Incubate in lysis buffer w Proteinase K	Sediment soil
Incubate with SDS at 65°C	Incubate supernatant with Chelex 100 at 56°C
Centrifuge and incubate supernatant on ice with PVP	Sediment Chelex 100
Microcon 30 concentration	Concentrate sample
QIAamp Tissue Kit	Heat to 95°C
	Isocode procedure
4 hours	2 hours

PCR analysis: Conventional PCR analysis was performed using primers that specifically amplified 23S rDNA. Two, five, or ten µl of template was added per 100 µl assay. PCR products were analyzed on a 3% Nusieve 3:1 gel prepared in TBE buffer and stained with ethidium bromide. Photodocumentation was done with the Alpha Innotech Imaging System.

Results

Up to 10 µl of template from the simplified procedure could be used in a PCR reaction for soil suspensions of 10% through 60% without any observable PCR inhibition. Although 2 µl was not inhibitory, both 5 and 10 µl of eluate from the standard procedure had significant inhibition at higher percent soil suspensions. We attribute the inconsistent degree of inhibition at 60% compared to 30-50% suspensions to the variability in sampling of those aliquots because the high soil content interfered with consistent pipetting. Because of this variation in pipetting, 50% suspensions were used for future extractions.

One hundred milligrams of soil (200 µl of a 50% soil suspension) can be extracted using the standard procedure without any inhibition whereas 250mg (500 µl of a 50% soil suspension) can be extracted using the simplified procedure without any inhibition.

The detection limit of the simplified procedure was 150 CFUs and was independent of whether the samples were extracted immediately after preparation or after storage for one week at 4°C. The detection limit of the standard procedure was also 150 CFUs although the intensity of the resulting PCR product was less than the equivalent samples prepared by the simplified procedure, and was also not affected by whether the samples were extracted immediately after preparation or storage for one week at 4°C.

CONCLUSIONS

We have developed a new procedure for the extraction of *B. anthracis* spores from soil that is simpler and more efficient in removing inhibitors from these samples. As a consequence, we are able to successfully extract DNA from a larger sample of soil, 500 versus 250 μL , without PCR inhibitory contaminants and with at least equal endpoint detection limits, effectively increasing the specific detection limit of the assay. An added advantage of this method is that its simplicity may make it adaptable to automated DNA extraction procedures.

HONEY BEES SCAVENGE AIRBORNE BACTERIA FROM THE ATMOSPHERE

Kevin Prier^{1,2}, Bruce Lighthart^{1,2}, Gerald Loper³, Jerry Bromenshenk²

¹Microbial Aerosol Research Laboratory LLC, 10975 Doll Rd., Monmouth, OR 97361

²Division of Biological Sciences, University of Montana, Missoula, Montana 59812

³USDA, Agriculture Research Service, Carl Hayden Bee Center, Tucson, AZ 85719

ABSTRACT

Can honey bees be used as collectors of atmospheric microbial agents of harm? Individual tethered honey bees were flown in a mini wind tunnel and exposed to a cloud of aerosolized bacterial spores (an Anthrax simulant). The bees adsorbed bacterial spores proportional to the measured electrostatic charge on the bee and to the aerosol exposure dose. Based on these laboratory observations, we have formulated a mathematical model for the adsorption of spores onto a bee in flight. We then tested this model on free-flying bees in a greenhouse.

1. INTRODUCTION

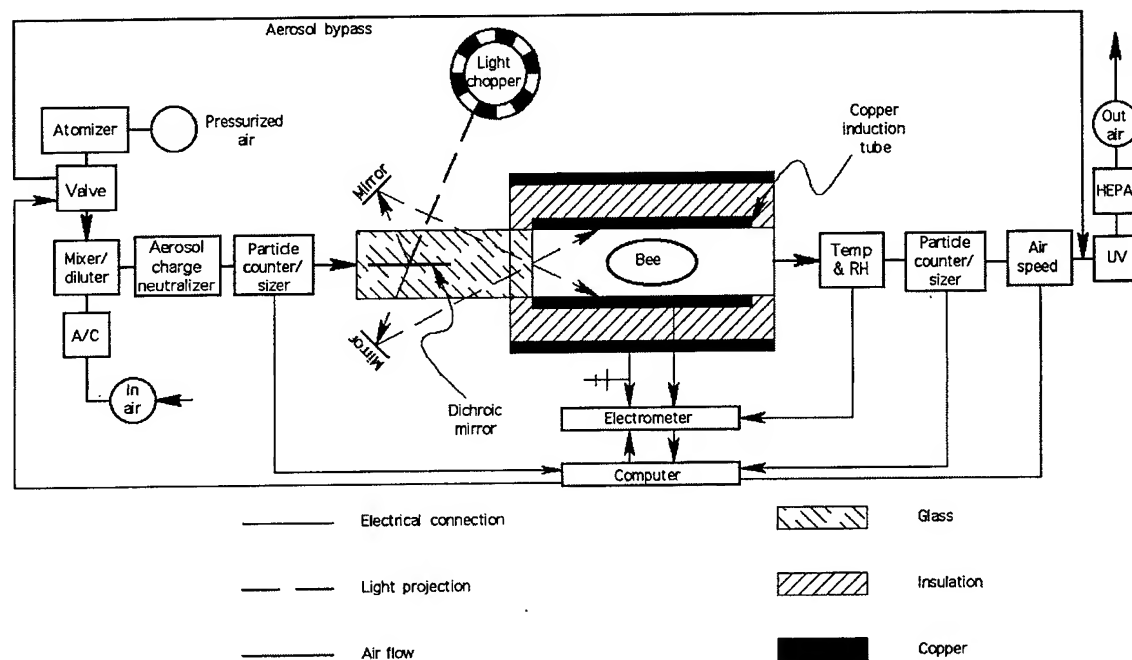
Honey bees (*Apis mellifera*) are electrostatically charged during flight (Erikson, 1975; Yes'kov & Sapozhnikov, 1976). This charge is useful for the bee in collecting pollen (Corbet *et al.*, 1982), as the charge on the bee attracts particles of opposite charge. It is our hypothesis that a flying bee will tend to collect any oppositely charged particulate material that they fly through, including aerosolized bacterial spores.

We have therefore been studying whether honey bees can be used to collect measurable quantities of bacterial spores from the air through which they fly. The purpose of this research is to investigate the possibility of using honey bees to detect the presence of biowarfare/bioterrorism agents or to detect the presence of plant pathogens before the appearance of disease symptoms.

2. METHODS

We have designed a wind tunnel system in which we can tether a single bee and measure its electrostatic charge as it flies (Figure 1). In addition to the charge on the bee, we measure the temperature, wind speed, relative humidity, and concentration of airborne particles in the system. Controllable parameters in the wind tunnel are wind speed, temperature, and the timing and duration of exposure to a continuously generated bacterial spore aerosol (*Bacillus subtilis* var. *niger* (BG)). A typical experiment is at a temperature of 22°C, a wind speed of 9.5–10km/hr, and 3 pulses of aerosol of 45 seconds each. After exposure to the aerosol, the bee is removed from the wind tunnel and sonicated in two rinses of 7ml sterile deionized water. The rinse water is heated to 70°C for 10 minutes to kill any vegetative bacteria and then filtered. The filter is placed

(A)



(B)

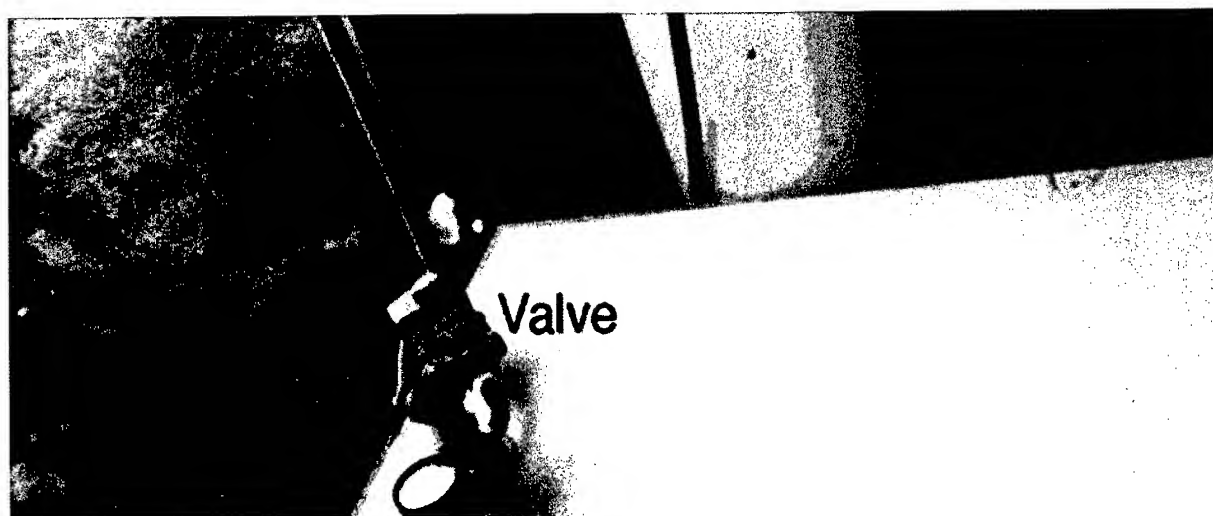


Figure 1. (A) Schematic diagram of the wind tunnel setup. (B) Photograph of the wind tunnel setup.

spore side up on a nutrient agar plate and incubated at 30°C overnight. The number of colonies on the filter is then counted and compared to the particle count from the wind tunnel to determine what percentage of the bacterial spore exposure adhered to the bee. All wind tunnel measurements and controls are controlled through a computer using LabVIEW.

3. RESULTS

3.1 *Bees adsorb bacterial spores in proportion to their static charge*

We have discovered that aerosolized bacterial spores are adsorbed onto flying bees and that the percentage of the spore exposure dose adsorbed is proportional to the electrostatic charge on the bee (Figure 2). We hypothesize that the static charge produces an attractant field around the bee and that the greater the static charge, the larger the attractant sphere around the bee, and therefore the bee has a larger effective scavenging volume as it flies (Lighthart *et al.*, 2000).

We have also discovered an as yet unidentified seasonal effect on the bees' ability to adsorb bacterial spores from the air (Figure 2), independent of the charge on the bee. "Winter" bees were taken from inside the hive, whereas "Summer" bees were caught as they left the hive. One contributing factor may be the age of the bees, as wintering bees tended to be older than summer foraging bees and had fewer hairs for spores to get "caught" in.

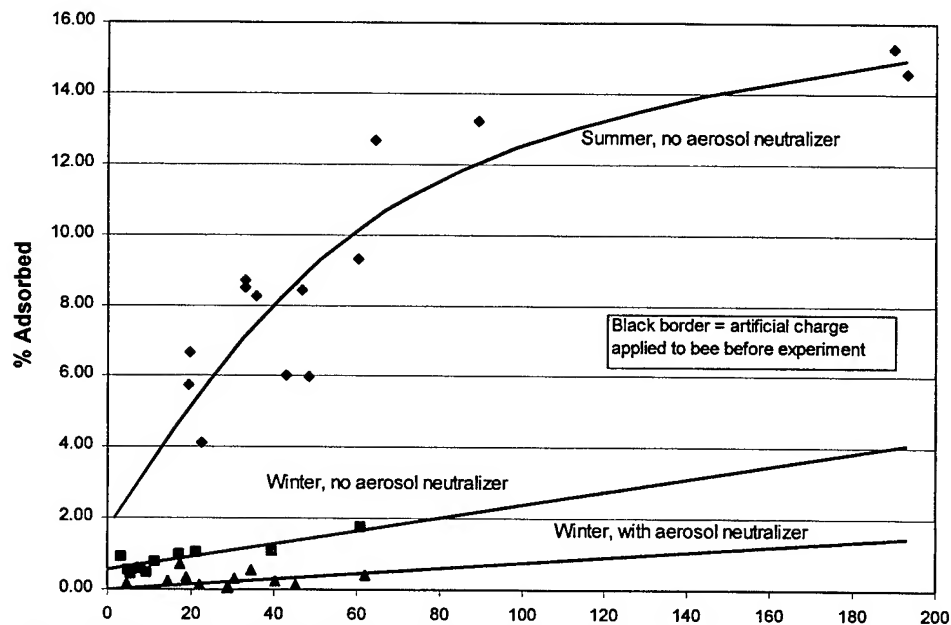


Figure 2. The effects of electrostatic charge and season on the percentage of spore dose adsorbed onto flying bees.

3.2 A model for adsorption of aerosolized bacterial spores in the field

The foregoing discoveries, along with the need to predict the amount a bee will adsorb in field tests, led us to develop a model to predict the amount of spores that can be collected from bees that have flown through a continuously generated plume of aerosolized bacterial spores originating from a point source. In field tests, the bees will be trained to fly across the aerosol plume to a feeder target and back to the hive (Figure 3). The model uses a normal distribution model (Pasquill) for the cloud particulate distribution (Figure 4), including a settling factor for the particles and adjustment for the bees flying perpendicular to the wind (thus increasing their flight path length). An additional factor calculates how many of the particles in the plume will adhere to the bee during each meter of flight, based on laboratory observations (Figure 5). The formula is integrated over the flight path, crossing the plume twice (once on the way to the target and once on the way back). It is further assumed that a certain percentage of the particles adsorbed onto the bee will be desorbed during each meter of flight, and this is also included in the calculation.

The parameters included in the calculation of the number of spores recovered from a bee at the hive are presented in Table 1. A graph of the particles being adsorbed and desorbed during each meter of flight, as well as the total particles on each bee, is presented in Figure 6.

3.3 Collection of spores from bees returning to the hive

The difficulty in assaying bacteria in the field is the recovery of spores from the bees as they return to the hive. The most efficient method would be to capture all returning bees and rinse them as a batch and then culture the rinse water as in the laboratory experiments. The obvious disadvantage of this approach is the death of all the returning bees. This may be acceptable in an emergency scenario where maximum recovery/sensitivity is necessary, but it would be impractical for hives used as long term monitoring stations.

We have designed a non-invasive method of collecting spores from returning bees by modifying a standard under-hive pollen trap (Figure 7). Returning bees must work through two mesh screens to enter the hive. The screens knock off pollen balls and other particles as the bees go through. A cyclone sampler is hooked up to the back of the hive and air is being continuously pulled through the bottom of the hive. The small spore particles will be caught in the air flow and pulled into the sampler while the heavier pollen balls will fall to the bottom of the pollen trap.

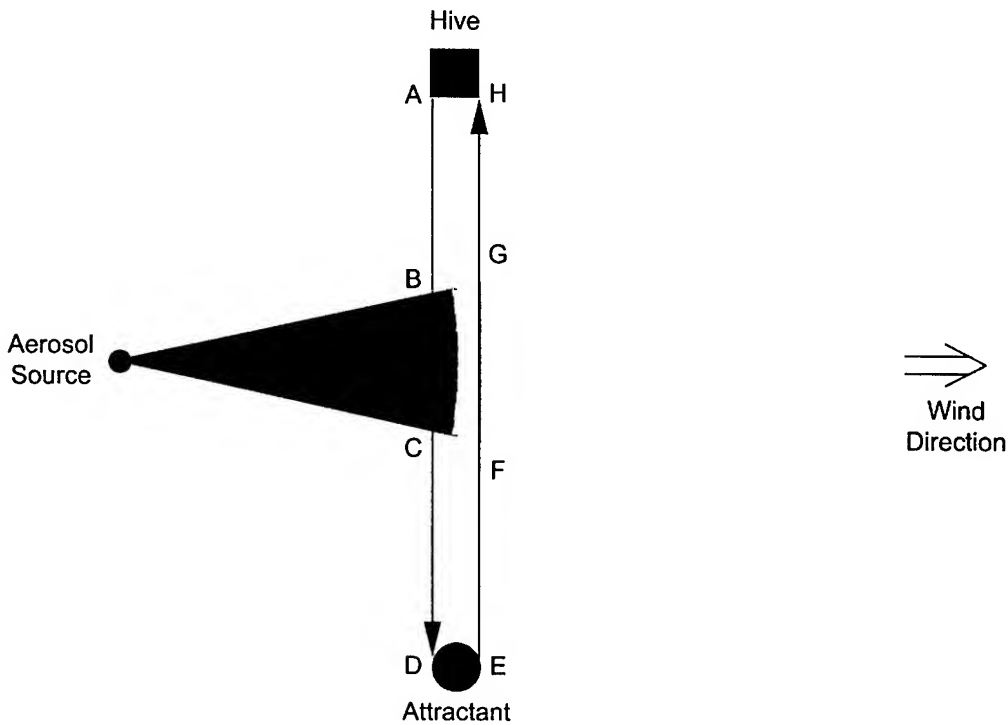


Figure 3. Outdoor test scenario where bees are trained to fly across an aerosol plume to a feeding station and back to the hive.

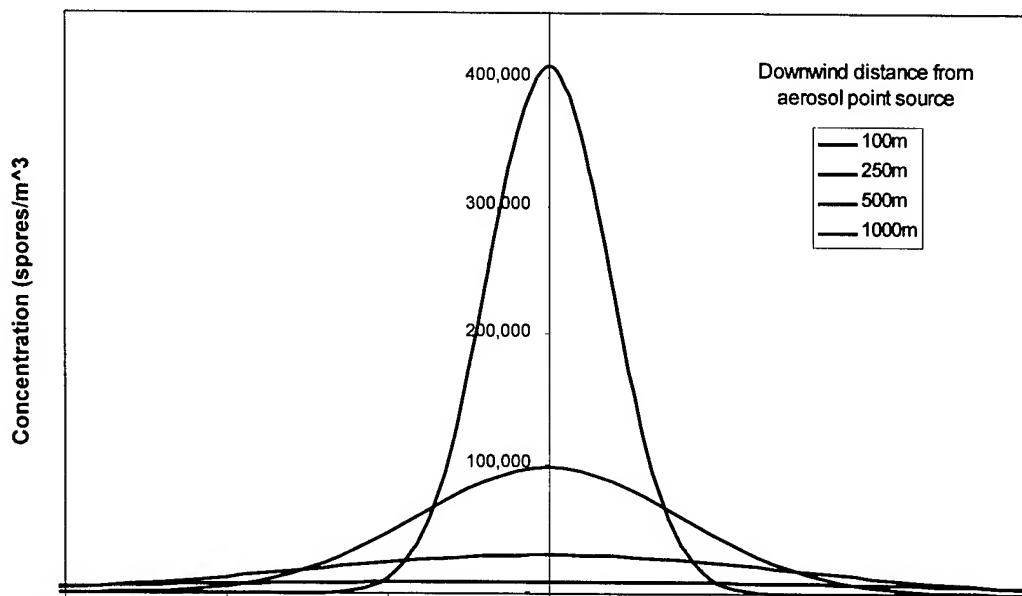


Figure 4. Bacterial spore concentration 10m above the ground at various distances from the point source, with moderately turbulent air and a wind speed of 2m/s.

$$(A \cdot K \cdot V) \left(\frac{Q \cdot R}{2 \cdot \pi \cdot w \cdot \sigma_y \cdot \sigma_z} \right) e^{-\frac{(y^2) \cdot [(w^2/b^2)+1]}{2 \cdot \sigma_y^2}} * \left\{ e^{-\frac{(z-h)^2}{2 \cdot \sigma_z^2}} + e^{-\frac{(z+h)^2}{2 \cdot \sigma_z^2}} \right\} e^{-\frac{[(h-(0.000035 \cdot x/w))^2]}{2 \cdot \sigma_z^2}}$$

term 1
adsorption
factor

term 2
aerosol distribution across flight
path

term 3
settling factor

Turbulence=	High	Moderate	Low
$\sigma_y =$	$0.4 \cdot x^{0.91}$	$0.36 \cdot x^{0.86}$	$0.31 \cdot x^{0.71}$
$\sigma_z =$	$0.4 \cdot x^{0.91}$	$0.33 \cdot x^{0.86}$	$0.31 \cdot x^{0.71}$

This value is integrated over the flight path, with two foci for $y=0$ (crossing the plume on the way to the target and on the way back), and with the additional modification of subtracting D^* (total accumulation for the previous meter) at each meter.

The final result is multiplied by ($C \cdot S$ = the percent collected at the hive times the number of bees returning).

Figure 5. Equation for the number of spore particles adsorbed onto a bee in each meter of flight.

Parameter (with variable notation)	Units	Range	Weather conditions		
			High turbulence	Mod. turbulence	Low turbulence
Source concentration (Q)	spores/ml	10^{11} - 10^{12}	$1E+11$	$1E+11$	$1E+11$
Source output rate (R)	ml/sec	0.01	0.01	0.01	0.01
Source output ($Q \cdot R$)	spores/sec	$f(Q, R)$	$1.00E+09$	$1.00E+09$	$1.00E+09$
Source height above ground (h)	m	0-10	2	2	2
Distance from aerosol source (x)	m	100-1000	250	250	250
Adsorption efficiency of bee (A)	%/pC	0.12	0.001	0.001	0.001
Charge on bee (K)	pC	10-100	50	50	50
Bee scavenging volume/meter flight (V)	m^3/m	0.001	0.001	0.001	0.001
Desorption rate (D)	%/m	.01-.1	0.0005	0.0005	0.0005
Bee flight altitude (z)	m	2-50	10	10	10
Bee flight velocity (b)	m/s	1-10	5	5	5
Wind velocity (w)	m/s	0-10	5	2	1
Hive to target distance (2y)(plume axis @ $y=0$)	m	500-1000	750	750	750
Approximate cross-section of plume @ 'x' m	m	$f(x)$	244	178	69
Length of flight path through plume	m	$f(x, b, w)$	344	191	70
Hive-to-plume flight path length	m	$f(x, b, w)$	358	308	347
Plume-to-target flight path length	m	$f(x, b, w)$	358	308	347
Total flight path length from hive to target	m	$f(b, w, y)$	1061	808	765
% collected at hive (C)	%	0-100	0.5	0.5	0.5
# of bee "sorties" (S)	-	0-10,000	200	200	200
Spores collected:			11,136	63,875	279,743

Table 1. Model parameters for the prediction of the number of spores collected by bees flying through a point-source plume of bacterial spores.

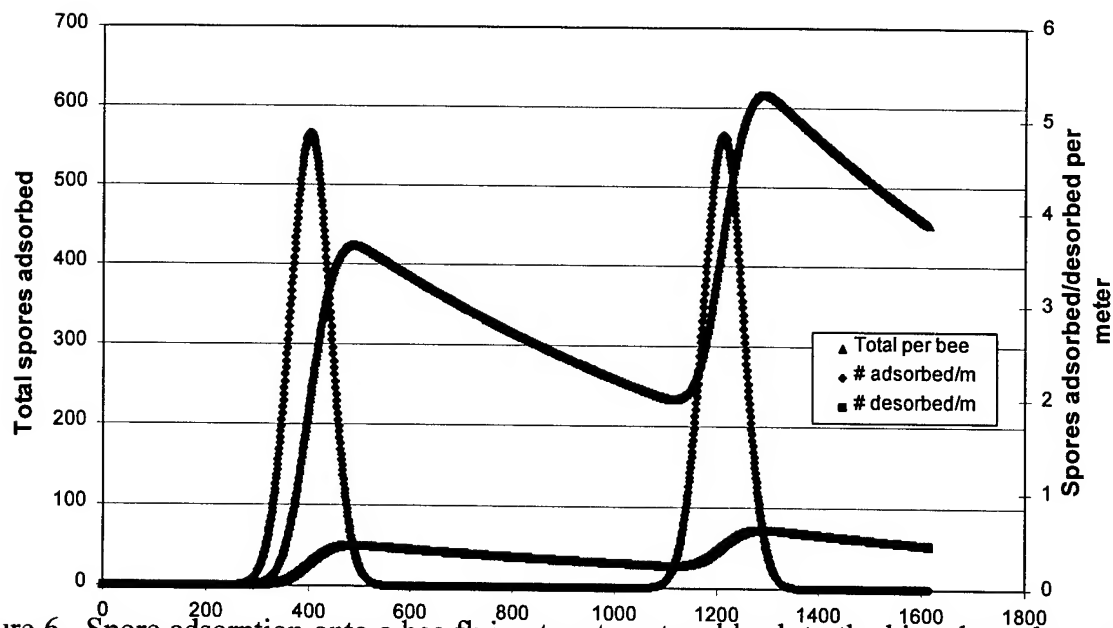


Figure 6. Spore adsorption onto a bee flying to a target and back to the hive through an aerosol plume, 250m from the point source, with moderately turbulent air and a wind speed of 2m/s.

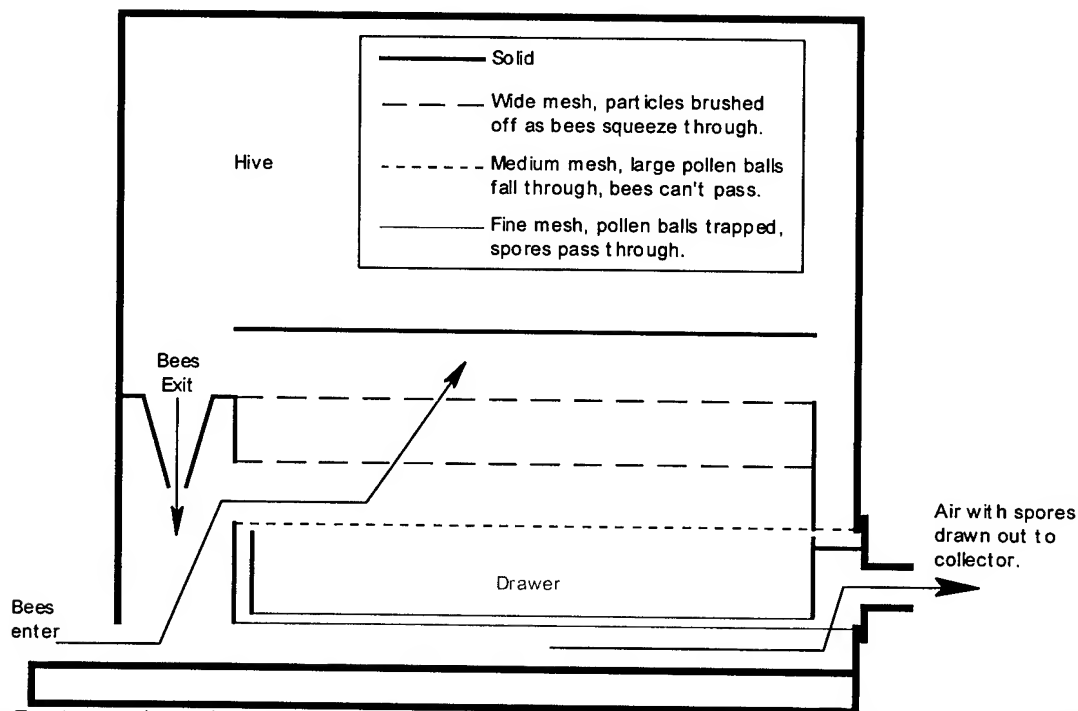


Figure 7. A non-invasive bacteria collection system: Bacterial spores and pollen are brushed off of bees as they squeeze through the wire mesh. Pollen balls are caught in the fine mesh in the drawer, while smaller spore particles are drawn into an air stream to a collector. Pollen balls can later be removed from the drawer for examination for spores.

3.4 System Disadvantages

The main problem in the system is contamination: once a positive result is obtained, it is impossible to tell if future positives are from the environment or from residual contamination from the hive. In most cases, though, this should not be a problem. In an acute scenario, for example looking for anthrax, the hive would be destroyed after a positive result. In domestic use in monitoring for crop pathogens the field would be treated after a positive result and by the time the treatment regimen was finished the hive should have been cleaned out by the bees and any remaining bacteria immobilized in wax or propolis.

For military applications, a styrofoam nucleus hive could be filled with five frames from a clean stock hive and then transported to the test site. After a period of flight, the entire nucleus hive could be sacrificed to test for the suspected pathogen without sacrificing the queen from the stock hive, which would then be able to recover the lost workers.

4. CONCLUSIONS

Honey bees may make a effective tool for the detection of harmful bacterial spores in the atmosphere. Because of their long flight range (up to 3km), and large numbers, one hive can cover a significant area. In addition to military use in detecting the presence of biowarfare agents, the honey bee system shows good potential for domestic applications such as monitoring crops for plant pathogens. Especially during pollination periods, the bees would have a close association with the crop plants, and would tend to pick up particulates, including pathogens, from the plants themselves as well as the air around them, making them an even more effective collection and detection tool.

5. REFERENCES

- Corbet, S. A., J. Beament, & D. Eisikowitch, 1982: Are electrostatic forces involved in pollen transfer? *Plant, Cell, and Environment* 5:125-129.
- Erikson, E. H., 1975: Surface electric potentials on worker honeybees leaving and entering the hive. *J. Apicultural Res.* 14:141-147.
- Lighthart, B., K. Prier, G. Loper, & J. Bromenshenk, 2000: Bees scavenge airborne bacteria. *Microbial Ecol.* (in press).
- Yes'kov, Y. K., and A. M. Sapozhnikov, 1976: Mechanisms of generation and perception of electric fields by honey bees. *Biofizika* 21:1097-1102.

ADDENDUM – Greenhouse trials

To test our model, we ran some experiments in a greenhouse with free-flying bees. In our first experiment, beehives were located inside the greenhouse, which had been sealed with plastic sheeting and HEPA filters, and then generated an aerosol cloud in the greenhouse. The hives were fitted with traps which allowed bees to leave the hive but which would isolate returning bees in a separate container. Upon generation of the aerosol cloud, the hive exits were closed off and the bees that were already outside were allowed to fly until they returned to the hive, where they were trapped. A number of bees that did not return to the traps were captured from various sites inside the greenhouse. Three sets of bees were then tested for the presence of adsorbed bacterial spores: bees which were not allowed to leave the hive into the aerosol

(control), bees which returned to the hive and were trapped, and bees which remained in the aerosol through the entire experiment before being captured. As shown in Table 2, the control bees had very little contamination. The trapped bees had many more spores on them, but predictably, not as many as the bees that were exposed for the entire duration of the experiment. The bees with the most spores adsorbed were those caught at or near feeding stations.

In a second experiment, new, clean hives were located outside the sealed area. An aerosol cloud was generated inside the greenhouse before the introduction of bees. The bees were then introduced from their hives through plastic tubes into the sealed area and were kept flying for a fixed period of time. The bees were collected from various sites inside the greenhouse and tested for adsorption of spores. Again, the bees with the most spores adsorbed were those caught at or near feeding stations (Table 2). It may be that these bees were actively foraging and had produced a higher static charge than the bees flying elsewhere. It was not possible in these experiments to measure individual charges on bees.

The average spore concentration for each experiment was about 250 spores/liter. Based on exposure time, bees with a charge of 10–50pC should have adsorbed from 512 to 2,559 spores each, which fits quite well with the observed results. If the bees near the feeders had a higher charge, for example 80–120pC, they should have picked up 4,094–6,142 spores, which also fits well with the observed results.

Expt.	Collection Site	Replicate	# Spores	# Bees	Spores/bee		
					Control	Test	Adjusted*
1	Hive egress (Control)	1	240	59	4		
		2	450	53	8		
		3	1,290	20	65		
					15		
Mean**							
2	Hive ingress (trap)	1	12,630	16		789	774
		2	8,190	60		137	122
		3	12,720	8		1,590	1,575
						M	399
	Side wall	1	6,180	10		618	603
		2	40,650	9		4,517	4,502
	Door		10,230	19		538	523
	Feeder -a		39,810	4		9,953	9,938
	Feeder -b		22,950	10		2,295	2,280
						M	4,483
	Alighted on collection tube	1	965	1		965	950
		2	671	1		671	656
		3	1,086	1		1,086	1,071
						M	907
	Side wall	1	740	1		740	725
	Side wall	2	925	1		925	910
Side wall	3	27,980	22		1,272	1,257	
Side wall	4	40,530	26		1,559	1,544	
					M	1,404	
Cyclone stand		25,710	4		6,428	6,413	

* Adjusted for control average.

** Weighted for number of bees in set

Table 2. Aerosolized bacterial spores in a greenhouse adsorbed onto free-flying honey bees collected at the indicated sites in a greenhouse.

AN INTEGRATED FIBER-OPTIC SYSTEM FOR IDENTIFYING BIOLOGICAL AGENTS

Yifu Guan, Jeffrey T. Ives and *James H. Bechtel*
IPITEK, 2330 Faraday Ave. Carlsbad, CA 92008
Phone: 760-438-1010, ext. 3326, Fax: 760-438-2412
e-mail: yguan@ipitek.com

ABSTRACT

An integrated fiber-optic detection system was designed for identifying biological agents. This system is a compact, fieldable, automated unit and operates in a continuous in-line mode. With this approach, there is no need for time-consuming and delicate sample preparation. Fundamental to our approach is the sandwich-hybridization between 16s ribosomal RNA (rRNA) of target agents (bacteria or viruses) and oligonucleotides. These oligonucleotides are designed to be fully complementary to specific regions of the rRNA of interest in order to differentiate microorganisms. We conducted a series of theoretical and experimental studies to investigate the hybridization stability. To determine sequences of oligonucleotides, GenBank has been mined, and mismatched regions of 16s rRNA of target microorganisms have been identified. RNA extraction methods have been tested, oligonucleotide immobilization has been studied, and rRNA hybridization has been evaluated.

INTRODUCTION

Biological warfare (BW) agents have become an increasing threat to military personnel and civilians in recent years.¹ Countering this threat is an extremely challenging task due to the diversity of BW agents, ranging from bacteria like *Bacillus anthracis*, to viruses such as hantavirus, to protein toxins such as botulinum. Although protective suits, respirators, vaccines, and antibodies can be useful in protecting against BW agents, the expense and cumbersome physical limitations make them generally impractical for widespread and continual use. Therefore, defenses against BW agents rely on warning systems to indicate what, when and where protective measures should be taken. The ideal warning systems should be able to identify low concentrations of biological agents without false alarms and as quickly as possible, since early warning can initiate immediate defensive action and significantly improve the safety of personnel in the threatened locations.

Developing detection systems needs an extra effort. In addition to the wide diversity of BW agents, their detection is further complicated by their existence in multiple forms, either floating in the ambient air, dissolved in water or stuck on the surface, as well as by the interference from such as dust particles, air pollutants, soil crystals, and other organic matter. These potential interferants could cause either positive or negative responses to trigger false alarms. Also these interferants often exceed the BW agents in number. For instance, aerosol particle density near the ground surface is measured ranging from less than 1000 particles/ml in clean marine environments to greater than 10^6 particles/ml in urban environments, with local environmental effects, such as dust clouds causing orders of magnitude changes in these numbers.

Although protein toxins are dangerous materials, our attention focuses on the detection of bacteria and viruses. They possess a more serious threat since their infection can lead to growth and multiplication for increased disability, chronic conditions, and further infectious spreading. These microorganisms also have protective coats that provide increased survival between hosts and facilitate their dispersal as offensive weapons. The ability of these agents to multiply and create protective coats is coded in their nucleic acids, and identifying this genetic information will detect the specific organism.

Nucleic acid identification is also valuable and probably essential for genetically modified microorganisms where a typically innocuous or non-recognized outer coat is used to transport pathogenic nucleic acid.

The nucleic acid polymers, DNA and RNA, combine to create all the proteins in an organism, and thereby define the function, including pathogenicity, of the cell and microorganism. For viruses, their structure as protein-coated nucleic acids makes the role of the nucleic DNA or RNA particularly obvious and critical. Depending on the type of virus, the viral genetic material may be single or double stranded and either DNA or RNA. DNA and RNA have very similar chemical compositions, which allows hybridization between strands of either molecules. This is an important feature because it allows hybridization-based methods to be universally applicable, independent of the target microorganisms. Methods to detect bacterial or viral nucleic acids have been investigated.² Typically, these methods rely on the polymerase chain reaction (PCR) to amplify and selectively purify specific regions of the genomic DNA, and are widely used in laboratories. However, these approaches are time-consuming, and require expensive instruments and delicate handling by trained personnel.

Utilizing new developments in optoelectronics, fiber-optics and sensor technology, we are developing compact, fieldable systems for detecting BW agents. One of these sensors is able to detect bacteria and viruses based on the sensitive fluorescence detection of rRNA of the target species. Fundamental to our approach is the sandwich-hybridization of the 16s rRNA of target biological agents and oligonucleotides in a sequence-specific manner. The first group of oligonucleotides is immobilized on the microarray surface through covalent attachment, and the second group is dye-labeled. Microorganism samples are injected directly into the detection system and cells are lysed. The released rRNAs are then bound to the surface-immobilized oligonucleotides through oligo:RNA hybridization. The bound rRNA molecules are further hybridized with dye-labeled oligonucleotides to form oligo:RNA:oligo complex. These oligonucleotides are of approximately 20 nucleotides in length, and are designed so specifically that they are fully complementary to the target rRNA. After removing unbound molecules, the oligo:RNA:oligo complexes are irradiated with a laser and the fluorescence from the fluorescent dyes are measured. The whole detection could be accomplished in less than 20 minutes. Figure 1 depicts the sandwich-hybridization process conceptually.

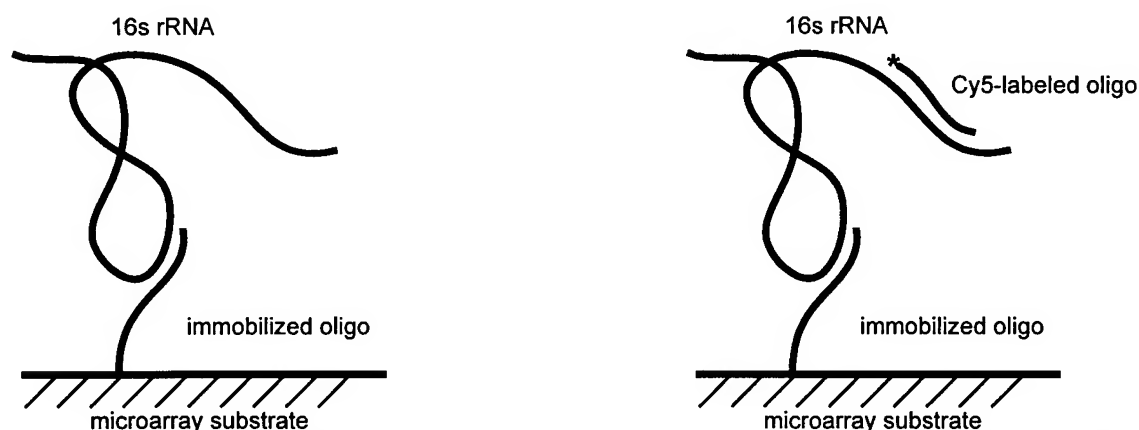


Figure 1. Schematic diagram showing the sandwich-hybridization of target RNA and oligonucleotide probes.

Our integrated fiber-optic system could have multiple applications and benefits. A typical scenario is the identification of food pathogens. Statistical data showed that more than 70,000 cases of food poisoning were caused by contamination of *E. coli* bacteria alone each year. The present methods for detecting these germs in food and dairy products entail making bacterial cultures and takes 12-48 hours to deliver a diagnosis. Sensitive, accurate and rapid methods of identifying contaminated food products can minimize product recalls or processing line shut-downs, which could save the food and dairy industry millions of dollars each year. The ability to detect low analyte concentrations in complex samples would allow early diagnosis of individuals exposed to infectious diseases or with cancer. This identification could also have applications in airports and border crossings where people and packages are in transit and concealed hazards are in low concentrations.³

EXPERIMENTAL RESULTS

A) System design

Our integrated fiber-optic system is composed of an optoelectronic board and a microfluid module. The optical block mounted on the optoelectronic board hosts a 635 nm diode laser for excitation, a dichroic filter set for directing the laser beam to the sample and separating the fluorescence emission from the excitation light, and a semiconductor photodetector for transducing the fluorescent light into electronic signals. Figure 2 shows a photograph of the optoelectronic board and control panel of the compact system. Photodetector output is integrated, digitized, and processed with a 20-bit A/D converter (DDC101, Burr-Brown) and a 12 MHz microcontroller. The electronic signals are then forwarded to a personal computer via an RS-232 connector. The data display and parameter setting are implemented on the computer with a simple GUI (Graphical User interface) program. To detect the Cy5-labeled oligonucleotides that are immobilized on the flat substrate surface inside the hybridization chamber, the excitation laser beam is directed downward by a 45 degree mirror and focused onto the substrate surface inside the hybridization chamber that is located about 10 mm below the fluorometer board. Fluorescence emission from Cy5-labeled oligonucleotide is collected by the same focusing lens before passing through the dichroic filter that blocks the backscattered excitation light. The emission filter used in conjugation with the dichroic beamsplitter can achieve a 1.0×10^{-7} rejection of the excitation light. From the transmission spectra of the dichroic filter and emission filter, 33 percent of the total emission energy of Cy5 dye is expected to be collected by this detection system. This optical block was tested in our prototype fluorometer to support the fiber-optic probe for monitoring the chemical contaminants in underground water, and the detection limit in the part-per-billion range was measured.⁴

The microfluid module consists of a reaction chamber, a hybridization chamber and solution reservoirs. It was designed to process the biological samples in a continuous in-line manner. The crude samples are mixed with permeabilization reagent in the reaction chamber. The released nucleic acids are then pressured to pass through a filter to enter the hybridization chamber and leave cellular fragments behind. Five minutes later, the hybridization chamber is eluted and the second hybridization of the bound rRNA with dye-labeled oligonucleotides starts. The whole process is designed to accomplish in less than twenty minutes. The pumps and valves are synchronized to direct the sample, solvents, buffers, and waste to the expected destinations.

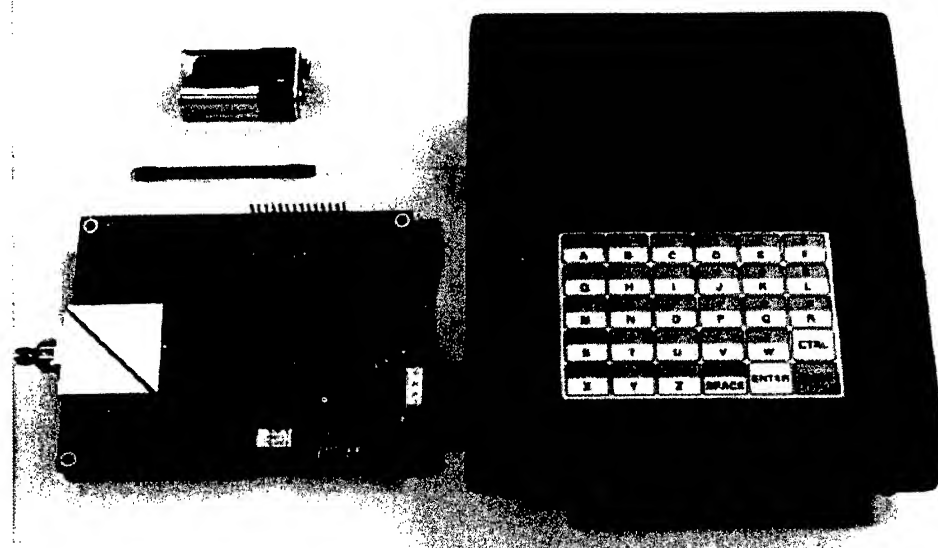


Figure 2. Photograph of the prototype fiber-optic system for identifying microorganisms. The optical block (white) is mounted on the optoelectronic board (shown on the left). The black case is the control panel.

B) Oligonucleotide determination

The determination of oligonucleotide sequences used for the target agents started with the fundamental analyses of how the oligonucleotide length, the base composition, the number of mismatches affect the hybridization specificity. The calculated results indicated that oligonucleotides about 15 bases long provide a reasonable compromise between room temperature stability of the oligo:RNA duplexes and sensitivity to single base mismatch. The calculated results also showed that differentiation based on oligonucleotide hybridization becomes more accurate and reliable as the number of mismatched nucleotides between the target RNA and potential interferants increases.

The 16s rRNA sequences of *E. coli*, *Bacillus*, and *Erwinia* were obtained from GenBank. Sequence alignments were carried out to identify the mismatched regions of nucleotide sequences. During the alignment, the programs were able to shift the sequences relative to each other to obtain the positions of optimal match. When two sequences matched, a solid line was created, such that two identical sequences created a 45° line. When the sequences had no significant similarity, an open space was created. The sequences of the selected oligonucleotides were determined from the open spaces. If an open space showed multiple mismatches, it received a high priority for consideration since the identification specificity could be enhanced.

The oligonucleotides of 15-20 nucleotides in length were designed to be fully complementary to the identified regions with the maximum mismatches. For those oligonucleotides to be immobilized on microarray substrates, a spacer of ten A nucleotides is added to the 5'-end, ensuring that the oligonucleotides are flexible enough, even after immobilization, to provide full accessibility to target 16s rRNA to achieve an efficient hybridization. The (A)₁₀-capped oligonucleotides is further derivatized at the 5' end with primary amine group to prepare for further crosslinking reactions. The oligonucleotides used for fluorescence probing will be labeled at 5'-end with either Cy5 dyes.

C) RNA extraction

Conventional methods of extracting and purifying RNA from microorganisms involve an extended series of centrifugation, precipitation, and related steps that require approximately more than two hours.⁵ To scale the process down to a few minutes in a compact, automated microfluid module, we are developing methods that could be operated in a continuous in-line mode. In addition, this new procedure for RNA preparation should protect the target RNA from digesting by RNase enzymes, and purify the target RNA while removing other nucleic acids, proteins, and cellular debris. The effectiveness of the method was evaluated by the survival percentage of the cells after being exposed to permeabilization reagents. The released genomic DNA and rRNA was confirmed by 1.5% agarose denaturing electrophoresis gel.

We tested physical methods to lyse the cells, and found that neither of sonication, electroporation nor magnetic beads blasting could lyse cells effectively, since either the released rRNA was fragmented or the releasing efficiency was very low. Therefore, permeabilization reagents were evaluated. They included hybridization buffer, extraction buffer, and an equal-volume mixture of hybridization and extraction buffers, SDS solution, and Triton X100. Heating was also used to assist the lysis process in some cases. *E. coli* and *B. subtilis* were used as the models for Gram negative and Gram positive bacteria, respectively.

As expected, all the reagents used were effective enough to release *E. coli* rRNA, as indicated by the survival percentage shown in Figure 3. In contrast, the Gram positive bacteria were more resistant to disruption. Either hybridization buffer, extraction buffer or Triton X100, alone could not efficiently lyse the cells. However, heating in conjunction with Triton X100 presented less survival of cells. Further results showed that Triton X100 plus heating can also disrupt the more lysis-resistant *B. cereus*. The RNA preparation process could be accomplished in 3-5 minutes (See Figure 4).

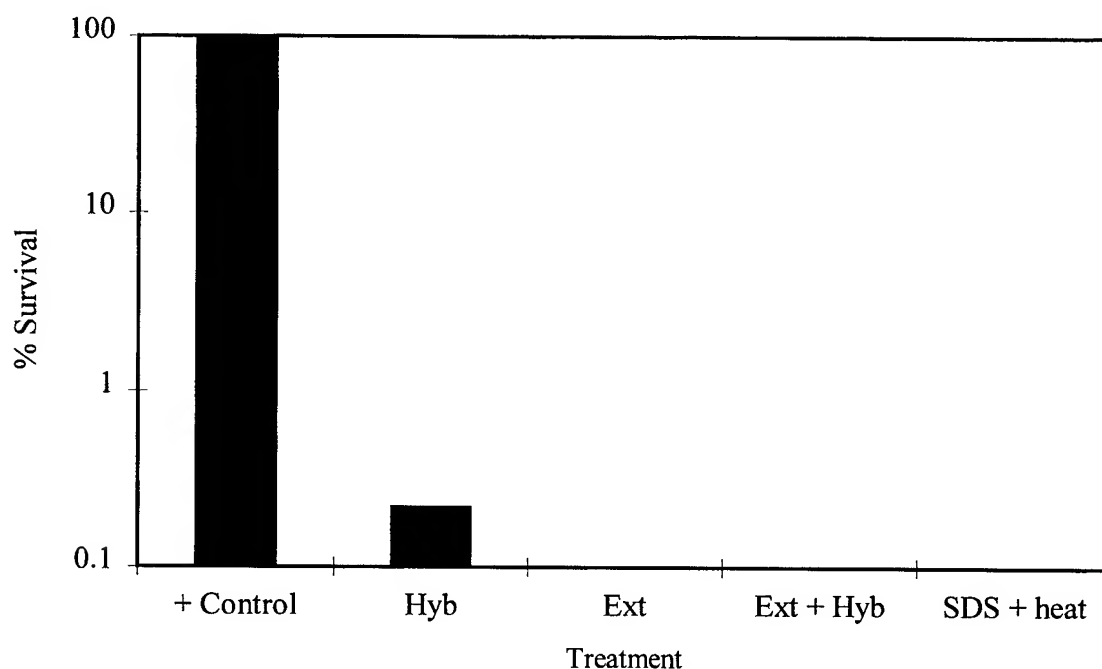


Figure 3. Effect of different buffers on lysing *E. coli* cells.

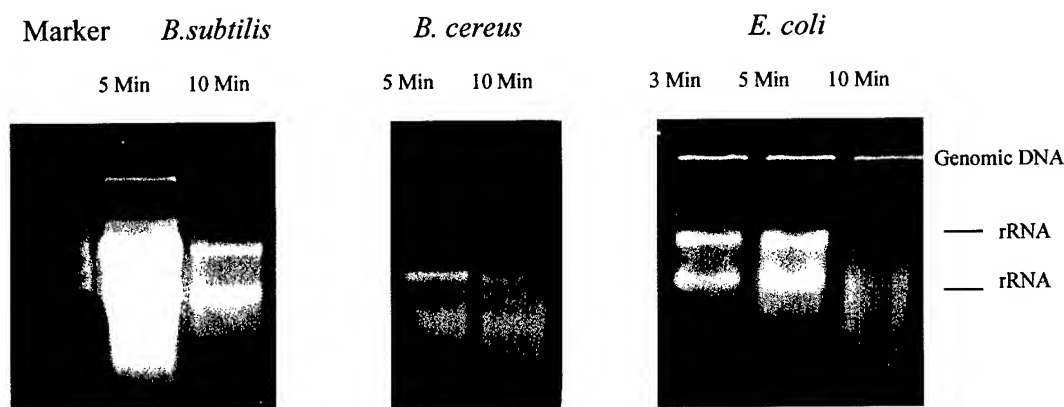


Figure 4. Denaturing agarose gel illustrating the release of genomic DNA and rRNA using Triton-X/heating treatments

D) Immobilization and hybridization

We immobilized oligonucleotides on the microarray substrate using chemical crosslinking protocol. Covalent binding is the preferred method of attaching molecules to a substrate surface since it is more stable and durable than other molecular interactions (for instance, hydrophobic interactions in simple physical deposition), and can be accomplished using a variety of surface chemistries and crosslinking reagents.⁶

In our experiments, amine-coated microscope glass slides were immersed in a homobifunctional crosslinker. After the surface was rinsed thoroughly, Cy3-labeled IgG antibody solution was deposited on this micro slide, and covered with a piece of slide cover. The micro slides were then sealed in a hybridization chamber. Primary amines of Cy3-labeled IgG react with another terminal functional group of the crosslinker that covalently attached on the micro slides. After a designated period, the micro slides were rinsed vigorously to remove all unbound molecules and naturally dried. The fluorescent images of Cy3-labeled IgG immobilized on micro slides were recorded on a fluorescence imaging system. This instrument is equipped with a diode at 532 nm for excitation and a filter at 585 nm, which match the adsorption and emission maxima of Cy3 dye, respectively. The substitution of dye-labeled IgG for 5'-aminated oligonucleotides is to attempt to evaluate the immobilization and hybridization efficiencies separately. And the successful immobilization of antibodies can be adapted for 5'-aminated oligonucleotides without modification.

Preliminary results demonstrated the success of Cy3-labeled IgG immobilization on a microarray substrate with the help of a crosslinker. Square-shaped fluorescent images were observed from the crosslinker-treated micro slides (Figure 5, left), but not the micro slides without crosslinker treatment (Figure 5, right). The influence of organic solvents and immobilization duration on the immobilization efficiency were also evaluated, and no obvious difference of fluorescence images was observed.



Figure 5. Fluorescence images of Cy3-labeled IgG immobilized on micro slides. Left: two square-shaped fluorescence images of Cy3-labeled IgG are observed from the crosslinker-treated micro slide. Cy3-labeled IgG immobilization was accomplished in 30 (top) and 60 minutes (bottom), respectively. Right: no fluorescence images of Cy3-labeled IgG can be detected from the micro slide that was not treated in the crosslinker solution.

The hybridization experiments were carried out on a porous transfer membrane. After rRNA binds on the membranes, the membranes were blocked by immersion in the hybridization solution, followed by the addition of oligonucleotide probes. Hybridization periods of overnight, 15 and 5 minutes were used. A series of steps for colorimetric detection were performed after rinsing the membrane. The visual images did indicate that a hybridization time as short as 5 minutes was feasible. Concentrations of digoxigenin-labeled oligonucleotides that are complementary to *B. subtilis* 16s rRNA were varied to determine the optimal concentration of probes.

The ability to discriminate closely related rRNA from different species is critical to the success of the proposed approach. The purified 16s rRNA for *B. subtilis* and *B. cereus* were spotted on membranes, and the membranes were probed with the same 15-mer oligonucleotide that is perfectly matched to *B. subtilis* 16S rRNA, but has a single mismatch compared to *B. cereus* 16S rRNA. Figure 5 illustrates the distinct image differences. Much stronger signals for the perfectly matched *B. subtilis* rRNA were observed. For comparison, Figure 6 also includes results obtained with an oligonucleotide that contains five mismatches for *B. cereus* 16S rRNA. As expected, the signal was much weaker.

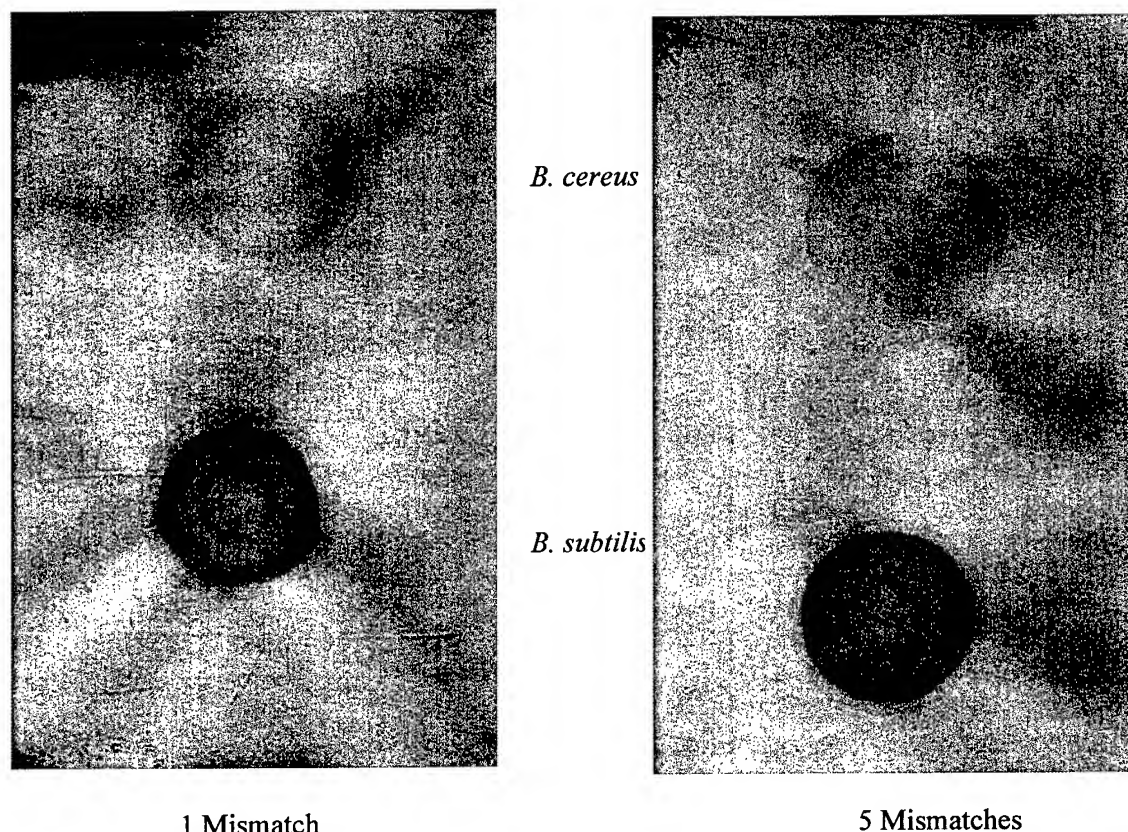


Figure 6. Hybridization of oligonucleotides with one (left) and five (right) mismatches for *B. cereus* 16S rRNA (top) versus perfect matches to *B. subtilis* 16S rRNA (bottom)

CONCLUSIONS

To accomplish the goal of identifying bacterial pathogens and viruses at the detection point accurately, quickly and sensitively, we designed a fiber-optic system that measures the fluorescence of the sandwich-hybridized 16S rRNA of target microorganisms. After evaluating rRNA preparation protocols, we developed a method that can scale the time-consuming and delicate sample preparation down to a few minutes and work in a continuous in-line mode. The oligonucleotides that are complementary to the specific sequences of target rRNA were successfully immobilized on a substrate surface using crosslinking reagents, and target rRNA were hybridized with the oligonucleotides. Hybridization data indicated that the target microorganisms could be differentiated even by a single mismatch in rRNA sequences.

ACKNOWLEDGMENTS

This work has been supported in part by the U.S. Air Force contract #F41624-99-C-9003 monitored by Dr. Burt Bronk. The support and advice are greatly appreciated.

REFERENCE

1. Simon, J. D., J. Amer. Med. Assoc. **278**, 428 (1997).
2. Service, R. F., Science **268**, 26 (1998).
3. Falkinham, III, J. O., in Methods for General and Molecular Bacteriology, American Society for Microbiology, Washington, D. C. (1984).
4. Ives, J., Doss, H., Sullivan, B., Stires, J. and Bechtel, J., SPIE, **3540**, 36 (1998).
5. Norris, J. R. and Ribbons, D. W., eds. Methods in Microbiology, Academic Press, London (1971).
6. Schena, M., DNA Microarray, Oxford University Press, Oxford (1999).

PRODUCTION OF MONOCLONAL ANTIBODIES: VALIDATION OF PROCESSES AND PRODUCTS FOR CRITICAL REAGENT REPOSITORY

Tracy H. Coliano^{1*}, Jun T. Park², Karen S. Heroux², Sarah Cork², Ameneh M. Arasteh¹,
Suzanne K. Kracke², and Peter A. Emanuel¹

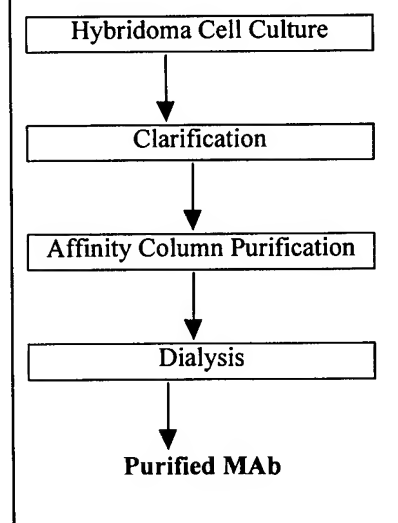
¹U.S. Army Edgewood Chemical Biological Center, Process Engineering Facility,
Aberdeen Proving Ground, MD 21010

²Geo-Centers, Inc., P.O. Box 68, Aberdeen Proving Ground, MD 21010

Edgewood Chemical Biological Center (ECBC) recently marked the opening of the Critical Reagent Repository (CRR) at the Process Engineering Facility (PEF). The Joint Program Office for Biodefense (JPOBD) established the CRR to store and validate all immunological and DNA based biodetection reagents for the DOD. This facility includes a 1500-gallon liquid nitrogen tank, which supplies uninterrupted coolant to archived hybridoma cell lines as well as remote facility monitoring, backup generator, and secured access. The program is housed in four areas covering 1215 cubic feet of the facility. This includes a validation lab that will perform quality control and quality assurance on antibody reagents destined for fielded systems such as the Portal Shield and the BIDS. The Hybridoma Production Laboratory has been established to expand hybridoma cell lines for long-term cryopreservation and to produce monoclonal antibodies (MAb) in cell culture supernatants. The Antibody Recovery/Purification Laboratory purifies MAb from these cell culture supernatants, which are subsequently used for supporting antibody validation activities. The process diagram for the production and purification of monoclonal antibodies is shown in Figure 1.

Hybridoma cell lines were acquired through the JPO Biodefense Critical Reagent Program (CRP) cryorepository. Cell lines were thawed, washed and resuspended in either Iscove's Modified Dulbecco's Medium (IMDM) or BDCell Mab Medium Quantum Yield. Both media were supplemented with 17.6% fetal calf serum, 100 µg/ml penicillin-streptomycin and 1 mM Sodium Pyruvate. In addition, BDCell media was supplemented with 2 mM L-glutamine (IMDM already contains L-glutamine). These media are referred to as "Complete" media. Hybridoma cells were expanded until a sufficient number of cells existed for seeding Integra CL1000 bioreactors. Bioreactors were seeded with 24×10^6 cells in 15 ml of medium. MAbs are secreted into the cell compartment of the bioreactor and are harvested periodically as the hybridoma cells are removed, split, fed and returned to the bioreactor. The cell chamber is separated from the larger media chamber by a semi-permeable membrane. When cells/antibodies are harvested, the 1 liter of Nutrient media (Complete media containing only 1% serum) in this chamber is replaced with fresh media.

Figure 1. Schematic Diagram of the Production and Purification of Monoclonal Antibodies



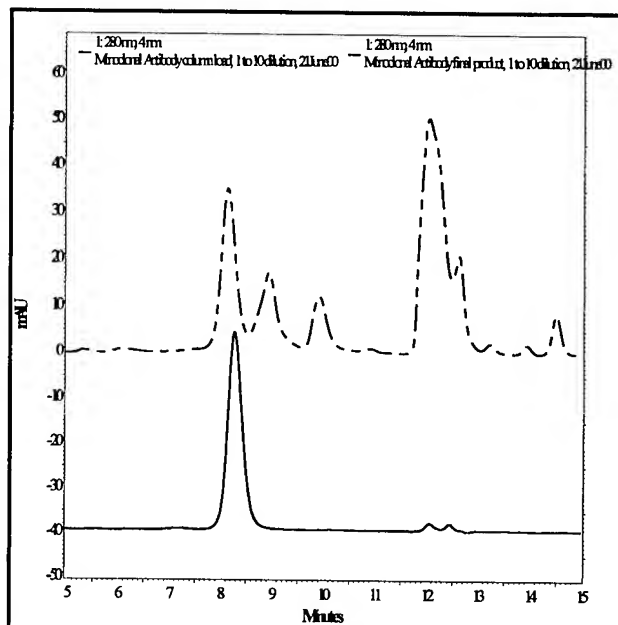
Purification of MAbs is a simple, single column process using the affinity resin, recombinant Protein-A (Pharmacia, Sweden). Following clarification by centrifugation and pH adjustment, the cell supernatant is filtered through a 0.2 µm filter. The supernatant is loaded onto a rProtein-A column and eluted at low pH. To preserve the protein activity, elution is into fraction tubes containing 1 M Trizma Base to neutralize the pH quickly. The antibody fractions are pooled and dialyzed into a final formulation, generally phosphate buffered saline (PBS) or Tris buffered saline (TBS). Protein-A column equilibration

with phosphate buffers works well for most of the MABs we have purified although some will precipitate out of solution. In those cases, Tris- based buffers maintain solubility better than phosphate based buffers.

The activity of purified MAB is measured by an Enzyme-Linked Immunosorbent Assay (ELISA) with a specific antigen. Antibody concentration is determined by Bio-Rad Protein Assay (Bio-Rad, Hercules, CA). The purity of MABs is measured by an analytical gel permeation chromatography (GPC) column (TosoHaas TSG-G3000SWXL) with a Beckman HPLC system and a SDS-PAGE method. Figure 2 shows the chromatograms obtained from the analytical GPC system: a) a sample collected after clarification and b) a final purified MAB sample.

It was found that most of the MABs we have produced are IgG type 2 or 3 from mouse cell lines. The simple process can purify these antibodies without any significant MAB loss, which is mentioned in Figure 1.

Figure 2. Analytical GPC chromatograms of a column load sample (dashed line) and a purified monoclonal antibody (solid line).



Monoclonal antibodies produced from hybridoma cells have substrate specificity that is superior to polyclonal antibodies. This increased specificity makes them ideal for use in biodefense for Army. JPOBD has successfully established the program to work closely with all players within the biodefense community in order to foster standardization of methods, accessibility of the information, and validation of processes and products. ECBC is proud to play a role in what will surely prove to be beneficial to the DOD and instigate more effective use of resources.

PEPTIDE EPITOPES AND MIMETICS

Roy G. Thompson*, Akbar S. Khan, Ameneh M. Aresteh and James J. Valdes
U.S. Army Soldier Biological Chemical Command, Edgewood Chemical and Biological Center,
Aberdeen Proving Ground, MD 21010-5424

ABSTRACT

The objective of this project is two-fold: 1) to identify relatively short peptide sequences (12 mers) that mimic the ability of an antibody to bind to a specific antigen and could thus be used as a substitute for antibodies in various assay formats 2) to identify peptide sequences that may mimic an epitope binding site of a given antigen that could then be used as a positive control in testing antibody – antigen interactions. A combinatorial random peptide library displayed in *E. coli* was screened against two biological toxins, staphylococcal enterotoxin B (SEB) and ricin, and against two monoclonal antibodies generated against SEB and ricin. After five rounds of sequential panning the library against the target ligand, colonies of individual *E. coli* clones were screened through ELISA assays to identify those clones interacting most strongly with the target ligand. The DNA insert encoding for the peptide in each positive clone was then sequenced and converted into the corresponding peptide sequence. Of ten clones selected from each screening protocol, sequences are presented for the clones showing the highest inhibition of antibody-antigen binding in the ELISA.

Introduction

Present methods for the point detection of biothreat agents depend heavily on the use of polyclonal or monoclonal antibodies for recognizing and binding to specific biological antigens. As relatively large, complex proteins with secondary and tertiary structural requirements for maintaining their optimal activity, the use of whole antibodies imposes a significant logistic tail in meeting requirements for production, storage and use in detection platforms outside controlled environments. The traditional hybridoma approach in developing antigen-specific antibodies is also extremely costly and labor intensive and may only access 10^6 of the 10^9 estimated antibody variants thought to be encoded in the immunological systems genome¹. The use of whole antibodies also impose a limit on the detection sensitivity in some sensor platforms, where sensitivity is dependent on the concentration of molecules that can be immobilized in a given area.

Advances in genetic technologies have enabled scientists to clone gene fragments encoding for antibody specificity into host expression vectors, such as bacteriophage^{2,3} and rapidly screen the library of random gene combinations to identify those fragments of the whole antibody molecule that mediate an antibody's specific recognition of a given antigen^{4,5}.

Further reductionism in defining the molecular determinants of antibody specificity for antigen has been pursued by using combinatorial random peptide displays to map the specific amino acid sequences of the hypervariable region of the antibody that actually binds to the antigen epitope. It has been shown that the essential binding domains of an antibody may be as small as 5-15 amino acids^{6,7,8,9}. Random peptide display libraries can be applied to two significant issues in the requirements for biodetection: 1) the design of molecular recognition elements that are smaller than whole antibodies and antibody fragments, and 2) the design of peptide sequences that can mimic the epitope binding sites on antigens and thus be used as positive controls for the antigen in assay validation. We have employed a random dodecapeptide library to screen for peptide sequences that may mimic the binding of antibody to the ricin

and staphylococcal enterotoxin B (SEB) toxins and to monoclonal antibodies generated against ricin and SEB.

METHODS

Random Peptide Library. The FliTrx random peptide library was obtained commercially from Invitrogen. The library is composed of 1.77×10^8 primary clones of *E. coli* with the dodecamer peptide sequence inserted within the Thioredoxin (TrxA) active site loop. The TrxA peptide fusion is cloned into the nonessential domain of the major bacterial flagellin protein (FliC) under control of a P_L promoter from bacteriophage λ . When induced, the peptide sequence is expressed on the surface of the *E. coli* flagella with the N- and C- terminal ends constrained by a disulfide bond. Greater than 90% of peptide fusions are generally assembled into functional flagella where they can represent up to 20% of total cellular protein¹⁰ (see Fig. 1).

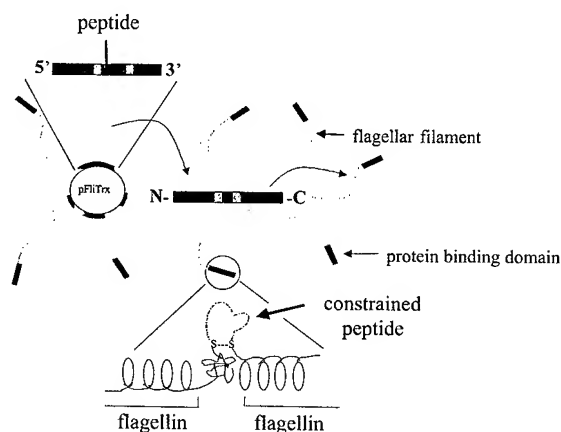


Fig. 1. Schematic of peptide library construction and display

Antigens and Antibodies. The library was screened against two complementary antigen-antibody targets. The two antigens – whole ricin and SEB toxins were obtained from Sigma Chemical Company. The monoclonal antibodies to ricin and SEB were provided by Dr. Peter Emanuel of the ECBC.

Cell culture and library expression. Two mls of the stock FliTrx library was added to IMC medium containing 100 ug/ml carboxycillin and grown by shaking at 25 °C for 15 hrs. Expression of the peptide fusion was then induced by adding approximately 1×10^{10} cells to IMC media containing carboxycillin and 100 ug/ml tryptophan and shaken at 25 °C for 6 hrs.

Reagent Immobilization. The target antigen or antibody was diluted to 20 ug/ml in sterile water and adsorbed onto 60 mm tissue culture plates (Nunc, Delta) by gentle agitation at 50 rpm for 1 hr. The plates were rinsed with 10 ml sterile water followed by gentle agitation for 1 hr with a blocking solution containing 100 ug/ml carboxycillin, 1% non-fat dry milk, 150 mM NaCl and 1% α -methylmannoside.

Panning. After decanting the blocking solution, 10 ml of the induced cell culture in media containing 1% nonfat dry milk, 150 mM NaCl and 1% α -methylmannoside was added to the culture plates, the plates gently agitated at 50 rpm for 1 min followed by 1 hr of incubation with no agitation. The cell media was then decanted and the plate gently washed X5 with IMC media. Cells bound to the plate were eluted into 10 mls fresh culture media by placing the plate on a vortex to shear the flagella and release the cells to the media. The cells were then cultured overnight and the complete procedure repeated for five rounds of panning.

ELISA. 100 μ l phosphate buffered saline (PBS) containing 1 μ g/ml of the antigen or antibody target ligands was added to microtiter plates and incubated overnight at 4 °C. A blocking solution of PBS /0.5% BSA was added, the plates incubated at room temperature for 1 hr and then washed X3 with PBS/0.025% Tween - 20. $10^9 - 10^{10}$ bacterial cells in 100 μ l assay buffer (PBS/0.25%BSA/ .05% Tween-20) was added to each well and incubated for 1 hr at 25 °C. The wells were then rinsed X3 with the assay buffer, followed by the addition of 100 μ l of Anti-Thio antibody (Invitrogen) at 1:5000 dilution and incubation at 25 °C for 30 min. The wells were then rinsed with buffer X3 and 100 μ l of horseradish peroxidase – labeled (HRP) anti-rabbit IgG (Pharmacia Biotech) added and allowed to incubate for 30 min at 25 °C. The plates were washed X3 before adding 100 μ l of substrate solution ABTS to the wells for 10 min at room temperature. Absorbance at 405 nm was measured in a microplate reader. For competitive ELISA, antigen or antibody ligands were added to compete with the binding of the peptide clones.

DNA isolation and sequencing of positive clones. After the fifth round of panning, culture and peptide induction, cells were streaked onto RMG coated plates and incubated overnight at 37 °C. Individual clones that tested positive in the ELISA were selected and amplified at 30 °C for 16 hrs with shaking. Plasmid DNA was isolated using the S.N.A.P Miniprep Kit. The plasmids were sequenced by the Biopolymer Laboratory at the University of Maryland using the FliTrx Forward Sequencing primer supplied by Invitrogen.

RESULTS

SEB Antibody. Figure 2 presents the ELISA results from screening peptide clones against the monoclonal antibody for SEB. Five of the ten clones selected after five rounds of biopanning show an ability to inhibit the binding of SEB to the anti-SEB antibody.

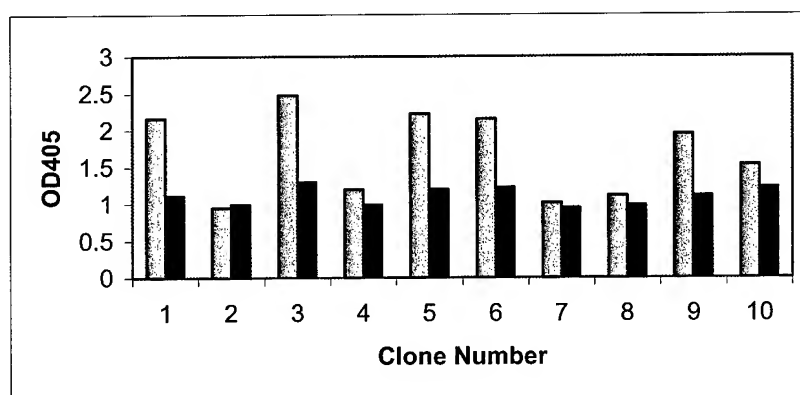


Fig. 2. ELISA selection of peptide clones against the monoclonal antibody to SEB. Non-competitive ELISA results are presented as the shaded bars. Solid bars represent the competitive ELISA where 1 μ g/ml of SEB was added to each well to compete with the binding of the peptide clones.

SEB. Figure 3 shows the ELISA screening results obtained from peptide binding to the SEB toxin. Four of the ten clones show significant interactions with the SEB toxin, as measured by the inhibition of peptide binding in the presence of a monoclonal antibody to SEB.

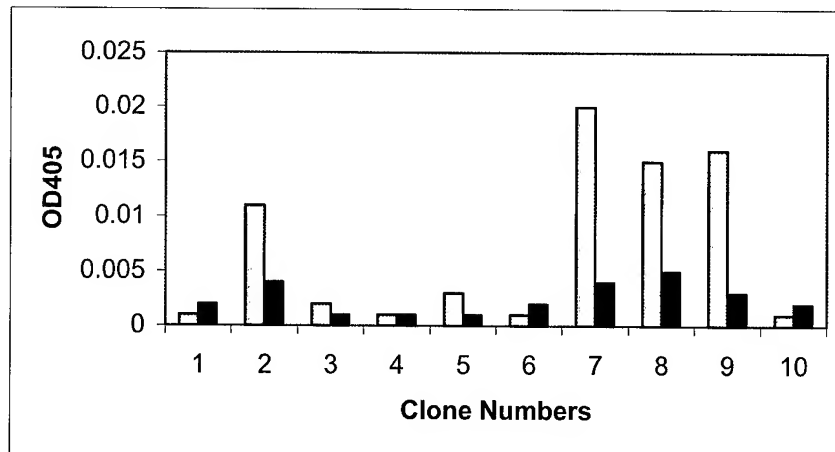


Fig 3. ELISA screening of peptide clones against SEB toxin. Noncompetitive ELISAs are indicated by the shaded bars. Solid bars represent the inhibition of peptide-SEB interaction in the presence of the SEB monoclonal antibody.

Ricin Antibody. The results of panning the peptide library against a monoclonal antibody to ricin are presented in Figure 4. Of ten clones selected after by five rounds of biopanning against the target antibody, four of the ten show significant activity in the ELISA screen to indicate specific interactions with ricin.

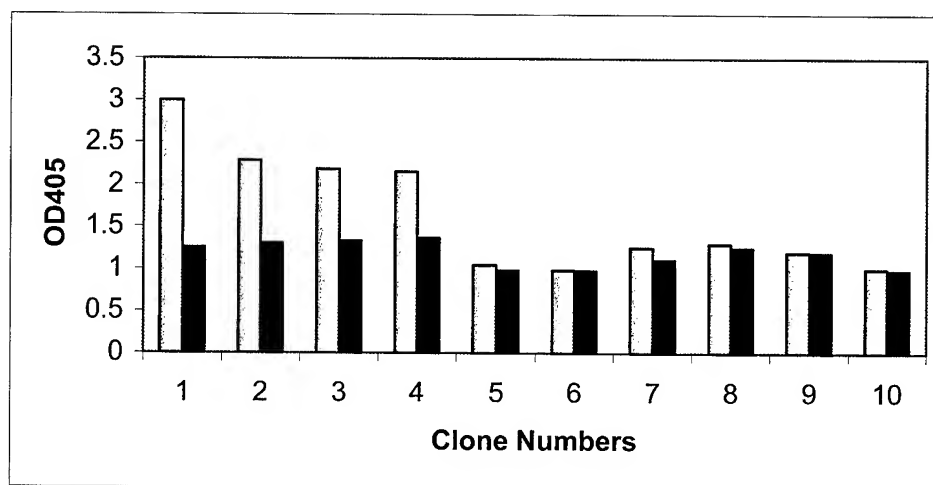


Fig. 4. ELISA screening of peptide clones against a monoclonal antibody to whole ricin. Shaded bars represent the direct binding of peptides to the antibody. Solid bars represent peptide binding to the antibody in the presence of whole ricin.

Whole Ricin. Figure 5 shows the ELISA results obtained from peptide clones panned against whole ricin. Four of the ten peptide clones show significant activity in inhibiting the binding between ricin and a monoclonal antibody.

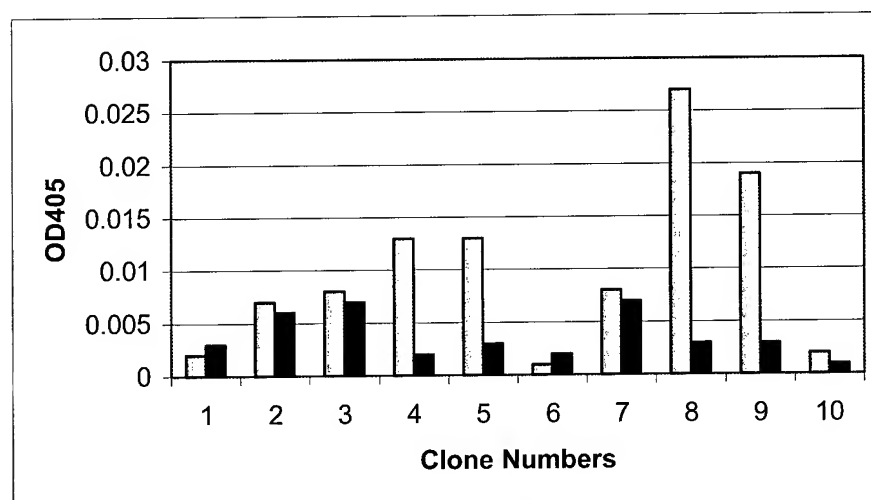


Fig. 5. ELISA results from screening peptide clones against whole ricin. Shaded bars indicate peptide binding to ricin. Solid bars indicate peptide binding to ricin in the presence of 1 µg ricin monoclonal antibody.

The peptide sequences of clones that showed specific inhibition of ligand binding in the ELISA assay are presented in Table 1.

TABLE 1. Peptide sequences derived from DNA of positive clones

Target	Ligand	Clone#	Amino Acid Sequence
SEB		2	ser-val-gly-ala-gly-ala*-arg-cys-val-val
		7	ser-arg-leu-val-arg-gly-val-arg-gly-leu-ser-try
		8	ala-cys-tyr-ser-asp-phe-gly-phe-ser-phe-ala-try
		9	thr-val-iso-cys-met-ala-leu-leu-leu-arg-gly-phe
SEB _{AB}			iso-ser-pro-ala-gln-tyr-arg-pro-iso-leu-leu
Ricin		4	asp-asp-leu-val-val-gln-ser-arg-val-leu-arg
		5	met-thr*-arg-leu-leu-cys-arl-val-leu-arg
		8	glu-val-ser-ser-gly-gly-ala-thr-gly-ser-gly
		9	arg-val-thr-arg-asp-glu-arg*-val-phe-val-ser
Ricin _{AB}		1	met-asp-arg-val-val-gly-val-ser-arg-leu-val
		2	met-arg-phe-ala-gly-arg-arg-leu-ala-arg-phe
		3	asp-phe-val-iso-asp-arg-met-cys-arg-arg-leu
		4	leu-glu-leu-gly-leu-val*-iso-glu-gly-val

Discussion

We have screened a 12 mer random peptide display library for binding to the toxigenic antigens SEB and whole ricin to identify peptide sequences that may be used to replace the use of whole antibodies in various point detection platforms. We have also screened the library against monoclonal antibodies specific for SEB and ricin to identify peptide sequences that may mimic the epitope binding site on the antigens. From the results obtained to date, we have identified up to four peptide sequences for each target that are candidates for further analysis.

None of the isolated peptide clones that show competitive inhibition in the ELISA for a given target ligand evidence a common homology in their amino acid residue sequence. This finding is usually interpreted to indicate that the peptides are either binding to different structural motifs of the target, or that the binding site of the target exhibits a discontinuous epitope that can be recognized by a variety of peptide sequences. The absence of sequence homology is not unexpected. One would expect multiple peptide binding sites to be present on large protein toxins as well as whole antibody molecules, based on their composition from multiple subunits. Ricin, for example, is composed of two structurally and functionally distinct subunits while an IgG antibody is composed of four distinct subunits.

One needs to consider whether the use of FLITRx peptide library, expressed on the flagella of *E. coli* bacteria, may be less efficient for identifying positive clones compared to the procedures using the much smaller phage expression vectors. The *E. coli* bacterium is orders of magnitude larger than phage and may impose certain physical restraints on the peptide gaining access and binding tightly enough to the targeted epitope so as not to be washed away during any of the rinse stages. One would predict from this scenario that the FLITRx library would require more rounds of successive panning against the target ligand to gain the same enrichment of positive clones in the final culture as that reported for the smaller phage vectors. We performed five successive rounds of selection and amplification compared to the average of three rounds performed with phage. It is possible that a consensus sequence in positive clones would appear if more than ten colonies had been selected from the final plated culture, though it is just as probable- given multiple epitopes on the whole toxins and antibodies- that we would identify even more unique sequences.

Further discrimination between which structural motif the peptides are binding to, and their degree of specificity for a single site will require screening the positive clones against smaller fragments of the target molecule. We have begun to undertake these studies as well as having the peptide sequences synthesized to enable specific peptide-ligand binding studies to measure binding affinity and cross-reactivity with other epitopes.

CONCLUSIONS

Screening a randomly displayed peptide library against toxin and antibody target ligands has identified a number of unique peptide sequences that can be further analyzed for their ability to specifically bind to a single epitope on the ligand. The peptide sequences derived from panning the library against the SEB and ricin toxins will be further tested on their ability to mimic the specificity and affinity of SEB and ricin antibodies for binding to their respective target, and their ability to substitute for antibodies as the critical molecular recognition element in various biodetection platforms. The peptide sequences derived from panning the library against SEB and ricin antibodies will be further tested for their ability to act as effective antigenic epitopes in replacing the use of actual toxins as positive controls for validating assay specificity and sensitivity.

REFERENCES

1. Winter, G. and C. Milstein. 1991. *Nature*, 349: 293-299.
2. Smith, G.P. 1985. *Science*, 228:1315-1317.
3. Parmley, S.F. and G.P. Smith. 1988. *Gene*, 73: 305-308
4. Krebber, C., S. Spada, D. Desplancq and A. Pluckthun. 1995. *FEBS Letters*, 377: 227-231.
5. Davies, J. and L. Riechmann. 1995. *FEBS Letters*, 339: 285-290.
6. Devlin, J.J., L.C. Pangariban and P.E. Devlin. 1990. *Science*, 249:404-406.
7. Davies, J. and L. Riechmann. 1995. *Bio/Technology*, 13: 475-479.
8. Horwell, D.C. 1995. *TIBTech*, 13:
9. Luzzago, A., F. Felicir, A. Tramanteno, A. Pessi and R. Cortese. 1993. *Gene*, 128: 51-57.
10. Lu, A., K.S. Murray, V. VanCleave, E.R. LaVallie, M.L. Stahl and J.M. McCoy. 1995. *Bio/Technology* 13: 366-372.

RAPTOR: A PORTABLE, AUTOMATED BIOSENSOR

George P. Anderson*, Chris A. Rowe-Taitt, and Frances S. Ligler

Center for Bio/Molecular Science and Engineering,
Naval Research Laboratory, Washington DC 20375

The RAPTOR is a portable automated fiber optic biosensor for detection of biological threat agents. It performs rapid (3 to 10 minute), fluorescent sandwich immunoassays on the surface of short polystyrene optical probes for up to four target analytes simultaneously. The optical probes can be reused up to forty times, or until a positive result is obtained, reducing the logistical burden for field operations. Numerous assays for toxins, such as SEB and ricin, and bacteria, such as *Bacillus anthracis* and *Francisella tularensis*, have been developed. Research International has commercialized the RAPTOR, and development of a second-generation instrument, sponsored by the US Marine Corps, is now in progress.

INTRODUCTION

The fiber optic biosensor has developed over the last decade from a single channel laboratory breadboard into a portable, automated 4-channel sensor.¹⁻⁷ While the optical, electronic, and mechanical workings have evolved significantly, the assay methodology has remained essentially the same, consisting of a sandwich fluoroimmunoassay. Capture antibodies are immobilized onto the surface of an optical fiber. When sample flows over the fiber probes, immobilized antibody captures any analyte present. The amount of analyte bound is determined by a later step where the binding of a fluorescent tracer antibody to the bound analyte forms a fluorescent complex or "sandwich". The biosensor monitors this complex formation by evanescently exciting surface-bound fluorophores with a diode laser. The optical probe captures a portion of the emitted fluorescence, which returns back up the fiber to the photodiode detector. Since the excitation intensity and efficiency of fluorescence recovery falls exponentially with distance from the fiber probe surface, the system is highly discriminatory for the surface bound fluorophores.⁸

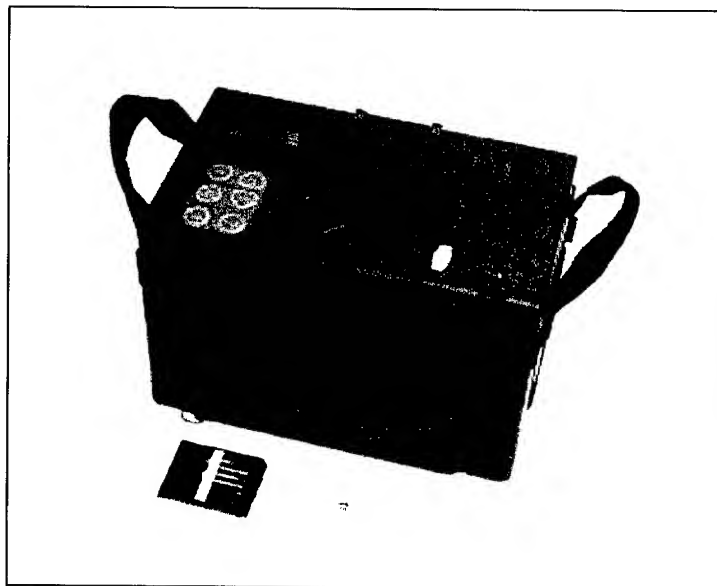


Figure 1. RAPTOR Fiber Optic Biosensor

The RAPTOR (Figure 1) is the only fiber optic biosensor commercially available (Research International, Woodinville, WA) that is designed to withstand the rigors of

*Correspondence: Email: ganderson@cbmse.nrl.navy.mil; Telephone: 202 404 6033; Fax 202 767 9594

field-testing. The system employs a separate 635 nm diode laser to excite each of the four fiber optic probes. To match this excitation wavelength, the fluorescent dye Cy5 is used to tag the tracer antibody. Since the sensor performs a two-step sandwich assay, fluorescent tracer reagent is not contaminated by sample and negligible signals are obtained from optical probes when negative samples are analyzed. Hence, both the fiber probes and fluorescent reagent can be reused until a positive is obtained. This makes the RAPTOR ideal for continuous monitoring applications. If a positive sample is detected, the user need only replace the coupon which holds the four capture antibody-coated optical probes. The optical probes are injection-molded polystyrene, which permits inexpensive mass production. These probes are easily coated with antibody by passive adsorption, over-coated with a stabilizing solution, and dried while being glued into the coupon, thereby providing an extended shelf life. Each coupon is marked with a bar code that tells the sensor the appropriate assay protocol and the identity of the antibody on each of the probes. To use, the coupon is inserted into the holder on the RAPTOR, and sample and reagents are introduced through blunt tipped needles, which connect to the coupon upon closure of the top door. From its initial design, the RAPTOR was made to be field hardened and very simple to use, even for an operator with no technical background. It can be battery operated and accepts samples introduced either manually or automatically from an attached air particle collector.

Data analysis is also completely automated, which removes any subjective bias of the user. After the data are collected and analyzed using preloaded software, with user modifiable settings, the results are displayed on the LCD screen of the instrument in a simple display specifying the assays performed and the instrument's assessment of the results. While the results are displayed in a qualitative, easy-to-read format (negative, suspect, positive, high positive), quantitative data can be downloaded through a serial port to a computer for further analysis.

The RAPTOR and the fiber optic biosensors from which it evolved have been used to detect and quantify a variety of hazardous substances in numerous sample matrices; this work includes detection of explosives,⁹⁻¹¹ toxins,^{6,7,12-14} bacteria,^{6,7,13,15,16} and viruses,^{6,7} in ground water,¹⁰ soil extracts,¹¹ air extracts,¹⁶ meat homogenates,^{12,13} and clinical fluids.^{15,17} A summary of the limit of detections for several different analytes is shown in Table 1.

TABLE 1. Limits of detection for toxins and pathogens using a 10-minute assay performed with RAPTOR

Hazard	Type	Limit of Detection
Staphylococcal enterotoxin B (SEB)	Toxin	1 ng/ml
Ricin	Toxin	10 ng/ml
Cholera toxin	Toxin	1 ng/ml
<i>Yersinia pestis</i> F1	Bacterial surface protein	10 ng/ml
<i>Bacillus anthracis</i>	Gram positive bacterium (vegetative form)	50 cfu/ml
<i>Bacillus globigii</i>	Gram positive bacterium (spore)	5 x 10 ⁴ spores/ml
<i>Brucella abortus</i>	Gram negative bacterium	7 x 10 ⁴ cfu/ml
<i>Francisella tularensis</i>	Gram negative bacterium	5 x 10 ⁴ cfu/ml
<i>Giardia lamblia</i>	Protozoan cysts	3 x 10 ⁴ cysts/ml

EXPERIMENTAL

Buffers and Reagents

Anti-*Giardia* antibody (Mab 7D2 ascites) and antigen were provided by Dr. Ted Nash (NIH, Bethesda, MD).¹⁹ Mab 7D2 IgG was purified using MEP-HyperCel (Life Technologies). Additional anti-*Giardia* antibody (Mab AG1 and Cy5-labeled AG1) was purchased from Waterborne, Inc. (New Orleans, LA). The anti-cholera toxin IgG was purchased from Biogenesis (Brentwood, NH); cholera toxin antigen was purchased from Calbiochem (La Jolla, CA). Ricin, ovalbumin, *B. anthracis* Sterne strain, *F. tularensis* LVS and all antibodies directed against these antigens were provided by Naval Medical Research Command, Silver Spring, MD. Affinity-purified sheep anti-SEB IgG and SEB antigen were purchased from Toxin Technology (Sarasota, FL). RAPTOR wash buffer consisted of phosphate buffer (Sigma, 8.3 mM, pH 7.3) containing 0.05% (v/v) Triton X-100 (TX-100) and 0.01% (w/v) sodium azide (PBT). Casein and bovine serum albumin (BSA) were purchased from Sigma (St. Louis, MO).

Probe and Coupon Preparation

Capture antibodies were immobilized onto fiber optic probes by passive adsorption. Injection-molded, polystyrene fiber optic probes (Research International) were first blackened at their distal ends to prevent reflection of excitation light. Probes were then placed into capillary tubes (100 μ l, cut to 4 cm length) pre-filled with 36 μ l of the appropriate antibody solution, in general, 100 μ g/ml IgG in 0.1 M sodium carbonate buffer (pH 9.6). After overnight incubation at 4°C, unbound IgG was rinsed off the probes by brief immersion in dH₂O, and the probes were incubated for 15-30 minutes in immunoassay stabilizer solution (ABI, Columbia, MD). The probes were then mounted and glued into the disposable coupons (Figure 2), as described in detail previously.¹⁴

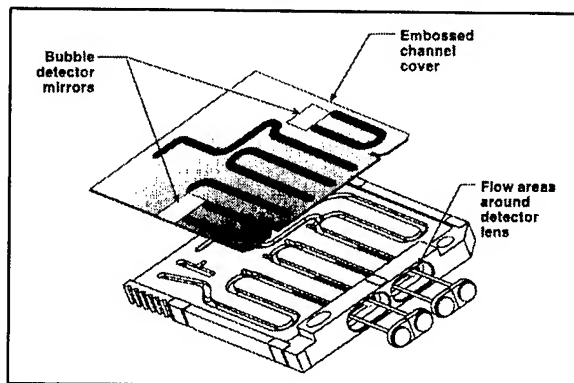


Figure 2. Schematic of assay coupon showing four fiber optic probes, adhesive channel cover and bubble detector mirrors.

Preparation of Cy5-labeled Antibodies

Cy5-conjugated antibodies were prepared by reacting 3 mg of protein (1 mg/ml) in 50 mM sodium tetraborate, 40 mM NaCl, pH 9.0 with one vial bisfunctional Cy5-reactive dye (Amersham Life Science Products, Arlington Heights, IL) for 30 minutes at room temperature in the dark. Subsequently, labeled protein was separated from unincorporated dye by size-exclusion chromatography. Dye to protein ratios ranged from 2 to 4 Cy5 molecules per IgG.

RAPTOR Design and Operation

Insertion of the assay coupon into the RAPTOR coupon compartment aligns all necessary optical paths and engages all fluidic connections required for sample analysis. A pneumatic pump moves buffer, air, fluorescent reagent (from on-board reservoirs), or sample within the system. Serpentine channels in the coupon provide a common path across the probe surfaces. Bubble detectors, which monitor liquid-to-air interfaces, control introduction of sample and fluorescent reagent (Figure 2).

During the two-step sandwich immunoassay, sample is flowed over the four fiber optic probes mounted in the assay coupon. Antigen present in the sample binds to the fiber optic probe coated with

capture antibody specific for that antigen; unbound material is washed away by a brief rinse with PBT. Fluorescently labeled antibody is next introduced and binds to the antibody-antigen complexes on the probe surface, completing the sandwich assay. This tracer reagent is maintained at a suitable temperature in an onboard thermal storage module and recovered after each assay cycle, allowing multiple sequential analyses to be performed. Excitation light from four 5 mW Sanyo laser diodes (635 nm) within the RAPTOR is focused into the fiber optic waveguides. An evanescent wave is created along each probe, exciting the fluorescent emission of specifically bound Cy5-labeled antibodies. The portion of the fluorescence captured by the optical probe is collimated by the probe's molded lens and focused onto a photodiode using a ball lens, chosen for its light-gathering power and short focal length (Figure 3). A long-pass dichroic filter (665 nm) rejects reflected laser light. If each fiber optic probe has been coated with capture antibodies with differing specificities, one sample is interrogated for four different analytes simultaneously.

Assay Procedure

Each assay consists of multiple steps, which are performed automatically by the RAPTOR. Immediately after loading the coupon into the instrument, prior to analyte challenge, the RAPTOR automatically initiates a five-minute baseline protocol. The probes are briefly rinsed with PBT (for hydration), and are then incubated for 90 seconds with fluorescent tracer antibody. After tracer reagent is returned to its compartment, the probes are rinsed with PBT and an initial background wash value is determined. This background rate represents the rate of nonspecific binding of the fluorescent antibody to the probe surface and must be determined before samples are analyzed.

To analyze a sample, it is first loaded into the sample port using a 1 ml syringe equipped with a blunt-tipped needle or a transfer pipette. After the coupon is rinsed briefly with PBT, the sample is flowed into the coupon and is incubated with the probes for a seven minutes. A subsequent wash with PBT eliminates unbound material; the RAPTOR automatically flushes the sample port with PBT at the same time as the PBT wash, thus preventing sample carryover. Next, the coupon is cleared with air to prevent dilution of the incoming tracer reagent. Cy5-antibody reagent is flowed into the coupon and incubated for 90 s to interrogate the amount of antigen bound to the probes. The tracer reagent is returned to its reservoir for reuse and a final PBT wash completed. The entire standard assay cycle, including all wash steps, is completed in ten minutes.

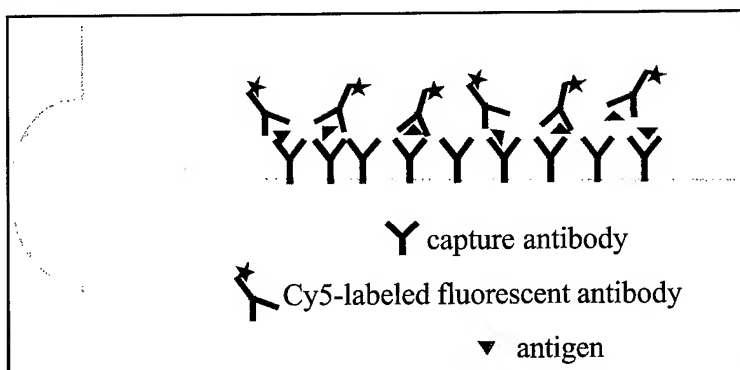


Figure 3. Schematic of optical probe and immunoassay

The rate of fluorescence increase during incubation with the Cy5-antibody is calculated ("assay rate"), and a final reading is taken to determine the increase in fluorescence due to Cy5-antibody bound during the entire assay cycle ("wash delta"). While one parameter is sufficient for strongly positive samples, use of both factors greatly reduces the number of false positives obtained.^{6,7} Assay data are stored by the RAPTOR and can be downloaded through a serial port for quantitative analysis. Samples are considered positive if the both values are greater than the means of the background values plus three standard deviations.

RESULTS

The RAPTOR has been used to detect a number of different toxins and pathogens. In a recent trial, we set up coupons of two different types: a pathogen coupon, which tested for *B. anthracis*, *Giardia*, and *F. tularensis*, and a toxin coupon, which tested for ricin, cholera toxin, and SEB. In addition to the agent-specific probes, each coupon also contained a positive control probe coated with an anti-ovalbumin IgG. The control probe was utilized to check the activity of the coupon and tracer reagent prior to sample testing and again at the completion of a series of tests to confirm that both the probe and tracer reagent retained their activity.

To test that pathogen and control assays (ovalbumin, *B. anthracis*, *F. tularensis*, and *Giardia*) were compatible for use in a single assay coupon, 10 µg/ml of each Cy-5 labeled tracer antibody (40 µg/ml total) was mixed and placed in the reagent bag. This fluorescent reagent cocktail was then used in assays performed with multi-analyte coupons housing one fiber directed against each of the above analytes. To ensure that all components of the system were functional, a control containing a low concentration of ovalbumin was analyzed at the beginning of each trial. An additional

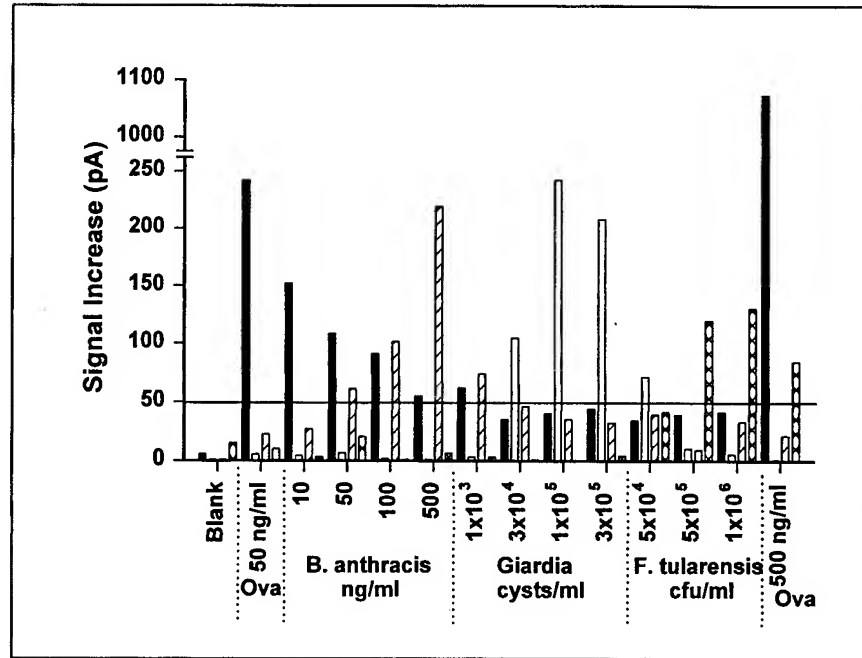


Figure 4. Dose response curve for each analyte on the pathogen coupon assay set. The signal increase obtained after being challenged with increasing amounts of each analyte is shown for each probe. Ovalbumin: solid, Giardia: open, *B. anthracis*: hatched, *F. tularensis*: cross-hatched.

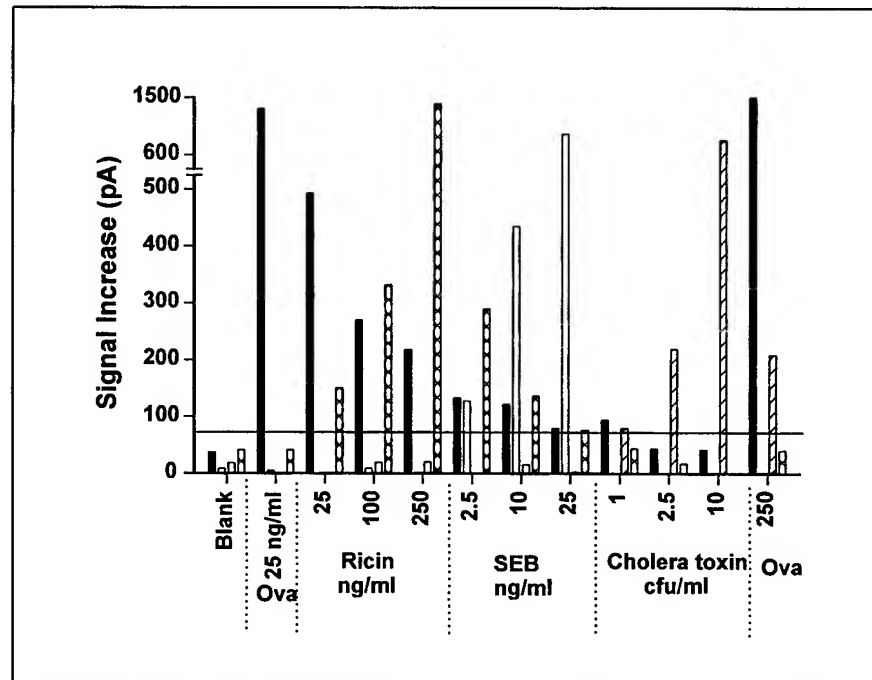


Figure 5. Dose response curve for each analyte on the toxin coupon assay set. The signal increase obtained after being challenged with increasing amounts of each analyte is shown for each probe. Ovalbumin: solid, Cholera toxin: hatched, SEB: open, Ricin: cross-hatched.

ovalbumin control was included at the end of each trial as a final test to gauge coupon and reagent activity. Each of the other analytes was tested sequentially and a dose response curve for each determined (Figure 4). For each analyte, both the wash delta (shown in Figure 4) and the assay rate remained above background levels (>0) during subsequent analyses, even in the absence of additional analyte. These results indicated that the surface-bound capture antibody: antigen complexes were not saturated with tracer antibody until after several additional incubations with tracer antibody (cocktail). The magnitude of this effect may vary depending on tracer affinity and avidity, the number of binding sites on the antigen, and reaction kinetics. However, since coupons would normally be used only until the first positive is achieved, the lack of saturation does not present a problem for field-testing.

An analogous experiment was carried out using the toxin coupon, which contained probes specific for ricin, SEB, cholera toxin, and an anti-ovalbumin IgG control probe. As was seen for the pathogen coupon the control probe for ovalbumin gave strong positive responses at both the beginning and end of the trial (Figure 5). Then each target was tested at concentrations near the predetermined limits of detection (Table 1) and a dose-response curve for each determined.

For both the pathogen coupon and the toxin coupon, no significant cross reactivity was observed at the concentrations tested. As the concentration of analyte increased the response for the probe specific for that analyte increased. Had the concentration of analyte been increased further the signal would continue to rise. Signals can go to as high as 20,000 pAmps, before the instrument's range is exceeded. This is observed best with the toxin assays, as the pathogen/bacterial assays do not generally result in such large signals. This large range permits a good dynamic range for each assay, from ng/ml to μ g/ml. Even if a sample were introduced at a huge excess it would not cause a problem; since the assay is a two-step process, no hook effect will occur.

At the completion of the assay validation, fifty coupons of each type and thirty vials of lyophilized reagent were prepared. These materials, along with two RAPTORs, are now in the field to provide an enhanced threat detection capability and produce data on long-term system and assay endurance.

CONCLUSIONS

The RAPTOR fiber optic biosensor is well suited for testing for pathogens and toxins and can be used as an in-line monitor or to analyze discrete samples. Only minimal sample preparation (e.g. dilution or coarse filtration) is required. Disposable coupons can be made with optimum assay combinations, allowing multiple samples to be analyzed for multiple pathogens without changing probes or reagents. Assay procedures and data analyses are both fully automated, but can be modified by the user to fit the user's specifications. Furthermore, antibody-coated probes and fluorescent reagents can be stored for over 1 year. The RAPTOR is portable (12 lb) and can be operated on batteries for use in the field. The assays are fast (3-10 min assays) and sensitive (limits of detection = 1-10 ng/ml, 50-5000 cfu/ml, depending on the antibody:analyte combinations). The second-generation device, which will be available in late 2000, will utilize custom-built peristaltic pumps instead of pneumatic pressure for liquid movement. It is expected that this change, along with other improvements, will increase both RAPTOR's sensitivity and reliability for field operation.

ACKNOWLEDGEMENTS

This work was funded in part by the Office of Naval Research and by the U.S. Marine Corps. The views expressed here are those of the authors and do not represent the opinions of the U.S. Navy, the U.S. Department of Defense, or the U.S. Government.

REFERENCES

1. TB Hirschfeld and MJ Block, "Fluorescent immunoassay employing optical fiber in capillary tube," US Patent 4,447,546, 1984.
2. J.D Andrade and R Vanwagenen, "Process for conducting fluorescence immunoassays without added labels and employing attenuated internal reflection," US Patent 4,368,047, 1983.
3. BJ Tromberg, MJ Sepaniak, T Vo-Dinh, and GD Griffin, "Fiber-optic chemical sensors for competitive binding fluoroimmunoassay," *Anal. Chem.* **59**, pp. 1225-1230, 1987.
4. BI Bluestein, M Craig, R Slovacek, L Stundtner, C Urciuoli, I Walczak, and A Luderer, "Evanescent wave immunosensors for clinical diagnostics." In: *Biosensors with Fiberoptics*, (DL Wise and LB Wingard, Jr., eds.) pp. 181-223 Humana Press, NJ, 1991.
5. FS Ligler, JP Golden, LC Shriver-Lake, RA Ogert, D Wijesuria and GP Anderson, "Fiber-optic biosensor for the detection of hazardous materials," *Immunomethods*, **3**, pp. 122-127, 1993.
6. GP Anderson, KD King, KL Gaffney, and LH Johnson, "Multianalyte detection using the fiber optic biosensor," *Biosensors & Bioelectronics*, **14**, pp. 771-777, 2000.
7. KD King, JM Vanniere, JL LeBlanc, KE Bullock, and G.P. Anderson, "Automated fiber optic biosensor for multiplexed immunoassays," *Environ. Sci. & Tech.* **34**, pp. 2845-2850, 2000.
8. GP Anderson, JP Golden, and FS Ligler, "An evanescent wave biosensor – fluorescent signal acquisition from step-etched fiber optic probes" *IEEE Transactions on Biomedical Engineering*, **41**, pp. 578-584, 1994.
9. IB Bakaltcheva, FS Ligler, CH Patterson, and LC Shriver-Lake, "Multi-analyte explosive detection using a fiber optic biosensor," *Anal. Chim. Acta*, **399**, pp. 13-30, 1999.
10. SK Van Bergen, IB Bakaltcheva, JS Lundgren, and LC Shriver-Lake, "On-site detection of Explosives in groundwater with a fiber optic biosensor," *Environ. Sci. & Tech.* **34**, pp. 704-708, 2000.
11. LC Shriver-Lake, C.H. Patterson, and S.K. van Bergen, "New Horizons: Explosive detection in soils with a fiber optic biosensor," *Field Anal. Chem. Tech.* In press. 2000.
12. LA Tempelman, KD King, GP Anderson, and FS Ligler, "Quantitating staphylococcal enterotoxin B in diverse media using a portable fiber optic biosensor," *Anal. Biochem.* **223**, pp. 50-57, 1996.
13. DR DeMarco, EW Saaski, DA McCrae, and DM Lim, "Rapid detection of *Escherichia coli* O157:H7 in ground beef using a fiber-optic biosensor," *J. of Food Protection*, **62**, pp. 711-716. 1999.
14. KD King, GP Anderson, KE Bullock, MJ Regina, EW Saaski, and FS Ligler, "Detecting staphylococcal enterotoxin B using an automated fiber optic biosensor," *Biosensors & Bioelectronics*, **14**, pp. 163-170. 1999.
15. LK Cao, GP Anderson, FS Ligler, and J Ezzell, "Detection of *Yersinia pestis* F1 antigen by a fiber optic biosensor," *J. Clin. Micro.* **33**, pp. 336-341, 1995.
16. FS Ligler, GP Anderson, PT Davidson, RJ Foch, JT Ives, KD King, G Page, DA Stenger, and JP Whelan, "Remote sensing using an airborne biosensor," *Environ. Sci. & Tech.* **32**, pp. 2461-2466, 1998.
17. GP Anderson, KD King, LK Cao, M Jacoby, FS Ligler, and J Ezzell, "Quantifying serum anti-plague antibody using a fiber optic biosensor," *Clin. Diag. Lab. Imm.* **5**, pp. 609-612, 1998.
18. RD Adam, "The biology of *Giardia* spp." *Microbiol. Rev.* **55**, pp. 706-732, 1991.
19. JH Boone, JH, TD Wilkins, TE Nash, JE Brandon, EA Macias, RC Jerris, and DM Lyerly, "TechLab and Alexon *Giardia* enzyme-linked immunosorbent assay kits detect cyst wall protein" *J. Clin. Micro.* **37**, pp. 611-614, 1999.

DEMONSTRATION OF A RAPID, PORTABLE EVANESCENT WAVE BIOLOGICAL AGENT IDENTIFIER

Stephen J. Krak, Anthony A. Boiarski¹, Richard L. Hall, and Herbert S. Bresler

Battelle Memorial Institute
505 King Avenue
Columbus, Ohio, 43201, USA
¹ BioSense Consulting

Evanescent wave technology remains one of the leading contenders for rapid, automated, portable biological agent sensing and monitoring applications. This technology offers sensitivity and logistical benefits including the ability to eliminate wash steps and reuse the sensor surface after negative test results. We report on progress of an evanescent wave biological agent identifier for the US Marine Corps' Small Unit Biological Detector (SUBD). Efforts have so far focused on Bidiffractive Grating sensor technology initially developed by Roche Diagnostics. Competitive detection sensitivities have been demonstrated at the Joint Field Trials (JFT5) and third-party blind trials. Since JFT5, the identifier has been radically redesigned to accommodate twelve channels rather than three, to remove all moving parts and to avoid the need for optical alignment.

Introduction

Optical evanescent wave technology has been used to address needs of the biological warfare agent detection community for several years. Optical evanescent field sensing techniques under investigation have included grating couplers [1], waveguide interferometers [2][3], waveguide and fiber optic fluorescence [4], and surface plasmon resonance (SPR) sensors [5]. These approaches propose to leverage the many potential advantages of evanescent wave technology: sensitivity, speed, compactness, ruggedness, and low logistical burden. In this paper, we present the most recent developments in the advancement of the Bidiffractive Grating technology. The design improvements reported here demonstrate advances in multi-analyte measurement capability and ruggedness without compromises in detection sensitivity. The result is a demonstration unit with a new read head, fluidics delivery and software control that represent an important step towards a field-deployable sensor for bioagent detection and identification.

History

The identifier work presented here centers on the Bidiffractive Grating technology adapted from work originally developed by Roche Diagnostics Division in Basel, Switzerland[6][7][8]. The Bidiffractive Grating (BDG) biosensor consists of a mass-producible sensor (waveguide) and an optoelectronic instrument to interrogate the sensor. Immunoassay chemistries are immobilized on the sensor surface using protocols developed by Roche and Battelle.

The first stages of BDG development consisted of building a fluidics delivery system and computer control around a single-channel read head designed by Roche and Zeiss Optics (Jena, Germany). Using this instrument, assays were developed with biological agent simulants and other agents of biological origin (ABO). The results of ABO assay development conducted by the Navy Medical Research Center (NMRC) demonstrated that the BDG approach delivered promising limits of detection, comparable to state-of-the-art immunoassay sensors [9]. Simulant assay development included Ovalbumin (Ova), B.

globigii (BG), MS-2 (bacteriophage) and Erwinia Herbicola (Eh). This work culminated in participation at the 1999 Joint Field Trials (JFT5) and a round of blind trials conducted by NMRC at the request of the program sponsor. These exercises confirmed the promising performances observed in the ABO studies.

While the performance of the BDG approach was acceptable, it also became obvious that the precision laboratory instrument was not amenable to field use. Three channels on a sensor surface were not adequate for multi-analyte detection. As a refractometer, the instrument was also susceptible to other physical phenomena including temperature and pressure. Finally, interrogating multiple channels required mechanical translation and re-alignment for each channel location. Therefore, work began that would lead to a more rugged and fieldable approach, thereby making the resulting instrument a better choice for military applications. As a consequence, the Laboratory Attenuation Identifier (LAI) was designed and built in a very short timeframe. The LAI is a demonstration unit intended for laboratory use and is an important step toward a field-ready instrument. In this paper, we present improvements demonstrated by the LAI over the previous BDG configuration, as well as current performance status and plans for the future.

Approach

For the design of the LAI, three fundamental modifications were made to the previous BDG instrument. An attenuation approach replaced the refractive index measurement previously used. The sensor flow cell configuration was redesigned to accommodate 12 channels rather than three. And the read head optics were redesigned to interrogate all 12 channels simultaneously without the need for mechanical motion. Finally, the LAI was tested to ensure that the limits of detection had not been compromised.

The resulting instrument is a liquid-sample identifier that can simultaneously perform up to 12 immunoassays to detect and identify the presence of biological warfare agents in the sample. A photograph of the system is shown in Figure 1. The major elements of the LAI are the disposable sensor (flow cell assembly), a fluidics system, an optical read head, and software and electronic elements.

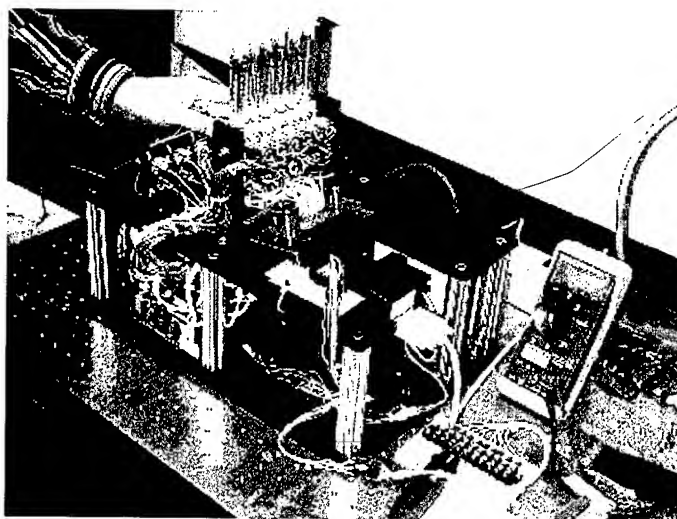


FIGURE 1. Laboratory Attenuation Identifier (LAI).

A schematic diagram of the LAI is provided in Figure 2. As a demonstration unit, the LAI has not been optimized for size, weight, or power consumption. For reference, the present unit dimensions are

16.5" H x 11" W x 11" L, it weighs approximately 40 pounds, and consumes roughly 66 Watts. Recent changes in the fluidics design will reduce these numbers, particularly power consumption, in the very near future. Optimizations planned for future efforts will focus on substantially reducing the size, weight, and power consumption, while further increasing the ruggedness and field-usability of this device.

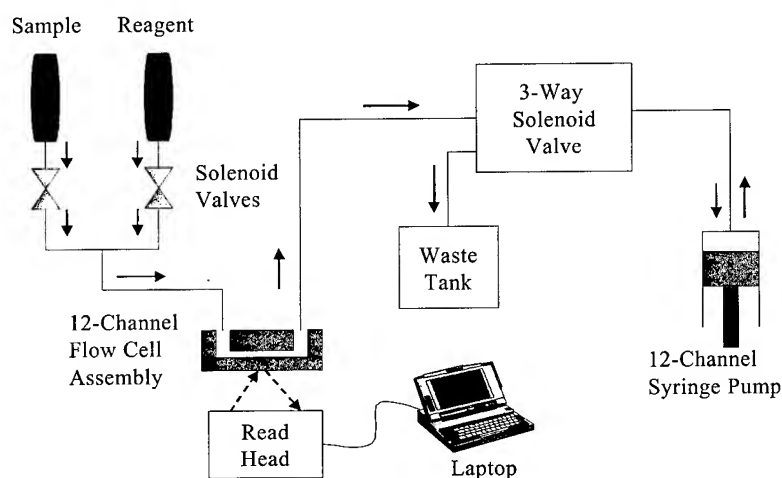


FIGURE 2. LAI functional schematic.

The precise alignment of the waveguide, light source, and signal sensing device required for the LAI is accomplished by an integrated read head subassembly. To perform the desired functions simply and ruggedly in a compact package, the design had to incorporate the ability to simultaneously read 12 channels with no moving parts and require no alignment steps. Finally, it had to contain only solid state electronics and commercially available optics.

The read head that emerged from this work not only meets all of these criteria, but is also rugged, compact, and weighs only 8 pounds. This read head provides a strong foundation for future development of a field-ready identifier based on the LAI operating principles. Figure 3 shows the assembled read head. Optical elements were assembled into four mechanical subassemblies that were precisely connected using a series of interlocking features. These elements allow the read head to be assembled without the need for special alignment tools or procedures.

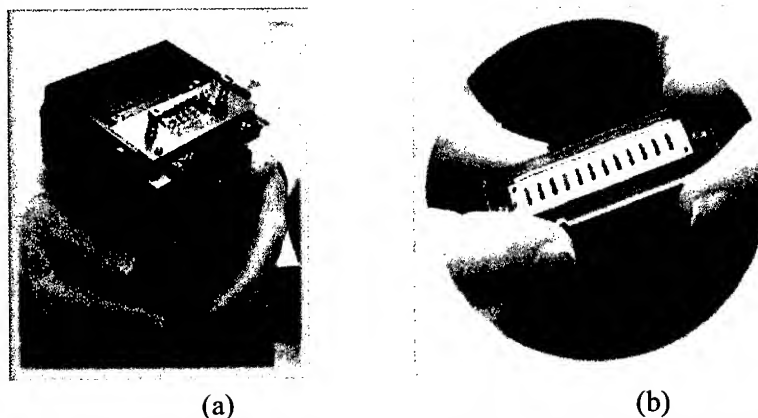


FIGURE 3. Assembled read head (a), and Sensor flow cell assembly (b).

The fluidics interface seen at the top of Figure 3a is a significant improvement to previous BDG designs as well. In the present embodiment, the sensor flow cells assembly in Figure 3b is dropped into a paddle roughly the size of a floppy disk. The handle at the top of Figure 3a is rotated to lift the interface and allow for the paddle to be inserted. The handle is rotated into a locked position, sealing the 24-port interface with the sensor flow cell. No other alignment is required for either fluidics sealing or optical throughput.

This application requires a pump with 12-channels working simultaneously. Early in the development work, we determined that no commercial syringe pumps were suitable for this application based on size, weight, and power considerations. As a result, Battelle developed a compact 12-channel syringe pump specifically for this application (Figure 4). A U.S. Patent application has been filed for this design.

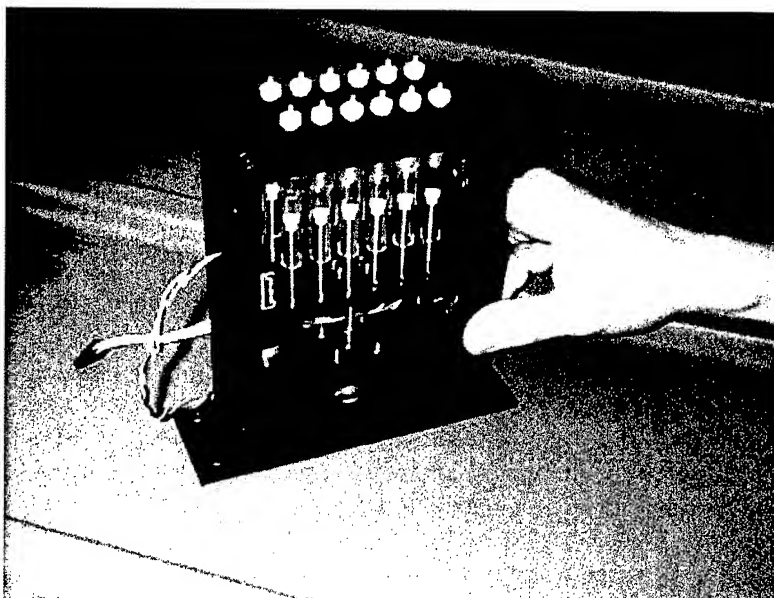


FIGURE 4. 12-Channel syringe pump assembly.

The hardware surrounding the BDG technology has undergone significant design changes for this application. The new design demonstrates that the technology can be applied in a multi-analyte, portable and robust platform.

Performance Evaluation

Performance measurements for the LAI were made using the same chemistry techniques as those used for the BDG-index approach, namely, a sandwich assay including a gold-labeled secondary antibody. However, significant progress has also been made in the area of chemistry development for the BDG technology. The result is a reproducible, covalent chemistry in which immobilized capture antibody can be stored on the sensor surface in a dry state. The surface can be re-hydrated rapidly, and accelerated aging studies on this dry-storage chemistry are producing very promising results.

Only the detail for the Ovalbumin assay will be provided in this paper. Assays for the remaining simulants (BG, MS-2 and Eh) were very similar.

Ovalbumin (Ova) antigen response data were determined for various sample concentrations ranging from 1 to 100 ng/mL. Extensive blank response measurements (plain buffer – 0 ng/mL) were also obtained to determine the assay cut-off (CO) value, where:

$$\text{CO} = \text{Mean of Blank Responses} + 2 \times (\text{Standard Deviation of Blank Responses}) \quad (1)$$

A typical attenuation versus time plot, obtained during the Ovalbumin testing, is shown in Figure 5, where det Ab OD = 3. Figure 5a shows the results of a two-step assay, blank sample test (i.e., Ovalbumin concentration = 0) for the first four flow-cell channels. Figures 5b and 5c are attenuation versus time plots for 10 and 100 ng/mL of Ovalbumin respectively. In this case, the 10 ng/mL Ova sample was flowed through flow cell channels five through eight, and the 100 ng/mL Ova sample was flowed through channels nine through twelve. Using this multi-channel flow approach, at least four replicate measurements were simultaneously obtained for a given Ova concentration.

In these figures, the first 650 seconds of read head output is for Step 1 of the two-step sandwich assay (sample flowing through flow cell for 10 minutes). No attenuation should occur during this first step. From 650 seconds to 885 seconds, the second assay step is performed where detector antibody is introduced into the flow cells for a 3-minute period. For the blank sample (0 ng/mL in Figure 5a, we expect no change in signal for Step 2. For a positive sample (non zero antigen concentration) we expected and measured an increased amount of attenuation with time as gold-labeled detector antibody binds to the capture antigen. As shown in Figures 5b and 5c, the slope, S_2 , of the output during this second step increases with antigen concentration level.

Note that the slope, S_2 , moderates with time, indicating the onset of saturation. For this reason we used the initial slope in our analysis algorithm. The attenuation response is determined from Figure 5 using the following equation:

$$\text{Response} = S_2 - S_1, \quad (2)$$

which is the difference in slope of the output signal that occurs following the addition of the detector antibody (see Figure 5c).

Results

The LAI performance compared well to the BDG index approach. As in the last section, detailed analysis will be shown only for the Ovalbumin assay. Other simulants having been analyzed in a like manner. Finally, a table showing limits of detection for all simulants will be discussed.

Using the blank data from channels 1 – 4 described above and other blank response determinations, the mean blank response was equal to 0.03 %/min (theory = 0). The standard deviation in blank response was, however, equal to 0.76 %/min. The cut-off for these tests, calculated using Equation (1), is $\text{CO} = 1.56$. This cut-off value was later reduced to less than 0.8 %/min by equipment modifications.

The mean response and standard deviation were also calculated for channels 5 – 8 (10 ng/mL) and channels 9 – 12 (100 ng/mL). The results of these calculations are:

$$\text{Response (10 ng/mL)} = 3.83 \pm 1.26 \text{ \%/min, and} \quad (3)$$

$$\text{Response (100 ng/mL)} = 6.24 \pm 1.81 \text{ \%/min} \quad (4)$$

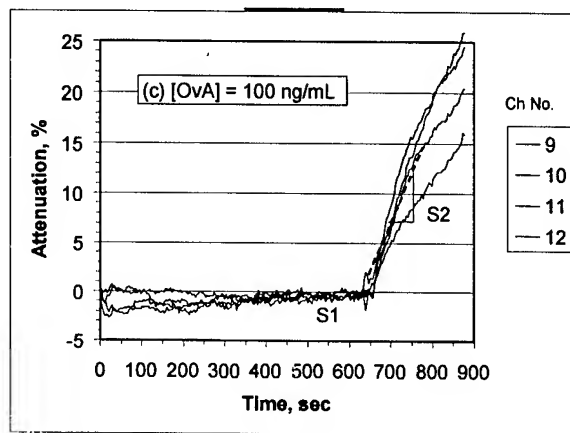
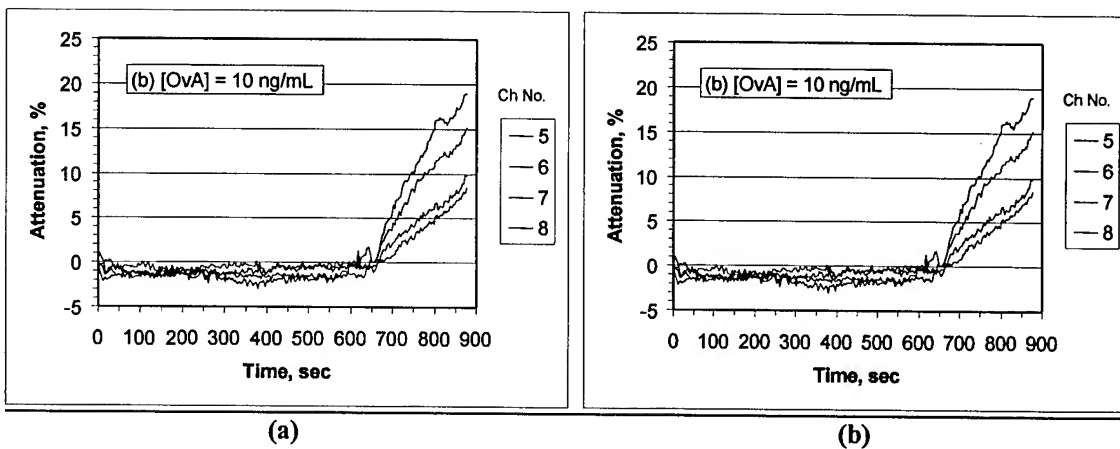


FIGURE 5. Test results for Ova.

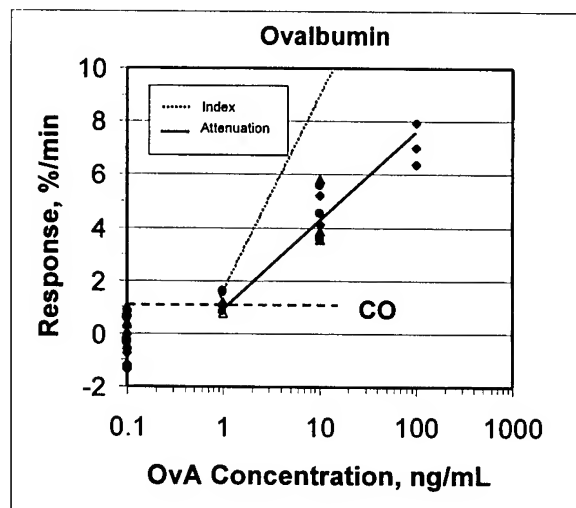


FIGURE 6. Dose response for Ova.

The standard deviation in the positive response values is a measure of the Coefficient of Variation (CV) of the assay data, where:

$$CV = 100 \times (\text{Standard Deviation}/\text{Mean}) \quad (5)$$

The data in the calculations above indicate that the assay CV is less than 33%. This CV value is typical of past assay testing and represents variations due to a variety of effects including capture antibody coating density variations, waveguide thickness changes, and random drift effects.

Results from previous testing indicates that the index response is approximately 3 times greater than the attenuation response for Ovalbumin antigen (Figure 6). However, the limits of detection (point where response equals CO) is approximately the same for the two modes of BDG operation. Results indicate that the limit of Ovalbumin detection is between 1 and 10 ng/mL for both the index and attenuation mode.

The limits of detection (LOD) for each simulant were estimated based on their dose response plots. The LOD values in this table were determined by extrapolating the response curves to the lowest concentration value where the following condition occurred:

$$\text{Mean Response} \times (1 - CV/200) > \text{Cut-off} \quad (6)$$

This equation uses the coefficient of variation, CV, for each assay to account for the variability in the positive responses and the cut-off value to account for variable output drift and non-specific binding effects. Consequently, the LOD values given in Table 1 represent less than 2% false positive readings and greater than 98% detection probability. These limits of detection are comparable to other immunoassay approaches and very encouraging for the future of this technology.

TABLE 1. LAI Limits of Detection

Simulant	LAI Limit of Detection
Ovalbumin	2 (ng/mL)
MS2	3×10^8 (pfu/mL)
B. globigii	2×10^4 (cfu/mL)
Erwinia herbicola	2×10^6 (cfu/mL)

Future development work on the LAI will focus on additional improvements of the technology. Surface chemistry will be improved to increase instrument sensitivity. Upgrading optics, fluidics, software and electronics will enhance ruggedness, utility and operational stability while reducing size, weight, power consumption and reagent volumes. In addition, fluidic elements, software and chemistry protocols developed for this technology will be applied to other promising bio-detection and identification approaches.

CONCLUSIONS

The Laboratory Attenuation Identifier (LAI) is a demonstration instrument developed to show in principle that an evanescent waveguide approach to biological identification can be made rapid, portable and rugged. We have demonstrated promising immunoassay limits of detection for up to twelve channels

simultaneously with a new, compact optical read head. The new read head uses commercially available components, makes sensor flow cell assembly replacement simple and fast, and requires no optical alignment. New advances in LAI fluidics are shrinking the size and power consumption of the unit and resulting in at least one U.S. Patent application. Future efforts will continue to move the design towards the goal of a field-ready Small Unit Biological Detector.

Acknowledgements

This project was funded by Government Contract Number SP00700-00-D-3180 for the Marine Corps Systems Command.

REFERENCES

1. D. Clerc and W. Lukosz, Integrated optical output grating coupler as refractometer and (bio-)chemical sensor, *Sensors and Actuators B*, 11 (1993) 461-465.
2. J. Ingenhoff, B. Drapp and G. Gauglitz, Biosensors using integrated optical devices, *Fresenius J. Anal. Chem.*, 346 (1993) 580-583.
3. R. Heidemann, R. Kooyman and J. Greve, Performance of a highly sensitive optical waveguide Mach-Zehnder interferometer immunosensor, *Sensors and Actuators B*, 10 (1993) 209-217.
4. R. M. Wadkins, J. P. Golden, and F. S. Ligler, "Simultaneous Measurement of Cy5.5-Labeled Capture Antibodies and Cy5-Labeled Antigens in a Fiber Optic Biosensor," *Proc. SPIE-Int. Soc. Opt. Eng.*, 2676 (Biomedical Sensing, Imaging, and Tracking Technologies I), 148-155 (1996).
5. P. Daniels, J. Deacon, M. Eddowes and D. Pedley, Surface plasmon resonance applied to immunosensing, *Sensors and Actuators*, 15 (1988) 11-18.
6. Fattinger, C., Mangold, C., Gale, M. T., Helmut, S., Bidiffractive grating coupler: universal transducer for optical interface analytics, *Opt. Eng.*, 34 (1995), 2744-2753.
7. Fattinger, C., Surface-selective optical microdetection, *The 7th Cyprus Conference on New Methods in Drug Research*, Limassol, Cyprus (1996), pp. 1-7.
8. Spinke, J., Oranth, J., Fattinger, C., Koller, H., Mangold, C., Voegelin, D., The bidiffractive grating coupler: application as an immunosensor., *Anal. Biochem* (1997), 253, 112-122.
9. O'Brien, T., Johnson, L. H., Aldrich, J. L., Allen, S. G., Liang, L., Plummer, A. L., Krak, S. J., Boiarski, A. A., The development of immunoassays to four biological threat agents in a bidiffractive grating biosensor, *Biosensors & Bioelectronics* 14 (2000) 815-828.

DISSOCIATION ENHANCED LANTHANIDE FLUOROIMMUNO ASSAYS (DELFI[®]A) FOR DETECTION OF FOODBORNE PATHOGENS AND AGENTS OF BIOLOGICAL ORIGIN

Emily D. Myers

Science and Technology Corporation
Edgewood, MD 21040 USA

Deborah L. Menking, Michael T. Goode, and Alan W. Zulich
U.S. Army Edgewood Chemical and Biological Center
Aberdeen Proving Ground, MD 21010 USA

The Biosensors Team has a continuing effort geared toward providing the Army with improved immunological and DNA-based biosensors and their assays with the capability of rapidly and accurately detecting and identifying toxins, viruses, and bacterial pathogens. In addition, the team continues to develop and evaluate emerging and next-generation sensors and assay technologies. This work has encompassed, in-part, the hardware and assay assessment of a detection technology called Dissociation Enhanced Lanthanide Fluoroimmuno Assays (DELFI[®]A) that uses Time Resolved Fluorescence (TRF) to interrogate for the presence of biological agents.

Introduction: Time Resolved Fluorescence (TRF) of lanthanide probes was evaluated using Perkin Elmer's 1420 VICTOR²_™ Multilabel Counter. TRF technology distinguishes between short and long decay components by using a gated fluorometer with time-resolution capability that employs appropriate delay, counting, and cycle times. It is possible to distinguish between long decay and short decay (intrinsic background fluorescence and scattering) fluorescence emissions by the use of sensitive lanthanide chelates in combination with time-resolved fluorescence in the study of biological macromolecules. The difference between the wavelengths of excitation and emission maxima (Stokes Shift) indicates the energy dissipated during the lifetime of the excited state before it returns to the ground state. During the excited state, the lanthanide chelate emits fluorescence at a determined wavelength that is 200-300 nm longer than its excitation wavelength. The 1420 VICTOR²_™ Multilabel Counter can distinguish between the fluorescence emission of the lanthanide chelate and the background fluorescence because the latter has a shorter Stokes Shift (30 – 50 nm). The scope of this effort involved the evaluation of time resolved fluorescence using a lanthanide probe, europium chelate of N¹-[p-isothiocyanatobenzyl]-diethylene-triamine-N¹, N², N³-tetra-acetic acid (DTTA), using Perkin Elmer's 1420 VICTOR²_™ Multilabel Counter as a biodetector. The effort was initiated by a collaboration between Biosensors Team and Perkin Elmer (formerly EG&G Wallac). The following agents of biological origin and foodborne pathogens were evaluated on the 1420 VICTOR²_™ Multilabel Counter: *Bacillus subtilis* var. *niger*, *Bacillus anthracis*, *Yersinia pestis*, *Clostridium botulinus* A and B toxins, *Staphylococcus enterotoxin* B, and *Escherichia coli* O157: H7. The focus of this work was to establish the dynamic range and quantify the limit of detection for these antigens in DELFI[®]A Assay Buffer. Future work will address the issue of sample preparation and antigen extraction from food samples relative to detection sensitivities.

Materials and Methods. Reagent preparation for *Bacillus subtilis* var. *niger*, *Bacillus anthracis*, *Yersinia pestis*, *Clostridium botulinus* A and B toxins, *Staphylococcus enterotoxin* B, and *Escherichia coli* O157: H7 consisted of labeling specific antibodies with biotin and europium (Eu⁺³) for use as capture and reporter molecules, respectively, for TRF-based sandwich assays. Specifically, one goat anti-*Bacillus subtilis* IgG polyclonal, one rabbit anti-*Bacillus anthracis* IgG polyclonal, and one rabbit anti-*Yersinia pestis* IgG polyclonal were used for both capture and reporter for their respective antigens.

Clostridium botulinus toxin assay preparations consisted of labeling two Granite Diagnostics goat polyclonal antibodies (individually specific to toxin serotypes A and B) with biotin and Eu^{+3} and one recombinant anti-*C. botulinus* B F(ab')₂ antibody with biotin. Reagent preparation for TRF assay development of *Staphylococcus* enterotoxin B consisted of labeling one rabbit polyclonal antibody with biotin and one monoclonal (Mab) antibody with Eu^{+3} . An *E. coli* O157:H7 TRF DELFIA[®] assay was developed using commercially available antibody from Kirkegaard & Perry Laboratories, Inc (KPL, Gaithersburg, MD). The BacTrace[™] affinity purified antibody (Cat # 01-95-90) was isolated from a serum pool from goats immunized with whole cells of *E. coli* serotype O157:H7 and is highly specific for *E. coli* O157:H7. KPL has minimized cross-reactivity of this antibody to other *E. coli* strains through extensive adsorption using non-O157:H7 serotypes of *E. coli*. Perkin Elmer provided europium-labeling services for rabbit anti-BG, rabbit anti-*B. anthracis*, rabbit anti-*Y. pestis*, goat anti *C. botulinum* A and B, monoclonal anti-SEB, and goat anti-*E. coli* O157:H7. Molar incorporations ratios (MIR) for detector proteins ranged from 6.1 to 15.9 moles of europium to 1 mole of IgG. Capture antibodies were labeled in-house with Molecular Device's Corporations (MDC, Sunnyvale, CA.) ImmunoLigand Assay (ILA) Biotin Label (Product # R9002). Dinitrophenol (DNP)-biotin N-hydroxysuccinimide (NHS) ester was rehydrated with 1 ml of dimethylformamide (DMF) to a final stock concentration of 0.0058 $\mu\text{M}/\mu\text{l}$. The only exception was the recombinant anti-*C. botulinus* B F(ab')₂. PE provided biotin-labeling services for this antibody. To achieve a molar coupling ratio (MCR) of 10:1 moles of biotin to IgG, 11.47 ml of biotin NHS ester was added to a 1 mg/ml preparation of each capture protein. Following a 2-hour incubation in the dark at ambient room temperature (ART), the conjugate was separated on a Pharmacia PD-10 Sephadex G-25 column. Ten 0.5 ml fractions were eluted and absorbance reads at 280 nm and 362 nm (presence of DNP for biotin trace) were made using a Beckman DU 650 spectrophotometer. MIRs for capture proteins ranged from 2.4 to 11.3 moles of biotin to protein for assay development. Each biotinylated conjugate antibody was diluted in 1X Threshold Assay Buffer for stabilization.

Preparation of antibody dilutions. All antibody conjugates were diluted for use in DELFIA[®] Assay Buffer (Wallac, Product # 1244-111) for TRF assay development (Tris-HCl buffered NaCl solution [pH 7.8] containing <0.1% NaN_3 , bovine serum albumin, bovine gamma globulins, Tween 40, diethylenetriaminepentaacetic acid [DTPA], and an inert red dye). Assay development consisted of determining the optimum amounts of capture and detector conjugates needed to elicit maximum endpoint sensitivity in the shortest period of time. Preliminary antibody loading studies were designed in matrix fashion by incorporating 50 to 400 ng/test (in 100 μl volume) of each biotinylated conjugate. Europium labeled conjugates were incorporated from 50 to 200 ng/test (in 20 μl volume). The dynamic range of the assay was monitored from 0 – 1×10^7 cfu/ml for BG, *B. anthracis*, *Y. pestis*, and *E. coli* O157:H7 assays. *C. botulinus* A, *C. botulinus* B, and *Staphylococcus* enterotoxin B assays were evaluated from 0 to 250 ng/ml of toxin.

Preparation of antigens. *Bacillus subtilis* var. *niger* Pine Bluff field grade spores used in assay development were obtained from Dugway Proving Ground. The antigen dilution range consisted of a fresh preparation of BG spores from 0 – 1×10^7 cfu/ml in DELFIA[®] Assay Buffer. *Bacillus anthracis* Sterne spores were obtained from the Air Force Institute of Pathology (AFIP) @ 9.5×10^6 cfu/ml. This spore preparation was cobalt gamma irradiated. The antigen dilution range consisted of a fresh preparation of spores from 0 – 1×10^6 cfu/ml in DELFIA[®] Assay Buffer. *Yersinia pestis* CO92 was also obtained from AFIP @ 1×10^8 cfu/ml and was also cobalt gamma irradiated. The antigen dilution range consisted of a fresh preparation from 0 to 1×10^6 cfu/ml of antigen in DELFIA[®] Assay Buffer. *C. botulinus* Toxin A solution at 0.5 mg (0.5 ml) Product # 025-08173 and *C. botulinus* Toxin B Solution at 0.5 mg (0.5 ml) Product # 9810137 were purchased from Wako Pure Chemicals Industries, Ltd. (Osaka, Japan). The antigen dilution range consisted of a fresh preparation of toxins from 0 – 250 ng/ml in DELFIA Assay Buffer. *Staphylococcus* enterotoxin B Cat # S 4881 was purchased from SIGMA (St.

Louis, MO) and reconstituted in 0.01 M Phosphate Buffered Saline (PBS) + 0.05% sodium azide for a final concentration of 1 mg/ml. The antigen range consisted of a fresh preparation from 0 to 25 ng/ml of antigen in DELFIA[®] Assay Buffer. Two *E. coli* O157:H7 cell preparations were used for development of TRF assays with the KPL antibody conjugates. The application for using each cell preparation is described hereafter, however the antigenic expression in the form of Shiga-like toxins I and II, flagella, and/or specific lipopolysaccharides cannot be determined for all cell preparations evaluated. The antigen preparations used were (1) KPL *Escherichia coli* O157:H7 Positive Control (Cat. # 50-95-90) and (2) ATCC *Escherichia coli* O157:H7 Number 43888. KPL *Escherichia coli* O157:H7 Positive Control was used as a model assay system where it provided verification of the functionality of the assay system. The product was ideally suited for use as a positive control in immunoassays designed for *Escherichia coli* O157:H7 detection. The material was provided as heat-killed *Escherichia coli* O157:H7 cells at approximately 7×10^9 cells/ml (1 ml of approximately 2% wet packed cell w/v) in dextran solution. The lyophilized product was rehydrated with a 50% glycerol solution and stored at -35 °C long term or 4 °C short term (2 weeks). The organism *Escherichia coli* (Migula) Castellani and Chalmers, designation CDC B6914-MS1 [3417-86; CIP 105917], was purchased from ATCC in a freeze-dried form. The antigenic properties are reported to demonstrate characteristics common to serotype O157:H7 isolated from human feces. This particular organism does not produce either Shiga-like toxin I or II and does not possess the genes for these toxins. Propagation of this material is achieved by growth on Trypticase Soy Agar at 37 °C. The parent strain 43888 was plated and an individual colony was isolated (Isolate Number 3, lot # 00-0009-141) and used as an inoculum for future bacterial fermentations. The *E. coli* O157:H7 used for the duration of TRF assay development was manufactured on Tryptic Soy Broth with a concentration of 6.65×10^9 cfu/ml. The antigen dilution range consisted of a fresh preparation of 0 to 1×10^7 cfu/ml of each antigen in DELFIA[®] Assay Buffer.

DELFIA[®] Assay Protocol. All optimized DELFIA[®] experiments performed on the VICTOR²_™ were 75-minute assays. DELFIA[®] Streptavidin Microtitration Strip plates (Wallac, Product # C122-105) were pre-washed three times with a 1X solution of DELFIA[®] Wash Solution (Wallac, Product # 1244-114), followed by the addition of 100 µl of biotinylated antibody at 200 ng/well. The biotinylated antibody was incubated in the streptavidin-imbued microtiter plate for 30 minutes at 37 °C at 400 rpm with orbital shaking using a VorTemp 56 Plate Shaker/Incubator, Cat # S2056 (Denville Scientific, NJ). Subsequent to incubation of immunoreactants, the separation of the free and bound fraction was accomplished by extensive washing of the solid phase surface with a 1X solution of DELFIA[®] Wash Solution. After washing the plates three times, each respective antigen and reporter antibody labeled with europium at 50 ng /20 µl were sequentially added to the microtiter well and incubated at 37 °C for 30 minutes with 400 rpm shaking. Once the immunocomplex was immobilized in the plate, the final step in the assay was the dissociation of the lanthanide ion from the immunocomponent on the solid phase into a solution where a highly fluorescent lanthanide chelate was formed. This reaction was driven by the addition of DELFIA[®] Enhancement Solution (Wallac, Product # 1244-105), which has a low pH and contains β-diketones that chelates the Eu^{+3} from the antibody. The solution dissociates Eu^{+3} from solid-phase bound Eu^{+3} - labeled antibodies during a time period of a few minutes to form a homogeneous and highly fluorescent Eu^{+3} -(2-NTA)₃ (TOPO)₂₋₃ micellar chelate solution. The newly formed chelate was then measured by the time-resolved fluorometer. In the case of Eu^{+3} , the fluorescence was initiated by excitation at 340 nm with emission at 613 nm. The europium-labeled antibody conjugate was pre-filtered immediately before use with a Sterile 0.2 µm 13 µm HT Tuffryn[®] Membrane Acrodisc[®] Syringe Filter (Pall Gelman Laboratory, Cat # 4454).

Results. Statistical analysis for *Bacillus subtilis* var. *niger*, *Bacillus anthracis*, *Yersinia pestis*, *Clostridium botulinus* Toxins A and B, *Staphylococcus* enterotoxin B, and *Escherichia coli* O157: H7 DELFIA® assay development on the VICTOR™ Multilabel Counter is performed by calculating the standard deviation (STD), percent coefficient of variation (%CV), and Signal to Noise (S/N) ratio for the mean antigen concentrations for each assay. The % CV was calculated by dividing the standard deviation for the assay by the mean counts per second (cps) value for the assay. The assay endpoint sensitivity cutoff was determined by subtracting the assay cps mean background value (plus 3X the standard deviation) from the raw signal in cps for each dilution. At least four replicates were run for each antigen concentration with fluorescence values represented in cps. Current endpoint sensitivity for *Bacillus subtilis* var. *niger* is 1×10^4 cfu/ml, indicated in Table 1. The BG assay was generated with incorporation of 400 ng of biotinylated goat anti-BG and 200 ng of Eu⁺³ labeled goat anti-BG. Due to time constraints, BG was never evaluated using the current optimized protocol for TRF, which lowered the biotin and Eu⁺³ conjugate concentrations. Better sensitivity and lower backgrounds will be achieved once these conditions are tested. Table 2 shows the endpoint sensitivity for *Bacillus anthracis* TRF assay generated with incorporation of 200 ng of biotinylated rabbit anti-*B. anthracis* and 50 ng of Eu⁺³ labeled rabbit anti-*B. anthracis*. Current endpoint sensitivity for *B. anthracis* is 2×10^3 cfu/ml. Endpoint sensitivity for *Yersinia pestis* TRF assay is shown in Table 3. The *Y. pestis* assay was generated with incorporation of 200 ng of biotinylated rabbit anti-*Y. pestis* and 50 ng of Eu⁺³ labeled rabbit anti-*Y. pestis*. Current endpoint sensitivity for *Y. pestis* is 2×10^3 cfu/ml. Figure 1 describes the assay endpoint sensitivity for *C. botulinus* A and B toxin TRF assays. *C. botulinus* A toxin assay was generated with incorporation of 100 ng of biotin anti-*C. botulinus* F(ab)₂ and 50 ng of Eu⁺³ labeled goat anti-*C. botulinus* A. *C. botulinus* B toxin assay was generated with incorporation of 200 ng of biotinylated anti-*C. botulinus* F(ab)₂ and 50 ng of Eu⁺³ labeled goat anti-*C. botulinus* B. Current endpoint sensitivity for both *C. botulinus* A and B TRF assays is between 0.1 and 0.5 ng/ml. Table 4 demonstrates *Staphylococcus* enterotoxin B TRF detection endpoints generated with incorporation of 200 ng of biotinylated rabbit anti-SEB and 50 ng of Eu⁺³ labeled Mab anti-*Staphylococcus* enterotoxin B. The *Staphylococcus* enterotoxin B assay endpoint sensitivity was determined to be 0.05 ng/ml. The KPL *E. coli* O157:H7 and ATCC *E. coli* O157:H7 assay endpoint sensitivities were calculated as shown in Tables 5 and 6, respectively. The limit of detection for each *E. coli* assay was 80 cfu/ml.

TABLE 1. Final Assay Endpoint Sensitivity for TRF DELFIA® *Bacillus subtilis* var. *niger*.

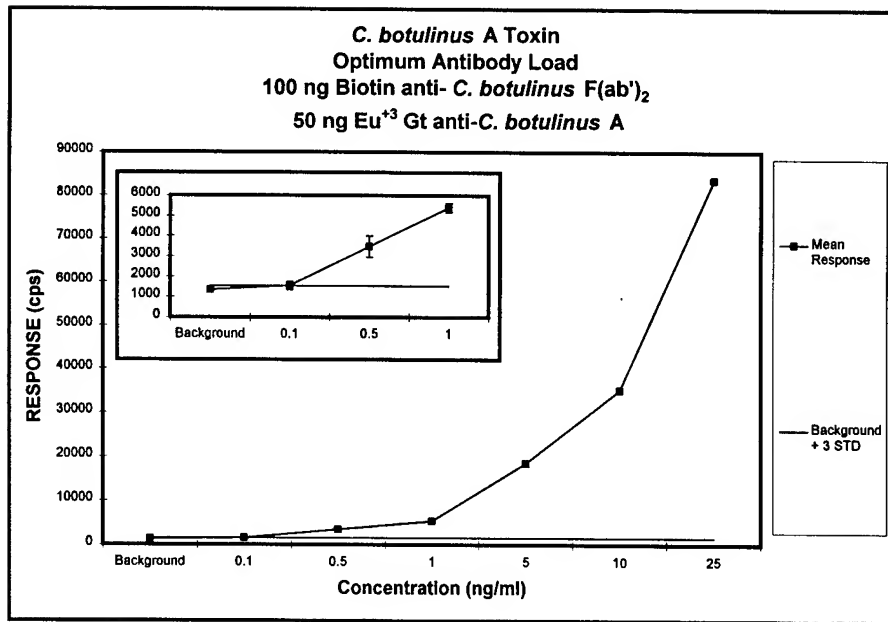
<i>Bacillus subtilis</i> var. <i>niger</i> Field Grade Spores			
Supplied by Dugway Proving Ground			
Protocol B			
Capture Antibody: Biotin Goat anti-BG (DPG)			
400 ng / well / 100 µl DELFIA Assay Buffer			
Antigen: 0 - 1×10^7 cfu / mL in DELFIA Assay Buffer (100 µl / well)			
Detection Antibody: Eu ⁺³ Goat anti-BG (DPG)			
200 ng / well / 20 µl DELFIA Assay Buffer			
Incubate 30 minutes @ 37°C 400 rpm			
WASH 6 x NUNC Washer			
Background + 3 STD: 6387			
LLD: 1.00E+04 cfu / mL			
	Counts	Counts - Bkgd + 3 STD	CV %
0	3496	-2891	27.8
1.00E+01	3093	-3284	13.8
1.00E+02	4572	-1815	19.3
1.00E+03	3823	-2564	17.5
1.00E+04	8082	1695	43.4
1.00E+05	45782	39375	2.4
1.00E+06	227393	221006	2.2
1.00E+07	228842	222455	5.5

TABLE 2. Final Assay Endpoint Sensitivity for TRF DELFIA® *Bacillus anthracis* Assay.

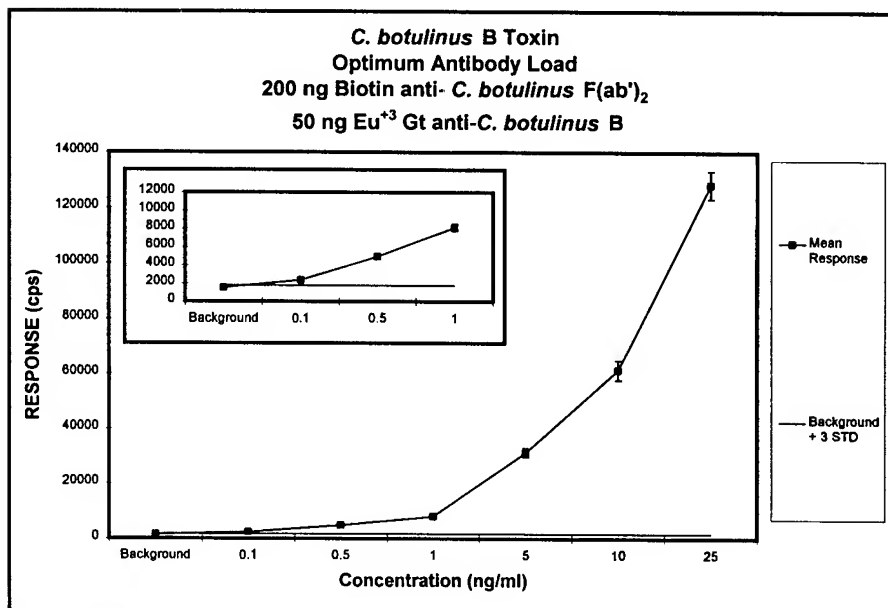
<i>Bacillus anthracis</i> STERNE spores Supplied by Air Force Institute of Pathology (AFIP)			
Capture Antibody: Biotin Rbt anti <i>B. anthracis</i> 200 ng / well / 100 µl DELFIA Assay Buffer Incubate 30 minutes @ 37°C 400 rpm WASH 3 x DELFIA washer			
Antigen: 0 - 1 x 10 ⁸ cfu / mL in DELFIA Assay Buffer (100 µl / well) Detection Antibody: Eu ³ Rbt anti <i>B. anthracis</i> 50 ng / well / 20 µl DELFIA Assay Buffer Incubate 30 minutes @ 37°C 400 rpm WASH 6 x DELFIA washer			
Background + 3 STD: 1153 LLD: 2.00E+03 cfu/ml			
	Counts	Counts - Bkgd + 3 STD	CV %
0	923	-230	8.3
1.00E+01	846	-307	7.5
1.00E+02	861	-292	6.0
1.00E+03	1234	81	6.8
2.00E+03	3376	2223	16.7
5.00E+03	6163	5010	8.9
1.00E+04	6660	5507	11.2
1.00E+05	26473	25320	16.6
1.00E+06	11708	10555	5.67

TABLE 3. Final Assay Endpoint Sensitivity for TRF DELFIA® *Yersinia pestis* Assay.

<i>Yersinia pestis</i> CO92 Supplied by Air Force Institute of Pathology (AFIP)			
Capture Antibody: Biotin Rbt anti <i>Y. pestis</i> 200 ng / well / 100 µl DELFIA Assay Buffer Incubate 30 minutes @ 37°C 400 rpm WASH 3 x DELFIA washer			
Antigen: 0 - 1 x 10 ⁸ cfu / mL in DELFIA Assay Buffer (100 µl / well) Detection Antibody: Eu ³ Rbt anti <i>Y. pestis</i> 50 ng / well / 20 µl DELFIA Assay Buffer Incubate 30 minutes @ 37°C 400 rpm WASH 6 x DELFIA washer			
Background + 3 STD: 2498 LLD: 2.00E+03 cfu / mL			
	Counts	Counts - Bkgd + 3 STD	CV %
0	2007	-490	8.1
1.00E+01	1665	-833	2.4
1.00E+02	1605	-892	11.2
1.00E+03	2350	-148	5.3
2.00E+03	2682	184	1.9
5.00E+03	3397	898	5.7
1.00E+04	7331	4833	6.3
1.00E+05	45019	42521	4.5
1.00E+06	190952	188455	9.6



A



B

Figure 1. Graphic representation of *C. botulinus* A and B toxin assays using the optimum antibody loads determined in preliminary assay development optimization. Graph A describes *C. botulinus* A toxin endpoint sensitivity between 0.1 and 0.5 ng/ml with optimum antibody concentrations at 100 ng biotin anti-*C. botulinus* F(ab')₂ and 50 ng Eu⁺³ Goat anti-*C. botulinus* A. Graph B demonstrates *C. botulinus* B toxin endpoint sensitivity is between 0.1 and 0.5 ng/ml with optimum antibody concentrations at 200 ng biotin anti-*C. botulinus* F(ab')₂ and 50 ng Eu⁺³ Goat anti-*C. botulinus* B.

TABLE 4. Final Assay Endpoint Sensitivity for TRF DELFIA® SEB Assay.

<u>Staphylococcal Enterotoxin B</u> <u>SIGMA (Cat # S 4881)</u>			
Capture Antibody: Biotin Rbt anti SEB 200 ng / well / 100 µl DELFIA Assay Buffer Incubate 30 minutes @ 37°C 400 rpm WASH 3 x DELFIA washer			
Antigen (SEB): 0 - 25 ng/mL in DELFIA Assay Buffer (100 µl / well) Detection Antibody: Eu ³ Mab anti SEB 50 ng / well / 20 µl DELFIA Assay Buffer Incubate 30 minutes @ 37°C 400 rpm WASH 6 x DELFIA washer			
Background + 3 STD: 1726 LLD: 0.05 ng/mL			
	Counts	Counts - Bkgd + 3 STD	CV %
0	996	-730	24.4
0.005	1327	-399	4.5
0.01	1848	-79	6.1
0.05	4320	2594	3.7
0.1	8348	6622	6.9
0.5	37431	35705	6.3
1	74999	73273	2.8
5	347108	345382	4.3
10	704717	702991	3.0
25	1713253	1711527	3.7

TABLE 5. Final Assay Endpoint Sensitivity for TRF DELFIA® KPL Positive Control *Escherichia coli* O157:H7 Assay.

<u>Escherichia coli O157:H7</u> <u>Kirkegaard & Perry Positive Control Cat. # 50-95-90</u>			
Capture Antibody: Biotin Goat anti- <i>E. coli</i> O157:H7 b/p: 5.3 (KPL Cat # 10-95-90) 200 ng / well / 100 µl DELFIA Assay Buffer Incubate 30 minutes @ 37 °C 400rpm WASH 3 x DELFIA washer			
Antigen (<i>E. coli</i> : O157:H7) 0 - 1 x 10 ⁷ CFU/ml in DELFIA Assay Buffer (100 µl / well) Detection Antibody: Eu ³ Goat anti- <i>E. coli</i> O157:H7 Eu ³ /p: 10.9 (KPL Cat # 10-95-90) 50 ng / well / 20 µl DELFIA Assay Buffer Incubate 30 minutes @ 37 °C 400 rpm WASH 6 x DELFIA washer			
Bkgd + 3 STDEV: 2404 LLD: 8 x 10¹ CFU/ml			
CFU/ml	Counts	Counts - Bkgd + 3STDEV	CV %
0	1792	-612	11.4
1 x 10 ¹	2056	-348	11.2
2 x 10 ¹	2357	-47	6.1
8 x 10 ¹	3087	683	6.8
1 x 10 ²	3403	999	6.9
8 x 10 ²	5171	2767	6.2
1 x 10 ³	6420	4016	8.8
5 x 10 ³	16469	14065	4.3
1 x 10 ⁴	29921	27517	2.6
1 x 10 ⁵	310714	308310	2.8
1 x 10 ⁶	3021265	3018861	1.2
1 x 10 ⁷	4134518	4132114	2.2

TABLE 6. Final Assay Endpoint Sensitivity for TRF DELFIA® ATCC *Escherichia coli* O157:H7 Assay.

<i>Escherichia coli</i> O157:H7			
ATCC Number 43888			
Capture Antibody: Biotin Goat anti- <i>E. coli</i> O157:H7 b/p: 5.3 (KPL Cat # 10-95-90) 200 ng / well / 100 µl DELFIA Assay Buffer Incubate 30 minutes @ 37°C 400rpm WASH 3 x DELFIA washer			
Antigen (<i>E. coli</i> O157:H7) 0 - 1 x 10 ⁷ CFU/ml in DELFIA Assay Buffer (100 µl / well) Detection Antibody: Eu ⁺³ Goat anti- <i>E. coli</i> O157:H7 Eu ⁺³ /p: 10.9 (KPL Cat # 10-95-90) 50 ng / well / 20 µl DELFIA Assay Buffer Incubate 30 minutes @ 37°C 400 rpm WASH 6 x DELFIA washer			
Bkgd + 3 STDEV: 2534 LLD: 8 x 10¹ CFU/ml			
CFU/ml	Counts	Counts - Bkgd + 3STDEV	CV %
0	2105	-429	6.8
1 x 10 ¹	2840	306	10.6
2 x 10 ¹	2388	-146	4.0
5 x 10 ¹	3339	805	2.0
5 x 10 ²	3860	1326	9.6
8 x 10 ²	5867	3333	4.3
1 x 10 ³	7742	5208	6.0
5 x 10 ³	11825	9291	7.3
1 x 10 ⁴	15870	13336	8.4
1 x 10 ⁵	1228278	1225744	10.6
1 x 10 ⁶	1186687	1164153	6.9
1 x 10 ⁷	3697437	3694903	6.3

CONCLUSIONS

Both bacterial spore assays, *Bacillus subtilis*, var *niger* and *Bacillus anthracis*, exhibited sensitive levels of detection. Even though each spore assay used polyclonal antibodies for both capture and detector, the assay still proved to be very sensitive. A monoclonal antibody, for both BG and *B. anthracis*, was not available to add specificity to the assay. The BG assay was not completely optimized for biotin and Eu⁺³ conjugate concentrations. Further analysis will probably yield better sensitivity and lower backgrounds once these conditions are tested. The *Yersinia pestis* TRF assay also demonstrated a sensitive level of detection using a polyclonal antibody for both capture and detector during the evaluation. As expected, sensitive detection was achieved for all TRF toxin assays. The use of a monoclonal detector antibody in the SEB assay and a recombinant F(ab')₂ protein in the *C. botulinus* immunocomplex provided assay specificity as well as sensitive toxin detection. The *Escherichia coli* O157:H7 assay demonstrated very sensitive detection using a europium-labeled polyclonal immunoglobulin from KPL. The same antibody was used as the capture (biotin) and detector (europium) components in the sandwich assay due to the unavailability of securing a monoclonal antibody or a more suitable counterpart for target site specificity. It is probable that this polyclonal is capable of detecting the LPS and O somatic antigens, as well as the flagellar filaments and Shiga-like toxins secreted from the bacteria. According to KPL product specifications, the goat anti-*E. coli* O157:H7 is highly specific for *E. coli* O157:H7 and cross-reactivity to other *E. coli* strains has been minimized through extensive adsorption using non-O157:H7 serotypes of *E.*

coli. In the case of the ATCC *E. coli* O157:H7 preparation, the bacteria may possess the LPS and somatic antigen components, as well as filamentous flagellar portions. It is known that this antigen preparation does not carry the genes required to secrete the Shiga-like toxin I or II associated with *E. coli* O157:H7. It is probable that the antibody did recognize the LPS and O somatic antigen sites for immunocapture to elicit such sensitive *E. coli* detection at 80 cfu/ml. KPL Positive Control Antigen performed sufficiently for development of a "model" *E. coli* O157:H7 assay. The actual antigenic determinations (i.e., presence of LPS, O antigens, Shiga-like toxins, etc.) are not given for this preparation. The antigen did serve as a suitable positive control for TRF assay development by validating the integrity of the antibody conjugates used to perform the *E. coli* assays in the presence of the KPL Positive Control Antigen (80 cfu/ml).

REFERENCES

1. EG & G Wallac. Time-Resolved Fluorescence Label Technologies for Pharmaceutical Screening Assays. *LANCE™ News*, May 1997.
2. EG & G Wallac. Advice for Setting Up Robust DELFIA Binding Assays, *Wallac Drug Discovery*, Application Note No. 002.
3. McKane, Larry and Judy Kandel. "Diseases Acquired Through the Alimentary Tract," *Microbiology Essentials and Applications*. New York: McGraw-Hill, Inc., 1996, 2nd edition, Chapter 22, pp. 571-572.
4. Mageau, Richard P, 1998. "Immunoassays for the Detection and Quantitation of Staphylococcal Enterotoxins from Meat and Poultry Products and/or Broth Culture Fluids," *United States Department of Agriculture Food Safety and Inspection Service, Microbiology Laboratory Guidebook*, 3rd Edition, Chapter 15.
5. Soini, E., and Lovgren, T., 1987. Time-resolved fluorescence of lanthanide probes and applications in biotechnology, *CRC Critical Reviews in Analytical Chemistry*, **18**, Issue 2, PP. 105-112.
6. Sharer, Amelia K. and Bonnie E. Rose, 1998. "Detection, Isolation, and Identification of *Escherichia coli* O157:H7 and O157:NM (Nonmotile) from Meat and Poultry Products," *United States Department of Agriculture Food Safety and Inspection Service, Microbiology Laboratory Guidebook*, 3rd Edition, Chapter 5.
7. U. S. Department of Health and Human Services. *Botulism in the United States 1899-1996*. Handbook for Epidemiologists, Clinicians, and Laboratory Workers. Centers for Disease Control and Prevention, National Center for Infectious Disease, Division of Bacterial and Mycotic Diseases, 1998, pp. 1-17.

MICROORGANISM IDENTIFICATION BY MASS SPECTROMETRY AND PROTEIN DATABASE SEARCHES — AN ANALYSIS

Ravi P. Lall and A. Peter Snyder
R&T Directorate US Army Edgewood Chemical Biological Center
Aberdeen Proving Ground, MD 21010-5423 USA

ABSTRACT

The potential for the identification of microorganisms based on information contained in prokaryotic genome and protein sequence databases is explored and evaluated. Protein biomarkers for various bacteria can be determined by combining biological sample processing methodologies with mass spectrometry. The experimental mass spectra have been matched with protein databases available on the Internet. Further, the organisms have been ranked according to the matched peaks. The literature has reported on the masses of a set of ions by MALDI TOF mass spectrometry of intact or treated cells. These experiments included *B. subtilis* and *E. coli*, because of their completely sequenced genomes. This has been verified and extended by an in -depth evaluation, especially for the limitations caused by the statistical factors. Most of the matches obtained were very good. This report extended the protein database matching with experimental, liquid chromatography coupled with Electrospray ionization, mass spectra of the bacterial extracts. For the vast majority of bacteria, proteomic databases are not available. The limitations of this method have been revealed by conducting protein database matching for the protonated species from LC-ESI of *B. megaterium* and *C. freundii* (trifluoro acetic acid extracts), respectively. Eliminating the common protein entries from different organisms may improve this approach to some extent.

INTRODUCTION

The various biological identification approaches are essential for support of the mission to develop and demonstrate an advanced Biological Sample Preparation System for incorporation with leading biological identification technologies. The BSPS will be used in conjunction with ESI- mass spectrometry for biological identification purposes. The development of these technologies with concurrent advances in biological identification systems, will permit more rapid and reliable responses to biological threats on the battlefield as well as in applications related to Domestic Preparedness , intelligence gathering , and treaty verification issues.

There are various reports in the literature probing into the suitability of several MS approaches for rapid identification and characterization of microorganisms. All of these approaches are based on the detection of unique biomarkers and combinations thereof. Cell wall lipids have been employed as bacterial biomarkers.^{1,2} Many reports have suggested the use of proteins expressed in microorganisms as biomarkers. Organism identification and classification has been attempted by using the mass spectra of protein mixtures obtained on matrix assisted laser desorption/ionization (MALDI) time of flight (TOF) instruments as well as on electro spray ionization instruments.³⁻⁷ The fingerprint protein profile for different organisms i.e. the pattern of observed mass spectral peaks typically in the mass range of 4-15 kDa is generally used for identification purposes. The critical requirement is mass spectral reproducibility. However, it is known that the spectra of such complex mixtures depend in intricate ways on a number of instrumental and microbiological factors- among these are bacterial culture growth times⁸ and sample pretreatment⁵ Also the fingerprint mass spectral library of microorganisms is shaped by both the ionization technique and mass analyzer.

Presently DNA sequences for all species are being added on to the databases, which can be easily searched on the Internet. Complimentarity exists between the genome of the organism and the respective proteome. Characterization of such organisms can be achieved through knowledge of their complete genome or complimentary proteomes. MS based procedures for identity assignment of individual proteins are available.⁹⁻¹⁴ Software is available for protein identification on-line based on peptide mapping and sequence database strategies.¹⁵

There has been reports addressing the possibility of exploiting the information contained in prokaryotic genome and protein sequence databases to rapidly identify microorganisms.¹⁶ Specifically the authors demonstrated that microorganisms can be identified when the constituents of a set of proteins, represented by their molecular masses in a mass spectrum, are each identified in a sequence database along with their organism sources. Two organisms with completely sequenced genomes, *Bacillus subtilis* and *Escherichia coli*, (a gram-positive and a gram-negative bacterium, respectively) were studied in this referenced report. The organisms were ranked according to matched peaks. This has been verified and extended by an in -depth evaluation, especially for the limitations caused by the statistical factors. The studies have been extended on the protein database matching of experimental LC-ESI mass spectra of the bacterial extracts. Also we went further in developing a relatively unique bacterial protein matrix and used that to rank the organisms by matched peaks. For the vast majority of bacteria, proteomic databases are not available. Attempts have been made to study the limitations of this method by conducting protein database matching for the protonated species from LC-ESI of *B. megaterium* and *C. freundii* (trifluoroacetic acid extracts), respectively.¹⁷ Very few genomic proteins for these are available in the protein databases.

EXPERIMENTAL SECTION

For the purpose of this study protein biomarkers for various organisms have been obtained by different biological sample processing methods in combination with mass spectrometry. MALDI TOF mass spectrometry as well as LC-ESI mass spectrometry has been employed. For some illustrations organisms with different growth times have been used.

First various protein molecular weights obtained from different mass spectra were listed and then searches made in the SWISS PROT/TrEMBL database from the Swiss Bioinformatics Institute. The sequence retrieval system was used for the purpose. Web sites can be accessed by first going to www.expasy.ch. The web sites include SWISS PROT and SRS. A search was made either by query form or by alternate query form. A selection was made for the bacteria in general and the molecular weight range by selecting the window of ± 3 Da for a mass obtained by mass spectrometry. In some cases a ± 5 Da window was applied for the purpose of illustration. For the purpose of making relatively unique bacterial protein matrix, a list of 20 bacteria was selected. Six of the bacteria have a genome known and include, *Escherichia coli*, *Bacillus subtilis*, *Borrelia burgdorferi*, *Haemophilus influenzae* and *Helicobacter pylori*. Their protein entries from the SWISSPROT and TrEMBL databases, were listed in excel format. Unique protein entries for each bacterium relative to the other nineteen bacteria were found and hence we named it as a mass specific bacterial database. Masses from the experimental mass spectra were matched with the proteins in the SWISSPROT and TrEMBL databases. Also the masses from experimental mass spectra were matched with the protein entries from the mass-specific matrix, for all of the 20 bacteria. We have used the masses from 1K to 18k Da, from the experimental spectra,

RESULTS AND DISCUSSION

We discuss the results by describing each case. Each case ranks the organisms according to matched peaks of the specific experimental mass spectra. A proton mass of one mass unit was subtracted from the protonated masses in the experimental mass spectra before making the matches with the protein databases. Only the organisms corresponding to a significant number of matches are shown in the tables below. The matches corresponding to the first rank in the reference database (SWISS PROT & TrEMBL),

are shown in the bold letters and the ones corresponding to the mass specific bacterial database are shown in underlined, in the corresponding observed mass tables. The SWISS-PROT and TrEMBL databases are updated periodically. In the recent update there are more protein entries, shown for *Vibrio cholerae* and *Bacillus Halodurans*, The genome study for these organisms is complete and it is expected that the protein entries corresponding to complete proteome set will be available shortly. In case 1 and 2, we have also shown protein matches found corresponding to these organisms, in Sw/Tr database

CASE 1

Positive Ion MALDI mass spectra from *Bacillus subtilis* from Figure 2A Ref 16.

A proton mass of one unit mass was subtracted from the original observed masses in *B. subtilis* mass spectrum to obtain the masses, as shown in TABLE 1A. First we match the observed masses in TABLE 1A with the protein entries available for bacteria, in the SWISS-PROT/TrEMBL databases (Sw/Tr db). We used ± 3 Da mass window to find the matches. We used each mass shown in TABLE 1A, turn by turn with ± 3 Da mass range to get the results. The result of the search gives us the names of the organisms and the mass of the protein entry corresponding to each match. We repeat this process for matching the observed masses in TABLE 1A with the mass specific bacterial matrix as described earlier. The results are summarized in TABLE 1B. The first column of this TABLE lists all the organisms with significant number of matches found with the protein entries in SWISS-PROT/TrEMBL database, as well as mass specific bacterial matrix. We have shown the matches with proteins from *vibrio cholerae* and *Bacillus halodurans* also. As described earlier, the organism with highest number of matches found is listed first and so on. Second and third column lists the total number of matches found corresponding to each organism, with the protein entries in SWISS-PROT/TrEMBL and mass specific bacterial matrix respectively. In the TABLE 1B, in the column for mass specific bacterial database, a symbol "/" is used corresponding to the organism for which no data has been compiled.

TABLE 1A
Observed masses in *B. subtilis* mass spectrum (Figure 2A Ref.1)

<u>3988</u>	<u>4506</u>	4947	<u>5247</u>	6098	6582	6664	<u>9888</u>
<u>4302</u>	<u>4877</u>	<u>4993</u>	<u>5892</u>	<u>6510</u>	<u>6623</u>	<u>7724</u>	

TABLE 1B
Ranking of organisms according to matched peaks in *B. subtilis* mass spectrum (Fig. 2 A Ref 16)

Name of the organism	No of matches SW/Tr db	No of matches - Mass specific db	Genome study complete	Total no. of protein entries from SW/Tr db
<i>B. subtilis</i>	11	9	Yes	4606
<i>E. coli</i>	7	3	Yes	9244
<i>Pseudomonas aeruginosa</i>	6	/	Yes	6998
<i>B. Burgdorferi</i>	6	3	yes	2231
<i>Vibrio cholerae</i>	5	2	yes	4460
<i>Bacillus halodurans</i>	5	/	yes	4237
<i>M. tuberculosis</i>	4	4	Yes	4355
<i>H. Pylori</i>	2	1	Yes	4166

We can discuss the example of *B.subtilis*. As shown in the TABLE 1B, the observed masses in TABLE 1A give 11 total matches with the protein entries in SWISS PROT/TrEMBL database corresponding to *B.subtilis*. This is higher number of matches than any other organism listed in this table. So *B.subtilis* ranks first. Same way as we see in the third column corresponding to *B.subtilis*, we have 9 matches for the protein entries for *B.subtilis* found in Mass specific Bacterial matrix. This is also the highest number for *B.subtilis* than any other organism listed in the TABLE 1B. So this ranks first with the mass specific bacterial matrix also. In TABLE 1A the masses corresponding to the first rank with respect to Sw/Tr (in this case: *B.subtilis*) is shown in Bold. The masses corresponding to the first rank with respect to mass specific bacterial matrix (in this case: *B.subtilis*) are underlined. As described earlier the mass specific bacterial matrix is made to eliminate any common entries of one bacteria with the rest of the bacteria belonging to the matrix. This may narrow down the ranking and help in better identification of the organisms with the help of protein database searches.

TABLE 1B also lists whether the genome study for that particular organism is complete or not. The total number of protein entries available in the SW/Tr database, corresponding to each organism, is also recorded as shown. This helps in determining the quality of ranking since the number of microorganisms whose proteomes are completely known is limited. Also the more is the number of protein entries, the more is the probability of a match, even if the protein entry may or may not be identical to the one in the experimental mass spectra. As we refer to TABLE 1B, *Bacillus subtilis* ranks first. The total number of matches corresponding to this organism in SW/Tr is 11. The second rank is *E.coli* with total number of matches of 7. At the same time the number of SW/Tr protein entries for *B.subtilis* is approximately half that for *E.coli*. This tells positive about this ranking. Again referring to this TABLE 2B we see that the total number of matches for the observed masses w.r.t mass specific bacterial matrix proteins, for *B.subtilis* is 9, and that for *E.coli* is 3. So the first ranking of *B.subtilis* over *E.coli* is improved in this case by using this relatively unique proteins for each organism. The ratio of matches for *B.subtilis* compared with *E.coli* is 3 while the same ratio for the Sw/Tr Database is 11/7. So the mass specific bacterial database clearly improves the ranking of *B.subtilis*.

We cannot assess the statistical overlapping in this case, as some of the organisms with large number of protein entries are showing less number of matches. But as the number of protein entries in the protein databases is being updated, we get more organisms with significant number of matches as is seen in table 1B for the protein matches from *Bacillus halodurans*, *Pseudomonas aeruginosa* and *vibrio cholerae*

CASE 2

This deals with the published MALDI mass spectra of the same organism, *E.coli*. A direct comparison of these mass spectra shows that they do not match with each other as is seen from the corresponding tables for the observed masses. But *E.coli* gets the first ranking in both of these two cases when their corresponding experimental mass spectra is matched with the protein data bases, as is seen below.

CASE 2.1: MALDI spectra of Escherichia coli (ATCC9637). Figure 1b of Ref. 5

As is seen in the TABLE 2.1B, *E. coli* has a first ranking. The second ranking corresponds to *B.subtilis*. The mass specific database did not help in this case in the better identification of *E. coli* as is seen in the TABLE 2.1 B. The *B.subtilis* matched protein entries in this case is 5 which is the same in number as those of *E.coli*. Also as is seen in TABLE 2B, selecting the +/-5 MW window does not help in better identifications, as the relative number of matches for the first and second rank remains similar.

TABLE 2.1A
Observed masses in *E.coli* mass spectrum (Figure 1b of Ref. 5))

<u>4362</u>	5076	<u>6255</u>	7708	9067	10464
<u>4711</u>	5752	<u>7272</u>	<u>8447</u>	9424	10760

TABLE 2.1B

Ranking of organisms according to matched peaks of *E. coli* mass spectrum (Fig 1b of ref. 5)

Name of the Organism	No of matches SW/Tr db (+/- 5 Da)	No of matches SW/Tr db (+/-3 Da)	No of matches - Mass specific db	Total no of protein entries From SW/Tr db	Genome study complete
<i>E.coli</i>	10	8	5	9244	Yes
<i>B.subtilis</i>	7	6	5	4606	Yes
<i>Vibrio cholerae</i>	7	6	None	4460	No
<i>H.Influenzae</i>	6	4	2	2035	Yes
<i>H. Pylori</i>	4	4	2	4166	Yes
<i>Rhizobium sp.</i>	4	2	/	/	No
<i>B. burgdorferi</i>	4	1	None	2231	Yes
<i>M.Leprae</i>	3	3	/	1538	No
<i>Synochoccus sp.</i>	3	3	/	/	No
<i>M. tuberculosis</i>	3	2	1	4355	Yes
<i>S. typhimurium</i>	3	3	/	1687	No

CASE 2.2: Direct MALDI mass spectra of E.coli (Figure 1a of Ref 6)

As is shown in the TABLE 2.2B the *E. coli* has a first ranking and recent update shows *vibrio cholerae* and *bacillus subtilis* are very close in matches to *E.coli*. The window of +/- 5 MW does not show any advantage over Window of +/-3MW. The rankings stay similar with the mass specific database, as shown in TABLE 2.2 B.

TABLE 2.2A

Observed masses in *E.coli* mass spectrum (Figure 1a of Ref 6)

3636	4532	6547	7333	9535	13093
4365	4769	7271	9061	9737	

TABLE 2.2B

Ranking of organisms according to matched peaks in *E.coli* mass spectrum (Figure 1a of Ref 6)

Name of the organism	No. of matches SW/Tr db (+/- 5 Da)	No of matches SW/Tr db (+/-3 Da)	No of matches - Mass specific db
<i>E.coli</i>	8	7	6
<i>B.subtilis</i>	6	6	5
<i>Vibrio cholerae</i>	7	3	None
<i>Bacillus halodurans</i>	6	4	/
<i>H. Pylori</i>	6		2
<i>Rhizobium sp.</i>	3	1	
<i>B. burgdorferi</i>	4	4	2
<i>H.Influenzae</i>	3	3	2
<i>Synechococcus sp.</i>	1	1	/
<i>M. tuberculosis</i>	2	1	1
<i>S. typhimurium</i>	3	1	/

CASE 3

The observed masses in case 3.1 and 3.2 are quite different as seen in the corresponding observed mass tables. These are two different samples studied at two different times. But as we will see in the tables 3.1 B and 3.2 B, *E.coli* gets a clear first rank when matched with protein entries in either the Sw/Tr database and mass specific bacterial database.

Case 3.1 : LC-ESI of *E.coli* 9637 TFA extract (REF 17, Table 2)

As we see in TABLE 3.1A, there are 49 mass entries. As is seen in TABLE 3.B *E.coli* gets a clear first rank with 37 mass entries matching with the protein entries in Sw/Tr database. 28 masses match with the protein entries in mass specific database as shown in TABLE 3.1B,. SW/Tr protein matches are shown from only six organisms having complete genome and proteome study. These were among the bacteria used to build the mass specific database as described earlier.

TABLE 3.1A
Observed masses in *E.coli* mass spectrum (Ref. 17, Table 2)

<u>1086.3</u>	<u>2138.0</u>	<u>3623.7</u>	<u>6253.9</u>	<u>7780.6</u>	<u>9263.5</u>	<u>10458.1</u>
1160.3	2374.3	3792.1	<u>6314.7</u>	<u>7854.4</u>	<u>9517.2</u>	<u>11223.0</u>
<u>1193.3</u>	2415.2	<u>4479.8</u>	6329.3	<u>9063.3</u>	<u>9535.3</u>	11296.0
<u>1214.5</u>	<u>2430.5</u>	<u>5035.7</u>	<u>7139.0</u>	<u>9190.7</u>	<u>9609.0</u>	<u>11780.5</u>
<u>1234.3</u>	2503.9	<u>5095.7</u>	<u>7271.1</u>	9208.1	<u>9683.0</u>	13092.9
2007.0	2734.9	5169.8	<u>7273.2</u>	<u>9225.4</u>	<u>9739.2</u>	<u>15692.3</u>
<u>2122.0</u>	3508.6	<u>5549.1</u>	<u>7706.3</u>	<u>9229.5</u>	<u>10385.1</u>	<u>15766.1</u>

TABLE 3.1 B
Ranking of organisms according to matched peaks in *E.coli* mass spectrum (Ref 17, Table 2)

Name of the organism	No of matches SW/Tr db	No of matches - Mass specific db
<i>E.coli</i>	<u>37</u>	<u>28</u>
<i>B.subtilis</i>	<u>18</u>	<u>13</u>
<i>M. tuberculosis</i>	<u>11</u>	<u>7</u>
<i>H. Pylori</i>	<u>9</u>	<u>6</u>
<i>B. burgdorferi</i>	<u>4</u>	<u>4</u>
<i>H. Influenzae</i>	<u>1</u>	<u>None</u>

Case 3.2: LC-ESI of *E.coli* (10 h incubation) (Ref 18 Table No. 6)

As we see in the TABLE 3.2 A there are total 43 mass species. Looking at TABLE 3.2B, *E.coli* gets a clear first ranking with 32 masses matching the protein entries in Sw/tr database and 27 mass entries matching the protein entries in the mass specific database. Mass specific database improves the ratio of

the number of protein matches of *E.coli* vs *B.subtilis*. In TABLE 3.2 B, SW/Tr protein matches are shown from only six organisms having complete genome and proteome study. As described earlier, these were among the bacteria used to build the mass specific database as described earlier.

TABLE 3.2 A
Observed masses in *E.coli* mass spectrum (Ref. 18 Table No. 6)

2429.1	6409.3	8876.2	9737.7	14099.9
2471.1	6412.8	8991.8	10298.2	15407.2
2980.0	6854.4	9062.2	11122.3	15690.8
4362.6	7269.7	9189.3	11184.4	16684.6
5018.0	7272.5	9224.6	11686.2	17513.2
5094.8	7331.2	9421.1	11779.2	18161.0
5379.1	7705.8	9534.3	11975.0	18771.4
6253.2	7867.3	9538.8	12768.5	
6314.1	8324.2	9551.9	13126.3	

TABLE 3.2 B
Ranking of organisms according to matched peaks in *E.coli* mass spectrum (Ref 18 Table6)

Name of the organism	No of matches SW/Tr db	No of matches - Mass specific db
<i>E.coli</i>	32	27
<i>B.subtilis</i>	19	14
<i>H. Pylori</i>	9	7
<i>M. tuberculosis</i>	7	2
<i>H. Influenzae</i>	4	4
<i>B. burgdorferi</i>	4	4

CASE 4.

LC-ESI of *E.coli*, 6 h incubation (Ref. 18 Table 2)

This has total 18 mass entries. As we see there is some variation in the masses when compared to 10 hrs incubation as seen in TABLE 3.2 A. But as we see in the Table 4B *E.coli* has a clear 1st ranking over the next one that is *B.subtilis*. There were 16 matches with protein database entries for *E.coli*. Mass specific database does not seem to have any significant effect in improving the ranking in this case as shown in TABLE 4B. In TABLE 4.2 B, SW/Tr protein matches are shown from only six organisms with complete genome and proteome study as described earlier.

TABLE 4A
Observed masses in *E.coli* mass spectrum -6 h incubation, (Ref. 18, Table 2)

<u>2329.5</u>	<u>5018.5</u>	<u>7331.5</u>	<u>11778.9</u>
<u>2370.5</u>	<u>5379.2</u>	<u>7868.7</u>	<u>15691.0</u>
<u>2980.1</u>	<u>6314.2</u>	<u>9224.6</u>	<u>17513.5</u>
3791.2	<u>6409.2</u>	<u>9534.0</u>	
<u>4362.5</u>	<u>7270.2</u>	<u>11184.1</u>	

TABLE 4B
Rankings of organisms according to matched peaks in *E.coli* mass spectrum (Ref 18, Table 2)

Name of the organism	No of matches SW/Tr db	No of matches - Mass specific db
<i>E.coli</i>	16	16
<i>B.subtilis</i>	7	6
<i>H. Pylori</i>	5	4
<i>B. burgdorferi</i>	3	2
<i>M. tuberculosis</i>	2	1
<i>H. Influenzae</i>	1	1

CASE 5

The purpose of this case is to show the limitations of this method by ranking the organisms according to matched peaks of *C.Freundi* and *B.magnaterium* spectra. This is true that very few protein entries for these organisms are known on the database, due to the incomplete study of their genomes. So not any significant matches for these organisms are expected on the Sw/Tr protein database. But we see large no. protein matches for *E.coli* as shown below. About 9000 protein entries for *E.coli* are there on the Sw/Tr database. This includes redundant protein entries. Though it is difficult to be certain, many of these matches may be the result of the statistical overlap.

Case 5.1: LC-ESI of *B. megaterium* TFA extract (Ref 17, Table 3)

As shown in the TABLE 5.1B there are 41 matched protein entries for *E.coli* out of a total of 50 mass entries. This indicates the magnitude of statistical limitations of, protein database searches approach for Bacterial identification. The matched Protein entries for *E.coli* are reduced to 26 with mass specific database. In TABLE 5.1 B, SW/Tr protein matches are shown from only six organisms having complete genome and proteome study as described earlier.

TABLE 5.1A
Observed masses in *B.megaterium* mass spectrum (Ref. 17, Table 3)

<u>1193.3</u>	6274.7	<u>7109.7</u>	7709.5	<u>9766.8</u>	<u>11611.3</u>
<u>1231.3</u>	<u>6314.5</u>	<u>7156.4</u>	<u>9330.5</u>	<u>9827.5</u>	<u>11725.3</u>
<u>1350.2</u>	6334.7	<u>7278.7</u>	<u>9334.0</u>	<u>9883.1</u>	<u>12044.9</u>
<u>3046.5</u>	<u>6351.1</u>	7423.9	9348.2	<u>10024.6</u>	12118.9
<u>3185.9</u>	<u>6388.0</u>	<u>7450.4</u>	9351.4	<u>10043.7</u>	<u>12406.7</u>
<u>4378.2</u>	<u>6391.7</u>	<u>7452.5</u>	9619.1	<u>10451.6</u>	
<u>4740.1</u>	<u>6447.7</u>	<u>7465.9</u>	<u>9692.9</u>	<u>10695.4</u>	
<u>4815.3</u>	<u>6576.6</u>	<u>7518.3</u>	9746.4	<u>11061.9</u>	
6260.9	<u>6896.3</u>	7647.9	<u>9753.0</u>	<u>11537.0</u>	

TABLE 5.1B

Ranking of organisms according to matched peaks in *B. megaterium* mass spectrum. (REF 17, Table 3)

Name of the organism	No of matches SW/Tr db	No of matches - Mass specific db
<i>E.coli</i>	<u>41</u>	<u>26</u>
<i>B.subtilis</i>	<u>20</u>	<u>10</u>
<i>M. tuberculosis</i>	<u>18</u>	<u>7</u>
<i>B. burgdorferi</i>	<u>16</u>	<u>3</u>
<i>H. Influenzae</i>	<u>8</u>	<u>7</u>
<i>H. Pylori</i>	<u>6</u>	<u>4</u>

CASE 5.2 : LC-ESI of *C.Freundi* TFA extract (Ref 17, Table 4)

There are 46 observed masses in the experimental ESI mass spectrum. Out of these 46 mass entries, 26 protein matches are found for *E.coli* in the SW/Tr database.

CONCLUSIONS

Most of the matches found for examples of *B.subtilis* and *E.coli* were good. In a number of cases discussed, a direct comparison of published mass spectra of the same organism; *E.coli*, showed that there was variation between each other. However searching the proteome database, for masses observed in each spectrum, leads to the positive identification of the bacteria, in each case. This was true of cases involving the use of MALDI TOF as well as ESI mass spectrometry. In a case that deals with LC-ESI of *B.megaterium*, we see that there are 41 matches found for *E.coli* corresponding to 50 mass entries matched from the experimental mass spectra of *B.megaterium*. Even though at this time very few protein entries for this organism are available it gives the magnitude of statistical limitations of this approach. Also eliminating the common protein entries from the different organisms may in some cases improve this approach for biological identification, using mass spectrometry and protein database searches. More bacteria with complete genome and proteome study can be included in compiling the database for relatively unique proteins for different bacteria. So the biological identification of organisms with the help of mass spectrometry and database searches can provide a complement to fingerprint method presently used. More insight into this method will be known as more and genomes and proteomes for various organisms are known. That will unfold more statistical limitations of this method as well.

REFERENCES

1. Anhait J.P; Fenselau. C. Anal. Chem. 1975. 47. 219-225
2. Heller. D; Fenselau. C; Cotter R; Demirev P; Olthoff J; Uy. M; Tanaka T; Kishimoto. Y. *Biochem. Biophys. Res. Commun.* 1987, 142. 194-199.
3. . Krishnamurthy, T.; Ross, P.; Rajamani, U. *Rapid Commun. Mass Spectrom.* 1996, 10, 883-888.
4. Arnold, R.; Reily, J. *Rapid Commun. Mass spectrum.* 1998, 12, 630-636.
5. Wang, Z.; Russon, I.; Li, L.; Roser, D.; Long, S.R. *Rapid Commun. Mass. Spectrum.* 1998, 12, 456-464.
6. . Dai, Y.; Li, L.; long, S.R. *Rapid Commun. Mass Spectrum.* 1999, 13, 73-78
7. Krishnamurthy, T.; Davis, M.T.; Stahl, D.C.; Lee, T.D. *Rapid Commun. Mass Spectrom.* 1999, 13, 39-49.

8. Arnold, R.; Reily, J. *A Study of Bacterial Culture Growth By MALDI-MS of Whole Cells*; Proceedings of the 46th ASMS Conference on Mass Spectrometry and Allied Topics. Orlando, Fl. May 31-June 4, 1998; p 180.
9. Henzel, W.; Billeci, T.; Stults, J.; Wong, S.; Grimley, C.; Watanabe, C. *Proc. Natl. Acad. Sci. U.S.A.* 1993, 90, 5011-5015.
10. Mann, M.; Hojrup, P.; Roepstorff, P. *Biol. Mass. Spectrom.* 1993, 22, 338-345.
11. Pappen, D.; Hojrup, P.; Bleasby, A. *Curr. Biol.* 1993, 3, 327-332
12. James, P.; Quadroni, M.; Caratoli, E.; Gonnet, G. *Biochem. Biophys. Res. Commun.* 1993, 195, 58-64
13. Yates, J. R. III; McCormick, A; Eng, J. *Anal. Chem.* 1996, 68, 534A-540A.
14. Fenyo, D.; Qin, J.; Chait, B. *Electrophoresis* 1998, 19, 998-1005.
15. (a). prospector.ucst.edu, www.proteometrics.com. (b) www.mann.enbl.embl-heidelberg.de/services/PeptideSearch. (C) cbrg.inf.ethz.ch/MassSEarch.html expasy.hcuge.ch. (d) www.seqnet.dl.ac.uk/mowse.html
16. Demirev, P.A.; HO, Y.; Ryzhov, V.; Fensalau, Catherine. *Anal. Chem.* 1999, 71, 2732-2738
17. Liang, Li. LCMSBacteria report submitted to Edgewood Chemical Biological Center, 12, 1999.
18. Dunlop, Kevin.; Liang, Li. Report submitted to ECBC, APG MD, 8, 2000.

ADVANCEMENTS IN DETECTION CAPABILITIES AND DATA ANALYSIS WITH THE IMPROVED PYROLYSIS GAS CHROMATOGRAPHY-ION MOBILITY SPECTROMETER BIODETECTOR

Ashish Tripathi¹, Waleed Maswadeh¹, Philip A. Coon² and A. Peter Snyder²

1- Geo Centers Inc, P. O. Box 68, Gunpowder Branch, APG, MD 21010

2- SBCCOM, U. S. Army, Gunpowder Branch, APG, MD 21010

ABSTRACT

Pyrolysis-gas chromatography-ion mobility spectrometry (Py-GC-IMS) is a biological point detection device, developed by Edgewood Chemical Biological Center (ECBC) at U.S. Army Edgewood Area Aberdeen Proving Grounds.

The Py-GC-IMS can be described as a pyrolysis based biological agent detector, which employs a gas chromatography column to resolve the gaseous pyrolyzate into its constituent components and a standard U.S. Army Improved Chemical Agent Monitor (ICAM) to detect the separated components. Because the ICAM is a proven chemical agent detector, Py-GC-IMS can also be used as a chemical agent detector.

Recently, Py-GC-IMS was field tested at the Joint Field Trials VI (JFT VI). These trials were held at Defense Research Establishment Suffield (DRES), Medicine Hat, Alberta, Canada. The trials were administered during the daytime. *Bacillus globigii* (v. niger), MS-2 bacteriophage virus, *Erwinia herbicola* and Ovalbumin were used as biological agent simulants. Some interferents were also used. During the trials, test windows varied from 45 min to 180 min. During a test window a particulate dissemination was performed (start time, nature and duration of dissemination were hidden from participants). The trial participants were required to report the nature of biological agents disseminated, time of detection and duration of biological dissemination. During a test window, at the digressions of test directors, multiple dissemination of the same or different biological simulants were performed.

Contrasting the JFT VI with JFT IV (held in Dugway Proving Grounds) where only BG spores and *E. herbicola* vegetative bacteria were sprayed (never sprayed together), it became imperative to upgrade the detection capabilities and data analysis to accommodate for four biological simulants, which may or may not be disseminated together. To achieve this objective, the requirement is that in the Py-GC-ion mobility data space each of these biological simulants should produce at least one unique peak. That is to say, if a biological simulant A produces a unique peak A in the data space, whenever that peak A is found (irrespective of numerous other peaks not specific to simulant A), it can be ascertained with high confidence that simulant A was detected. Such a requirement was satisfied for all the four agents used in JFT VI, by incorporating a flow-through pyrolyzer, which greatly reduces secondary degradation of pyrolyzate and critical adjustments of various pneumatic flows within the Py-GC-IMS system.

This poster presents the improvements in detection of the four agents (compared to two in JFT IV) and their unique Py-GC-IMS patterns. This is the first step for a fully automated and largely simplified data analysis.

INTRODUCTION

The requirement for classification/detection of the four simulants namely, *Bacillus globigii* (v. niger), *Erwinia Herbicola*, MS-2 bacteriophage virus and Ovalbumin, is that the pyrolyzate biomarker for each of the simulant should have at least one detectable component unique to that agent. That is, each simulant should have at least one unique peak in the pyrolysis-gas chromatography-ion mobility data space. To achieve this objective, the pyrolysis step should be executed in order to yield as much of

primary pyrolysis products (defined as the very first generation of pyrolysis products formed at the start of pyrolysis) as the Py-GC-IMS instrument allows.

Elution and capture of primary pyrolysis product in itself is not sufficient. The pyrolyzate should be resolved into its constituents moieties with the use of a fast gas chromatography system. The resolution of pyrolyzate into its constituents is imperative for many reasons, most important of which is the use of Improved Chemical Agent Monitor (ICAM), an ion mobility spectrometer (IMS). Since IMS produces non-linear response from ions, also multiple components simultaneously entering the IMS cell compete for ionization and tend to produce mixed response, which is different from their individual responses. Therefore, it becomes imperative that at a given time only one pyrolyzate constituent enter the IMS cell.

These are the two parts of Py-GC-IMS instrument (shown in Figure 1) where improvements are made. The effect of these improvements is used to compare with the earlier version of the instrument as described elsewhere (1).

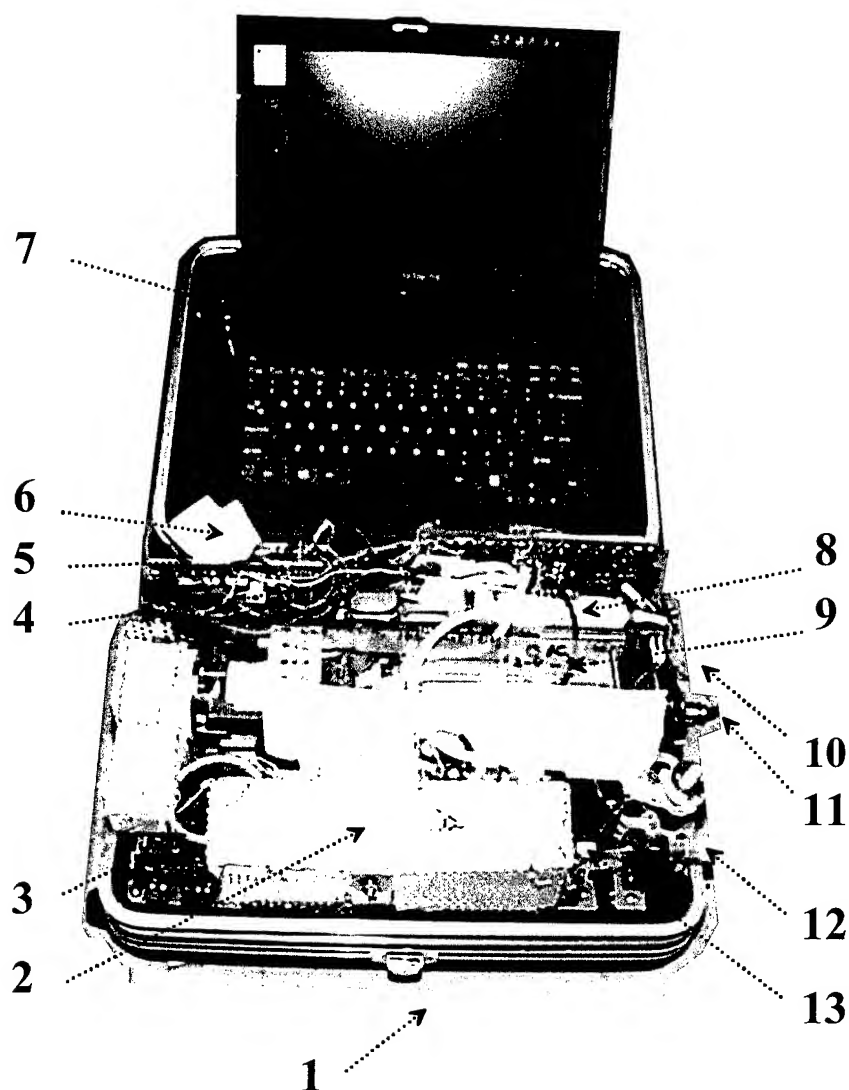
APPROACH

Improvements in Pyrolyzer Design

The process of pyrolysis can be viewed as series of two processes. The first process involves the thermal decomposition of the pyrolysis sample (be it liquid or solid) into vapor phase moieties (called pyrolyzate). The first process is a heterogeneous process. This step is followed by removal of pyrolyzate from the hot pyrolysis region. The second process is a homogeneous process occurring in gaseous phase. If the gaseous pyrolyzate is not removed from hot pyrolyzate, it starts to undergo secondary degradation into low molecular weight moieties. Additional degradation of pyrolysis products adds complexity in identification of the parent source of the daughter products. Figure 2 shows the process of pyrolysis as applied to dipicolinic acid (a highly labile biomarker of Gram positive bacterial spores). As the process of secondary degradation continues dipicolinic acid decomposes into picolinic acid and finally pyridine. The process of secondary degradation of pyrolysis products was investigated. A direct probe pyrolyzer (CDS pyroprobe) was modified to allow for flow of air through the quartz tube pyrolyzer (as shown in Figure 3). The pyrolyzate eluting from the pyrolyzer was introduced directly into the corona discharge ionization region of a triple quadrupole mass spectrometer (APCI III from Perkin Elmer). The pyrolyzer was set to reach a temperature of 500 °C in five seconds. A 0.2 µl aliquot of 1 mg/ml aqueous solution of DPA was deposited on the quartz wool. The sample was pyrolyzed. Multiple pyrolysis runs were performed while only changing the airflow rate through the pyrolyzer. Figure 4 shows the effect of change of airflow rate through the pyrolyzer on dipicolinic acid (DPA) pyrolysis. As the sweep airflow rate is reduced from 36 ml/min to 0 ml/min the DPA pyrolysis product distribution changes from being only DPA to only pyridine. The reason is that as the flow rate of air is increased through the pyrolyzer, the air sweeps the air borne pyrolyzate faster and thereby reducing the residence time of pyrolyzate in the heated pyrolysis region and thus reducing the secondary degradation. The same principal is applied to the quartz tube pyrolyzer, where at the time of maximum pyrolyzate formation the flow through the pyrolyzer tube is increased to 40 ml/min.

Another improvement made was to increase the heating rate of pyrolyzer such that it reaches a temperature of 350 °C in less than four seconds. The advantages of using higher heating rate pyrolyzer for Py-GC-IMS system are as follows:

1. Py-GC-IMS is a point detection field instrument. Therefore, it is designed to work with multiple biological samples. Since different samples reach their maximum pyrolysis degradation temperature (T_{MAX}) at different temperatures, it becomes imperative that these T_{MAX} occur within a short span of time (Time span within which the T_{MAX} occur = Δt_{TMAX}). Essentially Δt_{TMAX} should be shorter than the time it takes to inject the pyrolyzate into the GC-column (injection time = t_{inj})



1- 12 x 9 x 5 inch carrying case; 2- high temperature 3-way GC-injection valve and pump connection to draw aerosol particulate onto the quartz filter; 3- programmable GC ring; 4- diaphragm vacuum pump; 5- electronic control boards; 6- 50-pin interface to PCMCIA data acquisition card; 7- Hitachi mini-notebook with Data acquisition card (PCMCIA) from National Instruments; 8- molecular sieve packs; 9- voltage-gated ion source and ion mobility spectrometer components of airborne vapor monitor (AVM) (Graseby-Dynamics, Watford, Herts, UK); 10- coaxial cable for Ethernet/serial PC card communications; 11- DC power in; 12- aerosol inlet; 13- pyrex filter aerosol collector in a quartz tube/pyrolysis source.

Figure 1. The lunchbox version of Py-GC-IMS system.

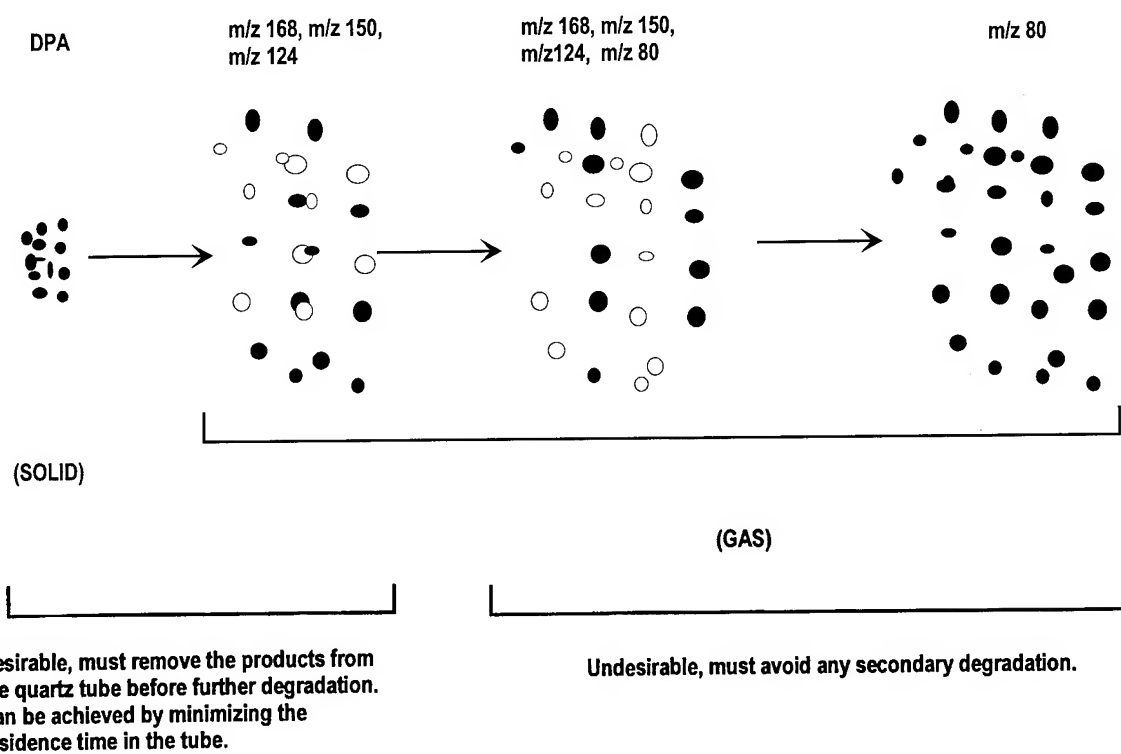


Figure 2. The two process involved in pyrolysis. Notice that as the second step is prolonged the product distribution is altered.

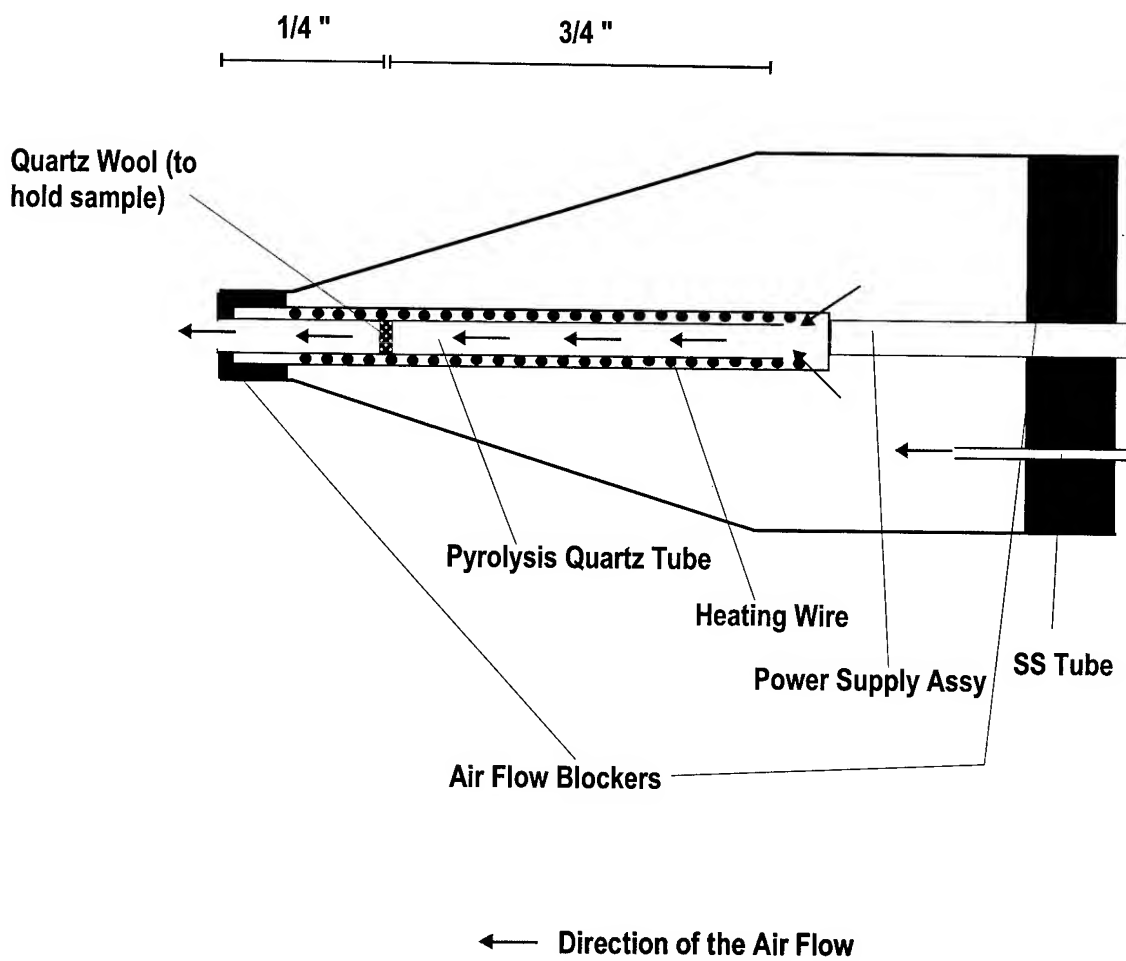


Figure 3. The modified CDS pyroprobe that allows air to flow through the quartz tube pyrolyzer.

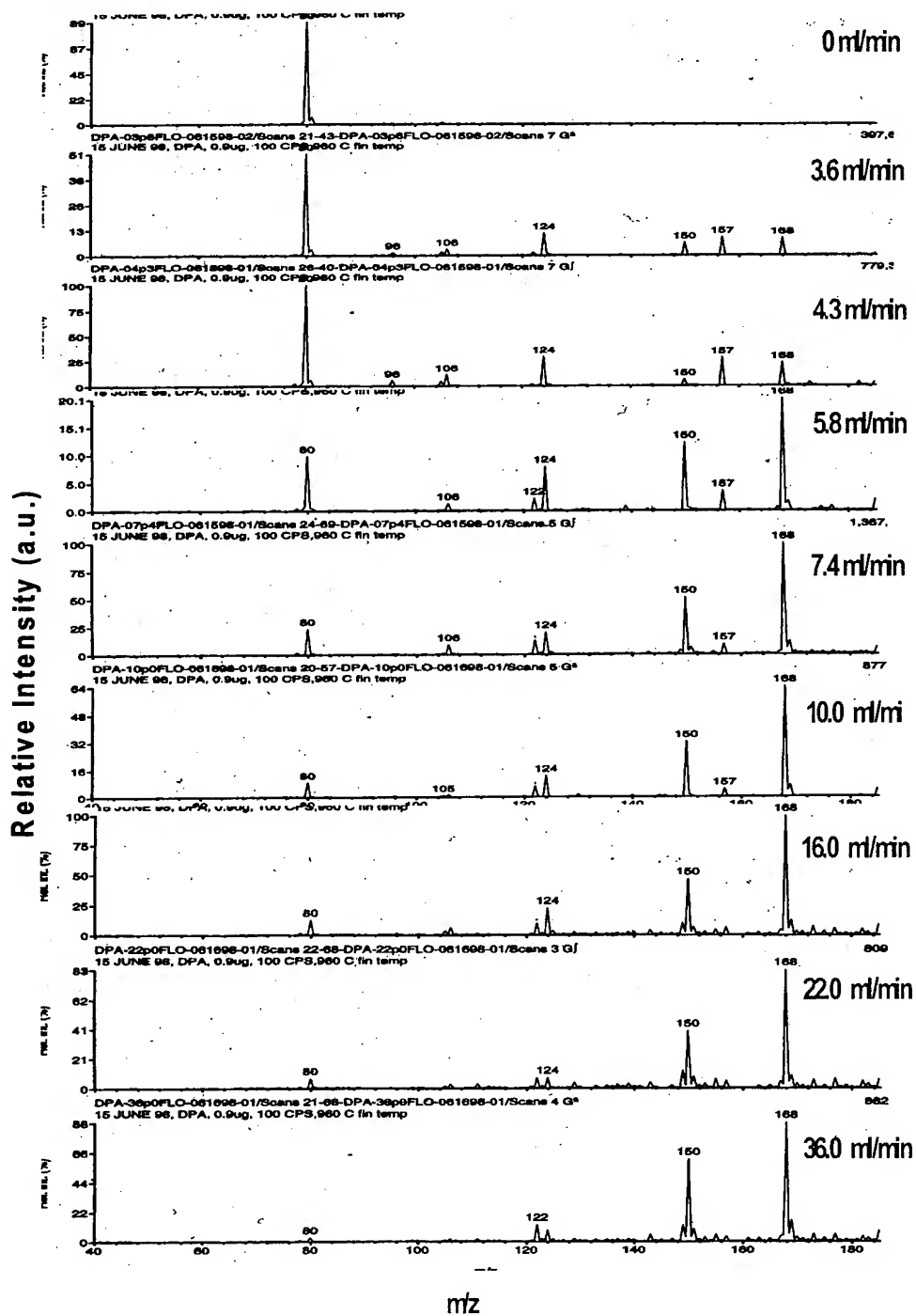


Figure 4. Effect of sweep airflow rate on DPA pyrolysis.

$$t_{inj} > \Delta t_{TMAX}$$

If the above condition is not met then Py-GC-IMS will not be able to detect all the target analytes with one instrument setting, because while one of the target analyte will elute pyrolyzate within the time of injection, other may elute its pyrolyzate outside the time of injection.

2. The faster the pyrolysis is brought about, the lesser the extent of time the pyrolysis sample spends at high temperature, therefore lesser the extent of secondary degradation in solid phase.
3. The faster the pyrolysis, the shorter the time duration in which pyrolyzate elute, thereby increasing the peak height of the pyrolyzate in intensity scale. This increases the system sensitivity

Two-Step GC Heating

The Py-GC-IMS system described by Snyder et al (1) was set up such that the GC column was heated in a linear heating rate from 40 °C to 140 °C at 120 C/min. Figure 5a shows the time-temperature profile for the GC column. The advantage of such a heating rate is primarily a shorter processing time. The disadvantage is that while all the useful chemical information is obtained within first 27 sec, most of the useful information is obtained in first 20 seconds. The injection into the GC- column is at eight seconds from the start. From this perspective of all the useful information is contained in 20 seconds space of a data space, which is 50 seconds long. That means that more than half the portion of the data space is being not used. To elucidate the above explanation consider Figure 5b, which shows typical BG, spore Py-GC-ion mobility spectra. It is evident that most of the Py-GC-IMS data space is not being utilized. There is another undesirable side effect that results from this setup. Since most of the chemical species are eluted from the GC-column within a span of 20 seconds there competition for protons in the ionization region of IMS causes a merging effect on peaks, making them difficult, if not impossible, to be resolved from one another. This adds another degree of non-linearity in detection. To side step this undesirable setting, GC-Column was setup in a way that it maintains a temperature of 40 °C for the first 12 seconds after which it ramps up to a temperature of 140 °C at a heating rate of 150 C/min. This, essentially, is a *two-step GC-column* heating procedure. The heating rate is profiled in Figure 6a. The point of injection occurs at GC-Column temperature of 40 °C (compared to 66 °C for the single step ramp heating). The less polar species are show improved resolution by GC-column. Figure 6b shows the Py-GC-ion mobility spectra of B. G Spore obtained with two-step heating of the GC-column. Comparing Figure 6b with Figure 5b, it is clear that peak resolution is improved considerably with two-step heating because the last useful peak is observed at 37 seconds mark. More importantly, the improved resolution of less polar peaks in retention time, reduces the non-linear effects of overlapping components.

RESULTS AND DISCUSSION

The four simulants

In the JFT VI the four biological simulant used are: *Bacillus globigii* (v. niger) spore, Ovalbumin, MS-2 bacteriophage virus and *Erwinia herbicola* (in 1 % sucrose solution). After incorporating the outlined improvements into the Py-GC-IMS system a database library was developed by multiple pyrolysis of these four simulants.

Figure 7 shows the Py-GC-ion mobility data space of 1 µg of BG spore. It is observed that there are peaks found in peak space marked 1, 2 and 3. Peak 1 is the response of Py-GC-IMS system to picolinic acid (a degradation products of DPA, which is found as calcium salt in the cell wall structure of Gram positive bacterial spores). Peaks 2 and 3 share a monomer and dimer relationship. The chemical source of peaks 2 and 3 are yet to be investigated. No detectable peak activity is detected in areas marked 4, 5, 6, 7 and 8.

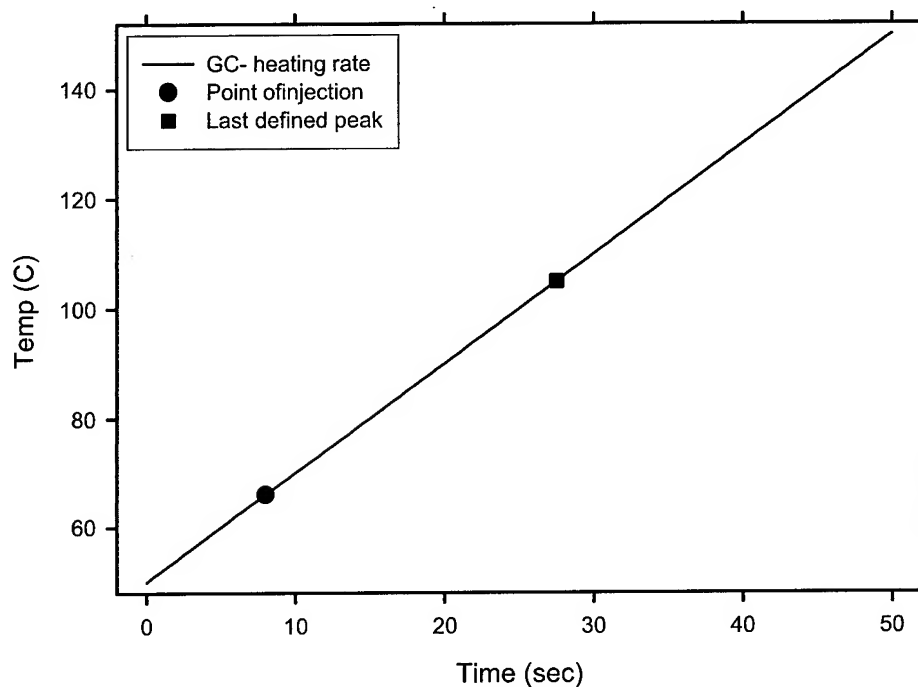


Figure 5a. The time-temperature profile of the GC column. The GC column is heated from 40 to 140 C @ 120 C/min. Notice that the point of injection (big circular dot) and the point where last recognizable peak was detected (big square dot) are only about 20 seconds apart. In a dataspace, which is about 50 seconds wide, only 40 % is being utilized for any meaningful purpose.

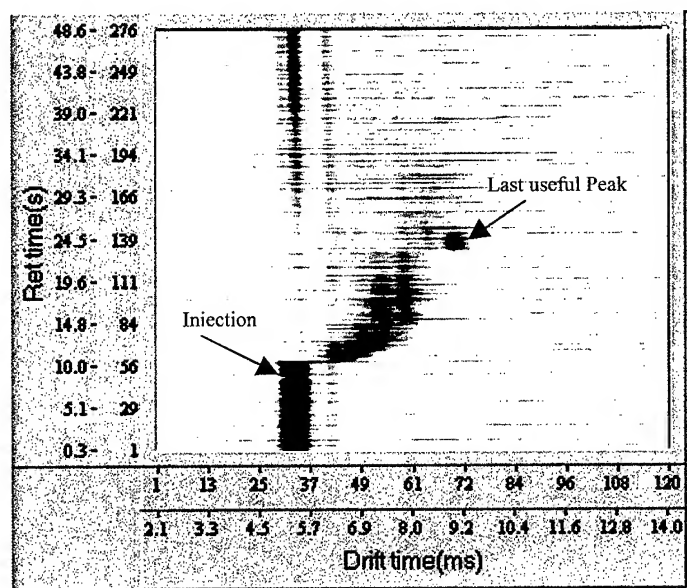


Figure 5b. BG Spore Py-GC-ion mobility spectra. Notice all of the useful data is obtained before 30-second mark in the GC-retention time.

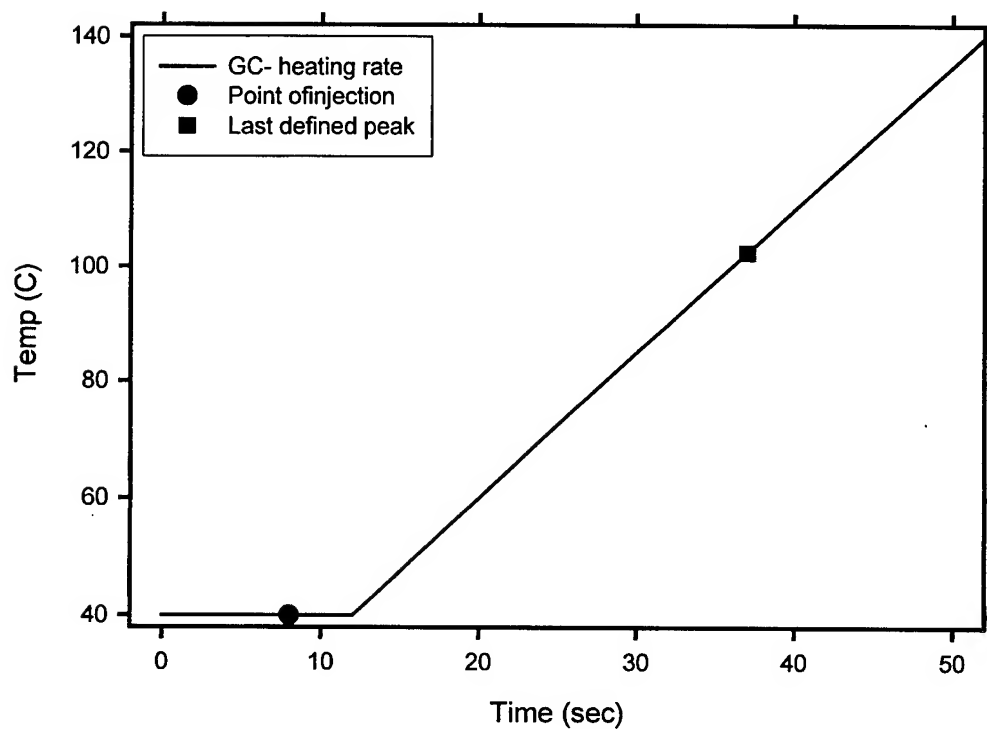


Figure 6a. The time-temperature profile of the GC column. Notice that the point of injection (big circular dot) and the point where last recognizable peak was detected (big square dot) are now about 30 seconds apart.

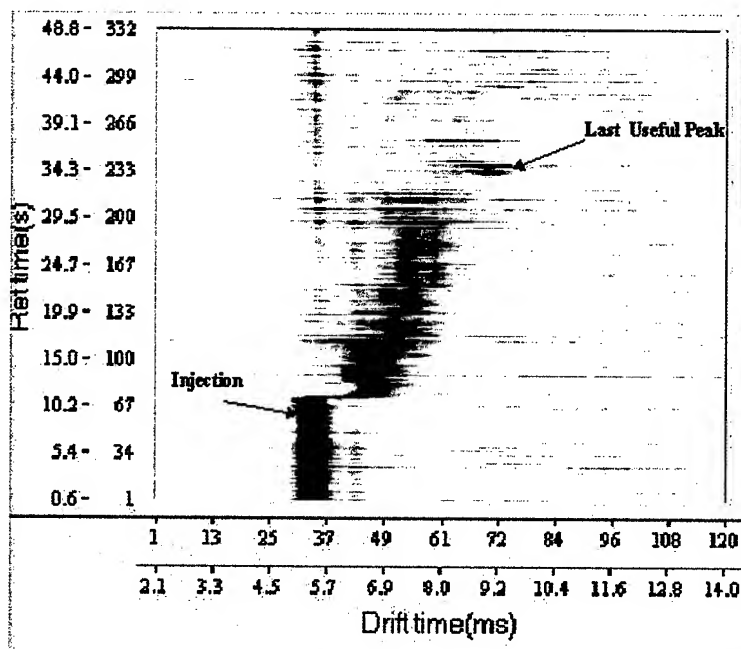


Figure 6b. BG Spore Py-GC-ion mobility spectra obtained with two-step GC heating. Notice that "last useful peak" has now shifted to 35-second mark compared to 25 seconds with high heating of GC-column (Figure 5b)

1 μ g *Bacillus Globii* (v. niger) Spore

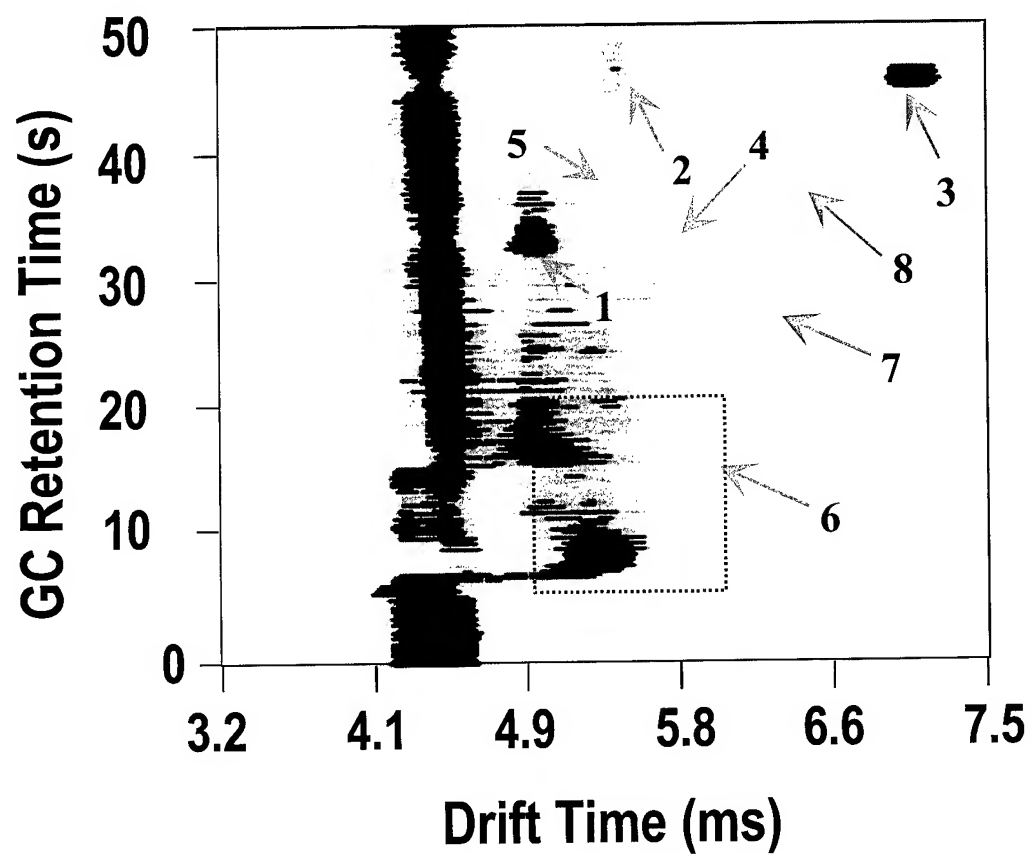


Figure 7. The Py-GC-IMS data space of BG spore. Notice that peak activity is observed in peaks marked 1, 2 and 3.

Figure 8 shows the Py-GC-ion mobility data space of 1 μ g of MS-2 bacteriophage virus. Notice that there is peak activity observed in areas marked 4 and 5 (chemical makeup of these peaks are unknown at present, but is under investigation). However, unlike BG spore no detectable activity is found in peak areas marked 1, 2 and 3 and like BG spore no activity is detected in areas marked 7, 8. Therefore, MS-2 bacteriophage virus can easily be differentiated from BG spore.

Figure 9 shows the Py-GC-ion mobility data space of 1 μ g of ovalbumin protein. Like MS-2 bacteriophage virus there is peak activity found in areas marked 4 and 5. Added to that there is peak activity found in region 6. The differentiation between MS-2 bacteriophage virus and ovalbumin can be obtained based on activity in region marked 6. The reason for similarity of the Py-GC-ion mobility data space of MS-2 bacteriophage virus and ovalbumin could be related to high protein content in both. It is also observed that no activity is detected in areas 1, 2, 3, 7 and 8.

Figure 10 shows the Py-GC-ion mobility data space of 1 μ g of *Erwinia herbicola* pyrolyzed with 1 μ g of sucrose. The reason for adding sucrose is that at JFT VI trials *Erwinia herbicola* is sprayed in 1 % sucrose solution. There is peak activity observed in region marked 7 and 8. However, unlike BG, ovalbumin and MS-2 bacteriophage virus no activity is detected in regions marked 1, 2, 3, 4, 5 and 6.

Examining the four Py-GC-IMS data spaces, it is possible to construct a simple logic chart that differentiates between the four data space. Such a logic chart is depicted in Table 1.

Table 1. The peaks loading of the four biological simulants.

<i>Simulant</i>	Peak 1	Peak 2	Peak 3	Peak 4	Peak 5	Peak 6	Peak 7	Peak 8
BG Spore	Yes	Yes	Yes	No	No	No	No	No
MS-2	No	No	No	Yes	Yes	No	No	No
Ovalbumin	No	No	No	Yes	Yes	Yes	No	No
EH	No	No	No	No	No	No	Yes	Yes

The effect of advancements on Py-GC-IMS system

The advancements made in the pyrolysis step and GC separation step provides ample support to start investigating the possibility of fully automated data analysis. A starting point would be to calculate peak areas in the regions marked 1 through 8 and used these numbers for a multivariate analysis based factorial analysis and investigate if a factorial separation can be obtained. That is one of the planned investigations for the upcoming year. The results of such an investigation will be field-tested.

The effect of advancements made can be seen on a comparative study between before and after the advancements. Figure 11 shows the comparison between BG spore Py-GC-IMS data space as reported by Snyder et al (1) before the advancements and after the advancements. Clearly the Py-GC-ion mobility data space of BG spore had better resolved and richer peak loadings than before. Similarly, the comparison of *Erwinia herbicola* Py-GC-ion mobility data spaces before and after the advancements reveals improved peak details in the first 30 seconds of GC retention time while adding peak loadings after 30 second retention time(as shown in Figure 12).

CONCLUSIONS

Advancements in the pyrolysis steps show that more detectable pyrolyzate components can be obtained from a fast heating flow through pyrolyzer because of reduction of secondary degradation and sharper pyrolyzate elution, which improves instrument sensitivity. The two-step gas chromatography column heating provides an improved retention-time resolution over the 50 seconds data space than one-step GC heating. One set of instrument operation condition provides four distinct Py-GC-ion mobility data spaces for the four simulants. It is now possible that an automated data analysis procedure can classify the four simulants based on targeted peak loadings.

1 μ g MS-2 Bacteriophage Virus

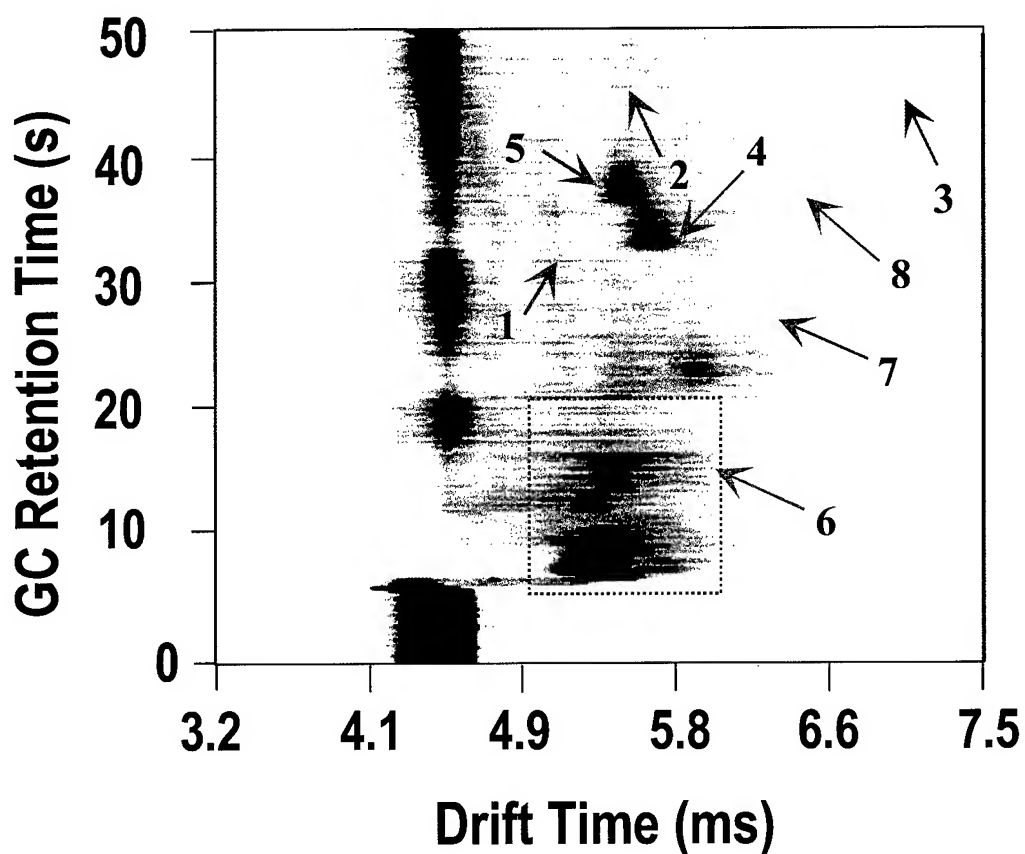


Figure 8. The Py-GC-IMS data space of MS-2 bacteriophage virus. Notice that while no detectable peak activity is observed in peaks marked 1, 2 and 3, there is peak activity in areas marked 4 and 5.

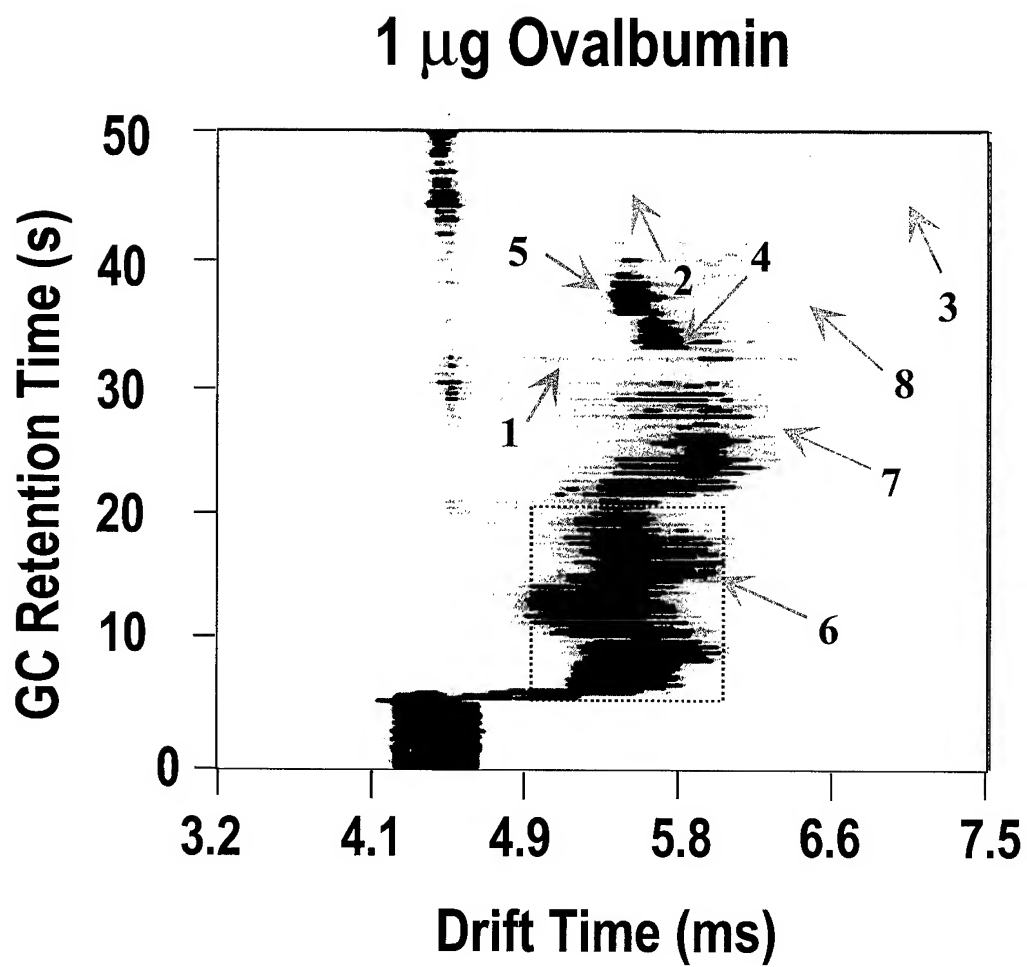


Figure 9. The Py-GC-IMS data space of ovalbumin protein. Notice that while no detectable peak activity is observed in peaks marked 1, 2 and 3, there is peak activity in areas marked 4, 5 and 6.

1 μg *Erwinia Herbicola* + 1 μg sucrose

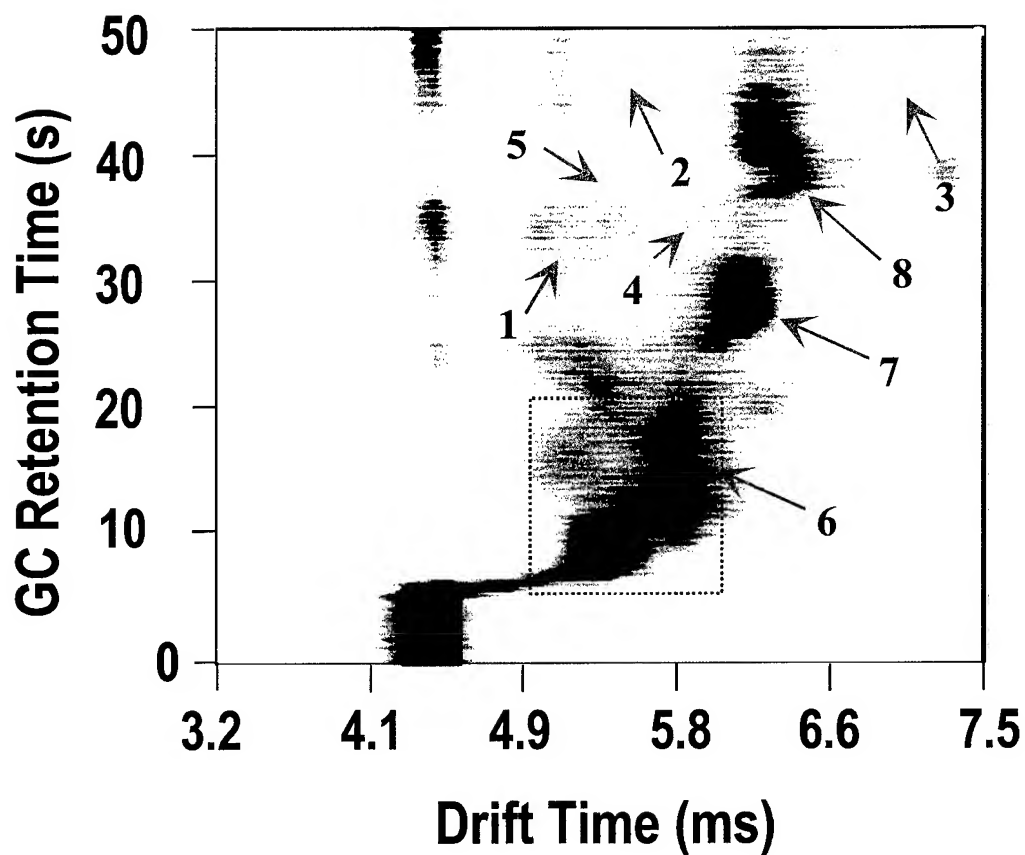


Figure 10. The Py-GC-IMS data space of *Erwinia herbicola* in sucrose. Notice that while no detectable peak activity is observed in peaks marked 1, 2 and 3, 4, 5 and 6, there is peak activity in areas marked 7 and 8.

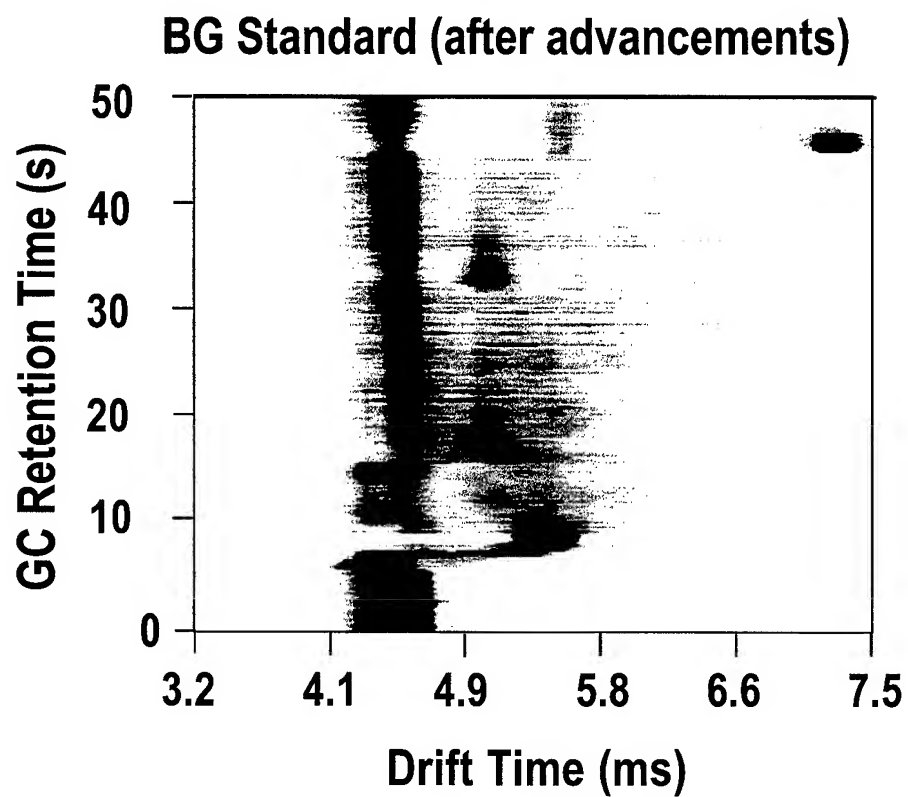
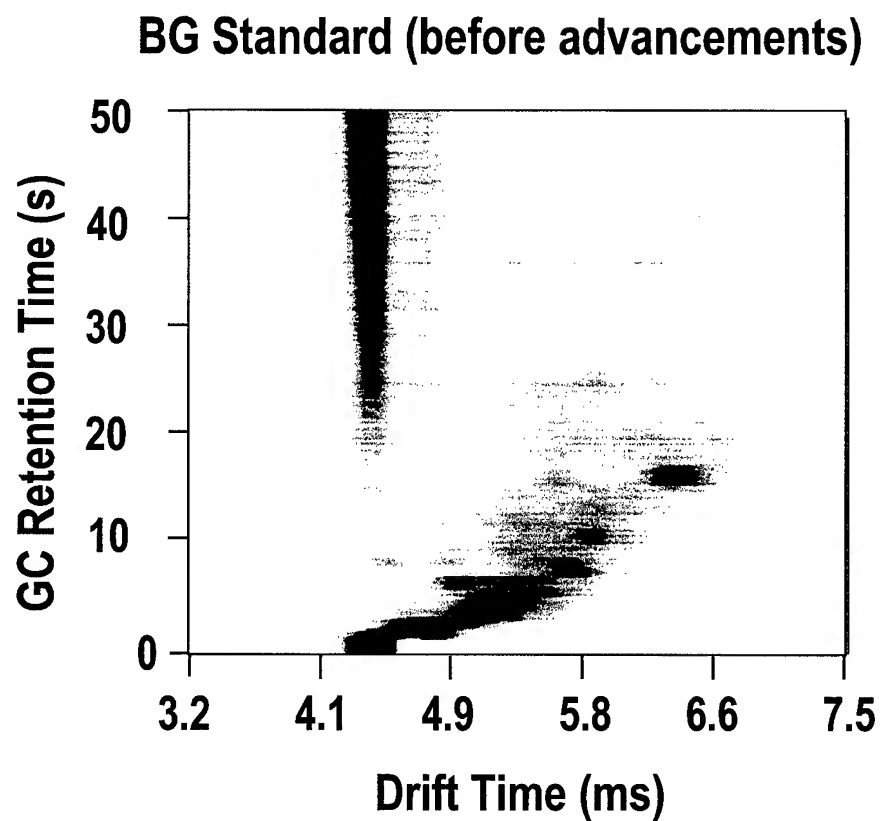


Figure 11. Comparison between Py-GC-ion mobility data space of BG spore before and after the advancements.

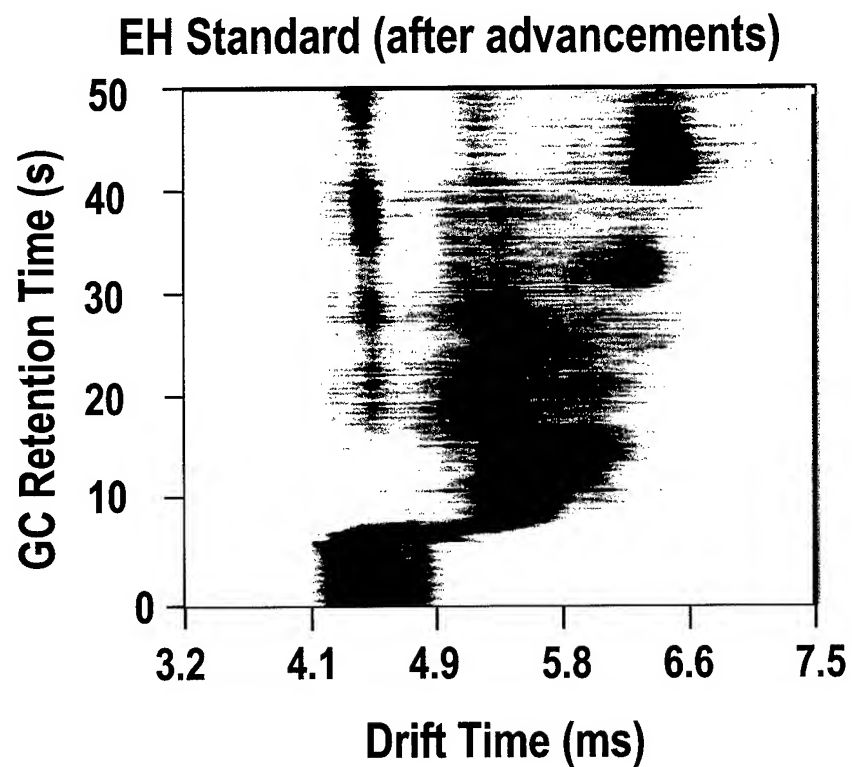
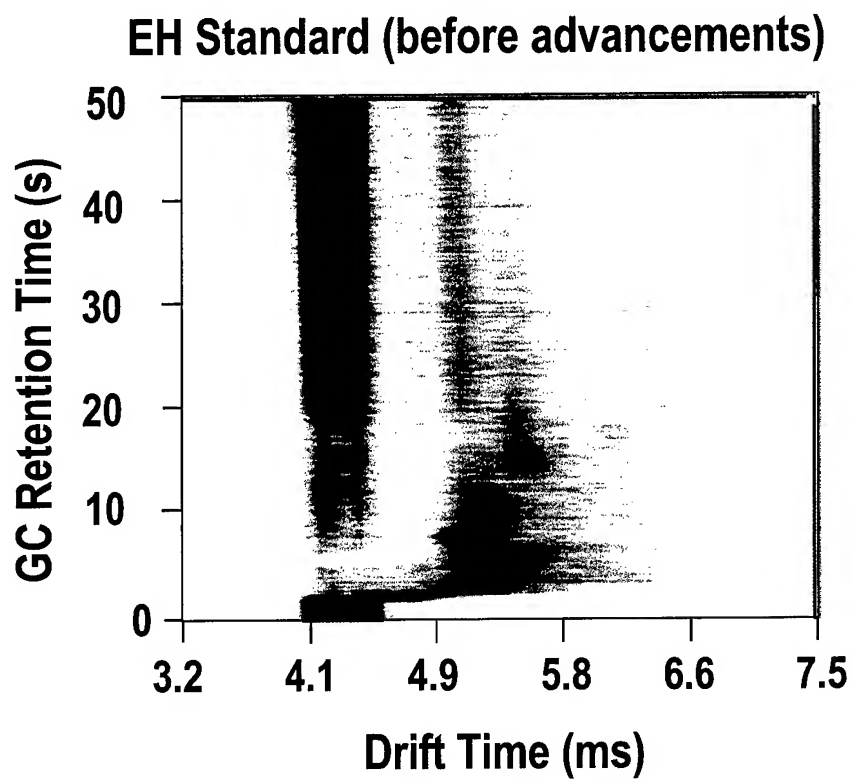


Figure 12. Comparison between Py-GC-ion mobility data space of EH standard before and after the advancements.

REFERENCE

1-Snyder, A. P., Maswadeh, W. M., Parsons, J. A., Tripathi, A., Meuzelaar, H. L. C., Dwarzanski, J. P. and Kim, M., *Field Analytical Chemistry and Technology*, Vol. 3, Issue 4-5, p 315- 326.

UPGRADING A CHEMICAL MONITOR INTO A BIODETECTOR

Waleed M. Maswadeh, Ashish Tripathi and John A. Parsons

GEO-Centers, Inc., Gunpowder Branch, P.O. Box 68, Aberdeen Proving Ground, MD, 21010-0068; and

Ken Barry, Charles S. Harden, A. Peter Snyder

U.S. Army Edgewood Biological Chemical Center, Aberdeen Proving Ground, MD, 21010

ABSTRACT:

This paper presents the steps and design considerations that were taken to upgrade a regular chemical monitor into a Bio-detector. The upgrade had extended the monitor capabilities to monitor chemicals as well as monitor and detect biological compounds. Two modular were added which consist of gas chromatography (GC) and pyrolysis. The first step taken was to resolve the mixture detection deficiency of the chemical monitor by introducing a mixture separation step using gas chromatography (GC). The second step involved careful transformation of biological compounds or its biomarkers from the solid phase into a gas phase by pyrolysis.

A handheld ion mobility spectrometer (IMS) used for chemical agent monitoring (I-CAM) was upgraded to detect biological agent particulate by adding a front-end interface. The front-end interface consists of aerosol trapping/pyrolysis quartz-tube (Py) and a patented temperature-programmable gas chromatography ring (GC). The detector unit is about the size of a lunchbox, that is, 12x9x5 inch. The upgrade did not eliminate the IMS device it's ability to detect chemical agents by the IMS. Due to the unique design of the aerosol trapping/pyrolysis quartz tube, the Py-GC-IMS system is capable of analyzing various samples, in gas, liquid and solid form without any prior sample preparation. Similar upgrade designs can be applied to other chemical monitors.

INTRODUCTION:

In recent years, there have been considerable developments and interests in making a compact, handheld biological monitor for outdoor field tests. In the literature, many attempts were made to develop a handheld biological monitor that can give an alarm in a reasonable time frame, less than 5 minutes. The majority of biological monitors take a good amount of time to produce reliable results in the 20-minute frame or more. One of the first attempts was made by Meuzelaar and Co-workers [1]. In their attempt, a Curie point wire was used to transform biological sample into a gas phase and pyrolysis products are injected into a short transfer line into an I-CAM.

This paper presents the major three steps and design considerations that were taken to upgrade a chemical monitor into a biological monitor. The improved-chemical agent monitor (Graseby Ionics, Watford, Herts, UK) was chosen for this upgrade.

Discussion and Results:

Not any chemical monitor can be considered as a candidate to be upgraded into a biological monitor. There are certain criteria a chemical detector should have before it can be upgraded to a biological monitor. Some of these criteria a chemical monitor should have are fast response (few milliseconds), preferably spectral output, specificity to polar compounds, compact, minimum maintenance, preferably no special buffer gas or carrier gas required, low power consumption, and low weight. Some of the chemical monitors available commercially that can be considered biologically upgradeable are miniature mass spectrometer (TOF, ion trap, quadrupole), ion mobility spectrometer (improved-chemical agent monitor; I-CAM), and UV fluorescence detector. Majority of these chemical monitors accepts only chemical samples in the vapor phase. In addition, majority of these chemical monitors cannot function properly when monitoring a mixture of chemicals because the chemical monitor produces complex signature that requires complex multivariable data analysis technique to decipher the signature. Analyzing various chemical monitors or detectors available commercially, two devices were chosen that met most of the above listed criteria for a bio-upgradeable chemical monitor. The first candidate is the I-CAM and the second is the TOF mass spectrometer. In this paper, the I-CAM was chosen to show the steps taken to transform it from a chemical monitor into a biological monitor. Similar steps can be applied to other chemical monitors/detectors such as mass spectrometers to transform it to a biological monitor.

The majority of chemical monitors commercially available detect chemical compounds in the vapor (gas) phase. The majority of biological monitors use complex sample preparation and detection of biological compounds or agents and are carried out in a liquid stationary matrix.

One of the main criteria to upgrade a chemical monitor into a biological monitor is the ability to transform the biological compounds or fragments (biomarkers) to the gas phase. Why should chemical monitor be upgraded to monitor biological compounds? Because chemical monitors are more superior in their response time, selectivity and sensitivity when compared with biological monitors available commercially. To apply such superior features of the chemical monitor onto the biological monitor, one should find away to transform biological compounds into the gas phase.

Three major steps were applied to upgrade a handheld ion mobility spectrometer (Improved-Chemical Agent Monitor, I-CAM) to monitor biological agents such as B.G. spores. Briefly, the I-CAM is an ion mobility spectrometer where chemical vapor molecules are drawn into and ionized in the ionization region. A fraction of the ionized vapor molecules is injected into the drift tube where ions are separated by the net effect of electric fields and drift drag, the resistance of atmospheric pressure neutral molecules [2]. In ion mobility spectrometry, the ionization region is always full of ions of the reactant buffer gas (normally water cluster ions) and called reactant ion peak (RIP). Chemical vapor molecules are ionized by the proton transfer from reactant ions to vapor molecules.

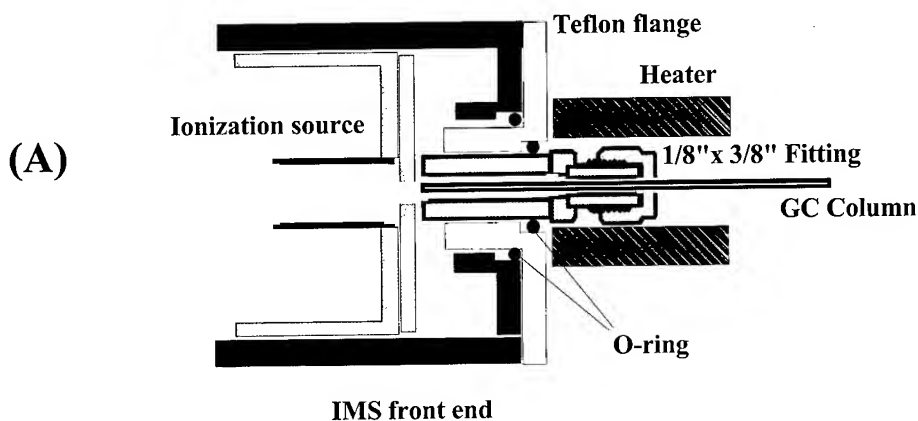
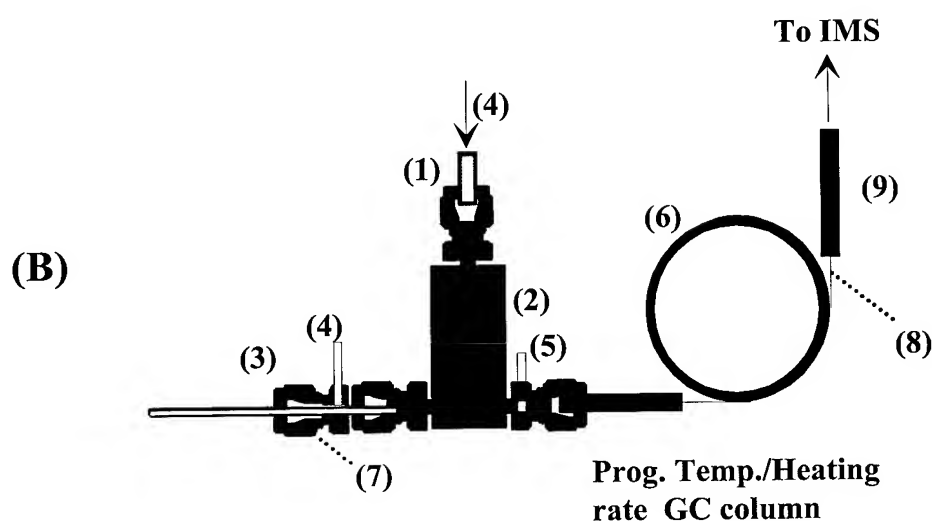


Diagram of the GC-IMS interface



- 1) 1/8" o.d. x .03" i.d lined S.S. high temperature, 3-way valve with 1/8" swagelock fittings, 3) 1/16" glass lined S.S. tube., 4) Clean, dry air, 5) Vacuum, 6) Patented ring GC oven, 7) 1/8" swagelock-1/8" tube reducer with 1/16" side S.S. tube, 8) High Temp S.S. GC column 4m long x .5mmx.25um, 9) interface heater.

Figure 1A shows a schematic diagram of the GC-IMS interface and how close the GC column relative to the ionization source. Figure 1 B shows a schematic diagram of the GC-IMS setup.

Careful considerations are taken to insure that the chemical vapors are eluted in the center of the ionization region, as shown in Figure 1A. Such consideration will eliminate any condensation, dramatic dilution and maximize the ionization efficiency. Unfortunately, all types of monitors and detectors have very low resolution when challenged with vapor mixtures. To

overcome such deficiency, it is important to have a pre-separation of the vapor mixture where separated vapors are introduced to the monitor or detector one by one. One of the simplest and most common ways used in vapor mixture separation is gas chromatography. A temperature-programmable gas chromatography ring (patent 5,856,616) was carefully interfaced onto the I-CAM. The GC column outlet is positioned close to the central entrance of the I-CAM ionization region. The choice of the GC column was such to provide optimum flow rate into the I-CAM ionization region, produce maximum separation for chemical compounds on interest, rigidity, extend its life of operation and fast heating/cooling rates. The GC column is temperature-programmed to ramp from room temperature to 150 °C (2 °C /sec) so as to expand the spectrum of chemical compounds that can be analyzed and to reduce column degradation during stand by operation. The GC column inlet is connected to a high-temperature 3-way valve (General Valve, Fairfield, NJ, USA) for sample injection. The sample injector temperature was set to at least 20°C higher than the maximum GC column temperature. The 20°C higher temperature will eliminate the condensation of chemical compounds inside the sample injector internal surfaces prior the GC column. The interface region of the sample injector and GC column inlet was designed in a way to reduce the interface dead volume by fast purging of the interface internal volume after sample injection. Such fast purging of the interface produces sharp injection of vapor sample into the GC column with no tailing. Figure 1B shows a schematic diagram of the ring type GC column connected to an I-CAM system. The combination of I-CAM with gas chromatography (GC-IMS) produces a true two-dimensional data space that is similar to GC-MS (mass spectrometry). Figure 2 shows typical GC-IMS data space of a mixture of phosphonate compounds (DMMP, DIMP and DEEP). The water fall figure can be presented by a more powerful format that is called contour plot as shown in Figure 3.

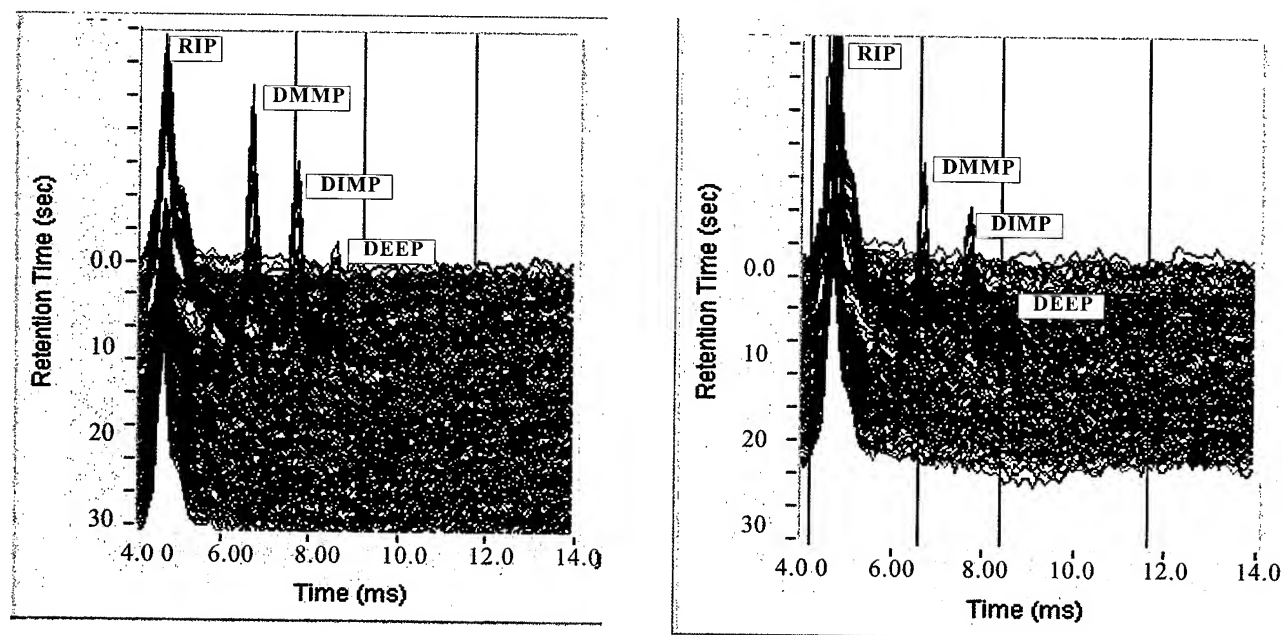


Figure 2 shows a duplicate analysis of the phosphonate mixture using the lunchbox Py-GC-IMS system. The water fall display shows the separation of Dimethyl methy phosphanate, Diisopropyl methyl phosphonate (DIMP), and Diethyl ethyl phosphonate (DEEP).

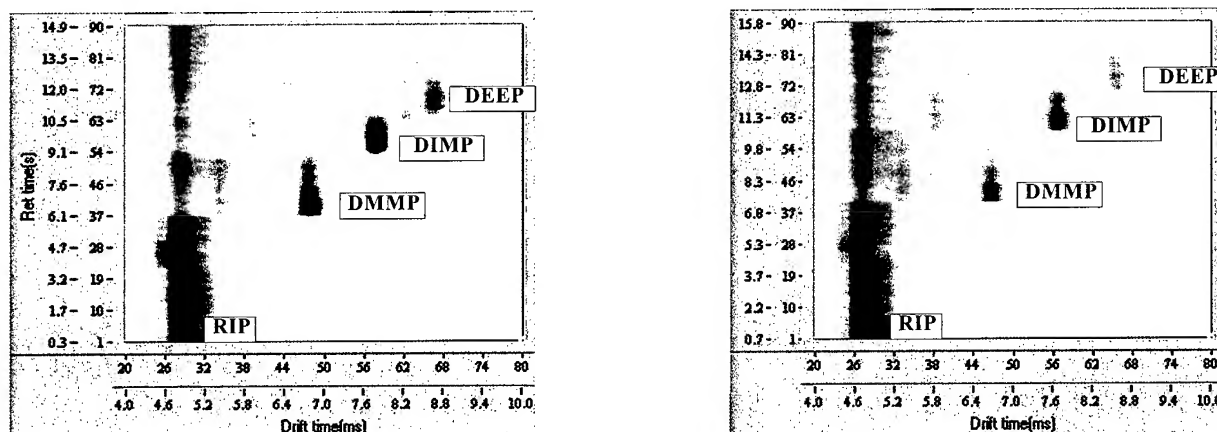


Figure 3 shows a duplicate GC-IMS contour plot of phosphonate mixture, Dimethyl ethylphosphonate (DMMP), Diisopropyl methyl phosphonate (DIMP) and Diethyl ethylphosphonate (DEEP). Note, the good separation and sharp elution of the three compounds.

As had been mentioned earlier, biological compounds or fragments need to be transformed into the gas phase for the GC-IMS system to detect. Majority of biological compounds are solid in nature. Also, some of the biological agents are made of living cells such as bacteria. A unique quartz tube was designed to accept various biological samples (even in aerosol format) and fragments of biological sample are transformed into the gas phase. Figure 4 shows the quartz trap/pyrolyzer tube (Py). The pyrolyzer tube (Py) consists of a quartz tube with frit (average pore size of 150-200um) mounted inside the center of the quartz tube. The frit serves as a filter support for the micro fiber quartz filter disc (< 1 um pore size). The function of the micro fiber quartz filter is to retain aerosol particulates in the range of one um in diameter and higher, a base for direct injection of solid suspension and to prevent any contamination down streams of the pyrolysis region. A fast heating wire is coiled and placed on the center of the quartz tube (1/4 inch diameter x 1 inch length) that quickly transfer biological sample into the gas phase. It is very important that biological sample or fragments are removed away from the hot pyrolysis region to the GC column inlet to minimize thermal degradation of biological fragments. A small flow of carrier gas was introduced during the fast biological sample heating and transformation across the micro fiber quartz filter into the down stream of the hot zone. Figure 5 shows a schematic diagram of the sample trap/pyrolysis tube (Py) connected to the GC-IMS setup (Figure 1B).

The Py-GC-IMS system (Figure 6) is compact (12x9x5 in), light weight (10 Lbs.), requires no liquid consumables or gas cylinders, and analyzes both chemical and biological samples in all gas, liquid or solid form.

One of the major advantages of the sample trap/pyrolysis quartz tube is that it accepts any form of sample (aerosol, solid suspension, liquid as well as vapors), requires no sample preparation and very low maintenance. Figure 7 shows biological GC-IMS data space of a direct injection of B.G. spores in liquid suspension using the improved Py-GC-IMS system shown in Figure 6.

For the analysis of aerosol particulates in the range of 1-5 ACPLA (agent containing per liter of air), an additional aerosol particle concentrator is needed and interfaced with the Py-GC-IMS system inlet. During outdoor trials, bacterial aerosols and background particulates in the range of 2 to 10 μm -diameter range were concentrated from a 1000-to-0.7 L/min (air-to-air) and retained by a micro-fiber quartz filter in a quartz tube. A multi-stage rapid heating (normally two-step heating) of the quartz tube

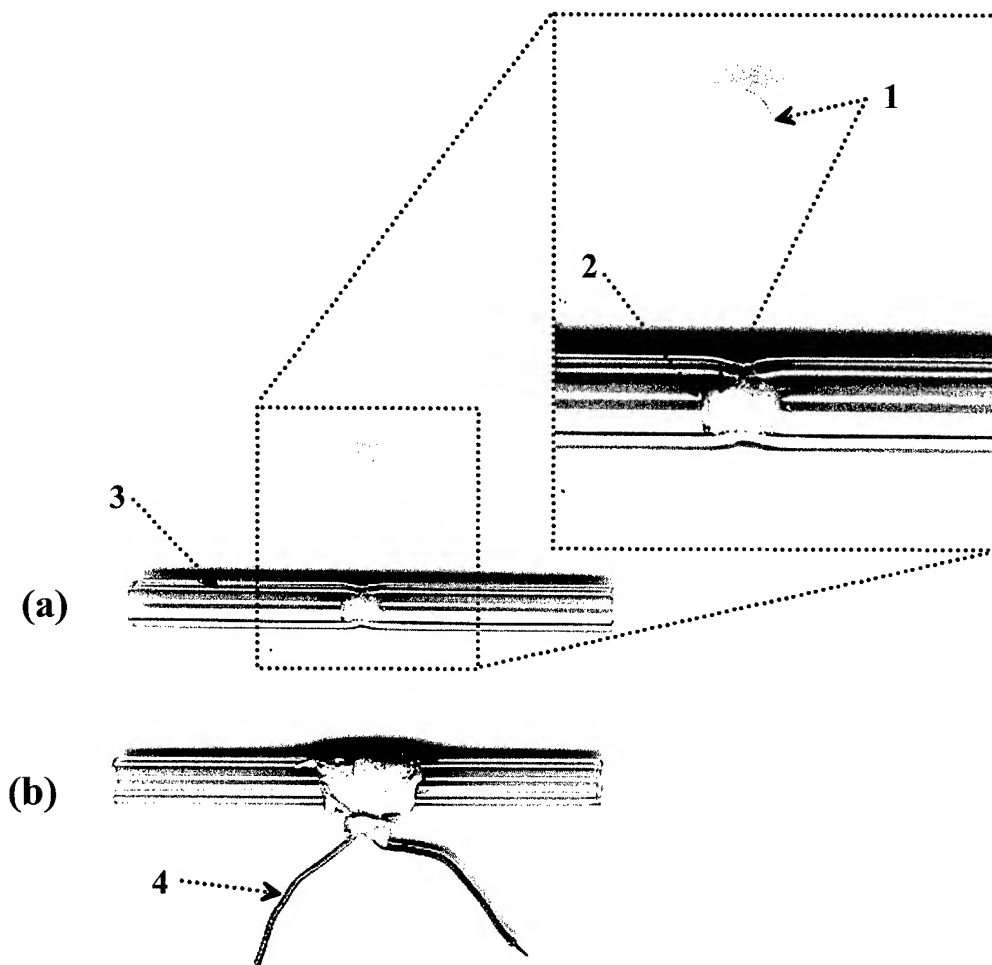
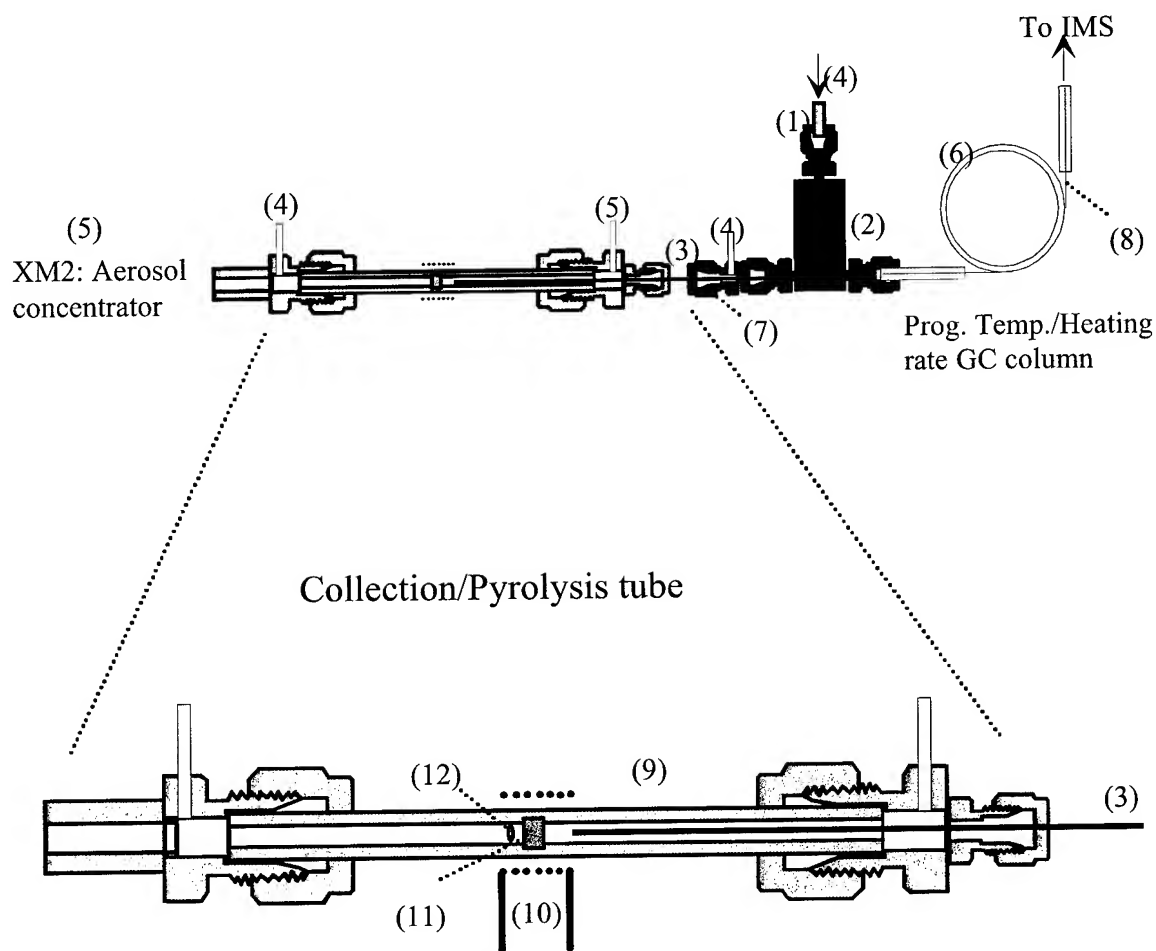


Figure 4 shows the quartz trap/pyrolyzer tube (Py). The pyrolyzer tube (Py) consists of a quartz tube with frit (average pore size of 150-200 μm) mounted inside the center of the quartz tube. The frit serves as a filter support for the micro fiber quartz filter quartz filter disc (< 1 μm pore size).



- 1) 1/8" o.d. x .03" i.d lined S.S. high temperature, 3-way valve with 1/8" swagelock fittings, 3) 1/16" glass lined S.S. tube., 4) Clean, dry air, 5) Vacuum, 6) Patented ring GC oven, 7) 1/8" swagelock- 1/8" tube reducer with 1/16" side S.S. tube, 8) High Temp S.S. GC column 4m long x .5mmx.25um, 9) Injection liners, frit quartz tube, 72x6.3mm, 10) Pyrolyzer heater wire, 11) 1 um quartz filter, 12) Retainer spring.

Figure 5 shows the a schematic diagram of the biological Py-GC-IMS system and an enlarged schematic diagram of the collector/Pyrolyzer tube. in JFT-4, Dugway P.G.

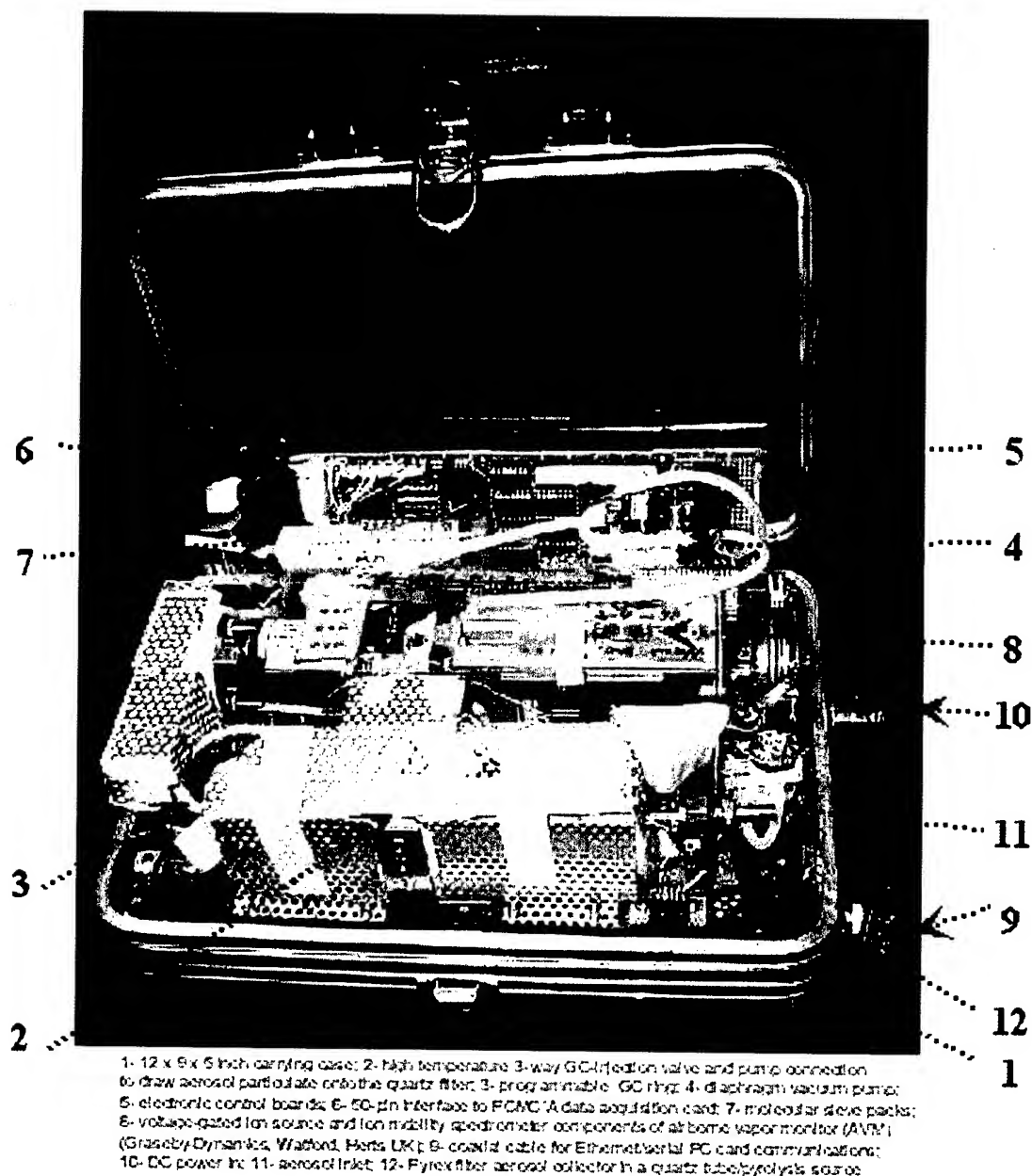


Figure 6 shows a photo of the lunchbox Py-GC-IMS system. The Py-GC-IMS system is compact (12x9x5 inch), light weight (10 Lbs. with mini Laptop computer), requires no liquid consumables or gas cylinder, and analyzes both chemical and biochemical samples

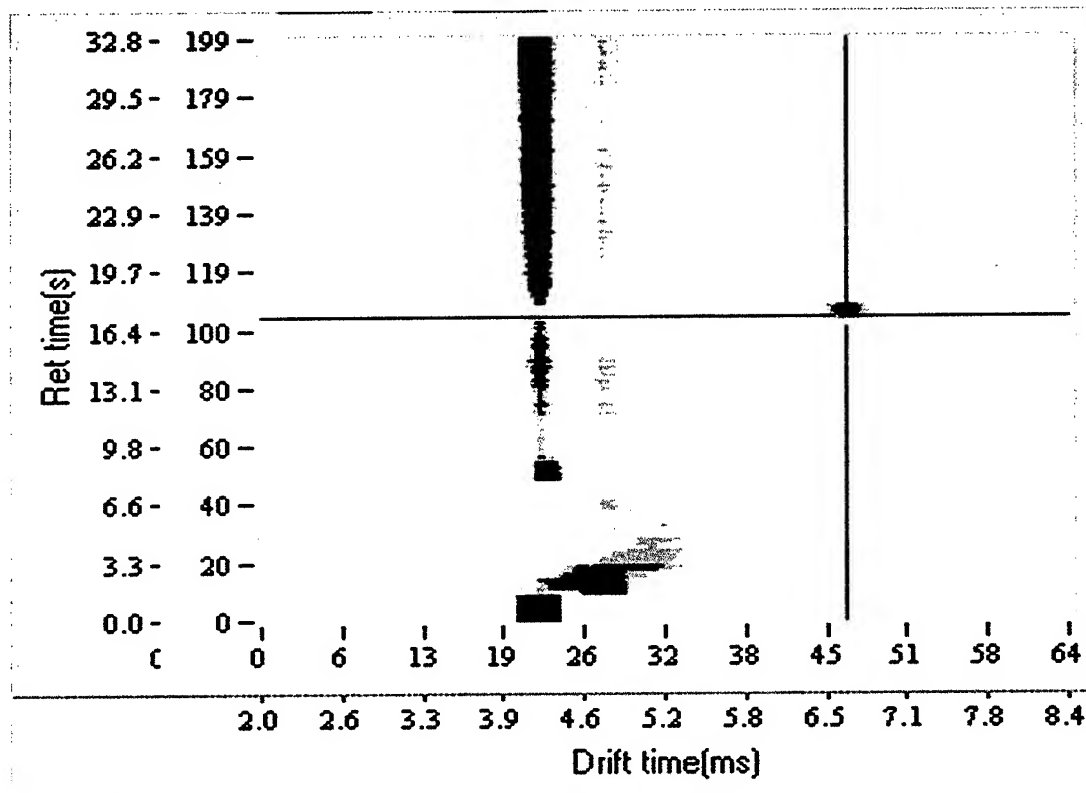


Figure 7 shows the GC-IMS data space of a direct injection of BG sample (suspension) at Dugway Proving Ground using a direct injection of BG suspension. The (a) symbol indicates the GC elution of picolinic acid and the (b) symbol indicates the GC elution of highly volatile pyrolysis products.

to 100°C and 300°C in 10 seconds and 4 seconds, respectively, effected vaporization, and a portion of the pyrolyzate was directed into a GC ring column. The GC separated eluate was detected by the atmospheric pressure-based IMS. Various standards give distinct peaks in the acquired GC-IMS data space. The sensitivity of the Py-GC-IMS system during outdoor trials was down to three ACPLA. Figure 8 shows a sequence of four GC-IMS data space during the fourth outdoor Joint Field Trials (JFT-4) and the detected activity of BG spores presence.

Extensive programming was written to create a user-friendly interface panel, as shown in Figure 9, as well as to remotely control the Py-GC-IMS system. Certain software considerations were applied for optimum data retrieval [3]. Also, the program generates all control protocol and scans functions necessary for the continuous operation of the Py-GC-IMS system. Figure 10 shows a typical scan functions used to operate various modules in the Py-GC-IMS system.

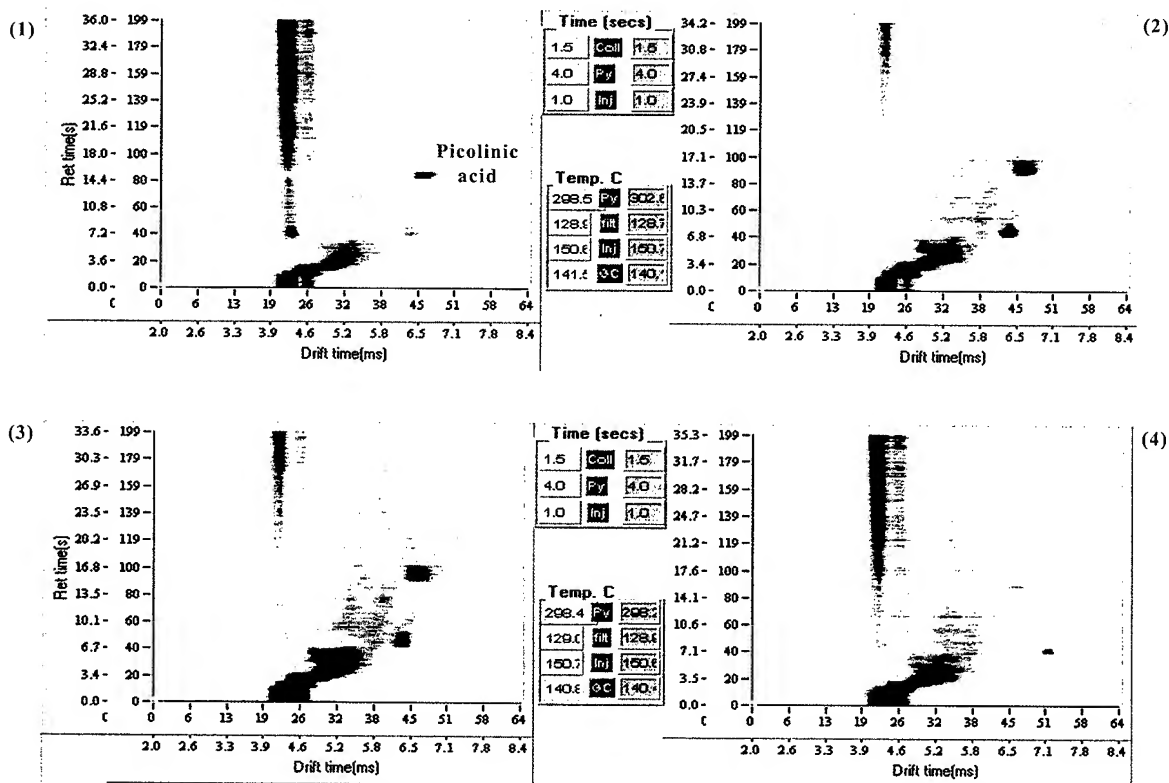


Figure 8 shows a sequence of GC-IMS data spaces during the 4th outdoor Joint Field trials (JFT-4). A significant BG spores activity is detected (the presence of picolinic acid) during an active window.

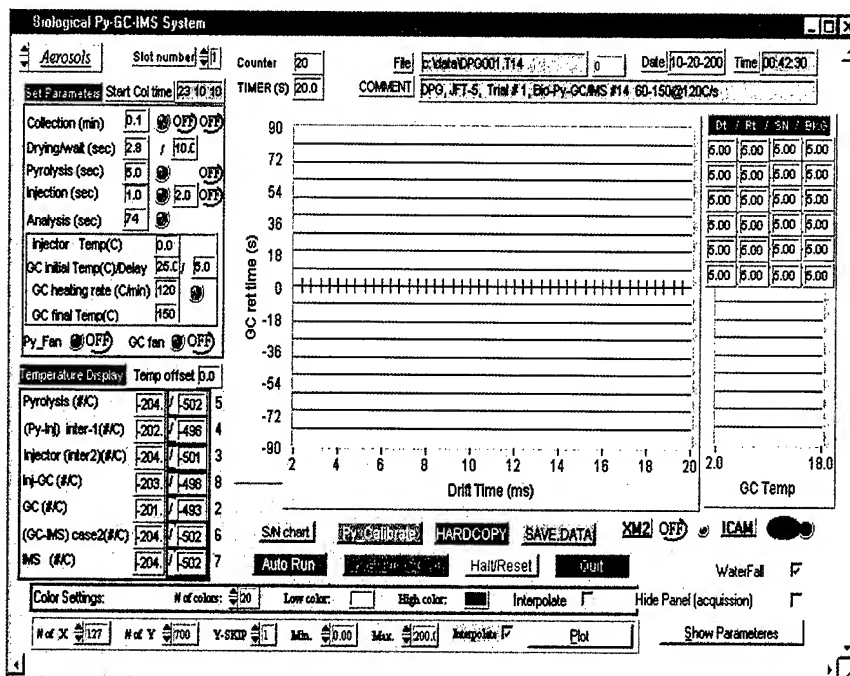


Figure 9 shows the user-friendly interface panel that is used to operate the Py-GC-IMS system.

Cycle Elements

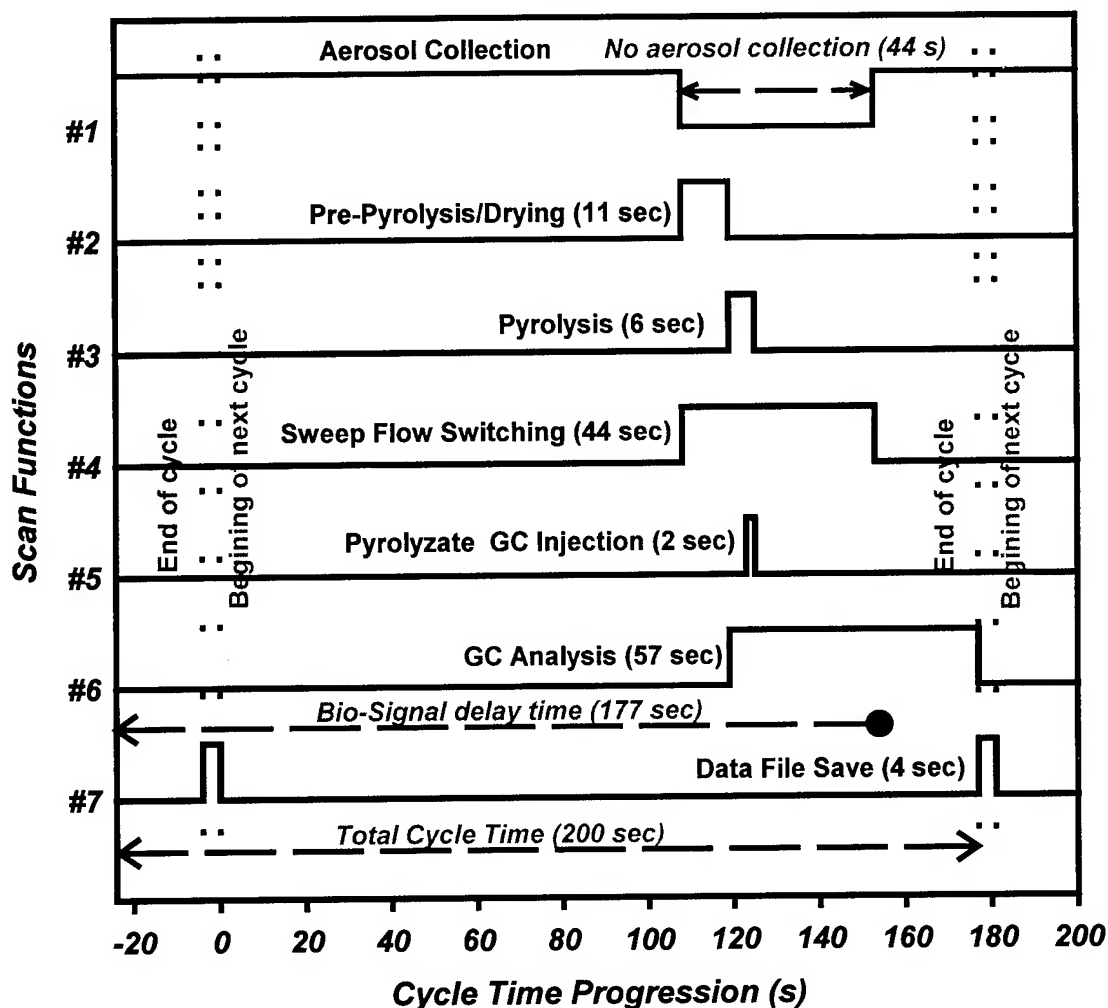


Figure 10 shows the six scan functions in time used to control the biological Py-GC-IMS system. The two double-dotted lines represent a single run while beyond this area represents the end of a cycle-run (left) and the beginning of a new cycle-run during the AUTO-RUN option.

CONCLUSIONS

This paper presented the steps and design considerations that were taken to upgrade a regular chemical monitor into a Bio-monitor. A handheld chemical agent monitor (I-CAM) was used in this bio-monitor upgrade because the I-CAM offers certain advantages over other handheld chemical monitors devices. The combination of I-CAM with gas chromatography (GC-IMS) produces a true two-dimensional data space that is similar to GC-MS (mass spectrometry).

The controlled heating of the pyrolyzer device was used to transform biological compounds from the solid phase into the gas phase. This was also accomplished by using a special trap/pyrolyzer tube (Py) with continuous internal flow. Such a design of a pyrolyzer tube gives minimum decomposition of biomarkers that are produced during pyrolysis. Also, the pyrolyzer tube was designed to trap aerosol particulates and liquid droplets for further analysis.

The Py-GC-IMS system is the only bio-monitor available that is compact (12x9x5 in), light weight (10 Lbs.), requires no liquid consumables or gas cylinders, and analyzes both chemical and biological samples in any sample form; gas, liquid or solid form. No sample preparation is required in this handheld Py-GC-IMS system. Sensitivity of the Py-GC-IMS system during outdoor Joint Field Trials was down to three ACPLA.

REFERENCES

- 1- Snyder, A.P., Harden, C.S., Brittain, A.H., Kim, M.-G., Arnold, N.S. and Meuzelaar, H.L.C., *Anal.Chem.* , 65, 299-306 (1993).
- 2- Eiceman, G.A. and Karpas, Z., *Ion Mobility Spectrometry*, CRC Press, Boca Raton, Fl. 1994
- 3- Davis, D.M., Maswadeh, W.M., Shoff, D.B., Harden, C.S. and Snyder. A.P., *3rd international Workshop on IMS*, Galveston, TX, Oct. 16-19, 1994.

SEMI-SELECTIVE OPTICAL SENSORS FOR REAL-TIME DETECTION OF BIOLOGICAL WARFARE AGENTS

Han Chuang, AnCheng Chang, Laura Taylor, and *Mary Beth Tabacco*
Echo Technologies, Inc.
451 D Street
Boston, MA 02210 USA

Abstract

ETI is developing a suite of optical sensors to detect and distinguish classes of microorganisms. This approach is a departure from other developmental sensors designed to identify a single organism and is therefore referred to as *semi-selective*. The sensors are based on molecular recognition and fluorescence spectroscopy. Detection of bacteria and spores, in both liquid and aerosolized samples, has been demonstrated. Sensors are also being developed for detection of viruses (MS2) and toxins. Class selectivity has been demonstrated in the presence of potential ambient biological and non-biological interferents. A handheld prototype having 3 independent optical sensor modules has been fabricated.

Introduction

Many sensor development efforts are focussed on identification of specific microorganisms that could be used in biological warfare. Very elegant work has been done using antibodies, and more recently DNA probes, for detection of pathogenic microorganisms in water [1-3]. These assays are however inherently complex, requiring sample preparation, addition of solvents, and washing steps. Even when these steps systems are automated, they necessitate the development and maintenance of fluid handling systems, reagent reservoirs, and generate chemical waste. Also, a significant drawback to these approaches is that the exact nature of the chemical/biological threat must be known in advance, so that an appropriate antibody, or complementary DNA strand, can be produced and immobilized on the sensor. In addition, producing high quality antibodies is a costly, time-consuming process, and they are subject to non-specific binding. This further implies that these techniques will be limited when faced with an unknown or genetically modified organism.

The novel concept of the semi-selective sensor array has been applied to detection of chemical vapors [4] and metal ions in solution [5]. Its application to detection of microorganisms is a new idea, and is presently being used by ETI for detection of air and water-borne pathogens. The technical approach departs from the conventional "one-sensor, one-analyte" paradigm and will demonstrate the utility of an array of *semi-selective* optical transducers for detection of broad classes of microorganisms. This approach is particularly useful when the specific nature, or concentration, of the biological contaminant may not be known in advance. In this paper we present an overview of the approach with data from sensors to detect bacteria and spores. Data is also presented which validates the *semi-selective* detection concept in laboratory studies.

Technical Approach

ETI is presently developing sensors to detect and discriminate classes of Biological Warfare (BW) threats such as bacteria, spores, viruses and toxins. Using a multi-sensor array, as shown in Figure 1, the nature of the threat can be assessed and distinguished from non-biological material, and from the naturally occurring biological background (e.g., airborne dead bacteria, fungi, molds and humic matter). Detection of broad classes of chemical and biological threats is particularly well suited to situations where the nature of the contaminants is not known in advance. The data from multiple sensors in an array are analyzed as an ensemble using chemometric algorithms, thereby providing more information than an individual sensor for a single analyte.

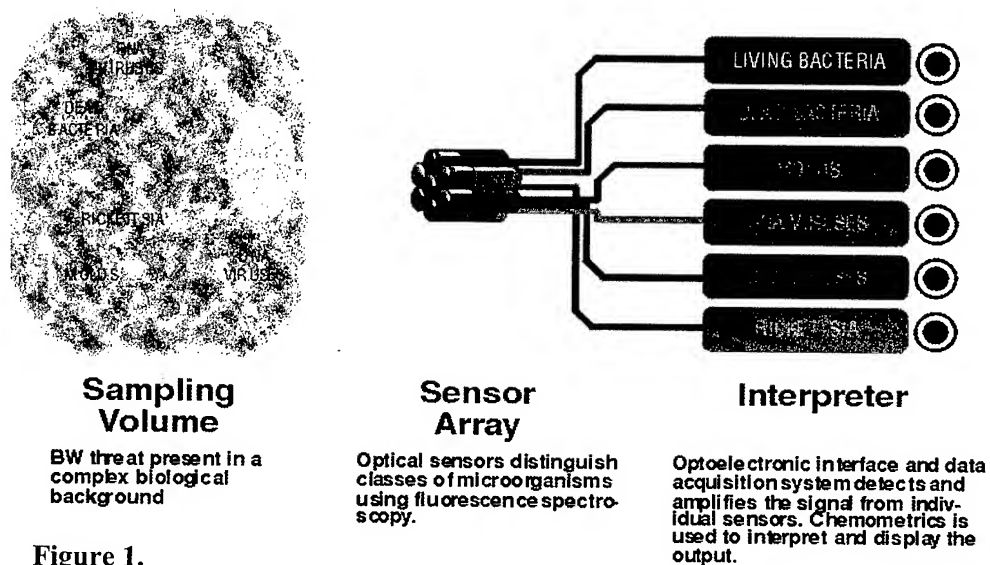
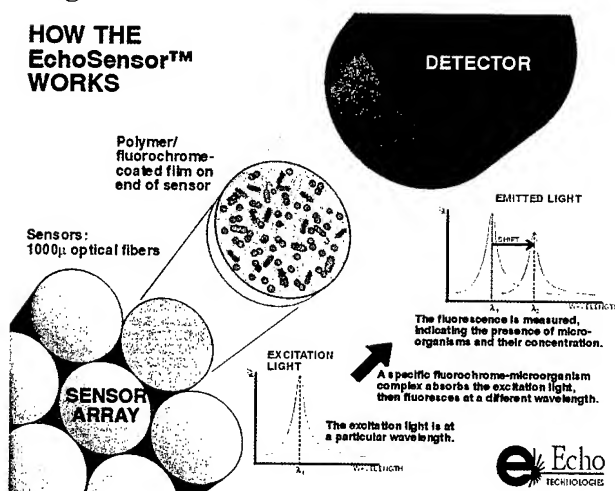


Figure 1.

Figure 2.

HOW THE EchoSensor™ WORKS



The sensors are optical transducers that use molecular recognition and fluorescent reporter molecules configured on optical substrates as shown in Figure 2. These substrates can be waveguides or silica coupons. The sensors offer inherent simplicity, and unlike antibody or DNA probes, require no consumable reagents or sample preparation. The optoelectronic design is modular so that new sensing capability can be added easily and cost effectively. Also, the use of miniature, off-the-shelf integrated optical and electronic components ensures low power requirements and system reliability.

General Methods

The semi-selective sensors have three fundamental components: a molecular recognition compound and fluorescent reporter molecule; a polymer membrane for immobilization of the reagents; and an optical substrate. The molecular recognition and fluorescence signaling are generally performed by one and the same molecule although in some cases they can be two distinct molecules. Polymer membranes are generally hydrophilic materials that are chemically compatible with the fluorescent reagents. The optical substrates used can be large diameter optical fibers, planar waveguides or silica coupons.

Fluorescent reporters. The fluorophore/molecular recognition elements interact with the target organisms by one of several mechanisms:

- diffusion through cell membranes to stain nucleic acids, e.g., bacteria;
- interaction with chemicals expressed on the surface of the organism, e.g., spores, toxins, bacterial metabolites;
- selective diffusion through compromised cell membranes, e.g., live/dead bacteria, toxins;
- staining of DNA/RNA, e.g., viruses.

The fluorescent reagents can exhibit fluorescence enhancement, quenching, wavelength shifts, or go from an inherently non-fluorescent state to a fluorescent state. Each of these has been successfully demonstrated in our laboratory. As an example, there are several classes of nucleic acid fluorescent dyes that have been developed for use in cell biology. These stains diffuse through the cell membranes of cells and intercalate into the DNA resulting in a change in the fluorescence intensity. The total change in fluorescence signal from a sensor is related to the numbers of microorganisms present on the sensor surface (as shown in Figure 3 in the Results section). We have also demonstrated that combinations of nucleic acid reactive dyes can be used to improve the sensor response over the life cycle of bacterial cells. This has resulted in both an increase in total fluorescence signal, but also mitigated the effects of cell aging on sensor response. Sensors to detect bacterial endospores are fabricated using ionophores or luminescent lanthanides that interact with chemicals uniquely expressed by the spores.

Polymer membranes. Polymer membranes are used to immobilize the detection chemistry and serve as an interaction medium for the reaction between the fluorescent reporter molecules and the microorganisms. The film ensures a homogeneous surface, thereby improving sensor reproducibility and enhancing coupling of excitation/emission light into the sensing region. Equally important is the ability to tailor the microenvironment to impart specific chemical or physical properties, which facilitate reaction between the organism and the reporter molecule. Polymers that we have used successfully in the laboratory are listed below with a short description of their properties.

- Alginate acid - biopolymer/bacterial adhesin
- HEMA (hydroxyethylmethacrylate) – hydrogel/crosslinked
- PVP (polyvinylpyrrolidone) – hydrolytically stable
- PIB (polyisobutylene) – hydrophobic/bacterial adhesion
- DOW – hydrophobic siloxane

Preliminary work with alginate acid and HEMA indicates that they are good matrices for the DNA-reactive fluorophores. Sensors for bacteria, spores and biochemical toxins have been successfully demonstrated using alginate polymers. PVP is presently being tested as an alternative matrix for spore detection. PIB has been used for detection of bacteria in aqueous flow systems.

Microorganisms. The cultivation, transfer and preparation procedures for all microorganisms are performed in a Class II, Type A laminar flow biosafety cabinet (Baker Co., Sanford, ME) using aseptic techniques. Bacteria and virus (MS2) were generally a product of the American Type Culture Collection (ATCC, Rockville, MD). SPORDEX® *Bacillus subtilis* (*globigii*) spore suspensions [ATCC 9372] were obtained from AMSCO Sterility Products (Apex, NC) or from Dugway Proving Ground. Toxins and simulants were obtained from Sigma or American Peptide.

Instrumentation. Sensors are evaluated in the laboratory using one of three instruments. The samples are generally introduced as microdroplets (2-10 μ L) or in aerosol form using a bioaerosol chamber and nebulizer. Initial screening of new sensors and chemistry is done using a double monochromator system with fiber optic interface (Acton Research Corporation, Acton, MA). The fluorescence signal is collected by a SpectraPro-300 monochromator with a photomultiplier tube (PMT). Appropriate filters are used to purify the excitation and emission light. Sensors can also be tested using an Ocean Optics S2000 Fiber Optics Spectrometer (Dunedin, FL) with either a blue LED or white light source. This system also has a fiber optic probe, which can be directly interfaced with a bioaerosol chamber for measuring sensor response to aerosolized bacteria or spores. Alternatively, sensors are tested using a custom detection instrument designed by ETI composed of an optical module with dual-LED excitation, and fully integrated data acquisition and signal processing electronics. [This custom instrument is shown as a handheld detector in Figure 7 in the Results section.]

Results

The key to the *semi-selective* detection concept is to design sensors that will respond generically to members of each class of BW threat (i.e., bacteria, bacterial spores, toxins and viruses) while not significantly cross-reacting with members of another class. Also, the sensors should not respond to potential ambient biological and non-biological interferents (e.g., fungal spores, ragweed, dust, soot, and clay). Some cross reactivity may be allowable when using an array of sensors (as shown in Figure 1) because when analyzed as an ensemble the data from the array will provide more information than from an individual sensor.

As an example, in Figure 3 six calibration curves for the bacterial sensors are presented. The bacteria samples were delivered as microdroplets in these experiments. This figure summarizes the sensor responses to bacteria that differ greatly in their microbiological characteristics encompassing gram positive and negative, rods and cocci, and differing size. This data shows that the sensors respond similarly to each bacterial genus and species over a sensing range of greater than three orders of magnitude. Although not included in Figure 3, similar calibration curves have been developed for other bacteria including *Micrococcus*, *Burkholderia*, and other species of *Erwinia* and *Bacillus*.

In Figure 4 the response of the bacterial sensor to aerosolized samples of *Pseudomonas aeruginosa* is presented and shows an excellent response time of 2 minutes or less to see a significant change in fluorescence intensity. Note, a water control shows no fluorescence enhancement. This data suggests that the sensors could potentially be used for direct sampling from the air eliminating the need to bring the sample into a liquid matrix as required by several other sensor types.

Sensors have also been developed and well characterized for detection of bacterial spores based on detection of chemicals uniquely expressed in the spore coat. The fluorescence emission spectra as a function of *Bacillus subtilis* spore number are shown in Figure 5. In this experiment spore samples were introduced to the sensor as 10 μ L aqueous droplets. Preliminary work has also been done to verify detection of aerosolized spores.

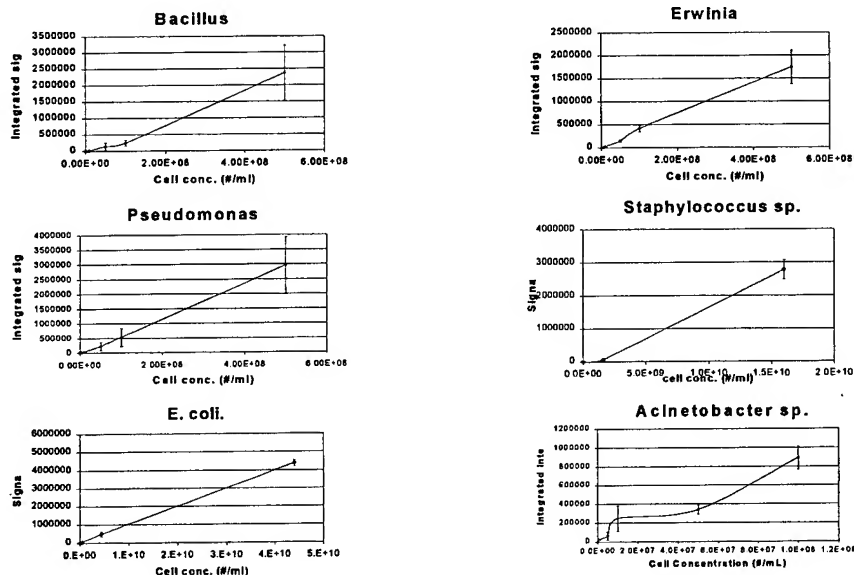


Figure 3. Calibration curves demonstrating quantitative response of semi-selective bacterial sensors. Sensors respond generically to several genera and species including gram positive and negative, and rods and cocci.

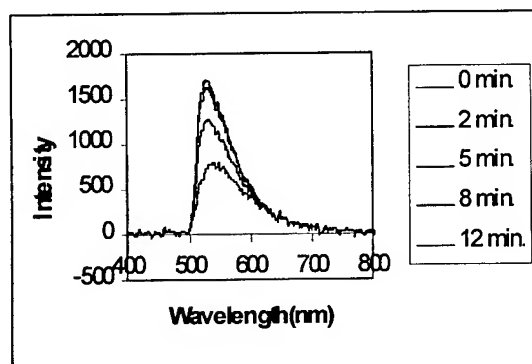


Figure 4. Response of a bacterial sensor to aerosolized *P. aeruginosa*. The approximate number of cells

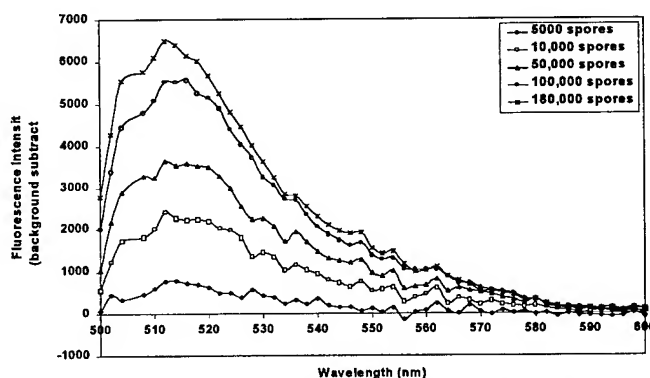


Figure 5. Fluorescence emission spectra as a function of *Bacillus subtilis* spore concentration. Spore samples were introduced to the sensor as 10 μ L droplets.

As suggested by Figure 1, the full potential of the semi-selective detection concept will be realized using an array of sensors that can detect and discriminate classes of potential BW threats. In Figure 6 laboratory data is presented which provides preliminary validation of the approach. The bar graph combines data from three different sensor types for detection of bacteria, bacterial spores and fungal spores (a potential ambient biological material). The response of each sensor type to the target organism is presented along with the sensor response to other BW classes and to potential biological interferents.

For example, the solid bar graph on the left shows the response of a bacterial sensor to *Erwinia*, and the corresponding immunity or small response to MS2 virus, ovalbumin (toxin simulant), ragweed, fungal spores, and *Bacillus subtilis* spores. The bar graph on the far right is the response of the spore sensor to *Bacillus subtilis* spores and, reading to the left, its relative immunity to the other challenges. Combining this data (and possible that from a sensor channel designed specifically to detect a biological interferent) you can begin to describe the environment both in terms of what is, and what is not, present. Work is continuing to improve sensors for toxins and viruses and to determine their selectivity. Future work will include investigation of mixtures of materials and field testing to further validate the approach.

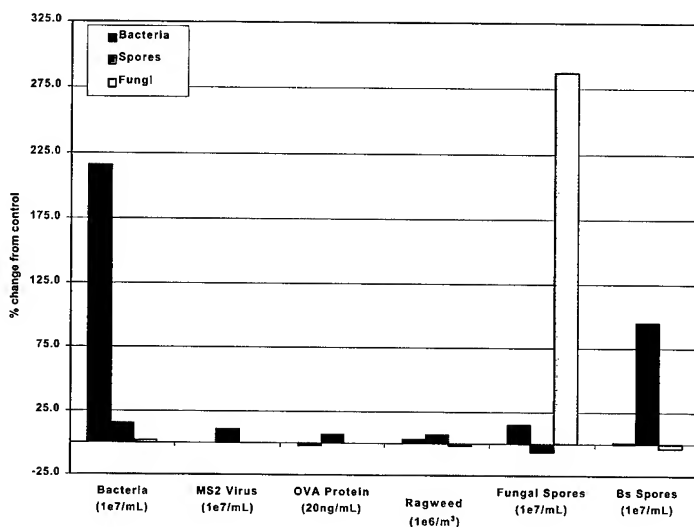


Figure 6. A multichannel array to detect and discriminate biological agents. The responses of three different sensor types (for bacteria, fungal spores, and bacterial spores) to the target organism are shown. Also, the sensor immunity to the other BW classes and potential biological interferents is shown.

A handheld prototype BW detection system has been fabricated and is shown in Figure 7. Three optical modules which house the sensors, dual LED light sources, photodiode detector and all filters, are capable of interrogating up to six unique sensor types. A fully integrated optoelectronic interface and data acquisition system has been designed so that the system requires no user expertise and can operate unattended. The system is being evaluated in the laboratory using liquid and aerosol samples of bacteria and spores.

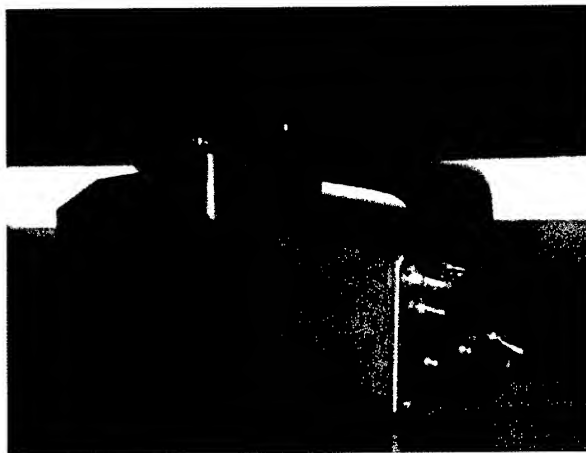


Figure 7. Handheld EchoSensor
Biological Detector.

CONCLUSIONS

The concept of *semi-selective* detection of Biological Warfare Agents has been presented. Summary data has been presented which demonstrates semi-quantitative detection of bacteria, such as *E. coli*, *Bacillus* and *Erwinia herbicola*, and bacterial spores such as *Bacillus subtilis*. Rapid sensor response time to aerosolized bacteria samples was also shown. This will potentially eliminate the need to bring air samples into a liquid matrix as required by many other sensor technologies. Laboratory data was presented to show both the class selectivity of three sensor types and their relative immunity to potential biological interferences. Development of sensors to detect toxins and viruses is continuing. A handheld EchoSensor Biological Detector has been prototyped and is being evaluated in the laboratory. The sensors are simple in design and the optoelectronic interface uses all COTS components, which should result in a system, which is very inexpensive. A potential use for the *semi-selective* detectors could be as a screening tool in conjunction with a more sophisticated analytical device.

Acknowledgement

This work was supported with funding from the MARCORSYSCOM (Contract No. N66001-97-D-8504) and the Army Research Laboratory (Contract No. DAAL01-98-C-0077).

References

1. Cao, K.L., Anderson, G.P., Ligler, F.S., and Ezzel, J., "Detection of Yersinia pestis Fraction 1 antigen with a fiber optic biosensor," J.Clin. Microbiol., 33, 336-341 (1995).
2. Wadkins, R.M., Golden, J.P., Pritsiolas, L.M., and Ligler, F.S., "Detection of multiple toxic agents using a planar array immunosensor," Biosensors & Bioelectronics, 13, 407-415 (1998).
3. Stahl, D. "Development of DNA Microarrays for the Rapid identification of Novel microbial Agents in Biologically Complex Settings," presentation to the Biological Agent Detection and Identification

Program Overview, DARPA Biological Warfare Defense Program, Defense Sciences Office, April 27-30, 1999 Santa Fe, NM.

4. Dickinson, T.A., Walt, D.R., White, J., and Kauer, J.S., "Rapid Analyte Recognition in a Device Based on Optical Sensors and the Olfactory System," *Anal. Chem.*, **68**, 2191-2202 (1996).
5. Tabacco, M.B., Chadha, S., Hammond, J.D., and Walt, D.R., "Multivariate Analysis of Cross-reactive Fluorescent Indicators for Analysis of Metal-ion Mixtures," in preparation (1999).

DEMONSTRATION OF SURFACE ENHANCED FLUORESCENCE WITH BACTERIAL BIOSENSORS

Han Chuang, Jaimie Russo, Mary Beth Tabacco
Echo Technologies, Inc., 451 D Street Boston, MA 02210

James B. Gillespie
Army Research Laboratory, Adelphi, MD 20783

Abstract

Echo Technologies is developing optical sensors for microorganisms detection based on fluorescence spectroscopy and molecular recognition. Bacteria react with nucleic acid fluorophores resulting in an increase in the fluorescence intensity recorded by the sensor. The sensitivity demonstrated to date is comparable or superior to other detection methods such as immunoassay, bioluminescence, microcalorimetry, Coulter counter, surface plasmon resonance and electrochemical techniques.¹ However, increased sensitivity is desirable in situations where an early-warning system for microorganism contamination is critical. In this study, we report preliminary results using Surface Enhanced Fluorescence (SEF) techniques for sensitivity enhancement in sensors to detect *Pseudomonas aeruginosa*.

Introduction

In the past few years, researchers have observed that with proper preparation silver colloid particles may increase fluorescence intensity at surfaces due to an increased electromagnetic field on the silver particle surface.² Another common surface phenomenon is fluorescence quenching which is a result of non-radiative energy transfer between excited fluorophores and quencher molecules. Because the metal can serve as a quencher, the magnitude of the SEF effect may depend on the distance between the fluorophore molecule and the metal particle. The use of various spacer molecules has been proposed to control this distance. Proper thickness control of the spacer layer may maximize the fluorescence enhancement while minimizing the fluorescence quenching effect. Useful spacer materials that have been reported in literature include octadecanoic acid, BSA-biotin/avidin and silica.² In addition to optimization

of the SEF effect, a silica layer protects the silver colloid from attack by solution-borne chemicals, thus extending the lifetime of the colloid particles.

In this paper, we will show that incorporation of silver colloid into bacterial sensing films results in higher fluorescence signals due to the SEF effect and that this enhancement can be greater still using colloidal particles coated with a silica spacer layer.

Experimental

Preparation of metal colloids. Silver colloid was prepared by a citrate reduction method. 22.5 mg of AgNO_3 (Sigma) was dissolved in 125 mL of deionized distilled water. The solution was heated to a boil while 2.5 mL of 1% sodium citrate (Aldrich) was added under constant agitation. The mixture was boiled for 15 minutes and was then cooled to room temperature. The solution was passed through a 0.2 μm syringe filter (Pall Gelman Laboratory) to obtain nanometer-size silver particles. A spectrometer (Spectronic 20D, Milton Roy, Ivyland, PA) with a set wavelength of 440 nm was used to measure a 10 \times dilution of the silver colloid suspension. The optical density (OD) of the freshly-prepared suspension was calculated to be around 70.

Silica-coated silver colloid was prepared starting with a suspension that was first diluted to OD50 with deionized distilled water. 185 μL of the diluted suspension was mixed with 5 mL of 2-propanol (Sigma), 169 μL of ammonium hydroxide (EM Science) and 5.8 μL of 10% tetraethyl orthosilicate (TEOS, Aldrich). The mixture was incubated at 40° C for a period from 2 to 24 hours during which the silica layer forms around the colloid. Following incubation, the mixture was centrifuged at 6000 rpm for 20 minutes. The supernatant was removed and the pellet resuspended in 2 ml of isopropanol. This step was repeated and the final pellet was resuspended in 2 ml of sterile water.

Sensor preparation. Both SYTO 13 and SYTOX Green (Molecular Probes, Inc., Eugene, OR) nucleic acid stains were used in the sensing films. The sensing chemistry was prepared by mixing water or the silver colloid suspension (OD50) with concentrated fluorophore stock solution so that the final concentration in the sensing chemistry was 25 μM . Aliquots (10 μL each) of the sensing chemistry were pipetted onto the surface of disposable microscope cover glasses, which were placed at the distal end of the optical fibers (Figure 1). 10 μL aliquots of water or *Pseudomonas aeruginosa* cell suspension were then individually pipetted onto the sensor coupons. The mixture was allowed to incubate in the dark at room temperature for at least 10 min., followed by individual fluorescence measurement.

Bacteria. The *Pseudomonas aeruginosa* bacteria (herein referred to as Pa) used in this study were obtained from the American Type Culture Collection (Rockville, MD, strain # 10145). The Pa cultivation, transfer and preparation procedures were performed in a Class II, Type A laminar flow

biosafety cabinet (Baker Co., Sanford, ME) using aseptic techniques. Cells were grown on Trypticase Soy Agar (Becton Dickinson, Cockeysville, MD) plates and incubated at 30°C for 18 to 24 hrs. Pa cells were harvested from TSA, suspended in 2 mL of sterile water, and centrifuged at 5,000 rpm for 15 min. The supernatant was carefully removed and the pellet washed twice in sterile water and resuspended in 2 ml sterile water. The final Pa concentration was approximately 5×10^8 cells/mL, based on an acridine orange direct count using epifluorescence microscopy.³

Instrumentation. A double monochromator equipped with a photomultiplier tube (PMT) detector and a fiber optic interface probe were used to interrogate the sensors (Figure 1).

A 16× microscope objective was used to focus the excitation light beam on an 800 μm (core diameter) optical fiber. The fiber optic was used to carry the excitation light to the distal end and to transport the emitted fluorescence signal to the detector. Prior to assembly, serial polishing steps were applied to the distal ends of all optical fibers, and a 0.3 μm lapping film was used for the final polishing step. The excitation light to the sensor was provided by a 75 W Xe-arc lamp, coupled to an Acton Research Corporation (Acton, MA) SpectraPro-150 monochromator. The fluorescence signal was collected through an ARC SpectraPro-300 monochromator with the PMT operated at 600 V. The excitation and fluorescence wavelengths were set at 485 nm and 525 nm, respectively. To purify the excitation beam and to eliminate stray light from the source, optical filters were used on the source monochromator exit slit (475 RDF 40, Omega Optical, Inc., Brattleboro, VT) and the detector monochromator entrance slit (GG 495, SCHOTT Glass Technologies Inc., Duryea, PA). A desktop computer with ARC SpectraSense v1.04 data acquisition software was used for data acquisition. An ARC NCL controller box was used as the computer-spectrometer interface.

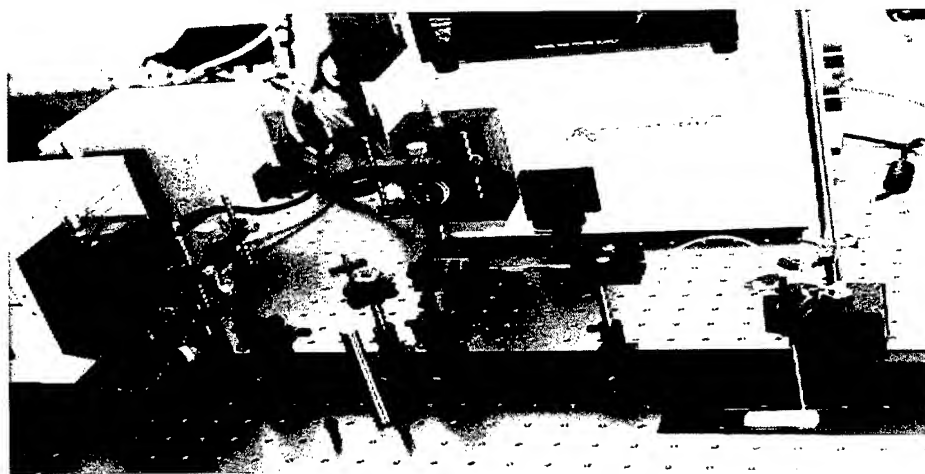


Figure 1. Instrumentation for the fiber optic bacterial sensor.

Scanning electron microscope (SEM) images of silver particles were collected using a Stereoscan-240 supplied by Cambridge Instruments (currently LEO Electron Microscopy, Thornwood, NY), operated at 30 kV. The SEM images were used to determine the size of the silver colloid and to estimate the thickness of the silica layer. Gold sputter coating on the silver particles was not performed prior the SEM image acquisition because of silver's inherent high electron density.

Results and Discussion

Figure 2 demonstrates the sensor response and fluorescence signal enhancement due to incorporation of uncoated silver colloid into the sensing membrane. The test sample was a 5×10^8 cells/ml Pa

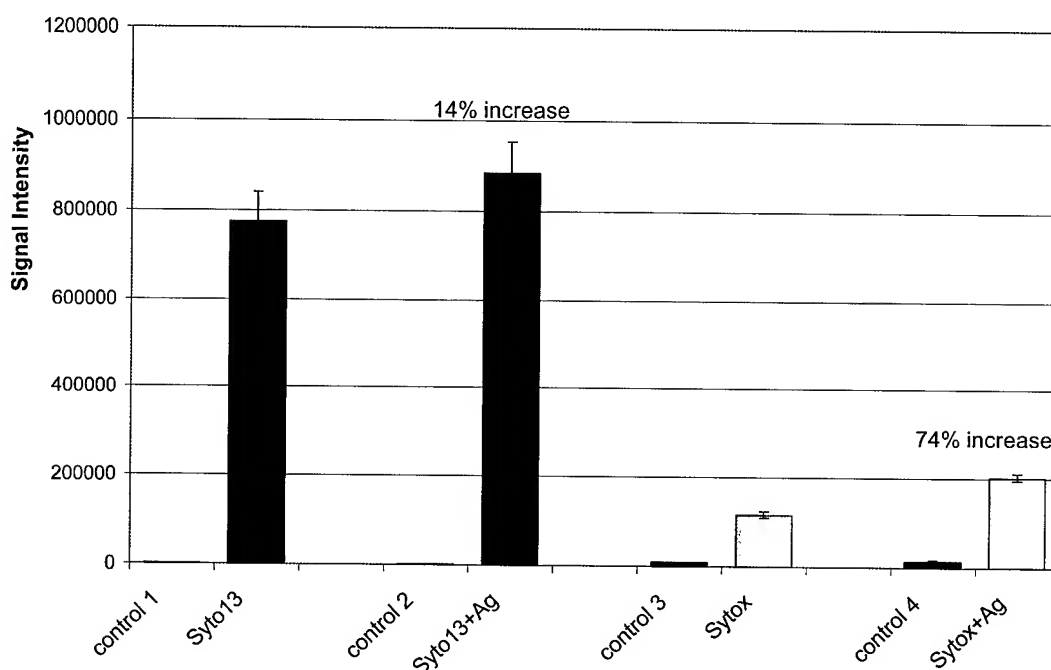


Figure 2. Fluorescence signal enhancement on a bacterial sensor using silver colloid. In the plot, "Ag" refers to chemistry containing silver colloid, and "control" refers to blank measurements which use water as the sample. The error bars represent one standard deviation from three replicate measurements.

suspension in water. The signal enhancements were 14% and 74%, respectively, using SYTO 13 and SYTOX Green chemistry when uncoated silver colloid was incorporated in the sensor. The fluorescence signal increase was small compared to a 20-fold increase reported in the literature, where silver colloid was coated with a spacer layer.² Addition of a spacer layer on the silver colloid surface should minimize fluorescence quenching and result in greater fluorescence enhancement.

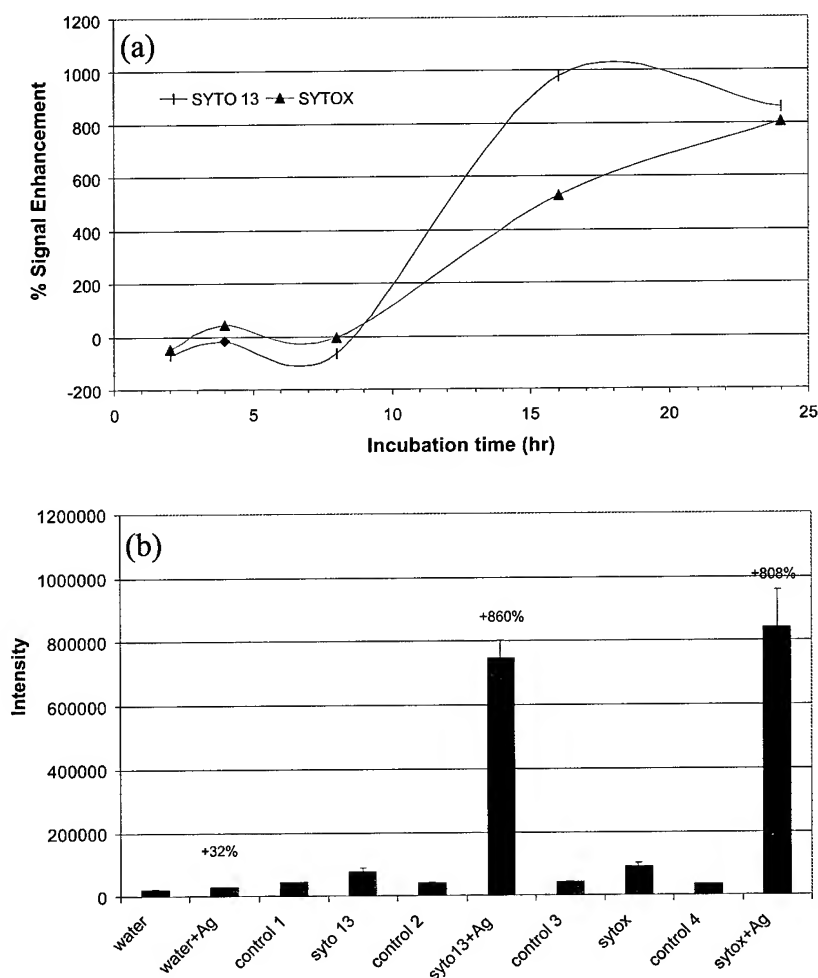


Figure 3. Fluorescence enhancement using coated silver colloid. (a) effect of incubation time on signal enhancement, and (b) a plot showing maximized signal enhancement with 24 hr incubation time. In the plot, "Ag" refers to sensors which contain silica-coated silver colloid.

There are many parameters that determine the thickness of the silica spacer layer including reagent concentration and incubation time. The effect of incubation time on the silica formation process was studied and the results are presented in Figures 3a and 3b. In Figure 4 SEM images of the silica-coated colloid are presented. An incubation time of at least 16 hrs was necessary to obtain significant fluorescence enhancement (Figure 3a), which was 800% or greater (Figure 3b). We believe that better signal enhancement can be achieved by fine tuning the silica coating process or the sensing chemistry formulation. This may include optimization of reagent concentrations and processing variables used to coat the colloid, and dye or colloid concentrations in the sensing chemistry.

CONCLUSIONS

Significant signal enhancement in optical bacterial sensors has been demonstrated. The signal increases arise from Surface Enhanced Fluorescence resulting from incorporation of silver colloid into the sensing film. Addition of a silica coating on the silver colloid particles as a spacer layer results in a signal increase of 8-fold or greater. The SEF effect can be even greater after optimization of reagent concentrations and layer thickness. Procedures for preparation of silica-coated silver colloid are simple, therefore this technique should be applicable to many other fluorescence-based sensing methods.

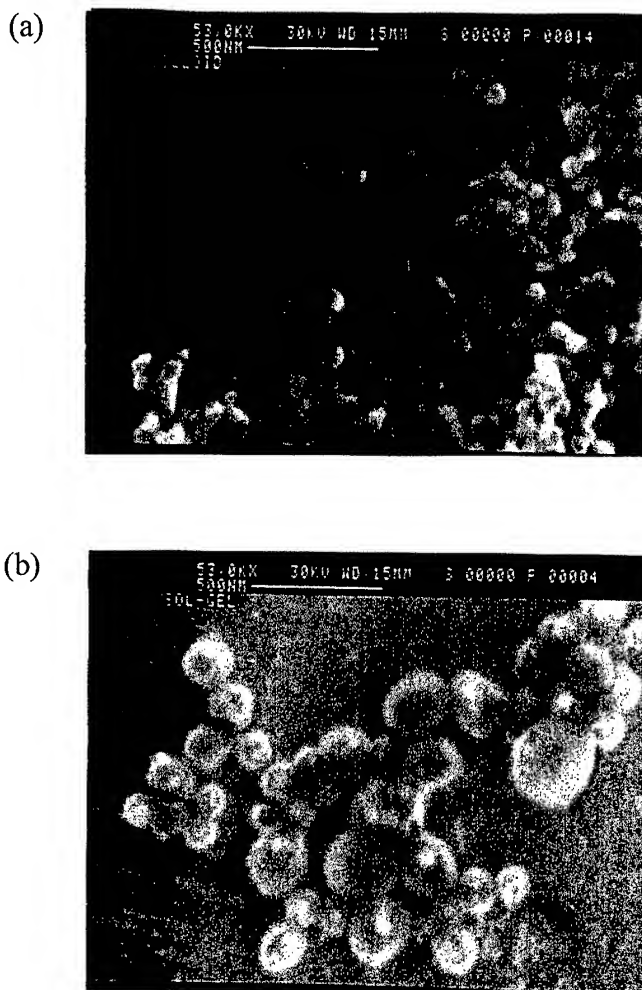


Figure 4. SEM image of (a) uncoated silver colloid particles and (b) silica-coated silver colloid particles. The thickness of the silica coating is approximately 30 μ m or more.

ACKNOWLEDGEMENT

We would like to thank Army Research Laboratory for their financial support of this project, under contract number DAAL01-98-C-0077.

REFERENCES

1. *Hobson, N. S.; Tothill, I.; Turner, A. P. F. Biosensors & Bioelectronics* **1996**, *11*(5), 455-477.
2. *Sokolov, K.; Chumanov, G.; Cotton, T. M. Anal. Chem.* **1998**, *70*, 3898-3905.
3. *Mittelman, M. W., Greesey, G. G., Hite, R. R. Microcontamination* **1983**, *1*(2), 32-37.

NON-INTRUSIVE ANALYSIS OF CHEMICAL AGENT IDENTIFICATION SETS (CAIS) USING A PORTABLE FIBER-OPTIC RAMAN SPECTROMETER

Steven D. Christesen, Brian MacIver, Lawrence Procell, and David Sorrick
Research and Technology Directorate, U.S. Army Edgewood Chemical Biological Center
Aberdeen Proving Ground, MD 21010-5424

Michael Carrabba [†] and Job Bello
EIC Laboratories, Inc.
Norwood, MA 02062

ABSTRACT

Portable fiber-optic Raman systems are being used to analyze chemical agents and other toxic chemicals in sealed glass containers. These containers include ampoules and bottles that are contents of chemical agent identification sets (CAIS) developed for use in training military personnel in chemical agent identification, safe handling, and decontamination. Real-time non-intrusive analysis of these sets is required so that the items containing chemical agents can be identified for proper disposal. This paper details the laboratory measurement of Raman spectra of CAIS chemicals and the analysis of CAIS items in the field. We also discuss the evaluation of man-portable Raman instruments for CAIS assessments.

[†] Present address: Chromex, P.O. Box 3190 Albany, OR 97321-0706.

1. INTRODUCTION

The army used chemical agent identification sets (CAIS) from 1928 to 1969 to train military personnel in the identification, safe handling, and decontamination of chemical warfare agents. These sets, which were produced in large quantities and distributed widely, contain samples of chemical warfare agents as well as other hazardous chemicals (Table 1). Of the chemicals found in the sets, only mustard, nitrogen mustard, and lewisite are still classified as chemical warfare material.

The U.S. Army Program Manager for Non-Stockpile Chemical Materiel (PMNSCM) is responsible for the disposal of recovered CAIS. Comprising chemicals in sealed in glass ampoules or bottles; the CAIS are stored at military sites throughout the country awaiting final disposition. In order to dispose of these samples, the ampoules and bottles containing military chemical agents (mustard, lewisite, and nitrogen mustard) need to be segregated from those containing only industrial compounds (phosgene, cyanogen chloride, GA simulant, chloroacetophenone, adamsite, triphosgene, and chloropicrin). The industrial chemicals can be disposed of as "normal" hazardous waste, while the chemical agents must first undergo chemical neutralization.

The identification of the CAIS contents is being accomplished with the use of a portable, fiber optic Raman spectrometer system operating in the near IR spectral region.¹ The laser energy and the Raman scattered radiation are readily transmitted through the glass so that the analysis can be accomplished without opening the ampoule or bottle. The fiber optic probe allows for the placement of the Raman instrument up to 25 meters from the CAIS ampoules themselves.

**Table 1: Contents of CAIS
STORED IN AMPOULES**

5% sulfur mustard (HD, H, or HS) in chloroform
5% lewisite (L) in chloroform
10% nitrogen mustard (HN-1 or HN-3) in chloroform
neat phosgene (CG)
neat cyanogen chloride (CK)
50% chloropicrin (PS) in chloroform
GA simulant

STORED IN BOTTLES

neat sulfur mustard
sulfur mustard adsorbed on charcoal
lewisite adsorbed on charcoal
nitrogen mustard (HN-1 or HN-3) adsorbed on charcoal
chloropicrin adsorbed on charcoal
solid chloroacetophenone (CN)
solid triphosgene (CG simulant)
solid adamsite (DM)

Spontaneous Raman spectroscopy can be used to identify molecules via their characteristic vibrational signatures. Until recently, however, Raman analysis has been confined to the analytical or physical chemistry laboratory. With the advances in charge coupled device (CCD) detectors, optical filters, diode lasers, and fiber optics, Raman spectroscopy has broken out of the laboratory and become an analytical technique for field use.²⁻⁵ Numerous companies, including EIC Laboratories, Ocean Optics/Boston Advanced Technologies, and Multichannel Instruments, are now building small, portable Raman instruments that were inconceivable only 10 years ago. The CCD array detectors have eliminated the need to scan mirrors or gratings and the need for an exit slit. Without moving parts, the Raman instruments have become much less prone to misalignments, and can be made quite rugged. A Raman system has even been designed for deployment on a lander or rover for analysis of extraterrestrial rocks and soil.⁵

In this paper, we discuss laboratory measurements of known samples (CAIS standards) and actual field measurements of recovered CAIS items. Some of the recovered items were returned to the Edgewood Chemical Biological Center (ECBC) for laboratory analysis using normal gas chromatography (GC) and gas chromatography with mass spectrometry (GC/MS). These intrusive analyses allowed us to assess the accuracy of the non-intrusive Raman analyses.

Although a desired goal, the Raman instrument need not specifically identify the CAIS contents. It is required only to provide sufficient information to determine whether or not the CAIS item contains a chemical agent (mustard, nitrogen mustard, or lewisite).

1. CHEMICAL AGENT IDENTIFICATION SETS

1.1. CAIS Description

Several different kinds of chemical agent identification sets were developed and fielded. Liquid samples in the sets were sealed in glass ampoules or 4 ounce bottles, and the solid samples were stored only in glass bottles. Two ampoule sizes were used; 1.875 inches in diameter by approximately 4.625 inches long and 1 inch diameter by 7.5 inches long. The contents of the bottles were typically etched in the glass and remained legible. Paper labels were used with the ampoules and were missing in almost all of the samples studied. Some of those that had labels were found to be labeled incorrectly when analyzed by the Raman system.

When initially prepared, the contents of the liquid items in the CAIS were either colorless or had a slight yellow tint. Over the years of storage, however, many of the items have degraded and are now

highly colored. Unfortunately, the color is not necessarily indicative of the contents. Based on the analyses of recovered CAIS items, the contents of an ampoule containing a clear liquid could be anyone of 4 different chemicals or mixtures. Recovered CAIS items containing lewisite in chloroform have ranged in color from clear to brown while mustard in chloroform samples have been either clear or dark red to black. Some phosgene samples have also been red.

1.2. CAIS Chemicals

Detailed descriptions of the physical, chemical, and toxicological properties of the CAIS chemicals are contained elsewhere.⁶ Only a brief description of these compounds will be given here.

Mustard (H or HD), lewisite (L), and nitrogen mustard (HN-1 or HN-3) are highly toxic vesicants or blister agents. These agents affect the eyes and lungs and blister the skin. As little as 30 drops of lewisite applied to unprotected skin can be fatal. HD, or distilled mustard, is mustard (H) that has been purified by washing and vacuum distillation. H can contain up to 30 percent sulfur impurities.

Although toxic, the remaining CAIS chemicals are not considered chemical warfare agents. Phosgene and chloropicrin attack the respiratory tract. In extreme cases, phosgene can cause membranes to swell and the lungs to become filled with fluid resulting in death due to lack of oxygen. Chloropicrin irritates the lungs, eyes, and skin and can also cause coughing, nausea, and vomiting. Cyanogen chloride is also a lung irritant in addition to producing the effects of cyanide poisoning. Adamsite (vomiting agent) and chloroacetophenone (tearing agent) are riot control agents and are less toxic than the other chemicals found in the identification sets.

2. CAIS STANDARDS

2.1. Chemicals

The laboratory studies were performed at the U.S. Army's Edgewood Chemical Biological Center in a chemical agent surety facility. All chemical surety materials were handled in an approved surety laboratory hood by Chemical Personnel Reliability Program (CPRP) certified personnel. The CAIS standards containing chemical warfare agents were prepared from spectrophotometric grade chloroform (Fisher) and CASARM (chemical agent standards analytical reference material) grade distilled mustard (HD), lewisite (L), and nitrogen mustard (HN-1). The GA simulant comprised (by volume) 46.4% ethyl myristate (Fluka), 31.7% diethyl malonate (Fluka), and 21.9% ethyl caprylate (Fluka). Chloropicrin and chloroacetophenone were purchased from Kodak and Aldrich, respectively. The adamsite, cyanogen chloride, and phosgene used were of unknown origin.

2.2. Reference Spectra

Commercial spectral search software (SpectralID™ from Galactic Industries) is used to provide a preliminary identification of the CAIS contents. The software searches a spectral database comprised of Raman spectra of the CAIS standards described above. A Raman spectroscopist familiar with the CAIS spectra confirms the identification prior to any disposition of the CAIS item. Raman spectra of most of the possible contents of the chemical agent identification sets were measured in the laboratory (triphosgene was not available), and some of these spectra are shown in Figure 1. Raman spectra of HD have previously been reported in the literature.^{7,8} The liquid samples were placed in glass ampoules identical to those used for the actual CAIS items.

Glass vials were used as sample holders for the solid samples (CN and DM). Spectra of the solid samples contained intense fluorescence backgrounds. Even with this background, however, the spectra yielded identifiable Raman lines for analysis.

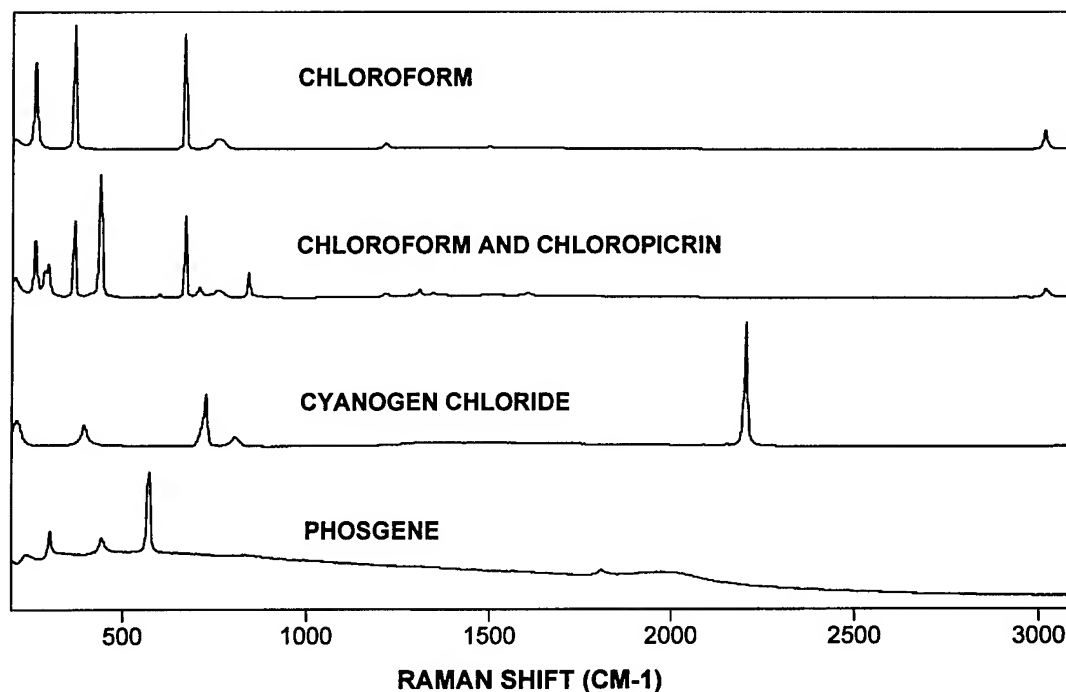


Figure 11: Library spectra of chloroform, 50:50 mixture of chloroform and chloropicrin, cyanogen chloride, and phosgene

3. RAMAN ANALYSIS OF RECOVERED CAIS

A portable fiber optic Raman system was taken to Tooele Army Depot (Utah), Ft. Devons (Massachusetts), Ft Polk (Louisiana) and the former Ft. Ord (California) for field analyses of suspect CAIS ampoules. A total of 136 CAIS items have been analyzed by Raman spectroscopy of which 67% have been identified (Table 2). In all of the items that were not positively identified, the Raman spectrum did identify the presence of chloroform. Because no CAIS ampoules were ever filled with neat chloroform, these items were assumed to contain HD, L, PS, HN-1 or HN-3 in addition to the chloroform. Some of the samples that were identified as "Unknown" (containing chloroform) by the Raman system were subsequently analyzed in the laboratory. Of the 17 samples analyzed, 13 were found to contain HD in chloroform ranging in concentration from 1.3% to 8.7%, and 4 contained L in chloroform at concentrations from 2.6% to 9.4% (an example is shown in Figure 2). Twenty items classified as unknowns were not analyzed further.

As previously stated the Raman instrument need only be able to differentiate chemical agent containing items from those that contain only industrial chemicals. Therefore, when a spectrum indicates the presence of chloroform but nothing else, the item is assumed to also contain chemical agent; either L, HD, HN-1, or HN-3. In the samples analyzed to date, this has always been the case. The spectra of chloropicrin in chloroform items have always displayed discernible peaks from both chloroform and chloropicrin.

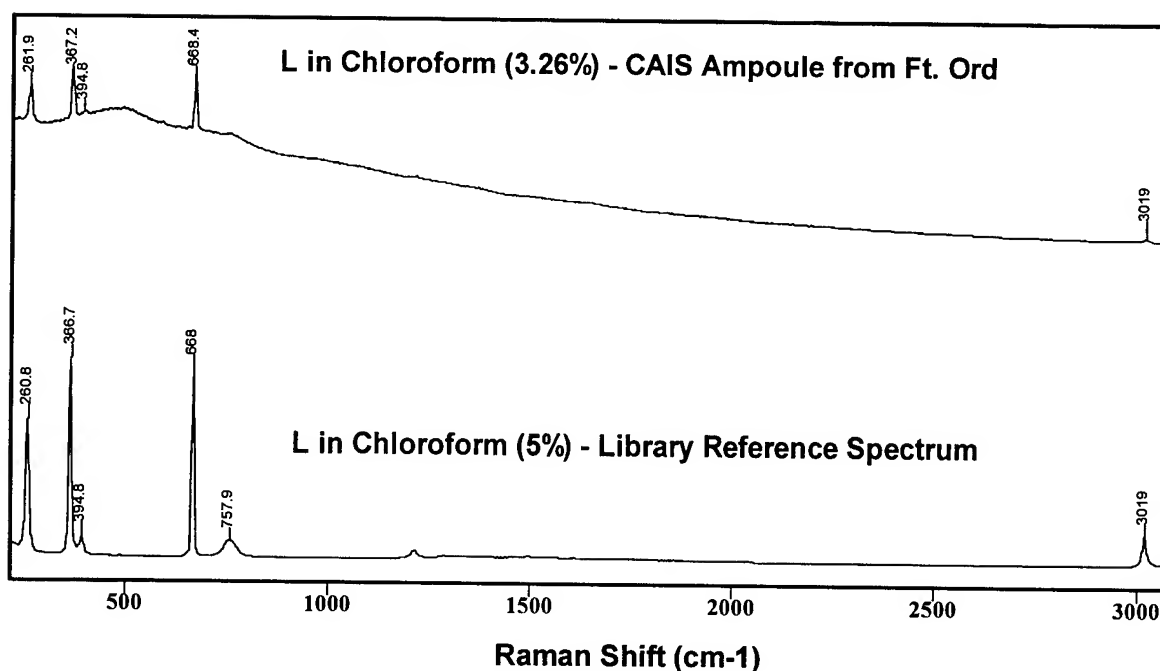


Figure 12: L in chloroform: CAIS item (upper spectrum) and reference sample (lower spectrum). The peak at 394.8 cm^{-1} is due to L, the other peaks are from chloroform.

The charcoal samples presented the biggest challenge for the Raman system. The large fluorescence background from the charcoal obscured any signal from the liquid, and no Raman analyses of these samples were possible. Luckily, the bottles containing the charcoal samples were clearly etched with the identity of the contents.

Table 2: Raman analysis of CAIS items

CAIS Item	Number of Samples	Number Identified by Raman	% Identified
L in Chloroform	20	16	80
HD in Chloroform	22	3	14
CG	30	30	100
PS in Chloroform	36	36	100
Neat PS	2	2	100
Solid CN	6	4	67
Unknowns*	20	0	0
TOTAL	136	91	67

* Raman analyses of these items showed the presence of chloroform only. They were not analyzed further.

4. RAMAN ANALYSIS OF NON-CAIS ITEMS

The Raman system has also been used to identify the contents of ampoules that appear to be items from chemical agent identification sets but are not. These ampoules have been found to contain the fumigant methyl bromide (at the former Black Hills Army Depot) and neat chloropicrin used in safe protection devices (at Ft. McCoy and the Oakcreek, WI police station). Raman spectra of these items are shown in Figure 3.

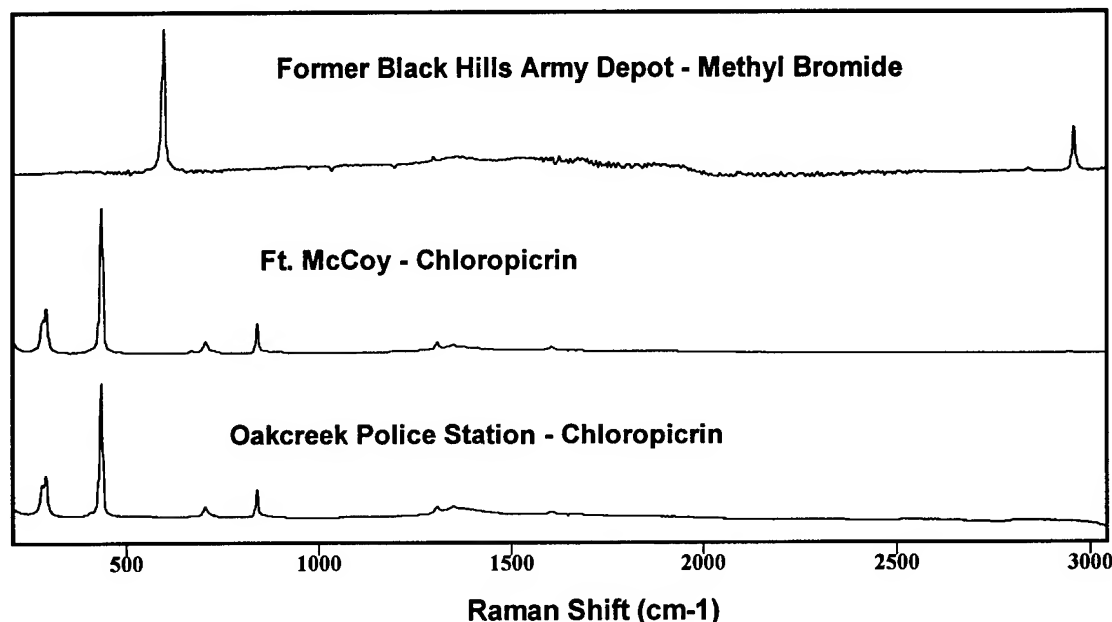


Figure 13: Spectra of non-CAIS items.

5. COMPARISON OF NEW PORTABLE RAMAN INSTRUMENTS FOR CAIS ANALYSIS

PMNSCM has developed a mobile Rapid Response System (RRS) for on-site characterization and disposal of recovered CAIS. Housed in a mobile trailer, personnel identify the agent contained in each CAIS ampoule and bottle using a fiber-optic Raman spectrometer, segregate the ampoules and bottles according to their identified chemical contents, and treat the segregated agents on-site.

In addition to the Raman system in the RRS, PMNSCM has a need for a truly man-portable instrument for assessing small numbers of suspect CAIS at military and non-military sites where deployment of the full RRS is not required. To determine the best instrument for this application, we tested 3 commercially available Raman instruments and compared their performance to the Raman system currently in the RRS (EIC Laboratories, Inc. Model RS2000). The details of that comparison can be found in reference 9. The instrument descriptions and results of the comparison are given in Tables 3 and 4.

6. CONCLUSIONS

Raman spectroscopy has been used to non-intrusively analyze the contents of glass ampoules and bottles from chemical agent identification sets. A portable, fiber-optic Raman spectrometer was taken to several locations for on-site analysis of recovered CAIS items. After transport, the Raman instrument required no recalibration and was set up and operational within 30 minutes. The portability and ruggedness of the Raman system makes it an ideal instrument for this application where low-level detection is not required.

Not all of the recovered CAIS items could be positively identified, as strong fluorescence backgrounds obscured the HD and L peaks in some of the liquid samples tested. For the recovered CAIS ampoules analyzed, only the HD and L in chloroform items were unidentified. In each of these cases, however, the chloroform was detected. When only chloroform is detected, the CAIS items are treated as if they also contained chemical agents. All CAIS items containing industrial compounds were positively identified.

Originally envisioned only as an assessment tool for the RRS, Raman spectroscopy has proven useful for analyzing of suspect CAIS items in the field. Due to the successful Raman assessment operations at the former Ft. Ord, Ft. Devons, Ft. Polk, Ft. McCoy, and Oakcreek, PMNSCM will field a man-portable Raman system capable of shipment by commercial aircraft.

REFERENCES

1. Christesen, S., MacIver, B., Procell, L., Sorrick, D., Carrabba, M., and Bello, J., "Nonintrusive Analysis of Chemical Agent Identification Sets Using a Portable Fiber-Optic Raman Spectrometer," *Appl. Spectrosc.*, Vol. 53, No. 7, pp.850-855, July 1999.
2. Angel, S.M., Cooney, T.F., and Skinner, H.T., "Applications of Fiber Optics in NIR Raman Spectroscopy", in *Modern Techniques in Raman Spectroscopy*, J.J. Laserna, Ed. (John Wiley & Sons, Ltd., Chichester, England, 1996), Chap. 10, pp. 387-417.
3. Chase, B., "A New Generation of Raman Instrumentation", *Appl. Spectrosc.*, Vol. 48, No. 7, pp. 14A-19A, July 1994.
4. Lewis, I.R. and Griffiths, P.R., "Raman Spectrometry with Fiber-Optic Sampling," *Appl. Spectrosc.*, Vol. 50, No. 10, pp. 12A-30A, October 1996.
5. Wang, A., Haskin, L.A., and Cortez, E., "Prototype Raman Spectroscopic Sensor for in Situ Mineral Characterization on Planetary Surfaces," *Appl. Spectrosc.* Vol. 52, pp. 477-487, April 1998.
6. Marrs, T.C., Maynard, R.L., and Sidell, F.R., *Chemical Warfare Agents: Toxicology and Treatment* (John Wiley & Sons Ltd., Chichester, England, 1996), Chaps. 6-10, pp. 139-227.
7. Christesen, S., "Raman Cross Sections of Chemical Agents and Simulants," *Appl. Spectrosc.*, Vol. 42, No. 2, pp. 318-321, February 1988.
8. Christesen, S., "Vibrational Spectra and Assignments of Diethyl Sulfide, 2-Chlorodiethyl Sulfide and 2,2'-Dichlorodiethyl Sulfide," *J. Raman Spectrosc.* Vol. 22, pp. 459-465, 1991.
9. Christesen, S., Procell, L., Sorrick, D., and MacIver, B., "Comparison of Portable Raman Instruments for Use in the Single CAIS Access and Neutralization (SCANS) Project," ECBC-TR-102, August 2000.

Table 3: Raman Instruments Specifications

	<i>InPhotonics Inphotote</i>	<i>Chromex Sentinel</i>	<i>INEEL Chromex</i>	<i>EIC RS2000</i>
Spectrometer				
Dimensions (in)				
Height	9	8	18½	8
Width	10	15	27¼	16
Length	16	18	34¼	26
Weight (lbs)	20	25	<150	50
Resolution (cm ⁻¹)	~6	~6	7	2
Wavenumber Range (cm ⁻¹)	234 to 2590	300 to 1850 ^a	117 to 3300 ^b	-720 to 3092
Calibration Procedure	On demand (automatic)	Continuous, automatic	On demand (automatic)	Not automatic
Laser				
Dimensions (inches)	Included in Spectrometer	Included in Spectrometer	Included in Spectrometer	10" x 3½" x 5½"
Wavelength (nm)	785	~810	785	785
Power (mW)	300	115	300	300
Other Instrumentation	None	None	None	CCD Controller 13¼" x 6¼" x 8"
Fiber Optic Probe				
Size	0.5" diam, 4" length	8" x 3" x 2.5"	8" x 3" x 2.5" ^c	0.5" diam, 4" length
Fiber Cable Type	1 excitation & 1 collection	1 excitation & 1 collection	1 excitation & 1 collection	1 excitation & 1 collection
Exc. Fiber Diam. (µm)	90	50	50	90
Emiss. Fiber Diam. (µm)	200	600	600	200
Focal Length (mm)	10	50	50	10
Cable Length Tested	25	4	25	25

Notes

- a. Sentinel Range Upgradable to 2900 cm⁻¹
- b. Due to movement of the detector, the actual range for the test was -873 to 2771 cm⁻¹
- c. The INEEL system was tested with both probe designs

Table 4: PMNSCM Portable Raman Requirements Checklist

	InPhotonics InPhotote	Chromex Sentinel	EIC RS2000	Chromex Raman 2000
Sensitivity	✓	✓	✓	✓
Resolution	✓	✓	✓+	✓
Spectral Coverage	✓	✓	✓+	✓
Size and Weight	✓+	✓	✓-	✓
Calibration	✓	✓+	✓-	✓

✓ : Meets PMNSCM requirements. ✓+: Surpasses PMNSCM requirements. ✓-: Does not meet PMNSCM requirements

DETECTION AND IDENTIFICATION OF CHEMICAL AGENTS IN WATER USING SURFACE ENHANCED RAMAN SPECTROSCOPY (SERS) ON GOLD AND SILVER DOPED SOL-GELS

*Steven D. Christesen** and Kate K. Ong

Research and Technology Directorate, U.S. Army Edgewood Chemical Biological Center
Aberdeen Proving Ground, MD 21010-5424

M. Edward Womble
Raman Systems, Inc.
Boston, MA 02215

Richard Clarke and Ranjith Premasiri
Boston University
Boston, MA 02215

ABSTRACT

The military has identified a need to detect, identify and quantify chemical and biological contaminants in water. The system currently in use (the M272 Chemical Agent Detection Kit) does not meet the current water monitoring standards. The M272 test procedures require 30-40 minutes to complete and are difficult to perform while wearing chemical protective clothing. We have undertaken a program to develop a chemical agent water monitor based on surface Enhanced Raman spectroscopy (SERS). Using SERS, we have demonstrated detection of chemical agent simulants in water at levels as low as 500 ppb.

1. INTRODUCTION

The Operational Requirements Document for a Joint Chemical/Biological Agent Water Monitor (JCBAWM) states that there is an immediate need for a device that will detect, identify, and quantify chemical and biological (CB) agents in water supplies during water point selection, production, storage, and distribution to consumers (including shower points and personnel decontamination stations). The M272 cannot detect chemical contaminants at the required levels to ensure treated water supplies meet the Tri-Service field drinking water standards nor at concentrations necessary to accurately forecast water purification equipment performance. Table 1 lists the detection requirements in $\mu\text{g/L}$ of water for water consumption rates of 5L/day and 15L/day. Also listed are the current capabilities of the M272. Current M272 Chemical Agent Test Kit procedures also require 30-40 minutes to complete a series of analyses for chemical agents. The assorted tests required to analyze for chemical agents are difficult to perform in a mission oriented protective posture (MOPP) level 4 ensemble increasing the potential for errors.

1.1. Surface Enhanced Raman Spectroscopy

We use Surface Enhanced Raman Spectroscopy (SERS) to identify the contaminating agents in water. Two properties make Raman Spectroscopy particularly well suited to measuring organic contaminants against a water background. First, similar to traditional mid-infrared spectroscopy, Raman Spectroscopy uses the characteristic vibrational features of the contaminants to provide their identity; however, Raman uses inelastic light scattering, instead of transmitting light through the sample. Second, unlike traditional infrared spectroscopy in which the vibrational fingerprint region used for identifying organic

contaminants is masked by the strong infrared absorbance of water, Raman scattering is unaffected by the presence of the water background and reports only the contaminant sample.

Table 5: DOD Tri-Services Field Water Quality Standards. Values are in $\mu\text{g/L}$.

CW Agent	Water Consumption		Sensitivity
	5 L/day	15 L/day	M272
Nerve Agents			20
VX	15	5	
GD	12	4	
GB	28	9.3	
GA	140	46	
Hydrogen Cyanide	6,000	2,000	20,000
Sulfur Mustard	140	47	2,000

The downside to Raman Spectroscopy has always been the relatively inefficient scattering and subsequent weakness of the Raman signal. In our program we use a technique known as Surface Enhanced Raman Scattering (SERS) to amplify the Raman signal to a level that allows ppm/ppb detection of the target chemical contaminants. In this approach a three to six order of magnitude increase in sensitivity, as compared to conventional Raman spectroscopy is obtained by allowing the target molecule to adsorb onto the surface of the metal. The interaction of the conducting electrons of the metal with the electrons of the adsorbed molecule creates a large change in the polarizability for the adduct, resulting in a significant increase in the scattering efficiency by the target molecule.

1.2. Metal-Doped Sol-Gels

Immobilized reagents are used in many important chemical processes like in separation science and in many catalytic processes. Sol-gel technology is one of unique ways that allows immobilization or encapsulation of chemical reagents, usually without any chemical modification to the immobilized species, under ambient processing conditions within a porous matrix. Sol-gels have many attractive characteristics like optical transparency (down to ~ 300 nm), thermal stability, chemical inertness, and tunability of its pore size, surface area, and shape.

Making sol-gel is a simple three-step process: hydrolysis, condensation, and polycondensation. The metal alkoxide precursor, alcohol (as a cosolvent), water, and an acid (as the catalyst) are mixed. Hydrolysis is initiated, and the sensing reagent (gold or silver in our case) can be added directly into the solution during this step. Next, condensation between an unhydrolyzed alkoxide group and a hydroxyl group or between hydroxyl groups occurs and a colloidal mixture called the sol forms. Finally, polycondensation between these colloidal sol particles and additional networking results in a porous, glasslike, three-dimensional lattice called the gel. The wet gel is then aged and dried to form a porous, transparent solid. The color of the solid depends the encapsulated chemical reagent.

1.3. Raman Instrumentation

Raman instruments continue to get smaller and cheaper. A number of companies including Ocean Optics and InPhotonics are building portable Raman systems. Boston University and Bruker Daltronics have built a prototype SERS based water monitor that is hand held and battery operated. The spectra

reported here were measured with a fiber-optic Raman system with 785-nm diode laser excitation (manufactured by either Kaiser or EIC Laboratories, Inc.).

2. SERS OF CHEMICAL AGENTS AND SIMULANTS

We have tested a number of different SERS active substrates including gold colloids, gold nanostructures, and sol-gels impregnated with gold and silver particles. Of these substrates, the gold sol-gels have shown the best sensitivity for the agent simulant methyl phosphonic acid (MPA). Figure 1 shows the surface enhanced Raman spectrum of 50 ppb (by mass) MPA in water with the gold sol-gel. Without surface enhancement, MPA is not detected in water at concentrations below 1 part-per-thousand. As shown in Figure 2, the SERS intensity is linear with concentration over the range from 500 ppb to 8000 ppb. More studies will determine the extent to which this linear relationship holds.

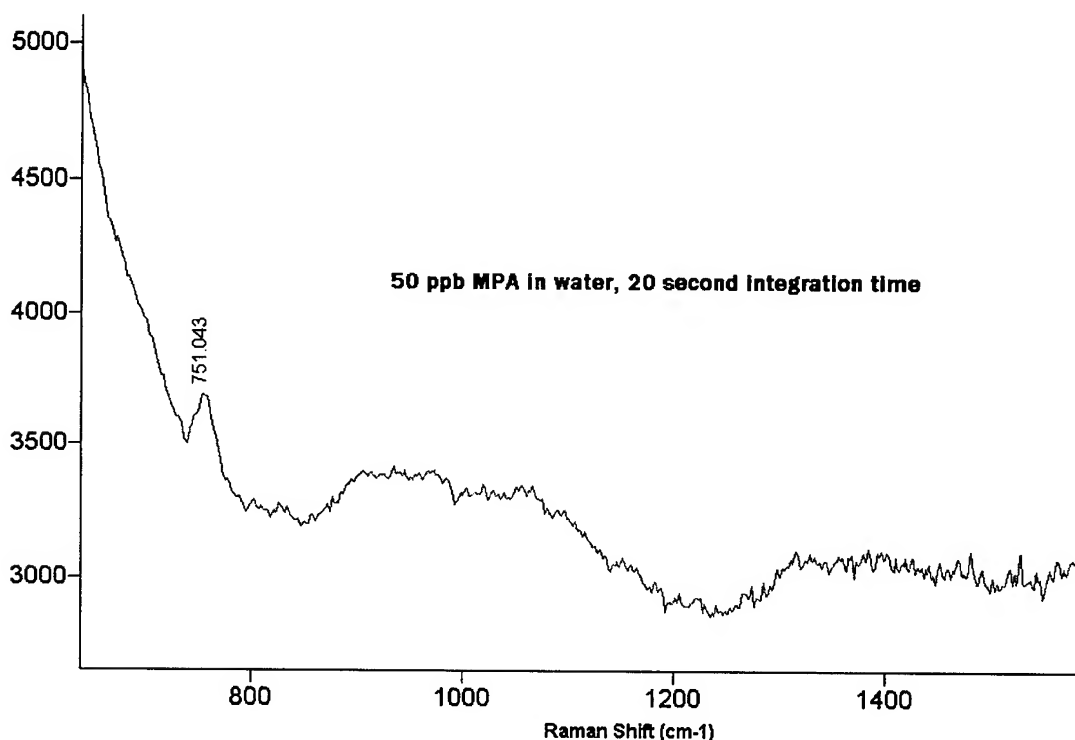


Figure 14: SERS spectrum of 50 ppb MPA in water using the gold-doped sol-gel.

We have also made preliminary SERS measurements of chemical agents in water. Figure 3 shows the SERS spectrum of GA using the gold sol-gel.

3. CONCLUSIONS

In our studies so far we have been able to detect agent simulants down to 50 ppb with Au-doped sol-gels. We have also found that gold provides greater enhancement than Ag for the agents and simulants studied. In preliminary studies, Au-doped sol-gels exhibit only modest enhancement for GA and GB. Lessons learned from these experiments, however, give us confidence that the sensitivity can be improved significantly. More chemical agent testing is to be performed with sol-gels and other SERS substrates.

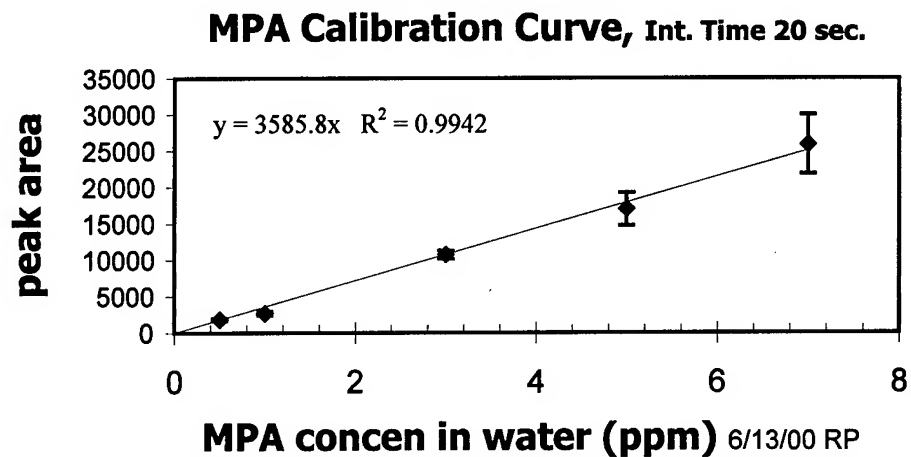


Figure 15: Calibration curve for MPA in water.

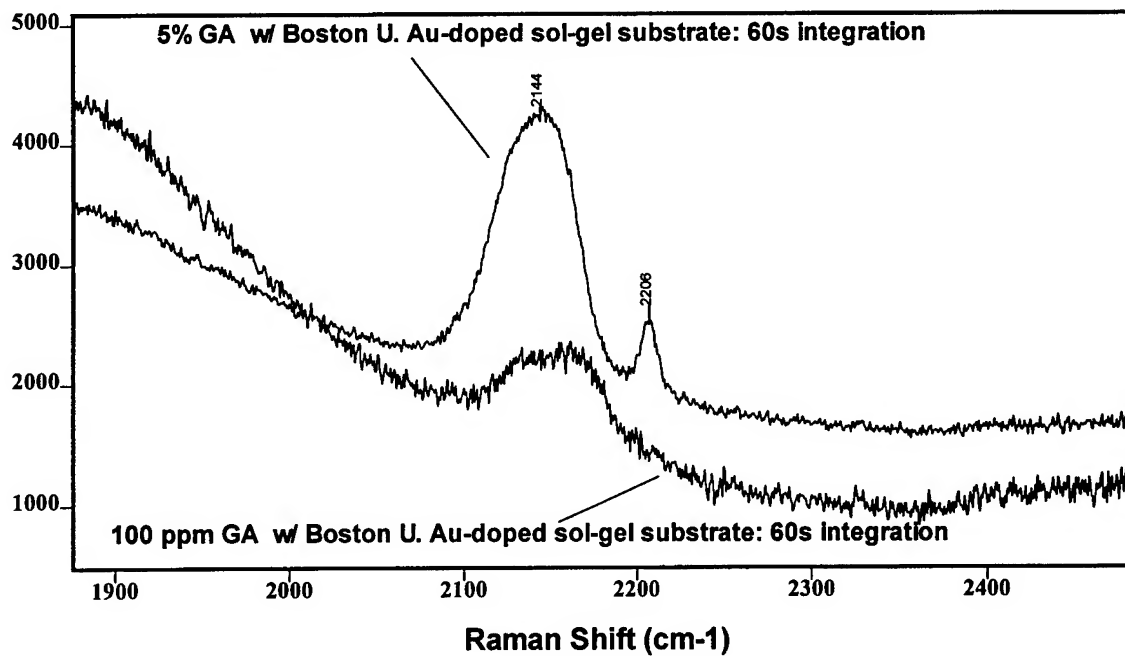


Figure 16: SERS spectrum of the chemical agent GA in water using the gold-doped sol-gel.

Acknowledgements

We would like to thank Lawrence Procell and David Sorrick (Edgewood CB Center) for their preparation of the agent samples and Dr. Stuart Farquharson and Dr. Yuan Lee (Real-Time Analyzers) for the Ag-doped sol-gels.

DETECTION OF CHEMICAL AND BIOLOGICAL AGENTS OF DEATH WITH MOLECULAR SPECIFICITY THROUGH QUANTIFIED RAMAN SPECTROSCOPY (QRS)

J. Kirchoff, J. Lucke, S. McLeod, *F. Nottke*, D. Obergh, J. Pollard

Pima Community College (West Campus Chemistry), The University Of Arizona Optical Sciences Center
and
Opto-Forensic Technologies/Wizard of Ink & Co. (OFT/WOI)
1830 East Broadway Blvd. #124-343, Tucson, Arizona, USA 85719-5968

ABSTRACT

By utilizing advances in photonics (optical) technology and creating Quantified Raman Spectroscopy (QRS), OFT/WOI introduces a technology that will greatly aid in the verification and authentication of chemical or biological agents of death (AOD). OFT, in collaboration with the University of Arizona Optical Sciences Center, is researching and developing the LVARs (Laser Verification and Authentication Raman Spectrometer™) line of spectroscopic forensic analysis/detection devices. OFT products using QRS photonics technology will prevent financial instrument/document fraud and detect agents of death before they can strike. Prevention, through detection, is the cheapest insurance money can provide in cases of fraud and death.

*These AODs are: I) Explosives and Pyrophorics; II) Chemical Agents; III) Biological Agents; IV) Drugs/Narcotics. See Appendix.

PRESENTATION

When it comes to the threat of death, prevention-through detection-is the most cost effective insurance money can provide. No amount of money can buy human life, let alone thousands of lives. But money must be paid for medical care, burial, cleanup, recovery, etc. whenever death occurs. And that cost can be substantial-it can even bring an agency to the door of ruin financially.

This "insurance" presentation deals with prevention of death through detection. Prevention is achieved whenever any agent of death-chemical or biological, natural or anthropogenic-is detected and stopped before it can unleash its action. Once that action is unleashed, all questions about the "cost" of prevention become moot. The cost of a single jumbo jet combined with the lawsuit costs after its loss, are more than the cost of all the security devices in every airport in the country. This ignores the cost, in human terms, of the loss of life. No money can satisfy that. While money saved from a disaster prevented is substantial, the value of the lives saved is beyond price.

This is not to imply that the cost of any prevention can be infinitely borne. To be widely used, any insurance technology must be effective and affordable. With the cost of x-ray and ion mobility explosive detectors in the \$100,000 to the \$1 million range, any new technology must be equal to or lower in price to compete effectively in the marketplace. Fortunately, advances in materials, science, quantum mechanics, lasers, opto-electronics and the like have created a situation where a new technology has arisen to compete successfully in both cost and effectiveness. This "new" technology we present today is really based on an old discovery dating back almost 70 years: Raman Scattering.

In 1928 at the dawn of modern quantum theory a young Indian Scientist, C.V. Raman, discovered that sometimes photons (light "particles") were not *absorbed* by an atom or molecule, but *scattered* from them. Such scattering, similar to bouncing a ball off another target "ball" (moving or stationary) could give considerable information on the nature of the other "ball". Raman won the Nobel Prize for this discovery, named after him, which was applicable to solids, liquids and gases. Because each and every

"ball"-atom or molecule-is different, the information provided is unique (like snowflakes). This atomic and molecular specificity makes Raman one of the most powerful analytical tools in chemistry and physics. But best of all, it is non-destructive. Analysis based on scattering (photon, electron, neutron, etc.), if done properly, is non-destructive because it imparts no energy to the atom or molecule being analyzed. For this reason, Raman spectroscopy (chemical study using Raman) is exploding in popularity for: medicine, forensic science (questioned document, anti-counterfeiting, drug analysis, etc.), chemical/biological/explosive agent detection, archaeology, art analysis and DWDM fiberoptic communications.

The research my scientists and students at Pima Community College and the University of Arizona, Tucson, Optical Sciences Center are conducting is in Raman Spectroscopy. By no means are we alone: substantial and important Raman research is being carried out by a number of institutions or companies (Boston University Photonics Center, Nicolet/Thermo Electron Corporation, Perkin-Elmer, InPhotonics, Renishaw, Andor, Jobin Yvon Horiba Group, Foster + Freeman, The University of Tennessee, Pfizer, Purdue University, The University of Arizona). These groups represent the gamut of research discussed earlier. Our research is in the areas of Quantified Raman Spectroscopy (QRS) and opto-electronic engineering.

Our goals include: the development of instrumentation to do QRS on a wide variety of samples; extending Raman Spectroscopy to other regions of the electromagnetic/nuclear spectrum; and the discovery of novel opto-electronic materials for Raman applications in communications, electronics, lasers, medicine and threat assessment.

Raman Spectroscopy can be used to study, verify and authenticate samples. The strengths of Raman Spectroscopy lie in the fact that:

1. It is non-destructive and non-invasive.
2. It works with water because water does not cause interference.
3. It works at wavelengths from ultraviolet to infrared (possibly all wavelengths).
4. It can be used with solids, liquids and gases.
5. It can be used with organic, inorganic and biological (living) material.
6. It can be used to determine: stability, energies, structure, functions, catalytic action, multi-component identities and various chemical/physical constants.
7. No need/requirement for vacuums, fans, pumps, special gases/atmospheres, forced air, etc.
8. It can distinguish levels of aging by analysis of oxidation and decomposition products.
9. It works through glass, quartz, most plastics; so dangerous/unstable materials can be analyzed *in situ* (bag, bottle, blisterpak)
10. Excellent spatial resolution-can be focused to analyze very small samples or parts of samples (down to a few micrometers), and thus "map" the spectral composition of a sample.
11. Very high-resolution spectroscopy can be done (less than 1 cm^{-1}), even using diode lasers.
12. Can be made a mobile unit with low power requirements with no moving parts (extremely rugged).

The high resolution, flexibility and non-destructiveness of Raman clearly distinguish it as the technique of choice for a wide range of future applications.

Because Raman Spectroscopy is a non-destructive technique that also possesses the additional advantages of being transparent to water (i.e. water does not interfere with analysis because the technique "sees" through it), and is applicable over a wide range of wavelengths, the number of potential applications of LVARs technology is quite expansive. The following nine areas represent a survey of these applications:

1. Medical - as an invasive and noninvasive diagnostic tool, in such areas as diabetes, blood cell disorders, blood analysis, cancer detection, and Pap-smear analysis (see *Anal. Chem.* **2000**, *72*, 3771-3775); detection of agents of death.
2. Dental - can be used to find dental cavities and gum abnormalities instead of x-ray.

3. Environmental - rapid, easy in-field analysis of environmental contaminants; in-line analysis of waste flows; in-line analysis of combustion smoke (cars, airplanes, and power plants); analysis of atmospheric pollutants.
4. Aerospace (Civilian) - analysis of materials for stress, corrosion, wear, etc.
5. Geological (USGS/NASA) - analysis of terrestrial and extra-terrestrial materials, including gems.
6. Military - submarine detection; detection of weapons of mass destruction (chemical and biological); detection of agents of death.
7. Manufacturing (Quality Control) - analysis and characterization of raw materials and in-flow processes.
8. Counterfeit Goods - the verification and authentication of genuine and counterfeit manufactured items (perfumes, clothing, medicine, replacement parts).
9. Optical Sciences - the analysis and characterization of compact disks, lens, fiber optics, mirrors, inks, and coatings; the use of LVARS technology to develop the next generation of high-speed Internet hardware and financial media; DWDM.

Advanced lasers, opto-electronic detectors and ingenious new techniques are only now overcoming some of the difficulties in Raman Spectroscopy:

- 1) Interference by fluorescence is avoided by use of coherent Raman techniques, spatial/temporal correlation, mathematical functions (such as Fourier Transform) and newer lasers which offer wavelengths previously unavailable. This also reduces chances of photo-activation/degradation.
- 2) Weak Raman signal intensities are overcome by stronger lasers, wavelength-specific highly sensitive detectors, surface enhancement to metals (SERS), and spatial focusing to the specific area to be analyzed, and such techniques as multiple vibrational enhancement.
- 3) Need for external calibration has been reduced by functions like Fourier Transform; QRS needs no external calibration at all because of its internal library.
- 4) Reduction of the mechanically and optically complex path that the laser and signal must travel inside the instrument.

The LVARS is a fully instrumental, non-destructive QRS device for the analysis and verification/authentication of the optical and electromagnetic properties (OEMP) of: printing agents (inks, dyes, thin films, plastics, toners, paper, fixatives, paints) used in documents and financial instruments, and agents of death (chemical or biological). The instrument is quantitative in nature so as to correlate compositional data (elemental, isotopic, structure) with Raman optical spectra. The LVARS design consists of a computer-controlled spectrometer with a microscope-guided grid head containing the laser excitation source and detector and optics. The spectrometer contains signal processing electronics which sends a stream of data to the computer for analysis and correlation with the library database. With advances in computer memory brought about by the demand in consumer electronics for audio and video, all the reference library database can be contained in a hand held device.

Because of these advantages, QRS, in the LVARS, is particularly suited for the detection of explosives and chemical warfare agents it can identify with *molecular specificity* not only what is there (qualitative analysis)- even in the presence of water or smoke or diesel fuel (common battle condition contaminants)- but also how much is there (quantitative analysis). No other technique or device currently available is as cost-effective, reliable, easy to use, safe, and versatile.

Appendix 1: Agents of Death(AOD)

The AOD'S that QRS can examine will be grouped by class for consideration. The agents are primarily anthropogenic, although some are natural or were modified from forms found in nature. There are four basic categories.

I. Explosives and Pyrophorics

A. Nuclear (the only area Raman cannot do!)

B. Chemical (low=burn, primary or high=detonate)

1. Low Explosives(propellants-solid and liquid)

- a. black powder
- b. smokeless powder
- c. liquid gasses
- d. low grade materiel

2. Primary Explosives(initiators)

- a. fulminates
- b. azides
- c. picrates, perchlorates
- d. unstable mixtures: metal salts or ions, amines

3. High Explosives

- a. nitro or nitrate compounds(TNT, nitro)
- b. TATP, C4, Detasheet
- c. Tetryl, PETN, RDX, HDX, and similar
- d. mixtures(dynamite, SEMTEX(RDX+PETN)), etc.

C. Pyrophorics

1. *Pyrophoric material* is anything that can burn or cause fires.

2. Fuel (munitions)

3. Accelerants (mainly organic fuels or solvents)

4. Incendiary agents

- a. Thermite (TH)
- b. Magnesium
- c. White & Red phosphorus (WP) (RP)
- d. Oils
- e. Thickened gasoline

5. Smokes

Zinc Chloride Smokes (HC)

- a. Zinc chloride and HCl
- b. Zinc oxychlorides
- c. Chlorosulphonic Acid (CSA)

II. Chemical Agents (including warfare)

A. Industrial (example: Insecticide and Herbicide Compounds; there are 14 *million* of these)

1. Compound One:

Sodium Cacodylate
Cacodylic acid or Dimethylarsenic acid
Water and sodium chloride

2. Compound Two:

Tri-isopropanolamine salt of 4-amino-3,5,6-tri-chloropicolinic acid (Picloram)
Tri-isopropanolamine salt of 2,4-dichlorophenoxyacetic acid (2,4,D)*
Unidentified by manufacture other than for the presence of water and a surfactant

3. Compound Three:

n-butyl ester of 2,4-d*
n-butyl ester of 2,4,5-tri-chlorophenoxyacetic (2,4,5-T*)
Isobutyl ester of 2,4,5-T*

4. Compound Four:

n-butyl ester of 2,4-D*
n-butyl ester of 2,4,5-T*

*2,4,-d and 2,4,5,-t may be contaminated with dioxins, some of which are very toxic.

B. Warfare

1. NERVE AGENTS (NA)

- a. Tabun (GA):O-ethyl dimethylamidophosphorylcyanide
- b. Sarin (GB):isopropyl methylphosphonofluoridate
- c. Soman (GD):pinaco methylphosphonofluoridate
- d. Methylphosphonothioic acids (GF & VX series:X, E, G, M, S)

2. VESICANT AGENTS 1 (blister)

Sulphur mustard (HD)

- a. N-ethyl-2,2' di(chloroethyl)amine, (HN1)
- b. N Methyl-2,2' di(chloroethyl)amine, (HN2)
- c. 2,2',2'' tri(chloroethyl)mine, (HN3)

2. Nitrogen mustard (HN)

3. Lewisite (L)

4. Halogenated Oximes

3. VESICANT AGENTS 2 (arsenicals-Lewisite)

- 1. 2-Chlorovinyl-dichloroarsine, $\text{ClCH}=\text{CH}-\text{AsCl}_2$

4. LUNG DAMAGING AGENTS (Choking Agents)

- 1. Phosgene (CG)
- 2. Diphosgene (DP)
- 3. Chlorine (Cl)
- 4. Chloropicrin
- 5. Perfluoroisobutylene (PFIB)
- 6. halogen acids (HA, A=Cl, Br, F, I)

5. CYANOGEN AGENTS (Blood Agents)

1. Hydrogen Cyanide (AC)
2. Hydrogen Sulphide
3. Cyanogen Halides
4. Halogen Moiety
5. Cyanogen Chloride (CK)
6. Cyanogen Bromide

6. INCAPACITANTS AND PSYCHOTOMIMETRIC AGENTS (see also IV)

1. Anticholinergics (CNS depressants), 3-quinuclidinyl Benzilate (BZ)
2. LSD, PCP (CNS stimulants), D-lysergic acid diethylamide
3. Amphetamines

C. Riot Control Agents

1. Orthochlorobenzylidene malononitrile (CN)
2. Chloracetophenone (CN)
3. Dibenzoxazepine (CR)
4. Arsenical smokes (sternutators)
 - a. Diphenylchlorarsine (DA) (Vomiting Agent)
 - b. Diphenylaminearsine chloride (Adamsite (DM)) (Vomiting Agent)
 - c. Diphenylcyanarsine (DC) (Vomiting Agent)
5. Bromobenzyl Cyanide (CA)
6. Bromoacetone (BA)

D. Other Potential Agents

1. Mutagens
2. Teratogens
3. Carcinogens
4. Pyrogens
5. Cytotoxins(cytolysins, shiga and like, see also III G)
6. Allergenics

III. Biological Agents (inc. warfare, genetically altered organisms, extremeophiles)

A. *Virus (Coxiella burnetti (Qfever), Vibrio cholera, Tularemia, etc?)

B. *Bacteria-Anthrax(*Bacillus anthracis*), Salmonella typhi, *Clostridium perfringens/botulinum*, Bubonic plague (Yersinia pestis)

C. *Fungi (and Lichens)

*Above three of these types includes extremeophiles.

D. Rickettsia- *Rickettsia prowasecki* (Typhus)

E. Prions (Bovine Spongiform Encephalitis)

F. Mycotoxin Agents (ATA)

G. Toxins(ricin, Staphylococcal Enterotoxin B (SEB), Botulinum, cholera, Diphtheria, cyanobacterial, other endo/exo-toxins, hemorrhagins, etc.)

H. Animal Diseases

1. Venezuelan Equine Encephalitis
2. BSE (see Prions)
3. Influenzas (avian, bovine)

I. Venoms (Animal, Insect, Plant, Sea Creature)

IV. Drugs and Narcotics

A. Legal

1. OTC

1. Pain Relievers (aspirin, ibuprofen, acetaminophen, naprox)
2. Allergy/Cold Medications (including those diverted to illegals)

2. Prescription (top ten as example)

1. Codone
2. Amoxacilline
3. Claritin
4. Albuterole
5. Propoxyphene
6. Premarine
7. Lipitor
8. Zithromax
9. Prilosec
10. Ortho-tricyclen

B. Illegal

1. THC and derivatives
2. Opiates (heroin, morphine, hash) and derivatives
3. Coca and derivatives
4. Synthesized drugs (PCP, crystal meth, amphetamines, etc)

PORPHYRINS AS DETECTORS OF CB AGENTS

H. James Harmon

Department of Physics

Department of Microbiology and Molecular Genetics

Oklahoma State University

Stillwater, OK 74078

ABSTRACT

Organic molecules including chemicals and constituents of CB agents alter the spectrophotometric characteristics of water soluble porphyrins. The absorbance spectrum of tetraphenylporphyrinsulfonate (TPPS) is shown to be changed on interaction with chemical analytes including aromatic, polyaromatic hydrocarbons, proteins, and the nerve gas and mustard simulants thiodiglycol, methylphosphonic acid, and triethanolamine. Detection limits as low as 250 ppt can be detected in less than 15 seconds.

INTRODUCTION

The detection of chemical agents and related molecules has been accomplished by numerous means including SAW/QCM devices, fluorescence and UV/Vis/IR spectroscopy, and electrochemical/enzymatic means. Specificity, sensitivity, and rapidity of detection are key desirable characteristics of any detection/sensing protocol. The reports that porphyrins are capable of interacting with numerous molecules with specific changes in their absorbance spectra suggest their utility as a rapid specific optical indicator of molecules including CB agents; the former are N- or S-mustards, organophosphates, or oximes while the latter are biological agents such as viruses, bacteria, spores, or toxins.

Porphyrins are nitrogen-containing compounds derived from the parent molecule tetrapyrroleporphin. Porphyrins are classified on the nature of the side chains replacing the hydrogens at positions 1-8; methyl, ethyl, vinyl, and propionic acid are common substituents. Complexation of porphyrins with metal alters the absorbance spectrum of the porphyrins. It is of interest to note that the wavelength of metallo-/porphyrins is dependent on the metal as well as the solvent used. The absorbance spectrum and the extinction coefficient (absorptivity) of metallo-/porphyrins are affected by the solvent and other molecules in the immediate environment. It is possible to isolate the effect of different analytes using one or more of the Soret (or B-bands (400-500 nm) or alpha band (Q-bands) from 550-650 nm absorbances. The basis for these spectral changes is similar to the basis of the change in the wavelengths absorbed by altering the groups substituting at positions 1-8 on the porphyrin ring. Factors which increase the pi-electron orbitals at the periphery of the porphyrin tend to cause red shifts of the absorbance and fluorescence (if present) bands. As pi electrons are withdrawn from the periphery, the spectrum blue shifts to shorter wavelengths. Just as the energy transitions for absorbance of photon energy are altered, so are the energy transitions involved in photon emission of absorbed energy. Thus, the fluorescence spectrum of porphyrins is altered, each having its unique spectrum (1,2).

An increasing number of publications report the chemical alteration of organic molecules by the catalytic activity of porphyrins and porphyrin-like heterocyclic compounds. In view of the intense light absorbance by these molecules, some of the catalytic processes are light-activated and light-dependent;

others may require the presence of a reductant as well. The chronicle of porphyrin-catalyzed reactions will not be exhaustive here; a sampling of the literature is provided in references 3 to 38. The intent here is to pinpoint the importance of the observation of porphyrin-catalyzed reactions. The crux of the phenomenon is that in order for porphyrins to catalyze an organic reaction, the porphyrin must bind, "dock", or somehow interact physically with the organic at least once during the catalytic process (a collisional encounter between substrate and catalyst).

Docking of the organic, analogous to the formation of an enzyme-substrate complex, should result in a distortion of the electron distribution of both molecules. Since the pi-electron distribution of the porphyrins is responsible for their intense visible light absorbance, we expect to see alterations of porphyrin spectra upon organic ligation. This idea is consistent with the changes in ϵ and λ_{\max} of the Soret (400- 450 nm) band (B-band) of the porphyrins by 1) alteration of the porphyrin sidechain constituents of the porphyrin ring, and 2) alteration of the spectral properties due to solvent polarity and hence differences in the electron distribution around the porphyrin plane as described earlier.

Alteration of the spectrophotometric characteristics of porphyrins has been reported by Mauzerall (2) and also by Shelnutz (39). In these studies, aromatic heterocyclic compounds such as phenanthrolines were complexed with porphyrin molecules; changes in pi-orbital density were observed, leading to changes in visible light absorbance, fluorescence, and Raman spectra. Close interaction of porphyrins and organics can quench porphyrin absorbance (40,41) and fluorescence spectra (40-42). Porphyrins have also been used in the shape-selective separation of aromatics and are particularly useful in the separation of fullerenes (43-45). A seminal paper indicates the Soret λ_{\max} change in the presence of organic polycyclics (46), the shift in λ_{\max} proportional to the energy of association with the porphyrin. Wavelength shifts in colorimetric indicators have been used to detect pentachlorophenol (47), cysteine and histidine (48), quinones (49-51), dinitrobenzoic acid (50,51), CO, NO₂, and H₂S (52-55) and herbicides (56).

The use of porphyrins and phthalocyanines as chemical sensor indicators is gaining in popularity. Wavelength shifts as colorimetric indicators have been used to sense the presence of pentachlorophenol (47), cysteine and histidine (48), and quinones (49-51). Hayashi, et al., and others (49,50) indicated that the binding of the quinone was via multiple H-bonds between the quinone and the OH-naphthyl subgroups of the porphyrin as well as between the quinone and the COO⁻ groups of Zn- porphyrin dinitrobenzoic acid. A gas sensor using metalloporphyrin Langmuir-Blodgett films deposited on a field-effect transistor (52) can measure CO, NO₂, and H₂S (53,55) and herbicides (56). In addition, the spectral properties of porphyrins are altered by the presence of proteins (57), nucleic acids (58,59), and amino acids (60,61), and lectins (62) similar to ricin with specific spectral changes for each analyte.

Metal chelates such as bipyridyl (and porphyrins and phthalocyanines) can oxidize nerve agents (63); this oxidation necessarily requires the docking of the agent to the metal chelate. Similarly, the binding of organophosphate nerve agent simulants to copper bound to self-assembled monolayer carboxylic acid has been reported (64). Thus, alteration in the electron density due to interaction and/or binding with another molecule, even at the periphery of then porphyrin, results in spectroscopic changes. This is the physical basis of our porphyrin-based sensor system.

The changes in the spectrophotometric characteristics of tetraphenylporphyrinsulfonate (TPPS) were measured in the presence of organic molecules, proteins, and chemical agent analogues. Methylphosphonic acid (MPA) is the hydrolysis product of phosphofluoro compounds such as GB (Sarin) and GD (Soman) as well as the phosphothionic acid compound VX. Thiodiethanol (thiodiglycol; TDG) is an analog/simulant of sulfur mustard and is after one chemical step becomes H. Triethanolamine (TEA) is a precursor to and thus a simulant of the nitrogen mustard HN1 and other nitrogen mustards.

MATERIALS AND METHODS

Absorbance spectra were recorded using either a split-beam CARY 4E or dual wavelength SDB-3 (Johnson Research Foundation, Univ. of Pennsylvania) spectrophotometer at room temperature. Spectra were recorded digitally and processed using GRAMS/32 (Galactic Industries) software. Difference spectra were obtained by recording the absolute spectra of $1.33\ \mu\text{M}$ (4 nmoles in 3 ml) in 0.05 sodium phosphate (Sorensen) buffer at pH 7.4 in the presence and absence of the analyte and digitally subtracting the 2 spectra to obtain the TPPS plus analyte *minus* TPPS difference spectrum.

Tetraphenylporphyrin sulfonic acid (TPPS) was purchased from Porphyrin Products (Logan, UT), used without further purification, and dissolved in dH_2O at $1\ \text{mg/ml}$ ($0.833\ \text{mM}$) concentration as a "stock" solution. Proteins were purchased from Sigma (St. Louis, MO) and used as provided. Organic molecules such as thiodiglycol (TDG) and methylphosphonic acid (MPA) were obtained from Aldrich (Milwaukee, WI). Formaldehyde (Sigma), naphthalene (Baker), benzene (Baker), and triethanolamine (TEA) (Fisher) were purchased at the highest purity available and used without further purification. Naphthalene and benzene were dissolved in ethanol at 3000 ppm; a small ($10\text{--}30\ \mu\text{l}$) aliquot was added to the sample such that the ethanol concentration was less than 1% w/v. In those samples where the agent was added as an ethanol solution, an equal volume of ethanol was added to the reference sample. A solution of naphthalene was made by stirring water or 0.05 M sodium phosphate buffer in the presence of excess solid naphthalene until a saturated solution (30 ppm) was obtained; this was diluted to obtain the desired concentration as an alternative method to corroborate the spectral shifts obtained with naphthalene dissolved in ethanol. Proteins were dissolved in 0.05 M sodium phosphate (Sorensen) buffer at $10\ \text{mg/ml}$ and diluted with the same buffer to attain the desired concentration.

TPPS was immobilized by placing $0.833\ \text{mM}$ TPPS onto cellulose membrane for one hour, followed by drying overnight at room temperature, and washing non-bound TPPS off the membrane with $1\ \text{M}$ NaCl and $0.1\ \text{N}$ HCl prior to storage at room temperature until used. Spectra were recorded by placing a $1\ \text{X}\ 2\ \text{cm}$ membrane strip against the inside of a 3 ml cuvette and either adding the desired solution or placing $50\ \mu\text{l}$ of a pure organic such as benzene into the cuvette (not touching the film), sealing the cuvette, and recording the spectrum after 15 minutes. The absorbance maximum of immobilized TPPS is red-shifted as indicated in Table 1.

RESULTS

The spectrum of the water-soluble porphyrin tetraphenylporphyrin sulfonate (TPPS, Fig 1)

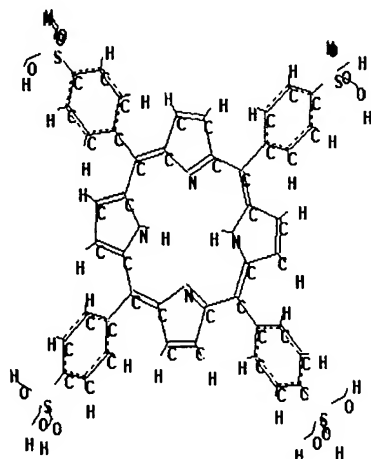


Figure 1. Structure of Tetraphenylporphyrinsulfonate (TPPS).

consists of 5 absorbance bands in the visible light region: an intense absorbance (β band) in the "Soret" region centered at 413 nm and 4 Q-bands centered at 515, 550, 580, and 633 nm as shown in Figure 2. As seen in Figure 2, interaction of TPPS with an analyte such as naphthalene or benzene cause a shift in the wavelength of the bands, normally to a longer wavelength due to the perturbation of the electron density in the TPPS by interaction with the electron clouds of the analyte present. Interaction of benzene with soluble TPPS causes shifts in the wavelength maxima to 419, 517, 553, 588, and 646 nm (cf. Fig. 3). In the difference spectrum, the presence of a new peak is seen as a peak and the loss of the original peak of TPPS upon complexation is seen as a trough; thus the difference spectrum results in a "first derivative"-looking spectrum if wavelength shifts have occurred.

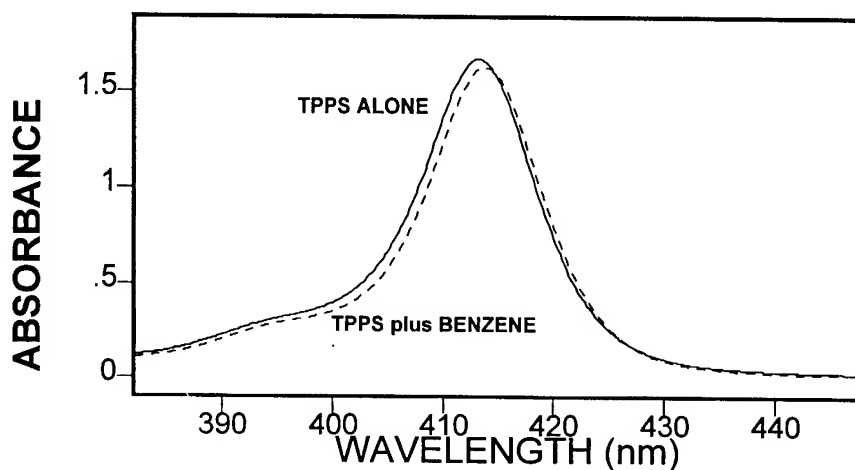


Figure 2. Absolute Spectra of TPPS and TPPS plus Benzene.

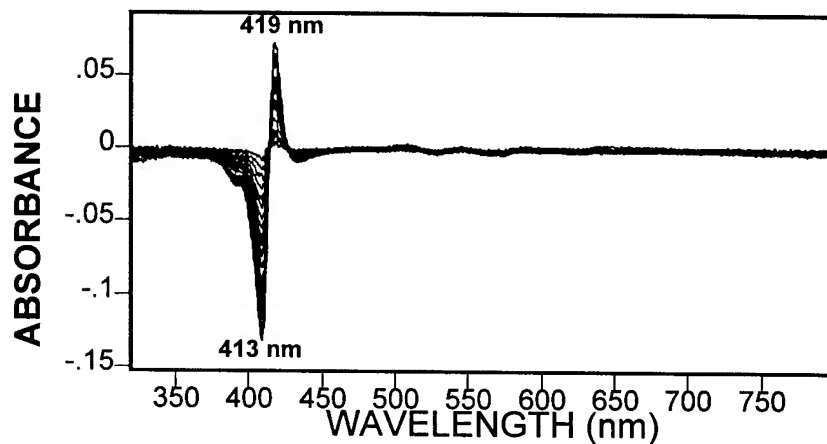


Figure 3. Difference Spectra of TPPS Plus Benzene minus TPPS at Different Benzene Concentrations.

The advantage of using difference spectra is that small shifts in wavelength, especially those involving only a fraction of the porphyrin population, are easily detected. Another advantage of using difference spectra is that small shifts in wavelength, especially those involving only a fraction of the porphyrin population, are easily detected. The new wavelength peak identifies the analyte; the absorbance change indicates quantity of analyte.

Using 5 visible light absorbance peaks of a typical porphyrin, the possibility of changing the wavelength and/or absorptivity (extinction coefficient) of each band which acts independently of the

others allows over 5^6 (7700) possible combinations of spectra; the actual number is far greater than this since each analyte shifts the spectrum and changes the absorptivity by a different value. Thus, each analyte has its own "unique" spectral signature that can be identified and utilized for determining which and what analyte is bound

Different analytes can induce shifts in other bands differently, as seen in Tables 1 and 2. In the presence of naphthalene, the Soret band is observed at 426 nm, for example.

Table 1 illustrates the great selectivity and specificity of analyte detection due to the increase in absorbance in the Soret due to complexation of analytes. It is apparent that some analyte-porphyrin complexes have similar wavelengths in the Soret band. However, when absorbance as well as wavelength differences at the Soret and the Q-bands are recorded, each analyte is different. It can also be seen from the data in Table 2 that the sensor surface is also responsive to analytes in vapor form as well.

Table 1. Changes in Soret Absorbance of TPPS in Presence of Analytes

	Absorbance	Absorbance	Immobilized	Medium
Isopropanol	431 nm	421 nm	yes	air
acetone	434	423	yes	air
methanol	429	418	yes	air
formaldehyde	431	421	yes	air
ethanol	427	416	yes	air
naphthalene	413	426	no	H ₂ O
benzene	413	419	no	H ₂ O
ANALYTE	413	434	no	"
naphthalene	424	422	yes	"

Proteins change the absorbance of porphyrins, each protein displaying a characteristic "signature". Some examples and the shifted wavelengths are shown in Table 2. The LOD values for some proteins are shown (concentration at 0.001A). TPPS interacts with the surface of the proteins, a desirable trait since we want to detect the determinants on the surface of a biological agent.

Table 2. Wavelength Shift of TPPS by Proteins

PROTEIN	"413" nm	"515" nm	"550" nm	"580" nm	"630" nm	LOD
Lysozyme	426	-----	-----	-----	650	214 ppb 15 nM
Luciferase	424.25	-----	-----	597	647	ND
ApoMyoglobin	422.5	-----	-----	-----	648	ND
Myoglobin	424	532	-----	598	649	87 ppb 5 nM
Insulin	421.4	-----	-----	-----	-----	ND
RNAase	424.6	529	560	600	653	547 ppb 40 nM
Poly-L-lysine	397	-----	562	596	649	ND
Protamine Sulfate	402.6	525	559	597	653	ND
Bovine Serum Albumin	421.5	-----	-----	592	646	ND

The Soret absorbance of aqueous TPPS changes from 413 nm to 431 nm in the presence of triethanolamine, 423 nm with a 428 nm shoulder with thiodiglycol, and 424 nm with MPA. Because of

the small absorbance changes observed and the fact that the absorbance of the Soret band is at least 5-fold greater than the other bands, absorbance changes in the Soret were recorded at the above-stated wavelengths.

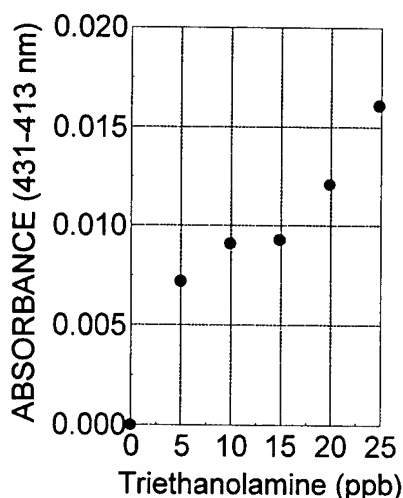


Figure 4. Triethanolamine Concentration vs. Absorbance.

The interaction of triethanolamine with soluble TPPS causes a decrease in 413 and an increase in 431 nm absorbance. At concentrations of 25 ppb or higher, a decrease in 515 nm absorbance is also seen with an accompanying increase at 537 nm. As seen in Figure 4, the magnitude of the combined 413 nm decrease and 432 nm increase is linearly dependent on the concentration of TEA present. The calculated LOD is 750 ppt.

The presence of the sulfur mustard simulant TDG (thiodiglycol, thiodiethanol) shifts the TPPS absorbance to 423 nm with a shoulder at 428 nm. As seen in Figure 5, the magnitude of the absorbance difference at 413 and 420 nm is linearly proportional to TDG at low (< 5 ppm) concentrations. The lower limit of detection (which we define as corresponding to 0.001 A change) is approximately 250 ppt.

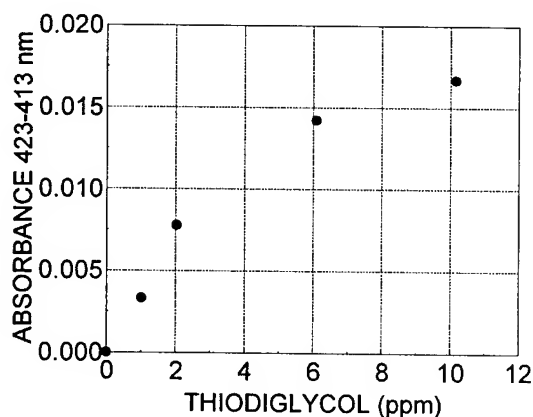


Figure 5. Thiodiglycol Concentration vs. Absorbance.

Methylphosphonic acid (MPA) is a hydrolysis product of organophosphates. In contrast to TEA and TDG where the spectral changes associated with interaction with TPPS are complete within 15 seconds, the interaction of MPA with TPPS is time-dependent. The loss of 413 nm absorbance and the

increase at 425 nm (the TPPS plus PMA *minus* TPPS difference spectrum shows a split trough at 413 and 416 nm and a 425nm peak with 430 nm shoulder) is linear with time over 45 minutes after which time no further absorbance change is observed. After 45 minutes incubation time, the extent of absorbance change is linear up to 6 μ M (576 ppb) MPA. The estimated LOD (0.001 A change) is 8 ppb (cf. Figure 6).

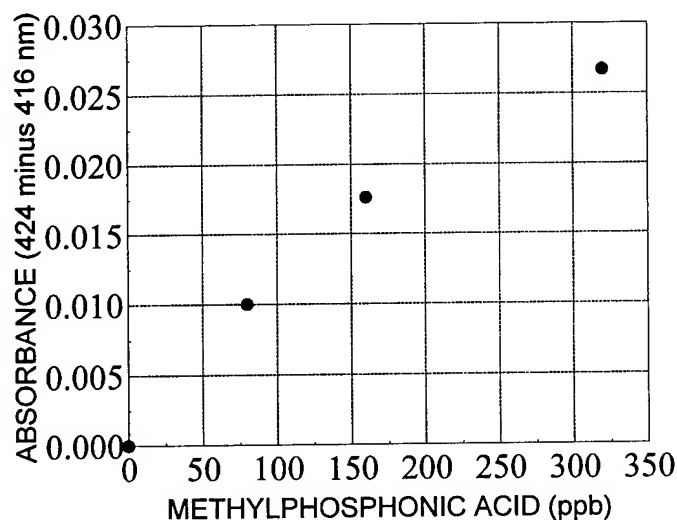


Figure 6. Methylphosphonic Acid Concentration vs. Absorbance.

CONCLUSIONS

While a porphyrin such as TPPS has 5 absorbance bands (Soret and 4 "Q" bands), the ratios of extinction coefficients are 530:17:7.5:7.1:3.7. While 7700 combinations of spectral changes of the 5 bands are possible, only changes in the absorbance of the prominent highly absorbing Soret band can be used at low (<50 ppb) analyte concentrations. The lower limit of detection is determined by the spectrophotometer used. We have specified LOD's based on 0.001 A changes which are not difficult to accurately measure using our equipment. At higher analyte levels, changes in the Q-bands can be measured as well, allowing greater specificity in the response and identification of the agent. That over 7700 combinations are possible is a valid conclusion since, as seen in Table 2, the absorbance bands act independently of each other. This is apparent from the observations that with some analytes not all bands are affected and those that are affected are not affected to the same extent. Thus, the availability of multiple absorbance bands grants considerable specificity while the large absorptivity allows considerable sensitivity.

Although biological agents per se were not used, the ability of proteins to alter the spectrophotometric characteristics of porphyrins has been demonstrated. The surface of viruses, bacteria, and spores contain proteins. Differences between different strains of cells or viruses are the result of differences in surface proteins. That new influenza strains are not neutralized by our immune system is due to slight changes in the structure of surface proteins such as neuraminidase that are not "recognized" by antibodies against the protein antigens of earlier strains. Because different pathogens have different surface protein components, we believe that porphyrins can potentially identify and differentiate between biological agents. In addition, some toxins are proteins. Thus, the presence of a pathogen or its toxin can be detected by its specific spectral changes.

REFERENCES

- 1) Igarashi, S. and Yotsuyanagi, T. (1993) *Analytica Chimica Acta* 281, 347-351.
- 2) Mauzerall, D. (1965) *Biochem.* 4, 1801-1810.
- 3) Karasevich, I.E., Anisomova, B. L., Rubailo, V.L., and Shilov, A.E. (1993) *Kinetics and Catalysis* 34, 651-657.
- 4) Kuroda, Y., Suzuki, Y., and Ogoshi, H. (1994) *Tetrahedron Letters* 35, 749-750.
- 5) Grinstaff, M.W., Hill, M.G., Labinger, J.A., and Gray, H.B. (1994) *Science* 264, 1311-1313.
- 6) Banfi, S., Maiocchi, A., Moggi, A., Montanari, F., and Quici, S. (1990) *J. Chem. Soc., Chem. Commun.*, 1794-1796.
- 7) Battioni, P., Renaud, J.-P., Bartoli, J.F., and Mansuy, D. (1986) *J. Chem. Soc., Chem. Commun.*, 341-343.
- 8) Traylor, T.G., Fann, W-P., and Bandyopadhyay, D. (1989) *J. Am. Chem. Soc.* 111, 8009-8010.
- 9) Anelli, P.L., Banfi, S., Montanari, F., and Quici, S. (1989) *J. Chem. Soc., Chem. Commun.*, 779-789.
- 11) Banfi, S., Legramandi, F., Montanari, F., Pozzi, G., and Quici, S. (1991) *J. Chem. Soc., Chem. Commun.*, 1285-1287.
- 11) Mansuy, D., Battioni, P., and Renaud, J-P. (1984) *J. Chem. Soc., Chem. Commun.*, 1255-1257.
- 12) Renaud, J-P., Battioni, P., Bartoli, J.F., and Mansuy, D. A (1985) *J. Chem. Soc., Chem. Commun.* 888-889.
- 13) Miki, K. and Sato, Y. (1993) *Bull. Chem. Soc. Japan* 66, 2385-2390.
- 14) Akasaka, T., Haranaka, M., and Ando, W. (1993) *J. Am. Chem. Soc.*, 115, 7005-7006.
- 15) Ostovic, D., He. G-X., and Bruce, T.C. (1994) in "Metalloporphyrins in Catalytic Oxidations" (R.A. Sheldon, ed.) pp 29-68. Marcell Dekker, Inc., New York.
- 16) Zheng, T.-C. and Richardson, D.E. (1995) *Tetrahedron Lett.* 36, 833-836.
- 17) Zheng, T.-C. and Richardson, D.E. (1995) *Tetrahedron Lett.* 36, 837-840.
- 18) Hennig, H., Behling, J., Meusinger, R., and Weber, L. (1995) *Chem. Ber.* 128, 229-234.
- 19) Gilmartin, C., and Smith, J.R.L. (1995) *J. Chem. Soc. Perkins Trans.* 2, 243-251.
- 20) Shukla, R.S., Robert, A., and Meunier, B. (1996) *Journal of Molecular Catalysis A: Chemical* 113, 45-49.
- 21) Ohtake, H., Higuchi, T., and Hirobe, M. (1995) *Heterocycles* 40, 867-903.

- 22) Appleton, A.J., Evans, S., and Smith, J.R.L. (1996) *J. Chem.Soc. Perkins Trans* 2, 281-285.
- 23) Bolzonella, E., Campestri, S., Di Furia, F., and Ghiotti, P. (1996) *J. Phys. Org. Chem.* 9, 539-544.
- 24) Maldotti, A., Molinari, A., Bergamini, P., Amadelli, R., Battioni, P., and Mansuy, D. (1996) *J. Molecular Catalysis A: Chemical* 113, 147-157.
- 25) Takeuchi, M., Kodera, M., Kano, K., and Yoshida, Z. (1996) *J. Molecular Catalysis A: Chemical* 113, 51-57.
- 26) Weber, L., Hommel, R., Behling, J., Haufe, G., and Hennig, H. (1994) *J. Am. Chem. Soc.* 116, 2400-2408.
- 27) Cooke, P.R. and Smith, J.R.L. (1994) *J. Chem. Soc. Perkins Trans* 1, 1913-1923.
- 28) Martinez-Lorente, M.A., Battioni, P., Kleemiss, W., Bartoli, J.F., and Mansuy, D. (1996) *J. Molecular Catalysis A: Chemical* 113, 343-353.
- 29) Gold, A., Jayaraj, K., Ball, L.M., and Brust, K. (1997) *J. Molecular Catalysis A: Chemical* 125, 23-32.
- 30) Meunier, B. and Sorokin, A. (1997) *Accounts of Chemical Research* 30, 470-476.
- 31) Maldotti, A., Bartocci, C., Varani, G., Molinari, A., Battioni, P., and Mansuy, D. (1996) 35, 1126-1131.
- 32) Hampton, K.W. and Ford, W.T. (1996) *J. Molecular Catalysis A: Chemical* 113, 167-174.
- 33) Bhyrappa, P., Young, J.K., Moore, J.S., and Suslick, K.S. (1996) *J. Molecular Catalysis A: Chemical* 113, 109-116.
- 34) Kamp, N.W.J. and Smith, J.R.L. (1996) *J. Molecular Catalysis A: Chemical* 113, 131-145.
- 35) Wang, X. and Woo, L.K. (1998) *J. Org. Chem* 63, 356-360.
- 36) Anzenbacher, P., Jr. and Kral, V. (1995) *J. Molecular Catalysis A: Chemical* 96, 311-315.
- 37) Anzenbacher, P., Jr. and Kral, V., Jursikova, K., Gunterova, J., and Kasal, A. (1997) *J. Molecular Catalysis A: Chemical* 118, 63-68.
- 38) Abatti, D., Zanicelli, M.E.D., Iamamoto, Y., and Idemori, Y.N. (1997) *Thin Solid Films* 310, 296-302.
- 39) Shelnutt, J.A. (1983) *J. of Phys. Chem.* 87, 605-616.
- 40) Sato, T., Ogawa, T., and Kano, K. (1984) *J. Phys. Chem* 88, 3678-3682.
- 41) Kano, K., Nakajima, T., and Hashimoto, S. (1987) *J. Phys. Chem.* 91, 6614-6619.
- 42) Kano, K., Takei, M. and Hashimoto, S. (1990) *J. Phys. Chem.* 94, 2181-2187.

- 43) Kibbey, C.E. and Meyerhoff, M.E. (1993) *J. Chromatography* 641, 49-55.
- 44) Kibbey, C.E., Savina, M.R., Parseghian, B.K., Francis, A.H., and Meyerhoff, M.E. (1993) *Anal. Chem.* 65, 3717-3719.
- 45) Xiao, J., Savina, M.R., Martin, G.B., Francis, A.H., and Meyerhoff, M.E. (1994) *J. Am. Chem. Soc.* 116, 9341-9342.
- 46) Schneider, H.-J. and Wang, M. (1994) *J. Org. Chem.* 59, 7464-7472.
- 47) Zhao, S. and Luong, J.H.T. (1995) *J. Chem. Soc., Chem. Comm.* 1995, 663-664.
- 48) Sekota, M. and Nyokong, T. (1997) *Polyhedron* 16, 3279-3284.
- 49) Hayashi, T., Miyahara, T., Koide, N., Kato, Y., Masuda, H., and Ogoshi, H. (1997) *J. Am. Chem. Soc.* 119, 7281-7290.
- 50) Hayashi, T. and Ogoshi, H. (1997) *Chem. Soc. Reviews* 26, 355-364.
- 51) D'Souza, F., Deviprasad, G.R., and Hsieh, Y.-Y. (1997) *Chem. Commun.* 1997, 533-534.
- 52) Kawakami, T. and Igarashi, S. (1996) *Anal. Chim. Acta* 333, 175-180.
- 53) Vaughn, A.A., Baron, M.G., and Narayanaswamy, R. (1996) *Anal. Comm.* 33, 393-396.
- 54) Gu, C., Sun, L., Zhang, T., and Li, T. (1996) *Thin Solid Films* 284-285, 863-865.
- 55) Inagaki, N., Tasaka, S., and Sei, Y. (1996) *Polymer Bull.* 36, 601-607.
- 56) Alvarez, J., Souto, J., Rodriguez-Mendez, and Saja, J.A. (1998) *Sensors and Actuators B. Chemical* 48, 339-343.
- 57) Harmon, H.J. (2000) *Biosensors and Bioelectronics*, submitted.
- 58) Korri-Youssoufi, H., Garnier, F., Srivastava, P., Godillot, P., and Yassar, A. (1997) *J. Am. Chem. Soc.* 119, 7388-7389.
- 59) Wandrekar, V., Trumble, W.R., and Czuchajowski, L. (1996). *J. Heterocyclic Chem.* 33, 1775-1783.
- 60) Sekota, M. and Nyokong, T. (1997). *Polyhedron* 16, 3279-3284.
- 61) Hayashi, T., Miyahara, T., Koide, N., Kato, Y., Masuda, H., and Ogoshi, H. (1997) *J. Am. Chem. Soc.* 119, 7281-7290.
- 62) Arimori, S. Takeuchi, M., and Shinkai, S. (1996) *J. Amer. Chem. Soc.* 118, 245-246.
- 63) Xie, Y. and Popov, B.N. (2000) *Anal. Chem.* 72, 2075-2079.
- 64) Crooks, R.M. and Ricco, A.J. (1998) *Acc. Chem. Res.* 31, 219-227.

ROTATIONAL SIGNATURES OF CHEMICAL AGENTS AND RELATED COMPOUNDS

R. D. Suenram, A. R. Hight Walker, G. T Fraser, and D. F. Plusquellic
Optical Technology Division
National Institute of Standards and Technology
Gaithersburg, MD 20899

R. S. DaBell, P. M. Chu, and G.C. Rhoderick
Analytical Chemistry Division
National Institute of Standards and Technology
Gaithersburg, MD 20899

and

Alan C. Samuels, James O. Jensen, Michael W. Ellzy, and J. Michael Lochner
Edgewood Chemical Biological Center
Edgewood Area, Aberdeen Proving Ground, MD 21010-5424

Abstract: The rotational spectra of more than twenty different chemical-warfare agents, precursors, and decomposition products have been studied using the technique of Fourier-Transform MicroWave (FTMW) spectroscopy. The compounds studied include the four common G-agents (GA, GB, GD, and GF). Here, we describe FTMW spectroscopy, which is a high sensitivity technique (better than $\mu\text{mol/mol}$, i.e. 1 ppm), with near real-time response (down to 1 s) and 100 % certain chemical identification. The development of FTMW for gas analysis builds upon a long history at NIST in the quantitative analysis of gas mixtures.

Introduction: Over the past several years we have been assessing the feasibility of using Fourier-transform microwave spectroscopy for chemical analysis. Interest has been expressed in this technique by practicing analytical chemists from regulatory agencies, automobile manufacturers, and the chemical weapons community. These interests are motivated in large part by the need for new and improved measurement tools to accurately and unambiguously quantify various hydrocarbons, oxygenated hydrocarbons, chemical-warfare agents etc. For instance, in the automobile industry, real-time concentration measurements of the automobile exhaust-gas composition could potentially provide feedback on the complex chemistry in the engine and exhaust system, which in turn, could be used to improve fuel formulations and engine performance, while reducing emissions.

In the chemical agent arena, the rotational spectra of more than twenty different chemical warfare agents, precursors, and decomposition products have been studied, including the four common G-agents (GA, GB, GD, and GF). Here, we describe the technique of Fourier-Transform MicroWave (FTMW) spectroscopy, which is a high sensitivity technique (better than $\mu\text{mol/mol}$, i.e. 1 ppm) with near real-time response (down to 1 s) and 100 % certain chemical identification. The development of FTMW for gas analysis builds upon a long history at NIST in the quantitative analysis of gas mixtures, which includes standard reference gas mixtures, and more recently the development of a quantitative infrared spectral database of common air pollutants.¹

FTMW spectroscopy was originally developed approximately 20 years ago by Balle and Flygare (1981)² for the measurement of the microwave rotational spectra of trace exotic chemical species, such as weakly bound dimers, hydrogen-bonded complexes, diatomic molecules ablated from refractory materials, and free radicals. The high sensitivity of the technique and its unprecedented accuracy in species identifications motivated the beginning of an effort to assess the potential of FTMW spectroscopy

for the quantitative chemical analysis of complex gas mixtures. Initial studies along these lines by Andresen *et al.* (1994)³ and Lovas *et al.* (1994)⁴ demonstrated the ability of the technique to deliver a linear response for a single trace-gas impurity in a nitrogen gas stream. Since that time we have demonstrated the generality of the technique for the potential quantification of a variety of impurities in nitrogen or rare-gas streams at concentration levels less than 1 $\mu\text{mol/mol}$ ⁵. Some of the studied compounds relevant to the chemical weapons community are listed in Table I below. Of particular interest are the rotational spectra of the various G agents. In total, more than 20 compounds have been studied for this project.

Table I. Agents and Related Compounds Studied by FTMW Spectroscopy	
<i>G-Agents</i>	<i>Mustard Related Compounds</i>
Tabun (GA)	Diethyl sulfide (DES)
Sarin (GB)	Chloroethylethylsulfide (CEES)
Soman (GD)	Thiodiglycol (TDG)
Cyclohexyl Sarin (GF)	2-Hydroxyethylethylsulfide (HOEES)
<i>Simulants</i>	N-Ethyldiethanol amine
Dimethylmethylphosphonate (DMMP)	<i>Agent precursors</i>
Diethylmethylphosphonate (DEMP)	Pinacolyl alcohol
Diisopropylmethylphosphonate (DIMP)	Pinacolone
	DF

Experimental: Figures 1 and 2 show a photograph and a schematic diagram, respectively, of one of the FTMW spectrometers at NIST. Briefly, a molecular beam of a sample is injected coaxially into a high- Q Fabry-Perot microwave resonator using a pulsed-molecular-beam valve. Once the molecules reach the center of the cavity, a short (approximately 1 μs) pulse of microwave radiation resonant with one of the TEM_{00} modes of the cavity is applied to the molecular beam. If the molecules have a resonance overlapping the 500 kHz bandwidth of the cavity, a macroscopic polarization is induced. The electric field due to this polarization is detected as a function of time using a super-heterodyne receiver. The detected signal is digitized and then Fourier-transformed to obtain a spectrum. Such a spectrum is illustrated in Figure 3 for the $J = 2 - 1$ rotational transition of OC^{36}S in natural abundance in a 1 % by volume carbonyl sulfide in argon gas mixture. The natural abundance of ^{36}S is 0.015%. The "Doppler-doublet" structure is a consequence of the unidirectional molecular beam interacting with the two traveling wave components of the cavity standing wave. It should be noted that the technique is not directly applicable to molecules such as benzene, naphthalene, methane, and carbon dioxide, which lack a permanent electric dipole moment, and light hydrides such as HF or OH, which do not have any absorption lines in the microwave spectral region.

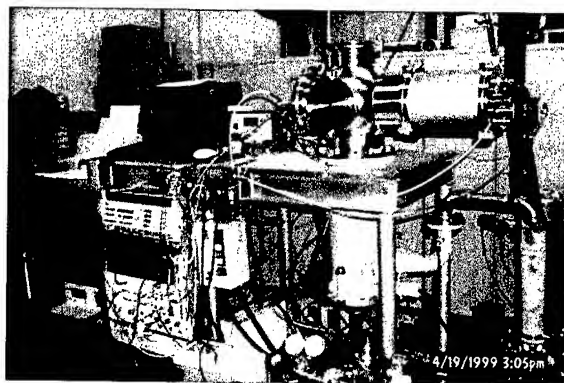


Figure 1. Photograph of FTMW Spectrometer

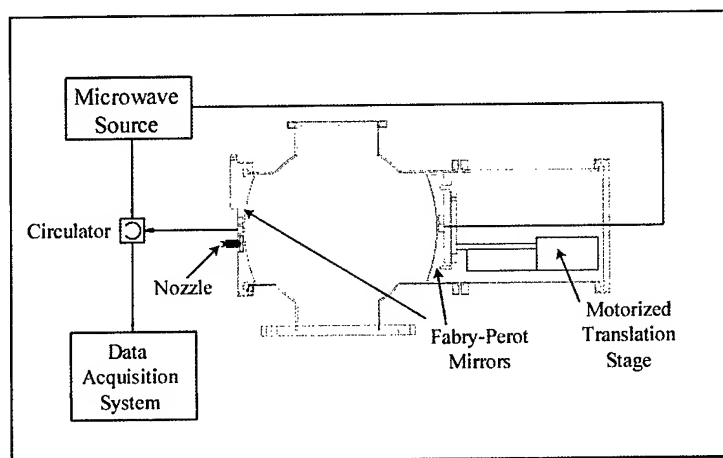


Figure 2. Schematic Diagram of the FTMW Spectrometer.

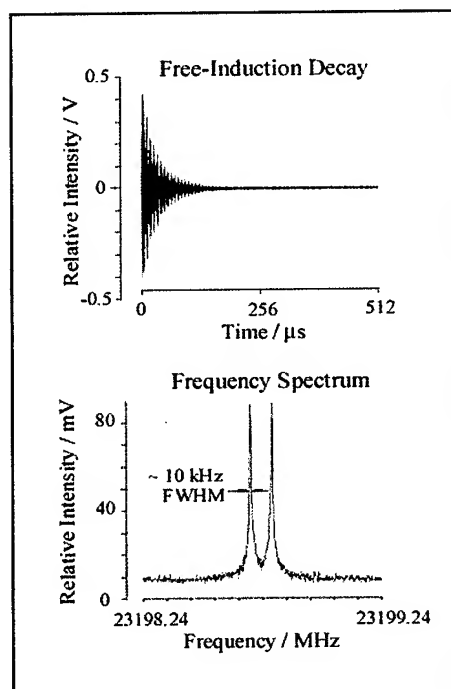


Figure 3. Free-induction decay signal and its Fourier Transform

The high spectral resolution (5 kHz FWHM) relative to the approximately 10 GHz operating range of the instrument and the unique qualities of the rotational spectrum of a molecule give the instrument effectively 100 % species selectivity. This selectivity is illustrated in Figure 4 for the structural isomers pinacolone and pinacolyl alcohol. The instrument also provides a rapid, near-real-time response. The time response of the instrument is limited by the 5 Hz to 10 Hz nozzle pulse rate, the flow rate of the gas to the nozzle, and the gas-line passivation. A typical time-response is shown in Figure 5 for a 10 $\mu\text{mol/mol}$ (10 ppmv) sample of acetaldehyde in N_2 with Ne/He added for increased sensitivity. We have more recently

demonstrated the capabilities of FTMW spectroscopy for the detection of chemical warfare agents. Figure 6 shows survey microwave spectra for the nerve agents Sarin^{6,7} and Soman as recorded using a FTMW spectrometer established in a surety laboratory at Aberdeen Proving Grounds.

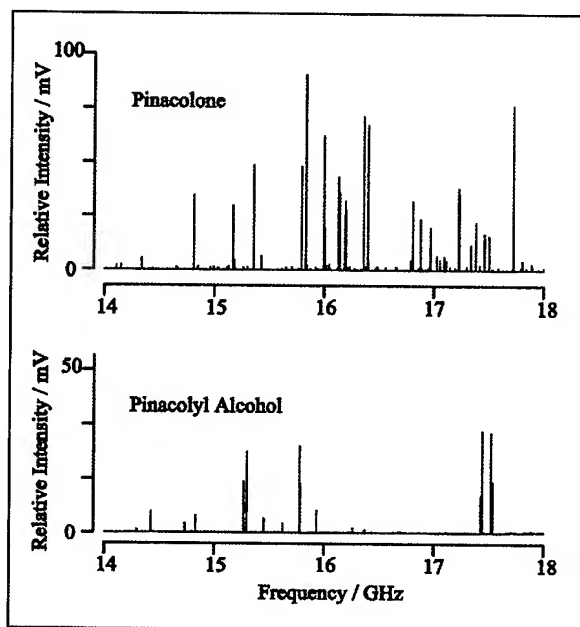


Figure 4. FTMW spectra of the two structural isomers, pinacolone and pinacolyl alcohol.

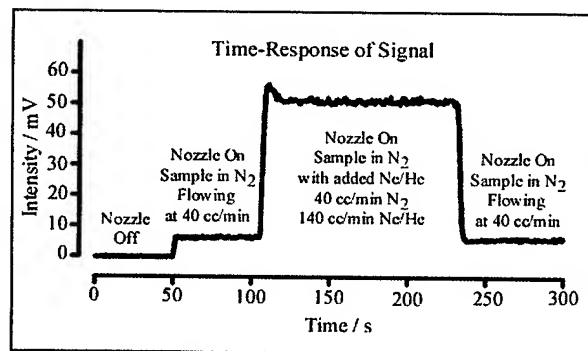


Figure 5. Illustration of the time response of the spectrometer for a sample of acetaldehyde in N₂ with Ne/He added.

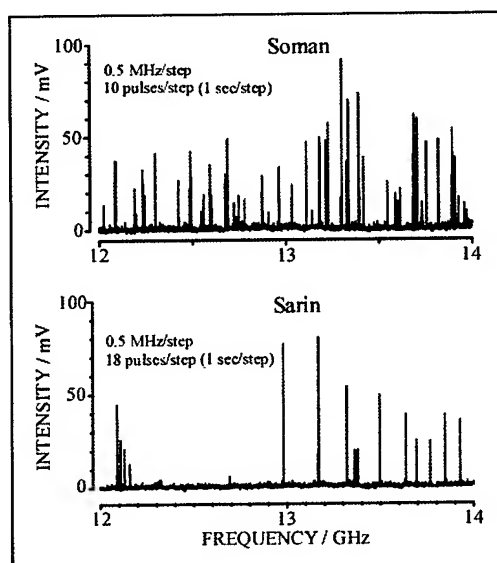


Figure 6. Survey FTMW spectra of the nerve agents Soman and Sarin.

Present efforts are directed at validating FTMW spectroscopy for the quantitative analysis of complex mixtures of gases, such as several trace gas impurities in air. Of particular concern is gas condensation and non-thermal equilibrium in the supersonic nozzle expansion, processes that are more pronounced in complex gas mixtures. In addition, we will be examining in more detail the linearity, frequency variation, effects of humidity, and short and long-term reproducibility of the instrument, as well as addressing the needs for gas-mixture standards.

As part of this effort we have tested the ability of FTMW spectroscopy to positively identify a series of trace impurities in a nitrogen gas sample. The researcher performing the measurements and analysis was not aware of the contents of the sample, except that it consisted of one or more components from a selected group of 16 oxygenates. FTMW was able to correctly identify all the components of the gas mixture, with no false positives. In addition, by comparing the signal intensities to known standards when available, consisting of a single trace gas in nitrogen, reasonable estimates for the concentrations of the impurities in the unknown were obtained. The results from this study are summarized in Table II. It is important to emphasize the preliminary nature of these results. The unknown concentrations were assigned with only one calibration standard and further work is required to validate the instrument response function under the present operating conditions.

Table II. Identified trace gas impurities				
Compound	Ratio	Concentration (ppm)	Concentration (%)	Concentration (ppm)
Acetaldehyde	16/1	0.086	$0.202 \pm 0.5 \%$	13.0
Ethanol	170/1	60	$60.3 \pm 0.2 \%$	70.54
Ethyl- <i>t</i> -butyl ether	10/1	---	$5.19 \pm 0.5 \%$	---
Methyl ethyl ketone	44/1	---	$5.22 \pm 0.2 \%$	---

^aStandard uncertainties are given as a percentage of the given concentration.

The results in Table II demonstrate the potential of FTMW spectroscopy for trace gas analysis of multicomponent mixtures. For instance, with 1 min of signal averaging FTMW appears capable of detecting acetaldehyde and ethanol at concentration levels of approximately 5 nmol/mol (5 ppb) and 0.4 nmol/mol (0.4 ppb). These preliminary successful results certainly show the promise of FTMW for automobile emissions monitoring, and are a motivating force for our continuation of this effort.

In a second study, a sample of eight different chemical agent related compounds were prepared at a concentration of approximately 100 $\mu\text{mol/mol}$ (100 ppmv) in a neon carrier gas. The pulse conditions for each compound was then optimized and stored using the software that controls the instrument. Once stored, the software was used to check for each species in turn using a 1 s burst of gas pulses, *ie.* 10 gas pulses. Using this technique, all eight compounds were identified in approximately 1 minute of total time. Figure 7 shows a two GHz spectral survey scan of this mixture. It is apparent that even for a mixture of eight different compounds, the overall spectrum is not very dense, hence it should be possible to analyze mixtures containing many more than eight compounds using this technique without any pre-separation.

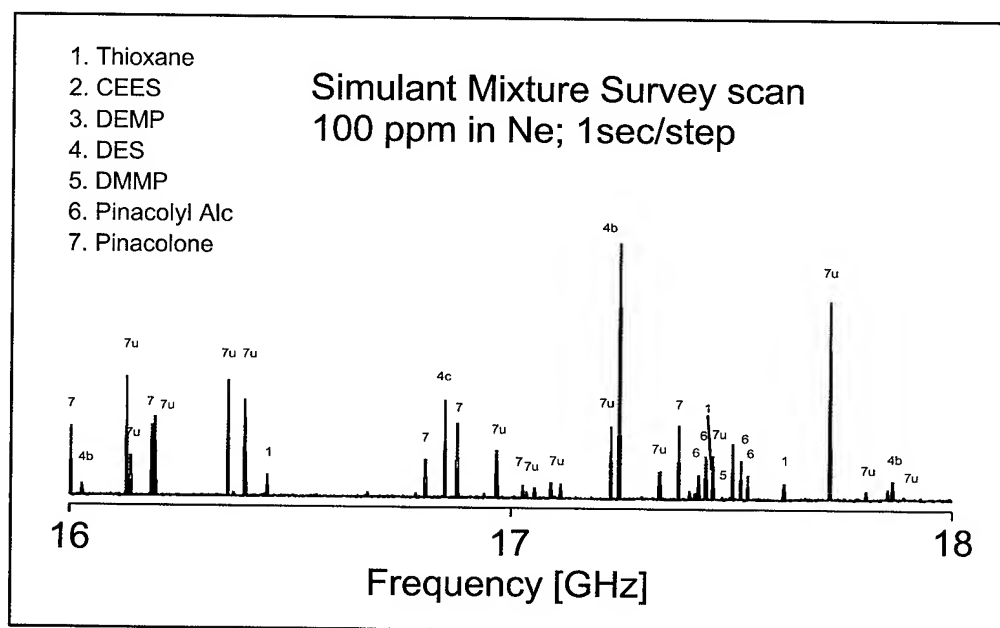


Figure 7. Survey scan of simulant mixture

CONCLUSIONS

The technique of Fourier transform microwave spectroscopy has been described. The application of the technique to the quantitative analysis of trace amounts of chemical agents in the vapor phase appears promising. The technique has the capability to provide analytical chemists with a sensitive ($<1 \mu\text{mol/mol}$), near-real-time monitor of chemical agents with unambiguous chemical identification. Potential applications include the real-time monitoring of agents or related compounds at destruction sites or during a treaty verification process.

REFERENCES

1. Chu, P. M., Guenther, F. R., Rhoderick, G. C., and Lafferty, W. J., "The NIST Quantitative Infrared Database," *J. Res. Natl. Inst. Stand. Technol.* **104**, 59 (1999).
2. Balle, T. J. and Flygare, W. H., "Fabry-Perot cavity pulsed Fourier transform microwave spectrometer with a pulsed nozzle particle source," *Rev. Sci. Instrum.* **52**, 33 (1981).
3. Andresen U., Dreizler H., Kretschmer U., Stahl W., and Thomsen C., "A molecular-beam Fourier-transform microwave spectrometer developed for analytical purposes," *Fres. J. Anal. Chem.* **349**, 272 (1994).
4. Lovas, F. J., Pereyra, W., Suenram, R. D., Fraser, G. T., Grabow, J. -U., and Hight Walker, A. R., "Using Fourier transform microwave spectroscopy to detect hazardous air pollutants," in *Proc. 1994 U.S. EPA/A&WMA Intern. Symp. - Optical Sensors for Environmental and Chemical Process Monitoring*, (1994).
5. Suenram R. D., Grabow J. -U., Zuban A., and Leonov I., "A portable, pulsed-molecular-beam, Fourier-transform microwave spectrometer designed for chemical analysis," *Rev. Sci. Instrum.* **70**, 2127 (1999).
6. Hight Walker, A. R., Suenram, R. D., Samuels, A. C., Jensen, J. O., Woolard, D., and Wiebach, W., "Fourier Transform Microwave Spectroscopy of Chemical Warfare Agents and their Synthetic Precursors," *SPIE Proceeding*, **3533**, (1998).
7. Hight Walker, A. R., Suenram, R. D., Samuels, A. C., Jensen, J. O., Ellzy, M. W., Lochner, J. M., and Zeroka, D., "Detection of the Chemical Warfare Agent Sarin by Microwave Spectroscopy," *J. Chem. Phys.*, submitted, (2000).

INFRARED, FAR INFRARED, AND MILLIMETER WAVE SPECTROSCOPIC MEASUREMENTS ON BIOLOGICAL MATERIALS: BACTERIAL SPORES, POLLENS, AND MOLD

Alan C Samuels, James O. Jensen, William R. Loerop,
Michael Ellzy, J. Michael Lochner, Dorothea Paterno, and Kate K. Ong

*Edgewood Chemical and Biological Center
Edgewood, MD 21010 USA*

Dwight Woolard

*Army Research Office
Research Triangle Park, NC 27709 USA*

Tatiana Globus

*University of Virginia
Charlottesville, VA 22903*

Abstract: We describe a technique for the quantitative preparation and spectroscopic transmission measurement of films containing biological spores, pollens, and molds. The films prepared in this fashion were measured spectroscopically at infrared, far infrared, and millimeter wave frequencies, and the results of these measurements are presented. The study encompasses two spore-forming bacteria, *Bacillus subtilis* var. *niger*, and *Bacillus thuringiensis*, and five varieties of pollen and mold commonly found in the environment. The spectrally-resolved extinction per unit mass of the film is analyzed and the spectra of the different biological materials is contrasted. The potential for detection and discrimination between these different biological materials using spectroscopy is discussed in the context of the observed spectrally-resolved extinction.

INTRODUCTION

Environmental monitoring for hazardous materials of biological origin presents a significant technical and technological challenge. Currently, technologies that are fielded or in development for field biological warfare agent monitoring rely on harvesting a sample of the atmosphere to be monitored and processing the sample through sophisticated assays to effect identification. Less sophisticated optical techniques have been developed that rely on back-scattering principles and/or on ultraviolet fluorescence to identify potential threat aerosols; however these systems are bulky, power hungry, and limited in their capability to discriminate between harmful versus innocuous biological materials.

We have been investigating the feasibility for monitoring biological materials using infrared spectroscopy. Naumann has demonstrated that the use of careful data analysis of the mid- and long wave infrared spectra of biological microorganisms affords a significant capability to discriminate between species¹. Additionally, the theoretical predictions of van Zandt et al.²⁻⁴ as well as the experimental measurements of Woolard et al.⁵⁻⁶ have supported the notion that biological materials exhibit spectral properties in the far infrared and millimeter wave region of the electromagnetic spectrum. In mid- and

long wave infrared measurement, the phenomenology is of course related to the chemical composition of the material under study. Specifically, absorption bands observed in the mid- and long wave infrared region are associated with the fundamental molecular vibration modes of the various functional groups that constitute the proteins and other biomolecules in the microorganism. While these basic building blocks are common to all materials of biological origin, the multicomponent manifold of spectral signatures that result from the spectroscopic investigation of intact microorganisms, spores, and biomaterials may demonstrate a unique quality that can be correlated to the type of organism.

In the far infrared and millimeter wave spectral region, the data are even more sparse. This is primarily due to experimental difficulties with measuring the spectroscopy of materials at these wavelengths. The underlying phenomenology is purported to be the low frequency vibrations associated with long-range structure in large molecules and molecular lattices, such as the helical structure of deoxyribonucleic acid and the secondary and tertiary structure of proteins. The natural frequency of vibrations of this nature has been predicted to be below 30 cm^{-1} , which is more commonly known as the gigahertz and terahertz region of the time domain.

EXPERIMENTAL METHODS

We have established a protocol for preparing uniform samples of certain biological and microbiological organism films that facilitates the quantitative preparation of these materials for infrared spectroscopic study. The technique capitalizes on the availability of membrane filters made of materials that are essentially transparent in the spectral regions under investigation. Microorganism films of controlled thickness and quantitative content may be prepared very reproducibly using this protocol, and they are amenable to spectroscopic measurement throughout most of the infrared, far infrared, and millimeter wave spectral region due to the low absorptivity of the polycarbonate material in this region.

Bacillus subtilis variant Niger (BG) was acquired from a Dugway Proving Ground stock source, originally manufactured by Merck in 1956. The material was subjected to a succession of wash/centrifugation cycles using saline buffer solution prior to spray-drying. *Bacillus thuringiensis* subsp. Kurstaki (ATCC 35646) was cultured on a nutrient sporulating (NSM) agar media consisting of Lab-Lemco Agar 23 g/L, Bacto Agar 2 g/L, Yeast Extract 3 g/L, Tryptone 3 g/L, and $\text{MnCl}_2 \cdot 4\text{H}_2\text{O}$ (1%) 1-mL/L. The spores harvested from the NSM agar plates was subjected to four cycles of wash/centrifugation cycles using $18.0 \pm 0.1\text{ M}\Omega$ filtered water. Pollen and mold samples were obtained from Greer Laboratories (Lenoir, NC) and used as received.

Lyophilized or spray-dried samples of the microorganisms or particulates under study were weighed to $\pm 0.1\text{-mg}$ on a microbalance, then suspended in $18.0 \pm 0.1\text{ M}\Omega$ filtered water (Nanopure, inc.), which was filtered through a $0.2\text{-}\mu\text{m}$ filter immediately prior to use. Typically, suspensions on the order of 1-mg/mL of the microorganisms or particulates were prepared in this fashion. The suspensions were kept uniform with frequent vortexing. Known volumes of the suspension were then transferred to a filtration assembly, along with a small aliquot of water (typically 2-mL) to ensure uniform distribution of the particulates on the surface of the membrane filter.

Porous track-etched polycarbonate (PC) membrane filters (Poretics, inc.) with $0.4\text{-}\mu\text{m}$ pores were utilized as the substrate material. In addition, a cellulose nitrate membrane filter pad with $0.2\text{-}\mu\text{m}$ pores was used as a buffer pad between the PC filter membrane and the fritted glass filter support. This measure was found to be necessary in order to eliminate long range structure in the filtered films resulting from the coarse porosity of the fritted glass filter support. The PC membrane and its associated filtrate were mounted in a film sample card (Spectra-Tech, Inc.) and dried in a 70°C oven for a minimum of 24-hours prior to measurement in the infrared or far infrared.

Millimeter wave measurements are somewhat more difficult than infrared measurements, so a separate procedure for sample preparation was established for the W-band waveguide measurements. Thin waveguide sections that are typically used as phase-shifters for waveguide characterizations were employed in this study. These components are thin (1-mm and 2-mm thick) sections of gold-plated brass machined to match the W-band waveguide. In these experiments, the waveguide section was fully packed with the dry solid under study. In some cases, the packed material in the waveguide section had sufficient integrity that the solid slug formed was essentially free standing; in these instances we were able to conduct full two-port transmission measurements on the sample. In all cases, we conducted single-port reflection measurements through the material by setting up a waveguide short in a horizontal fashion (see figure 1).

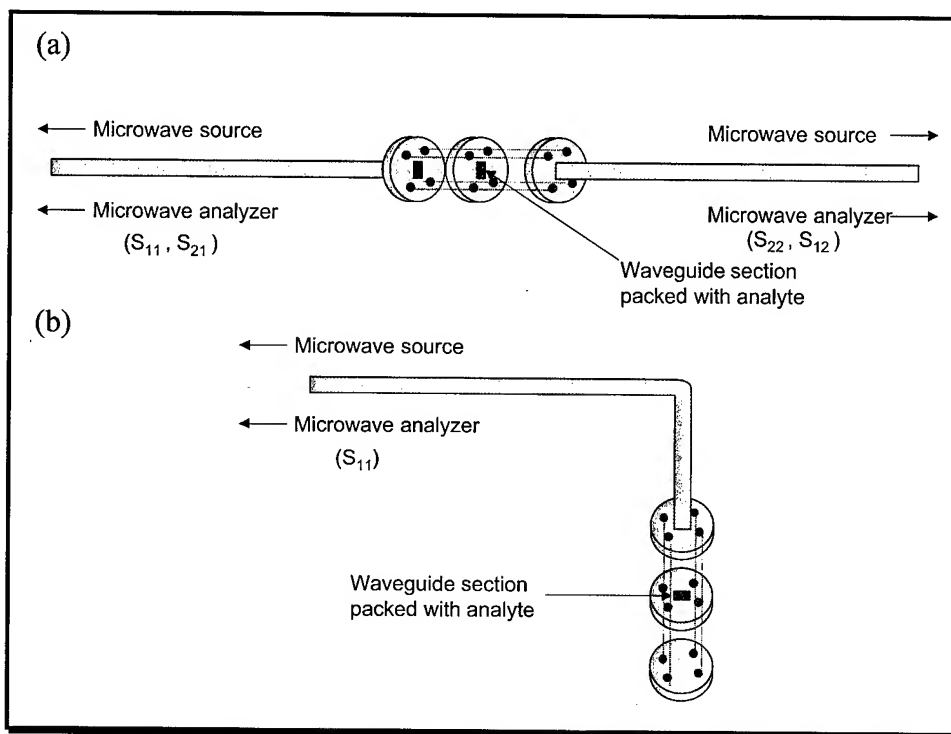


Figure 1. Experimental setup for W-band transmission mode (a) and reflection mode (b) measurements with the HP8510C Vector Network Analyzer.

Infrared spectra were collected at 0.5-wavenumber resolution using a Nicolet-800 Fourier transform spectrometer employing a mercury-cadmium-telluride detector and averaging 32 scans per interferogram. Far-infrared spectra were collected at 0.25-wavenumber resolution using a Bruker IFS-66 system equipped with mercury arc lamp source and a liquid-helium-cooled Si-bolometer ($T = 1.7^\circ \text{ K}$) for signal detection and averaging 128 scans per interferogram. All infrared and far infrared spectra were made relative to a blank PC membrane filter, which was collected as a background measurement. Millimeter-wave (W-band, 75-110 GHz) measurements were made on a Hewlett-Packard model 8510C vector network analyzer equipped with a W-band test set, at a resolution based on the number of points in the data sweep (201 in the case of the data presented here, which corresponds to 0.175-GHz). The network analyzer was calibrated to the plane of the sample insertion point, and measurements of empty waveguide segments were made to verify that no waveguide mismatch situations existed.

Calculations of refractive index n and extinction coefficient k

The measurements obtained in this study were used to derive the high-frequency dielectric properties of the biological materials under consideration. Here, the investigation seeks to resolve the frequency-dependent nature of the material that results directly from the microscopic resonant phenomenon. When optically-active resonance is present in any material a frequency-dependent, lossy, dielectric characteristic will result. Such a dielectric will exhibit an effective permittivity of the form

$$\varepsilon(\nu) = \varepsilon_{real} + i\varepsilon_{imag} = \varepsilon_{\infty} + \sum_j \frac{S_j \nu_j^2}{(\nu_j^2 - \nu^2) - i\gamma_j \nu}, \quad (1)$$

where ε is the complex dielectric function, ν is the frequency in wavenumbers, and ε_{real} and ε_{imag} are the real and imaginary parts, respectively. The last term in Eq. (1) explicitly gives the complex permittivity in terms of the high-frequency dielectric constant, ε_{∞} , and a sum over the Lorentz oscillator states. Here, S_j is the oscillator strength, ν_j is the eigenfrequency and γ_j is the full width at half maximum associated with each harmonic oscillator. The dielectric properties of the films may be equivalently characterized by the complex index of refraction defined by

$$N(\nu) = n + ik, \quad (2)$$

where the real part, n , is the refractive index and the imaginary part, k , is the extinction coefficient. In almost all materials (i.e., nonmagnetic) the index of refraction and the dielectric constant are defined according to $N = \sqrt{\varepsilon/\varepsilon_0}$ where ε_0 is the permittivity of a vacuum, hence, the individual terms in Eqs. (1) and (2) are related by

$$\varepsilon_{real} = n^2 - k^2, \quad (3)$$

$$\varepsilon_{imag} = 2nk. \quad (4)$$

Lossy dielectrics, with nonzero ε_{imag} and k , introduce an exponential damping factor (i.e., $\exp(-\alpha z)$) to the propagating electromagnetic wave with an attenuation constant defined by⁷

$$\alpha = \frac{4\pi k}{\lambda_0} = \frac{2\pi \varepsilon_{imag}}{\lambda_0 n}, \quad (5)$$

where $\lambda_0 = c/f = \nu^{-1}$ is the wavelength in free space. In theory, if one seeks to derive a frequency-dependent attenuation (or extinction) coefficient from *very* uniform films then the effects of interference must be addressed. Specifically, films that sufficiently uniform and thin can be expected to exhibit frequency-dependence both in their transmission and reflectance spectra due to fringing effects. In this situation, the effects of geometrical interference must be subtracted from the spectra to derive the true frequency-dependence of the material parameters. When fringes are observed in measurements, interferometric techniques (i.e., vary wavelength or thickness) must be employed directly to determine the dielectric properties. Furthermore, numerical iterations are necessary to discriminate the natural wavelength-dependence of the material from those produced by the geometry of the film⁸.

Fortunately, the effects of geometrical fringing can be artificially excluded by precise control of film thickness variations (e.g., lapping in semiconductor film measurement) or naturally diminished by random variations introduced by imperfections. In such situations where fringes are not resolved, an average transmission can be defined, and measured that resolves the dependence of the dielectric (or optical) parameters on spectral wavelength. Specifically, the average transmission through a non-fringing film of randomly varying thickness is given by⁷

$$\langle T \rangle = \frac{(1 - R_s)^2 (1 - k^2/n^2)}{\exp(\alpha d) - R_s^2 \exp(-2 \alpha d)}, \quad (6)$$

where d is the average thickness of the film and R_s is the surface-reflectance (i.e., of an equivalent air and infinite-film interface) given by

$$R_s = \frac{(n-1)^2 + k^2}{(n+1)^2 + k^2}. \quad (7)$$

If the material is sufficiently lossy such that

$$\exp(2 \alpha d) \gg R_s^2, \quad (8a)$$

$$k^2 \ll n^2, \quad (8b)$$

are true then Eqs. (6) and (7) simplify to

$$\langle T \rangle = (1 - R_s)^2 \exp(-\alpha d). \quad (9)$$

$$R_s = \frac{(n-1)^2}{(n+1)^2}. \quad (10)$$

Data collected for two samples of different average thickness can now be used to eliminate the surface-reflectance and define the absorption coefficient as

$$\alpha = \frac{\log(\langle T_1 \rangle / \langle T_2 \rangle)}{(d_2 - d_1)}. \quad (11)$$

where $\langle T_1 \rangle$ and $\langle T_2 \rangle$ are the average-transmission measurements for samples of thickness d_1 and d_2 , respectively. Once the transmission and the absorption coefficients have been determined over some

frequency-band of interest, Eqs. (9) and (10) can be used sequentially to extract the refractive index, $n(\nu)$ and Eq. (7) can be used to determine the extinction coefficient, $k(\nu)$. The assumptions utilized from (8) can now easily be verified for accuracy.

In the results reported here, simultaneous measurements of optical transmission through samples of different thickness, prepared under the same conditions, were used to determine the absorption and refractive index spectra. For most of the data presented the effects of specimen imperfections and/or spectral bandwidths were such that the material characteristics were derived using the non-fringing procedure described above. In addition, the materials studied possessed sufficient loss to justify the use of Eqs. (9) and (10). This procedure allowed for the interrogation of narrow spectral features in the dielectric characteristics.

RESULTS AND DISCUSSION

Infrared spectra of the materials studied taken with the Nicolet-800 FTIR spectrometer are shown in figures 2 and 3. The data in figure 2 demonstrate the potential for the infrared spectroscopic approach to discriminate between the various biomaterials, as well as identify biological as opposed to mineral material. Comparison of figures 2 and 3 reveals evidence for a capability to discriminate between bacterial spores and the common pollens and molds as well as mineral dust. Figure 3 also provides some insight as to the potential for spectroscopic discrimination between two species of bacterial spore. Figure 3 also presents a validation of the sample preparation procedure by demonstrating the scalability of the signal as a function of the quantity of BG or Bt spores applied to the surface of the film.

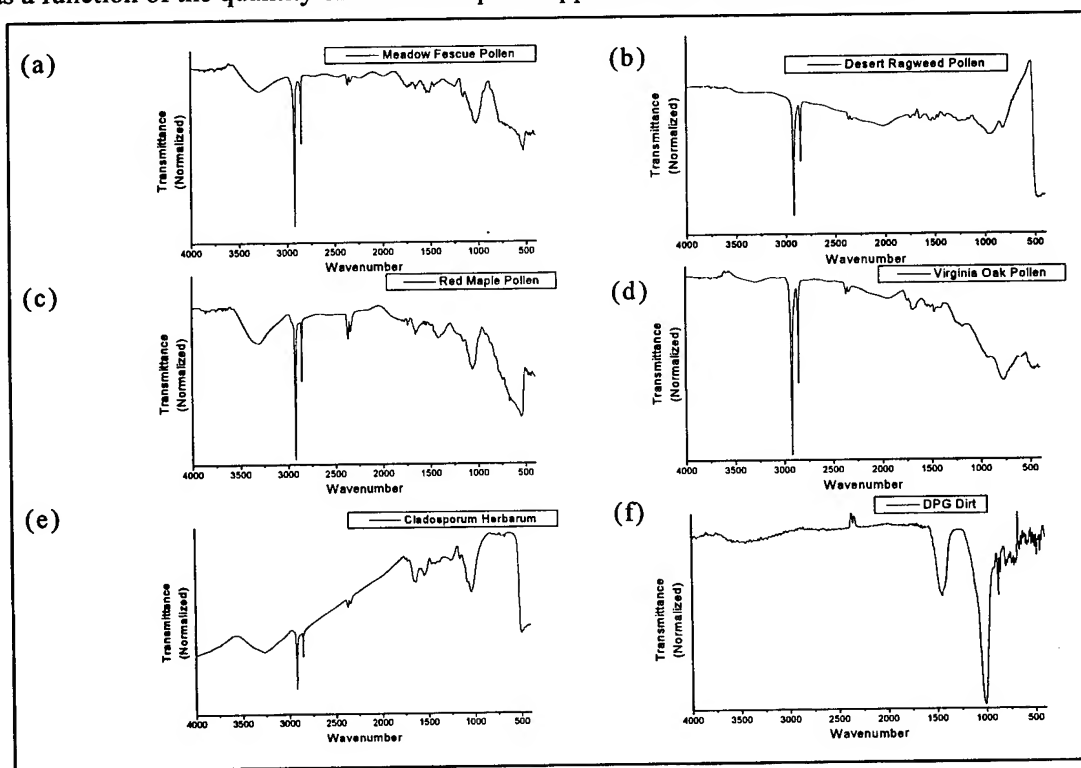


Figure 2. Infrared spectra of meadow fescue (a), desert ragweed (b), red maple (c), and Virginia oak (d) pollens, and cladosporium herbarum, a common mold (e), and some dirt from Dugway proving ground topsoil (f).

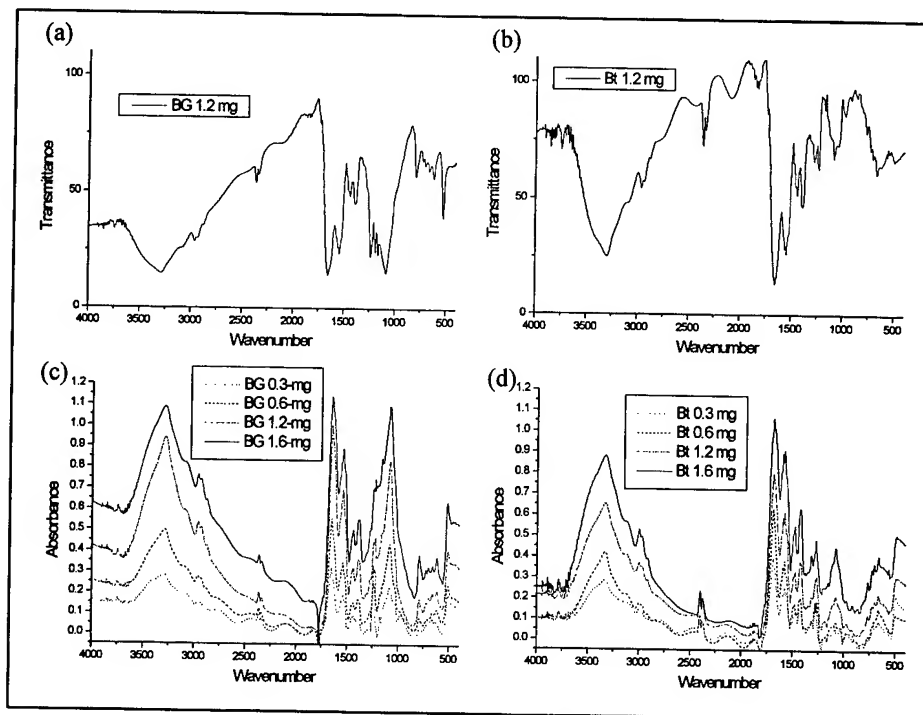


Figure 3. Infrared spectra of BG (a) versus Bt (b) in the mid infrared, and concentration-dependent absorbance spectra of BG (c) and Bt (d).

Far infrared spectra of BG are shown in figures 4 and 5. A notable feature visible in several of the spectra at 18 wavenumbers is due to the presence of water in some of the samples, and should be disregarded. What remains is a set of extremely weak bands that are near the noise floor of the instrument. The films prepared for this measurement were of very low concentration, but are comparable to the lowest concentration films measured in the mid infrared experiments. The effect of increasing the concentration of the spores in a BG film is presented in figure 5(c). It is clear from this data that there are indeed pronounced, reproducible peaks in the biological materials; however, the quantity of material required to exhibit a useful signal level is significantly higher than that which is needed for mid infrared analysis.

W-band spectra of the materials under study are presented in figures 6 and 7. Much of the variance in the different data sets was found to be due to the density of the material rather than its molecular makeup. It is probable that the dielectric properties of these materials are a unique characteristic of each; however, the data do not provide a substantial amount of variance indigenous to the various materials to demonstrate any utility for W-band spectroscopy to detect or identify the materials. The reflection and transmission data are both affected by the mechanics of packing the powdery materials into the waveguide section. It is difficult to treat the surfaces of the pellet such that a completely smooth surface is presented to the network analyzer, so some variance is apparent particularly in the S_{11} and S_{22} data in the transmission experiment (figure 7). Much of the curvature evident in the scattering parameters is likely to be due to the expected interference effects of packing a slab of dielectric material into the waveguide. With an estimate of the refractive index of the material, it is possible to deconvolute this effect and hence isolate the actual spectral response of the material under study. Analysis of the data presented here is now underway to further elucidate these results.

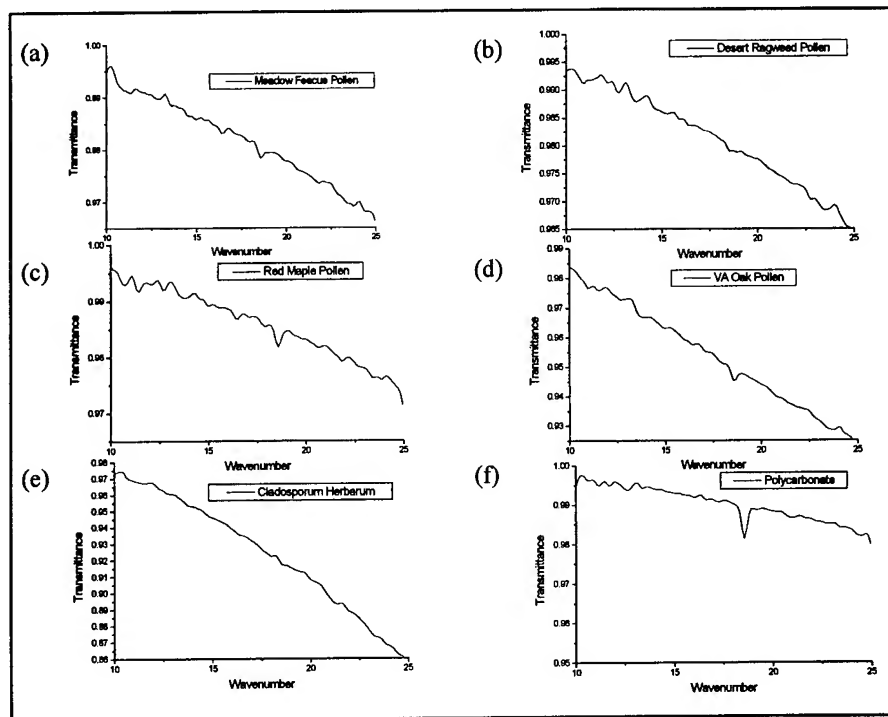


Figure 4. Far infrared spectra of meadow fescue (a), desert ragweed (b), red maple (c), and Virginia oak (d) pollens, and cladosporium herbarum, a common mold (e), and a blank polycarbonate membrane (f). The strong feature that appears at ca. 18 wavenumbers is a water vapor line.

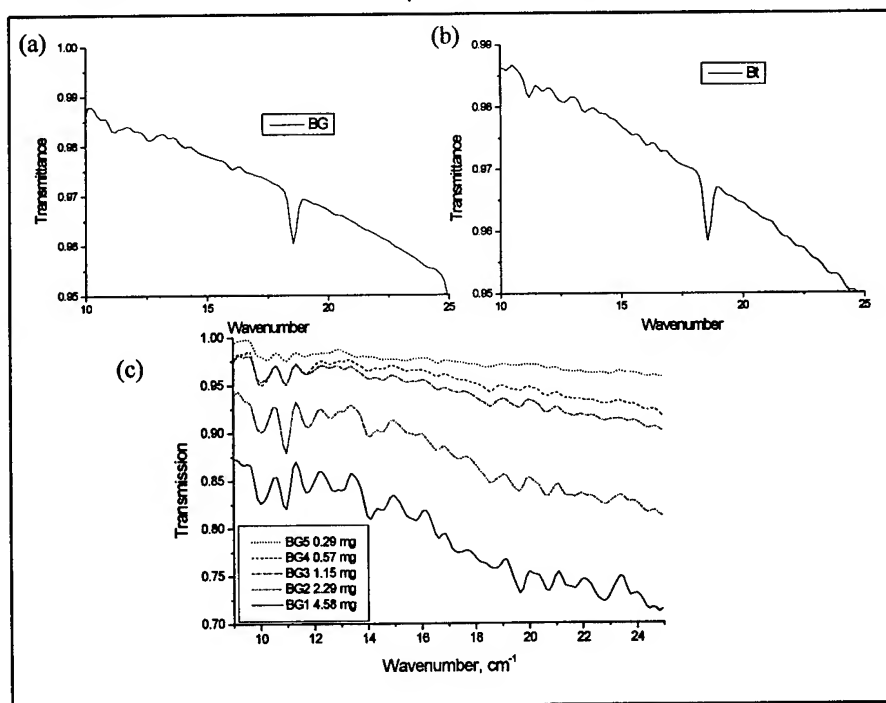


Figure 5. Far infrared spectra of BG (a) and Bt (b). The strong feature at ca. 18 wavenumbers is a water vapor line. The far infrared spectra of BG were also taken as a function of mass of the BG film (c).

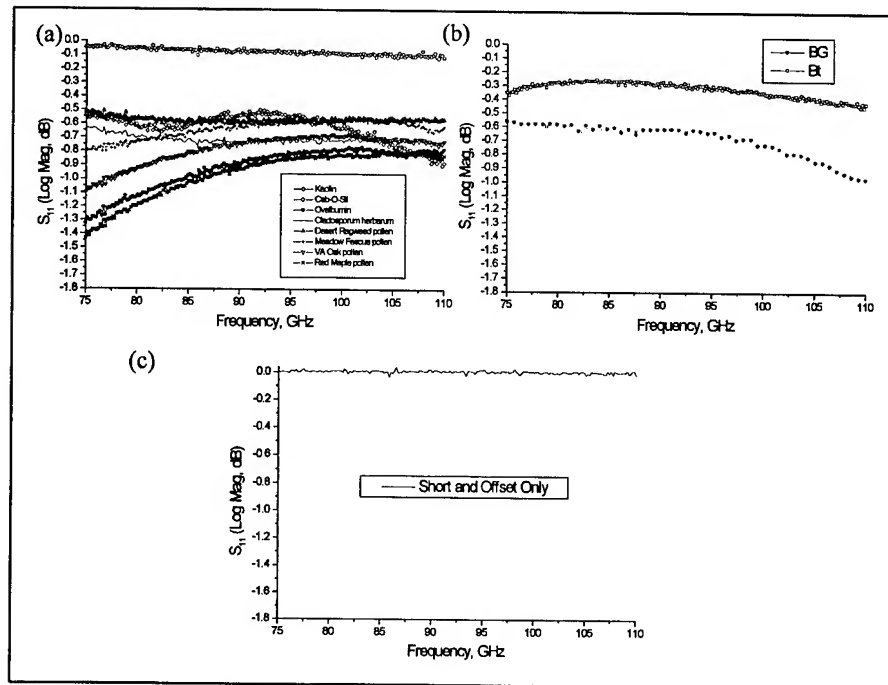


Figure 6. (a) W-band spectra in reflection mode of Kaolin, a common clay mineral, Cab-O-Sil, a form of silica dessicant/fluidizer, ovalbumin, a protein derived from chicken egg white, and the mold and pollens described elsewhere. (b) W-band spectra (reflection mode) of BG and Bt. (c) W-band spectra (reflection mode) of the empty short and offset.

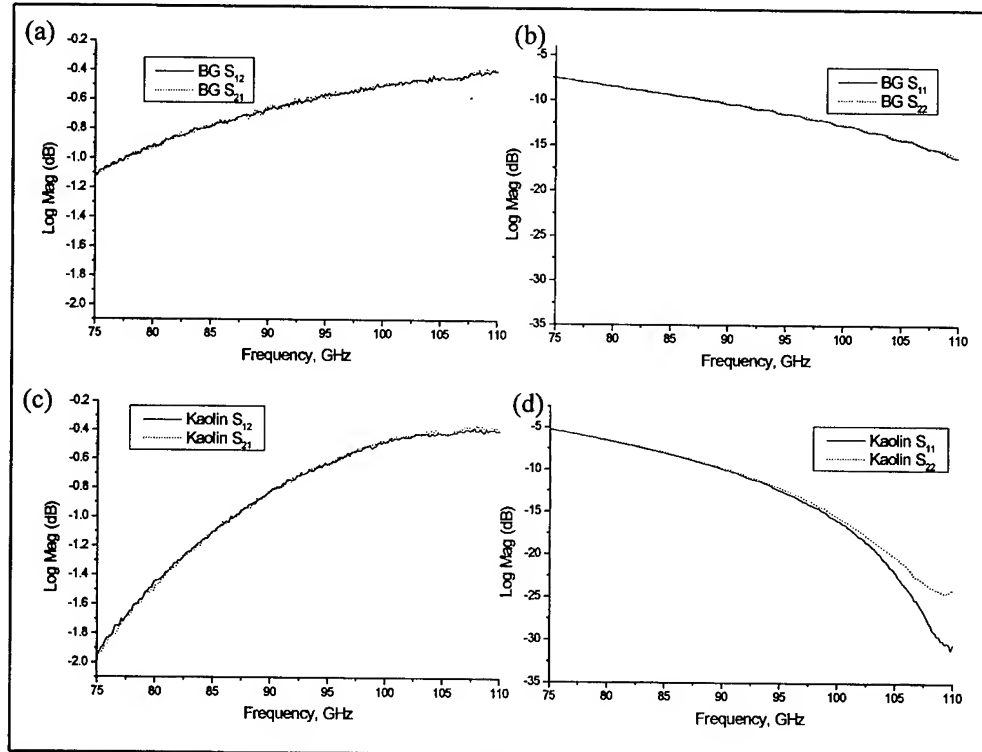


Figure 7. W-band spectra in transmission mode of BG (top) and Kaolin (bottom).

CONCLUSIONS

We have collected infrared, far infrared, and millimeter wave data on a variety of bacterial spores and some common environmental constituents. The data demonstrate a significant level of promise for infrared spectroscopy in particular to be developed into a unique and reasonably specific detector for biological materials in the ambient environment. A quantitative analysis of the data and signal to noise levels achievable in currently available instrumentation is underway to establish the ultimate detection limits possible and the obstacles that must be addressed in order to achieve a real-time environmental monitor for threat aerosol concentrations in a field environment.

Although the far infrared results presented here demonstrate very low extinction, the approach may yet have merit in a mode in which the sensor employs a pre-concentrator to accumulate solid particles from the atmosphere, perhaps even directly onto a polycarbonate substrate. When an adequate amount of material has been collected, distinct and potentially highly unique spectral signatures of the materials will emerge, as demonstrated with the higher concentration BG film data in Figure 5(c). These signatures are likely to be even more specific than the mid-infrared spectra by virtue of the fact that the secondary structure of the constituent molecules in the material is responsible for the observed spectral lines. Additionally, it is possible to employ coherent sources and diode heterodyne detectors with resonator cavities to key in on low levels of signals, potentially bringing out the weak spectral lines with highly enhanced sensitivity. These measurements should be taken as an early demonstration of the fact that there is some exploitable phenomenology in the far infrared spectral region.

The W-band data present very little distinction between the various species, leading to the conclusion that the utility for environmental sensing would be limited.. It must be pointed out, however, that the bandwidth coverage in this frequency regime is extremely narrow. The full 35 GHz band corresponds approximately to only one wavenumber, which is on the order of the linewidth of the spectral lines observed in the far infrared measurements! Thus, the data analysis that is underway to deconvolute sample structure effects from the W-band data may be very revealing. Other frequency bands need to be studied as well. For instance, Belyaev et al. have observed indirect evidence for the interaction of genomic DNA in microorganisms with radiation in the 40-60 GHz frequency range⁹⁻¹⁰. This frequency range is accessible with the 8510C, and experiments are planned to elucidate the spectral response of these biomaterials in this spectral region as well.

ACKNOWLEDGMENTS

The authors acknowledge the support of the Defense Advanced Research Projects Agency (Dr. Steve Buchsbaum) for support under the SIMBAD program.

REFERENCES

1. D. Naumann, C.P. Schultz, D. Helm, "What can infrared spectroscopy tell us about the structure and composition of intact bacterial cells?", *Infrared Spectroscopy of Biomolecules* (1996), 279-310. Editor(s): Mantsch, Henry H.; Chapman, Dennis. Publisher: Wiley-Liss, New York, N.Y.
2. V.K. Saxena, L.L. van Zandt, and W.K. Schroll, Atomic Motions and High Frequency Cutoff in Biological Macromolecules, *Chem. Phys. Lett.*, **164**(1), 82 (1989).
3. V.K. Saxena and L.L. van Zandt, Local Modes in a DNA Polymer with Hydrogen Bond Defect, *Biophys. Journal*, **67**, 2448 (1994).

4. W.N. Mei, M. Kohli, E.W. Prohovsky, L.L. van Zandt, "Acoustic Modes and Nonbonded Interactions of the Double Helix," *Biopolymers*, **20** 833 (1981).
5. D. L. Woolard, T. Koscica, D.L. Rhodes, H.L. Cui, R.A. Pastore, J.O. Jensen, J.L. Jensen, W.R. Loerop, R.H. Mittleman and M.C. Nuss, "Millimeter Wave-induced Vibrational Modes in DNA as a Possible Alternative to Animal Tests to Probe for Carcinogenic Mutations," *Journal of Applied Toxicology*, **17**(4) pp. 243-246 (1997).
6. D.L. Woolard, F.J. Crowne, T.R. Globus, M. Bykhovskaia, J.L. Hesler, T.W. Crowe, N. Paravastu, A.C. Samuels, J.O. Jensen, J.L. Jensen, W.R. Loerop, "Feasibility of submillimeter-wave technology for the identification of biological warfare agents", Fourth Joint Workshop on Standoff Detection for Chemical and Biological Agents, Williamsburg, VA, Oct. 1998.
7. T.S. Moss, G.J. Burrell, B. Ellis. Semiconductor Opto-electronics. (1973). Publisher: Butterworth & Co. Ltd., Durban, South Africa..
8. Y. Z. Chen, A. Szabo, D. F. Schroeter, J. W. Powell, S. A. Lee and E. W. Prohofsky, *Phys. Rev. E*, **55**, 7414-7423 (1997).
9. I.Y. Belyaev, Y.D. Alipov, V.S. Shcheglov, and V.N. Lystsov, "Resonance Effect of Microwaves on the Genome Conformational State of *E. coli* Cells," *Z. Naturforsch.* **47c**, 621-627 (1992).
10. I.Y. Belyaev, V.S. Shcheglov, Y.D. Alipov, and V.A. Polunin, "Resonance Effect of Millimeter Waves in the Power Range From 10^{-19} to 3×10^{-3} W/cm² on *Escherichia coli* Cells at Different Concentrations," *Bioelectromagnetics*, **17**, 312-321 (1996).

ARTIFICIAL NEURAL NETWORKS FOR INFRARED SPECTRAL CLASSIFICATION

Howard T. Mayfield

Air Force Research Laboratory
AEF Technologies Division, 139 Barnes Drive, Suite 2, Tyndall AFB, FL 32403

Larry W. Burggraf and DeLyle Eastwood

Air Force Institute of Technology
Department of Engineering Physics, 2950 P Street, Wright Patterson AFB, OH, 4543

ABSTRACT

Artificial neural networks and classical pattern recognition methods were compared for classifying infrared spectra. Qualitative infrared spectra of nerve agents, their precursors, and hydrolysis products were obtained from US Army, SBCCOM⁴ and their contractors. Bio Rad/Sadtler Laboratories provided spectra of organophosphorus pesticides. Additional spectra were obtained from the NIST Gas Phase Infrared Library. The spectra were obtained in a variety of digital formats including the JCAMP-IR format, ASCII X, Y formats, and Nicolet and Grams proprietary formats. Prior to conducting classification experiments, the spectra were translated to a common ASCII format. The spectra were pretreated for the classification experiments by expressing them in the absorbance mode and in the frequency domain, translating them into a common ASCII format, trimming the spectra to a common frequency range, and normalizing the absorbances. The pretreated spectra were transduced into data vectors by a "binning" process in which the frequency axis was divided into a set of ranges or bins of equal width, and the average absorbance within each bin was assigned to the corresponding element of the spectral data vector. Due to the limited number of spectra available, some test/evaluation set spectra were obtained by adding calculated noise to the authentic spectra before transducing the noise degraded spectra. All spectra were used over the same frequency range, but binning the available infrared spectra into different numbers of spectral bins provided several data sets. The computer classification experiments used the classical k-nearest neighbor (KNN) classification technique, feed forward artificial neural networks (ANNs) and radial basis function networks (RBFNs) to divide the spectra into classes according to the compound's expected use a pesticide, or as a military nerve agent, precursor, or hydrolysis product. Experiments relating to false positive classifications were made using spectra from the NIST library, of compounds that were not organophosphorus in nature.

INTRODUCTION

Infrared spectroscopy provides a powerful and widely available methodology for detection of chemical contaminants, including industrial pollutants and chemical warfare materials. These capabilities may provide critical measurements and warnings in the event of deliberate military use of chemical warfare agents, in cases of terrorist attack, or in cases of industrial accidents which may endanger military and civilian personnel over wide areas. Infrared spectroscopy is a rapid technique, with the well-developed capability of providing entire infrared spectra of samples or remote beam paths within a period of seconds. Infrared spectra arise from electromagnetic interactions with molecular vibrational energy levels and they are thus fundamental properties of molecules. As such they can provide information for identifying and/or classifying substances.^{1,2}

⁴ Support for this project was given by the Joint Services Chemical and Biological Defense Committee, US Army SBCCOM, Aberdeen Proving Ground, MD.

The potential to identify or classify a substance from its infrared spectrum offers the use of the infrared spectrum to provide warning if a hazardous chemical is released and to minimize false alarms through the identification of the chemical. A common approach is to present the spectrum of a detected compound to a library search system, which compares the spectrum in turn with a series of stored spectra until the spectrum most closely resembling the unknown is determined. This approach was traditionally costly in computer time and it required the mass storage space necessary to store all the spectra of the library. If a warning was desired from the detection of certain hazardous substances, the identified compound had to be checked against a list of hazardous substances and an alarm declared if the substance was on the list.³

Given the computer capacity necessary for performing a library search and also for performing a Fourier transform to support FT/IR instruments, an alternative approach for declaring an alarm is to use computerized classification techniques to determine if a detected spectrum belongs to a chemical in a hazardous class. This approach may be faster than that of identifying the detected substance, and it requires less examination of the spectrum. The classification approach may also be useful for nonproliferation inspections, as are authorized in the recent Chemical Warfare Convention (CWC), where analytical results from samples collected in an on-site inspection are not to be displayed unless they indicate the sample contains a substance banned in the convention⁴.

Classification or sorting of samples by computers based on chemical analysis results has been a goal of analytical chemists who are practitioners of chemometrics, a discipline of statistical and mathematical interpretation of chemical analysis data. Traditionally, pattern recognition techniques were applied to classification problems, including the techniques of *k*-Nearest Neighbor (KNN), linear learning machines, and Bayesian techniques.⁵⁻⁷ These were supplemented with techniques based on principal components analysis such as Soft Isostructural Modelling for Class Analysis (SIMCA).⁸ More recently artificial neural networks (ANNs) have been proposed to solve classification problems.⁹

Artificial neural networks process multivariate data to produce additional multivariate results by forming networks in which individual variables or nodes are functions of the nodes in higher level layers of the network. Such networks often contain three layers, an input layer that is derived from multivariate input data, a hidden layer whose nodes are formed from combinations of the input layer nodes, and an output layer, whose nodes are derived from the hidden layer nodes. The interconnections between nodes in an ANN are illustrated in Figure 1. ANNs with more than one hidden layer are possible but additional layers often add needless complexity. A hidden layer node is formulated as shown in Equation 1. Here m is the number of input nodes, N_j is the value of node j , x_i is the value of input node i , w_i is the value of corresponding weight, b_j is the bias of the node, and f_j is known as the transfer function. Typical transfer functions used in classification problems include the log-sigmoid function (Equation 2), the tan-sigmoid function (Equation 3), or linear functions (Equation 4).^{10,11}

$$N_j = f_j\left(\sum_{i=1}^m w_i x_i + b_j\right) \quad \text{Equation 1}$$

$$f(x) = \frac{1}{1 + e^{-x}} \quad \text{Equation 2}$$

$$f(x) = \frac{2}{1 - e^{-2x}} - 1 \quad \text{Equation 3}$$

$$f(x) = x \quad \text{Equation 4}$$

For classification problems, an ANN uses as many input nodes as there are features or measurements in the data vectors to be classified. One input layer node is directly obtained from each element of the

data vector. One output layer node is used for each class in the data set being classified. When calibrated, or trained, the ANN should yield a value of 1 in the node corresponding to each data vector's true class, and a value of 0 in the nodes of all other classes. The calibration, or training, involves setting the values of the weights and biases of the ANN. This is done in an iterative process using a set of data vectors, called the training set, whose true classes are known. The weights and biases are usually set to random values initially. Then a series of iterations are made where the training set is classified and the errors between the true output node values and those calculated in each iteration are used to recalculate an improved set of weights and biases. Once the ANN has been trained a second set of data vectors called the test set or the evaluation set may be used to test the ANN's performance on additional data.^{10,11}

Radial Basic Function Networks (RBFNs) are similar in structure and concept to ANNs, utilizing interconnections between network nodes to transfer information from an input layer, through a hidden layer, to an output layer. However, the nodes are formulated differently, Equation 5 shows the general form of an RBFN Node. In Equation 5, N_j is node j , R is the radial basis transfer function, $\|x - w_j\|$ is the Euclidean vector norm of the difference between the vector of input nodes x and the node's weight vector w_j , and b_j is the bias of the node. The Gaussian function, shown in Equation 6 is the most common radial basis transfer function.^{11,12}

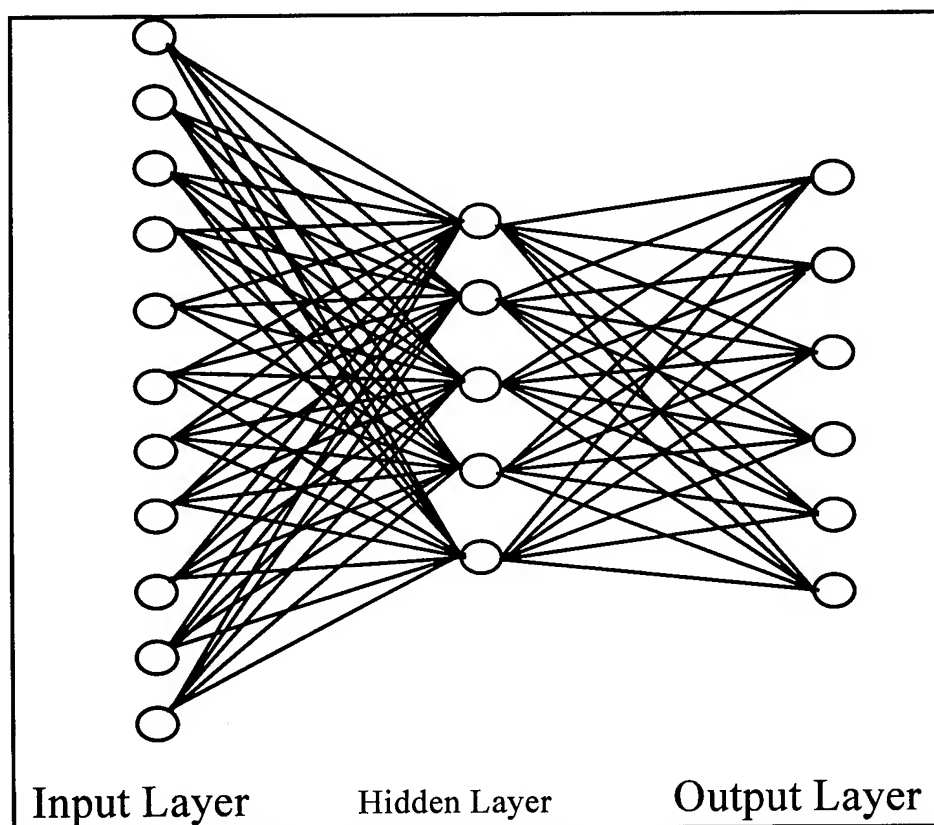


Figure 17. Diagram of an Artificial Neural Network, showing interconnections between the nodes.

$$N_j = R(\|x - w_j\|xb_j)$$

Equation 5

$$R(x) = e^{-x^2}$$

Equation 6

As training set vectors are presented to a generation routine for a RBFN, a new hidden layer node, or "center" is usually added for each training set vector, and the weights and biases of the node are mathematically determined to generate the appropriate output.^{11,12} A critical difference between RBFNs and ANNs is produced by the form of the transfer functions, whose typical forms are plotted in Figure 2. RBFN transfer functions tend to act on data which is concentrated near the center of an expected range, while ANN transfer functions react to data over a wider range, often concentrating the data into the range between 0 and 1 or -1 and 1.¹⁰⁻¹²

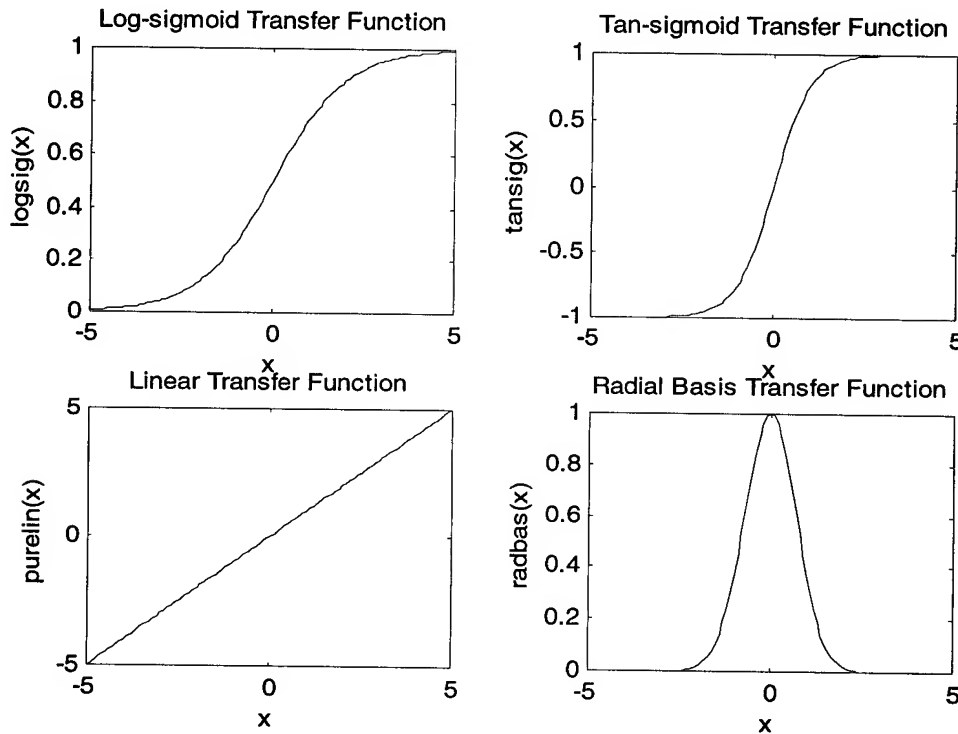


Figure 18. Typical transfer functions used in artificial neural networks and radial basis function networks.

In effort to evaluate the effects of preprocessing on neural network classifiers, Fisher weights were calculated for selected trials. Fisher weights are indications of the discriminating power of the features exhibited by a data set. Larger Fisher weights are indications of greater discriminating power between the classes for a given feature. To calculate Fisher weights, pairwise Fisher weights are calculated between each pair of classes in the training set. The pairwise Fisher weight for a feature I between two classes j and k is given in Equation 7. For data sets with more than two classes, the overall Fisher weight for each feature is the average of the pairwise Fisher weights for the feature.

$$F_{j,k} = \frac{|\bar{x}_{i,j} - \bar{x}_{i,k}|}{1/n_j \sum (x_{i,j} - \bar{x}_{i,j})^2 + 1/n_k \sum (x_{i,k} - \bar{x}_{i,k})^2}$$

Equation 7

EXPERIMENTAL

Condensed phase Mid-infrared spectra of organophosphorus pesticides were provided by Bio-Rad/Sadtler Inc and were used with their permission. The US Army SBCCOM and government contractors provided spectra of chemical warfare agents, simulants, precursors, and hydrolysis products. These spectra were obtained as computer files in a variety of digital formats. The files were translated to a common ASCII format prior to use. Additional spectra of a wide variety of industrial and environmentally significant chemicals were purchased from the National Institute of Standards and Technology (NIST) as their Vapor Phase Infrared Library, which was purchased in the JCAMP format. The NIST library consists of two major portions, one originally collected under the leadership of the US EPA, and the other collected by NIST in their laboratories. The EPA portion of the library will be termed the EPA Vapor Phase Library.

In order to utilize the spectra from a diversity of sources, they were trimmed to a common frequency range of 650 to 2500 cm^{-1} , as was dictated by the most restrictive set of the supplied spectra. The absorbance ranges were normalized to absorbance values between 0 and 1. Data vectors were produced from the trimmed and normalized spectra by binning. The frequency range was divided into a number of "bins" or frequency regions that were equal in terms of frequency width. The average of the normalized absorbance within each bin was assigned as the corresponding element of that spectrum's data vector. Sixty-seven spectra from nerve agents, precursors, hydrolysis products, and simulants were processed to generate data vectors that were designated Class 1 in the training set. Forty-eight spectra of organophosphorus pesticides were processed to generate data vectors for Class 2 of the training set. Four training sets were generated by varying the number of bins used. Training sets were generated with 25, 50, 100, and 200 bins. For three-class experiments, Class 3 training set spectra were the first 100 spectra of the EPA Vapor Phase Library. Class 3 was intended to represent innocuous compounds that would be encountered by inspectors or early warning instruments more often than the pesticides or Class 1 compounds. Although some pesticides and other organophosphorus compounds are included in the EPA Vapor Phase Library, none of the first 100 spectra were from compounds containing phosphorus.

Synthetic noise was added to the trimmed and normalized training set spectra from Class 1 and Class 2 to generate additional spectra for the test set. The noise was generated using the infrared spectral noise model developed by Schuchardt¹⁴ to generate noise for an average signal-to-noise ratio of 5 for each spectrum. The noise-degraded spectra were transduced into test set data vectors in the same manner as the training set vectors. For situations where a third spectral category was included, additional spectra from the EPA Vapor Phase Library were transduced and submitted as unknowns.

Preprocessing and neural network calculations were carried out on personal computers running the MATLAB matrix mathematics package, plus the Neural Network Toolbox and Statistics Toolbox (The Mathworks, Inc.). Calculations were made under the control of locally developed m-files. ANNs could be allocated, initialized, and trained using routines in the Neural Network Toolbox. The general strategy of backpropagation of errors was followed with three training algorithms supplied in the Neural Network Toolbox, the Gradient Descent Algorithm¹⁵, the Robust Backpropagation Algorithm¹⁶, and the Levenberg-Marquardt Algorithm¹⁷. Details of these are available in the references cited.

RESULTS

Calculation and application of Fisher weights did improve the apparent separation of classes in principal components maps of the data sets. A principal components map of the 100-bin training set, after Fisher weights were applied, is shown in Figure 3. The corresponding maps for the 200-bin, 50-bin, and 25-bin training sets were qualitatively similar.

Precise comparisons of the effects of data preprocessing for the ANN classifiers proved to be difficult. Due to the random initialization and optimization of weights and biases of the ANNs, a different set of weights and biases was produced from each initialization and training, and this produced

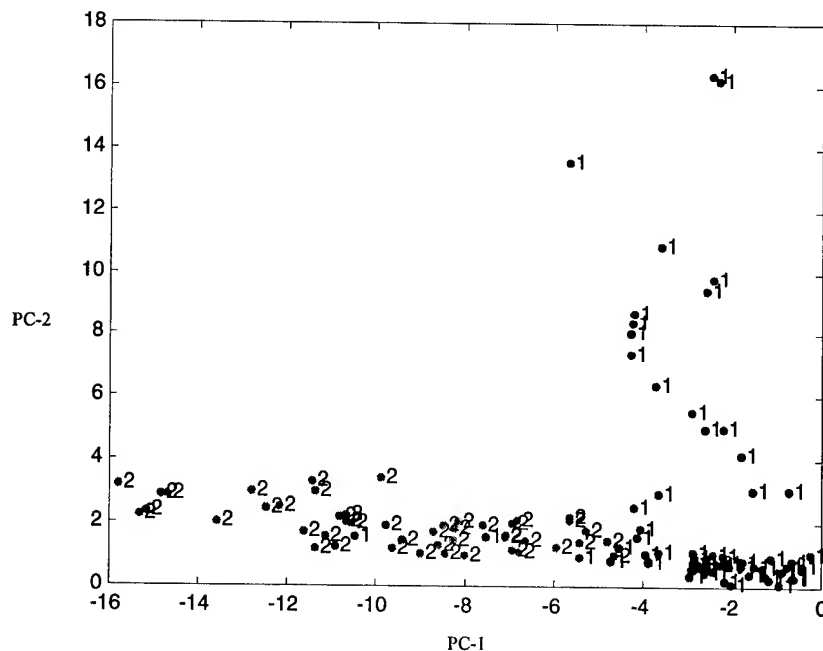


Figure 19. Principal components map of 100-bin, 2-class data set with Fisher weights applied.

corresponding differences in the final classifications. Results for a set of 5-trials of ANN classifiers with “raw” or unweighted data sets are summarized in Table 1. ANN classifiers based on the gradient descent algorithm exhibited the greatest tendency not to converge numerically to a specified root-mean-square error value, and they were the only classifiers tested with the two-category data that produced erroneous classifications from the training set after the ANN had been trained. ANN classifiers based on the robust backpropagation algorithm exhibited better convergence to a given error value and they suffered no misclassifications of the training set data vectors after the ANN had been trained. ANN classifiers based on the Levenberg-Marquardt training algorithm made greater demands of the personal computer memory than other training systems. On a PC equipped with 64 Mbytes of RAM, the Levenberg-Marquardt ANNs could be implemented only for the 25-bin data set. ANN classifiers trained by the Levenberg-Marquardt algorithm converged efficiently and produced no training set errors for the 25-bin case, and they exhibited the lowest frequency of error for the 25-bin, 2-class data set.

In effort to improve both the stability and accuracy of the neural network classifications, experiments were conducted with committee classifiers which used five ANNs trained with the robust backpropagation technique, and which averaged the output layers before rounding the results to the nearest integer for evaluation of the predicted class. Greater stability was needed before the effects of feature weighting and feature selection could be explored. Classification results from a series of 2-class trials using robust backpropagation committee classifiers, using raw data, Fisher weighted data, and selecting features with high Fisher weights are summarized in Table 2. These trials indicated that there was improvement in most cases in using the committee classifiers, but little was gained in applying Fisher weights, and accuracy was usually lost when a subset of the features was selected on the basis of Fisher weights.

Table 6. Summary of results from single ANN classifiers with raw data.

Feed Forward Neural Network Results, Number of Trials=5	200-bin		100-bin		50-bin		25-bin	
	Test	Train	Test	Train	Test	Train	Test	Train
Back-propagation of Errors								
Total Number Misclassified	12	11	20	14	19	22	43	40
Avg. Misclassification Frequency	0.021	0.019	0.035	0.024	0.033	0.038	0.075	0.07
Robust Back-propagation								
Total Number Misclassified	8	0	3	0	12	0	30	0
Avg. Misclassification Frequency	0.014	0	0.005	0	0.021	0	0.052	0
Levenberg-Marquardt Training								
Total Number Misclassified							17	0
Avg. Misclassification Frequency							0.03	0

Table 7. Summary of results comparing single ANN and ANN committee classifiers.

Data Set	Single Network Classifiers, Raw Data	5-Network Committee Classifiers, Raw Data	5-Network Committee Classifiers, Fisher Weighted Data	5-Network Committee Classifiers, Fisher Weights 3.0
200-bin	0.140	0.007	0.005	0.070
100-bin	0.005	0.014	0.003	0.035
50-bin	0.021	0.003	0.005	0.056
25-bin	0.520	0.012	0.012	0.050

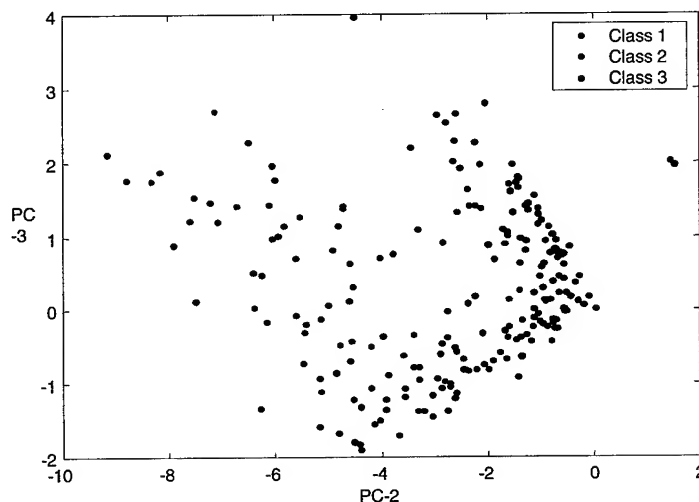


Figure 20. Principal components map of 25-bin, 3-class data set.

Experiments remain underway for the 3-class data sets. These are intended to test the effects on an ANN-based classifier when spectra are presented which were poorly represented in the training set. Figure 4 shows the plot of principal components 2 versus 3 for the 3-class, 25-bin data set. Class separation is more easily perceived between principal components 2 and 3 than between principal components 1 and 2 or 1 and 3 despite the greater variance information in the earlier principal components. Initial experiments with the 25-bin 3-class data set yield classification of the training set spectra without error. The trained 3-class ANN classifiers locate the phosphorus containing compounds and pesticides in the EPA vapor phase library, but they falsely classify about 5% of the innocuous compounds from the library in either class 1 or class 2.

CONCLUSIONS

The ANN classifiers appear to classify the mid-infrared spectra of organophosphorus compounds between pesticides and nerve agent-related compounds with a high degree of accuracy. Stability and accuracy of the ANN classifiers is enhanced by a committee approach in which several ANNs are trained and their output results averaged to form the final committee classification. The Fisher weighting technique appears to offer little improvement for the ANN classifiers. This is somewhat surprising in view that this technique has been used for some time to improve classical pattern recognition classifications. The explanation may lie in the weights and biases that make up an ANN, and which are adjusted for optimum classification results when the network is trained.

ACKNOWLEDGEMENTS

This work was supported as an in-house effort by Air Force Institute of Technology, Department of Engineering Physics and by Air Force Research Laboratory, AEF Technologies Division. The work was funded by the Department of Defense Joint Committee for Chemical and Biological Defense with project administration by the US Army, SBCCOM. We also thank US Army ERDEC and Bio-Rad Laboratories, Inc., Sadtler Division for providing infrared spectra used in this work. We are also grateful to other organizations and workers who provided infrared spectra or technical assistance but asked to remain unacknowledged.

DISCLAIMER

Certain instruments and software have been identified by brand name to fully document the work. Such mention does not imply recommendation or endorsement by the Air Force nor does it imply that the items identified are the best available for the purpose

REFERENCES

1. P. R. Griffiths and J. A. de Haseth, *Fourier Transform Infrared Spectroscopy*, John Wiley & Sons, New York, NY, 1986.
2. H. H. Willard, L. L. Merritt, Jr., J. A. Dean, and F. A. Settle, Jr., *Instrumental Methods of Analysis*, 7th Ed., Wadsworth Publishing Company, Belmont, CA 1988.
3. S. L. Emery, *IRSPEC Version 1.0: An IR Database Program*, Chemical Research Development and Engineering Center, Aberdeen Proving Ground, MD, CRDEC-TR-88128, September, 1988.
4. CONVENTION ON THE PROHIBITION OF THE DEVELOPMENT, PRODUCTION, STOCKPILING AND USE OF CHEMICAL WEAPONS AND ON THEIR DESTRUCTION, (Corrected

version in accordance with Depositary Notification C.N.246.1994.TREATIES-5 and the corresponding Procès-Verbal of Rectification of the Original of the Convention, issued on 8 August 1994).

5. P. C. Jurs and T. L. Isenhour; *Chemical Applications of Pattern Recognition*, John Wiley and Sons, New York, NY, 1975.
6. B. R. Kowalski and C. F. Bender, *Journal of the American Chemical Society* **94**, 5632 (1972).
7. B. R. Kowalski and C. F. Bender, *Journal of the American Chemical Society* **95**, 686 (1973).
8. M. A. Sharaf, D. L. Illman, and B. R. Kowalski, *Chemometrics*, John Wiley & Sons, New York, NY, 1986.
9. J. R. Long, H. T. Mayfield, M. V. Henley, and P. R. Kromann, *Analytical Chemistry* **63**, 1256 (1991).
10. S. Haykin, *Neural Networks. A Comprehensive Foundation*, Macmillan College Publishing Company, New York, NY, 1994.
11. H. Demuth and M. Beale, *Neural Network Toolbox for Use with MATLAB. User's Guide Version 3*, The Mathworks, Inc., Natick, MA, 1998.
12. S. Chen, C. F. N. Cowan, and P. M. Grant, *IEEE Transactions on Neural Networks*, **2**, 302 (1991).
13. M. A. Sharaf, D. A. Illman, and B. R. Kowalski, *Chemometrics*, John Wiley & Sons, New York, NY, 1986.
14. G. D. Schuchardt, *Automated Infrared Detection of Organophosphorus Compounds in Multicomponent Solutions*, MS Thesis, Air Force Institute of Technology, Wright-Patterson AFB, OH, 1995.
15. D. E. Rumelhart, G. E. Hinton, and R. J. Williams, *Nature* **323**, 533 (1986).
16. M. Reidmiller and H. Braun, "A direct adaptive method for faster backpropagation learning: The RPROP algorithm," *Proceedings of the IEEE international Conference on Neural Networks*, 586 (1993).
17. M. T. Hagan and M. Menhaj, , *IEEE Transactions on Neural Networks*, **5** 989 (1994).

POLARIZED LIGHT SCATTERING TO PROVIDE SIZE DISTRIBUTIONS OF MICROORGANISMS

by Burt V. Bronk¹, Merrill E. Milham², Zhao Z. Li³, and Jozsef Czege³

1. AFRL/HST at SBCCOM, A.P.G. MD, 21010-5424

2. ECBC at SBCCOM, A.P.G., MD 21010-5424

3. USUHS, Bethesda, MD 20814-4799

Abstract:

Calculations for Mueller matrix elements for polarized light scattering are made for particles in the size ranges appropriate for microorganisms. For spherical particles or randomly oriented particles whose regularity (symmetry) is adequate for their scattering properties to be approximated well by spheres, there are only four non-zero elements. We examine these elements for spherical particles in water and using parameters which are in ranges typical for many single microorganisms. Of these we find that the graph for the normalized S34 element (i.e., S34/S11) shows the most interesting effects for small changes in the parameters. The parameters examined are size, optical constants, and variance in size (i.e., standard deviation of a distribution). We fit the graph obtained using a very much simplified model of a spore, to data obtained by light scattering from a suspension of *Bacillus cereus* spores and find that the model fits the data well enough using reasonable parameters to indicate utility.

Introduction:

This presentation indicates in outline form a poster given at this conference. Most of the figures are derived from calculations of Mueller matrix elements for light scattering from small particles. The mathematics used in these calculations as well as the experimental methods may be obtained from reference 1 or 2. Examples of a biological application and other references are given in reference 3.

The scattering apparatus in Fig. 1 is a much simplified diagram. The definition of the Stokes Vector is shown in terms of the parameters for the E-field (electric field) for a coherent light beam. On the bottom of the figure we see the definition of the Mueller matrix, whose elements we calculate and discuss in this effort. For a randomly oriented collection of identical (or almost identical) particles, there are only six non-zero (or non-negligible) elements for this matrix. We will consider particles which are sufficiently well approximated by homogeneous spheres that we may consider only the four independent parameters which are non-zero for such spheres. These are $S_{11}=S_{22}$; $S_{12}=S_{21}$; $S_{33}=S_{44}$; $S_{34}=-S_{43}$.

We examined each of these four matrix elements as a function of the scattering angle, Θ . We use a wavelength of 633 nm and assume the scattering particles are in water unless otherwise noted. All calculations are for a population of particles distributed in size (diameter, since we are modeling the particles with spheres) according to a Gaussian with a Coefficient of Variation (CV) of 0.2 unless otherwise noted. We use a refractive index similar to that for a bacterial spore in these examples ($n = 1.52 + .015i$).

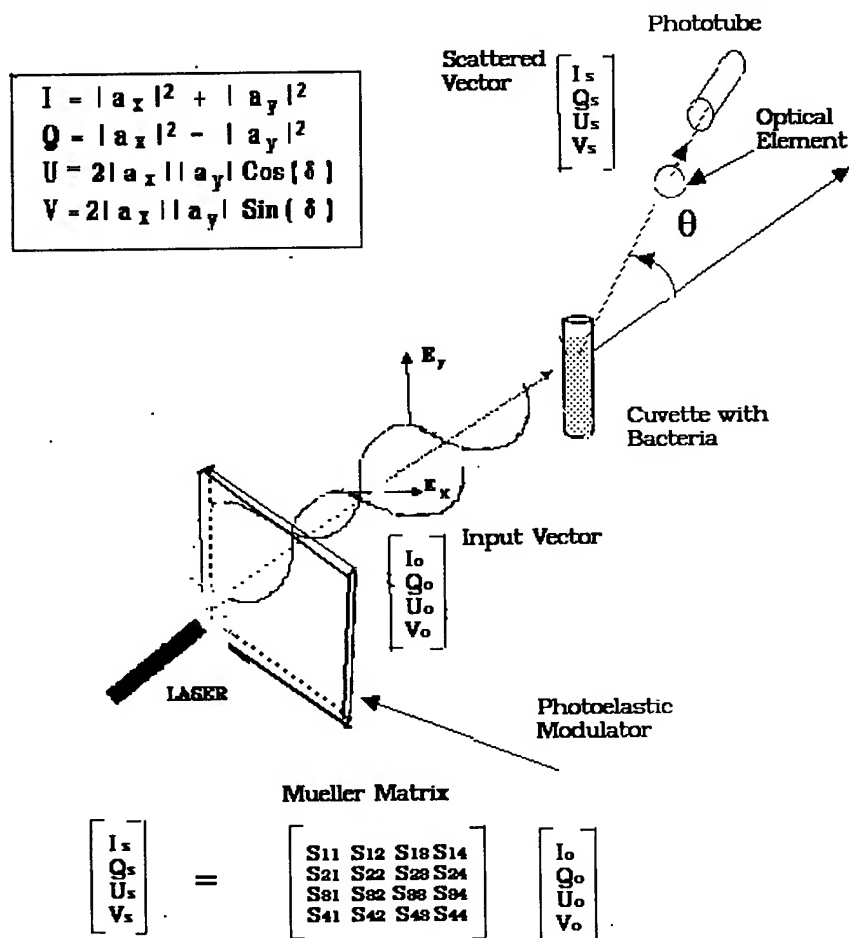


Figure 1: Stokes vector, Mueller matrix, and simplified sketch of experimental setup

For the present purpose and to define the angles used in the graphs presented, a sketch of the experimental setup is shown in Fig. 1. A much more detailed explanation of a similar experimental setup is given in reference 2.

Results: We plot the graphs of the four non-zero elements for a few sizes in the appropriate range for single microorganism particles. In the first example of this series, we plot normalized S_{11} or $S_{11}/S_{11}(0)$ vs angle in Fig 2. We see that as expected, the forward scattering increases relative to back scattering for larger particles.

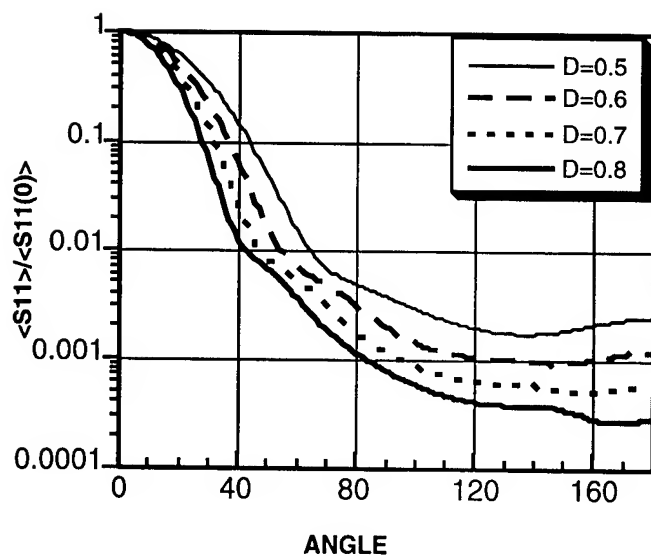


Figure 2: Average S11 normalized by average S11(theta=0).

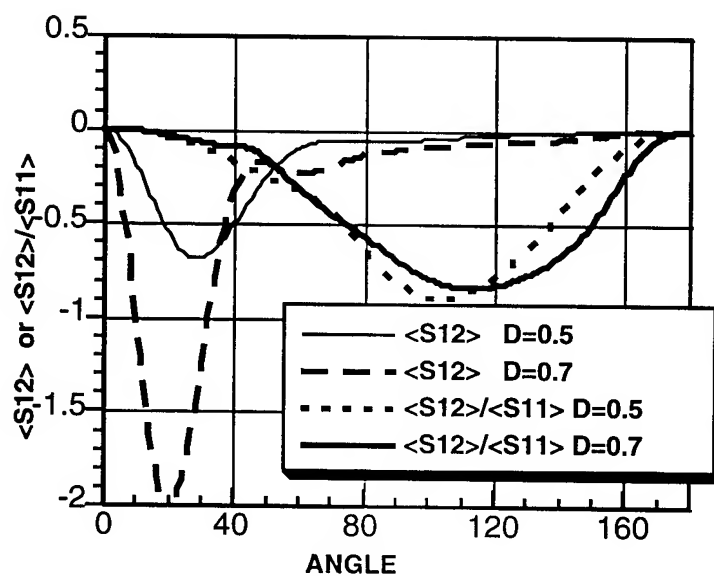


Figure 3: $\langle S_{12} \rangle / \langle S_{11} \rangle$ or $\langle S_{12} \rangle$ vs Angle

In Fig 3 we plot averages for both the unnormalized element, S_{12} , and the normalized element, S_{12}/S_{11} . The graphs become more symmetrical as the diameter becomes smaller. We

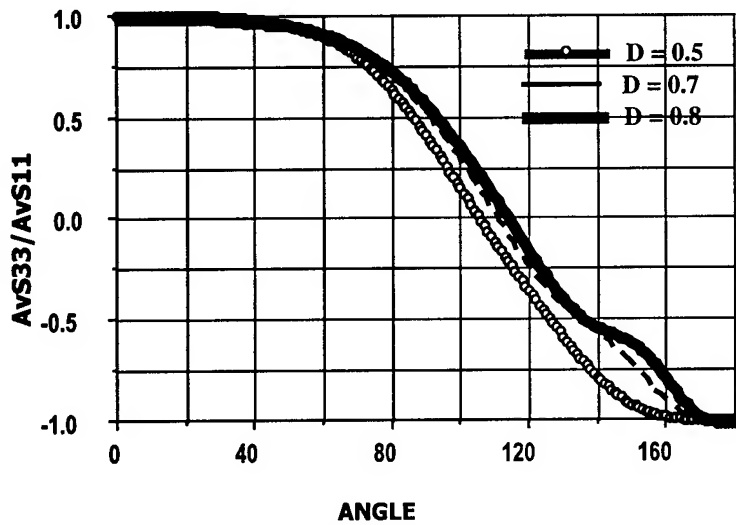


Figure 4: $\langle S_{33} \rangle / \langle S_{11} \rangle$ vs Angle

note that the unnormalized element's graph reveals additional features for this particular element. In Fig 4 we plot the normalized matrix element $\langle S_{33} \rangle / \langle S_{11} \rangle$. The changes for this element with size are rather small in the present parameter range. In Fig 5 we plot $\langle S_{34} \rangle / \langle S_{11} \rangle$. Calculations with this element give graphs showing quite prominent changes in appearance with small size change.

In Figure 6 we plot $\langle S34 \rangle / \langle S11 \rangle$ for a population of 0.9 micron bacteria (index = 1.37 + 0i)

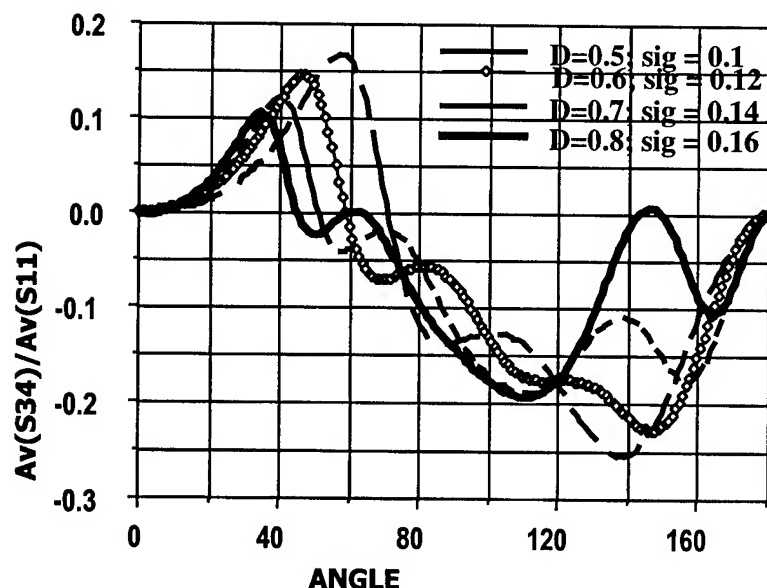


Figure 5: $\langle S34 \rangle / \langle S11 \rangle$ vs angle for spores of various average diameter

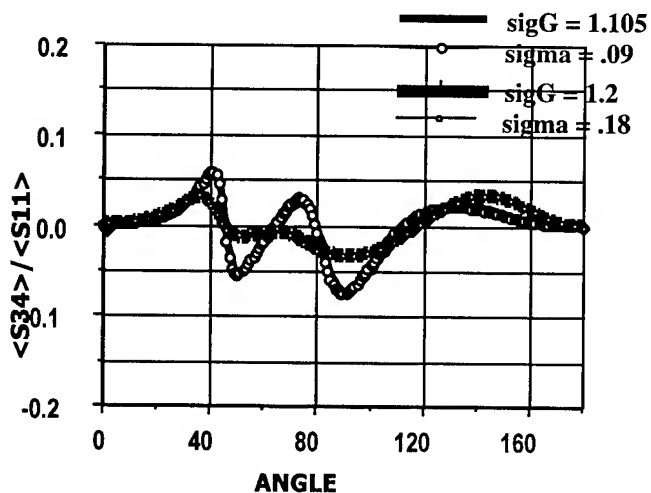
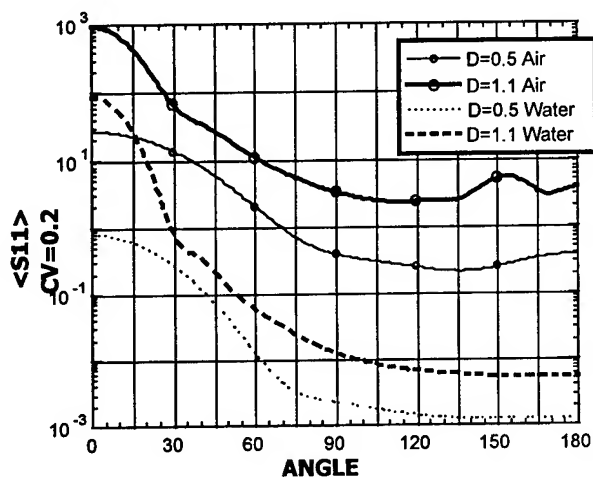


Figure 6: $\langle S34 \rangle / \langle S11 \rangle$ vs Angle for Gaussian or Equivalent Log Normal Distributions

suspended in water calculated with a Gaussian or a Log Normal distribution. In each case the SigmaG for the Lognormal is chosen to be equivalent to the sigma (Standard Deviation) for the Gaussian. with a CV of either 0.1 or 0.2. We see that for CV's up to ~20%, the results from the two rather different distributions are close to identical. However, the CV itself is important in determining the shape of the graph.

Scattering from Vegetative Bacteria in Air or Water



Vegetative Bacteria Compare in Air vs Water

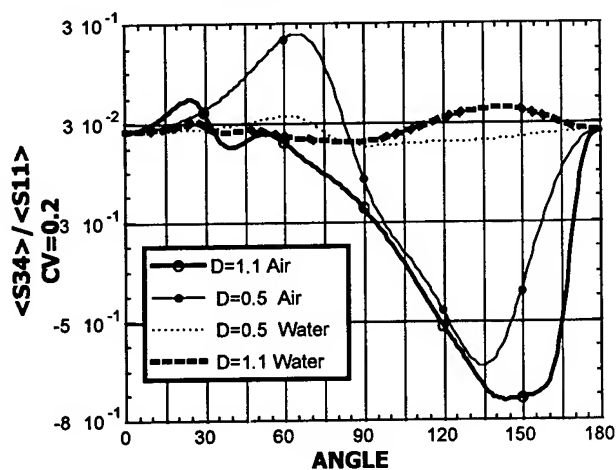


**Figure 7: Vegetative Bacteria in Air or Water. Top, S_{11}
Bottom, S_{34}/S_{11}**

In Fig 7 we compare S_{11} or S_{34}/S_{11} for a population of vegetative bacteria of two different average sizes either in air or in water. The logarithmic $\langle S_{11} \rangle$ graph retains much the same shape, although the scattering as expected is much larger in air since the contrast in refractive index is larger in air. The graph of $\langle S_{34} \rangle / \langle S_{11} \rangle$ shows much more amplitude in air, and a change in shape as well.

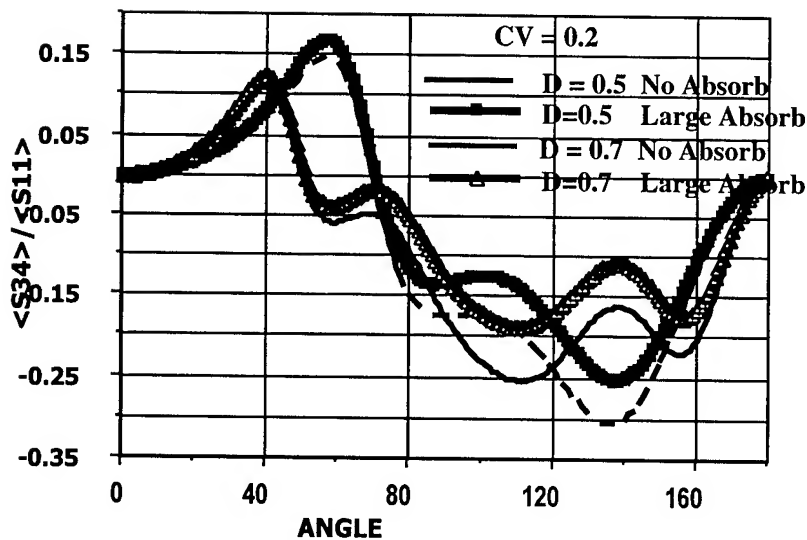


Figure 8: Effect of absorption on $\langle S_{34} \rangle / \langle S_{11} \rangle$.

In Fig 8 we examine the effect of absorption (large, index = $1.52 + 0.015i$) vs no absorption for spores in water. The log scale graph of S_{11} (not shown) does not show much change except for a slight lowering for backward angles, and overall scatter is of course reduced. On the other hand we see in Fig 8 that the change in the normalized S_{34} element is quite noticeable for angles between about 80 and 160 degrees, with the values obtained with absorption larger.

In Fig 9 we show how the $\langle S_{34} \rangle / \langle S_{11} \rangle$ graph for a 0.5 micrometer average diameter vegetative cell in water varies depends on the σ_G of the Log Normal distribution of sizes. It is evident that the amplitude reduces (and the extrema shift) as the variation of sizes increases. We also see that for a CV of 10% the Gaussian gives results indistinguishable in practice from a Log Normal distribution with a σ_G of 1.105. For a $\sigma = 0.0$, (Log Normal $\sigma_G = 1.0$). S_{34}/S_{11} is very peaked with its maximum at 87 degrees in contrast to the distribution with $\sigma = 0.05$ and the same average size, which is smooth and has its maximum at ~77 degrees.

In Fig 10 we diagram the complex structure of a bacterial spore such as *Bacillus cereus* after electron micrographs from several sources. The exosporium is commonly seen only in cereus or anthracis bacilli.

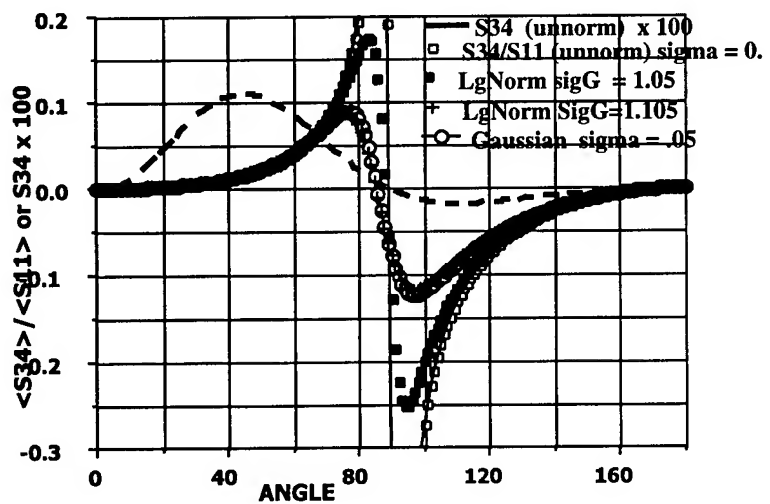


Figure 9: $\langle S34 \rangle / \langle S11 \rangle$ for a vegetative 0.5 micron bacterium in water for various size distributions.

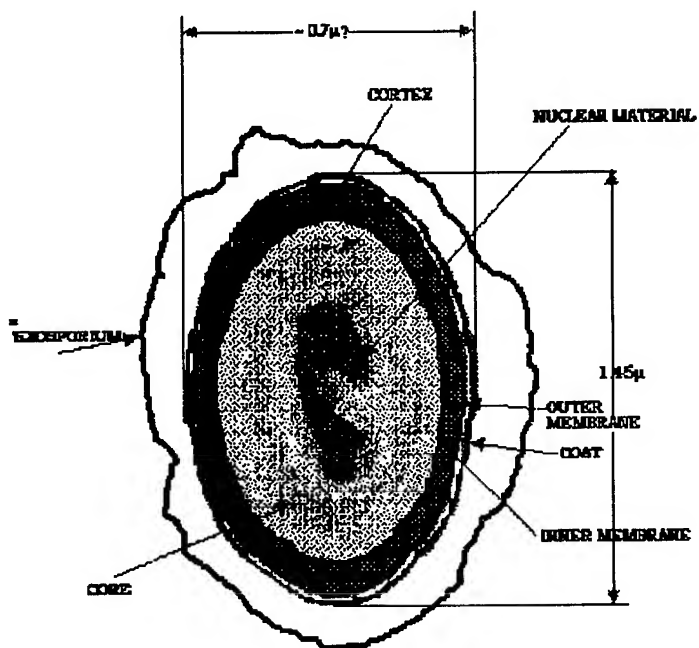


Figure 10: Diagram of a typical *Bacillus cereus* spore.

In Fig 11, we show an attempt to fit the experimental graph of $\langle S_{34} \rangle / \langle S_{11} \rangle$ measured with *B. cereus* spores in water suspension using a much-simplified model which assumes a homogeneous sphere with diameter < 1 micron. In this fit we used a value for the refractive index ($n = 1.52 + .000025i$) in which the two numerical parameters were obtained from data (unpublished) measured by other methods with *B. cereus* spores. The average diameter and the sigma (standard deviation) of the distribution were allowed to vary. The result in Fig 11 shows that the model with the parameters used can be related significantly to experimental data

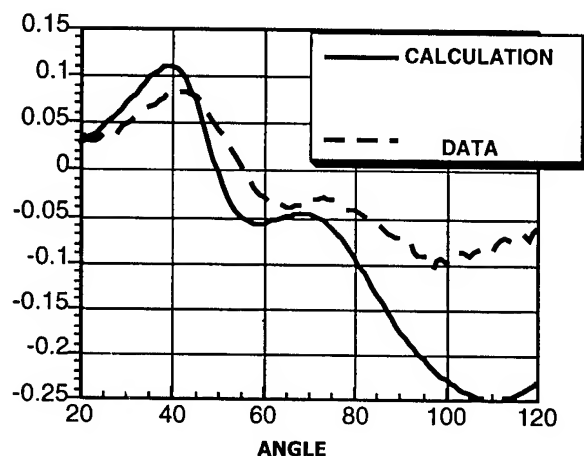


Figure 11: Experimental data from *B. cereus* spores in water fitted with much simplified model.

In another attempt at a fit, in addition to the above parameters, the imaginary index was allowed to vary. In this case, as can be seen in Fig 8, increasing the imaginary index causes an increase in large angle values for S_{34}/S_{11} . In this way we obtained an excellent fit still using this very simple model, however we arrived at a very high value, $0.015 i$ for the imaginary part of the refractive index. It may be that allowing such a high value for this parameter accounts for some of the ignored complexity of the spores structure as diagrammed in Fig 10, or it may be that more complex mathematical models (e.g., layered spheres) are required to relate the experiment closely to the calculations.

Conclusions:

- The graph of the normalized Mueller matrix element, S_{34}/S_{11} , vs angle has a structure with sufficient complexity to fit it to several parameters important for micron-sized biological particles. Changes of the graphs for the other normalized elements examined are not as dramatic or easily characterizable for small variations in the parameters ranges studied here, but may be useful in other parameter ranges.
- Absorbance by the particle makes a significant change in the graph of S_{34}/S_{11} vs angle, as does the particles real index and the index of the medium in which the particles are immersed..

- Previous studies showed that for randomly oriented axisymmetric particles, the graphs of S34/S11 vs angle are closely correlated with the small diameter of the particle, but not with its length. The average diameter (D) of such a collection of particles may be measured by obtaining these graphs. In the present study we see that small changes in the coefficient of variation $\{SD/\langle D \rangle\}$ (where SD is the standard deviation) of the size distribution make large and noticeable changes in the graph of S34/S11. The graph is not very sensitive to whether a logarithmic or a Gaussian distribution of particle sizes was used.
- Applying a much-simplified model of a bacterial spore to determination of S34/S11 allowed a satisfactory fit of the graph to experimental data using reasonable parameters for *Bacillus cereus* spores.

References:

1. C. F. Bohren and D. R. Hoffman, (1983) *Absorption and Scattering of Light by Small Particles*, John Wiley & Sons, New York,.
2. B. V. Bronk, W. P. Van De Merwe, D. R. Huffman, (1992). "Polarized Light Scattering as a Means for Detecting Subtle Changes in Microbial Populations", in "Modern Techniques for Rapid Microbiological Analysis" editor: W. Nelson, VCH Publishers, N.Y., pp 171-197.
3. Burt V. Bronk, Stephen D. Druger, Jozsef Czege and Willem P. Van De Merwe, (1995) "Measuring Diameters of Rod Shaped Bacteria in Vivo with Polarized Light Scattering", *Biophysical J.*, vol. 69 1170-1177.

SHIPBOARD AUTOMATIC LIQUID AGENT DETECTOR (SALAD)

Diane LaMoy
US Navy, NSWC Dahlgren
Chemical Biological Systems Defense Branch
Dahlgren, VA 22448

Abstract The U.S. Navy developed a Shipboard Automatic Liquid Agent Detector (SALAD) to detect and differentiate 200-micron liquid nerve (G series and VX) and liquid blister (HD and L) agents. This paper describes the design of the SALAD system, which uses M8 paper as the detection media, and Charged Coupled Device (CCD) imaging technology. Digitized images are captured using light from the visible spectrum, which is produced from a halogen illumination source. Optically coupling the light through 13 continuous wavelength pass band filters produces 13 different spectral images of the target area. These images are processed and analyzed for the presence of chemical agent. The electronics system is based on a PC/104 back plane architecture with embedded C language software for system control and image analysis.

This paper provides an overview and functional description of the SALAD system

Salad Overview

SALAD is a fixed point detection system used by Naval forces to detect and alarm for liquid chemical agent contamination of the ship's exterior. The system responds to nerve (G, V) and blister (H) chemical warfare agents. The most important operational feature of SALAD is that it monitors the ship's exterior in real time and automatically detects and differentiates liquid agents at low concentrations. A alarm occurs in less than 60 seconds.

The system provides alarm and agent identification to the Bridge and Damage Control Central (DCC) or Central Control Station (CCS). This data can be used to advise the Commanding Officer of the occurrence of a chemical attack.

The SALAD system is designed to work in conjunction with the Improved Point Detection System (IPDS). IPDS detects chemical warfare agents in vapor form, while SALAD detects chemical warfare agents in liquid form. Together, these systems provide an automatic detection and warning system in all threat conditions.

SALAD is designed to be used as a permanently mounted shipboard system that is operated during heightened chemical warfare (CW) threat conditions or for training.

System Description

SALAD (figures 1 and 2) consists of an external detector unit (DU), a Control Display Unit (CDU), and a Remote Display Unit (RDU). The DU continuously monitors for liquid chemical agents with a specially designed detector paper that stains upon contact with liquid chemical agent droplets. The DU uses spectrophotometry technology to view the sample and, if chemical agent droplets are detected, provides digital signals to activate visual and audible alarms at the CDU and RDU.

System Hardware

Detector Unit (DU)

The DU (figures 3 and 4) continuously advances the detector paper past a fixed aperture exposing the paper to liquid chemical agent droplets falling from the atmosphere. The DU consists of an automatic door that opens when the system is activated exposing a 4 inch x 4 inch area of detector paper. Inside the DU is a Detector Paper Cassette, two (2) Optical Scanner Assemblies, an Illuminator Assembly, and electronics and mechanical hardware that control the operation of the DU.

The DU continuously scrolls paper within the Detector Paper Cassette past the open aperture. Once exposed, the detector paper takes between 30 and 60 seconds to be fed from its exposed location to the Optical Scanner Assembly for analysis.

The Illuminator Assembly provides color-specific illumination to both Optical Scanner Assemblies via fiberoptics. The optical scanner takes video images to measure the ratio between the stain intensity and unstained intensity for up to thirteen different color positions. This video data is digitized by the DU electronics and analyzed using a detection algorithm. Digital signals are sent from the DU to the CDU and RDU to provide the appropriate messages or alarms.

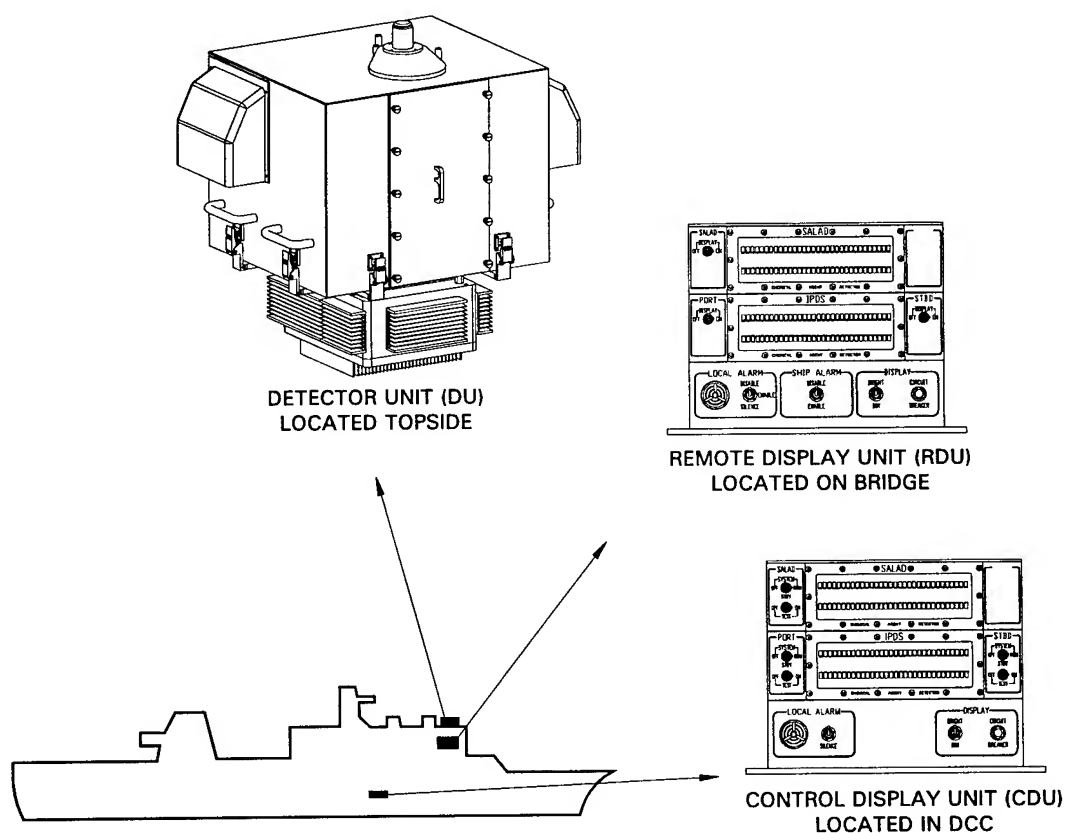


Figure 1. Shipboard Automatic Liquid (Chemical) Agent Detector (SALAD)

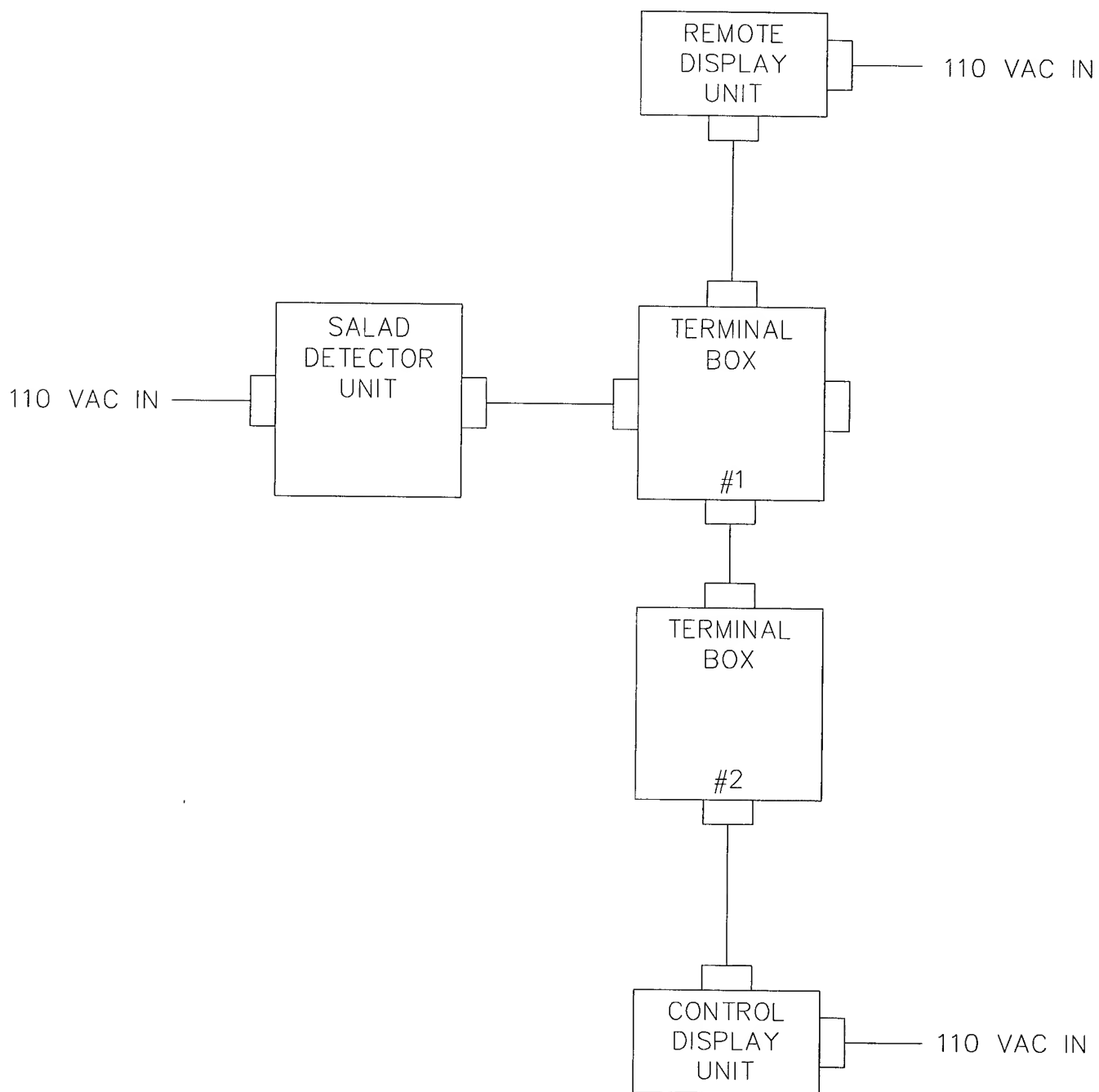


Figure 2. SALAD Interconnection Diagram

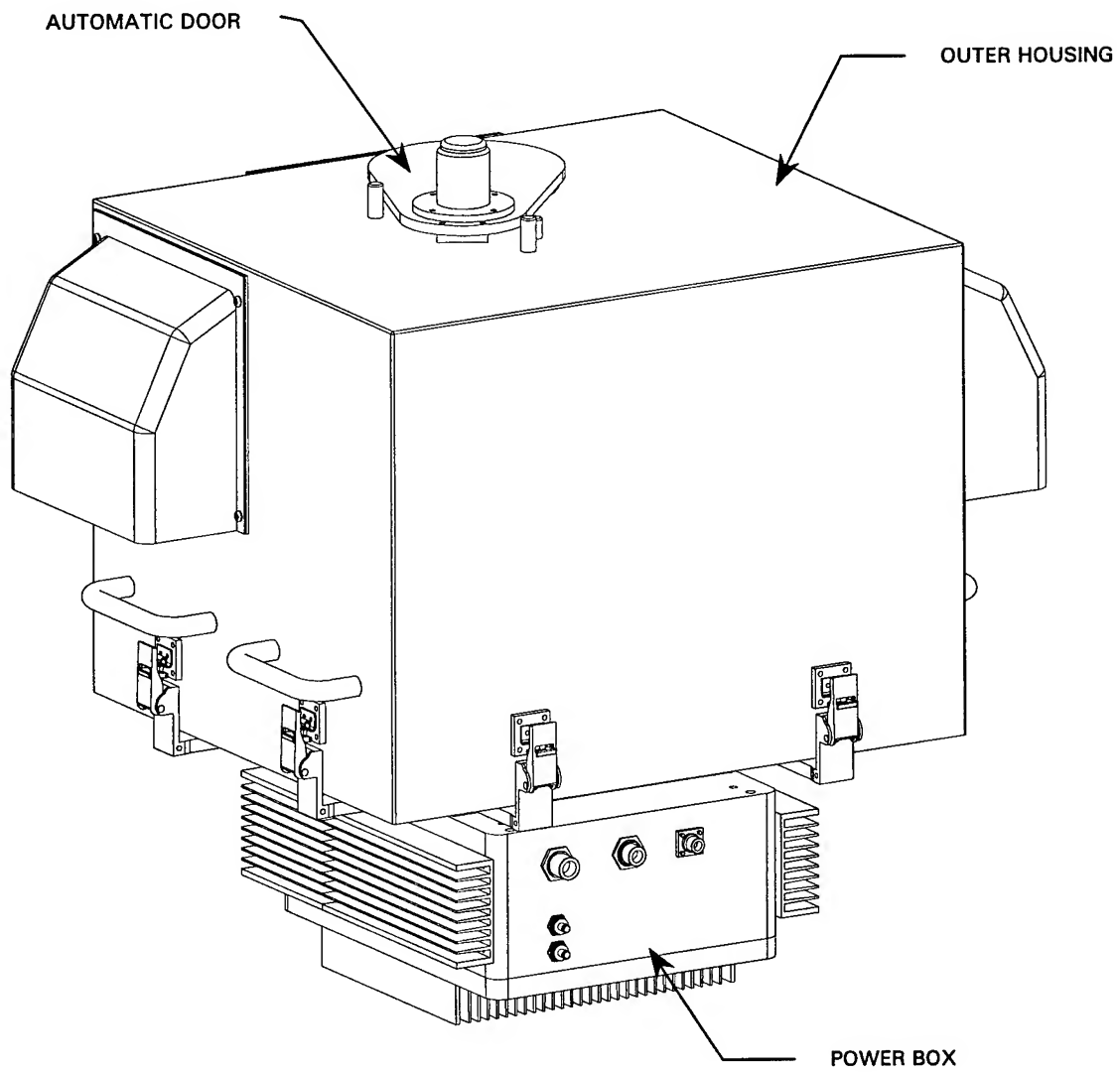


Figure 3. Detector Unit (DU)

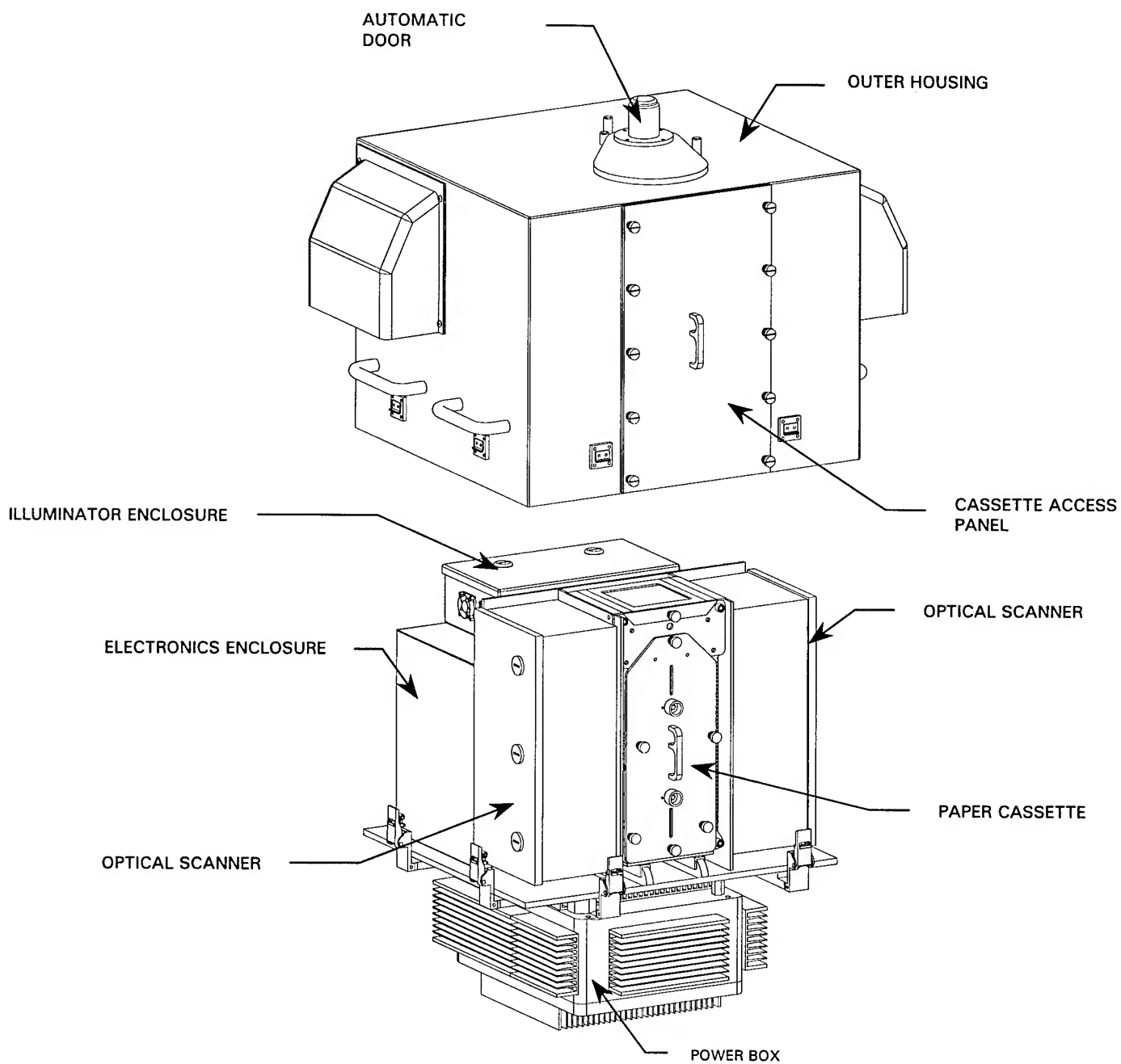


Figure 4. Detector Unit (DU) with Outer Housing Removed

Control Display Unit (CDU) and Remote Display Unit (RDU) The CDU (figure 5) contains all control switches for the operation of the system, and responds with printed messages and audible alarms as directed by the DU. It is normally mounted in Damage Control Central (DCC) or Central Control Station (CCS).

The RDU (figure 6) is normally mounted on the Bridge, and is similar to the CDU except that it has no system switches and thus cannot control the system. It responds with the same printed messages and audible alarms as the CDU.

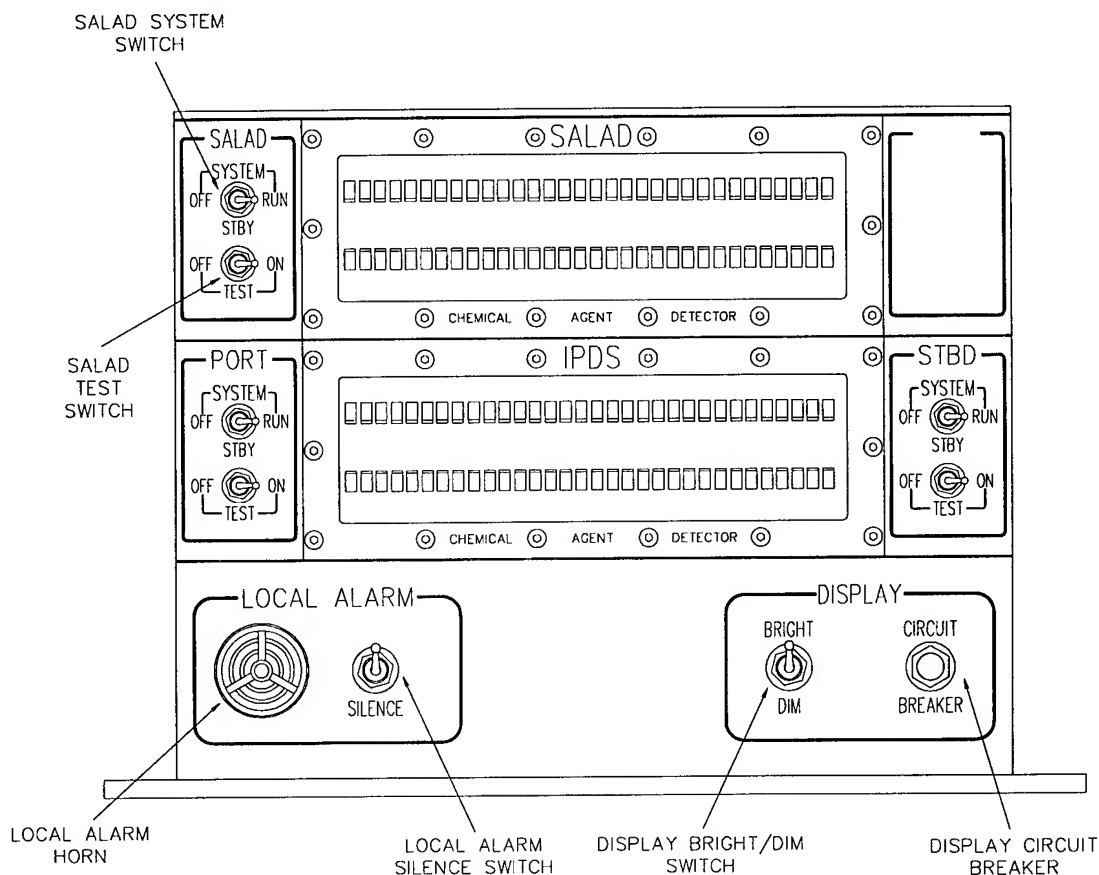


Figure 5. Control Display Unit (CDU)

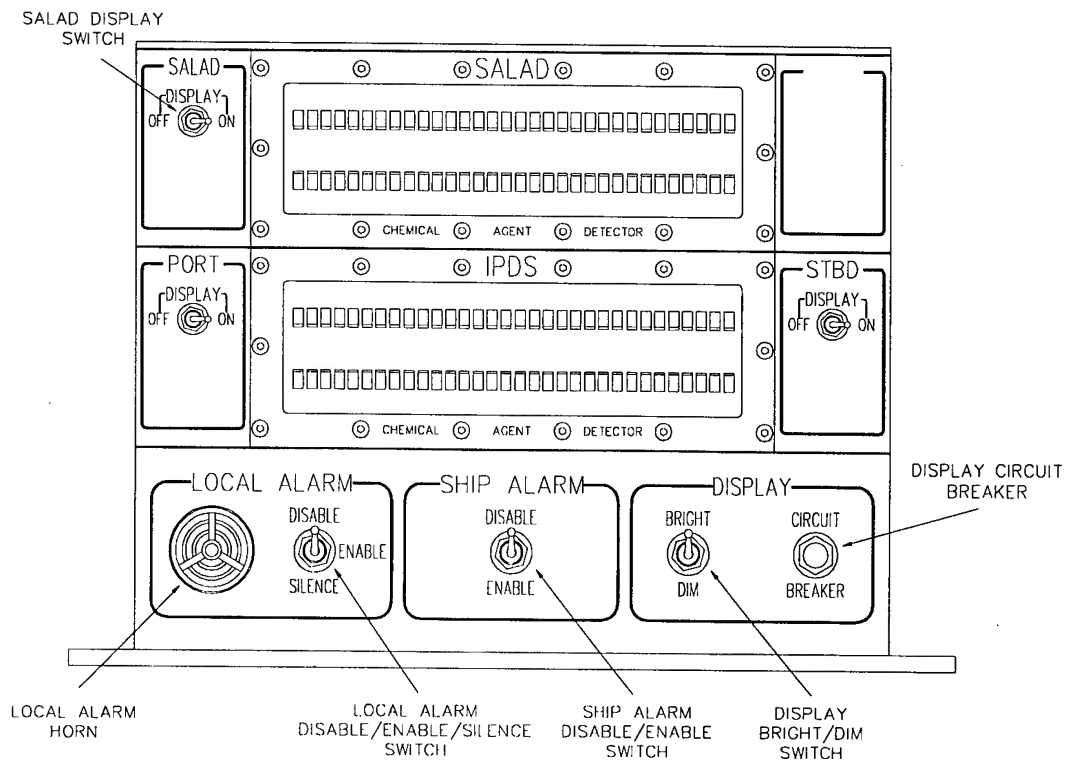


Figure 6. Remote Display Unit (RDU)

Table 1. Reference Data

Equipment	Power Requirements	Sensitivity	Operating Temperature	Storage Temperature	Shelf Life
Detector Unit (DU)	110 VAC	Alarm against nerve (G,V) and blister (H) liquids at 0.5-0.6mm droplet size or larger	-28° C (-18° F) to 50° C (122° F) *	-40° C (-40° F) to 70° C (158° F)	Useful ship life
Control Display Unit (CDU)	110 VAC	N/A	-28° C (-18° F) to 50° C (122° F)	-40° C (-40° F) to 70° C (158° F)	Useful ship life
Remote Display Unit (RDU)	110 VAC	N/A	-28° C (-18° F) to 50° C (122° F)	-40° C (-40° F) to 70° C (158° F)	Useful ship life
Terminal Box	N/A	N/A	N/A	N/A	Useful ship life

*Table 2. Shipboard Automatic Liquid (Chemical) Agent Detector
System Equipment, Accessories, and Documents Supplied*

Nomenclature	Quantity	Overall Dimensions			Weight (lb)
		Length (in)	Width (in)	Height (in)	
Detector Unit (DU) Assembly	1	24.3	22	30	240
Control Display Unit (CDU) Assembly	1	14	12	10	15
Remote Display Unit (RDU) Assembly	1	14	12	10	15
Paper Cassette	2	8.1	7.5	17.3	8
Paper Roll Assembly	6	6.8	6.0	6.0	3
Terminal Box	2	14	12	10	15

System Operation

SALAD is designed to be operated continuously during periods of elevated threat of chemical attack, for up to 30 days. The paragraphs that follow describe normal operating procedures for SALAD system. The system is activated and controlled at the CDU (figure 5) located in DCC/CCS.

Detection of Liquid Chemical Agents If the DU determines that it has found and validated a chemical agent, it will send that information to the CDU, and the CDU will enter an alarm state. In this state, the LOCAL ALARM horn (figure-5) will sound a continuous audible signal. The following alarm message will be shown on the alphanumeric display (6), blinking at a rate of two times per second:

SALAD DETECTOR AGENT WARNING

There are three agent types recognized by the DU. Alternating with the warning message above, the display will also show the type of agent that has been detected, as follows:

*NERVE AGENT DETECTED -TYPE G
NERVE AGENT DETECTED -TYPE VX
BLISTER AGENT DETECTED -TYPE HD*

The LOCAL ALARM horn will not sound again unless the DU detects another agent type or if the DU detects an agent again after at least one minute of absence. The alphanumeric display will continue to show the agent detection messages above for 1 minute after the last detection. If another type of agent is detected within this one minute time, the LOCAL ALARM will sound again, and that agent will be displayed. After one minute passes without detecting an agent, the system will automatically go back to scan mode.

The LOCAL ALARM horn will not sound in response to an unknown stain.

DU Status Self-Monitoring

The DU will periodically check its operational status and send updated status information to the CDU for display.

If there are any conditions outside the proper operating parameters, the CDU will beep intermittently and display the first error or warning shown.

The audible LOCAL ALARM horn (5) will sound the Alert Signal (beeping on and off every ¼ sec) until manually reset by the operator.

Simulant Test Mode

Simulant test mode is used to provide confidence that the system is working properly and capable of detecting liquid chemical agents. Chemical agent simulant droplets are intentionally placed onto the detector paper and, if the system is operating properly, the DU will detect, alarm, and identify the simulants.

Diagnostic Mode

To determine the operational status of the system at any time, the operator may initiate a Built-In-Test (BIT). The results of the BIT will be shown on the alphanumeric display (figure 5).

Spectrophotometry

The SALAD DU employs the concept of spectrophotometry to measure spectral reflectance relative to wavelength. Spectral reflectance is the ratio between the intensity measurement of the stain and the intensity measurement of the unstained detector paper (reference) for specific wavelengths of illumination.

Inside the DU, the detector paper is imaged with a black and white CCD camera. Illumination of the detector paper is provided through up to thirteen different narrowband and long pass filters. Each filter is singly positioned in front of a white light source and permits specific wavelengths of light to pass. For each filter position, camera video data is digitized for the unstained detector paper and stored in a reference table. When a stain is introduced, the digitized video data is compared to the unstained reference data for each of the filters. The result is a reflectance ratio for each of the filter positions.

Each agent stain has a unique pattern of reflectance ratios, also called its signature, which permits the detection/differentiation of liquid G, H, and V class chemical agents. In addition, stains from unknown substances can be disregarded if their signatures do not match those in the "agent library".

FUNCTIONAL FLOW.

Overall Level.

Agent Sampling

The DU continuously advances the detector paper in the cassette past a fixed aperture exposing the paper to liquid chemical agent droplets in the atmosphere. If droplets land on the paper they chemically react with dyes embedded in the paper to create a colored stain. The detector paper advances into the field of view of the CCD camera where it is imaged using up to thirteen colors of illumination.

Signal Acquisition and Analysis

After the agent stain sample is imaged by the CCD camera, the video data for each of the filters is digitized by a frame grabber card. The CPU compares the digitized image to the reference video data collected for unstained paper. The resulting ratios for up to thirteen filters provide a signature for the agent sample. A software detection algorithm compares the sample's signature with a library of known agent signatures. If there is a match with a nerve or blister agent of interest, audible and written alarms are initiated on the system's display units to alert the ship's crew.

Major Function Level

Detector Unit

The major components of the DU are described in the following paragraphs. The location of the detector unit should be labeled on both the CDU and RDU. A functional diagram that relates the components can be found in figure 7.

Automatic Exposure Door

The automatic exposure door provides a weathertight cover on the paper exposure aperture during the detector "OFF" and "STANDBY" modes. When SALAD is switched to "RUN" mode, during heightened threat levels or for training, the automatic exposure door lifts and rotates to expose the detector paper. When SALAD is switched back to "STANDBY" mode the automatic exposure door lifts, rotates back, and drops to seal the exposure aperture.

Detector Paper

The detector paper is a 200' replaceable roll of M8 detector paper. To extend paper life, the roll is double spooled so that the paper can be moved bi-directionally. The M8 detector paper roll used for SALAD was specifically designed to detect G, H, and V class agents and withstand the shipboard environment.

Detector Paper Cassette

The detector paper cassette holds the roll of detector paper. It guides the paper past an exposure aperture for agent sampling at the top of the cassette and past two camera viewing apertures located on each side. The cassette is designed so that both the detector paper and/or cassette can be removed and replaced.

Paper Transport Stepper Motors

When the detector paper cassette is properly installed, the paper transport stepper motors will continuously scroll the detector paper past the exposure aperture. Any droplets that fall onto the paper during the exposure will create stains and be detected as the paper moves past the CCD camera in the optical scanner assembly. The paper transport stepper motors are located within the electronics enclosure of the DU. They move the paper bi-directionally in .4" increments.

Optical Scanner Assembly

There are two optical scanner assemblies per DU. Each optical scanner contains a CCD camera for imaging and a fiberoptic light line for providing illumination. The direction of the detector paper movement determines which optical scanner is providing stain detection video data to the detector unit electronics and which camera is providing pre-scan information.

Illuminator Assembly

The illuminator assembly uses a halogen lamp to provide filtered illumination to both optical scanners concurrently via fiberoptics. The halogen lamp illuminates through a fiberoptic cable, through the filter wheel, and onto another fiberoptic cable that feeds both optical scanners. The filter position is determined electronically using a pair of LED/phototransistors that operate through the spinning filter wheel. The halogen lamp is located inside the illuminator enclosure and the stepper motor driven filter wheel is located inside the electronics enclosure.

Detector Unit (DU) Electronics

The electronics that control the operation of the DU consist of five circuit boards; specifically, a commercial computer board, two video frame grabber boards, and two custom printed wiring boards. All boards are inside the electronics enclosure of the DU. The custom main I/O printed wiring board contains a microprocessor that controls the system functions. The custom I/O driver board provides the proper electronic signals to operate or drive the mechanical components. Each video frame grabber board digitizes the analog video from the CCD cameras. The computer board is an Intel (or equivalent) 486DX4 132MHz. It is loaded with the DU operation software and the agent detection algorithm. Communication with the CDU and RDU is provided via its RS422 port. In addition, the DU has an external RS232 port that allows for upgrading software or data logging.

Automatic Exposure Door Electronics

The automatic exposure door electronics are contained within the box mounted to the bottom of the DU. This box contains the high voltage electronics used to lift the automatic exposure door. It also contains a linear power supply that supplies power to the halogen lamp. The electronics are controlled by the detector unit electronics.

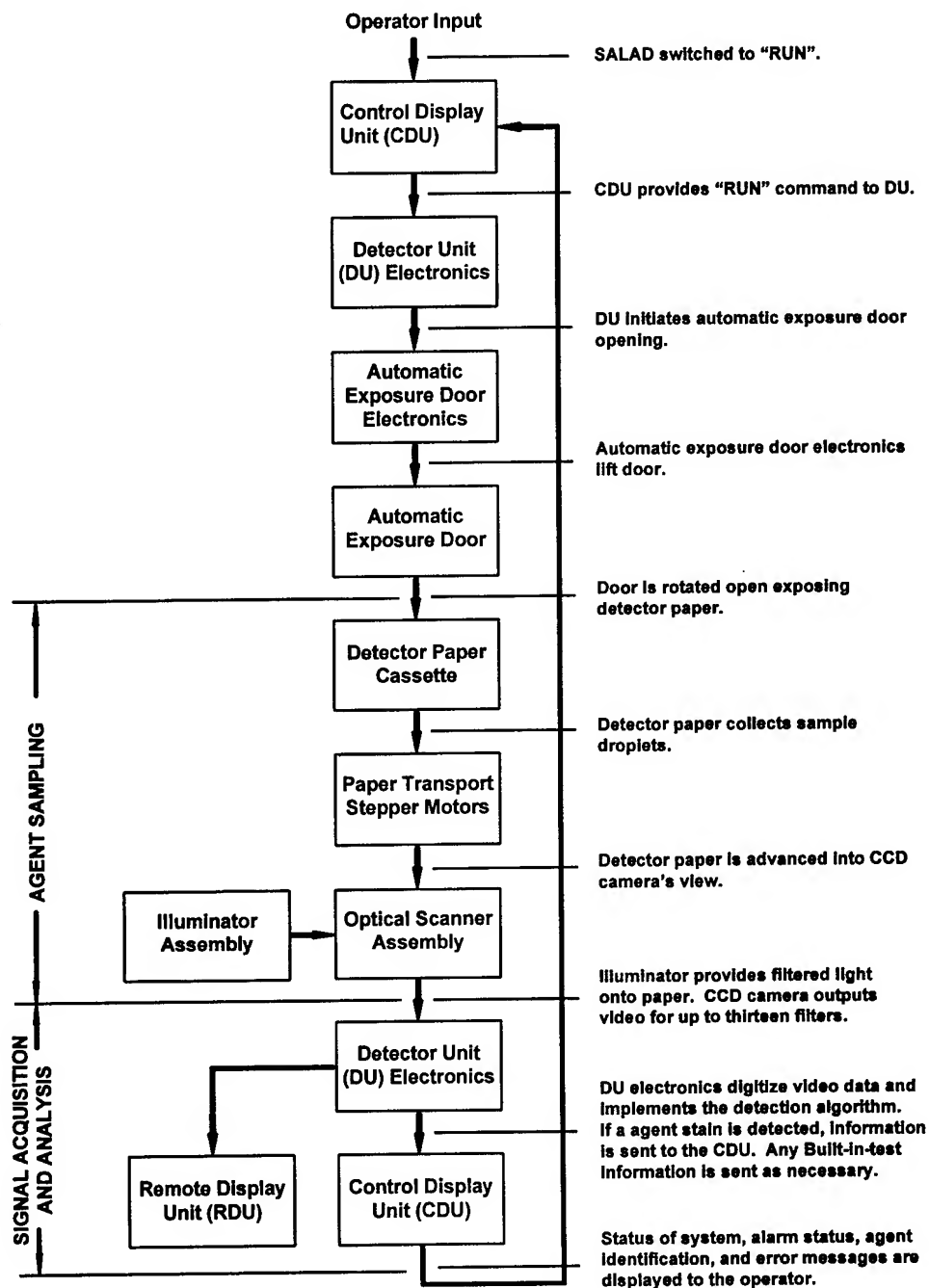


Figure 7. SALAD Detection Flow Chart

Conclusions

The SALAD system was tested and approved for production and installation on ships. SALAD provides reliable automatic liquid agent point detection. The technology for the SALAD uses standard Navy M8 chemical agent detection paper.

Other technologies are also being examined to detect liquid chemical agents. These technologies include optical Spectroscopy techniques such as Ramen and Fourier transform infrared (FT-IR).

AMBIENT BACKGROUND CHARACTERIZATION WEB SITE

Dorothea Paterno

DoD, SBCCOM ,ECBC

AMSSB-RRT-DP

Aberdeen Proving Ground, MD 21010 USA

Allen Smith

DoE, ORNL

Oak Ridge, TN 37831 USA

A comprehensive repository on the web of ambient biobackground characterization data gathered from TTCP CBD Group, TP-10 countries is in process of development. The US DoD Joint Science and Technology Panel for Chemical and Biological Defense (JSTPCBD) has funded ECBC to execute an effort which is limited in scope to the accumulation and development of a database of previously collected ambient background data, and the analysis thereof. The DoE Chemical and Biological Non-Proliferation Program has funded a special project for development of a website on which the data will reside.

The website will facilitate interactions and collaboration among individuals working on ambient background studies or for whom ambient background poses an impact on detector (or other methodology) development.

The goal to understanding the ambient biobackground is to develop a set of rules of the factors that influence fluctuations of the biological composition of the atmosphere at a given location.

The database will be UNCLASSIFIED; it is the responsibility of the "owners" of data to ensure the data is unclassified.

All material for posting on the web site will have the appropriate release documentation and approvals.

To facilitate the collection and transfer of the information into the web database contact Dorothea Paterno, DoD, ECBC , Program Point of Contact, all web information is sent to her; dorothea.paterno@sbccom.apgea.army.mil 410-436-4466; 410-436-1912 FAX; web site administrator is Dr Allen Smith, ut3@ornl.gov.

<http://bioback.ed.ornl.gov>



Ambient Biobackground Characterization



[Search](#) [Discussion](#) [Research](#) [Reference](#) [Contact](#)

[Site Map](#)

Welcome to the Ambient Background Characterization Web Page!

Access to the web site is to facilitate interactions and collaboration among individuals working on ambient background studies. Background poses an impact on detector (or other methodology) development.

[Purpose](#)

[Security Levels](#)

[Announcement/Invitational letter for Participation in Ambient Biobackground Characterization web site \(pdf\)](#)



The Technical Cooperation Program (TTCP) Subgroup 'E' TP 10

Dr. Peter Biggins, United Kingdom
Dr. Camille Boulet, Canada

Dr. Ralph Leslie, Australia
Dr. Randolph Long, United States

This web site contains information which is provided in confidence to the governments of the United States, the United Kingdom, Canada, Australia, and the Technical Cooperation Programme (TTCP) between these governments. This site may contain proprietary or commercially valuable information. The governments shall not treat it in any manner likely to prejudice the rights of any owner thereof, including the right to obtain patent or like statutory rights. Information may be used and disseminated only for evaluation for defence purposes within the recipient governments who shall ensure that no disclosure is made only with the prior written consent of each of the above governments.

Web site content point of contact: dorothea.paterno@sbccom.apgea.army.mil
For e-mail notification of news related to this site or to join the contact list contact: ut3@ornl.gov.

This page last modified on 21 March, 2000

[Security/Disclaimer](#)

Search - Netscape

File Edit View Go Communicator Help

Back Forward Reload Home Search Netscape Print Security Shop Stop

Bookmarks Location: <http://bioback.ed.ornl.gov/biomain/search.html>

Instant Message Secure Web Shop My Presario Compaq At Home Compaq Support Smart Update! RealPlayer

Ambient Biobackground Characterization - Search

[HOME](#) [Search](#) [Discussion](#) [Research](#) [Reference](#) [Contact](#)

Use the form below to search this site. Note that you may use boolean operators AND & OR and you may select c

Text to Search For:	<input type="text"/>
Boolean: <input type="text" value="AND"/>	Case <input type="text" value="Insensitive"/>
<input type="button" value="Search"/> <input type="button" value="Reset"/>	

[HOME](#) [Search](#) [Discussion](#) [Research](#) [Reference](#) [Contact](#)

[Security/Disclaimer](#)

Document Done

Biological Background Characterization Discussion Area

[HOME](#) [Search](#)[Research](#)[Reference](#)[Contact](#)[Forum Index](#) | [FAQ](#) | [New](#)**5 Registered Users****General Discussion****CBNP Discussion**

For discussion of issues relevant to the CBNP program.

0 Posts

Last Post: Ne

Air Sampling Apparatus

Discussion of Air Sampling Apparatus

1 Posts

Last Post: 11/

Indoor Air Quality Studies

Discussion of Indoor Air Quality Studies

1 Posts

Last Post: 11/

Outdoor Urban Environments

Discussion of Outdoor Urban Environments

1 Posts

Last Post: 11/

*** TP10 Discussion***

Reserved for TP10 representatives

0 Posts

Last Post: Ne

Test Area

Practice here...

1 Posts

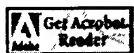
Last Post: 3/2

All times are EST

[Home](#)[Click here to e-mail the site administrator](#)Forums powered by [WWWThreads Free](#)

Ambient Background Characterization - Research

[HOME](#) [Search](#) [Discussion](#) [Research](#) [Reference](#) [Contact](#)



Some files may require Acrobat Reader - Download from Adobe

TTCP - TP10 Proceedings

Proceedings of the First TTCP Subgroup E - TP10 Bioaerosol Workshop - Feb. 1997 held at DERA, CBD, Porton Down, UK. "Characterisation of Ambient Bioaerosols"

PDF file - 8.2 MB

Excerpt from TP10 Aug 97 meeting minutes - 5 Tier Levels of Characterization

CANADA



Web Displays for Colin Watson Aerosol Layout (CWAL) DRES

UNITED KINGDOM



Univ of Birmingham. "BACE STUDY-EMR contract 2027/00r/CBD, BACE Campaign 1995/96, Aerosol biodiversity data"

UNITED STATES



Edgewood Chemical Biological Center (ECBC) Historical 1995-1997 Background Data

Naval Research Laboratory - The Aerobiology Project (Access pending clearance)

Portal Shield Particle Data - JPO-BioDefense Systems (Access pending clearance)

JPO-Bio Defense Portal Shield Info

[HOME](#) [Search](#) [Discussion](#) [Research](#) [Reference](#) [Contact](#)

[Security/Disclaimer](#)

Ambient Background Characterization - Reference

[HOME](#) [Search](#) [Discussion](#) [Research](#) [Reference](#) [Contact](#)

Population of Reference area is on-going. Check back for recent additions.

Contact Dorothea Paterno (dorothea.paterno@sbccom.apgea.army.mil) for submission information.

Click on a link below to "jump" to a specific section, or scroll down page:

[WWWSites](#)

[Australia](#)

[Canada](#)

[United Kingdom](#)

[United States](#)

UNITED STATES



TP-10 Representative - [Dr. S.R. Long](#)

WWW Sites

[Chemical & Biological Nonproliferation Program](#)

[Edgewood Chemical and Biological Center](#)

[Tri Agency CBNP Portal](#)

Journal Articles

An hypothesis describing the general temporal and spatial distribution of alfresco bacteria in the Earth's atmospheric surface layer. *Atmos. Environ.* 32(14/15):2491-2496, 1998.

The ecology of bacteria in the alfresco atmosphere (*FEMS Microbiology Ecology*, Volume: 23, Issue: 4) Lighthart, Bruce, pp. 263-274.

Effect of simulated solar radiation on mixed outdoor atmospheric bacterial populations (*FEMS Microbiology Ecology*, Volume: 26, Issue: 4) Tong, Yongyi, et al., pp. 311-316.

Increased Airborne Bacterial Survival as a Function of Particle Content and Size (*Aerosol Science and Technology*, Volume: 27, Issue: 3) Lighthart, Bruce; Shaffer, Brenda T., pp. 439-446.

Aerobiology Links

Aerobiologia - International Journal of Aerobiology: <http://www.wkap.nl/journalhome.htm/0393-5965>

AEROBIOLOGICAL ENGINEERING Bioaerosol Sampling and Detection: <http://www.engr.psu.edu/aewik/biodet.html>

Aerobiology International: <http://www.isao.bo.cnr.it/aerobio/ai/index.html>

Aerobiology Links (Italy): <http://www.isao.bo.cnr.it/aerobio/ai/AILINK.html>

Australian Pollen calendar http://www.dar.csiro.au/info/airwatch/appendix_5.htm

British Atmospheric Data Centre: <http://www.badc.rl.ac.uk/> The British Atmospheric Data Centre (BADc) is the Natural Environment Research Council's (NERC) Designated Data Centre for the Atmospheric Sciences. It is sited at the Rutherford Appleton Laboratory (RAL) in Oxfordshire, part of the Central Laboratory of the Research Councils (CLRC)

British Mycological Society: <http://www.ulst.ac.uk/faculty/science/bms/> British Mycological Society Details of the society, including links to journals, other societies etc.

Canadian Pollen Site <http://www.canoe.ca/Weather/pollen.html>

Ambient Biobackground Characterization - Contacts

[HOME](#) [Search](#) [Discussion](#) [Research](#) [Reference](#) [Contact](#)

Bioback Web Site Administration

Dorothea Paterno

Content Point of Contact

Physical Scientist

U.S. Army Soldier Biological Chemical Command

AMSSB-RRT-DP

APG, Maryland 21010-5423

Phone: 410-436-4466

Fax: 410-436-1912

e-mail: dorothea.paterno@sbccom.apgea.army.mil

Allen L. Smith

Bioback Web Site Administrator

Oak Ridge National Laboratory

MS 62066

Oak Ridge, TN 37831

phone: 865-574-5934

fax: 865-576-6661

e-mail: ut3@ornl.gov

[HOME](#) [Search](#) [Discussion](#) [Research](#) [Reference](#) [Contact](#)

[Security/Disclaimer](#)

BW DETECTION AND THE BACKGROUND BIOAEROSOLS – ISSUES, PROBLEMS AND RECOMMENDATIONS

Joint Conference on Point Detection for Chemical and Biological Defense
October 2000

By

Dr. Amnon Birenzvig and Dr. Charles Wick

Abstract

Detection of Biological Warfare (BW) agents presents a formidable task. BW agents are aerosol particles (mostly in the respirable range). The toxicity of BW agents is such that the detectors need to be extremely sensitive. In addition the sensors / detectors need to function in an environment that is rich in Bioaerosols. These Bioaerosols often interact with the detector in a manner that is similar to BW agents. In this paper we will discuss some past efforts to characterize the background, present some examples of these measurements, and propose future studies to gain better understanding on how the BW detectors function in the background and potential means to use the data generated by these sensors to detect the BW agents in the “noisy” background.

INTRODUCTION

In addition to the required high sensitivity of BW agents detectors, these detector need to operate in an environment which is rich in biological aerosol which may interfere with the detection process. Figure 1 is a conceptual description of the problem. Close to the point of release the number concentration of BW particles is much larger than the background particles. However, as the plume of the BW agent travels downwind and disperses, the relative concentration of the BW particles diminishes. Figure 2 illustrates the same thing in a slightly different way. Close to the point of dissemination (the triangle above the background level on the upper left-hand side of figure 2) the concentration of the agent is higher than the background and the agent can be easily detected. As the agent plume travels downwind the concentration of the agent diminishes and become comparable, and then much smaller than the background.

BACKGROUND CHARACTERISTICS:

The background is a complex mixture of biological, organic and non-organic aerosols of various sizes and shape. Factors affecting the background are local weather, local and distance (up wind) land use (such as agricultural activity, urban areas, desert, etc.), various human activities, time of year, time of day, and many others (many not well understood). Figure 3 is an example of the seasonal variation of Pollen, which is one class of the Bioaerosols that exist in the atmosphere. The point of this chart is to show that different species have different cycle and peak

at different time of the year. It is important to remember that figure 3 represents monthly averages of many years. Obviously within this averages the concentration can vary from year to year and from day to day or minute by minute.

Figure 4 shows an example of the diversity of Bioaerosols that can be found in nature. The top half of figure 4 is an example of the diversity of Bioaerosols sizes. These can range from sub- μm to several tens μm in diameter. The bottom half of figure 4 shows different common type of fungi. Figure 5 is an example how the concentration of Bioaerosols can vary within a short (2 minutes) period of time.

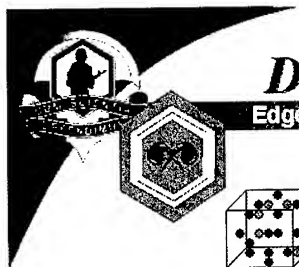
Figure 6 is represents an example of aerosol particles ($> 2\mu m$) concentration over a nine days period. As can be seen, aerosol concentration varies from few $\frac{\text{Particles}}{\text{liter}}$ to $10^4 \frac{\text{Particles}}{\text{liter}}$. Particles concentration can vary wildly over a very short period of time. Particles concentration exhibits a diurnal cycle of a sort. However deviation from the cycle are common. All concentration data have 1 minute Time Weighted Average (TWA). At any given time particle concentration can vary over a relatively short distances as can be seen in figure 7 which shows the time history and variability of particles concentration collected simultaneously with 10 sensor in an area of 600*300 meters.

Attempts to "smooth" the data by averaging the data over increasing periods prove to be unsuccessful as can be seen in figures 8-10. With a 9 days average some smoothing occurs (which for some reason break down in the second half of the day). However the day to day variability (as represented by the standard deviation) is significant.

CONCLUSIONS AND RECOMMENDATIONS:

The background atmosphere in which BW detectors have to operate contains Biological and non-Biological particles. These particles are highly variable in space and time. The behavior of the background aerosols and the factors (man made and natural) that contribute to them are not well understood. The BW detectors can, and usually do interact with these particles. In many cases the required sensitivity of the detectors fall within the background level and variability of the background.

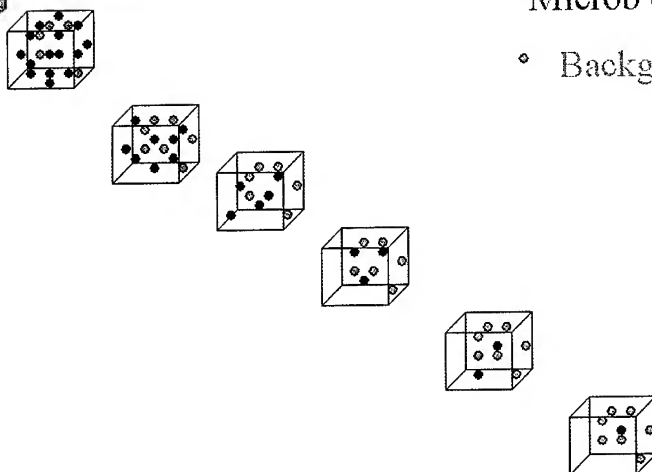
We recommend that developmental BW detectors be tested in a real world environment early in their development cycle. Different technologies need to be evaluated simultaneously to determine if and how they synergize each other by fusing their data. This will provide means to down select a suit of detectors that are most reliable. As technology change new detectors can be added to the mix. A cost benefit analysis can determine which of the new technologies should be perused.



Detection Problem and the Background

Edgewood Chemical Biological Center

- Microb of interest
- Background particle



3

UNCLASSIFIED

Figure 1

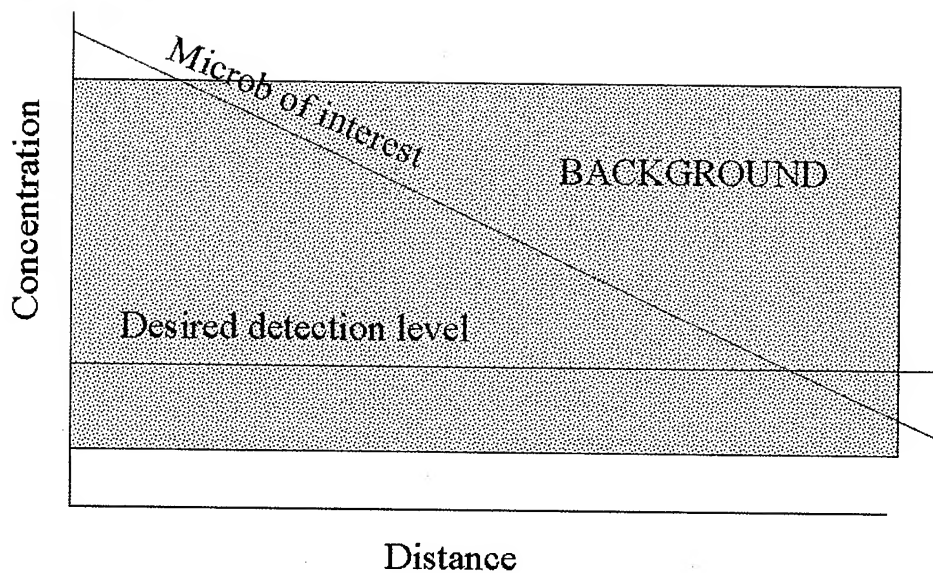
Conceptual description of the problem of BW detection in the real world



Detection Problem and the Background

Edgewood Chemical Biological Center

UNCLASSIFIED



4

UNCLASSIFIED

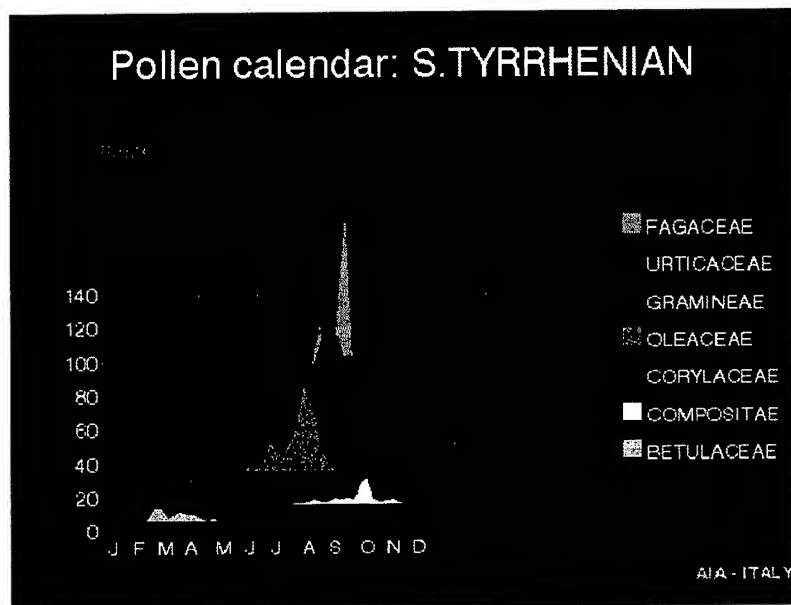
Figure 2
Required detection level and the background

UNCLASSIFIED



Typical Annual Distribution of Pollen

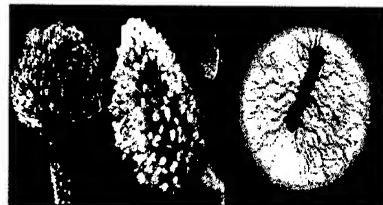
Edgewood Chemical Biological Center



5

UNCLASSIFIED

Figure 3
An example of seasonal variation of Pollen



Different particles size and shape



Agroclype



Didymella



Cladosporium



Stemphylium

Different Fungi Particles

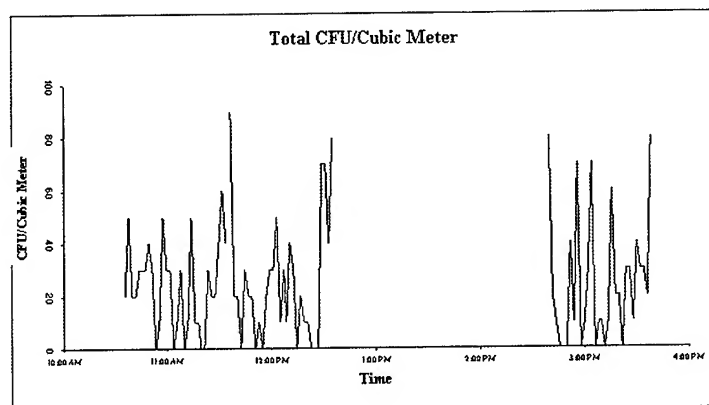
Figure 4
An example of different Bioaerosols found in the atmosphere



Bacteria variability with time

UNCLASSIFIED

Edgewood Chemical and Biological Center



6

UNCLASSIFIED

Figure 5
Short term variability of aerosols of Biological Nature

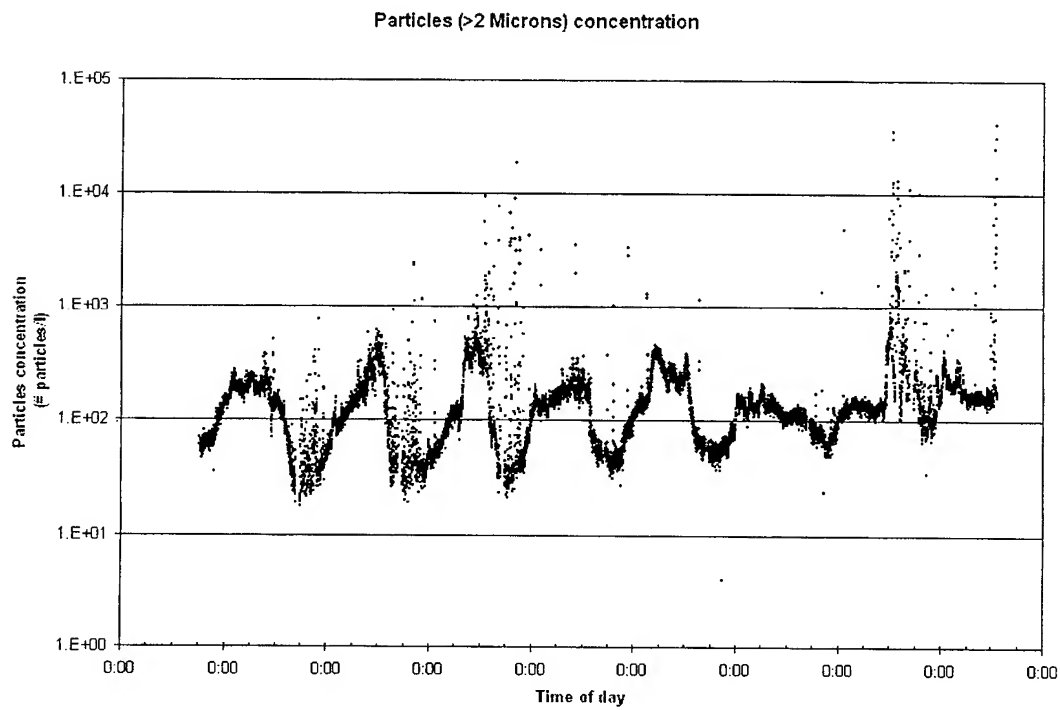


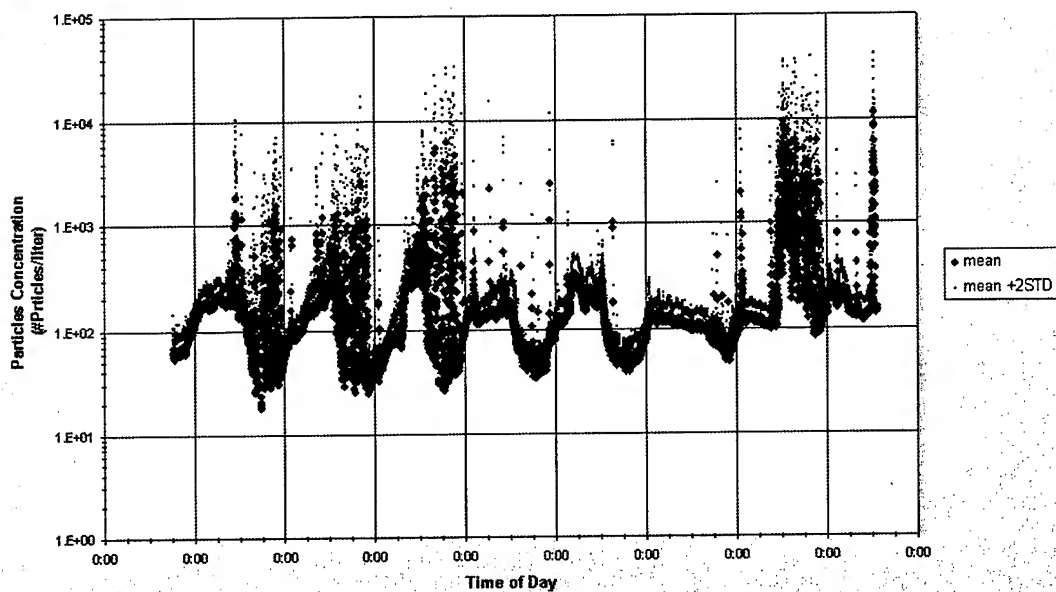
Figure 6
An example of variability of aerosols' concentration with time

UNCLASSIFIED



Edgewood Chemical Biological Center

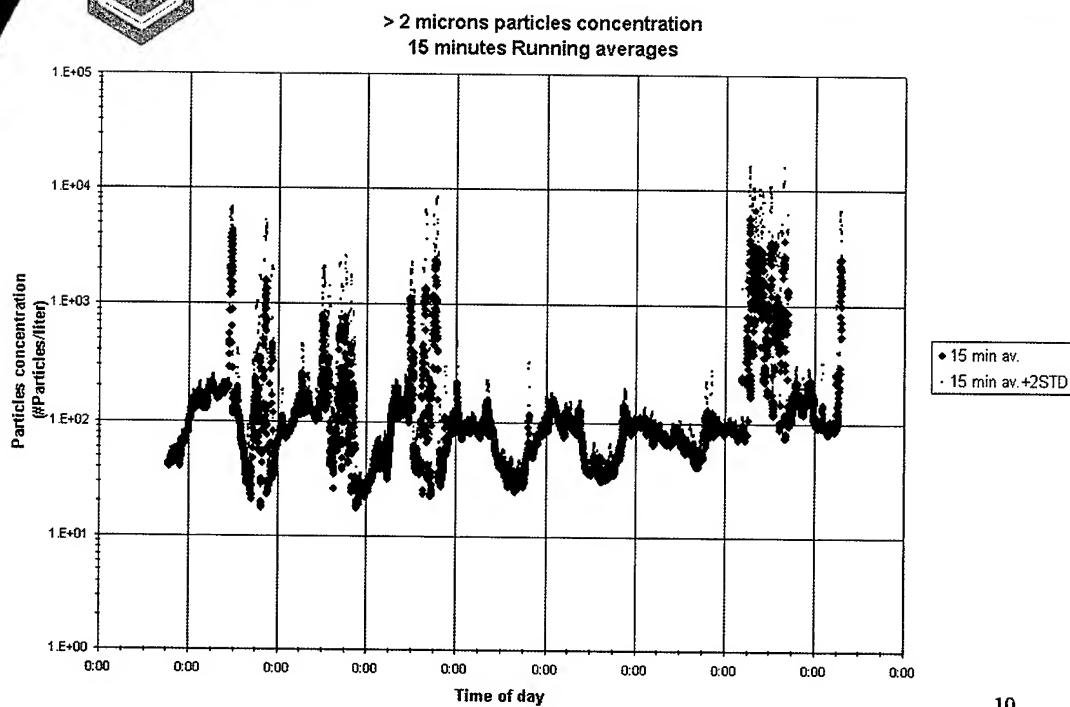
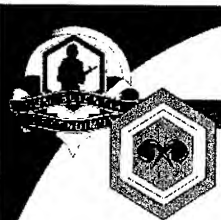
Spatial distribution of
aerosol particles > 2 microns.
1 min. TWA, 10 sensors, 600X300 meters area



8

UNCLASSIFIED

Figure 7
Spatial distribution of aerosol particles ($> 2\mu\text{m}$)

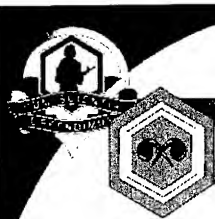


10

UNCLASSIFIED

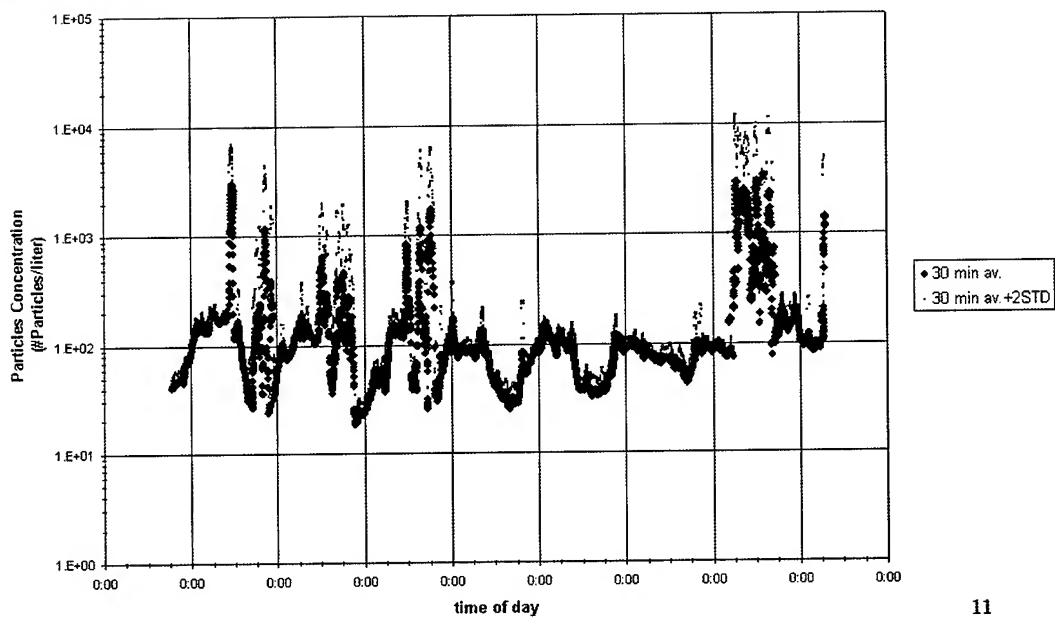
Figure 8
15 minutes running averages

UNCLASSIFIED



Edgewood Chemical & Biological Center

> 2 microns particles concentration
30 minutes Running averages



11

UNCLASSIFIED

Figure 9
30 minutes running averages

UNCLASSIFIED

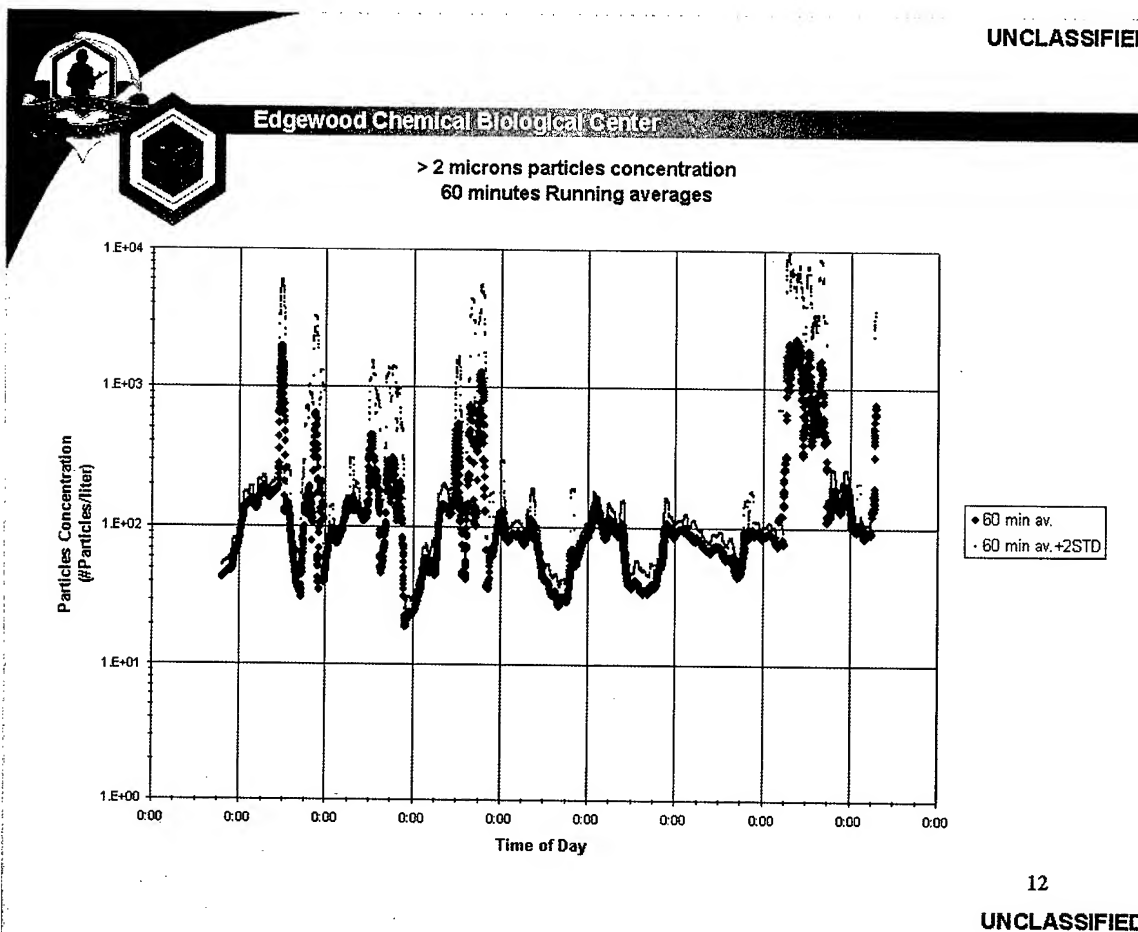


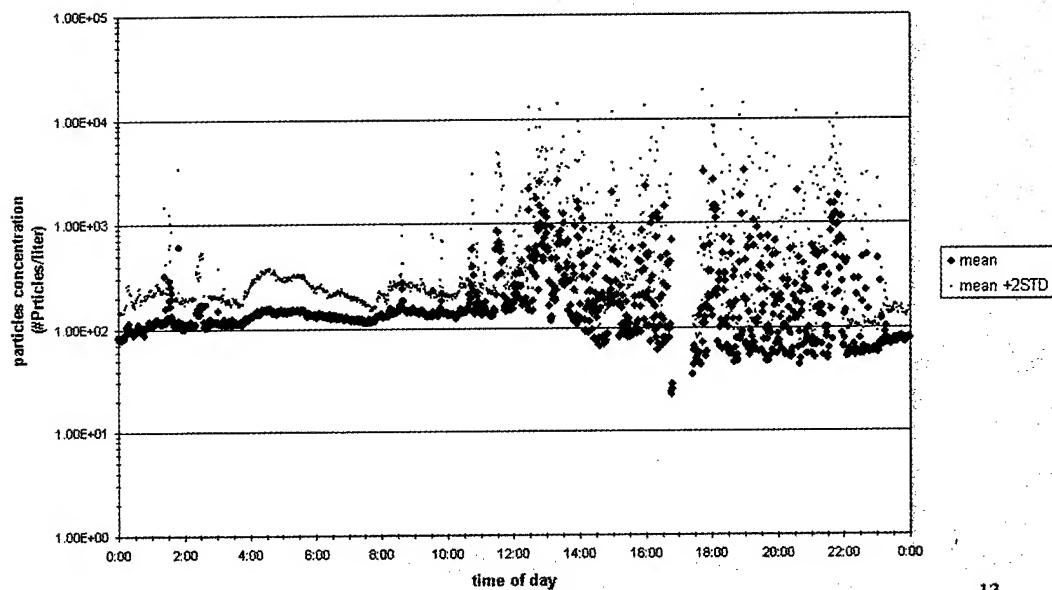
Figure 10
60 minutes running averages

UNCLASSIFIED



Edgewood Chemical Biological Center

Particles > 2 microns
Diurnal Cycle
average of 9 days



13

UNCLASSIFIED

Figure 11
9 days averages

CHEMICAL AND BIOLOGICAL AGENT POINT DETECTOR DATA ACQUISITION USING THE ENVIRONMENTAL SYSTEMS MANAGEMENT ANALYSIS AND REPORTING NETWORK

Anthony Gattuso and Roger Schlicht
General Atomics
San Diego, CA 92121

Joel Roark and Bob Hilley
Nomadics, Inc.
Stillwater, OK 74076

John D. Mills
Env. Mgmt. Office
Tinker AFB, OK 73110

Bruce J. Nielsen and Dennis Bernia
Air Force Research Lab.
Tyndall AFB, FL 32403

Point detection provides useful data at one location and at one time. If networked with other data sources over time, point detection data can be more powerful and provide area-wide information. The Air Force has been developing a network to automatically detect, monitor, and respond to environmental hazards. Known as the Environmental Systems Management, Analysis and Reporting neTwork (E-SMART[®]), the prototype system has been installed at Tinker AFB, Oklahoma. This paper describes the current program that will survey and integrate off-the-shelf, developmental, and former Soviet Union sensors and assess the E-SMART system applicability to chemical and biological agent detection and warning.

INTRODUCTION

Chemical and biological threats to our society are becoming more common and are the focus of US government initiatives for development of warning and protection systems. Conventional monitoring systems suffer from limited expandability and vendor-specific communications protocols that can lead to incompatibilities in hardware, software, and data format when equipment is supplied from more than one vendor. Research is being conducted in the US and other countries to advance sensor technology for detection of chemical and biological materials applicable to acts of terrorism or warfare. Many of these sensors and systems have specific application requirements or possess unique features that limit their use or deployment. The US and our allies need systems that can be rapidly deployed and are flexible to accommodate a wide range of sensor technologies.

The goal of the Environmental Systems Management, Analysis and Reporting neTwork program is to eliminate sensor incompatibilities by defining an open standard for constructing modular monitoring networks.[1] The Air Force Research Laboratory, Air Expeditionary Forces Technologies Division (AFRL/MLQ) has been developing capabilities to automatically detect, monitor, and respond to the presence of hazardous materials in the environment. The Energy Control and Monitoring System used by civil engineering to monitor and control installation-wide HVAC systems, and concepts for the cancelled "Fixed Site Detection Warning System" solicitation out of Wright-Patterson AFB (~1989), helped lead to the E-SMART concept. The E-SMART system serves as a network that connects multiple sensors, actuators, and other input and output devices deployed over a wide area to provide comprehensive,

accurate, and timely information to support analytical models and decision-making. E-SMART uses open software architecture, providing a non-proprietary protocol for development and integration of commercial off-the-shelf sensors, as well as unique sensors developed for specific applications. The system is designed for continuous, autonomous operation with central reporting and manual intervention as needed. The E-SMART concept was developed by General Atomics for the Air Force under a Broad Agency Announcement (1991) with funding from Armstrong Laboratory, Tyndall AFB (now AFRL/MLQ).

Development of E-SMART for dual-use applications continued under a White-House sponsored DARPA Technology Reinvestment Project (TRP) funded jointly by DARPA and a General Atomics-led team in a cost-sharing arrangement (\$5.4M, 1995). This contract was managed by the Department of Energy (DoE) Idaho with technical oversight by DOE/EM. Under the DARPA TRP, General Atomics and its partners developed and demonstrated a prototype E-SMART network at Tinker AFB, Oklahoma to further the readiness of E-SMART components for full-scale deployment. The project further developed and advanced the E-SMART standardized network protocol to include new sensors, sampling systems, and graphical user interfaces.

In the 1998 Defense Appropriation, Congress provided \$4 million to enhance the demonstration E-SMART system at Tinker AFB. E-SMART technology was extended to atmospheric and other environmental compliance monitoring, and to industrial process control for pollution prevention. The system at Tinker AFB is incorporating more than one hundred sensors collecting subsurface and other environmental data from around the base. This system integrates oxygen, hydrocarbon, barometric pressure, water level and pH sensors taking measurements at 15 minute intervals to provide a near real time assessment of the status of environmental conditions at Tinker AFB.

The Air Force Research Laboratory has conducted research and development (R&D) for a number of sensor technologies for detection and monitoring of chemicals in the environment that are similar to chemical/biological warfare agents. AFRL/MLQ is continuing to fill the E-SMART toolbox through the Small Business Innovation Research (SBIR) program. "Development and Integration of Micro-Electro-Mechanical Systems (MEMS) Based Sensor Technologies with E-SMART" led to two Phase I projects that integrated a suite of E-SMART compatible water quality sensors. The current Phase II follow-on project will use microfluidics and a MEMS-based spectrometer for analysis of a wide variety of analytes including agent simulants. Two other Phase I projects for "Perchlorate Sensing Technology," also developed E-SMART compatible systems. E-SMART promises to integrate advancements in sensor technology with proven communication, electronic control, and analysis technology to produce a reliable, versatile, intelligent, cost-effective, warning and response system.

In the fiscal year 2000 Defense Appropriation, Congress provided \$4M to continue development of the E-SMART system. Under the direction of AFRL/MLQ, the team of Tinker AFB Environmental Management Office, General Atomics (GA), Nomadics, Inc., Oklahoma State University College of Veterinary Medicine (OSU/CVM) and Department of Microbiology, University of New Mexico/New Mexico Engineering Research Institute (UNM/NMERI), and Auburn University Institute for Biological Detection Systems will survey the availability of off-the-shelf, developmental, and former Soviet Union (FSU) chemical/biological sensors, identify those capable of integration with E-SMART, integrate sensors, and demonstrate the capability.

The E-SMART Chemical and Biological Agent Detection Network program will lead to a basic deployed warning and response system. The purpose of this effort is to develop technology for improved force protection at fixed and forward military installations through sensing, and active and passive protection. This concept will be demonstrated by connecting an initial suite of existing and emerging chemical and biological sensors to the E-SMART system located at Tinker AFB. Sensors will be searched for and selected from present military and commercial-off-the-shelf (COTS) sources, emerging sensors from Department of Defense development programs, and from sensor technologies developed in the former Soviet Union. A matrix will be developed to down-select the most likely candidates for integration into the E-SMART system. Guidance will be provided by a diverse steering group established

for that purpose. Final sensor selection will be based on customer needs. Presently available COTS sensors will be directly integrated into the system. Promising sensors in development in the US or FSU will be taken to the deployable prototype stage for integration into the system. New sensor research will not be initiated. Laboratory tests will be conducted at licensed test cells prior to deployment at Tinker AFB for system validation.

E-SMART technologies were developed for environmental applications. This program will leverage past work to address applications to counter-proliferation of chemical and biological weapons. This program is accessing sensor technology from the FSU, possibly preventing chemical/biological weapons proliferation, i.e.: recruitment of FSU scientists by terrorist states. The FSU chemical and biological weapon's programs required sensor and monitoring technologies to be used in production of agents. It is the policy of the United States to assist the FSU in defense conversion where possible. Preliminary discussions at General Atomics with Russian scientists indicate technological opportunities in the FSU can be transferred to the E-SMART system.

THREAT

Threats emerging from the proliferation of nuclear, biological, and chemical (NBC) weapons have become one of today's foremost security challenges. Chemical and biological (CB) weapons are not limited to use as weapons of warfare among military forces. CB agents are accessible to and have been used by individuals and groups. This is the result of increasing availability of weapons of mass destruction (WMD) information technology to a wide range of possible adversaries of the United States. Current detection technologies are deficient and inadequate, particularly in the case of biological weapons (BW). Protection against accidents and threats from chemical and biological weapons unleashed by terrorists on civilian populations or in warfare may be enhanced by application of advances in chemistry, physics, modern molecular biology, genetic engineering and electrical engineering, and communications technologies.

The interrelationship between doctrine, requirements, and materiel development is critical and forms the baseline for all detection and identification warning network systems. The central thrust of the US doctrine is deterrence. This means being prepared and in possession of such capabilities that it offers no advantage to anyone to use such weapons against us. This is difficult without retaliatory capability and it places highly critical importance on a strong and impenetrable defense.

At the tactical level this same doctrine is overarching, but uses contamination avoidance as a major doctrinal concept. To avoid contamination, commanders must be provided with a network of systems that not only detects contamination, but also identifies the specific type of contamination. Critical, and implied in this doctrine, is the importance of knowing where contamination is not present, thus providing the commander with the freedom to choose where decisive, tactical, and strategic events can be planned. Equally critical, in the event contamination cannot be avoided, is the availability of protection and decontamination capabilities. The importance of rapidly and reliably connecting these matrices of systems into a coherent, automated reporting and analysis process is paramount if our leadership is to be provided with the tools to be informed and knowledgeable.

Dozens of NBC detection, identification, and warning systems exist. More are in various stages of development. Some systems depend on point source detection and identification, while others are configured to provide standoff detection. These systems involve Joint Programs, as well as Service-specific programs. The existing systems also involve numerous technologies, ranging from very sophisticated mass spectrometers, to computer-chip-embedded antibodies, to color-coded contact paper. A fully integrated network sensor and analysis system that extends across logistical and tactical operations within and between Services is needed. A system that provides a reliable flow of nuclear, biological, and chemical threat information to the appropriate commander in a near-real-time manner as input into the tactical and strategic decision process is critical. This system must be a smart network system that automatically channels threat information to the right people at the right time in a cost-effective manner if we are to reduce the threat to our national security.

SOLUTION

The need for integrated systems that will provide near-real-time information as to the presence of environmental concerns is more critical today than ever before. Not only are the harmful effects of these environmental materials dangerous to the health and welfare of our citizens, but the potential destruction and damage from either terrorist or military use of chemical and biological weapons systems against citizens and/or military forces could substantially impact our national security. The need for reliable and early warning, detection, and identification of these lethal substances is key to avoiding the potential effects of these weapons. A need exists today to develop large scale, distributed systems for warning, response, and protection against terrorist acts using CB materials and weapons. The E-SMART concept offers a platform where integration of currently available sensor technology, or adaptation of emerging sensor and enabling technologies, can be demonstrated to satisfy this need. Therefore, the objective of this program is to demonstrate the usefulness of the E-SMART technology for CB agent detection using mature technology, and to provide a technical transition path for new, advanced sensor technology for the future. The scope of the program involves a comprehensive effort to identify and deploy COTS technologies and/or to adapt, validate and optimize the performance of emerging sensor technologies and to demonstrate their applicability through laboratory and field demonstrations. This will be accomplished by integrating a suite of existing and emerging chemical and biological sensors to E-SMART.

The E-SMART program provides a novel approach to develop and demonstrate both valid and cost-effective technologies that can serve in the dual-purpose mode of airbase defense and homeland defense roles for advanced detection and warning of use of chemical and biological weapons of mass destruction. The USAF, in conjunction with General Atomics, has developed and demonstrated the E-SMART system as part of its on-going efforts to ensure successful environmental remediation of historically contaminated sites. The E-SMART system serves as a network that connects multiple sensors and other input devices (e.g., meteorological station) deployed over a wide area to provide a comprehensive, accurate, and easy-to-use system to support decision models. The goal of E-SMART is to eliminate vendor-specific incompatibilities by defining an open standard for a modular monitoring and reporting network.

The E-SMART concept of large distributed networks of "plug-and-play" sensors lends itself to integration of CB sensors for warning and protection systems. However, current CB sensor technologies are inherently bulky, complex, relatively slow, and require numerous proprietary standards and protocols for their operation. Additionally, major technical challenges exist in the areas of sample collection, detection, and identification, agent discrimination, interferents (i.e., false positive and negative alarms), size/weight and power consumption, and development of a remote/early warning sensing system.

Recent technological advances promise to address these challenges and will ultimately result in cost effective systems for wide-scale application. Miniaturization of chemical, biochemical and physical processes and their integration onto a single microchip (e.g. "lab-on-a-chip") will provide "microfactories" that, within minutes, can diagnose infectious agents or diseases by separation and detection of bacteria, toxins or viruses in blood or other samples. This technology will be particularly valuable for monitoring and warning systems. Thus, in systems that previously were limited to one or a few sensors, emerging technologies make it possible to conceive of millions of sensors integrated into systems to improve their performance, increase their lifetime, make them more flexible in use, and decrease their life cycle costs.

A primary objective of this program is to expand the suite of sensors for the E-SMART system to include devices for the detection of chemical and biological warfare agents. This program involves investigation into the state of the art in CB detection technology with applicability to the E-SMART network protocol. Technology development will focus on affordable, reliable, and supportable sensors that are capable of rapid CB agent identification within required detection sensitivity. The program will initially focus on commercial off-the-shelf devices compatible with the E-SMART concept. These systems will most likely be available from DoD inventory and will demonstrate the efficacy and system functionality as a distributed network of CB detection devices. Another objective of this program is to seek pertinent CB technology, where applicable, from the FSU. The technology of interest will be

emerging technology that has near-term application as a deployable system or is complementary to existing systems available in the United States. Development of emerging technology by Russian research and development organizations will be pursued, where applicable. The E-SMART team will direct such development and will conduct subsequent testing and validation at certified US facilities prior to integration into E-SMART.

The purpose of this program is to integrate emerging chemical and biological sensors developed in the US and in the FSU with the E-SMART system, and to demonstrate a fully integrated warning and response system for chemical and biological weapons. The program will provide a warning and response system to protect individuals, property and the environment from the threats of accidental or terrorist releases of chemical and biological agents. Specifically, the objective is to create an E-SMART Chemical and Biological Detection Network that evolves from an existing E-SMART system. E-SMART is a data acquisition system that uses "smart sensors" to detect and monitor chemical, biological, and physical parameters in a multitude of locations and media. A fundamental objective of this continuing program is to deploy (ready for field demonstration) state-of-the-art or emerging ("breakthrough") sensor technologies that will allow rapid identification of chemical and/or biological threat agents. E-SMART will monitor information from all detectors deployed in a network, collect data from these detectors and other sources of status information, and transmit via a communication system to command and control center(s). At the center(s), the data will be processed and displayed in a useable form to assist in making operational decisions.

The program will make use of the E-SMART Base-wide Demonstration System at Tinker Air Force Base in Oklahoma City for field validation testing of deployed sensor systems. Use of this system will leverage the investment in E-SMART technology already made by the Air Force. E-SMART allows integration of commercial off-the-shelf hardware into a single sensor management system. E-SMART is intended to be an open standard, available to any equipment manufacturer. The user is provided a standard network architecture on which a site-specific monitoring plan can be implemented using sensors and actuators from various manufacturers, and upgraded, as new monitoring devices become available.

SYSTEM ARCHITECTURE

E-SMART integrates diverse monitoring and control technologies by means of a modular, "building block" design approach to allow for flexible system configuration. The E-SMART network treats each smart device—whether a sensor, sampler, or actuator—as a black box that obeys the standard communication protocols and electrical interfaces for the network. Printers for personal computers provide an analogy for this type of interoperability; compatible printers are available from various manufacturers, allowing the user to select the printer best suited for their needs without requiring complex programming and network modifications. This approach allows multiple vendors to produce different sensors which meet the same functional specification and which can be interchanged on the network without impacting operation. Likewise, government or industry will be able to procure E-SMART compatible devices for a particular monitoring network based on a functional specification without fear of incompatibility between devices obtained from multiple vendors.

Each E-SMART sensor or actuator contains its own microprocessor "brain" which provides it with a means of storing calibration, control, status, and quality assurance data. This "brain" communicates using the network protocol, manages data and controls operation of smart device. Since the sensor manufacturer embeds the sensor specific information within the smart device, the E-SMART user is not required to develop calibration or control programs for specific sensors. The "brain" E-SMART devices make use of is the LONTalk™ communication protocol and "chip" developed by Echelon Corporation. LONTalk supports the widely used seven-layer Open Systems Interconnection (OSI) model for network communications. LONTalk is a sophisticated networking protocol that supports routers, gateways, bridges, and multiple communication media such as fiber optic, twisted pair, and radio frequency (RF). The use of this communication protocol by E-SMART allows the use of hundreds of smart sensors or actuators within a single monitoring network.

Once intelligence is distributed to sensors via microprocessors, sensors become able to not only sense environmental data, but to also perform "smart" functions. "Smart" functions include activities such as (1) self-calibration and calibration checking, (2) communication in a standardized protocol to other sensors on the monitoring network, (3) onboard data logging and data storage, and (4) plug-and-play installation.

The operator interface to an E-SMART network is provided by a personal computer running the appropriate E-SMART software. The computer communicates with the sensors on a network to collect and archive their data, and to provide straightforward, graphically based man-machine interaction via a graphical user interface (GUI). It can also aid the E-SMART operator with expert system and analytical software to enhance system operation and to support on-site decision-making. The computer system may be located remotely from the sensors that it controls. Data acquisition and sensor control capabilities may be provided by means of web-based internet access as well. The E-SMART System at Tinker AFB will consist of 8 nodes at deployment sites (see Fig. 1) and one node at Oklahoma State University integrated into one E-SMART network by means of radio frequency and Ethernet communication links.

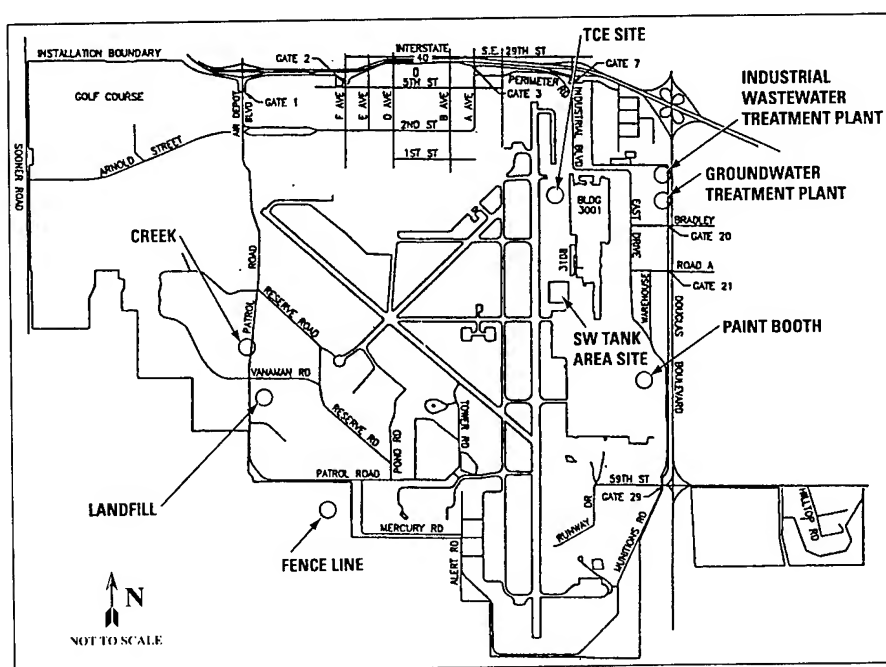


Figure 1. - E-SMART Deployment Sites at Tinker AFB.

Communication between E-SMART devices and the E-SMART computer system depends on the transmission of data "packets" constructed using the LONTalk protocol. Each data packet is constructed from a series of bytes (a byte consists of a string of eight binary digits, e.g. 01110010). LONTalk data packets contain address information, commands and data. Direct communication between E-SMART devices using the LONTalk Protocol (Echelon FTT-10 Transceiver) can occur via copper wires, radio frequency communication (49 MHz and 900 MHz), powerline transceivers, or fiber-optic transceivers. In addition, the existing base Ethernet network is utilized to link several of the E-SMART installation sites together. In this case, the LONTalk data packets are encapsulated within Ethernet data packets and sent from one E-SMART site to another by means of LONTalk to Ethernet Gateways. All of the communication equipment is based on commercially available technology.

Figure 2 illustrates the E-SMART Network Architecture for the project. As seen in the figure, the Southwest Tank Area (SWTA), the Groundwater Treatment Plants (GWTP 1 and 2), the Paint Shop, and the Industrial Waste Treatment Plant (IWTP) are linked via the existing Base Ethernet system. This

system facilitates high-speed communication across the base. Three of the selected sites (South Boundary, Stream Site, and the Landfill Site) are linked to the SWTA via Ethernet to GWTP2 and then via 900 MHz spread-spectrum radio relay. The 900 MHz radio relay system utilizes an existing wind-power generation tower. The tower will provide direct line of site for the radio transceivers to the Landfill, Stream, and the South Boundary Sites. The distance from the tower to the South Boundary Site is approximately one half mile. The 900 MHz radio modems should be able to communicate up to several miles apart. However, the actual performance of the units may be degraded by electromagnetic interference from base operations, weather conditions or other factors to be determined during the demonstration.

Forty-nine MHz transceivers are used to provide short-range (100-200 feet) links between individual sensors at the three RF-linked sites. The 49 MHz transceivers cost less and consume less power than the 900 MHz transceivers. Since all of the individual sensors at these sites are solar-powered, it is highly desirable to utilize low power components to conserve energy.

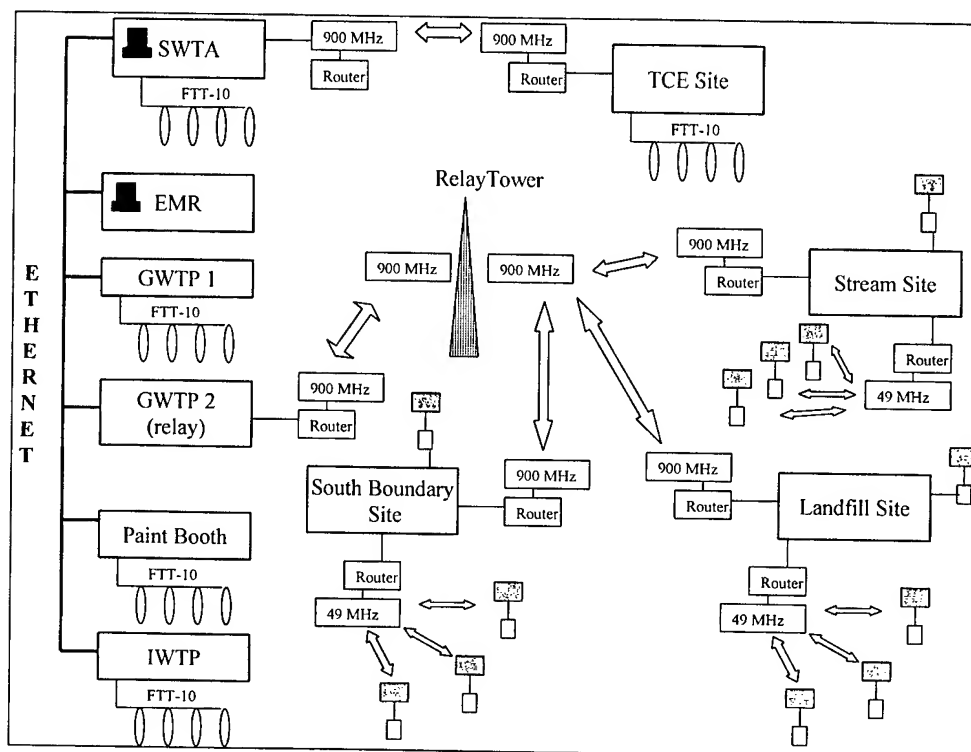


Figure 2. E-SMART System Network Architecture
(note that FTT-10 is a hardwired segment of the network).

APPROACH

Using the combined expertise of the team members, the E-SMART team will select and provide a suite of chemical and biological agent detectors and integrate them into the presently operating on-line network at Tinker AFB. The selection process will include a review of presently available and emerging technologies and sensors, including concentrators and species identification elements. The selected candidates will be laboratory-tested and configured for on-line utilization. Final development of some candidates may be required, however sensor research is not the thrust of this program. Those that are successfully tested will be integrated into the E-SMART network, field-tested, deployed and operated at Tinker AFB.

The E-SMART team will conduct both open and restricted literature search for relevant sensor and/or sensor systems technology that can be adapted or integrated into the E-SMART network technology for the detection of chemical and biological agents. A fundamental objective throughout the program will be integration of existing military sensors, commercial off-the-shelf sensors, sensors emerging from ongoing DoD funded research and development programs, with a special focus on sensor technologies available from the FSU. The E-SMART team, with the assistance of the USAF program managers, will secure and review current intelligence documents that are prepared by or for DoD, are tailored to the threat, and are essential for developing and updating requirements for chemical and biological defense programs.

The E-SMART team will update and review promising commercial or "pre-commercial" sensor technology from the private sector and from U.S. government-funded sensor programs. These will include four key Defense Advanced Research Projects Agency (DARPA) programs: Tissue-Based Biosensors Program, Microfluidic Molecular Systems Program, Pathogen Genome Sequencing Program, and the Protection Program. Several projects and technologies that will be investigated are shared by the U.S. Department of Energy and DARPA. Recent medical chemical defense R&D accomplishments, especially in advanced medical diagnostics, will be reviewed. Examples of potential government-funded systems include the Biological Aerosol Warning System (BAWS) tier I and III instruments and Joint Chemical Agent Detector (JCAD). Once selected, GA and Nomadics will integrate the COTS devices. These two organizations have prior experience with integrating off-the-shelf devices to E-SMART.

Team members will conduct laboratory validation tests of applicable sensor technology using simulants and/or live agents to demonstrate the capability and performance aspects of the sensor device(s) for which they are responsible. The validation tests will be conducted and evaluated in accordance with approved validation test plans. It is likely that preliminary testing and evaluation of sensors will be done using simulants of agents. The simulants are molecules whose structure and/or characteristics are similar to those of the agents themselves. Some are non-(or less) toxic than the agents themselves. Simulants are typically molecules that are either precursors of the agents or hydrolysis products of the breakdown of the agents. For example, exposure of personnel to agents is commonly determined by testing for the hydrolysis chemical products in urine or blood/plasma samples. Simulants of the organophosphates include methylphosphonic acid (MPA), dimethyl methylphosphonate (DMMP), and di-isopropyl methylphosphonate. Thiodiethanol (dithioglycol) is used as a simulant for the sulfur mustard agents. An additional simulant used for nerve gas is the insecticide Malathion and its more toxic cousin (close to that of Sarin/Tabun), Parathion.

The E-SMART team's academic partners, the Oklahoma State University, Auburn University (Institute for Biological Detection Systems), and NMERI will direct the development within the FSU or US communities and will validate the operation of the devices in laboratory tests. Device validation is expected to include limited testing with simulants or possibly with live agents at certified facilities. Our OSU team member has special laboratory facilities for conducting laboratory testing of devices against selected CB agents. OSU has two laboratories specifically designed for use of toxic organophosphate nerve agents. Nerve gas agent simulants are presently used in these laboratories. OSU also has several biological safety level three (BSL3) laboratories required for experimentation with the BW agents *Bacillus anthracis*, *Brucella* spp., and *Francisella tularensis*. OSU possesses several strains of these agents for use in laboratory validation of sensors for these BW agents.

Liquid solutions of the simulants can be made in the laboratory. Standardization of the solution is essential to adequately assess sensor performance. The difficulty and uncertainty of measurement increases as the concentration of the sample decreases. This can be somewhat overcome by initially generating a relatively concentrated solution, assay it via the desired methods, and then have an aliquot of the sample analyzed. Less concentrated solutions can be made by accurate dilution of this stock solution to the ppb range. Further dilutions of the stock solution can yield solutions to provide concentrations in the ppt range. Accurate dilution of the standardized solutions will provide adequately low concentration samples for testing.

The standardization and use of vapor or aerosol samples is more difficult. An integral part of this will be the commercial determination of a gas sample for reference that can be used with other technologies for comparison, just as with the dilution protocol of the liquid samples. The concentration of a vapor such as MPA or DMMP can also be determined from its vapor pressure, atmospheric pressure, temperature, etc., via chemical calculation using Raoult's and Henry's Laws. This will provide the mole fraction of the gas above a binary mixture such as an organic and water. Once the composition/mole fraction of the vapor above a solution is known, then this solution can be used as a standard gas mixture. Lower concentrations can be obtained by dilution of the binary liquid solution or by dilution of the gas mix with nitrogen or argon, just as a liquid solution is diluted with solvent. Dilution of a gas can be performed using a sealed vesicle of known volume filled with N₂ at atmospheric pressure, removing a fixed volume of the N₂ via syringe and then replacing that volume with the sample whose concentration is known. The dilution factor is the ratio of total volume/replaced volume.

As an example, an organophosphate nerve gas agent sensor candidate could be tested in the laboratory setting using two organophosphorus (OP) anticholinesterase simulants. The simulants have many characteristics similar to OP nerve agents such as Sarin. In addition, negative controls can be included in each test to evaluate sensor discrimination. Negative controls are selected depending on the particular type of sensor, e.g., sensors based on acetylcholinesterase inhibition use pseudocholinesterase-inhibiting OP agents. Laboratory testing is done by evaluating the sensitivity of the sensors at detecting OP simulants in aqueous solution. Because OPs are more sensitive to hydrolysis under alkaline conditions, concentrations of each simulant in orders of magnitude from 10⁻¹⁵ to 10⁻⁶ are prepared daily just before assay in buffers at two different pH values (pH 5 and pH 7). Each sensor is exposed to simulant or negative control for a range of times (0, 5, 15, 30, 60 and 120 seconds) and detection/discrimination evaluated.

Following are examples of laboratory testing of sensors for the biological species. Spores of *Bacillus anthracis* can be used to test the limits of sensitivity of the sensor. Known concentrations of *B. anthracis* spores are applied either in liquid for a liquid detector or via a nebulizer within a confined system for an airflow detector. Spore concentrations can be determined by colony forming unit (CFU) counts using the Miles-Misra technique on blood agar plates. A field strain and the Sterne strain can be used in separate assays. Spores of two closely related bacteria can be used to determine the specificity of the probe; known concentration of *Bacillus cereus* and *Bacillus mycoides* spores can also be tested in a manner analogous to that of *B. anthracis* spores. A similar method to that used for *B. anthracis* can be used to test the limits of sensitivity for *Francisella tularensis*. Live vegetative cells rather than spore suspensions are used, and blood glucose cysteine agar plates for growth of *Francisella* strains are used instead of blood agar plates. The same methods can be used to test the limits of sensitivity for *Brucella abortus*, *Brucella melitensis*, and/or *Brucella suis*.

Once the limits of sensitivity are determined for a sensor using pure cultures, additional testing can be done to determine the limits with mixed cultures. For each respective sensor, the selected agent in known concentrations is mixed with two additional species of bacteria, one related and one unrelated, in known concentrations and the limits of sensitivity determined.

Devices proven to be effective from validation tests will then be integrated into E-SMART. GA will perform this work at their development site in San Diego with subsequent field validation tests performed at Tinker AFB. Field validation may be accomplished using approved simulants, simulated signal conditioning and reporting to the E-SMART network, or through the node established at the OSU-certified facilities. Our academic team members will play a lead role in defining both laboratory and field validation test protocols and procedures. GA and Nomadics will perform the field validation work with some limited support from the remaining team members.

The major technical challenges are in the areas of biological collection, detection, and identification, including remote/early warning sensing, improved agent discrimination and quantification, sample processing, interferent (i.e., false positive and negative alarms) and ambient biological background rejection, and genetic probe development. Size, weight, and power reduction of detectors; power

generation and consumption; development of integrated biological and chemical detection systems; and the fusion of sensor data with mapping, imagery, and other data for near real-time display of events are other areas of challenge. Development efforts seek to optimize and balance system sensitivity, size/weight, cost, and power consumption, signature and false alarm rate.

The E-SMART team will conduct sensor development of emerging technologies from the US and FSU. This development is intended to take promising sensor technologies from bench-top or laboratory development to deployable prototypes that can be integrated with the E-SMART network. In partnership with the International Science and Technology Center (ISTC) in Moscow, General Atomics proposes to expand the project team by funding Partner Projects with organizations in states of the Former Soviet Union (FSU) that demonstrate advanced capability, experience, and off-the-shelf or emerging technology for near-term detection of chemical and/or biological threat agents. For Russian-based efforts, GA proposes using ISTC as the clearinghouse for technology development. GA will negotiate subcontracts with specific Russian organizations using ISTC support for the distribution of RFP solicitations.

In Phase I of the program the team will evaluate currently available and emerging sensor technology and determine the feasibility of integration with E-SMART. General Atomics will utilize its contacts in Russia for applicable Russian technology. General Atomics has worked with the ISTC to identify former Russian weapons scientists and technology for the purpose of transitioning these resources to peaceful applications and businesses in Russia or the U.S. General Atomics staff in coordination with NMERI, OSU and AU will evaluate applicable Russian technology in addition to technology available within the U.S. From these evaluations, a set of commercially available sensor devices and emerging sensor technology will be down-selected and recommended for integration and/or development for E-SMART. A system requirement specification will be written based on the results of the technology evaluation, customer requirement for the system deployment, and customer response to technology recommendations. A design report will be written to conclude Phase I.

The Phase II effort will focus on integration of commercially available sensors, emerging sensor technology development, and laboratory testing and validation. General Atomics will be the primary integrator of commercial devices, although industrial partners may in some cases provide engineering support to integrate their own devices. Active agent and simulant compound tests will be conducted as part of the Phase II activities. U.S. academic institutions will play a key role in the validation testing of all devices including Russian-supplied devices during this phase. OSU-CVM is internationally known for excellence in research of infectious diseases, particularly bacterial zoonotic diseases. Zoonotic bacterial diseases are those that infect both man and animals, among which are anthrax, brucellosis, and tularemia, bacterial diseases of particular concern as biological warfare agents.

Field validation tests will be conducted in Phase III of the program. An E-SMART demonstration system at Tinker AFB will be used for this purpose. Availability of the Tinker system reduces the cost of field validation of the chem/bio devices and enables longer-term reliability testing. Documentation of the field validation activity and a comprehensive final report will be written to conclude Phase III and the program.

E-SMART promises to integrate advancements in sensor technology with proven communication, electronic control, and analysis technology to produce a reliable, versatile, intelligent, cost-effective, environmental monitoring and control system. E-SMART is a "core technology" for sensor development bringing together many technologies that reduce the data acquisition and analysis burden, providing knowledge through modeling and graphical display, and empowerment to control operations.

CONCLUSIONS

This technical program is accelerating the state-of-the-art technologies that improve force protection and response. The use of a standard approach to network communications and data management for environmental sensors will permit the exchange of data and operating commands between sensors,

actuators, and control computer systems. Furthermore, a standard promotes the use of modular hardware and software components, and allows equipment from different manufacturers to be interconnected on a single monitoring network. The effort will demonstrate the efficacy of the E-SMART system as a deployable CB agent detection network capable of providing timely and accurate detection, modeling, and warning of attack.

REFERENCES

1. E-SMART Node Specification: Preliminary Release, General Atomics, May 1996.
2. "Final Report for E-SMART Prototype Environmental Monitoring System at Tinker Air Force Base", 31 Jul 97, Contract F34601-95-D-0374, Delivery Order 014, SOW EMR-96-001, Dynamics Research Corporation.
3. "E-SMART Basewide Demonstration At Tinker Air Force Base; Sensor Survey Report", General Atomics, January 1999, Document #GA-C23044, prepared under Contract GS06T98BNC0981 for Department of the Air Force Oklahoma City Air Logistics Center Environmental Management Directorate and General Services Administration.

First Joint Conference on Point Detection for Chemical & Biological Defense
Participants List

- A -

Mr. Philippe Adam
C.E.B.
B.P. 3
Vert le Petit, F-97710 France
Tel: +33 1 69 90 84 78
Fax: + 33 1 64 93 52 66

Mr. Wolf P. Altman
Battelle
505 King Avenue
Columbus, OH 43201
Tel: 614/424-4342
Fax: 614/424-4185
E-mail: altman@battelle.org

Dr. George P. Anderson
Naval Research Laboratory
Center for Bio/Molecular Science and Engineering
Washington, DC 20375-5348
Tel: 202/404-6033
Fax: 202/404-8897
E-mail: ganderson@cbmse.nrl.navy.mil

Dr. Joanne D. Andreadis
Naval Research Laboratory
Code 6910
4555 Overlook Ave, SW
Washington, DC 20375
Tel: 202/404-6046
Fax: 202/767-9594
E-mail: jxa@ccsalph4.nrl.navy.mil

COL Edwin A. Armitage
U.S. Army Medical Resch & Materiel Cmd
ATTN: MCMR-PLD
504 Scott Street
Fort Detrick, MD 21702-5012
Tel: 301/619-6936
E-mail: edwin.armitage@det.amedd.army.mil

Mr. Robert L. Armstrong
LASYS, Inc
821 Canterbury Arc
Las Cruces, NM 88005
Tel: 505-646-4308
Fax: 505-646-1034
E-mail: roarmstr@nmsu.edu

CPT Mohammad K. Asif
U.S. Air Force Research Lab
ATTN: AMSSB-RRT
5183 Blackhawk Road
Aberdeen Proving Ground, MD 21010-5424
Tel: 410/436-4348
Fax: 410/436-1912
E-mail: mohammad.asif.sbcom.apgea.army.mil

- B -

Mr. George Balunis
DTRA
8725 John J. Kingman Rd., MS 6201
Ft. Belvoir, VA 22060-6201
Tel: 703/767-5727
Fax: 703/767-5735

Mrs. Pamela B. Barrett
U.S. Army ECBC
ATTN: AMSSB-REN / E3549
5183 Blackhawk Road
Aberdeen Proving Ground, MD 21010-5424
Tel: 410/436-5875
Fax: 410/436-2991
E-mail: pamela.barrett@sbcom.apgea.army.mil

Mr. Jerry M. Bazzetta
U.S. Army Chemical School
401 Engineer Loop - Suite 1029
Fort Leonard Wood, MO 65473-8926
Tel: 573/596-0131x37673
Fax: 573/563-8063

Dr. James Bechtel
IPITEK
2330 Faraday Ave
Carlsbad, CA 92008
Tel: 760-438-1010
Fax: 760/438-2412
E-mail: jbechtel@ipitek.com

Dr. Andrew Bell
DERA
Chemical & Biological Defence Sector
Porton Down, SP4 0JQ UNITED KINGDOM
E-mail: AJBELL@dera.gov.uk

Mr. Cleve Benton
Naval Surface Warfare Center
300 Hwy 361
Crane, IN 47522
Tel: 812/854-5683
Fax: 812/854-5828
E-mail: benton-w@crane.navy.mil

Mr. Patrick L. Berry
U.S. Army ECBC
ATTN: AMSSB-ENE
5183 Blackhawk Road
APG, MD 21010-5424
Tel: 410/671-5541

Dr. Amnon Birenzvig
U.S. Army ECBC
ATTN: AMSSB-AST
5183 Blackhawk Road
APG, MD 21010-5424
Tel: 410/671-8431
E-mail: amnon.birenzvig@sbcom.apgea.army.mil

Mr. Neil Bloomfield
Graseby Dynamics
10640 Main Street, Suite 204
Fairfax, VA 22030
Tel: 703 218-0380
Fax: 703 926-1572
E-mail: nbcoom@gradyn.com

Mr. Gary Bodily
Mission Research Corporation
1780 North Research Parkway
Logan, UT 84341-1941
Tel: 435/753-8565x107or8422
Fax: 435/753-7462
E-mail: bodily@mrclogan.com

Mr. Brandon Boeglin
Naval Surface Warfare Center
300 Hwy 361
Crane, IN 47522
Tel: 812/854-1912
Fax: 812/854-5828
E-mail: boeglin-b@crane.navy.mil

Dr. Sal Bosco
Defense Threat Reduction Agency - Chem Bio
MS 6201, DTRA CB
8725 John Kingman Road
Ft. Belvoir, VA 22060-6201
Tel: 703/767-5818
Fax: 703/767-5735
E-mail: sal.bosco-contractor@DTRA.MIL

Mr. Jerold R. Bottiger
US Army ECBC
5183 Blackhawk Road
Aberdeen Proving Ground, MD 21010-5424
Tel: 410/436-1705
Fax: 410/436-2742
E-mail: jrbottig@sbccom.apgea.army.mil

Dr. B. Gerard Bricks
BSM, Inc.
32 Elmwood Drive
Kennett Square, PA 19348
Tel: 610/388-2411
Fax: 610/388-0309
E-mail: bgm1ksq@aol.com

Dr. John Brokenshire
Graseby Dynamics
10640 Main Street, Suite 204
Fairfax, VA 22030
Tel: 703 218-0380
Fax: 703 926-1572
E-mail: nbcoom@gradyn.com

Dr. Burt V. Bronk
U.S. Airforce Research Lab
ATTN: AMSSB-RRT-AL
Building E5951/17
5183 Blackhawk Road
Aberdeen Proving Ground, MD 21010-5424
Tel: 410/436-1813
Fax: 410/436-2742
E-mail: bvbbronk@sbccom.apgea.army.mil

Mrs. Marguerite Brooks
DTRA/SRF
6801 Telegraph Road
Alexandria, VA 22310-3398
Tel: 703-325-4226
Fax: 703-325-4329

Ms. Stacey M. Broomall
Science and Technology Corp.
500 Edgewood Road, Suite 205
Edgewood, MD 21040
Tel: 410/436-5719
Fax: 410/436-5807
E-mail: stacey.broomall@c-mail.apgea.army.mil

Mr. Tom Brown
Environmental Technologies Group, Inc.
1400 Taylor Ave.
Baltimore, MD 21234
Tel: 410 321-5200
Fax: 410 339-3175
E-mail: tbrown@envtech.com

Dr. Wayne A. Bryden
Applied Physics Laboratory
The Johns Hopkins University
11100 Johns Hopkins Road
Laurel, MD 20723-6099
Tel: 240/228-6210
Fax: 240/228-6904
E-mail: wayne.bryden@jhuapl.edu

Dr. Stephen Buchsbaum
DARPA SPO
3701 N. Fairfax Drive
Arlington, VA 22203
Tel: 703-812-1973
Fax: 703-516-7360
E-mail: sbuchsbaum@darpa.mil

Mr. Brett A. Burdick
Virginia Dept. of Emergency Management
10501 Trade Ct.
Richmond, VA 23236
Tel: 804/897-6500 x6569
Fax: 804/897-6576
E-mail: bburdick@vden.state.va.us

Dr. Larry W. Burggraf
Air Force Institute of Technology AFIT/ENP
Bldg. 640, 2950 P Street
Wright Patterson AFB, OH 45433-7765
Tel: 937/255-3636
Fax: 937/255-2921
E-mail: Larry.Burggraf@afit.af.mil

- C -

Dr. Jon J. Calomiris
U.S. Air Force Research Lab
ATTN: AMSSB-AL / E3549
U.S. Army SBCCOM
5183 Blackhawk Road
Aberdeen Proving Ground, MD 21010-5424
Tel: 410/436-5797
Fax: 410/436-5807
E-mail: jon.calomiris@sbccom.apgea.army.mil

Mr. Timothy W. Caraher
Scentzar Corp.
213 Taylor Street
Fredericksburg, VA 22405
Tel: 804/338-6264
Fax: 540/372-7576
E-mail: scentzar1@aol.com

Mr. Scott Carey
Naval Surface Warfare Center
ATTN: Code B53
17320 Dahlgren Road
Dahlgren, VA 22448
Tel: 540/653-8199
Fax: 540/653-8223
E-mail: careysa@nswc.navy.mil

Dr. John P. Carrico
SRI International
1611 N. Kent Street
Arlington, VA 22209
Tel: 703/247-8562
Fax: 703/247-8537
E-mail: carrico@wdc.sri.com

Dr. Gary W. Carriveau
SAIC
16701 West Bernardo Drive
San Diego, CA 92127
Tel: 858-826-9948
Fax: 858-826-9718
E-mail: gary.w.carriveau@saic.com

Mr. Tom Carter
SAIC
1227 S. Patrick Drive
Suite 110
Satellite Beach, FL 32937
Tel: 321-779-6024
Fax: 321-779-8715
E-mail: nancy.l.frey@saic.com

Mr. M.J. Castle
DERA (MOD)
CBD Porton Down
CB Systems, Bldg. 06b
Salisbury, Wilts. SP4 0JQ UNITED KINGDOM
Tel: 441980613271
Fax: 441980613769
E-mail: mcastle@dera.gov.uk

Ms. Elizabeth S. Catalano
U.S. Army SBCCOM
OPM for NBC Defense Systems
5183 Blackhawk Road
Building E3549
Aberdeen Proving Ground, MD 21010-5424
Tel: 410-436-5597
Fax: 410-436-6526
E-mail: elizabeth.catalano@SBCCOM.APGEA.ARMY.MIL

Mr. Michael V. Catalano
Program Manager for Chemical Demilitariz
ATTN: SFAE-CD-CE-S/M
5183 Blackhawk Road
Building E4586
Aberdeen Proving Ground, MD 21010-5424
Tel: 410-436-1460
Fax: 410-436-1111
E-mail: michael.catala@SBCCOM.APGEA.ARMY.MIL

Mr. Don Ceckowski
ITT Aerospace
Communications Division
P.O. Box 3700
Fort Wayne, IN 46801
Tel: 219/451-6010
Fax: 219/451-6033

Mr. David P. Charbonneau
General Dynamics Information System
8800 Queen Ave South
Bloomington, MN 55431
Tel: 952/921-6323
Fax: 952/921-6552
E-mail: david.p.charbonneau@gd-is.com

Dr. Jack Cheng
Booz Allen & Hamilton
4001 N. Fairfax Drive
Suite 750
Arlington, VA 22203
Tel: 703/465-5744
Fax: 703/525-3754
E-mail: cheng-jack@bah.com

Dr. Steven D. Christesen
U.S. Army SBCCOM
ATTN: AMSSB-RRT-DL, Building E5951
5183 Blackhawk Road
Aberdeen Proving Ground, MD 21010-5424
Tel: 410-436-1828
Fax: 410-436-2742
E-mail: steven.christesen@sbccom.apgea.army.mil

Dr. Han Chuang
Echo Technologies, Inc
451 D. Street
Boston, MA 02210
Tel: 617-443-0066
Fax: 617-204-3080
E-mail: hchuang@echotech.net

Dr. Russell Chung
Naval Research Laboratory
Code 6375
Washington, DC 20375
Tel: 202-404-1964
Fax: 202-767-5301
E-mail: rchung@ccf.nrl.navy.mil

Prof. James M. Clark
DERA, CBD
Detection, Building 6
DERA CBD Porton Down
Salisbury SP4 0JQ, UNITED KINGDOM
Tel: 44980613405
Fax: 44980613987
E-mail: jmclark@dera.gov.uk

Ms. Sandy Clark
Naval Surface Warfare Center
300 Hwy 361
Crane, IN 47522
Tel: 812/854-4050
Fax: 812/854-5828
E-mail: clark-s@crane.navy.mil

Dr. Cyril R. Clarke
Oklahoma State University
264 McElroy Hall
Stillwater, OK 74078
Tel: 405/744-8093
Fax: 405/744-8263
E-mail: clarke@okstate.edu

Dr. Jean Clarke
Nomadics, Inc.
1730 Cimmaron Plaza
Stillwater, OK 74075
Tel: 405 372-9535
Fax: 405 372-9537
E-mail: jclarke@nomadics.com

LTC David W. Coker
West Desert Test Center - Dugway Proving Ground
ATTN: CSTE-DTC-DP-WD
Dugway, UT 84022-5000
Tel: 435-831-5416
Fax: 435-831-5661
E-mail: decoker@dugway-emh3.army.mil

Mr. Robert V. Collins
Midwest Research Institute
425 Volker Blvd.
Kansas City, KS 64110
Tel: 816/753-7600x1537
Fax: 816/753-5519
E-mail: rvcollins@mrresearch.org

Ms. Stella Colucci
Yamada International Corporation
1235 Jefferson Davis Highway
Suite #708
Arlington, VA 22202
Tel: 703/416-0490
Fax: 703/416-0492
E-mail: scolucci@yamada.com

Dr. David Combest
Naval Special Warfare Development Group
2240 Sandfiddler Road
Virginia Beach, VA 23456
Tel: 757/492-7960x2270
Fax: 757/492-7962
E-mail: dai@nctamlant.navy.mil

Dr. David E. Cooper
SRI International
333 Ravenswood Avenue
Menlo Park, CA 94025-3493
Tel: 650/859-3742
Fax: 650/859-5036
E-mail: david.cooper@sri.com

Mr. Richard Cope
Nomadics, Inc.
1730 Cimarron Plaza
Stillwater, OK 74075
Tel: 405/372-9535
Fax: 405/372-9537
E-mail: rcope@nomadics.com

Dr. Joseph Corriveau
OSD/AT&L
DATSD (CBD)
3050 Defense Pentagon
Room 3C257
Washington, DC 20301-3050
Tel: 703-695-5486
Fax: 703-695-0476
E-mail: corrivjl@acq.osd.mil

Ms. Susan R. Coyne
US Army Medical Research Institute of Infectious Diseases
Diagnostics Systems Division
1425 Porter Street
Ft. Detrick, MD 21702-5011
Tel: 301-619-7193
Fax: 301-619-2492
E-mail: susan.coyne@amedd.army.mil

Mr. Terry R. Creque
Defense Threat Reduction Agency, CB
8725 John J. Kingman Road
MS 6201
Fort Belvoir, VA 22060-6201
Tel: 703/326-8764
Fax: 703/767-5735
E-mail: terry.creque@dtra.mil

Mr. Norbert J. Crookston
DSIC
4301 North Fairfax Drive
Arlington, VA 22203
Tel: 703/847-9368
Fax: 703/522-3888
E-mail: ncrook7821@aol.com

- D -

Prof. Christopher John Davis
Veridian Systems
1400 Key Boulevard
Suite 100
Arlington, VA 22209-2369
Tel: 703/516-6384
Fax: 703/524-2420
E-mail: cjdavis@psrw.com

MSgt Daniel L. Davis
U.S. Airforce Research Lab
ATTN: AMSSB-RRT
E3332
5183 Blackhawk Road
Aberdeen Proving Ground, MD 21010-5424
Tel: 410/436-3995
Fax: 410/436-2447
E-mail: Daniel.davis@sbccom.apgca.army.mil

Dr. Dennis M. Davis
U.S. Army ECBC
ATTN: AMSSB-RRT-DD
E3220/129
5183 Blackhawk Road
Aberdeen Proving Ground, MD 51010-5424

Mr. Paul D. Davis
Dugway Proving Ground
West Desert Test Center
ATTN: STEDP-WD-C-C
Dugway, UT 84074
Tel: 435/831-5407
Fax: 435/831-5432
E-mail: pdavis@dugway-emh3.army.mil

Mr. Peter J. Day
Graseby Dynamics
10640 Main Street
Suite 204
Fairfax, VA 22030
Tel: 703 218-0380
Fax: 703 926-1572
E-mail: nbcoom@gradyn.com

Mr. Mike Deckert
SBCCOM/PM-JBPDS
ATTN: SFAE-BD, E4470
Aberdeen Proving Ground, MD 21010
Tel: 410/436-7730
Fax: 410/436-4434
E-mail: michael.dekkert@sbccom.apgea.army.mil

Dr. Adarsh Deepak
Science and Technology Corp.
10 Basil Sawyer Drive
Hampton, VA 23666-1393
Tel: 757/766-5800
Fax: 757/865-1294
E-mail: a.deepak@stcnet.com

Dr. Richard DeFreez
Pacific Scientific Instruments
Photonics R&D
481 California Avenue
Grants Pass, OR 97526
Tel: 541-472-6630
Fax: 541-479-3057
E-mail: rick.defreez@pacsciinst.com

Mr. Paul DeLuca
US Army, ECBC
Bldg. E5951, AMSSB-RRT-TA
5183 Blackhawk Road
APG, MD 21010-2742
Tel: 410/436-7297
Fax: 410/436-2742
E-mail: paul.deluca@sbccom.apgea.army.mil

Dr. William A. Dement
U.S. Army Dugway Proving Ground
ATTN: CSTE-DTC-DP-TD
Office of the Technical Director
Dugway, UT 84022-5000
Tel: 435 831-5187
Fax: 435 831-3713
E-mail: dp-td@dugway-emh3.army.mil

Dr. Dominique Despeyroux
DERA
CBD Porton Down
Salisbury, Wilts., SP4 0JQ UNITED KINGDOM
Tel: 44-1980-613486
Fax: 44-1980-613987
E-mail: dddespeyroux@dera.gov.uk

Dr. Larry Deuser
BAE Systems
6500 Tracor Lane
Mail Drop 27-21
Austin, TX 78725
Tel: 512-929-2047
Fax: 512-929-4774
E-mail: larry.deuser@baesystems.com

Dr. John D. Ditmars
Argonne National Laboratory
EAD-900
9700 S. Cass Avenue
Argonne, IL 60439
Tel: 630/252-5953
Fax: 630/252-4611
E-mail: jditmars@anl.gov

Mr. Robert Doherty
U.S. Army ECBC
ATTN: AMSSB-RRT-TA
5183 Blackhawk Road
Aberdeen Proving Ground, MD 51010-5424
Tel: 410/436-1759
Fax: 410/436-7297
E-mail: paul.deluca@SBCCOM.APGEA.ARMY.MIL

Dr. Terry Donaldson
Oak Ridge National Laboratory
P.O. Box 2008
MS 6226
Oak Ridge, TN 37831-6226
Tel: 865-576-4853
Fax: 865-574-6442
E-mail: donaldsontl@ornl.gov

Mr. Alan Dorney
USARL - HRED
ATTN: AMSRL - HR - MM
Aberdeen Proving Ground, MD 21005-5425
Tel: 410/278-5933
Fax: 410/278-5933
E-mail: adorney@arl.mil

Dr. Joel Dubow
University of Utah
Dept. of Materials Science
1400 E 200 S
Salt Lake City, UT 84112
Tel: 801/581-8388
E-mail: Joel.Dubow@mc.utah.edu

Dr. H. Dupont Durst
ECBC
Aberdeen Proving Ground, MD 21010
Tel: 410-436-7291
Fax: 410-436-7317
E-mail: dupont.durst@sbccom.apgea.army.mil

- E -

Dr. Maria L. Embrey
Central MASINT Organization
3100 Clarendon Blvd.
Suite 300
Arlington, VA 22201
Tel: 703-907-0122
Fax: 703-907-0797
E-mail: afemmbmt@dia.osis.gov

Mr. Merlin L. Erickson
PM NBC Defense Systems
5183 Blackhawk Road
Aberdeen Proving Ground, MD 21010-5424
Tel: 410/436-4055
Fax: 410/436-1383
E-mail: mlericks@cbddcom.apgea.army.mil

Dr. Tom Evans
Battelle Dugway Operations
Dugway Proving Ground
P.O. Box 217
Dugway, UT 84022
Tel: 435/831-5528
Fax: 435/831-5922
E-mail: evanst@battelle.org

Dr. Jay D. Eversole
Naval Research Laboratory
Code 5615
4555 Overlook Avenue, S.E.
Washington, DC 20375
Tel: 202/767-9523
Fax: 202/404-8114
E-mail: eversole@nrl.navy.mil

Dr. Kenneth J. Ewing
Battelle Memorial Institute
2012 Tollgate Road
Suite 206
Bel Air, MD 21015
Tel: 410-569-0200
Fax: 410/569-0588
E-mail: ewing@battelle.org

- F -

Dr. Nicholas F. Fell
U.S. Army Research Laboratory
Attn: AMSRL-SE-EO
2800 Powder Mill Road
Adelphi, MD 20783
Tel: 301-394-2569
Fax: 301-394-0310
E-mail: nfell@arl.army.mil

Dr. Michael L. Finson
Physical Sciences Inc.
20 New England Business Center
Andover, MA 01810
Tel: 978 689-0003
Fax: 978 689-3232
E-mail: finson@psicorp.com

Ms. Angel A. Fitzgerald
Naval Surface Warfare Center
Dahlgren Division
17320 Dahlgren Road
Dahlgren, VA 22448-5100
Tel: 540/653-8414

Mr. Robert Fitzgerald
Naval Surface Warfare Center
ATTN: Code B53
17320 Dahlgren Road
Dahlgren, VA 22448
Tel: 540/653-3313
Fax: 540/653-8747
E-mail: fitzgeraldra@nswc.navy.mil

MSG Dennys E. Flores
US Army Special Operations Command
3939 Rosehill Road, Apt. 3216
Fayetteville, NC 28311
Tel: 910-432-1370
Fax: 910-432-5152
E-mail: floresd@soc.mil

Dr. J.L. Fobes
FAA
Naval Postgraduate School
Code AA.JF, Room 137
699 Dyer Road
Monterey, CA 93943
Tel: 831/656-1926
Fax: 831/656-2313
E-mail: jlfobes@nps.navy.mil

Mrs. Virginia Foot
DERA (MOD)
CB Systems, Bldg. 06b, CBD Porton Down
Salisbury, Wilts SP4 0JQ, SP4 0JQ UNITED KINGDOM
Tel: 441980613639
Fax: 441980613987
E-mail: vefoot@dera.gov.uk

Prof. Alvin Fox
University of South Carolina
School of Medicine, Dept. Microbiol. & Immunol.
Columbia, SC 29208
Tel: 803-733-3288
Fax: 803-733-3192
E-mail: afox@dcmsserver.med.sc.edu

Dr. Stephen Francesconi
Nova Research/NRL
4555 Overlook Ave., SW - Code 6115
Washington, DC 20375-5320
Tel: 202/404-1737
Fax: 202/404-8515
E-mail: scf@ccf.nrl.navy.mil

Dr. Gad Frishman
IIBR
P.O. Box 19
NESS-ZIONA, 74100 ISRAEL
Tel: 972 8 9381459

Dr. Julia Fruetel
Sandia National Laboratories
P.O. Box 969
MS 9951
Livermore, CA 94551
Tel: 925/294-2724
Fax: 925/294-3020
E-mail: jfruet@sandia.gov

- G -

Mr. Timothy Gainor
Office of the Special Assistant
for Gulf War Illnesses
5113 Leesburg Pike, Suite 901
Falls Church, VA 22041
Tel: 703/681-3269x137
Fax: 703/681-3321
E-mail: tgainor@gwillness.osd.mil

Dr. Eric Gard
Lawrence Livermore National Lab
5000 East Avenue
Mail Stop L-231
Livermore, CA 94550
Tel: 925/422-0038
Fax: 925/422-3160
E-mail: gard2@llnl.gov

Mr. Tom Gargan
Geo-Centers, Inc.
US Army Center For Environmental Health Research
568 Doughten Drive
Fort Detrick, MD 21702-5010
Tel: 301-619-2338
Fax: 301-619-7654
E-mail: thomas.gargan@amedd.army.mil

Mr. Bill Gates
Naval Surface Warfare Center
300 Hwy 361
Crane, IN 47522
Tel: 812/854-1576
Fax: 812/854-5828
E-mail: gates-bill@crane.navy.mil

Mr. Richard Gaylord
GEOMET Technologies, Inc.
8577 Atlas Drive
Gaithersburg, MD 20877
Tel: 301-417-9605
Fax: 301-990-1925
E-mail: rgaylord@geomet.com

CPT Tammy R. Gibb
USAMRIID
Diagnostic Systems Division
Ft. Detrick, MD 21702
Tel: 301-619-4735
Fax: 301-619-2492
E-mail: Tammy.Gibb@det.amedd.army.mil

Mr. Richard M. Gilligan
Science and Technology Corporation
500 Edgewood Road
Suite 205
Edgewood, MD 21040
Tel: 410/679-1612
Fax: 410-679-0369
E-mail: gilligan@stcnet.com

Mr. Jean-Louis Goasdoue
CEB
B.P. 3
Vert le Petit, 97710 France
Tel: +33 1 69 90 83 57

Mr. Michael T. Goode
U.S. Army, Edgewood Chemical Biological Center
ATTN: AMSSB-RRT-BI
5183 Blackhawk Road
E3549
Aberdeen Proving Ground, MD 21010-5424
Tel: 410 436-5530
Fax: 410 436-5807
E-mail: mtgoode@sbccom.apgea.army.mil

Mr. Norman Green
Science and Technology Corporation
500 Edgewood Road
Suite 205
Edgewood, MD 21040
Tel: 410/436-6625
Fax: 410/436-8363
E-mail: norman.green@sbccom.apgea.army.mil

Dr. Wayne H. Griest
Oak Ridge National Laboratory
P.O. Box 2008
Oak Ridge, TN 37831-6120
Tel: 865-574-4864
Fax: 865-576-7956
E-mail: griestwh@ornl.gov

Dr. Abraham Grossman
InVitro Diagnostics, Inc.
3960 Broadway
Suite 407
New York, NY 10032
Tel: 212-568-0365
Fax: 212-568-0469
E-mail: agrossma@ix.netcom.com

Dr. Yifu Guan
IPITEK
2330 Faraday Avenue
Carlsbad, CA 92008
Tel: 760/438-1010x3326
Fax: 760/438-2412
E-mail: yguan@ipitek.com

- H -

Prof. Emil Halamek
Military University
Department of Chemistry
CZ-682 03 bySkCU, CZECH REPUBLIC
Tel: 420 0507 421 3384
Fax: 420 0507 421 2297
E-mail: halamer@uus-pu.cz

Dr. Charles S. Harden
U.S. Army ECBC
ATTN: AMSSB-RRT-DD
E3220/125
5183 Blackhawk Road
APG, MD 21010-5424
Tel: 410/436-3758
Fax: 410/436-3753
E-mail: csharden@apea.army.mil

Dr. H. James Harmon
Oklahoma State University
306 LSE
Dept. of Physics
Dept. of Micro. & Molecular Genetics
Stillwater, OK 74078
Tel: 405/744-9692
Fax: 405/744-7421
E-mail: jharmon@okstate.edu

Ms. Jeanne Hawtin
SAIC
1309 Continental Drive
Suite F
Abingdon, MD 21009
Tel: 410/436-3303
Fax: 410/436-3054
E-mail: jeanne.p.hawtin@saic.com

Mr. Richmond Henriques
TRW
5111 Leesburg Pike
Suite 200
Falls Church, VA 22041
Tel: 703/681-3279x124
Fax: 703/681-3321

Dr. William Herzog
MIT Lincoln Lab
244 Wood Street
Lexington, MA 02420
Tel: 781-981-2558
Fax: 781 981-0602
E-mail: wherzog@ll.mit.edu

Ms. Linda A. Hightower
Mission Research Corporation
8560 Cinderbed Road, Suite 700
Newington, VA 22122
Tel: 703/339-6500x108
Fax: 703/339-6953
E-mail: lindah@mrcwdc.com

CWO5 Randy C. Himes
MCCDC NBC Requirements
3300 Russell Road
Quantico, VA 22134
Tel: 703-784-6210
Fax: 703-784-2532
E-mail: himesrc@mccdc.usmc.mil

Dr. Mark A. Hollis
MIT Lincoln Laboratory
244 Wood Street, Rm. E-118E
Lexington, MA 02420-9108
Tel: 781-981-7842
Fax: 781-981-3867
E-mail: hollis@ll.met.edu

Dr. Eric Holwitt
AFRL/HEDB (CMI)
2503 Gillingham Drive
Brooks AFB, TX 78235
Tel: 210-536-1192
Fax: 210-536-4716

Mr. James Horton
Horton Consulting
2 Belmont Court
Fredericksburg, VA 22405
Tel: 540/374-8509
Fax: 540/374-0997
E-mail: jbginc@erols.com
Mr. Joseph Houterman
General Dynamics
8800 Queen Ave South
Bloomington, MN 55431

Ms. Patricia Howard
234 S. Fraley Blvd.
Dumfries, VA 22026
Tel: 703 445-1616
Fax: 703 445-8185
E-mail: phowarpm@sverdrup.com

Mr. Alex Hryniewicz
Cdr, SBCCOM
ATTN: AMSSB-RBD-B
Building E3549
5183 Blackhawk Road
APG, MD 21010-5242
Tel: 410-436-5984
Fax: 410-436-3236

CPT Michael Hunter
Combat Developments
U.S. Army Chemical School
32 Williams Street
Ft. Leonard Wood, MO 65473
Tel: 513/596-0131x37103
Fax: 573/563-8000
E-mail: hunterm@wood.army.mil

- J -

Dr. Margo Jackisch
DGI
2034 Eisenhower Ave
Suite 115
Alexandria, VA 22314
Tel: 703/535-8720
Fax: 703/535-8723
E-mail: jackischm@defensegrp.com

Dr. Amanda Jenkins
U.S. Army Research Laboratory
ATTN: AMSRL-WM-MA
Building 4600
Aberdeen Proving Ground, MD 21005
Tel: 410-306-1911
Fax: 410/436-1051
E-mail: ajenkins@arl.army.mil

Ms. Janet L. Jensen
U.S. Army ECBC
ATTN: AMSSB-RRT
Building E5554
5183 Blackhawk Road
APG, MD 21010-5424
Tel: 410/436-5836
Fax: 410/436-1120
E-mail: janet.jensen@sbccom.apgea.army.mil

Dr. Thomas H. Jeys
MIT/Lincoln Laboratory
244 Wood Street
Lexington, MA 02420-9108
Tel: 781/981-0650
Fax: 781/981-0602
E-mail: jeys@ll.mit.edu

Mr. Bruce W. Jezek
SBCCOM
ATTN: AMSSB-BD
Building E4455
5183 Blackhawk Road
APG, MD 21010-5424
Tel: 410/436-2835
Fax: 410/436-4919
E-mail: bwjezek@cbdcom.apgea.army.mil

Mr. Gregory Johnson
Naval Surface Warfare Center
ATTN: Code B53
17320 Dahlgren Road
Dahlgren, VA 22448
Tel: 540-653-3323
Fax: 540-653-8747
E-mail: johnsongp@nswc.navy.mil

Dr. Anna Johnson-Winegar
Office of the Director
Defense Research and Engineering
The Pentagon - Room 3D129
Washington, DC 20301-3080
Tel: 703/693-9410
Fax: 703/697-1797
E-mail: johnoad@acq.osd.mil

Mr. Edward Joiner
INTELLITEC
2000 Brunswick Lane
Deland, FL 32724
Tel: 904 736-1700
Fax: 904 736-2250
E-mail: ejoiner@intellitec.com

Mr. Timothy V. Jones
Naval Surface Warfare Center
Dahlgren Division
16525A Governor Bridge Road, Apt. 308
Bowie, MD 20716
Tel: 540-653-6649
E-mail: jonest@nscw.navy.mil

MSgt William E. Jones
U.S. Marine Corps
NBC Requirements Chief
MCCDC
3300 Russell Road
Quantico, VA 22134
Tel: 703/784-6998
Fax: 703/784-2532
E-mail: joneswe@mccdc.usmc.mil

- K -

Dr. Jiri Kadlcak
Military Technical Institute of Protection
RYBKOVÁ 8
CZ-60200 BRNO, CZECH REPUBLIC
Tel: 420 5 41183086
Fax: 420 5 41182748
E-mail: jiri.kadlcak@telecom.cz

Ms. Kimberley Kalmes
Scentczar Corp.
213 Taylor Street
Fredericksburg, VA 22405-2909
Tel: 804-827-7000 x 461
Fax: 540-694-7409
E-mail: scentczar@excite.com

Mr. Kevin Kearns
U.S. Army ECBC
Attn: AMSSB-RRT-BI
E3549
5183 Blackhawk Road
Aberdeen Proving Ground, MD 21010-5424
Tel: 410/436-5413
Fax: 410/436-5807
E-mail: kevin.kearns@sbccom.apgea.army.mil

Mr. Frank W. Kelly
GEOMET Technologies, Inc.
8577 Atlas Drive
Gaithersburg, MD 20877
Tel: 301-417-9605
Fax: 301-990-1925
E-mail: fkelly@geomet.com

Mr. Jana Kesavan
US ARMY Contractor
ECBC
Aberdeen Proving Ground, MD 21010
Tel: 410-436-1819
E-mail: kesavan@mail.jhmi.edu

Mr. Edward Kessler
Science & Technology Research Inc.
5200 Potomac Drive
King George, VA 22485
Tel: 540-663-9101
Fax: 540-663-4057
E-mail: strdd@crosslink.net

Mr. Fred K. Knauert
USAMRIID
Diagnostics Systems Division
1425 Porter Street
Ft. Detrick, MD 21702-5011

Lt Col Les Koch
Joint Service Integration Group
ATTN: ATSN-CMZ-JS (Lt Col Koch)
401 Engineer Loop
Suite 1309
Ft. Leonard Wood, MO 65473
Tel: 573/596-0131x37754
Fax: 573/596-0131x37757
E-mail: kochl@wood.army.mil

Ms. Carrie Krahn
Environmental Technologies Group, Inc.
1400 Taylor Ave.
Baltimore, MD 21030
Tel: 410-321-5200
Fax: 410-339-3175
E-mail: ckrah@envtech.com

Mr. Stephen J. Krak
Battelle Memorial Institute
505 King Avenue
Columbus, OH 43201
Tel: 614-424-3839
Fax: 614-424-3962
E-mail: krak@battelle.org <mailto:krak@battelle>

Dr. Thaiya Krishnamurthy
U.S. Army ECBC
ATTN: SCBRD-RTE
Building E3835
Aberdeen Proving Ground, MD 21010-5424
Tel: 410-436-5909
Fax: 410-436-6536
E-mail: thaiya.krishnamurthy@sbccom.apgea.army.m

Mr. Dave Kuhlman
Naval Surface Warfare Center
300 Hwy 361
Crane, IN 47522
Tel: 812/854-1251
Fax: 812/854-5828
E-mail: kuhlman-dave@crane.navy.mil

Mr. Gary M. Kwitkoski
Defense Threat Reduction Agency/CB
8725 John J. Kingman Road, MS 6201
Fort Belvoir, VA 22060-6201
Tel: 703 767-5799
Fax: 703 767-5135
E-mail: gary.kwitkoski@dtra.mil

- L -

Mr. Charles E. Laljer
The MITRE Corp.
7323 Hwy 90 West, Suite 402
San Antonio, TX 78227
Tel: 210/675-9640
Fax: 210/675-1941
E-mail: laljer@mitre.org

Mr. Ravi P. Lall
U.S. Army ECBC - R&T Directorate
5183 Blackhawk Road
Aberdeen Proving Ground, MD 21010-5424
Tel: 410/436-8641
Fax: 410/436-3753
E-mail: ravinder.lall@sbccom.apgea.army.mil

Mr. Carlos E. Lama
Naval Surface Warfare Center.
Code B53 - Building 1356
17320 Dahlgren Road
Dahlgren, VA 22448
Tel: 540/663-3306
Fax: 540/653-8747
E-mail: klama@crosslink.net

Dr. Stephen A. Lammert
Oak Ridge National Laboratory
Chemical and Analytical Sciences Division
M/S 6365, Bldg. 5510
P.O. Box 2008
Oak Ridge, TN 37831-6365
Tel: 865-574-4879
Fax: 865-576-8559
E-mail: lammerts@ornl.gov

Ms. Diane LaMoy
Naval Surface Warfare Center
Dahlgren Division - Dept. B53
17320 Dahlgren Road
Dahlgren, VA 22448
Tel: 540/653-3307
Fax: 540/653-8747
E-mail: lamoydm@nswc.navy.mil

LTC Paul L. Langerhans
HQDA, ODCSOPS, DAMO-FDB
Chemical and NBC Defense
6708 Huntsman Blvd.
Springfield, VA 22152
Tel: 703 696-5752
Fax: 703 695-9156
E-mail: paul.langerhans@hqda.army.mil

Dr. Richard G. Langlois
Lawrence Livermore National Laboratory
BBRP, L-452
7000 East Ave
Livermore, CA 94551
Tel: 925-422-5616
Fax: 925-422-2282
E-mail: langlois@llnl.gov

Dr. Michael Languirand
MIT Lincoln Laboratory
244 Wood Street
Lexington, MA 02173-9108
Tel: 781/981-7756
Fax: 781/981-5398
E-mail: mlanguirand@ll.mit.edu

Mr. Alan R. Lee
US Army MANSCEN-DCD/CM DIV
320 Engineer Loop, Suite 141
Fort Leonard Wood, MD 65473-8929
Tel: 573-563-4025
Fax: 573-563-8000

Dr. Stephen J. Lee
U.S. Army Research Laboratory
P.O. Box 12211
Research Triangle Park, NC 27709-2211
Tel: 919/549-4365
Fax: 919/549-4310
E-mail: slee@aro-emhl.army.mil

MAJ John Lemondes
JOP-BD
5201 Leesburg Pike
Skyline #3, Suite 1200
Falls Church, VA 22041-3203
Tel: 703-681-5196
Fax: 703-681-3454
E-mail: lemondessj@jpoibd.osd.mil

Dr. Jay Lewington
Graseby Dynamics, Ltd.
1400 Taylor Ave.
Baltimore, MD 21030
Tel: 410-321-5385
Fax: 410-339-3175
E-mail: jay.lewington@grasebydynamics.com

Mr. John W. Lewis
Naval Surface Warfare Center
ATTN: Code B53
17320 Dahlgren Road
Dahlgren, VA 22448
Tel: 540/653-3658
Fax: 540/653-8223
E-mail: lewisjw@nswc.navy.mil

Mr. Patrick Lewis
Sandia National Laboratories
Microsensor R&D
MS 1425
P.O. Box 5800
Albuquerque, NM 87185-1425
Tel: 505-284-3315
Fax: 505-844-1198
E-mail: prlewis@sandia.gov

Dr. Bruce Lighthart
Microbial Aerosol Research Laboratory
10975 Doll Road
Monmouth, OR 97361
Tel: 503/838-2264
Fax: 503/606-0926
E-mail: lighthab@open.org

Mr. Scott Lilienthal
ITT Industries - AIS
2560 Huntington Ave
Alexandria, VA 22303
Tel: 703/715-4816
Fax: 703/960-7047
E-mail: dawson.cagle@itt.com

Dr. Duane Lindner
Sandia National Laboratories
Adv. Detection Technologies
Dept. 8101, MS 9951
Livermore, CA 94551
Tel: 925-294-3306
Fax: 925-294-3020
E-mail: dllindn@sandia.gov

Ms. Misty H. Lindsey
Science and Technology Corp.
500 Edgewood Road, Suite 205
Edgewood, MD 21040
Tel: 410-436-7752

Mr. Michael Lockhart
Pacific Sierra Research/Veridian
1115 5th Street
Charlottesville, VA 22902
Tel: 804-984-5657 x107
Fax: 804-984-5156
E-mail: mlockhart@psrw.com

Mr. William Loerop
U.S. Army ECBC
ATTN: AMSSB-RTE
5183 Blackhawk Road
APG, MD 21010-5424
Tel: 410/436-1743
Fax: 410-436-1120

Dr. S. Randolph Long
U.S. Army SBCCOM/ECBC
ATTN: AMSSB-RRT
Building E3330
5183 Blackhawk Road
Aberdeen Proving Ground, MD 21010-5424
Tel: 410/436-2262
Fax: 410/436-1912
E-mail: srlong@sbccom.apgea.army.mil

Dr. Richard A. Lorey
Naval Surface Warfare Center
ATTN: Code B50
17320 Dahlgren Road
Dahlgren, VA 22448
Tel: 540/653-8412
Fax: 540/653-8223
E-mail: loreyra@nswc.navy.mil

Mr. George Lozos
Environmental Technologies Group, Inc.
1400 Taylor Ave
Baltimore, MD 21234
Tel: 410/321-5385
Fax: 410 339-3175
E-mail: glozo@envtech.com

Mr. Sam S. Lucas
Graseby Dynamics
1400 Taylor Ave.
Baltimore, MD 21234
Tel: 410-321-5208
Fax: 410-321-5500
E-mail: slucass@aol.com

- M -

Dr. Raymond A. Mackay
U.S. Army ECBC
ATTN: AMSSB-RRT
5183 Blackhawk Road
APG, MD 21010-5424
Tel: 410 436-3250
Fax: 410 436-2649
E-mail: raymond.mackay@sbccom.apgea.army.mil

Dr. Frank Magnotta
Lawrence Livermore National Laboratory
P.O. Box 808
MS L-183
Livermore, CA 94551
Tel: 925/422-7285
Fax: 925/422-2499
E-mail: magnotta1@llnl.gov

Mr. Salvatore Maranto
U.S. Army SBCCOM
ATTN: AMSSB-REN-E.MC
Building E3549
5182 Blackhawk Road
Aberdeen Proving Ground, MD 21010
Tel: 410/436-4173
E-mail: sal.maranto@sbccom.apgea.army.mil

Mr. Charles W. Martin
Ares Corporation
1800 N. Kent Street, Suite 1230
Arlington, VA 22209
Tel: 703/525-0211
Fax: 703/525-1227
E-mail: chuck@arescorp.com

Mr. Francis A. Martin
SAIC
2109 Emmorton Park Road, Suite 121
Edgewood, MD 21040
Tel: 410-671-6772
Fax: 410-671-6720
E-mail: francis.a.martin@saic.com

Dr. Waleed Maswadeh
GEO-Centers, Inc / SBCCOM
Building E3220, Room 118
5183 Blackhawk Road
Aberdeen Proving Ground, MD 21010-5424
Tel: 410-436-2416
Fax: 410-436-3764
E-mail: wmmaswad@sbccom.apgea.army.mil

Mr. John Maxey
USAF/ILEXR
1260 Pentagon
Washington, DC 20330-1260
Tel: 703/604-0769
Fax: 703/604-4050
E-mail: john.maxey@pentagon.af.mil

Dr. Howard T. Mayfield
Air Force Research Laboratory
AEF Technologies Division
139 Barnes Drive, Suite 2
Tyndall AFB, FL 32403
Tel: 850-283-6049
Fax: 850-283-6090
E-mail: Howard.Mayfield@tyndall.af.mil

SSG Jeffrey L. McClendon
203rd MI BN
4727 Deercreek Loop
Aberdeen Proving Ground, MD 21005
Tel: 410-278-2446
E-mail: jmccclendon@bldg4727.apg.army.mil

Dr. Martin McDonnell
DERA
CBD Porton Down
Salisbury, Wilts, SP4 0JQ UK
Tel: 44 1980 613943
Fax: 44 1980 613912
E-mail: mbmcdonnell@dera.gov.uk

Prof. Andrew R. McFarland
Texas A&M University
Department of Mechanical Engineering
College Station, TX 77843
Tel: 979-845-2204
Fax: 979-845-1883
E-mail: arm@tamu.edu

Dr. R. Andrew McGill
NRL
Code 6375
4555 Overlook Avenue, S.W.
Washington, DC 20375
Tel: 202-767-0063
Fax: 202-767-5301
E-mail: amcgill@ccf.nrl.navy.mil

Mr. Vincent M. McHugh
U.S. Army ECBC
ATTN: AMSSB-RRT-DD
E3220/126
5183 Blackhawk Road
Aberdeen Proving Ground, MD 21010-5424

MAJ Christopher C. McLane
AF/ILEXR
1260 Pentagon
Washington, DC 20330-1260
Tel: 703/604-3943
Fax: 703/604-4050
E-mail: christopher.mclane@pentagon.af.mil

Mr. Michael P. McLoughlin
Johns Hopkins Univ. Applied Physics Laboratory
11100 Johns Hopkins Road
Laurel, MD 20723-6099
Tel: 240-228-5631
Fax: 240-228-5026
E-mail: mike.mcloughlin@jhuapl.edu

Mr. Thomas M. McMahon
Veridian
4455 Genesee Street
Buffalo, NY 14225
Tel: 716-631-6905
Fax: 716-631-4183
E-mail: tmcMahon@buffalo.veridian.com

Mr. Allister McNeish
BAE Systems
6500 Tracor Lane
Mail Drop 27-21
Austin, TX 78725
Tel: 512-929-4741
Fax: 512-929-4774
E-mail: allister.mcneish@baesystems.com

Mr. Darrel E. Menking
U.S. Army ECBC
ATTN: AMSSB-RRT-BM
Bldg. E3831
5183 Blackhawk Road
Aberdeen Proving Ground, MD 21010-5424
Tel: 410-436-5914
Fax: 410-436-6536
E-mail: darrel.menking@sbccom.apgea.army.mil

Ms. Deborah L. Menking
U.S. Army ECBC
Biosensors Team
Bldg. E3549
5183 Blackhawk Road
Aberdeen Proving Ground, MD 21010-5424
Tel: 410-436-5514
Fax: 410-436-5807
E-mail: deborah.menking@SBCCOM.APGEA.ARMY.MIL

Ms. Angela G. Mersiwsky
Naval Surface Warfare Center
Dahlgren Division
17320 Dahlgren Road
Dahlgren, VA 22448-5100
Tel: 540/653-3399

Mr. Gordon O. Moe
Veridian - PSR
1400 Key Blvd.
Arlington, VA 22209
Tel: 703/516-6201
Fax: 703/524-2420

Mr. Alan Moore
U.S. Navy
105 Kennedy Street
Alexandria, VA 22305
Tel: 703 /602-8841x402
Fax: 703/602-8393

Dr. Dan Morgan
National Research Council
2101 Constitution Ave., NW
HA 262/NMAB
Washington, DC 20418
Tel: 202/334-3496
Fax: 202/334-3718
E-mail: dmorgan@nas.edu

Mr. Jeff Morgan
SVERDRUP
234 S. Fraley Blvd.
Dumfries, VA 22026
Tel: 703-445-1616 x127
Fax: 703-445-8185
E-mail: morganjj@sverdrup.com

CPT Robert F. Mortlock
Joint Program Office for Biological Defense
5201 Leesburg Pike, Skyline #3 - Suite 1200
Falls Church, VA 2204103203
Tel: 703/681-9678
Fax: 703/681-3454
E-mail: mortlock@jpobd.osd.mil

LTC Timothy Moshier
PM, JBPDS
ATTN: SFAE-BD, Building 4470
Hoadley Road
Aberdeen Proving Ground, MD 21010
Tel: 410-436-7730
Fax: 410-436-4434
E-mail: tfmoshie@sbccom.apgea.army.mil

Ms. Emily D. Myers
Science and Technology Corp.
500 Edgewood Road, Suite 205
Edgewood, MD 21014
Tel: 410/436-5911
Fax: 410/436-5807
E-mail: emily.myers@SBCCOM.APGEA.ARMY.MIL

CPT James W. Myers
Air Force Research Laboratory
AFRL/SNJM
3109 P Street
Wright Patterson Air Force Base, OH 45433
Tel: 937/255-9614x298
Fax: 937/255-6489
E-mail: james.myers@wpafb.af.mil

Dr. Michael L. Myrick
University of South Carolina
Department of Chemistry and Biochemistry
631 Sumter St.
Columbia, SC 29208
Tel: 803/777-6018
Fax: 803/777-9521
E-mail: myrick@psc.sc.edu

- N -

Mr. Viet K. Nguyen
Naval Research Laboratory
Code 6375
Washington, VA 20375
Tel: 202/767-2536
Fax: 202/767-5301
E-mail: kvnguyen@ccf.nrl.navy.mil

Mr. Bruce Nielsen
AFRL/MLQ
Deployed Warning and Response
139 Barnes Dr
Suite 2
MS 37
Tyndall AFB, FL 32403-5323
Tel: 850-283-6227
Fax: 850-283-6064
E-mail: bruce.nielsen@tyndall.af.mil

Col (P) Patricia Nilo
U.S. Army Chemical School
401 Engineer Loop
Suite 1041
Ft Leonard Wood, MO 65473-8926
Tel: 573/563-8053
Fax: 573/563-8093
E-mail: nilop@wood.army.mil

Dr. David A. Norwood, Jr.
USAMRIID
Diagnostic Systems Division
Ft. Detrick, MD 21702
Tel: 301-619-4726
Fax: 301-619-2492
E-mail: David.Norwood@det.amedd.army.mil

Mr. Francis Anthony Nottke
OPTO-Forensic Technologies
1830 East Broadway Blvd., #124-343
Tucson, AZ 85719
Tel: 520-241-5698
E-mail: fanottke@worldnet.att.net

Mr. Daniel M. Nowak
U.S. Army SBCCOM
AMSSB-PM-RNN-A
5183 Blackhawk Road
Aberdeen Proving Ground, MD 51010-5424
Tel: 410-436-5631
Fax: 410-436-6526
E-mail: daniel.nowak@sbccom.apgea.army.mil

- O -

Mr. Kevin P. O'Connell
U.S. Army ECBC
ATTN: AMSSB-RRT-BM
5183 Blackhawk Road
Aberdeen Proving Ground, MD 21010-5424
Tel: 410-436-5999
Fax: 410-436-6536
E-mail: kevin.oconnell@sbccom.apgea.army.mil

Dr. Thomas E. Old
Mission Research Corporation
735 State Street
Santa Barbara, CA 93101
Tel: 805/963-8761 Ex.220
Fax: 805/962-8530
E-mail: old@mrcsb.com

Ms. Lisa D. Olsen
U.S. Geological Survey
Water Resources Division
8987 Yellow Brick Road
Baltimore, MD 21237
Tel: 410-238-4309
Fax: 410-238-4210
E-mail: ldolsen@usgs.gov

Mr. Jack O'Neil
The JGW Group
10640 Main Street, Suite 200
Fairfax, VA 22030
Tel: 703 352-3400
Fax: 703 385-6470
E-mail: awilson@jgwgroup.com

Ms. Kate K. Ong
U.S. Army ECBC
ATTN: AMSSB-RTE
5183 Blackhawk Road
APG, MD 21010-5424
Tel: 410/436-7730
Fax: 410/436-4434
E-mail: kate.ong@sbccom.apgea.army.mil

Dr. Chun-Sing Orr
National Institute for Occupational Safety and Health
1095 Willowdale Road
MS 3030
Morgantown, WV 26505
Tel: 304/285-6098
Fax: 304/285-6041
E-mail: corr8@cdc.gov

Ms. Danielle Ortelli
Center for Naval Analyses
4325 Mark Center Drive
Alexandria, VA 22311
Tel: 703/824-2991
Fax: 703/824-2256
E-mail: ortellid@cna.org

- P -

Mr. Dhirajlal G. Parekh
U.S. Army SBCCOM/ECBC
ATTN: AMSSB-RRT-DD
Bldg E3160
5183 Blackhawk Blvd.
APG, MD 21010-5424
Tel: 410-436-8400
Fax: 410-436-1912

Dr. Jun T. Park
Geo-Centers, Inc.
P.O. Box 68
Aberdeen Proving Ground, MD 21010
Tel: 410/436-5598
Fax: 410/436-6536
E-mail: jun.park@cmailsvr1.apgea.army.mil

Mr. Shawn Park
The Boeing Company
2401 E. Wardlow Road
MC C078-0315
Long Beach, CA 90807-5309
Tel: 562-593-6460
Fax: 562-593-8851
E-mail: shawn.h.park@boeing.com

Mr. Greg Parks
ACI
One International Plaza
Suite 600
Philadelphia, PA 19113
Tel: 610/362-1200x267
Fax: 610/362-1290
E-mail: gparks@aci-corp.org

Mr. Jerry C. Pate
DTRA
Technology and Materiel Division / CB
8725 John J. Kingman Road
MS 6201
Fort Belvoir, VA 22060-6201
Tel: 703/767-4588
Fax: 703/767-5735
E-mail: jerry.pate@dtra.mil

Ms. Dorothea A. Paterno
U.S. Army SBCCOM
ATTN: AMSSB-RTE
5183 Blackhawk Road
APG, MD 21010-5424
Tel: 410/436-4466
Fax: 410/436-1912
E-mail: dorothea.Paterno@sbccom.apgea.army.mil

Mr. Brian L. Patrick
Sverdrup Technologies
234 S. Fraley Blvd.
Suite 204
Dumfries, VA 22026
Tel: 703-445-1616

Ms. L. Michelle Peery
Midwest Research Institute
425 volker Blvd.
Kansas City, MO 64110
Tel: 816/753-7600x1272
Fax: 816/753-5359
E-mail: mpeery@mrresearch.org

Mr. Kirkman R. Phelps
CDR USA SBCCOM
ATTN: AMSSB-RRT E3332
5183 Blackhawk Road
APG, MD 21010-5424
Tel: 410/436-2675
Fax: 410/436-2447
E-mail: krphelps@cbddcom.apgea.army.mil

Mr. Michael Phillips
Orbital Sciences Corporation
2771 North Garey Ave
Pomona, CA 91769
Tel: 909/593-3581
Fax: 909/596-2301
E-mail: phillips.mike@orbital.com

Dr. Richard Pollina
Remote Sensing Lab
Bechtel Nevada MS RSL10
PO Box 98521
Las Vegas, NV 89193-8521
Tel: 702-295-8918
Fax: 702-295-8967
E-mail: pollinrj@nv.doc.gov

Mr. Michael Pompeii
Naval Surface Warfare Center
Dahlgren Division
ATTN: Code B53
Building 1369
17320 Dahlgren Road
Dahlgren, VA 22448-5000
Tel: 540/653-3326
Fax: 540/653-8747
E-mail: mpompeii@nswc.navy.mil

Mr. R. Pope
Booz-Allen & Hamilton Inc.
8283 Greensboro Drive
McLean, VA 22102
Tel: 703/917-2500

Dr. Timothy Postlethwaite
Constellation Technology
7887 Bryan Dairy Road
St. 100
Largo, FL 33777
Tel: 727-547-0600
Fax: 727-545-6150
E-mail: tpost@contech.com

Mr. Ronald Priest
Constellation Technology Corp.
7807 Bryan Dairy Road
Largo, FL 33777

Dr. Charles A. Primmerman
DTRA / ASCO
8725 John J. Kingman Road
MS 6201
Fort Belvoir, VA 22060
Tel: 703/767-5702
Fax: 703/767-5701
E-mail: charles.primmerman@dtra.mil

Dr. Paul Pulaski
University of New Mexico
Center for High Technology Materials
1313 Goddard SE
Albuquerque, NM 87106
Tel: 505-272-7944
Fax: 505-272-7801
E-mail: pulaski@unm.edu

- Q -

Mr. James M. Quarles
Battelle Crystal City
1725 Jefferson Davis Highway
Suite 600
Arlington, VA 22202
Tel: 703/413-7813
Fax: 703/413-8880
E-mail: mquarles@battelle-cc.org

- R -

Dr. Vipin K. Rastogi
GeoCenters, Inc.
Gunpowder Branch
P.O. Box 68
Aberdeen Proving Ground, MD 21010-0068
Tel: 410-436-4856
Fax: 410-436-2081
E-mail: vipin.rastogi@SBCCOM.APGEA.ARMY.MIL

Mr. Richard D. Read
Lockheed Martin
9500 Goodwin Drive
Manassas, VA 20110
Tel: 703/367-1546
Fax: 703/367-3061
E-mail: richard.read@lmco.com

Ms. Jennifer Reasor
Strategic Analysis Inc.
2626 Hillegass Avenue, Suite B
Berkeley, CA 94704
Tel: 703/608-4614
Fax: 510/841-4251
E-mail: jreasor@snap.org

Dr. Nelson W. Rebert
Central MASINT Organization
DIA/CMO 3100 Clarendon Blvd., Suite 300C
Arlington, VA 22201
Tel: 703-907-1592
Fax: 703-907-0797
E-mail: afrebnw@dia.osis.gov

COL Stephen V. Reeves
PM NBC Defense Systems
5183 Blackhawk Road
Aberdeen Proving Ground, MD 51010-5424
Tel: 410/436-2566
Fax: 410/436-1383
E-mail: stephen.reeves@sbccom.apgea.army.mil

Mr. Craig Reichow
HQ USAF/XONP(ANSER)
Suite 800
1215 Jefferson Davis Hwy
Arlington, VA 22202-3251
Tel: 703/416-8463
Fax: 703/416-3474
E-mail: reichowc@anser.org

Dr. I. Gary Resnick
DTRA-CB
8725 John Kingman Road
MS 6201
Ft. Belvoir, MS 22060-6201
Tel: 703 767-5722
Fax: 703-767-5800
E-mail: ruth.williamshunt@dtra.mil

Mr. Joel Roark
Nomadics, Inc.
1730 Cimarron Plaza
Stillwater, OK 74075
Tel: 405/372-9535
Fax: 405/372-9537
E-mail: jroark@nomadics.com

Dr. Hector G. Robert
Quantum Magnetix
7740 Kenamar Ct.
San Diego, CA 92122
Tel: 858-566-9200
Fax: 858-566-9388
E-mail: hrobert@qm.com

Dr. Joseph E. Roehl
Scentczar Corporation
213 Taylor Street
Fredericksburg, VA 22405-2909
Tel: 540/372-2004
E-mail: scentczar@aol.com

Ms. Toni Roehl
Scentczar Corp.
213 Taylor Street
Fredericksburg, VA 22405
Tel: 540/372-2004
Fax: 540/372-7576
E-mail: scentczar@aol.com

LT Jennifer Taylor Roever
Air Force Research Laboratory / SNJM
3109 P Street
Wright Patterson AFB, OH 45433
Tel: 937/255-9614
Fax: 937/255-6489
E-mail: jennifer.taylor@wpafb.af.mil

Dr. James E. Rogers
U.S. Army SBCCOM
Edgewood Chemical Biological Forensics Center
E3150
Aberdeen Proving Ground, MD 21010
Tel: 410/436-8990
Fax: 410/436-2081
E-mail: jerogers@sbccom.apgea.army.mil

Cpt. Doron Ronen
Israel MOD/NBC Protection Division
Hakiry Tel-Aviv, ISRAEL
Tel: 97236977650
Fax: 97236977683

Dr. Dennis Roser
Geo-Centers, Inc.
P.O. Box 68
Gunpowder Branch
Aberdeen Proving Ground, MD 21010-0068
Tel: 410/436-1820
Fax: 410/436-3764
E-mail: dennis.roser@sbccom.apgea.army.mil

Ms. Cindy Rossi
U.S. Army Medical Research Institute of Infectious Diseases
1425 Porter Street, DSD
Fort Detrick, MD 21702-5011
Tel: 301-619-7193
Fax: 301-619-2492
E-mail: cynthia.rossi@amedd.army.mil

Mr. Ian Rothwell
British Industrial & Research Assoc. Ltd
P.O. Box 2
1 Beach Road West
Portishead
Bristol, BS20 7JB UNITED KINGDOM
Tel: 44 (0) 1275 847787, :
Fax: 44 (0) 1275 847303
E-mail: I_rothwell@biral.com

Dr. Kelley Ruud
URS-Radian
8501 N. Mopac
Austin, TX 78759
Tel: 512/419-5934
Fax: 512/454-0109
E-mail: kelly_ruud@urscorp.com

- S -

Dr. Bohuslav Safar
Military Technical Institute of Protection
BYBKOVÁ 8
CZ-60200 BRNO, CZECH REPUBLIC
Tel: 420 5 41183189
Fax: 420 5 41182748
E-mail: jiri.kadlcak@telecom.cz

Dr. Gary Salzman
Los Alamos National Lab
Mail Stop D460
P.O. Box 1663
Los Alamos, NM 87945
Tel: 505-667-5503
Fax: 505-665-0854
E-mail: salzman@lanl.gov

Dr. Alan C. Samuels
U.S. Army ECBC
ATTN: AMSSB-RTE / E5554
5183 Blackhawk Road
Building E5554
APG, MD 21010-5424
Tel: 410/436-5874
Fax: 410/436-1120
E-mail: alan.samuels@sbccom.apgea.army.mil

Major Norman Saulnier
Canadian Embassy/NATIBO
Canadian Defence Liaison Staff (Washington)
501 Pennsylvania Ave., N.W.
Washington, DC 20001
Tel: 202-682-7633
Fax: 202-682-7643
E-mail: norman.saulnier@dfait-maeci.gc.ca

Mr. Brian Schimmoller
Radian
8501 N. Mopac Blvd.
Austin, TX 78720
Tel: 512/419-5288
Fax: 512/454-0109
E-mail: brian_schimmoller@urscorp.com

Mr. Roger Schlicht
General Atomics
3550 General Atomics Ct. - Bldg 30, Rm 102
San Diego, CA 92121-1122
Tel: 858-455-2509
Fax: 858-455-3231

Dr. John Schmidt
Environmental Technologies Group, Inc.
1400 Taylor Ave.
Baltimore, MD 21030
Tel: 410-321-5163
Fax: 410-339-3175
E-mail: jschm@envtech.com

Dr. Kristen Sellers
Veridian - PSR
1115 Fifth Street, SW
Charlottesville, VA 22902
Tel: 804/984-5657x142
Fax: 804/984-5156
E-mail: ksellers@psrw.com

Dr. Sanjiv R. Shah
Science & Technology Corp.
500 Edgewood Road, Suite 205
Edgewood, MD 21040
Tel: 410-436 5537
Fax: 410-436 5807
E-mail: shah@stcnet.com

Mr. Matthew J. Shaw
Battelle Memorial Institute
505 King Avenue
Columbus, OH 43201
Tel: 614-424-4075
Fax: 614-424-4185
E-mail: shawmj@battelle.org

Mr. Tommy R. Shedd
US Army Center for Environmental Health Research
568 Doughten Drive
Fort Detrick, MD 21702-5010
Tel: 301/619-7576
Fax: 301/619-7606
E-mail: tommy.shedd@amedd.army.mil

Mr. Donald B. Shoff
U.S. Army ECBC
ATTN: AMSSB-RRT-DD
E3220/127
5183 Blackhawk Road
Aberdeen Proving Ground, MD 21010-5424

Mr. David G. Shoffner
EAI Corporation
1308 Continental Drive
Suite J
Abingdon, MD 21009
Tel: 410/676-1449
Fax: 410/671-7241
E-mail: shoffner@eaicorp.com

LT James Simms
NAVFAC
6711 Hammond Ct
Marriottsville, MD 21104
Tel: 410-962-0684
Fax: 410-962-6751
E-mail: james.l.simms@usace.army.mil

Mr. Harold V. Smith
LaSys, Inc.
821 Canterbury Arc
Las Cruces, NM 88005
Tel: 505/525-8582
Fax: 505/525-8583
E-mail: hvsmith@zianet.com

Mr. Shane Smith
Microsensor Systems, Inc.
P.O. Box 609501
Orlando, FL 32860-9501
Tel: 407/884-3392
Fax: 407/886-7061
E-mail: ssmith@sawtek.com

Dr. A. Peter Snyder
U.S. Army ECBC
Research and Technology Directorate
Building E3220
Room 136
5183 Blackhawk Road
Aberdeen Proving Ground, MD 21010-5424
Tel: 410/436-2416
Fax: 410/436-3753
E-mail: apsnyder@sbccom.apgea.army.mil

Mr. Sam Sorice
SAIC
1227 S. Patrick Drive
Suite 110
Satellite Beach, FL 32937
Tel: 321-779-6041
Fax: 321-779-8715
E-mail: nancy.l.frey@saic.com

Mr. Sam Sorice, III
SAIC/CMO
1227 S. Patrick Drive
Suite 110
Satellite Beach, FL 32937
Tel: 321-494-8026
Fax: 321-779-4925
E-mail: soricesa@saic.com

Dr. Kevin M. Spencer
EIC Laboratories, Inc.
111 Downey Street
Norwood, MA 02062
Tel: 781-769-9450
Fax: 781-551-0283
E-mail: spencer@eiclabs.com

Ms. Debra Stephenson
General Dynamics Information Systems
8800 Queens Ave South
Bloomington, MN 55431
Tel: 952/921-6448
Fax: 952/921-6552
E-mail: debra.l.stephenson@gd-is.com

Mr. Douglas C. Stewart
Midwest Research Institute
425 Volker Blvd.
Kansas City, KS 64110
Tel: 816/753-7600x1261
Fax: 816/753-5359
E-mail: d.stewart@mriresearch.org

Dr. Robert Stirbl
Jet Propulsion Laboratory/NASA/Caltech
MS 306-438
4800 Oak Grove Drive
Pasadena, CA 91109
Tel: 818/354-5436
Fax: 818/393-4773
E-mail: robert.stirbl@jpl.nasa.gov

Dr. Peter J. Stopa
U.S. Army ECBC
ATTN: AMSSB-RIEN-E-MC, E3549
5183 Blackhawk Road
Aberdeen Proving Ground, MD 20101-5424
Tel: 410-436-5578
Fax: 410-612-5083
E-mail: pjstopa@apgea.army.mil

Dr. Micheline Strand
ARO
P.O. Box 12211
RTP, NC 27709-2211
Tel: 919-549-4343
Fax: 919-549-4399

Prof. Steven H. Strauss
Colorado State University
Department of Chemistry
Fort Collins, CO 80523
Tel: 970/491-5104
Fax: 970/491-1801
E-mail: strauss@chem.colostate.edu

Dr. Edward W. Stuebing
U.S. Army ECBC
ATTN: AMSSB-RRT-TA / E5951
5183 Blackhawk Road
Aberdeen Proving Ground, MD 20101-5424
Tel: 410/436-3089
Fax: 410/436-2742
E-mail: ewstuebi@sbccom.apgea.army.mil

Dr. Richard Suenram
NIST
Optical Technology Division
100 Bureau Drive, Stop 8441
Gaithersburg, MD 20899-8441
Tel: 301-975-2165
Fax: 301-975-2950
E-mail: richard.suenram@nist.gov

Lt. Joe Suhajda
311th NSW / YACN
7909 Lindbergh Drive
Bldg. 578
Brooks AFB, TX 78235-5352
Tel: 210/536-6364
Fax: 210/536-2993
E-mail: joseph.suhajda@brooks.af.mil

Dr. Jack A. Syage
Syagen Technology, Inc.
1411 Warner Avenue
Tustin, CA 92780
Tel: 714-258-4400x22
Fax: 714-258-4404
E-mail: jsyage@syagen.com

Dr. A.J. Syllaos
Raytheon
P.O. Box 660246, MS 35
Dallas, TX 75266
Tel: 972/344-3487
Fax: 972/344-3638
E-mail: syllaos@raytheon.com

Mr. James M. Sylvia
EIC Laboratories
111 Downey Street
Norwood, MA 02062
Tel: 781-769-9450
Fax: 781-551-0283

- T -

Dr. Mary Beth Tabacco
Echo Technologies, Inc.
451 D Street
Boston, MA 02210
Tel: 617-443-0066
Fax: 617-204-3080
E-mail: mtabacco@echotech.net

- V -

Ms. Rebecca Tanner
Science and Technology Corp.
500 Edgewood Road, Suite 205
Edgewood, MD 21040
Tel: 410 436-3471
Fax: 410 436-5807

Ms. Cindy Taylor
Environmental Technologies Group, Inc.
1400 Taylor Ave.
Baltimore, MD 21234
Tel: 410 321-5385
Fax: 410 339-3715
E-mail: ctayl@envtech.com

Dr. Jeffrey D. Teska
USAMRIID
Special Pathogens Branch
Diagnostic Systems Division
1425 Porter Street
Fort Detrick, MD 21702-5011
Tel: 301/619-7193
Fax: 301/619-2492
E-mail: jeffrey.teska@amedd.army.mil

Mr. Peter M. Tessier
University of Delaware
Department of Chemical Engineering
Newark, DE 19716
Tel: 302-831-6642
Fax: 302/831-1048
E-mail: tessier@che.udel.edu

Major Dany Theriault
National Defence Headquarters - Canada
DS/SPM 3-3
Major-General George R. Pearkes Bldg.
Ottawa, Ontario, K1A 0K2 Canada
Tel: 819-997-9760
Fax: 819-997-9685
E-mail: maj.d.theriault@debbs.ndhq.dnd.ca

Ms. Susan M. Thomas
Naval Surface Warfare Center
Dahlgren Division
17320 Dahlgren Road
Dahlgren, VA 2244805100
Tel: 540/653-2833

Dr. David Tratt
Jet Propulsion Laboratory
4800 Oak Grove Drive
MS 168-214
Pasadena, CA 91109
Tel: 818/354-2750
Fax: 818/393-6984
E-mail: dtratt@jpl.nasa.gov

Dr. Ashish Tripathi
Geo-Centers, Inc.
P.O. Box 68, Gunpowder Branch
APG, MD 21010
Tel: 410/436-2416
E-mail: axtripat@c-mail.apgea.army.mil

Dr. John Vitko, Jr.
Sandia National Lab/CA
PO Box 969
MS 9004
Livermore, CA 94551-0969
Tel: 925-294-2820
Fax: 925-294-3422
E-mail: ivitko@sandia.gov

Dr. Tuan Vo-Dinh
Oak Ridge National Laboratory
P.O. Box 2008
MS-6101
Oak Ridge, TN 37831-6101
Tel: 865/574-6249
Fax: 865/576-7651
E-mail: vodinh@ornl.gov

Mr. Bruce Voelker
Science and Technology Corp.
500 Edgewood Rd.
Suite 205
Edgewood, MD 21040
Tel: 410 436-5911
Fax: 410 436-5807
E-mail: btvoelker@c-mail.apgea.army.mil

- W -

Dr. Peter Watts
RSG Consulting
98 Firs Road, Firs Down
Salisbury, Wilts, SP5 1SP UNITED KINGDOM
Tel: 44 1980 862161
E-mail: pwatts.rsg@ukgateway.net

Dr. Michael A. Weibel
Battelle/Dugway Proving Ground
Bldg 4239
Dugway, UT 84022
Tel: 435 831-3888
Fax: 435 831-5432
E-mail: weibelm@battelle.org

Dr. Wayne Weimer
Zyvex Corporation
1321 N. Plano Road, Suite 200
Richardson, TX 75081x236
Tel: 972/235-7881
Fax: 972/235-7882
E-mail: wwweimer@zyvex.com

Dr. Charles H. Wick
U.S. Army ECBC
ATTN: AMSSB-RRT-DS
Bldg E3160
5183 Blackhawk Road
Aberdeen Proving Ground, MD 21010-5424
Tel: 410-436-3321
Fax: 410-436-1912
E-mail: chwick@apgea.army.mil

Dr. Peter L. Wick
NSWC
Code B20
17320 Dahlgren Road
Dahlgren, VA 22448-51--
Tel: 540-653-2794 f)
Fax: 540-654-8029
E-mail: WickPL@NSWC.NAVY.MIL

Mr. John Williams
Battelle Dugway Operations
Dugway Proving Ground
Dugway, UT 84022
Tel: 435-831-5862
Fax: 435-831-5922
E-mail: williamsjm@battelle.org

Mr. Michael Williamson
U.S. Army ECBC
ATTN: AMSSB-RRT-TA
5183 Blackhawk Road
Aberdeen Proving Ground, MD 21010-5424
Tel: 410/436-6701
Fax: 410/436-2742

Ms. Pat Wilson
Naval Surface Warfare Center
300 Hwy 361
Crane, IN 47522
Tel: 812/854-4917
Fax: 812/854-5828
E-mail: wilson-m@crane.navy.mil

Mr. Daniel Wise
U.S. Army ECBC
ATTN: AMSSB-RTB
5183 Blackhawk Road
APG, MD 21010-5424
Tel: 410/671-5403
Fax: 410/671-4048
E-mail: dgwise@sbccom.apgea.army.mil

Mr. Michael D. Wolozyn
LESCO
(Consultant for Army DCSLOG)
30 Francis Court
Stafford, VA 22554-7681
Tel: 703 697-2571
Fax: 703 614-7328
E-mail: michael.wolozyn@hqda.army.mil

Dr. Ngai M. Wong
U.S. Airforce Research Lab
ATTN: AMSSB-AL / E3332
5183 Blackhawk Road
Aberdeen Proving Ground, MD 21010-5424
Tel: 410/436-3111
Fax: 410/436-2447
E-mail: ngai.wong@sbccom.apgea.army.mil

- Y -

Ms. Susan Yim
US Army, Edgewood Biological Center
ATTN: AMSSB-RRT-BI
5183 Blackhawk Road (E3549)
Aberdeen Proving Ground, MD 21010-5424
Tel: 410-436-5530
Fax: 410-436-5807
E-mail: sxyim@sbccom.apgea.army.mil

Dr. Ray Yin
U.S. Army Research Lab
ATTN: AMSRL-WM
Building 4600
Aberdeen Proving Ground, MD 21005
Tel: 410 306-0680
Fax: 410 306-0676
E-mail: ryin@arl.army.mil

- Z -

Dr. Mitchell R. Zakin
Physical Sciences, Inc.
20 New England Business Center
Andover, MA 01810
Tel: 978-983-2252
Fax: 978-689-3232
E-mail: zakin@psicorp.com

Mr. Alan Zulich
U.S. Army, Edgewood Chemical & Biological Center
ATTN: AMSSB-RRT-BJ
5183 Blackhawk Road (E3549)
Aberdeen Proving Ground, MD 21010-5807
Tel: 410 436-3444
Fax: 410 436-5807
E-mail: awzulich@sbccom.apgea.army.mil

AUTHOR INDEX

-A-

Adkins, Douglas R., 140
 Akinyemi, Agnes, 328
 Allan, Cindy M., 199
 Altman, Wolf P., 52
 Anderson, George P., 408
 Anderson, Lawrence F., 140
 Arasteh, Ameneh M., 399, 401

-B-

Baker, William, 145
 Barry, Ken, 459
 Bechtel, James H., 390
 Beck, Heena S., 346
 Bello, Job, 486
 Bernia, Dennis, 586
 Birenzvige, Amnon, 573
 Black, R. S., 318
 Blethen, Gretchen, 122
 Bodily, Gary, 309
 Boiarski, Anthony A., 415
 Bottiger, Jerold R., 294, 328
 Bresler, Herbert S., 415
 Bright, Randy, 341
 Brittain, Alan M., 75
 Brock, Mary E., 222
 Brokenshire, John, 75
 Bromenshenk, Jerry, 380
 Bronk, Burt V., 542
 Brown, Steve, 227
 Brueck, S.R.J., 116
 Buonaugurio, Tom, 41
 Burckel, David, 116
 Burggraf, Larry W., 145, 533

-C-

Caraher, Timothy W., 123
 Carrabba, Michael, 486
 Catalano, Elizabeth S., 336
 Chandra, S., 318
 Chang, AnCheng, 471
 Chen, Jianzhu, 102
 Cheng, Tu-chen, 185
 Cherrier, Pierre P., 175
 Christensen, Deanna R., 195
 Christesen, Steven D., 486, 494
 Chu, P. M., 515
 Chuang, Han, 471, 479
 Chue, Calvin, 369
 Clapsaddle, Brady J., 158
 Clarke, Richard, 494
 Coliano, Tracy H., 399

Colston, Bill, 227
 Coon, Philip A., 341, 442
 Cork, Sarah, 399
 Coyne, Susan R., 373, 377
 Craw, Philip D., 373, 377
 Crocker, Robert, 131
 Czege, Jozsef, 543

-D-

DaBell R. S., 515
 Davis, Dennis M., 122
 Day, Peter J., 64
 DeFreez, Richard K., 175
 Deluca, Paul J., 294
 Doherty, Robert, 328
 Dubow, Joel, 309
 Dulleck, George R., 140
 Durst, H. Dupont, 109
 Dworzanski, Jacek P., 242

-E-

Eastwood, Delyle, 533
 Eldefrawi, Mohyee E., 204
 Ellzy, Michael W., 515, 522
 Emanuel, Peter A., 204, 369, 399
 Evans, Matthew D., 277
 Ezzell, John W., 199, 377

-F-

Fell, Jr., Nicholas F., 168
 Ferko, Scott, 131
 Fox, Alvin, 272
 Fox, Karen F., 272
 Fraser, G. T., 515
 Fruetel, Julia, 131
 Frye, Melissa S., 195
 Frye-Mason, Gregory C., 140

-G-

Gattuso, Anthony, 586
 Gibb, Tammy R., 195
 Gillespie James B., 168, 479
 Girvin, Kenneth L., 175
 Globus, Tatiana, 522
 Goode, Michael T., 212, 346, 423
 Gray, David, 341
 Green, Doug, 94
 Griest, Wayne H., 81
 Guan, Yifu, 390
 Guzelian, Andrew A., 151

-H-

Haglund, J. S., 318
Hall, Richard L., 415
Hanold, Karl A., 277
Harden, Charles S., 122, 459
Harmon, H. James, 505
Hart, Kevin J., 81
Hartman, Laurie J., 195
Hasselbrink, Charlie, 131
Hebert, Gretchen N., 158
Heller, Edwin J., 140
Henchal, Erik A., 195, 222, 373, 377
Heroux, Karen S., 399
Hight Walker, A. R., 515
Hilley, Bob, 586
Hohe, Donald R., 52
Hollis, Mark A., 102
Howard, Rob, 61
Hyrncewich, Alexander P., 81

-I-

Isley, Elizabeth A., 123
Ives, Jeffery T., 390

-J-

Jabbour, Rabih, 252
Janni, James A., 151
Jenkins, Amanda, 109
Jensen, James O., 515, 522
Jensen, Janet, 109
Johnson, Bernadette, 102
Johnson, Gregory P., 235
Johnson, Yvette A., 272
Johnson-Winegar, Anna, 28
Jones, Les, 227

-K-

Kalmes, Kimberly A., 123
Kerby, Stephen B., 195
Kesavan, Jana, 328
Khalil, Maha, 204
Khan, Akbar S., 204, 401
Kijek, Todd M., 222
Kim, Man-Goo, 242
Kirchoff, J., 498
Knauert, Fred K., 373, 377
Koch, Leslie, 17
Kottenstette, Richard J., 140
Kracke, Suzanne K., 369, 399
Krahmer, Mark T., 272
Krak, Stephen J., 415
Krishnamurthy, Thaiya, 252
Kyung, Jae H., 102

-L-

Laine, Bruno, 252
Lall, Ravi P., 432
Lammert, Stephen A., 81, 263
LaMoy, Diane, 552
Langlois, Richard G., 227
Lee, S. A., 318
Lee, Stephen J., 92
Lewis, Patrick R., 140
Li, Guangming, 145
Li, Zhao Z., 543
Lighthart, Bruce, 380
Ligler, Frances S., 408
Lindsey, Misty H., 346
Lochner, J. Michael, 515, 522
Loerop, William R., 522
Long, S. Randolph, 9
Loper, Gerald, 380
Lozos, George, 94
Lucke, J., 498
Ludwig, George V., 222
Luoma, Greg A., 175

-M-

MacIver, Brian, 486
Makrides, Savvas C., 151
Manginell, Ronald P., 140
Martinez, David, 140
Masquelier, Don, 227
Maswadeh, Waleed M., 242, 442, 459
Mathews, John, 309
Mathews, Richard H., 102
Mayfield, Howard T., 533
McBride, Mary, 227
McCubbin, Patrick E., 357
McFarland, Andrew R., 318
McHugh, Vincent M., 122
McLeod, S., 498
Mendenhall, Linda M., 102
Menking, Darrel E., 369
Menking, Deborah L., 212, 423
Meuzelaar, Henk L. C., 242
Milanovich, Fred, 227
Milham, Merrill E., 542
Mills, John D., 586
Moshier, LTC Timothy, 41
Mowry, Curtis D., 140
Myer, Pete, 227
Myers, Emily D., 212, 423

-N-

Nagpal, Madan, 272
Nargi, Frances E., 102
Nasarabadi, Shanavaz, 227

Nielsen, Bruce J., 586
Nilo, Patricia, 25
Norwood, David A., 195
Nottke, F., 498
Nowak, Daniel M., 61

-O-

O'Connell, Kevin P., 204
Obergh, D., 498
Odom, Matthew A., 158
Ong, Kate K., 494, 522

-P-

Palmacci, Steven T., 102
Park, Jun T., 399
Parsons, John A., 242, 459
Paterno, Dorothea, 522, 565
Pellegrino, Paul M., 168
Petrovick, Martha S., 102
Phan, H. N., 318
Phelps, Kirkman, 1
Piccioni, Marc A., 175
Plusquellic, D. F., 515
Pollard, J., 498
Potter, Michael A., 175
Premasiri, Ranjith, 494
Prier, Kevin, 380
Procell, Lawrence, 486
Pulaski, Paul D., 116

-Q-

Qin, Dujie, 109

-R-

Raelin, Jeremy A., 151
Ramponi, Albert J., 227
Rastogi, Vipin K., 185
Redus, Stephanie L., 199
Renzi, Ronald, 131
Rhoderick, G. C., 515
Rider, Todd H., 102
Roark, Joel, 586
Roehl, Joseph E., 123
Roser, Dennis C., 252
Rossi, Cindy A., 222
Rowe-Taitt, Chris A., 408
Rundell, Ann E., 102
Russo, Jaimie, 479

-S-

Salzmann, Jean-Pierre, 252
Samuels, Alan C., 515, 522

Sasaki, Darryl Y., 140
Schlicht, Roger, 586
Shah, Sanjiv R., 346
Shaw, Matthew J., 318
Shoemaker, David R., 373
Shoff, Donald B., 122
Shokair, Isaac, 131
Shopes, Robert, 204
Sickenberger, David W., 81
Smith, Allen, 566
Smith, Laura T., 102
Snyder, A. Peter, 242, 432, 442, 459
Sorricks, David, 486
Spencer, Kevin M., 151
Stamps, Jamie, 131
Stephens, Timothy, 102
Stephenson, James L., 263
Stinchcombe, Timothy J., 204
Stopa, Peter J., 289, 341
Strauss, Steven H., 158
Stuebing, Edward W., 294, 328
Suenram, R. D., 515
Swart, Remco, 252
Syage, Jack A., 277
Sylvia, James M., 151

-T-

Tabacco, Mary Beth, 471, 479
Tanner, Rebecca L., 212, 346
Taylor, Laura, 471
Teska, Jeffrey D., 199, 377
Thompson, Roy G., 401
Tripathi, Ashish, 242, 442, 459
Trudil, David, 341

-V-

Valdes, James J., 204, 369, 401
VanderNoot, Victoria, 131
Venkateswaran, Kodumudi, 227
Voelker, Bruce T., 212

-W-

Weber, Daniel, 328
Whitney, Ronald B., 175
Wick, Charles H., 357, 573
Wilson, Rod, 94
Wise, Daniel, 328
Wise, Marcus B., 81
Womble, M. Edward, 494
Wong, Alex S., 175
Wong, Ngai, 9
Woolard, Dwight, 522